

PRINCIPLES OF POLYMER SYSTEMS

SIXTH EDITION

Ferdinand Rodriguez
Claude Cohen
Christopher K. Ober
Lynden A. Archer



CRC Press
Taylor & Francis Group

PRINCIPLES OF
POLYMER SYSTEMS

SIXTH EDITION

PRINCIPLES OF
POLYMER SYSTEMS
SIXTH EDITION

Ferdinand Rodriguez
Claude Cohen
Christopher K. Ober
Lynden A. Archer



CRC Press

Taylor & Francis Group

Boca Raton London New York

CRC Press is an imprint of the
Taylor & Francis Group, an **informa** business

CRC Press
Taylor & Francis Group
6000 Broken Sound Parkway NW, Suite 300
Boca Raton, FL 33487-2742

© 2015 by Taylor & Francis Group, LLC
CRC Press is an imprint of Taylor & Francis Group, an Informa business

No claim to original U.S. Government works
Version Date: 20141017

International Standard Book Number-13: 978-1-4822-2379-8 (eBook - PDF)

This book contains information obtained from authentic and highly regarded sources. Reasonable efforts have been made to publish reliable data and information, but the author and publisher cannot assume responsibility for the validity of all materials or the consequences of their use. The authors and publishers have attempted to trace the copyright holders of all material reproduced in this publication and apologize to copyright holders if permission to publish in this form has not been obtained. If any copyright material has not been acknowledged please write and let us know so we may rectify in any future reprint.

Except as permitted under U.S. Copyright Law, no part of this book may be reprinted, reproduced, transmitted, or utilized in any form by any electronic, mechanical, or other means, now known or hereafter invented, including photocopying, microfilming, and recording, or in any information storage or retrieval system, without written permission from the publishers.

For permission to photocopy or use material electronically from this work, please access www.copyright.com (<http://www.copyright.com/>) or contact the Copyright Clearance Center, Inc. (CCC), 222 Rosewood Drive, Danvers, MA 01923, 978-750-8400. CCC is a not-for-profit organization that provides licenses and registration for a variety of users. For organizations that have been granted a photocopy license by the CCC, a separate system of payment has been arranged.

Trademark Notice: Product or corporate names may be trademarks or registered trademarks, and are used only for identification and explanation without intent to infringe.

Visit the Taylor & Francis Web site at
<http://www.taylorandfrancis.com>

and the CRC Press Web site at
<http://www.crcpress.com>

Contents

Preface.....	xvii
Authors.....	xix
Chapter 1 Introduction	1
1.1 Polymers.....	1
1.2 Applications of Polymers	2
1.3 Polymer-Based Industries	4
1.3.1 Plastics	5
1.3.2 Rubber.....	5
1.3.3 Fibers	7
1.3.4 Coatings	8
1.3.5 Adhesives	8
1.4 Feedstocks for Polymers	8
1.5 Polymer Science and Technology	12
1.6 Trends.....	16
Keywords.....	17
Problems	17
References	18
General References.....	19
Chapter 2 Basic Structures of Polymers	21
2.1 Classification Schemes.....	21
2.2 Bonding.....	22
2.3 Single Molecules	25
2.4 Network Molecules	28
2.5 Thermodynamics of Binary Systems.....	28
2.5.1 Entropy	29
2.5.2 Enthalpy	30
2.5.3 Free Energy.....	31
2.5.4 Swelling of Polymer Networks	31
2.6 CED and Solubility Parameters	35
2.6.1 Solubility Parameters of Polymers	36
2.6.2 Hydrogen-Bonding Index	41
2.6.3 Group Contribution Method	41
Appendix 2.A	42
Keywords.....	45
Problems	45
References	49
General References.....	50

Chapter 3	Physical States and Transitions	53
3.1	Physical States	53
3.2	Conformation of Single Chains in Solutions.....	53
3.3	Phase Separation in Polymer Mixtures	56
3.4	Transitions in Pure Polymers	61
3.5	Amorphous Polymers.....	64
3.6	Plasticization	70
3.7	Crystallinity.....	72
3.8	Conformation of Single Chains in Crystals	75
3.9	Spherulites and Drawing	77
3.10	Crystallization Kinetics.....	80
3.11	Transition Temperatures.....	83
3.12	Strain-Induced Crystallization	90
3.13	Block Copolymers	91
3.14	LC Polymers.....	93
3.15	Gels.....	95
	Keywords.....	97
	Problems	98
	References	103
	General References.....	105
Chapter 4	Polymer Formation.....	107
4.1	Polymerization Reactions.....	107
4.2	Functionality	108
4.3	Step- and Chain-Growth Polymerizations	111
4.4	Chain Polymerization.....	111
4.4.1	Kinetic Scheme.....	111
4.4.2	Individual Rate Constants.....	116
4.4.3	Molecular Size	120
4.4.4	Chain Transfer and Inhibition.....	121
4.4.5	Temperature Dependence	125
4.4.6	Conjugated Diene Monomers	126
4.5	Ionic Polymerization	127
4.5.1	Cationic Polymerization	127
4.5.2	Anionic Polymerization	132
4.6	Controlled Radical Polymerization	137
4.7	Insertion Polymerization	141
4.7.1	Ziegler–Natta Catalysts	141
4.7.2	Metallocene Catalysts.....	143
4.7.3	Supported Chromium Catalysts	144
4.7.4	Group Transfer Polymerization	145

4.8	Step-Growth Polymerization	146
4.8.1	Hyperbranched Polymers and Dendrimers	152
4.9	Ring-Opening Polymerization	154
4.9.1	Bis-Benzocyclobutane Resin	156
4.10	Chain Copolymerization	157
4.10.1	Assumptions	157
4.10.2	Material Balances	158
4.10.3	Special Cases	159
4.10.4	Other Copolymers	164
4.11	Biosynthesis of Polymers	165
4.12	Polymer Modification	169
	Keywords	171
	Problems	173
	References	181
	General References	183
Chapter 5	Polymerization Processes	187
5.1	Design Criteria	187
5.2	Bulk Polymerization	191
5.2.1	Quiescent Bulk Polymerization (Monomer Casting)	191
5.2.2	Stirred Bulk Polymerization	192
5.3	Solution Polymerization	196
5.4	Suspension Polymerization	202
5.5	Emulsion Polymerization	205
5.6	Polymerization Reaction Engineering	212
5.7	Comparison of Polymerization Methods	213
	Keywords	214
	Problems	214
	References	218
	General References	219
Chapter 6	Molecular Weight of Polymers	221
6.1	Molecular Weight Distribution and Average Molecular Weight	221
6.2	Theoretical Distributions	224
6.3	Empirical Distribution Models	229
6.4	Measurement of Distribution	232
6.5	Measurement of Molecular Weight	239
6.6	Number-Average Molecular Weight Methods	240
6.7	Weight-Average Molecular Weight Methods	247

Appendix 6.A	254
Appendix 6.B	254
Appendix 6.C.....	255
Keywords.....	256
Problems	257
References	263
General References.....	264
Chapter 7 Viscous Flow	267
7.1 Introduction.....	267
7.2 Viscosity.....	268
7.2.1 Definitions and Microscopic Origins	268
7.2.2 Non-Newtonian Viscosity.....	272
7.2.3 Models for the Viscosity of Non-Newtonian Fluids....	276
7.3 Viscometry.....	280
7.4 Polymer Shapes in Solution	285
7.4.1 Polymer Chain Statistics.....	285
7.4.2 Dilute Solution Viscous Properties.....	294
7.4.3 Polymer Molecular Weight and Intrinsic Viscosity	297
7.5 Effect of Concentration and Molecular Weight	301
7.6 Effect of Temperature and Pressure.....	308
7.7 Elongational Viscosity	310
7.8 Drag Reduction in Turbulent Flow	315
Keywords.....	319
Problems	321
References	328
Chapter 8 Rheometry and Viscoelastic Fluid Flow	331
8.1 Introduction.....	331
8.2 Normal Stress Differences in Shear.....	332
8.3 Poiseuille Flow in Tubes and Capillaries.....	336
8.4 Couette Shear Flow between Coaxial Cylinders	341
8.5 Torsional Shear between Parallel Plates	347
8.6 Shear between Cone-and-Plate Fixtures.....	350
Appendix 8.A Equations of Continuity for Incompressible Fluids under Isothermal Flow Conditions	355
Appendix 8.B Differential Equations of Motion.....	356
Keywords.....	357
Problems	358
References	360

Chapter 9	Mechanical Properties at Small Deformations	361
9.1	Introduction.....	361
9.2	Polymer Elasticity in Various Deformations	361
9.3	Viscoelasticity—Maxwell Model	365
9.3.1	Creep.....	366
9.3.2	Stress Relaxation	367
9.3.3	Constant Rate of Strain	368
9.3.4	Harmonic Motion	369
9.4	Dynamic Measurements	371
9.5	Polymers—Five Regions of Viscoelasticity.....	374
9.6	Generalized Maxwell Model	377
9.7	Coarse-Grained Molecular Models and Effect of Molecular Weight.....	381
9.8	Effect of Crystallinity	386
9.9	Rubber Elasticity.....	388
9.9.1	Ideal Rubber Elasticity	388
9.9.2	Modifications of the Ideal Rubber Model	393
9.9.3	Continuum Mechanics and Empirical Models of Rubber Elasticity.....	398
9.9.4	Viscoelasticity of Elastomers	401
9.10	Effect of Fillers	403
9.11	Other Transitions	403
Appendix 9.A	Harmonic Deformation of a Maxwell Element.....	405
9.A.1	Trigonometric Notation.....	405
9.A.2	Complex Notation.....	407
	Keywords	408
	Problems	409
	References.....	415
	General References.....	417
Chapter 10	Ultimate Properties	419
10.1	Failure Tests.....	419
10.2	Constant-Rate-of-Strain Tests.....	421
10.3	Breaking Energy	423
10.4	Creep Failure.....	424
10.5	Fatigue.....	425
10.6	Reduced-Variable Failure Correlations.....	426
10.7	Fracture of Glassy Polymers.....	428
10.8	Fracture of Elastomers	432
10.9	Heterophase Systems	434
10.9.1	Partly Crystalline Materials	434
10.9.2	Fibers	435

10.9.3	Rubber	438
10.9.4	Composites	441
	Keywords.....	445
	Problems	446
	References	446
	General References.....	447
Chapter 11	Some General Properties of Polymer Systems.....	449
11.1	Design Criteria.....	449
11.2	Compounding	449
11.3	Hardness	451
11.4	Density	452
11.5	Thermal Properties.....	453
11.6	Electrical Properties	455
11.7	Optical Properties	463
11.8	Diffusion in Polymers.....	466
	Keywords.....	469
	Problems	470
	References	472
	General References.....	473
Chapter 12	Degradation and Stabilization of Polymer Systems.....	477
12.1	Introduction	477
12.2	Degrading Agencies.....	477
12.2.1	Electromagnetic Waves	478
12.2.2	Oxidation	480
12.2.3	Moisture and Solvents	480
12.2.4	Biological Degradation.....	483
12.3	Phase Separation and Interfacial Failure.....	483
12.4	Polymer Degradation	484
12.4.1	Chain Scission	484
12.4.2	Depolymerization	486
12.4.3	Cross-Linking.....	487
12.4.4	Bond Changes.....	489
12.4.5	Side-Group Changes.....	491
12.5	Antioxidants and Related Compounds	491
12.6	Stabilizers for Irradiated Systems	496
12.7	Ablation	500
	Keywords.....	502
	Problems	503
	References	503
	General References.....	504

Chapter 13	Fabrication Processes	507
13.1	Fabrication.....	507
13.2	Raw Material Forms.....	507
13.3	Mixing.....	508
13.4	Coatings and Adhesives	513
13.4.1	Coatings	513
13.4.1.1	Nondiluent, Nonreactive.....	513
13.4.1.2	Nondiluent, Reactive.....	514
13.4.1.3	Diluent, Nonreactive.....	517
13.4.1.4	Diluent, Reactive	519
13.4.2	Adhesives	521
13.5	Photoresists: An Application of Polymers to Microelectronics.....	524
13.6	Polymeric Membranes.....	529
13.7	Applications of Polymers in Medicine.....	532
13.7.1	Hip Prosthesis	533
13.7.2	Vascular Grafts	535
13.7.3	Sutures.....	535
13.7.4	Controlled Drug Delivery Systems	536
13.7.5	Tissue Engineering.....	539
	Keywords.....	539
	Problems.....	540
	References	541
	General References.....	542
Chapter 14	Fabrication Processes: Extrusion and Molding	547
14.1	Extrusion in General	547
14.2	Extrusion of Flat Film, Sheet, and Tubing	551
14.3	Fibers	559
14.4	Laminates	564
14.5	Compression Molding	566
14.6	Injection Molding	568
14.7	Injection-Molding Simulations.....	573
14.7.1	Filling Stage	573
14.7.2	Packing Stage.....	576
14.7.3	Cooling Stage.....	577
14.8	Other Molding Processes	577
14.8.1	Reaction Injection Molding.....	577
14.8.2	Casting	578
14.8.3	Blow Molding and Sheet Molding	580

14.9	Foams	583
14.9.1	Polyurethane Foams.....	585
14.9.2	Rubber and Poly(Vinyl Chloride) Foams.....	586
14.9.3	Rigid Foams	590
14.10	Sheet Forming	593
	Keywords.....	596
	Problems.....	597
	References	597
	General References.....	599

Chapter 15 Polymers from Renewable Resources and Recycling

	of Polymers.....	603
15.1	Introduction	603
15.2	Polysaccharides	603
15.2.1	Selected Uses	607
15.3	Biological Polyamides.....	607
15.4	Biological Polyesters	611
15.5	Polymers from Renewable Resources	613
15.5.1	Polyesters.....	613
15.5.2	Polyols	615
15.5.3	Use of CO ₂ as Feedstock.....	616
15.5.4	Metabolic Engineering Production of Raw Materials	616
15.6	Waste Generation and Disposal	617
15.6.1	Disposal.....	617
15.6.2	Recycling of Paper, Glass, and Aluminum	619
15.7	Identification and Separation.....	620
15.7.1	Identification	620
15.7.2	Size Reduction	622
15.7.3	Direct Flotation.....	622
15.7.4	Froth Flotation.....	623
15.7.5	Water Removal.....	623
15.7.6	Paper Removal	623
15.7.7	Metal Removal.....	624
15.7.8	Dissolution	625
15.7.9	Combined Technology	625
15.8	Down-Cycling	626
15.8.1	Film Reclamation Process	627
15.9	Monomer Recovery	628
15.10	Hydrogenation, Pyrolysis, and Gasification	628
15.10.1	Hydrogenation (Liquid Product and Hydrogen Atmosphere)	629
15.10.2	Pyrolysis (Gaseous Product and Inert Atmosphere)	629

15.10.3	Gasification (Gaseous Product and Oxidizing Atmosphere)	629
15.11	Incineration with Energy Recovery.....	630
15.11.1	Power Plants	630
15.11.2	Incineration	631
15.11.3	Cement Kilns	631
15.12	Degradable Polymers	633
15.12.1	Photooxidation	633
15.12.2	Hydrolysis.....	633
15.12.3	Microbial Degradation (Biodegradation).....	634
15.12.4	Commercial and Near-Commercial Degradable Polymers	634
15.12.5	Applications	636
15.13	Prospects	636
	Keywords.....	638
	Problems.....	640
	References	641
	General References.....	643
Chapter 16	Carbon Chain Polymers	645
16.1	Introduction	645
16.2	The Polyolefins	646
16.2.1	Some Individual Polymers	646
16.2.2	Selected Uses	648
16.3	The Acrylonitrile–Butadiene–Styrene Group.....	648
16.3.1	Some Individual Polymers	649
16.3.2	Selected Uses	653
16.4	The Diene Polymers	653
16.4.1	Some Individual Polymers	654
16.4.2	Selected Uses	658
16.5	The Vinyls	658
16.5.1	Some Individual Polymers	659
16.5.2	Selected Uses	661
16.6	The Acrylics	661
16.6.1	Some Individual Polymers	661
16.6.2	Selected Uses	663
16.7	The Fluorocarbon Polymers.....	663
16.7.1	Some Individual Polymers	664
16.7.2	Selected Uses	665
Appendix 16.A	Generic Classification of Some Commercial Elastomers.....	666
Appendix 16.B	Classification and Properties of Principal Man-Made Fibers.....	667
Appendix 16.C	The Polyolefins	669
Appendix 16.D	The Acrylonitrile–Butadiene–Styrene Group	671

Appendix 16.E	The Dienes (Butadiene Included in Appendix 16.D).....	673
Appendix 16.F	The Vinyls.....	674
Appendix 16.G	The Acrylics.....	675
Appendix 16.H	The Fluorocarbon Polymers	676
Keywords.....		677
Problems.....		677
References		678
General References.....		679
Chapter 17	Heterochain Polymers	683
17.1	Introduction	683
17.2	Polyesters.....	683
17.2.1	Some Individual Polymers	683
17.2.2	Selected Uses	688
17.3	Polyethers	689
17.3.1	Some Individual Polymers	689
17.3.2	Selected Uses	693
17.4	Polyamides and Related Polymers	694
17.4.1	Some Individual Polymers	694
17.4.2	Selected Uses	700
17.5	Aldehyde Condensation Polymers.....	700
17.5.1	Some Individual Polymers	701
17.5.2	Selected Uses	701
17.6	Polymers Based on Isocyanate Reactions	703
17.6.1	Some Individual Polymers	703
17.6.2	Selected Uses	705
17.7	Silicones	706
17.7.1	Some Individual Polymers	706
17.7.2	Selected Uses	710
17.8	Polyphosphazenes	710
17.8.1	Some Individual Polymers	711
17.8.2	Selected Uses	712
17.9	Engineering Resins and High-Performance Polymers.....	712
17.10	Thermoplastic Elastomers.....	715
Keywords.....		718
Problems.....		719
References		720
General References.....		721
Chapter 18	Analysis and Identification of Polymers.....	725
18.1	Purpose of Polymer Analysis	725
18.2	IR and Ultraviolet Spectroscopy	725
18.3	Differential Thermal Methods	728

18.4	Other Methods of Thermal Analysis.....	734
18.5	Nuclear Magnetic Resonance Spectroscopy	736
18.6	X-Ray Methods	739
18.7	Miscellaneous Spectroscopic Methods	742
18.8	Chemical Tests and Identification Schemes	743
	Keywords.....	743
	Problems.....	744
	References	744
	General References.....	745
Appendix A	747
Appendix B	759
Appendix C	769
Appendix D	771
Appendix E	773
Index	775

Preface

The sixth edition of the book *Principles of Polymer Systems* contains new material and additional end-of-chapter problems. The team of authors who wrote the fifth edition has collaborated in revising the book. The basic structure of the book and the general level of treatment remain unchanged. We have continued to deepen and strengthen the fundamentals of chemistry, physics, materials science, and chemical engineering pertaining to polymer systems. The theoretical aspects remain at the level of a first course in polymers for senior undergraduates and beginning graduate students in several fields. Because the revisions required expansion of some topics and introduction of new ones, outdated or less relevant material was deleted to keep the book at a similar size as in the previous edition.

This edition includes a more detailed discussion of crystallization kinetics, strain-induced crystallization, block copolymers, liquid crystal polymers, and gels in Chapter 3. New, powerful radical polymerization methods such as atom transfer radical polymerization (ATRP), nitroxide-mediated polymerization (NMP), and reversible addition/fragmentation chain-transfer polymerization (RAFT) are introduced in Chapter 4. Chapter 5 on polymerization processes now includes additional flow sheets and discussion of the polymerization of polystyrene and poly(vinyl chloride). The topics of flow and deformation of polymer systems are now described in three chapters. Chapter 7 discusses viscous flow and viscosity models for non-Newtonian fluids and includes a new section on the elongational viscosity of polymers, a property of considerable importance in extension-dominated processes such as fiber spinning. Rheometry and viscoelastic flow are presented in Chapter 8. Coarse-grained bead-spring molecular and tube models are discussed in addition to the generalized mechanical model of Maxwell to describe viscoelasticity in Chapter 9. Models and experimental results of rubber elasticity have also been updated in Chapter 9. The ultimate properties in Chapter 10 have an expanded section on fracture of glassy and semicrystalline polymers and a new section on the fracture of elastomers. A new section on diffusion in polymers has been added to Chapter 11 on general properties and a section on membrane formation added to Chapter 13 on fabrication methods. The field of polymers from renewable resources has recently blossomed and has been elaborated upon in Chapter 15 that includes the topics of waste disposal and recycling of polymers. Chapter 18 on analysis and identification of polymers contains a new section on X-ray methods and a discussion of dielectric relaxation.

We hope that the integrated approach to polymer science and engineering presented here will also make the book a useful reference. The practitioner of polymers in traditional industries focused on plastics, fibers, coatings, and adhesives, as well as in newer applications such as in electronics, medicine, and membrane separations, would find the book useful. We are indebted to the insights of students and teachers over the years.

We are grateful for the comments and suggestions from many users and reviewers. We have corrected errors and typos in the previous edition and hope our readers will be forgiving for those that have escaped our attention in the present one.

Ferdinand Rodriguez

Cornell University

Claude Cohen

Cornell University

Christopher K. Ober

Cornell University

Lynden A. Archer

Cornell University

Authors

Ferdinand Rodriguez is professor emeritus of chemical engineering at Cornell University, Ithaca, New York. He was the author of the first edition of this textbook. His BS and MS degrees in chemical engineering were earned at Case Western Reserve University, Cleveland, Ohio. After serving in the US Army, he earned his PhD in chemical engineering at Cornell University. His research in the field of polymers resulted in over 150 journal articles, while he was on the Cornell faculty. Many of these were presented at meetings of the American Chemical Society, the American Institute of Chemical Engineers, and the Society of Plastics Engineers. In retirement he remains active in Cleveland chapters of these organizations. He has published a few original music compositions and is an active amateur musician in several Cleveland area groups.

Claude Cohen is the Fred H. Rhodes professor of engineering at Cornell University. He received his BS (with high honors) from the American University in Cairo, Egypt, and his PhD from Princeton University, Princeton, New Jersey. He was a Katzir-Katchalsky fellow at the Weizmann Institute of Science, Rehovot, Israel, and a research associate at Caltech, Pasadena, California. He joined Cornell School of Chemical Engineering Ithaca, New York in 1977 where he has been ever since except for sabbatical leaves in Strasbourg, Haifa, San Jose (California), and Paris.

Professor Cohen received an Excellence in Teaching Award for his course on polymeric materials based on this textbook. His research interests focus on the structure–property relationships of elastomers and the testing of theories of rubber elasticity and fracture. Previous research efforts were devoted to the study of suspensions and their applications. He was a co-principal investigator of the Cornell Injection Molding Program initiated under a grant from the National Science Foundation (NSF) and supported by an industrial consortium until 2000.

Christopher K. Ober joined Cornell University in 1986 after four years working in industry at the Xerox Research Centre of Canada on problems related to printer technology. He is now the Francis Bard professor of materials engineering and has served as chair of the department of materials science and engineering. More recently he has been associate dean of engineering for research and graduate studies and the interim dean of engineering at Cornell. He received his BSc Honours in Chemistry (Co-op) from the University of Waterloo, Waterloo, Ontario, in 1978 and his PhD in polymer science and engineering in 1982 from the University of Massachusetts at Amherst, Massachusetts. He has pioneered new materials for photolithography and studies the biology materials interface. An early contributor to the investigation of self-organizing systems, he studies liquid crystals and block copolymers. More recently he has begun to study nanoparticle materials. Professor Ober has reported the results of his research in more than 350 peer-reviewed publications, book chapters, and conference proceedings, and delivered more than 400 invited presentations.

A fellow of both the American Chemical Society and the American Physics Society, his awards include the 2013 SPS Japan International Award, the 2009 Gutenberg Research Award from the University of Mainz, the 1st Annual FLEXI Award in the Education Category (for flexible electronics) in 2009, a Humboldt Research Prize in 2007, and the 2006 ACS Award in Applied Polymer Science.

Lynden A. Archer is a professor of chemical engineering at Cornell University and the William C. Hoey director of the School of Chemical and Biomolecular Engineering Ithaca, New York. Since 2008, he has served as co-director of the KAUST-Cornell University (KAUST-CU) Center for energy and sustainability, which focuses on basic research and applications of polymer–nanoparticle composite materials.

Professor Archer received his BSc in chemical engineering (polymer science) from the University of Southern California in 1989 and his PhD in chemical engineering from Stanford University, Stanford, California, in 1993. His research focuses on transport properties of polymers and polymer–particle hybrids and their applications for electrochemical energy storage.

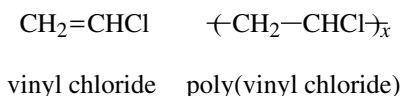
He is a fellow of the American Physical Society and the recipient of the 2013 National Science Foundation Special Creativity Award from the Division of Materials Research. Archer has published over 160 scientific papers on physical polymer science and nanomaterials science and applications.

1 Introduction

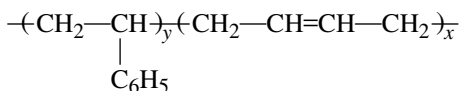
1.1 POLYMERS

In a literal sense, the term **polymer** denotes a molecule made up by the repetition of some simpler unit, the **monomer**. The term **macromolecule**, big molecule, also is used more or less as a synonym for polymer. Both terms are used in referring to more complex structures made up from more than one monomer. Some important polymers are linear, but branched, cross-linked, or even more complex architectures are also common.

In formulas representing polymers, the end groups are often ignored because they may not have a major effect on the properties of the polymer. For example, the polymer based on vinyl chloride is represented in the following way:

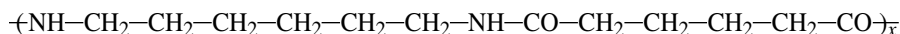


Also, the fact that several monomers are dispersed at random in a chain may not be explicit to allow us to abbreviate the structure, as in the random **copolymer** of styrene and butadiene:



Styrene-butadiene rubber copolymer

In nylon 6,6, the repeating unit is made up of a diamine and a diacid:



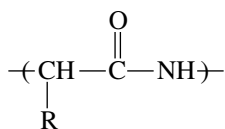
Nylon 6,6 (a polyamide based on hexamethylenediamine and adipic acid)

In some cases two monomers may be combined to form a **dimer**, three to form a **trimer**, and so on. The number of repeating monomer units is referred to as the **degree of polymerization**, indicated by x or y in the formulas shown (see also Section 4.4). When more than one monomer is present in the polymer, as in styrene-butadiene rubber (SBR), the overall degree of polymerization may be ambiguous. For low-molecular-weight polymers, the term **oligomer** (*oligo* being a prefix of Greek origin meaning “few”) is often used. Typically, oligomers might encompass degrees of polymerization of 2–20. The analogous term **oligosaccharide** usually includes molecules with 2–6 sugar units (see Figure 15.3).

Some naturally occurring polymers have a simple repeating unit. Starch, cellulose, and natural rubber are examples of such polymers, which are chains of a simple

unit repeated thousands of times. Cellulose, in the form of cotton, is useful as a textile fiber without chemical modification. The polymer-based industries all started with such naturally occurring materials. A second stage in industrial development has often been the modification of a natural polymer to make it more useful. Cellulose from wood and other sources was modified to make semi-synthetic fibers, plastics, and coatings. All industries have found that wholly synthetic polymers, built up from small molecules, such as ethylene and propylene, offer a broad spectrum of properties. Obviously, many natural materials still have a place in technology. However, when the idea arises of “tailoring” a polymer to certain end-use requirements, the wholly synthetic polymers often provide the most successful solution.

The study of naturally occurring complex polymers made great strides in the latter part of the last century. A relatively simple example is **insulin**, a hormonal protein that forms in the pancreas. It is best known as an agent to lower blood sugar in diabetic patients. The structure has repeating units with amide linkages (also called peptide linkages):



A macromolecule of insulin has a total of 51 such units with 16 variations of R. Proteins, nucleic acids (DNA, RNA), and enzymes generally are complex macromolecules (see Chapter 15).

1.2 APPLICATIONS OF POLYMERS

To the general public, plastics, fibers, rubber, adhesives, paints, and coatings all are familiar as consumer products. The fact that all of these are based on polymers, and that often the same polymer can be used for more than one application, is a much less familiar concept.

In Table 1.1 the usage of polymers in three major categories is summarized for two decades. Of course, in every category there are some specialty polymers that go into specific *niche* markets representing areas of growth and profit. The commodity polymers may dominate the statistics, but they do not always represent the items of greatest value to a particular company. For example, biodegradable sutures, contact lenses, and adhesives for microchips all use small volumes of expensive, special polymers.

Over the decades, the major uses of some materials have not changed much. Most fibers, both synthetic and natural, still go into clothing and house furnishings, just as they did over a century ago. Automobile parts including tires use over two-thirds of the rubber consumed in the United States, just as they did half a century ago. Protective and decorative coatings and the adhesives sold in hardware stores still resemble, at least superficially, the products sold for many decades. However, it is in the area of plastics that diversity of materials and of applications has grown most conspicuously.

New or expanded applications are the main reason for the consistent growth of plastics in the two decades (1980–2000), as seen in Table 1.1. In that period, the use of poly(vinyl chloride) for pipe, conduit, and siding in construction became common.

TABLE 1.1
Polymer Consumption in the United States (in Units of 10⁶ kg)

Category	1980	1990	2000
All plastics (sales)	15,826	26,859	42,893
Thermosets (total)	2,726	4,517	5,820
Alkyd	186	145	163
Epoxy	143	227	300
Phenolic	681	1,337	1,453
Polyester (unsaturated)	430	554	681
Urea and melamine	610	771	418
Polyurethane	676	1,482	2,806
Thermoplastics (total)	13,099	22,342	37,073
Acrylonitrile-butadiene-styrene	774	1,067	1,428
Acrylic	213	341	681
Cellulosics	46	36	n.a.
Nylon	124	253	640
Polyacetal	39	65	64
Polycarbonate	90	281	232
Polyester (thermoplastic)	437	853	2,320
Polyethylene (HDPE)	2,000	3,785	7,002
Polyethylene (LLDPE)	with LDPE	1,767	4,498
Polyethylene (LDPE)	3,310	3,294	3,626
Polyphenylene-based alloys	48	90	n.a.
Polypropylene and copolymers	1,656	3,773	7,009
Polystyrene and copolymers	1,649	2,341	3,051
Poly(vinyl chloride) and other vinyls	2,572	4,130	6,521
Thermoplastic elastomers	140	265	n.a.
Rubber (production figures)			
Natural rubber (consumption)	585	808	1,191
Synthetic rubber (total)	2,015	1,958	2,462
Styrene-butadiene rubber	1,074	791	874
Butadiene	311	431	605
Ethylene-propylene	144	208	346
Nitrile	63	69	89
Polychloroprene	151	79	64
Other	272	380	484
Fibers (mill consumption figures)			
Natural fibers			
Cotton	1,391	1,833	2,158
Wool	63	61	38
Synthetic fibers (total)	3,941	3,940	4,698
Cellulosics	366	230	158
Nylon	1,071	1,209	1,184
Polyester	1,811	1,451	1,757

(Continued)

TABLE 1.1
(Continued) Polymer Consumption in the United States (in Units of 10⁶ kg)

Category	1980	1990	2000
Acrylic	354	230	154
Polyolefin	340	822	1,446
Synthetic polymers (all categories)	21,781	32,757	50,053

Source: *Chemical and Engineering News; Fiber Organon; Chemical Marketing Reporter; Modern Plastics.* HDPE, high-density polyethylene; LDPE, low-density polyethylene; LLDPE, linear low-density polyethylene; n.a., not available.

The water and soft drink bottles made of poly(ethylene terephthalate) that now dominate grocery shelves have almost completely displaced glass bottles. It would come as a surprise to most consumers to find that soft drink bottles, video and audio tapes, and polyester apparel all are made from the same polymer. Likewise, polypropylene used in the casing for almost all automobile batteries has the same basic formula as the polymer used for indoor–outdoor carpeting, transparent overwrap films, lawn furniture, and *polyolefin* intimate apparel.

In the period 2002–2012, economic difficulties stalled the growth of plastics consumption in the United States except for high-density and linear low-density polyethylene [1]. However, the total world consumption of thermoplastics has continued to grow. A recent survey shows that in the period 2005–2012, the global polymer industry grew by an annual average of around 3% [2]. This occurs despite a decline in consumption over the same period in the Americas and Europe. The growth in world consumption was led by an average of around 6% growth in Asia, Africa, and the Middle East, and an even higher growth rate in Russia's commonwealth, that is, the Commonwealth of Independent States. Future growth outlook for the United States is positive, however, for two reasons: (1) better economic outlook and (2) the advent of viable shale gas technologies that would provide low-cost raw materials for polyethylene and polypropylene and their derivatives.

1.3 POLYMER-BASED INDUSTRIES

Until the 1920s and 1930s, the several industries that produced polymeric materials were independent of one another for the most part and were based on natural or modified natural materials. These industries can be identified in a broad sense as follows:

- Plastics
- Rubber
- Fibers
- Coatings
- Adhesives

In fact, it was not until after World War II that the dividing lines became so blurred as to make it difficult to classify some companies.

1.3.1 PLASTICS

The term *plastic* denotes a material that can be shaped. Polymers that can be formed repeatedly by application of heat and pressure are called **thermoplastics**. Those that can be formed only once are called **thermosets**. Before 1940, thermosets outsold thermoplastics. Although both categories continue to grow, thermoplastics have dominated the market for some time (Table 1.1).

During Civil War days, daguerreotype cases were molded out of compositions containing shellac, gutta-percha, or other natural resins along with fibrous materials. The compression molding machinery and dies that were used were quite similar in principle to those being used a 100 years later. Hyatt's discovery (1868) that nitrated cellulose mixed with camphor could be molded under pressure to give a hard, attractive material suitable for billiard balls and detachable collars is often cited as the start of the plastics industry. Others date it from 1907, when Baekeland patented the first wholly synthetic plastic (a thermoset) based on the reaction of phenol and formaldehyde. The industry has expanded continuously with scarcely a pause since 1930 (Figure 1.1). The capacity for styrene production as a result of the synthetic rubber program developed during World War II was an important factor. The need for polyethylene and poly(vinyl chloride) during the war also accelerated industrial know-how. By 1960, each of these three polymers had been produced at the rate of over a billion pounds per year.

1.3.2 RUBBER

Even before the voyages of Christopher Columbus, the natives of South and Central America made use of the latex obtained by puncturing the bark of certain trees. By coagulating the latex, a rubber ball could be produced that was used in the national sport of the Mayan Indians. Macintosh and Hancock in England and Goodyear in the United States (1839) discovered that mixing natural rubber with sulfur gave a moldable composition that could be heated and converted (vulcanized) to a useful, nontacky, stable material suitable for raincoats, waterproof boots, and solid tires for carriages. The general progress of the rubber industry soon became associated with the automobile. Even today, about 70% of all types of rubber ends up in tires and a good part of the remainder is used in hoses, gaskets, grommets, and other parts of the modern automobile. The pneumatic tire developed by John Dunlop in 1888 and the use of carbon black as a reinforcing filler and of organic accelerators for the sulfur cross-linking reactions were achieved with natural rubber. Since World War I, most natural rubber has been cultivated in Malaysia, Indonesia, Thailand, and several other tropical countries rather than the Americas. Between World Wars I and II the development of synthetic rubbers was pursued, especially in Germany and the United States. In Germany, emphasis was placed on general-purpose rubber to reduce dependence on far-flung sources of supply. In the United States, more emphasis was placed on specialty rubbers, such as ThiokolTM (polysulfide rubber) and NeopreneTM (polychloroprene), which are more resistant to swelling by nonpolar solvents than natural rubber.

During World War II, Germany and Russia had developed synthetic rubbers so as to be self-sufficient. In the United States, a crash program was instituted that was to affect

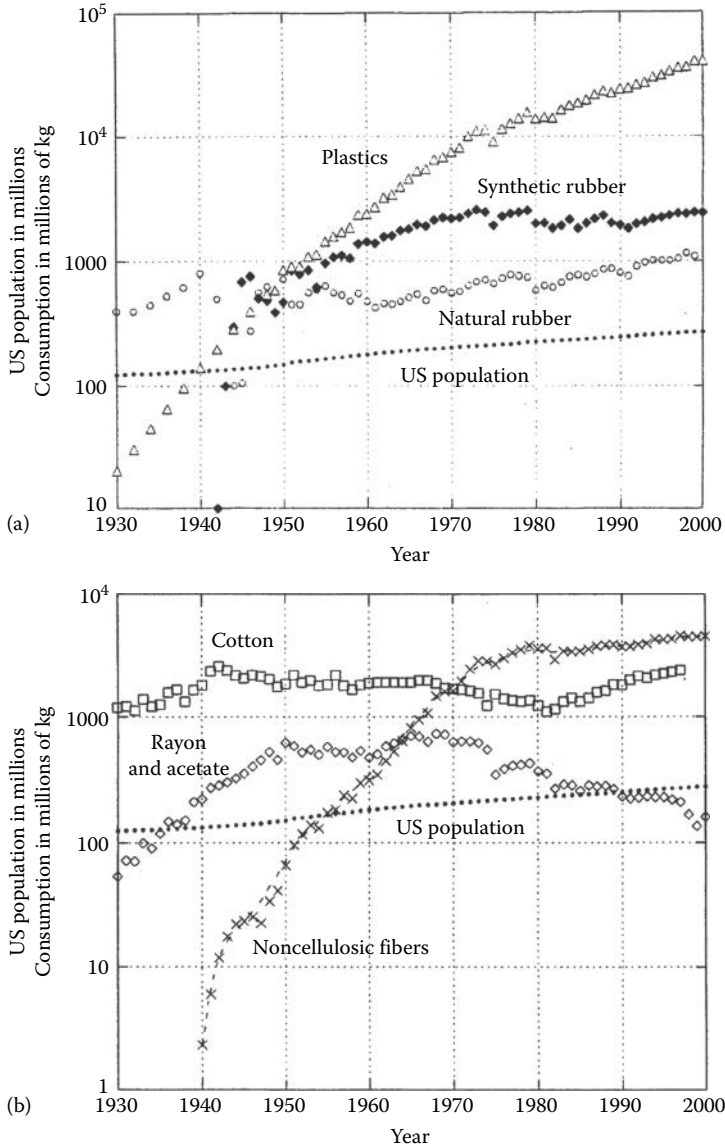


FIGURE 1.1 Polymer consumption compared with the population of the United States, which was about 275 million in 2000: (a) plastics and rubber; (b) fibers.

all other polymer-based industries eventually. Production of a SBR (originally called GR-S, for government rubber-styrene) went from zero in 1941 to over 700×10^6 kg in 1945. Figure 1.1a shows a drop in natural rubber consumption and the development of SBR during America's years in World War II (1941–1945). Despite a brief resurgence of interest in natural rubber after the war, the synthetic material remained in use. The primary results of the SBR program were as follows:

1. Tremendous production capacity for styrene and butadiene monomers
2. Independence of American industry from rubber imports for many uses
3. Availability of synthetic rubber latex for other uses
4. New insight into polymer production and characterization

Not the least of the accomplishments was the overnight conversion of many scientists and engineers into polymer engineers, polymer chemists, polymer physicists, and so on. After the war, their interest remained in the field, so that the rather thin prewar ranks of, for example, textile, rubber, and paint researchers suddenly swelled to large numbers of highly trained people who were not wedded to any one industrial viewpoint. The exchange of technology between industries that now is quite common can be credited in great measure to the proper recognition of the principles of polymer science and technology as the underlying basis for all these fields. Polymer research in university departments of chemistry, chemical engineering, and materials science has expanded as a consequence of industrial interest and government support.

Since the early 1970s per capita consumption of all forms of rubber in the United States has not changed much (Figure 1.1). SBR production peaked at 1.5×10^9 kg in 1973. Various factors have contributed to keep consumption from increasing despite significantly greater numbers of automobiles on the road. The trends to smaller automobiles and higher priced fuel all softened the demand for rubber in transportation. Moreover, the change in construction of tires had several effects. Belted radial tires use a higher ratio of natural rubber and *cis*-polybutadiene to SBR than the older bias-ply tires. The radial tires often wear longer, which helps to make up for their higher initial cost. The net result is a decreased demand for replacement tires. In the 1950s, a life of 20,000 mi (32,000 km) was considered acceptable for a bias-ply tire. Many radial tires now can be expected to last at least twice that long.

1.3.3 FIBERS

Natural polymers still are an important part of the fiber world. Regenerated cellulose (rayon) and cellulose acetate were introduced around 1900, but nylon was the only wholly synthetic polymer produced in quantity before World War II. In the 1960s, cotton and wool usage decreased, while polyester and nylon production boomed. Since about 1970, the cellulose (rayon and acetate) have diminished in importance (Figure 1.1; Table 1.1). Pollution problems inherent in conventional rayon manufacture caused some plants to close down in the 1970s. A factor favoring synthetic fibers has been the fashion trend to *easy-care* fabrics and garments. Cotton and wool require chemical treatment to compete on this basis. Synthetic fibers also have had a price advantage in recent years due partly to labor costs. Cotton and wool are *labor-intensive* materials compared to synthetics.

Although cotton consumption in US mills fluctuates from year to year, several points should be taken into account. A large fraction (as much as 50% in some years) of cotton production in the United States is exported rather than processed domestically into textiles. Also, a large amount of cotton (and other fibers) is imported in the form of finished apparel without being included in the mill consumption figure. About two-thirds of all apparel sold in the United States is imported [3].

In the United States, annual imports of silk from 1979 to 1993 averaged 0.5–1 million kg and usage of wool averaged about 75 million kg, both of which are small compared to the 1,000–2,000 million kg of cotton imported in the same period. On a worldwide basis in 1993, demand for fibers (in millions of kg) was as follows: cotton, 18,966; wool, 1,658; silk, 68; synthetic cellulose, 2,246; and synthetic noncellulose, 16,182 [4].

1.3.4 COATINGS

Decorative and protective polymeric coatings were based on unsaturated oils (linseed oil, tung oil) and natural resins (shellac, kauri gum) for centuries. In the 1930s, synthetic resins (alkyd resins), which really are modified natural oils, became important. The SBR program had its repercussions in the coatings industry, since styrene–butadiene latexes (with higher styrene content than rubber) were found to be useful film formers. Latex paints based on vinyl acetate and acrylic resins now have been developed for outdoor as well as indoor applications. Such water-thinnable coatings represent most of the interior coatings and about half the exterior paints for houses. In 2000, total shipments of coatings amounted to about 1.3 billion gal, a little over half of which were *architectural* sales and the remainder were industrial finishes (to manufacturers of products such as automobiles and appliances) and other special-purpose coatings. Legislation in most states now limits the solvents that can be used in commercial coating applications, both in type and in amount. Water-thinned and powdered coatings are being substituted for solvent-based paints and lacquers in many instances.

1.3.5 ADHESIVES

Since adhesives often must be specifically designed to bond to two different surfaces, an even greater diversity of products has been developed than in coatings.

In similar fashion to the coatings industry, the adhesives industry has made use of the latex technology developed during World War II. Many natural polymers are still used, but almost every new plastic and rubber developed has spawned a counterpart adhesive. The development of the highly advertised *super glues* based on the cyanoacrylates (see Section 13.4) was atypical in that the materials were used as adhesives first and not adapted from some prior application as plastics or coatings.

The starch and sodium silicate adhesives used to assemble paperboard materials still dominate the overall picture. Among the synthetics, phenolic and urea resins are widely used in plywood and particleboard manufacturing and in the surface treatment of fibrous glass insulation. Fibrous glass insulation has grown in importance as the United States has become more energy conscious. The phenolic resins used as binders for the glass give the characteristic pink color to the insulation.

1.4 FEEDSTOCKS FOR POLYMERS

Ethylene, even when considered only as the monomer for the homopolymer, is a very important commodity. More than that, it is an essential ingredient in vinyl chloride and styrene, the other two largest volume monomers for plastics (Figure 1.2).

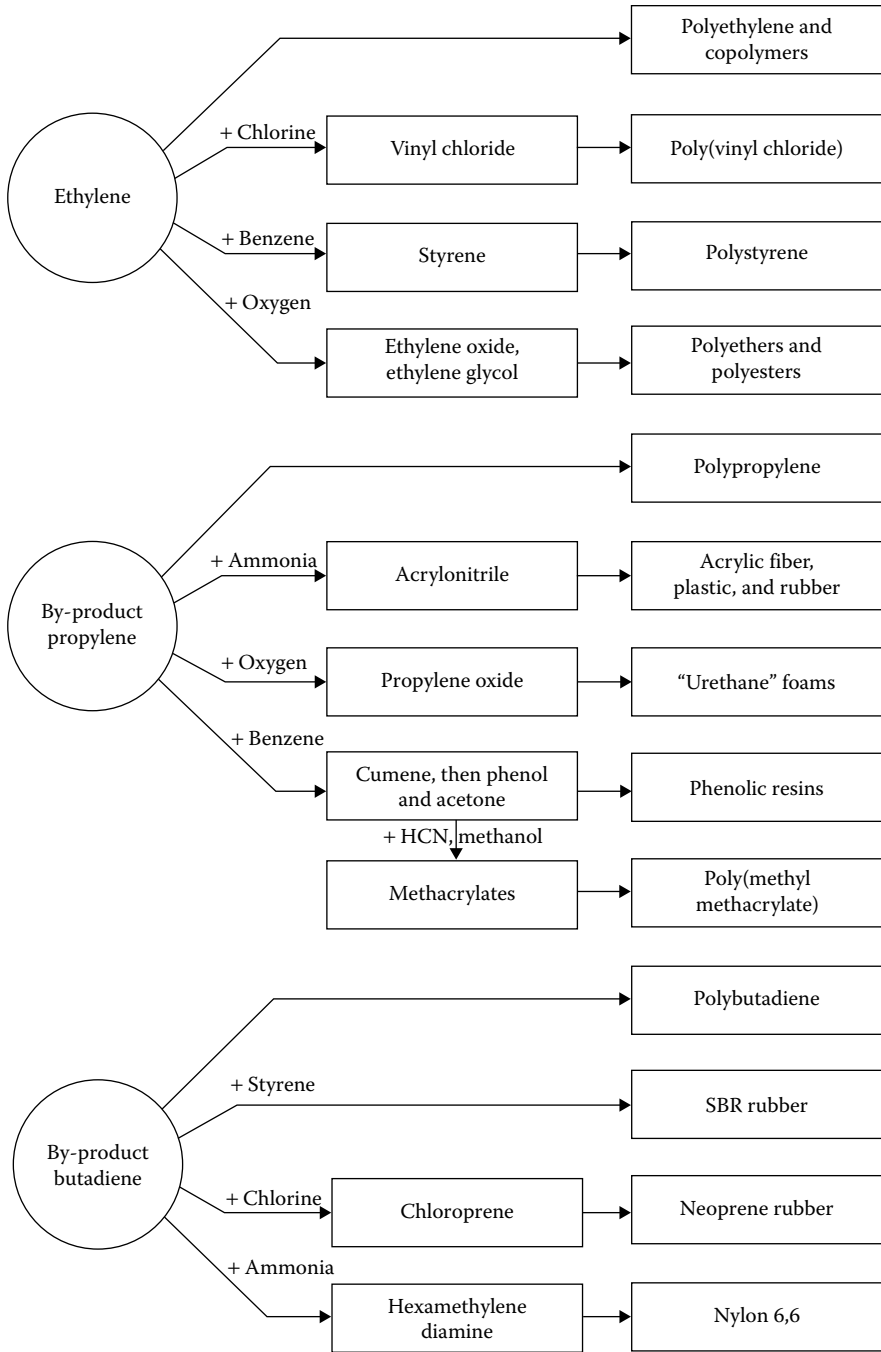


FIGURE 1.2 Major polymeric products derived from ethylene and their by-products. Not all reactants or products are shown.

Polymer-grade propylene and butadiene are made in large measures as by-products of ethylene manufacture. As seen in Figure 1.2, these two raw materials enter into the production of virtually all the other major plastic, rubber, and fiber polymers.

Table 1.2 shows a number of industrial organic chemicals that act as **building blocks** for polymers. With the exception of urea, it is obvious that the major use for each of them is in plastics, fibers, rubber, coatings, or adhesives. The capacity and usage estimates of many individual monomers and some polymers are updated periodically in *Chemical Market Reporter*.

Ethylene can be made from a variety of starting materials. Ethane recovered from natural gas is a *clean* feed, in that few by-products occur (Table 1.3). Natural gas was regarded as a diminishing resource in the 1970s, so almost all plants built then were made to use a variety of heavier feeds such as heavy naphtha (boiling range

TABLE 1.2
Building Blocks of Polymers

Chemical Name	US Capacity (in Units of 10 ⁶ kg)	Major Polymeric Uses as Fraction of Total
Ethylene	26,600	HDPE, 26%; LDPE (& LLDPE), 29%
Propylene	16,500	Polypropylene (PP), 39%; acrylonitrile, 14%; propylene oxide, 11%
Urea	10,700	Fertilizers, 86%; resins, 5%
Vinyl chloride	8,000	PVC, 98%
Formaldehyde	5,700	Urea-formaldehyde resins, 24%; phenol-formaldehyde resins, 16.5%; polyacetals, 13%; melamine-formaldehyde resins, 3%
Styrene	5,500	Polystyrene, 66%; ABS, 11%; SBR, 7%
Ethylene glycol	3,700	PET (bottle-grade) 34%; antifreeze, 26%; PET fibers, 24%; PET film, 4%
Propylene oxide	2,300	Urethane foams, 58%; propylene glycols, 22%
Phenol	2,200	Bisphenol-A, 35%; phenolic resins, 34%; caprolactam (nylon 6), 15%
Butadiene	2,000	SBR (& latex), 40%; polybutadiene, 20%; polychloroprene, 5%; ABS, 5%
Phosgene	2,000	Toluene diisocyanate, 40%; other isocyanates, 40%; polycarbonate resins, 13%
Vinyl acetate	1,700	Adhesives, 20%; paints, 18%; other latex products, 18%; Polyvinyl alcohol, 18%; Polyvinylbutyral, 11%
Acrylonitrile	1,600	Nylon intermediates, 30%; ABS, 28%; acrylic fibers, 25%
Acetic anhydride	2,700	Cellulose esters, 86%
Acrylic acid	1,200	Superabsorbent (& other water-soluble) polymers, 35%; <i>n</i> -butyl acrylate, 30%; ethyl acrylate, 20%
Methyl diphenyl diisocyanate	1,100	Rigid polyurethane foam, 80%; Reaction injection molding (RIM) applications, 13%; cast elastomers, 2%
Bisphenol A	1,050	Polycarbonates, 68%; epoxy resins, 24%
Adipic acid	1,030	Nylon 6,6 fibers, 72%; resins, 18%
Caprolactam	880	Nylon 6 fibers, 74%; resins and films, 26%

(Continued)

TABLE 1.2
(Continued) Building Blocks of Polymers

Chemical Name	US Capacity (in Units of 10 ⁶ kg)	Major Polymeric Uses as Fraction of Total
Methyl methacrylate	770	Polymeric sheet forms, 32%; molding powders, 15%; surface coatings, 24%
Phthalic anhydride	580	Plasticizers, 53%; unsaturated resins, 23%; alkyd resins, 13%
Toluene diisocyanate	450	Flexible urethane foams, 90%; coatings, 4%; cast elastomers, 2%
Fluorocarbons	430	Fluoropolymers, 28%; refrigerants, 46%; foamed polymers, 20%
Butene-1	380	Comonomer with ethylene, 65%; polybutene-1, 14%
Maleic anhydride	270	Unsaturated polyester resins, 63%; copolymers, 8%
Dicyclopentadiene	180	Unsaturated polyester resins, 45%; petroleum resins, 34%; EPDM, 11%
Carbon disulfide	160	Rayon, 49%; cellophane, 6%; rubber chemicals, 15%
Melamine	110	Surface coatings, 37%; laminates, 32%; molding compounds, 7%; paper coatings, 6%; wood adhesives, 6%; textile treatment, 4%

Source: Data based on periodic estimates appearing in *Chemical Market Reporter*.

ABS, acrylonitrile butadiene styrene; EPDM, ethylene-propylene diene monomer; HDPE, high-density polyethylene; LDPE, low-density polyethylene; LLDPE, linear low-density polyethylene; n.a., not available; PET, poly(ethylene terephthalate); Polyvinylbutyral, poly(vinyl butyral); PVC, poly(vinyl chloride); SBR, styrene-butadiene rubber.

TABLE 1.3
Typical Product Profile for Production of 1000 Parts by Weight of Ethylene from Various Feedstocks

Product	Feedstock				
	Ethane	Propane	Naphtha	Atmospheric Gas Oil	Crude Oil
Ethylene	1000	1000	1000	1000	1000
Acetylene	—	—	—	—	200
Propylene	24	375	420	557	135
Butadiene	30	69	141	187	90
Other C ₄ s and gasoline	24	158	848	1019	435
Fuel oil	—	—	195	729	600
Residue gases	172	659	521	457	—
Pitch	—	—	—	—	583
Total feed	1253	2260	3126	3951	3050

Source: Stinson, S.C., *Chem. Eng. News*, 57, 32, May 28, 1979.

of 100°C–220°C) or atmospheric gas oil (AGO; boiling range of 200°C–350°C). However, the 1980s saw a renewed interest in light feeds, including ethane.

Many factors enter into the choosing of a feedstock, including government regulations regarding natural gas prices; this is a touchy political matter since many voters heat their homes with natural gas. The development of new technologies in natural gas production (such as horizontal hydrofracking) is putting renewed interest in light feeds (ethane and propane) as sources of feedstocks. Actually, almost any hydrocarbon source is a possible feed. A heavy feed like AGO (Table 1.3) yields a variety of by-products that must be sold or used to make the process economical. Some chemical companies have explored the direct production of ethylene from crude oil, bypassing the usual oil refinery. By recycling various streams, the yield of ethylene can be optimized without having to market gasoline or fuel oil in competition with the traditional oil refiners.

The product distribution can differ from that listed in Table 1.3 for various reasons, especially the **severity** of the cracking process (temperature and residence time during processing). High-severity operations, which involve higher temperatures and longer residence times during cracking, usually increase conversion per pass. Moderate-severity operations usually produce more by-products but lessen the amount of feed converted into less valuable materials such as coke.

With almost any feed, the hydrocarbon source mixed with steam is pyrolyzed at 850°C or higher for up to 1 s by passage through a tube set in a **cracking furnace**. The steam is added to decrease formation of coke on the tube walls. The hot effluent gases are quenched with water or oil to stop the reaction. Separations using distillation and absorption are used to obtain pure products as well as to recycle some materials. The relative merits of various feedstocks and cracking processes have been the topics of numerous journal articles. As a measure of energy usage in the United States, it may be pointed out that the entire synthetic polymer industry (plastics, rubber, and fibers) produced about 50 billion kg in 2000 while about 8 times that weight of hydrocarbon was burned as fuel in motor vehicles [5].

For environmental reasons and sustainability, the past decade has seen large efforts in the development and commercialization of a number of polymers based totally or partially on renewable resources (see Chapter 15).

1.5 POLYMER SCIENCE AND TECHNOLOGY

The chemistry and physics of polymers lagged behind technology for many years. In 1920, Staudinger proposed his **macromolecular hypothesis**, saying that substances such as natural rubber were not colloidal, physical associations of small molecules but were truly long-chain molecules of extremely high molecular weight. Since such materials were not easily characterized by the methods used with small molecules, most chemists regarded polymer research as a rather undignified occupation. However, the studies of Emil Fischer on proteins, Meyer and Mark on cellulose, and Carothers on polycondensation had established a basis for acceptance of Staudinger's ideas by the 1930s. Once again, World War II must be recognized as a time when research accelerated sharply and theories started to catch up with practice. Debye's work on light scattering, Flory's work on viscous flow (as well as other areas), and Harkins's work on a theory of emulsion polymerization grew out of government-sponsored projects. The discovery by Ziegler of

synthetic catalysts that would give ordered polymers and the extension of such systems by Natta in the 1950s changed many fundamental ideas of polymer science, as did the discovery of large single crystals of high-molecular-weight polymers a few years later.

A capsule chronology of polymer technology and science is given in Table 1.4. Winfield [6] presented an annotated retrospective look at the history of plastics,

TABLE 1.4
Selected Chronology of Polymer Science and Technology

1770	Priestley is said to have given rubber its name because it can erase pencil marks
1806	Gough (England) experiments with elasticity of natural rubber
1838	Regnault (France) polymerizes vinylidene chloride via sunlight
1839	Goodyear (the United States), Macintosh and Hancock (England), vulcanization (cross-linking) of natural rubber
1859	Joule (England) demonstrates thermodynamic principles of elasticity of rubber
1860s	Molding of natural plastics such as shellac and gutta-percha
1868	Hyatt (the United States), celluloid (cellulose nitrate-molded articles)
1891	Chardonnet (France), regenerated cellulose via nitrate
1893–1899	Cross, Bevan, Beadle, and Stearn (England), viscose rayon fibers
1907	Baekeland (the United States), phenol–formaldehyde resins
1910	First rayon plant in the United States
World War I	Cellulose acetate solutions (<i>dope</i>) for aircraft Laminated plywood and fabric construction for aircraft fuselages
1884–1919	Emil Fischer (Germany) establishes formulas of many sugars and proteins
1920	Staudinger (Germany) advances macromolecular hypothesis
1928	Meyer and Mark (Germany) measure crystallite sizes in cellulose and rubber
1929	Carothers (the United States) synthesizes and characterizes condensation polymers
1920s	Cellulose nitrate lacquers for autos
1924	Cellulose acetate fibers
1926	Alkyd resins from drying oils for coatings
1927	Poly(vinyl chloride) Cellulose acetate plastics
1929	Polysulfide (thiokol) rubber Urea–formaldehyde resins
1930–1934	Kuhn, Guth, and Mark (Germany) derive mathematical models for polymer configurations; theory of rubber elasticity
1931	Poly(methyl methacrylate) plastics Neoprene (Duprene) synthetic rubber
1936	Poly(vinyl acetate) and poly(vinyl butyral) for laminated safety glass
1937	Polystyrene Styrene–butadiene (Buna S) and acrylonitrile–butadiene (Buna N) rubbers (Germany)
1938	Nylon 6,6 fibers
1939	Melamine–formaldehyde resins Poly(vinylidene chloride)
1940	Butyl rubber (the United States)
1941	Polyethylene production (England)

(Continued)

TABLE 1.4**(Continued) Selected Chronology of Polymer Science and Technology**

1942	Unsaturated polyesters for laminates
World War II	Debye, light scattering of polymer solutions Flory, viscosity of polymer solutions Harkins, theory of emulsion polymerization Weissenberg, normal stresses in polymer flow Silicones Fluorocarbon resins Polyurethanes (Germany) Styrene-butadiene rubber (the United States) Latex-based paints
1944	Carboxymethyl cellulose Filament winding
1945	Cellulose propionate Dielectric heating of polymers Fiber-reinforced boats
1946	Screw-injection molding Automatic transfer molding
1947	Epoxy resins
1948	ABS polymers
1950	Polyester fibers
1948–1950	Acrylic fibers
1949	Blow-molded bottles
1950	Poly(vinyl chloride) pipe
1950s	Ziegler, coordination complex polymerization Natta, tacticity in polymers Szwarc, living polymers; interfacial polycondensation Hogan and Banks, crystalline polypropylene; fluidized bed coating
1953	Staudinger receives the Nobel prize
1954	Polyurethane foams (the United States) Styrene-acrylonitrile copolymers
1955	Williams-Landel-Ferry equation for time-temperature superposition of mechanical properties
1956	Linear polyethylene Acetals [poly(oxymethylene)]
1957	Polypropylene Polycarbonates
1957	Keller and Till, single crystals of polyethylene characterized
1958	Rotational molding
1959	Chlorinated polyether Synthetic <i>cis</i> -polyisoprene and <i>cis</i> -polybutadiene rubbers
1960	T. Smith, the failure envelope
1960	Ethylene-propylene rubber Spandex fibers
1962	Phenoxy resins Polyimide resins

(Continued)

TABLE 1.4
(Continued) Selected Chronology of Polymer Science and Technology

1965	Poly(phenylene oxide) Polysulfones Styrene–butadiene block copolymers
1960s	Cyanoacrylate adhesives Aromatic polyamides Polyimides Silane coupling agents Thermoplastic elastomers (block styrene–butadiene copolymers) NMR applied to polymer structure analysis Maxwell, orthogonal rheometer Moore, Gel permeation chromatography (GPC) analysis for molecular weight distribution Differential scanning calorimetry Marvel, polybenzimidazoles Gilham, torsional braid analysis Ethylene–vinyl acetate copolymers Ionomers Natta and Ziegler share the Nobel prize (1963) Polysulfone Parylene coatings HDPE fuel tanks
1970s	Polybutene (isotactic) Poly(butyl terephthalate) Thermoplastic elastomers based on copolyesters Poly(phenylene sulfide) Polynorbornene (rubber) Polyarylates Polyphosphazenes Soft contact lenses Reaction injection molding Interpenetrating networks High-performance liquid chromatography Submicrometer lithography for integrated circuits Polyester beverage bottles Structural foams Kevlar aromatic polyamide Poly(ethersulfone) Reaction injection molding for auto fascia Unipol gas-phase polymerization Linear low-density polyethylene Polyarylates High-density polyethylene grocery bags Flory receives the Nobel prize (1974)

(Continued)

TABLE 1.4
(Continued) Selected Chronology of Polymer Science and Technology

1980s	Polysilanes Liquid crystal polymers High-modulus fibers Poly(etheretherketone) Conducting polymers Polyetherimide Poly(methylpentene) Pultrusion Replacement of fluorocarbon blowing agents Group transfer polymerization Differential viscometry
1990s	Metallocene catalysts Large-scale recycling of polyester and HDPE bottles Poly(ethylene-2,6-naphthalene dicarboxylate) Living cationic polymerization (Kennedy) Syndiotactic polystyrene commercialized Styrene–ethylene copolymers Nanocomposites de Gennes receives the Nobel prize (1991)
2000	Heeger, MacDiarmid, and Shirakawa share the Nobel prize

ABS, acrylonitrile butadiene styrene; HDPE, high-density polyethylene; NMR, nuclear magnetic resonance.

including many of the developments noted in Table 1.4. Two other extensive historical reviews appeared in *Modern Plastics* [7] and in *Rosato's Plastics Encyclopedia and Dictionary* [8]. A growing source of information on the history of polymers is the Beckman Center for the History of Chemistry in Philadelphia, which has a continuing program of receiving new material and publishing reviews.

1.6 TRENDS

The worldwide picture of plastics consumption indicates that the use of polymers is distributed throughout the developed and developing nations. The rate of growth in Latin America, Asia/Oceania, Africa/Mideast, and the Russian commonwealth over the period 1982–2013 was greater than that in North America and Europe. Different regions of the world are expected to grow at different paces, with Asia leading the growth according to a recent study [2].

Predictions of economic phenomena are notoriously inaccurate. However, there are a few known factors that will continue to affect the polymer industry in the next decade. The large-volume plastics will find ever-increasing use in automobiles, furniture, and housing. Polymers for special applications in electronics, medicine, and other fields will continue to develop. This is true for rubber, fibers, coatings, and adhesives

as well as for plastics. Fabrication techniques will be made more efficient and more environment-friendly. The global picture of polymer production has changed with the building of polymerization facilities in countries with access to raw materials (such as polyethylene plants in Saudi Arabia). Building a polymer industry is high on the list of goals for most developing countries. Despite the growth in polymer consumption in the developing countries, as mentioned above, the average consumption of polymers in the world is still far behind the usage in the industrialized nations. Political and social developments may alter some patterns. Importation of textiles and apparel into the United States has been a major factor in the slowdown of domestic production of synthetic fibers. Tariff barriers may protect some industries and hurt others.

Since 1980 the US chemical industry has undergone a great deal of restructuring. In general, there are fewer producers of each commodity polymer than there were a few decades ago. However, almost every company would like to participate in the specialty polymer market, where the profits are likely to be higher.

KEYWORDS

Polymer
Monomer
Macromolecule
Copolymer
Dimer
Trimer
Degree of polymerization
Oligomer
Oligosaccharide
Insulin
Thermoplastics
Thermosets
Building blocks
Cracking furnace
Severity
Cracking furnace
Macromolecular hypothesis

PROBLEMS

- 1.1 What are some large-scale uses of plastics and rubber in US construction industry that are obvious to the layman?
- 1.2 What are some obvious uses of rubber and plastics in the automotive industry (in addition to tires)?
- 1.3 What are some drawbacks of ordinary cellulose-based paper for books and newspapers compared with what might be expected from a material based on polyethylene? What disadvantages might the plastic have (in addition to the initial one of price)? What is the potential market for *synthetic* newsprint?

- 1.4** If every one of the 10 million or so automobiles produced in the United States in a single year suddenly were equipped with a thermoplastic polycarbonate windshield, what new selling price might be expected for the general-purpose material? Assume that the selling price scales with the 0.6 power of production volume.
- 1.5** What factors other than volume produced will affect the selling price of a polymer?
- 1.6** When plastics are used for a molded article, a specified volume of material must be used to achieve a certain effect. However, prices for plastics usually are given on a unit weight basis. If acetal resin is to compete on a cost-per-volume basis with polypropylene in a given application, what must the price ratio be on a weight basis (see Appendix C)?
- 1.7** The price of the polymer is only one factor in the selling price of a finished article containing that polymer. Some other items might include other ingredients: production labor, decorating, packaging, and distribution. Rank the following items in the order of increased dependence on polymer cost:
- Polyethylene garbage can
 - Nylon panty hose
 - Nylon guitar string
 - Tinted cellulose acetate sunglasses
 - Nylon pocket comb
 - Automobile tire
- What factors are important for each item?
- 1.8** Using data from any recent issue of *Chemical Marketing Reporter* (Schnell Publishing Co.), plot the lowest polymer price listed versus monomer price for ethylene, propylene, styrene, vinyl chloride, and bisphenol A (polycarbonate). Should the ratio of polymer price to monomer price increase or decrease with monomer price? Why?

REFERENCES

Production figures: *Statistical Abstract of the United States* issued annually by the Bureau of the Census, Department of Commerce, through the US Government Printing Office, Washington, DC. Summaries usually appear in *Chemical and Engineering News* (first week in June) and *Modern Plastics* (January). Occasionally, figures appear in *Chemical Market Reporter*. Detailed current prices of most plastics are reported in *Plastics Technology* and of many polymers and additives in *Chemical Market Reporter*.

1. Facts and figures: *Chem. Eng. News*, 91:25 (July 1, 2013).
2. Galie, F., and C. Trabucchi: World Polymers Outlook, *Chemical Information Services* (ICIS), Chemical Business Report, October 2013.
3. Reisch, M. S. *Chem. Eng. News*, 79:18 (July 23, 2001).
4. Facts and figures: *Fiber Organon*, 65:113 (1994).
5. Schedules 1087, 1103, and 1105, *Statistical Abstract of the United States*, U.S. Government Publications, 2001.

6. Winfield, A. G.: *Plastics Eng.*, 48(5):32 (1992).
7. Facts and figures: *Mod. Plast.*, 82:77 (January 1977).
8. Rosato, D. V.: *Rosato's Plastics Encyclopedia and Dictionary*, Hanser Publishers, New York, 1993.

GENERAL REFERENCES

History

- Elliott, E.: *Polymers & People: An Informal History*, CHOC, Philadelphia, PA, 1986.
- Morawetz, H.: *Polymers: The Origins and Growth of a Science*, Wiley, New York, 1985.
- Morris, P. J. T.: *Polymer Pioneers: A Popular History of the Science and Technology of Large Molecules*, CHOC, Philadelphia, PA, 1986.
- Mossman, S. T. I., and P. J. T. Morris (eds.): *The Development of Plastics*, CRC Press, Boca Raton, FL, 1994.
- Seymour, R. B., and I. Cheng (eds.): *History of Polyolefins*, Kluwer Academic Publishers, Norwell, MA, 1985.
- Seymour, R. B., and R. D. Deanin (eds.): *History of Polymeric Composites*, VNU Science, Utrecht, The Netherlands, 1987.
- Seymour, R. B., and G. S. Kirshenbaum (eds.): *High Performance Polymers: Their Origin and Development*, Elsevier Applied Science, New York, 1986.
- Seymour, R. B., and H. F. Mark (eds.): *Organic Coatings: Their Origin and Development*, Elsevier, Amsterdam, The Netherlands, 1989.

Introductory Textbooks and Handbooks

- Aggarwal, S. L., and S. Russo (eds.): *Comprehensive Polymer Science*, Pergamon Press, New York, 1992.
- Allcock, H. R., F. W. Lampe, and J. E. Mark: *Contemporary Polymer Chemistry*, 3rd edn., Prentice Hall, Upper Saddle River, NJ, 2003.
- Allen, G., and J. C. Bevington (eds.): *Comprehensive Polymer Science*, 7 vols., Pergamon Press, New York, 1988.
- Ash, M., and I. Ash (eds.): *Encyclopedia of Plastics, Polymers, and Resins*, 4 vols., Chemical Publishing Co., New York, 1987.
- Birley, A. W., B. Haworth, and J. Batchelor: *Physics of Plastics: Processing, Properties, and Materials Engineering*. Hanser Publishers, New York, 1992.
- Boyd, R. H., and P. J. Phillips: *The Science of Polymer Molecules*, Cambridge University Press, New York, 1994.
- Brandrup, J., E. H. Immergut, and E. A. Grulke (eds.): *Polymer Handbook*, 4th edn., Wiley, New York, 1999.
- Brazel, C. S., and S. L. Rosen: *Fundamental Principles of Polymeric Materials*, 3rd edn., Wiley, New York, 2011.
- Brydson, J. A.: *Plastics Materials*, 7th edn., Butterworth-Heinemann, Oxford, 1999.
- Carley, J. F. (ed.): *Whittington's Dictionary of Plastics*, 3rd edn., Technomic, Lancaster, PA, 1993.
- Carraher, C. E., Jr.: *Introduction to Polymer Chemistry*, Taylor & Francis Group, Boca Raton, FL, 2013.
- Cheremisinoff, N. P. (ed.): *Handbook of Polymer Science and Technology*, Marcel Dekker, New York, 1994.
- Coleman, M. M., and P. C. Painter: *Fundamentals of Polymer Science*, Technomic, Lancaster, PA, 1994.
- Cowie, J. M. G.: *Polymers*, 2nd edn., Chapman & Hall, New York, 1991.
- Craver, C. D., and C. E. Carraher, Jr. (eds.): *Applied Polymer Science 21st Century*, Elsevier, Oxford, 2000.

- David, D. J., and A. Misra: *Relating Materials Properties to Structure—Handbook and Software for Polymer Calculations and Materials Properties*, Technomic, Lancaster, PA, 1999.
- Elias, H. G.: *An Introduction to Polymers*, Wiley, New York, 1997.
- Gnanou, Y., and M. Fontanille: *Organic and Physical Chemistry of Polymers*, Wiley, New York, 2008.
- Harper, C. A. (ed.): *Handbook of Plastics, Elastomers, and Composites*, 2nd edn., McGraw-Hill, New York, 1992.
- Heath, R. J., and A. W. Birley: *Dictionary of Plastics Technology*, Chapman & Hall, New York, 1993.
- Hiemenz, P. C., and T. P. Lodge: *Polymer Chemistry*, 2nd edn., CRC Press, Boca Raton, FL, 2007.
- Jenkins, A. D., and J. F. Kennedy (eds.): *Macromolecular Chemistry*, vol. 3, Royal Society of Chemistry, London, 1985.
- Kleintjens, L. A., and P. J. Lemstra (eds.): *Integration of Fundamental Polymer Science and Technology*, Elsevier, New York, 1986.
- Kroschwitz, J. I. (ed.): *Encyclopedia of Polymer Science and Engineering*, 2nd edn., 17 vols., Wiley, New York, 1985–1990.
- Kumar, A., and R. K. Gupta: *Fundamentals of Polymer Engineering, Second Edition Revised and Expanded*, Marcel Dekker, New York, 2003.
- Mark, J. E. (ed.): *Physical Properties of Polymer Handbook*, Springer, New York, 2006.
- Nicholson, J. W.: *The Chemistry of Polymers*, CRC Press, Boca Raton, FL, 1991.
- Odian, G.: *Principles of Polymerization*, 4th edn., Wiley, New York, 2004.
- Painter, P. C., and M. M. Coleman: *Essentials of Polymer Science and Engineering*, 3rd edn., DEStech Publications, Lancaster, PA, 2008.
- Ram, A.: *Fundamentals of Polymer Engineering*, Plenum Press, New York, 1997.
- Ravve, A.: *Principles of Polymer Chemistry*, Plenum Press, New York, 1995.
- Rubin, I. I. (ed.): *Handbook of Plastic Materials and Technology*, Wiley, New York, 1990.
- Sperling, L. H.: *Introduction to Physical Polymer Science*, 4th edn., Wiley, New York, 2005.
- Stevens, M. P.: *Polymer Chemistry*, 3rd edn., Oxford University Press, New York, 2009.
- Strobl, G. R.: *The Physics of Polymers*, Springer, New York, 1996.
- Ulrich, H.: *Raw Materials for Industrial Polymers*, Hanser Publishers, New York, 1988.
- Ulrich, H.: *Introduction to Industrial Polymers*, 2nd edn., Hanser-Gardner, Cincinnati, OH, 1992.
- Young, R. J., and P. A. Lovell: *Introduction to Polymers*, 3rd edn., CRC Press, New York, 2011.

2 Basic Structures of Polymers

2.1 CLASSIFICATION SCHEMES

The study of any subject as vast as and as complex as polymers is simplified by gathering together the many thousands of examples that are known into a few categories about which generalized statements can be made. By speaking about polymers as a special topic, we already are categorizing molecular materials as low-molecular-weight or high-molecular-weight polymers. Within the polymer field, several classifications have been found to be useful. These classifications are based on the following:

1. *Molecular structure.* We can ask, for example, whether the polymer molecule is linear or branched. Is it made up of identical monomer units (homopolymer) or a mixture of two or more monomer units (copolymer, terpolymer). The polymer molecules may exist as separate individual molecules or they may be covalently linked to a macroscopic network.
2. *Physical state.* The polymer may be in the molten state with a viscosity characteristic of a liquid or the elasticity associated with a rubbery material. It may also be in a solid state that can have an amorphous glassy structure or a partially ordered crystalline structure. We shall see that the distinctions depend on the temperature, molecular weight, and chemical structure of the polymer.
3. *Chemical structure.* The elemental composition of a polymer, the chemical groups present (ether, ester, hydroxyl), or the manner of synthesis (chain propagation, transesterification, ring opening) may be used as a means of classifying polymers. A person or company attempting to exploit a unique raw material or process may profitably use such an approach for the development of a new class of polymers.
4. *Response to environment.* In the plastics industry, an important factor in economic usage and in end-use stability of a product is the behavior of the material at high temperatures. The term **thermoplastic** is applied to materials that soften and flow in response to the application of pressure and heat. Thus, most thermoplastic materials can be remolded many times, although chemical degradation may eventually limit the number of molding cycles. The obvious advantage is that a piece that is rejected or broken after molding can be ground up and remolded. The disadvantage is that there is a limiting temperature for the material in use above which it cannot be used as a

structural element. The **deflection temperature**, formerly termed the **heat distortion temperature**, is measured by a standard loading at a standard rate of temperature rise.

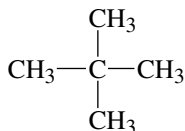
The term **thermoset** is applied to materials that, once heated, react irreversibly so that subsequent applications of heat and pressure do not cause them to soften and flow. In this case, a rejected or scrapped piece cannot be ground up and remolded. However, the limiting upper temperature in use often is considerably higher than the molding temperature. Once again, chemical stability becomes a limiting factor.

Other classifications can be applied to the response of polymers in contact with liquids and gases for applications in paints, food packaging, bottles, or gasoline tanks for automobiles.

5. *End use.* Within an industry, or within some other grouping, there may be an important difference in processing or end-use behavior. The various polymer-consuming industries tend to think of a new material as an adhesive, a fiber, a rubber, a plastic, or a coating, even though the material may be adaptable to all these applications.
6. *Cost of polymers.* In any application, one can differentiate between low-cost, general-purpose materials and high-cost, specialty materials. For engineers this is a very logical categorization as a first step to specifying a material for a given use.

2.2 BONDING

Polymers generally are held together as large molecules by covalent bonds, whereas the separate molecules, or nonneighboring segments of the same molecule, are attracted to each other by **intermolecular forces**, also termed *secondary* or *van der Waals* forces. Other types of bonds (secondary interactions), such as hydrogen and ionic bonds, can also occur in polymeric systems and may have dramatic effects on the properties. Covalent bonds are characterized by high energies (35–150 kcal/mol), short interatomic distances (0.11–0.16 nm), and relatively constant angles between successive bonds. Some important examples are given in Table 2.1. An apparent exception is the Si—O—Si bond, for which values from 104° to 180° have been reported. The flexibility of this bond, coupled with the ability of methyl groups attached to silicon to rotate about the Si—C bond, is responsible for poly(dimethylsiloxane) (PDMS) having the lowest glass-forming temperature of any polymer, −110°C [1]. Secondary forces are harder to characterize because they operate between molecules or segments of the same molecule rather than being localized to a pair of atoms. These forces increase in the presence of polar groups and decrease with increasing distance between molecules. One can see qualitatively the effect of polarity on intermolecular attraction in the boiling points (bp's) of the series methane (CH₄, bp −161°C), methyl chloride (CH₃Cl, bp −24°C), and methyl alcohol (CH₃OH, bp 65°C). Because the energy of interaction varies inversely with the sixth power of the distance, small differences in structure can have large effects. For example, compare the boiling points of the isomers, neopentane and *n*-pentane:



Neopentane
bp 9.5°C



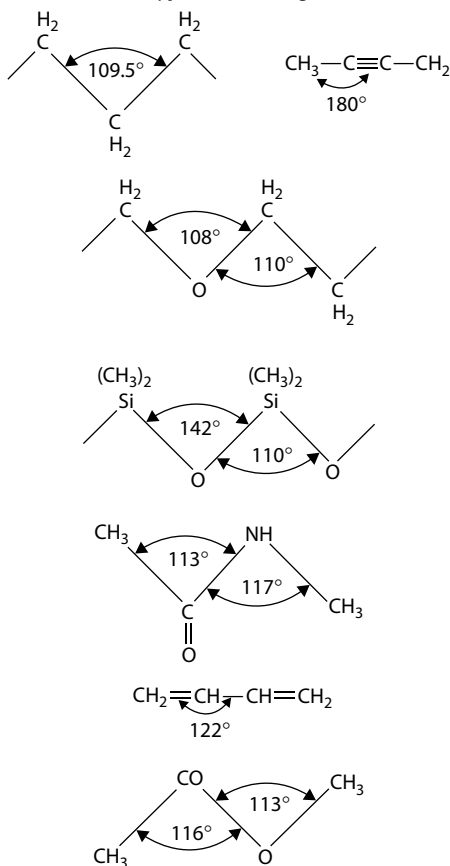
n-Pentane
bp 37°C

TABLE 2.1
Covalent Bonds

Dimensions and Energies^a

Bond	Typical Bond Length (Å) [2]	Typical Average Bond Energy (kcal/mol) [3]
C—C	1.54	83
C=C	1.34	147
C≡C	1.20	194
C—H	1.09	99
C—O	1.43	84
C=O	1.23	171
C—N	1.47	70
C=N	1.27	147
C≡N	1.16	213
C—Si	1.87	69
Si—O	1.64	88
C—S	1.81	62
C=S	1.71	114
C—Cl	1.77	79
S—S	2.04	51
N—H	1.01	93
S—H	1.35	81
O—H	0.96	111
O—O	1.48	33
Si—N	1.74	—

Some Typical Bond Angles [2]



^a 1 Å = 0.1 nm; 1 kcal = 4.185 kJ.

TABLE 2.2
Hydrogen Bonds

Bond	Typical Bond Length (Å)	Typical Bond Energy (kcal/mol)
O—H—O	2.7	3–6
O—H—N	2.8	
N—H—O	2.9	4
N—H—N	3.1	3–5
O—H—Cl	3.1	
N—H—F	2.8	
N—H—Cl	3.2	
F—H—F	2.4	7

Source: Pimentel, G. C., and McClellan, A. L., *The Hydrogen Bond*, Freeman, San Francisco, CA, 212, 224, 292, 1960.

Intermolecular distances can be estimated from crystal lattice dimensions in crystalline polymers and from the average density of amorphous polymers. Distances of 0.2–1.0 nm and energies of 2–10 kcal/mol predominate in small molecules. In a large molecule the energy is better characterized by the **cohesive energy density** (CED), which measures the energy per unit volume rather than per molecule (see Section 2.6). The hydrogen bond deserves special mention because its effect is so localized. Tables 2.1 and 2.2 summarize some typical values of bond energies and dimensions. Hydrogen bonding has a great influence on the properties of cellulose (cotton) and polyamides (nylon and proteins), among others. The multiplicity of strong hydrogen bonds in dry cotton gives cotton many of the properties associated with a covalent-bonded **network** leading to insolubility and infusibility despite the fact that its covalent bonds are combined into individual chains of glucose rings.

In general, covalent bonds govern the thermal and photochemical stability of polymers. Bond strength can be used as a clue to degradation mechanisms. For example, sulfur-vulcanized rubber is more likely to degrade at the comparatively weak S—S bonds than at the strong C—C bonds, both of which occur in the structure.

However, secondary forces determine most of the physical properties that are associated with specific low molar mass compounds. Melting, dissolving, vaporizing, adsorption, diffusion, deformation, and flow involve the making and breaking of intermolecular *bonds* so that molecules can move past one another or away from each other. In polymers, these forces play the same role in the movements of individual segments of the long-chain molecules.

The *arrangement* of the covalent structure in space leads to a convenient method of classification that helps explain polymer properties. Basically there are two such arrangements. The polymer may be present as *single* molecules, albeit of large individual size (i.e., molecular weight of 10^7), or as an *infinite network*. The distinction is important because only the separate molecules can exhibit plastic flow and solubility.

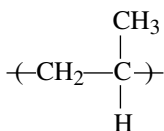
Accustomed as we are to thinking of the molecular scale as submicroscopic, it comes as something of a jolt to realize that the major portion of polymer in a tire or a bowling ball is really only one molecule. This is because all the separate molecules in the tire were connected to one another by sulfur cross-links during *vulcanization*. (Incidentally, the molecular weight of a bowling ball polymer on this basis is about 10^{28} !)

One can calculate that a single molecule with a molecular weight of 10^6 and a density of 1 g/cm^3 should form a sphere of 14.7 nm in diameter. This is large enough to be clearly visible by electron microscopy, and indeed such single molecules have been distinguished [5].

2.3 SINGLE MOLECULES

The single molecules may be **linear** or **branched** (Figure 2.1). An important consequence is that branching interferes with the ordering of molecules, so that crystallinity decreases. Also, the melt flow properties and the elastic behavior of polymers are greatly influenced by the degree of branching and size of the branches.

If the polymer chain contains carbon atoms with two different substituents, the two sides of the chain to which a carbon on the backbone chain is connected are different. That is, if we take the mirror image (the **enantiomer**) of such a substituted carbon, it cannot be superposed on the original without breaking covalent bonds. We refer to this as a **chiral** group and the carbon as the **chiral center**. In polymers such as polyethylene (PE) and polyisobutylene (with two methyl groups on every second carbon of a carbon chain), there is a plane of symmetry, so the groups are **achiral**. **Optical isomerism** is familiar in the organic chemistry of sugars, amino acids, and many other biologically important molecules. As an example, consider the case of polypropylene, with the repeat unit:



Although the above planar projection may make it appear that rotation about the C—C bond can exchange the positions of the CH_3 and the H on the chiral carbon, these groups will be on different sides of the chain backbone because the bonds on the carbon are tetrahedrally directed. Every other carbon is a chiral center and three structures can result. These are best visualized by looking at the main polymer chain in an extended planar zigzag conformation. In general, changes in structure caused by rotations about single bonds are termed **conformations**, and isomers that cannot be interchanged without bond breaking are termed **configurations**.

With polypropylene in the planar zigzag conformation, each pendent methyl group may be on one side of the chain, that is, all *d* or all *l*, using the terminology of stereochemistry. Using the terminology coined by Natta [6], this is an **isotactic structure** (Figure 2.2). The regularity of such an arrangement facilitates the molecular ordering necessary in crystalline materials. A regular alternation of pendent groups is called a **syndiotactic structure**. Random placement of the methyl group gives an **atactic structure**. Until the advent of coordination complex polymerization, it was

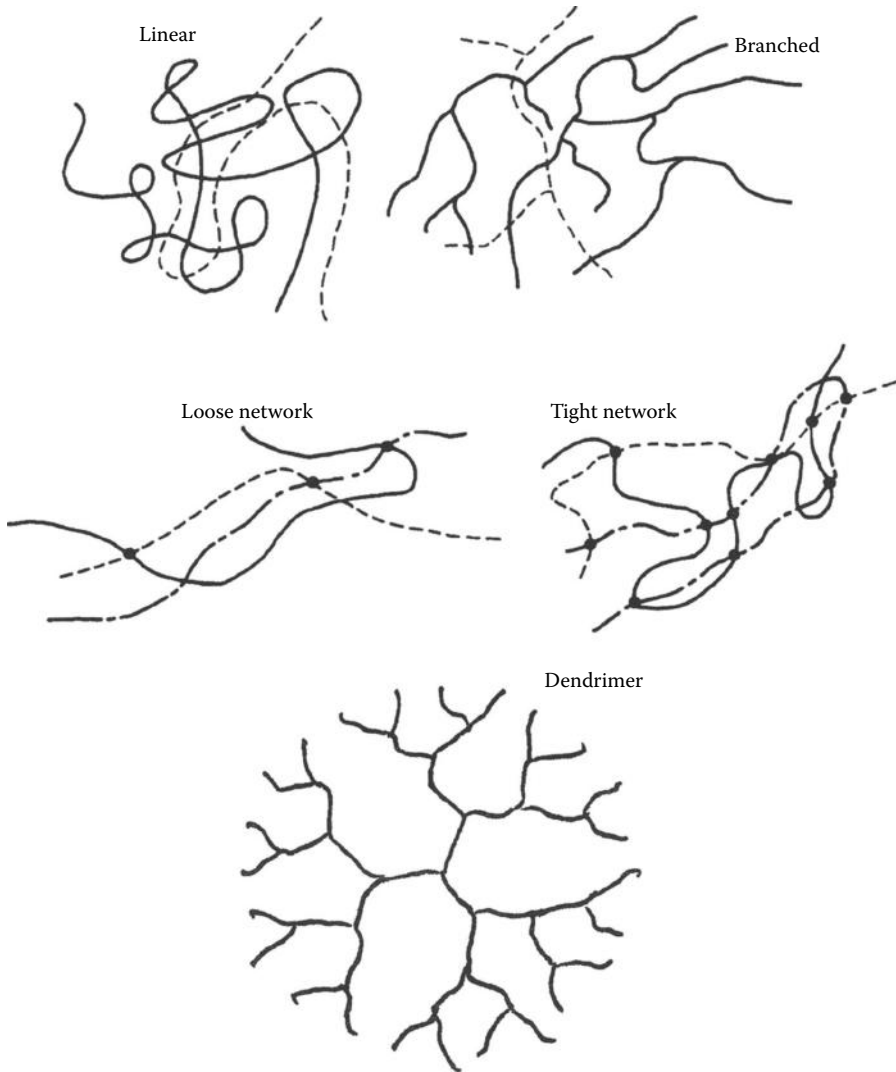


FIGURE 2.1 Polymer structures.

difficult to produce synthetically (with an optically inactive catalyst) any structure except the atactic. However, regular structures and more complex variants have since been produced with a variety of catalyst systems. In the amorphous, random-coil state, **tacticity** may be a minor factor in determining properties, but in crystal lattice formation, it often assumes a predominant role.

Poly(propylene oxide) is an example of a polymer that has a three-atom repeat unit in the chain. It has been made as all *d* or all *l* isotactic polymers, which are optically active, as the *d-l* isotactic mixture, and as the atactic polymer. In the planar zigzag presentation, the isotactic form has the pendent methyl group aligned in two rows (Figure 2.2a).

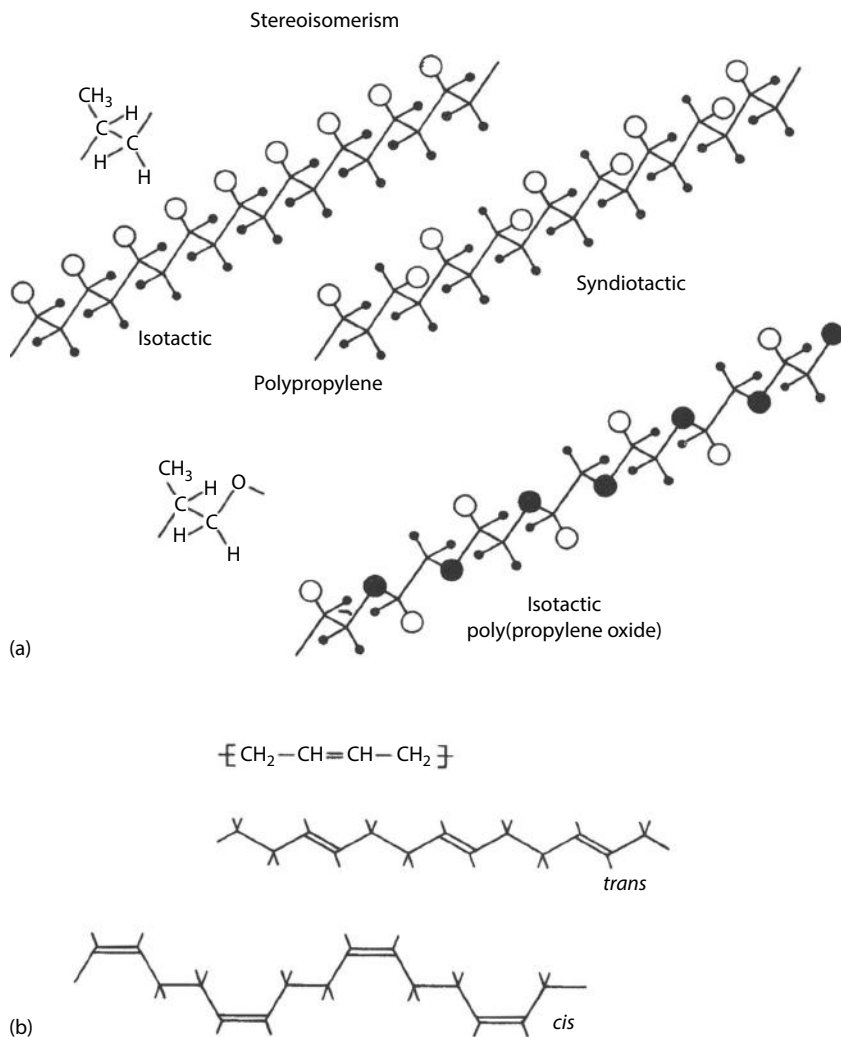


FIGURE 2.2 (a) Stereoisomers from asymmetric carbon. (b) Stereoisomers from double bonds in chains of 1,4-polybutadiene.

A second type of **stereoisomerism** is of the **cis–trans** variety familiar in small ethenic molecules. Because rotation is not free about a double bond, the substituents on either side can assume two attitudes (Figure 2.2b). When the chain parts are on opposite sides, we have a *trans* conformation, and when they are on the same side, we have a *cis* conformation. In this case also, the catalyst systems that permit production of all-*cis* or all-*trans* polymers were first developed in the 1950s [6].

Recent developments of new catalysts (metallocenes) have enabled the synthesis of branched polyolefins (e.g., PE and polypropylene) with controlled structures providing another way to control the properties of these polymers. Other promising new polymeric structures are hyperbranched polymers [7] and dendrimers [8].

These polymers tend to have globular shapes (Figure 2.1) and are being investigated as drug delivery systems and for other specialty applications.

2.4 NETWORK MOLECULES

A loose polymer network can result from cross-linking a linear or branched polymer. Natural rubber consists mostly of a linear polymer that can be cross-linked to a loose network by reaction with 1%–3% sulfur. The same polymer reacted with 40%–50% sulfur is *hard rubber*, a *tight* network polymer used for pocket combs and bowling balls (Figure 2.1). Networks may also be formed directly, without the intermediate linear stage.

It was pointed out earlier (Section 2.1) that **thermoplastic** polymers soften without chemical change when heated and harden when cooled, whereas **thermosetting** polymers, once formed, do not soften upon heating below their decomposition temperatures. We can identify the thermoplastic polymers with the linear and branched structures. The **thermosets** generally form network polymers upon being heated the first time. As with all generalizations in the field of polymers, there are numerous exceptions. Cellulose is essentially a linear polymer (cotton, rayon). However, because of the strong hydrogen-bonded structure, softening does not occur below the decomposition temperature. Therefore, it cannot be molded without breaking bonds.

A more complex arrangement results when two polymers form networks that overlap in space. One way of making such an **interpenetrating network (IPN)** is to swell a cross-linked polymer with a monomer. The IPN comes about when the monomer is polymerized into a second network, even though the two networks may have no covalent bonds in common [9–11]. Despite the fact that two polymers are not compatible when mixed as linear molecules, the IPN may exhibit no macroscopic phase separation and thus can be much stronger than a mechanical mixture.

Another kind of mixed network comes about when two linear polymers that are incompatible at room temperature are simultaneously cross-linked at a high temperature at which they are compatible. Phase separation on cooling may be inhibited by the covalent bonds, which limit the movement of polymer chains. The term **semi-IPN** can refer to a linear polymer trapped in a network of another polymer.

2.5 THERMODYNAMICS OF BINARY SYSTEMS

Polymers are often synthesized or used in solutions as mixtures with low-molecular-weight solvents. More recently, a number of polymer blends (mixtures of different polymers) with desirable properties have been commercialized. The ability of a polymer to dissolve in a solvent or to mix with another polymer to form a single-phase mixture depends on the free energy change ΔG_m upon mixing the two components. At a temperature T , thermodynamics allows us to express ΔG_m as

$$\Delta G_m = \Delta H_m - T\Delta S_m \quad (2.1)$$

where:

ΔS_m is the change of entropy upon mixing

ΔH_m is the change of enthalpy upon mixing

The change of volume upon mixing is denoted by ΔV_m and is usually quite small. For a polymer to dissolve in a solvent or another polymer, it is necessary to have $\Delta G_m < 0$. If $\Delta G_m > 0$, the mixing of a polymer with a solvent (or with another polymer) will result in two phases, each containing predominantly one of the two components. In Chapter 3, we will discuss phase separation in polymer solutions and blends. Here, we describe a simple thermodynamic analysis that helps to understand the basis of these phase separations in polymers.

2.5.1 ENTROPY

Boltzmann's relationship states that the entropy of a system is proportional to the logarithm of the number of different ways, Ω , the components (atoms or molecules) of that system can be rearranged without changing the state of the system (see Appendix 2.A). When the two components are small molecules comparable in size, they can fit interchangeably in space, visualized as a lattice arrangement. The relationship, usually derived in elementary physical chemistry texts, reduces in the ideal case ($\Delta H_m = 0$ and $\Delta V_m = 0$) to

$$\Delta S_m = -R(N_1 \ln x_1 + N_2 \ln x_2) \quad (2.2)$$

where:

R is the gas constant (8.31447 J/K · mol)

N and x are the number of moles and mole fractions of the two components, respectively

When a polymer replaces component 2 in the same lattice, account must be taken of the fact that the volume occupied by the polymer is very much greater than that of a lattice site taken to be equal to that of a solvent. In the simplest approach developed by Flory [12], the number of lattice sites occupied by the polymer is increased in proportion to the volume fraction of polymer in the mixture. Thus, the mole fractions in Equation 2.2 are replaced by the corresponding volume fraction of v each component:

$$\Delta S_m = -R(N_1 \ln v_1 + N_2 \ln v_2) \quad (2.3)$$

For the assumptions made in the derivation of the above equation, see Appendix 2.A. Equation 2.3 can also be used when both components 1 and 2 are polymers in the case of a polymer blend. The equation can be written in terms of the change in entropy per unit volume of the mixture as

$$\frac{\Delta S_m}{V} = -R \left(\frac{v_1}{V_1} \ln v_1 + \frac{v_2}{V_2} \ln v_2 \right) \quad (2.4)$$

where:

V_1 and V_2 are the volumes per mole of components 1 and 2, respectively

Note that ΔS_m is always positive because the volume fractions are less than unity. In a polymer blend, both V_1 and V_2 are much larger than the value of the molar volume of

a solvent of small molecules. Therefore, ΔS_m for a polymer blend is much smaller than that for a polymer–solvent mixture. Returning to Equation 2.1, it can now be seen that it is much harder to satisfy the condition of $\Delta G_m < 0$ for polymer blends than for polymer solutions. The blending of two polymers into a one-phase blend depends strongly on their enthalpy of mixing as their entropy of mixing is quite small.

2.5.2 ENTHALPY

In the simple thermodynamic model of Flory, the heat of mixing for polymer solutions (ΔH_m) is calculated using Hildebrand's regular solution theory [13] that gives

$$\frac{\Delta H_m}{V} = v_1 v_2 (\delta_1 - \delta_2)^2 \quad (2.5)$$

where:

δ_1 and δ_2 are known as the **solubility parameters** of components 1 and 2, respectively

In the older literature, a widely used dimension for the solubility parameter is $(\text{cal}/\text{cm}^3)^{1/2}$, called the hildebrand. Other units used are $(\text{J}/\text{cm}^3)^{1/2}$ and $(\text{MPa})^{1/2}$, which are identical. One hildebrand is the equivalent of $2.046 (\text{MPa})^{1/2}$. The solubility parameters for some common liquids are listed as δ_i in Table 2.4. We shall return to the meaning of solubility parameters and their application to polymers in Section 2.6.

For polymer solutions, as for simple solutions, the heat of mixing is the energy change involved in forming one contact between solvent and solute units at the expense of breaking a solvent–solvent contact and a solute–solute contact (ΔH_c) times the number of solvent–solute contacts in the mixture. A polymer chain is pictured as made up of x repeat units. Now, assume that the number of contacts (N_c) is proportional to the volume fraction of solvent multiplied by the number of repeat units (x) and the number of effective contacts per segment (Z). Then, for the mixing of N_2 moles of polymer with N_1 moles of solvent,

$$\Delta H_m = \Delta H_c N_2 N_c = \Delta H_c N_2 Z x v_1 \quad (2.6)$$

But the volume fractions are related to the number of lattice spaces taken up by each component:

$$\frac{v_1}{v_2} = \frac{N_1}{x N_2} \quad (2.7)$$

Thus, substituting in Equation 2.6,

$$\Delta H_m = \Delta H_c Z N_1 v_2 \quad (2.8)$$

When this equation is rewritten as

$$\Delta H_m = RT \chi_H N_1 v_2 \quad (2.9)$$

the symbol χ_H can be identified as the energy change in units of RT when a mole of solvent is transferred from a pure solvent to an infinite amount of polymer. Also, it is the energy in units of kT (where k is the Boltzmann's constant equal to 1.3807×10^{-23} J/K) when a molecule of solvent is transferred. Comparing Equation 2.9 with 2.5, one finds that in this simplest approach

$$\chi_H = \frac{V_1}{RT} (\delta_1 - \delta_2)^2 \quad (2.10)$$

2.5.3 FREE ENERGY

For polymer solutions, combination of Equations 2.1, 2.3, and 2.9 yields

$$\Delta G_m = RT(\chi_H N_1 v_2 + N_1 \ln v_1 + N_2 \ln v_2) \quad (2.11)$$

Experimentally, it is found that for polymer solutions, the entropy of mixing is substantially overestimated by the expression in Equation 2.3. To correct this problem, χ_H is replaced by an **interaction parameter** (χ) that comprises an entropic component independent of temperature and denoted by β and the enthalpic component (χ_H) such that a practical expression for ΔG_m is then

$$\Delta G_m = RT(\chi N_1 v_2 + N_1 \ln v_1 + N_2 \ln v_2) \quad (2.12)$$

where:

χ is given by

$$\chi = \beta + \frac{V_1}{RT} (\delta_1 - \delta_2)^2 \quad (2.13)$$

β , which is sometimes referred to as the lattice parameter, is usually around 0.35 ± 0.1

Furthermore, in comparison with experiments, it turns out that χ is also a function of concentration. Most listed values of χ are for the particular polymer in the given solvent at a stated temperature and at infinite dilution. Some values of χ are listed in Table 2.3 for polymers in what are known as *good* solvents. A number of more rigorous expressions for ΔS_m and ΔG_m have been presented over the years [15]. The predictions of various theories have been compared with Monte Carlo simulations [16,17] that are able to compute thermodynamic properties with fewer assumptions than in the original models.

2.5.4 SWELLING OF POLYMER NETWORKS

When a polymer network is placed in a solvent, it will swell and reach an equilibrium swelling in the presence of excess solvent. The free energy of a swollen network can be assumed to consist of the sum of the free energy of mixing the polymer network

TABLE 2.3
Polymer–Solvent Interaction Parameters at 25°C

Polymer	Solvent	Interaction Parameter χ	
<i>cis</i> -Polyisoprene	Toluene ($V_1 = 106$) ^a	0.391	
	Benzene ($V_1 = 89.0$)	0.437	
Polyisobutylene	Toluene	0.557	
	Cyclohexane ($V_1 = 108$)	0.436	
Butadiene–styrene (71.5:28.5)	Benzene	0.442	
	Cyclohexane	0.489	
Butadiene–acrylonitrile			
	82:18	Benzene	0.390
	70:30	Benzene	0.486
61:39	Benzene	0.564	

Source: Bristow, G. M., and Watson, W. E., *Trans. Faraday Soc.*, 54, 1731, 1958. See Orwoll, R. A., *Rubber Chem. Technol.*, 50, 451, 1977; Bandrup, I., and F. H. Immergut (eds.), *Polymer Handbook*, 3rd edn., Wiley, New York, 1989; Sheehan, C. J., and A. U. Bisio, *Rubber Chem. Technol.*, 39, 149, 1966 for more examples.

^a V_1 is in cubic centimeters per mole.

and the solvent and the elastic free energy of expanding the network. The free energy of mixing of the network and the solvent is given according to Equation 2.12 by

$$\Delta G_m = RT(\chi N_1 v_2 + N_1 \ln v_1) \quad (2.14)$$

where the last term in the parentheses of Equation 2.12 becomes negligible compared to the second term since the entire network consists of one molecule and N_2 approaches 0. In Chapter 8, we will see that the elastic free energy associated with isotropic swelling of a network sample can be obtained from the theory of rubber elasticity and is given by

$$\Delta G_{el} = \left(\frac{3}{2}\right) RT \zeta (\alpha^2 - 1) \quad (2.15)$$

where:

T is the absolute temperature

ζ is the number of moles of elastic polymer chain strands in the sample

$$\alpha = v_2^{-1/3}$$

An elastic polymer chain strand is defined as a chain attached to the network by cross-links at its two ends. The free energy of a swollen network or gel is then given by the sum of Equations 2.14 and 2.15 as

$$\Delta G_{el} = RT(\chi N_1 v_2 + N_1 \ln v_1) + \left(\frac{3}{2}\right) RT \zeta (v_2^{-2/3} - 1) \quad (2.16)$$

When the network swells to equilibrium in excess solvent, the chemical potential (partial molar free energy) of the solvent inside the gel (μ_1) is equal to the chemical potential of the pure solvent (μ_1^0) outside the gel. Thermodynamics gives the quantity ($\mu_1 - \mu_1^0$) as the derivative of ΔG_{el} with respect to N_1 at constant T , P , and N_2 . Setting the derivative of the expression in Equation 2.16 with respect to N_1 equal to 0 gives the following relation between v_2 , V_1 , χ , and N , where N is the number of moles of elastic polymer chain strands per unit volume of dry network:

$$\ln(1 - v_2) + v_2 + \chi v_2^2 = -NV_1 v_2^{1/3} \quad (2.17)$$

This equation can be thought of as the result of the balance between two types of forces: thermodynamic forces due to the solvent swelling the network (left-hand side of the equation) and elastic forces resisting the network expansion (right-hand side).

Equation 2.17 and similar equations have been used to derive the experimental values of χ from swelling data as v_2 can be independently measured, values of V_1 are listed in handbooks, and N is simply related to the elastic modulus of the network that can also be measured (see Chapter 8). Orwoll [18] has reviewed the theoretical basis for χ and the experimental procedures for its measurement. Osmotic pressure, vapor sorption, gas-liquid chromatography, light scattering, and other methods can be used. Although it may not be the best absolute measure of χ , equilibrium swelling is a very practical method and relates directly to an important application, namely, the selection of materials for use in the presence of solvents. Figure 2.3 shows data for values of χ extracted using Equation 2.17 from the swelling of different PDMS networks cross-linked in the melt versus the equilibrium polymer concentration of the networks in benzene. To achieve different cross-link densities, networks were prepared by end-linking precursor chains of different molecular weight [19]. The line in the figure represents the relationship between

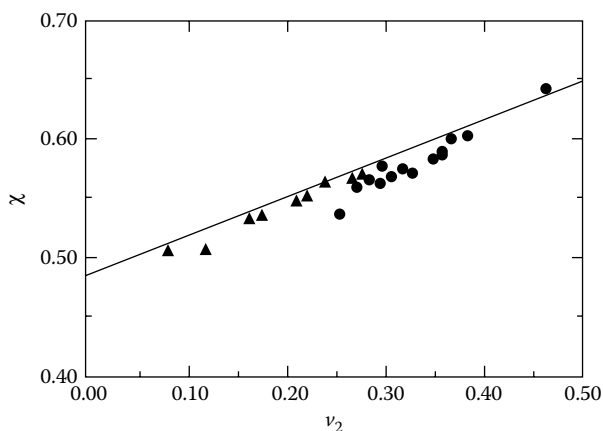


FIGURE 2.3 The interaction parameter χ as a function of polymer volume fraction v_2 for various PDMS networks of different structures and modulus swollen in benzene. The data points are calculated from the swelling results using Equation 2.17. The line represents data obtained for solutions of uncross-linked PDMS chains in benzene. (Data from Flory, P. J., and Shih, H., *Macromolecules*, 5, 761, 1972; Patel, S. K., Malone, S., Gilmore, J. R., and Colby, R. H., *Macromolecules*, 25, 5241, 1992.)

the interaction parameter and the polymer volume fraction of solutions of uncross-linked PDMS chains in benzene using vapor pressure measurements [20]. As shown in the figure, the agreement between data obtained from swelling and from more accurate methods is in general satisfactory, but discrepancies have been reported.

The following slightly different relation for equilibrium swelling was obtained by Flory [21]:

$$\ln(1 - v_2) + v_2 + \chi v_2^2 = - NV_1 \left[v_2^{1/3} - 2 \left(\frac{v_2}{f} \right) \right] \tag{2.18}$$

where:

f is the functionality of the cross-links

The additional term on the right-hand side of the above equation compared to Equation 2.17 is negligible for small values of v_2 or for cross-links of high functionality. Equations 2.17 and 2.18 can be represented in the form of nomographs for ease of determination of an unknown parameter given that the other parameters in the equation are known. Figure 2.4 represents such a nomograph based on Equation 2.18 for tetrafunctionally cross-linked networks ($f = 4$).

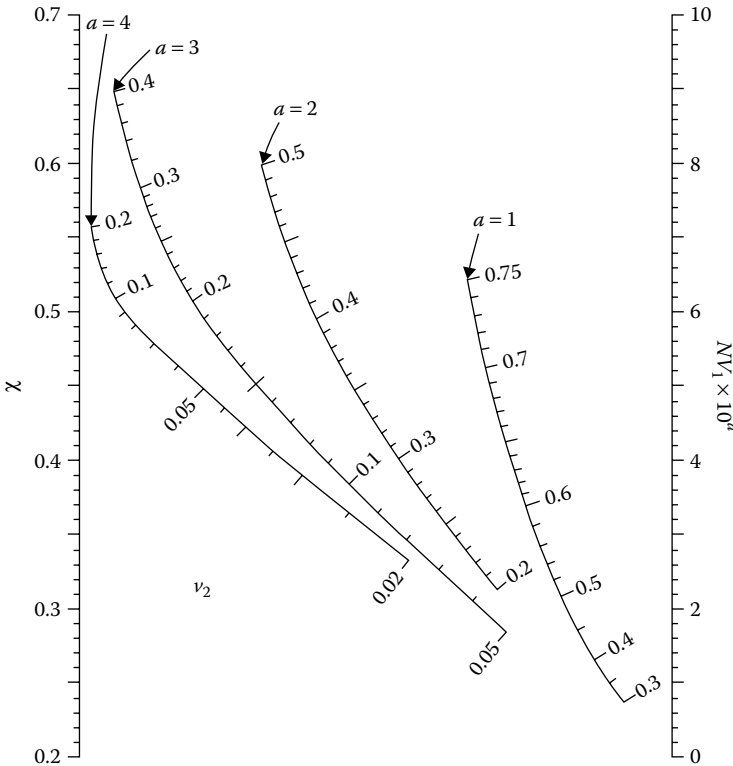


FIGURE 2.4 Nomograph for swelling (Equation 2.18 with $f = 4$). A straight line connects the compatible values of the variables on their corresponding scales. Note that the exponent a varies with the scale selected for v_2 . For example, for $\chi = 0.40$ and $v_2 = 0.3$, $NV_1 = 4.0 \times 10^{-2}$.

2.6 CED AND SOLUBILITY PARAMETERS

The unique properties of polymers can be attributed to the fact that polymer segments are held together by covalent bonds in one direction but by secondary bonds in the other two. A measure of the strength of secondary bonds is given by the CED:

$$\text{CED} = \frac{\Delta E_v}{V_l} \quad (2.19)$$

where:

ΔE_v is the molar energy of vaporization

V_l is the molar volume of the liquid

For small molecules, ΔE_v can be measured by conventional means. The energy necessary to separate molecules from one another from the close spacing typical of the liquid state to the distant spacing of the vapor is evaluated directly by calorimetric methods or indirectly by measuring the vapor pressure p as a function of absolute temperature T . The Clapeyron equation can be used to extract an enthalpy of vaporization ΔH_v :

$$\frac{dp}{dT} = \frac{\Delta H_v}{T(V_g - V_l)} \quad (2.20)$$

where:

V_g and V_l are the molar volumes of the compound in the vapor and liquid, respectively, at temperature T

The internal energy of vaporization ΔE_v is related to ΔH_v by

$$\Delta E_v = \Delta H_v - p(V_g - V_l) \quad (2.21)$$

The **solubility parameter** introduced in Section 2.5 is the square root of CED.

Example 2.1

What is the solubility parameter for *n*-hexane at 25°C? Since V_g is much larger than V_l , the second term in Equation 2.21 can be replaced by $\bar{R}T$ (assuming an ideal gas).

Data: Enthalpy of vaporization $\Delta H_v = 7540$ cal/mol; molar volume = $86.2/0.654 = 131.8$ cm³/mol

Solution:

$$\text{CED} = \frac{7540 - 1.987 \times 298}{131.8} = 52.7 \text{ cal/cm}^3$$

Solubility parameter = $\delta = 7.26$ hildebrands = 14.9 (MPa)^{1/2}

2.6.1 SOLUBILITY PARAMETERS OF POLYMERS

Liquids with similar solubility parameters are apt to dissolve the same solutes and to be mutually compatible. This leads to an indirect method of measuring δ for a polymer. The dissolution of a polymer in a low-molecular-weight liquid causes the random coil to expand and occupy a greater volume than it would in the dry, amorphous state. If the polymer is composed of single molecules, viscous flow can occur. For dilute solutions of polymers at the same concentration in different solvents, the viscosity will depend on the polymer expansion. It is expected that when the polymer and the solvent have the same δ , the maximum expansion will occur and therefore the highest viscosity (for a given concentration) will be obtained. By measuring the viscosity of solutions of the same polymer at the same concentration (usually dilute) in a variety of solvents, one should be able to deduce, in principle, a consistent value of δ_2 for the polymer.

We shall see in Chapter 7 how to obtain the values of the interaction parameter χ given theoretically in Equation 2.13 from the measurements of viscosity of dilute polymer solutions. If the polymer comprises a cross-linked network, solution cannot occur, but individual parts of the polymer chains, that is, polymer segments, can solvate to give a swollen gel. Once again, it is expected that the maximum swelling will take place when the value of δ_2 matches δ_1 of the solvent and the interaction parameter χ is at its minimum.

Although the foregoing statements are borne out qualitatively by experiments, specific (e.g., polar and hydrogen bonding) interactions and differences in molar volume of solvent make the estimation of δ_2 more complicated. The difficulty stems from the fact that the basis of Equation 2.10 is the theory of regular solutions that ignores strong interactions such as polar and hydrogen bonding interactions. Furthermore, Equation 2.10 assumes that a solvent-solute interaction energy can be written simply in terms of the product of pure solvent and pure solute solubility parameters and that ΔH_m is always positive. To take into account strong interactions and improve somewhat the situation, the total CED or equivalently the total solubility parameter δ_t is broken into different components— δ_d for dispersion (non-polar) forces present in regular solutions, δ_p for polar interactions, and δ_h for hydrogen bonding interactions—such that

$$\delta_t^2 = \delta_d^2 + \delta_p^2 + \delta_h^2 \quad (2.22)$$

Values for the three components have been estimated by various means, most of which yield similar but not identical numbers. Both experimental and calculation methods have been employed. When the total CED is estimated from the experimental enthalpy of vaporization, the polar and hydrogen-bonding parameters may be calculated using bond contribution methods. Values of these *Hansen parameters* are included in Table 2.4. In order to represent the solvent interaction with a polymer, a three-dimensional map is needed. An idealized representation is shown in Figure 2.5 for a hypothetical situation in which the solubility volume is centered at values of $\delta_d:\delta_p:\delta_h = 15:7:12$. The total solubility parameter is about 20.4. Also shown are the projections of the surface of the solubility volume on each of the

TABLE 2.4
Characteristic Parameters for Some Solvents at 25°C

Liquid	Formula Weight (g/mol)	Density (g/cm ³)	Solubility Parameter (MPa) ^{1/2}				H-Bonding Index γ
			δ_d	δ_p	δ_h	δ_t	
Acetic acid	60.1	1.044	13.9	12.2	18.9	26.5	–
Acetone	58.1	0.785	13.0	9.8	11.0	19.7	9.7
Acetonitrile	41.1	0.776	10.3	11.1	19.6	24.8	13.0
Acrylonitrile	53.1	0.801	10.6	12.5	14.0	21.6	12.7
<i>n</i> -Amyl alcohol	88.2	0.811	14.8	9.1	14.7	22.7	–
Benzene	78.1	0.874	16.1	8.6	4.1	18.7	0.0
Bromobenzene	157.0	1.486	18.4	8.2	0.0	20.1	–
<i>n</i> -Butanol	74.1	0.806	15.0	10.0	15.4	28.7	18.7
Carbon disulfide	76.1	1.256	10.9	16.6	4.3	20.3	0.0
Chlorobenzene	112.6	1.098	17.4	9.4	0.0	18.7	1.5
Chloroform	119.4	1.477	11.0	13.7	6.3	18.7	1.5
Cyclohexane	84.2	0.774	16.5	3.1	0.0	16.8	0.0
Cyclohexanone	98.2	0.942	15.6	9.4	11.0	21.3	8.4
<i>n</i> -Decane	142.3	0.725	15.8	0.0	0.0	15.8	0.0
Diacetone alcohol	116.2	0.934	10.7	11.4	12.6	20.0	13.0
Dibutyl phthalate	278.4	1.042	15.9	9.5	8.1	20.2	–
Diethyl ether	74.1	0.714	14.5	2.9	5.1	15.8	13.0
<i>N,N</i> -Dimethylformamide	73.1	0.944	17.4	13.7	11.3	24.8	11.7
Dimethyl sulfoxide	78.1	1.096	18.4	16.4	10.2	26.7	7.7
1,4-Dioxane	88.1	1.028	16.3	10.1	7.0	20.7	9.7
Ethanol	46.1	0.785	12.6	11.2	20.0	26.1	18.7
Ethyl acetate	88.1	0.894	13.4	8.6	8.9	18.2	8.4
Ethylbenzene	106.2	0.862	16.5	7.4	0.0	18.1	1.5
Ethylene dichloride (1,2-dichloroethane)	99.0	1.246	14.2	11.2	9.0	20.2	1.5
Ethylene glycol (EG)	62.1	1.110	10.1	15.1	29.8	34.9	20.6
EG monobutyl ether (or 2-butoxyethanol)	118.2	0.896	13.3	7.9	13.0	20.2	13.0
EG monoethyl ether (or 2-ethoxyethanol)	90.1	0.925	13.0	9.1	15.2	21.9	13.0
EG monoethyl ether acetate ester	132.2	0.968	14.4	9.0	8.9	19.1	9.4
Glycerol	92.1	1.258	9.3	15.4	31.4	36.2	–
<i>n</i> -Heptane	100.2	0.679	15.3	0.0	0.0	15.3	0.0
<i>n</i> -Hexane	86.2	0.654	14.9	0.0	0.0	14.9	0.0
1-Hexene	84.2	0.668	14.4	3.9	0.0	15.0	–
Isophorone	138.2	0.917	16.4	9.4	3.2	19.2	–
Isopropyl acetate	102.1	0.866	14.3	8.4	5.7	17.6	8.6
Isopropyl alcohol	60.1	0.781	14.0	9.8	16.0	23.4	18.7

(Continued)

TABLE 2.4
(Continued) Characteristic Parameters for Some Solvents at 25°C

Liquid	Formula Weight (g/mol)	Density (g/cm ³)	Solubility Parameter (MPa) ^{1/2}				H-Bonding Index γ
			δ_d	δ_p	δ_h	δ_t	
Methanol	32.0	0.786	11.6	13.0	24.0	29.7	18.7
Methylene chloride (dichloromethane)	84.9	1.316	13.4	11.7	9.6	20.2	1.5
Methyl ethyl ketone (2-butanone)	72.1	0.800	14.1	9.3	9.5	19.3	7.7
Methyl isobutyl ketone (3,3'-dimethyl 1-2-butanone)	100.2	0.796	14.4	8.1	5.9	17.6	7.7
Methyl methacrylate	100.1	0.930	13.5	10.1	8.5	18.9	–
N-Methyl pyrrolidone	99.1	1.020	16.5	10.4	13.5	23.7	–
Nitrobenzene	123.1	1.190	17.6	14.0	0.0	22.5	2.8
Nitroethane	75.1	1.045	19.0	13.0	0.0	23.0	2.5
1-Nitropropane	89.1	0.996	18.1	11.2	0.0	21.3	2.5
2-Nitropropane	89.1	0.985	16.5	10.4	6.6	20.6	2.5
n-Pentane	72.2	0.621	14.4	0.0	0.0	14.4	0.0
Perchloroethylene (tetrachloroethene)	165.9	1.611	11.4	15.2	0.0	19.0	–
Pyridine	79.1	0.978	17.6	10.1	7.7	21.7	18.1
Styrene	104.2	0.901	16.8	9.1	0.0	19.1	1.5
Tetrahydrofuran	72.1	0.882	13.3	11.0	6.7	18.5	–
Toluene	92.1	0.862	16.4	8.0	1.6	18.3	4.5
1,1,2-Trichloroethylene	131.4	1.455	11.7	14.0	4.4	18.7	–
Vinyl acetate	86.1	0.926	12.9	10.0	8.7	18.5	–
Water	18.02	0.997	12.2	22.8	40.4	48.0	39.0
p-Xylene	106.2	0.856	16.5	7.0	2.0	18.1	4.5

Source: Barton, A. F. M., *Handbook of Solubility Parameters and Other Cohesion Parameters*, CRC Press, Boca Raton, FL, 94–186, 1983.

three planes. In practice, the volume containing the good solvents may resemble an irregular sausage rather than a spheroid. However, the correlation is often more satisfactory, as one might expect with the additional parameters available. But the behavior of mixtures of solvents is not always predictable, and the molecular volume still can affect the correlation.

Consider the example of swelling of cross-linked butyl rubber [14] in 10 solvents (Figure 2.6). In this figure, v_2 is the volume fraction of rubber in the swollen sample. It is obvious that using $\beta = 0.45$, solvents with δ around 8 swell butyl rubber more effectively than do solvents with δ clearly below or clearly above 8, thus confirming that the selection of $\delta_2 = 8.1$ is a good estimate but not an exact value. Representative values of δ_2 obtained from swelling data are shown

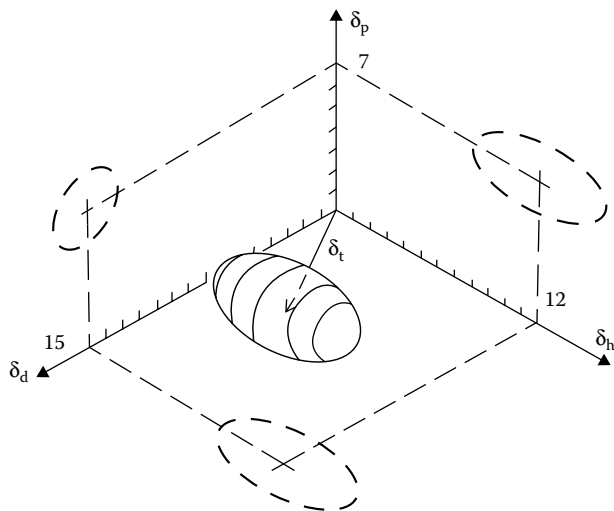


FIGURE 2.5 Solubility volume in three-dimensional solubility parameter space for a hypothetical situation where the solubility is a maximum at the coordinates indicated and the polymer is insoluble outside the limits of the skin of the football-shaped volume. The total solubility parameter is represented by the length of the arrow from the origin to the center of the volume.

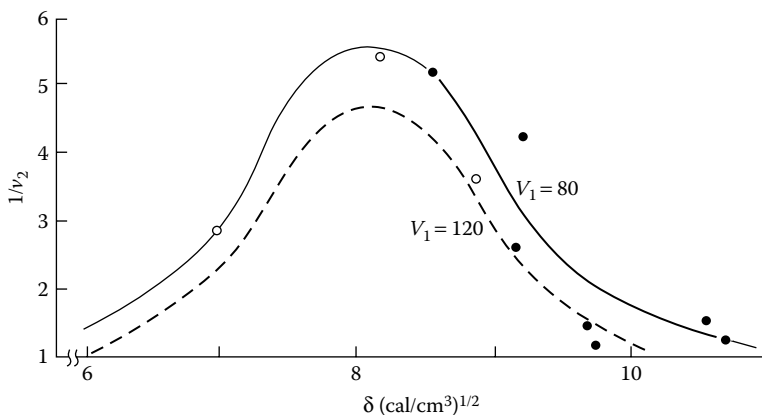


FIGURE 2.6 Swelling data for butyl rubber (Data from Bristow, G. M. and Watson, W. E., *Trans. Faraday Soc.*, 54, 1731, 1958.) in solvents with $100 < V_1 < 120$ (o) and with $80 < V_1 < 100$ (●). Curves for Equations 2.13 and 2.18 with $\beta = 0.45$, $N = 1.0 \times 10^{-4}$ mol/cm³, and $\delta = 8.1$ hildebrands.

in Table 2.5 and, in general, show an increase with the polarity of the polymer. Another use of solubility parameters is in choosing compatible polymers for use in blends in surface coatings and adhesives. Maximum compatibility is expected to occur between polymers with same δ_2 . Because of the important role ΔH_m plays in the compatibility of blends mentioned earlier, it has been found that a *negative*

TABLE 2.5
Three-Dimensional Solubility Parameters for Selected Polymers ([MPa]^{1/2})

Polymer	δ_d	δ_p	δ_h	$\delta_1 = \delta_2$
Cellulose acetate	18.6	12.7	11.0	25.1
Polyisobutylene	14.5	2.5	4.7	15.5
Polyisoprene (<i>cis</i>)	16.6	1.4	-0.8	16.7
Nylon 6,6	18.6	5.1	12.3	22.9
Poly(acrylonitrile)	18.2	16.2	6.7	25.3
Poly(ethylene terephthalate)	19.4	3.5	8.6	21.5
Poly(methyl methacrylate)	18.6	10.5	7.5	22.7
Polystyrene	21.3	5.7	4.3	22.5
Polysulfone (bisphenol A)	19.0	0.0	7.0	20.3
Poly(vinyl acetate)	20.9	11.3	9.7	25.7
Poly(vinyl chloride)	18.8	10.0	3.1	21.5

Source: Grulke, E. A., in J. Bandrup and E. H. Immergut (eds.), *Polymer Handbook*, 3rd edn. Wiley, New York, 556, 1989.

ΔH_m would insure compatibility. This has led to the chemical modification of some polymers to make them compatible with others.

Example 2.2

A cross-linked sample of polymer P swells to 4.55 times its original volume when immersed in solvent S at 27.0°C. Addition of a small amount of ethanol causes the swelling to decrease. If the polymer-solvent interaction parameter, χ_1 , for S and P is 0.500, what is the solubility parameter of P? The parameter β is 0.400.

Data for solvent S: Formula Weight (FW) = 216 g/mol, density = 1.00 g/cm³, and internal energy of vaporization = 63.2 kJ/mol

Solution:

$$\delta_s = (\text{CED})^{0.5} = \left(\frac{\Delta E_v}{V_l} \right)^{1/2} = \left(\frac{63,200}{216} \right)^{1/2} = 17.1 \text{ (MPa)}^{1/2}$$

Using Equation 2.13,

$$0.50 = 0.40 + [216/(8.31 \times 300)](17.1 - \delta_p)^2$$

$$\delta_p = 17.1 \pm 1.1$$

Since δ for ethanol > 17, δ_p must be less than δ_s . Thus,

$$\delta_p = 16.0 \text{ (MPa)}^{1/2}$$

2.6.2 HYDROGEN-BONDING INDEX

Because of the strong effect of hydrogen-bonding interactions on the solubility of polymers, another empirical approach was developed based on a parameter called the **hydrogen-bonding index**, γ . The change in hydrogen bonding that occurs when a solvent is mixed with deuterated methanol in specific proportions compared with the bonding when benzene is the solvent can be measured by the shift of a peak in infrared spectrum away from a value of 2681 per cm. By using a scale for the hydrogen-bonding parameter that ranges from 0 for benzene and other hydrocarbons to 18.7 for ethanol and up to 39.0 for water, swelling and compatibility of polymers and solvents can be better predicted than by using δ alone. Values of the relative hydrogen-bonding index for various solvents appear in Table 2.4. The parameter locations for some major groups of solvents are indicated in Figure 2.7. Such a map has great value in selecting solvents for a coating system or in judging probable resistance to swelling for a particular application.

2.6.3 GROUP CONTRIBUTION METHOD

The method of **group contribution** allows one to calculate the solubility parameter of a polymer without making experimental observations on the polymer. One defines a molar attraction constant F_i for each group on the polymer molecule. For polystyrene, for example, the chemical structure of the monomer unit is subdivided into three groups:

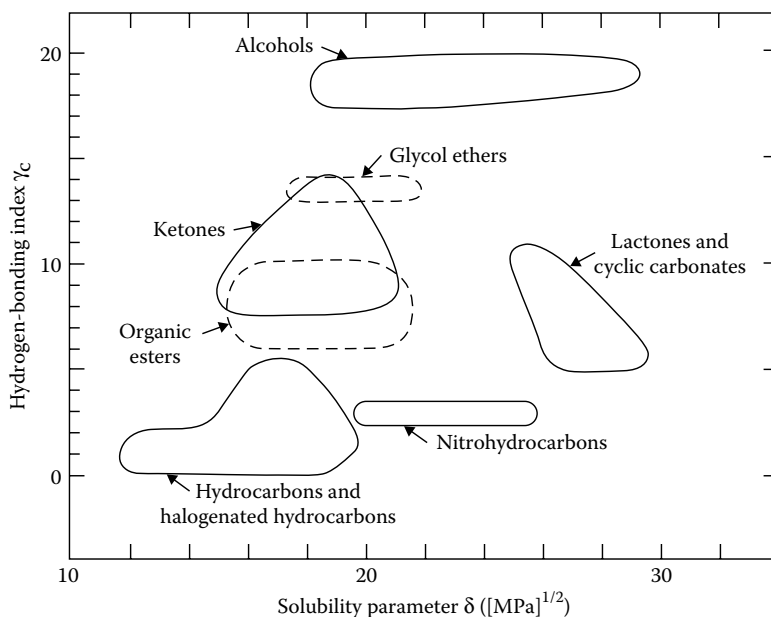
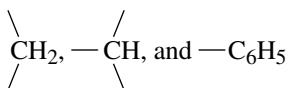


FIGURE 2.7 Parameter locations for major solvent groups. (Data from E. I. du Pont de Nemours and Co., *Solvent Formulating Maps for Elvacite Acrylic Resins*, PA 12-770, 1971.)

Van Krevelen [27] gives an extensive list of these group contributions to the solubility parameter. The values of F_i are in $\text{cal}^{1/2}/\text{cm}^{3/2}$ and are typically obtained from low-molar-mass compounds from the expression:

$$F_i = (\Delta E_i V_i)^{1/2}$$

where:

ΔE_i and V_i have been defined earlier as the CED and molar volume, except that here they pertain to the particular group i

Assuming that the contributions of different groups are additive, one writes

$$\delta = \rho \frac{\sum F_i}{\sum M_i}$$

where:

ρ and M_i are the density of the polymer and the molar mass of group i , respectively

Given that $F(-\text{CH}_2) = 135 \text{ cal}^{1/2}/\text{cm}^{3/2}$, $F(-\text{CH}) = 60 \text{ cal}^{1/2}/\text{cm}^{3/2}$, and $F(-\text{C}_6\text{H}_5) = 720 \text{ cal}^{1/2}/\text{cm}^{3/2}$, one calculates $\delta = 9.41 \text{ cal}^{1/2}/\text{cm}^{3/2}$ or $19.26 \text{ MPa}^{1/2}$ for polystyrene. This value is within 3% of the experimentally reported value of $18.72 \text{ MPa}^{1/2}$ [28].

Finally, we note that a dynamic property such as the dissolution rate of a polymer into a solvent depends on more than equilibrium thermodynamic properties. In the case of polymer dissolution, mass transfer considerations such as polymer diffusion in the solvent are important. For example, when water, a nonsolvent, is added to 2-butanone, poly(methyl methacrylate) dissolves more rapidly despite the fact that the solvent mixture is thermodynamically poorer than 2-butanone by itself [29].

APPENDIX 2.A

Flory and Huggins [30] derived independently the expression for the entropy of mixing a polymer and a solvent given in Equation 2.3 by using a lattice model (Figure 2.A.1). The calculation is performed by starting with an empty lattice and placing n_2 polymer molecules one at a time and segment by segment on the lattice, then filling the remaining vacant sites of the lattice with n_1 solvent molecules.

The assumption is that there is no volume change upon mixing polymer and solvent. If each polymer molecule consists of x segments and the size of the segment is assumed to be equal to that of the solvent, then the total number of sites n of the lattice is taken to be

$$n = n_1 + xn_2 \quad (2.A.1)$$

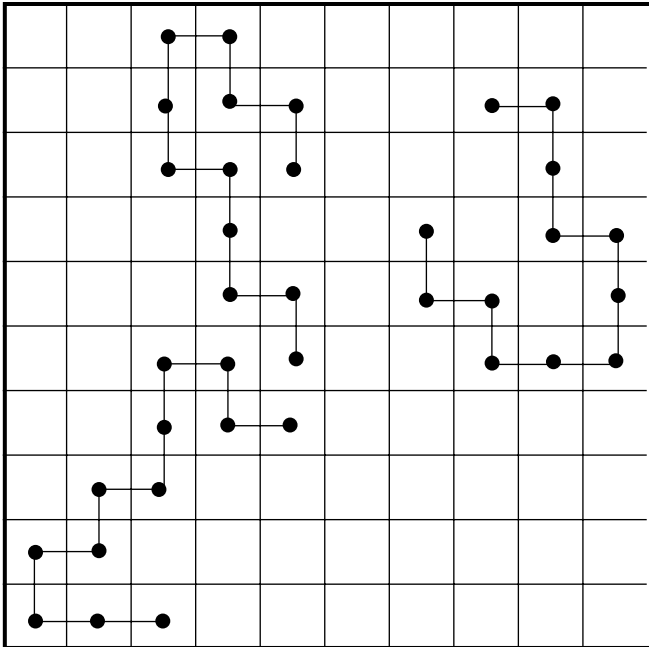


FIGURE 2.A.1 Schematic of polymer chains on a two-dimensional lattice.

The basis of the calculation for the entropy of the mixture is Boltzmann’s entropy expression:

$$S_M = k \ln \Omega_M \tag{2.A.2}$$

where:

k is Boltzmann’s constant

Ω_M represents the total number of possible configurations of such a filled lattice

Ω_M can be expressed as

$$\Omega_M = \frac{1}{n_2!} \prod_{n'_2=0}^{n'_2-1} \Omega_{n'_2+1} \tag{2.A.3}$$

where:

$\Omega_{n'_2+1}$ is the probability of placing the polymer molecule $n'_2 + 1$ on the lattice where n'_2 molecules are already placed on the lattice

The denominator $n_2!$ accounts for the fact that the n_2 polymer molecules are identical and therefore the order in which they are placed on the lattice is irrelevant. The symbol \prod represents a product of the probabilities of placing all the polymer molecules on the lattice.

To obtain an expression for $\Omega_{n'_2+1}$ one observes that (1) the number of ways of placing the first segment of the $n'_2 + 1$ molecule is $n - xn'_2$ since this is the number of vacant sites; (2) taking the coordination number of the lattice to be z , the number of ways of arranging the second segment will be $z(n - xn'_2)/n$, assuming that the probability of finding this site vacant is proportional to the fraction of vacant sites (mean-field approximation); (3) the number of configurations of the third segment is given by $(z-1)(n - xn'_2)/n$; and (4) the number of configurations for the succeeding $x-3$ segments is taken to be the same as for the third. In principle, this last number should be slightly decreasing as we add the segments of the $n'_2 + 1$ molecule, but the error is negligible. The number of configurations $\Omega_{n'_2+1}$ for the $n'_2 + 1$ molecule is the product of all the above probabilities and is then given by

$$\Omega_{n'_2+1} = (n - xn'_2) \frac{z(n - xn'_2)}{n} \left[(z-1) \frac{n - xn'_2}{n} \right]^{x-2} \quad (2.A.4)$$

For large z (Flory's approximation), one obtains

$$\Omega_{n'_2+1} \approx \frac{(z-1)^{x-1}}{n^{x-1}} (n - xn'_2)^x \quad (2.A.5)$$

Substituting in Equation 2.A.3, one obtains

$$\Omega_M = \frac{1}{n_2!} \prod_{n'_2=0}^{n'_2-1} \frac{(z-1)^{x-1}}{n^{x-1}} (n - xn'_2)^x \quad (2.A.6)$$

The last expression can be rewritten as

$$\Omega_M = \left(\frac{z-1}{n} \right)^{(x-1)n_2} \frac{x^{xn_2}}{n_2!} \left[\frac{(n/x)!}{(n/x - n_2)!} \right]^x \quad (2.A.7)$$

Substituting in Equation 2.A.2 and using the Sterling approximation,

$$\ln n_2! = n_2 \ln n_2 - n_2 \quad (2.A.8)$$

one obtains

$$S_M = -k \left[n_1 \ln \frac{n_1}{n_1 + xn_2} + n_2 \ln \frac{n_2}{n_1 + xn_2} \right] + k(x-1)n_2 [\ln(z-1) - 1] \quad (2.A.9)$$

The entropy change upon mixing the pure components 1 and 2 is given by

$$\Delta S_m = S_M - S_1 - S_2 \quad (2.A.10)$$

The expression for S_1 and S_2 for this lattice model can be obtained from the expression in Equation 2.A.9 by setting $n_2 = 0$ and $n_1 = 0$, respectively, to find

$$S_1 = 0 \text{ and } S_2 = kn_2 \left\{ \ln x + (x-1) [\ln(z-1) - 1] \right\} \quad (2.A.11)$$

Substituting (2.A.9) and (2.A.11) into (2.A.10), changing the number of molecules into the number of moles by dividing with Avogadro's number, simplifying, and taking x to represent the ratio of molar volumes, we recover Equation 2.3:

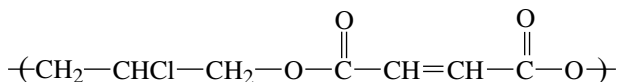
$$\Delta S_m = -R(N_1 \ln v_1 + N_2 \ln v_2)$$

KEYWORDS

Deflection temperature
 Heat distortion temperature
 Thermoset
 Intermolecular forces
 Cohesive energy density
 Network
 Linear (branched)
 Enantiomer
 Chiral
 Chiral center
 Achiral
 Optical isomerism
 Conformations
 Configurations
 Isotactic structure
 Syndiotactic structure
 Atactic structure
 Tacticity
 Stereoisomerism
 cis-trans
 Thermoplastic
 Interaction parameter (χ)
 Interpenetrating network (IPN)
 Solubility parameter, δ
 Hydrogen-bonding index
 Group contribution method

PROBLEMS

- 2.1** For a material with a density of 1.0 g/cm^3 , estimate the molecular weight of a sphere made up of one molecule with a diameter of (a) 100 \AA , (b) $1.0 \text{ }\mu\text{m}$, and (c) 1.0 cm . Avogadro's number = 6.02×10^{23} molecules/mol.
- 2.2** A polyester has the following repeat unit:



What stereoisomers are possible?

- 2.3** Estimate the repeat distance between methyl groups in the same row of isotactic poly(propylene oxide) in the planar zigzag form (Figure 2.2a). Repeat for the syndiotactic poly(propylene oxide).
- 2.4** A cross-linked sample of polyisobutylene swells 10 times its original volume in cyclohexane. What volume will it swell to in toluene?
- 2.5** A polymer of propylene oxide (PO), $\text{-(CH}_2\text{-CH(CH}_3\text{)-O)-}$, is cross-linked so that the average distance between cross-links is 5000 chain atoms. The polymer density after cross-linking is 1.20 g/cm^3 . What is the density of a swollen sample in a solvent for which $\chi = 0.40$ and solvent density is 0.80 g/cm^3 ? Assume additivity of volumes. Molecular weight of solvent is 102.
- 2.6** The gamma radiation of many polymers results in cross-linking. For a new polymer, assuming that cross-link density $N/2$ is directly proportional to radiation dose, deduce the cross-link density at the highest dose and χ , the interaction parameter.

Dose (mrad)	v_2 in <i>n</i> -Hexane at 25°C
1	0.090
2	0.110
4	0.138
8	0.177
16	0.225

- 2.7** Calculate the extended planar zigzag length (nm) of a molecule with 1000 repeat units of (a) $\text{-(Si(CH}_3\text{)}_2\text{-O)-}$, (b) $\text{-(CH}_2\text{-CO-O)-}$, (c) $\text{-(CH}_2\text{-CH}_2\text{)-}$, and (d) $\text{-(CH}_2\text{-O)-}$. Neglect the end-group contributions to length.
- 2.8** A single molecule of isotactic polypropylene has a molecular weight of 2×10^6 . Calculate the following:
- The length (cm) when the chain is extended (planar zigzag form)
 - The volume occupied if the molecule forms a single crystal with a density of 0.906 g/cm^3
- 2.9** Heating natural rubber with 0.100 mol of peroxide/1000 cm^3 gives a network that swells to 4.35 times its original volume in toluene (at 25°C). Each peroxide molecule yields one cross-link. Heating the same rubber with 28.0 g of sulfur/1000 cm^3 (instead of the peroxide) gives a network that swells to 3.45 times its original volume (at 25°C). If all the sulfur atoms react to form bridges with variable numbers of atoms between chains, how many sulfur atoms are there in an average cross-link? The atomic weight of sulfur is 32.0. Toluene: density = 0.867 g/cm^3 , FW = 92.14 g/mol.
- 2.10** A polymer P with a very high initial molecular weight (1×10^6) is cross-linked by agent A. Each molecule of A brings about one cross-link. The cross-link density is measured by swelling the sample in a *perfect*

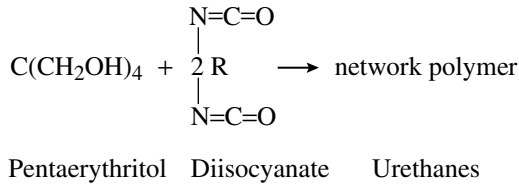
solvent (whose solubility parameter is equal to that of the polymer). If a 5.00-cm³ sample of P with 0.020 g of A/100 g of P swells to 75.0 cm³, what concentration of A will yield a 5.00-cm³ sample that swells to only 25.0 cm³? Parameter β of system = 0.475, $V_1 = 83.0$ cm³/mol. Agent A: FW = 205 g/mol.

- 2.11** A cross-linked rubber sample swells to 10 times its original volume when immersed in solvent A. Assuming that this is the best possible solvent for the polymer, what is the solubility parameter of solvent B, which is made up by adding a small amount of a lactone to solvent A? The sample swells only to 5 times its original volume in B. Both solvents A and B have a molar volume of 100 cm³ and the same value of the parameter β . All tests are made at 27°C. Solvent A: CED = 85.0 cal/cm³, $\chi = 0.33$.
- 2.12** A mixture of benzoyl peroxide (0.5 g) with poly(vinyl ethyl ether) (PVEE; 100 g) is heated to 175°C. Assuming that all the peroxide decomposes and that each molecule of peroxide extracts two hydrogen atoms to produce a single cross-link, calculate the following:
- The expected chain density N at 25°C in the final network
 - The swollen volume of 1 cm³ of polymer in benzene at 25°C
- Benzoyl peroxide: molecular weight (MW) = 242. PVEE: MW = 72 (repeat unit), $\rho = 0.97$ g/cm³, V_1 (benzene) = 89.0 cm³/mol, χ (PVEE, benzene) = 0.40
- 2.13** A silicone rubber sample is cross-linked by exposure to gamma radiation. The average number of chain atoms between cross-links determined by a mechanical test is 850. What volume (cm³) will be occupied by 1 g of rubber when it is equilibrated in *n*-octane at 20°C? The formula weight for dimethyl siloxane $-(\text{Si}(\text{CMe}_2)_2\text{O})-$ is 78. The solid rubber has a density of 1.00 g/cm³. The formula weight of *n*-octane is 114 and its density is 0.703 g/cm³. χ (20°C) is 0.49.
- 2.14** If the polymer sample described in Example 2.2 is placed in solvent Q, which has the same lattice parameter as S, to what extent will the sample swell at 27.0°C? Data for solvent Q: FW = 88.0 g/mol, density = 0.860 g/cm³, internal energy of vaporization = 29.9 kJ/mol.
- 2.15** A cross-linked polymer is swollen in three solvents. What is the predicted swollen volume in solvent C? Assume that the lattice parameter is 0.300 for all three solvents. All data are taken at 27°C.

Solvent	Molar Volume (cm ³ /mol)	Swollen Volume ^a (cm ³)	Solubility Parameter (hildebrands)
A	100	4.00	7.00
B	100	4.00	8.80
C	250	–	8.20

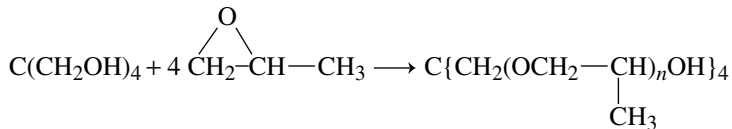
^a Swollen volume of gel starting with 1.00 cm³ of original polymer.

- 2.16** A network polymer is produced by reacting 2 mol of a diisocyanate (DI) with 1 mol of pentaerythritol (PE; the R group does not contain nitrogen):



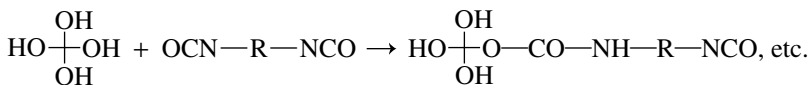
The network polymer has a density of 1.05 g/cm³ and, according to an elemental analysis, 2.10 g/l of nitrogen. What swollen volume can one expect from 1.00 cm³ of network polymer when it is equilibrated with chlorobenzene (density 1.10 g/cm³, MW = 112.5), for which system the polymer-solvent interaction parameter is 0.430?

- 2.17** A tetrafunctional telechelic polymer (possessing reactive end groups; see Section 4.5) is made by ring scission polymerization of propylene oxide (PO) on pentaerythritol (PE).



PE: FW = 136; PO: FW = 58.0

This is followed by network formation with the addition reaction of a low-molecular-weight diisocyanate (DI).



DI: FW = 110

Given the following information:

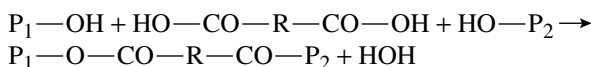
200 mol of PO and 2 mol of DI are used per mole of PE. Reaction is complete in each step.

Density of unswollen network polymer is 1.06 g/cm³.

The network polymer swells to 3.57 times its original volume in toluene (at 27.0°C), which has a solubility parameter of 8.90 hildebrands, an FW of 92.14, and a density of 0.862 g/cm³.

What is the *solubility parameter* of the network polymer if the lattice parameter β is 0.300?

- 2.18** A copolymer of allyl alcohol has some pendent OH groups. It is cross-linked through the OH groups by reaction with a negligible volume of a dicarboxylic acid:



The ester-cross-linked sample is then exposed to gamma radiation, which introduces covalent C—C cross-links in addition to the ester cross-links formed previously. When 10.0 cm³ of this *doubly cross-linked* polymer is placed in water, it swells rapidly to 55.6 cm³. However, after an extended time in water, all the ester bonds are hydrolyzed and now the same sample swells to 83.3 cm³. *What fraction of the cross-links present in the doubly cross-linked sample (before hydrolysis) was due to ester bonds?* The value of the polymer-solvent interaction parameter is 0.48.

- 2.19** Obtain an expression for the difference in chemical potential, $\mu_1 - \mu_1^0$, of a solvent inside and outside a network swollen in that solvent by differentiating Equation 2.16 with respect to N_1 , keeping T and N_2 constant. Note that the total volume of the swollen network, $V = N_1 V_1 + V_p$, where V_p is the volume of the dry network, depends on N_1 . Show that at equilibrium swelling, that is, when $\mu_1 - \mu_1^0 = 0$, you recover Equation 2.17.
- 2.20** (a) Rewrite Equation 2.A.6 as 2.A.7 by using the definition of a factorial:

$$n! = n(n-1)(n-2)(n-3)\dots(3)(2)(1)$$

(b) Derive Equation 2.A.9 from 2.A.2 and 2.A.7, using Sterling's approximation.

- 2.21** Obtain Flory's entropy of mixing, Equation 2.3, from Equations 2.A.9 through 2.A.11.
- 2.22** Use the group contribution method to calculate the solubility parameter of linear polyethylene (PE) and poly(vinyl chloride) (PVC) given the following molar attraction constants:

$$\begin{array}{l} F(-CH_2) = 135 \text{ cal}^{1/2}/\text{cm}^{3/2}, \quad F\left(-\overset{\text{H}}{\underset{\text{H}}{\text{C}}}\right) = 60 \text{ cal}^{1/2}/\text{cm}^{3/2}, \\ F(-Cl) = 230 \text{ cal}^{1/2}/\text{cm}^{3/2} \end{array}$$

The densities of PE and PVC are 0.86 and 1.39 g/cm³, respectively. Compare the values of δ you obtain with the observed values of 16.2 and 19.8 MPa^{1/2} for these two polymers.

REFERENCES

1. Barry, A. J., and H. N. Beck: chap. 5 in F. G. A. Stone and W. A. G. Graham (eds.), *Inorganic Polymers*, Academic Press, New York, 1962.
2. Bowen, H. J. M. et al.: *Tables of Interatomic Distances and Configurations in Molecules and Ions*, Chemical Society, London, 1958.

3. Pauling, L.: *The Nature of the Chemical Bond*, 3rd edn., Cornell University Press, Ithaca, NY, 1960, pp. 85, 189.
4. Pimentel, G. C., and A. L. McClellan: *The Hydrogen Bond*, Freeman, San Francisco, CA, 1960, pp. 212, 224, 292.
5. Richardson, M. I.: *Proc. R. Soc. (London)*, A279:50 (1964).
6. Natta, G. et al.: *J. Polym. Sci.*, 51:156 (1961).; *SPE Trans.*, 3:(1963).
7. Jikei, M., and M.-A. Kakimoto: *Prog. Polym. Sci.*, 26, 1233 (2001).
8. Frechet, J. M. J., C. J. Hawker, I. Gitsov, and J. W. Leon: *JMS Pure Appl. Chem.*, A33(10):1399 (1996).
9. Sperling, L. H.: *Macromol. Rev.*, 12:141 (1977).
10. Sperling, L. H.: *Interpenetrating Networks and Related Materials*, Springer, New York, 2012.
11. Klemmner, D. (ed.): *Polymer Alloys: Blends, Blocks, Grafts and Interpenetrating Networks*, Springer, New York, 2013.
12. Flory, P. J.: *Principles of Polymer Chemistry*, chap. 12, Cornell University Press, Ithaca, NY, 1952.
13. Hildebrand, J. H., and R. L. Scott: *The Solubility of Nonelectrolytes*, 3rd edn., Reinhold, New York, 1950.
14. Bristow, G. M., and W. E. Watson: *Trans. Faraday Soc.*, 54:1731 (1958).
15. Schweitzer, K. S., and J. G. Curro: *Adv. Polym. Sci.*, 116:319 (1994).
16. Dickman, R., and C. K. Hall: *J. Chem. Phys.*, 85:3023 (1986).
17. Binder, K.: *Adv. Polym. Sci.*, 112:181 (1994).
18. Orwoll, R. A.: *Rubber Chem. Technol.*, 50:451 (1977).
19. Patel, S. K., S. Malone, C. Cohen, J. R. Gillmor, and R. H. Colby, *Macromolecules*, 25:5241 (1992).
20. Flory, P. J., and H. Shih: *Macromolecules*, 5:761 (1972).
21. Flory, P. J.: *Principles of Polymer Chemistry*, chap. 13, Cornell University Press, Ithaca, NY, 1952.
22. Barton, A. F. M.: *Handbook of Solubility Parameters and Other Cohesion Parameters*, CRC Press, Boca Raton, FL, 1983, pp. 94–186.
23. Bandrup, I., and F. H. Immergut (eds.): *Polymer Handbook*, 3rd edn., Wiley, New York, 1989.
24. Sheehan, C. J., and A. U. Bisio: *Rubber Chem. Technol.*, 39:149 (1966).
25. Grulke, E. A.: in J. Bandrup and E. H. Immergut (eds.), *Polymer Handbook*, 3rd edn., Wiley, New York, 1989, p. 556.
26. E. I. du Pont de Nemours and Co.: *Solvent Formulating Maps for Elvacite Acrylic Resins*, PA 12-770, 1971.
27. van Krevelen, D. W.: *Properties of Polymers*, 2nd edn., Elsevier, Amsterdam, the Netherlands, 1976, p. 134.
28. Mangaraj, D., S. K. Bhatnagar, and S. B. Rath: *Makromol. Chem.*, 67:75 (1963).
29. Cooper, W. J., P. D. Krasicky, and F. Rodriguez: *J. Appl. Polym. Sci.*, 3(1):65 (1986).
30. Flory, P. J.: *J. Chem. Phys.*, 10:51 (1942); Huggins, M. L., *Ann. N. Y. Acad. Sci.*, 43:1 (1942).

GENERAL REFERENCES

- Barton, A. F. M.: *Polymer-Liquid Interaction Parameters and Solubility Parameters*, CRC Press, Boca Raton, FL, 1990.
- Barton, A. F. M.: *Handbook of Solubility Parameters*, 2nd edn., CRC Press, Boca Raton, FL, 1991.
- Coleman, M. M., P. C. Painter, and J. F. Graf: *Specific Interactions and the Miscibility of Polymer Blends*, Technomic, Lancaster, PA, 1991.

- Harris, F. W., and R. B. Seymour (eds.): *Structure–Solubility Relationships in Polymers*, Academic Press, New York, 1977.
- Mark, J. E., H. R. Allcock, and R. West: *Inorganic Polymers*, 2nd edn., Oxford University Press, New York, 2005.
- Monnerie, L., and U. W. Suter: *Atomistic Modeling of Physical Properties*, Springer-Verlag, Berlin, Germany, 1994.
- Olabisi, O., L. M. Robeson, and M. T. Shaw: *Polymer–Polymer Miscibility*, Academic Press, New York, 1979.
- Paul, D. R., and C. B. Bucknall: *Polymer Blends*, Wiley, New York, 2005.
- Paul, D. R., and L. H. Sperling (eds.): *Multicomponent Polymer Materials*, American Chemical Society, Washington, DC, 1986.
- Porter, D.: *Group Interaction Modeling of Polymer Properties*, Marcel Dekker, New York, 1995.
- Rempp, P., and G. Weill (eds.): *Polymer Thermodynamics and Radiation Scattering*, Huthig & Wepf, Basel, Switzerland, 1992.
- Seymour, R. B., and C. F. Carraher, Jr.: *Structure–Property Relationships in Polymers*, Plenum Press, New York, 1984.
- Thomas, E. L. (ed.): *Materials Science and Technology: Structure and Properties of Polymer*, VCH, New York, 1993.
- Urban M. W., and C. D. Craver (eds.): *Structure–Property Relations in Polymers: Spectroscopy and Performance*, American Chemical Society, Washington, DC, 1993.
- van Krevelen, D. W., and K. T. Nijenhuis: *Properties of Polymers*, 4th edn., Elsevier, Amsterdam, the Netherlands, 2009.

3 Physical States and Transitions

3.1 PHYSICAL STATES

The physical states in which a polymer can exist may be idealized by considering first a very long, regular polymer chain. Many of the physical properties and phase transitions of polymers can be described using physics concepts that ignore the actual chemical constitution of the chain, be it for example polyethylene, polystyrene (PS), or poly(methyl methacrylate) (PMMA). The reason is that these properties are dominated by the extreme length and chain-like structure of these molecules and not by their actual chemical composition. For more complex structures such as branched, cross-linked, or **block copolymers** for which the chains are inhomogeneous, new physical models need to be introduced to describe the general properties of these structures. The chemical composition and configuration of polymers play, however, a crucial role on how the molecules will pack in their pure state. Atactic PS, for example, is an amorphous solid (existing in a condition called a **glassy state**) at room temperature, whereas isotactic and syndiotactic PS exist in a **crystalline state**. Even though isotactic and syndiotactic PS have the same chemical composition as atactic PS, their regular configurations (see Section 2.3) enable their molecules to fit together in such a way that intermolecular (chemical) attractions stabilize the chains in a regular lattice, despite the weak intermolecular barriers to rotation around single bonds. As the temperature is lowered, intermolecular barriers to rotation become greater, and the crystal is more stable. However, as the temperature is increased, the ease of intermolecular rotation increases and the crystal structure eventually melts.

This chapter is devoted to various physical structures and transitions that occur in polymer systems. It covers simple binary polymer mixtures, amorphous polymers, and crystalline polymers, and discusses briefly diblock copolymers, **liquid crystal (LC) polymers**, and gels.

3.2 CONFORMATION OF SINGLE CHAINS IN SOLUTIONS

A very successful model that describes the shape of a linear polymer chain is that of a **random Gaussian coil** [1,2]. The molecule can be described as a long string made of a very large number of steps in which each step represents a segment of the molecule. The orientation of each segment (step) is random relative to the orientation of the preceding segment. The conformation of such a coil is constantly changing in solution and the probability that the chain will have a certain **end-to-end distance** (distance between the two ends of the chain) is given by a Gaussian probability distribution

(see Section 9.8). This model predicts that the end-to-end distance squared of a polymer molecule will be proportional to its molecular weight M , that is,

$$\left(\overline{r_0^2}\right) = \text{const} \times M \quad (3.1)$$

This prediction is in excellent agreement with experimental observations in polymer melts and concentrated solutions and provides a **scaling law** for the dependence of the average size R of the molecular coil

$$R = cM^{1/2} \quad (3.2)$$

where:

c is a proportionality constant that depends on the chemical structure of the polymer

When the polymer is in dilute solution in a good solvent, the coil will swell with the solvent and it will achieve an expanded size. Flory showed that in this case R becomes proportional to $M^{0.6}$. More recent physics calculations and experimental results demonstrated that Flory's exponent is correct to within a few percent. The melt conformation and the dilute solution conformation represent two limiting cases when the polymer volume fraction (v_2) approaches unity and 0, respectively. In dilute solutions, the polymer molecules do not interact with each other and remain on average far from one another (Figure 3.1). In concentrated solutions and in melts, however, the coils representing different molecules are highly interpenetrated and there are not enough solvent molecules to swell the chains.

An intermediate regime that has been extensively studied by physicists led by de Gennes [3] is the **semi-dilute** regime where the concentration of polymer is high enough such that the coils are interpenetrated (Figure 3.2) but small enough such that portions of the chains (called blobs) are still highly swollen and do not interact with each other. A scaling analysis of this situation leads to the following result:

$$R = \text{const} M^{1/2} v_2^{-1/4} \quad (3.3)$$

The power of the polymer volume fraction v_2 in the above expression has also been verified experimentally [4] with some indication that it holds well into the concentrated regime. The transition from dilute to semi-dilute behavior occurs when the concentration of polymers is such that the coils begin to overlap. This concentration has been denoted in the literature as the overlap concentration, c^* or v_2^* . For high-molecular-weight polymers, this concentration occurs at fairly low values, v_2^* of the order of 0.01. Solutions are generally considered concentrated when $v_2 \geq 0.1$. For good solvents, c^* scales with $M^{-4/5}$ [3]. Other scaling laws for polymer systems can be found in Reference 3.

As discussed in Chapter 2, the ability of a solvent to dissolve a polymer will depend on the difference in their solubility parameters or on Flory's interaction parameter. The interaction parameter depends on temperature (see Equation 2.13), and therefore the swelling of a coil by a solvent will also depend on temperature.

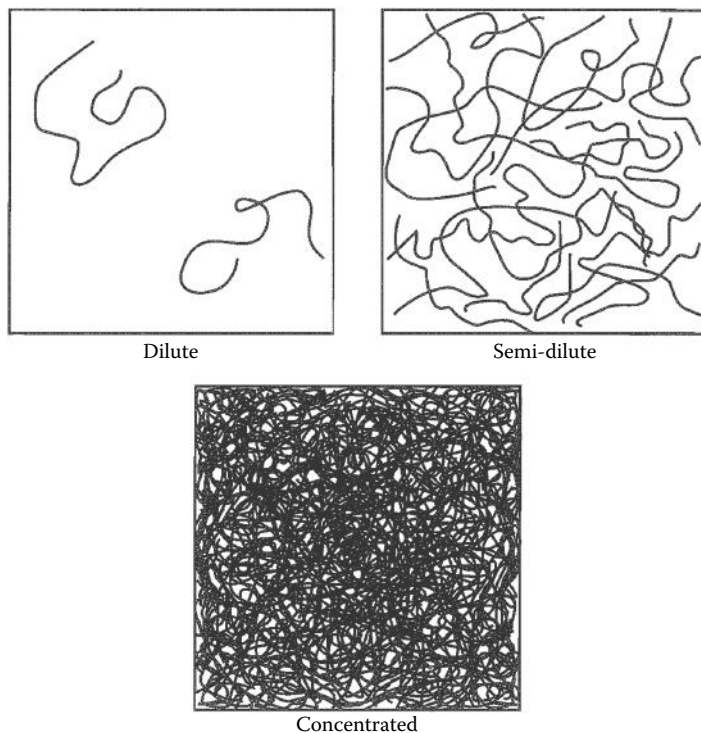


FIGURE 3.1 Illustrations of polymer chains in solutions at different concentrations.



FIGURE 3.2 Subdivision of a chain into blobs in semi-dilute solutions.

By varying the temperature, one changes the nature of the polymer–solvent interaction which can lead to precipitation (phase separation) of the polymer out of solution. Precipitation is a phase separation where one phase has a high polymer concentration (the precipitate) and the other phase (the supernatant) has a low polymer concentration.

3.3 PHASE SEPARATION IN POLYMER MIXTURES

The thermodynamic model of polymer binary solutions developed by Flory and presented in Chapter 2 predicts the coexistence of two phases (one rich in polymer and the other poor in polymer) when the temperature is lowered. **Equilibrium between the two phases** in a binary mixture requires that

$$\mu_1 - \mu_1^0 = \mu'_1 - \mu_1^0 \quad (3.4)$$

and

$$\mu_2 - \mu_2^0 = \mu'_2 - \mu_2^0 \quad (3.5)$$

where:

the primes indicate the chemical potentials in the second phase
the superscript 0 denotes the property of the pure compound

The chemical potentials of the pure compounds are constant at constant temperature and pressure and are subtracted for later convenience from μ_1 and μ_2 in Equations 3.4 and 3.5, respectively. To fulfill the requirements that the polymer concentration has two values for the same chemical potential indicating the coexistence of two phases, the chemical potentials μ_1 and μ_2 must pass through a minimum and a maximum between $v_2 = 0$ and $v_2 = 1$ as shown in Figure 3.3. The curves of different χ values plotted in Figure 3.3 are obtained from Flory's expression of the free energy of mixing (Equation 2.12) by differentiating this expression with respect to N_1 to obtain the following expression for $\mu_1 - \mu_1^0$:

$$\mu_1 - \mu_1^0 = \left(\frac{\partial \Delta G_m}{\partial N_1} \right)_{T,P} = RT \left\{ \ln(1 - v_2) + \left[1 - \left(\frac{1}{x} \right) \right] v_2 + \chi v_2^2 \right\} \quad (3.6)$$

and arbitrarily taking $x = 100$. Values of χ larger than χ_c will lead to the formation of two coexisting phases of different composition (see Equation 3.11). A complementary equation for $\mu_2 - \mu_2^0$ is obtained by differentiating ΔG_m with respect to N_2 :

$$\mu_2 - \mu_2^0 = \left(\frac{\partial \Delta G_m}{\partial N_2} \right)_{T,P} = RT \left[\ln v_2 - (x - 1) + (x - 1)v_2 + \chi x(1 - v_2)^2 \right] \quad (3.7)$$

For relatively small values of χ , $\mu_1 - \mu_1^0$ and $\mu_2 - \mu_2^0$ decrease monotonically with v_2 (Figure 3.3) and the polymer mixture remains in one phase. As χ increases, which can be achieved by decreasing the temperature, the same value of the chemical potential can be satisfied by three values of the polymer concentration (Figure 3.3). As in the case of the pressure–volume isotherm of the van der Waals equation of state, the intermediate region where the slope of the curve is positive represents unstable concentrations. We are then left with two stable polymer concentrations. The polymer concentrations at equilibrium must satisfy both Equations 3.4 and 3.5 and will be uniquely determined. Two polymer concentrations will then have the

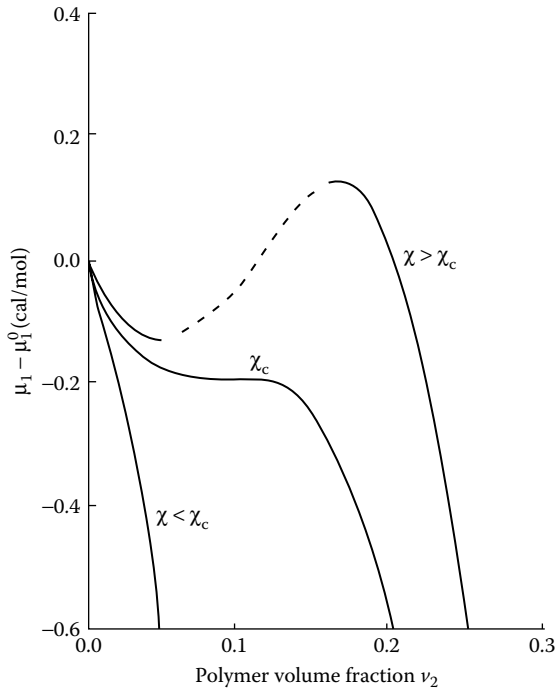


FIGURE 3.3 Plots of the chemical potential difference $\mu_1 - \mu_1^0$ as a function of polymer volume fraction for different values of χ . For $\chi < \chi_c$, this function is monotonically decreasing and the one-phase mixture is stable for all values of v_2 . For $\chi > \chi_c$, this function goes through a minimum and a maximum, and the mixture phase separates.

same chemical potentials for a given value of the temperature (or the interaction parameter). These concentrations define the **coexistence curve** or **binodal** in Figure 3.4. The **spinodal curve** in this figure represents the limits of stability given by the optima of the curves in Figure 3.3.

Above a certain temperature, the **upper critical solution temperature (UCST)**, the single-phase polymer solution is stable at all polymer concentrations. The critical point is reached when the optima of the chemical potential versus v_2 curve merges with the inflection point (represented by the curve χ_c in Figure 3.3). Mathematically, the critical conditions are given by

$$\left(\frac{\partial \mu_1}{\partial v_2} \right)_{T,P} = 0 \quad (3.8)$$

and

$$\left(\frac{\partial^2 \mu_1}{\partial v_2^2} \right)_{T,P} = 0 \quad (3.9)$$

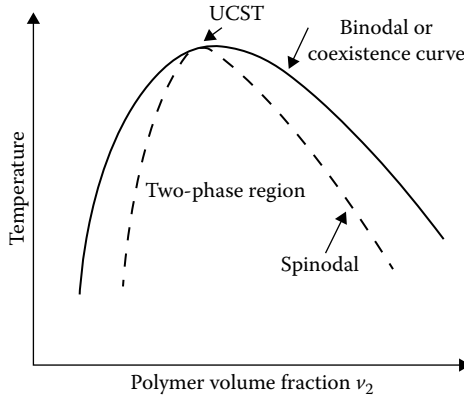


FIGURE 3.4 Schematic phase diagram for a binary polymer–solvent mixture showing a UCST.

Using Equation 3.6, the above criticality conditions yield two equations for the two unknown, $v_{2,c}$ and χ_c at the **critical point**. For large values of x , the results are

$$v_{2,c} = \frac{1}{1 + x^{1/2}} \quad (3.10)$$

and

$$\chi_c = \frac{1}{2} + \frac{1}{x^{1/2}} \quad (3.11)$$

Since $v_1 + v_2 = 1$, we also get

$$v_{1,c} = \frac{x^{1/2}}{1 + x^{1/2}} \quad (3.12)$$

The results of Flory's model are in qualitative agreement with experimental results. As the molecular weight of a polymer increases (i.e., as x increases), the value of the critical volume fraction $v_{2,c}$ moves closer to 0 and the value of χ_c approaches 0.5. Since the critical temperature increases as the molecular weight increases, the higher molecular weight samples are less soluble in a given solvent under similar conditions. Note that for the modest value of $x = 100$, $v_{2,c}$ is approximately 0.1 and χ_c is 0.6.

We saw in Section 2.5 that the thermodynamic approach used for polymer–solvent mixtures can be used for polymer blends (mixtures of two polymers). For simplicity, let us consider the case of two polymers that have the same molar volume. In the lattice model, this would correspond to chains with the same number of segments. The entropy per unit volume of the mixture given in Equation 2.4 can be written as

$$\frac{\Delta S_m}{NV_0} = -R \left(\frac{v_1}{V_1} \ln v_1 + \frac{v_2}{V_2} \ln v_2 \right) \quad (3.13)$$

where:

N and V_0 are the number of moles and molar volume of lattice sites, respectively

The entropy of mixing per mole of lattice site can then be expressed as

$$\frac{\Delta S_m}{N} = -R \left(\frac{v_1}{p} \ln v_1 + \frac{v_2}{p} \ln v_2 \right) \quad (3.14)$$

where:

$p = V_1/V_0 = V_2/V_0$ and represents the number of segments per molecule

The enthalpy of mixing given by Equation 2.9 can be written as

$$\frac{\Delta H_m}{N} = RT \left(\frac{\chi_H}{p} \right) v_1 v_2 = RT \chi v_1 v_2 \quad (3.15)$$

where:

χ now represents the polymer–polymer segmental interaction parameter

Combining Equations 3.14 and 3.15, we obtain for the free energy of mixing

$$\frac{\Delta G_m}{N} = RT \left(\frac{v_1}{p} \ln v_1 + \frac{v_2}{p} \ln v_2 + \chi v_1 v_2 \right) \quad (3.16)$$

To obtain the critical conditions for this case, we apply again Equations 3.8 and 3.9 and obtain after some algebra:

$$v_{1,c} = v_{2,c} = \frac{1}{2} \quad (3.17)$$

and

$$\chi_c = \frac{2}{p} \quad (3.18)$$

The result of Equation 3.17 is not surprising as we have taken the two polymers to have exactly the same size and thus would expect the coexistence curve to be symmetrical with respect to polymer concentration, unlike the polymer–solvent case (Equation 3.10) where $v_{2,c} \ll 1$. However, the result of Equation 3.18 is revealing as p is a large number and χ_c is approaching 0. Therefore, for two polymers to be **compatible** (i.e., form a homogeneous mixture), χ must be very small. As seen in Equation 3.14 and discussed in Section 2.4, the entropy of mixing two polymers is quite small (since p is large) and although it is positive, it cannot compensate in most cases for the enthalpy of mixing given in the free energy expression of the Flory model by $\chi v_1 v_2$. It was therefore thought for a long time that you could not mix two polymers into a homogeneous mixture. However, polymer binary systems with very small values of χ have been discovered and blends of some such polymers have been commercialized. An example of a homogeneous blend is that of PS and poly(phenylene oxide) (PPO) commercialized under the trade name of Noryl. The mixture possesses useful properties such as the lowering of the melt processability of PPO and the improvement on the mechanical properties of PS. It also turns out that for polymers that attract each other through hydrogen bonding or other types of secondary interactions, χ may be negative—contrary to the situation in regular solutions

given by Equation 2.10. The heat of mixing of these polymers is negative, guaranteeing a negative ΔG_m and insuring compatibility. The majority of commercial blends are however made from immiscible polymers with copolymers (compatibilizers) added in small amount to reduce the size of the phase-separated domains in the blend and improve processability and mechanical properties of the blend.

Some polymer mixtures de-mix (phase separate) as the temperature is increased contrary to the results of the Flory–Huggins model that predicts phase separation with decrease in temperature only. These mixtures are known to have a **lower critical solution temperature (LCST)**. Figure 3.5 shows experimental data for poly(*N*-isopropylacrylamide) (PIPPAm) in water with an LCST around 33°C below which the solution remains homogeneous and above which it phase separates. Several models have been developed to explain the existence of an LCST.

These models are based on the corresponding state theory, the free volume theory, or lattice models that include vacant sites to account for volume changes upon mixing [6,7]. The basic concept in all these models is that besides combinatorial entropy as calculated by Flory and Huggins, there is also noncombinatorial entropy from the packing of the molecules that leads to a volume change upon mixing. This noncombinatorial entropy, which in Section 2.5 was assumed for simplicity to be given by the constant β , has a temperature behavior opposite to that of the enthalpic interaction parameter. When the contribution of the noncombinatorial entropy is added to the enthalpic interaction parameter to correct for the overestimation of the Flory entropy expression, the resulting total interaction parameter goes through a minimum as a function of temperature as shown in Figure 3.6. This is because the enthalpic contribution dominates at low temperatures and the noncombinatorial entropy dominates at high temperatures. This temperature dependence of χ leads naturally to the prediction of both a UCST and

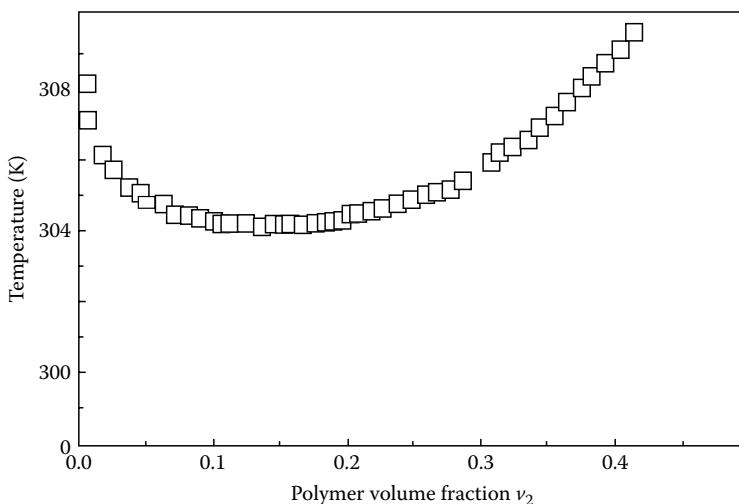


FIGURE 3.5 Phase diagram of poly(isopropylacrylamide) in water mixture at 1 atm showing an LCST. Above 304 K the system phase separates into two phases. (Reproduced with permission from Marchetti, M. et al., *Macromolecules*, 23, 1760, 1990. Copyright 1990 American Chemical Society.)

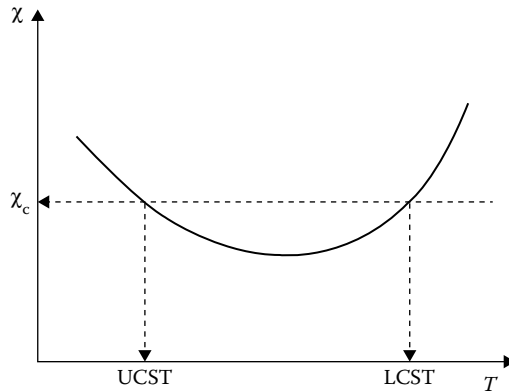


FIGURE 3.6 Illustration of the dependence of χ on temperature that leads to the existence of both a UCST and an LCST. For $\chi > \chi_c$, two phases coexist, but for $\chi < \chi_c$ (between UCST and LCST), there is no phase separation.

an LCST as illustrated in Figure 3.6. In most polymer–solvent systems, however, one observes one of these critical points only as the other one would be either at too high or at too low temperature for the solvent to remain in the liquid phase.

3.4 TRANSITIONS IN PURE POLYMERS

Depending on the temperature, the dynamics and conformations of polymer molecules—taken again for simplicity as long, regular chain consisting of a succession of single bonds—can be very different. Three states that are well recognized are as follows:

1. *The melt state.* At relatively high temperatures, free rotation around each bond allows the chain to assume an infinite number of conformations in space and the molecules are continuously changing their conformation and are able to translate (diffuse) in space. The higher the temperature, the more intense is the molecular motion.
2. *The glassy state.* At some sufficiently low temperatures, rotations around single bonds become impossible because of the energy barriers that a substituent on one chain atom encounters when trying to move past the substituent on an adjacent chain atom. Even hydrogen atoms on adjacent carbons interfere with one another at low enough temperatures. The polymer molecules become frozen in an entangled, disordered state.
3. *The crystalline state.* As described in Section 3.1, the chemical composition and configuration of a polymer may allow it to pack in a regular lattice and achieve a *long-range* order as the polymer is cooled from the **melt state**. Rotations around bonds are prevented by intermolecular interactions that lead to the formation of stable crystalline domains.

Factors that affect the physical state of a polymer or the temperature at which transitions occur are as follows:

1. The polymer chain may contain double or triple bonds or rings, which do not permit rotation at any temperature without actual bond breaking.
2. The polymer may be branched or cross-linked.
3. The polymer may be short or long.
4. The polymer may not be homogeneous; parts may be in various states.
5. The polymer may be dissolved in a lower molecular weight liquid or in another polymer.
6. A polymer that is stressed may be oriented and not completely isotropic in the melt. Rapid cooling of the melt may preserve the orientation even when the stress is removed.

Two major transition temperatures are the glass transition temperature (T_g) and the melting temperature (T_m). T_g is the temperature below which free rotations cease because of intramolecular energy barriers. Values of T_g most often listed for polymers correspond to the stiffening temperature. Simple bending of a rod might be the criterion. The timescale of the test is important. Even hindered rotation around single bonds may be sufficient to allow adjustment to new conformations over a long time. A plastic that is brittle when hit with a hammer may sag under its own weight over a period of weeks at the same temperature. It is a glass in the first test, but a melt (of sorts) in the second.

Although we have implied that the glassy state is homogeneous, the results of recent research indicate that most glass-forming materials, including polymers, may be fairly heterogeneous with domains on the order of 2–10 nm. NMR experiments and fluorescence probe diffusion measurements [8,9] have been interpreted in support of the existence of heterogeneities, but recent neutron scattering results have been interpreted in terms of either homogeneous structures [10] or inhomogeneous structures [11]. This is an area of ongoing research and is the subject of debates in the literature. A good review of the status of the field has been presented by Sillescu [12].

If the long polymer chains are interconnected by widely separated cross-links, the portions of chains between the cross-links can still assume the three states mentioned. In the case of melt state, a loosely cross-linked melt is called a **rubber**. The extent to which the original molecules can assume new conformations is limited because of the topological constraints of the cross-links. If the number of cross-links is increased, the portions of chains between cross-links become shorter. Finally, these sections of chains may be so short that rotations around single bonds and segmental diffusion are no longer possible and the system resembles a permanent glass even at temperatures at which an uncross-linked polymer would be a melt.

The difficulty of fitting an entire polymer into a lattice leads to a generalization that crystallinity is never perfect. In fact, many *crystalline* polymers may have amorphous contents of 20%–50%. This is many orders of magnitude greater than the imperfections associated with common metals. The amorphous portion may be glass, melt, or rubber, depending on the temperature, timescale of testing, or cross-linking.

Another conceptual difficulty that may arise concerns the previously discussed phenomenon of tacticity (Section 2.3). Free rotation around single bonds does not imply interchangeability of two substituents on a chain atom. Thus, an isotactic polymer (as in Figure 2.2) may undergo an infinite number of rotations around each of the bonds in the main chain. However, when the chain is once again put in the planar

zigzag form, all of the pendant groups will fall into exactly the same positions as they had before the rotations.

Before going on to discuss in greater detail the characteristics of these three basic states (glass, melt, and crystal), it might be well to describe some interrelations. Since no long-range molecular rearrangement is possible below T_g , it follows that if crystals are to form, crystallization will have to take place above that temperature. The highest temperature at which a crystal lattice is stable is the melting temperature (T_m). If no crystal lattice is stable, or if the material is quenched from the melt to a temperature well below T_g , behavior of the sort indicated by line $A-B$ (Figure 3.7) is possible.

Ordinary atactic PS and PMMA are two polymers that do not form crystals and, on cooling below their T_g 's (both about 100°C), go directly from an easily deformed melt to a rigid, transparent, amorphous glass. Common nylon (nylon 6,6) quenched to room temperature might follow the same path. However, if nylon is cooled at a constant rate (say, 1°C/s) from the melt, it might follow path $A-C$. Some crystals form when the temperature falls below T_m . At a temperature below T_g , the crystals that form are surrounded by a matrix of amorphous glass. If the glass is the major constituent, the material may be quite brittle. When polyethylene is cooled to room temperature, it remains well above its T_g . As indicated by line $A-D$, the polymer may be highly crystalline with amorphous melt outside the crystalline regions. In response to a stress, the amorphous parts are rather easily deformed. Of course, above T_m , there are no crystals.

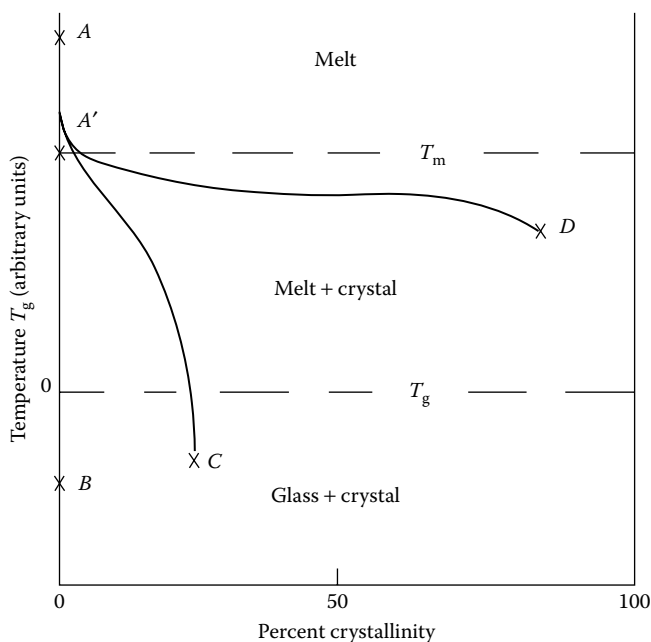


FIGURE 3.7 Examples of cooling from the melt. Point A : All curves go through A' on cooling. Point B : Room-temperature state of PS cooled at any rate from the melt and also typical state of nylon 6,6 that has been quenched from the melt to a temperature below T_g . Point C : Typical final state of nylon 6,6 cooled at 1°C/s to a temperature below its T_g . Point D : Linear polyethylene cooled to room temperature (which is well above its T_g).

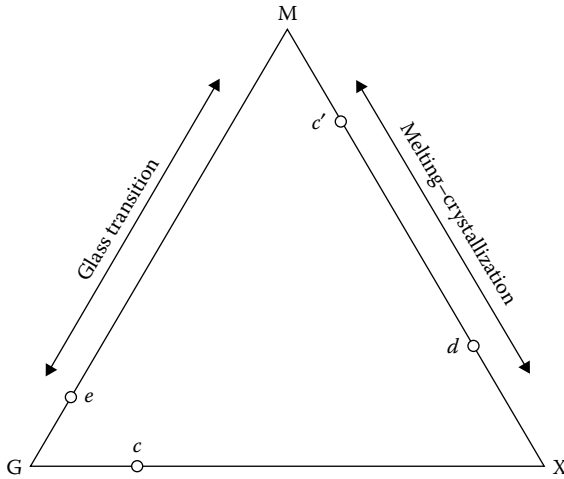


FIGURE 3.8 Composition diagram. Point c corresponds to C of Figure 3.7 and d to D . Composition c or c' may be rubbery even in the absence of covalent cross-links. Point e is possible only when two portions of the same molecule have separate values of T_g . G, glass; M, melt or rubber; X, crystal.

Figure 3.8 is another attempt to interrelate the various physical states. Compositions C and D are near points c and d , respectively, in Figure 3.8. It is possible to have a melt with low crystallinity (point c'). If the crystals are large enough and strong enough to act as massive cross-links connecting high-molecular segments, the melt will act like a rubber as long as the temperature is between T_g and T_m . Recently developed thermoplastic elastomers of polypropylene synthesized with metallocene catalysts are examples of such materials. The crystallinity arises from portions of the chains that have isotactic configurations. A composition in which parts of molecules can be glassy whereas other parts remain in the melt (point e) is achieved by the technique of block copolymerization (Section 4.9). Once again, rubbery behavior is attainable if the glassy domains act as cross-links. Such a polymer is really two homopolymers tied together, each exhibiting its own T_g . Because they are tied together, they cannot segregate macroscopically, but can only do so on a microscopic basis. The thermoplastic elastomer based on styrene and butadiene is one commercial example of a system with two T_g 's: one below room temperature and the other above (see Section 4.5).

3.5 AMORPHOUS POLYMERS

An amorphous polymer is easy to imagine. A bowl of spaghetti is a fair analogy. A bucket of long worms or snakes is even better, because polymer molecules are constantly in motion. To be analogous to some common polymers, the worms would have to be 10^3 – 10^4 times longer than they are thick (i.e., 5 mm diameter, 10 m long!). Obviously, the constant motion one notes in the bucket is not of whole worms at once, but of individual segments. The analogous **segmental Brownian motion** in polymers is very important in explaining flow and deformation. As mentioned in Section 3.4, the segments themselves move by virtue of rotations around single bonds in the main chain

of the polymer. The intensity of the motion increases with temperature. Below a certain temperature (T_g), the polymer segments do not have sufficient energy to move past one another. Rotations around single bonds become very difficult. If the material is stressed, the only reversible response can be for bond angles and distances to be strained, since no gross movements of segments can take place. Such a material is a **glass**. Only if the temperature is above T_g the segments can rearrange to relieve an externally applied stress. This important parameter, T_g , can be characterized also as an inflection point in the specific volume–temperature curve (Figure 3.9). The **glass transition temperature** T_g resembles a second-order transition, because the change in volume is not discontinuous as it is with T_m . The abruptness of the transition can be rationalized by the concept of free volume (see Section 3.6). The segmental energy has to exceed a certain barrier value before a *hole* of segmental dimensions can be created for diffusion.

It has long been believed that the glass transition is not a thermodynamic transition but simply a kinetic effect caused by our inability to make measurements under infinitesimally small cooling rates. Kauzmann pointed out [14] that based on the extrapolated data of several glass-forming liquids, the entropy of such supercooled liquids will drop below the values of their corresponding crystals. This is, of course, unphysical and is known as the Kauzmann paradox. Gibbs and DiMarzio [15] put forward a statistical thermodynamic model that explains the existence and some of the characteristics of the glass transition. These authors evaluate the conformational entropy of chains placed on a lattice with vacancies; as the temperature is decreased, the density of the system increases and the conformational entropy decreases until it reaches 0 (i.e., the conformation of the chains is frozen). The temperature at which this occurs is denoted by T_2 that turns out to have the same dependence on molecular weight as the experimental T_g . Although the theoretical T_2 is a second-order

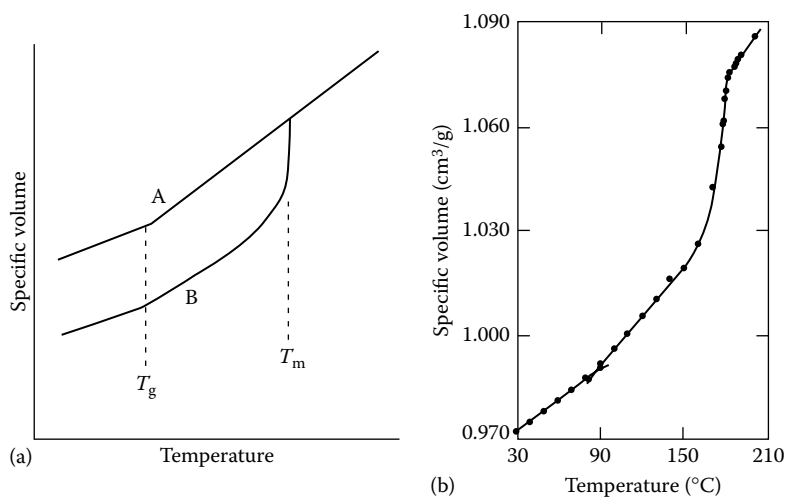


FIGURE 3.9 (a) Specific volume versus temperature for A, an amorphous polymer, and B, a partly crystalline polymer. (b) Volume–temperature curve for pure poly(*N,N'*-sebacoyl piperazine), for which T_g is 82°C and T_m is 180°C–181°C. (Data from Flory, P. J., and H. K. Hall, *J. Am. Chem. Soc.*, 73, 2532, 1951.)

transition temperature and obeys the thermodynamic interrelations among changes in heat capacity, expansion coefficient, and compressibility, T_g does not obey these interrelations [16]. In summary, the model implies that some of the material properties mimic at T_g what happen theoretically at T_2 if it was possible to cool the liquid infinitely slowly, that is, avoids freezing in a nonequilibrium state.

Experimentally, T_g itself depends on the timescale of the experiment in which it is measured. As pointed out by Bueche [17], a 100-fold increase in heating rate when volume change is being measured increases the apparent T_g of PS only about 5°C. Molecular weight affects T_g also. Theoretical equations of some complexity have been proposed [18]. An empirical correlation can be obtained in the form

$$T_g = T_{g,\infty} - \frac{K_g}{M_n} \quad (3.19)$$

where:

T_g for a finite molecular weight M is related to that for an infinitely long polymer, $T_{g,\infty}$. For example, the data of Beevers and White [18] for PMMA can be fitted by $K_g = 2.1 \times 10^5 \text{C}\cdot\text{mol/g}$ and $T_{g,\infty} = 114^\circ\text{C}$ when M_n exceeds 10^4 . Likewise, PS data are fitted by $K_g = 1.7 \times 10^5 \text{C}\cdot\text{mol/g}$ and $T_{g,\infty} = 100^\circ\text{C}$ down to molecular weights of less than 3×10^3 [17]. In both cases the maximum difference in T_g due to differences in M_n are small above $M_n = 5 \times 10^4$.

If we store energy in an amorphous polymer by stressing it and then attempt to recover the work we put in, there is always a certain amount of mechanical energy loss. This loss may be small above or below T_g , but it is always a maximum at T_g . In fact, this often is a more sensitive measurement of T_g than volume change on heating. The rationalization is not difficult. In the glass the stress is stored by bond distortions, which are easily recovered. Above T_g , polymer chains can be uncoiled readily from their random conformation by rotations about successive single bonds. Only at T_g is the uncoiling hindered by intermolecular forces. The discussion of deformation and flow of amorphous polymers is continued in Chapters 7 through 9.

Segmental mobility is highly dependent on chain stiffness and somewhat dependent on intermolecular forces. It is expected that polymers with high polarity or high cohesive energy density should have higher transition temperatures than nonpolar materials. This is borne out approximately in Table 3.1. However, regularity, which is so important to crystallizability, counts for little in the amorphous transition. Since the segmental motion implies the concerted movement of many chain atoms (10–50 atoms), bulky side groups, which hinder rotation about single bonds, should also raise T_g . An interesting series in this respect is afforded by the vinyl ether polymers. As the polar ether linkage is diluted by longer alkyl side groups from methyl to butyl, T_g decreases. However, when the alkyl group is bunched up next to the chain, as with *tert-butyl* ether, rotation about the single bonds in the chain is made difficult and T_g is raised dramatically. Chain stiffness and, consequently, T_g are increased if single bonds in the polymer chain are replaced by multiple bonds about which there can be no rotation. Ring structures in the main chain contribute inflexibility as

TABLE 3.1
Transition Temperatures for Selected Polymers

Monomer Unit	T_g (°C)	T_m (°C)	Total Solubility Parameter [(MPa) ^{1/2}]
Ethylene (linear)	-125	141	16.2
Propylene			
(isotactic)	-7	187	-
(syndiotactic)	-9	150	-
(atactic)	-10	-	-
Butene-1 (isotactic)	-24	140	-
Isobutylene	-73	-	15.5
4-Methylpentene-1 (isotactic)	30	166	-
Styrene			
(isotactic)	100	240	-
(syndiotactic)	-	270	-
(atactic)	100	-	22.5
α -Methyl styrene	130	-	-
Butadiene			
(1,4 polymer) (<i>cis</i>)	-102	12	-
(1,4 polymer) (<i>trans</i>)	-50	142	-
Isoprene			
(1,4-polymer) (<i>cis</i>)	-70	39	167
(1,4-polymer) (<i>trans</i>)	-50	80	-
Acrylonitrile	125	-	-
Chloroprene (1,4 polymer)	-50	80	18.8
Vinyl chloride (syndiotactic)	81/98	273	21.5
Vinyl acetate	32	-	19.2
Vinylidene chloride	-18	190	-
Vinyl alcohol	85	265	-
Vinyl methyl ether	-31	144	-
Vinyl ethyl ether	-43	86	-
Vinyl <i>n</i> -butyl ether	-55	64	-
Vinyl <i>iso</i> -butyl ether	-20	115	-
Methyl methacrylate	105	-	18.6
Ethyl acrylate	-24	-	-
Acrylic acid	106	-	-
Vinyl fluoride	41	200	-
Vinylidene fluoride	-40	171	-
Chlorotrifluoroethylene	100	220	-
Tetrafluoroethylene	117	330	-

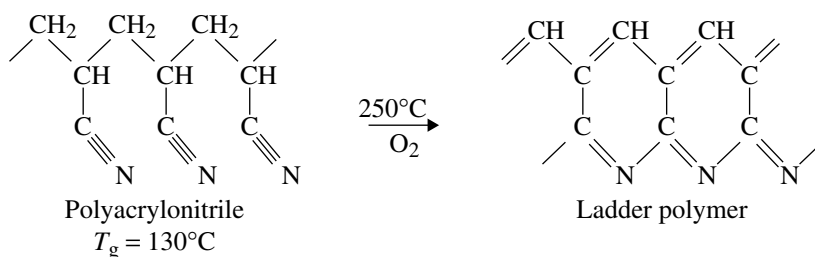
(Continued)

TABLE 3.1
(Continued) Transition Temperatures for Selected Polymers

Monomer Unit	T_g (°C)	T_m (°C)	Total Solubility Parameter [(MPa) ^{1/2}]
Ethylene terephthalate	60/85	280	21.5
Caprolactone	-60	64	-
Ethylene oxide	-41	69	-
1,2-Propylene oxide	-72	-	-
1,3-Propylene oxide	-78	75	-
Formaldehyde (osymethylene)	-82	184	-
Acetaldehyde (isotactic)	-30	165	-
Tetramethylene oxide	-84	57	-
Phenylene sulfide	97	-	-
Cellulose tributyrate	115	-	-
Ethyl cellulose	43	-	21.1
Nylon 6	50/100	270	-
Nylon 6,6	50	280	-
Dimethyl siloxane	-127	-54	14.9

Source: Runt, J. P., *Encycl. Polym. Sci. Tech.*, 4, 487, 1986; Brandrup, J., and Immergut, F. H. (eds.), *Polymer Handbook*, 3rd edn., Wiley, New York, 1989; Lewis, O. G., *Physical Constants of Linear Homopolymers*, Springer-Verlag, New York, 1968.

in poly(ethylene terephthalate) (PET) or cellulose derivatives. **Ladder polymers** have been synthesized in which there are no single bonds in the polymer chain. For example, pyrolysis of polyacrylonitrile gives an aromatic structure of high thermal stability:



This particular material is so stable that it can be held directly in a flame in the form of woven cloth and not be changed physically or chemically [22]. When polyacrylonitrile is used as the precursor for carbon fibers, the ladder structure is often an intermediate [23]. The ladder polymer is subjected to carbonization (graphitization) typically at 1200°C–1400°C under nitrogen followed by additional heat treatment and special surface oxidation to improve adhesion. The carbon fibers so produced have stiffness moduli as high as 500 GPa (about 75×10^6 psi) and are widely used in high-performance composites.

For a copolymer in which the monomer units are distributed in a random fashion, polarity and chain stiffness of the copolymer are roughly the averages of those for the individual homopolymers. Various thermodynamic approaches suggest rules for predicting the glass transition temperature of a copolymer in terms of the weight fraction of each monomer and the T_g of each homopolymer. However, the following empirical equation due to Gordon and Taylor [24] is widely used:

$$T_g(\text{copolymer}) = \frac{w_1(T_g)_1 + kw_2(T_g)_2}{w_1 + kw_2} \quad (3.20)$$

where:

k is a fitted constant [20]

When $k = 1$, a linear relationship results. When $k = (T_g)_1/(T_g)_2$ (using absolute temperatures), a reciprocal relationship will be derived:

$$\frac{1}{T_g(\text{copolymer})} = \frac{w_1}{(T_g)_1} + \frac{w_2}{(T_g)_2} \quad (3.21)$$

The relationship can be extended to systems with more than two monomers by adding another constant for each additional monomer.

Example 3.1

Monomers A and B are copolymerized with the following results:

Weight Fraction A in Polymer	T_g (°C)
1.000	108.0
0.850	75.0
0.260	28.0

What value of k fits these data to Equation 3.20? If A forms a copolymer with equal weights of A and C, and the same k applies, what T_g can be expected? The T_g of C is -37.0°C .

Solution: Substituting in Equation 3.20 and solving for $k(T_g)_B$,

$$75.0 = \frac{0.850(108.0) + 0.150k(T_g)_B}{0.850 + 0.150k}$$

$$28.0 = \frac{0.260(108.0) + 0.740k(T_g)_B}{0.260 + 0.740k}$$

$$k(T_g)_B = \frac{75.0(0.850 + 0.150k) - [0.850(108.0)]}{0.150} \text{ etc.}$$

$$k(T_g)_B = 75.0k - 187 = 28.0k - 31$$

so

$$k = 3.32 \text{ and } (T_g)_B = 18.7^\circ\text{C}$$

Then

$$(T_g)_{\text{new}} = \frac{0.500 (108.0) + 0.500 (3.32) (-37.0)}{0.500 + 0.500 (3.32)} = -3.4^\circ\text{C}$$

3.6 PLASTICIZATION

The glass transition temperature marks the onset of segmental mobility for a polymer. In the **free volume** approach, one pictures the movement of the segments due to a concentration gradient (diffusion) or due to a stress (viscous flow) as a jumping phenomenon. A segment moves or diffuses in a concerted manner into a vacancy or hole adjacent to it, leaving a hole of dimensions behind. We know that the specific volume of a polymer increases as the temperature increases, as shown by the normal coefficient of expansion. However, the increase in volume is not uniform, and the local density on a molecular scale fluctuates to give an overall population of holes or *free volume*. As mentioned in Section 3.5, one experimental method of determining T_g is to note the temperature at which the coefficient of expansion changes. This greater increase in volume with temperature above T_g represents the addition of free volume for segmental movement. In Section 7.6, a quantitative measure of free volume is given in the form of the Williams, Landel, and Ferry (WLF) equation. It turns out that the WLF equation can also be derived from Gibbs and DiMarzio entropy model [25].

If we mix two materials of different T_g 's, we can imagine that each would contribute to the free volume of the system in proportion to the amount of material present. In this way we can rationalize that T_g should be a linear function of composition for copolymers. Likewise, if we mix a polymer with a solvent or another compatible polymer, we expect a T_g that is the weighted average of each component (Equation 3.20 or 3.21). An important application of this principle is in **plasticization**. A plasticizer is a nonvolatile solvent that usually remains in the system in its ultimate use. Since solvent and polymer are not chemically bound to one another, the term *external plasticizer* is sometimes used to distinguish this case from copolymerization, where a comonomer of low T_g may be used to lower the T_g of the system (so-called internal plasticization). Poly(vinyl chloride) (PVC) is very versatile because it is compatible with a variety of plasticizers and because the plasticized polymer remains quite stable both physically and chemically for long periods of time. The dependence of T_g on composition for several plasticizers is indicated by the behavior of the **flex temperature**, which is close to T_g , for amorphous polymer (Figure 3.10). The efficiency in lowering T_g is not the only criterion for selecting a plasticizer. Cost, odor, biodegradability, high-temperature stability, and resistance to migration may be important in specific applications. Since stiffness of a polymer at temperature T decreases as

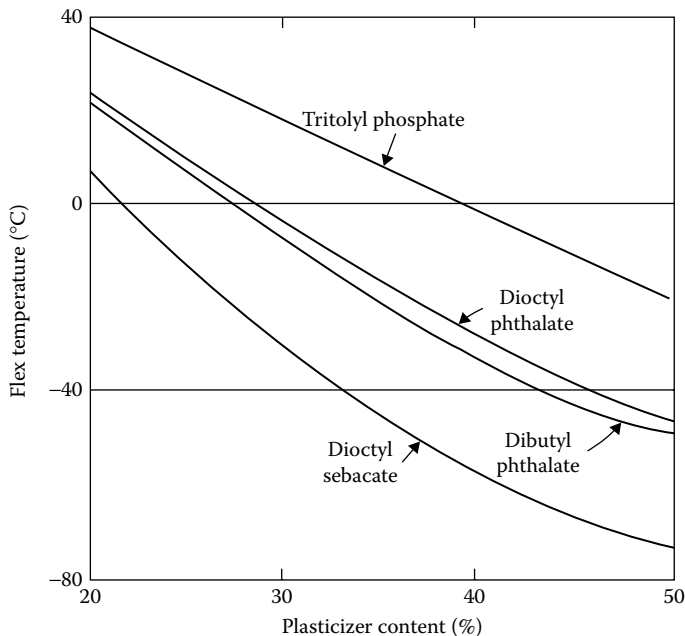


FIGURE 3.10 Effect of plasticizers on cold flex temperature of PVC compounds. The temperature is that at which torsional stiffness reaches some arbitrary value. (Data from Lannon, D. A., and E. I. Hoskins, chap. 7 in P. D. Ritchie, ed., *Physics of Plastics*, Van Nostrand, Princeton, NJ, 1965.)

$T - T_g$ increases, plasticization efficiency may also be judged by the lowering of the stiffness modulus at room temperature (Figure 3.11).

Many commercial fibers are plasticized by small amounts of water. The familiar process of ironing a garment generally takes place between T_g and T_m so that creases can be controlled without destroying the overall structure due to crystallinity. In steam ironing, moisture lowers T_g allowing a lower ironing temperature.

Another property that changes at the glass transition is the specific heat. The technique of differential scanning calorimetry (DSC) is often used to measure transitions (see Section 18.3). The method is convenient since it makes use of small samples and is an automated procedure. Using the method of DSC, the temperature range over which the transition occurs can be measured. Paul and coworkers [27] have observed that miscible polymer blends may be characterized by narrow or broad transitions. A broad transition does not mean that there is thermodynamic phase segregation but that there are large composition fluctuations in addition to the usual fluctuations in density in pure components. Thus, blends that are compatible in that only one glass transition is observed and which are transparent in both glassy and melt states may vary in the affinity of the components for each other without leading to phase separation. Most miscible polymer blends exhibit an LCST and phase separate on heating. The reason is that since the enthalpic contribution to the interaction parameter of blends is small for miscibility to occur, the total interaction parameter is dominated

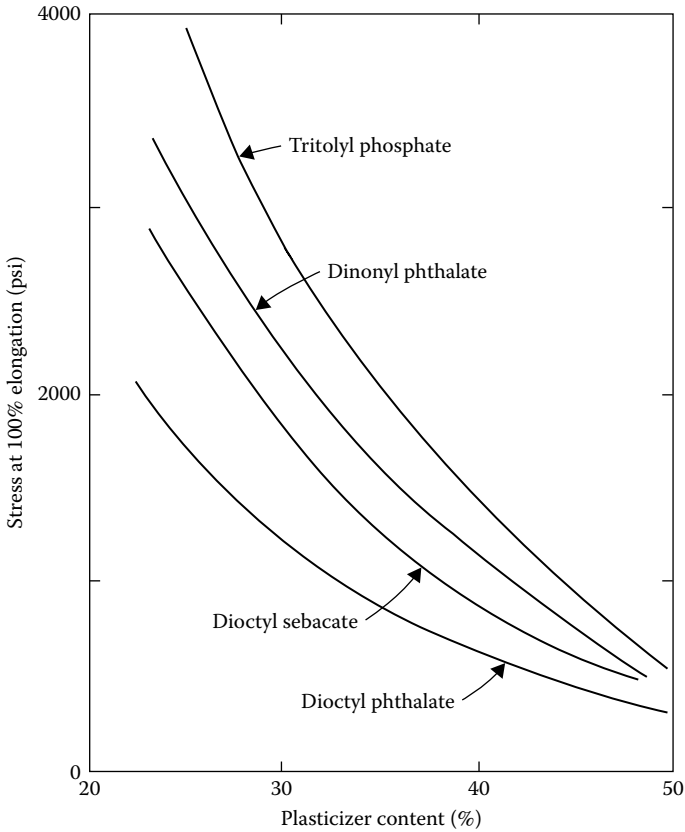


FIGURE 3.11 Effect of plasticizers on 100% modulus (stress at 100% elongation) of PVC compounds. (Data from Lannon, D. A., and E. I. Hoskins, chap. 7 in P. D. Ritchie, ed., *Physics of Plastics*, Van Nostrand, Princeton, NJ, 1965.)

by the noncombinatorial entropic contribution that increases χ as the temperature increases (see Section 3.3 and Figure 3.6). As an example, a mixture with equal weights of PMMA and poly(epichlorohydrin) is miscible at room temperature but becomes cloudy (indicating phase separation) at about 250°C [27].

3.7 CRYSTALLINITY

Polymers in the solid state can be completely amorphous, partially crystalline, or almost completely crystalline. Polymer crystals have the requirement that they must accommodate the covalent axis within an ordered structure. For some time the interpretation of X-ray diffraction patterns was that individual polymer molecules were partly crystalline and partly amorphous. The longest dimension of the **crystallites** in polycrystalline materials is usually about 5–50 nm, which is a small fraction of the length of a fully extended polymer molecule. A graphical representation of this once popular model is shown in Figure 3.12. Here a long polymer chain wanders

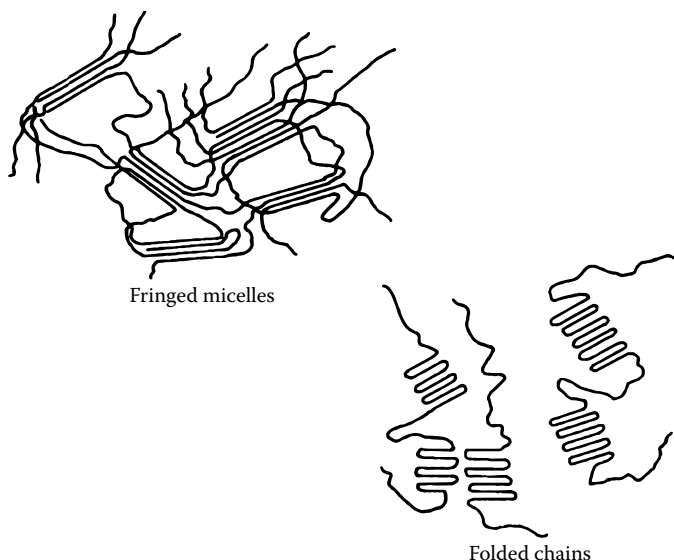


FIGURE 3.12 Crystallite arrangements.

successively through disordered, random regions, and through bundles of organized regions (micelles) of successively amorphous and ordered structures. For a polymer that can be extended to a length of 5000 nm with crystal and amorphous domains averaging 10 nm, a single polymer thread might tie together a hundred or more crystallites. Although this **fringed micelle** model may be adequate in some ways for samples crystallized rapidly from the melt, it is inadequate for samples crystallized slowly from melts or solutions. In these cases, density arguments, as well as X-ray and NMR evidence, indicate that the chains fold on themselves with amorphous regions consisting of relatively tight folds. Such chain folding is clearly seen in single crystals.

For many years the statement could be made that all polymer crystals were sub-microscopic. However, Till [28] and Keller [29] in 1957 produced single crystals of polyethylene up to 10 μm in one dimension. Subsequently, single crystals of many other polymers were obtained. A surprising feature of most of these crystals is that the covalent axis of the polymer chains is perpendicular to the longer dimensions of the crystals (Figure 3.13). The explanation is that the polymer folds over on itself after about a hundred chain atoms have entered the lattice. The crystal thickness increases with the temperature of crystal formation or with subsequent annealing at a higher temperature. A polyethylene crystal with a thickness of 10 nm may be formed at 100°C. Heating the crystal at 130°C for several hours will increase the thickness to about 40 nm.

Both thermodynamic and kinetic arguments have been propounded to explain the spontaneous formation of the folded-chain structure [30]. The kinetic theory currently favored by some workers views the folding as a means of increasing the crystallization rate, even though crystals with completely extended chains might be more stable under equilibrium conditions. Indeed, polyethylene samples with molecular weights of less than 10,000 exhibit crystal thicknesses approximating the length of extended

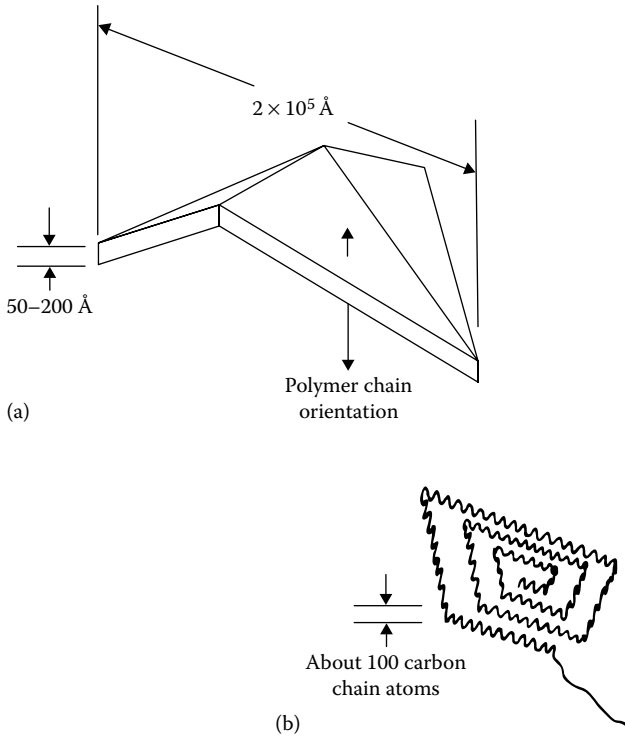


FIGURE 3.13 (a) A large single crystal of polyethylene might have the dimensions indicated here. (b) The growth mechanism involves the folding over of the planar zigzag chain on itself at intervals of about every 100 chain atoms. A single crystal may contain many individual molecules.

chains [31]. The four-sided hollow pyramidal crystal is only one form found for polyethylene. Ridged crystals, truncated pyramids, and fibrillar forms are also known. Other materials show other features. Poly(oxyethylene) gives flat hexagonal crystals and polypropylene gives lath-like crystals. Polypropylene is an example where the folded chains are not derived from planar zigzag ribbons but from helices (see Section 3.8). The single-crystal evidence showing folded-chain structures for a variety of polymers leads one to think that the same structures also occur in polycrystalline materials.

The mechanical properties of crystalline materials can be viewed from two extreme positions. Materials of low crystallinity may be pictured as essentially amorphous polymers with the crystallites acting as massive cross-links, about 5–50 nm in diameter. The cross-links restrain the movement of the amorphous network just as covalent cross-links would. However, unlike the covalent bonds, the crystal cross-links can be melted or mechanically stressed beyond a rather low yield point. At the opposite end of the crystallinity spectrum, one can regard a highly crystalline material as a pure crystal that contains numerous defects such as chain ends, branches, folds, and foreign impurities. Mechanical failure of highly crystalline nylon, for example, bears a great resemblance to that of some metals, with deformation bands rather than the ragged failure typical of amorphous polymers.

X-ray and electron diffraction studies of unoriented polymers allow the calculation of some interplanar distances in the crystalline domains. Diffraction by oriented fibers gives more information, since the axis of the fiber usually parallels one of the crystallographic axes. Both the conformation of single chains and the arrangement of the chains in the crystal lattice can be deduced, although the methods of analysis are neither simple nor unambiguous.

3.8 CONFORMATION OF SINGLE CHAINS IN CRYSTALS

The planar zigzag conformation has been used to illustrate tacticity (Section 2.3). Some polymers assume this conformation in the crystal, for example, polyethylene and 1,4-(*cis*-polybutadiene). Isotactic polymers in which the pendant group is bulky often assume a **helical conformation** [32]. Polypropylene forms an $H,3_1$ helix, that is, a helix in which three monomer units give one complete turn (Figure 3.14). This simple helix can be generated by imagining the successive bonds being wrapped around a triangular mandrel, every other bond lying on a face and the alternating bonds lying on an edge. As seen in an end view (Figure 3.14), the pendant methyl groups form a second triangular prism that contains the smaller one. Helices with more than three repeat units per turn are common. The α -helix assumed by many polymers of amino acids has about 18 units per five turns. This helical form of the single molecule may persist even in solution.

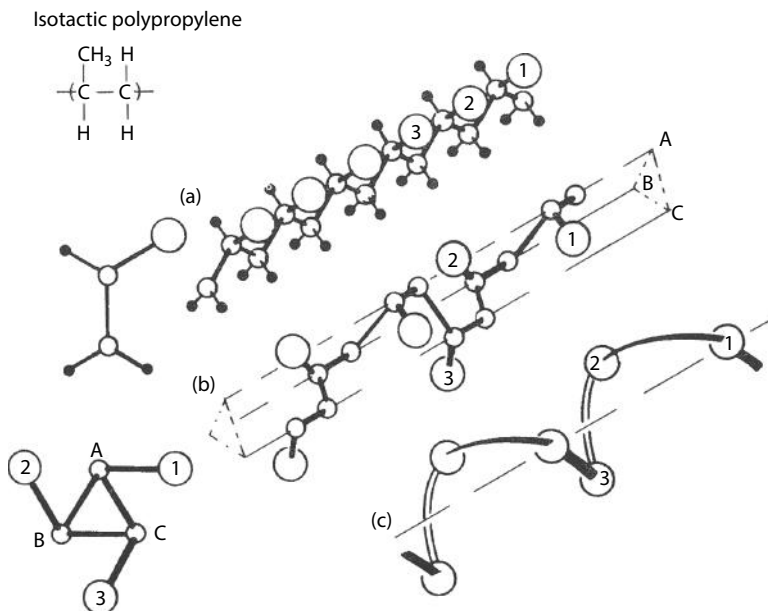


FIGURE 3.14 (a) Isotactic polypropylene. The large spheres represent the pendant methyl groups. (b) The $H,3_1$ helix with hydrogens omitted. (c) The pendant methyl groups as a helix. (Data from Rodriguez, F., *J. Chem. Educ.*, 45, 507, 1968.)

Other helices are favored by syndiotactic polymers and some symmetrically substituted materials. A helix designated as $H_{2,1}$ can be generated by wrapping a chain around a mandrel with a square cross section. It must be emphasized that only single-bond rotations and not bond bending or stretching are involved in achieving these conformations. Specific interactions between pendant groups, such as hydrogen bonding in polymers of amino acids, or specific hindrances, such as repulsion between adjacent pendant methyl groups, often dictate the conformation with the most favorable free energy.

The fitting together of the chains in a lattice can take many forms. The **unit cell** of polyethylene (planar zigzag chains) is shown in Figure 3.15. With some polymers, especially atactic, polar ones, crystallites may be formed that are lamellar. For example, they may have a helical form as individual chains and pack into a lattice in one direction, but not have a well-defined periodicity in the third dimension.

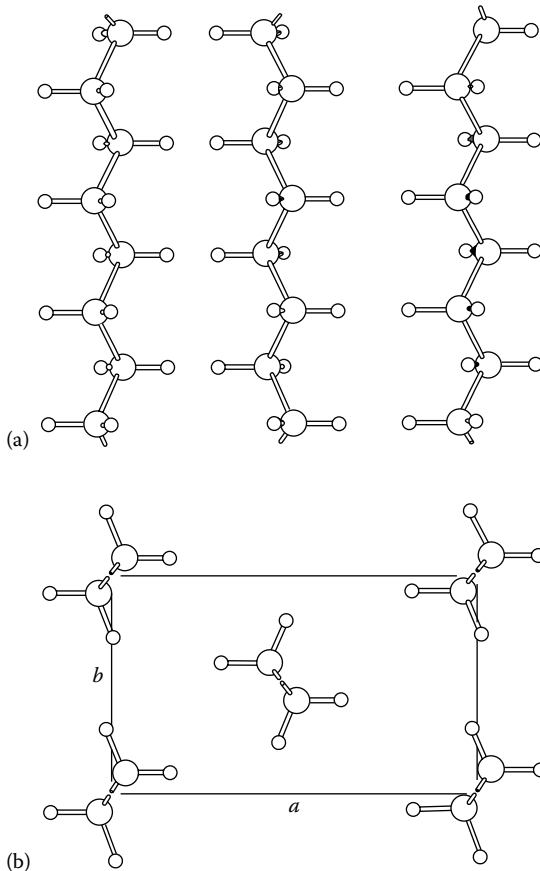


FIGURE 3.15 (a) Side view and (b) top view of the three-dimensional lattice model of the packing in the crystal structure of polyethylene in which $a = 7.4 \text{ \AA}$, $b = 4.94 \text{ \AA}$, and successive pendant atoms are 2.55 \AA apart along the chain axis. (Data from Natta, G., and P. Corradini, *Rubber Chem. Technol.*, 33, 703, 1960.)

3.9 SPHERULITES AND DRAWING

Quiescent crystallization of a polymer from the melt or solution often results in a peculiar form of crystalline growth with a preferred chain orientation relative to a center (nucleus). For example, cooling poly(ethylene oxide) in a thin film results in the growth of circular areas emanating from nuclei, the growth stopping only when advancing fronts meet. When completely cooled, the areas may be as large as a centimeter in diameter (Figure 3.16). Polarized light reveals that the polymer chains are oriented tangentially around each nucleus despite the fact that the domain (a **spherulite**, since it extends in three dimensions) consists of a multitude of crystallites and is not a single crystal. In most materials the **spherulites** do not exceed 100 μm in diameter.

When a highly crystalline material is stressed, a certain amount of energy can be stored by bond bending and stretching and other lattice distortions. Beyond the elastic limit (usually at a low elongation), rearrangement of the polymer chains often takes place so that chains are oriented in the direction of stress. This destroys the spherulitic pattern if it exists. This process of orientation by stretching (**drawing**) is used for most textile fibers (nylon, rayon, polyacrylonitrile). The oriented crystalline structure gives high strength and low elongation in the direction of the fiber axis. Drawing of crystalline materials often has another unusual feature, **necking**. If a sample of spherulitic nylon is stretched, elongation does not occur uniformly over the whole sample as it does when a rubber band is stretched. After a slight overall elongation (about 5%), a neck appears (Figure 3.17) and grows if stretching is continued.

Spherulites at the shoulder are pulled apart, and polymer chains are oriented in the direction of stress as they enter the neck. The orientation is permanent, since the new crystalline form is stable. Thus, it is not inconsistent that molded (spherulitic) nylon may be listed as having an elongation at break of about 300%, whereas drawn



FIGURE 3.16 Spherulitic structure of poly(ethylene oxide) seen between crossed polarizing sheets.

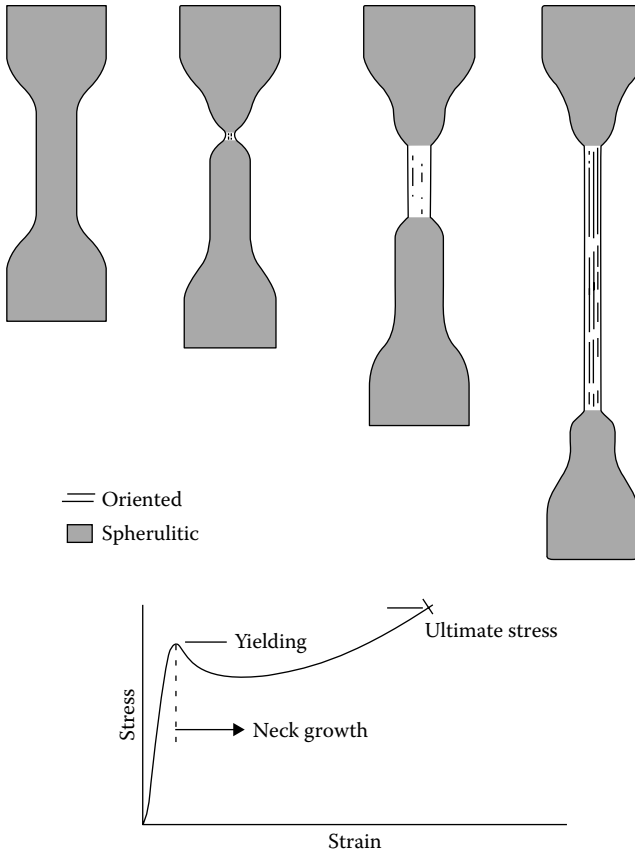


FIGURE 3.17 Successive stages in the drawing (elongation) of a spherulitic polymer.

nylon fibers (oriented) have an ultimate elongation of only 20%. However, in drawn polyethylene, folded chains persist in oriented crystallites with tie molecules connecting the folded chain packets (Figure 3.18).

The process just described involves going from random crystallites (short-range order and long-range disorder) to oriented crystallites (short- and long-range order). There are numerous polymers, which, although amorphous in the unstressed state, on uniaxial stretching exhibit sharp X-ray patterns characteristic of oriented crystals. Usually the pattern disappears on release of the stress as the polymer goes back to the amorphous state. Characteristic repeat distances from X-ray patterns of these and stable crystalline materials allow estimation of unit cell dimensions, the crystal system, and also the ultimate density of perfectly crystalline material.

The organization of the crystals in a spherulite has been investigated for numerous materials. For example, single crystals have been observed to grow faster in one direction than another with branching so as to assume a sheaflike appearance and ultimately to form the nucleus of a spherulite [30]. The individual arms of the spherulite

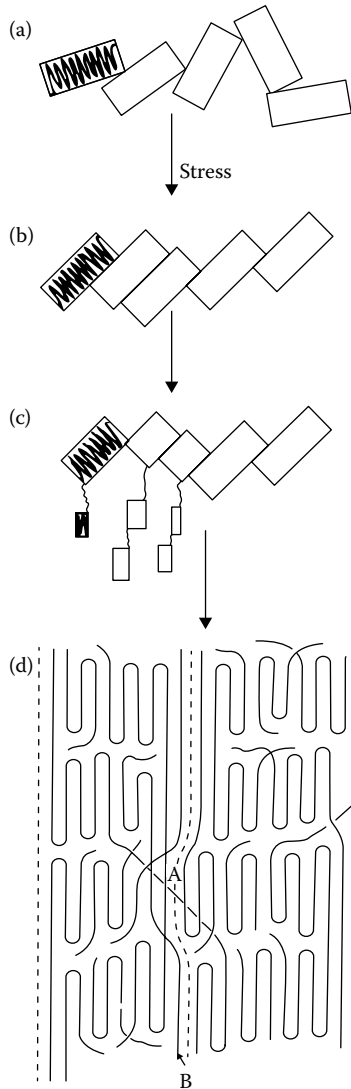


FIGURE 3.18 The drawing process. (a) Twisted crystal lamellae that make up the spherulitic structure are pulled into (b) tilted pre-deformed lamellae during the pre-necking period. (c) The tilted lamellae are torn into blocks and tie molecules that make up the microfibrils (d) with interfibrillar A and intrafibrillar B tie molecules in the fully drawn state as proposed by Peterlin for polyethylene. (Data from Peterlin, A., *Text. Res. J.*, 42, 20, 1972; Perkins, W. G., and R. S. Porter, *J. Mater. Sci.*, 12, 2355, 1977.)

may have twists that lead to concentric rings or bands (Figure 3.19). More commonly the nucleus of a spherulite is a solid impurity such as a catalyst residue. Such adventitious nuclei can be augmented or obscured by intentionally adding materials to act as nuclei. This can result in highly crystalline materials with spherulites so small as not

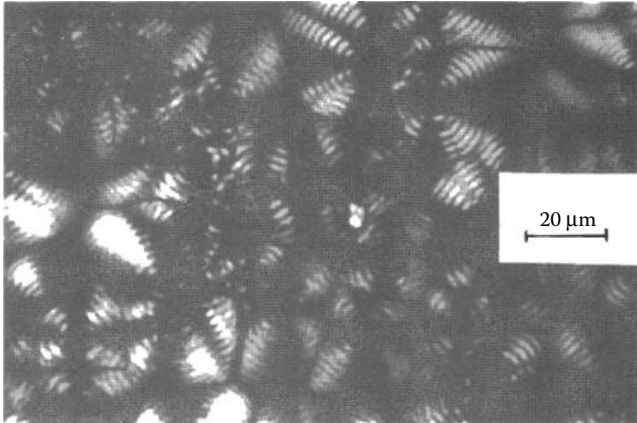


FIGURE 3.19 Slowly formed spherulites of linear polyethylene show a characteristic banded structure when observed between crossed polarizers.

to scatter light appreciably. *Nucleated* materials are available commercially, where the mechanical advantages of crystallinity are desired without the opacity that comes from light scattering at the boundaries of large spherulites.

When crystallization occurs under stress, interesting new forms are seen. In particular, nucleation along flow lines in polyethylene results in a *shish kebab* structure, so-called because folded chain lamellae (the *kebabs*) grow out at intervals from a center shaft of oriented polymer. While not all are as dramatic as the polyethylene case, *row structures* in which a central fibril acts as a contiguous source of nuclei are not uncommon when crystallization takes place in extrusion and molding, even under conditions of low melt stress [36].

3.10 CRYSTALLIZATION KINETICS

The tendency for a polymer to crystallize is enhanced by **regularity** and **polarity**. The molecules must fit together neatly, as well as attract one another, since most of the intermolecular energies vary inversely with the sixth power of the distance between molecules. Examples of the effect of regularity are given in Table 3.2.

The isotactic form is not always the most crystalline. In poly(vinyl alcohol), for example, the syndiotactic form crystallizes more readily than the isotactic because there are strong repulsive forces between adjacent hydroxyl groups [37] in the isotactic form.

Examples of the effect of polarity are as follows:

Nonpolar: Polypropylene (atactic), noncrystalline

Polar: Poly(vinyl alcohol) (atactic), somewhat crystalline

Very polar: Polyamide (nylon 6), very crystalline

Although crystallization and melting are reciprocal of each other and occur at the same temperature for small molecules, this is rarely the case for polymers. The reason is that

TABLE 3.2
Effect of Regularity on Polymer Crystallinity

Irregularity	Polymer	Typical Percent Crystallinity
Copolymer	Linear polyethylene	70
	Isotactic polypropylene	70
	Linear random copolymer	0
Tacticity	Isotactic polypropylene	70
	Atactic	0
<i>cis-trans</i>	<i>trans</i> -1,4-Polybutadiene	40
	<i>cis</i> -1,4-Polybutadiene	30 (at 0°C, long times)
	Random <i>cis</i> and <i>trans</i>	0
Linearity	Linear polyethylene	70
	Branched polyethylene	40

kinetics (rather than just thermodynamics) plays an important role in the crystallization of entangled macromolecular chains. The theory of homogeneous nucleation for crystal formation suggests that, at equilibrium, liquid fluctuations allow critical size nuclei to form and be stable for growth. Whereas this occurs for low-molar-mass molecules at their melting temperature, such fluctuations are very rare in entangled polymers at their equilibrium T_m because of the very high activation energy needed. Supercooling below T_m decreases the free energy for alignment of polymer segment into critical size nuclei. However, an opposing effect that decreases the occurrence of the needed fluctuations is the fact that the viscosity increases at lower temperatures. The interplay of these two effects leads to optimal rates of crystallization between T_g and T_m .

Most polymer crystallizations occur via a heterogeneous nucleation mechanism where extraneous nuclei such as dust particles, catalytic residues, or intentionally added nucleating agents initiate the crystallization. For either homogeneous or heterogeneous nucleation, the volume of a crystallite at time t will be $V(t, \tau)$, where τ represents the start of nucleus growth. Under isothermal conditions, one may assume that in isotropic growth, $V(t, \tau)$ obeys the relation:

$$V(t, \tau) = \frac{4}{3} \pi C^3 (t - \tau)^3 \quad (3.22)$$

where:

C is a constant rate of change of a linear dimension (e.g., the radius of a spherulite)

In homogeneous nucleation where the nucleation process occurs at random times, the mass fraction of a crystallizable material (m_c/m_0), at time t is given by

$$\frac{m_c}{m_0} = \frac{\rho_c}{\rho_l} \int_0^t V(t, \tau) \dot{n} d\tau \quad (3.23)$$

where:

\dot{n} is the average rate of nuclei generation of critical size for growth per unit volume and is assumed constant

The densities of the crystal phase and of the liquid phase are represented by ρ_c and ρ_l , respectively. Substitution of Equation 3.22 into 3.23 and integration yield

$$\frac{m_c}{m_0} = \frac{\pi\rho_c C^3 \dot{n} t^4}{3\rho_l} \quad (3.24)$$

This result is valid only at the initial stages of crystallization because as time progresses, the rate will slow and stop when growing crystallites come into contact with each other. If we define dm_c as the amount of material crystallized during time dt and dm'_c as the amount crystallizable under unrestricted growth during the same differential time increment, we can assume

$$dm_c = \left(\frac{1 - m_c}{m_0} \right) dm'_c \quad (3.25)$$

By applying Equation 3.24 to dm'_c , the above equation becomes

$$dm_c = \left(\frac{1 - m_c}{m_0} \right) \left(\frac{4\pi m_0 \rho_c C^3 \dot{n} t^3}{3\rho_l} \right) dt \quad (3.26)$$

Integration from zero to t gives

$$\ln \frac{m_0 - m_c}{m_0} = \frac{\pi\rho_c C^3 \dot{n} t^4}{3\rho_l} \quad (3.27)$$

or

$$\frac{m_c}{m_0} = 1 - \exp\left(-\frac{\pi\rho_c C^3 \dot{n} t^4}{3\rho_l}\right) \quad (3.28)$$

Equation 3.28 is often expressed in the general form:

$$\frac{m_c}{m_0} = 1 - \exp(-Kt^n) \quad (3.29)$$

and is known as the **Avrami equation**, where K is a rate constant and the exponent n is equal to 4 for homogeneous crystallization. For heterogeneous crystallization caused by seeding, all crystallites may be assumed to grow simultaneously at $\tau = 0$. In that case, the integration of Equation 3.23 is not needed and one has instead

$$\frac{m_c}{m_0} = \frac{\rho_c}{\rho_l} V(t)N \quad (3.30)$$

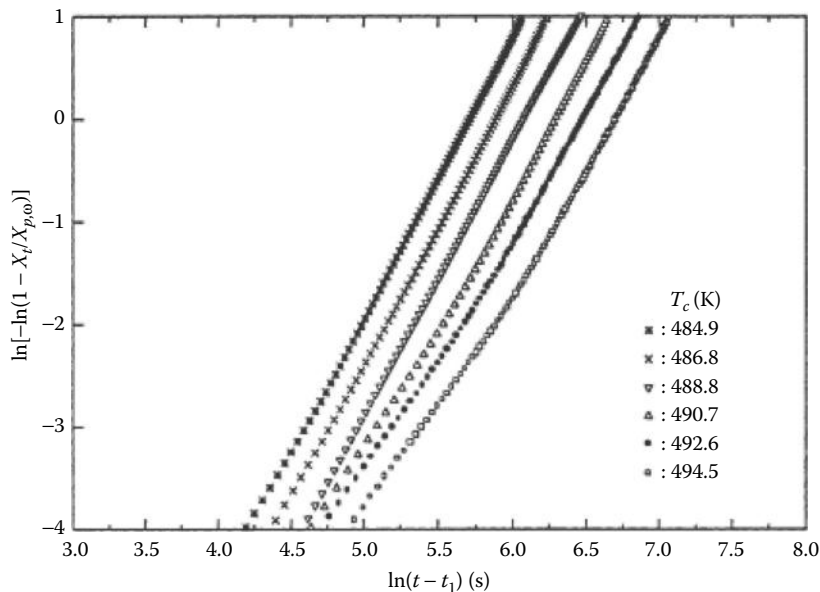


FIGURE 3.20 Data for the primary isothermal crystallization of PET at different temperatures analyzed on the basis of the Avrami equation: where $X_t/X_{p,\infty}$ represents m_t/m_0 . Deviation from linearity indicates a varying value of n with extent of crystallization. (Data from Lu, X. F., and J. N. Hay, *Polymer*, 42, 9423, 2001. With permission.)

where:

N is the seed concentration per unit volume

It is then easy to show that the exponent in Equation 3.29 will be equal to 3. In practice, a value of n between 3 and 4 is often observed. The assumption that the start of crystal growth at random points and at either random times (homogeneous) or all at once (heterogeneous) does not usually hold. Further complexities arise from the shape of the initiating critical nuclei that may lead to nonisotropic crystal growth. Values of n lower than 3 are predicted for crystallite growth in the form of discs or rods. Despite these difficulties, the Avrami equation is regularly used as a semiempirical tool to characterize polymer crystallization rates. The value of n can be determined from the knowledge of ρ_c and ρ_l and the use of **dilatometry** that measures the change in volume with time (see Section 5.1). DSC and integrated X-ray scattering intensities have also been used to determine n . Based on Equation 3.29, the results in Figure 3.20 for PET show that n may be considered constant over a wide range of extent of crystallization, but clearly not over the entire process [38].

3.11 TRANSITION TEMPERATURES

DSC has become the most popular analytical tool for determining transition temperatures as well as the degree of crystallinity (see Section 16.3). Small samples (5–15 mg) are sufficient, and a temperature scanning rate of 20°C/min is often

feasible. Heat transfer is usually less efficient in dilatometers or mechanical testing devices than in DSC. Both calorimetry and dynamic mechanical analysis are regarded as standard tests (ASTM D3418). Many other techniques have been applied to establish the upper temperature limit for dimensional stability, such as softening points (ASTM D1525) or microindenter penetration [39].

For most polymers, there is a single temperature (in an experiment with a given timescale) at which the onset of segmental motion occurs; it is termed the glass transition temperature T_g . Similarly, for those polymers that crystallize to any extent, there is a single melting temperature T_m (which does depend to some extent on molecular weight). However, in both the amorphous and crystalline phases, additional rearrangements or relaxation processes can occur. Usually these do not result in obvious changes in properties. Sometimes they are observed as peaks in damping versus temperature plots resulting from oscillatory mechanical or electrical stresses (see Sections 9.7 and 9.10).

Since crystallinity depends strongly on regularity, but T_g does not, it is conceivable that some copolymers might form glasses before they can crystallize. This is the case for ethylene-propylene random copolymers of roughly equimolar proportions. When polymerized by a catalyst that gives highly crystalline, linear polyethylene, or highly crystalline, isotactic polypropylene, a mixture of the monomers gives an amorphous, rubbery material that does not crystallize but only forms a glass on cooling to about -60°C . Another example is shown in Figure 3.21. Here, adding about 20% of phenylmethylsiloxane is sufficient to destroy the crystallinity of poly(dimethylsiloxane) without substantially raising the T_g .

It is obvious from the foregoing that, for partially crystalline materials, T_m is always greater than T_g and that the difference is a maximum for homopolymers. An examination of these parameters for many homopolymers leads to the generalization that [41]

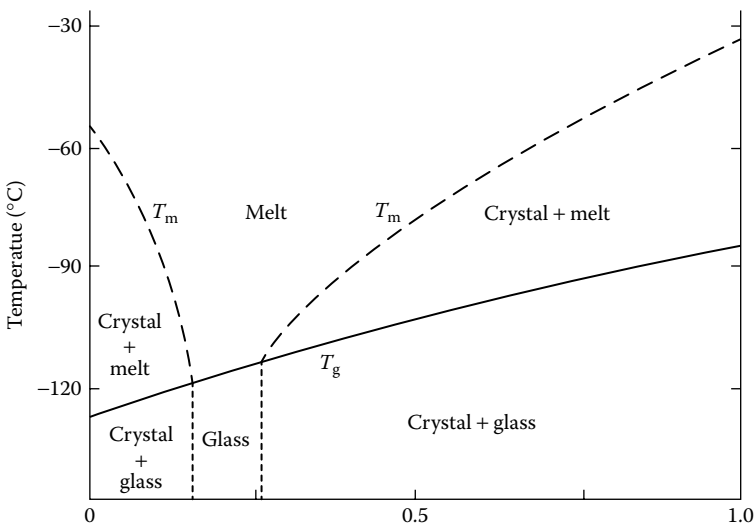


FIGURE 3.21 Loss of crystallinity by copolymerization of phenylmethyl siloxane with dimethyl siloxane. (Data from Polmanteer, K. E., and M. J. Hunter, *J. Appl. Polym. Sci.*, 1, 3, 1959.)

$$1.4 < \frac{T_m}{T_g} < 2.0 \quad (3.31)$$

The ratio generally is higher for symmetrical polymers such as poly(vinylidene chloride) than it is for unsymmetrical polymers such as isotactic polypropylene.

Some other generalizations can be made in light of what has been said so far. The rate of polymer crystallization increases as the temperature is lowered from T_m . However, no crystallization takes place effectively below T_g . Consequently, the maximum rate of crystallization occurs at a temperature between T_m and T_g (Figure 3.22). The maximum rate occurs about halfway between T_g and T_m for natural rubber, but it

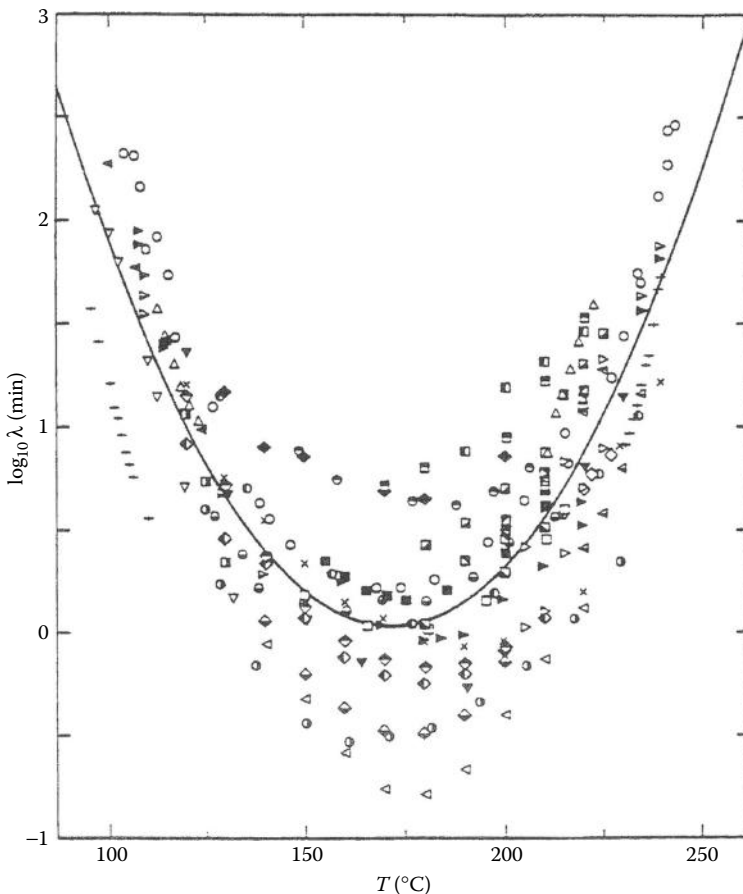


FIGURE 3.22 Cumulative data for the isothermal crystallization of PET from numerous experimental data collected by Hieber and fitted to an empirical equation. λ represents the time needed to achieve half the maximum amount of crystallinity. Despite the large scatter from the various experiments, the data clearly show that the rate of crystallization rises to a maximum between $T_g = 60/80^\circ\text{C}$ and $T_m = 260/280^\circ\text{C}$. (Reproduced from *Polymer*, 36, Hieber, C. A., 1455. Copyright 1995, with permission from Elsevier.)

can be much closer to T_m for some polymers such as poly(dimethylsiloxane) or polyethylene. If a sample of molten polymer is quenched rapidly to a temperature below T_g , a metastable glass may be obtained. Warming the sample just above T_g can increase crystallinity, making the sample stiffer. In the interesting situation that then arises, a glassy polymer is heated, becoming progressively softer as the temperature increases, suddenly stiffens, and then softens again as the T_m is approached (Figure 3.23; see also Figure 18.6).

The **melting point** T_m of a polymer usually is more properly termed a melting range, because a single specimen consists of more than one molecular weight and more than one crystal size. Decreasing either molecular weight or crystal size lowers T_m somewhat. Besides determining T_m by the disappearance of opacity (seen by transmitted light) and polymer orientation (seen by transmitted polarized light), T_m can be characterized by the abrupt change in specific volume V that occurs (a first-order transition) (Figure 3.24).

Chain stiffness also has an effect on T_m . Two linear, nonpolar polymers are linear polyethylene and isotactic PS. The bulky phenyl groups hinder rotation around single bonds in the PS backbone. Since this rotation is the source of chain flexibility, it is not surprising that PS is much stiffer than polyethylene. This shows up in melting points: PS, $T_m = 230^\circ\text{C}$; polyethylene, $T_m = 137^\circ\text{C}$. Qualitatively, one can picture the effect of stiffness by comparing (1) the detachment of a leather strap from a wall to which it is nailed with and (2) the peeling of a stiff wooden board, also nailed. In the first, nails are stressed sequentially, whereas in the second, all nails are stressed simultaneously. The molecular analogy for a nail is the intermolecular bond. Some typical values for T_m are summarized in Table 3.1.

Adding a solvent to a polymer decreases T_m in a manner predictable by the following equation [44]:

$$\frac{1}{T_m} - \frac{1}{T_m^0} = \frac{R}{\Delta H_u} \frac{V_u}{V_1} (v_1 - \chi v_1^2) \quad (3.32)$$

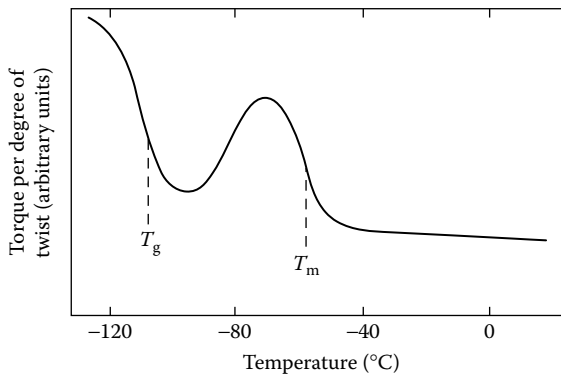


FIGURE 3.23 Quenched sample of silicone copolymer being heated from below T_g . Recrystallization between T_g and T_m increases the stiffness, which then disappears when T_m is exceeded. (Data from Polmanteer, K. E., and M. J. Hunter, *J. Appl. Polym. Sci.*, 1, 3, 1959.)

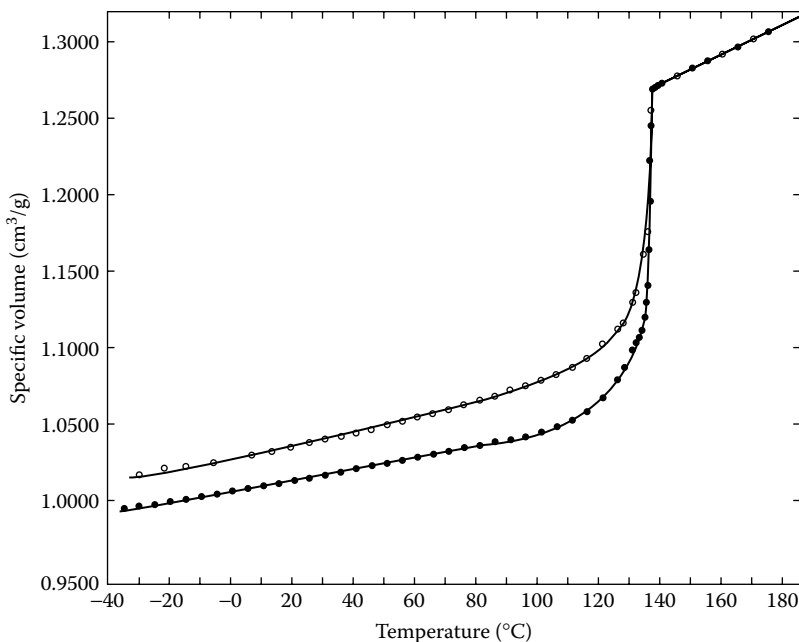


FIGURE 3.24 Specific volume–temperature relations for linear polyethylene (Marlex 50). Specimen slowly cooled from melt to room temperature prior to experiment (\circ) and specimen crystallized at 130°C for 40 days and then cooled to room temperature prior to experiment (\bullet). (Data from Mandelkern, L., *Rubber Chem. Technol.*, 32, 1392, 1959.)

where:

V_u is the molar volume of the polymer repeat unit in the pure liquid state

ΔH_u is the heat of fusion per polymer repeat unit

V_1 is the molar volume of the solvent

v_1 is the volume fraction of the solvent

χ is the polymer–solvent interaction parameter

R is the gas constant

T_m^0 is the melting point of the pure polymer (see Figure 3.25 and Table 3.3)

Most of the time, the depression of T_m by a small amount of solvent is modest.

Example 3.2

If three volumes of poly(ϵ -caprolactone), $-(\text{CH}_2)_5-\text{CO}-\text{O}$, are diluted with one volume of a good solvent for which $V_1 = V_u$ and $\chi = 0.400$, what is the depression in the melting point? Properties of the polymer are given in Table 3.3.

Solution:

$$\Delta H_u = 142 \times 114 = 16.2 \text{ kJ/mol}$$

$$\frac{1}{T_m} - \frac{1}{337\text{K}} = \left(\frac{8.314 \text{ J/mol} \cdot \text{K}}{16.2 \times 10^3 \text{ J/mol}} \right) (0.25 - 0.4 \times 0.25^2) = 1.155 \times 10^{-4} \text{ K}^{-1}$$

$$T_m = 324\text{K} = 51^\circ\text{C}$$

so

$$\Delta T_m = 64 - 51 = 13^\circ\text{C}$$

A sizable increase in density with crystallization is characteristic of almost all materials. Only water, bismuth, and a few polymers are exceptions. The density of perfectly crystalline materials can be derived from X-ray measurements. The amorphous material is easily measured above its melting point and the density extrapolated to lower temperatures. Knowing these densities at any temperature together with the actual density of a sample gives a convenient estimate of the degree of crystallinity. The percent crystallinity is given by the ratio:

$$\frac{\text{Sample density} - \text{amorphous density}}{\text{Perfect crystal density} - \text{amorphous density}} \times 100$$

Because chain atoms are involved in chain folding and in chain ends, it has been argued that even a single crystal could not be 100% crystalline on the basis described.

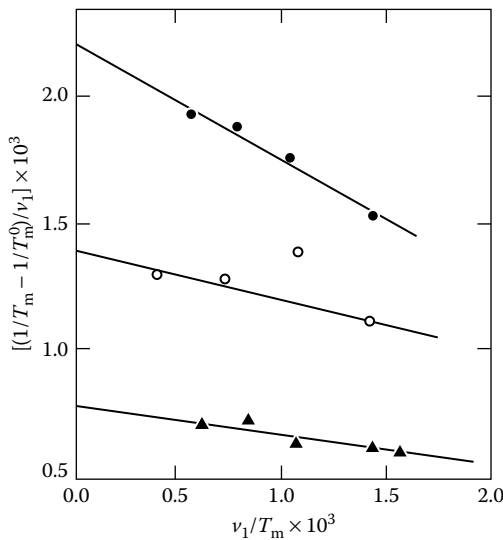


FIGURE 3.25 Temperature reduction as $(1/T_m - 1/T_m^0)/v_1$ plotted against v_1/T_m for cellulose tributyrate mixed with hydroquinone monoethylether (○), dimethyl phthalate (●), and ethyl laurate (▲). Linearity would not be greatly affected by replacing v_1/T_m by v_1 . (Data from Mandelkern, L., and P. J. Flory, *J. Am. Chem. Soc.*, 73, 3206, 1951.)

TABLE 3.3
Heat of Fusion for Selected Polymers

Monomer Unit	ΔH_u (J/g)	T_m (°C)	Density ^a (g/cm ³)		Repeat Unit (g/mol)
			Amorphous	Crystalline	
Ethylene (linear)	293	141	0.853	1.004	28.05
Propylene (isotactic)	79	187	0.853	0.946	42.08
Butene-1 (isotactic)	163	140	0.859	0.951	56.12
4-Methylpentene-1 (isotactic)	117	166	0.838	0.822	84.16
Styrene (isotactic)	96	240	1.054	1.126	104.15
Butadiene (1,4 polymer) (<i>cis</i>)	171	12	0.902	1.012	54.09
Butadiene (1,4 polymer) (<i>trans</i>)	67	142	0.891	1.036	54.09
Isoprene (1,4 polymer) (<i>cis</i>)	63	39	0.909	1.028	68.13
Isoprene (1,4 polymer) (<i>trans</i>)	63	80	0.906	1.051	68.13
Vinyl chloride (syndiotactic)	180	273	1.412	1.477	62.50
Vinyl alcohol	163	265	1.291	1.350	44.06
Ethylene terephthalate	138	280	1.336	1.514	192.18
ϵ -Caprolactone	142	64	1.095	1.194	114.14
Ethylene oxide	197	69	1.127	1.239	58.08
Formaldehyde (oxymethylene)	326	184	1.335	1.505	72.11
Nylon 6	230	270	1.090	1.090	113.16
Nylon 6,6	301	280	1.091	1.241	226.32

Source: Runt, J. P., *Encycl. Polym. Sci. Tech.*, 4, 487, 1986; Brandrup, J. and F. H. Immergut (eds.): *Polymer Handbook*, 3rd edn. 1989. Wiley, New York; Springer Science+Business Media: *Physical Constants of Linear Homopolymers*, 1968, Springer-Verlag, New York, Lewis, O. G.

^a Near 25°C.

It should be obvious that characterization of a partly crystalline polymer is much more complex than mere specification of the fraction that is crystalline. Some factors that need to be taken into account have been listed by Magill [47] as follows:

1. Crystallite size, crystallite distribution, and crystallite perfection
2. Constraints on amorphous regions (matrix) that perturb it from its truly disordered condition
3. Defects or distortions in the paracrystalline sense
4. Presence of voids and surface stresses
5. Polymer chain chemistry, where induced chain irregularities prevent the system from attaining its lowest energy state
6. Transient and permanent entanglements in the amorphous regions
7. Inherent strains that give rise to nonrandom states
8. Chain length and chain ends

9. Nature of interzonal or surface layer with distance
10. Distribution of spherulite sizes
11. The relative sequence lengths for a block copolymer

3.12 STRAIN-INDUCED CRYSTALLIZATION

The early studies of **strain-induced crystallization** involved cross-linked rubber and polymer used to make elastomers. Imposing a tensile strain on a crystallizable amorphous polymer induces crystallization that enhances its mechanical properties. The imposed strain is expected to facilitate the alignment of polymer segments in the direction of the deformation and thus promotes crystallization. At a given temperature, the state of greater order represents a state of lower entropy and higher free energy. As a consequence, to melt the crystals formed under strain will require a higher temperature than the crystals formed under unstressed conditions. Early careful measurements in which T_m is extrapolated to a limiting value for perfect crystallites are shown in Figure 3.26. Available theories based on just the increase in free energy are unsuccessful in predicting these results. The small increase in free energy predicted cannot justify the large increase in melting temperatures observed. Nonetheless, the conjecture that strain causes local alignment of short part of the

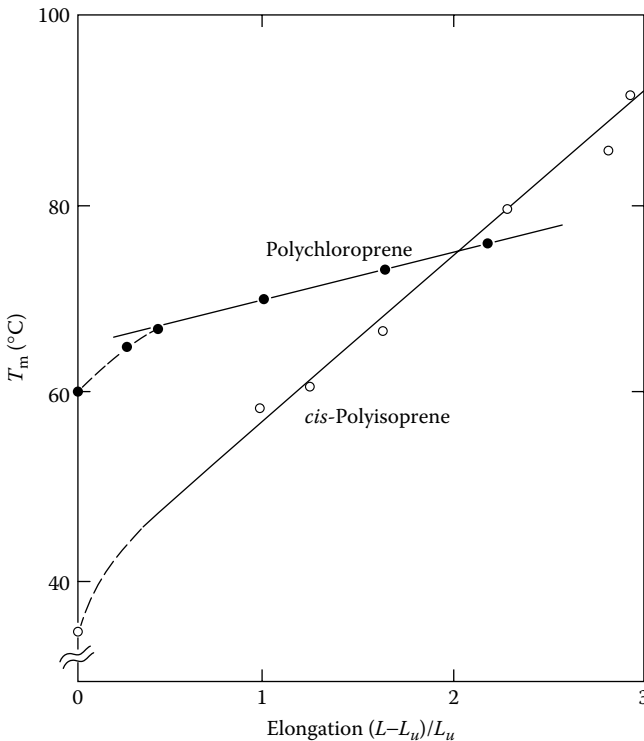


FIGURE 3.26 Strain-induced crystallization (L_u) is the unstretched length. (Data from Krigbaum, W. R. et al., *J. Polym. Sci.*, A2(4), 475, 1966.)

chain that leads to the formation of thin fringed micelles that act as threadlike nuclei is well supported by experimental evidence [48].

In recent years, there have been a very large number of studies on flow-induced crystallization under a variety of shear conditions such as rotational viscometers with transparent parallel plates or pressure flow between transparent beryllium plates that allowed X-rays and/or birefringence measurements. Studies of crystallization during flow in a rectangular duct where samples were subjected to a variety of shearing time and temperature history shed some light on the formation of nuclei and, more importantly, their long persistence after the shear has stopped [49]. The renewed interest in this topic stems from its relevance in polymer processes, and in particular injection molding of polyolefins and polyesters. The complexities of strain-induced crystallization have been recently reviewed and discussed in a monograph by Janeschitz-Kriegl [48] and there is continued research interest in this field.

3.13 BLOCK COPOLYMERS

We have previously alluded to two major commercial applications of block copolymers: the addition of AB diblock copolymers in blends of homopolymers, A and B, to improve the processability and mechanical properties of the mixture, and the use of ABA-type triblock copolymers as thermoplastic elastomers when block A (e.g., PS) is below its glass transition, whereas block B (e.g., polybutadiene) is above its glass transition at ambient temperature. Other products made from block copolymers include pressure-sensitive adhesives, oil additives, and automobile parts.

Because the different blocks are typically incompatible, they phase separate. However, they are linked via covalent bonds and cannot separate themselves entirely. As a result the phase separation process leads to the formation of microdomains, the nature of which depends on the relative volume fraction f of different components and the size of which depends on the degree of polymerization of the block segments, N . Finally, the morphologies that can be achieved are very diverse and depend on the Flory–Huggins segment–segment interaction parameter χ for blends introduced earlier. For block copolymers with fairly narrow molecular weight distribution (i.e., low dispersity; see Section 6.1), specific morphologies of different symmetry with long-range order can be achieved depending primarily on the relative composition given by f . Figure 3.27 shows some of the different morphologies that can be obtained with diblock copolymers. Most block copolymers studied to date have similar block materials from the point of view of phase separation. This situation is a result of the use of anionic polymerization, which until recently has been the best method for block copolymer formation. As a result, the limited number of monomers possible with anionic polymerization led to block copolymers usually being made from nonpolar-hydrocarbon-like polymers such as styrene, butadiene, and isoprene. The resulting properties are still interesting however. In triblock copolymers such as the PS-*block*-polybutadiene (PBD)-*block*-PS, thermoplastic elasticity is achieved when the end PS blocks are fairly short compared to the middle PBD blocks. The PS phase separates in nearly spherical domains that are glassy at ambient temperature and act as multifunctional cross-links for the PBD. Besides the composition f , the temperature also plays a role in the observed morphologies when one approaches the transition

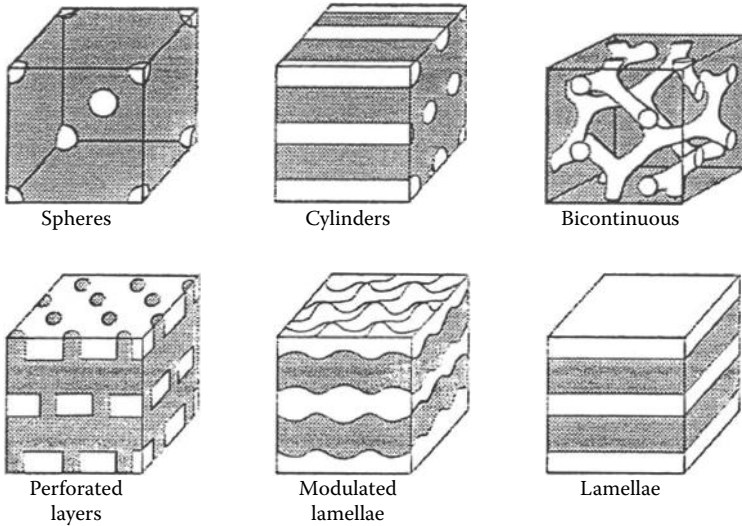


FIGURE 3.27 Examples of ordered-state morphologies found in low polydispersity diblock copolymers. Shaded and unshaded regions represent the two different blocks. (Data from Bates, F. S. et al., *Faraday Discuss.*, 1994, 98: 7. Reprinted by permission from the Royal Society of Chemistry.)

temperature at which the blocks become compatible (the order–disorder transition [ODT]), which is found to depend on the product χN [51]. Because of the chemical similarity of butadiene and styrene, even though there is phase separation, it is in the weak segregation limit, and as a result the phases possible with this system are relatively large, 25 nm or so (χN does not favor phase separation at small block size).

Most recent developments in block copolymer applications make use of the fact that the phase-separated microstructures are of nanometer length scales, periodic in nature, and in many cases porous if one of the phases is removed. The use of block copolymers is especially advantageous if these length scales cannot be readily accessed via other means. The following three examples will illustrate the opportunities and challenges in using block copolymers.

In the first example, the microelectronics industry is intensely exploring the use of block copolymers to form patterns on length scales under 20 nm. The process known as directed self-assembly (DSA) makes use of the phase separation of block copolymers in thin layers. Periodic spheres make dots and periodic cylinders or lamellae make lines, and by using these microstructures and guiding their assembly, it is possible to draw circuits. The challenge of this approach is that microstructures do not readily bend, jog, or change direction like a circuit pattern unless there is a defect, achieving microstructure perfection is difficult due to strong surface interactions, and the formation of long-range structures takes more time than a typical lithographic process step.

At the present time, remarkable progress is being made in tackling these issues largely using PS-*block*-PMMA (PS-*b*-PMMA). By incorporating homopolymers into a block copolymer, it is possible to more easily create microstructures that can bend and change direction to form a circuit. Guiding the assembly process has

been carried out by creating patterns on *neutral* layers, that is, periodic changes in surface energy have been shown to direct the assembly of block copolymers. Surface topography also enables alignment of microstructure. This assembly process that can take hours to carry out can be sped up using solvent vapor annealing as well as rapid laser heating methods. New polymers other than PS-*b*-PMMA have been developed that reside in the strong segregation limit and very small structures (<10 nm) have been produced. The DSA guiding structure can be larger than the ultimate pattern making it easier to make the smallest of periodic features. At the present time, low defect densities are still difficult to achieve, but it is expected that within the next couple of years DSA lithography will be used to produce memory devices and microprocessors.

The complex microstructures possible with block copolymers also offer possibilities to produce new functional materials. In addition to the typical spheres, cylinders, and lamellae, gyroid phases and more complex structures are possible. By incorporating multiple phases into a block copolymer (three or more blocks), a remarkable range of small (<20 nm) structures can be formed. With proper selection of nanoparticles, it is possible to deposit a metal or ceramic phase within one of the block copolymer domains. By then heating the nanocomposite, porous structures can be formed by removing the phase without the inorganic component. Applications ranging from fuel cell and battery membranes, and water reverse osmosis membranes for water purification are being explored.

Block copolymers are also strongly surface-active materials and can be used to modify coatings and even act as large size surfactants. By incorporating a block copolymer in a coating, it is possible to direct its segregation to the surface or an interface. For example, coatings designed to resist fouling in a marine environment have been created using block copolymers that effectively prevent growth of barnacles or seaweed on these surfaces without the use of toxins. When block copolymers are added to a solution, they can act as surfactants and will even form micelles and vesicles. If amphiphilic materials are used, such block copolymers may be dissolved in water and self-associate in solution to encapsulate a nonpolar phase in the core of a micelle. Such materials have been studied for drug delivery and used as tracers in medical diagnostics.

3.14 LC POLYMERS

Several intermediate states are possible between the three-dimensional crystal that has long-range order and the amorphous, isotropic liquid or glass that does not. To describe phases that have organization and order between these two extremes, the term **mesophase** (from the Greek *mesos* meaning “middle”) has been coined. Three types of mesophases have been identified: LCs, plastic crystals (PCs), and conformationally disordered (condis) crystals (CCs) [52]. These mesophases are differentiated according to the degree of disorder present that can be positional in the case of LCs, orientational in the case of PCs, and conformational in the case of CCs. The best-known polymeric materials that exhibit a mesophase are rigid rod-like polymers that form LCs. These polymers are typically polyaramids that contain aromatic groups in the main chain linked by amide bonds and polyesters that also contain aromatic groups in the main chain. These polymers are different because the

polyaramids are liquid crystalline in the presence of a solvent, whereas the aromatic polyesters are liquid crystalline in the melt.

Liquid crystallinity is not restricted to polymer molecules. Some relatively simple molecules such as sodium stearate, a soap, exhibit varying degrees of liquid crystallinity. In fact, the name of one LC form, the **smectic** state, derives from the Greek word *smectos* meaning “soap-like.” Another common LC form is the **nematic** state (from the Greek word *nematos* meaning “threadlike”). It is therefore convenient to distinguish between **polymer LCs** (PLCs) and low-molar-mass (or monomer) LCs (MLCs) [53]. Transitions from an isotropic liquid phase to a liquid crystalline phase may be induced by lowering temperature in **thermotropic** LCs, or a mesophase may be induced by concentration in **lyotropic** LCs [54,55]. Using such classification one can see that the polyaramids mentioned above are lyotropic and the aromatic polyesters are thermotropic. It has also been shown that the LC transition may be brought about by pressure [56].

Using a tool such as DSC (Section 18.3) or polarized-light microscopy, a progression can be seen for some materials going from the three-dimensional crystal and melting to the two-dimensional smectic state or the one-dimensional nematic state and, finally, to the isotropic liquid state (Figure 3.28). In the nematic phase, there is orientation alignment of the rodlike molecules, but, unlike the smectic state, the centers of gravity of the molecules are not located within layers [57]. There are several subgroups of the smectic phase depending on the precise nature of the organized state.

The nematic phase is the most common of the mesomorphic phases and most rigid rod polymers show nematic LC behavior. When a solution of a lyotropic polyaramid (such as Kevlar) is extruded from a sulfuric acid solution, a highly oriented structure results and gives the recovered solid polymer a very high modulus and a high tensile strength. Normally lyotropic polymers cannot be melt processed because strong hydrogen bonds between polymer chains lead to extraordinarily high melting temperatures. Breaking

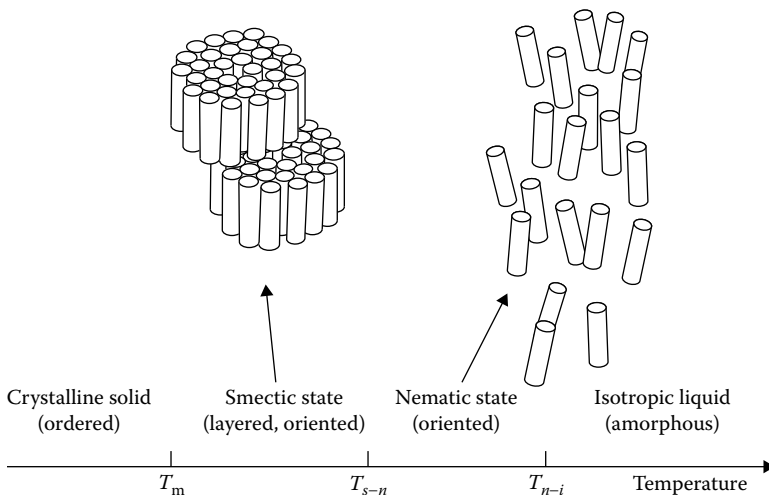


FIGURE 3.28 Schematic visualization of possible mesomorphic transitions as temperature increases in an LC system showing the organization of mesogens (represented as cylinders) in the smectic and nematic states.

up these hydrogen bonds and permitting processing in solution can often involve aggressive highly acidic solvents such as the sulfuric acid mentioned above. The polyaramid in this case is the polyamide based on terephthalic acid and *p*-phenylenediamine and it is used to make ropes of incredible strength and woven items such as bulletproof vests. New lyotropic polymers such as poly(benzoxazole) or poly(benzthiazole) have even greater modulus and upper use temperature. Fibers of these materials are used in flameproof apparel and as the fiber component in advanced composites.

Most LC polymers in the market are linear, highly aromatic thermotropic polyesters. They combine chemical stability with chain rigidity and retain dimensional stability (remain as glasses) up to 200°C or 300°C and are also very chemically stable (resistant to oxidation). These types of PLCs, such as the commercial Vectra and Xydar, are usually processed in the melt state with conventional fabrication techniques such as extrusion and molding (see Chapter 14). A major advantage of such polymers is that they can be melt processed and form extremely precise molded structures that do not shrink on cooling. They have been used in molded parts for microelectronics and in mounting brackets for optical communications.

To keep the desirable properties of rigid-rod polymers and facilitate the processing of such materials by lowering melting temperatures or making them more readily soluble, blocks of stiff molecules known as **mesogenic groups** may be incorporated either along the main chain of a polymer molecule or as pendant groups. The **mesogens** are separated from each other by segments of flexible chains, so they may act as somewhat independent LCs and still remain part of the overall polymer molecule. In these cases, the orientation corresponding to a smectic or nematic state may be induced by an orienting field and include flow, temperature, or the action of an electric or magnetic field. These materials have better mechanical properties than common or reinforced engineering plastics and also have lower thermal expansion coefficient and higher resistance to chemicals and high temperatures. Despite their higher cost, they have found use in electronic devices and automotive components.

3.15 GELS

The term **gels** is associated with highly swollen polymer networks. A gel thus typically consists of a cross-linked polymer network holding a large amount of liquid in place. The nature of the cross-links can vary. They are usually generated by small molecules (cross-linkers) that covalently link flexible elastic chains into a network. They can also be caused by the segregation in a copolymer where constituents A and B have very different interaction with the solvent. The maximum amount of liquid that a network can hold will depend on the structure of the network and the affinity of the polymer to the liquid. We saw earlier (see Section 2.5) that these factors are represented by N , the number of moles of elastic polymer chain strands per unit volume, and χ , the Flory interaction parameter. Knowing N and χ , the amount of maximum swelling may be estimated by calculating the polymer volume fraction v_2 using Equation 2.18 or Figure 2.4. If N is unknown, it can be determined from the knowledge of χ and v_2 . The effect of χ on the v_2 (which is inversely related to the swelling) is illustrated in Figure 3.29 for different values of N . Equilibrium curves 2, 3, and 4 are for increasing values of N (i.e., increase in cross-link density). As N increases,

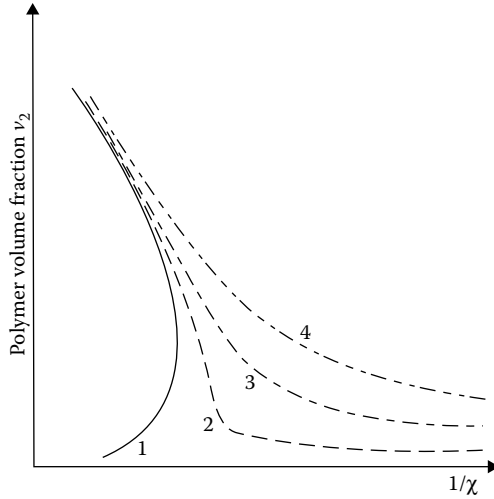


FIGURE 3.29 Schematic representation of the effect of cross-link density on the swelling of networks. Curve 1 represents the coexistence curve of an UCST polymer solution and curves 2, 3, and 4 are for gels with increasing cross-link density.

v_2 increases and the equilibrium swelling decreases for a given value of χ . Because χ^{-1} can also be thought of as the effect of temperature (see Equation 2.13), curve 1 is the coexistence curve of uncross-linked polymer of a finite large molecular weight.

In **hydrogels**, the liquid is water and the network is made from water-soluble polymers that are chemically or physically cross-linked. Physical cross-links may consist of crystallites, associations due to hydrogen bonding, or aggregates of hydrophobic moieties in an otherwise hydrophilic polymer. Physical gels are reversible, meaning that the association leading to the network connectivity can be dissolved often by heat and the network loses its rigidity. The structure of a hydrogel is affected by a large number of parameters such as the extent of charge, the extent of crystallinity, and the degree of association due to hydrophobic moieties on the chains. This versatility of structures and ensuing properties has led to a number of specialized applications in foods, water absorbents, and contact lenses. Extensive research with biocompatible hydrogels is being pursued in bioengineering and biomedical applications such as in bioseparations, tissue engineering, and drug delivery [58–60]. Water-soluble polymers such as poly(ethylene oxide) (PEO) or hydrolyzed polyacrylamide or modifications thereof have polar groups or ionic charges along their chains that enhance their uptake of water.

The presence of charges on the polymer also leads to an interesting transition in the gel from highly swollen to highly deswollen (collapsed) as a function of temperature (or interaction parameter), pH, and electric field. Figure 3.30 shows the original demonstration of this transition as a function of temperature for a network made of the copolymer *N*-isopropylacrylamide (IPPA_m) and sodium acrylate. As shown earlier, PIPPA_m has an LCST such that it precipitates from water at high temperatures. Gels made of PIPPA_m with various amounts of sodium acrylate that will impart ionic charges to the chains exhibit a high degree of swelling in water at low temperatures and deswell (collapse) at high temperatures. The swelling ratio V/V_0 is the ratio of

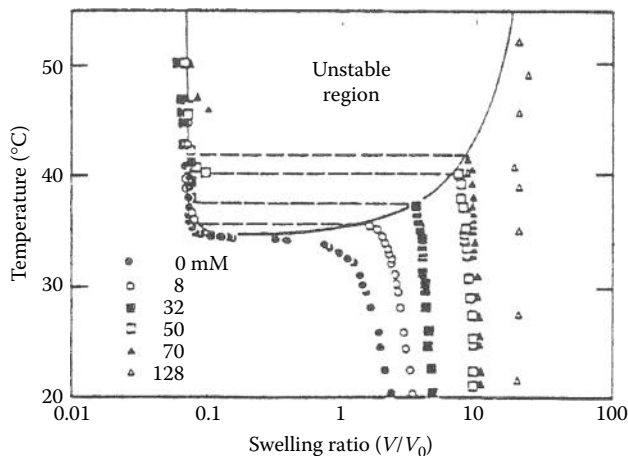


FIGURE 3.30 Effect of the degree of ionization on the swelling of gels of copolymer *N*-isopropylacrylamide and sodium acrylate in water. The concentrations listed in the legend are those of the sodium acrylate in the copolymer. (Reproduced with permission from Hirotsu, S. et al. 1987. *J. Chem. Phys.* 87:1392. Copyright 1987, American Institute of Physics.)

the volume of the gel to its volume in the original preparation state. As the amount of charges (sodium acrylate content) increases, the volume change at the transition is larger and the transition temperature increases. These experimental results can be predicted qualitatively by adding terms to the free energy of swollen networks given by Equation 2.16 that incorporate the effect of volume changes upon mixing polymer and solvent [62] and the free energy of ionic charges [44,63]. Gels made from polymers that exhibit an LCST also show the curious effect that they swell more under increased isotropic pressure [62]. Since these earlier works, the swelling behavior of charged hydrogels has been studied extensively experimentally, theoretically, and more recently by Monte Carlo computer simulations [64]. The swollen–collapse transition of charged hydrogels can be the basis of controlled drug delivery methods (see Section 13.7.4).

KEYWORDS

Block copolymers
 Glassy state
 Crystalline state
 Liquid crystal polymer
 Random Gaussian coil
 End-to-end distance
 Scaling laws
 Semi-dilute
 Equilibrium between phases
 Coexistence curve or bimodal
 Spinodal curve
 Upper critical solution temperature (UCST)

Critical point conditions
Compatible polymers
Free volume
Lower critical solution temperature (LCST)
Melt state
 T_m , T_g
Rubber
Segmental Brownian motion
Glass
Glass transition temperature
Ladder polymer
Flex temperature
Plasticization
Crystallite
Fringed micelle
Helical conformation
Unit cell
Spherulite
Drawing
Necking
Regularity
Polarity
Avrami equation
Dilatometry
Melting point
Mesophase
Strain-induced crystallization
Smectic
Nematic
Polymer LCs
Thermotropic
Lyotropic
Mesogenic groups
Mesogen
Gels
Hydrogels

PROBLEMS

- 3.1** When a saturated paraffin such as polymethylene $-(\text{CH}_2)_n-$ is chlorinated, chlorine replaces hydrogen at random. Invariably, small amounts of chlorine (10–50 wt% Cl) cause a lowering of softening point. Large amounts (about 70%) *raise* the softening point. Rationalize on the basis of intermolecular forces.
- 3.2** Polymers that are oriented on stretching may crystallize, since the molecules are then able to fit into a lattice more easily. How does this help

explain why a rubber band heats up on stretching to near its breaking point? (Try this by holding a rubber band to your lips and suddenly stretching it.)

- 3.3** Copolymers of monomers A and B have the following stiffening temperatures:

Weight Fraction of B	Stiffening Temperature (°C)
0.00	60.0
0.10	36.0
0.15	20.5
0.25	-8.0
0.35	-3.0
0.50	+5.0

Estimate T_g for homopolymers of B and A. Explain your assumptions.

- 3.4** For the polyethylene of Figure 3.24 (indicated by lower curve), calculate the fraction of crystalline material at 20°C, assuming that the coefficient of expansion for amorphous material is the same above and below T_m and that the density of perfect crystal can be obtained from Figure 3.15.
- 3.5** Compare graphically the temperatures of Table 3.1 with Equation 3.31. Also plot T_m and T_g versus δ_2 . Rationalize extraordinary points.
- 3.6** From the data of Figure 3.10, calculate the ratio of T_g for tritolyl phosphate to that for dioctyl sebacate.
- 3.7** What is wrong with describing a sample of polyisobutylene as *predominantly cis* or *syndiotactic*?
- 3.8** The following data are obtained when linear polyethylene is mixed with α -chloronaphthalene [65].

T_m (°C)	Volume Fraction of Solvent v_1
137.5	0.00
134.5	0.06
131.0	0.16
125.0	0.32
120.0	0.52
115.0	0.75
110.0	0.95

Densities of amorphous polyethylene and solvent are approximately 0.8 and 1.1 g/cm³, respectively. Estimate the heat of fusion of polyethylene and the polymer-solvent interaction parameter.

- 3.9** When held at a constant temperature, spherulites grow at a constant radial velocity. Crystallization rate may be studied by following the overall volume of a large sample containing many spherulites, each growing from a separate nucleus. Derive a formula for the change in density ρ with time t for a sample in which no new nuclei are formed after crystallization starts and in which the constant radial growth rate is $(dr/dt)_0$. Assume that we

follow the density only during the time in which spherulites do not grow large enough to touch each other. Let densities of crystalline and amorphous polymer be ρ_c and ρ_a , respectively.

- 3.10** What melting temperature can be expected for poly(ethylene oxide) mixed with water when the volume fraction of solvent is 0.01, 0.02, and 0.05? Assume that $\chi = 0.45$. See Table 3.3 for additional data.
- 3.11** The T_g of nylon 6,6 is lowered by water or methanol. Using Equation 3.21, estimate for the two liquids assuming that the temperature at which $E' = 2.0$ GPa is near T_g (Figure 9.15).
- 3.12** How much plasticizer with $T_g = -80^\circ\text{C}$ would have to be added to a film of nylon 6,6 in order for T_g to be 25°C ? If $V = 200$ cm³/mol and $\chi = 0.40$, what would be the effect on T_m of this amount of plasticizer? Data: $\Delta H_u = 301$ J/g, $\rho = 1.091$ g/cm³, $T_m = 280^\circ\text{C}$, $T_g = 50^\circ\text{C}$.
- 3.13** Two copolymers of ethylene ($\text{CH}_2=\text{CH}_2$) and propylene ($\text{CH}_2=\text{CHCH}_3$) have the same ratio of monomers. However, one is rubbery at room temperature and does not stiffen until the temperature is lowered to about -70°C , whereas the other is rather stiff, tough, and opaque at room temperature. Explain the difference.
- 3.14** What kind of isomerism might you expect in polymers of 1-butene ($\text{CH}_2=\text{CHCH}_2\text{CH}_3$)? Which form is likely to be least crystalline? What kind of isomerism do you expect in 1,4 polymerization of chloroprene ($\text{CH}_2=\text{CClCH}=\text{CH}_2$)? Which isomer should be most crystalline?
- 3.15** Why does an injection-molded PS protractor show a complicated pattern when viewed in polarized light?
- 3.16** Poly(ϵ -caprolactone) has $T_g = -60^\circ\text{C}$ and $T_m = +60^\circ\text{C}$. In the study of biodegradability at 25°C , it would be desirable to vary the degree of crystallinity holding all other variables constant. Why is this difficult with poly(ϵ -caprolactone)? Why should it be easier with poly(ethylene terephthalate), which has $T_g = +60^\circ\text{C}$ and $T_m = 250^\circ\text{C}$?
- 3.17** The Gordon–Taylor equation (Equation 3.20) can represent the glass transition temperature T_g of a two-component system in terms of weight fractions of components.
- Show that $[(T_g)_1 - T]w_1/w_2 = \phi = kT - k(T_g)_2$.
 - Plot ϕ versus T to get k and $(T_g)_2$, assuming $(T_g)_1 = 113^\circ\text{C}$ for the system described by Anderson, who determined transition temperatures for blends of poly(methyl methacrylate) (1) with poly(epichlorohydrin) (2) [66]:

Weight Fraction of 2	Transition Temperature ($^\circ\text{C}$)
0.000	113
0.200	52
0.300	42
0.430	11
0.700	-3
1.000	-19

- 3.18** Styrene forms a homopolymer with a T_g of 100.0°C . The rubbery copolymer with butadiene commonly called styrene–butadiene rubber (SBR) has a T_g of -60°C , whereas the copolymer used for coatings has a T_g of 28.0°C . If a copolymer is made with equal weights of butadiene and vinyl acetate (T_g of polyvinylacetate = 28°C), what T_g is expected for this new copolymer? Assume the validity of the Gordon–Taylor equation with the same k for any pair of monomers as long as monomer 1 is butadiene. SBR is 25.0 wt% styrene; copolymer (coatings) is 25.0 wt% butadiene.
- 3.19** When 100 g of PVC is mixed with 25 g of plasticizer Z, the glass transition temperature is lowered from 87°C (for PVC) to 0°C . A mixture of 100 g of PVC with 50 g of Z shows a glass transition temperature of -25°C . What glass transition temperature is to be expected from a mixture of 100 g of PVC with 100 g of Z?
- 3.20** The equilibrium uptake of water into Nafion[®] was measured by Tobias Wheeler (PhD thesis, Cornell University, 2008) at different relative humidity (from 20% to 100%) corresponding to different water activity. The equilibrium water uptake was achieved by placing disk samples of Nafion in a closed environment in the presence of different salt solutions to achieve different relative humidities.
- Using Equation 3.6 show that the activity a_1 of a solvent defined by the relation: $\Delta\mu_1 = RT \ln a_1$ is given by $a_1 = (1 - v_2) \exp(v_2 + \chi v_2^2)$ assuming $x \gg 1$.
 - From the selected data of measured water activity a_w listed below, calculate and plot the values of χ as a function of v_2 .

a_w	0.2	0.32	0.75	0.84	0.89	0.94	0.97	1.00
v_1	0.063	0.08	0.15	0.19	0.22	0.26	0.27	0.33

- Is there a range of v_2 for which Flory’s original assumption of almost constant χ holds?
 - (Optional: extra credit) The Nafion series of polymers are ionomer copolymers (charged polymers). Can you provide an interpretation for the above behavior of χ as a function of v_2 ?
- 3.21** The critical conditions, v_{2c} and χ_c , of a polymer–solvent mixture are obtained by applying Equations 3.8 and 3.9 to the chemical potential expression in Equation 3.6. Perform the necessary differentiations and show that, for large x , your results reduce to Equations 3.10 and 3.11.
- 3.22** Show that the critical conditions (Equations 3.10 and 3.11) are also obtained from the complementary equations $(\partial\mu_2/\partial v_2)_{T,P} = 0$ and $(\partial^2\mu_2/\partial v_2^2)_{T,P} = 0$ using Equation 3.7.
- 3.23** (a) What are the values of v_{2c} and χ_c if the ratio of polymer to solvent molar volume is 516?
- Plot the value of $\mu_1 = \mu_1 - \mu_1^0$ for different solvents having the same molar volume but with $\chi = 0.9\chi_c$, $\chi = \chi_c$, and $\chi = 1.2\chi_c$ at $T = 300\text{ K}$. What is the value at the inflection point of $\Delta\mu_1$ versus v_2 at $\chi = \chi_c$, and $\chi = 1.2\chi_c$?

(c) Obtain analytically the values of v_2 at the maximum and minimum of $\Delta\mu_1$ versus v_2 at $\chi = 1.2\chi_c$.

(d) Such a polymer solution with $v_2 = 0.1$ and $\chi = 1.2\chi_c$ will separate into two phases. Explain why the dilute phase will have a polymer concentration v_2 lower than 0.01.

3.24 The Flory free energy of mixing two polymers with number of segments p_1 and p_2 is given by

$$\frac{\Delta G_m}{N} = RT \left(\frac{v_1}{p_1} \ln v_1 + \frac{v_2}{p_2} \ln v_2 + \chi v_1 v_2 \right)$$

Determine the critical conditions, v_{2c} and χ_c , by applying Equations 3.8 and 3.9. Show that your results reduce to Equations 3.17 and 3.18 when $p_1 = p_2$. All other parameters are defined in Section 3.3.

3.25 The coexistence curve of linear PIPPAm chains in water at 1 atm is shown in Figure 3.5. At a higher pressure, the coexistence curve shifts upward to higher temperatures making the polymer soluble at all concentrations in water at higher temperatures.

(a) Consider a PIPPAm gel of low cross-link density. Sketch its swelling curves at 1 atm and at the higher pressure. It will be helpful to sketch first the coexistence curves at 1 atm and at a higher pressure and then draw the swelling curves of the gel relative to these coexistence curves (see Figure 3.29).

(b) Does the gel swell more or less at the higher pressure?

3.26 One has the following thermodynamic condition at equilibrium between a crystalline phase and a liquid phase:

$$\mu_u^c - \mu_u^0 = \mu_u^l - \mu_u^0$$

where μ_u^c , μ_u^l , and μ_u^0 correspond to the chemical potential of a polymer repeat unit in the crystalline phase, the liquid phase, and the reference pure liquid phase at the same T and P , respectively. Flory [44] used the above relation and writes for the left-hand side of the above equation:

$$\mu_u^c - \mu_u^0 = -\Delta H_u \left(1 - \frac{T}{T_m^0} \right)$$

where ΔH_u is the enthalpy of melting for a repeat unit because at $T = T_m^0$, $\mu_u^c = \mu_u^0$. To obtain an expression for $\mu_u^l - \mu_u^0$, that is, the right-hand side of the first equation, Flory used Equation 3.7 for the chemical potential of a polymer-solvent mixture, assuming that x is large. Reproduce Flory's steps to obtain Equation 3.32. Note: Need to distinguish between the molar volume of a repeat unit and that of a solvent molecule.

3.27 The following rates of crystallization of a PET sample at half the maximum amount of maximum crystallinity were published in 2001 [39]:

Low T (Cold Crystallization)		High T (Hot Crystallization)	
T (K)	λ (min)	T (K)	λ (min)
391.0	11.40	484.9	4.41
392.9	9.26	486.8	5.22
394.8	6.57	488.8	6.33
396.7	5.42	490.7	7.71
398.6	4.25	492.6	8.72
400.6	3.45	494.5	10.10

- (a) Plot these data in the form of $\log \lambda$ (min) versus T ($^{\circ}\text{C}$). Do they follow the same trend as reported in Figure 3.22?
- (b) Assuming that the maximum rate of crystallization of the present sample occurs as predicted by the empirical fit in Figure 3.22, that is, $\log \lambda = 0$ at $T = 173^{\circ}\text{C}$, interpolate the data plotted in part (a) into a quasi-continuous curve to predict data of faster crystallization rates than the researchers of the present data were able to achieve.

REFERENCES

1. Flory, P. J.: *Principles of Polymer Chemistry*, chap. 10, Cornell University Press, Ithaca, NY, 1952.
2. De Gennes, P. G.: *Scaling Concepts in Polymer Physics*, chap. I, Cornell University Press, Ithaca, NY, 1979.
3. De Gennes, P. G.: *Scaling Concepts in Polymer Physics*, chap. III, Cornell University Press, Ithaca, NY, 1979.
4. Daoud, M. et al.: *Macromolecules*, 8:804 (1975).
5. Marchetti, M., S. Prager, and E. L. Cussler: *Macromolecules*, 23:1760 (1990).
6. Patterson, D.: *Rubber Chem. and Technol.*, 40:1 (1967); *Macromolecules*, 2:672 (1969).
7. Sanchez, I. C., and R. H. Lacombe: *Macromolecules*, 11:1145 (1978).
8. Schmidt-Rohr, K., and H. W. Spiess: *Phys. Rev. Lett.*, 66:3020 (1991).
9. Hall, D. B. et al.: *Phys. Rev. Lett.*, 79:107 (1997).
10. Arbe, A. et al.: *Phys. Rev. Lett.*, 81:590 (1998).
11. Kanaya, T., and K. Keisuke: *Adv. Polym. Sci.*, 154:87 (2001).
12. Sillescu, H.: *J. Non-Cryst. Solids*, 243:81 (1999).
13. Flory, P. J., and H. K. Hall: *J. Am. Chem. Soc.*, 73:2532 (1951).
14. Kauzmann, W.: *Chem. Rev.*, 43:219 (1948).
15. Gibbs, J. H., and E. A. DiMarzio: *J. Chem. Phys.*, 28:373, 807 (1958); DiMarzio, E. A., and J. H. Gibbs: *J. Polym. Sci.*, 40:121 (1959).
16. Gordon, M.: chap. 4 in P. D. Ritchie (ed.), *Physics of Plastics*, Van Nostrand, Princeton, NJ, 1965.
17. Bueche, F.: *Physical Properties of Polymers*, chaps. 4 and 5, Wiley, New York, 1962.
18. Beevers, R. B., and E. F. T. White: *Trans. Faraday Soc.*, 56:744 (1960).
19. Runt, J. P.: *Encycl. Polym. Sci. Tech.*, 4:487 (1986).
20. Brandrup, J., and F. H. Immergut (eds.): *Polymer Handbook*, 3rd edn., Wiley, New York, 1989.

21. Lewis, O. G.: *Physical Constants of Linear Homopolymers*, Springer-Verlag, New York, 1968.
22. Sorenson, W. R., and T. W. Campbell: *Preparative Methods of Polymer Chemistry*, 2nd edn., Wiley, New York, 1968, p. 237.
23. Riggs, J. P.: in H. F. Mark, N. M. Bikales, C. G. Overberger, and G. Menges (eds.), *Encyclopedia of Polymer Science and Engineering*, vol. 2, 2nd edn., Wiley, New York, 1985, p. 640.
24. Gordon, M., and J. S. Taylor: *J. Appl. Chem.*, 2:493 (1952).
25. Adams, G., and J. H. Gibbs: *J. Chem. Phys.*, 43:139 (1965).
26. Lannon, D. A., and E. I. Hoskins: chap. 7 in P. D. Ritchie (ed.), *Physics of Plastics*, Van Nostrand, Princeton, NJ, 1965.
27. Fernandes, A. C., J. W. Barlow, and D. R. Paul: *J. Appl. Polym. Sci.*, 32:5481 (1986).
28. Till, P. H.: *J. Polym. Sci.*, 24:301 (1957).
29. Keller, A.: *Phil. Mag.*, 2:1171 (1957).
30. Keller, A.: *Rept. Progr. Phys.*, 31:623 (1968).
31. Anderson, F. R.: *J. Polym. Sci.*, C3:123 (1963).
32. Miller, M. L.: *The Structure of Polymers*, chap. 10, Reinhold, New York, 1966.
33. Rodriguez, F.: *J. Chem. Educ.*, 45:507 (1968).
34. Natta, G., and P. Corradini: *Rubber Chem. Technol.*, 33:703 (1960).
35. Peterlin, A.: *Text. Res. J.*, 42:20 (1972); Perkins, W. G., and R. S. Porter: *J. Mater. Sci.*, 12:2355 (1977).
36. Clark, F. S., and C. A. Garber: *Intern. J. Polym. Mater.*, 1:31 (1971).
37. Fujii, K. et al.: *J. Polym. Sci.*, A2:2347 (1964).
38. Rodriguez, F., and T. Long: *J. Appl. Polym. Sci.*, 44:1281 (1992); Cheremisinoff, N. P., and P. N. Cheremisinoff (eds.): *Handbook of Advanced Materials Testing*, chap. 18, Dekker, New York, 1995.
39. Lu, X. F., and J. N. Hay: *Polymer*, 42:9423 (2001).
40. Polmanteer, K. E., and M. J. Hunter: *J. Appl. Polym. Sci.*, 1:3 (1959).
41. Boyer, R. F.: *Rubber Chem. Technol.*, 36:1303 (1963).
42. Hieber, C. A.: *Polymer*, 36:1455 (1995).
43. Mandelkern, L.: *Rubber Chem. Technol.*, 32:1392 (1959).
44. Flory, P. J.: *Principles of Polymer Chemistry*, chap. 13, Cornell University Press, Ithaca, NY, 1952.
45. Mandelkern, L., and P. J. Flory: *J. Am. Chem. Soc.*, 73:3206 (1951).
46. Krigbaum, W. R., J. V. Dawkins, G. H. Via, and Y. I. Balta: *J. Polym. Sci.*, A2(4):475 (1966).
47. Magill, J. H.: in J. M. Schultz (ed.): *Treatise on Materials Science and Technology*, vol. 10A, Academic Press, New York, 1977.
48. Janeschitz-Kriegl, H.: *Crystallization Modalities in Polymer Melt Processing*, Springer-Verlag, Vienna, Austria, 2010.
49. Janeschitz-Kriegl, H. and G. Eder: *J. Macrom. Sci. B Phys.*, 46:591 (2007).
50. Bates, F. S., M. F. Schulz, A. K. Khandpur, S. Forster, and J. F. Rosedale: *Faraday Discuss.*, 98:7 (1994).
51. Schultz, M. F., and F. S. Bates: chap. 32 in J. E. Mark (ed.), *Physical Properties of Polymers Handbook*, American Institute of Physics Press, Woodbury, NY, 1996.
52. Wunderlich, B., and J. Grebowicz: *Adv. Polym. Sci.*, 60/61:1 (1988).
53. Samulski, E. T.: *Faraday Discuss.*, 79:7(1985).
54. Goodby, J. W.: *Science*, 231:350 (1986).
55. Ober, C. K., J.-I. Jin, and R. W. Lenz: *Adv. Polym. Sci.*, 59:103 (1984).
56. Hsiao, B. S., M. T. Shaw, and E. T. Samulski: *Macromolecules*, 21:543 (1988).
57. Ballauff, M.: chap. 5 in R. W. Cahn, P. Haasen, and E. J. Kramer (eds.), *Materials Science and Technology*, vol. 12, VCH, New York, 1993.

58. Ottenbrite, R. M., S. J. Huang, and K. Park (eds.): *Hydrogels and Biodegradable Polymers for Bioapplications*, American Chemical Society, Washington, DC, 1996.
59. Peppas, N. A., Y. Huang, M. Torres-Lugo, J. H. Ward, and J. Zhang: *Ann. Rev. Biomed. Eng.*, 2:9 (2000).
60. Saltzman, M. W.: *Drug Delivery: Engineering Principles for Drug Therapy*, Oxford University Press, Oxford, 2001.
61. Hirotsu, S., Y. Hirokawa, and T. Tanaka: *J. Chem. Phys.*, 87:1392 (1987).
62. Marchetti, M., S. Prager, and E. L. Cussler: *Macromolecules*, 23:3445 (1990).
63. Tanaka, T. et al.: *Phys. Rev. Lett.*, 45:1636 (1980).
64. Yin, D.-W., Q. Yan, and J. J. de Pablo: *J. Chem. Phys.*, 123:174909 (2005); Yin, D.-W., F. Horkay, J. F. Douglas, Q. Yan, and J. J. de Pablo: *J. Chem. Phys.*, 129:154902 (2008).
65. Quinn, F. A., Jr., and L. Mandelkern: *J. Am. Chem. Soc.*, 80:3178 (1958).
66. Anderson, C. C., and F. Rodriguez: *Proc. ACS Div. Polym. Mat. Sci. Eng.*, 51:609 (1984).

GENERAL REFERENCES

- Bassett, D. C. (ed.): *Developments in Crystalline Polymers—I*, Elsevier Applied Science, New York, 1985.
- Bicerano, J.: *Computational Modeling of Polymers*, Dekker, New York, 1992.
- Bicerano, J.: *Prediction of Polymer Properties*, Dekker, New York, 1993.
- Birley, A. W., B. Haworth, and J. Batchelor: *Physics of Plastics: Processing, Properties and Materials Engineering*, Hanser-Gardner, Cincinnati, OH, 1992.
- Carfagna, C. (ed.): *Liquid Crystalline Polymers*, Pergamon Press, New York, 1994.
- Craver, C. D., and T. Provder (eds.): *Polymer Characterization: Physical Property, Spectroscopic, and Chromatographic Methods*, American Chemical Society, Washington, DC, 1990.
- Fleer, G. I., M. A. C. Stuart, J. M. H. M. Scheutjens, T. Cosgrove, and B. Vincent: *Polymers at Interfaces*, Chapman & Hall, New York, 1993.
- Geil, P. H.: *Polymer Single Crystals*, Wiley-Interscience, New York, 1963.
- Gelin, B. R.: *Molecular Modeling of Polymer Structures and Properties*, Hanser-Gardner, Cincinnati, OH, 1994.
- Gordon, M., and N. A. Plate (eds.): *Liquid Crystal Polymers III/III*, Springer-Verlag, New York, 1984.
- Gruenwald, G.: *Plastics: How Structure Determines Properties*, Hanser-Gardner, Cincinnati, OH, 1992.
- Harland, R. S., and R. K. Prud'homme (eds.): *Polyelectrolyte Gels: Properties, Preparation, and Applications*, American Chemical Society, Washington, DC, 1992.
- Hartwig, G.: *Polymer Properties at Room and Cryogenic Temperatures*, Plenum Press, New York, 1995.
- Haward, R. N. (ed.): *The Physics of Glassy Polymers*, Wiley, New York, 1973.
- Hope, P. S., and M. J. Folkes (eds.): *Polymer Blends and Alloys*, Chapman & Hall, New York, 1993.
- Hunt, B. J., and M. I. James (eds.): *Polymer Characterization*, Chapman & Hall, New York, 1993.
- Koenig, J. L.: *Chemical Microstructure of Polymer Chains*, Wiley, New York, 1980.
- Kovarskii, A. L. (ed.): *High-Pressure Chemistry and Physics of Polymers*, CRC Press, Boca Raton, FL, 1994.
- Mark, J. F., A. Eisenberg, W. W. Graessley, L. Mandelkern, E. T. Samulski, J. L. Koenig, and G. D. Wignall: *Physical Properties of Polymers*, 2nd edn., American Chemical Society, Washington, DC, 1993.
- McArdle, C. B. (ed.): *Side Chain Liquid Crystal Polymers*, Chapman & Hall, New York, 1989.
- McArdle, C. B.: *Applied Photochromic Polymer Systems*, Chapman & Hall, New York, 1991.

- Mitchell, J., Jr. (ed.): *Applied Polymer Analysis and Characterization*, Hanser-Gardner, Cincinnati, OH, 1992.
- Monnerie, L., and U. W. Suter: *Atomistic Modeling of Physical Properties*, Springer-Verlag, Berlin, Germany, 1994.
- Paul, D. R., and C. B. Bucknall: *Polymer Blends*, Wiley, New York, 2000.
- Peterlin, A. (ed.): *Plastic Deformation of Polymers*, Dekker, New York, 1971.
- Plate, N. A. (ed.): *Liquid-Crystal Polymers*, Plenum Press, New York, 1993.
- Porter, D.: *Group Interaction Modelling of Polymer Properties*, Dekker, New York, 1995.
- Robeson, L., and L. M. Robeson: *Polymer Blends: A Comprehensive Review*, Hanser-Gardner, Cincinnati, OH, 2007.
- Roe, R.-J.: *Methods of X-ray and Neutron Scattering in Polymer Science*, Oxford University Press, New York, 2000.
- Sawyer, L., D. T. Grubb, and G. F. Meyers: *Polymer Microscopy*, 3rd edn., Springer, New York, 2008.
- Schröder, E., G. Müller, and K.-F. Arndt: *Polymer Characterization*, Hanser-Gardner, Cincinnati, OH, 1989.
- Seymour, R. B., and C. F. Carraher, Jr.: *Structure–Property Relationships in Polymers*, Plenum Press, New York, 1984.
- Sharma, K. R.: *Polymer Thermodynamics: Blends, Copolymers and Reversible Polymerization*, CRC Press, Boca Raton, FL, 2011.
- Stroeve, P., and A. C. Balazs (eds.): *Macromolecular Assemblies in Polymeric Systems*, American Chemical Society, Washington, DC, 1992.
- Struik, L. C. F.: *Internal Stresses, Dimensional Instabilities and Molecular Orientations in Plastics*, Wiley, New York, 1990.
- Thomas, E. L. (ed.): *Materials Science and Technology: Structure and Properties of Polymers*, VCH, New York, 1993.
- Urban, M. W., and C. D. Craver (eds.): *Structure–Property Relations in Polymers: Spectroscopy and Performance*, American Chemical Society, Washington, DC, 1993.
- Utracki, L. A.: *Polymer Alloys and Blends*, Hanser-Gardner, Cincinnati, OH, 1990.
- Utracki, L. A. (ed.): *Two-Phase Polymer Systems*, Hanser-Gardner, Cincinnati, OH, 1991.
- van Krevelen, D. W., and K. T. Nijenhuis: *Properties of Polymers*, 4th edn., Elsevier, Amsterdam, The Netherlands, 2009.
- Weiss, R. A., and C. K. Ober (eds.): *Liquid-Crystalline Polymers*, American Chemical Society, Washington, DC, 1990.
- Woodward, A. F.: *Atlas of Polymer Morphology*, Hanser Publishers, New York, 1988.
- Wunderlich, B.: *Macromolecular Physics/Crystal Melting*, Academic Press, New York, 1980.
- Yang, H. (ed.): *Polymer Morphology*, Nova Science Publications, Hauppauge, NY, 2002.

4 Polymer Formation

4.1 POLYMERIZATION REACTIONS

Polymerization is the process of joining together small molecules by covalent bonds to produce high-molecular-weight polymers. Both natural and synthetic polymers are built from these simple small molecular units known as monomers. However, the range of properties that can be achieved depends on the strategy used to assemble these units. This chapter covers many of the synthetic strategies used to build polymers and provides examples of several of the commercial polymers made with these techniques.

There are basically two approaches to polymer formation: **chain-growth** and **step-growth** polymerization. Chain-growth polymerization involves combining monomers with similar reactive functions starting from a single reactive site and growing the polymer chain from that site. The reactive chain site can be a cation, an anion, or a radical. The type of chain-growth polymerization selected depends on the monomer to be used and the requirements of the target polymer. Among the recent inventions in polymerization chemistry has been *living polymerization* that permits the growth of polymer chains with identical molecular weights and enables the creation of block copolymers or other polymers with well-controlled structures.

Certain transition metals will also catalyze polymer formation with hydrocarbon vinyl monomers. This work resulted in the Nobel Prize in Chemistry in 1955. Such polymers include polyethylene and polypropylene and are among the largest volume polymers produced. More recently the 2000 Nobel Prize in Chemistry has been awarded for the discovery of conducting polymers, also first made by metal-catalyzed chain-growth polymerization. More recently again, the 2005 Nobel Prize in Chemistry has been awarded for work on ring-opening metathesis polymerization and the development of new functional group-tolerant catalysts for this polymerization reaction. These prizes indicate that polymer chemistry continues to be a vibrant, rapidly evolving field.

Step-growth polymerization involves the combination of monomer units with other units having complementary chemical functions. Most natural polymers such as proteins or polysaccharides are made from enzymatically mediated step-growth processes. Most high-performance synthetic polymers (e.g., high strength, high thermal stability, high thermal conductivity) are prepared using these methods because step-growth processes enable the introduction of robust species in the polymer backbone. Most liquid crystalline polymers, such as those used to make bulletproof or fire-resistant articles, fall in this category. The formation of these and other polymers will be discussed in this chapter.

Around the turn of the last century, chemists were reluctant to accept the idea of rubber, starch, and cotton as long, linear chains connected by covalent bonds. A popular alternative was the idea of an *associated colloidal* structure. As a matter of fact, some small molecules do exhibit such behavior. Soap molecules will associate into complex liquid crystalline structures and are used as the basis for the formation of mesoscopic solids. Other surfactant molecules such as the phospholipids present in the wall of many living cells will form micelles and vesicles. However, the effective molecular weight of such structures varies with concentration and temperature, whereas the molecular weights of true polymers with covalent links do not.

The reactions by which some complex, naturally occurring macromolecules are formed are not completely understood. Even *cis*-polyisoprene, natural rubber, which can be made in a single step from isoprene in the laboratory, is synthesized by a rather complex series of reactions in the rubber tree.

The ultimate starting materials for synthetic polymers are few in number. Petroleum, natural gas, coal tar, and cellulose are the main sources. In recent years, ethylene and propylene from natural gas and petroleum refining have been used as a starting point for a variety of monomers as well as serving as key monomers. The process of building up polymers from simple repeating units (monomers) can proceed with many variations. We can classify some of these as follows:

1. By the kinetic scheme governing the polymerization reaction: chain versus stepwise reactions
2. By the functionality, that is, the number of bonds each monomer can form in the reaction used
3. By the chemical reaction used to produce new bonds: vinyl addition, esterification, amidation, ester interchange, and so on
4. By the number of monomers used in the final polymer: homopolymer, copolymer, terpolymer, and so on
5. By the process used in the polymerization: bulk, solution, suspension, or emulsion polymerization

4.2 FUNCTIONALITY

While the kinetic scheme of polymerization is the most important method for classifying polymerization types, it is important to understand monomer functionality before we continue. Monomer can be converted to polymer by any reaction that creates new bonds. Fundamental to any polymerization scheme is the number of bonds that a given monomer can form. Carothers, focusing largely on step-growth polymers, defined this number of bonds as the functionality of a monomer in a given reaction. Examples are given below in Figure 4.1. It should be obvious that a functionality of 2 can lead to a linear structure. For example,

a monomer with one acid and one amine group has a functionality of 2. While monomers that polymerize through such functional groups have easily recognizable functionality, that is not always the case. For example, vinyl groups have an intrinsic functionality of 2, and thus ethylene polymerization can lead to a linear polymer even though only one functional group is involved. The necessity for

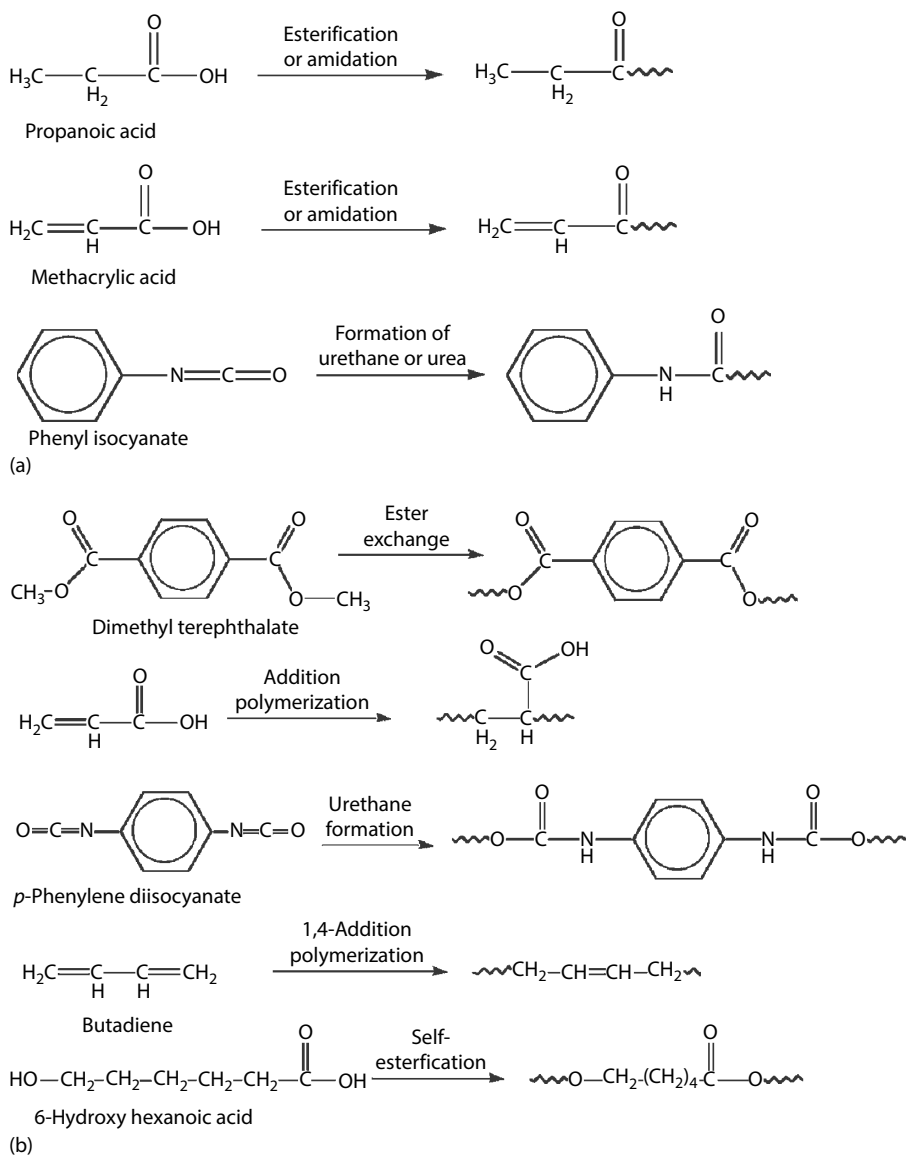


FIGURE 4.1 Functionality and structure. (a) Functionality of 1 (A—); (b) functionality of 2 (—B—);

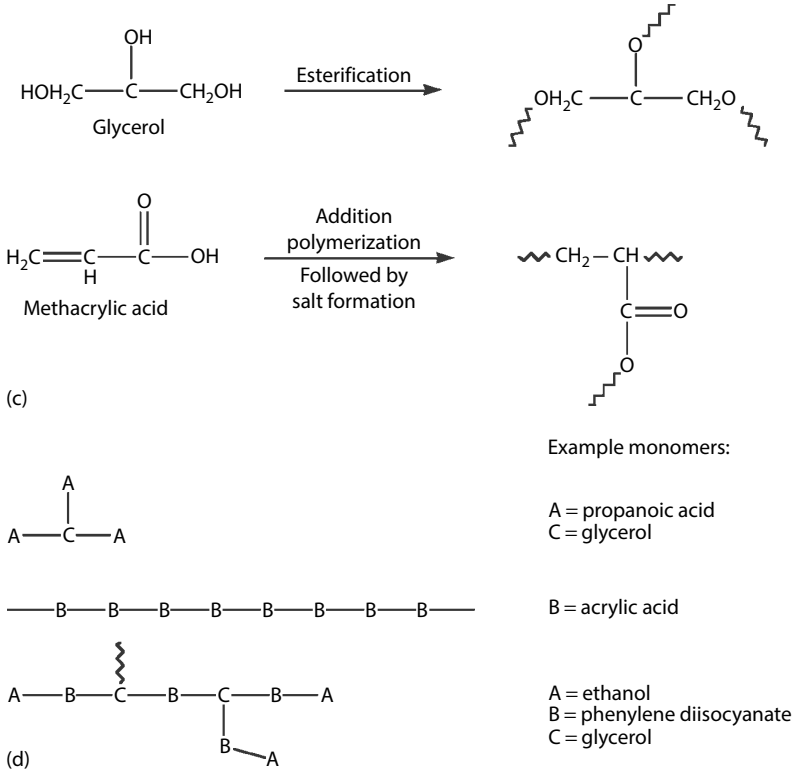
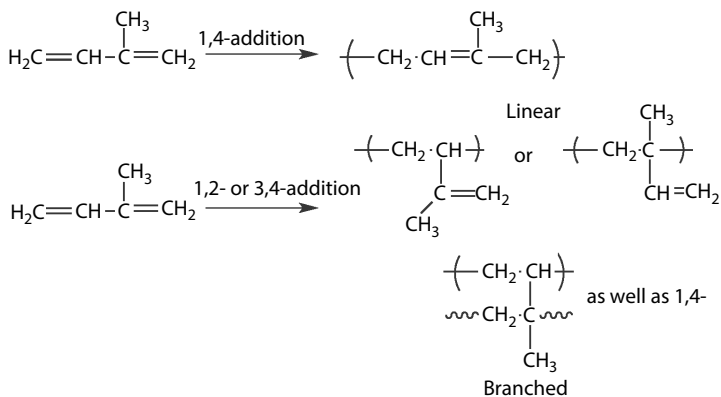


FIGURE 4.1 (Continued) (c) functionality of 3 ($\text{---}\overset{|}{\text{C}}\text{---}$); (d) structures.

specifying the reaction is emphasized by a monomer such as isoprene, which can react in several ways. Natural rubber is a form of 1,4-polyisoprene as shown in the following scheme:



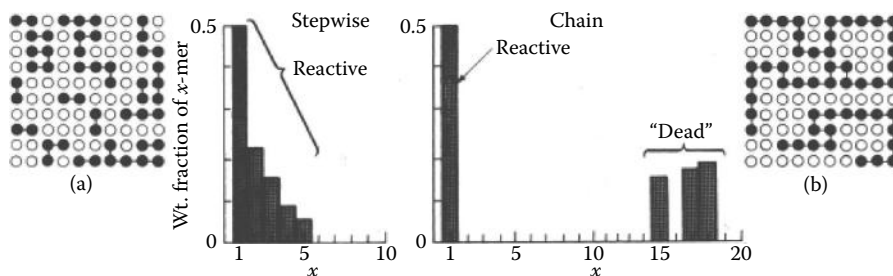


FIGURE 4.2 Histograms of weight fraction versus degree of polymerization (x) for the examples of step-growth polymerization and chain polymerization. Inset (a) shows many small chains formed during step-growth polymerization, whereas inset (b) shows the fewer large chains formed during the initial stages of chain-growth polymerization.

4.3 STEP- AND CHAIN-GROWTH POLYMERIZATIONS

We can imagine two extremes of simplified behavior in the conversion of monomer to polymer. In a typical stepwise polymerization, each polymer strand formed can react further with monomer or other polymers. In order to describe the size of a polymer, often the degree of polymerization, x , is used. This refers to the number of monomer repeat units in the polymer. Each dimer ($x = 2$), trimer ($x = 3$), and so on is just as reactive as a monomer. By contrast, in a typical chain polymerization each polymer is formed in a comparatively short time, and then is *dead* and remains unchanged by reaction with any remaining monomer. Growing chains can add monomer, but neither monomer itself nor dead polymer can add monomer. Monomer, growing polymer, and dead polymer are quite different from one another in terms of reactivity.

The initial distribution of molecular size is quite different for the two cases (Figure 4.2). Further reaction of the stepwise polymer will gradually change the distribution toward higher values of x , the number of monomer units in a polymer. Further reaction in the chain polymer system will diminish the monomer concentration, but will also increase the quantity of polymer at high values of x .

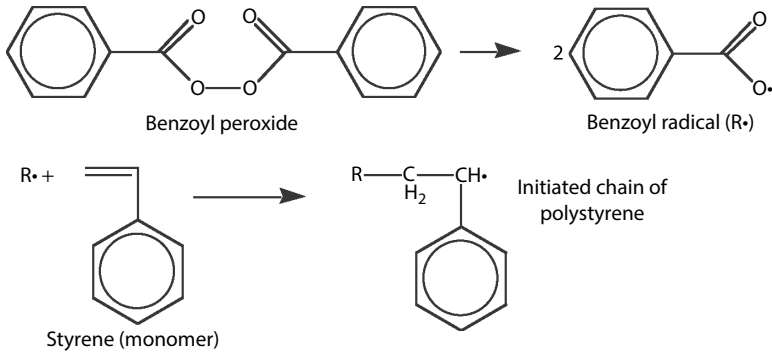
While these extremely simplified cases are met in practice, some very important exceptions occur that show the need for caution in making generalizations. For example, nylon 6 would normally be considered as a step-growth polymer because it is a polyamide. However, it can also be produced by a ring-opening polymerization that is a kind of chain-growth polymerization. Thus, these definitions are useful but can sometimes be misleading.

4.4 CHAIN POLYMERIZATION

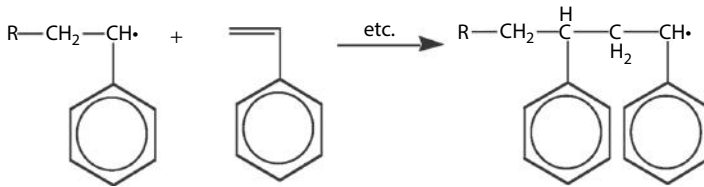
4.4.1 KINETIC SCHEME

Ethenic polymerization is an economically important class of polymer-forming reactions whose kinetics typifies chain-growth polymerization [1]. The terms *vinyl*, *olefin*, or *addition polymerization* are often used, although they are more restrictive. Usually three stages are essential to the formation of a useful high polymer.

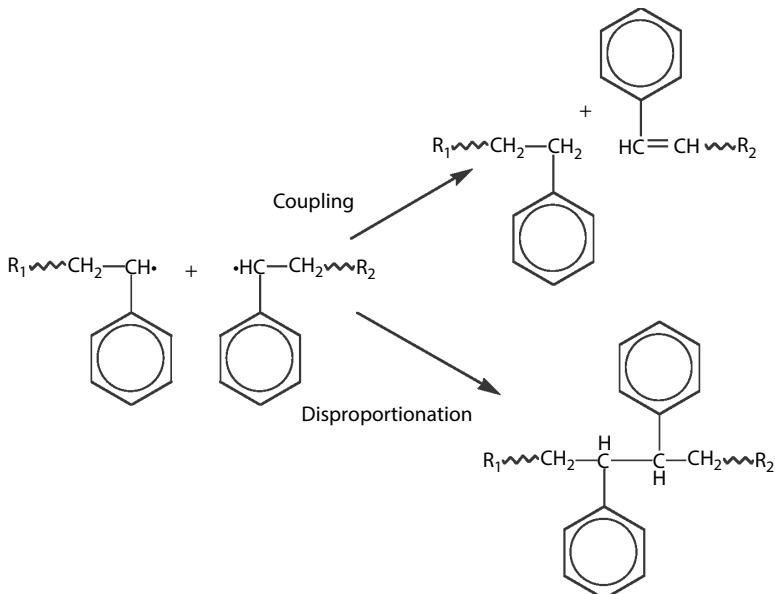
1. **Initiation** is the creation of an *active* center such as a free radical, a carbanion, or a carbonium ion. For example, radicals formed by the thermal dissociation of benzoyl peroxide can initiate the chain polymerization of styrene.



2. **Propagation** involves the addition of more monomer to the reactive site at the growing chain end—usually the final molecular weight can be achieved very rapidly (e.g., a degree of polymerization of 10^5 can be achieved in 0.1 s).

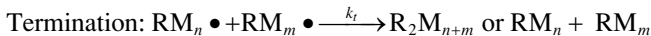
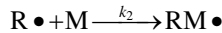
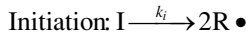


3. **Termination** is the disappearance of an active center.



The mode of termination can have an effect on final molecular weight. If termination is through coupling, then the final molecular weight is twice what would be expected if termination occurs through disproportionation. Other propagating systems are described in Sections 4.5 and 4.6.

A shorthand notation for these reactions is as follows:



As seen here, each reaction is characterized by a rate constant. It is a cornerstone of polymerization theory that the reactivity of a growing polymer chain depends almost completely on the last unit added and not on previously added units or on the length of the chain. Therefore, k_p is the same for a chain of any length.

The kinetic model consistent with this mechanism is simple, provided that the following assumptions are valid (quantities in brackets are concentrations, e.g., moles per liter):

1. Reaction proceeds slowly enough that a steady state is reached where the radical population does not change rapidly with time.

$$\left(\frac{d[R \bullet]}{dt} \text{ and } \frac{d[M \bullet]}{dt} = 0 \right)$$

Material balances then give

$$2k_i[I] - k_2[R \bullet][M] = \frac{d[R \bullet]}{dt} = 0 \quad (4.1)$$

$$k_2[R \bullet][M] - 2k_t[M \bullet]^2 = \frac{d[M \bullet]}{dt} = 0 \quad (4.2)$$

2. The propagation reaction occurs so much more often than the other reactions that it is effectively the only process that consumes monomer.

$$\text{Rate of polymerization} = R_p = \frac{-d[M]}{dt} = k_p[M \bullet][M] \quad (4.3)$$

Under these conditions, we get first-order dependence on monomer and half-order dependence on initiator:

$$R_p = k_p \left(\frac{k_i}{k_t} \right)^{0.5} [M][I]^{0.5} \quad (4.4)$$

If only a certain fraction f of initiator fragments can successfully react with monomer, we have

$$R_p = k_p \left(\frac{fk_i}{k_t} \right)^{0.5} [M][I]^{0.5} \quad (4.5)$$

As a first approximation, f will be assumed here to be unity. Actual values often are in the range of 0.8 ± 0.2 .

Frequently in experimental studies the monomer concentration is measured as a function of time for various starting concentrations of monomer and initiator and at various temperatures. When making high-molecular-weight polymers, relatively few initiator molecules will be consumed compared to the number of monomer molecules. If $[I]$ can be assumed to be essentially constant, Equation 4.4 can be integrated to give

$$\ln \frac{[M]_0}{[M]} = k_p \left(\frac{k_i}{k_t} \right)^{0.5} [I]^{0.5} t \quad (4.6)$$

A semilog plot of concentration versus time should give a line with an intersection for $t = 0$ at the initial concentration and a slope related to the rate constants and initiator concentration (Figure 4.3). For various reasons, such as diffusion-controlled reaction or more complex mechanisms, the experimental order for a polymerization may be more or less than one. We shall see later (Section 5.5) that an emulsion polymerization may be zero order in overall monomer concentration. If conversion is

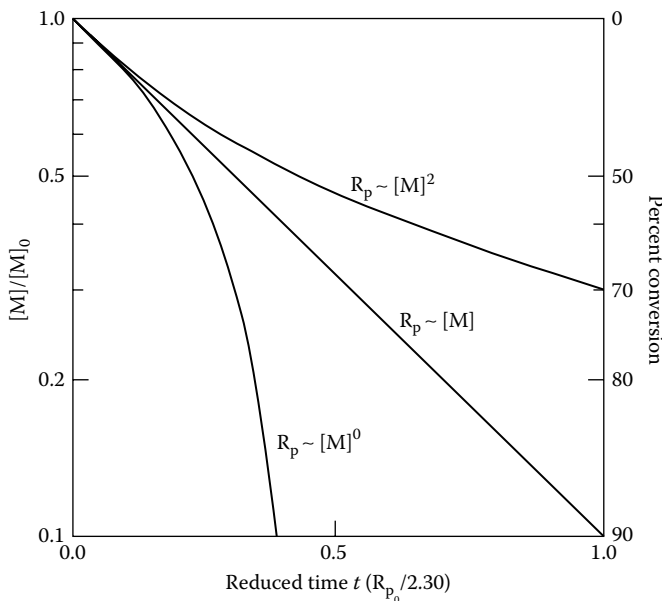


FIGURE 4.3 Concentration–time plots for three polymerizations having the same rate of monomer consumption, initially R_{p_0} but having a rate that depends on monomer concentration to the zero, first, or second power.

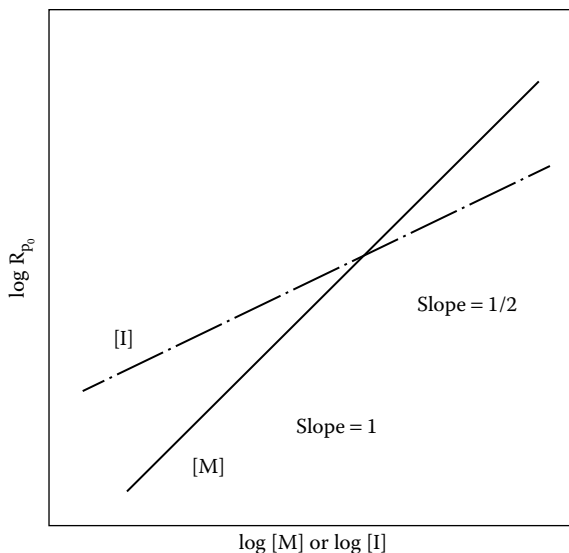


FIGURE 4.4 Expected correlation of initial rate R_{p_0} , with initial concentrations of initiator I or monomer M.

followed only to 50% conversion (Figure 4.3), the slight curvature presented by zero to second-order reactions may not be readily seen. However, systematic errors in concentration analysis, heat transfer, or induction periods can produce curvature in such plots, which then relate to no fixed order. The deviations of many polymerizations from first-order kinetics (and half-order in initiator) often are a valuable clue to unraveling the sequence of reaction steps. Another check on the order is to plot the polymerization rate, often the initial rate, against the initial concentration of monomer and initiator (Figure 4.4). This is also a strategy used to determine kinetic information during chain copolymerization reactions, discussed later in Section 4.10. The complication of simultaneous depletion of monomer and initiator is minimized here.

Example 4.1

In the laboratory, 100 g of monomer M and 1.00 g of peroxide Z are dissolved to make 1.000 l of a solution in toluene. After 15.0 min at 70°C, the polymerization is stopped and the polymer is precipitated by the addition of methanol. After drying, the yield of polymer is 20.0 g. Assuming that the concentration of initiator and the density of the solution change negligibly, what percentage conversion can be expected in 2.00 h for a plant batch that consists of 200 kg of monomer with 1.50 g of peroxide in 2500 l of solution in toluene at 70°C?

Solution: Let K be the rate constants lumped together and FW be the formula weight of the peroxide. Then, in the laboratory preparation (using Equation 4.6),

$$\ln 1.25 = K \left(\frac{1.00}{\text{FW}} \right)^{1/2} 15.0$$

In the plant batch,

$$\ln \left(\frac{[M]_0}{[M]} \right) = K \left(\frac{1.50}{2.50 \times \text{FW}} \right)^{1/2} 120$$

Thus,

$$\ln \left(\frac{[M]_0}{[M]} \right) / \ln 1.25 = \left(\frac{1.50}{2.50} \right)^{1/2} \frac{120}{15.0}$$

$$\frac{[M]_0}{[M]} = 3.99$$

$$\text{Percentage conversion} = \frac{100([M] - [M]_0)}{[M]_0} = 74.9\%$$

4.4.2 INDIVIDUAL RATE CONSTANTS

The individual rate constants in Equations 4.4 and 4.5 are not determined by the experiments described so far. The initiation rate k_i can be evaluated from studies using no monomer. The decomposition of a typical initiator is a first-order process:

$$-\frac{d[I]}{dt} = k_i[I] \quad (4.7)$$

The integrated form is

$$\ln \left(\frac{[I]}{[I]_0} \right) = -k_i t \quad (4.8)$$

Another way of expressing the rate constant is by specifying the time it takes for the concentration of undecomposed initiator to fall to half its original value. The *half-life* is

$$t_{1/2} = \frac{0.693}{k_i} \quad (4.9)$$

As is the case with most of the rate constants, the temperature dependence of k_i can be correlated by an Arrhenius expression:

$$k_i = A \exp \left(\frac{-E_i}{RT} \right) \quad (4.10)$$

where:

E_i is the energy of activation for the decomposition process

Some typical values of $t_{1/2}$ as a function of temperature for organic peroxides are shown in Figure 4.5. In Table 4.1 a few other radical sources are compared with two commonly used peroxides.

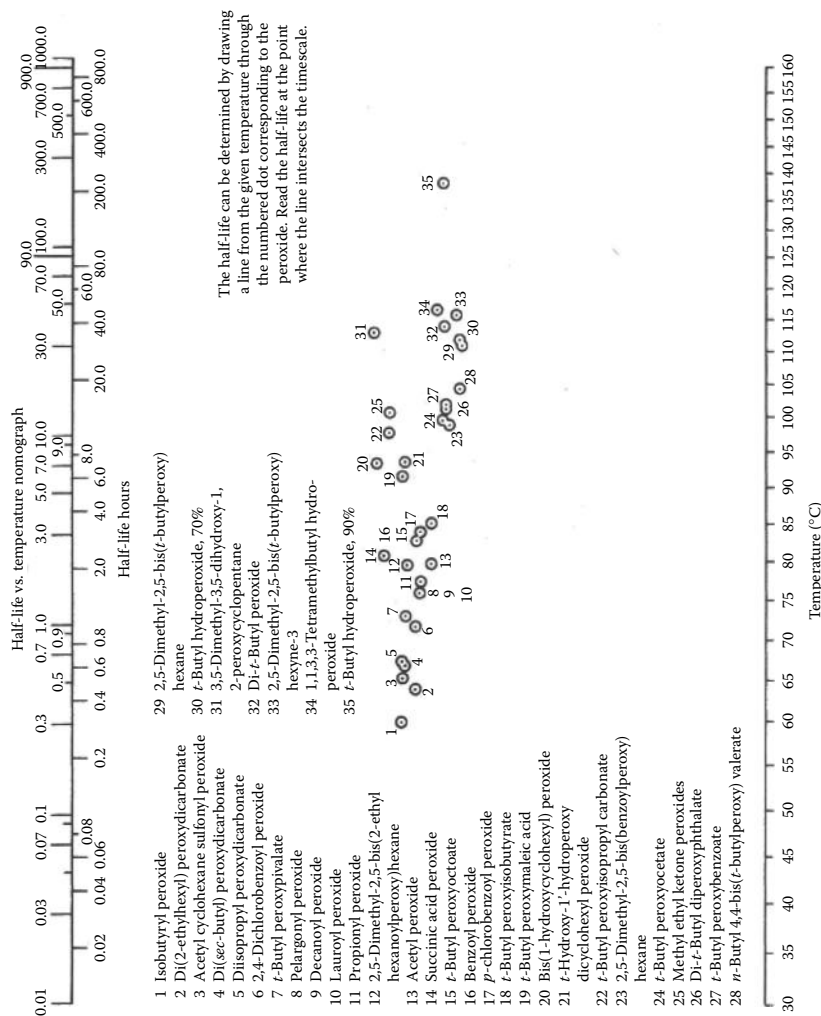


FIGURE 4.5 Thermal stability of organic peroxides as indicated by time for decomposition of 50% of the original charge (half-life for first-order reaction). (Data from Wallace and Trieman Company, *Lucidol Organic Peroxides*, Lucidol Division, Wallace and Trieman, Buffalo, NY, 1968.)

TABLE 4.1
Typical Rate Constants for Selected Free-Radical Initiators

Name and Formula	FW	<i>T</i> (°C)	<i>k_i</i> (s ⁻¹)	<i>E_i</i> (kJ/mol)
2,2'-Azobisisobutyronitrile CH ₃ C(CN)—N=N—C(CN)CH ₃	164.2	60	9.15 × 10 ⁻⁶	129
Benzoyl peroxide (C ₆ H ₅ CO) ₂ O ₂	242.2	60	2.76 × 10 ⁻⁶	124
Dicumyl peroxide [C ₆ H ₅ C(CH ₃) ₂] ₂ O ₂	270.4	115	2.05 × 10 ⁻⁵	159
4,4'-Azobis(4-cyanovaleric acid) ^a HOOCCH ₂ CH ₂ C(CH ₃)(CN)—N=N—C(CN) (CH ₃)CH ₂ CH ₂ COOH	280.3	80	8.97 × 10 ⁻⁵	141
Potassium persulfate ^a K ₂ S ₂ O ₈	270.3	30	8.83 × 10 ⁻¹⁰	139

Source: Brandrup, J., and E. H. Immergut: *Polymer Handbook*, 3rd edn. 1989. New York. Copyright Wiley-VCH Verlag GmbH & Co. KGaA; Kolthoff, I. M., and I. K. Miller, *J. Am. Chem. Soc.*, 73, 3055, 1951.

^a Water soluble.

The integrated form of the polymerization equation (Equation 4.6) can be modified to take into account the time dependence of initiator concentration. Equation 4.8 is rewritten as

$$[I] = [I]_0 \exp(-k_i t) \quad (4.11)$$

This result combined with Equation 4.4 yields

$$-\frac{d[M]}{dt} = \left(\left[\frac{k_p^2}{k_t} \right] \right)^{0.5} (k_i)^{0.5} [M][I]^{0.5} \exp\left(-\frac{k_i t}{2}\right) \quad (4.12)$$

The following equation is then obtained by integration between time 0 and *t* (and letting *y* = *k_it*):

$$\ln \left(\frac{[M]}{[M]_0} \right) = \left(\frac{k_p^2}{k_t} \right)^{0.5} [I]_0^{0.5} \left(\frac{2}{y} \right) \left[1 - \exp\left(-\frac{y}{2}\right) \right] \quad (4.13)$$

When *y* is very small, Equation 4.13 reduces to Equation 4.6. For example, when *y* = 0.1, the quantity (2/*y*)[1 - exp(-*y*/2)] = 0.975. Although the equation is more exact than Equation 4.6, it is not explicit in time. However, a trial-and-error solution for time will usually converge rapidly.

Example 4.2

When peroxide A is heated at 60°C in an inert solvent, it decomposes by a first-order process. An initial concentration of 5.00 mmol/liter changes to 4.00 mmol/liter after 1.00 h. Next, a solution of peroxide (0.400 mmol/liter) and monomer is held at 60°C. Additional data: $k_p = 1.8 \times 10^4$ liter/mol s and $k_t = 1.45 \times 10^7$ liter/mol s.

- (a) What is the concentration of initiator after 10.0 min?
 (b) What fraction of monomer should remain unconverted after 10.0 min?

Solution:

- (a) From Equation 4.8,

$$\ln 0.800 = -k_i 3600 \text{ while } k_i = 62.0 \times 10^{-6} \text{ s}^{-1}$$

In the polymerization,

$$\ln\left(\frac{[I]}{4.00}\right) = -62.0 \times 10^{-6} \times 600 = 0.0372; [I] = 0.385 \text{ mmol/liter}$$

- (b) From Equation 4.13,

$$\frac{2}{y} \left[1 - \exp\left(\frac{-y}{2}\right) \right] = 0.991$$

$$\ln\left(\frac{[M]}{[M]_0}\right) = (1.8 \times 10^4) \left(\frac{62.0 \times 10^{-6} \times 4.00 \times 10^{-4}}{1.45 \times 10^7} \right)^{1/2} 600 \times 0.991$$

$$-\ln\left(\frac{[M]}{[M]_0}\right) = 0.443$$

$$\frac{[M]}{[M]_0} = 0.642 \text{ (unconverted fraction of monomer remaining)}$$

A complication in using tabulated values for k_t is that not every radical produced initiates a chain. To measure the effective number of radicals, it is necessary to carry out an actual polymerization or a reaction with a compound that is known to react in the same way as monomer but more easily analyzed. If k_t is known with confidence from one monomer reaction, it can be used in others in order to separate a value of $k_p/(k_t)^{0.5}$ for the individual monomer. Some of the latter are listed in Table 4.2. A further separation of k_p from k_t is more difficult, but it can be attained by several methods. One of these is intermittent photoinitiation, which gives a measure of chain-growth rate [5]. Another method is emulsion polymerization with a known particle population (Section 5.5). Some experimentally derived values for k_p and k_t are given in Table 4.2.

TABLE 4.2
Selected Propagation and Termination Rate Constants

Monomer	Temperature (°C)	k_p^2/k_t ($\times 10^3$ liter/ mol-s)	k_p (liter/ mol-s)	k_t ($\times 10^{-6}$ liter/ mol-s)	E_p (kcal/mol)	E_t (kcal/mol)
Acrylamide	25	22,000	28,000	14.5		
Methyl acrylate	30	120	720	4.3	7	5
	60	460	2,090	9.5		
Methyl methacrylate	30	3.0	251	21	5	0.5
	60	10	515	25.5		
	80	21	800	30.5		
Styrene	50	0.38	209	115	7	2
Vinyl acetate	60	240	9,500	280	7	5
Vinyl chloride	25	35	6,200	1,100	4	4

Source: Brandrup, J., and E. H. Immergut: *Polymer Handbook*, 2nd edn. 1975. New York, 11.47–11.52. Copyright Wiley-VCH Verlag GmbH & Co. KGaA.

4.4.3 MOLECULAR SIZE

The molecular weight that results from a chain polymerization with simple kinetics can be deduced from the scheme outlined so far. First, it is necessary to define the kinetic chain length and the degree of polymerization. The **kinetic chain length** v_n is the number of monomer units converted per initiating radical, so that

$$v_n = \frac{\text{Rate of monomer consumption}}{\text{Rate of radical formation}} = \frac{R_p}{2k_t[I]} \quad (4.14)$$

Using Equation 4.5 with $f = 1$, we get

$$v_n = \frac{k_p}{2} (k_i k_t)^{-0.5} [M][I]^{-0.5} \quad (4.15)$$

The number-average degree of polymerization x_n is

$$x_n = \frac{\text{Total monomer units in system that have reacted}}{\text{Total molecules in system}} \quad (4.16)$$

The corresponding molecular weight (M_n) is simply x_n multiplied by the formula weight of the repeat unit (the monomeric molecular weight).

It should be noted that, by convention, in stepwise polymerization, unreacted monomer is included in the numerator of Equation 4.16. However, in chain polymerization, unreacted monomer usually is not included. Likewise, unreacted monomer molecules are counted in the denominator for step-growth polymerization but not for chain polymerization. The rationale for this is based on the usual discontinuity

between monomer and polymer in chain polymerizations (Figure 4.2), while we must keep track of all unreacted chemical functions on both monomer and polymer in the step-growth polymerization. If termination is by **disproportionation**, x_n is the same as v_n ; if by coupling, $x_n = 2v_n$. Both mechanisms are important in practice. For example, styrene terminates almost exclusively by coupling, whereas methyl methacrylate (MMA) typically terminates 58% by disproportionation and 42% by coupling [7].

Example 4.3

Assume that methyl acrylate terminates by coupling, $(k_p^2/k_t) = 0.460$ liter/mol s at 60°C (Table 4.2). If an azo initiator compound with a half-life of 10.0 h at this temperature is used to initiate polymerization of a solution of 260.0 g of monomer in toluene (to make 1.000 liter), what concentration of initiator will give an initial number-average molecular weight of 500,000? What will be the initial rate of conversion?

Solution:

$$x_n = \frac{500,000}{86.09} = 5,810 \text{ repeat units per molecule}$$

$$k_t = \frac{0.693}{36,000} = 19.3 \times 10^{-6} \text{ s}^{-1}; [M]_0 = \left(\frac{260.0}{86.09} \right) = 3.02 \text{ mol/liter}$$

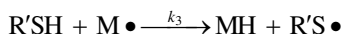
In Equation 4.15, $x_n = 2v_n$ and

$$5810 = \left(\frac{0.460}{19.3 \times 10^{-6}} \right)^{1/2} \times 3.02 [I]_0^{-1/2}; [I]_0 = 80.2 \text{ mmol/liter}$$

$$\begin{aligned} -\left(\frac{d[M]}{dt} \right)_0 &= [0.460 \times (19.3 \times 10^{-6}) \times (80.2 \times 10^{-3})]^{1/2} \times 3.02 \\ &= 2.55 \times 10^{-3} \text{ mol/liter-s or } 9.18 \text{ mol/liter-h} \end{aligned}$$

4.4.4 CHAIN TRANSFER AND INHIBITION

It often happens that x_n is much smaller than v_n in a chain polymerization. A major reason for this is **chain transfer**. For example, a molecule such as dodecyl mercaptan ($C_{12}H_{25}SH$ or $R'SH$) is widely used as a **chain transfer agent** (CTA) where it is desirable to decrease molecular weight in radical polymerization. The agent enters the propagation scheme by giving up a proton to the growing radical chain, terminating it, but possibly initiating a new chain.



If $k_3 \cong k_4 \cong k_p$, the interposing of such an agent will not change v_n , but it will decrease x_n , since more than one dead polymer chain has been formed from one initiating

fragment ($R\bullet$). In the commercial production of styrene-butadiene rubber, dodecyl mercaptan might be added at a ratio of 1 part of mercaptan to 200 parts monomer, enough to reduce the average molecular weight severalfold. Of course, other species present during polymerization can act as CTAs. Solvent, initiator, monomer, or polymer sometimes are involved. In the simple case of only one transfer reaction with constant k_3 and with k_4 large compared to k_3 , the rate of radical termination leading to new molecules is increased by the number of times the radical is transferred:

$$\text{Rate of molecule generation} = Yk_t [M\bullet]^2 + k_3 [R'SH][M\bullet] \quad (4.17)$$

where:

Y has a value of 1 if termination is by coupling and a value of 2 if termination is by disproportionation

Then the degree of polymerization becomes

$$x_n = \frac{k_p [M][M\bullet]}{\text{Rate of molecule generation}} \quad (4.18)$$

Rearranging and substituting Equation 4.17 into 4.18,

$$(x_n)^{-1} = \frac{Yk_t [M\bullet]}{k_p [M]} + \frac{k_3 [R'SH]}{k_p [M]} \quad (4.19)$$

or

$$(x_n)^{-1} = (x_n)_0^{-1} + \frac{C_s [R'SH]}{[M]} \quad (4.20)$$

where:

$(x_n)_0$ is the number-average degree of polymerization that would occur in the absence of any chain transfer

A plot of $(x_n)^{-1}$ versus $[R'SH]/[M]$ will give a straight line with an intercept of $(x_n)_0^{-1}$ and a slope of C_s , the **chain transfer constant**. The chain transfer constant is specific for a given monomer and agent combination under particular conditions of solvent composition and temperature. In the more general case, chain transfer can take place between radical chains and many other species such as monomer, solvent, or even dead polymer. Any molecule from which a hydrogen atom can be abstracted to terminate one chain and to leave behind a radical of adding monomer is a possible CTA. A broader form of Equation 4.20 for the general case is

$$(x_n)^{-1} = (x_n)_0^{-1} + \sum \frac{C_i [A_i]}{[M]} \quad (4.21)$$

where:

C_i is the chain transfer constant for the agent A_i present at concentration $[A_i]$

Example 4.4

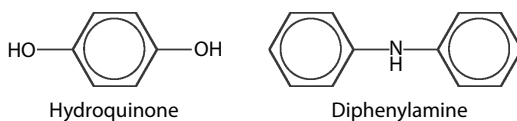
Listed below is data generated by the experimental polymerization of MMA. The initial concentration of MMA, $[M]_0$, is assumed to be 9.35 mol/liter. The %-CTA is the mole percent CTA with respect to monomer. The CTA used was lauryl mercaptan.

Sample	M_n	M_w/M_n
0% CTA	183,000	1.52
0.5%	11,500	3.19
1%	6,500	2.80
1.5%	3,500	3.58
2.0%	3,100	3.02

Using data on the effect of chain transfer on molecular weight (MW), calculate C_s , the chain transfer constant

Solution: The degree of polymerization, x_n , can be calculated from M_n . The value of %-CTA can be used to determine $[S]/[M]$. If $(x_n)_0$ is the degree of polymerization with 0% CTA, then following Equation 4.20, a plot of $(x_n)^{-1}$ versus $[S]/[M]$ can be used to obtain C_s . The value of C_s calculated from the slope of the plot is 1.66.

If $k_4 < k_p$, the overall rate will be decreased by chain transfer. This is *degradative* chain transfer. In fact, if k_4 is so small as to be negligible, chain transfer results in inhibition and the agent is a free-radical sink, or **inhibitor**. Almost all ethenic monomers are stored and shipped containing such a material to prevent adventitious polymerization. Hydroquinone and diphenylamine are compounds that at concentrations of 10–200 ppm are effective inhibitors. The radicals that result from these compounds are unreactive toward monomer. These inhibitors have many features in common with additives required for **living radical polymerization**, discussed later.



Dissolved oxygen in a polymer system often acts as an inhibitor by reacting with radicals to give stable species. The variable induction periods that result can be annoying. Free-radical polymerizations usually are carried out under an inert atmosphere for this reason. Some early workers sought to eliminate the need for deaeration in commercial reactors by adding reducing agents to act as scavengers for oxygen. The greatly increased rates that resulted when that was done were later explained by the fact that, while oxygen scavenging was not very efficient, the reducing agent–oxidizing initiator combination produced radicals much faster than the oxidizing agent could by itself. Such **redox couples** now are commonly employed to obtain fast rates at low temperatures by *reduction activation*. For example, the initial rate of polymerization of acrylamide with oxidizing agent (persulfate) is increased sevenfold by a modest amount of reducing agent (thiosulfate) (Figure 4.6).

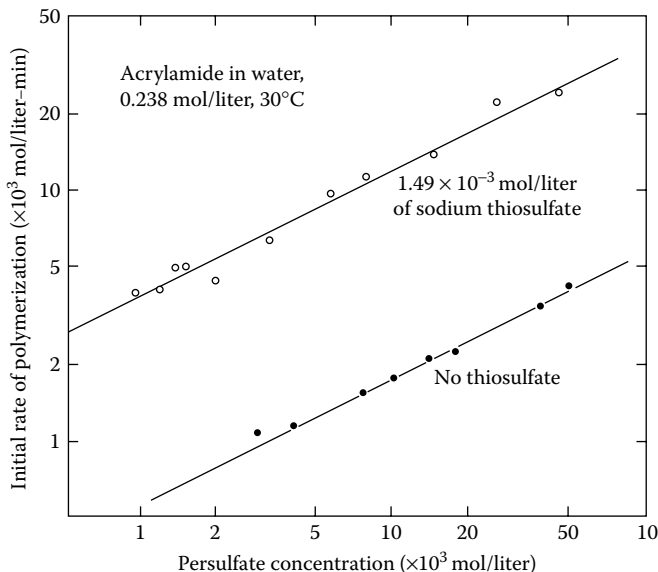
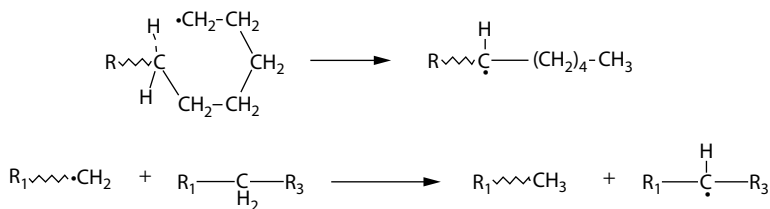
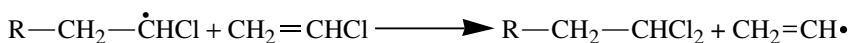


FIGURE 4.6 Increase in polymerization rate by addition of reducing agent, $\text{Na}_2\text{S}_2\text{O}_3$, to reaction initiated by $\text{K}_2\text{S}_2\text{O}_8$. Slope of log-log plot is 0.5 in either case. (Data from Riggs, J. R., *The Aqueous Phase Polymerization of Acrylamide: A Kinetics and Mechanism Study*, PhD thesis, Cornell University Press, Ithaca, NY, 1964.)

In many systems a polymer can be dead to the usual addition of monomer, but alive in the sense that it can act by a different mechanism as a transfer agent. At high temperatures and pressures, growing polyethylene chains abstract protons from themselves (*backbiting*) or from other dead polymers.



These two processes result in short and long branches, respectively, because each new radical can add to monomer. This polymer is known as low-density polyethylene because it has a lower density and a lower melting temperature than polyethylene produced by other methods due to branching. Monomer itself can be a CTA. It is hard to tell whether vinyl chloride ($\text{CH}_2=\text{CHCl}$) terminates by coupling or by disproportionation, since most chains are terminated by having a growing radical abstract a chlorine atom from a monomer molecule.



The resultant radicals are not thought to initiate chains but rather to combine to form butadiene that subsequently copolymerizes with vinyl chloride [9].

4.4.5 TEMPERATURE DEPENDENCE

The temperature dependence of the reaction rate constants k_i , k_p , and so on can be expressed as conventional Arrhenius equations:

$$k = A \exp\left(-\frac{E_a}{RT}\right) \quad (4.22)$$

where:

- E_a is the **activation energy**
- A is the collision frequency factor
- R is the gas constant
- T is the absolute temperature (K)

The temperature dependence of the overall polymerization rate R_p follows from Equation 4.4:

$$k_p \left(\frac{k_i}{k_t}\right)^{1/2} = A_p \left(\frac{A_i}{A_t}\right)^{1/2} \exp\left(\frac{E_i/2 - E_p - E_i/2}{RT}\right) \quad (4.23)$$

As an example, E_i for persulfate decomposition in water is 33.5 kcal/mol and $E_p - E_i/2$ for acrylamide polymerization is 1.5 kcal/mol. The calculated activation energy for R_p , 18.25 kcal/mol, is in fair agreement with a measured value of 16.9 kcal/mol [8].

Generally, the overall rate of polymerization increases with temperature. However, the variation of degree of polymerization with temperature follows from Equation 4.15:

$$\frac{d(\ln x_n)}{dT} = \frac{d(\ln v_n)}{dT} = \frac{E_i/2 - E_p - E_i/2}{RT^2} \quad (4.24)$$

Example 4.5

Solution polymerization of monomer A initiated by peroxide P at two temperatures (using the same concentrations of A and P) gives the following results:

	35.0°C	53.0°C
Conversion in 30 min	25.0%	65.0%
Initial molecular weight	500,000	300,000

What is the energy of activation, E_i , for the decomposition of P?

Solution: We can abbreviate Equations 4.6 and 4.15 as

$$\ln\left(\frac{[M]_0}{[M]}\right) = K(k_i)^{1/2}[I]^{1/2}t$$

and

$$M_n = M_0 X_n = \frac{M_0 K}{(k_t)^{1/2} [I]^{1/2}}$$

where:

M_0 is the formula weight of a repeat unit

Only K and k_t depend on temperature

At 35.0°C (condition A):

$$\ln\left(\frac{1}{0.75}\right) = K_A (k_t)_A^{1/2} [I]^{1/2} 30 \text{ and } 500,000 = \frac{M_0 K_A}{(k_t)_A^{1/2} [I]^{1/2}}$$

so that

$$\frac{\ln(1/0.75)}{500,000} = \frac{(k_t)_A (30)}{M_0}$$

At 53.0°C (condition B):

$$\ln\left(\frac{1}{0.35}\right) = K_B (k_t)_B^{1/2} [I]^{1/2} 30 \text{ and } 300,000 = \frac{M_0 K_B}{(k_t)_B^{1/2} [I]^{1/2}}$$

so that

$$\frac{\ln(1/0.35)}{300,000} = \frac{(k_t)_B (30)}{M_0}$$

The ratio $(k_t)_B / (k_t)_A = 6.08$ (all other terms cancel out), so

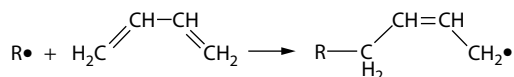
$$\ln\left[\frac{(k_t)_B}{(k_t)_A}\right] = 1.805 = \left(\frac{E_t}{8.3145} \text{ J/mol-K}\right) \left(\frac{1}{308} \text{ K} - \frac{1}{326} \text{ K}\right)$$

and

$$E_t = 83.7 \text{ kJ/mol}$$

4.4.6 CONJUGATED DIENE MONOMERS

This discussion of chain polymerization has centered on free-radical polymerization of an ethenic monomer. Conjugated dienes such as 1,3-butadiene often polymerize as bifunctional monomers with 1,4-addition rather than as tetrafunctional monomers.



One double bond remains in the main chain for each monomer that reacts. Free-radical polymerization can also produce a 1,2 form of addition at the same time, so that the polymer that results may have some unsaturated side groups and perhaps even some network formation. Ionic and coordination complex schemes of

polymerization, described in Section 4.5, not only can give almost all 1,4 addition with butadiene, but also can be tailored to give all *cis* or all *trans* polymers as well. Free-radical polymerization usually gives a mixture of isomeric forms.

4.5 IONIC POLYMERIZATION

Ionic polymerization is a commercially important class of polymer-forming reactions. A key aspect of the ionic polymerization process is the requirement for a counterion to be present in addition to the charged reactive site to lead to overall charge neutrality. This is not necessary in a radical chain polymerization. Due to the instability of needed reactive intermediates, ionic polymerization is also usually more complicated than radical polymerization, and thus the former plays a somewhat smaller role in the formation of commercial polymer processes. There exist however some important monomers that can be polymerized only by ionic methods. The reactivity of ethenic monomers to polymerization by radicals, ions, and coordination catalysts varies with the structure in a manner that can be correlated though not always quantitatively predicted. A convenient classification is that by Schildknecht (Figure 4.7). It can be seen that for the vinyl monomer ($\text{CH}_2=\text{CHX}$), cationic initiation is favored when X is electron donating and anionic when X is electron withdrawing. In radical polymerization, the steric hindrance of the methyl group next to the double bond causes methacrylates, ($\text{CH}_2=\text{C}(\text{CH}_3)(\text{COOR})$), to react much more slowly than the corresponding acrylates, $\text{CH}_2=\text{CH}(\text{COOR})$.

A major difference between radical polymerization and the various ionic methods is that, in the latter, the incoming monomer must fit between the growing chain end and an associated ion or complex. The growing radical chain, however, has no such impediment at the growing end although the precise nature of the growing chain end in radical and *living radical* polymerization is not completely understood.

4.5.1 CATIONIC POLYMERIZATION

The most important polymer formed using cationic polymerization is polyisobutylene. Cationic polymerizations tend to be very rapid even at low temperatures. The polymerization of isobutylene (IB) with AlCl_3 or BF_3 is carried out commercially at -100°C (see Chapter 5). An estimate of the lifetime of a growing chain of IB in this case is about 10^{-6} s [11]. This is much shorter than the usual lifetime of a free-radical chain such as vinyl acetate, which may be several seconds. If ionic catalysis is used in a heterogeneous system (e.g., insoluble catalyst, soluble monomer, and polymer), the rate of diffusion of monomer to and polymer from the surface may control the overall rate. In such cases, intensity of agitation, catalyst particle size, and viscosity of solvent can become very important. Usually a cocatalyst is involved. For example, water is the cocatalyst with BF_3 (Figure 4.8) and it is $(\text{BF}_3 \text{OH})^-$ that forms the *gegen ion* (also called the *counter ion*) at the growing end of the chain. The fitting of the incoming monomer unit between chain and gegen ion can lead to stereoregularity, as when vinyl alkyl ethers are polymerized at very low temperatures [12].

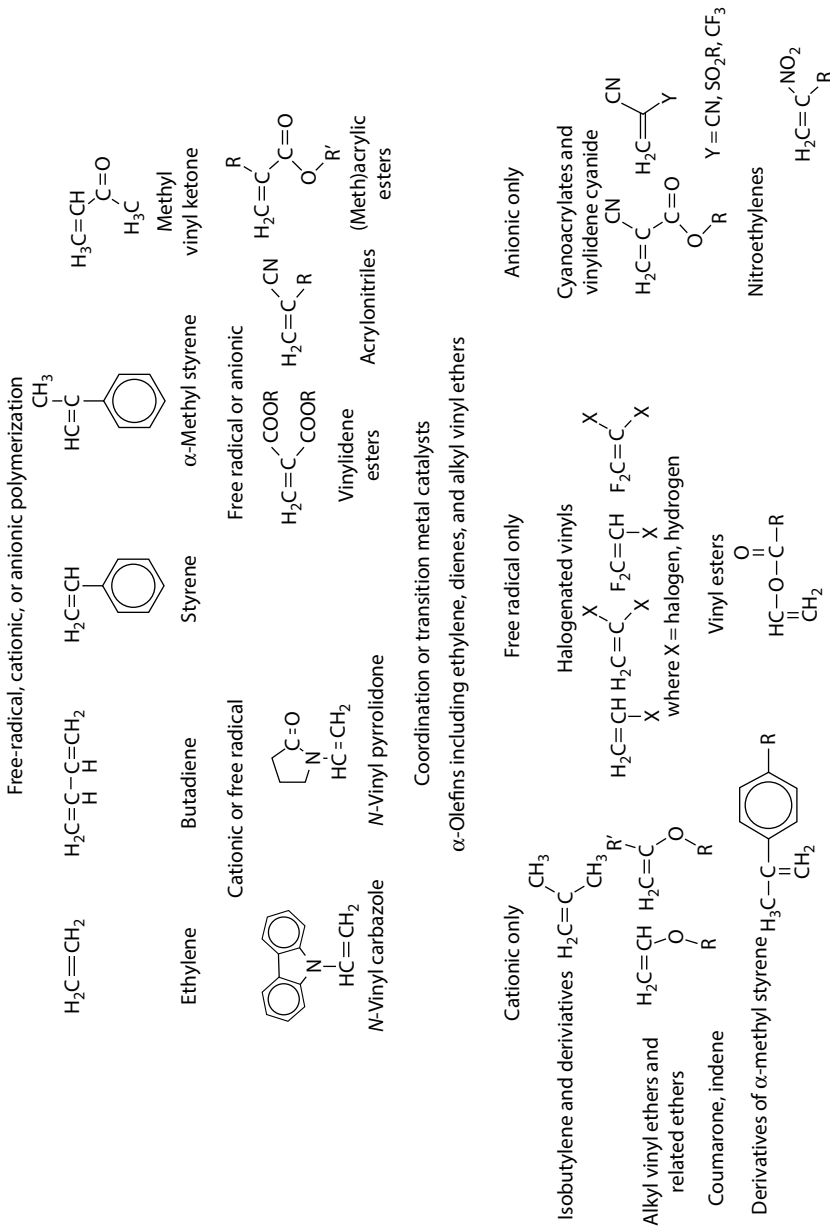
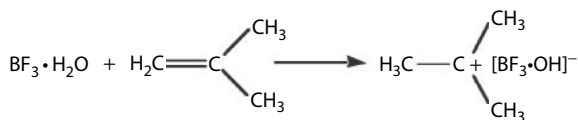


FIGURE 4.7 Type of chain polymerization suitable for common monomers. (Data from Billmeyer, E. W., Jr.: *Textbook of Polymer Science*. 1962. New York, 292. Copyright Wiley-VCH Verlag GmbH & Co. KGaA. Reproduced with permission.)

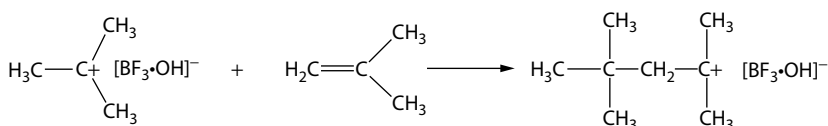
Carbocation (cationic polymerization) [13]

Initiation



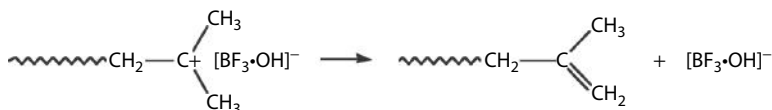
Flory, P. J., *Principles of Polymer Chemistry*, Cornell University Press, Ithaca, NY, 220, 1953.

Propagation



Flory, P. J., *Principles of Polymer Chemistry*, Cornell University Press, Ithaca, NY, 220, 1953.

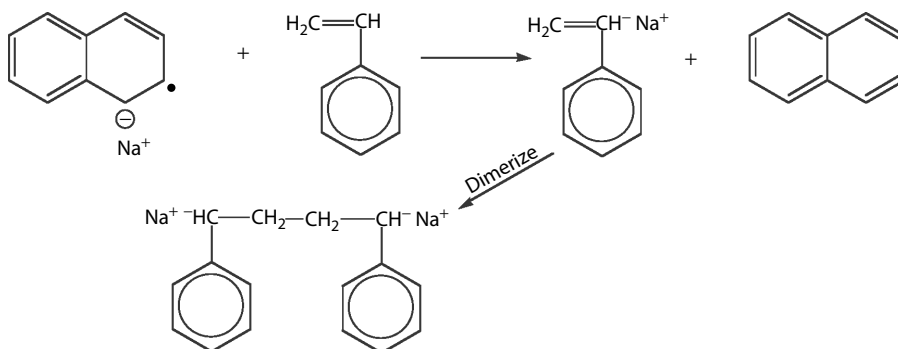
Termination



Flory, P. J., *Principles of Polymer Chemistry*, Cornell University Press, Ithaca, NY, 220, 1953.

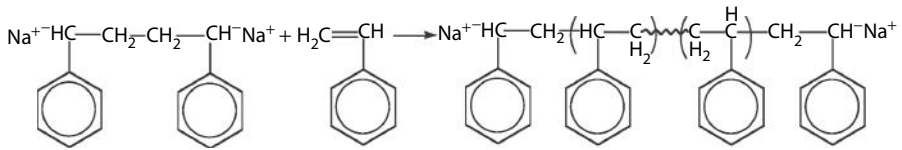
Carbanion (anionic polymerization) [10]

Initiation



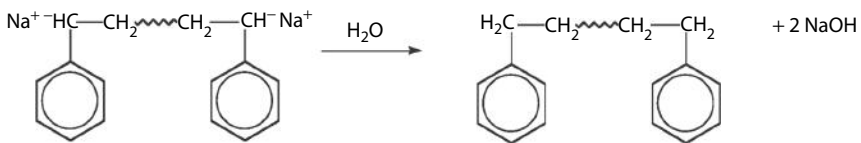
Billmeyer, E. W., Jr., *Textbook of Polymer Science*, Wiley, New York, 292, 1962.

Propagation



Billmeyer, E. W., Jr., *Textbook of Polymer Science*, Wiley, New York, 292, 1962.

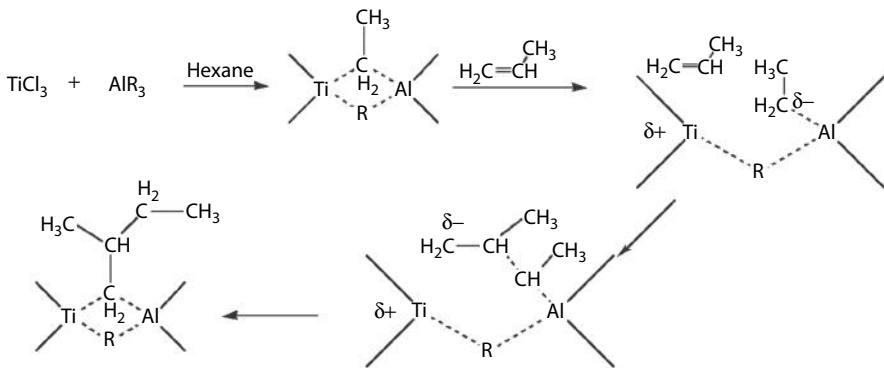
Termination



Billmeyer, E. W., Jr., *Textbook of Polymer Science*, Wiley, New York, 292, 1962.

Transition metal-catalyzed polymerization (Ziegler catalyst) [14]

Initiation and propagation



Termination

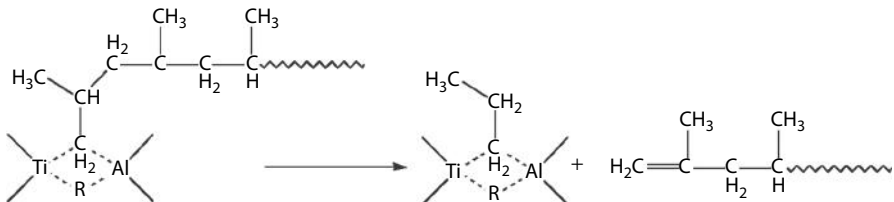


FIGURE 4.8 Some chain polymerization systems. (Data from Lenz, R. W.: *Organic Chemistry of Synthetic High Polymers*. 1967. New York, 623. Copyright Wiley-VCH Verlag GmbH & Co. KGaA. Reproduced with permission.)

As recently as 1975, it seemed unlikely that cationic polymerization would lead to a *living* system. A living polymerization can be defined as one with no termination mechanism. The growing end of the living polymer remains reactive after all the monomer (say monomer A) has been added. If a new monomer, B, is introduced into the system, it may add to the living end and result in a block of polymer B being covalently attached to the previously existing block of A. Cationic initiation was long regarded as having *built-in* termination and chain transfer mechanisms that would not allow keeping the end group reactive. However, it has been found that certain combinations of cationic initiators and modifiers will indeed allow the formation of living polymers [15,16].

Kennedy [16] has described the formation of a triblock polymer with a center block based on IB and end blocks based on indene. By using an initiator that is difunctional, the center block has two living ends so that both end blocks are added simultaneously. In one example shown in Figure 4.9, IB can be initiated from a

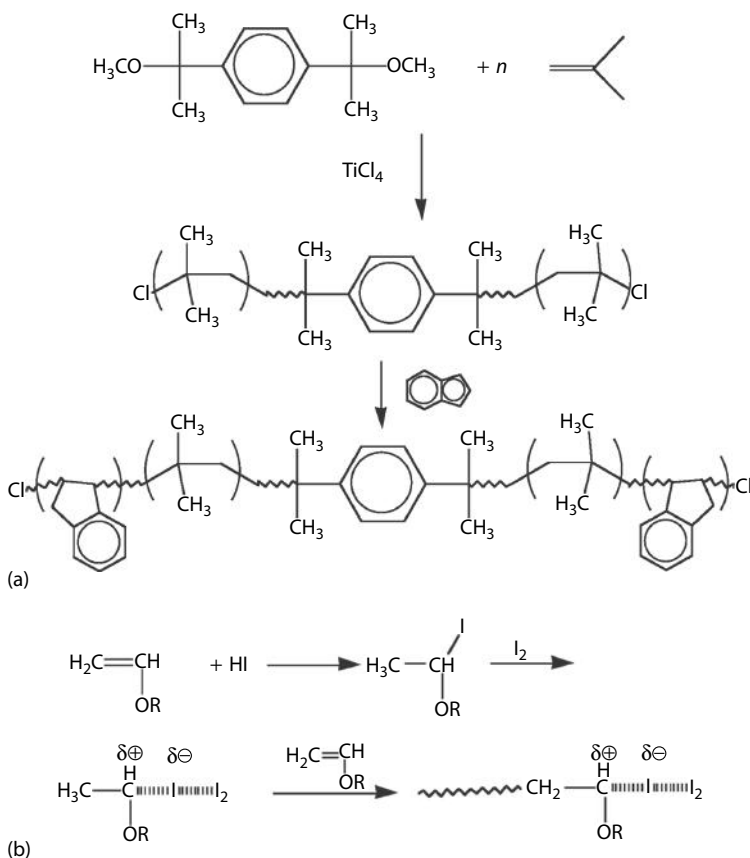


FIGURE 4.9 (a) Synthesis of a triblock copolymer of IB and indene (In) by cationic polymerization. (Data from Kennedy, J. P., and B. Ivan, *Designed Polymers by Carbocationic Macromolecular Engineering*, Hanser Publishers, New York, 1992.) (b) Synthesis of poly(vinyl ether) using living cationic initiator. (Data from Teyntjens, W. G. S., and E. J. Goethals, *Polym. Adv. Technol.*, 12, 107, 2001.)

difunctional initiator formed by the reaction of dicumyl ether (DCE) and TiCl_4 . The living character of the process can be demonstrated by the attachment of a block of indene when it is added to the reaction mixture after consumption of all IB. The molecular weight obtained is close to the theoretical value predicted from the initial concentrations of DCE, IB, and indene. If the process is *living*, that is, no termination takes place and initiation is much faster than propagation, then each molecule of DCE generates one molecule of polymer. Under Section 4.5.2, the molecular weight of the mid-segment should be equal the molar ratio of IB to DCE times the formula weight of IB (this will be discussed again in the section on living anionic polymerization):

$$M_n(\text{predicted}) = 56.1 \times \frac{[\text{IB}]}{[\text{DCE}]} = 56.1 \times \frac{1.45}{0.0016} = 51,000$$

A similar calculation predicts $M_n = 78,000$ for the triblock, which is somewhat lower than the measured value. As will be seen later (see Section 6.2), a ratio of M_w/M_n much less than 2 is indicative of a narrow molecular weight distribution and is typical of living polymers. The steps are summarized in Figure 4.9.

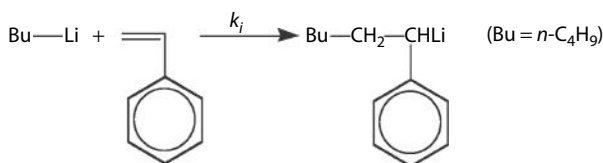
More recently, other types of **living cationic polymerizations** have been discovered by Sawamoto and colleagues [17]. The important realization that made this work possible was the need to slow down the rate of polymerization with respect to initiation. This is difficult in view of the fast rate of polymer growth in cationic polymerizations. To do this, a mixture of hydroiodic acid and iodine was used to initiate vinyl ethers. Initiation is slow (over hours) but the rate of polymerization is slower (days), and thus in the absence of transfer reaction, a living polymer is formed. This lesson has been extended to many other types of vinyl ethers. It has now been found that Lewis acids such as ZnI_2 or ZnCl_2 , or the addition of controlled amounts of non-nucleophilic counterions such as BF_4 or ClO_4 , can provide sufficient activation. As a result, many methods now exist for the synthesis of bifunctionally growing living polymers using cationic polymerization [18]. There has been recent focus on living cationic polymerization because of the development of coatings for drug-eluting stents. In particular, block copolymers that contain polyisobutylene blocks have been found to be very effective for this application.

Other kinds of polymerizations such as those that involve opening rings can be initiated by cationic mechanisms. A variety of main chain polyethers such as polytetrahydrofuran are made this way. Photogenerated acids can also be used to open oxirane rings, for example, and this is a very valuable method of photo-cross-linking epoxy groups.

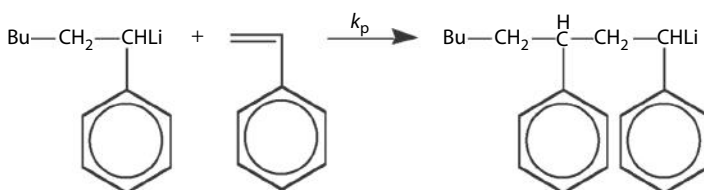
4.5.2 ANIONIC POLYMERIZATION

Although there are several mechanisms by which living polymers can be prepared, anionic polymerization to date represents the most successful commercial application. The particular usefulness of lithium alkyls has been with dienes to give *cis*-polyisoprene and *cis*-polybutadiene, although they can yield isotactic or atactic polymers of styrene and MMA. It is a peculiarity of polymerizations with lithium alkyl that there is no termination step. The rate of polymerization depends on the amount of initiator and monomer present [19].

Initiation



Propagation



If the rate of initiation is much faster than the rate of propagation, each initiator should start one polymer chain. If all these chains start at time zero and grow to consume all the monomer, a narrow molecular weight distribution (Poisson) results (see Section 6.2). The number-average degree of polymerization is given by $x_n = [M]/[I]$, where $[M]$ is the initial monomer concentration and $[I]$ is the initiator and, therefore, also the polymer concentration in moles per unit volume. This concept of initiation being faster than propagation and there being negligible termination is a key common element of all forms of living polymerization.

When butyl lithium is added to a monomer solution, the rates of initiation and propagation both depend on monomer concentration. If, however, the initiator is *seeded* by adding some monomer and then added to the remaining monomer, only the propagation step is observed. Under these circumstances, the reaction is first order in monomer (Figure 4.10), the straight line corresponding to

$$-\frac{d[M]}{dt} = k_p [M] [R_s] \quad (4.25)$$

or

$$\ln \frac{[M]_0}{[M]} = k_p t [R_s] \quad (4.26)$$

where:

$[M]$ is the monomer concentration at time t

$[M]_0$ at time $t = 0$ and $[R_s]$ is the concentration of growing polymer *seeds*. The rate is usually proportional to the initiator concentration to the first power in tetrahydrofuran and to the second power in hydrocarbon solvents. This is because the lithium is associated in nonpolar solvents as a complex.

Since the polymer chains are *alive*, a second monomer can be grown on a *seed* made from a different monomer, much as described earlier for living cationic polymerization. The final step of the polymerization is decomposition of the lithium alkyl

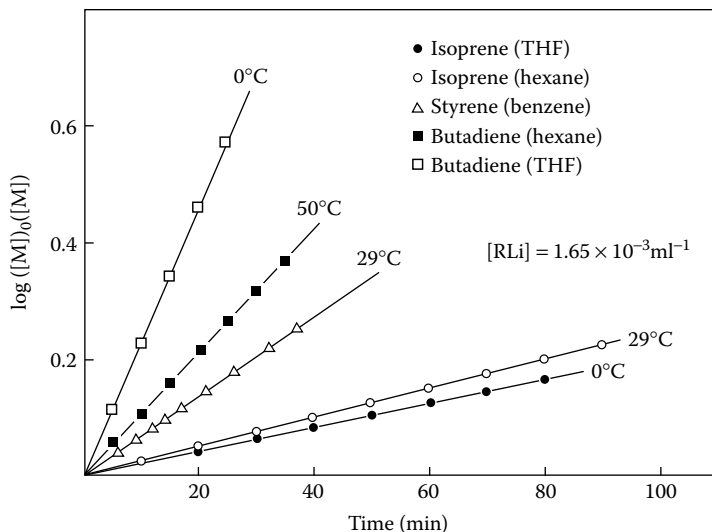


FIGURE 4.10 First-order rate plots for *seeded* butyl lithium polymerizations for monomers in benzene, hexane, or tetrahydrofuran. (Data from Morton, M., *AIChE Symp. Polymer Kinetics Catalyst Systems*, December 1961.)

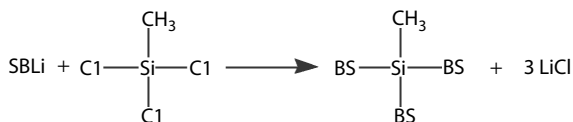
by addition of water or alcohol. Various end groups can be added to the living chains by employing a reagent to *kill* the polymer and simultaneously add a chemical function such as —COOH or —OH groups. Low-molecular-weight polymers (oligomers) of styrene, α -methylstyrene, and diene monomers have been produced with end groups as diverse as carboxyl, hydroxyl, and amine. These then can be used as blocks in other polymers by appropriate reactions such as esterification or amide formation.

Commercial copolymers based on styrene with either butadiene or isoprene have been prepared by this method. Both the random (both monomers present) and block (first one monomer added then the next) copolymers are available.

In one example [20], styrene (S) (60 g) in benzene (1400 g) is polymerized using 0.003 mol of *sec*-butyl lithium at 40°. Then isoprene (I) (450 g) is added and polymerized. Finally, an additional 60 g of styrene (S) is added and polymerized. Alcohol can then be added to cap the chain end and to precipitate the polymer. The chain thus made has the triblock copolymer structure SIS, where each letter in the abbreviation represents a *block* of monomer. These triblock copolymers with identical end blocks are generically known as ABA triblock copolymers. A somewhat different ABA block copolymer can be made by coupling together **living polymers** instead of merely capping them. Careful removal of moisture and air is necessary in either case [21]. Cyclohexane (40 cm³) is added followed by styrene (16 g) and *sec*-butyl lithium. After 40 min at 70°C in a tumbling rack, the bottle is cooled to 40°C and butadiene (B) (24 g) is added. At this point the orange-colored polystyryl anion is converted to the colorless polybutadienyl anion. Another hour at 70°C gives essentially complete conversion. The final step is to add a coupling agent that will join the living polymers together. If a difunctional agent such as diiodomethane or dimethyl dichlorosilane is used, a linear block copolymer is formed.



Methyl trichlorosilane is a trifunctional linking agent capable of producing a three-arm star polymer. There are a number of linking agents capable of forming star polymers from the coupling of living chains.



In either case the coupling is highly efficient, over 90% of the SBLi chains being incorporated into the block copolymer. The examples cited here are useful as **thermoplastic elastomers**.

At room temperature these thermoplastic elastomers act as though they were covalently cross-linked, exhibiting high resilience and low creep. However, they flow when heated above 100°C, like true thermoplastics. The reason is that the large polystyrene blocks form glassy aggregates that function as massive cross-links (Figure 4.11). The independent behavior of the polybutadiene portion is made evident by the fact that the polymer exhibits two widely separated values of T_g . Block copolymers can be made with tensile strengths of over 3000 psi (20 MPa) and high elongations. By contrast, conventional styrene–butadiene rubber cannot be made to exceed 1 or 2 MPa whether cross-linked or not unless a reinforcing filler is added.

When the initiator is based on the reaction product of sodium and naphthalene (Figure 4.8), the growing chain is difunctional. It is possible to put various functional groups on both ends of a single chain in a single step. In fact, if done correctly, this initiator can be used to produce ABA polymers directly by polymerization of one monomer followed by addition of a second type.

Polar monomers present a problem with the sodium and lithium initiators described above. For example, MMA does not initiate satisfactorily due to side reactions such as cyclization and side reactions. A number of modified initiating systems have been found that do result in high-molecular-weight, narrow-distribution polymers of methacrylates and acrylates. Moreover, there is some control over tacticity. Workers at Imperial Chemical Industries described the polymerization of methacrylates using a modified lithium initiator [22]. The living nature of the growing polymer chain was demonstrated unequivocally in one experiment in which monomer was added in separate portions. Between additions the molecular weight was measured showing good conversion.

It is obvious that all the polymer chains remained *alive* throughout the entire process. Also, M_w/M_n remained at about 1.1 throughout the experiment. The fact that the measured molecular size is around 1.5 times the ratio of monomer to initiator indicates that not all the lithium was available for initiation. The explanation given is that there are two types of complexes in equilibrium. The polymer produced in this experiment was about 70% syndiotactic and 3% isotactic. Block and random copolymers can be prepared with this initiating system.

Other workers [23] have used modified lithium initiators to polymerize acrylates in addition to methacrylates in a living fashion. The polymerizations are complete

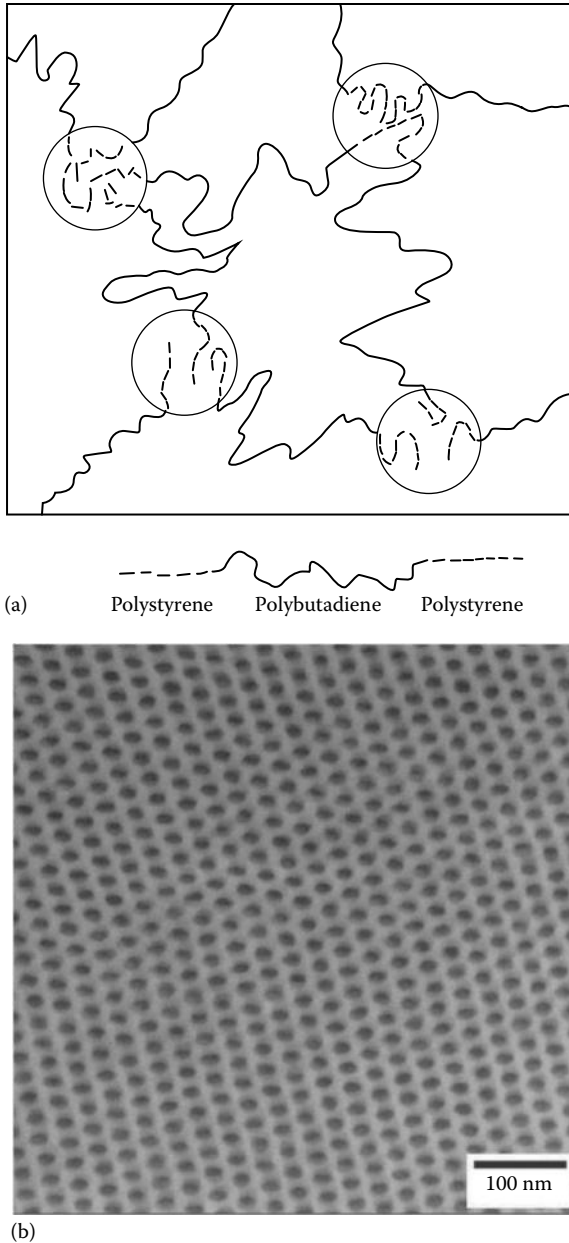


FIGURE 4.11 Typical ABA triblock thermoplastic elastomer. (a) Circles are glassy domains of polystyrene acting as temperature-sensitive cross-links holding the polybutadiene segments in place; (b) a typical transmission electron microscope (TEM) micrograph of a SEBS sample (Shell Kraton G1652) with 29 wt% polystyrene block, showing a hexagonally packed cylinder morphology. This image was taken on a microtomed ultrathin cross section (~60 nm) of a bulk sample. The polystyrene cylinder phase was preferably stained by RuO₄ vapor and appears dark. (Courtesy of Xuefa Li, Cornell University, Ithaca, New York.)

in 10 min even though the temperature is typically under -80°C . Today, with sufficiently pure monomers using correct protecting groups to limit unwanted reactions, the anionic polymerization of methacrylate monomers has become routine.

4.6 CONTROLLED RADICAL POLYMERIZATION

The newest form of living polymerization and potentially the most versatile is **living radical polymerization**, more formally known as **controlled radical polymerization**. First discovered for the polymerization of low-molecular-weight methacrylates, it can be applied to styrenics, acrylates, methacrylates, and a variety of other vinyl monomers. A major advantage over anionic polymerization is the relative insensitivity to functional groups. Like all living polymerizations, it was important to establish rapid initiation with slower overall rate of polymerization and at the same time to inhibit any termination or transfer reactions. Normally, this is very complicated in a radical polymerization, so a radical trap is used in combination with high temperatures. The molecules used have much in common with the inhibitors used to stabilize monomers and prevent premature polymerization.

Three basic classes of living radical polymerization have been developed in laboratories around the world in the 1990s: (1) those using nitroxide-based materials (e.g., TEMPO [2,2,6,6-tetramethylpiperidinyloxy]) are largely used for styrene and diene polymerizations [24,25] and this type of polymerization is often called nitroxide-mediated polymerization (NMP), whereas (2) those using the Cu-complex control agents are largely used for methacrylates and acrylates and this type of polymerization is known as atom transfer radical polymerization (ATRP) [26]. Examples of the controlled radical polymerizations of styrene (NMP) and methyl methacrylate (ATRP) are given in Figure 4.12a and b, respectively. (3) Reversible addition/fragmentation chain transfer (RAFT) involves the use of compounds such as dithioesters or thiocarbamates to carry out the same role of taming the reactive radical [27]. A scheme for this polymerization is given in Figure 4.12c. Each requires at some stage the introduction of a radical initiator to start the reaction that is quickly stabilized by the presence of these key additives. All of them (nitroxide, copper halide, sulfur compounds) are known as radical inhibitors and it was the understanding that living polymerization involved fast initiation relative to polymerization with the absence of termination learned from living cationic polymerization that made this development in radical polymerization possible [18].

In the case of the TEMPO-mediated polymerization of styrene (Figure 4.12a), the product of a single monomer is formed when the typical reaction temperature of initiation for a radical source such as benzoyl peroxide is used (e.g., 70°C). Only by reaching temperatures as high as 130°C will the TEMPO–polymer bond weaken sufficiently to permit insertion of a monomer. Even so, the rate of polymerization is relatively slow and termination and side reactions are much slower still. The chain end remains sufficiently living that a second monomer can be added to the polymerization mixture and form a second block. Typically, the polymerization is carried out in the melt, but high boiling point solvents such as *o*-dichlorobenzene can also be used.

More recently, new nitroxide compounds have been developed that permit a broader range of monomers to be used. By fine-tuning the stability of the radical and the

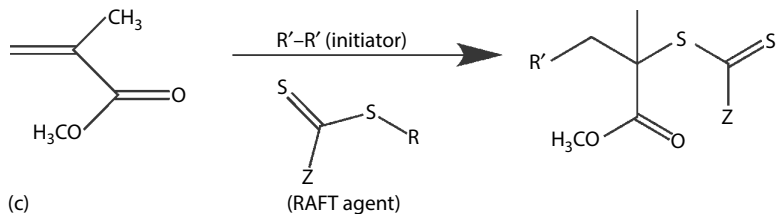
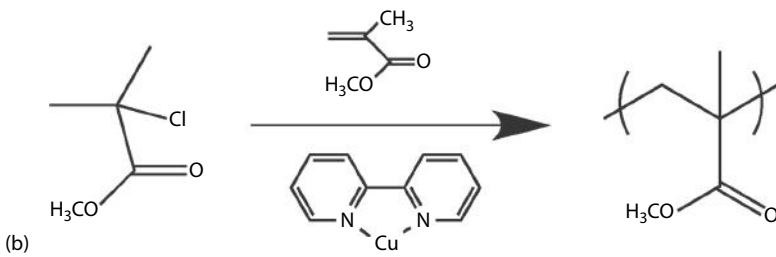
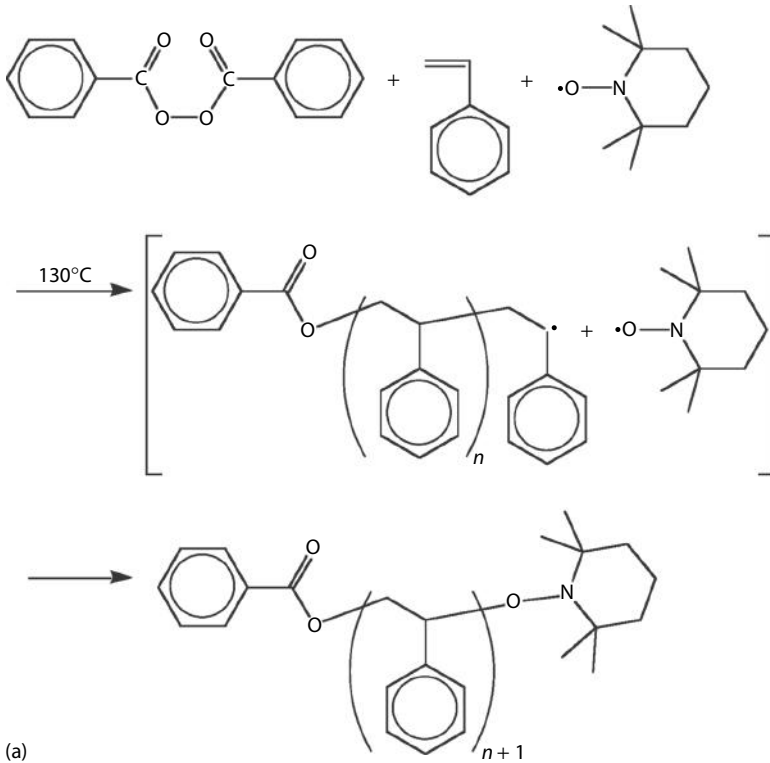
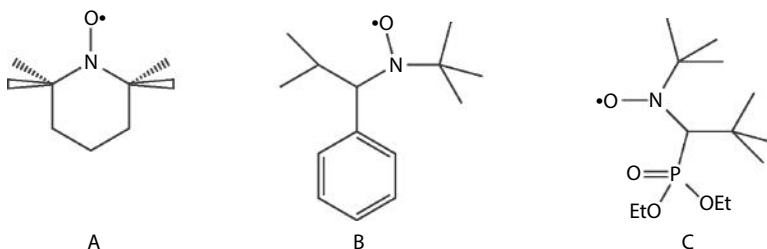


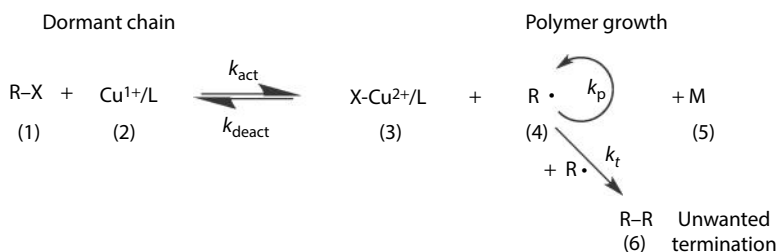
FIGURE 4.12 (a) The radical polymerization of styrene in the presence of TEMPO stable free radical, (b) the polymerization of methyl methacrylate in the presence of Cu^{I} bipy, and (c) the polymerization of methyl methacrylate in the presence of a RAFT agent. All additives serve to stabilize the radical by forming a bond with the radical chain end. Polymerization only takes place in the short time the capping agent is off the chain.

steric environment of the nitroxide compounds, it is possible to reduce polymerization temperature and to expand suitable monomers to the methacrylate series as well as the styrene monomers. Examples of alternate nitroxide compounds are shown below. Compound A is TEMPO; B is 2,2,5-trimethyl-4-phenyl-3-azahexane-3-nitroxide; and C is a nitroxide compound known commercially as BlocBuilder.

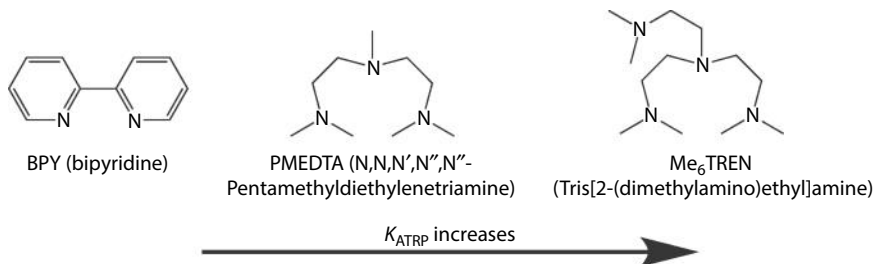


ATRP, like the NMP reaction described above, depends on the ability of a capping atom (in this case a halogen) to stabilize the reactive chain end and reduce the possibility of chain termination and side reaction [28]. Typically a halogen-terminated analog of the monomer is created, often by *in situ* processes but sometimes by the reaction of an acid or acid halide with the monomer. This alone does not enable polymerization. Instead, Cu and a ligand are added to the reaction mixture that weakens the carbon–halogen bond enough that monomer insertion (polymerization) can take place. As such, the Cu-mediated ATRP of MMA works effectively by creating an activated bond at the growing chain end. The presence of Cu activates the chain end, and depending on the reaction temperature and the stability of the bond, the halogen hops on and off the chain end sufficiently often that monomer can be inserted (Figure 4.12b).

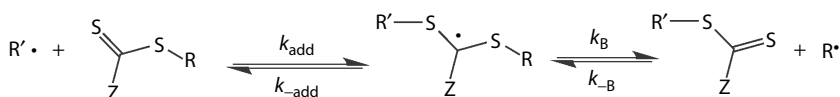
The method is sufficiently versatile that methacrylates, acrylonitriles, dienes, and styrenes all are copolymerized. The proposed mechanism for ATRP is shown in the scheme below. The figure shows three possible activities for the radical: (1) dormant—most of the time the radical is capped and unreactive, and (2) polymer formation—the radical is active and the halogen is complexed with the copper enabling the insertion of monomer. This state is short lived enough that side reactions and termination are unlikely. Finally (3) unwanted reactions such as termination may occur. Again the chance of these latter reactions are minimized enough that the polymerization can be considered living, that is, without termination.



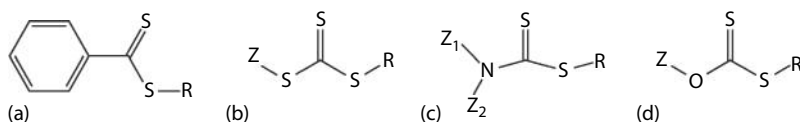
The role of the ligand and other components is very important in the progress of the reaction. While understanding of the detailed mechanisms involving the precise role of copper in the reaction is still evolving, the importance of the ligand is quite clear. For example, in the three ligands shown below, it is possible to change the relative time the radical is active. The value of $K_{\text{ATRP}} (= k_{\text{act}}/k_{\text{deact}})$, which is the ratio of the rate constant for activation versus deactivation, increases in going to ligands that more strongly bind the copper [29].



Like those methods of living radical polymerization described above, the molecular weight of a polymer made in a RAFT process can increase linearly with conversion, molecular weight distributions are narrow, and at any given time, the majority of the polymer chains are capped and therefore dormant. The reactions involved in RAFT are those of classical chain polymerization (initiation, propagation, and termination) in addition to the chain transfer step. Termination is not fully suppressed in RAFT, and it is the retention of the sulfur groups in the product that provide the living character and makes the process suitable for making block copolymers and end functional polymers. The polymerization reaction is shown in Figure 4.12c and the different process steps are shown below [27].



Not all RAFT agents are equal and proper selection of a given monomer or application will be critical. However, there exist a broad range of agents to select from. Generally, RAFT polymerizations are divided into two groups: those involving more activated monomers (MAMs) such as methacrylates, acrylates, and acrylamides, and those involving less activated monomers (LAMs) such as vinyl acetate, *N*-vinylpyrrolidone, or *N*-vinylcarbazole. Appropriate RAFT agents are commercially available and have been tabulated in a number of sources. Such RAFT agents are shown below and fall into four basic categories: (1) dithiobenzoates, (2) trithiocarbonates, (3) dithiocarbonates, and (4) xanthates [30].



Switchable RAFT agents have been developed and permit the combination in block copolymer form of LAM- and MAM-type monomers in a single polymer.

By transforming reactivity and then introducing a new monomer, it is possible to make block copolymers that would otherwise be nearly impossible. This has special advantages in tailoring new polymers for applications in advanced technology areas such as biomedical uses.

These living radical processes permit the formation of new block and graft polymers using simple monomers in a versatile manner. Applications of block copolymers are described in some detail in Chapter 3. In addition, the development of living radical polymerization tools has permitted the study of polymer brushes grown from a surface initiator. **Star polymers**, for example, require the creation of multifunctional initiators, but this is readily possible with some thought given to the number of chains desired and the reactivity of the starting core molecule. Polymer brushes and many other architectures that are being produced using these new polymerization methods also require new initiator molecules. In the case of polymer brushes, the initiator needs to be designed to bond to a specific surface. Often these surfaces might be oxides such as silica or glass or might be metals such as gold. Along with complex structures, like all living methods narrow molecular weight distribution is possible and this may itself be a reason to use this process. Typical molecular weights with narrow distribution are currently possible up to ~50,000 g/mol. Commercialization of ATRP polymers has taken place and is to date focused on coatings and sealants. New products from such polymers could be imagined in future.

4.7 INSERTION POLYMERIZATION

The term **coordination complex polymerization** was used for some time to embrace many systems that could give some control over the stereochemistry of the product. However, **insertion polymerization** is a more general description of polymerizations that include a *hindered propagation site*.

4.7.1 ZIEGLER–NATTA CATALYSTS

A revolution occurred in the realm of polymer chemistry in 1955 when Giulio Natta demonstrated conclusively that stereospecific polymers could be produced with synthetic catalysts [31]. The systems he employed were primarily α -olefins polymerized by Ziegler catalysts—a discovery of Karl Ziegler. In recognition of this work, Natta and Ziegler shared the Nobel Prize in Chemistry for 1963. Since that early work, isotactic, syndiotactic, *cis*, and *trans* polymers have been made by using ionic and even some free-radical initiators at low temperatures with various types of monomers.

Many systems other than free-radical or ionic initiators have been investigated for the production of polymers. Several have assumed commercial importance because they lead to structures that cannot be achieved easily by free-radical or ionic routes. Ziegler-type catalysts [29] originally involved the formation of a complex precipitate from triethylaluminum and titanium tetrachloride:



Ethylene bubbled into the suspension at room temperature polymerizes very rapidly to give a high-molecular-weight, linear polyethylene. The linearity leads to higher crystallinity than a branched polymer, so that the product differs significantly from high-pressure, free-radical polyethylene. With propylene, an isotactic polymer can be produced. The mechanism may proceed as outlined in Figure 4.8, the stereospecificity stemming from the local topography of the catalyst at the site where monomer is inserted. For a time it was postulated that a heterogeneous catalyst would be needed for stereospecific activity, but this was refuted by subsequent work with similar catalysts, which, though complex, were soluble.

With diolefins such as butadiene and isoprene, both *cis*- and *trans*-1,4 polymers can be obtained. Variations in transition halide and/or ratio of alkyl to halide give different structures. For example, $\text{TiCl}_4\text{-AlR}_3$ with $\text{Al/Ti} > 1$ gives 96% *cis*-polyisoprene and with $\text{Al/Ti} < 1$ gives 95% *trans*-polyisoprene [32].

It is instructive to see how the Ziegler–Natta catalyst has evolved with respect to its use for the polymerization of propylene. Goodall [33] identifies three generations of catalysts. The first, dating to the 1950s, resulted from the reaction of TiCl_4 with triethylaluminum in cold hydrocarbons. The resulting slurry was slowly heated to 160°C – 200°C for several hours to convert $\beta\text{-TiCl}_3$ (brown) to $\gamma\text{-TiCl}_3$ (purple), which had been shown to be essential for propylene polymerization. A cocatalyst that alkylates the Ti atoms generating active centers (usually diethylaluminum chloride) should also be present. Early on it was found that electron donors such as ethers, esters, and amines would enhance the polymerization by reacting with the closely related ethylaluminum dichloride, which, unlike the monochloride, poisons the catalyst.

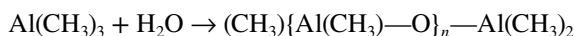
A second generation was developed in the 1970s. It was found that ether extraction of the brown precipitate to remove AlCl_3 followed by heat treatment at 60°C – 100°C in the presence of excess TiCl_4 gave a catalyst with smaller, more active crystallites.

In the third generation, during the 1980s, MgCl_2 was used as a support for the catalyst. Since over 400 patents on catalyst preparation were granted in the decade before 1985, it was difficult to identify one optimum process. Goodall describes a *common* method as starting by ball milling anhydrous MgCl_2 with ethyl benzoate to make a catalyst support to which is added TiCl_4 with a diluent such as hexane. After washing the solid with more hexane, the *precatalyst* is dried in a vacuum. The final polymerization system requires the presence of trialkylaluminum and a Lewis base such as ethylbenzoate.

The three generations can be characterized by the fraction of isotactic polypropylene produced and the productivity in kilograms of polypropylene per gram of Ti. The first generation yielded polypropylene that was only about 92% isotactic. A separate solvent extraction of atactic polymer was required to give a suitable product. The subsequent generations yielded 96% isotactic polymer, eliminating the extraction step. In the first two generations, productivities of 15 kg polypropylene/g Ti were typical. With the third generation, as much as 1500 kg/g Ti can be obtained. In a laboratory preparation, a third-generation-type catalyst yielded 25 kg polypropylene/g Ti in 1 h at 63°C and 4 bar pressure [33]. The polypropylene was 93% isotactic.

4.7.2 METALLOCENE CATALYSTS

Although they have been described as a type of Ziegler–Natta catalyst, the *metallocenes* have given rise to polyolefins of such novel properties as to merit a separate category. A simple metallocene is defined as the cyclopentadienyl derivative of a transition metal. In practice, the metallocene is used in conjunction with a methyl aluminoxane (MAO). When cyclopentadiene loses a hydrogen from a singly bonded carbon in the ring, a very stable π -bonded structure similar to benzene is formed, but with an overall negative charge present (Figure 4.13). Kaminsky [34] reported the polymerization of propylene, ethylene, and various comonomers using Cp_2ZrCl_2 and similar soluble metallocenes with a large excess of coactivator MAO. The MAO is produced by the controlled partial hydrolysis of trimethylaluminum.



The structure of MAO with n in the range of 4–20 apparently varies with the method of preparation. Branched chains and rings have been postulated in addition to the linear form shown above. The typical ratio of Al in the MAO to transition metal in the metallocene is of the order of 100–10,000.

The dicyclopentadiene compound yielded atactic polypropylene as demonstrated by extraction with hydrocarbon solvents. However, when Kaminsky replaced the π -bonded cyclopentadienyl ligands by ethylene-bridged indenyl rings (Figure 4.13), isotactic polymer was produced, and less than 1% of the polymer was extractable. Furthermore, the productivity at 21°C over an 8-h period was about 400 kg polypropylene/g Zr.

Commercialization of metallocene technology has taken the form of several competing product lines. Recently several resins have been commercialized that are made from metallocene/MAO catalysts with the addition of a noncoordinating anion such as tri(pentafluorophenyl) boron, said to provide charge balance and to stabilize the catalyst cation [35]. Because the metallocenes are soluble and well defined, they are termed *single-site* catalysts as opposed to the conventional heterogeneous Ziegler–Natta catalyst, which has a multiplicity of reaction sites differing in activity. Where the Ziegler–Natta-based polymers have broad molecular weight distributions and uneven comonomer distributions (for ethylene–hexene copolymerization, for example), the metallocene-based polymers have narrow molecular weight distributions and uniform comonomer distributions. Crystalline polymers of propylene and amorphous copolymers of ethylene with propylene have also appeared. In one

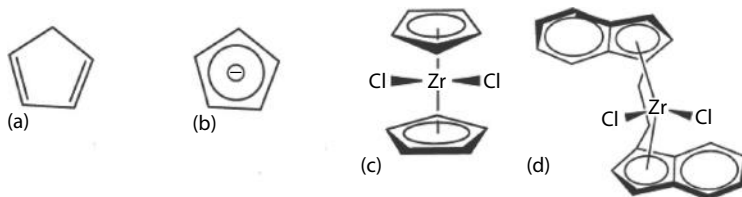


FIGURE 4.13 Structures of (a) cyclopentadiene (Cp), (b) Cp^- , (c) Cp_2ZrCl_2 , and (d) *rac*-ethylene(indenyl)zirconium dichloride.

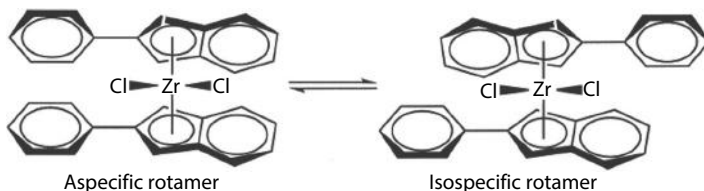


FIGURE 4.14 Oscillating metalocene catalyst. (Data from Coates, G. W., *Chem. Rev.* 100, 1223, 2000.)

example [36], a reaction mixture with MAO yielded 2.5 kg polypropylene/g Ti in 1 h at 30°C.

In the 1950s, Natta described the formation of polypropylene polymers that were a mixture of stereoisomers. It was possible to isolate three fractions from the product mixture, one of which was described as a blocky polymer. This polymer has elastomeric properties due to alternating blocks of isotactic (or syndiotactic) units with blocks of atactic units. Being able to produce such materials as the principle product would have major economic importance. In recent years, several strategies have been identified to make such blocky hydrocarbon polymers and include (1) asymmetric (C1 point group) catalysts, (2) oscillating catalysts, and (3) binary catalyst mixtures [37]. While all approaches provide the desired materials, perhaps the most interesting strategy involves the oscillating catalytic site (see Figure 4.14). By freeing the link normally found between the metallocene ligands, the catalyst can switch between two states, one of which provides an amorphous product (a specific rotamer) and other of which gives crystalline polypropylene (isospecific rotamer). Since the site can switch during the polymer forming process, the polymer has a blocky, crystalline–amorphous character that provides elastomer properties.

4.7.3 SUPPORTED CHROMIUM CATALYSTS

Metal oxides have been used to give linear polyolefins, although they have not been used for isotactic structures. Nickel, cobalt, chromic, or vanadium oxides supported on silica alumina have been found effective for ethylene and α -olefin copolymers at low temperatures. In 1975 it could be said that most linear polyethylene being marketed was being produced using the catalyst developed by the ConocoPhillips (Bartlesville, Oklahoma) (essentially chromium oxide on a silica–alumina base) [38]. The $\text{SiO}_2/\text{Al}_2\text{O}_3$ support is saturated with an aqueous CrO_3 solution. When this material is activated by heating in air at 500°C–800°C, chromates and dichromates form by reaction with support surface hydroxyl groups. Reduction of the chromium by monomer or hydrogen leads to a site where ethylene can attach to form a chromium–ethyl bond. Polymerization results from insertion of monomer units at the chromium–alkyl bond.

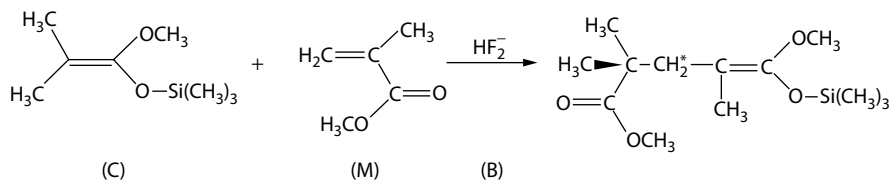
Marsden has reviewed industrial catalysts that typically contain 1% by weight of chromium on the surface of the silica support [39]. The preparation of the silica support is critical, since each catalyst particle creates a polymer particle much larger than itself. It is vital that the support fragment as polymerization proceeds so that access to active sites can continue. Surface areas can range from 50 to 1000 m^2/g , and pore volumes can range from 0.4 to 3 cm^3/g . High pore volume generally increases

productivity. Active catalysts fracture rapidly to particles in the 7- to 10- μm range within the first few minutes of polymerization. Since as much as 5000 g of polymer can grow on 1 g of catalyst, it is obvious that the original surface would become inaccessible to incoming monomer after a short time if it were not for the fragmentation that disperses the catalyst throughout the polymer particle. Many patents have specified the addition of titanium, zirconium, aluminum, boron, or fluorides in order to enhance the metal oxide activity. Whether incorporated on the surface or in the bulk of the support, titanium, in particular, can affect the molecular weight of the polyethylene made and also the productivity of the catalyst.

J. Paul Hogan and Robert L. Banks (ConocoPhillips, Bartlesville, Oklahoma) had observed the formation of crystalline polypropylene as well as linear polyethylene in 1951 using their own metal oxide catalyst system. In fact, about half a dozen companies filed patent applications in 1953 covering crystalline polypropylene. The consequent, technically complex legal battles for priority extended over a period of three decades. Finally, in 1983, the US patent on crystalline polypropylene was issued to Phillips. Hogan and Banks received the Perkin Medal in 1987 in recognition of their achievement.

4.7.4 GROUP TRANSFER POLYMERIZATION

It has been mentioned that linear polymers of olefins, diolefins, and styrene with narrow molecular weight distributions are possible when anionic *living polymer* systems are used. Anionic methods have only recently been successful with acrylic monomers. **Group transfer polymerization** is a method for producing linear, living polymer systems from acrylates and methacrylates using organosilicon initiators [40]. The mechanism appears to be an anion-catalyzed polymerization with the initiator consisting of a ketene silyl acetal. The insertion point is different from the usual metal-carbon bond site of other anionic systems. Typically, the starting material is methyl trimethylsilyl dimethyl ketene acetal (C), which adds a monomer such as methyl methacrylate (M) in the presence of a nucleophilic activator such as bifluoride ion (B):



Propagation takes place by insertion of additional monomer at the position marked with an asterisk. In a clean system, there is no termination, so a block of one monomer, perhaps MMA, can be formed followed by a block of a second monomer, for example, glycidyl methacrylate and so on. Many chemical functions can be present in the polymerization making the process very versatile. Molecular weight distributions can be very narrow, although the molecular weights that can be achieved are generally less than 50,000 g/mol, a value less than possible with anionic polymerization. The termination step can be controlled to put a reactive site at one or both ends of the final polymer. In one example, two living chains are coupled by reaction with

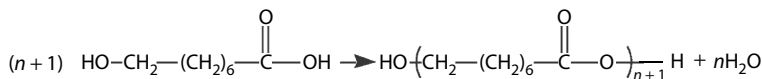
1,4-bis(bromomethyl)benzene followed by *quenching* the silyl group with tetrabutylammonium bromide. The result is a single polymer molecule with a carboxyl group at each end. Polymers with reactive end groups have been called **telechelic**, based on the Greek words *tele* meaning “far off” and *chele* meaning “claw.” Such polymers are useful in subsequent chain-extension reactions. Although syndiotactic units tend to be favored in group transfer polymers, a great deal of random tacticity usually is also found. Brittain has reviewed the mechanism of group transfer polymerization, especially as it is used to produce random and block copolymers [41]. Generally, the polymer forming reaction is thought to have an anionic character.

4.8 STEP-GROWTH POLYMERIZATION

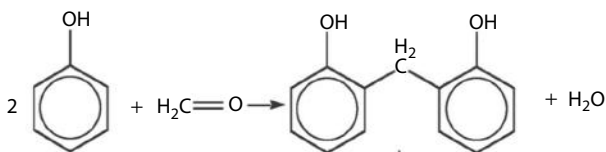
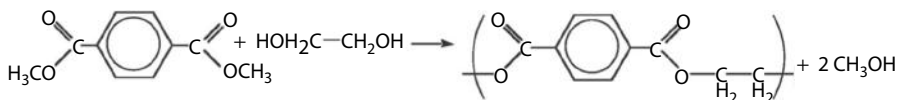
Step-growth polymerization is a process that is used for making many useful polymers. There are important differences between step-growth and chain-growth polymerization. It is important to realize that in chain reactions, propagation to final molecular weight is very rapid. In a styrene polymerization, for example, we might start a bulk polymerization with a peroxide and stop it after only 1% of the monomer is converted to polymer. Analysis would show that the mixture consisted of 99% of unreacted monomer and 1% of high-molecular-weight polymer, a result shown in Figure 4.2. Conversion of the remaining monomer to polymer would not affect the already formed material, which, with the exception of some *living* polymer systems, is dead. We cannot ordinarily make a low-molecular-weight polymer by addition polymerization and then increase its molecular weight by more of the same reaction. By contrast, step-growth polymerization involves the slow buildup of polymer chains from monomers, dimers, and trimers. The principle of equal reactivity regardless of molecular weight is fundamental to stepwise polymerization also. Furthermore, no high-molecular-weight polymer is formed until virtually all the monomer is consumed. This is a major point of difference between chain and step-growth polymerization.

There are also important differences in the nature of the polymer backbone formed by these processes. Olefin addition reactions lead to polymer chains containing aliphatic carbon as the backbone. Most step-growth reactions instead form polymer chains or rings containing *heteroatoms* (noncarbon atoms) in addition to aliphatic carbon in the backbone. The presence of heteroatoms can provide remarkable enhancements in polymer performance and often leads to polymers with higher glass transition temperatures and thermal stability leading to such properties as conductivity or electroluminescence.

Some step-growth reactions involve condensation in that some part of the reacting system is eliminated as a small molecule (Figure 4.15). A good example is esterification, in which water is eliminated during reaction between an acid and an alcohol. Because there is an equilibrium between reactants and products, the rate of conversion can be controlled by the rate of removal of one of the products (in this case, water).



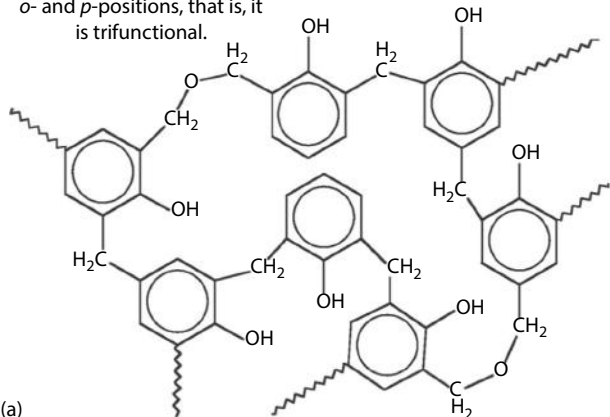
Of the six common plastics that are currently being recycled, only one, polyethylene terephthalate (PETE), is a polyester formed by step-growth processes. The others,



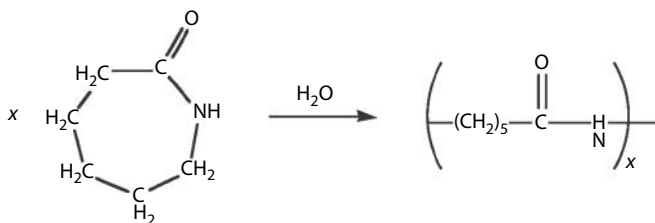
Phenol Formaldehyde

etc.

Phenol is active at the *o*- and *p*-positions, that is, it is trifunctional.



(a)



(b) Caprolactam

FIGURE 4.15 Step-growth polymerization systems: (a) condensation; (b) ring opening;

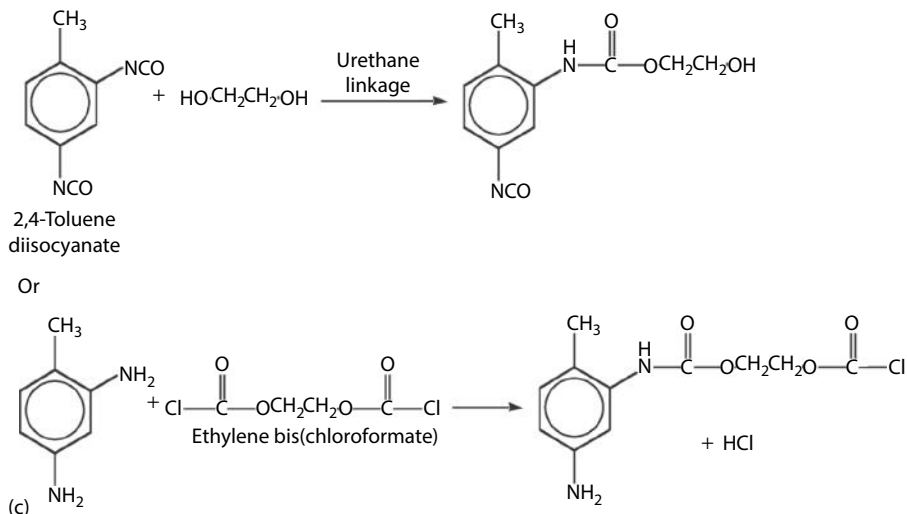
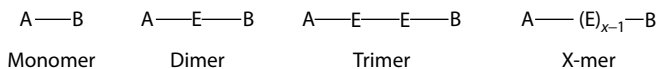


FIGURE 4.15 (Continued) (c) pseudocondensation.

polystyrene, polyvinyl chloride, polypropylene, high-density polyethylene, and low-density polyethylene, are formed by chain polymerization. However, this situation is more a reflection of the cost of the products and not their properties. In fact, most high-performance engineering thermoplastics are made by step-growth polymerization and include polycarbonate, polyaramid, polyether ketone, and polyimide, for example. Polycarbonate has excellent impact properties and is used as a shatterproof transparent glass replacement. Polyaramid is a liquid crystalline, high-temperature cousin of nylon and is used where great strength and light weight are needed. For example, ropes that pull oil-drilling rigs are made of this polymer, as are several kinds of bulletproof vests. Polyether ketone is another high-performance polymer often used in automotive applications and polyimide is a polymer with thermal stability exceeding 350°C making it attractive for uses where high-temperature, lightweight insulators are needed. Nylon is a common textile polymer invented in the 1930s and still used today for stockings, because of its excellent performance. PETE (or PET) is used for food packaging, drinking bottles, and textile fibers, and as the base of photographic films. It is easily recycled, because it can be broken down into its monomer building blocks and repolymerized to make a new, clean polymer.

Turning again to polyester formation, if we represent reactive hydroxyl groups by A, carboxyl groups by B, and ester groups by E, we can write the formulae for monomer, dimer, trimer, and x -mer as shown in the scheme below:



It is apparent that each successive member of the series has the same reactive groups as the monomer despite its larger size. With the principle of equal reactivity for all molecular sizes, a further condensation reaction is as likely to involve an x -mer as it

is monomer. Starting with N_A molecules and forming N_E ester groups, we can define the extent of polymerization p as

$$p = \frac{N_E}{N_A} \quad (4.27)$$

This parameter is 0 for pure monomer, and it reaches a value of 1 when every end group has been reacted. The number of molecules left in the system when N_E groups have been formed, N_R , is

$$N_R = N_A - N_E \quad (4.28)$$

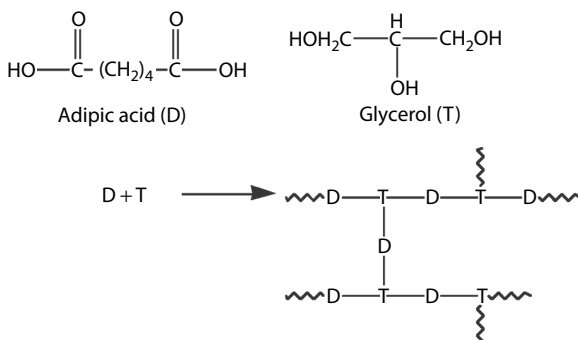
The number-average degree of polymerization x_n becomes

$$\bar{x}_n = \frac{N_A}{N_R} = \frac{1}{1-p} \quad (4.29)$$

We shall use this example to derive a distribution of molecular weights later in Section 6.2.

Note that it is possible to form polymer with a mixture of monomers that have reactive groups A and B on different monomers, for example, A–A monomers can be mixed with an equal number of B–B monomers. Many commercially important polyesters and polyamides are made in this way by combining two dissimilar monomers of functionality 2, with different functionalities A and B, such that A will react only with B and not with itself, and vice versa. The result is something like a copolymer. However, since it is perfectly alternating, it is more convenient to think of it as a **dyadic homopolymer**. PETE and nylon 6,6, for example, exhibit the regularity and crystallinity typical of homopolymers and are useful as fibers as well as other uses. If one were to use a mixture of diacids rather than a single one in making a polyamide, the result would no longer be a perfect dyadic polymer. The regularity would be disrupted and the tendency to crystallize diminished as in normal random copolymerization.

When polyfunctional monomers are involved, successively higher conversion of monomer to polymer increases the probability of forming a network. It is important to be able to predict the maximum degree of conversion to which it is safe to go before network or gel formation occurs. A simple condensation between a trifunctional molecule T, which does not react with itself but does react with a bifunctional molecule D, has been analyzed [42]:



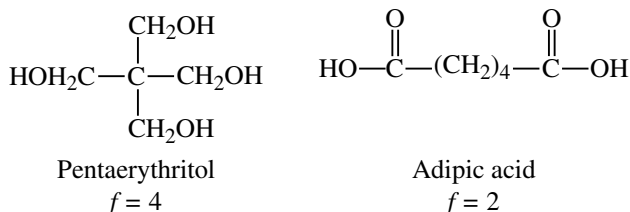
If the initial ratio of hydroxyl groups to carboxyl groups is ρ and the initial number of hydroxyl groups and carboxyl groups is N_T and N_D , respectively, incipient gelation will take place when $(N_E)_g$ ester groups have been formed, where

$$(N_E)_g = N_T(2\rho)^{-0.5} \quad (4.30)$$

At this point the probability that each polymer molecule is connected to another one becomes 1, that is, an infinite network has been formed. However, only part of the system is in this network. A substantial amount of polymer remains free and soluble. Further reaction rapidly reduces the soluble, extractable portion. For a monomer of functionality f reacting with that of functionality 2, the fraction of reactive higher functionality groups that have been consumed at the gel point p_F is given by

$$\left(\frac{1}{p_F}\right)^2 = \rho(f-1) \quad (4.31)$$

For example, take the case of the esterification of 1.1 mol of pentaerythritol with 2 mol of adipic acid:



The ratio of reactive groups ρ is $4.4/4.0 = 1.1$. Equation 4.31 indicates that if more than 55% of the hydroxyl groups are reacted ($p_f \geq 0.55$), the system will form a gel. Since ρ is constant, the fraction of carboxyl groups reacted p_B is simply ρp_F , or 0.605. In actual experiments, the predictions based on this equation are somewhat conservative because some of the cross-links formed are intramolecular and do not contribute to total network formation. When there are N kinds of polyfunctional reactants in the same system, an average functionality can be used, where ρ_i is the ratio of the reactive groups on reactant i of functionality f_i to all groups that react the same way:

$$\bar{f} = \sum_1^N f_i \rho_i \quad (4.32)$$

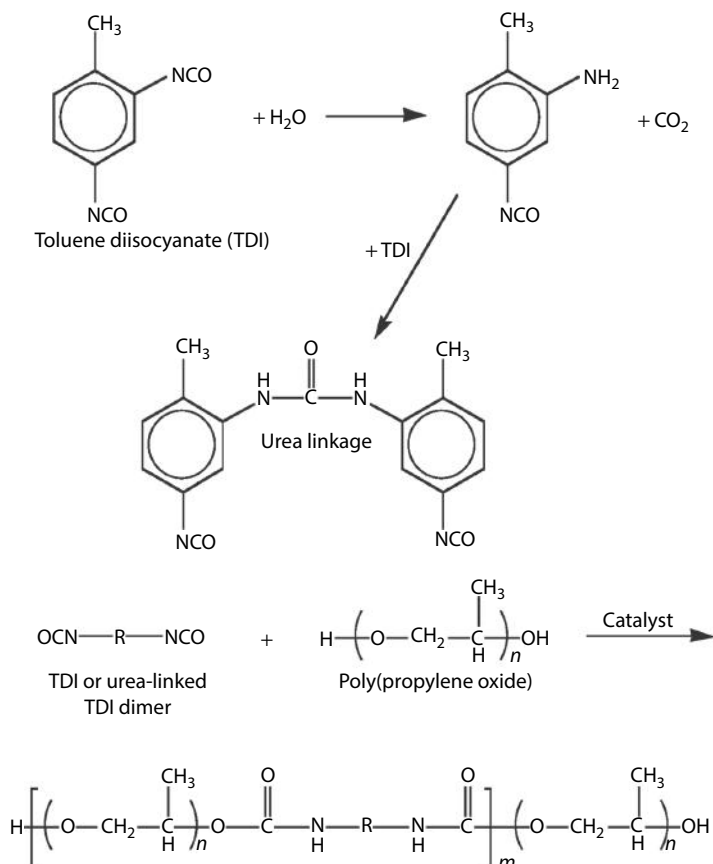
In this way, 1/3 mol of sorbitol, f_i being six hydroxyl groups per molecule, with 1 mole of ethylene glycol, f_i being two hydroxyl groups per molecule, would be the equivalent of 1 mol of pentaerythritol, both in number of available hydroxyl groups and in average functionality (Table 4.3).

Stepwise reactions can offer special problems in controlling reaction rate and molecular weight. In **ring-opening polymerization**, there may be a thermodynamic equilibrium that varies with temperature, as in making nylon 6 from caprolactam (see Section 4.9).

TABLE 4.3
Stepwise Reactions with Polyfunctional Monomers

	Functionality, f_i	Initial Moles of Reactant	Moles of Functional Group	ρ_i
1. Two reactants, $r = 1.1$				
Pentaerythritol	4	1.1	4.4	1.0
Adipic acid	2	2.0	4.0	1.0
2. Two alcohols, $r = 1.0$				
Sorbitol	6	0.33	2	0.5
Ethylene glycol	2	1	2	0.5
Adipic acid	2	2.0	4	1.0

In many isocyanate systems, reactions can be so rapid as to present problems in control. Isocyanate foam production involves the following reactions to form CO_2 as foaming agent and then the polymer network:



These reactions are so rapid at room temperature that special machinery had to be developed to bring the ingredients (and others) together in a matter of seconds, giving a continuous mat of foam product, that is, the urethane polymer indicated. The important point here is that despite the condensation with ejection of a small molecule, the reaction is not easily controlled.

Stepwise polymerization can sometimes be stopped at an early stage and completed in a separate piece of equipment. Such two-stage polymerizations are quite common. In the isocyanate example above, the polypropylene oxide is a low-molecular-weight ($x_n = 15$), ring-opening polymer that then becomes part of the isocyanate foam by a different reaction.

Network polymers often are made in two stages, which may use the same reaction. One of the first synthetic polymers was based on the product of phenol and formaldehyde. Even today, more than 100 years later, this polymer plays an important role in the microelectronics industry as the basis of photoresists. Phenol-formaldehyde condensation is carried out in two stages (Figure 4.15). The first produces a mixture of low-molecular-weight linear and branched polymers that are still fusible and soluble in organic solvents. (It is this product that is used for photoresists.) This reaction may be carried out in a large glass-lined reactor. Final production of the cross-linked network uses the same reaction carried out concurrently with the final molding operation. This is necessary because a thermoset material like this cross-linked network cannot be remolded. (Nor can it be easily removed from a 5000-gal reactor if the first stage proceeds too far too fast.)

Other technologically important network polymers include epoxy thermosets used in the printed circuit board manufacture, a variety of rubber materials as sealants and adhesives, and cross-linked, high durability coatings.

4.8.1 HYPERBRANCHED POLYMERS AND DENDRIMERS

Many years ago, Flory described the behavior of a polymer constructed from AB_2 monomers [42]. Normally multifunctional monomers will lead to cross-linking. If this monomer is used, each B group will react with an A group to form a branch. This branching will go on indefinitely until all monomers are used up. However, cross-linking does not occur. In fact, nature uses such polymer architectures in starch and glycogen. The resulting polymer resembles a bush where the starting monomer is the stem of the bush and the additional units are the branches on the bush. This **hyper-branched** molecule is very compact and has a smaller radius of gyration than linear polymers of the same degree of polymerization. Thus, it could be very efficient for storing energy as nature does. Flory also showed that the molecular weight distribution of such polymers is extremely broad.

More recently molecular materials based on this branching idea have been produced in which the starting point is a multifunctional central molecule. Hyperbranched structures grow from this central point. Typically, each repeat unit contains a branch and a large number of identical units lie at the chain ends. This class of polymer-like materials is known as **dendrimers**, the name coined by Tomalia to describe a family of polyamidoamines [43]. Dendrimers are globular materials with diameters of a few nanometers making them about the size of a virus. The branched structure

can be used to entrain metal ions, drugs, or other materials and carry the contents into a variety of environments. The dendrimers are small enough that cells can capture them during endocytosis. In this fashion, drugs trapped in the confines of the dendrimer can be delivered. The melt viscosity of dendrimers has been shown to be lower than that of polymers of similar molecular weight because of their compact size. Generally dendrimers have narrow molecular weight distributions because of the stepwise way in which they are built [44].

There are two approaches to dendrimer synthesis. The first, now known as the divergent strategy, involves growing branches from a central point to a layer of monomer units. A chemical reaction is used that stops after each layer is added and then the periphery of the dendrimer must be reactivated. Only about four layers or generations can be added before the growth process becomes too inefficient due to steric crowding. A synthetic scheme for preparation of such dendrimers is shown in Figure 4.16. The molecular structure shown is commercially available in large quantities and is based on polypropylene imine [45]. Via Michael addition, acrylonitrile is added to a multifunctional amine core, and since each amine group is difunctional and the vinyl group is monofunctional, we have an AB_2 unit added for each acrylonitrile unit. Only a single generation of units can be added at a time. Subsequent to the growth of each layer, the nitrile groups are hydrogenated to regenerate the amine groups on the outside of the dendrimer. The next layer is added by an additional reaction of acrylonitrile followed again by hydrogenation. This is repeated until it can go no further and usually produces a dendrimer of about four generations. While the resulting dendrimer has a narrow molecular weight, imperfections in the hydrogenation and Michael addition steps lead to side products.

An alternate approach involves a **convergent** synthetic scheme. In this case, a wedge-shaped unit is prepared consisting of AB_2 repeat units [46]. These wedges are then connected to a central point at the wedge A unit to form the dendrimer. Usually, the central unit has two, three, or four branches. While in principle it should be possible to add many generations of growth to each dendrimer molecule, in fact their growth is limited by the same steric crowding present in the divergent strategy, and thus dendrimers are limited to approximately four generations. One of the most

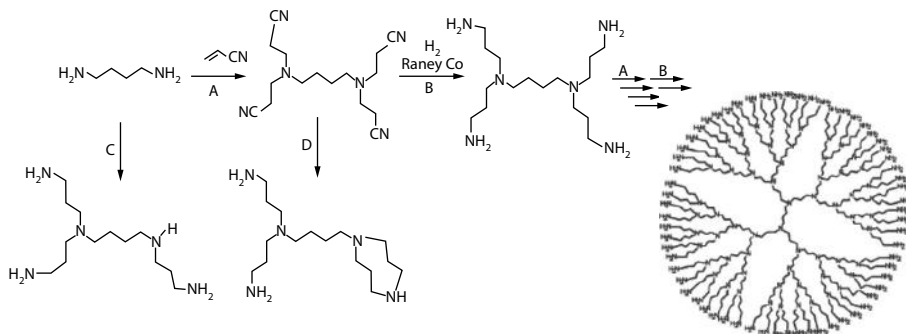


FIGURE 4.16 The formation of a dendrimer using the divergent approach involving Michael addition of acrylonitrile to an amine core. Each addition step is followed by a hydrogenation to reform amine functions for subsequent addition of acrylonitrile.

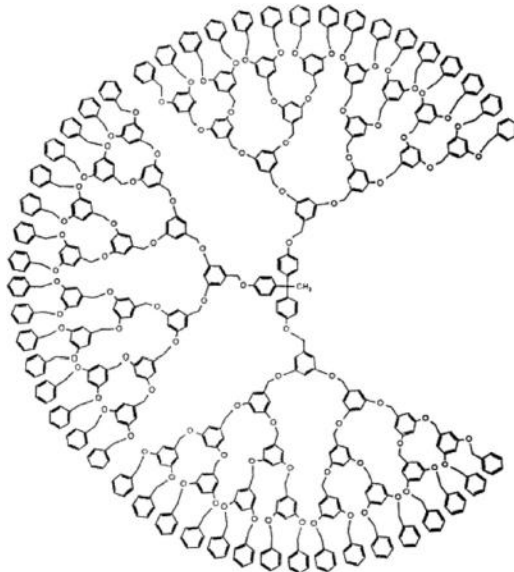


FIGURE 4.17 A dendrimer built from three dendrons using the Fréchet approach to convergent dendrimer synthesis.

successful approaches to the divergent strategy has been using benzylic groups. In this approach, the AB_2 unit is a 3,5-dihydroxy benzyl alcohol. The phenolic groups are protected and the benzyl alcohol is converted to a benzyl bromide. This group is used to form an ether link to a phenolic group and so the growth of each wedge or dendron is started. Once each dendron is formed, it can be linked to a central core of several junction points. As shown in Figure 4.17, these wedges are linked to a three-arm structure.

An interesting effect of this synthetic scheme is that populations of dendrimers can be made to have a single molecular weight. This property is in contrast to synthetic polymers that consist of populations of polymers with a distribution of different molecular weights. The monodisperse nature of dendrimers has been demonstrated by using such methods as matrix-assisted laser desorption-ionization time-of-flight (MALDI-TOF) mass spectroscopy as other methods intended for polymers are not sufficiently sensitive. When dendrimers of precise molecular weight are studied, it can be shown that solution viscosity roughly increases with dendrimer generation, but that viscosity is less than what would be expected for a polymer of similar molecular weight.

4.9 RING-OPENING POLYMERIZATION

When a ring is opened to form a linear polymer, the propagation step may resemble either chain or stepwise polymerization. It was pointed out in Section 4.8 that an equilibrium may be set up between open-chain and ring structures when the monomer (i.e., the ring) is as reactive as growing polymer. In making nylon 6 from caprolactam, no condensation is involved because the product has the same

composition as the reactants (Figure 4.15b). At 220°C with 1 mol of water to 10 mol of monomer initially, an equilibrium is reached rather rapidly in which the reaction mixture contains about 5% unchanged monomer, even though the number-average degree of polymerization is nearly 100 [47]. The residue of monomer can present a problem in purification. It may be necessary to inactivate the equilibration catalyst and then remove the unreacted monomer by vacuum stripping or solvent extraction.

Usually only small rings are involved in such equilibria. The silicones are an exception in that a continuous series of rings of increasing sizes are formed. Silicone rings can be isolated with up to 80 ring atoms (see Section 17.7). The polymerization of cyclopentene with a tungsten catalyst also leads to an equilibrium among large rings. A catalyst can be formed when WCl_6 with tetraalkyl tin modified by ethyl ether. The combination bears some resemblance to the Ziegler system (Section 4.6). The reactions are summarized in Figure 4.18. The term **olefin metathesis** has been applied to this reaction [48]. When an acyclic olefin is introduced, the large rings are interrupted and made into open-chain polymers. In one example, monomer

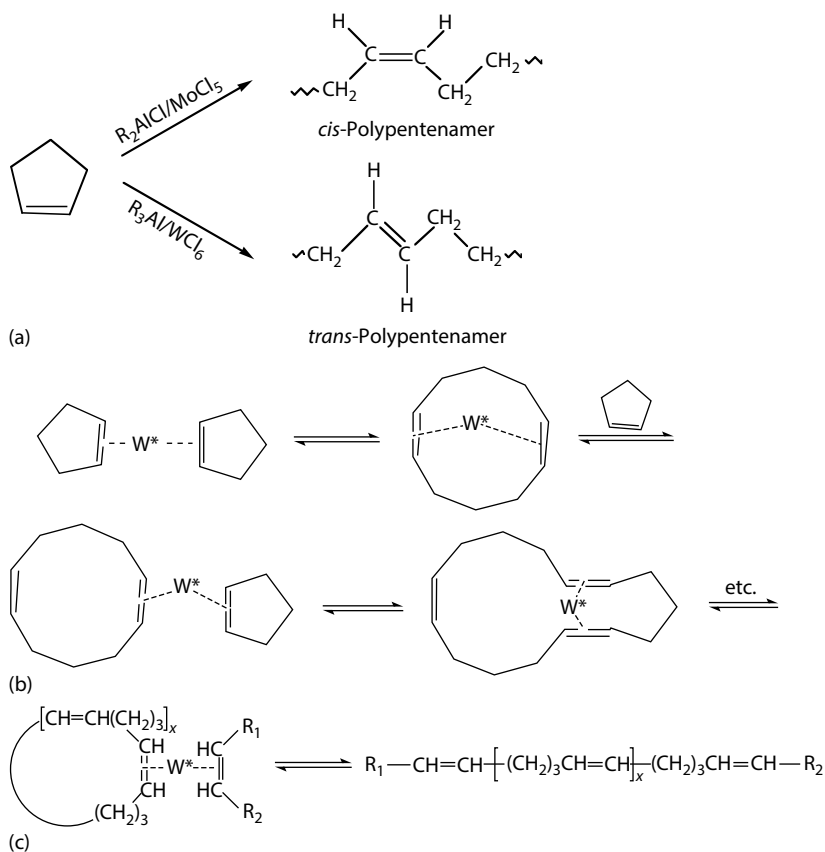


FIGURE 4.18 Ring opening by olefin metathesis. (Data from Calderon, N., and R. L. Hinrichs, *Chem. Tech.*, 4, 627, 1974.) (a) Polymerization of cyclopentene; (b) olefin metathesis; (c) cross metathesis with acrylic olefin.

is completely converted to polymer in 30 min at 0°C with a ratio of monomer to tungsten of about 10,000. The low temperature is needed to keep the equilibrium concentration of cyclopentene down. In general, higher temperatures favor rings over open-chain polymers.

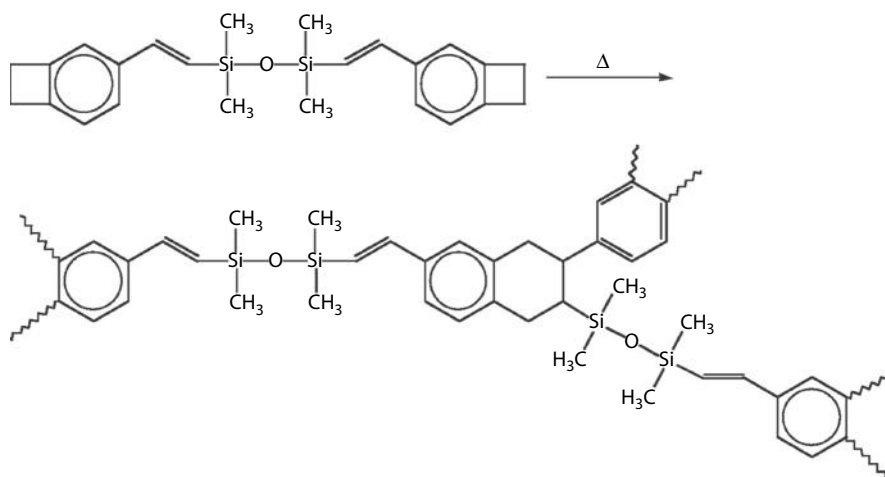
Recently researchers have examined the polymerization of polycarbonates and polyesters from macrocycles, ring structures made up of dozens of repeat units. The advantage of this approach is that a low-melting-point, low-viscosity macrocycle can be molded in shape and then converted to a polymer [49]. This process has not yet been commercialized.

Another common feature of most ring-opening schemes is the low heat of polymerization. Polybutadiene has a very similar structure to polypentenamer, but the isothermal conversion of butadiene to polymer requires removal of 74.9 kJ/mol, whereas conversion of cyclopentene to polymer requires removal of only 18.4 kJ/mol. A commercial polyalkenamer and other polymers made from metathesis and ring-opening metathesis polymerization are described in Section 16.4.

For strained rings with only three or four atoms, ring opening is easy and the heat of polymerization is comparatively large. In going from liquid monomer to amorphous, solid polymer, the heat of polymerization is 94.5 kJ/mol for ethylene oxide and 105 kJ/mol for a cyclobutane ring. The reactions of epoxy resins containing the three-membered oxirane ring are described in Section 13.4 both as coatings and as adhesives.

4.9.1 BIS-BENZOCYCLOBUTANE RESIN

Much newer are thermosetting resins containing the cyclobutane ring [48]. To polymerize the monomer ($T_m = 152^\circ\text{C}$), it is first melted by heating at 160°C . When the temperature is raised to 200°C , polymerization occurs rapidly to form a network structure with no added catalyst [50]. Most often the resin is used in composites with large amounts of glass fibers or other reinforcement. The temperature stability of the chemical structure shown below is high enough, so that it can be used as an insulating material in microelectronic circuit manufacture.



4.10 CHAIN COPOLYMERIZATION

When more than one monomer is polymerized at the same time, a variety of structures can result. In a step-growth polymerization with more than one monomer but the same pair of functional groups, the reaction rate can be assumed to be the same for each monomer. Thus, they react in a statistical manner that leads to a random distribution of monomers in the final polymer.

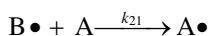
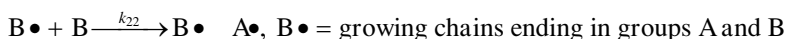
In the simple case of two monomers A and B in a chain polymerization, the rate of polymerization of each monomer is rarely the same. One can derive relationships that will help answer some questions about the degree of heterogeneity of the products made under various conditions:

1. What is the composition of a polymer made from the limited conversion of a mixture of two monomers?
2. How will two monomers that never have copolymerized before interact?

The first is answered by introducing relative reactivities. The second is approached by the Alfrey–Price *Q–e* scheme. To express the relationship of polymer composition to the monomer composition from which it is being formed, we go back to the kinetic scheme of Section 4.4. If we can assume that we achieve a *steady-state* population of chain radicals that grow to high molecular weight, the material balances for various species are few and simple for a binary system.

4.10.1 ASSUMPTIONS

1. Over any short time interval, the concentration of free radicals does not change appreciably with time, that is, $d[\text{radical}]/dt = 0$.
2. A growing polymer chain's reactivity is determined solely by the last monomer unit added. This reactivity is independent of the molecular weight.
3. The only monomer-consuming reactions taking place, together with their rate constants, are as follows:



That is, a growing chain whose last added unit was monomer A has reactivity determined by A only. This chain can add another A, in which case reactivity is unchanged; it may also react with B, in which case the new reactivity is determined by B.

4. Propagation is the only reaction of importance, since it is repeated many times for each initiation or termination step.

4.10.2 MATERIAL BALANCES

1. Rate of creation of radicals ($t = \text{time}$):

$$\frac{d[A\bullet]}{dt} = k_{21}[B\bullet][A] - k_{12}[A\bullet][B] = 0 \quad (\text{assumption 1}) \quad (4.33)$$

or

$$\frac{[A\bullet]}{[B\bullet]} = \frac{k_{21}[A]}{k_{12}[B]}$$

2. Rate of consumption (disappearance) of monomers A and B:

$$-\frac{d[A]}{dt} = k_{11}[A\bullet][A] + k_{21}[B\bullet][A] \quad (4.34a)$$

$$-\frac{d[B]}{dt} = k_{12}[A\bullet][B] + k_{22}[B\bullet][B] \quad (4.34b)$$

We define the **relative reactivities** as $r_1 = k_{11}/k_{12}$ and $r_2 = k_{22}/k_{21}$. In both cases, these ratios are the ratio of the reactivity of the monomer toward itself to the reactivity of the monomer toward the other monomer. Now at the instant when monomer concentrations are $[A]$ and $[B]$ (moles per liter), the rates at which monomer is entering a growing polymer chain are

$$-\frac{d[A]}{dt} \quad \text{and} \quad -\frac{d[B]}{dt}$$

The mole fraction of monomer A being added to the growing polymer at this instant, F_1 , then is

$$F_1 = \frac{d[A]/dt}{d[A]/dt + d[B]/dt} \quad (4.35)$$

Of course,

$$\frac{F_1}{F_2} = \frac{d[A]}{d[B]} \quad (4.36)$$

Now we let

$$f_1 = \frac{[A]}{[A] + [B]} \quad \text{and} \quad \frac{f_1}{f_2} = \frac{[A]}{[B]} \quad (4.37)$$

Combining Equations 4.33 through 4.37 gives

$$\frac{F_1}{F_2} = \frac{(r_1 f_1 / f_2) + 1}{(r_2 f_2 / f_1) + 1} \quad (4.38)$$

or

$$\frac{F_1}{1 - F_1} = \frac{r_1 f_1 / (1 - f_1) + 1}{r_2 (1 - f_1) / f_1 + 1}$$

Thus, we have related the *instantaneous* copolymer composition F_1 to the instantaneous monomer composition f_1 by two parameters r_1 and r_2 . We say *instantaneous* because if A and B are consumed at different rates so that $F_1 \neq f_1$, the value of f_1 will change as monomer is converted to polymer in a batch operation.

4.10.3 SPECIAL CASES

Several cases simplify Equation 4.38. If k_{12} and k_{21} are 0, no copolymer is formed, but only a mixture of homopolymers is formed. If k_{11} and k_{22} are 0, only perfectly alternating copolymer is formed ($F_1 = F_2 = 0.5$). If $r_1 = r_2 = 1$, then $F_1 = f_1$. An interesting special case is $r_1 r_2 = 1$, when Equation 4.38 becomes

$$\frac{F_1}{1-F_1} = \frac{r_1 f_1}{1-f_1} \quad (4.39)$$

This resembles the vapor y -liquid x composition at constant relative volatility α_r :

$$\frac{y}{1-y} = \frac{\alpha_r x}{1-x} \quad (4.40)$$

In such *ideal* copolymerization, the F_1 - f_1 curve never crosses the F_1 - f_1 diagonal, whereas when $r_1 r_2 \neq 1$, there can be a point where they cross to give an *azeotrope* at which $F_1 = f_1$ (Figure 4.19). Equation 4.38 can be rewritten as

$$Y = r_1 X \frac{1+r_1 X}{r_1 r_2 + r_1 X} \quad (4.41)$$

where:

$$Y = F_1/(1-F_1) \text{ and } X = f_1/(1-f_1)$$

r_1 and r_2 are the relative reactivities

Terpolymers (three monomers) require six relative reactivities and can be handled conveniently only in special cases or by computer methods.

Example 4.6

The reactivity of a combination of monomers depends a great deal on the nature of the polymerizing center. For example, the reactivity ratios of butadiene (1) and styrene (2) are quite different in an anionic copolymerization ($r_1 = 5$, $r_2 = 0.04$) and in a radical copolymerization ($r_1 = 1.39$, $r_2 = 0.78$). If a copolymerization is performed with a 50/50 mixture of the two, what are the initial compositions of the polymers formed in the two cases?

Solution: Using Equation 4.38, the equation that provides the *instantaneous* copolymer composition, F_1 , for the anionic polymerization case is

$$\frac{F_1}{1-F_1} = \frac{5 \times 0.5(1-0.5) + 1}{0.04 \times (1-0.5)/0.5 + 1}$$

Rearranging and solving for F_1 gives a value of 86% butadiene in the polymer. In fact, this method is used commercially to form a pseudo-block copolymer, since once the butadiene is used up, then only styrene is added to the living end of the growing polymer chain. Similarly, using the reactivity ratios for a radical polymerization, then a polymer with 58% butadiene is produced.

For the simple case of only two monomers, the problem of calculating F_1 as a function of degree of conversion and initial monomer composition is analogous to the situation in differential distillation of a binary mixture. Monomer is converted to polymer irreversibly just as volatile liquids are distilled out from a pot irreversibly. A material balance gives the Rayleigh equation [51] (also called the Skeist equation):

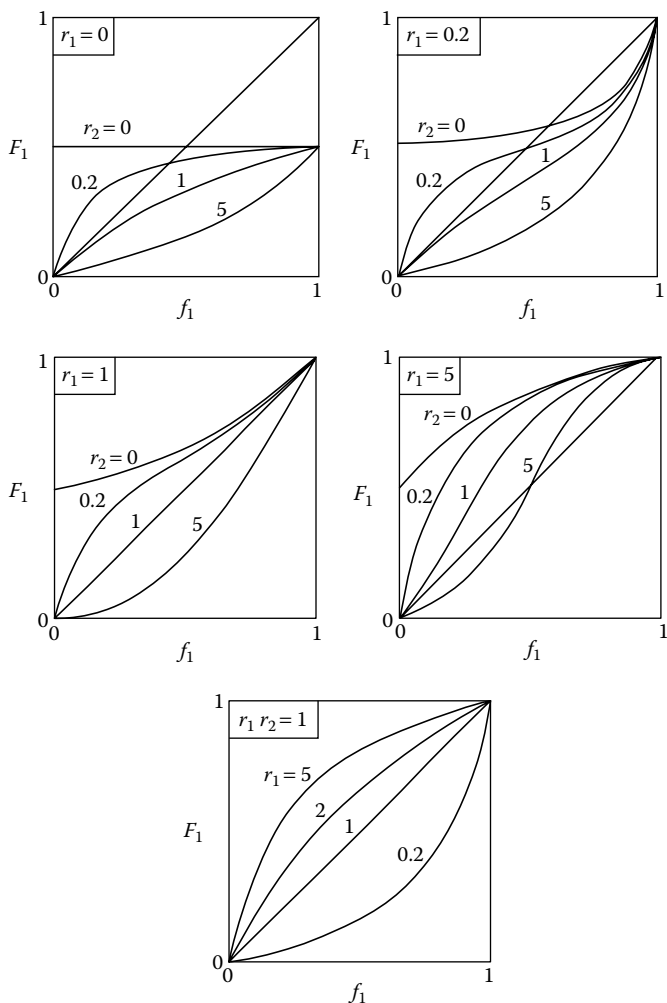


FIGURE 4.19 F_1 being the mole fraction of monomer 1 in polymer formed when f_1 is the mole fraction of monomer 1 in the feed for various combinations of the relative reactivity ratios.

$$\ln\left(\frac{N}{N_0}\right) = \int_{(f_1)_0}^{f_1} \frac{df_1}{F_1 - f_1} \quad (4.42)$$

where:

N/N_0 is the mole fraction of all monomer present initially that is still unreacted
 $(f_1)_0$ and f_1 are the mole fractions of component A initially and at N/N_0 . This can be integrated graphically or analytically, although the analytic result is not tidy except when $r_1 r_2 = 1$. For that case,

$$\left(\frac{N}{N_0}\right)^{r_1-1} = \frac{f_1}{(f_1)_0} \left[\frac{1 - (f_1)_0}{1 - f_1} \right]^{r_1} \quad (4.43)$$

Also

$$\frac{N_1}{(N_1)_0} = \left[\frac{N_2}{(N_2)_0} \right]^{r_1} \quad (4.44)$$

where:

N_1 and N_2 are the number of moles of monomers A and B still in the monomer phase at any time. In the general case [52],

$$\frac{N}{N_0} = \left[\frac{f_1}{(f_1)_0} \right]^\alpha \left[\frac{f_2}{(f_2)_0} \right]^\beta \left[\frac{(f_1)_0 - \delta}{f_1 - \delta} \right]^\gamma \quad (4.45)$$

where:

$$\alpha = \frac{r_2}{1 - r_2}$$

$$\beta = \frac{r_1}{1 - r_1}$$

$$\gamma = \frac{1 - r_1 r_2}{(1 - r_1)(1 - r_2)}$$

$$\delta = \frac{1 - r_2}{(2 - r_1 - r_2)}$$

At $(f_1)_0 = \delta$, an azeotrope is formed.

Some results of an equimolar monomer feed of vinyl acetate and vinyl laurate are shown in Figure 4.20. Although the average polymer composition $\bar{1}$ is never changed much and eventually has to equal the original monomer ratio, the polymer being made at high conversions may approximate pure vinyl laurate. This is a real problem in polymerization methods that attempt complete conversion. Partial conversion with recycling of unreacted monomer and makeup of the more reactive monomer is one method of regulation. Another is to add the more reactive monomer during the reaction to maintain the same monomer and therefore the same polymer composition [53]. Some examples (Table 4.4) are typical in that $r_1 r_2$ seldom exceeds unity. A comprehensive set of relative reactivity ratios has been published by Alfrey

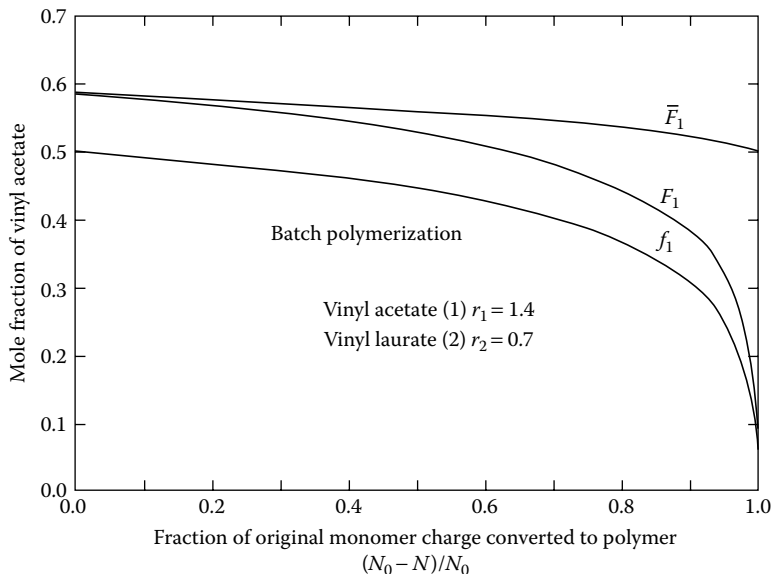


FIGURE 4.20 Polymer and monomer compositions as functions of conversion. F_1 is the mole fraction of monomer 1 in the polymer being formed at a point where the feed composition has shifted to f_1 . \bar{F}_1 is the average composition of all polymer generated up to that point.

and Young [54] and is more extensively tabulated in *Polymer Handbook*. However, it is desirable to have some parameters associated with a single monomer that would allow prediction of r_1 and r_2 for various combinations with that monomer just as bond contribution, and atomic radii are used to estimate bond strengths and interatomic distances. According to the Alfrey–Price relationship [52,53], each monomer can be characterized by values of Q and e that are related to relative reactivities by

$$\ln r_1 = \ln \left(\frac{Q_1}{Q_2} \right) - e_1(e_1 - e_2) \quad \text{and} \quad \ln r_1 r_2 = -(e_2 - e_1)^2 \quad (4.46)$$

Please note the so-called Q – e scheme is rarely used these days, but is included here because some of the concepts are useful. The parameter Q_1 is mainly affected by the relative stability of the polymer chain radical resulting from the addition of monomer 1 to the growing end. As a point of reference, styrene is assigned values of $Q = 1$ and $e = -0.80$. Resonance-stabilized monomers such as 1,3-butadiene are expected to have high Q values, whereas nonconjugated monomers such as ethylene ($Q = 0.015$, $e = -0.20$) have low Q values. The parameter e is expected to reflect the polarity of the monomer and the polymer radical resulting from the addition of the monomer. An electron-donating substituent on the end of a polymer radical, as in *p*-methoxystyrene ($Q = 1.36$, $e = -1.11$), decreases e , while an electron-withdrawing substituent, as in *p*-nitrostyrene ($Q = 1.63$, $e = 0.39$), increases e . The Q – e scheme is analogous to, but not identical with, the linear free-energy relationship, the Hammett equation, which is so important to the physical organic chemistry of small molecules. It should be noted that only a few monomers are tabulated and that the scheme is only moderately

TABLE 4.4
Relative and Copolymerization Parameters

Radical	1,3-Butadiene	Maleic Anhydride	Styrene	Vinyl Chloride	Methyl Methacrylate	Acrylonitrile	Q	e
1,3-Butadiene	1.0	—	1.4	8.8	0.53 ^a	0.35	2.39	-1.05
Maleic anhydride	—	1.0	0.0 ^b	0.008 ^c	0.03 ^b	0 ^b	0.23	2.25
Styrene	0.5	0.01 ^b	1.0	35	0.50 ^b	0.37	1.00	-0.80
Vinyl chloride	0.035	0.296 ^c	0.077	1.0	0 ^b	0.074	0.044	0.20
Methyl methacrylate	0.06 ^a	3.5 ^b	0.50 ^b	12.5 ^b	1.0	23 ^b	0.74	0.40
Acrylonitrile	0.0	6 ^b	0.070	3.7	0.0	1.0	0.60	1.20

Source: Alfrey, T., Jr., and C. C. Price, *J. Polym. Sci.*, 2, 101, 1947.

Notes: All data at 50°C except

a 5°C

b 60°C

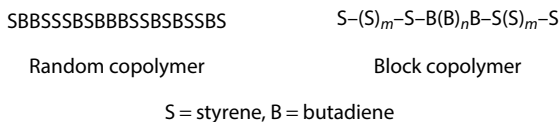
c 75°C

Example: for styrene (1) and acrylonitrile (2), $r_1 = 0.37$ and $r_2 = 0.070$.

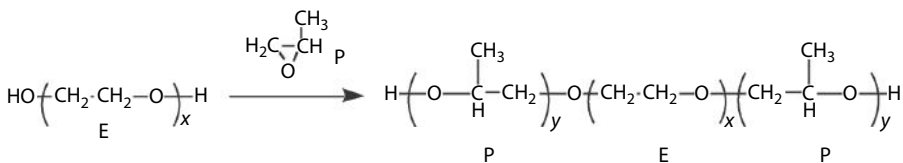
successful, but it is useful where experimental data are sparse. Average values have been calculated and tabulated by Young [54].

4.10.4 OTHER COPOLYMERS

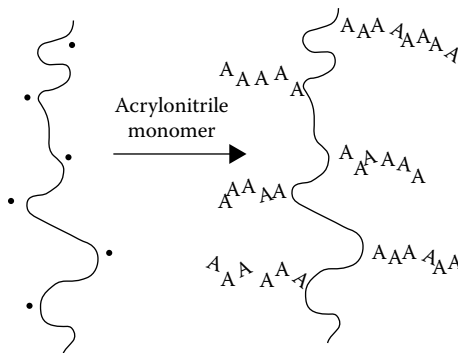
The copolymers discussed so far are *random* in that we polymerize a mixture of monomers and they are arranged in some uniform way along the polymer chain. Even in this case, long runs of one monomer or the other may occur, especially when one monomer is present in higher proportion than the other. We have already mentioned the interesting properties of styrene–butadiene block copolymers used as thermoplastic elastomers. There are many other uses for block copolymers. Template synthesis of mesoporous ceramics is currently being investigated [56]. The self-assembly characteristics of these materials is of importance.



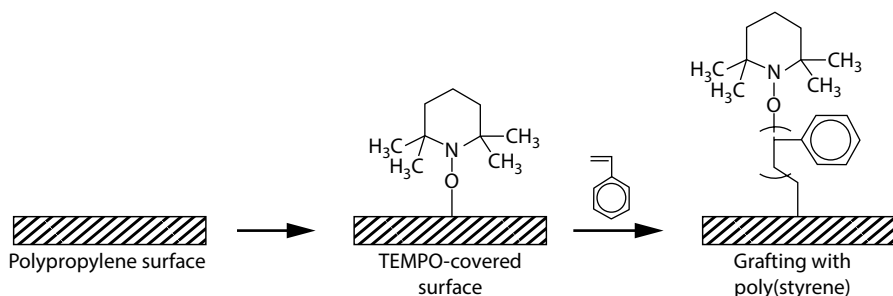
Even low-molecular-weight block copolymers have values for this process. If an ethylene oxide (E) polymer terminating in hydroxyls is used to start a propylene oxide (P) polymerization, a block polymer results with hydrophilic (E) and hydrophobic (P) portions. The products at molecular weights of 1000–2000 are useful as surface-active agents.



A third variety is the **graft** copolymer. In this case, branches of one monomer are grown on a main stem of a previously formed polymer molecule. For example, polyethylene can be irradiated in air with gamma rays or accelerated electrons, which leave peroxides or free radicals *trapped* on the polymer backbone. Exposed to a reactive monomer such as acrylonitrile ($\text{CH}_2=\text{CHCN}$), polymerization is initiated at the free-radical sites, and branches of polyacrylonitrile grow on the polyethylene crystal stem [57].

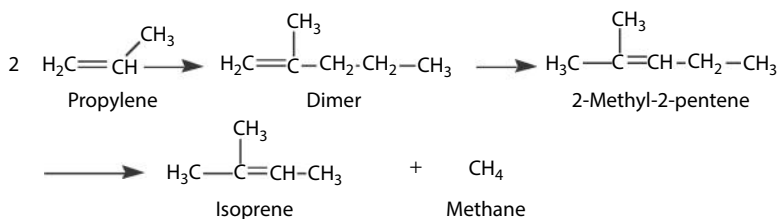


Recently, the growth of tailored surfaces for a variety of applications including biomedical uses have benefited from the understanding of the grafting of polymers. As above, polypropylene can be exposed to radiation to generate radicals. If the surface is immediately exposed to a solution with TEMPO, the radicals can be trapped [58]. The resulting TEMPO-covered surface can be used to initiate the growth of polymer brushes from the surface in which all the chains have the same molecular weight. While a polypropylene surface is shown here, it is also possible to attach the initiator to glass or silicon oxide surfaces and grow brushes from the surface. Initiators based on ATRP or RAFT mechanisms are also possible and a considerable literature has developed around these methods, particularly applied to biomedical applications and studies.



4.11 BIOSYNTHESIS OF POLYMERS

Polymers produced by biological routes invariably are made by some kind of step-wise polymerization rather than a chain polymerization. An interesting example is afforded by *cis*-1,4-polyisoprene. Isoprene can be made from propylene through a sequence of dimerization, isomerization, and steam demethanization [59]:



In a synthetic polymerization, the monomer is easily converted to the *cis*-1,4 polymer by using a butyl lithium initiator in a hydrocarbon solvent (Section 4.5). The identical structure is produced in the plant tissues of the rubber tree *Hevea brasiliensis*. Although over 2000 species of plants produce polyisoprenes, only the one cited is utilized on a large commercial scale, mainly in the warm climates of Malaysia, Indonesia, and Liberia. Brazil, original home of the plant, no longer contributes significantly to the world's supply. Like other plants, the tree contains tubes or vessels that convey water and salts from the roots to the leaves and a second system that carries soluble sugars down from the leaves in the sap. Unlike most other plants, the rubber tree has a third system of vessels in which the sugars

are converted into a latex, a stabilized emulsion of rubber particles along with the other compounds necessary to the process such as enzymes, sterols, and lipids. The function of the rubber in the tree is unknown. Apparently it does not serve as a food reserve in the way that starch does in other systems. The primitive raw material used in the latex formation is acetic acid [60,61]. Many intermediate products have been isolated or demonstrated by incorporation of ^{14}C -labeled compounds in the growing plant. A number of enzymes and other catalysts are necessary. Some stages in the conversion of biomolecular precursors to polyisoprene are indicated in the sequence of Figure 4.21. The manner in which the pyrophosphate adds to the growing chain and the specific enzyme that is involved is not known with certainty.

Although most commercially important polysaccharides are recovered from plants and trees, progress has been made in producing some by controlled fermentations in conventional plant equipment. Raw cotton contains over 85% cellulose, which is the linear polymer of β -D-glucopyranose (Figure 4.22). The formal indication of the structure for the pyranose unit is somewhat misleading, since the rings are not planar and

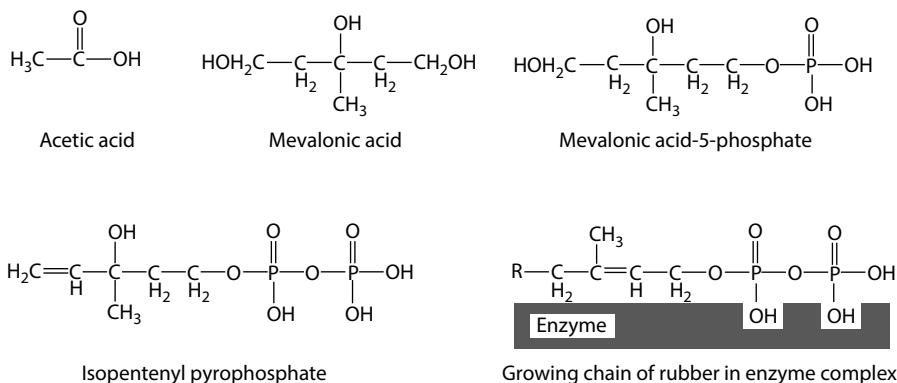


FIGURE 4.21 Intermediates in the biosynthesis of rubber. (Data from Archer, B. L. et al.: chap. 3 in L. Bateman, ed., *The Chemistry and Physics of Rubber-Like Substances*. 1963. New York. Copyright Wiley-VCH Verlag GmbH & Co. KGaA. Reproduced with permission.)

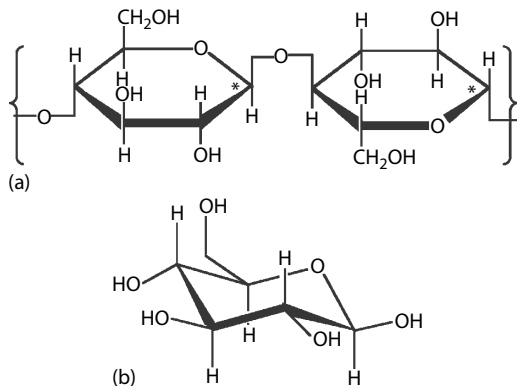


FIGURE 4.22 (a) Cellulose repeating structure, β -D-glucopyranose unit; (b) D-glucose.

the bond angle at the oxygen connecting successive rings is distorted. The important feature to note is that all of the ring carbons are asymmetric and therefore give rise to possible stereoisomers. The changes in physical properties can be great. For example, the unbranched component of starch, amylose, differs only in that the carbon marked with an asterisk in Figure 4.22 has the oxygen below the ring rather than above as in cellulose. However, amylose dissolves in water but cellulose does not. As in the case of rubber, phosphates appear to be intermediates in the biosynthesis of polysaccharides. Glucose-1-phosphate in the presence of an enzyme extracted from potato juice can be converted to amylose. The energy for carrying out polymerization is obtained by the oxidation of some of the starting monosaccharide. A variety of microorganisms can produce cellulose from sugar in the proper culture medium. However, cellulose from such an operation cannot compete economically with polymer from cotton or wood.

The biopolymers discussed here have a relatively simple structure in which a single or a very few repeat units are involved. The enzymes that catalyze these reactions are complex proteins. A large number of laboratories work today on the structure of proteins and other polymeric components of living organisms such as ribonucleic acid (RNA) and deoxyribonucleic acid (DNA). The importance of nucleic acids (combinations of phosphoric acid, sugars, and nitrogenous bases) is that they, in cooperation with proteins, are the main constituents of viruses and genes, and occur in all living cells. Synthesis of these materials is remote but conceivable.

A close approximation to test tube creation of a biologically active substance was made at Stanford University [59]. Using a tritium-labeled (+) DNA as a template, workers were able to make an artificial (–) DNA from modified monomer units. The resulting (–) DNA was different from that usually found in nature, but it was able to act as a reverse template to reproduce (+) DNA identical with the starting material. This experiment does not demonstrate the total synthesis of living matter from the elements. It does show that genetic modification by chemical means is a distinct possibility. Total syntheses of **enzymes** have been reported (see Section 15.3).

Often it is worthwhile to be able to make proteins and other biopolymers synthetically. The composition and molecular weight control possible in a natural polymer are very difficult synthetically. Merrifield developed a synthetic method that permits the formation of short polymer segments of controlled composition by working out a protection–deprotection strategy on supported catalysts [62]. A typical reaction sequence is shown in Figure 4.23 and involves first attaching a protected monomer to a cross-linked, insoluble polymer bead (shown as the circle in the figure) [63]. After attachment the end group of the monomer on the bead is deprotected. The next step is the attachment of the next monomer (here alanine) and removal of the dimer from the bead as well as removal of the protecting group on the amine function. Larger polypeptides of defined length and composition can be prepared by repeating the process many, many times. It is the only synthetic process that rivals nature in its ability to control molecular weight and composition with high precision. Merrifield won the Nobel Prize for this process that even today is still important. The chemistry invented for this synthesis has found many other uses and was instrumental in enabling advanced photoresists. Once the target polymer is produced, then it is removed from the polymer bead. Robotic synthesizers are available, so that polymer synthesis can be carried out by simply programming a machine.

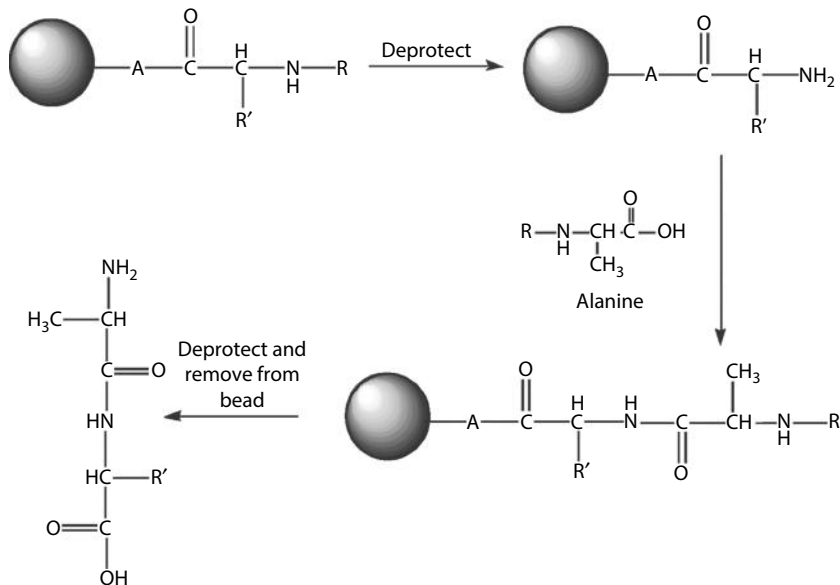


FIGURE 4.23 The Merrifield synthesis of an oligopeptide dimer.

More recently, scientists have learned to make polymers by harnessing the machinery of life. One approach is to make an artificial genome and insert it into *Escherichia coli* bacteria. Then the **genetically engineered bacteria** produce the desired protein in large quantities as outlined in Figure 4.24. The resulting polymer has a precise sequence and preselected molecular weight. A limitation of the **Merrifield route** is low molecular weight, which is easily overcome in the bacterial approach. Interestingly, to make the artificial genome inserted in bacteria for protein synthesis requires the use of the kind of polymer synthesis described above. While it is possible to use the naturally occurring amino acids, it is also possible to contemplate the use of artificial amino acids [62]. Work to form liquid crystalline fluoropolymers from artificial proteins has been carried out, as well as the production of proteins with organic conducting segments.

Several families of bacteria actually store energy in the form of a plastic rather than fat or starch, as do other living systems. Thus, if bacteria that produce a polymer of interest are identified, they can be grown and the polymers harvested. One such polymer produced by the bacterium *Pseudomonas oleovorans* that has achieved near commercialization is based on hydroxybutyric acid that is polymerized by the bacteria to form a polyester [64]. Such polyesters have the advantage that they are biodegradable. The precise polymer that is produced by the bacteria depends on the chemical feed, essentially set by what the bacteria are eating. Polymers ranging from rubber to thermoplastic have been produced and tests of their use in recyclable packaging have been carried out. The structure of a bacterial elastomer is shown in the scheme below. The polymer as shown is a low T_g material that will flow at room

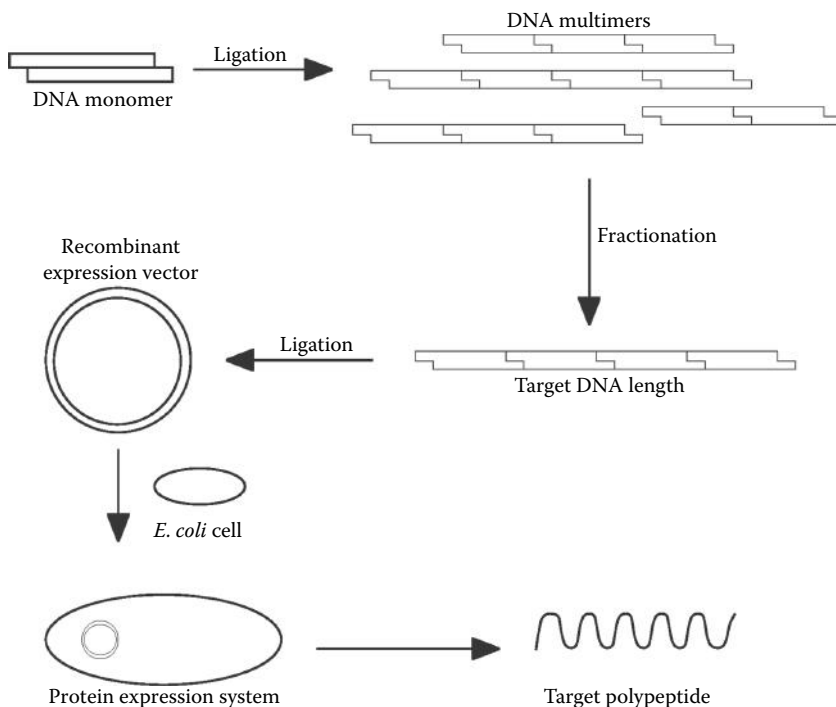
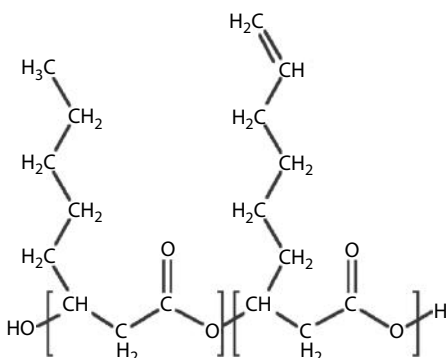


FIGURE 4.24 Engineering new polymers via bacterial cell growth.

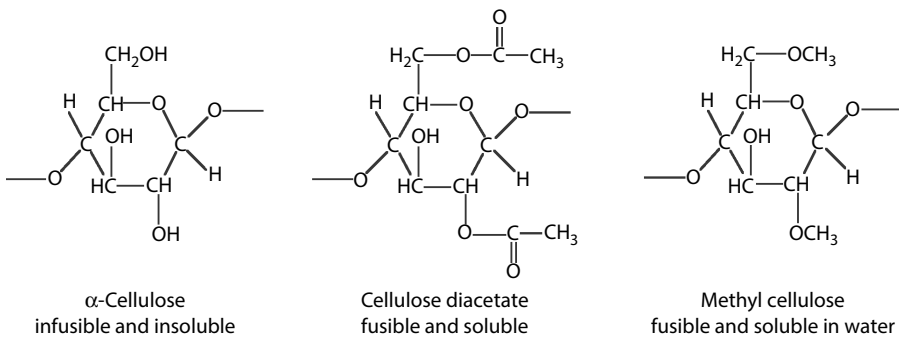
temperature. Cross-linking to the elastomer takes place through the pendant double bond and can make use of many radical curing processes.



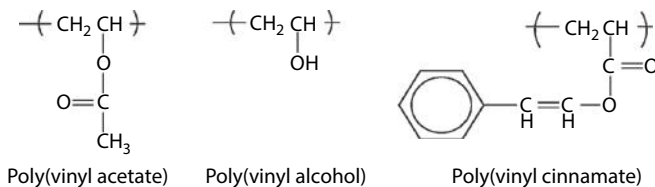
4.12 POLYMER MODIFICATION

Whenever a polymer is formed in several stages, each subsequent stage is a kind of polymer modification. All cross-linking reactions (vulcanizations) of rubber would fall in this category, together with the molding of network polymers such as the phenol formaldehyde resins. However, the term *polymer modification* is used here to

mean changes wrought by the polymer manufacturer in an operation separate from the final molding, spinning, or formation. Modifications are feasible when a polymeric raw material that can have its value enhanced substantially by the operation is available. Two naturally occurring polymers in this category are α -cellulose and natural rubber. In the form of cotton, α -cellulose is already valuable as a fiber. Even with cotton, the chemical treatment to give wash-and-wear properties may amount to a polymer modification. But cotton linters, the short fibers remaining from cotton ginning, and also α -cellulose from wood pulping are not easily utilized. The hydrogen-bonded structure of cellulose prevents it from melting or dissolving below its decomposition temperature. Permanent reaction of these hydroxyl groups by esterification or etherification results in materials that are soluble and fusible—and therefore capable of being molded or cast in useful forms.



Sometimes several purposes can be served at once. Chlorination of natural rubber decreases the flammability of the polymer. At the same time, it raises the T_g so that the polymer can be used as a binder for traffic paints. Nitration of cellulose allows the native cotton to be plasticized and molded. Flammability is enhanced at the same time. This may be a disadvantage to makers of molded articles for decoration and apparel. However, the munitions manufacturer regards the flammability and propellant power of guncotton, cellulose nitrate, as its most important advantage. Most often a polymer modification is economically justifiable only when the original polymer occurs naturally or as a by-product. Sometimes modification is the only good way to make a material. A case in point is the photosensitive polymer polyvinyl cinnamate.



An attempt to polymerize vinyl cinnamate would give a cross-linked network, since the functionality is 4. Even polyvinyl alcohol cannot be made directly, because the monomer is unknown (isomeric with acetaldehyde). Thus, it is necessary first to polymerize vinyl acetate, then to hydrolyze the polymer to the polyalcohol. Finally, the alcohol

TABLE 4.5
Typical Polymer Modifications

Purpose of Modification	Initial Polymer	Chemical Reactions	Example of Final Form
Change physical form	α -Cellulose	Regeneration via xanthate	Rayon, cellophane
Change solubility	α -Cellulose	Esterification	Cellulose acetate
		Etherification	Cellulose nitrate
			Hydroxy ethyl cellulose
			Carboxy methyl cellulose
			Ethyl cellulose
	Polyvinyl acetate	Hydrolysis	Methyl cellulose
	Polyvinyl alcohol	Acetal formation	Polyvinyl alcohol
Introduce cross-linking sites	Butyl rubber	Bromination	Polyvinyl butyral
	Polyvinyl alcohol	Esterification	Polyvinyl formal
Increase flammability	α -Cellulose	Esterification	Brominated butyl rubber
Decrease flammability	Natural rubber	Chlorination	Polyvinyl cinnamate
Change mechanical properties	Natural rubber	Graft copolymerizations of methyl methacrylate	Cellulose nitrate (guncotton)
			Chlorinated rubber
			Graft copolymer

is esterified by cinnamic acid (functionality of 1 in an esterification). Exposure of a film of polyvinyl cinnamate to ultraviolet light causes rapid formation of a cross-linked, insoluble network (see Section 13.5). It has been used as a *photoresist* to establish etched patterns on lithographic plates. Some other typical modifications are listed in Table 4.5.

KEYWORDS

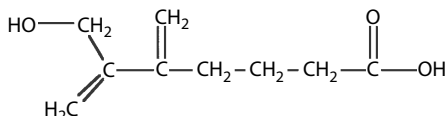
Functionality
 Step-growth polymerization
 Chain polymerization
 Initiation
 Initiator
 Propagation
 Termination
 Coupling
 Disproportionation
 Free-radical polymerization
 Half-life
 Kinetic chain length
 Degree of polymerization
 Chain transfer
 Chain transfer agent
 Inhibition

Inhibitor
Living radical polymerization
Redox initiation
Activation energy
Cationic polymerization
Living cationic polymerizations
Gegen ion
Anionic polymerization
Living polymer
Block copolymer
Thermoplastic elastomer
Living radical polymerization
Nitroxide-mediated polymerization (NMP)
Atom transfer radical polymerization (ATRP)
Reversible addition/fragmentation chain transfer (RAFT)
Block copolymer
Star polymers
Coordination complex polymerization
Insertion polymerization
Group transfer polymerization
Ziegler–Natta catalysis
Telechelic
Metallocene
Step-growth
Condensation
Ring opening
Pseudocondensation
Dyad
Hyperbranched
Dendrimers
Ring-opening polymerization
Olefin metathesis
Copolymerization
Random copolymer
Graft polymer
Q–e scheme
Relative reactivity
Azeotrope
Biosynthesis
Hevea brasiliensis
Enzymes
Escherichia coli
Merrifield synthesis
Genetically engineered bacteria
Pseudomonas oleovorans
Polymer modification

PROBLEMS

4.1 What structures can occur in the polymer when chloroprene, $\text{CH}_2=\text{CCl}-\text{CH}=\text{CH}_2$, is polymerized?

4.2 Consider this monomer:



- (a) What is the functionality of this monomer in a free-radical or ionic polymerization? Name and describe the isomeric forms expected in linear polymers formed by such reactions.
- (b) What is the functionality of this monomer in a polyesterification? Name and describe the isomeric forms expected in linear polymers formed by such a reaction.
- (c) Which would you expect to have the higher T_g , linear polymer from (a) or (b)? Why?
- 4.3 What is the energy of activation for the decomposition of di-*tert*-butyl peroxide (Figure 4.5)? For bis(1-hydroxy cyclohexyl) peroxide?
- 4.4 Two monomers are polymerized in homogeneous solution with the following results:

Series I	Monomer A	Monomer B
Initial monomer concentration (mol/liter)	0.100	0.200
Time to convert 5% of original monomer charge to polymer (h)	0.100	0.300
Initiator concentration (mol/liter)	0.0397	0.0397

In a second series at the same temperature, it is desired that both polymers produced initially have the same degree of polymerization. It can be assumed that both polymers terminate exclusively by coupling. In this second series, both monomers initially are 0.300 mol/liter. What should be the ratio of concentration of initiator for monomer B compared with that for monomer A in this second series?

4.5 The following data are obtained for the polymerization of a new monomer. Predict the time for 50% conversion in run D. Calculate the energy of activation for the polymerization. $R = 1.987 \text{ cal/mol}\cdot\text{K}$.

Run	Temperature (°C)	Conversion (%)	Time (min)	Initial Monomer Concentration (mol/liter)	Initial Initiator Concentration (mol/liter)
A	60	50	500	1.00	0.0025
B	80	75	700	0.50	0.0010
C	60	40	584	0.80	0.0010
D	60	50	—	0.25	0.0100

- 4.6** The table gives the initial rate of polymerization $(-d[M]/dt)_0$ for each combination of monomer and peroxide in mmol/liter-min. In each case, initial concentrations of monomer and initiator are 0.100 and 0.00100 mol/liter, respectively. Calculate the rates (a) and (b).

Monomer	Peroxide I		Peroxide II	
	30°C	80°C	30°C	80°C
A. Styrene	1.00	2.00	0.500	1.50
B. Methyl methacrylate	2.00	5.00	(a)	(c)
C. Vinyl acetate	3.00	(b)	(d)	7.50

- 4.7** Using k_i based on Figure 4.5 and $k_p/(k_t)^{0.5}$ from Table 4.2, calculate the time needed to convert half of a charge of MMA to polymer using benzoyl peroxide as the initiator in benzene solution at 60°C. What number-average degree of polymerization do you expect initially? Initial charge per 100 ml of solution: 10 g MMA and 0.1 g benzoyl peroxide. What fraction of the initiator has been used after 50% conversion of monomer?
- 4.8** When peroxide P is held at 70°C for 10 h, 90% of the original peroxide remains undecomposed. Now if a 5% solution of ethyl mercurate containing 0.000100 mol/liter of peroxide P is polymerized at 70°C, 40% of the original monomer charge is converted to polymer in 1 h. How long will it take to polymerize 90% of the original monomer charge in a solution containing 10% ethyl mercurate (initially) with 0.0100 mol/liter of peroxide P?
- 4.9** Initiator B has twice the half-life that initiator A has at 70°C. Monomer C polymerizes 3 times as fast as monomer D at 70°C when initiator A is used and all the concentrations are the same. If both C and D terminate by coupling, what is the ratio of degree of polymerization for case I to that for case II?

	Case I	Case II
Monomer	C	D
Initiator	A	B
Concentration of monomer	1 mol/liter	2 mol/liter
Concentration of initiator	0.001 mol/liter	0.005 mol/liter

- 4.10** When peroxide A is heated to 60°C in an inert solvent, it decomposes by a first-order process. An initial concentration of 5.0 mmol/liter of peroxide changes to 4.0 mmol/liter after 1.0 h.
- (a) In the following system, what fraction of the monomer should remain unconverted after 10 min at 60°C?
- (b) What is the concentration of initiator after 10 min? System parameters (all at 60°C) are as follows:
- $$k_p = 1.8 \times 10^4 \text{ liter/mol-s}$$
- $$k_i = 1.45 \times 10^7 \text{ liter/mol-s}$$
- Initiator concentration = 4.0×10^4 mol/liter

- 4.11** Methyl acrylate (1.0 mol) is polymerized in benzene (1.0 l of solution) using succinic acid peroxide (1.0×10^{-3} mol) at 60°C . How long will it take to convert 10% of the monomer to polymer? How long will it take to convert 90% of the monomer to polymer? If the polymerization were carried out adiabatically, how much would the temperature have risen after 10% conversion? Assume that the specific heat of the benzene solution is $370 \text{ cal}/^\circ\text{C}\cdot\text{l}$.
- 4.12** When monomer M is polymerized at 50°C using 0.0200 mol/liter of initiator and 2.00 mol/liter of monomer, the molecular weight formed initially is 100,000 g/mol. The same molecular weight is produced at 63°C with the same amount of initiator but with a monomer concentration of 4.55 mol/liter. What concentration of initiator should be used at 70°C to get a molecular weight of 150,000 g/mol if the monomer concentration is 6.00 mol/liter?
- 4.13** Solution polymerization of monomer A initiated by peroxide P at two temperatures (using the same concentrations of A and P) gives the following results:

Temperature	35.0°C	53.0°C
Conversion in 30 min (%)	25.0	65.0
Initial molecular weight	500,000	300,000

What is the energy of activation (E_a) for the decomposition of P?

- 4.14** The decomposition of benzoyl peroxide is characterized by a half-life of 50 h at 60°C and an activation energy of 27.3 kcal/mol. How much peroxide (mol/liter) is needed to convert one-third of the original charge of vinyl monomer (original concentration of 2 mol/liter) to polymer in 85 min at 70°C ? Data: $[k_p^2/k_t] = 128 \text{ liter}/\text{mol}\cdot\text{h}$ at 70°C .
- 4.15** Monomer M (FW = 156) is polymerized using peroxide P. Termination is by disproportionation. The peroxide has a half-life of 1.00 h at 90°C and an activation energy of 30.0 kcal/mol. In a run at 60°C where the initial charge to the reactor is 1.00×10^{-3} mol of P and 2.00 mol of M in a total volume of 2500 ml, the reaction is stopped after 35.0 min, at which time 12.5 g of polymer has been formed. What number-average molecular weight is expected of the polymer?
- 4.16** Monomer M is to be polymerized using a peroxide initiator, I. The peroxide has a half-life of 6.00 h at 70°C . The polymerization is to be carried out with the following requirements:

Polymerization time	2.00 min
Polymerization temperature	70°C
Conversion	2.00%
Initial degree of polymerization	1200

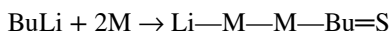
If the efficiency (f) = 1.00, and termination is by coupling, what concentration of peroxide should be used (in mol of peroxide/mol of monomer)?

- 4.17** Peroxide G has twice the half-life that peroxide H has at the same temperature, 65°C. Monomer K polymerizes 3 times as fast as monomer L at 65°C when initiator H is used with either monomer and all the concentrations are the same. If both K and L homopolymers terminate by coupling, what is the ratio of the initial degree of polymerization for case I to that for case II as described in the following table? That is, what is $(x_n)_I/(x_n)_{II}$?

Initial Concentrations of Reactants, Polymerizations at 65°C

Reactant	Case I	Case II
Monomer	[K] = 1.00 mol/liter	[L] = 2.00 mol/liter
Initiator	[H] = 0.00100 mol/liter	[G] = 0.00500 mol/liter

- 4.18** An aliphatic acrylate was polymerized by a free-radical mechanism and terminated by coupling. A peroxide characterized by a half-life of 1.0 h at 90°C and an activation energy of 30.0 kcal/mol was used for initiation. A polymer with a number-average degree of polymerization of 10,000 was produced by polymerization at 70°C using an initiator concentration of 3.5×10^{-4} mol/liter. If 2.00% of the initial monomer present was converted to polymer in 45.0 min, what was the initial monomer concentration?
- 4.19** When radicals are produced by photoinitiation, the rate of radical production can be independent of the temperature. Thermal decomposition of a peroxide is, of course, temperature dependent. When styrene is photopolymerized in two experiments in which only the temperature is varied, the time it takes to convert 20.0% of the original charge of monomer to polymer is 20.0 min at 60°C and 18.0 min at 70°C. However, when an organic peroxide is the thermal initiator, the corresponding times for 20.0% conversion are 40.0 min at 70°C and 23.0 min at 80°C. If the half-life of the peroxide at 90°C is 10.0 h, what is its half-life at 60°C?
- 4.20** When monomer M is polymerized using peroxide Q at 57.0°C, 5.00% of the monomer is converted to polymer after 3.00 h. At 82.0°C, 15.00% is converted after only 1.00 h. The molecular weight initially produced at the higher temperature has exactly one-half the value of that produced at the lower temperature. If the energy of activation of the termination reaction is negligible, what is the energy of activation for the propagation reaction? The same starting concentrations of monomer and peroxide are used at both temperatures.
- 4.21** If one reacts butyl lithium (BuLi) with a small amount of monomer, a seed of living polymer is produced.



Now we mix 10^{-3} mol of S with 2 mol of fresh monomer M and find that the reaction is first order in M. Half the monomer, 1 mol, is converted to polymer in 50 min at 25°C. Estimate k_p . Total volume of system is 1 liter. There is no termination reaction.

- 4.22** A vinyl monomer ($\text{CH}_2=\text{CHY}$, $\text{MW} = 213$) is polymerized by a free-radical initiator in the presence of dodecyl mercaptan ($\text{C}_{12}\text{H}_{23}\text{SH}$). Analysis of the purified polymer shows the following:

$$\text{Number-average degree of polymerization} = 430$$

$$\text{Sulfur content} = 5.45 \times 10^{-6} \text{ g-atoms/g}$$

$$\text{Terminal unsaturation} = C \text{ mol/g}$$

If half the kinetic chains are terminated by coupling and half by disproportionation, what is the expected value of C ?

- 4.23** Show how the copolymer equation can be rearranged to give

$$\frac{Y-1}{X} = r_1 - \left(\frac{Y}{X^2} \right) r_2$$

Derive r_1 and r_2 from a plot of these data by Dainton [65] for acrylamide (1):methacrylamide (2).

Compositions	
Feed $f_1/(1 - f_1)$	Polymer $F_1/(1 - F_1)$
0.125	0.150
0.250	0.358
0.500	0.602
1.000	1.33
4.000	4.72
8.000	10.63

Plot F_1 versus f_1 and compare the data with the copolymer equation on these coordinates.

- 4.24** Draw curves (on the same plot) of polymer composition (F_1) versus monomer composition (f_1) for the following systems:
- Butadiene (1), styrene (2), 60°C , $r_1 = 1.39$, $r_2 = 0.78$
 - Vinyl acetate (1), styrene (2), 60°C , $r_1 = 0.01$, $r_2 = 55$
 - Maleic anhydride (1), isopropenyl acetate (2), 60°C , $r_1 = 0.002$, $r_2 = 0.032$

Assuming that one starts with an equimolar mixture of monomers in each case, which will contain more of monomer (1), the polymer formed first of the polymer formed later?

- 4.25** Compare the experimental values of r_1 and r_2 from Table 4.4 with those calculated by using Q and e values from the same table for several pair of monomers.
- 4.26** Acrylonitrile, 1 mol, is copolymerized with methyl vinyl ketone, 2 mol, at 60°C . Regarding acrylonitrile as monomer 1, $r_1 = 0.60$ and $r_2 = 1.66$. Calculate the mole fraction of acrylonitrile in polymer made initially. What

is the mole fraction of acrylonitrile in the polymer being formed when 2 mol of monomer have been converted to polymer?

- 4.27 In the copolymerization of monomers 1 and 2, $r_1 = 1.0$ and $r_2 = 0.5$. Initially $f_2 = 2f_1$
- Which monomer predominates in the polymer formed initially?
 - After 10% of the monomer charge is converted to polymer, does the polymer being made have more or less of monomer 1 than the polymer that was made initially? Show your calculations and reasons.
- 4.28 Using the data given below, select concentrations of initiator and CTA that will give poly(vinyl acetate) with an initial molecular weight (assuming coupling) of 15,000. The polymerization (at 60°C) should be 50% complete in 8 min.

Reactant	FW	Initial Concentration (g/l)
Monomer: vinyl acetate	86.09	500.0
Initiator: 2,2'-azo-bis-2-isobutyl-4-methylvaleronitrile	332	–
Transfer agent: benzyl mercaptan	124.21	–

Solvent: methanol (to make 1 liter), $k_t = 3.78 \times 10^{-4} \text{ s}^{-1}$, $k_p = 15 \times 10^3 \text{ liter/mol-s}$, $k_t = 600 \times 10^6 \text{ liter/mol-s}$, $C_s = 0.885$ (dimensionless) (Brandrup and Immergut 1989).

- 4.29 The following chain transfer constants are reported for the polymerization of styrene at 60°C (Brandrup and Immergut 1989):

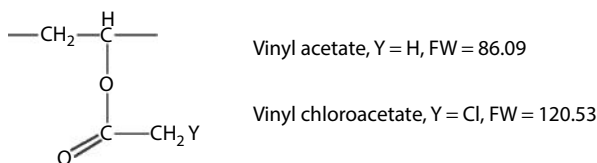
Reagent	Chain Transfer Constant	Molecular Weight (g/mol)	Density (g/cm ³)
Toluene	Essentially zero	92.1	0.866
Styrene	0.60×10^{-4}	104.1	0.903
Acetone	1.5×10^{-4}	58.08	0.792
Isopropyl alcohol	3.1×10^{-4}	60.09	0.789
Carbon tetrachloride	92.0×10^{-4}	153.34	1.595

Under a certain set of conditions, one can produce polystyrene with a degree of polymerization (x_n) of 5000. The conditions are that a peroxide-type initiator is used at 60°C and the initial concentration of monomer is 2.00 mol/liter with toluene as the only solvent. What concentration of additive (g/liter) would reduce the x_n to 800? Note: concentration is in terms of the additive taking the place of part of the toluene and keeping the initial monomer concentration at 2.00 mol/liter. Calculate separately for each of the three additives. Assume additivity of volumes.

- 4.30 The molecular weight of polymer when vinyl butyrate is polymerized in an inert solvent is 500,000. With all other conditions the same, addition of 5 g/liter of 1-dodecanethiol decreases the molecular weight to 150,000.

What concentration of 1-dodecanethiol will give a molecular weight of 275,000 (other conditions remaining the same)?

- 4.31** When monomers A and B are copolymerized, an azeotrope (polymer composition same as feed) is formed at a ratio of 7 mol of A to 3 mol of B. If monomer B is known not to homopolymerize,
- What polymer composition (mole fraction of A) will result initially when a mixture of 9 mol of A and 1 mol of B is polymerized?
 - Will polymer formed after 50% conversion from an initial mixture of 4 mol of A and 6 mol of B contain
 - More A than polymer formed at 1% conversion?
 - Less A than polymer formed at 1% conversion?
 - Same fraction of A as polymer formed at 1% conversion?
- 4.32** A random copolymer of vinyl chloroacetate (1) and vinyl acetate (2) is made with $F_1 = 0.00500$ and a density of 1.04 g/cm^3 . Then each chlorine is removed by reaction with metallic zinc to form zinc chloride (removed by a water wash) and a carbon-carbon cross-link (one for each pair of chlorines). Assuming a complete network with no loose ends, what swollen volume will 2.80 g of cross-linked copolymer occupy in a solvent with a molar volume of $82.5 \text{ cm}^3/\text{mol}$ and $\chi = 0.520$?



- 4.33** Homopolymer A has a T_g of 120°C . Homopolymer B has a T_g of -40°C . A and B are copolymerized (to very low conversion) and the glass transition temperatures of the copolymers are measured. For a monomer feed of 50:50 (mole ratio), the T_g is 74°C . For a monomer feed of 25:75 (A:B), T_g is 36°C .
- What is the expected T_g when the monomer feed is 85:15 (A:B)? Assume that
- There is a linear relationship between T_g and weight fraction of A in the polymer.
 - Density does not change with composition.
 - Monomers A and B have the same molecular weight.
- 4.34** When monomers A and B are copolymerized in a mole ratio of 2 of A to 5 of B, the polymer formed (initially) has a composition exactly the same as the monomer feed. However, when the monomer ratio is 5 of A to 1 of B, the polymer has a ratio of 5 mol of A to 3 of B. What monomer feed composition (mole fraction of A) will yield a polymer (initially) with equal moles of A and B?
- 4.35** Monomers A and B copolymerize to give an azeotropic composition in which the weight fraction of B is 0.750. A copolymer with a weight

fraction of A equal to 0.750 can be made when the monomer feed has a weight fraction of A equal to 0.810. What mole fraction of A will be contained in a copolymer made from a monomer mixture with 10 mol each of A and B?

Monomer A: FW = 104

Monomer B: FW = 171

- 4.36** Monomers A, B, and C are polymerized together. Illustrate all the possible propagation reactions with equations and constants. Define the relative reaction rates (r_i). What set of values for r_i describes production of mixtures of homopolymers?
- 4.37** Monomers A and B are copolymerized under various conditions. Predict the composition (mol% of A) initially formed at the start of a copolymerization with an equimolar feed.

Data

Run I: Feed—99 mol A, 1 mol B; initial polymer—0.50 mol% B.

Run II: Feed—1 mol A, 99 mol B; initial polymer—2.00 mol% A.

- 4.38** An equimolar mixture of methyl acrylate and styrene is copolymerized. It is found that polymer radicals based on methyl acrylate add methyl acrylate monomer at a rate that is only 18% of the rate at which they add styrene. Polymer radicals based on styrene add methyl acrylate at a rate that is 133% of the rate at which they react with styrene. For what feed composition will a copolymer be produced that is uniform in composition (does not change with conversion)?
- 4.39** The reaction of 1.00 mol of monomer A with 4.00 mol of monomer B yields an azeotrope with a T_g of 15.0°C. It is also established that a polymer made from a monomer feed of equimolar quantities of A and B has a T_g of 30.0°C. A nonazeotropic polymer is made from a monomer feed with 4.00 mol of A and 1.00 mol of B. Given that the T_g of A is 125.0°C and the T_g of B is 0.0°C, what is the T_g of the nonazeotropic polymer? Monomers A and B have the same formula weight and density.
- 4.40** Monomers A and B yield homopolymers with glass transition temperatures of 210.0°C and 20.0°C, respectively. When they are copolymerized, an equimolar feed yields a polymer with a mole fraction of A = 0.800 and a glass transition temperature of 95.0°C. Monomer A has a formula weight of 124 and monomer B has a formula weight of 102. The copolymerization is *ideal* in that $r_1 r_2 = 1$. If a copolymer is made from a feed with a mole fraction of A = 0.300, what glass transition temperature is expected for the polymer?
- 4.41** The reaction rate of an isocyanate with a primary alcohol may be given by

$$-\frac{d[B]}{dt} = -\frac{d[A]}{dt} = k[A][B]$$

where:

[B] and [A] are concentrations of isocyanate and hydroxyl groups, respectively, in moles per liter

For the following mixture, estimate the time required for gel to form. Assume $k = 0.50$ liter/mol-h:

3,3'-Dimethylphenylmethane-4,4'-diisocyanate ($C_{17}H_{14}N_2O_2$)	2 mol
2-Ethylhexanol ($C_8H_{18}O$)	1.5 mol
Trimethylolpropane ($C_6H_{14}O_3$)	1 mol
Benzene	To make 1 liter

4.42 Polymer A is mixed with a small amount of peroxide P in order to carry out a cross-linking operation. It can be assumed that each peroxide molecule that decomposes produces two radicals that, together, introduce one cross-link into the polymer. Thus, decomposition of one molecule of peroxide brings about one cross-link. The polymer/peroxide mixture is divided into three portions, and cross-linking is carried out at various temperatures for various times. In order to characterize the reaction, samples are swollen in a solvent for which the polymer-solvent interaction parameter is 0.400. From the data furnished below, calculate the activation energy for peroxide decomposition. An additional assumption is that the peroxide decomposes at the same rate that it would decompose in the absence of polymer.

Cross-Linking Temperature ($^{\circ}C$)	Time (h)	Volume Fraction of Polymer in Swollen Gel, v_2
110	0.500	0.340
110	1.000	0.390
135	0.500	0.380

REFERENCES

1. Flory, P. J.: *Principles of Polymer Chemistry*, Cornell University Press, Ithaca, NY, 1953, pp. 106, 132.
2. Wallace and Tiernan Company: *Lucidol Organic Peroxides*, Lucidol Division, Wallace and Tiernan, Buffalo, NY, 1968.
3. Brandrup, J., and E. H. Immergut (eds.): *Polymer Handbook*, 3rd edn., Wiley, New York, 1989.
4. Kolthoff, I. M., and I. K. Miller: *J. Am. Chem. Soc.*, 73:3055 (1951).
5. Flory, P. J.: *Principles of Polymer Chemistry*, Cornell University Press, Ithaca, NY, 1953, pp. 148-158; M. S. Matheson, E. E. Auer, E. B. Bevilacqua, and E. J. Hart: *J. Am. Chem. Soc.*, 71:497 (1949).
6. Brandrup, J., and E. H. Immergut: *Polymer Handbook*, 2nd edn., Wiley, New York, 1975, pp. 11.47-11.52.
7. Bevington, J., and H. Mellville: *J. Polym. Sci.*, 12:449 (1954).
8. Riggs, J. R.: The Aqueous Phase Polymerization of Acrylamide: A Kinetics and Mechanism Study, PhD thesis, Cornell University Press, Ithaca, NY, 1964.
9. Razuvayev, G. A. et al.: *Polym. Sci. USSR*, 1020 (1962).
10. Billmeyer, E. W., Jr.: *Textbook of Polymer Science*, Wiley, New York, 1962, p. 292.
11. Kennedy, J. R., and R. M. Thomas: *J. Polym. Sci.*, 49:189 (1961).

12. Russell, K. E., and G. J. Wilson: in C. E. Schildknecht (ed.), *Polymerization Processes*, Wiley, New York, 1977.
13. Flory, P. J.: *Principles of Polymer Chemistry*, Cornell University Press, Ithaca, NY, 1953, p. 220.
14. Lenz, R. W.: *Organic Chemistry of Synthetic High Polymers*, Wiley, New York, 1967, pp. 418, 623.
15. Kennedy, I. R., S. Midha, and Y. Tsunogae: *Macromolecules*, 26:429 (1993).
16. Kennedy, J. P., and B. Ivan: *Designed Polymers by Carbocationic Macromolecular Engineering*, Hanser Publishers, New York, 1992.
17. Teyntjens, W. G. S., and E. J. Goethals: *Polym. Adv. Technol.*, 12:107 (2001).
18. Deng, H., S. Kanaoka, M. Sawamoto, and T. Higashimura: *Macromolecules*, 29:1772 (1996).
19. Morton, M.: *AIChE Symp. Polymer Kinetics Catalyst Systems*, December 1961.
20. Holden, G., and R. Milkovich: US Patent 3,265,765 (assigned to Shell Oil Company), August 9, 1966.
21. Hsieh, H. L.: *Rubber Chem. Technol.*, 49:1305 (1976).
22. Ballard, D. G. H., R. I. Bowles, D. M. Haddleton, S. N. Richards, R. Sellens, and D. L. Twose: *Macromolecules*, 25:5907 (1992).
23. Bayard, R., I. R. Teyssie, S. Varshney, and J. S. Wang: *Polym. Bull.*, 33:381 (1994).
24. Georges, M. K., R. Veregin, P. Kazmaier, and G. Hamer: *Macromolecules*, 26:2987 (1993).
25. Hawker, C. J., A. Bosman, and E. Harth: *Chem. Rev.*, 101:3661 (2001).
26. Matyjaszewski, K.: *Macromol. Symp.* 174:51 (2001).
27. Moad, G., E. Rizzardo, and S. H. Thang: *Aust. J. Chem.*, 58:379 (2005).
28. Wang, J. S., and K. Matyjaszewski: *Macromolecules*, 28:7901 (1995).
29. Tang, W., Y. Kwak, W. Braunecker, N. V. Tsarevsky, M. L. Coote, and K. Matyjaszewski: *J. Am. Chem. Soc.*, 130:10702 (2008).
30. Rizzardo, E., M. Chen, B. Chong, G. Moad, M. Skidmore, and S. H. Thang: *Macromol. Symp.*, 248:104 (2007).
31. Natta, G. et al.: *J. Polym. Sci.*, 16:143 (1955).
32. Cooper, W.: in I. C. Robb, and F. W. Peaker (eds.), *Progress in High Polymers*, vol. 1, Heywood, London, 1961, p. 279.
33. Goodall, B. L.: *J. Chem. Educ.*, 63:191 (1986).
34. Guyot, A., C. Bobichon, R. Spitz, L. Duranel, and J. L. Lacombe: in W. Kaminsky, and H. Sinn (eds.), *Olefin Polymerization*, Springer-Verlag, New York, 1987, p. 13.
35. Tait, R. I. T.: in W. Kaminsky, and H. Sinn (eds.), *Olefin Polymerization*, Springer-Verlag, New York, 1987, p. 309.
36. Kaminsky, W.: in T. Keii, and K. Soga (eds.), *Catalytic Polymerization of Olefins*, Elsevier, New York, 1986, p. 293.
37. Coates, G. W.: *Chem. Rev.*, 100:1223 (2000).
38. McMillan, F. M.: in J. K. Craver, and R. W. Tess (eds.), *Applied Polymer Science*, ACS, Washington, DC, 1975, p. 328.
39. Marsden, C. E.: *Plast. Rubber Comp. Proc. Appl.*, 21:193 (1994).
40. Webster, O. W., W. R. Hertler, D. Y. Sogah, W. B. Farnham, and T. V. RajanBabu: *J. Am. Chem. Soc.*, 105:5706 (1983).
41. Brittain, W. J.: *Rubber Chem. Tech.*, 65:580 (1992).
42. Flory, P. J.: *Principles of Polymer Chemistry*, chap. 9, Cornell University Press, Ithaca, NY, 1953.
43. Tomalia, D. A., H. Baker, J. R. Dewald, M. Hall, G. Kallos, S. Martin, J. Roeck, J. Ryder, and P. Smith: *Polym. J. (Tokyo)* 17:117–141 (1985).
44. Hawker, C. J.: *Advances in Polymer Science*, vol. 147, Springer-Verlag, Berlin, Heidelberg, Germany, 1999.

45. Bosman, A. W., H. M. Janssen, and E. W. Meijer: *Chem. Rev.*, 99:1665–1688 (1999).
46. Emrick, T., and J. M. J. Fréchet: *Curr. Opin. Colloid Interface Sci.*, 4:15–23 (1999).
47. Tobolsky, A. V.: *Properties and Structure of Polymers*, chap. 6, Wiley, New York, 1960.
48. Calderon, N., and R. L. Hinrichs: *Chem. Tech.*, 4:627 (1974).
49. Brunelle, D. J., and T. G. Shannon: *Macromolecules*, 24(11): 3035 (1991).
50. Experimental Benzocyclobutene for Aerospace Applications, Dow Chemical Company, Midland, MI, 1992. <http://www.dow.com/cyclotene/>.
51. McCabe, W., J. C. Smith, and P. Harriott: *Unit Operations of Chemical Engineering*, 4th edn., McGraw-Hill, New York, 1985, p. 507.
52. Meyer, V. E., and G. G. Lowry: *ACS Polym. Div. Preprints*, 5:60 (1964); *J. Polym. Sci.*, A3:2843 (1965).
53. Hanna, R. J.: *Ind. Eng. Chem.*, 49:208 (1957).
54. Alfrey, T., Jr., and L. J. Young: chap. 2 in G. E. Ham (ed.), *Copolymerization*, Wiley, New York, 1964.
55. Alfrey, T., Jr., and C. C. Price: *J. Polym. Sci.*, 2:101 (1947).
56. Simon, P. F. W., R. Ulrich, H. W. Spiess, and U. Wiesner, *Chem. Mater.*, 13(10):3464 (2001).
57. Hoffman, A. S., and R. Bacskaï: chap. 6 in G. E. Ham (ed.), *Copolymerization*, Wiley, New York, 1964.
58. Miwa, Y., K. Yamamoto, M. Sakaguchi, and S. Shimada: *Macromolecules*, 32(24):8234 (1999).
59. Archer, B. L. et al.: chap. 3 in L. Bateman (ed.), *The Chemistry and Physics of Rubber-Like Substances*, Wiley, New York, 1963.
60. Jirgensons, B.: *Natural Organic Macromolecules*, Pergamon Press, New York, 1962, p. 116.
61. Goulian, M., A. Kornberg, and R. L. Sinsheimer: *Proc. Natl. Acad. Sci. USA*, 58:2321 (1967).
62. Merrifield, R. B., and J. M. Stewart: *Nature*, 207(4996):522 (1965).
63. Atherton, E., and R. C. Sheppard: *Solid Phase Peptide Synthesis: A Practical Approach*, IRL Press, Oxford, 1989.
64. Kim, Y. B., R. W. Lenz, and R. C. Fuller: *J. Polym. Sci. Part A: Polym. Chem.*, 33(8):1367 (1995).
65. Dainton, E. S., and W. D. Sisley: *Trans. Faraday Soc.*, 59:1385 (1963).
66. Kirchhoff, R. A., and K. I. Bruza: *Prog. Polym. Sci.*, 18:85 (1993).
67. Hydrocarbon processing and petroleum refiner, 46(11):192 (November 1967).
68. Dessipri, E., D. A. Tirrell, and E. D. T. Atkins: *Macromolecules*, 29(10):3545–3551 (1996).

GENERAL REFERENCES

- Aggarwal, S. L. (ed.): *Block Polymers*, Plenum, New York, 1970.
- Akelah, A., and A. Moet: *Functionalized Polymers*, Chapman & Hall, New York, 1990.
- Albright, L. E.: *Processes for Major Addition-Type Plastics and Their Monomers*, McGraw-Hill, New York, 1974.
- Allen, N. S. (ed.): *Photopolymerisation and Photoimaging Science and Technology*, Elsevier, New York, 1989.
- Allen, R. E. M., and C. R. Patrick: *Kinetics and Mechanisms of Polymerization Reactions*, Wiley, New York, 1974.
- Bailey, E. E., Jr., and I. V. Koleske (eds.): *Alkylene Oxides and Their Polymers*, Dekker, New York, 1991.
- Bamford, C. H., and C. E. H. Tipper: *Comprehensive Chemical Kinetics*, vol. 14, Elsevier, New York, 1976.

- Benham, I. L., and J. E. Kinstle (eds.): *Chemical Reactions on Polymers*, ACS, Washington, DC, 1988.
- Biederman, H., and Y. Osada: *Plasma Polymerization Processes*, Elsevier, New York, 1992.
- Bodanszky, M.: *Principles of Peptide Synthesis*, Akad.-Verlag, Berlin, Germany, 1984.
- Boor, I., Jr.: *Ziegler-Natta Catalysts and Polymerizations*, Academic Press, New York, 1979.
- Brunelle, D. I. (ed.): *Ring-Opening Polymerization*, Hanser-Gardner, Cincinnati, OH, 1993.
- Butler, G. B.: *Cyclopolymerization and Cyclocopolymerization*, Dekker, New York, 1992.
- Carraher, C. E., and M. Tsuda (eds.): *Modification of Polymers*, ACS, Washington, DC, 1980.
- Casale, A., R. S. Porter, and W. H. Sharkey: in H. I. Cantow (ed.), *Polymerization*, Springer-Verlag, New York, 1975
- Cassidy, R. E.: *Thermally Stable Polymers—Synthesis and Properties*, Dekker, New York, 1980.
- Ceresa, R. I. (ed.): *Block and Graft Copolymerization*, vol. 1, Wiley, New York, 1973; vol. 2, 1976.
- Chien, J. C. W. (ed.): *Coordination Polymerization*, Academic Press, New York, 1975.
- Chum, H. L. (ed.): *Polymers from Biobased Materials*, Noyes, Park Ridge, NJ, 1991.
- Cowie, J. M. G. (ed.): *Alternating Copolymers*, Plenum, New York, 1985.
- Culbertson, B. M., and J. E. McGrath (eds.): *Advances in Polymer Synthesis*, Plenum, New York, 1985.
- Dickstein, W. H.: *Rigid Rod Star-Block Copolymers*, Technomic, Lancaster, PA, 1990.
- Dragutan, V., A. T. Balaban, and M. Dimonie: *Olefin Metathesis and Ring-Opening Polymerization of Cyclo-Olefins*, Wiley, New York, 1986.
- Elias, B. (ed.): *Chemistry and Technology of Epoxy Resins*, Chapman & Hall, New York, 1993.
- Elias, H.-G.: *Macromolecules, Synthesis, Materials, and Technology*, 2nd edn., Plenum, New York, 1984.
- Erusalimskii, B. L.: *Mechanisms of Ionic Polymerization*, Plenum, New York, 1986.
- Fontanille, M., and A. Guyot (eds.): *Recent Advances in Mechanistic and Synthetic Aspects of Polymerization*, Kluwer Academic, Norwell, MA, 1987.
- Frisch, K. C., and S. L. Reegen (eds.): *Ring-Opening Polymerization*, Dekker, New York, 1969.
- Goethals, E. J. (ed.): *Telechelic Polymers: Synthesis and Applications*, CRC Press, Boca Raton, FL, 1988.
- Ham, G. E.: *Copolymerization*, Wiley-Interscience, New York, 1964.
- Ham, G. E. (ed.): *Vinyl Polymerization*, part 1, Dekker, New York, 1967; part 2, 1969.
- Haward, R. N. (ed.): *Developments in Polymerisation—1*, Elsevier Applied Science, New York, 1979.
- Haward, R. N. (ed.): *Developments in Polymerisation—2*, Elsevier Applied Science, New York, 1979.
- Haward, R. N. (ed.): *Developments in Polymerisation—3*, Elsevier Applied Science, New York, 1982.
- Hogen-Esch, T. E., and J. Smid (eds.): *Recent Advances in Anionic Polymerization*, Elsevier Applied Science, New York, 1987.
- Ivin, K. J., and T. Saegusa (eds.): *Ring-Opening Polymerization*, 3 vols., Elsevier Applied Science, New York, 1984.
- Jenkins, A. D., and A. Ledwith (eds.): *Reactivity, Mechanism, and Structure in Polymer Chemistry*, Wiley-Interscience, New York, 1974.
- Kaminsky, W., and H. Sinn (eds.): *Transition Metals and Organometallics as Catalysts for Olefin Polymerization*, Springer, New York, 1988.
- Kennedy, J. P.: *Cationic Polymerization of Olefins: A Critical Inventory*, Wiley-Interscience, New York, 1975.
- Kennedy, J. R., and B. Ivan: *Designed Polymers by Carbocationic Macromolecular Engineering Theory and Practice*, Hanser-Gardner, Cincinnati, OH, 1992.
- Ketley, A. D.: *The Stereochemistry of Macromolecules*, vols. 1 and 2, Dekker, New York, 1967.

- Kricheldorf, H. R. (ed.): *Handbook of Polymer Synthesis, Parts A and B*, Dekker, New York, 1991.
- Kucera, M.: *Mechanism and Kinetics of Addition Polymerizations*, Elsevier, New York, 1991.
- Lazar, M., T. Bleha, and I. Rychly: *Chemical Reactions of Natural and Synthetic Polymers*, Prentice Hall, Englewood Cliffs, NJ, 1989.
- Lenz, R. W.: *Organic Chemistry of Synthetic High Polymers*, Wiley, New York, 1967.
- Lenz, R. W., and E. Ciardelli (eds.): *Preparation and Properties of Stereoregular Polymers*, Reidel, Hingham, MA, 1979.
- McGrath, J. (ed.): *Ring-Opening Polymerization*, ACS, Washington, DC, 1985.
- Meier, D. J. (ed.): *Block Copolymers*, Gordon & Breach, New York, 1983.
- Millich, F., and C. E. Carraher (eds.): *Interfacial Synthesis*, Dekker, New York, 1973.
- Morgan, P. W.: *Condensation Polymers by Interfacial and Solution Methods*, Wiley, New York, 1965.
- Morton, M.: *Anionic Polymerization: Principles and Practice*, Academic Press, New York, 1983.
- Mulvaney, J. E.: *Macromolecular Syntheses. A Periodic Publication of Methods for the Preparation of Macromolecules*, vol. 6, Wiley, New York, 1977 (with various editors and years of issue).
- Nonhebel, D. C., and J. C. Walton: *Free Radical Chemistry*, Cambridge, New York, 1974.
- Noshay, A., and J. E. McGrath: *Block Copolymers: Overview and Critical Survey*, Academic Press, New York, 1976.
- Odian, G.: *Principles of Polymerization*, 3rd edn., Wiley, New York, 1991.
- Paleos, C. M. (ed.): *Polymerization in Organized Media*, Gordon & Breach, New York, 1992.
- Platzer, N. A. J. (ed.): *Polymerization Kinetics and Technology*, ACS, Washington, DC, 1973.
- Platzer, N. A. I. (ed.): *Polymerization Reactions and New Polymers*, ACS, Washington, DC, 1973.
- Platzer, N. A. I. (ed.): *Copolymers, Polyblends, and Composites*, ACS, Washington, DC, 1976.
- Plesch, R. H.: in I. C. Robb, and F. W. Peaker (eds.), *Progress in High Polymers*, vol. 2, Heywood, London, 1968.
- Pomogailo, A. D., and V. S. Savost'yanov: *Synthesis and Polymerization of Metal-Containing Monomers*, CRC Press, Boca Raton, FL, 1994.
- Quirk, R. R. (ed.): *Transition Metal Catalyzed Polymerization*, Gordon & Breach, New York, 1983.
- Rempp, R., and E. W. Merrill: *Polymer Synthesis*, Huethig & Wepf, Mamaroneck, NY, 1986.
- Roberts, A. D. (ed.): *Natural Rubber Science and Technology*, Oxford University Press, New York, 1988.
- Sadhir, R. K., and R. M. Luck (eds.): *Expanding Monomers: Synthesis, Characterization, and Applications*, CRC Press, Boca Raton, FL, 1992.
- Saegusa, T., and E. Goethals (eds.): *Ring-Opening Polymerization*, ACS, Washington, DC, 1977.
- Sandler, S. R., and W. Karo: *Polymer Synthesis*, vol. 1, Academic Press, New York, 1974.
- Sawada, H.: *Thermodynamics of Polymerization*, Dekker, New York, 1976.
- Schildknecht, C. E., and I. Skeist (eds.): *Polymerization Processes*, Wiley, New York, 1977.
- Semlyen, I. A. (ed.): *Cyclic Polymers*, Elsevier Applied Science, New York, 1986.
- Soga, K., and M. Terano (eds.): *Catalyst Design for Tailor-Made Polyolefins*, Elsevier, Amsterdam, The Netherlands, 1994.
- Solomon, D. H. (ed.): *Step-Growth Polymerizations*, Dekker, New York, 1972.
- Sorenson, W. R., and T. W. Campbell: *Preparative Methods of Polymer Chemistry*, 2nd edn., Wiley, New York, 1968.
- Stang, R. J. (ed.): *Vinyl Cations*, Academic Press, New York, 1979.
- Starks, C.: *Free Radical Telomerization*, Academic Press, New York, 1974.
- Swarc, M., and M. Van Beylens: *Ionic Polymerization*, Chapman & Hall, New York, 1993.

- Takemoto, K., Y. Inaki, and R. M. Ottenbrite (eds.): *Functional Monomers and Polymers*, Dekker, New York, 1987.
- Tsurata, T., and K. E. O'Driscoll (eds.): *Structure and Mechanism in Vinyl Polymerization*, Dekker, New York, 1969.
- Uglea, C. V., and I. A. Negulescu: *Synthesis and Characterization of Oligomers*, CRC Press, Boca Raton, FL, 1991.
- Ulrich, H.: *Raw Materials for Industrial Polymers*, Hanser-Gardner, Cincinnati, OH, 1988.
- Van der Ven, S.: *Polypropylene and Other Polyolefins: Polymerization and Characterization*, Elsevier, New York, 1990.
- Vandenberg, E. J., and J. C. Salamone (eds.): *Catalysis in Polymer Synthesis*, ACS, Washington, DC, 1992.
- Vogl, O., and I. Furukawa (eds.): *Polymerization of Heterocyclics*, Dekker, New York, 1973.
- Yamashita, Y.: *Chemistry and Industry of Macromonomers*, Huthig & Wepf, Basel, Switzerland, 1992.
- Yasuda, H.: *Plasma Polymerization*, Academic Press, New York, 1985.
- Yocum, R. H., and E. B. Nyquist (eds.): *Functional Monomers*, 2 vols., Dekker, New York, 1973.

5 Polymerization Processes

5.1 DESIGN CRITERIA

Whether a polymerization is carried out on a small scale in the laboratory or on a commercial scale in an industrial complex, one must deal with certain issues. The viscosity of the reaction mixture and the control of temperature are the most prominent. Usually the larger the scale of production, the more difficult it becomes to maintain uniform conditions.

Many of the problems that attend mechanical design of polymerization systems are common to ordinary organic reactions. Toxic and flammable monomers and catalysts, noxious odors, and sticky solids are dealt with routinely in chemical and petroleum plants. Some notable examples in the field of commercial polymer processes are as follows:

Toxicity. Acrylonitrile ($\text{CH}_2=\text{CH}-\text{CN}$) has the toxicity of inorganic cyanides. A maximal concentration of 20 ppm in air is recommended for 8-h exposures.

Flammability. Many Ziegler catalysts involve aluminum triethyl, which is pyrophoric (bursts spontaneously into flames on exposure to air).

Odors. The lower acrylates can have odors that are penetrating and disagreeable even in low concentrations. Special catalytic systems may be installed to destroy traces of monomer in effluent gas streams.

In most cases the polymers themselves do not present these problems. However, unlike low-molecular-weight products, polymers are not generally subjected to purification by extraction, distillation, or crystallization after they have been formed. The ingredients present during formation often remain as part of the final product. Various techniques, bulk, solution, suspension, and emulsion are used to produce polymers. Some of the criteria for using these techniques are connected with thermal effects.

The conversion of a double bond to a single bond is accompanied by an exothermic **heat of polymerization** on the order of 10–20 kcal/mol. With monomers of molecular weight of about 100 and specific heat of about 0.5 cal/°C-g, this means an adiabatic temperature rise of 200°C–400°C. Removal of this heat of polymerization often limits the rate at which the reaction can be carried out, especially because most monomers and polymers are poor conductors of heat. As pointed out earlier, a higher temperature often gives a lower molecular weight. Because of this, a variable temperature widens the distribution of molecular weights. Also, a rise in temperature increases the rate of reaction and the rate of heat generation. Highly substituted monomers have more steric repulsion in the polymer form. This is reflected in lower heats of polymerization. Table 5.1 presents a comparison of vinyl monomers including comparison of monomers such as styrene with α -methyl styrene and acrylates with methacrylate.

TABLE 5.1
Heats of Polymerization and Changes in Volume (Liquid Monomer to Amorphous Polymer in the Range of 20°C–25°C)

Monomer	Structural Unit	FW (g/mol)	$-\Delta H_p$			Monomer	Polymer
			(kJ/mol)	(kJ/g)	Density (g/cm ³)		
Ethylene	$-\text{CH}_2-\text{CH}_2-$	28.05	102	3.62	Gas	0.853	
Propylene	$-\text{CH}_2-\text{CH}(\text{CH}_3)-$	42.07	84	0.50	0.519	0.853	
Isobutylene	$-\text{CH}_2-\text{C}(\text{CH}_3)_2-$	56.11	48	0.86	0.594	0.914	
Butene-1	$-\text{CH}_2-\text{CH}(\text{C}_2\text{H}_5)-$	56.11	84	1.49	0.595	0.859	
Isoprene	$-\text{CH}_2-\text{C}(\text{CH}_3)=\text{CH}-\text{CH}_2-$	68.12	75	1.10	0.681	0.909	
Styrene	$-\text{CH}_2-\text{CH}(\text{C}_6\text{H}_5)-$	104.15	70	0.67	0.906	1.047	
α -Methyl styrene	$-\text{CH}_2-\text{C}(\text{CH}_3)(\text{C}_6\text{H}_5)-$	118.18	35	0.30	0.908	1.066	
Vinyl chloride	$-\text{CH}_2-\text{CHCl}-$	62.50	96	1.54	0.911	1.412	
Vinyl acetate	$-\text{CH}_2-\text{CH}(\text{C}_2\text{H}_5\text{O}_2)-$	86.09	88	1.02	0.932	1.190	
Acrylonitrile	$-\text{CH}_2-\text{CH}(\text{CN})-$	53.06	78	1.46	0.806	1.184	
Methyl methacrylate	$-\text{CH}_2-\text{C}(\text{CH}_3)(\text{C}_2\text{H}_5\text{O}_2)-$	100.12	56	0.56	0.944	1.190	
Ethyl acrylate	$-\text{CH}_2-\text{CH}(\text{C}_2\text{H}_5\text{O}_2)-$	100.12	78	0.78	0.924	1.120	
Methyl acrylate	$-\text{CH}_2-\text{CH}(\text{C}_2\text{H}_5\text{O}_2)-$	86.09	78	0.91	0.953	1.220	
Acrylamide	$-\text{CH}_2-\text{CH}(\text{CONH}_2)-$	71.08	79	1.12	1.122	1.300	
Tetrahydrofuran	$-\text{CH}_2-\text{CH}_2-\text{CH}_2-\text{CH}_2-\text{O}-$	72.11	23	0.32	0.886	0.985	
1,3-Butadiene	$-\text{CH}_2-\text{CH}=\text{CH}-\text{CH}_2-$	54.09	73	1.35	0.621	0.902	
Chloroprene	$-\text{CH}_2-\text{C}(\text{Cl})=\text{CH}-\text{CH}_2-$	88.54	68	0.77	0.958	1.243	
Ethylene oxide	$-\text{CH}_2-\text{CH}_2-\text{O}-$	44.05	95	2.15	Gas	1.127	

Source: Brandrup, J., and E. H. Immergut (eds.): *Polymer Handbook*, 3rd edn., Sections II and IV, Wiley, New York, 1989; Runt, J. P., *Enc. Polym. Sci. Eng.*, 4, 487, 1986.

As a monomer is converted to a polymer in a homogeneous system, the **viscosity** can increase rapidly. In a highly viscous medium, small monomer molecules still can diffuse readily to growing chains so that k_p remains relatively constant, but large growing chains cannot diffuse easily toward each other, so that k_t can decrease considerably. According to Equation 4.5, the rate should increase. Also, according to Equation 4.15, the degree of polymerization should increase. This sudden increase in rate, **autoacceleration** or the **Trommsdorff effect**, is pronounced when high-molecular-weight polymer is formed, since the viscosity of the solution increases in proportion to the molecular weight raised to somewhere between the second and fourth power in many cases. The transition from normal kinetics to autoacceleration can be quite sharp. It is aggravated by the higher rate of heat generation, which can raise the temperature and further increase the rate. The addition of large amounts of initiator to give a lower molecular weight or the presence of a solvent to keep the viscosity down can delay the onset of autoacceleration. However, the addition of a polyfunctional monomer will bring about branching and perhaps gel formation with early onset of the effect.

Polymers invariably are more dense than their monomers even when both are amorphous. The **shrinkage** on polymerization can be as much as 10%–20%. In a batch polymerization, this often means a variable vapor volume above the reacting liquids. The agitation systems may be complicated, as in the suspension polymerization of styrene or methyl methacrylate, where monomer is lighter than water and must be drawn down into the agitated core, but polymer is heavier than water and must be pulled off the bottom of the reactor. This change in volume is the basis for kinetic measurements based on **dilatometry**. Even in dilute (1%–5%) solutions of monomer in an inert solvent, the increase in density as polymerization proceeds is enough to provide a measure of conversion. The extent of reaction is followed by measuring the volume of the system. Usually the density is directly proportional to conversion, simplifying calculations.

The dilatometer shown in Figure 5.1 was used for photoinitiated polymerizations. It has a reaction cell with flat faces in order to ensure uniform illumination by UV light [3]. For example, a monomer such as methyl methacrylate can be dissolved in toluene with an initial concentration of 2% monomer in a stirred reaction cell with a working volume of 50 cm³. A change in height of 50 mm in a 1-mm diameter capillary tube can correspond to a conversion to polymer of 10%–20% of the initial monomer charge. Quite sensitive measurements of polymerization rates are possible as long as temperature and viscosity changes can be controlled.

Example 5.1

Two cylinders are filled to a depth of 10.0 cm with (1) methyl methacrylate and (2) styrene. When both are polymerized completely, what will be the average depth of polymer in each cylinder (assuming no lateral shrinkage)?

Solution: Using data from Table 5.1,

$$\text{Methyl methacrylate: } 0.944 \times 10 \text{ cm}/1.19 = 7.9 \text{ cm}$$

$$\text{Styrene: } 0.906 \times 10 \text{ cm}/1.047 = 8.7 \text{ cm}$$

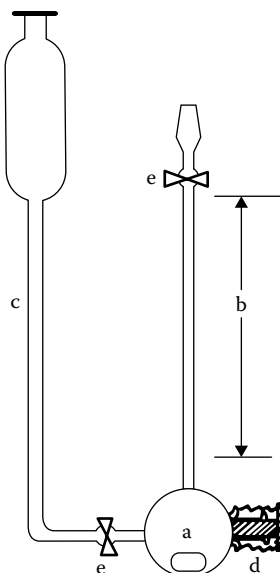
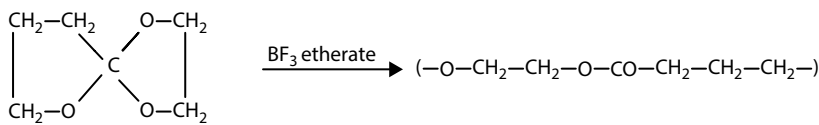


FIGURE 5.1 Dilatometer: (a) reaction bulb; (b) graduated capillary tube; (c) filling tube; (d) plug; (e) fluorocarbon stopcocks. (Data from Joshi, M. G., and F. Rodriguez, *J. Appl. Polymer Sci.*, 27, 3151, 1982.)

Certain classes of monomers do not shrink and may even expand on polymerization [4]. One of the first examples reported was a spiro orthoester that was polymerized to a polymer with an estimated molecular weight of 25,000 using a boron trifluoride etherate initiator [5]. In this case, there was no measurable shrinkage on polymerization. The monomer is made by reacting ethylene oxide with α -butyrolactone:



1,4,6-Trioxaspiro[4,4]nonane

Polymerization may be carried out with monomer alone (**bulk**), in a solvent (**solution**), as an emulsion in water (**emulsion**), or as droplets, each one comprising an individual bulk polymerization, suspended in water (**suspension**). All four methods are commercially applied to radical-initiated chain polymers such as polystyrene. Most ionic and coordination complex systems are inactivated by water, so that only bulk or solution methods can be used. Also, rather few condensations are carried out in emulsion or suspension. However, ethylene dichloride and sodium polysulfide are condensed to give ethylene polysulfide rubber and sodium chloride in an aqueous emulsion. Gas-phase polymerization and interfacial condensation are special techniques, which are mentioned in Section 5.3.

5.2 BULK POLYMERIZATION

In **bulk polymerization**, also called **mass** or **block** polymerization, monomer and polymer (and initiator) are the only components. When only part of the monomer charge is converted to polymer, however, the problems encountered are more typical of the solution method, which is discussed next. We can differentiate between quiescent and stirred bulk polymerizations. Both methods are applied to systems where polymer is soluble in monomer and progressively increases in viscosity with conversion. In quiescent systems, gel formation, corresponding to infinite viscosity, can occur. Because of the heat of polymerization and autoacceleration, the reaction rate is difficult to control. Heat removal is impeded by high viscosity and low thermal conductivity. The removal of traces of unreacted monomer from the final product is difficult because of low diffusion rates. Conversion of all monomer is difficult for the same reason.

5.2.1 QUIESCENT BULK POLYMERIZATION (MONOMER CASTING)

Typically, nonstirred polymerizations are used to produce materials in useful shapes. Whenever a cross-linked thermoset is molded, the final reaction is carried out without agitation. As an example, phenol–formaldehyde condensation carried out in a mold under pressure has been mentioned earlier. The casting of methyl methacrylate in a closed mold to make large sheets has several advantages. For example, the Trommsdorff effect gives a large fraction of extremely high-molecular-weight molecules. These in turn make for a tough material with high melt viscosity that is ideal for sheet-forming operations. It would be hard to make this material in another form and then mold it as sheet because of this high melt viscosity. The major problems involved are (1) heat removal to prevent boiling of monomer, which would leave bubbles in the sheet; (2) conversion of all monomer; and (3) accommodation of the 21% shrinkage that occurs on polymerization. Problems 1 and 3 are alleviated somewhat by starting with a degassed syrup of low-molecular-weight polymer (10%–30% of syrup) and benzoyl peroxide (0.02%–0.05%) in methyl methacrylate rather than with monomer alone. A simple mold consists of two glass plates separated by a flexible gasket, typically poly(vinyl alcohol) that is also the confining wall of the mold. After filling, the entire assembly is placed in an air oven. A typical time-temperature profile would show an exotherm due to autoacceleration after about 18 h. The shrinkage is accommodated by the flexible mold wall. Virtually complete conversion of monomer is assured by a 10-h *soak* at 85°C. The unattractive feature of this process is the long holdup time in the mold.

A continuous sheet-casting operation has obvious advantages over the batch process [6]. The casting syrup is confined between stainless-steel belts by using a flexible gasket as in the batch process (Figure 5.2). The belts run progressively through polymerization and annealing zones. It is important that pressure be maintained (by external rollers) so that monomer boiling will not occur. Since a higher temperature can be used, the total time for polymerization is decreased compared to the batch operation. The molecular-weight distribution that results from continuous polymerization will differ from that for the batch-cast polymer,

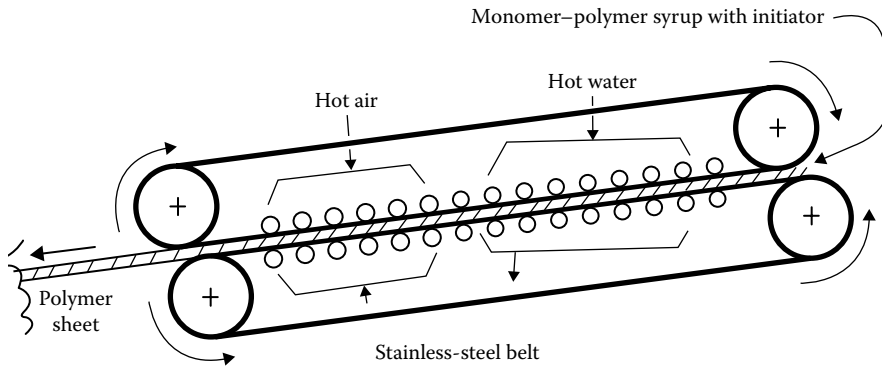


FIGURE 5.2 Continuous casting of poly(methyl methacrylate) sheet. (Data from Opel, C. J., and P. H. Bottoms, US Patent 3,376,371, Swedlow, Inc., 1968.)

so the products are not identical. Sheet thickness for the continuous casting process usually is limited to the range of 2–12 mm [7]. An example described in the original patent [8] used a belt that was 41 m long and 1.4 m wide. The two successive temperature zones were maintained at about 70° and 105°C, and the belt moved at 1 m/min.

5.2.2 STIRRED BULK POLYMERIZATION

Bulk polymerizations that are stirred have been used for various commercial polymers. Some, such as free-radical-initiated polyethylene, are carried out to low conversion so that the unreacted monomer acts as a diluent. These are, in effect, solution polymerizations and are treated in Section 5.3. Equipment that will handle liquids progressively from monomer (~0.01 poise) to polymer (~10⁵ poise) with efficient heat removal is usually designed specifically for a given installation. Conventional turbine- or propeller-agitated vessels can handle a limited degree of conversion. With low-molecular-weight condensation polymers, the completed polymer melt may be transferable by gear pumps or merely extruded from the reactor by application of moderate pressure.

Styrene can be polymerized to a high conversion if a small amount, say 20%, of an unreactive solvent is present. It is often referred to as a bulk polymerization even though some solvent is present. Most **atactic polystyrene** is produced by free-radical polymerization in this manner. Several continuous processes have been described in some detail [9]. In one process, linear-flow reactors are used in series (Figure 5.3). Each reactor contains a series of sections that are agitated and provided with heat transfer tubes. A free-radical initiator may be used. In order to lower viscosity, especially in the latter stages, a solvent, typically ethyl benzene, is present to the extent of about 20%. Polymerization to high conversion is obtained in the last reactor as the temperature is increased

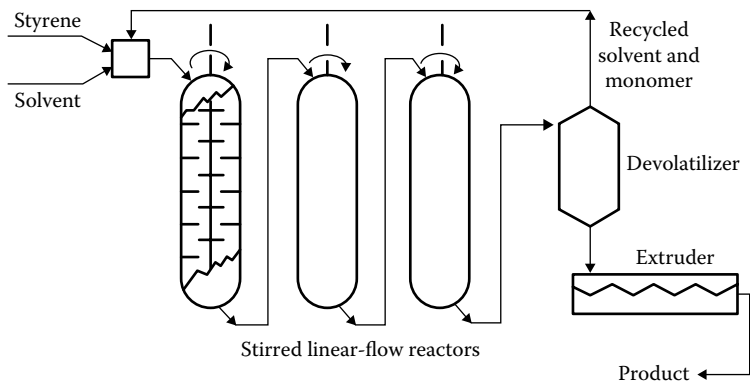


FIGURE 5.3 Continuous polymerization of polystyrene.

from 100°C to 200°C. A vacuum tank (devolatilizer) removes unreacted styrene together with almost all of the solvent that then is recycled. Finally, an extruder forms the product into molding pellets. A twin-screw extruder reactor has also been suggested for the continuous bulk polymerization (Figure 5.4). Such a reactor can handle more highly viscous polymer melts than the tower-like reactors.

A continuous process for **nylon 6,6** in which hexamethylenediamine is mixed and heated with an excess of adipic acid in an agitated tank has been described in a patent [10]. The low-viscosity mixture is then directed to the top of a towerlike reactor containing perforated plates and an agitator to help mix vapor and melt (near the bottom) (Figure 5.5). Diamine vapor is introduced at various places near the bottom so that it is available for reaction as it rises through the tower. With careful control of flow rates and temperatures, the product issuing from the bottom of the reactor can be maintained at a uniform molecular weight (number average) of about 10,000. A reactor about 8 m tall with an inside diameter of 0.4 m was used to make 90 kg/h of polymer. Reactor temperatures increased from 178°C in the top stage to 276°C in the bottom (eighth) stage.

Nylon 6,6 also can be produced continuously using an extruder reactor like that in Figure 5.4. Most poly(vinyl chloride) is produced by a batchwise suspension polymerization in reactors like the one shown in Figure 5.13; however, bulk polymerization has the advantage that no suspending or emulsifying agent is left in the resin to detract from optical clarity, an advantage for packaging applications that account for as much as 5% of all poly(vinyl chloride). A two-stage, bulk batch process (Figure 5.6) operation has been described [12]. *Prepolymerization* in a stirred tank (0.016% azodiisobutyronitrile, 130 rpm, 60°C, 1 MPa) is carried to about 10% conversion. Further reaction to about 75% conversion occurs in a scraped surface autoclave with slow agitation over a period of 10–12 h or more. Porous particles with diameters of 100–200 μm result after monomer is blown off and the polymer is recovered.

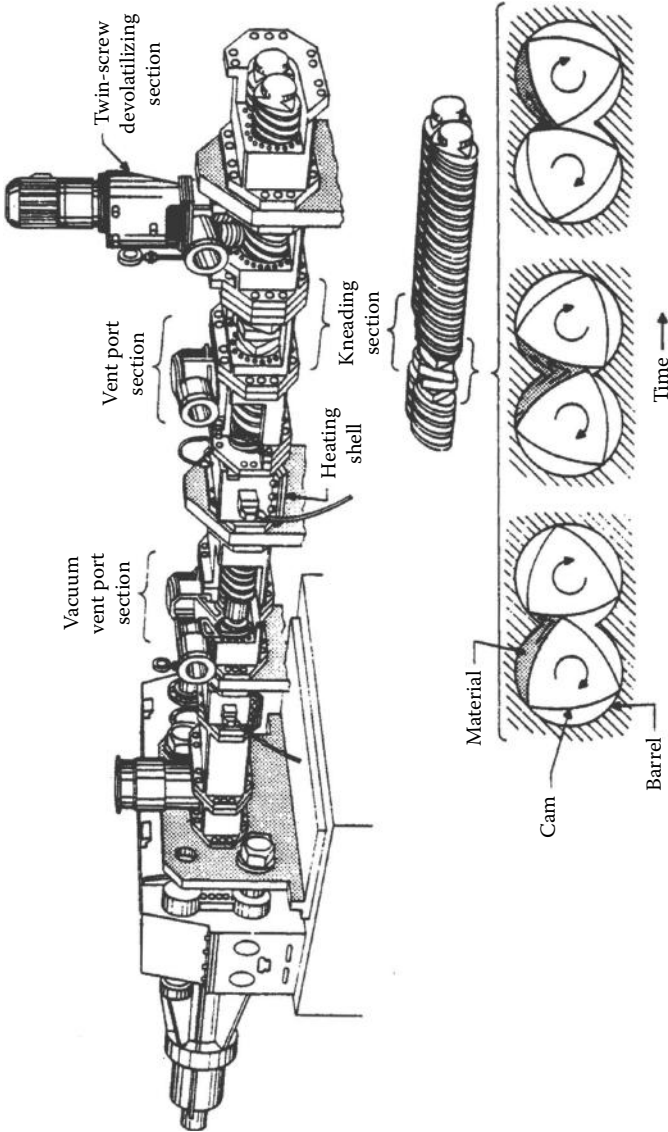


FIGURE 5.4 Twin-screw extruder reactor. (Courtesy of Mack, W. A., and R. Herter, *Extruder Reactors for Polymer Production*, Werner & Pfleiderer Corporation, Waldwick, NJ, 1975.)

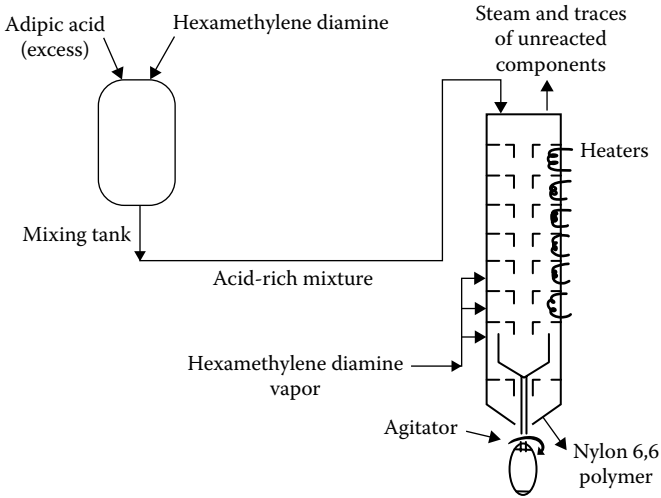


FIGURE 5.5 Continuous polymerization of Nylon 6,6. Polymer of increasing molecular weight is formed as the acid-rich mixture contacts a countercurrent flow of diamine vapor. (Data from Brearly, A. M. et al., US Patent 5,674,974, E. I. Du Pont de Nemours and Company, 1997.)

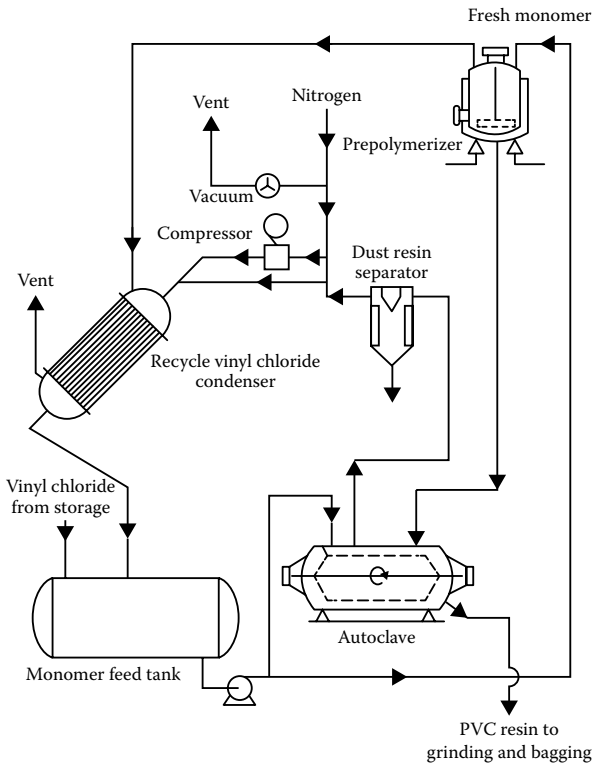


FIGURE 5.6 Continuous bulk polymerization of vinyl chloride. PVC, poly(vinyl chloride). (Data from Krause, A. *Chem. Eng.* 72, 117, 1965.)

5.3 SOLUTION POLYMERIZATION

When a monomer is diluted in an inert solvent, there are several advantages over bulk polymerization. The main one is that the heat of polymerization is taken up by a greater mass, thus minimizing the exotherm. Also, the viscosity increase is minimized. A solvent that is more volatile than the monomer can be refluxed to remove heat from the system and, in some cases, to keep the reaction at a constant temperature. We can subdivide solution polymerizations by the phases present. Invariably, monomer and diluent are miscible, so the combinations are listed in the table below:

Reactant	1	2	3	4
Monomer and diluent	Soluble	Soluble	Soluble	Soluble
Initiator	Soluble	Insoluble	Insoluble	Soluble
Polymer	Soluble	Soluble	Insoluble	Insoluble

Some physical schemes to carry out these reactions can be illustrated with specific examples.

1. *All components soluble.* This probably is the most widely used system for the laboratory preparation of new polymers and copolymers. It is applicable to most free-radical and ionic propagation schemes. Low viscosity enhances temperature control. The obvious disadvantage is that the recovery of the polymer or its purification involves handling a large amount of extraneous material. Adding a nonsolvent in order to precipitate the polymer can remove unreacted monomer at the same time. On an industrial scale, handling large amounts of solvents may be unavoidable. The laboratory preparation of a block copolymer with anionic initiation was mentioned in Section 4.5.2. In commercial production, both economic and ecological considerations make it necessary to recover and purify the solvents and diluents, usually by fractional distillation.

When monomer conversion is limited with recycling of a large amount of unreacted monomer after the polymer is removed, the system is, in effect, a solution polymerization in which part of the monomer is acting as a solvent. One large-scale industrial application illustrating this scheme is the free-radical polymerization of ethylene at extremely high pressures. The conditions lead to a highly branched structure because of chain transfer to polymer. Large quantities of low-density polyethylene (**LDPE**) are produced in tubular reactors. In a typical scheme (Figure 5.7), 10%–30% of the monomer might be converted in a single pass at 1000–3000 atm and 100°C–200°C. Although a peroxide might be used as the free-radical source, a small amount (~0.05%) of oxygen can serve as an effective initiator. Under these conditions, the ethylene is well above its critical temperature and pressure, and the polymer is dissolved in monomer. Conversion can be increased to 40% or so by periodic

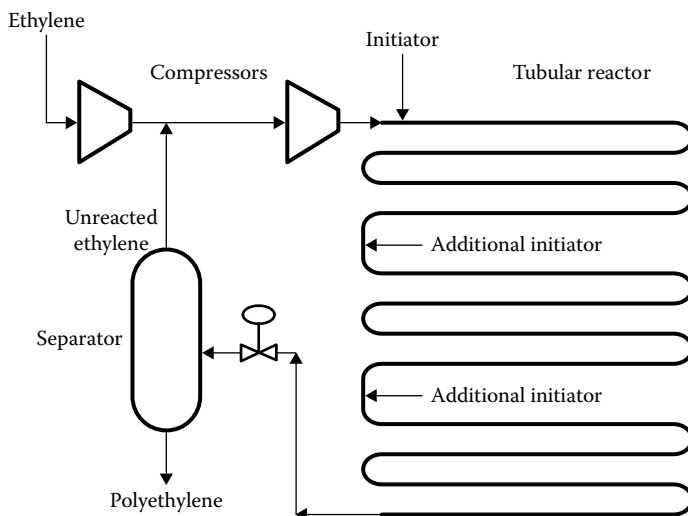


FIGURE 5.7 Tubular reactor for high-pressure, free-radical polymerization of ethylene. (Data from Doak, K. W., *Enc. Polym. Sci. Tech.*, 6, 386, 1986.)

addition of initiator at positions along the tube. Ethylene is continuously pumped into the tube and the product is periodically released from the other end to approximate plug flow through the tube and to decrease the buildup of polymer on the walls. At the end of this **peristaltic flow**, the pressure is reduced, the unreacted monomer flashes off and is recycled, and the polymer is recovered. For a single train system with a capacity of 100×10^6 kg/yr, the tube might be over 1 km long with an inside diameter of 5 cm and an outside diameter of 15 cm. Stirred autoclaves operating at similar pressures are sometimes used in place of the tubular geometry.

2. *Insoluble initiator.* An interesting, though not commercially important, example has been described in which the catalyst is in the form of a fixed bed and the polymer that is formed remains in solution [14]. A chromia-silica-alumina catalyst (an initiator that can be regenerated) will convert ethylene to linear polymer at moderate pressures. In this case, a dilute (2%–4%) solution of ethylene in an inert carrier (saturated hydrocarbon) is passed over a fixed bed of catalyst at 150°C – 180°C and 300–700 psi (2.1–4.8 MPa) (Figure 5.8). Conversion may be high, but there is considerable volume of solvent to recover and recycle. Periodic reactivation of catalyst at about 50-h intervals is required.
3. *Insoluble initiator and polymer.* With a polymerizing system of ethylene and an agitated catalyst suspension at lower temperatures, polyethylene and catalyst may be insoluble in an inert diluent and form a slurry that is removed continuously. The **loop** (or **double-loop**) reactor developed by Norwood [15] has been widely used for the slurry process. Turbulent circulation in

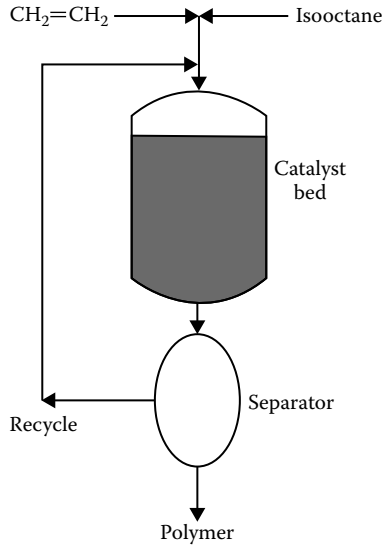


FIGURE 5.8 Fixed-bed reactor.

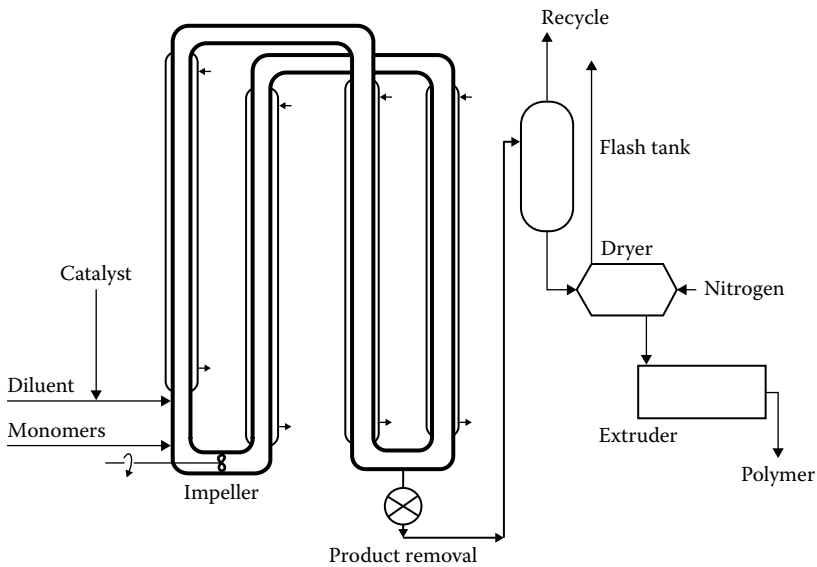


FIGURE 5.9 Double-loop slurry reactor for high-density polyethylene. (Data from Norwood, D. D., US Patent 3,248,179, Phillips Petroleum Co., 1966; Benham, E., M. P. McDaniel, and F. W. Bailey, US Patent 4,966,951, Phillips Petroleum Co., 1990.)

the loop is maintained by an impeller (Figure 5.9). The geometry provides a considerable area for heat removal through the jacketed pipes that comprise the loops. In making a copolymer of ethylene and 1-hexene, the preferred catalyst is chromia on a silica–titania support [16]. The cocatalyst, a trialkyl boron compound and the diluent, isobutane, are introduced into the loop

and the product is removed as a slurry from the loop. The temperature is kept below 100°C and the pressure is about 40 atm.

A **fluidized-bed, gas-phase polymerization** bears some resemblance to the process just described. Fine catalyst particles are contacted with rapidly upward moving ethylene vapors below the melting point of polyethylene (Figure 5.10). This has become an important commercial process with definite economic advantages over solvent-based systems (see Section 16.2). In one installation [17] with a capacity of 100×10^6 kg/yr, the fluidized bed reactor (Figure 5.10) has a diameter of 4.3 m (14 ft). Purified ethylene and powdered catalyst (modified chromia on silica) are fed continuously, and polyethylene fluff is removed intermittently from the reactor through a gas lock chamber. Reactor pressure is about 20 atm and the temperature is 85°C–100°C. Heat of polymerization is removed as the gas is circulated through external coolers. Only about 2% or 3% of the monomer is converted per pass, but overall monomer loss is kept below 1% of the feed by recycling. The growing particles remain in the reactor 3–5 h and attain a final diameter of about 500 μm . Since as much as 600,000 kg of polymer can be formed per kilogram of chromium, catalyst removal is not necessary for many applications. Molecular weight can be decreased using hydrogen as a chain transfer agent. Some process changes have enabled the conversion per pass to be as high as 6%.

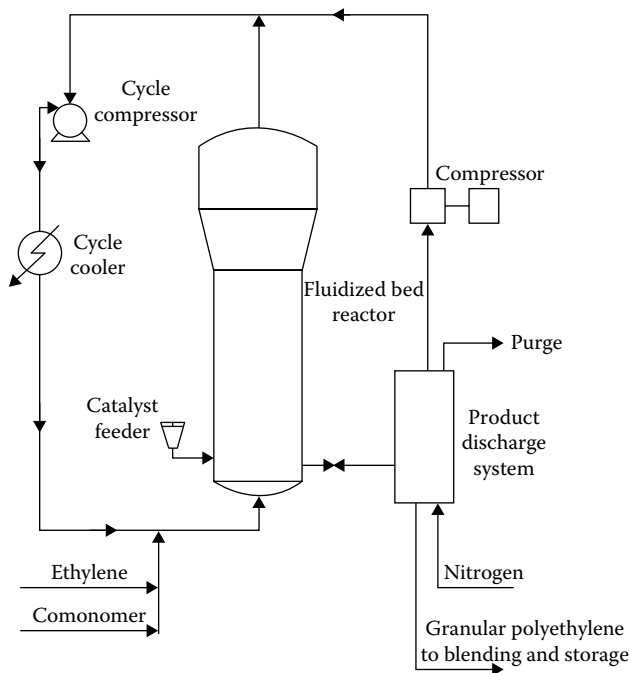


FIGURE 5.10 Gas-phase polymerization of ethylene. (Data from *Chem. Eng.*, 86, 83, December 3, 1979.)

In the 1980s, the fluidized bed process was modified to produce a copolymer similar in density to polyethylene produced by the older, high-pressure process. Copolymerization of ethylene with 1-butene or other normal alpha olefins introduces short pendant chains that decrease crystallinity. In the plastics business, the terms **high-density, or linear, polyethylene** and **LDPE** (or branched polyethylene) are now supplemented by linear LDPE (**LLDPE**). While all the properties of the high-pressure polymer are not achieved by the newer material, the economics of the low-pressure, solvent-free process are such that LLDPE competes successfully in many of the markets once dominated by branched LDPE. The fluidized bed itself is only one of several gas-phase polyolefin processes. Stirred beds, arranged either horizontally or vertically, do not depend on gas velocity and are less sensitive to uniformity of gas flow. The stirred beds have been used primarily for polypropylene [19]. However, the fluidized bed has also been adapted for production of polypropylene and propylene copolymers.

4. *Insoluble polymer.* Heating an aqueous solution of acrylonitrile with persulfate as initiator at 80°C results in a stringy precipitate of polyacrylonitrile that can be filtered out and dried. The process is successful because the precipitate is relatively dry and does not form large agglomerates.

There are some dramatic contrasts between the cationic polymerization to make **polyisobutylene** and the free radical and coordination complex (both Ziegler and Phillips) methods. Few free-radical processes can be operated below room temperature. Even when the radicals can be generated, the rate of propagation is low. However, the cationic growth of isobutylene proceeds rapidly at -65°C. Like the coordination complex systems, most cationic catalysts are inactivated by water. Unlike them, however, the radical life is short, so long reactor residence times are not necessary. The major engineering problem becomes that of heat removal at a low temperature. Although isobutylene is homopolymerized commercially, the production process is similar to the slurry used for making **butyl rubber**, a copolymer with isoprene [20]. The isoprene introduces a residual unsaturation in the polymer that can be used with conventional sulfur-based cross-linking agents. Jackets around cooling tubes in the reactor contain boiling ethylene for heat removal (Figure 5.11). The continuous feed to the reactor consists of two solutions: the monomers (25% isobutylene, 2%–3% isoprene, balance methyl chloride) and the catalyst (0.4% AlCl_3 in methyl chloride). About 3 parts of the latter are sprayed into 10 parts of the former solution. The exothermic reaction is almost instantaneous with conversion of as much as 95% of the isobutylene and 85% of the isoprene. A slurry of fine polymer particles (5–30 μm in diameter) is formed. At this point additives may be introduced to stabilize the slurry and decrease the fouling of the reactor. Slurry then overflows into an agitated flash tank with an excess of hot water.

The methyl chloride and any unreacted hydrocarbons are flashed off and sent to a recovery system. An antioxidant and a lubricant (zinc stearate) are added to the slurry in the flash tank also. Screening, filtering, and drying in a tunnel dryer are followed by a forming operation and packaging. The copolymer has been chlorinated and brominated to provide a different reactive group for cross-linking. Metal oxide

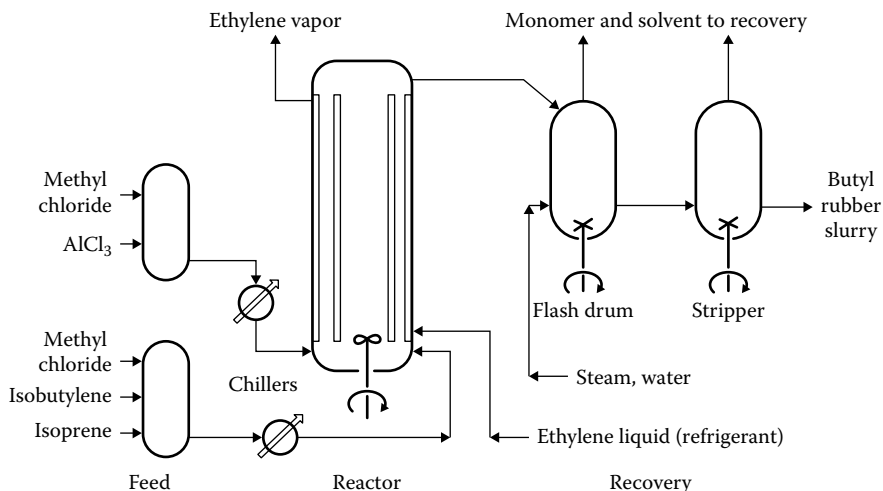
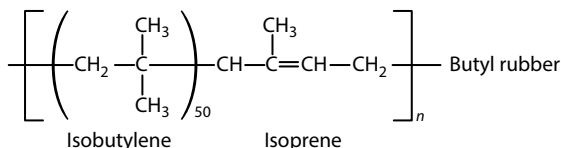
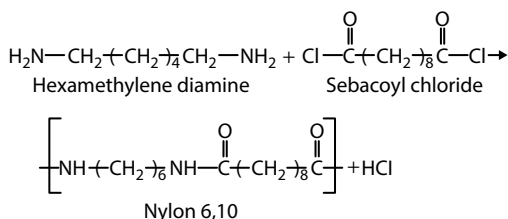


FIGURE 5.11 Butyl rubber production.

cross-linking when a halogenated group is present gives a structure that is more stable at high temperatures than sulfur cross-linking usually employed with residual unsaturation. Production of the homopolymer of isobutylene uses a similar process. Low-molecular-weight polyisobutylene is used in many adhesives.



An interesting example of condensation polymerization in this general category is **interfacial condensation**. A diacid chloride is dissolved in a heavy, dense solvent such as tetrachlorethylene. As a stagnant layer above it is poured a solution of diamine in water. At the interface a layer of polyamide (nylon) is formed almost immediately. But the reaction stops because of the slow diffusion of reactants to each other through the polymeric interface. However, as the interface is pulled out, reactants contact each other and form more polymers (Figure 5.12). Within limits, the rate of reaction is controlled by the rate of interface removal. With pure sebacoyl chloride and hexamethylene diamine, nylon 6,10 is formed from which fibers or films can be made.



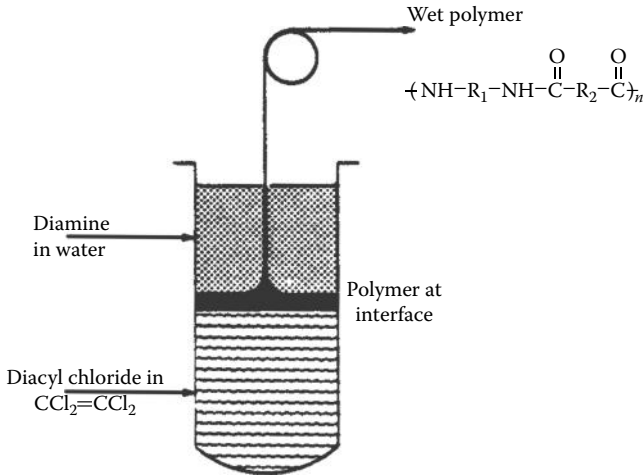


FIGURE 5.12 Interfacial condensation.

The demonstration based on the apparatus of Figure 5.12 has been popularized under the name *the nylon rope trick* [21,22]. It has been used at countless science fairs and at all levels of sophistication from elementary school to university. However, it is not very convenient even for laboratory preparations. A typical preparative method starts with the same ingredients as the nylon rope trick. The aqueous phase is placed in a high-speed stirrer (blender) and the organic phase added while the system is stirred at high speed. Suspending agents or surfactants may be added to stabilize the polymer–solvent dispersion that results. Plant-scale operations also use stirred tanks rather than quiescent interfaces.

For all these systems, a conventional glass-lined or stainless-steel reactor is suitable for batch operations when reaction pressures and product flow characteristics are within certain limits (Figure 5.13). Temperature can be controlled by liquid circulating in a jacket around the reactor or through coils within the reactor. Scraped-surface, stainless-steel reactors have been built that will handle pressures from a full vacuum to 6 atm and viscosities of 1 mPa·s to 10 kPa·s for large batches.

5.4 SUSPENSION POLYMERIZATION

If the monomer is insoluble in water, bulk polymerization can be carried out in suspended droplets. The water phase becomes the heat transfer medium. Since it is the continuous phase, viscosity changes very little with conversion, so that heat transfer to the reactor walls can be efficient. The behavior inside the droplets is very much like the bulk polymerizations described in Section 5.2. But because the droplets are only 10–1000 μm in diameter, more rapid reaction rates can be tolerated without boiling the monomer. To keep the droplets from coalescing as they proceed from liquid to solid states via a sticky phase, a so-called **protective colloid** (suspending agent) and careful stirring are used. Poly(vinyl alcohol) dissolved in the aqueous phase is a typical suspending agent, although many other agents including inorganic

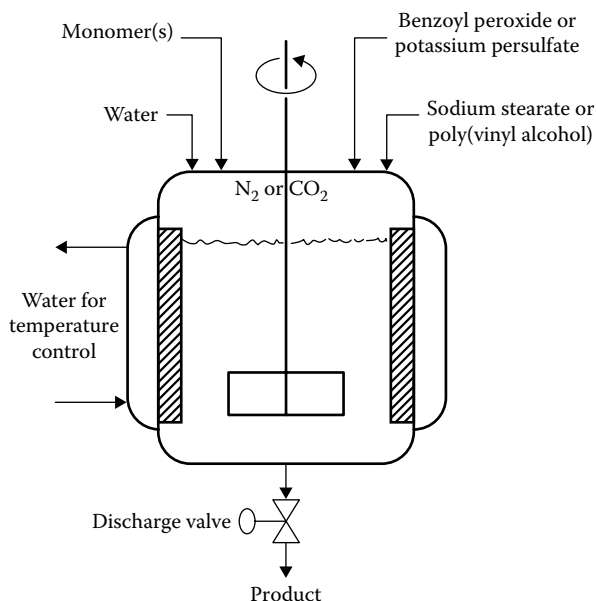


FIGURE 5.13 Basic stirred, jacketed batch reactor. For solution polymerizations, solvent, monomer, and initiator are charged. For suspension polymerization, water and a protective colloid such as poly(vinyl alcohol) form one phase, whereas the monomer and initiator form a second phase. In emulsion polymerization, a water-soluble initiator such as potassium persulfate is used together with a surfactant such as sodium stearate.

powders have been used. It is necessary that the agent be insoluble in the monomer-polymer particle so that a coating forms on the surface of the particle, thus retarding coalescence. However, this usually does not prevent the particles from rising (creaming) together if agitation is stopped so an interruption in the stirring can lead to massive agglomeration when the particles are at an intermediate state of conversion.

The particle size and size distribution are affected by the suspending agent and stirring rate. Particle size decreases with impeller diameter and speed [23]. A typical vessel suitable for suspension or emulsion polymerization like that shown in Figure 5.13 can be adapted for various processes by modifying the impeller geometry.

A simple suspension polymerization can be carried out in a glass flask with agitation.

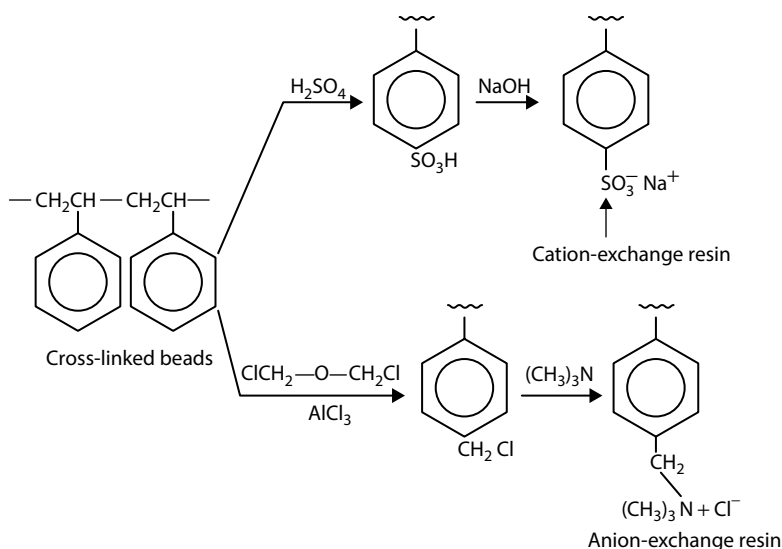
Aqueous Phase	
Water	400 ml
Poly(vinyl alcohol) ^a	1 g
Oil Phase	
Methyl methacrylate	100 g
Benzoyl peroxide	1 g

^a Copolymer with about 17% vinyl acetate.

Under a nitrogen atmosphere, the aqueous phase is heated to 80°C. The oil phase is added with stirring at about 150–300 rpm with a paddle agitator. After an hour or so, a slight exotherm, 5°C–10°C, is noted. Particles of the slurry examined before this time are sticky and usually agglomerate on cessation of stirring. After the exotherm, when most conversion has taken place, the particles are hard and do not agglomerate. Initially the monomer phase is lighter than water and agitation near the surface is essential. After the exotherm, enough polymer has been formed to make the oil phase heavier than water, so that settling out occurs if stirring is inadequate. Final recovery of the beads, which are 100–1000 μm in diameter, is by filtration and washing.

In most suspension polymerizations, conversion of monomer is nearly complete and pearl-like beads of polymer result, especially if the polymer is amorphous and below its glass transition temperature. Two important exceptions are vinyl acetate and vinyl chloride. Vinyl acetate can be polymerized to give a stable suspension of about 50% solids content if the particle size is kept small (1–15 μm in diameter). Plasticized with castor oil so that the polymer (partly hydrolyzed to the corresponding alcohol) will be above T_g at room temperature, the suspension makes an excellent quick-setting adhesive for wood, paper, and cloth. Most poly(vinyl chloride) is produced by suspension polymerization. The polymer is insoluble in its monomer. Suspension polymerization can be carried to 70%–90% conversion under moderate pressure (6 atm) and temperature (80°C) by using an oil-soluble initiator such as lauroyl peroxide or azoisobutyronitrile. During this period, polymer precipitates in the droplets. Release of pressure and stripping of monomer by pulling a vacuum leaves the polymer portion of the droplets as porous particles that can be recovered by filtration and drying or directly by spray drying. Such porous particles are ideally suited for adsorbing plasticizers in *dry-blending* operations.

Suspension polymerization of styrene in a batch process might require 8–12 h at 70°C–100°C. Coagulation is not necessary, since the particles are large enough to be filtered out directly after steam treatment to remove unreacted monomer. Although not much used for general-purpose polystyrene, suspension polymerization is ideal for producing the cross-linked beads required for gel permeation chromatography columns (Section 6.4) or for ion-exchange resins. Moore [24] described the copolymerization of styrene with divinyl benzene as a 20% solution in toluene with peroxide initiator. All these ingredients are suspended in water. In the presence of about 10% divinyl benzene, the monomer beads are gelled at a low conversion, triggering the Trommsdorff effect (Section 5.1). This cuts the time for almost 100% conversion down to about 2.5 h. From the 1000-gal, glass-lined reactors (similar to that shown in Figure 5.13), the beads (0.30–1 mm in diameter) are transferred after washing and drying to separate kettles, where they are reacted with sulfuric acid or chloromethyl ether followed by trimethylamine, making a quaternary ammonium group to make strong ion-exchange resins. A weak anion-exchange group results if dimethyl amine is used instead.



5.5 EMULSION POLYMERIZATION

At first glance, emulsion polymerization looks very much like suspension polymerization [25]. The same reactor (Figure 5.13) can be used but the mechanisms differ greatly (as do some of the ingredients). Suspension polymerization can be seen as a bulk polymerization carried out in suspended droplets of monomer and polymer. The end product comprises beads that are about the same size as the original monomer droplets.

However, some important distinctions between emulsion and suspension polymerizations are as follows:

1. Emulsions usually are composed of small particles (0.05–5 μm) compared with suspensions containing particles of 10–1000 μm in diameter.
2. Water-soluble initiators are used rather than monomer-soluble ones.
3. The end product usually is a stable latex—an emulsion of polymer in water rather than a filterable suspension.

Because of these conditions, the mechanism of polymerization is basically different. The essentials of an emulsion polymerization system are a monomer, a surface-active agent (surfactant), an initiator, and water. Initially, the surfactant is in the form of **micelles**, spherical or rodlike aggregates of 50–100 surfactant molecules with their hydrophobic *tails* oriented inward and their hydrophilic *heads* outward. These micelles form whenever the concentration of surfactant exceeds a rather low critical micelle concentration. The manner in which the **critical micelle concentration** for a given surfactant is measured is instructive for our purposes. If a dilute

aqueous solution of an oil-soluble dye such as eosin is titrated with a dilute soap solution, a soap concentration is reached where the color suddenly disappears. The explanation is that the dye has dissolved in or has been extracted by the micellar interiors. This is the same point at which surface tension stops decreasing rapidly with added soap. If monomer is added to a micellar dispersion, most of it remains as rather large droplets, but some of it dissolves in the micelles just as the dye does. Since they are smaller, the micelles present much greater surface area than do the droplets. Consequently, when free radicals are generated in the aqueous phase, the micelles capture most of them. After a few percentage conversion, the system consists of (1) stabilized, monomer-swollen polymer particles rather than micelles and (2) monomer, which is still mainly in droplets, although it constantly diffuses to replenish the swollen particles where polymerization continues. The result is, when monomer is quite water insoluble,

$$R_p = k_p[M][M\bullet] \quad (5.1)$$

where:

$[M]$ now is the concentration of monomer in the swollen polymer particles

Since this concentration, moles per liter of swollen particles, may remain constant from low conversions up to 70% or 80% conversion, R_p should be independent of the total concentration of monomer, that is, moles per liter of emulsion. This means that the superficial reaction rate is pseudo-zero order in monomer. Now, it can be shown that a polymer particle cannot tolerate more than one growing chain at a time. Two radicals in the same particle mutually terminate almost instantaneously. Therefore, on average, half the particles will contain radicals at any instant. As an analogy, picture a group of cups standing in the rain. Each cup has received either an odd or an even number of raindrops. With enough cups and enough rain, the chances are that half the cups have received an even number of drops and the other half an odd number. If the raindrops are initiating radicals and the cups are polymer droplets, only the half that have received an odd number of droplets are growing, the even cases having been stopped by mutual termination.

Therefore, $[M\bullet]$ is simply $N_p/2$, where N_p is the number of particles per unit volume of emulsion and

$$R_p = \frac{k_p[M]N_p}{2} \quad (5.2)$$

Similar reasoning, disregarding chain transfer and assuming termination by coupling, gives

$$x_n = \frac{k_p N_p [M]}{d[M\bullet]/dt} \quad (5.3)$$

where:

$d[M\bullet]/dt$ is the rate of radical formation (not the *net* rate) and may be proportional to the square root of initiator concentration in the aqueous phase

Example 5.2

Assume that during the emulsion polymerization of isoprene (FW = 68.12) with 0.10 potassium laurate at 50°C, during stage 2, the growing swollen particles contain 200 g of monomer per liter of swollen polymer particles. Assume also that the final latex has 400 g of polymer per liter with particles of 45.0 nm in diameter. The polymer has a density of 0.90 g/cm. Using Figure 5.14, estimate k_p (liter/mol-h).

Solution: The slope of the appropriate line in Figure 5.14 is 100% conversion per 30 h. Complete conversion amounts to $400/68.12 = 5.87$ mol/liter of isoprene. Thus,

$$R_p = \frac{5.87}{30} = 0.196 \text{ mol/liter-h} \quad (5.4)$$

In the particles, $[M] = (200/68.12) = 2.94$ mol/liter. The mass of each particle is

$$\frac{\pi D^3 \rho}{6} = \frac{\pi (45.0 \times 10^{-7} \text{ cm})^3 0.90 (\text{g/cm}^3)}{6} = 4.29 \times 10^{-17} \text{ g} \quad (5.5)$$

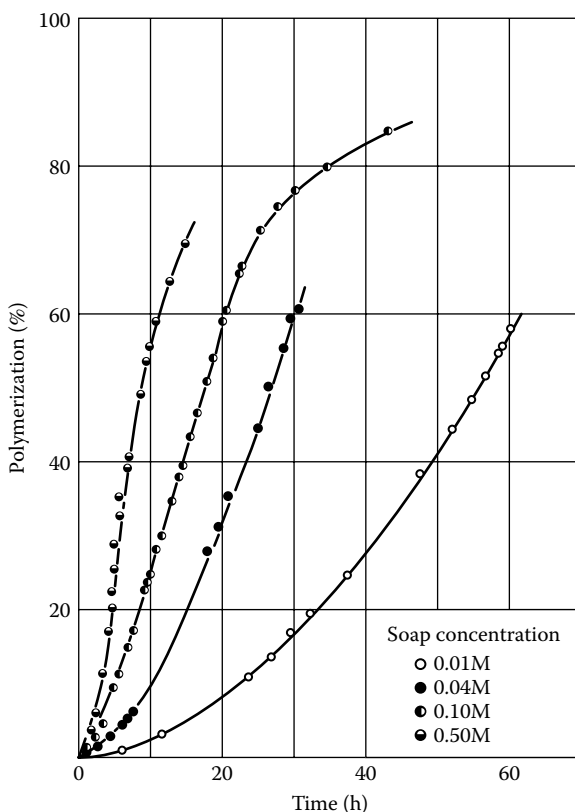


FIGURE 5.14 Polymerization of isoprene at 50°C for four concentrations of emulsifier (potassium laurate). (Data from Harkins, W. D., *J. Am. Chem. Soc.*, 69, 1428, 1947.)

Therefore,

$$N_p = \frac{400}{4.29} \times 10^{-17} = 9.3 \times 10^{18} \text{ particles per liter} \quad (5.6)$$

Divide N_p by Avogadro's number (6.02×10^{23}) to get moles per liter:

$$k_p = \frac{2R_p}{[M]N_p} = \frac{2 \times 0.196 \times (6.02 \times 10^{23})}{2.94 \times 9.3 \times 10^{18}} = 8.6 \times 10^3 \text{ liters/mol-h} \quad (5.7)$$

(The literature value is 10×10^3 liters/mol-h [2].)

One can distinguish three major stages in the typical emulsion polymerization (Figure 5.15). In the first two stages, large monomer droplets act as reservoirs supplying monomer to micelles as they are converted to monomer-swollen polymer particles. In the second stage, all the surfactant is on the surface of polymer particles with none left to form polymer-free micelles. This is the pseudo-zero-order stage corresponding to Equation 5.2. In the third stage, monomer droplets are exhausted so that only the monomer-swollen particles are left leading to essentially first-order kinetics.

The number of particles per unit volume (N_p) can be related to the concentrations of surfactant and initiator. The derivation can be complex, but the **Smith–Ewart** approach [25,26] introduces a number of simplifying assumptions. It is assumed that the entire process of establishing N_p takes place during the first part of polymerization, when the surfactant is still present in the form of micelles. Each effective radical generated from the initiator converts a micelle into a swollen polymer particle, which then grows at a constant rate ($\mu = dv/dt$). The capture of radicals by particles in competition with micelles is ignored for the moment. Every particle formed grows in area as well as in volume. Each increment of area requires a coating of surfactant, which is obtained from unreacted micelles. Thus, micelles disappear for two reasons: (1) some are converted to polymer particles and (2) some supply surfactant to growing particles.

At some time t_1 , all the surfactant in the system has coated the surface of particles, leaving none in the form of micelles. At that point, N_p no longer changes and the rate of polymerization is given by Equation 5.2. If effective radicals are being generated at a constant rate ρ_r , and each one starts a particle, then at t_1 ,

$$N_p = \rho_r t_1 \quad (5.8)$$

Next, we can relate t_1 to the surface area of particles being formed.

1. A single particle is formed at time τ and then grows until time t_1 . The volume of this particle (neglecting the initial volume of the micelle) at this time will be

$$v(t_1, \tau) = \mu(t_1 - \tau) \quad (5.9)$$

The surface area of the particle is related to the volume by geometry:

$$a(t_1, \tau) = (36\pi)^{1/3} [\mu(t_1 - \tau)]^{2/3} \quad (5.10)$$

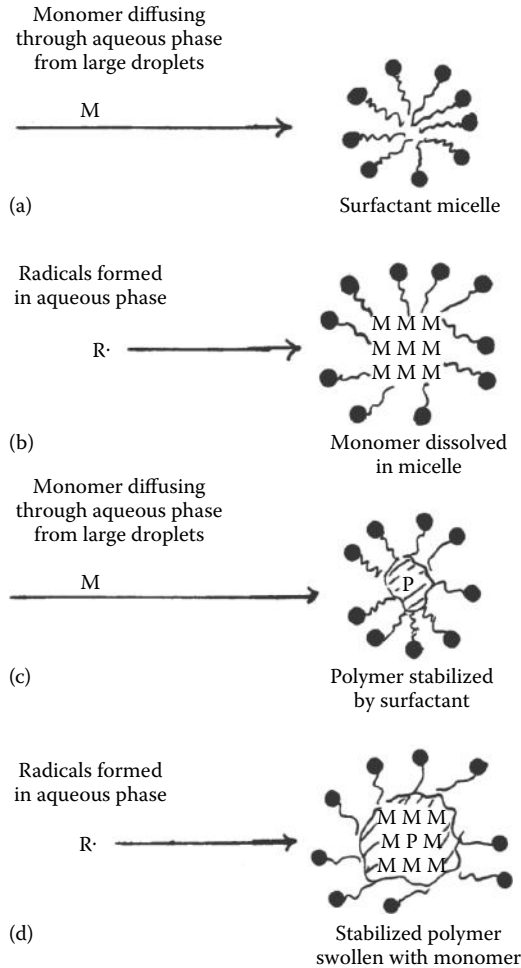


FIGURE 5.15 Emulsion polymerization. Stage 1: Surfactants form micelles (a) in which monomer can dissolve (b). Radicals from the aqueous phase convert the monomer to polymer (c). In the Smith–Ewart derivation, only steps (a) and (b) are considered to create polymer particles in stage 1. Stage 2: Micelles no longer exist and all surfactants are used to stabilize monomer-swollen polymer particles that undergo further growth through successive swelling (c) and polymerization (d). Stage 3: Monomer droplets are used up so only the monomer already dissolved in the particles is left to polymerize.

2. The number of particles generated in the time interval $d\tau$ is $\rho_r d\tau$. Thus, the total surface area of particles at t_1 , using Equation 5.6, is

$$A_t = \int_0^{t_1} a(t_1, \tau) \rho_r d\tau = (36\pi)^{1/3} (0.6\rho_r) \mu^{2/3} t_1^{5/3} \quad (5.11)$$

3. The total area at t_1 is also given by

$$A_t = a_s [S] \quad (5.12)$$

where:

a_s is the surface area occupied by a mole of surfactant

[S] is the surfactant concentration (in mol/l)

4. Combining Equations 5.4, 5.7, and 5.8, we can eliminate A_t and t_1 :

$$N_p = 0.53 \left(\frac{\rho_r}{\mu} \right)^{0.4} (a_s [S])^{0.6} \quad (5.13)$$

The total number of particles per liter should vary with surfactant concentration to the power of 0.6 and with initiator concentration (via ρ_r) to the power of 0.4. As noted earlier, at time t_1 (usually corresponding to a very small fraction of conversion), N_p no longer increases and the rate of polymerization reverts to Equation 5.2.

This derivation can be modified to take into account radicals entering particles in competition with micelles. The only change is that the factor 0.53 becomes 0.37. More serious differences occur when particles are large and may contain more than one growing polymer radical (slow termination rate), when initiator decomposition is very slow, or when the monomer is partly soluble in water or insoluble in polymer [26,27]. However, the form of Equation 5.9 often holds even though the proportionality factor and the values of the exponents must be determined experimentally.

An increase in surfactant concentration increases N and, therefore, increases R_p and x_n (Figure 5.14). High molecular weights are possible in emulsion polymerization because initiation is in one phase, water, and termination is in another phase, monomer-polymer. The combination of high molecular weight with high rate is one reason for the popularity of this method. **Seeded polymerizations** can be useful for making large-particle-size latexes. A completed *seed* latex is diluted to give the desirable value of N_p particles per liter of emulsion. No additional surfactant is added, so no new particles are formed. Monomer is fed in and initiator is added. Polymerization occurs in the previously formed particles, so that each one grows as monomer diffuses to it and is converted (Figure 5.16). When the seed monomer and the added monomer are different, graft copolymers may be formed, provided that the dead polymer in the seed can react by means of residual unsaturation or chain transfer.

A small amount of water solubility can alter the polymerization characteristics. Vinyl acetate dissolves in water only to the extent of 2%, but this is enough to give a combination of emulsion and solution polymerization when emulsion polymerization is attempted (Figure 5.16). The rate also is proportional to the initiator concentration [29]. Another exceptional case is vinylidene chloride, where monomer is almost insoluble in polymer but is adsorbed on the surface of polymer particles. Under these circumstances, faster stirring can accelerate the reaction (Figure 5.17) [30].

The latex that results from emulsion polymerization may be the desired form for the intended end use. Some paints and adhesives can use latexes directly. However, if massive polymer is desired, recovery may involve coagulation by heating, freezing, salt or acid addition, spray drying, or mechanical turbulence. Surfactants, coagulants,

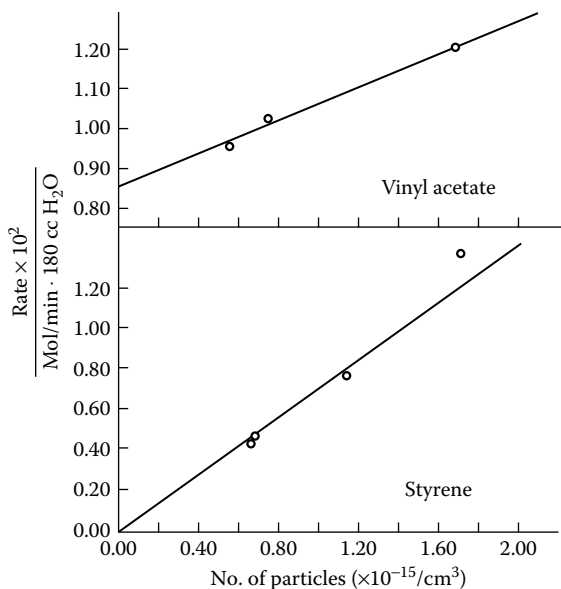


FIGURE 5.16 Rate of polymerization of styrene and vinyl acetate versus number of particles using a seed of poly(vinyl acetate) latex. (Data from Patsiga, R., M. Litt, and V. Stannett, *J. Phys. Chem.*, 64, 801, 1960.)

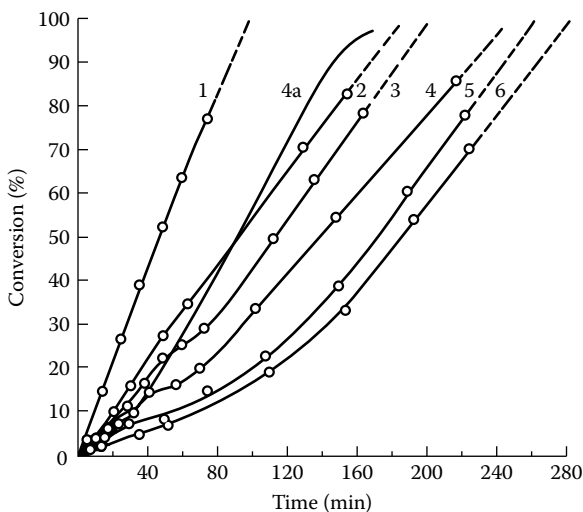


FIGURE 5.17 Effect of surfactant concentration on emulsion polymerization of vinylidene chloride at 36°C. (Data from Hay, P. M. et al., *J. Appl. Polym. Sci.*, 5, 23, 1961.) Initiator is 0.15 g $(\text{NH}_4)_2\text{S}_2\text{O}_8$ and 0.15 g $\text{Na}_2\text{S}_2\text{O}_5$ /100 g monomer. Sodium lauryl sulfate concentration of (1) 10.0 g, (2) 5.0 g, (3) 3.0 g, (4 and 4a) 2.0 g, (5) 1.0 g, and (6) 0.50 g/100 g monomer. The stirring rate is 285 rpm except for 4a, which is 756 rpm.

and initiator fragments often remain as impurities in the final product under these circumstances. In the production of styrene–butadiene rubber (SBR), sodium soaps of fatty acids are used as emulsifiers. Acidification of the final latex simultaneously destroys the surfactant and deposits free fatty acid in the coagulum, where it is a valuable adjunct to the sulfur cross-linking reaction used later on for vulcanization. Both **SBR** and **polychloroprene rubber** have been produced in continuous systems in which a number of stirred reactors are connected in series. The schematics of the flow sheets for their production and details of the processes involved are considered in Sections 16.3 and 16.4.

Several variants of suspension and emulsion polymerization can be used to produce particles with almost uniform particle size. Careful control of an emulsion polymerization in the absence of a separate surfactant can produce almost monodisperse (uniform size) latex particles with diameters as large as 0.5 μm . Swelling such a seed latex with additional monomer and continuing the polymerization, but now with a monomer-soluble initiator, can produce much larger, monodisperse particles [31]. Another route to uniform particles is **dispersion polymerization** in an organic solvent. For example, polymerization of styrene with benzoyl peroxide as the initiator produces a precipitate when the medium (a mixture of alcohols) is not a solvent for the polymer. If hydroxypropyl cellulose is present as a stabilizer (such as the protective colloid in usual suspension polymerization), essentially monodisperse particles can be produced [32]. Perhaps the most elegant method of producing highly monodisperse particles with diameters of 3–30 μm involves sending a reactor into space [33]. The microgravity environment in a space shuttle craft has been used to make polystyrene latexes. The technique starts with a seed latex, which is swollen with an additional monomer. The initiator is a combination of water-soluble persulfate and monomer-soluble azo compound. The particles actually produced in space have been marketed as microscopy standards by the US National Institute for Standards and Technology.

5.6 POLYMERIZATION REACTION ENGINEERING

In Chapter 4, we discussed the kinetics of chain growth and the number-average chain size in stepwise and chain polymerization. The results depended on such variables as the temperature (through the rate constants), the monomer, the initiator, and the transfer agent concentrations. As these parameters vary during an ensuing polymerization, the rate of chain growth and average chain size will change. To obtain polymers with a set of desired properties, the field of **reaction engineering** as applied to polymers was developed to try to predict the effect of changes in these variables during polymerization rather than relying on trial-and-error procedures. Under isothermal conditions and in a batch reactor, the molecular-weight distributions such as the **most probable distribution** and **Poisson distribution** (see Section 6.2) were derived early on by several leaders in the field for the case of stepwise and living chain polymerization, respectively [34–36]. A decade later, a breakthrough occurred when Denbigh [37] realized that the previous works on batch reactors apply to continuous tubular reactors when the length variable in a tubular reactor is replaced by time in a batch reactor. This opened up the field later for computer finite element calculations making use of

numerical techniques to solve the relevant coupled differential equations. When the kinetic constants, thermal and diffusion coefficients, and velocity profile in the reactor are known, numerical predictions can be compared to experimental results [38]. When predictions are not satisfactory, the input data are either incomplete or incorrect. This had led, in some instances, to an improved understanding of the reaction mechanisms involved [39, 40]. Although the problems can be quite complex such as in the case of gas–solid fluidized bed (Figure 5.10), efforts are being pursued to couple information of multiphase flow extracted from computational fluid dynamic software package with polymerization kinetics [41].

5.7 COMPARISON OF POLYMERIZATION METHODS

Bulk polymerization offers real hazards. The thermal conductivities of monomers and polymers are low, and the viscosity buildup limits heat transfer by forced convection. Removal of unreacted monomer from the final product is difficult because of the low surface-to-volume ratio. However, the level of impurities can be held down by use of low initiator levels and diligent monomer removal.

Solution polymerization offers easier temperature control because of (1) added heat capacity of solvent and (2) lower viscosity. Removal of last traces of solvent and unreacted monomer can be difficult. Level of impurities can be very low, since the initiator residues can be extracted.

Temperature control is more convenient in **emulsion polymerization**, because the viscosity changes very little with conversion. Also, thermal conductivity and specific heat of water are higher than those for organic solvents. It is possible in many cases to strip off unreacted monomer without coagulating the latex. However, impurity levels are usually rather high because surfactant and coagulant residues are much harder to remove. The agglomeration processes tend to give porous particles that trap some of the aqueous phase with its dissolved salts and surfactant.

As stated earlier, **suspension polymerization** is essentially a bulk polymerization carried out in droplets. Temperature control can be complicated by the unstable nature of the suspension. Agitation is critical. Often, as the viscosity within the beads rises, the reaction rate increases suddenly (Trommsdorff effect). This leads to a surge in heat generation, which does not usually occur in solution or emulsion polymerization. However, the viscosity of the continuous phase (water) does not change during the reaction, so that heat removal from the reactor is easier than in bulk polymerization. Monomer recovery parallels that in emulsion polymerization. Polymer recovery is simple and usually leads to lower impurity levels than with emulsion polymers.

Polymer processing after the reaction step varies with the solubility, the physical state, and the desired final form of the polymer, as well as with the extent of conversion of monomer to polymer. Coagulation of latexes and filtration of suspension polymers have been mentioned. Additional flow sheets for industrial processes in Chapters 16 and 17 illustrate a wide variety of processing operations. Washing to remove catalyst residues, low-molecular-weight polymer, or atactic fractions may be practical for a polymer such as polypropylene, which can be handled as a slurry of relatively hard particles. Recrystallization is a common procedure for low-molecular-weight organic compounds but not for polymers. Purification by dissolving and precipitation

is avoided because of the expense involved with copious quantities of solvents. Even deionized water can be ruinously expensive if 100 volumes are used for a single volume of polymer. Most polymers recovered by precipitation separate as slimy, sticky masses that are hard to handle. Heating, cooling, and pumping viscous melts and solutions require the same attention to power input and surface scraping as polymerization design. Final removal of liquids, whether solvent, diluent, or unreacted monomer, is complicated by the high viscosities and low diffusivities characteristic of most polymers. Vacuum evaporators, latex strippers, and vented extruders are used, as well as belt, pan, spray, and rotary kiln types of dryers.

KEYWORDS

Heat of polymerization, ΔH_p

Viscosity

Autoacceleration

Trommsdorff effect

Shrinkage

Dilatometry

Bulk polymerization

Solution polymerization

Emulsion polymerization

Atactic polystyrene

Nylon 6,6

Peristaltic flow

Loop (double-loop) reactor

Gas-phase polymerization

Polyisobutylene

Butyl rubber

Interfacial polymerization

Suspension polymerization

Protective colloid

Micelle

Critical micelle concentration

Smith–Ewart approach

Surfactant

Seeded polymerization

Latex

Styrene–butadiene rubber

Polychloroprene rubber

Dispersion polymerization

PROBLEMS

- 5.1 One kilogram of a 20% (by weight) solution of acrylamide in water at 30°C is polymerized adiabatically with a redox initiator. The peak temperature reached is 80°C. What is the molar heat of polymerization?

- Molecular weight (monomer) = 71
- Heat capacity (monomer and polymer) = 0.5 cal/g-°C
- Heat capacity (water) = 1.0 cal/g-°C
- Heat capacity of container, stirrer, and so on = 0.1 kcal/°C

5.2 In a particular adiabatic solution polymerization, the temperature (T) is found to vary with time (t) according to the expression:

$$\frac{1}{(T - T_0)} = \frac{A}{t} + B$$

For a run in which the initial monomer concentration is 0.800 mol/l and the initial temperature is 50.0°C, $A = 12.5 \text{ min/}^\circ\text{C}$ and $B = 0.0550^\circ\text{C}^{-1}$. If the specific heat of the solution is 0.650 cal/°C-ml and the volume of the solution remains constant with conversion, calculate the following:

- (a) The heat of polymerization
 - (b) The time for 10% conversion of monomer to polymer
- 5.3 (a) In what basic way is emulsion polymerization similar to suspension polymerization? (b) What advantage does this give over solution polymerization? (c) In what way do emulsion and suspension polymerizations differ basically? (d) In an unstirred, bulk polymerization that proceeds to 100% conversion, how can the effects of shrinkage and heat of polymerization be handled?
- 5.4 Why would one expect the apparent order (in monomer) of an emulsion polymerization to rise from 0 after 80% or 90% conversion? What maximum value should it reach?
- 5.5 What order of the rate dependence would be expected in a suspension polymerization initially? Why might the rate change abruptly after 5%–20% conversion?
- 5.6 According to Figure 5.16, the rate of emulsion polymerization for styrene varies directly with the number of particles at 60°C. Taking k_p (at 50°C) from Table 4.2, calculate the dynamic concentration of monomer in particles under these conditions. The experimental value of 5.2 mol/l has been found by M. Morton et al. [42].
- 5.7 Company Y has available a 5% (by weight) latex of poly(methyl methacrylate) containing particles that average 0.40 μm in diameter. In order to grow these to a larger size, 8 kg of monomer will be fed into the latex per kilogram of polymer as polymerization proceeds without further addition of emulsifier. The reaction is carried on until all monomer is added to the reactor and the ratio of monomer to polymer in the reactor has decreased to 0.1. Then the unreacted monomer will be steam stripped and recovered. Estimate the time required for the reaction in hours, the rate of heat removal initially (W/m^3 of original latex), and the final particle diameter.

Data:

- Isothermal reaction at 70°C
- $\Delta H_p = -13.0 \text{ kcal/mol}$ (54.4 kJ/mol)
- Density (polymer) = 1.2 g/cm³
- Density (monomer) = 0.9 g/cm³

$$k_p = 640 \text{ liter/mol-s}$$

Dynamic solubility of monomer in polymer = 1 g monomer/2 g polymer

- 5.8** In an emulsion polymerization, all the ingredients are charged at time $t = 0$. The time to convert various amounts of monomer to polymer is indicated in the following table. Predict the time for 30% conversion. Polymerization is *normal* (no water solubility or polymer precipitation).

Fraction of Original Charge of Monomer Converted to Polymer	Time (h)
0.05	2.2
0.12	4.0
0.155	4.9

- 5.9** Using the information in Figure 5.14, estimate the power of the dependence of N_p on surfactant concentration. In plotting the estimates of the stage 2 rates, use error bars on the graph to indicate the range of uncertainty. Hint: What should be plotted and why?
- 5.10** Assume that during the emulsion polymerization of isoprene with 0.10M potassium laurate at 50°C, during stage 2, the growing swollen polymer particles contain 20 g of monomer per 100 ml of swollen polymer. Assume also that the final latex has 40 g of polymer per 100 ml with particles of 45 nm in diameter. The polymer has a density of 0.90 g/cm³. Using Figure 5.14, estimate k_p (l/mol-h).
- 5.11** The following ingredients are charged to a reactor:

Poly(vinyl acetate) Particles (latex)	5.00 g, 2.00×10^{18} Particles
Styrene monomer	100 g
Water	0.900 liter
Initiator	Sufficient
Total volume about 1	

- (a) According to Figure 5.16, how long will it take to convert 50.0 g of styrene to polymer?
- (b) If the particle density is 1.05 g/cm³, what is the particle diameter of the original poly(vinyl acetate) seed?
- (c) If the particle density does not change with further polymerization, what is the particle diameter after 50.0 g of styrene has been polymerized and the unreacted monomer has been vacuum stripped off?
- 5.12** Monomer M can be polymerized using peroxide P in solution at 60°C. The half-life of P at that temperature is 5 h. When the initial monomer concentration is 0.400 mol/liter and the initial peroxide concentration is 4.00×10^{-2} mol/liter, 30.0% of the monomer is converted to polymer in 25.0 min. The conversion rate (at 60.0°C) for the same monomer in an emulsion of 1.00×10^{-6} mol/liter of particles is 13.6 mol/h-liter. The concentration of monomer in the particles is constant at 4.00 mol/liter. What is the termination rate constant?

- 5.13** Propylene is polymerized in a slurry reactor by an equimolar mixture of aluminum triethyl and titanium tetrachloride. The catalyst residue remains with the polymer in a hydrolyzed form. If a customer specifies a maximum ash content of 0.10 wt% in product, what productivity (moles of monomer converted per mole of catalyst) must be achieved? Assume that the ash is entirely Al_2O_3 and TiO_2 .
- 5.14** If 20,000 kg of vinyl chloride is polymerized in a 40-m³ jacketed reactor with 25 m² of the heat transfer area, what overall rate of heat transfer is needed when the reaction takes place in 6 h? If the jacket-side coefficient is 6,000 W/m²·°C and the temperature difference is 40°C, what inside coefficient is necessary? Neglect wall resistance.
- 5.15** In an adiabatic tubular reactor, styrene is converted partially to polymer at high pressure and the mixture of monomer and polymer is sprayed into a vacuum chamber with evaporation of monomer and recovery of polymer. If the heat of vaporization is 355 J/g and the monomer enters the tube at 50°C, what fraction can be converted to polymer per pass and still allow polymer recovery at 50°C?
- 5.16** Monomer A is polymerized at 80°C by two methods in two separate runs: (a) in an inert solvent (no chemical interactions) and (b) as an aqueous suspension. If the *initial* rate of polymerization for 1 l of solution is 0.057 mol/h, what is the expected *initial* rate for 1 l of suspension (in mol/h)?

Reactants	Solution (1 liter)	Suspension (1 liter)
Monomer	50 g (0.50 mol, 60 cm ³)	same
Benzoyl peroxide	1.0×10^{-3} mol (negligible volume)	1.0×10^{-4} mol (negligible volume)
Diluent	940 cm ³ of benzene	940 cm ³ of water
Additives	none	0.1 g of poly(vinyl alcohol)

- 5.17** In a solution polymerization, heat removal may be complicated by an increase in viscosity as polymerization proceeds. For the following situation, the heat of polymerization can be handled initially by a temperature difference between contents and jacket of 20°C. What temperature difference is required when half the charge has been converted to polymer? Conditions are as follows:
- The initial charge of monomer is 100 kg/m³ of solution.
 - The overall coefficient of heat transfer is 2000 W/m²·°C at the start of the reaction. It varies with viscosity of contents to the inverse one-third power.
 - (Viscosity of solution)/(initial viscosity) = $\exp(0.05c)$, where c is the concentration of polymer in kg/m³.
 - The rate of polymerization changes with concentration according to Equation 4.4 with initiator concentration held constant.
- 5.18** For the conditions of Problem 5.17, if the monomer is acrylamide, the solvent is water, and the time for 50% conversion is 35 min, what heat transfer area is required per cubic meter of solution?

REFERENCES

1. Runt, J. P.: *Enc. Polym. Sci. Eng.*, 4:487 (1986).
2. Brandrup, J., and E. H. Immergut (eds.): *Polymer Handbook*, 3rd edn., Sections II and IV, Wiley, New York, 1989.
3. Joshi, M. G., and F. Rodriguez: *J. Appl. Polym. Sci.*, 27:3151 (1982).
4. Takata, T., and T. Endo: *Prog. Polym. Sci.*, 18:839 (1993).
5. Bailey, W. J., and R. L. Sun: *Polymer Preprints*, 13(1):281 (1972).
6. Nauman, E. B.: *Enc. Polym. Sci. Eng.*, 2:500 (1985).
7. Harbison, W. C.: chap. 1 in J. I. Kroschwitz (ed.), *Encyclopedia of Polymer Science and Engineering*, vol. 2, Wiley, New York, 1985, p. 692.
8. Opel, C. J., and P. H. Bottoms: (Swedlow, Inc.), US Patent 3,376,371 (1968).
9. Priddy, D. B.: *Kirk-Othmer. Encycl. Chem. Tech.*, 22:1015 (1997).
10. Brearly, A. M. et al.: (E. I. Du Pont de Nemours and Company), US Patent 5,674,974 (1997).
11. Mack, W. A., and R. Herter: *Extruder Reactors for Polymer Production*, Werner & Pfleiderer Corp., Waldwick, NJ (1975).
12. Krause, A.: *Chem. Eng.*, 72:117 (1965).
13. Doak, K. W.: *Enc. Polym. Sci. Tech.*, 6:386 (1986).
14. Sittig, M.: *Polyolefin Resin Processes*, Gulf Publishing, Houston, TX, 1961.
15. Norwood, D. D.: (Phillips), US Patent 3,248,179 (1966).
16. Benham, E., M. P. McDaniel, and F. W. Bailey: (Phillips), US Patent 4,966,951 (1990).
17. *Chem. Eng.*, 80:72 (November 26, 1973).
18. *Chem. Eng.*, 86:83 (December 3, 1979).
19. Sinclair, K. B.: *Hydrocarbon Proc.*, 64(7):81 (1985).
20. Kresge, E. N., R. H. Schatz, and H.-C. Wang: Isobutylene Polymers, in *Encyclopedia of Polymer Science and Engineering*, vol. 8, 2nd edn., Wiley, New York, 1986, p. 423.
21. Sorenson, W. R., and T. W. Campbell: *Preparative Methods of Polymer Chemistry*, 2nd edn., Wiley, New York, 1968, p. 92.
22. Morgan, P. W., and S. L. Kwolek: *J. Chem. Ed.*, 36:182, 530 (1959).
23. Dawkins, J. W.: in G. Allen and J. C. Bevington (eds.), *Comprehensive Polymer Chemistry*, vol. 4, Pergamon Press, New York, 1989, p. 231.
24. Moore, J. C.: *J. Polym. Sci.*, A2:835 (1964).
25. Flory, P. J.: *Principles of Polymer Chemistry*, Cornell University Press, Ithaca, NY, 1953, pp. 203–217.
26. Blackley, D. C.: *Emulsion Polymerization*, Halsted-Wiley, New York, 1975, p. 99.
27. Kumar, A., and R. K. Gupta: *Fundamentals of Polymer Engineering*, chap. 7, 2nd edn., Dekker, New York, 2003.
28. Harkins, W. D.: *J. Am. Chem. Soc.*, 69:1428 (1947).
29. Patsiga, R., M. Litt, and V. Stannett: *J. Phys. Chem.*, 64:801 (1960).
30. Hay, P. M. et al.: *J. Appl. Polym. Sci.*, 5:23 (1961).
31. Ugelstad, J., and P. C. Mork: *Adv. Coll. Int. Sci.*, 13:101 (1980).
32. Ober, C. K., and M. L. Hair: *J. Polym. Sci. Chem. Ed.*, 25:1395 (1987).
33. Vanderhoff, J. W., M. S. El-Aasser, F. J. Micale, E. D. Sudol, C.-M. Tseng, H.-R. Sheu, and D. M. Kornfeld: *ACS Polym. Preprints*, 28(2):455 (1987).
34. Flory, P. J.: *J. Am. Chem. Soc.*, 58:1877 (1936).
35. Schultz, G. V.: *Z. Physik. Chem.*, B30:184 (1935).
36. Dostal, H., and H. Mark: *Trans. Faraday Soc.* 32, 1936: 54.
37. Denbigh, K. G.: *Trans. Faraday Soc.*, 43:648 (1947).
38. Kumar, A., and R. K. Gupta: *Fundamentals of Polymer Engineering*, chap. 6, 2nd edn., Dekker, New York, 2003.

39. Campell, J. D., M. Morbidelli, and F. Teymour: *Macromolecules*, 36:5502 (2003).
40. Simon, L. C., C. P. Williams, J. B. P. Soares, and R. F. de Souza: *Chem. Eng. Sci.*, 56:4181 (2001).
41. Ray, W. H., J. B. P. Soares, and R. A. Hutchinson: *Macromol. Symp.*, 206:1 (2004).
42. Morton, M., P. P. Salatiello, and H. Landfield: *J. Polym. Sci.*, 8:279 (1952).

GENERAL REFERENCES

- Athey, R. D., Jr.: *Emulsion Polymer Technology*, Dekker, New York, 1991.
- Chern, C.-S.: *Principles and Applications of Emulsion Polymerization*, Wiley, New York, 2008.
- Daniels, E. S., E. D. Sudol, and M. S. El-Aasser (eds.): *Polymer Latexes: Preparation, Characterization, and Applications*, ACS, Washington, DC, 1992.
- Dotson, N. A., R. Galvan, R. L. Laurence, and M. Tirrell: *Polymerization Process Modeling*, VCH, New York, 1996.
- Evans, D. F.: *Polymerization Process Modeling*, VCH, New York, 1995.
- Fontanille, M., and A. Guyot (eds.): *Recent Advances in Mechanistic and Synthetic Aspects of Polymerization*, Kluwer Academic Publishers, Norwell, MA, 1987.
- Lovell, P. A., and M. S. Aasser (eds.): *Emulsion Polymerization and Emulsion Polymers*, Wiley, New York, 1997.
- McCrum, N. G., C. P. Buckley, and C. B. Bucknall: *Principles of Polymer Engineering*, Oxford University Press, New York, 1988.
- McGreavy, C. (ed.): *Polymer Reaction Engineering*, Chapman & Hall, New York, 1993.
- Paleos, C. M. (ed.): *Polymerization in Organized Media*, Gordon & Breach, New York, 1992.
- Radian Corporation: *Polymer Manufacturing: Technology and Health Effects*, Noyes Data, Park Ridge, NJ, 1986.
- Reichert, K.-H., and W. Geiseler (eds.): *Polymer Reaction Engineering*, Huethig & Wepf, Mamaroneck, NY, 1986.
- Ryan, M. E. (ed.): *Fundamentals of Polymerization and Polymer Processing Technology*, Gordon & Breach, New York, 1983.
- Sadhir, R. K., and R. M. Luck (eds.): *Expanding Monomers: Synthesis, Characterization, and Applications*, CRC Press, Boca Raton, FL, 1992.
- Schildknecht, C. E., and I. Skeist (eds.): *Polymerization Processes*, Wiley, New York, 1977.
- Schork, F. J., P. B. Deshpande, and K. W. Leffew: *Control of Polymerization Reactors*, Dekker, New York, 1993.

6 Molecular Weight of Polymers

6.1 MOLECULAR WEIGHT DISTRIBUTION AND AVERAGE MOLECULAR WEIGHT

All synthetic homopolymers are really mixtures of different molecular weights. Some polymers, such as polyethylene, poly(ethylene oxide), and dimethyl silicones, are commercially available in sizes ranging almost continuously from monomer or dimer up to molecular weights in the millions. Although there is no sharp dividing line, we can draw an imaginary one at a molecular weight of about 2000, because it is near the limit of convenient purification by distillation or extraction. For compounds below this molecular weight, the term *oligomer* (Section 1.1) is often used. Except for smaller members of each series, each of these products is a mixture of different-sized molecules having a distribution of molecular weights and an average molecular weight, which we can define and measure in several ways. Polymers with high molecular weights are responsible for many of the properties that make polymers valuable as a class of materials. For high-molecular-weight polymers, differences between members of a homologous series differing in steps of 100 or so (the molecular weight of a typical monomer) become so slight as to prevent clean separations. Distributions of molecular weights are determined routinely using chromatographic techniques.

If someone wanted to drop into your hand, from a height of 1 ft, a series of 1000 steel balls with an average diameter of 2.4 in, you might agree to help him in his playful experiment. After all, a 2.4-in diameter steel ball weighs only about 2 lb. However, if he said that the average diameter was 23.6 in, your attitude might be less cooperative. Both numbers could refer to the same series of balls, the difference being in the manner in which the *average* diameter is calculated. If the population is as shown in Table 6.1, we can calculate an average diameter in several ways:

The average diameter D_L based on length (one dimension) is

$$\bar{D}_L = \frac{\sum N_i D_i}{\sum N_i} = \frac{2400}{1000} = 2.4 \text{ in}$$

The average diameter D_A based on area (two dimensions) is

$$\bar{D}_A = \frac{\sum N_i D_i^2}{\sum N_i D_i} = \frac{33,400}{2400} = 13.9 \text{ in}$$

TABLE 6.1
Hypothetical Distribution of Balls

Number of Balls N_i	Diameter D_i (in)	Length $N_i D_i$	Area ($\times 1/\pi$) $N_i D_i^2$	Volume ($\times 6/\pi$) $N_i D_i^3$
900	1	900	900	900
50	5	250	1,250	6,250
50	25	1250	31,250	781,250
$\Sigma N_i = 1000$		$\Sigma N_i D_i = 2400$	$\Sigma = 33,400$	$\Sigma = 788,400$

The average diameter D_V based on volume (three dimensions) is

$$\bar{D}_V = \frac{\sum N_i D_i^3}{\sum N_i D_i^2} = \frac{788,400}{33,400} = 23.6 \text{ in}$$

Although D_L reflects the preponderant number of small balls, the 1-in balls represent only about 0.1% of the total volume. D_V reflects the importance of the few large balls, which represent 99% of the volume (and weight) of the system. Incidentally, each 25-in ball weighs about 1 ton.

Let us now imagine a population of polymers with molecular weights distributed as in Table 6.1, where N is now the number of molecules of molecular weight $M = D$. The quantity we called $N_i D_i$ before is now $N_i M_i = W_i$, the weight of species with molecular weight M_i . Each of these species i is **monodisperse** (single size or weight), whereas the mixture of the species will be **polydisperse**. As seen in the previous example, we introduce here the concept of a **number-average molecular weight** M_n :

$$M_n = \frac{\text{Total weight of the system}}{\text{Molecules in the system}} \quad (6.1)$$

In terms of any population, then

$$M_n = \frac{\sum N_i M_i}{\sum N_i} = \frac{\sum W_i}{\sum (W_i/M_i)} \quad (6.2)$$

As in the case of the steel balls, M_n is very sensitive to the concentration of low-molecular-weight species. The **weight-average molecular weight** M_w is defined as

$$M_w = \frac{\sum N_i M_i^2}{\sum N_i M_i} = \frac{\sum W_i M_i}{\sum W_i} \quad (6.3)$$

In correlating such important polymer properties as viscosity or toughness, M_w is often a more useful parameter than M_n . Higher averages are defined as

$$M_z = \frac{\sum N_i M_i^3}{\sum N_i M_i^2} = \frac{\sum W_i M_i^2}{\sum W_i M_i} \quad (6.4)$$

$$M_{z+1} = \frac{\sum N_i M_i^4}{\sum N_i M_i^3} = \frac{\sum W_i M_i^3}{\sum W_i M_i^2} \quad (6.5)$$

These are used less often than M_n and M_w . The ratio of M_w to M_n is a measure of the broadness of a distribution, since each is influenced by an opposite end of the population. The quantity M_w/M_n is the **polydispersity index (PDI)**.

Example 6.1

A polymer shipment is to be made up by blending three lots of polyethylene, A, B, and C. How much of each lot is needed to make up a shipment of 50,000 kg with a weight-average molecular weight of 250,000 and a PDI of 3.65? Let $w_i = W_i/\Sigma W_i$.

Lot	M_w	PDI
A	500,000	2.50
B	250,000	2.00
C	125,000	2.50

Solution:

$$M_w = \sum w_i (M_w)_i \text{ from Equation 6.3}$$

$$250,000 = 500,000w_A + 250,000w_B + 125,000(1 - w_A - w_B) \quad (6.6)$$

$$2.50 = 5.00w_A + 2.50w_B + 1.25(1 - w_A - w_B)$$

$$w_A = 0.333 - 0.333w_B$$

and

$$\frac{1}{M_n} = \sum \frac{w_i}{(M_n)_i} \text{ from Equation 6.2}$$

(For convenience, divide molecular weights by 1000.)

$$(M_n)_i = \left(\frac{M_w}{\text{PDI}} \right)_i$$

$$\frac{1}{68.5} = \frac{w_A}{200} + \frac{w_B}{125} + \frac{1 - w_A - w_B}{50} \quad (6.7)$$

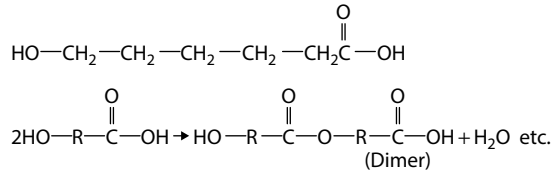
Solving simultaneously Equations 6.6 and 6.7, we get

$$w_A = 0.058; w_B = 0.314; w_C = 0.628$$

Amounts needed are 2,900 kg of A, 15,700 kg of B, and 31,400 kg of C.

6.2 THEORETICAL DISTRIBUTIONS

With the possible exception of some naturally occurring proteins, all polymers are mixtures of many molecular weights (*polydisperse*). This is a consequence of the random nature of polymerization reactions. For example, take the case analyzed by Flory [1] in which the monomer is an ω -hydroxy acid (see also Section 4.7).

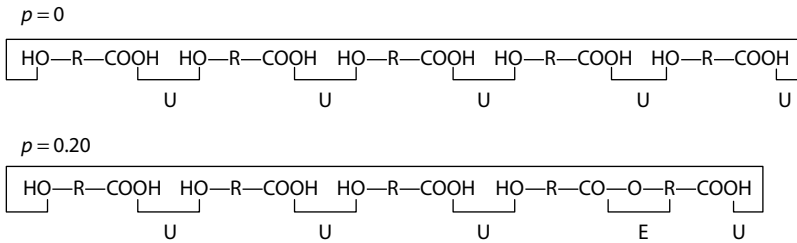


where: $-\text{CH}_2-\text{CH}_2-\text{CH}_2-\text{CH}_2-\text{CH}_2-$ in the first formula has been replaced by $-\text{R}-$ in the dimerization reaction. This is a typical stepwise polymerization in which each successively higher molecular-weight dimer, trimer, and so on is just as reactive as monomer. An important parameter is the fraction converted, p . If we have a population of such monomers, each can react to form an ester group. Each esterification eliminates one carboxyl and one hydroxyl group. With five monomers (Figure 6.1), there would be a maximum of five esterifications ($p = 1$). Initially, p is 0. After one reaction, $p = 0.20$. Abbreviating the unreacted sites by the symbol U and the esterified sites by the symbol E , we can generate a distribution of molecular weights by random reaction of 50 out of 100 sites ($p = 0.5$). If we had alternated sites of reaction with unreacted sites, we would have generated 50 dimers and no other species. Another possible extreme would be to generate 49 monomers and 1 polymer molecule with a degree of polymerization x of 51. We have 50 molecules in either case. With random reaction (Figure 6.1), monomers predominate in the number of molecules N_x , although not necessarily in weight xN_x . If our sample population were much larger, as it is in any macroscopic polymerization, we could assign a probability $(P_r)_x$ that a monomer unit selected at random is a part of a polymer with degree of polymerization x . We expect this to be a function of p , which is the probability that any particular reactive site has been esterified. The probability that a monomer unit is still unreacted varies from 1 when $p = 0$ to 0 when $p = 1$. We surmise that

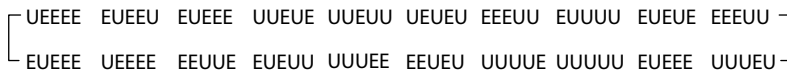
$$(P_r)_1 = 1 - p \tag{6.8}$$

The probability $(P_r)_2$ of picking a dimer at random from the mixture is the product of the probability p that the carboxyl group of the first monomer is esterified times the probability $(P_r)_1$ that the carboxyl group of the second monomer is unreacted. As we go to higher degree of polymerization, each esterified unit brings an additional factor of p to the probability since the cumulative probability is represented by a product of the probabilities of each step. Thus, we see that

Population of five monomers



Population of 100 monomers



Summary:

	x	N_x	xN_x
Monomer (—UU—)	1	25	25
Dimer (—UEU—)	2	15	30
Trimer (—UEEU—)	3	2	6
Tetramer (—UEEU—)	4	4	16
Pentamer (—UEEU—)	5	2	10
Hexamer (—UEEU—)	6	1	6
Heptamer (—UEEU—)	7	1	7
		<u>50</u>	<u>100</u>

FIGURE 6.1 Generation of molecular weight distribution by random reaction.

$$(P_r)_x = (1 - p)p^{x-1} \tag{6.9}$$

Also,

$$\sum_{x=1}^{\infty} (P_r)_x = \sum_{x=1}^{\infty} (1 - p)p^{x-1} = 1 \tag{6.10}$$

Now we can call $(P_r)_x$ the **mole fraction** of x -mer, since it is a normalized probability (i.e., the summation over all values of x is unity). According to Equation 6.9, the degree of polymerization with the largest mole fraction is *always* 1, namely, monomer. Keep in mind that we are dealing with a particular polymerization scheme in which all species are at equilibrium. The number-average degree of polymerization x_n for a distribution represented by Equation 6.9 is

$$x_n = \sum x(1 - p)p^{x-1} = \frac{1}{1 - p} \tag{6.11}$$

The last result is derived in Appendix 6.A. Disregarding the contribution to molecular weight made by the end groups, the molecular weight of a polymer M is related to the **degree of polymerization** x by $M = M_0x$, where M_0 is the molecular weight of a monomer unit in the chain. The number-average molecular weight M_n is then given by

$$M_n = M_0 x_n = \frac{M_0}{1-p} \tag{6.12}$$

We can write Equation 6.9 for x and x_n and combine the two to give

$$\ln \frac{(P_r)_x}{(P_r)_{x_n}} = (x - x_n) \ln p \tag{6.13}$$

But for sufficiently large values of p , $-\ln p \cong 1-p = 1/x_n$, so

$$\ln \frac{(P_r)_x}{(P_r)_{x_n}} \cong 1 - \frac{x}{x_n} \tag{6.14}$$

This *normalized* equation for mole fraction as a function of degree of polymerization is shown in Figure 6.2.

A second kind of average degree of polymerization can be defined as

$$x_w = \frac{\sum W_x x}{\sum W_x} \quad x=1,2,3,\dots \tag{6.15}$$

where:

W_x is proportional to the weight of x -mer

x_w is the **weight-average degree of polymerization**

The weight of x -mer from Equation 6.9 is

$$W_x = x(1-p)p^{x-1}M_0 \quad \text{and} \quad M_n = \sum W_x = \frac{M_0}{1-p} \tag{6.16}$$

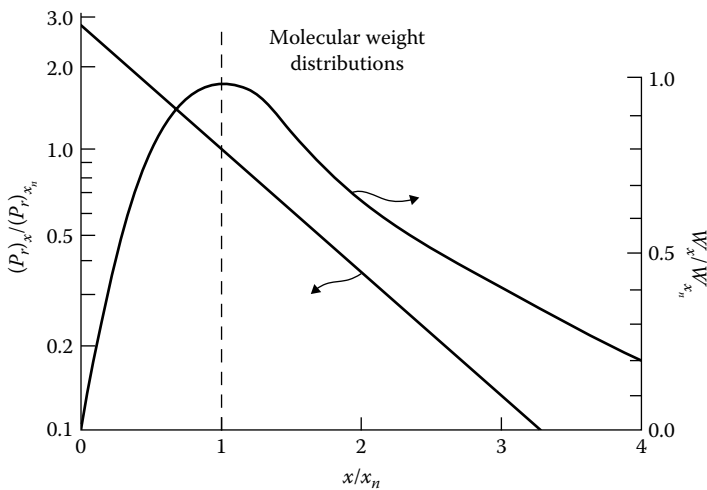


FIGURE 6.2 Normalized distributions according to Equations 6.14 and 6.19.

From Equations 6.15 and 6.16, we get

$$x_w = \frac{\sum (P_r)_x x^2}{\sum (P_r)_x x} = \frac{\sum x^2(1-p)p^{x-1}}{\sum x(1-p)p^{x-1}} = \frac{1+p}{1-p} \quad (6.17)$$

The last result is derived in Appendix 6.B. The weight fraction of x -mer w_x is given by

$$w_x = \frac{W_x}{\sum W_x} = x(1-p)^2 p^{x-1} \quad (6.18)$$

As in Equation 6.14, we can have a normalized distribution:

$$\ln \frac{w_x}{w_{x_n}} = \ln \frac{x}{x_n} + (x - x_n) \ln p \cong \ln \frac{x}{x_n} - \frac{x}{x_n} + 1 \quad (6.19)$$

This is also plotted in Figure 6.2. Higher averages of degree of polymerization are sometimes useful:

$$x_z = \frac{\sum (P_r)_x x^3}{\sum (P_r)_x x^2} \quad (6.20)$$

$$x_{z+1} = \frac{\sum (P_r)_x x^4}{\sum (P_r)_x x^3} \quad (6.21)$$

What we have been describing is sometimes called **the most probable distribution**.

It gives $x_w/x_n = 1 + p$. The ratio of 2 when p approaches unity is found experimentally for many stepwise and also for many chain polymerizations, although the reasoning can be different. Under conditions of chain polymerization with all polymers initiated and growing simultaneously, the distribution can be much narrower. For example, in a butyl lithium-initiated polymerization to give living polymers, the simultaneous growth of polymer chains gives a **Poisson distribution** [2]:

$$(P_r)_x (\text{mole fraction of } x\text{-mer}) = \frac{e^{1-x_n} (x_n - 1)^{x-1}}{(x-1)!} \quad (6.22)$$

or

$$\ln(P_r)_x = 1 - x_n + (x-1) \ln(x_n - 1) - \ln[(x-1)!] \quad (6.23)$$

$$w_x (\text{weight fraction of } x\text{-mer}) = \frac{x(P_r)_x}{x_n} \quad (6.24)$$

The PDI of the Poisson distribution is given by

$$\frac{x_w}{x_n} = 1 + \frac{x_n - 1}{x_n^2} \quad (6.25)$$

TABLE 6.2
Analysis of Distribution from Figure 6.1

Degree of Polymerization x	Number of Moles N_x	Mole Fraction $P_r = N_x/\Sigma N_x$	Relative Number of Monomer Units in x -mer $W_x/M_0 = x(P_r)z$	Weight Fraction $w_x = W_x/\Sigma W_x$	xw_x	x^2W_x
1	25	0.50	0.50	0.25	0.25	0.25
2	15	0.30	0.60	0.30	0.60	1.20
3	2	0.04	0.12	0.06	0.18	0.54
4	4	0.08	0.32	0.16	0.64	2.56
5	2	0.04	0.20	0.10	0.50	2.50
6	1	0.02	0.12	0.06	0.36	2.16
7	1	0.02	0.14	0.07	0.49	3.43
Total	50	1.00	2.00	1.00	3.02	12.64

$$x_n = \frac{\sum x(P_r)_x}{\sum (P_r)_x} = \frac{2.00}{1.00} = 2.00$$

$$x_w = \frac{\sum x^2(P_r)_x}{\sum x(P_r)_x} \quad \text{or} \quad \frac{\sum xw_x}{\sum w_x} = \frac{3.02}{1.00} = 3.02$$

$$x_z = \frac{\sum x^3(P_r)_x}{\sum x^2(P_r)_x} \quad \text{or} \quad \frac{\sum x^2w_x}{\sum xw_x} = \frac{12.64}{3.02} = 4.19$$

It can be seen that even when x_n is small, say about 100, x_w/x_n is nearly unity. Polymers can be produced on a commercial scale with

$$\frac{M_w}{M_n} = \frac{x_w}{x_n} < 1.1$$

by using butyl lithium as the initiator. Most *living polymerization* systems, such as those using Ziegler–Natta, metallocene, group transfer, and some cationic initiation, can yield narrow distributions when impurities are carefully avoided.

We can further illustrate the differences in the various averages by examining the sample of Figure 6.1 (Table 6.2). In this example, monomer ($x = 1$) has the highest mole fraction but not the highest relative weight (W_x). The average degrees of polymerization are also calculated according to the equations presented. As mentioned earlier, the usefulness of each of these numbers may depend on the particular property we are looking at. The reactivity of a urethane prepolymer may depend entirely on x_n . However, the viscosity of a polymer melt often varies more directly with x_w .

Example 6.2

Ten thousand elephants, while crossing the Alps in single file, are thrown into a panic by the sudden blast of a Punic trumpet. Each animal that panics entwines its trunk firmly about the tail of the preceding beast. In a quick but accurate

survey, Hannibal finds that there are now as many elephants that are part of strung-together trios as there are singles (unattached elephants). How many of the ponderous pachyderms panicked?

Solution: We assume a most probable distribution for which Equation 6.18 applies. According to Hannibal, the total weight of elephants in trios, w_3 , is the same as that in singles, w_1 , assuming that all elephants weigh the same. Thus,

$$w_1 = 1(1-p)p^0 = w_3 = 3(1-p)p^2$$

and

$$p = \left(\frac{1}{3}\right)^{1/2} = 0.577$$

That is, 57.7% of the elephants panicked.

6.3 EMPIRICAL DISTRIBUTION MODELS

The distribution of molecular weights has been shown to be important in many diverse applications, including flow of melts and solutions, aging and weathering behavior, adhesion, and flocculation. Because of the difficulties involved in measuring a distribution in detail, one shortcut has been to postulate a reasonable mathematical form or model for the distribution and then evaluate the parameters from x_w and x_n [3]. In general, such a model would give w_x , the weight fraction of x -mer, as a function of x , x_w , x_n , and perhaps other parameters. The *most probable* distribution (Equation 6.9) has only one parameter p that can be evaluated from either x_n (Equation 6.11) or x_w (Equation 6.17). If the experimentally determined ratio of x_w/x_n is not nearly 2 for high-molecular-weight material, the model cannot be used. The **Schulz distribution** is a more general form of the most probable distribution:

$$w_x = \frac{a}{x_n \Gamma(a+1)} \left(\frac{ax}{x_n}\right)^a \exp\left(-\frac{ax}{x_n}\right) \quad (6.26)$$

where:

$$x_w/x_n = (a+1)/a \text{ and } \Gamma(a+1) \text{ is the gamma function of } a+1$$

When $a = 1$ and x is large, this becomes the same as the most probable distribution, since $x_n = 1/(1-p)$ and $(x-1)\ln p \cong -x/x_n$. However, any value of x_w/x_n can be inserted. Qualitatively, the curves will resemble Figure 6.2 except that the overall breadth will reflect the influence of the PDI.

It will be seen in Section 6.4 that some experimental methods for measuring distribution result in a cumulative distribution function $W(x)$ describing a continuous distribution of x values, from which the **differential distribution** $w'_x = dW/dx$ can be derived. We are speaking now of distributions in the higher ranges of x_n , where the approximation $W = \int w'_x dx$ is applicable. It has been observed that a plot of $W(x)$ against x on logarithmic probability paper often gives a straight line. In terms of w'_x , this becomes the **Wesslau distribution** (or **logarithmic normal distribution**):

$$w'_x = \frac{1}{\beta\pi^{1/2}} \frac{1}{x} \exp\left[-\frac{1}{\beta^2} \ln^2\left(\frac{x}{x_0}\right)\right] \quad (6.27)$$

where:

$$\beta^2 = \ln(x_w/x_n)^2$$

$$x_0 = x_n \exp(\beta^2/4)$$

Once again, specification of x_w and x_n defines the entire distribution. As with the Schulz model, only the central value of the distribution, reflected by x_n , and the breadth, measured by x_w/x_n , can be changed. On a cumulative weight [$W(x)$] basis, the Schulz and Wesslau models give similar curves (Figure 6.3). On a differential (w_x) basis, qualitative differences become apparent (Figure 6.4).

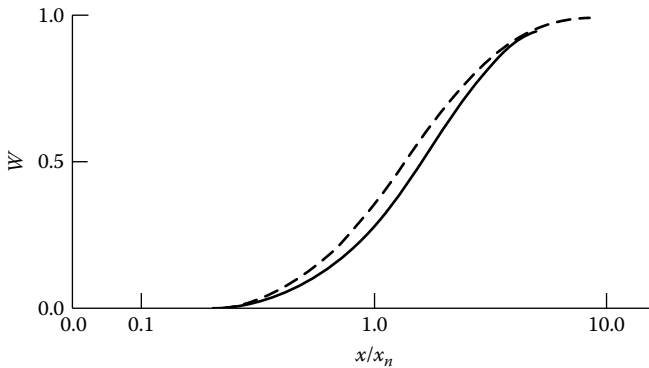


FIGURE 6.3 Cumulative weight fraction W as a function of ratio of degree of polymerization to number-average value for Schulz (solid line) and Wesslau (dashed line) models.

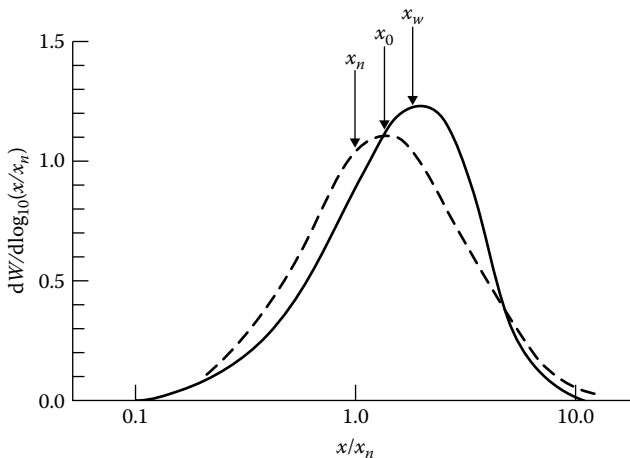


FIGURE 6.4 Differential distribution curves for models of Figure 6.3.

Example 6.3

The molecular weight distribution for a certain polymer can be described as

$$w_x = \frac{kx}{10 + x^2}$$

where:

$x = 1, 2, \text{ and } 3$ only

w_x is the weight fraction of polymer with degree of polymerization x

What is the value of k ? What is x_w ? What is x_n ?

Solution: The condition for k is that

$$\sum w_i = 1 = k \sum \left(\frac{x}{10 + x^2} \right)$$

$$k \left(\frac{1}{11} + \frac{2}{14} + \frac{3}{19} \right) = 0.392k = 1$$

so

$$k = \frac{1}{0.392} = 2.55$$

In analogy with Equations 6.3 and 6.2,

$$x_w = \sum w_i x_i = 2.55 \left(\frac{1}{11} + \frac{4}{14} + \frac{9}{19} \right) = 2.17$$

$$\frac{1}{x_n} = \sum \left(\frac{w_i}{x_i} \right) = 2.55 \left(\frac{1}{11} + \frac{1}{14} + \frac{1}{19} \right) = 0.548$$

$$x_n = 1.82$$

When dealing with high molecular weights ($x > 100$), it becomes convenient to treat distributions as being continuous rather than finite. As an example, let us assume that the cumulative weight fraction $W(x)$ of a polymer with degree of polymerization less than x is given by

$$W(x) = 0.01(x - 10) \text{ for } 10 < x < 110$$

$$W(x) = 0 \quad \text{for } x < 10 \quad (6.28)$$

$$W(x) = 1 \quad \text{for } x > 110$$

The **differential weight distribution** w'_x then is

$$w'_x = \frac{dW(x)}{dx} = 0.01 \quad (6.29)$$

The degree of polymerization is obtained by integration and normalization.

$$x_n = \frac{\int_1^\infty w'_x dx}{\int_1^\infty (w'_x/x) dx} = \frac{\int_{10}^{110} 0.01 dx}{\int_{10}^{110} (0.01/x) dx} = 41.7 \quad (6.30)$$

$$x_w = \frac{\int_1^\infty x w'_x dx}{\int_1^\infty w'_x dx} = \frac{\int_{10}^{110} 0.01 x dx}{\int_{10}^{110} 0.01 dx} = 60.0 \quad (6.31)$$

The continuous models are particularly useful when analyzing experimental data obtained for distributions where a cumulative weight is obtained first and must be converted mathematically to a differential distribution.

6.4 MEASUREMENT OF DISTRIBUTION

Both x_w and x_n can be measured independently (Sections 6.6 and 6.7) in order to get some idea of polydispersity. The ultracentrifuge, when applicable, gives a distribution directly. However, until the advent of gel permeation chromatography (GPC), **fractionation** of polymer from dilute solution was used. Polymers decrease in solubility with increasing molecular weight as predicted by the Flory–Huggins theory (Section 3.3). Figure 6.5 illustrates the variation of the coexistence curve with molecular weight for polystyrene in methylcyclohexane. A polymer can then be put in dilute solution and progressively precipitated by the addition of increments of a nonsolvent [5].

The highest-molecular-weight species will precipitate first. The method involves adding a nonsolvent slowly until the appearance of a precipitate. Then the system is heated to a temperature at which it is homogeneous, after which it is slowly cooled over a period of hours to a standard temperature. A variation is to cool the solution to successively lower temperatures and separate a fraction at each temperature rather than at each increment of nonsolvent. The polymer-rich phase that separates, the so-called **coacervate**, usually is a small volume compared to the total volume of the system and is viscous or gelatinous. One drawback of this process of coacervation is that low-molecular-weight polymer is occluded in the coacervate even under the conditions of slow cooling. Because this is more serious with higher molecular weights and higher starting concentrations, a rule of thumb may be employed that the beginning concentration should be less than 1% polymer regardless of molecular weight and also that the concentration times the intrinsic viscosity (Section 7.4) should be less than 1. Another scheme is to redissolve each fraction and reprecipitate it under the same conditions of solvent/nonsolvent ratio and temperature. Figure 6.6 shows the relationship between the degree of polymerization of material remaining in solution and solvent composition when poly(vinyl acetate) is precipitated from an acetone solution by addition of a methanol–water mixture.

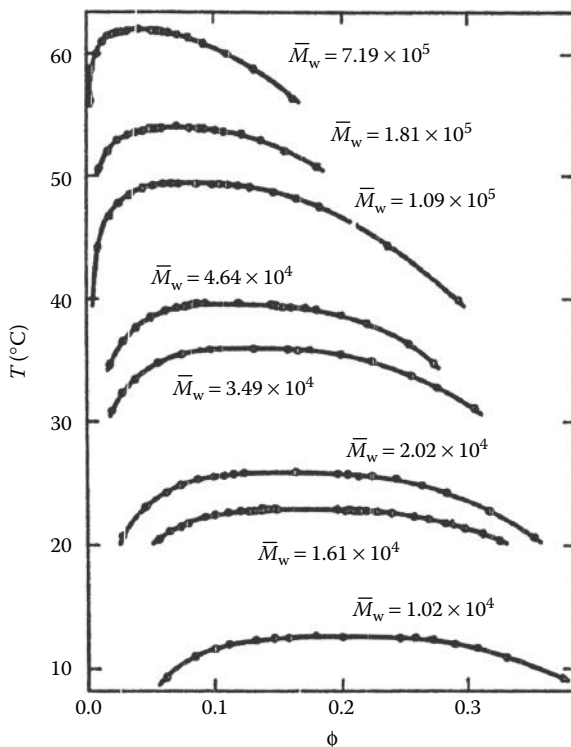


FIGURE 6.5 Coexistence curves of low polydispersity polystyrene in methyl cyclohexane. The volume fraction of polymer v_2 is denoted here by ϕ . (Reprinted with permission from Dobashi, T., M. Nakata, and M. Kaneko, *J. Chem. Phys.* 72, 6692, 1980. Copyright 1980 American Institute of Physics.)

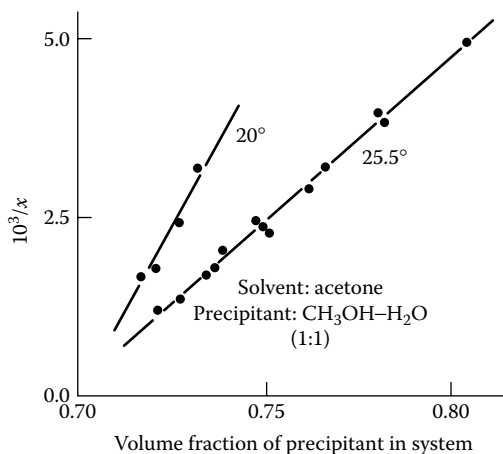


FIGURE 6.6 Decrease in solubility of poly(vinyl acetate) with added nonsolvent, increasing degree of polymerization x and decreasing temperature. (Data from Kotera, A., in M. J. Cantow, ed., *Polymer Fractionation*, Academic Press, New York, 1967.)

The procedure is tedious, because hours or days are required for clean separation of each fraction. Even then, each fraction is heterogeneous with $x_w/x_n = 1.05-1.2$ at best. Rather than precipitating the polymer from a dilute solution, it is possible to dissolve a solid polymer fractionally [7]. Diffusion through the solid polymer is slow, so it is essential that the material be spread out in a very thin film. A typical technique for fractionating polyethylene uses a 2-in-diameter column about 2 ft long packed with ordinary sand (40–200 mesh). A hot solution of polyethylene in xylene is introduced and cooled so that the entire charge of polymer, a few grams, is precipitated on the surface of the sand, giving a thin film. Then a solvent or a solvent mixture is added to elutriate the low-molecular-weight portion of the polymer. When no more polymer is elutriated at the solvent composition or temperature, the solvent-to-nonsolvent ratio is increased or the temperature is raised so that a higher molecular-weight fraction can be extracted. Columns of this type can be automated with a few solenoid-operated valves and a fraction collector in order that fractionation of a sample into 10–20 fractions can be carried out overnight without immediate supervision. In this column method, one does not have to wait for gravitational settling out of coacervate, and it is the speed with which fractionation can proceed, which is its advantage.

In both precipitation and dissolution methods, a single equilibrium stage of separation is achieved. Multistaged separations are not usually convenient. In either case, the raw data consist of a series of i fractions, each of weight w_i and an average molecular size x_i . A cumulative curve can then be plotted in which the ordinate is $\Sigma w_{i-1} + w_i/2$ and the abscissa is x_i . A smooth line through the points gives a curve that is a good approximation to $W(x)$, the cumulative molecular weight distribution function. Differentiation of this curve then gives $w'_x = dW(x)/dx$, the differential molecular weight distribution function. The reason that the raw values of w_i and x_i cannot be plotted as a histogram is that the intervals of both variables are not uniform. An example (Table 6.3; Figure 6.7) shows the long high-molecular-weight tail typical

TABLE 6.3
Analysis of Typical Fractionation Data

Raw Experimental Data			Calculated Results		
Fraction Number i	Fraction of Total Weight Recovered w_i	Degree of Polymerization $x_i (\times 10^{-3})$	Σw_i	$\Sigma w_{i-1} + w_i/2 = W_i$	$(dW/dx)_i (\times 10^3)$
1	0.050	1.1	0.050	0.025	0.040
2	0.100	2.5	0.150	0.100	0.060
3	0.120	4.1	0.270	0.210	0.063
4	0.083	5.8	0.353	0.313	0.052
5	0.075	7.4	0.428	0.390	0.043
6	0.110	9.4	0.538	0.483	0.039
7	0.120	12.5	0.658	0.598	0.030
8	0.130	17.5	0.788	0.723	0.0165
9	0.130	29.0	0.918	0.853	0.0072
10	0.082	64.0	1.000	0.959	0.0013

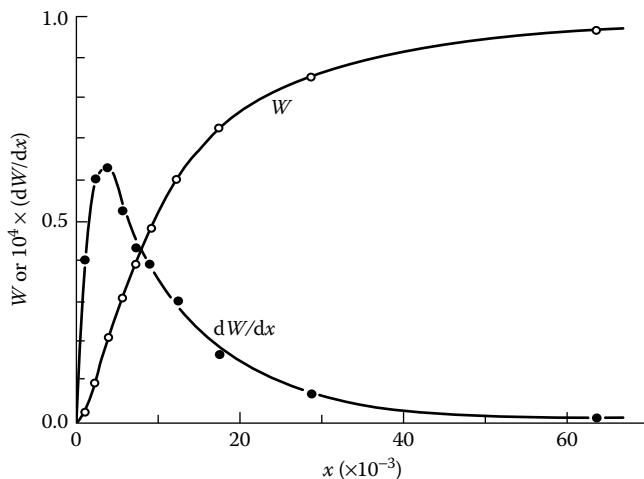


FIGURE 6.7 Differential and cumulative weight fraction plotted against degree of polymerization for distribution of Table 6.3.

of most polymers. The uncertainty in the slope at the high end also is apparent. In Figure 6.8, the advantage of a logarithmic plot in showing greater symmetry is seen.

The most popular technique for measuring distributions of molecular weights is known as **gel permeation chromatography** or **size exclusion chromatography** (SEC). The technique was first called *gel filtration* by Flodin and coworkers [8] who applied it to the separation obtained when water-soluble polymers are elutriated from a column packed with swollen, cross-linked, hydrophilic dextran (Sephadex) beads. The GPC name was coined by Moore [9] to describe the separation of organic-soluble polymers in columns packed with swollen, cross-linked, lyophilic polystyrene beads. All these names are somewhat misleading, since a gel is not necessary, porous glass beads being equally applicable; filtration is not part of the process as small molecules are retarded in the columns and large ones pass rather than the other way around; and chromatography classically implies formation of colors, which seldom occurs in this technique. The term **size exclusion chromatography** has been recommended although GPC is still widely used.

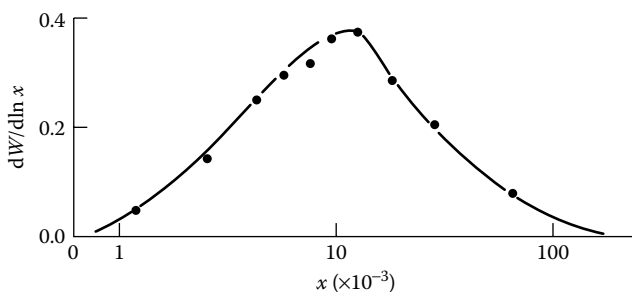


FIGURE 6.8 Data of Table 6.3 plotted as differential distribution on a logarithmic basis.

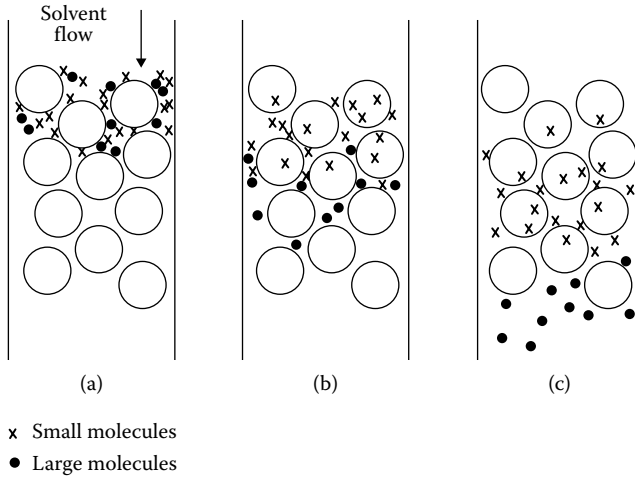


FIGURE 6.9 Process of GPC/SEC: (a) sample injection; (b) elution; (c) continued elution. (Data from Terry, S. L., and F. Rodriguez, *J. Polym. Sci. C*, 21, 191, 1968.)

The principle of the method is illustrated in Figure 6.9, where a mixture of small and large molecules has been deposited at one end of a column packed with porous beads. Initially there is a concentration gradient causing diffusion of polymer into the bead. However, the large molecules cannot penetrate the beads. A continuous flow of solvent sweeps the large molecules along and reverses the concentration gradient for the small ones so that they now diffuse back out of the beads. This process is repeated again and again as the sample moves through the column. Eventually, when the sample is elutriated from the other end, large molecules will emerge first and the small ones, retarded by the diffusion in and out of the packing, will emerge last. This is just the opposite from what adsorption or filtration would have accomplished, as in gas chromatography. When porous glass beads (about 100 mesh) are used as packing, the pore sizes can be measured by mercury intrusion. Pore diameters of 10–250 nm are useful for polymers in the 10^3 – 10^7 molecular weight range. More common is packing composed of swollen, cross-linked polymer beads. Such particles can be produced by suspension polymerization of a mixture of styrene, divinyl benzene, and a hydrocarbon diluent. Under conditions of constant temperature, flow rate, and concentration, for the same physical system, the retention volume V_r , the volume of solvent that must be elutriated from the system between the time the sample is introduced and the time it appears in the effluent, is a function only of the molecular size of the polymer.

The calibration procedure for SEC is illustrated in Figures 6.10 and 6.11. Two runs are made with injections of mixtures of polystyrene (narrow) molecular weight standards into a series of two columns that are packed with cross-linked polystyrene particles of about 10 μm in diameter. Each of the columns has an inside diameter of 7.5 mm and a length of 300 mm. Tetrahydrofuran (THF) flows at 1.0 ml/mm with a total pressure drop over the columns of about 20 atm at room temperature. When the times for elution at each of the 10 peaks are plotted against the logarithm of the corresponding molecular weights, a very linear calibration curve results covering

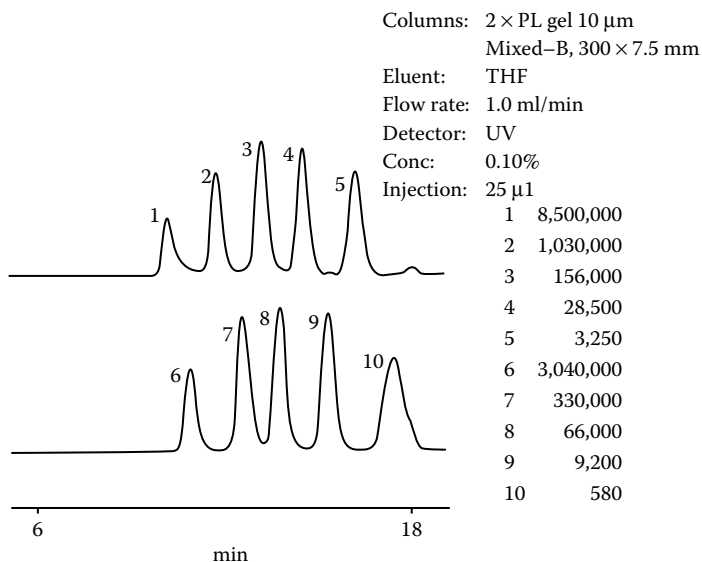


FIGURE 6.10 Injection of two solutions (five polymers in each) in separate runs yields chromatograms in which ultraviolet (UV) absorption is used to measure the concentration of polymer in the effluent. PL, Polymer Laboratories. (Courtesy of Polymer Laboratories Ltd., Amherst, MA.)

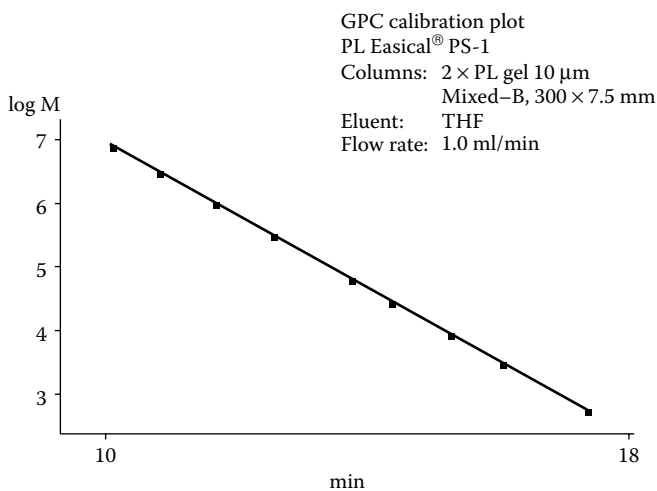


FIGURE 6.11 The calibration plot based on the 10 samples used in Figure 6.9 is linear over a range of four decades. (Courtesy of Polymer Laboratories Ltd., Amherst, MA.) The construction of the plot is carried out using a computer program. (EasiCal is a registered trademark of Polymer Laboratories.)

four decades of *polystyrene-equivalent* molecular weight. The entire calibration procedure takes less than 1 h. Of course, the pumping rate must be very reproducible in order for the elution times to be meaningful measures of molecular size.

The molecular weight distribution of a new sample can be estimated by the relative concentration of polymer at each effluent volume, which now corresponds to a known molecular weight. Some workers have found that calibration curves in which $M[\eta]$ is plotted against V_r coincide for polymers that differ in branching or in composition, thus giving a **universal calibration** [11]. The quantity $[\eta]$, the intrinsic viscosity, is discussed in Section 7.4.

The elements of a basic system are shown in Figure 6.12. The packed columns may each be 30–60 cm long. Often two or three will be placed in series. Even with swollen beads, there will be a void volume of around 30%. Solvent flow is maintained at a constant rate by a precision pump. A sample is injected after a flat baseline has been established. Concentration is measured by a detector, often a differential refractometer. Other devices are also used. Most commercial models for GPC/SEC use a laboratory computer to plot the concentration eluent volume data and also to calculate the appropriate molecular weight averages, the calibration data having been stored in the computer's memory. In addition to the differential refractometer, concentration can be detected by conductivity, radioactivity, light absorbance, or light scattering. Another detection device used in conjunction with a refractometer is a differential viscometer (see Section 7.3).

Infrared absorbance as a measure of concentration adds another dimension to the distribution analysis, because one can choose a band in the infrared region specific to one functional group and therefore to one component in a mixture or in a copolymer. For example, the ratio of hydroxyl to ether group in poly(ethylene oxide) varies with the molecular size.

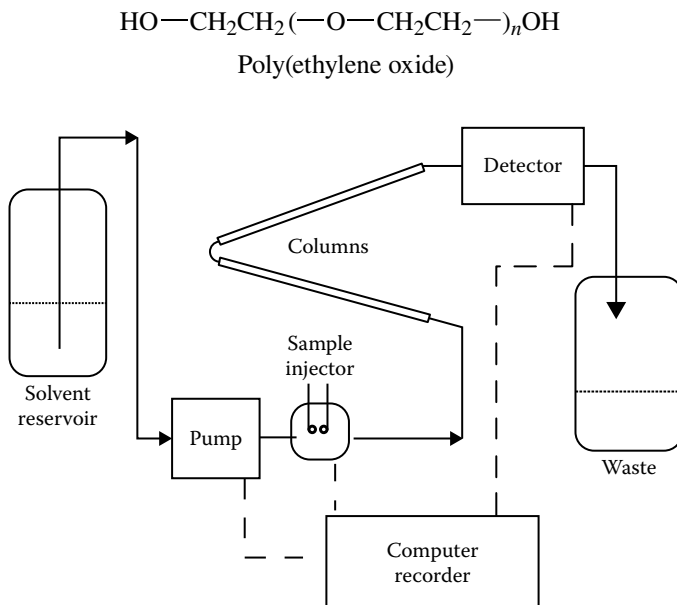


FIGURE 6.12 Basic layout for GPC/SEC.

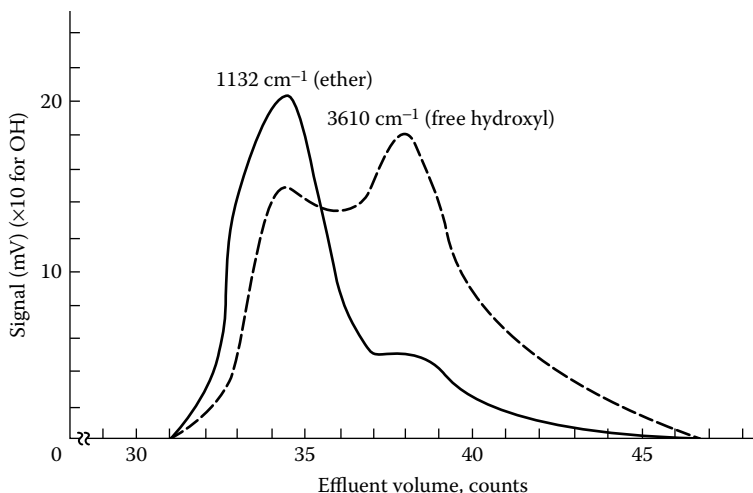


FIGURE 6.13 Mixture of poly(ethylene oxide) with molecular weights of 300 and 4000 analyzed at ether and end group wave numbers (maximum signal for OH, 1.8 mV). (Data from Terry, S. L., and F. Rodriguez, *J. Polym. Sci. C*, 21, 191, 1968.)

By measuring the concentration of hydroxyl and ether groups in the effluent from successive runs in the same system, the ratio of hydroxyl to ether, and therefore the molecular size, is obtained directly (Figure 6.13). The distribution of a monomer within a copolymer distribution can also be measured by this technique. More than one analyzer can be used to monitor the output simultaneously. For example, a laser light scattering apparatus (see Section 6.7) can be used in tandem with a differential refractometer. The refractometer gives a measure of the concentration, and the light scattering (together with the concentration) gives a measure of the molecular weight of the polymer in absolute terms. This does away with the need for a separate calibration since the system now is yielding a distribution curve directly. Column chromatography for molecular weight determination usually uses only one solvent at one temperature. In more general terms, high-performance liquid chromatography is used for the analysis of mixtures of drugs, natural products, or other complex materials. Often solvent temperature or composition is programmed to change over the analysis time.

6.5 MEASUREMENT OF MOLECULAR WEIGHT

Methods for determining molecular weight can be relative or absolute. Many properties of polymers that depend on molecular weight, such as solubility, elasticity, adsorption on solids, and tear strength, can be correlated with an average molecular weight. Once correlated, the property can be used as a measure of molecular weight. In practice, viscosity of melts and dilute solutions is the most often used relative method (see Section 7.3). Absolute methods can be categorized by the kind of average they measure.

Before the 1920s, many chemists were reluctant to believe that such large, covalently bonded structures were possible. The molecular weights were regarded as *apparent* values brought about by a physical association of smaller molecules in a *colloidal* state. Herman Staudinger was the first to strongly advocate the existence of large synthetic macromolecules and proposed the chain structure of polystyrene in 1920. We accept nowadays as the valid indication of molecular size the molecular weights of polymers measured by the different techniques described in Sections 6.6 and 6.7. No measurement is foolproof however, and it is unrealistic to specify the molecular weight of a polymer in the hundred–thousand range to four or five figures. Even the so-called absolute methods we are about to discuss rely on extrapolations that depend on some physical model expressed in mathematical form.

6.6 NUMBER-AVERAGE MOLECULAR WEIGHT METHODS

The measurement of the concentration of end groups when one knows the exact number per molecule is a method of counting the number of molecules. In the hydroxyacid ester example, a simple titration by standard sodium hydroxide would give the total number of free carboxyl groups. Since there is but one such group for each polymer molecule, we have a molecule-counting method. End group counting can be more sophisticated, as in the use of infrared or isotopic analysis. In any of these, we derive a number-average molecular weight M_n given by (see Equation 6.12)

$$M_n = x_n M_0 \quad (6.32)$$

where:

M_0 is the molecular weight of a repeating unit in the polymer

Because the relative concentration of end groups is smaller for higher molecular-weight polymers, this method becomes less sensitive as the molecular weight increases.

The magnitude of the depression of the melting point or the elevation of the boiling point of a solvent by a nonionized solute depends on the number of solute molecules present but not on their chemical nature. These colligative properties are used to estimate the molecular weight of a solute. The melting point depression is widely used in organic chemistry for the characterization of small molecules. The lowering of the melting temperature, $T_f - T$, is related to the normal melting temperature of the solvent T_f , its heat of fusion ΔH_f , and its molecular weight M_1 , and is also related to the molecular weight of the solute M_2 and the relative weights of solvent and solute w_1 and w_2 , respectively [13]:

$$T_f - T = \frac{RT_f^2}{\Delta H_f} \frac{M_1}{M_2} \frac{w_2}{w_1} \quad (6.33)$$

where:

R is the gas constant

For a solution of 1 g of polyethylene with $M_2 = 500$ in 100 g of camphor ($T_f = 178.4^\circ\text{C}$, $\Delta H_f = 2.58$ kcal/mol, $M_1 = 152$), $T_f - T$ is 0.48°C . As the molecular weight of the solute increases, measurement of the temperature lowering demands more sensitive equipment and the method becomes impractical. In order to measure the number of molecules by colligative methods, it is necessary to use dilute solutions. In practice, we often extrapolate results to infinite dilution by some suitable linearizing techniques.

Osmotic pressure is sufficiently sensitive to make it a useful measuring method for macromolecular solutions. We place on opposite sides of a semipermeable membrane (typically cellophane) a polymer solution and a pure solvent (Figure 6.14). The membrane is selected to pass solvent but not polymer. Because of the concentration gradient across the membrane, solvent will diffuse from the solvent side to the solution side until a pressure head (the osmotic pressure) is reached at equilibrium. Either by waiting for equilibrium or by measuring and compensating for pressures automatically, osmotic pressure can be measured at several concentrations. According to thermodynamics, the osmotic pressure π is related to the chemical potential of the solvent by the relation:

$$\pi = -\frac{\mu_1 - \mu_1^0}{V_1} \quad (6.34)$$

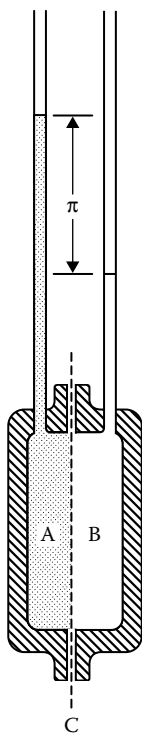


FIGURE 6.14 Osmotic pressure cell containing polymer solution A and solvent B separated by a semipermeable membrane C. The osmotic pressure is π .

where:

π is the osmotic pressure that can be expressed in $(\text{g}/\text{cm}^2) = h\rho$

h is the difference in liquid levels at equilibrium (cm)

ρ is the density of the solvent (g/cm^3)

μ_1, μ_1^0 are the chemical potential of the solvent in the solution and the pure solvent, respectively

V_1 is the molar volume of the solvent

By analogy to the pressure of a gas, the osmotic pressure of a solution of concentration c is expressed in terms of a **virial expansion**:

$$\frac{\pi}{c} = \frac{RT}{M_n} (1 + A_2 M_n c + A_3 M_n^2 c^2 + \dots) \quad (6.35)$$

where:

c is the concentration (g/cm^3)

T is the absolute temperature (K)

M_n is the number-average molecular weight (g/mol)

R is the gas constant $(8.48 \times 10^4 \text{ g}\cdot\text{cm}/\text{mol}\cdot\text{K})$

A_2, A_3, \dots are the second, third, ... **virial coefficients**

In the limit of infinite dilution, the above equation reduces to

$$\left(\frac{\pi}{c} \right)_{c=0} = \frac{RT}{M_n} \quad (6.36)$$

At small enough concentrations when the second virial term is small and the higher order terms negligible, one can write

$$\left(\frac{\pi}{c} \right)^{1/2} = \left(\frac{RT}{M_n} \right)^{1/2} \left(1 + \frac{A_2 M_n c}{2} \right) \quad (6.37)$$

Plots of $(\pi/c)^{1/2}$ versus concentration often are linear (Figure 6.15) and allow extrapolation to infinite dilution to extract the value of M_n . The fact that it is the number-average molecular weight that is measured by osmometry can be demonstrated by starting, for example, from the Flory–Huggins free energy of mixing expression of a polydisperse solution (Problem 6.29). The second virial coefficient A_2 is obtained from such plots by dividing the slope by the intercept and $M_n/2$. It arises primarily from the inhibition of molecules to move in the volume occupied by other molecules (referred to as **excluded volume**). If we consider for simplicity the polymer molecules as encompassed by spheres of radius R , then for a dilute polymer solution in a good solvent, each polymer molecule will resist the approach of another molecule such that the center of the approaching molecule is excluded from a volume equal to 8 times the volume of the molecule (see Figure 6.16). A_2 can be thought of as the total excluded volume of the solution and is given by [15,16]

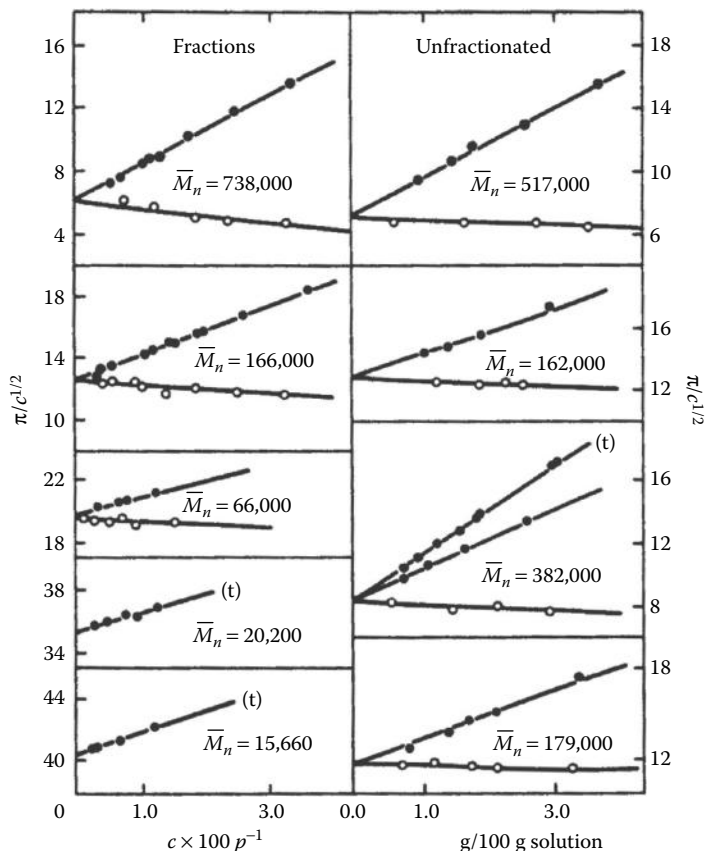


FIGURE 6.15 Osmotic pressure plotted according to Equation 6.37 for poly(methyl methacrylate) in toluene (\blacksquare), acetone (\bullet), or acetonitrile (\circ). (Data from Fox, T. G., J. B. Kinsinger, H. F. Mason, and E. M. Schuele, *Polymer*, 3, 71, 1962.)

$$A_2 = \frac{N_{AV} u_x}{2M^2} \quad (6.38)$$

where:

N_{AV} is Avogadro's number

u_x is the excluded volume per molecule

In Section 3.2, we saw that the radius of a flexible linear polymer chain in a good solvent grows with the molecular weight to the power of 0.6. This means that the excluded volume grows with molecular weight to the power of 1.8 and A_2 scales with molecular weight according to Equation 6.38 to the power of -0.2 . This scaling result has been verified experimentally in good solvents when the molecular weights are large.

A solvent can be of intermediate quality where the polymer molecules do not resist interpenetration in dilute solution (and do not attract each other as in the case

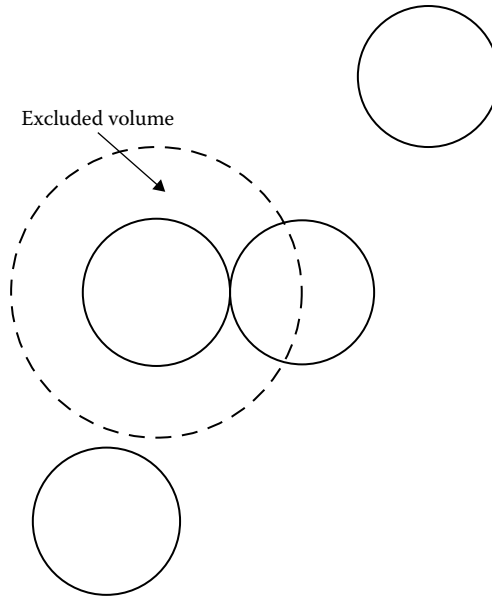


FIGURE 6.16 The excluded volume per particle for spherical particles in dilute solutions is 8 times the volume of the particle.

of a poor solvent). The excluded volume and the second virial coefficient of very large molecules (theoretically of infinite molecular weight) in such a solvent are zero. Such a solvent is called a **theta** solvent and sometimes it is referred to as a **Flory solvent** (See Section 7.4.1).

What happens to the osmotic pressure when the polymer concentration is in the semi-dilute regime is interesting. The virial expansion applicable to dilute solutions is no longer valid. An examination of Figure 3.1 for the cases of semi-dilute and concentrated polymer solutions suggests that the identity of single molecules becomes lost in this network structure of interpenetrated chains. One would then expect that the thermodynamic properties of the solution would become independent of the molecular weight of the polymer and would depend only on the polymer volume fraction (i.e., concentration). Based on this premise, scaling concepts applied to semi-dilute solutions of polymer in a good solvent predict that the osmotic pressure in this concentration regime obeys the relation [17]:

$$\pi = \text{const} \times v_2^{9/4} \quad (6.39)$$

The experimental results for poly(α -methyl styrene) of various molecular weights in toluene shown in Figure 6.17 demonstrate that at high concentrations the osmotic pressure becomes indeed independent of molecular weight, whereas at low concentrations (in the dilute regime) it is proportional to concentration. The data in the high concentration regime do not appear to have converged yet to the asymptotic limit predicted by Equation 6.39. If the Flory–Huggins model (Equation 3.8) was to be applied to the semi-dilute regime, it would predict a power law of 2.0 (see Problem 6.27).

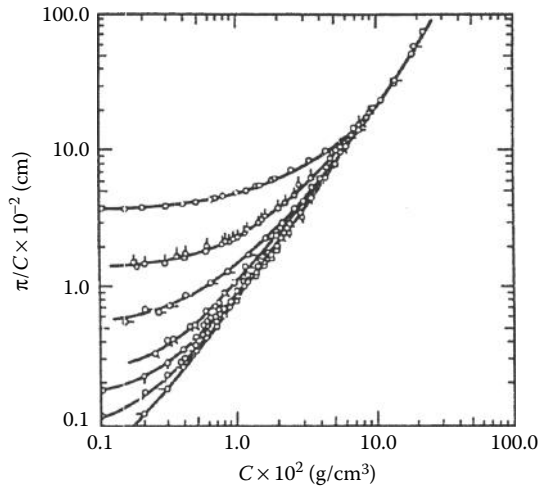


FIGURE 6.17 The dependence of the osmotic pressure of poly(α -methyl styrene)-toluene solutions for different low-polydispersity molecular weights (7, 20, 50.6, 119, 182, 330, and 774 in units of 10^4 g/mol). (Reprinted with permission from Noda, I., N. Kato, T. Kitano, and M. Nagasawa, *Macromolecules*, 14, 668, 1981. Copyright 1981 American Chemical Society.)

For polymer solutions in semi-dilute concentrations in a theta solvent, the power-law exponent in the equation corresponding to (6.39) is predicted by the scaling laws to be 3.0. This is in good agreement with reported experimental results [19].

Example 6.4

The following data are available for polymer A at 27°C. At a polymer concentration of 6.60 g/l, the osmotic pressure (π) is 1.82 cm of solvent. At a concentration of 14.0 g/l, the osmotic pressure (π) is 5.44 cm of solvent. Solvent density = 850 kg/m³. Estimate M_n and the second virial coefficient.

Solution: There are various ways to handle the data. However, if R is expressed as J/mol·K, the other units should be used in a compatible way. It is useful to remember that the unit Pa is equivalent to J/m³. Convert pressures to Pa:

$$(1.82 \times 10^{-2} \text{ m}) \times 850 \text{ kg/m}^3 \times 9.81 \text{ N/kg} = 152 \text{ Pa}$$

and

$$c = 6.60 \times 10^3 \text{ g/m}^3$$

Thus,

$$\frac{\pi}{c} = 23.03 \times 10^{-3} \text{ J/g}$$

Similarly, 5.44 cm of solvent = 454 Pa and $\pi/c = 32.43 \times 10^{-3}$ J/g. Using Equation 6.37 for each point and then simplifying,

$$\frac{RT}{M_n} = \frac{23.03 \times 10^{-3}}{\{1 + [(A_2 M_n \times 6.60 \times 10^3)/2]\}^2}$$

$$= \frac{32.43 \times 10^{-3}}{(1 + A_2 M_n \times 14.00 \times 10^3/2)^2}$$

$$(1.408)^{1/2} \{1 + [(A_2 M_n \times 6.60 \times 10^3)/2]\} = [1 + (A_2 M_n \times 14.00 \times 10^3)/2]$$

$$1.187 - 1.000 = (A_2 M_n/2)(14.00 \times 10^3 - 1.187 \times 6.60 \times 10^3)$$

$$\frac{A_2 M_n}{2} = \frac{0.187}{6.17 \times 10^3} = 30.3 \times 10^{-6} \text{ m}^3/\text{g}$$

Going back to Equation 6.37,

$$\frac{RT}{M_n} = \frac{23.03 \times 10^{-3}}{\{1 + [(30.3 \times 6.60 \times 10^{-3})/2]\}^2} = 19.0 \times 10^{-3} \text{ J/g}$$

where:

$$R = 8.3145 \text{ J/molK}$$

$$T = 300 \text{ K}$$

$$M_n = 131 \times 10^3 \text{ g/mol}$$

Therefore,

$$A_2 = \frac{2 \times 30.3 \times 10^{-6}}{131 \times 10^3} = 4.63 \times 10^{-10} \text{ m}^3 \text{ mol/g}^2$$

Osmotic pressure probably is the most popular of the colligative methods. However, membrane preparation is tricky, equilibrium may be slow to be reached, and the effect observed (π) decreases as M increases. The procedure has been automated in various ways. In one modern automatic recording membrane **osmometer**, the osmotic pressure can be measured in 5–30 min. The upper cell (Figure 6.18) is flushed with several volumes (a few milliliters) of solution. Diffusion of solvent from the lower cell through the membrane causes the flexible stainless-steel diaphragm to move. This, in turn, decreases the pressure in the lower cell until equilibrium is reached. The strain gauge indicates the corresponding osmotic pressure on the recorder via a calibrated circuit. With care, molecular weights of 5000–500,000 can be measured with about 1% accuracy. Below 5000, many polymers can penetrate the common membrane materials. When a low-molecular-weight polymer is placed in an osmometer, the rate of diffusion of the polymer through the membrane is discernible, since it results in a drift in the pressure necessary to maintain a null flow of solvent. Because the rate of diffusion decreases with increasing molecular size, the drift in osmotic pressure with time can be calibrated to yield the molecular weight of a specific polymer despite membrane penetration [20]. This is not an absolute method, of course.

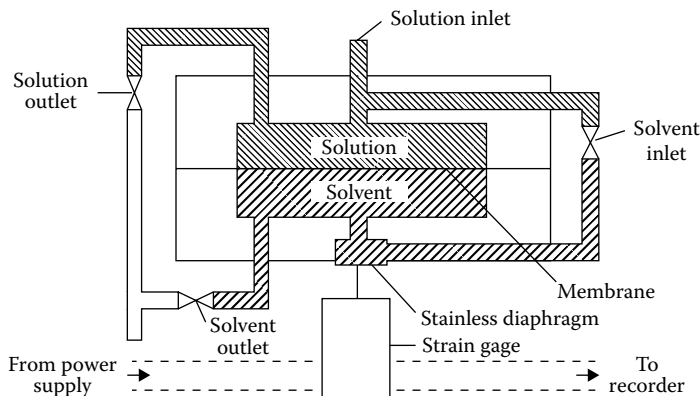


FIGURE 6.18 Schematic of a recording automatic membrane osmometer. The cell volume for solution and solvent is about 0.5 ml each. (Courtesy of Wescan Instruments, Inc., Santa Clara, CA.)

For molecular weights less than about 20,000, another technique has been automated. In the so-called vapor pressure osmometer, there is no membrane [21]. A drop of solution and a drop of pure solvent are placed on adjacent thermistors. The difference in solvent activity brings about a distillation of solvent from the solvent bead to the solution. The temperature change that results from the differential evaporation and condensation can be calibrated in terms of the number-average molecular weight of the solute. The method is rapid, although multiple concentrations and extrapolation to infinite dilution are still required.

6.7 WEIGHT-AVERAGE MOLECULAR WEIGHT METHODS

A standard technique for measuring weight-average molecular weight is light scattering where the intensity of light scattered at a certain scattering angle from a polymer solution at a given concentration is compared to the incident beam intensity. As described below (Figure 6.19), several measurements need to be performed and extrapolation of the data is needed to extract the desired information. Scattering of light from fluids and fluid mixtures is due to the fact that, even at equilibrium, fluids are inhomogeneous at very small length scales due to thermal fluctuations. These heterogeneities cause visible light (300–600 nm) to be scattered. The theory of light scattering from fluids goes back to Rayleigh who used electromagnetic theory of light to obtain an expression for scattered light from a fluid of small molecules.

For an incident beam of light of intensity I_0 , the scattered intensity from a scattering volume V is given by [22]

$$\frac{I_s}{I_0} = \frac{2\pi^2 n^2 V (1 + \cos^2 \theta)}{\lambda^4 R^2} \langle (\delta n)^2 \rangle \quad (6.40)$$

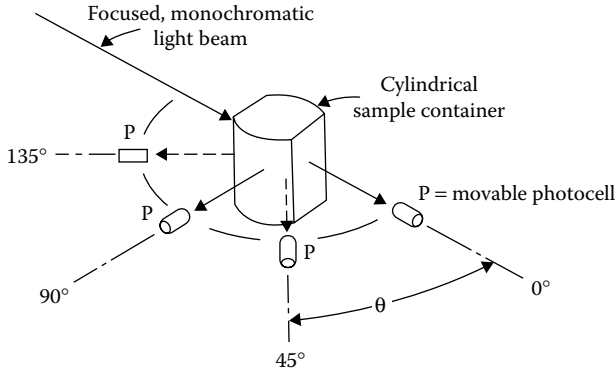


FIGURE 6.19 Photocell P senses light intensity I_s at angle θ .

where:

I_s is the intensity of the scattered light at a scattering angle θ

λ is the wavelength of light

R is the distance from the sample to the detector

n is the refractive index of the scattering medium

the brackets represent an average over the fluctuations of the refractive index

In a binary mixture, when the fluctuations in refractive index are due primarily to fluctuations in solute concentration, one can write

$$\frac{I_s}{I_0} \approx \frac{2\pi^2 n^2 V (1 + \cos^2 \theta)}{\lambda^4 R^2} \left(\frac{\partial n}{\partial c} \right)^2 \langle (\delta c)^2 \rangle \quad (6.41)$$

where:

$(\partial n / \partial c)$ represents the variation of refractive index with concentration and the average is now over concentration fluctuations

Statistical mechanics provides us with an expression for these equilibrium concentration fluctuations that allows us to link them to the thermodynamic properties of the solution. These equilibrium concentration fluctuations are given by [23]

$$\langle (\delta c)^2 \rangle = \frac{kT}{(\partial^2 G_m / \partial c^2)_{P,T}} \quad (6.42)$$

From thermodynamics, we can write (see Appendix 6.C)

$$\langle (\delta c)^2 \rangle = \frac{kT}{(\partial^2 G_m / \partial c^2)_{P,T}} = \frac{-kTcV_1}{V(\partial \mu_1 / \partial c)_{P,T}} = \frac{kTc}{V(\partial \pi / \partial c)_{P,T}} \quad (6.43)$$

and

$$\langle(\delta c)^2\rangle = \frac{1}{VN_{AV}} \left[\frac{1}{cM} + 2A_2 + \dots \right]^{-1} \quad (6.44)$$

In the above equation, we have used the virial expansion of the osmotic pressure of a monodisperse solution to obtain the last equation. Substituting Equation 6.44 into 6.41, we obtain

$$\frac{I_s}{I_0} = \frac{2\pi^2 n^2 (1 + \cos^2 \theta)}{N_{AV} \lambda^4 R^2} \left(\frac{\partial n}{\partial c} \right)^2 \left[\frac{1}{cM} + 2A_2 + \dots \right]^{-1} \quad (6.45)$$

The above result is for solute molecules that are much smaller than the wavelength of light. When the solute consists of large molecules such as polymers, the intensity of scattered light is reduced due to interference caused by phase differences in the scattered light coming from different parts of the molecule. In this case, the expression for the scattered light becomes

$$\frac{I_s}{I_0} = \frac{2\pi^2 n^2 (1 + \cos^2 \theta)}{N_{AV} \lambda^4 R^2} \left(\frac{\partial n}{\partial c} \right)^2 \left[\frac{1}{cMP(\theta)} + 2A_2 Q(\theta) + \dots \right]^{-1} \quad (6.46)$$

Expressions for $P(\theta)$ and $Q(\theta)$ have been obtained by Debye [24] for a linear polymer chain modeled as a Gaussian coil and expressions for other structures are also available [25]. In practice, Equation 6.46 is represented simply as

$$\frac{Kc}{R_\theta} = \frac{1}{MP(\theta)} + 2A_2 Q(\theta)c \quad (6.47)$$

where:

K is a lumped constant

R_θ is known as the Rayleigh ratio

The expressions for K and R_θ are given by:

$$K = \frac{2\pi^2 n^2}{N_{AV} \lambda^4} \left(\frac{\partial n}{\partial c} \right)^2 \text{ and } R_\theta = R^2 \frac{I_s}{I_0 (1 + \cos^2 \theta)} \quad (6.48)$$

K includes the refractive index of the solvent as well as the change in refractive index with polymer concentration for the particular system being investigated. The values of these properties for an extensive list of polymer/solvent systems are tabulated in *Polymer Handbook* [26]. They can also be measured in separate experiments using a refractometer and a differential refractometer. The intensity of scattered light is measured at various angles θ and for various dilute concentrations c . Both $P(\theta)$ and $Q(\theta)$ go to unity as θ approaches zero. A double extrapolation of the data to $\theta = 0$ and $c = 0$ allows for the determination of M , the second virial coefficient A_2 , and a complex function of molecular shape $P(\theta)$. We can see that in these two limits, Equation 6.47 reduces to

$$\lim (\theta \rightarrow 0) \frac{Kc}{R_\theta} = \frac{1}{M} + 2A_2c \quad (6.49)$$

and

$$\lim (c \rightarrow 0) \frac{Kc}{R_\theta} = \frac{1}{MP(\theta)} \quad (6.50)$$

From the first extrapolation of the data, one obtains $1/M$ as the intercept and $2A_2$ as the slope from a plot of Kc/R_θ versus c . From the second extrapolation and knowing M , one obtains $P(\theta)$ from a plot of Kc/R_θ versus θ . For a linear flexible polymer chain, Debye [23] showed that

$$\lim (c \rightarrow 0) \frac{Kc}{R_\theta} = \frac{1}{MP(\theta)} = \frac{1}{M} \left(1 + \frac{q^2}{3} R_g^2 \right) \quad (6.51)$$

where:

R_g^2 is the average of the square of the radius of gyration of the polymer coil, $\langle s^2 \rangle$
 $q = (4\pi/\lambda)n \sin \theta/2$ is known as the scattering wave vector

Equation 6.51 is the result of a Taylor series expansion in $q^2 R_g^2$ and holds when this product is much less than unity that is always achievable, in principle, as one goes to small scattering angles.

Both extrapolations of the data to $\theta = 0$ and $c = 0$ are carried out simultaneously in a **Zimm plot** (Figure 6.20). The abscissa consists of the two variables $\sin^2 \theta/2$ and c . The variable c is usually multiplied by an arbitrary constant to spread out the data in the plot. The bottom lower data in the Zimm plot are extrapolated data at $\theta = 0$, and the fit to this data has an intercept of $1/M$ and a slope of $2A_2$. As in osmotic pressure, measurements in a theta or poor solvent could give a zero or negative slope. The outermost left data in the plot are extrapolated data at $c = 0$ with an intercept of $1/M$ and a slope from which one can determine the radius of gyration using Equation 6.51.

In one commercial instrument, 15–18 photodiode detectors are arranged in fixed positions to measure laser light scattered at angles between 0° and 180° . For batch testing, a cell volume of 10 ml is used. The separate determination of change in refractive index with concentration, dn/dc , still is needed. In another model, a flow-through cell volume of only 67 μl is used to monitor light scattered as part of a SEC. A differential refractometer (which can also be used for measuring dn/dc) is placed in series to measure the concentration on the same stream. In either case, software is available which simplifies greatly the manipulation of experimental results. Using four concentrations in successive batch runs, all the intermediate parameters and a Zimm plot can be achieved in minutes when the apparatus output is fed directly to a personal computer. An example of the application of light scattering with SEC illustrates the increased scattering intensity at the highest molecular size (lowest retention volume) (Figure 6.21). Volumes of 50 μl each of three samples were injected at concentrations of 0.1, 0.2, and 0.3 g/l for molecular weights of 600, 200, and 30×10^3 , respectively.

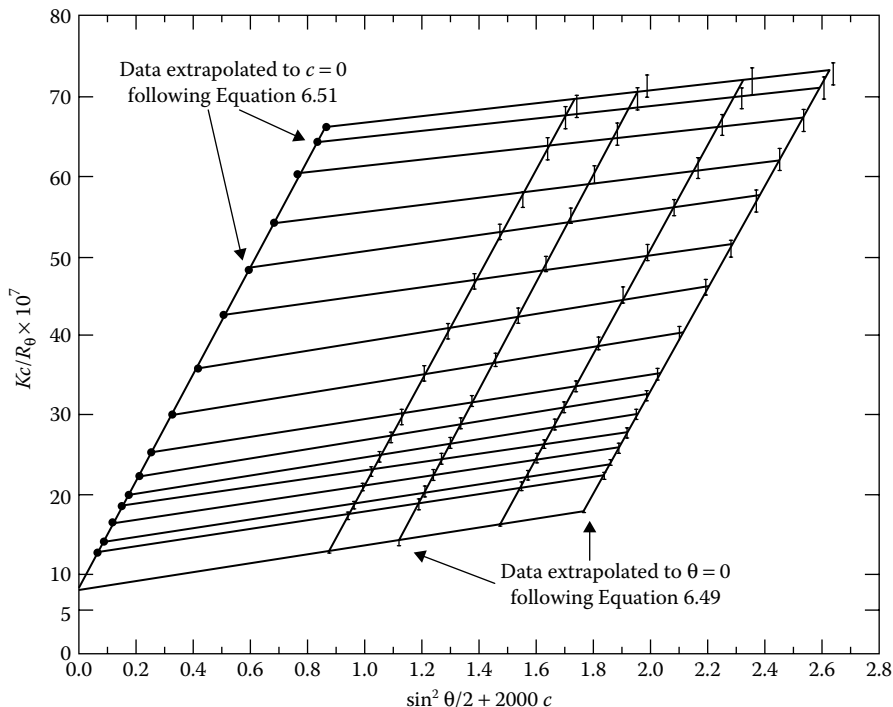


FIGURE 6.20 Zimm plot for cellulose nitrate in acetone at 25°C. The filled circles are extrapolated data to $c = 0$ and the filled triangles are extrapolated data to $\theta = 0$. (Reprinted with permission from Benoît, H. C., A. M. Holtzer, and P. Doty: *J. Phys. Chem.*, 58, 635, 1954. Copyright 1954 American Chemical Society.)

The size of the signal seen by the differential refractive index detector reflects the concentrations. The size of the signals seen by the photodetectors is greatest for the highest molecular weight at all angles (which ranged from 19.0° to 132.5°) [28].

The extrapolation to $\theta = 0$ can be eliminated if the scattered light intensity is measured at forward angles of less than 2° from the incident beam. This becomes possible when the light source is a small, single transverse-mode laser [29]. The optical diagram for this low-angle laser light scattering (LALLS) is relatively simple since no provision needs to be made for varying the angle of measurement. As in the case of the osmometer, the apparatus can be very compact. The weight-average molecular weight can be derived conveniently from this arrangement. However, when additional information such as the shape and size of the polymer molecules in solution is desired, the measurement of the angular dependence of scattered light intensity must be made. Another method of obtaining shape and size of polymer molecules which is based on very similar principles as light scattering is the technique of **neutron scattering**. Rather than scattering of light caused by differences in refractive index, neutron scattering is based on difference in scattering efficiencies between hydrogen atoms and deuterium atoms. By using deuteration of one

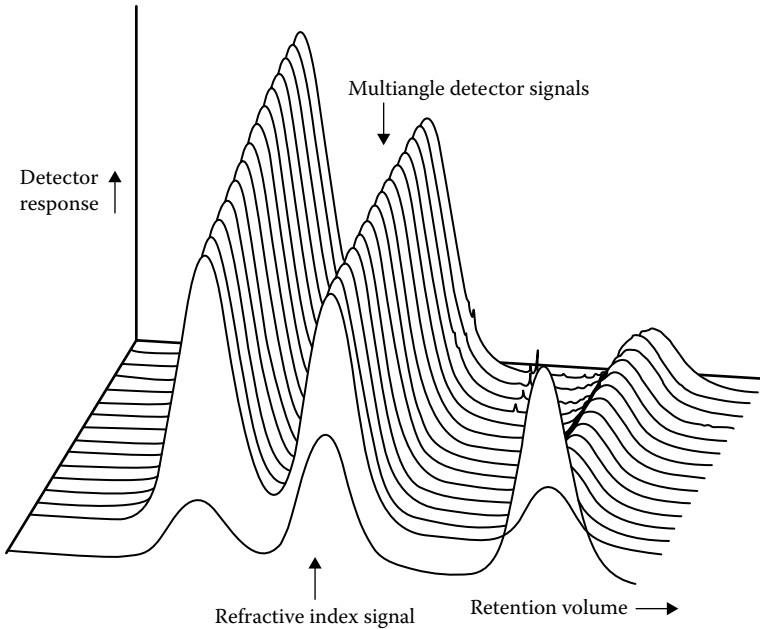


FIGURE 6.21 A three-dimensional plot of light scattering for three almost monodisperse polystyrenes (600,000, 200,000, and 30,000) measured by GPC/SEC in toluene at concentrations of 0.1, 0.2, and 0.3 g/l, respectively. The differential refractive index signal is in the foreground. The signals from the DAWN photodetectors can be converted to a Zimm plot by a computer program, ASTRA. (Courtesy of Wyatt Technology Corporation, Santa Barbara, CA; ASTRA software and DAWN light scattering apparatus are registered trademarks of Wyatt Technology.)

of the components, Zimm plots and structural information can be obtained [25]. The advantage of neutron scattering is that it can be used on melts where a small concentration of chains is deuterated. The method was instrumental in establishing that chains in melts have the same Gaussian conformation as in dilute theta solvents [30] as originally argued by Flory, but that remained controversial till then.

To see what kind of average molecular weight is measured by light scattering, one can examine the contributions made by individual species to the factor R_{θ} . For a monodisperse polymer i at $\theta = 0$,

$$\frac{Kc_i}{R_{\theta,i}} = \frac{1}{M_i} \quad (6.52)$$

For a polydisperse polymer, we then have

$$\frac{Kc}{R_{\theta}} = \frac{1}{\bar{M}} \quad (6.53)$$

where:

$c = \sum c_i$ is the total concentration

\bar{M} is the observed average molecular weight

R_θ is the total scattered intensity given by

$$R_\theta = \sum R_{\theta,i} = \sum Kc_iM_i \quad (6.54)$$

Substituting the above equation into (6.53), we find that

$$\bar{M} = \frac{R_\theta}{Kc} = \frac{\sum Kc_iM_i}{Kc} = \frac{\sum c_iM_i}{c} = \sum w_iM_i = M_w \quad (6.55)$$

Thus, the average molecular weight measured by light scattering is the weight-average molecular weight.

A major practical problem in light scattering is the presence of dust particles or gelled polymer particles. A small concentration of these obscures the scattering by ordinary polymer particles and results in an infinitely large M_w . Removal of dust by filtration is usually sufficient, but ultracentrifugation may be necessary, making this a rather expensive tool. Fortunately, solutions being eluted from a SEC usually have already been cleaned up to the point where dust particles have been eliminated. Kim and Cotts compared several light scattering devices as adjuncts to a GPC/SEC system. They concluded that a low-angle device was convenient, but that a multiple-angle detector supplied more information [31].

In the above light scattering measurements and analysis, we considered the **static light scattering** which we related to the molecular weight, the radius of gyration, and the second virial coefficient (a thermodynamic property). A more recent development in light scattering due to the advent of the laser and electronic handling of the data is **dynamic light scattering**. In this technique, dynamic properties of the polymer solution can be measured. A commonly determined property that can be obtained with this technique is the diffusion coefficient of a polymer in dilute solution. In this experiment, one measures the fluctuations in the scattered intensity with time on very short timescales (microsecond to millisecond). As was shown for the static light scattering case, these fluctuations are related to the fluctuations of concentrations. By performing a correlation of the time-dependent scattering intensities, one determines how concentration fluctuations decay in time and an analysis of the data provides information about the diffusion coefficient of the polymer in the solution [32]. One can extract a **hydrodynamic radius** of gyration (R_g^H) from the measured diffusion coefficient by using the established **Stokes–Einstein** relation and write

$$D = \frac{kT}{6\pi\eta R_g^H} \quad (6.56)$$

where:

η is the solvent viscosity

k and T have their usual meaning

We note that R_g^H is obtained from a dynamic property and its value may differ appreciably from the structural (static) $R_g = \langle s^2 \rangle^{1/2}$ [33].

An ultracentrifuge can be used to measure a molecular weight distribution. Under exceptionally high gravitational fields, polymers will settle out of a solution just as macroscopic beads fall through a viscous liquid according to Stokes' law. In an ultracentrifuge [34], the Brownian motion of the molecules is balanced against a centrifugal field and either the rate of settling or the equilibrium in the field is observed. A cell holding the solution is placed in a head that rotates on air bearings up to 70,000 rpm. The concentration gradient across the cell is estimated using refractive index as a measure. Because extrapolation to $c = 0$ is still necessary and the difference in refractive index between the solution and the solvent must be large, the ultracentrifuge has been very successful only with certain classes of polymers, for example, proteins. It has not been as widely used as osmometry or light scattering as an absolute measure of molecular weight. A definite advantage of the ultracentrifuge is that the entire distribution is obtained, not just one lumped average molecular weight. Not only M_w is measured but M_n, M_z, \dots , are also measured directly, without recourse to a mathematical model. However, the large size of the apparatus involved and the very high cost of the necessary instrumentation make the ultracentrifuge method an uncommon method of molecular weight determination.

APPENDIX 6.A

From Equation 6.10, we have

$$\sum_{x=1}^{\infty} p^{x-1} = \frac{1}{1-p} \quad (6.A.1)$$

Differentiating with respect to p both sides of the equation yields

$$\sum_{x=2}^{\infty} (x-1)p^{x-2} = \frac{1}{(1-p)^2} \quad (6.A.2)$$

Note that we have written the summation from $x = 2$ rather than 1 because the $x = 1$ term is 0. We can now change the running index x to $x + 1$ to obtain

$$\sum_{x=1}^{\infty} xp^{x-1} = \frac{1}{(1-p)^2} \quad (6.A.3)$$

The last equation can be rewritten as Equation 6.11.

APPENDIX 6.B

Differentiating Equation 6.A.3 with respect to p yields

$$\sum_{x=2}^{\infty} x(x-1)p^{x-2} = \frac{2}{(1-p)^3} \quad (6.B.1)$$

Changing the running index from x to $x + 1$, we get

$$\sum_{x=1}^{\infty} x(x+1)p^{x-1} = \frac{2}{(1-p)^3} \quad (6.B.2)$$

so that

$$\sum_{x=1}^{\infty} x^2 p^{x-1} = \frac{2}{(1-p)^3} - \sum_{x=1}^{\infty} xp^{x-1} = \frac{2}{(1-p)^3} - \frac{1}{(1-p)^2} = \frac{1+p}{(1-p)^3} \quad (6.B.3)$$

Equation 6.17 is obtained by combining Equations 6.A.3 and 6.B.3.

APPENDIX 6.C

From the thermodynamics expression for the differential change in free energy,

$$dG = -SdT + VdP + \mu_1 dN_1 + \mu_2 dN_2 \quad (6.C.1)$$

we have at constant T and P

$$dG = \left[\left(\frac{\mu_1 dN_1}{dN_2} \right) + \mu_2 \right] dN_2 \quad (6.C.2)$$

Assuming no volume change upon mixing, so that

$$\frac{dN_1}{dN_2} = -\frac{V_2}{V_1} \quad (6.C.3)$$

The above equation becomes

$$dG = [\mu_2 - \mu_1(V_2/V_1)] dN_2 = [\mu_2 - \mu_1(V_2/V_1)] V dc/M \quad (6.C.4)$$

where:

the relation $c = N_2 M/V$ is used

We obtain by differentiating the last equation twice

$$\left(\frac{\partial^2 G}{\partial c^2} \right)_{P,T} = \frac{V}{M} \left[\left(\frac{\partial \mu_2}{\partial c} \right)_{P,T} - \left(\frac{\partial \mu_1}{\partial c} \right)_{P,T} \frac{V_2}{V_1} \right] \quad (6.C.5)$$

From the Gibbs–Duhem relation,

$$N_1 d\mu_1 + N_2 d\mu_2 = 0$$

we find that

$$\left(\frac{\partial \mu_2}{\partial c} \right)_{P,T} = -\frac{N_1}{N_2} \left(\frac{\partial \mu_1}{\partial c} \right)_{P,T} \quad (6.C.6)$$

Substitution in Equation 6.C.5 yields

$$\left(\frac{\partial^2 G}{\partial c^2}\right)_{P,T} = -\frac{V}{M} \left(\frac{N_1 V_1 + N_2 V_2}{N_2 V_1}\right) \left(\frac{\partial \mu_1}{\partial c}\right)_{P,T} = -\frac{V^2}{MN_2 V_1} \left(\frac{\partial \mu_1}{\partial c}\right)_{P,T} = -\frac{V}{c V_1} \left(\frac{\partial \mu_1}{\partial c}\right)_{P,T}$$

from which Equation 6.43 follows. μ_1 and π are related by Equation 6.34.

KEYWORDS

Monodisperse
 Polydisperse
 Number-average molecular weight
 Weight-average molecular weight
 Degree of polymerization
 Polydispersity index (PDI)
 Mole fraction
 Degree of polymerization
 Most probable distribution
 Poisson distribution
 Schulz distribution
 Differential distribution
 Wesslau distribution
 Logarithmic normal distribution
 Differential weight distribution
 Fractionation
 Coacervate
 Gel permeation chromatography (GPC)
 Size exclusion chromatography (SEC)
 Colligative property
 Universal calibration
 Osmotic pressure
 Virial expansion
 Virial coefficients
 Excluded volume
 Theta (Flory) solvent
 Osmometer
 Light scattering
 Zimm plot
 Neutron scattering
 Static and dynamic light scattering
 Hydrodynamic radius
 Stokes–Einstein

PROBLEMS

- 6.1** A polymer sample contains an equal number of moles N of species with degrees of polymerization $x = 1, 2, 3, 4, 5, 7, 8, 9$, and 10 . What is x_n ?
- 6.2** Three samples of polymer are mixed without reaction. Calculate M_n and M_w for the mixture:

Sample	M_n	M_w	Weight of Mixture (g)
A	1.2×10^5	4.5×10^5	200
B	5.6×10^5	8.9×10^5	200
C	10.0×10^5	10.0×10^5	100

- 6.3** The molecular weight of a certain polymer can be described as

$$w_x = \frac{k(x)^{1/2}}{5+x} \quad x=1, 4, 9, \text{ and } 16 \text{ only}$$

where:

w_x is the weight fraction of polymer with degree of polymerization x
 What is the value of k ? What is the weight-average degree of polymerization, x_w ? What is x_n ?

- 6.4** A polymer sample has a molecular weight distribution described by

$$w_x = kx^2 \quad x = 1, 2, 3, \text{ and } 4 \text{ only}$$

where:

w_x is the weight fraction of polymer with degree of polymerization x
 Calculate x_n and x_w .

- 6.5** One gram of polymer A ($x_n = 2000$, $x_w = 5000$) is mixed with 2 g of polymer B ($x_n = 6000$, $x_w = 10,000$). Calculate the degree of polymerization of the mixture that would be derived from osmotic pressure measurements at several concentrations.
- 6.6** A polymer blend is made up of four lots of polymers, A, B, C, and D (with $k = 1, 2, 3$, and 4 , respectively), which can be described by

$$x_w = 2800k^{1.5}, \quad x_n = 1400k$$

The blend contains $1000/k^2$ g of each lot. For the blend,

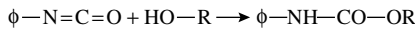
- What degree of polymerization can be expected from measurements made using a light scattering apparatus?
- What degree of polymerization can be expected from measurements of osmotic pressure at various concentrations?

- 6.7** A polymer sample is made up by evaporating together equal volumes (50.0 ml each) of three polymer solutions, A, B, and C. All three solutions are characterized by osmotic pressure measurements in a Flory *theta* solvent. What is the PDI of the mixture?

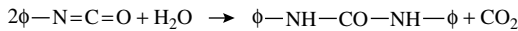
Polymer Identity	Concentration (g/dl)	Osmotic Pressure (cm of Solvent)	Distribution Type
A	1.250	4.000	Monodisperse
B	0.730	3.250	Most probable ^a
C	0.308	3.600	Most probable ^a

^a In each case, $x_n > 100$.

- 6.8** The molecular weight of a polymer is 10,000 according to an osmotic pressure experiment in a theta solvent. What osmotic pressure (atm) do you expect to encounter at a concentration of 1.18 g/dl? A light scattering experiment in a good solvent gives a molecular weight of 34,500. Why is there a difference in measured molecular weight? Would the difference be smaller or greater if the osmotic pressure were measured in a good solvent? ($R = 0.08206$ l-atm/mol·K and $T = 303$ K.)
- 6.9** Phenyl isocyanate (FW = 119) is expected to react quantitatively with primary alkyl hydroxyl groups to form urethanes and with water to form diphenyl urea.



Isocyanate Alcohol Urethane



Diphenyl urea

Analysis of 100 g of poly(ethylene oxide) with two hydroxyls per molecule results in 5.923 g of isocyanate being consumed with the evolution of 210 cm³ (at 1 atm, 25°C) of CO₂. Estimate x_n and the weight fraction of water in the polymer.

- 6.10** The following data are available for polymers A and B in the same solvent at 27°C:

Concentration c_A (g/dl)	Osmotic Pressure π_A (cm of Solvent)	Concentration c_B (g/dl)	Osmotic Pressure π_B (cm of Solvent)
0.500	1.25		
0.800	2.40	0.400	1.60
1.100	3.91	0.900	4.44
1.300	4.94	1.400	8.95
1.500	6.30	1.800	13.01

Solvent density = 0.85 g/cm³; polymer density = 1.15 g/cm³.

- (a) Plot $(\pi/c)^{1/2}$ versus c .
 (b) Estimate M_n and the second virial coefficient for each polymer.
 (c) Estimate M_n for a 25:75 mixture of A and B.
 (d) If $M_w/M_n = 2.00$ for A and B, what is M_w/M_n for the mixture of part (c)?
- 6.11** For a water-soluble polymer, what would be the upper limit on molecular weight measurable by freezing-point depression?
- 6.12** Plot the Schulz distribution in cumulative form on logarithmic probability paper for $x_w/x_n = 2$. What parameter for the Wesslau model gives the best fit?
- 6.13** In a particular reactor, polymerization appears to occur by two simultaneous mechanisms that give rise to two separate molecular weight distributions (as seen by chromatography). A high-molecular-weight portion (62.5 wt% of the total batch) can be resolved by solvent fractionation. It has $M_w = 550,000$ and $M_n = 210,000$. The entire batch has $M_w = 360,000$, but M_n cannot be measured unequivocally. Assuming that the lower molecular-weight portion (37.5 wt% of the total batch) has a *most probable* distribution, find the M_n of the lower molecular-weight portion and the M_n of the entire batch. It can be assumed that the lower molecular-weight portion has M_n high enough so that p is essentially equal to 1.
- 6.14** A polymer has a continuous cumulative distribution given by

$$W(x) = \ln(ea^2x^2 + 1) - \ln(a^2x^2 + 1)$$

where:

e is 2.7183

a is an adjustable parameter

Derive expressions for the differential weight distribution and for x_w and x_n in terms of a . What is x_w/x_n ?

- 6.15** Compare the cumulative distribution of Problem 6.14 with the Wesslau model on logarithmic probability paper using the product ax as the measure of molecular weight.
- 6.16** How could the model of Problem 6.14 be modified to allow x_w/x_n to be an independent variable?
- 6.17** Show that the cumulative weight distribution for the Wesslau model (Equation 6.27) is given by

$$W_x = \int_0^x w_x dx = \frac{1 + \operatorname{erf}(Y/\beta)}{2}$$

where:

$Y = \ln(x/x_0)$

erf is the normalized error function

- 6.18** A polymer sample has a molecular weight distribution described by

$$w_x = k(x)^{1/2} \quad x = 1, 2, 3, 4, \text{ and } 5 \text{ only}$$

where:

w_x is the weight fraction of x -mer

Calculate \bar{x}_n , \bar{x}_w , and the PDI.

- 6.19** Polymers A and B are monodisperse polystyrenes. Polymer A has a molecular weight 3 times that of B. Polymer C, however, is a polydisperse polystyrene for which M_w is 2.0×10^5 . Deduce the M_n for polymer C from the following measurements on a mixture of all three polymers: the mixture contains 25 g of A, 50 g of B, and 25 g of C. Light scattering gives a molecular weight of 112,500, whereas osmotic pressure gives a molecular weight of 60,000.
- 6.20** The molecular weight distributions of polymers A and B each can be represented by the *most probable* distribution. Also, $x_n > 100$ for each of them. When 200 g of A is mixed with 100 g of B, the PDI is $(x_w/x_n) = 4$ for the mixture. What is $(x_w)_A/(x_w)_B$?
- 6.21** By fractional precipitation, a polymer P with the *most probable* distribution and a number-average molecular weight $M_n = 150,000$ is cut into only two fractions, A and B, with $M_w = 250,000$ and 325,000, respectively. If the PDI of A is the same as that of B, what is the weight of fraction A obtained from 200 g of initial polymer P? What is the polydispersity of A and B?
- 6.22** A monodisperse polyester with a degree of polymerization of 1.00×10^5 is partly hydrolyzed by reaction with water. A total of 10.0 g of water is reacted with 0.0100 mol of polymer. Random scission occurs.
- What is the weight-average degree of polymerization of the final, partly hydrolyzed polymer?
 - What is the weight fraction of trimer in the resulting polymer?
- 6.23** In a polyesterification, 10-hydroxydecanoic acid is heated and water is removed. In run A: 4.5 mol of water is removed from 5 mol of monomer. In run B, 4.9 mol of water is removed from 5 mol of monomer.
- What are x_w and x_n for the polymer of run B?
 - If the two resultant polymers are combined without reaction, what is the x_w and x_n of the mixture?
- 6.24** A polymer solution with PDI = 1.52 is fractionated into three fractions. The weight-average molecular weight of each fraction, its PDI when measured, and its mass concentration (%) in the original sample are given in the table below.

Sample	$M_w \times 10^{-3}$ g/mol	PDI	Total (wt%)
Unfractionated	–	1.52	100
Fraction 1	360	1.20	20
Fraction 2	230	1.30	30
Fraction 3	130	–	50

- Calculate the PDI of fraction 3.
- What would be the value of the molecular weight of the unfractionated polymer and that of fraction 3 if obtained from osmotic pressure measurements?

6.25 A molecular weight distribution is given by

$$W = \log x - 1 \quad 10 < x < 100$$

$$W = 0 \quad x < 100$$

$$W = 1 \quad x > 100$$

where:

W is the cumulative weight fraction of polymer above the degree of polymerization x

Calculate x_w and x_n .

6.26 A molecular weight distribution is represented by

$$\frac{dW}{dx} = Bxe^{-ax} \quad 0 < x < \infty$$

- Express B in terms of x_n .
 - Determine the ratio of x_w to x_n .
 - Plot $dW/d(x/x_n)$ versus $\log(x/x_n)$ for the range $0.1 < (x/x_n) < 10$.
- 6.27** Use the Flory–Huggins expression for the solvent chemical potential in Equation 3.8 to show that in the semi-dilute regime, $v_2 \ll 1$ and therefore $\ln(1 - v_2) \approx -v_2 - v_2^2/2$, this model would predict that for high-molecular-weight polymers the osmotic pressure would scale as v_2^2 . Compare with the scaling law result. To what can you attribute the difference?
- 6.28** Consider the results of Figure 6.17:
- Discuss the molecular weight dependence of π/c versus c at both low and high concentrations.
 - How would you extract the molecular weight of the different samples and explain why there is an upper limit in the molecular weight that can be determined by osmometry.
- 6.29** The free energy of mixing expression for a polydisperse solution can be obtained by generalizing the Flory–Huggins Equation 2.12 to write

$$\Delta G_m = RT \left(\chi N_1 v_2 + N_1 \ln v_1 + \sum N_i \ln v_i \right)$$

where:

$$v_2 = \sum v_i$$

$$v_1 + v_2 = 1$$

- Use the above equation to show that the osmotic pressure in this model would be given by

$$\pi = -\frac{\mu_1 - \mu_1^0}{V_1} = -\frac{1}{V_1} \left(\frac{\partial \Delta G_m}{\partial N_1} \right)_{T,P} = -\frac{RT}{V_1} \left[\ln(1 - v_2) + \left(1 - \frac{1}{x_n} \right) v_2 + \chi v_2^2 \right]$$

where:

x_n is the number-average degree of polymerization

(b) Assume that this expression for π can be applied to dilute solutions and use $\ln(1 - v_2) \approx -v_2 - v_2^2/2$ to show that, in the limit of v_2 going to 0, a plot of π/v_2 versus v_2 will give an intercept proportional to the inverse of the number-average molecular weight.

6.30 A laboratory researcher synthesizes 200 g of a polymer by complete conversion of a monomer in a stepwise polymerization. She has only a membrane osmometer at her disposal and she measures a molecular weight of 150,000 g/mol for her product. She assumes that the molecular weight distribution is the *most probable* distribution (good assumption), and to reduce the polydispersity of the polymer obtained, she fractionates the entire sample (200 g of dry polymer) into three parts. The first precipitated fraction is removed and found to have a molecular weight of 300,000 g/mol and weighs 80 g dry. The second precipitated fraction is also removed and is found to have a molecular weight of 175,000 g/mol. The third part of the original 200 g remained in the solution and its molecular weight was measured to be 100,000 g/mol. She assumes that the PDIs of the three fractions (the two removed or precipitated fractions and the one remaining in solution) are the same, and she calculates

(a) The expected weight of polymer in the second and third fractions.

(b) The polydispersity of the fractions.

What are the values she obtains?

6.31 An empirical relation for the osmotic pressure π of a polymer solution at mass concentration c was proposed based on the van der Waals equation of state. It was written as

$$\frac{\pi M}{cRT} = \frac{1}{1 - sc}$$

where:

$$s = k_1 \pi^{-\alpha} \text{ with } \alpha < 1$$

M is the molecular weight

k_1 and α are constants

R and T have their usual meaning

The quantity s represents the specific van der Waals volume occupied by solute particles.

(a) Explain that according to the above equation, π depends on M and increases as c increases up to a limiting behavior when the product sc approaches unity. In the limit $sc \rightarrow 1$, show that one has then $\pi = (k_1 c)^{1/\alpha}$ which is independent of M . The attractiveness of this empirical relation for π is that it can describe both dilute and higher concentration behaviors.

(b) Old data on polyethylene oxide in water and nitrocellulose in acetone have been reanalyzed to show that in these cases, $\alpha = 0.43$ and 0.45 , respectively. Both systems are very good solvent-polymer mixtures. How do these values of α compare with the scaling law of semi-dilute solutions (Equation 6.39)?

6.32 Debye's expression for the intramolecular scattering interference factor $P(\theta)$ for a linear flexible coil modeled as a Gaussian coil is given by

$$P(x) = \left(\frac{2}{x^2} \right) \left[e^{-x} - (1-x) \right]$$

where:

$$x = q^2 R_g^2$$

$$q = (4\pi/\lambda)n \sin \theta/2$$

Obtain Equation 6.51 from 6.50 by expanding the exponential in the above expression in a Taylor series expansion in x for small x and keeping only the linear term in x for $P(x)$.

REFERENCES

1. Flory, P. J.: *Principles of Polymer Chemistry*, chap. 8, Cornell University Press, Ithaca, NY, 1953.
2. Swarc, M.: *Polymerization and Polycondensation Processes*, ACS, Washington, DC, 1962, p. 96.
3. Tung, L. H.: in M. J. Cantow (ed.), *Polymer Fractionation*, chap. E, Academic Press, New York, 1967.
4. Dobashi, T., M. Nakata, and M. Kaneko: *J. Chem. Phys.*, 72:6692 (1980).
5. Kotera, A.: in M. J. Cantow (ed.), *Polymer Fractionation*, chap. B.1, Academic Press, New York, 1967.
6. Blease, R. A., and R. F. Tuckett: *Trans. Faraday Soc.*, 37:571 (1941).
7. Elliott, J. H.: in M. J. Cantow (ed.), *Polymer Fractionation*, chap. B.2, Academic Press, New York, 1967.
8. Porath, J., and P. Flodin: *Nature*, 183:1657 (1959); Flodin, P.: *Dextran Gels and Their Applications in Gel Filtration*, Pharmacia, Uppsala, Sweden, 1962.
9. Moore, J. C.: *J. Polym. Sci.*, A2:835 (1964).
10. Rodriguez, F., R. A. Kulakowski, and O. K. Clark.: *Ind. Eng. Chem. Prod. Res. Develop.*, 5:121 (1966).
11. Grubisic, Z., P. Rempp, and H. Benoît: *Polym. Lett.*, 5:753 (1967).
12. Terry, S. L., and F. Rodriguez: *J. Polym. Sci. C*, 21:191 (1968).
13. Glasstone, S.: *Textbook of Physical Chemistry*, 2nd edn., Macmillan, London, 1962, p. 645.
14. Fox, T. G., J. B. Kinsinger, H. F. Mason, and E. M. Schuele: *Polymer*, 3:71 (1962).
15. Atkins, P.: *Physical Chemistry*, 6th edn., W. H. Freeman, New York, 1998, p. 682.
16. Flory, P. J.: *Principles of Polymer Chemistry*, chap. 12, Cornell University Press, Ithaca, NY, 1953.
17. De Gennes, P.-G.: *Scaling Concepts in Polymer Physics*, chap. 3, Cornell University Press, Ithaca, NY, 1979.
18. Noda, I., N. Kato, T. Kitano, and M. Nagasawa: *Macromolecules*, 14:668 (1981).
19. Stepánek, P., R. Perzyski, M. Delsanti, and M. Adam: *Macromolecules*, 17:2340 (1984).
20. Hudson, B. E., Jr.: *ACS Div. Polym. Chem.*, 7:467 (1966).
21. Neumayer, J. J.: *Anal. Chem. Acta*, 20:519 (1959).
22. Van de Hulst, H. C.: *Light Scattering by Small Particles*, 2nd edn., Wiley, New York, 1981.

23. Landau, L., and E. M. Lifshitz: *Statistical Physics*, Part I, 3rd edn., Pergamon Press, New York, 1980, p. 350.
24. Debye, P.: *J. Phys. Coll. Chem.*, 51:18 (1947).
25. Higgins, J. S., and H. C. Benoît: *Polymers and Neutron Scattering*, Clarendon Press, Oxford, 1994.
26. Brandrup, J., and E. H. Immergut: *Polymer Handbook*, 3rd edn., Wiley, New York, 1989.
27. Benoît, H. C., A. M. Holtzer, and P. Doty: *J. Phys. Chem.*, 58:635 (1954).
28. Wyatt, P. J.: *Anal. Chim. Acta*, 272:1 (1993).
29. McConnell, M. L.: *American Laboratory*, 10:63 (May 1978).
30. Benoît, H. C., D. Decker, J. S. Huggins, C. Picot, J. P. Cotton, B. Farnoux, and G. Jannink: *Nature*, 245:13 (1973).
31. Kim, S. H., and P. M. Cotts: *J. Appl. Polym. Sci.*, 42:217 (1991).
32. Berne, B. J., and R. Pecora: *Dynamic Light Scattering*, chap. 5, Wiley, New York, 1976.
33. Fetters, L. J., N. Hadjichristidis, J. S. Lindner, and J. W. Mays: *J. Phys. Chem. Ref. Data.*, 23:619 (1994).
34. Flory, P. J.: *Principles of Polymer Chemistry*, Cornell University Press, Ithaca, NY, 1953, p. 303.

GENERAL REFERENCES

- Brown, W., and K. Mortensen (eds.): *Scattering in Polymeric and Colloidal Systems*, Gordon and Breach, Amsterdam, The Netherlands, 2000.
- Carroll, B. (ed.): *Physical Methods in Macromolecular Chemistry*, Dekker, vol. 1, New York, 1969; vol. 2, 1972.
- Cazes, J., and X. Delamare (eds.): *Liquid Chromatography of Polymers and Related Materials II*, Dekker, New York, 1980.
- Dawkins, J. V. (ed.): *Developments in Polymer Characterization—I*, Applied Science, London, 1978.
- Epton, R. (ed.): *Chromatography of Synthetic and Biological Polymers*, 2 vols., Wiley, New York, 1978.
- Glöckner, G.: *Polymer Characterization by Liquid Chromatography*, Elsevier Applied Science, New York, 1987.
- Hamilton, R. J., and P. A. Sewell: *Introduction to High Performance Liquid Chromatography*, Wiley, New York, 1978.
- Huglin, M. B. (ed.): *Light Scattering from Polymer Solutions*, Academic Press, New York, 1972.
- Hunt, B. J., and S. R. Holding (eds.): *Size Exclusion Chromatography*, Chapman & Hall, New York, 1989.
- Hunt, B. J., and M. J. James (eds.): *Polymer Characterization*, Chapman & Hall, New York, 1993.
- Janca, J. (ed.): *Steric Exclusion Liquid Chromatography of Polymers*, Dekker, New York, 1983.
- Kratochvil, P.: *Classical Light Scattering from Polymer Solutions*, Elsevier Applied Science, New York, 1987.
- Pecora, R. (ed.): *Dynamic Light Scattering: Applications of Photon Correlation Spectroscopy*, Plenum Press, New York, 1985.
- Peebles, L. H., Jr.: *Molecular Weight Distributions in Polymers*, Wiley, New York, 1971.
- Provdar, T. (ed.): *Size Exclusion Chromatography*, ACS, Washington, DC, 1984.
- Provdar, T. (ed.): *Detection and Data Analysis in Size Exclusion Chromatography*, ACS, Washington, DC, 1987.
- Provdar, T. (ed.): *Chromatography of Polymers—Characterization by SEC and FFF*, ACS, Washington, DC, 1993.
- Remp, P., and G. Weill (eds.): *Polymer Thermodynamics and Radiation Scattering*, Hüthig & Wepf, Basel, Switzerland, 1992.

- Roe, R. J. (ed.): *Computer Simulation of Polymers*, Prentice Hall, Englewood Cliffs, NJ, 1991.
- Slade, P. E. (ed.): *Techniques and Methods of Polymer Evaluation, vol. 4: Polymer Molecular Weights*, Part II, Dekker, New York, 1975.
- Smith, C. G., W. C. Buzanowski, J. D. Graham, and Z. Iskandarani (eds.): *Handbook of Chromatography: Polymers*, vol. 2, CRC Press, Boca Raton, FL, 1993.
- Smith, C. G., N. E. Skelly, C. D. Chow, and R. A. Solomon: *Handbook of Chromatography: Polymers*, CRC Press, Boca Raton, FL, 1982.
- Snyder, L. R., and J. J. Kirkland: *Introduction to Modern Liquid Chromatography*, Wiley, New York, 1979.
- Tung, L. H.: *Fractionation of Synthetic Polymers—Principles and Practices*, Dekker, New York, 1977.
- Wu, C.-S. (ed.): *Handbook of Size Exclusion Chromatography*, Dekker, New York, 1995.
- Yau, W., J. J. Kirland, and D. Bly: *Modern Size-Exclusion Liquid Chromatography*, Wiley, New York, 1979.

7 Viscous Flow

7.1 INTRODUCTION

Polymers are shaped into useful objects using a variety of **forming processes**. In Chapters 13 and 14, we will study engineering aspects of polymer manufacturing in several of these processes, including calendaring, compression molding, extrusion, fiber spinning, film blowing, injection molding, and spin coating, all of which are used to fashion polymers into objects with defined size, shape, and surface finishes. In many of these processes, a liquid or molten polymer is forced through channels under the action of external forces to transport a specified amount of the flowing material to one or more specially shaped molds. In the mold, the polymer must flow into even smaller openings to imprint a desired shape. Subsequent cooling of the mold or molten polymer exiting the mold solidifies the material and produces solid articles in specified shapes [1,2]. An important recent extension of this approach involves the use of printing technology to create intricate three-dimensional objects [3]. This so-called **3D printing** methodology builds up a macroscopic object layer by printed layer. By using liquid polymer and colloidal suspension *inks* in a variety of chemistries, it is able to create objects with well-defined, spatially resolved material compositions not possible with conventional polymer forming processes. As with conventional polymer processing, however, the method takes advantage of the ability of polymers to flow in a specified manner under an applied load to control the thickness, spatial distribution, and chemical makeup of the finished article. The force required to fill a mold in a preset time or to achieve a specified flow rate in a print head nozzle or channel with known dimensions influences capacity and production rates in all polymer forming processes. It is therefore important to understand the fundamental physical variables that govern polymer resistance to flow.

Whenever matter is subjected to external forces, the response involves flow or deformation of some sort. **Rheology** is defined as the science of deformation and flow of matter. The breadth of the field is evident from the motto of the *Society of Rheology*. This motto is a quotation from the Greek philosopher Heraclitus, who said “Everything flows.” While many forms of matter are indeed studied by rheologists, polymers in the form of melts, solutions, and suspensions have always been of great interest since the founding of the society in 1929. This interest can be readily traced to the coupling of polymer flow properties with their molecular structure, thermodynamics, and morphology. It is sustained by the unique sensitivity of bulk rheological properties of many materials to their micro- and mesoscale features, as well as by the ease with which rheological information about many complex materials can be accessed from straightforward measurements.

This chapter provides an introduction to viscous flow properties of polymers. The emphasis will be on measurement techniques for characterizing the viscous flow of polymer solutions and melts, and on interpretation of data obtained from such

measurements. Simple models for viscous polymer flows are useful for deducing structural information such as molecular weight, random coil size, and branching from such measurements, and are therefore also treated in the chapter. Chapter 8 extends this coverage to elastic properties of polymers, which can be as important as viscous flow properties in fabrication processes. Chapters 9 and 10 describe mechanical properties and failure characteristics of polymers.

7.2 VISCOSITY

7.2.1 DEFINITIONS AND MICROSCOPIC ORIGINS

We have used the term *viscosity* up to now without a strict definition. The magnitude of a fluid's **viscosity** provides a measure of its resistance to flow. Viscosity is also related to the energy dissipated by a fluid in motion under the action of an applied force. In polymers, energy dissipation arises fundamentally from friction between molecules as they slide by each other in flow. Both the geometry of the polymer repeat unit and the strength of intermolecular forces between these units therefore determine the magnitude of the viscosity. Polymer solutions are generally less viscous than their melts because solvent present in the former mediate and in many cases lubricate sliding contacts between molecules. Polymer liquids made up of higher molecular-weight molecules are also usually more viscous because of the larger number of repeat units per polymer chain, which increases the overall friction. Thermodynamic state variables such as pressure and temperature can also affect viscosity. Typically the viscosity of polymer melts decreases with increasing temperature and increases with pressure. The flow resistance of a polymer during a fabrication process is therefore a function of the unique chemical characteristics of the material and the processing conditions such as temperature and applied force.

The device depicted in Figure 7.1. is termed a **planar Couette shear** cell. It provides a simple means for measuring the viscosity of a polymer and also allows for an operational definition of viscosity. In this device, a liquid is sandwiched between two parallel planes separated by a distance d in the y direction. The bottom plane is held stationary and the top plane moves in the x direction with an average speed U in the

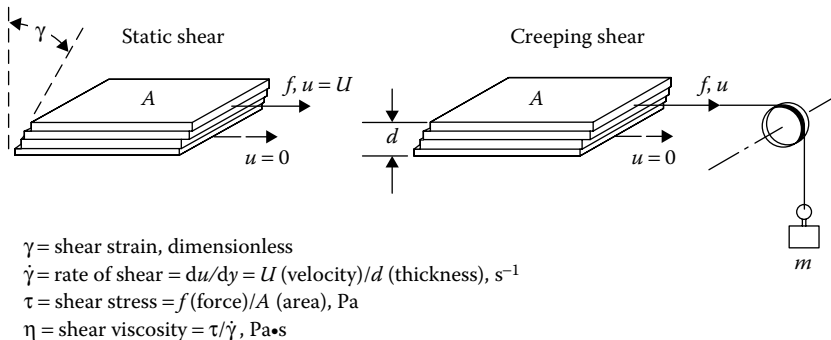


FIGURE 7.1 Arrangement for producing laminar, unidirectional shear flow between parallel plates (see Table 7.1).

direction x , parallel to the applied force $f_x = mgh$, where g is the gravitation constant and h is the vertical distance. If U is maintained small, fluid planes will slide by each other with speeds u_x between 0 and U , but always remain parallel to the direction of the applied force. This type of flow is termed a rectilinear **laminar flow**, and the speed at any point in the fluid is a linear function of its location y between the top and bottom planes:

$$u_x(y) = \frac{U}{d}y \quad (7.1)$$

Because u_x varies only in the direction y , perpendicular to the direction in which fluid planes slide, this type of flow is also termed a laminar **shear flow**. The force per unit area is the same everywhere in the fluid and is termed the **shear stress** $\tau_{yx} = \tau_s$:

$$\tau_s = \frac{f_x}{A} \quad (7.2)$$

The rate of change of velocity along y is also constant throughout the fluid $du_x/dy = U/d$ and is termed the **shear rate** $\dot{\gamma}$.

$$\dot{\gamma} = \frac{U}{d} \quad (7.3)$$

The ratio of shear stress to shear rate defines the fluid's shear viscosity:

$$\eta \equiv \frac{\tau_s}{\dot{\gamma}} \quad (7.4)$$

The viscosity of a fluid therefore determines the amount of force that must be applied to maintain the motion of the moving plane. The force resisting motion is for this reason termed the **viscous drag** and is analogous to the more familiar friction force that resists the relative motion of two solid bodies in contact. As with friction between solid bodies, the viscosity transforms mechanical work to heat and a vessel containing a high-viscosity polymer will become noticeably warm upon persistent shearing of the polymer.

Provided laminar shear flow can be maintained in the apparatus and the heat dissipated by viscous flow is removed at a fast enough rate to maintain the temperature of the fluid constant, the apparatus in Figure 7.1 provides a simple tool for measuring viscosity. In particular, if the velocity U and the force f acting on the upper plane are measured, the shear stress τ_s and the shear rate $\dot{\gamma}$ can be determined from Equations 7.2 and 7.3, and the viscosity of the fluid obtained as the slope of a plot of τ_s versus $\dot{\gamma}$. This method for measuring viscosity is limited to fluids with high enough viscosities that can be maintained in the gap during measurements. Other methods for measuring viscosity of low- and high-viscosity liquids will be discussed later.

Units for rheological variables introduced in this section are provided in Table 7.1. On dimensional grounds, it is possible to write down an expression for the rate of energy dissipated by viscous drag (**viscous dissipation**) per unit volume of fluid \dot{q}_T . From Equation 7.2, the shear stress has dimensions of force per unit area. Thus, $[\tau] = [f/A] = M/LT^2$, where M , L , and T are the fundamental dimensions of mass,

TABLE 7.1
Viscosity in Laminar, Unidirectional Flow

		SI Units	Metric Units	Engineering Units
Given:	Mass, m	0.454 kg	454 g	1.00 lb _m
	Velocity, U	0.305 m/s	30.5 cm/s	1.00 ft/s
	Gap width, d	61×10^{-6} m	6.1×10^{-3} cm	2.00×10^{-4} ft
	Area, A	9.3×10^{-4} m ²	9.3 cm ²	0.0100 ft ²
Then:	Constant, g	9.81 m/s ²	981 cm/s ²	32.2 ft/s ²
	Stress, τ	4.79 kPa	4.79×10^4 dyne/cm ²	3.22×10^3 lb _m /ft·s
	Shear rate, $\dot{\gamma}$	5.00×10^3 s ⁻¹	5.00×10^3 s ⁻¹	5.00×10^3 per s
	Viscosity, η	0.958 Pa·s	9.58 poise	0.644 lb _m /ft·s

length, and time, respectively. Likewise, $[\dot{\gamma}] = T^{-1}$, $[\eta] = M/LT$, and $[\dot{q}_T] = M/LT^3$. Comparing dimensions we see $[\dot{q}_T] = [\tau\dot{\gamma}]$, implying that $[\dot{q}_T] = k\tau\dot{\gamma}$, where k is a dimensionless constant with value of unity in this case. We therefore finally obtain

$$\dot{q}_T = \tau\dot{\gamma} = \eta\dot{\gamma}^2 = \frac{\tau^2}{\eta} \quad (7.5)$$

In a well-insulated polymer forming process, it is this dissipated energy generated by viscous flow that produces the previously referenced rise in temperature. Because of the high shear rates accessed in many polymer forming processes (see Table 7.2), the amount of viscous energy dissipated during processing can be so large that provided the equipment is properly insulated, no external heating is required to maintain the polymer above its melting point.

Energy dissipated by viscous flow in a macroscopic polymer forming process originates from friction between microscopic repeat units that constitute the polymer chain. The friction coefficient per repeat unit, the **monomeric friction coefficient** (ζ_m), is a function of the geometry of the repeat unit and its chemistry. Molecules such as polystyrene and poly(methyl methacrylate) that possess stiff,

TABLE 7.2
Shear Rates for Representative Polymer Forming Processes

Compression molding	$\dot{\gamma} = 1 - 10$ s ⁻¹
Calendering	$\dot{\gamma} = 10 - 100$ s ⁻¹
Extrusion	$\dot{\gamma} = 100 - 1,000$ s ⁻¹
Injection molding	$\dot{\gamma} = 1,000 - 10,000$ s ⁻¹

Source: Pezzin, G., *Materie Plastiche ed Elastomerie*, Instron Corporation, Canton, MA, August 1962 (English translation).

bulky repeat units have high monomeric friction coefficients, $\zeta_{m,PS} = 2.9 \times 10^{-6}$ and $\zeta_{m,PMMA} = 5.3 \times 10^{-5}$ in units of Pa-s-m at 125°C [5]. However, molecules such as poly(dimethyl siloxane) and polybutadiene made up of flexible, less bulky repeat units possess quite low monomeric friction coefficients, $\zeta_{m,PDMS} = 2.2 \times 10^{-12}$ and $\zeta_{m,PBD} = 1.6 \times 10^{-11}$ again in units of Pa-s-m at 125°C. Monomeric friction coefficients for molecules, such as poly(vinyl chloride) and poly(vinyl acetate), which possess compact polar repeat units that can interact via strong dipole-dipole secondary bonds, are typically intermediate between these extremes, $\zeta_{m,PVC} = 2.7 \times 10^{-8}$ Pa-s-m and $\zeta_{m,PVAc} = 1.1 \times 10^{-9}$ Pa-s-m at 125°C. A more complete listing of ζ_m values for polymers and the methods used to determine them are provided by Ferry [5].

In the simplest polymer systems, for example, melts of low-molecular-weight polymers, motion of individual polymer chains is completely decoupled from neighboring molecules. For these systems, the overall friction coefficient of a single molecule ζ_p is simply obtained by summing over all monomers present in that molecule:

$$\zeta_p = \sum_{i=1}^x \zeta_{m_i} = x\zeta_m \quad (7.6)$$

where:

$x = M/M_0$, the degree of polymerization of the polymer

M is the molar mass of the polymer

M_0 is the repeat unit molar mass

Friction is generated at the microscopic level by relative motion between polymer molecules in flow. In a simple shear flow such as that introduced in Section 7.2.1, the relative velocity between a polymer molecule and its surroundings can be estimated as $v_c = \dot{\gamma} R_g$, where R_g is the polymer coil radius in the melt. If the rate of shear is so small that it does not perturb the polymer shape, the rate of viscous dissipation per molecule \dot{q} is therefore given by

$$\dot{q} = \zeta_p v_c^2 = \zeta_p \dot{\gamma}^2 R_g^2 \quad (7.7)$$

The rate of viscous dissipation per unit volume \dot{q}_T is related to the rate of dissipation per molecule by

$$\dot{q}_T = \Gamma \dot{q} \quad (7.8)$$

where:

Γ is the number of polymer molecules per unit volume

Substituting for ζ_p and \dot{q} in Equation 7.8 yields

$$\dot{q}_T = \Gamma x \zeta_m R_g^2 \dot{\gamma}^2 \quad (7.9)$$

Equating Equations 7.5 and 7.9 yields the final result:

$$\eta = x \Gamma R_g^2 \zeta_m \quad (7.10)$$

The macroscopic shear viscosity η of the polymer melt is therefore determined by the monomer chemistry and geometry, packing density, and molecular size. Later we will see that in melts $R_g^2 \approx xa^2$ and $\Gamma = \rho N_{AV}/M$, implying that

$$\eta = A' \frac{\rho x^2 N_{AV} a^2 \zeta_m}{M} \quad (7.11)$$

where:

a is the characteristic size of a polymer repeat unit or segment

N_{AV} is the Avogadro's number

ρ is the mass density of the melt

A' is a numerical factor of order 1/6

Thus, the shear viscosity is predicted to increase linearly with molecular weight and monomer friction coefficient, which is consistent with experimental observations for low-molecular-weight polymer melts.

If the polymer is in solution, several other effects become important. For example, friction between solvent molecules also makes a contribution to the measured viscosity. The overall solution viscosity can therefore be written as $\eta^p + \eta_s$, where η^p is the polymer contribution and η_s is the solvent contribution. Solvents can cause swelling (good solvents) or collapse (poor solvents) of polymer chains in solution, which changes the expressions relating R_g and Γ to x and a . Finally, the above results were computed under the assumption that each segment of a polymer chain is in the **free draining** limit wherein it experiences the local velocity imposed by an imposed flow field. In polymer solutions, motion of a polymer chain segment can affect the solvent velocity around it, which will in turn affect the velocity of neighboring segments. This effect, termed **hydrodynamic interaction**, couples the frictional drag between molecular segments at remote locations on the same molecule, as well as between segments on separate molecules.

7.2.2 NON-NEWTONIAN VISCOSITY

For many low-molecular-weight liquids, viscosity is a **material property** and, by definition, only depends on thermodynamic state variables such as temperature, pressure, and concentration. These fluids are collectively termed **Newtonian Liquids** because they satisfy Newton's law of viscosity, $\tau_s = \mu(du_x/dy) = \mu\dot{\gamma}$, where μ , the Newtonian viscosity, is independent of τ_s or $\dot{\gamma}$. The viscosity of many polymer melts and solutions depends on thermodynamic state variables and flow conditions (τ_s and $\dot{\gamma}$, in the above example). In these systems, viscosity is not a material property because it cannot be uniquely defined from the knowledge of the thermodynamic state of the fluid alone. It is nonetheless possible to define an **apparent viscosity**, $\eta(\dot{\gamma}) \equiv \tau_s(\dot{\gamma})/\dot{\gamma}$, that quantifies the shear rate-dependent flow resistance. A plot of $\eta(\dot{\gamma})$ versus $\dot{\gamma}$ for a particular fluid is therefore termed its **flow curve**.

Figure 7.2 depicts $\tau_s(\dot{\gamma})$ versus $\dot{\gamma}$ and the resulting flow curves for a variety of non-Newtonian fluids. The broken lines in the figure are the expected behavior for a Newtonian (N) fluid. The simplest type of non-Newtonian behavior is displayed

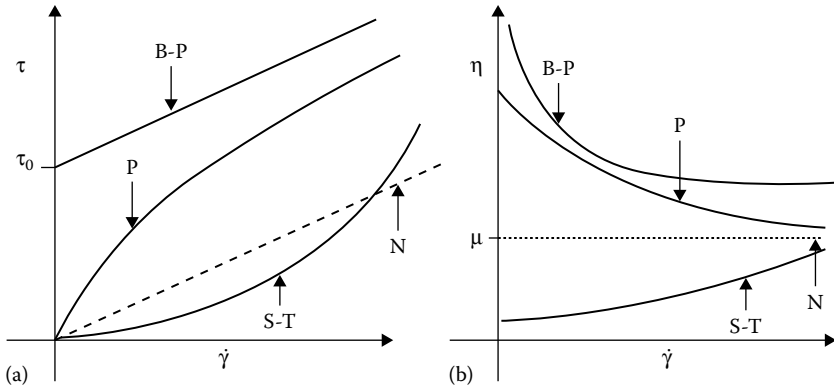


FIGURE 7.2 Newtonian and non-Newtonian fluids: (a) Shear stress versus shear rate; (b) apparent viscosity versus shear rate. B-P, Bingham plastic; N, Newtonian; P, pseudoplastic or shear thinning; S-T, shear thickening.

by a group of materials collectively termed **Bingham plastics** (B-Ps). This type of material initially responds to an applied shear stress in much the same way as a solid would, that is, by deforming but not flowing. When the shear stress exceeds a critical value $\tau_s = \tau_0$ known as the yield stress, the material flows in an analogous way to a simple Newtonian liquid, $\tau_s(\dot{\gamma}) = \mu\dot{\gamma}$, where μ is the viscosity. Thus, if a B-P is placed in the shear apparatus depicted in Figure 7.1 and the applied force $f_x = mgh$ gradually increased from 0, say by slowly varying m , the average velocity U of the upper plane would be 0 until the condition $f_x/A \geq \tau_0$ is achieved. By Equation 7.3, the shear rate in the material will therefore be zero up to the yield stress and then begin to increase linearly with the shear stress. Although B-Ps such as blood, toothpaste, ketchup, mayonnaise, and many paints are quite commonplace in nature, this type of behavior is rarely observed in pure synthetic polymers. Highly filled polymer melts, polymer–nanoparticle composites, and solutions of ultrahigh-molecular-weight polymers possess such large viscosities that their flow rates at low stresses can be well below the resolution of industrial measurement equipment, producing apparent B-P flow behavior. However, in these materials, the flow response at stresses above the apparent yield stress is non-Newtonian, so that the second requirement for B-P behavior is typically not met.

It is evident from Figure 7.2 that for some fluids the apparent viscosity $\eta(\dot{\gamma})$ is an increasing function of shear rate. For these fluids, the higher the rate of shear the larger is the measured fluid resistance. This type of fluid is therefore termed **shear thickening** (S-T). S-T behavior is not commonly observed in polymer melts or solutions in good solvents. Some S-T materials also expand, or dilate, in response to an applied shear stress. The term **dilatant** is therefore sometimes used to describe S-T fluids. S-T behavior is most often observed in multiphase materials, for example, suspensions, emulsions, slurries, and polymer blends, and is often a result of shear-induced changes in structure. For example, in suspensions sheared at high rates, shear promotes particle–particle collisions and coalescence. The large, so-called lubrication forces produced by fluids trapped between the particles can lead to a viscosity increase. Fluids for which $\eta(\dot{\gamma})$ is a

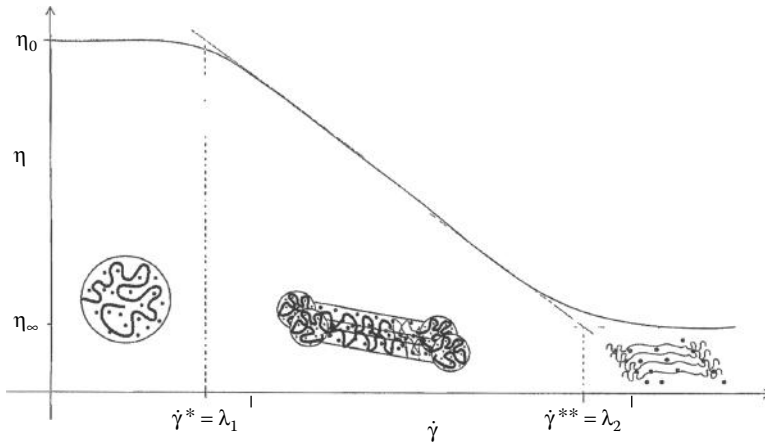


FIGURE 7.3 Flow curve for a shear-thinning polymer solution. η and $\dot{\gamma}$ are both plotted on logarithmic scales for clarity. The cartoon provides a simplified view of how polymer structure evolves in flow. Dots in the figure represent the surrounding molecules.

decreasing function of shear rate offer less resistance to shear at higher shear rates. This type of fluid is therefore termed **shear thinning** or **pseudoplastic (P)**. The vast majority of non-Newtonian fluids are shear-thinning liquids; most polymer melts and solutions of commercial interest also manifest shear-thinning properties in the shear rate range where they are typically processed (Table 7.2).

The flow curve for a representative shear-thinning polymer solution is depicted in greater detail in Figure 7.3. Depending on the shear rate, either Newtonian or non-Newtonian behavior can be observed. For example, at shear rates well below a first critical value $\dot{\gamma}^*$, the fluid exhibits Newtonian flow response. The viscosity η_0 in the limit of zero-shear rate is termed the **zero-shear viscosity** and is a material property. At a given temperature and pressure, η_0 is a function of polymer molecular weight, architecture, solution concentration, repeat unit chemistry, and structure. At shear rates above $\dot{\gamma}^*$, the fluid is a shear-thinning liquid. The rate of decrease of apparent viscosity with shear rate, $n(\dot{\gamma}) = -d \log \eta(\dot{\gamma}) / d \log \dot{\gamma}$, is an important fluid characteristic. In many polymers, $n(\dot{\gamma})$ is constant, $n(\dot{\gamma}) = n < 1$, particularly at high shear rates, and is termed the **shear-thinning exponent**. Generally, n is a function of polymer molecular weight, molecular-weight distribution, solution concentration and architecture. Typically, n is larger for high-molecular-weight polymer melts and solutions than for low-molecular-weight ones. Narrow molecular-weight distribution polymer melts and solutions are also usually more shear thinning than polydisperse or branched melts and solutions. Newtonian behavior is again observed at shear rates above a second critical value $\dot{\gamma}^{**}$. This last type of behavior is more commonly seen in polymer solutions than in melts. The low-shear-rate and high-shear-rate Newtonian flow regions of the curve are designated the **lower Newtonian regime** and the **upper Newtonian regime**, respectively. The viscosity η_∞ in the upper Newtonian regime is strictly a material property and is typically many orders of magnitude lower than η_0 , but usually larger than the solvent viscosity η_s . η_∞ is also not as sensitive to polymer molecular weight and concentration as is η_0 .

The cartoon in Figure 7.3 provides a reasonable, if oversimplified, explanation of why shear thinning occurs and for why polymers are especially susceptible to shear thinning. The main premise is that polymer molecules are dynamic objects and the structure they adopt in shear reflects a balance between the randomizing effect of thermal forces, which favor the ball-like or **random coil structure** on the extreme left, and the ordering effects of shear forces, which tend to align molecules to produce the elongated, cigar-like structures on the extreme right. When the rate of shear $\dot{\gamma}$ falls below the intrinsic rate λ_1^{-1} at which molecules recover their random coil structure, this structure is preserved in flow. λ_1^{-1} is therefore termed the characteristic polymer relaxation rate and λ_1 the longest polymer **relaxation time**. The flow resistance offered by each molecule at shear rates $\dot{\gamma} < \lambda_1^{-1}$ can, therefore, be crudely described as Stokes drag on a polymer sphere with diameter $2R_h$, where R_h is termed the **hydrodynamic radius** of the sphere.

At low shear rates, R_h does not change with flow rate and the fluid's flow resistance is the same at all rates. Newtonian fluid behavior is therefore observed. At higher shear rates, shear becomes more competitive with relaxation, and a combination of three effects is seen. First, shear tends to orient polymer molecules along the flow direction. Second, shear reduces the degree to which neighboring molecules intertwine or entangle. Finally, shear increases the separation distance between the two ends (**end-to-end distance**) of a polymer molecule. The first two effects render polymer molecules more streamlined, which reduces their resistance to flow and causes the apparent viscosity to decrease relative to η_0 . The third effect increases the flow resistance for reasons that will become clear later, but is generally smaller than the first two. Thus, as the shear rate is increased progressively above λ_1^{-1} , flow resistance falls as polymer molecules become more oriented and less entangled, explaining the gradual reduction in apparent viscosity observed. Eventually, at shear above $\dot{\gamma}^{**}$, molecules become nearly perfectly aligned and fully unentangled, so that further decreases in flow resistance are no longer possible. A second Newtonian flow regime with viscosity $\eta_\infty \ll \eta_0$ is therefore observed.

The ratio of the fluid relaxation time λ_1 to the timescale for flow t_f defines a dimensionless group termed the **Deborah number**, $De = \lambda_1/t_f$. This group has been used in the literature to characterize deviations from Newtonian flow behavior in polymers [6]. Specifically, in flows such as simple steady shear flow where a single flow time $t_f = \dot{\gamma}^{-1}$ can be defined, it has been observed that for $De \ll 1$, a Newtonian fluid behavior is observed, whereas for $De \gg 1$, a non-Newtonian fluid response is observed. However, in flows where multiple timescales can be identified, for example, shear flow between eccentric cylinders, the Deborah number is clearly not unique. In this case, it is generally more useful to discuss the effect of flow on polymer liquids in terms of the relative rates of deformation of material lines and material relaxation. In a steady flow, this effect can be captured by a second dimensionless group termed the **Weissenberg number**, $Wi \equiv \dot{\kappa}\lambda$, where $\dot{\kappa}$ is a characteristic deformation rate and λ is a characteristic fluid relaxation time. For polymer liquids, λ is typically taken to be the longest relaxation time λ_p , and for steady shear flow, $\dot{\kappa} = \dot{\gamma}$, which leads to $Wi \equiv \dot{\gamma}\lambda_p$.

Wi therefore characterizes the relative intensity of fluid relaxation and shear-induced molecular alignment. Thus, for $Wi \ll 1$, relaxation outcompetes shear-induced orientation and disentanglement, so shear has little effect on polymer structure and a Newtonian fluid behavior is observed. However, for $Wi \gg 1$, polymer molecules are

highly oriented by shear and non-Newtonian, shear-thinning fluid behavior observed. In flows characterized by very high Weissenberg numbers, polymer molecules are deformed so quickly that no relaxation is possible. This causes the material to exhibit solid-like properties. This relationship between the Weissenberg number and the fluid response is not necessarily limited to polymer liquids. Even simple fluids sheared under conditions where $Wi \gg 1$ could be expected manifest non-Newtonian properties. As an illustration, water has a relaxation time of order 3×10^{-12} s at 20°C . A shear rate of order 3.3×10^{13} s^{-1} is therefore required for the condition $Wi \approx 1$ to be achieved in a simple shear flow. This shear rate is well outside the range accessible to experiment, so water may be safely regarded as a Newtonian fluid. Polymer melts and solutions typically possess relaxation times in the range of 10^{-3} – 10^3 s; it therefore not at all surprising that their non-Newtonian flow characteristics are readily observed.

7.2.3 MODELS FOR THE VISCOSITY OF NON-NEWTONIAN FLUIDS

Numerous models have been proposed for non-Newtonian flow of polymer liquids. These models, collectively termed **constitutive equations**, range in complexity from simple multiparameter generalizations of observed behavior (phenomenological models) to detailed molecular theories that relate macroscopic observables such as shear stress and normal stress differences to polymer properties. Although significant progress has been made recently in the development of accurate molecular theories for polymer deformation in flow [7–12], molecular constitutive equations for non-Newtonian flow are not as widely used and require aspects of mathematics that are beyond the scope of a first course in polymer science. We will therefore focus primarily on phenomenological models for non-Newtonian fluids. To the engineer, a mathematical model for viscosity is a means to an end. Among other quantities, bulk flow rates in pipes and other conduits are usually desirable. The simple problem of deriving an equation for the velocity profile in laminar flow, for example, becomes such a formidable task with some models that, regardless of their accuracy, these models are of limited practical use.

The most effective model for non-Newtonian flow is the Ostwald–de Waele two-parameter, **power-law fluid** model [13]. The popularity of this model is easily traced to its tractability in mathematical manipulations. In the power-law model, the apparent viscosity $\eta = \tau_{xy}/|du_x/dy| = \tau/\dot{\gamma}$ of a polymer fluid subject to a simple steady shear flow is given by

$$\eta = K \dot{\gamma}^{n-1} \quad \text{or} \quad \tau = K \dot{\gamma}^n \quad (7.12)$$

where:

K has units of $\text{Pa}\cdot\text{s}^n$ in the SI system and is termed the fluid consistency

n is a dimensionless number related to the shear-thinning exponent introduced earlier and is termed the power-law index

Apart from its simplicity, the power-law model is attractive because it can reproduce Newtonian ($n = 1$), shear-thinning ($n < 1$), and S-T ($n > 1$) flow characteristics. It can be seen from the flow curves for a polymer melt (Figure 7.4) that Equation 7.12 would serve well over several decades of shear rate but would fail as the melt approaches

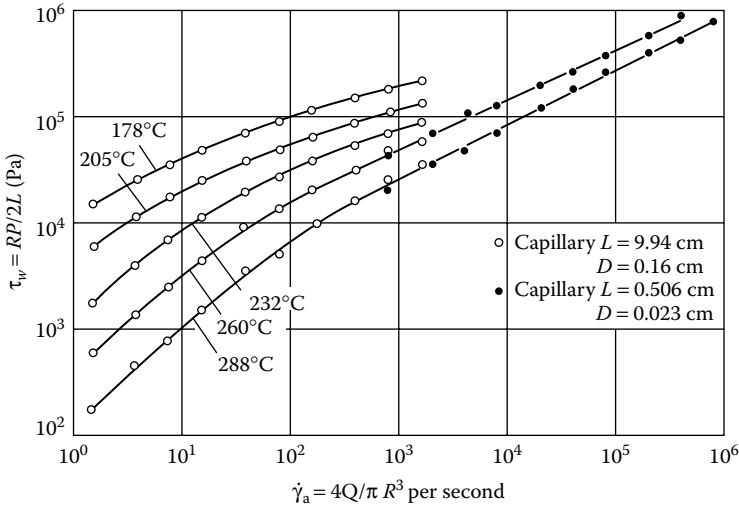


FIGURE 7.4 Flow curves for a commercial sample of polystyrene at various temperatures obtained using capillary rheometry.

the Newtonian flow regime. In polymer solutions (Figures 7.5 and 7.6), the power law fluid model is only adequate over a decade or so of shear rate. In the case of solutions, the lines are therefore drawn according to a different mathematical model [16]. As stress or rate of shear becomes small, the viscosities of almost all polymer melts, solutions, latexes, and some other dispersions appear to approach a constant

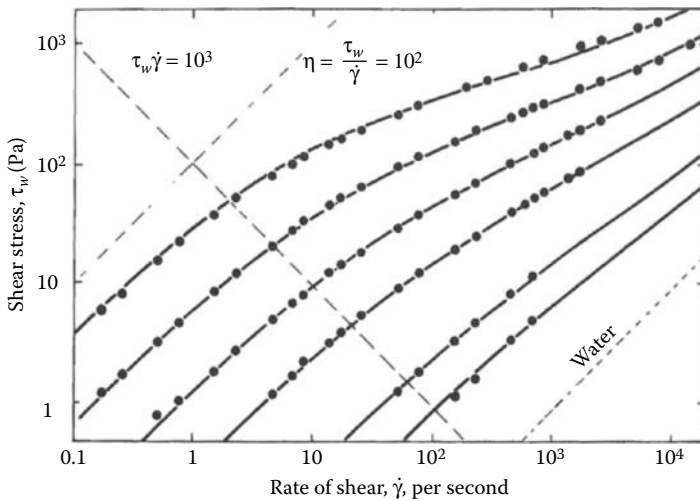


FIGURE 7.5 Flow curves for six concentrations of polyacrylamide in water. The lines through the data are model predictions. (Data from Rodriguez, F. and L. A. Goettler, *Trans. Soc. Rheol.*, 8, 3, 1964.)

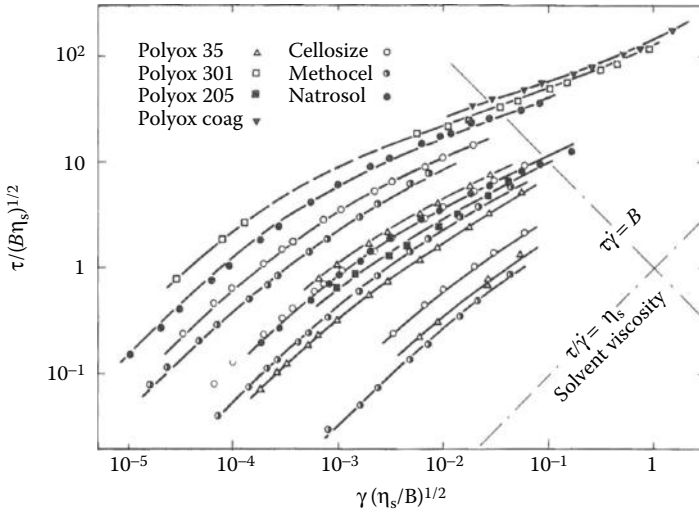


FIGURE 7.6 Flow curves for polyethylene oxide solutions in water. The lines through the data are model predictions. (Data from Rodriguez, F., *Trans. Soc. Rheol.*, 10, 169, 1966.)

value η_0 , which is not predicted by the power-law model. Instead, the model predicts an infinite viscosity when either τ or $\dot{\gamma}$ goes to 0.

The **Ellis model** is a three-parameter model and can be thought of as a mathematical combination of a Newtonian fluid model at low values of τ and a power-law model at high values of τ [17].

$$\left(\frac{\eta_0}{\eta} - 1 = k\tau^s \right) \text{ or } \eta_0 \dot{\gamma} = \tau + k\tau^{1+s} \tag{7.13}$$

Although this model correctly predicts a transition to Newtonian fluid behavior at low shear stresses or shear rates, at high rates the apparent viscosity goes to 0. However, as discussed in Section 7.2.2, there is evidence that the apparent viscosity of polymer solutions approaches a constant value η_∞ less than η_0 but greater than the solvent viscosity η_s as $\dot{\gamma}$ becomes very large. Other three-parameter models have been proposed by Williamson [18], Krieger and Dougherty [19], Eyring and Powell [20], and Reiner-Philippoff [21] that can describe fluids with finite values of both η_∞ and η_0 . Some years ago, Denny and Brodkey proposed an equation based on kinetic theories that included both η_0 and η_∞ [22]. The equation contains four other parameters. However, when two of these parameters are set equal to each other, the equation reduces to

$$\frac{\eta_0 - \eta}{\eta - \eta_\infty} = (\lambda \dot{\gamma})^s \tag{7.14}$$

Cross used this equation to correlate the flow properties of silicones and polyurethanes in both steady and oscillatory flows, and the expression is now termed the **Cross model**. The constant λ has units of time, and Cross demonstrated that it can

be regarded as a **characteristic relaxation time** for a non-Newtonian fluid [23]. A similar four-parameter expression, termed the **Carreau model**, was proposed by Carreau [24] which can fit the entire flow curve of many polymer solutions:

$$\frac{\eta_0 - \eta}{\eta - \eta_\infty} = [1 + (\lambda\dot{\gamma})^2]^{[(s-1)/2]} \quad (7.15)$$

In the above equation, the variable λ may again be regarded as the characteristic relaxation time. In polymer melts, η_∞ is often very difficult to measure experimentally because of the very high shear rates needed and resulting viscous heating. As a result, Equation 7.15 with $\eta_\infty = 0$ is often used to fit experimental data.

Example 7.1

Assume that the flow data for the most concentrated polyacrylamide solution in Figure 7.5 can be approximated by the Cross model (Equation 7.14 with $\eta_\infty = 0$) with $\eta_0 = 25$ Pa·s. What is the characteristic relaxation time λ for this solution?

Solution: The stresses at shear rates of 10 and 10^4 s⁻¹ are roughly 130 and 1700 Pa, respectively. The corresponding apparent viscosities are 13 and 0.17 Pa·s. Substituting in Equation 7.14 yields

$$\frac{25}{13} = 1 + (10\lambda)^b \quad \text{and} \quad \frac{25}{0.17} = 1 + (10^4\lambda)^b$$

Eliminating λ by taking ratios yields

$$\left(\frac{10^4}{10}\right)^b = \frac{146}{0.92} \Rightarrow b = 0.73 \quad \text{and} \quad b^{-1} = 1.37$$

Then,

$$10\lambda = \left(\frac{25}{13} - 1\right)^{1.37} \Rightarrow \lambda = 0.90 \text{ s}$$

Often polymer properties only in a narrow range of shear rates or stresses is important. In molecular weight characterization, for example, only η_0 is used. In capillary flow at high shear rates, the shear stress falls off rapidly away from the wall. Whether the viscosity at the centerline is finite or infinite may therefore have little effect on polymer flow calculations this geometry. Thus, the power law fluid model can be quite adequate in calculating such things as true shear rate at the wall for a non-Newtonian fluid. In most cases, η_0 can be estimated with more confidence than η_∞ . Mechanical degradation [25], static pressure effects [26], melt fracture [27], and viscous heating [28,29] compromise high-shear rate data in melts. However, often a reliable measurement of η_0 usually is limited only by the patience of the investigator and the long-term stability of the system being measured. It follows that η_0 should precede η_∞ in importance when attempting to fit any constitutive equation with four or more unknown parameters to

experimental data. One note of caution is that many values of η_0 in the literature were not measured directly but extrapolated from other data using an assumed model. Care must therefore be exercised in using published η_0 values for data reduction.

7.3 VISCOMETRY

The most common instrument used for viscosity measurements in low-viscosity liquids is the capillary viscometer. In this instrument, a liquid is made to flow under its own potential head through a narrow capillary with a well-defined length and cross section. The volumetric flow rate Q of a simple Newtonian liquid undergoing laminar flow in a capillary of diameter d and length l is given by Poiseuille's equation:

$$Q = \frac{\pi d^4 \Delta p}{128 \eta l} \quad (7.16)$$

where:

η is the viscosity of the liquid

Δp is the pressure difference between the fluid at the inlet and the outlet

Several viscometer configurations have been used for polymer solutions. The simplest is the Ostwald viscometer depicted in Figure 7.7. In this instrument, the lower bulb is first filled with liquid of interest. The liquid is then sucked slowly into the upper bulb until its lower meniscus rises slightly above the upper etch mark. Because the volume of the lower bulb is typically much larger than that of the upper one, it is not emptied

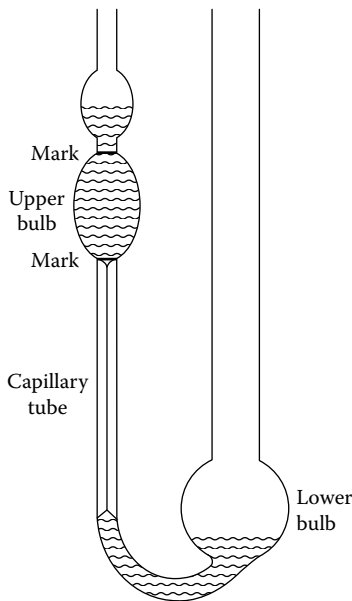


FIGURE 7.7 Ostwald viscometer. Viscosity is determined by measuring the time t required for fluid level to fall from the upper to the lower mark.

by this process. The viscometer is then typically immersed in a constant temperature bath for a sufficiently long time so that the temperature of the liquid in both bulbs equilibrates with the bath fluid. The liquid in the upper bulb is subsequently allowed to flow back into the lower one under the action of gravity and the time t required for the meniscus to travel from the upper to the lower etch mark recorded.

If the volume of fluid in the upper bulb is V , the average volumetric flow rate of fluid during the measurement is $\bar{Q} = (V/t) = \pi d^4 \rho g \bar{h} / 128 \eta l$, where \bar{h} is the average head of liquid driving flow during the period of observation and ρ is the liquid's density. This equation can be rearranged to give

$$\eta = A \rho t \quad (7.17)$$

where:

$A = \pi d^4 g \bar{h} / 128 V l$ is a constant that depends on the geometry of the instrument and can be determined from calibration experiments using liquids with known η and ρ

Thus, by simply measuring t , the **kinematic viscosity** $\nu = \eta/\rho$ of any low-viscosity Newtonian liquid can be determined. It is important to note that because the lower bulb contains liquid during the measurement, \bar{h} depends on the liquid level in both arms of the viscometer. Calibration experiments must therefore be performed with the same initial head of liquid as the actual measurements to yield accurate results. In practice, Equation 7.17 leads to small but systematic errors in viscosity data, particularly for low viscosity liquids. The source of errors can be traced to omission of the energy required to accelerate the liquid as it enters and leaves the capillary. When this effect is taken into account, Equation 7.17 reads [30]

$$\nu = A t + \frac{B}{t^2} \quad (7.18)$$

where:

B is the geometric constant that can also be determined by a calibration experiment

One disadvantage of the **Ostwald viscometer** is that viscosity measurements at multiple solution concentrations can be quite time consuming. As discussed in Section 7.4.2, the intrinsic viscosity of a polymer solution can only be determined if polymer solution viscosity data are available at multiple concentrations. Although the Ostwald viscometer can in principle be used to collect such data, the instrument must be emptied, cleaned, dried, and refilled after each experiment. The capillary and fluid reservoir sections of an **Ubbelohde viscometer** (Figure 7.8) are separated during measurements. The volume of fluid in the reservoir is therefore immaterial. An initial charge of solution can be diluted many times over to facilitate the viscosity data over a rather broad range of solution concentrations. The semiautomatic Ubbelohde viscometer includes additional features that further simplify solution viscosity measurements. The flow time t , for example, is recorded by means of photocells, which sense the passage of the fluid meniscus, reducing the influence of human errors on the accuracy of the measurements. Commercial devices are also available

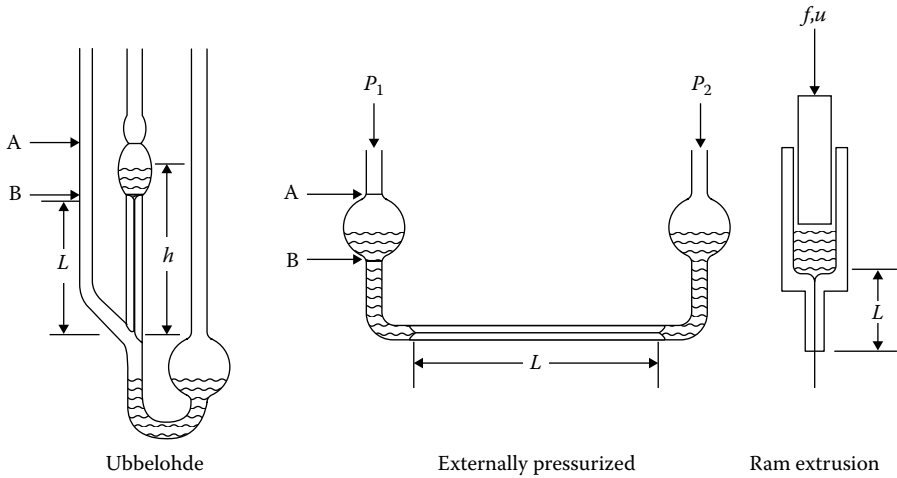


FIGURE 7.8 Capillary flow configurations for measuring viscosity. h and L are length scales defined in the figures; P_1 and P_2 are pressures; and f and u are the force and velocity, respectively with which the piston travels.

for carrying out automatically the entire procedure of filtering, charging, measuring flow time, and flushing out. The cost of these rather elaborate systems can be justified when a great many samples must be run, as in the quality control department of a large polymer-producing plant.

Another device that simplifies the measurement of dilute solution viscosity is the **differential viscometer**. One design [31] consists of two capillary tubes in series (Figure 7.9). When fluid is pumped at a constant rate through the two tubes, the pressure drops are sensed by differential pressure transducers, DPT-1 and DPT-2. With

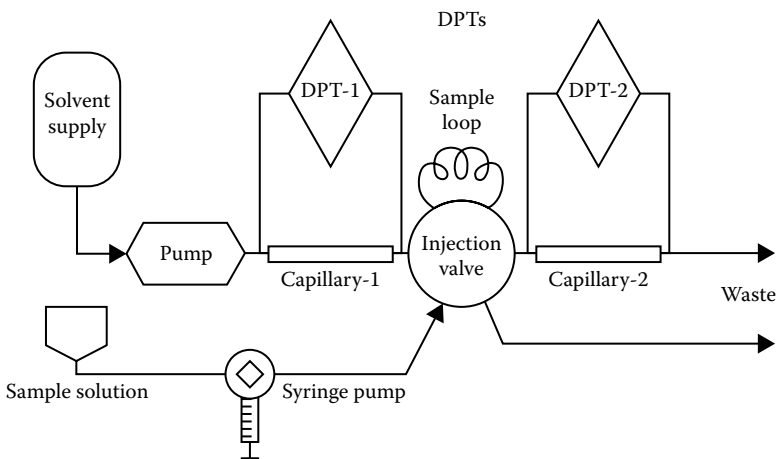


FIGURE 7.9 Schematic diagram of a differential viscometer (Viscotek Y-501). (Data from Hitchcock, C. D. et al., *Am. Lab.*, 26, 26, 1994.)

solvent flowing, the ratio of the two pressures, $(P_1/P_2)_s$, is a constant for a given piece of apparatus. Now a dilute polymer solution is placed in the sample loop. By turning the injection valve, the solvent continues to flow through the first tube, but the polymer solution flows through the second tube, giving rise to a new ratio of pressures (P_2/P_1) . The relative viscosity is then simply

$$\eta_r = \left(\frac{P_1}{P_2} \right)_s \left(\frac{P_2}{P_1} \right)_p \quad (7.19)$$

A more complicated version of the same apparatus has been used as a detection device for column chromatography [32]. In one example, an in-line differential viscometer was used together with a differential refractometer to measure the relative viscosity and the concentration, respectively. Because of the very low polymer concentrations, extrapolation to infinite dilution is not needed.

The viscous (DV) and refractometer (DRI) signals for a polystyrene sample in 1,2,4-trichlorobenzene at 145°C are shown in Figure 7.10. The data have been corrected (normalized) for the volume delay between the two detectors [33]. As one would expect, the viscosity signal peaks sooner than the concentration, since the higher molecular weights contribute more to the viscosity. Also, it can be noted that there will be an unavoidable uncertainty in the inherent viscosity, $\ln(\eta_r)/c$ at either end of the chromatogram, where the signal from one detector or the other merges

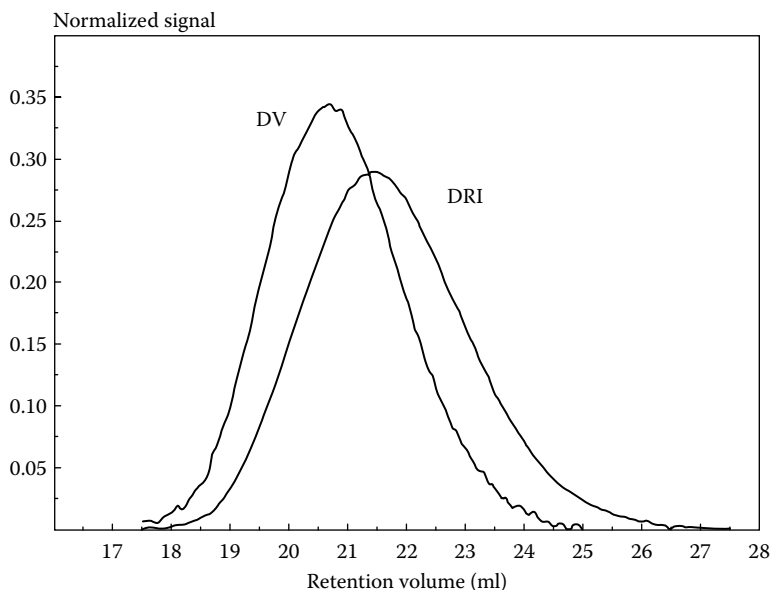


FIGURE 7.10 Normalized chromatographic signals from a differential viscometer (DV) and differential refractive index (DRI) monitor for a polystyrene sample with a broad molecular weight distribution ($M_w = 123,000$; $M_w/M_n = 2.24$). (From R. Lew, D. Suwanda, S. T. Balke, and T. H. Moury, *J. Appl. Polym. Sci.: Appl. Polym. Symp.* 52, 125, 1993. Copyright Wiley-VCH Verlag GmbH & Co. KGaA. Reprinted with permission.)

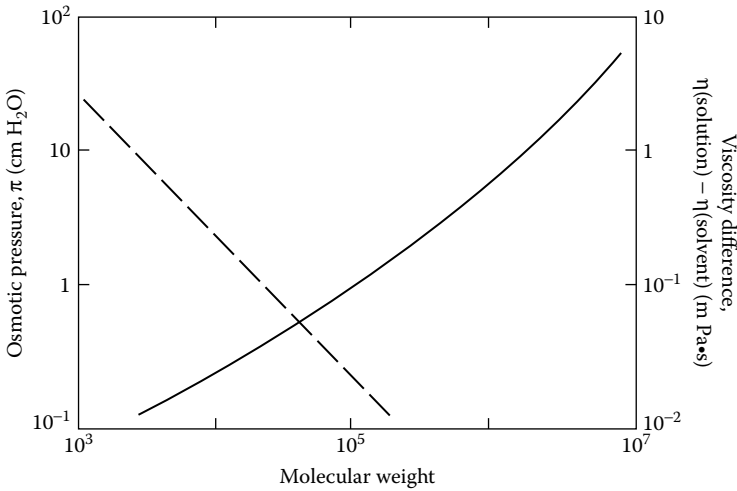


FIGURE 7.11 Effect of polymer molecular weight on observed quantities for two molecular weight measurement techniques.

with noise in the output. In comparison with light scattering, viscosity measurements involve far less time and equipment. Compared with osmotic pressure, viscosity has the advantage that the observable quantity increases as molecular weight increases (Figure 7.11). Of course, some absolute method such as light scattering or osmotic pressure measured on fractions where x_w/x_n is small (e.g., $x_w/x_n < 1.1$) must be used to *calibrate* Equation 7.19 for a given polymer and solvent.

The molecular size of polyolefins is conventionally reported in terms of the **melt index**, referring to the grams of polymer extruded in 10 min through a die that is 2.1 mm in diameter and 8.0 mm in length. The temperature and pressure must be specified (ASTM D1238). Instead of weighing the extrudate, the rate of movement of the plunger forcing the polymer through the die can be sensed and indicated. Typically, a force of 298 kPa is used at a temperature of 190°C for polyethylene and 230°C for polypropylene. The actual test time can vary from 15 s to several minutes, but the result is expressed as the flow that would take place in a 10-min period. Melt indexes of 0.1–50 are common. Based on the preceding discussions about the effect of polymer molecular weight on relaxation times and hence Wi (Section 7.2.2), normal stress effects in extrusion (Section 8.2), and kinetic energy losses at the entrance and exit of tubes during Poiseuille flow, there are justifiable concerns about using melt index data for purposes other than simple quality control measurements. The method nonetheless yields quick results, and is cheap and easy to use, making it quite popular in industry. Because the die is short, the flow resistance is dominated by losses as fluid enters and leaves the die. Because the flow in these regions has a strong extensional flow component (Section 7.7), the melt index of a polymer is sensitive to its elongational viscosity. Molecular characteristics, such as long-chain branching in polyolefins, that lead to high-transient elongational viscosity can therefore sometimes be diagnosed from a combination of melt index and shear rheology measurements.

7.4 POLYMER SHAPES IN SOLUTION

7.4.1 POLYMER CHAIN STATISTICS

A polymer molecule in solution is not a stationary piece of string as commonly depicted in cartoon representations, but instead is a constantly coiling and uncoiling chain whose conformation in space is ever changing. In a very dilute solution, the individual molecules can be considered as acting independently. Each molecule can be pictured as a string of beads with a tendency to form a spherical cloud having radial symmetry. It is possible to analyze this situation mathematically to determine how the polymer coil size depends on polymer molecular weight, monomer size, and solution conditions. The starting point is Figure 7.12 where the x repeat units of a polymer molecule are depicted by vectors r_1 to r_x , which specify the orientation of the individual units in space. The resultant vector,

$$\underline{R} \equiv \sum_{i=1}^x r_i \quad (7.20)$$

termed the polymer **end-to-end vector**, provides an overall measure of the configuration of repeat unit orientation vectors in a given molecule. In general, we are interested in macroscopic flow properties of polymers, which reflect averages over many molecules. The average end-to-end vector $\langle \underline{R} \rangle = \langle \sum_{i=1}^x r_i \rangle$ of an ensemble of polymer chains is therefore a more relevant measure of polymer configuration than the end-to-end vector of a single molecule.

To determine how the average size of the molecular cloud changes with molecular weight, several approaches with varying levels of realism can be used. For example, if the orientation adopted by a repeat unit (e.g., r_2 in Figure 7.12) is unhindered by the orientation of polymer repeat units to which it is connected (e.g., r_1 and r_3 in the figure), the polymer chain may be described as freely jointed or as a random flight of discrete monomeric units. In the **freely jointed chain** or **random flight model**, the orientations of repeat unit vectors are completely uncorrelated and

$$\langle \underline{R} \rangle = \sum_{i=1}^x \langle r_i \rangle = 0 \quad (7.21)$$

This result follows from the fact that for large x , there is an equal likelihood of finding polymer repeat units oriented in opposite directions in an ensemble of polymer

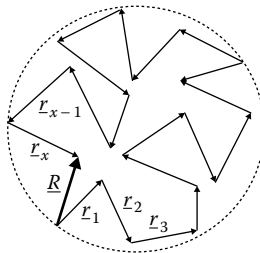


FIGURE 7.12 Equilibrium configuration of a single polymer chain in solution.

molecules. Thus, the two ends of a freely jointed polymer chain are oriented at random with respect to each other. The average separation of polymer chain ends does not need to be 0, however. To see this, let us define a different measure of the average separation between the ends of a polymer chain, $(\bar{r}_0^2)^{1/2} \equiv \langle \underline{R} \bullet \underline{R} \rangle^{1/2}$, which is formally termed the **root-mean-squared (rms) end-to-end distance** of the polymer. Substituting for \underline{R} in this expression and invoking the freely jointed chain model yield

$$\left(\bar{r}_0^2\right) = \left\langle \sum_{i=1}^x \underline{r}_i \bullet \sum_{j=1}^x \underline{r}_j \right\rangle = \sum_{i=j}^x \left\langle \underline{r}_i \bullet \underline{r}_j \right\rangle + 2 \sum_{i \neq j}^x \left\langle \underline{r}_i \bullet \underline{r}_j \right\rangle \quad (7.22)$$

But

$$\sum_{i=1}^x \left\langle \underline{r}_i \bullet \underline{r}_i \right\rangle = \sum_{i=1}^x \left\langle \underline{r}_i \bullet \underline{r}_i \right\rangle = x \left\langle |\underline{r}|^2 \right\rangle = x \bar{a}^2 \quad (7.23)$$

where:

\bar{a} is the average length of a polymer repeat unit

The second term can be expanded in the same manner to yield

$$\sum_{i \neq j}^x \left\langle \underline{r}_i \bullet \underline{r}_j \right\rangle = \sum_{i \neq j}^x \left\langle \underline{r}_i \right\rangle \bullet \left\langle \underline{r}_j \right\rangle = 0 \quad (7.24)$$

Our final result is therefore

$$\left(\bar{r}_0^2\right) = x \bar{a}^2 \quad (7.25)$$

which implies that the rms end-to-end distance increases as the square root of the degree of polymerization and in proportion to the average repeat unit length.

Example 7.2

Calculate the rms end-to-end distance of polyethylene with an average molecular weight of 140,000 g/mol. Compare your result with the fully extended length of this polymer. What is the physical significance of your result?

Solution: Polyethylene is made up of methylene groups, CH_2 , of molecular weight 14 g/mol, separated by a bond distance of about 1.54 Å. Therefore, $\bar{a} = 1.54 \text{ Å}$, $x = 10,000$, and

$$\left(\bar{r}_0^2\right)^{1/2} = 15.4 \text{ nm}$$

The fully stretched out length of this same polymer is

$$L_T = x \bar{a} = 1.54 \mu\text{m}$$

Comparing the two results, we see $L_T \gg (\bar{r}_0^2)^{1/2}$, which is consistent with the assumption that links between polymer repeat units are quite flexible.

A limitation of the freely jointed chain model is that the bond angle θ' linking polymer repeat units is constant (e.g., $\theta' = 109.5$ for tetrahedrally connected carbons), which results in some degree of correlation between repeat unit orientations. A model termed the **freely rotating chain model** fixes the bond angle between repeat units, but allows free rotation about bonds connecting them (Figure 7.5). In this case, it can be shown that

$$\left(\overline{r_0^2}\right) = x\bar{a}^2 \left(\frac{1 + \cos\theta}{1 - \cos\theta}\right) \quad (7.26)$$

where:

$$\theta = 180 - \theta'$$

For the polyethylene of our previous example, $\theta' = 109.5$ and $(r_0^2) = 2x\bar{a}^2$, so $(r_0^2)^{1/2} = 21.8$ nm. We are nevertheless still assuming the free rotation about each bond that ignores the energy required to rotate even one methylene group past another, as in the paraffins. Because there are energy barriers to rotation, certain chain conformations are preferred. The ratio of the measured value of (r_0^2) for a polymer to the value computed using Equation 7.26 is termed the **steric factor** σ of the polymer. Table 7.3 summarizes experimental and theoretical $(r_0^2)^{1/2}$ data, as well as σ values for a variety of polymers. It is clear from the table that σ is generally larger than unity, implying that rotation from one conformation to another is not free, but is restricted by the energy barrier to changes in conformation.

The probability of rotation from one conformation to another nonetheless increases with temperature. The **trans conformation** depicted in Figure 7.13 is, for example, more favored than any of the others. The **gauche positions** are more favorable than the *cis* position, or any other eclipsed conformation, but not as favorable as the *trans* position. These ideas can be formally integrated into a third model, which we here term the **symmetric restricted rotation model**. The mean-squared end-to-end distance is

$$\left(\overline{r_0^2}\right) = x\tilde{a}^2 \left(\frac{1 + \cos\theta}{1 - \cos\theta}\right) \left(\frac{1 + b}{1 - b}\right) \quad (7.27)$$

$$b = \langle \cos\phi \rangle$$

Notice that the progressive refinement of the model for repeat unit orientation yields expressions for the mean-squared end-to-end distance of the form

$$\left(\overline{r_0^2}\right) = x\left(\tilde{a}^2\sqrt{C_\infty}\right)^2 = xa^2 \quad (7.28)$$

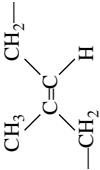
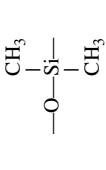

where:

a is the effective step length of the freely jointed chain and is termed the **statistical segment length**

$C_\infty \equiv a^2/\tilde{a}^2$ is termed the **C-infinity** value or **chain stiffness**

TABLE 7.3
Unperturbed Molecular Dimensions for Representative Polymers

Polymer	Repeat Unit	M/unit (n)	Temperature (°C)	$K' \times 10^5$ $K' = [\eta]_0/M^{0.5}$	$(\bar{r}_0^2/M)^{0.5} \times 10^{11}$ cm exp. ^a	$(\bar{r}_0^2/M)^{0.5} \times 10^{11}$ cm exp. ^b	σ Steric Factor ^c	$(\bar{r}_0^2/n)^{1/2}$ (Å) ^d exp.	$(\bar{r}_0^2/n)^{1/2}$ (Å) ^e cal.
Polyisobutylene	$\begin{array}{c} \text{CH}_3 \\ \\ -\text{CH}_2-\text{C}- \\ \\ \text{CH}_3 \end{array}$	56 (2)	24 95	106 91	795 757	412 412	1.93 1.84	4.21 4.01	2.18 2.18
Polystyrene	$\begin{array}{c} -\text{CH}_2-\text{CH}- \\ \\ \text{C}_6\text{H}_5 \end{array}$	104 (2)	70	75	710	302	2.35	5.12	2.18
Poly(methyl methacrylate)	$\begin{array}{c} \text{CH}_3 \\ \\ -\text{CH}_2-\text{C}- \\ \\ \text{C}=\text{O} \\ \\ \text{OCH}_3 \end{array}$	100 (2)	50	65	680	310	2.20	4.81	2.18
cis-Polyisoprene	$\begin{array}{c} \text{CH}_3 \quad \text{H} \\ \diagdown \quad / \\ \text{C}=\text{C} \\ / \quad \diagdown \\ \text{CH}_2 \quad \text{CH}_2- \end{array}$	68 (4)	0-60	119	830	485	1.71	3.42	2.00

<i>trans</i> -Polyisoprene		68 (4)	60	532	1030	703	1.46	4.25	290
Poly(dimethyl siloxane)		74 (2)	20	81	730	456	1.60	4.44	277
Polyethylene [37]		28 (2)	100	100	1030	582	1.77	3.85	218

Note: exp, experimental; calc, calculated/theoretical.

Source: Flory, P. J., *Principles of Polymer Chemistry*, Cornell University Press, Ithaca, NY, 618, 1953.

^a $(r_0^2/M)^{0.5} - (K'/\phi)^{1/2}$, where $\phi = 2.1 \times 10^{21}$ dl/mol.cm³; 1 Å = 0.1 nm.

^b From known angles and bond distances with free rotation.

^c The ratio of exp.-to-calc. value is $(r_0^2)^{0.5}$.

^d From $(r_0^2/M)_{\text{exp}}$

^e From $(r_0^2/M)_{\text{calc}}$

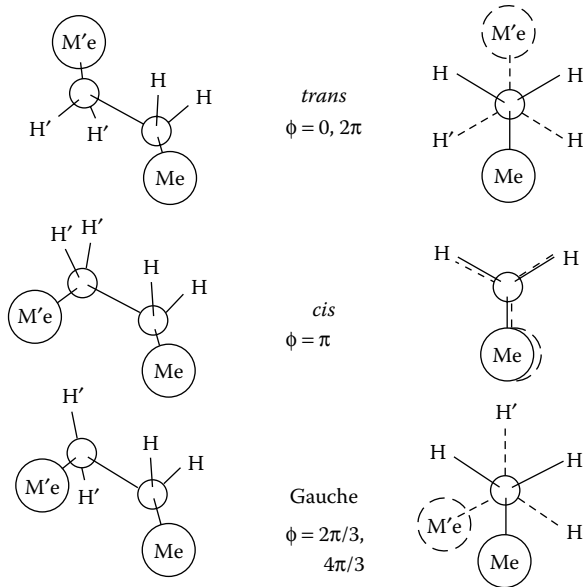


FIGURE 7.13 Conformation about a single bond for butane.

From the restricted rotation model, $C_\infty = (1 + \cos \theta)/(1 - \cos \theta) (1 + b)/(1 - b)$, whereas from the freely rotating chain model, $C_\infty = (1 + \cos \theta)/(1 - \cos \theta)$. Thus, the restricted motion at the junctions connecting polymer repeat units has the physical effect of stiffening the links, which increases the number of links along a chain one must travel before orientation vectors become uncorrelated. C_∞ values for some common polymers are provided in Table 7.4. A more extensive list is available in the *Polymer Handbook* [37]. It is apparent from the table that polymers such as polystyrene, which possess naturally bulky repeat units, have large C_∞ values, whereas polymers connected by flexible links (e.g., polyethylene oxide and polyisoprene) have the lowest C_∞ values.

The rms end-to-end distance $(\overline{r_0^2})^{1/2}$ does not directly report the coil size of a polymer molecule. Consider a polymer chain composed of x segments, each ending at a node labeled x (see Figure 7.14). Let the position vectors $\underline{R}_1 \cdot \underline{R}_n$ represent the location of all nodes with respect to a common origin. The center of mass of the molecule is located by the vector $\underline{R}_G = (1/x) \sum_{k=1}^x \underline{R}_k$. The rms distance between the nodes and their common center of mass defines the **radius of gyration**:

$$R_g = \langle s^2 \rangle^{1/2} = \frac{1}{x^{1/2}} \sum_{k=1}^x \langle (\underline{R}_k - \underline{R}_G)^2 \rangle^{1/2} = \frac{1}{\sqrt{6}} \sqrt{xa} \quad (7.29)$$

In the above equation, we have taken the polymer chain to be freely jointed with a statistical segment length $a = \sqrt{C_\infty} \bar{a}$. Notice that the radius of gyration is related to

TABLE 7.4
 C_∞ Values of Several Polymer/Solvent Pairs

Polymer	T	Solvent	C_∞
Polyacrylamide	30	Water	14.8
Polyacrylonitrile	30	Dimethylformamide	11.1
1,4-Polybutadiene	40	Cyclohexane	5.4
Polycarbonate (bisphenol A)	25	Chlorobenzene	3.55
Poly(dimethyl siloxane)	25	Toluene	6.25
Polyethylene	140	<i>p</i> -Xylene	6.8
Poly(ethylene oxide)	25	Benzene	4.25
Polyisobutylene	24	Benzene	6.5
1,4-Polyisoprene	20	Benzene	5.0
Poly(methyl methacrylate) (atactic)	21	Toluene	9.0
Polypropylene (atactic)	30	Toluene	6.2
Poly(propylene oxide)	25	Benzene	5.05
Polystyrene (atactic)	35	Cyclohexane	9.85
Poly(vinyl acetate)	29	Various	9.0
Polyvinyl alcohol	30	3-Heptanone	11.3
Poly(vinyl carbazole)	25	Tetrahydrofuran	15.9
Polyvinyl chloride	25	Tetrahydrofuran	6.7
Polyvinyl chloride	25	Tetrahydrofuran	6.7
Polyvinyl pyrrolidone	25	Water	12.3

Source: Cannon, M. R. et al., *Anal. Chem.*, 32, 355, 1960.

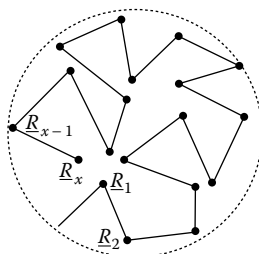


FIGURE 7.14 Bead stick representation of a polymer chain in solution.

the mean-squared end-to-end distance of the polymer coil, $\langle s^2 \rangle = \overline{(r_0^2)}/6$. Branching of the polymer chain has the effect of decreasing $\langle s^2 \rangle$ for the same overall degree of polymerization. This effect can be described in terms of the ratio of mean-squared radius of gyration of a branched polymer $\langle s^2 \rangle_{br}$ to that of a linear polymer $\langle s^2 \rangle$ with the same molecular weight:

$$\frac{\langle s^2 \rangle_{\text{br}}}{\langle s^2 \rangle} = g \quad (7.30)$$

For a star-shaped polymer (Figure 7.15) with f arms per molecule, g can be calculated using a model proposed by Zimm and Stockmayer [38]:

$$g_{\text{star}} = \frac{3f-2}{f^2} \quad (7.31)$$

The mean-squared radius of gyration of a three-arm star polymer is therefore about 22% lower than that of a linear polymer of the same molecular weight, whereas the mean-squared radius of gyration of a six-arm star polymer is just 56% that of a linear polymer with the same molecular weight. The Zimm–Stockmayer theory can be extended to compute $\langle s^2 \rangle$ for more complicated long-chain branched polymer structures, such as the *pom–pom* structure depicted in Figure 7.15 [39,40]. Defining the ratio of the molecular weight of the linear connector molecule to that of the total polymer as β , and the number of arms per branch point as f :

$$g_{\text{br}} = \beta^3 + 3\beta^2(1-\beta) + \frac{3}{2} \left(\frac{f+1}{f} \right) \beta(1-\beta)^2 + \frac{3f-1}{2f^2} (1-\beta)^3 \quad (7.32)$$

Our analysis of polymer chain statistics has up to this point tacitly assumed that only polymer segments located at most C_∞ units away from a test segment can influence its conformation. This assumption is not necessarily correct, because remote segments along the same chain, as well as segments on neighboring chains, can be located close enough to the test segment to exert steric constraints on its orientation. This effect tends to swell the polymer chain and can be captured by introducing an **expansion coefficient**:

$$\alpha = \left(\frac{\overline{r^2}}{r_0^2} \right)^{1/2} \quad (7.33)$$



FIGURE 7.15 Schematic of a six-arm star polymer (left) and a multiarm branched polymer (right).

where:

$(\overline{r^2})$ is the actual mean-squared end-to-end distance of the polymer
 $(\overline{r_0^2})$ is the value determined in the absence of the expansion effect

The expansion factor can be determined by assigning to each polymer segment a volume v into which no other segment can enter. The **excluded volume** v of the segment and the interactions that give rise to it are termed excluded volume interactions. The excluded volume is a function of segmental geometry, segment–solvent interactions, and temperature. A simple equation summarizing all three effects was derived by Flory [36]:

$$v = v^0 \left(1 - \frac{\theta_f}{T} \right) \quad (7.34)$$

where:

v^0 is a constant for a given polymer–solvent combination

T is the absolute temperature

θ_f is the **theta temperature** or **Flory temperature**

The theta temperature is approximately the temperature at which polymer of infinite molecular weight precipitates from a solvent. This is logical because this is the point where polymer segments just begin to associate more with each other than they do with the solvent. Like the interaction parameter, θ_f is characteristic of a given polymer–solvent system. Values of θ_f for a number of polymer–solvent pairs are provided by Kurata and Stockmayer [41].

Notice that at $T = \theta_f$, $v = 0$ and the excluded volume effects disappear. The expansion factor can be related to v through the following series expansion [42]:

$$\alpha^2 = \left(1 + \frac{4}{3}z - 2.075z^2 + 6.297z^3 - 25.057z^4 + \dots \right) \quad (7.35)$$

where:

$$z = \sqrt{x} \left(\frac{3}{2\pi} \right)^{3/2} \frac{v^0 [1 - (\theta_f/T)]}{a^3} \quad (7.36)$$

Substituting $T = \theta_f$ in the above equation yields $\alpha = 1$ and $(\overline{r^2}) = (\overline{r_0^2})$. At the theta temperature, polymer chain statistics are therefore well described by the random flight model. As the temperature is progressively increased above θ_f , v increases toward v^0 and polymer chains adopt more expanded structures in solution. These conditions are termed good solvent conditions and correspond to large z values. Under these circumstances, it can be shown that the expansion factor increases weakly with x , $\alpha \sim x^{0.1}$, and

$$(\overline{r^2})^{1/2} = x^{3/5} a \quad (7.37)$$

However, if T is lowered below θ_f , the solvent becomes progressively poorer and polymer molecules take up more collapsed structures in solution. An analogous expression to Equation 7.37 can be written in this case as $(r^2)^{1/2} = x^\xi a$, where ξ is typically in the range of 0.45–0.3.

7.4.2 DILUTE SOLUTION VISCOUS PROPERTIES

The **intrinsic viscosity** $[\eta]$ provides a sensitive measure of polymer size and architecture in dilute solution. Equation 7.38 can be used to determine the intrinsic viscosity of a polymer solution from measurements of the solution viscosity η and the solvent viscosity η_s :

$$[\eta] = \lim_{c \rightarrow 0} \frac{\eta - \eta_s}{c\eta_s} = \lim_{c \rightarrow 0} \frac{\eta_r - 1}{c} = \lim_{c \rightarrow 0} \frac{\eta_{sp}}{c} \quad (7.38)$$

where:

c is the concentration of polymer in solution

η_r/η_s is termed the **reduced viscosity**

$\eta_{sp} \equiv (\eta - \eta_s)/\eta_s = \eta_r - 1$ is designated the specific viscosity of the solution

Although η_r and η_{sp} are dimensionless, $[\eta]$ has units of reciprocal concentration, typically deciliter per gram. Methods for measuring the viscosity of dilute polymer solutions were introduced in Section 7.3. If either η_{sp}/c or $\ln(\eta_r)/c$ (the so-called **inherent viscosity**) is plotted against c , a straight line is observed (Figure 7.16) at low solution concentrations. The lines can be described by the following **Huggins** [43] and **Kraemer** [44] equations:

$$\text{Huggins equation: } \frac{\eta_{sp}}{c} = [\eta] + k'[\eta]^2 c \quad (7.39)$$

$$\text{Kraemer equation: } \frac{\ln(\eta_r)}{c} = [\eta] - k''[\eta]^2 c \quad (7.40)$$

The intercept and slopes therefore yield $[\eta]$, k' , and k'' . For many polymers in good solvents, $k' = 0.4 \pm 0.1$ and $k'' = 0.05 \pm 0.05$.

Equations 7.39 and 7.40 are applicable only in dilute solutions where η_r is less than about 2.

In analogy to the treatment of osmotic pressure, results obtained at higher solution concentrations can be linearized using an equation of the form [45]:

$$\left(\frac{\eta_{sp}}{c} \right)^{1/2} = [\eta]^{1/2} + \frac{k'''}{2} [\eta]^{3/2} c \quad (7.41)$$

This equation and Equation 7.50 are compared with the Huggins and Kraemer equations in Figure 7.16 and Table 7.5 for a set of experimental data.

Staudinger proposed on empirical grounds that $[\eta]$ is proportional to the molecular weight of a given polymer–solvent combination [46]. A more general expression

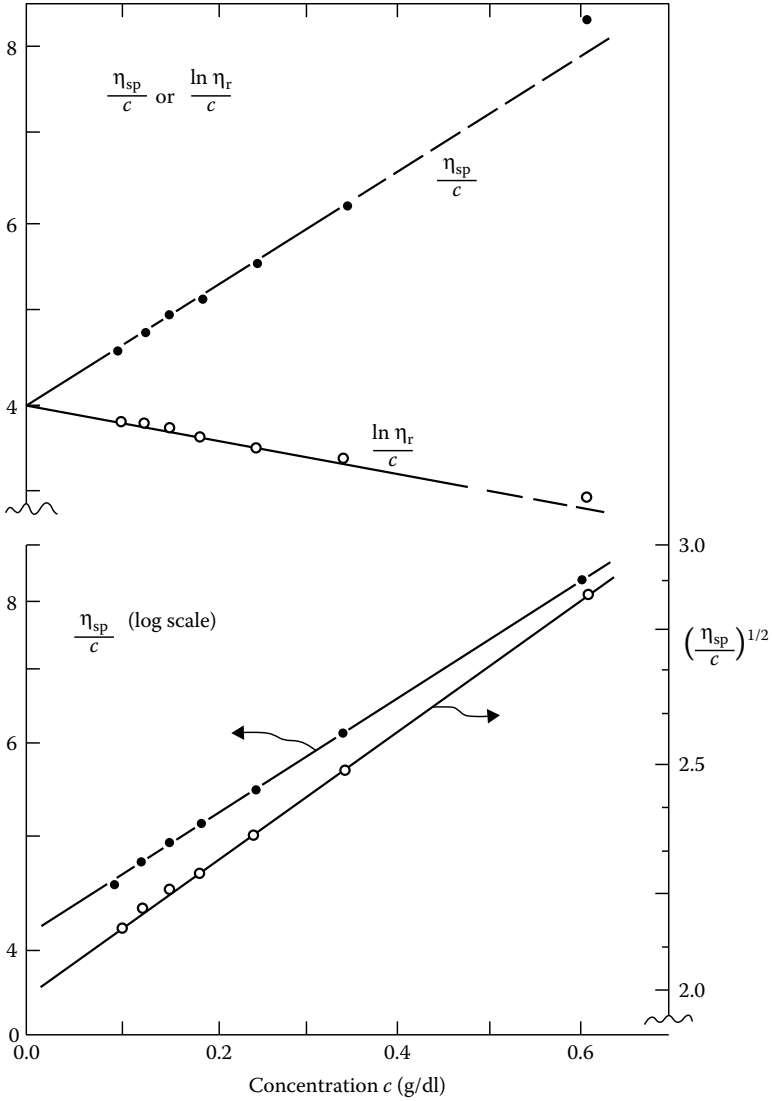


FIGURE 7.16 Viscosity correlations for dilute solutions.

TABLE 7.5
Parameters for Figure 7.16

Equation	$[\eta]$	Slope Factor
7.39	3.95	$k' = 0.41$
7.40	3.97	$k'' = 0.12$
7.41	3.99	$k''' = 0.36$

known as the **Mark–Houwink–Sakurada relationship** [47] yields the following power-law expression:

$$[\eta] = K'M^a \quad (7.42)$$

with $0.5 < a < 1$. Typical values of the constants K' and a for several polymer–solvent pairs are provided in Table 7.6. It is important to keep in mind that these values are only correct at the corresponding temperatures listed in the table.

On dimensional grounds, we would expect the intrinsic viscosity of a polymer in dilute solution to be proportional to the ratio of its hydrodynamic volume to its molecular weight:

$$[\eta] = \frac{\widehat{\Phi}_v R_g^3}{M} = \frac{\Phi_v \overline{(r^2)}^{3/2}}{M} \quad (7.43)$$

where:

Φ_v is termed the **Flory–Fox parameter** and is a constant of order (0.35–0.48) N_{AV} [48,49] for a given polymer–solvent system and N_{AV} is the Avogadro's number

TABLE 7.6
Parameters for the Mark–Houwink–Sakurada Equation

Polymer	Solvent	Temperature (°C)	$K' \times 10^5$	a
Cellulose triacetate	Acetone	25	8.97	0.90
Styrene-butadiene rubber	Benzene	54	0.66	
Natural rubber	Benzene	30	185	0.74
	<i>n</i> -Propyl ketone	14.5	119	0.50
Polyacrylonitrile	Water	30	68	0.66
Polyacrylonitrile	Dimethylformamide	25	23.3	0.75
Poly(dimethyl siloxane)	Toluene	20	20.0	0.66
Polyethylene	Decalin	135	62	0.70
Polyisobutylene	Benzene	24	107	0.50
	Benzene	40	43	0.60
	Cyclohexane	30	27.6	0.69
Poly(methyl methacrylate)	Toluene	30	7.1	0.75
Polystyrene				
Atactic	Toluene	30	11.0	0.725
Isotactic	Toluene	30	10.6	0.725
Poly(vinyl acetate)	Benzene	30	22	0.65
	Ethyl- <i>n</i> -butyl ketone	29	92.9	0.50
Poly(vinyl chloride)	Tetrahydrofuran	20	3.63	0.92

Source: Kurata, M. and W. H. Stockmayer, *Fortschr. Hochpolymer. Forsch.*, 3(2), 196, 1963.

Introducing Equation 7.33 into 7.43 yields

$$[\eta] = \hat{\Phi}_v \left(\frac{\bar{r}_0^2}{M} \right)^{3/2} M^{1/2} \alpha^3 \quad (7.44)$$

The intrinsic viscosity in any solvent is therefore predicted to vary as $M^{1/2}$ at the theta point ($T = \theta_f$). Comparing Equations 7.42 and 7.44 indicates that $a = 0.5$ for all polymer solutions at the theta temperature. Under good solvent conditions, $\alpha \sim M^{0.1}$ and $a = 0.8$. These values of a are in remarkably good accord with predictions from a molecular theory proposed by Zimm [48,49] under theta and good solvent conditions. In the **Zimm theory**, a polymer molecule such as that depicted in Figure 7.14 is modeled as a collection of friction centers or **beads**, located at the nodes in the figure, and elastic connectors or springs, located along the connecting rods in the figure. When a solution is subjected to shear, the bead separation is maintained by local elastic spring forces, and disturbances to the local fluid velocity created at one bead propagate to remote bead locations on the same polymer chain, as well as to beads on neighboring chains, by hydrodynamic forces. The resultant hydrodynamic interactions captured in the Zimm theory are therefore precisely the ones neglected in our earlier free-draining analysis of polymer friction. The Zimm theory is therefore said to describe the polymer solutions in the **nondraining** or **non-free draining** limit. Agreement between Equations 7.42 and 7.44, and the Zimm predictions is important because it provides a fundamental basis for the validity of the Mark–Houwink–Sakurada equation. Specifically, based on the Zimm theory, it is apparent that the friction between polymer segments and solvent and hydrodynamic interaction between segments are the source of the unique Mark–Houwink–Sakurada exponents in different polymer–solvent pairs.

As was the case for the radius of gyration, branching typically reduces the intrinsic viscosity of polymers. The intrinsic viscosities of branched $[\eta]_{br}$ and linear $[\eta]$ polymers of equal molecular weight can in fact be related using an expression analogous to Equation 7.30:

$$\hat{g} = \frac{[\eta]_{br}}{[\eta]} \quad (7.45)$$

In the above equation, \hat{g} is related to g by a power law, $\hat{g} = g^\iota$, where the exponent ι depends on the polymer architecture. Values of ι ranging from 0.5 to 3 have been reported in the literature. For example, in dilute solutions of star polymers, $\iota \approx 0.6$, whereas for H-shaped multiarm polymers, that is, multiarms with $f = 2$, ι values ranging from 1.3 to 2.6 have been reported [40].

7.4.3 POLYMER MOLECULAR WEIGHT AND INTRINSIC VISCOSITY

The practical importance of intrinsic viscosity cannot be overstated. It is the most common measure of polymer molecular weight. The relationship between the intrinsic viscosity and the molecular weight can be determined as follows. Consider a polymer liquid consisting of a distribution of molecules, each with molecular weight

M_i and weight fraction w_i . From the definition of the intrinsic viscosity, we can define an intrinsic viscosity $[\eta]_i$ for each component of the distribution and an average intrinsic viscosity, as follows:

$$\overline{[\eta]} = \sum_i w_i [\eta]_i \quad (7.46)$$

for the entire liquid. Using the above equation, we may therefore write $[\eta]_i = K' M_i^a$ and $\overline{[\eta]} = K' M_v^a$, where M_v is termed the **viscosity-averaged molecular weight**. Substituting for $[\eta]_i$ and $\overline{[\eta]}$ in Equation 7.46 yields an expression for M_v :

$$M_v = \left(\sum_i w_i M_i^a \right)^{1/a} \quad (7.47)$$

Notice that M_v approaches M_w as a approaches 1.0; for values of a in the typical range $0.5 < a < 1$, M_v is intermediate between M_n and M_w , but typically closer to M_w .

The quantity $[\eta]M$ has dimensions of volume and is termed the **hydrodynamic volume** of a polymer in solution. As already pointed out, it is directly proportional to the volume occupied by a polymer molecule and is related to the quantity Γ introduced in Equation 7.8, $\Gamma = \phi/([\eta]M)$, where ϕ is the volume fraction of polymer in solution. It was noted in Chapter 6 that this quantity is a useful parameter for the *universal* calibration of gel permeation chromatography (GPC) used for measuring polymer molecular weight; hence, it is evident that molecular weight by itself does not necessarily correlate with the ability of a molecule to diffuse in and out of the porous packing in a GPC column. However, the size of the molecule as represented by the hydrodynamic volume is closely related to its diffusing ability. Even then, the universal calibration may not take into account specific interactions that may occur between the polymer being analyzed and the polymer constituting the packing. The intrinsic viscosity for purposes of calibration has to be measured in the same solvent and at the same temperature as used for the chromatographic separation. Thus, the absolute molecular weight of a new polymer can be estimated from the GPC elution curve, provided that the apparatus is calibrated, say, with polystyrene standards of known intrinsic viscosity and molecular weight. A rather elegant combination consists of a differential viscometer, a light scattering instrument, and a differential refractometer, all monitoring the effluent of a GPC/size exclusion chromatography (SEC) apparatus. A universal calibration curve, $[\eta]M$ versus effluent volume, can be obtained directly from such an arrangement as long as the signals are appropriately calibrated and coordinated [50].

Although (η_0^2/M) is a function of temperature and solvent character, in many cases it is not very sensitive to either variable at temperatures near the theta temperature. The ratio of $[\eta]$ to $[\eta]\theta_f$ therefore provides a good estimate of α^3 , no matter what solvent was used to measure $[\eta]\theta_f$. Taking values of K' and a from Table 7.6, we find for polyisobutylene in cyclohexane at 30° (see Table 7.7):

TABLE 7.7
Dependence of α^3 on Molecular Weight
Polyisobutylene in Cyclohexane at 30°C

Molecular Weight $\times 10^{-3}$	Intrinsic Viscosity (dl/g)	
		$\alpha^3 = [\eta]/[\eta]_0$
9.5	0.145	1.39
50.2	0.47	1.96
558.0	2.48	3.10
2720.0	7.9	4.16

Source: Hitchcock, C. D. et al., *Am. Lab.*, 26(11), 26, 1994.

$$\alpha^3 = \frac{[\eta]}{[\eta]_{\theta f}} = \frac{K'M^a(\text{cyclohexane, } 30^\circ\text{C})}{K'M^a(\text{benzene, } 24^\circ\text{C})} = 0.258M^{0.19} \quad (7.48)$$

Therefore, for $M = 10^6$ g/mol, $\alpha^3 = 3.56$, that is, the individual polymer molecules occupy almost 4 times the volume in cyclohexane than they do in any theta solvent. It was mentioned in Section 2.5 that polymers in contact with solvents of like solubility parameter δ should show the greatest solvation effects, that is, swelling of networks or enhancement of viscosity of solutions. Now we can identify this solvating ability with α , the expansion factor.

Example 7.3

Polymers of monomer m are made in several molecular sizes and dissolved in solvent A or B. From the information given below, calculate the expansion factor and the hydrodynamic volume in solvent A for a polymer with a molecular weight of 10,000,000. Assume that the polymers are monodisperse.

Molecular Weight	Intrinsic Viscosity (dl/g)	
	In A	In B
1,000,000	4.000	2.000
200,000	1.100	–
50,000	–	0.447

Solution: Establish Mark–Houwink–Sakurada parameters.

$$\ln A: \frac{4.000}{1.100} = \left(\frac{1,000,000}{200,000} \right)^a \quad a = 0.802$$

$$\ln B: \frac{2.000}{0.447} = \left(\frac{1,000,000}{50,000} \right)^b \quad b = 0.500$$

Therefore, we surmise that B is a theta solvent. For a molecular weight of 10,000,000,

$$\ln A : \frac{[\eta]_A}{4.000} = \left(\frac{10,000,000}{1,000,000} \right)^{0.802}$$

$$[\eta]_A = 25.35 \text{ dl/g}$$

$$\ln B : \frac{[\eta]_B}{2.000} = \left(\frac{10,000,000}{1,000,000} \right)^{0.500}$$

$$[\eta]_B = 6.325 \text{ dl/g}$$

The expansion factor is

$$\alpha = \left(\frac{[\eta]_A}{[\eta]_B} \right)^{1/3} = 1.59$$

The hydrodynamic volume is

$$[\eta]_A M = 10,000,000 \times 25.35 = 253.5 \times 10^6 \text{ dl/mol}$$

Example 7.4

Polystyrene with a molecular weight of 1,000,000 in a theta solvent (ethylcyclohexane, 70°C) has an intrinsic viscosity of 0.75 dl/g. Calculate the steric factor.

Solution: Calculate the number of repeat units in a polymer with a molecular weight of 1,000,000:

$$\begin{aligned} n = \text{number of steps} &= 2 \times \text{repeat units} = 2 \times \frac{1,000,000}{104} \\ &= 19,230 \end{aligned}$$

The length of each step is 0.154 nm (the carbon–carbon bond length):

$$\left(\overline{r^2} \right)^{1/2} = (2 \times 19,230)^{1/2} \times 0.154 = 30.2 \text{ nm}$$

Calculate the rms end-to-end distance from the intrinsic viscosity in a theta solvent:

$$0.75 \text{ dl/g} = 2.1 \times 10^{21} \times \frac{\left(\overline{r^2} \right)^{3/2}}{1,000,000}$$

$$\left(\overline{r^2} \right)^{3/2} = 3.57 \times 10^{-16} \text{ cm}^3$$

$$\left(\overline{r^2} \right)^{1/2} = 7.09 \times 10^{-6} \text{ cm} = 70.9 \text{ nm}$$

The steric factor is

$$\sigma = \frac{70.9}{30.2} = 2.35$$

7.5 EFFECT OF CONCENTRATION AND MOLECULAR WEIGHT

At low solution concentrations, Equations 7.39 through 7.41 adequately describe the effect of concentration on polymer solution viscosity. In this same concentration range, Equations 7.42, 7.43, and 7.48 correctly describe the effect of polymer molecular weight on viscosity. These equations are inadequate, however, for predicting the viscosity of more concentrated polymer solutions. Several empirical expressions have been proposed in the literature for this purpose (see the work of Ott and Spurlin in Reference 51). An expression due to Lyons and Tobolsky [52] is particularly noteworthy:

$$\eta_{sp} = c[\eta] \exp\left[\frac{k'_L[\eta]c}{1-bc}\right] \quad (7.49)$$

This equation has been shown to reproduce the zero-shear viscosity of some polymers all the way from the dilute solution state to the melt. An equation of similar form has also been derived using free volume arguments [53,54]. The constant b in Equation 7.49 may be either negative or positive, and at low solution concentrations, the constant k'_L is the same as k' in Equation 7.39. A simpler form, in which b is zero, was used earlier by Martin [51]:

$$\log \frac{\eta_{sp}}{c} = \log[\eta] + K''[\eta] c \quad (7.50)$$

This equation is popular for fitting solution viscosity data because it is a two-parameter equation, yet provides good quality fits at high solution concentrations (see Figure 7.16).

In a melt of short chains, Equation 7.11 yields $\eta = \eta_0 = \rho x^2 N_{AV} a^2 \zeta_m / 6M$. A more rigorous calculation that takes into account the time-dependent conformational changes that can occur in an isolated polymer chain (**Rouse chain motion**) [55,56] gives

$$\eta_0 = \frac{\rho x^2 N_{AV} a^2 \zeta_m}{36M} \quad (7.51)$$

The shear viscosity of a polymer melt is therefore predicted by both methods to increase linearly with molecular weight $M = M_0 x$ and monomeric friction coefficient, ζ_m , where M_0 is again the repeat unit molecular weight. Except for very small M , experiments do indicate a linear increase of η with weight-average molecular weight $\overline{M_w} = M_0 \overline{Z_w}$ (Figure 7.17). However, beyond a certain critical molecular weight M_c , or a critical degree of polymerization Z_c , that varies from polymer to polymer, η_0 is observed to increase much more rapidly with polymer molecular weight, typically $\eta_0 \sim M^{3.5 \pm 0.3}$ [57–59]. Thus, for each section of a viscosity versus molecular weight curve, we may write

$$\log \eta_0 = A \log \overline{M_w} + B \quad (7.52)$$

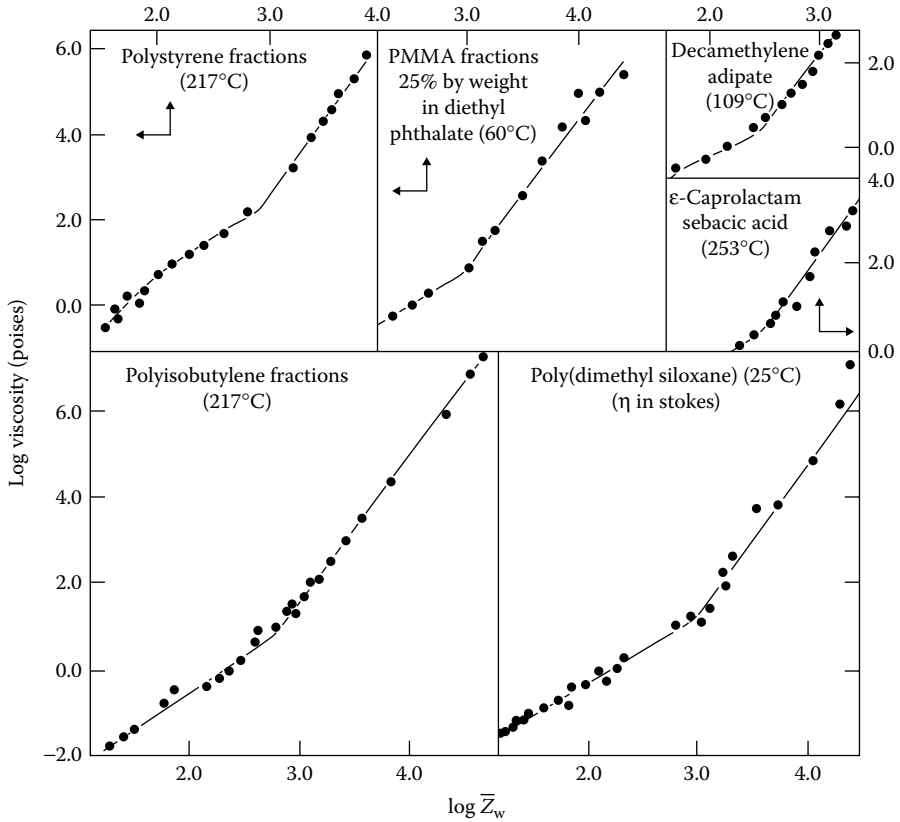


FIGURE 7.17 Logarithmic plots of viscosity η versus weight-average degree of polymerization Z_w for six polymers. 1 poise = 0.1 Pa-s. (Data from Fox, T. G. et al., chap. 12 in F. R. Eirich, ed., *Rheology*, vol. 1, Academic Press, New York, 1956.)

where:

$$A = 1.3 \pm 0.2 \text{ for } \overline{M}_w < M_c \text{ and } A = 3.5 \pm 0.3 \text{ for } \overline{M}_w > M_c$$

A similar effect is observed in polymer solutions, except in that case the transition is at a critical polymer volume fraction $v_{2c} = (M_c/M)\epsilon$, where $3/4 \leq \epsilon \leq 1$ [59,60], $v_2 = c/\rho$, ρ is the polymer density in the melt state, and c its concentration in solution. Values of $Z_c = M_c/m_0$ for several polymers are provided in Table 7.8. M_c data for a broader variety of polymers are available in Reference 59.

Example 7.5

A monodisperse polymer with a molecular weight of 133,000 has an intrinsic viscosity in a theta solvent at 35°C of 2.10 dl/g and a melt viscosity at 200°C of 250 kPa-s. What will be the value of the intrinsic viscosity (same solvent and temperature as earlier) for a new sample made from the same monomer but with a melt viscosity (at 200°C) of 835 kPa-s?

Solution: Assume Equation 7.52 with a slope of 3.5 and a molecular weight M_2 for the second sample:

$$\log\left(\frac{825}{250}\right) = 3.5 \log\left(\frac{M_2}{133,000}\right)$$

$$M_2 = 187,000$$

In a theta solvent,

$$\frac{[\eta]_2}{[\eta]_1} = \left(\frac{187}{133}\right)^{1/2}$$

$$[\eta]_2 = 2.49 \text{ dl/g}$$

Deviations from a linear relationship between η and M in polymer melts with small M are generally believed to arise from a molecular weight dependence of ζ_m at small M . This **chain-end effect** [59] saturates for polymer chains composed of 100 or more repeat units and therefore cannot explain the observed transition in viscosity above M_c . To understand the transition in viscosity when $M > M_c$ in polymer melts and for $\nu_2 > \nu_{2c}$ in solutions, we examine the assumption of an isolated polymer chain motion used to derive Equation 7.11. Specifically, if the number of polymer molecules per unit volume is Γ and each molecule occupies a volume V_p , then we would expect this assumption to fail when $V_p\Gamma \geq 1$, that is, as molecules begin to overlap. Substituting $V_p = (4/3)\pi R_g^3$ and $\Gamma = (cN_{AV})/M$ leads to a critical polymer concentration termed the **overlap concentration** for isolated molecules to begin to overlap:

$$c^* = \rho\nu_2^* = \frac{3M}{4\pi N_{AV}R_g^3} \quad (7.53)$$

We have already seen that in a good solvent $R_g \sim M^{3/5}$ and $c^* \sim M^{-4/5}$; whereas in a theta solvent, $R_g \sim M^{1/2}$ and $c^* \sim M^{-1/2}$. The overlap concentration for high-molecular-weight molecules can therefore be quite low, indicating that the isolated chain assumption can break down even for moderately high-molecular-weight polymers.

At even higher solution concentration, molecular overlap becomes so strong that the effect begins to strongly influence polymer rheology. In 1971, P. G. de Gennes proposed that the transition in molecular weight dependence of η arises from an additional contribution from **topological constraints** that highly overlapping polymer chains exert on one another [60]. The **critical molecular weight** M_c required for the transition is then related to the minimum number of repeat units required for molecules to invade each other's space and intertwine or entangle. Molecules such as polystyrene ($Z_c = M_c/M_0 \approx 365$) and poly(methyl methacrylate) ($Z_c \approx 295$) that possess somewhat stiff, bulky repeat units would then be expected to have higher Z_c values than molecules such as polyethylene ($Z_c \approx 135$) and poly(ethylene oxide) ($Z_c \approx 100$) that possess more flexible compact repeat units, which is indeed the case [59]. De Gennes specifically contended that in the presence of **entanglements**,

TABLE 7.8
Applicability of the Empirical Relationship $\log \eta = 3.4 \log Z_w + K$ for Describing Viscosity Data
for Various Long-Chain Polymer Melts

Polymer-Solvent Pair	[Polymer], Weight Fraction, f	Range of Applicability			Temperature Range Studied (°C)	Polymers and Molecular Weight Detm(N)
		$v_2 Z_c$ Break ^a	Highest Z Studied			
Linear nonpolar polymers						
Polyisobutylene	1.0	610	53,000		-9 to 217	$f(\eta)$
Polyisobutylene-xylene	0.05-0.20	~1400	140,000		25	W and $f(\eta)$
Polyisobutylene-decalin	0.05-0.20	-	140,000		25	W and $f(\eta)$
Polystyrene	1.0	730	7,300		130-217	$f(\eta)$
Polystyrene-diethyl benzene	0.14-0.44	~1000	22,500		30-100	$f(\eta)$
Poly(dimethyl siloxane)	1.0	~950	34,000		25	$W; \pi, LS$

Linear polar polymers					
	0.25	208	24,000	60	$f_c(\eta)$
Poly(methyl methacrylate)-diethyl phthalate	1.0	290	960	80-200	W:E
Decamethylene sebacate	10	280	1,320	80-200	W:E
Decamethylene adipate	10	290	990	80-200	W:E
Decamethylene succinate	10	290	1,190	0-200	W:E
Decamethylene adipate	1.0	<326	1,443	90	W:E
ω -Hydroxy undecanoate					
Effect of branching					
Poly(ϵ -caprolactam)					
Linear	1.0	324	2,300	253	W:E
Terachain	1.0	390	1,560	253	W:E
Octachain	1.0	550	2,000	253	W:E

Source: Ott, E. et al., *Cellulose and Cellulose Derivatives*, part III, Wiley, New York, 1216, 1955.

^a Z_c is the lowest chain length for which equation is valid for the solution wherein v_2 is the volume fraction of polymer. Detm(N), determination; f_c , fraction; W, whole polymer chain lengths were determined as indicated from intrinsic viscosity, (η) ; osmotic pressure, (π) ; LS, light scattering; E, end-group analysis.

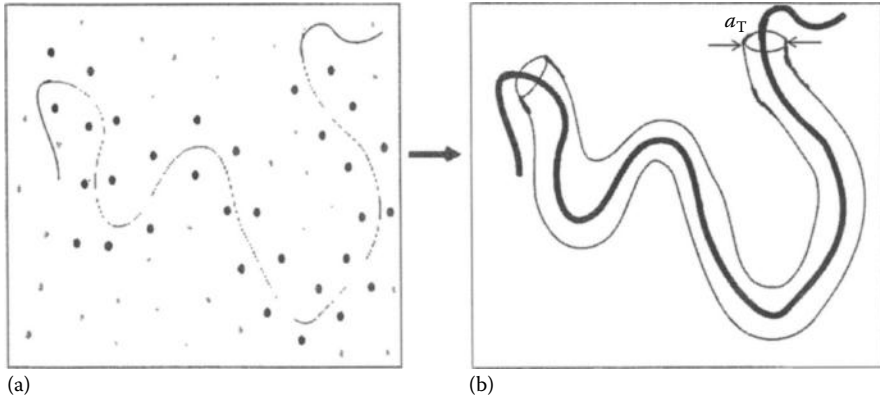


FIGURE 7.18 A single polymer chain in an entangled solution. (a) Distribution of entanglements (large dots) and solvent molecules (small dots) along the chain contour. (b) Topological constraints produced by entanglements confine diffusion of the polymer chain to a tubelike region; diameter $a_T = \sqrt{x_e}a$ and curvilinear length $L_c = (x/x_e)a_T$.

long-range translational diffusion of any individual polymer molecule in a melt or solution of similar molecules is confined to a tubelike region of diameter $a_T = \sqrt{x_e}a$ and length $L_c = a_T(x/x_e)$ (Figure 7.18). The terms a_T and L_c are designated the **tube diameter** and the polymer **contour length**, respectively, in the many papers and texts that analyze rheology and dynamics of entangled polymers. The variable $x_e = Z_c/q$ is termed the **entanglement spacing** and q typically ranges from 2 to 4 [61].

The tube envisaged in the **de Gennes tube** model framework is not an empty channel as one might summarize from textbook cartoons such as Figure 7.18b. It is instead filled with segments of neighboring molecules (Figure 7.18a) as required for the density to remain uniform. Thus, once in the tube, motion of any single molecule is resisted by the same friction forces as it would experience in a melt of short, unentangled polymers. The **friction coefficient** per molecule for motion along the tube is therefore the same as that for an unentangled polymer chain $\zeta_{p,T} = x\zeta_m$, but the time required by the molecule to renew its configuration is longer [60,62]. To see how this affects η_0 , we begin by writing down an expression for the elastic modulus or so-called **plateau modulus** (see Section 9.4) for the temporary polymer network created by entanglements about a randomly selected molecule [59,62,63]:

$$G_N^0 = \frac{4\rho N_{AV}kT}{5M_e} \quad (7.54)$$

where:

$$M_e = M_0x_e$$

The lifetime of the network is the time required for it to disappear spontaneously (by diffusion of the molecules forming the network) or the time required for the test molecule to escape by diffusion along the tube. Except in highly polydisperse polymers, the former time, termed the **constraint-release time** λ_{CR} [64], is substantially longer

than the latter, termed the tube diffusion time λ_{Rep} (or **reptation time**, by analogy to the constrained sliding motion of a snake). Therefore, the reptation process dominates.

If the friction coefficient for motion of entangled polymer chains along the tube is $\zeta_{\text{P,T}} = x\zeta_{\text{m}}$, as assumed by de Gennes, then the **self-diffusion coefficient** for reptation can be computed using Einstein's formula:

$$D_{\text{T}} = \frac{kT}{\zeta_{\text{P,T}}} = \frac{kT}{x\zeta_{\text{m}}} \quad (7.55)$$

The time λ_{Rep} required to escape the tube is therefore given by

$$\lambda_{\text{Rep}} = \frac{L_{\text{c}}^2}{D_{\text{T}}} = x^2 \frac{x}{x_{\text{e}}} \frac{a^2 \zeta_{\text{m}}}{kT} \quad (7.56)$$

An expression for the zero-shear viscosity follows from the definition of λ_{Rep} :

$$\eta_0 = \beta G_{\text{N}}^0 \lambda_{\text{Rep}} = \beta G_{\text{N}}^0 \left(\frac{L_{\text{c}}^2}{D_{\text{T}}} \right) = \frac{4}{5} \beta \frac{\rho N_{\text{AV}} a^2 \zeta_{\text{m}}}{M_0} x \left(\frac{x}{x_{\text{e}}} \right)^2 \quad (7.57)$$

where:

β is a constant of order 0.3 for narrow molecular weight distribution polymers.

Thus, the shear viscosity of an entangled polymer is predicted to increase much more strongly with molecular weight M than that of an **unentangled polymer**.

A similar conclusion can be reached from an older, more literal theoretical approach for calculating the viscosity of **entangled polymers** [65]. In this theory, entanglements between molecules are thought to form slippery knots that literally couple their motion. Thus, when a polymer liquid is subjected to shear flow, individual molecules respond by instinctively attempting to drag their entangled neighbors along with them. This action is resisted by the network of entanglements on surrounding molecules. This so-called **drag-coupling model** therefore yields a molecular friction coefficient that increases in proportion to the number of entanglements per molecule x/x_{e} [66,67]:

$$\zeta_{\text{p}} = x\zeta_{\text{m}} \left(1 + s \frac{x}{x_{\text{e}}} \right) \quad (7.58)$$

where:

s is a so-called **slippage factor** that ranges from 0 (no entanglement coupling) to 1.0 (perfect coupling)

An *ad hoc* argument due to Bueche [65] suggests that $s \approx 4/9$ for polymers in solution. In polymer melts, however, the slippage factor may vary with the strength of secondary bonds between polymer chains, for example, $s \rightarrow 1$ for molecules that interact via strong hydrogen bonds, whereas $s \rightarrow 4/9$ for molecules that interact only by weak van der Waals forces. Thus, for x/x_{e} greater than about 3, the second term in Equation 7.58 would begin to dominate and by $x/x_{\text{e}} \approx 10$, $\zeta_{\text{p}} \approx sx(x/x_{\text{e}})\zeta_{\text{m}}$.

The zero-shear viscosity can be determined by a similar procedure as for Equation 7.11 to obtain [66,67]

$$\eta_0 = L_c^2 s \Gamma \frac{x}{x_e} x \zeta_m = s \frac{\rho N_{AV} a^2 \zeta_m}{m_0} x \left(\frac{x}{x_e} \right)^2 \quad (7.59)$$

Both approaches (Equations 7.57 and 7.59) therefore yield $\eta_0 \sim x^3$ for $(x/x_e) \gg 1$.

An analysis by Doi [62,69] shows that the somewhat stronger than cubic exponent observed experimentally emerges from molecular-weight-dependent **fluctuations** in L_c due to thermal motion of polymer segments near the chain ends. More recent work [69] has confirmed that such tube length fluctuations are likely responsible for the larger than cubic exponent in η versus x plots obtained from experiments.

7.6 EFFECT OF TEMPERATURE AND PRESSURE

Viscous flow in a dense polymer liquid can be pictured as taking place by the movement of molecules or segments of molecules in jumps from one place in a lattice to a vacant hole. The total *hole concentration* can be regarded as space free of polymer, or **free volume**. Doolittle proposed that the viscosity should vary with the free volume in the following manner [70]:

$$\log \eta = A + \frac{BV_0}{V_f} \quad (7.60)$$

where:

A and B are constants

V_f is the free volume equal to $V - V_0$

V is the specific volume (per unit weight)

V_0 is the specific volume extrapolated from the melt to 0 K, without change of phase

The fractional free volume $f' = V_f/V$ is expected to vary with temperature as follows:

$$f' - f'_g = \alpha \Delta T \quad (7.61)$$

where:

α is the difference between the expansion coefficients for melt and glass

$\Delta T = T - T_g$

f'_g is the fractional free volume at T_g

For many polymers, α is about $4.8 \times 10^{-4} \text{ K}^{-1}$.

Williams, Landel, and Ferry [71] found empirically that the viscosity of a molten polymer at arbitrary temperature T can be related to its viscosity η_g at the glass transition temperature T_g by

$$\log \left(\frac{\eta}{\eta_g} \right) = \frac{-17.44(T - T_g)}{51.6 + (T - T_g)} = \frac{-17.44\Delta T}{51.6 + \Delta T} \quad (7.62)$$

This equation is known as the **WLF equation**. Equations 7.60 through 7.62 can be combined if V_0 in Equation 7.60 is replaced by V . This approximation is not unreasonable because unlike V_f , V does not change too rapidly with temperature. We begin by writing Equation 7.60 in difference form to eliminate the constant A :

$$\log\left(\frac{\eta}{\eta_g}\right) = \frac{B(f' - f'_g)}{f'_g f'} \quad (7.63)$$

Substituting for f' from Equation 7.61 gives

$$\log\left(\frac{\eta}{\eta_g}\right) = \frac{-(B/f'_g)\Delta T}{(f'_g/\alpha) + \Delta T} \quad (7.64)$$

Comparing Equations 7.64 and 7.62, we see $(f'_g = 51.6\alpha) \approx 0.025$. Thus, the glass transition is predicted to occur at a temperature where the fractional free volume is 2.5%. Remarkably, the empirical relationships used in deriving this result have been found to apply for most glass-forming compounds (polymers and inorganic glasses, low-molecular-weight compounds)! And, the inferred relationship between T_g and the fractional free volume is currently considered universal for glass-forming liquids.

When $T > 100^\circ\text{C} + T_g$, Equation 7.62 does not work as well as the more general expression [57]:

$$\log\left(\frac{\eta}{\eta_R}\right) = B' \left(\frac{1}{T^\xi} - \frac{1}{T_R^\xi} \right) \exp\left(-\frac{\beta}{M}\right) \quad (7.65)$$

where:

- η_R is the viscosity at a reference temperature T_R for a molecular weight M
- ξ is typically an integer
- B' and β are fitted constants

Some typical results for glass-forming polymers and molecular liquids are provided in Figure 7.19.

One would expect compression of a polymer melt to decrease its free volume and, consequently, increase its viscosity. Figure 7.20 summarizes the effect of upstream pressure in a capillary on the viscosity of polystyrene and polyethylene melts at temperatures above their respective glass transition temperatures T_g . The figure indicates that while pressure generally increases viscosity, the effect can be quite different for polymers with dissimilar monomer structure. Because increasing pressure will increase the glass transition temperature, it is possible to capture this effect using Equation 7.62 with a pressure-dependent T_g [73,74]. For several polymers, dT_g/dP is reported to be in the range of 0.16–0.43°C/MPa. Polystyrene, for example, has a value of 0.3°C/MPa [73]. It is harder to generalize about the temperature and pressure dependence of viscosity for polymer solutions.

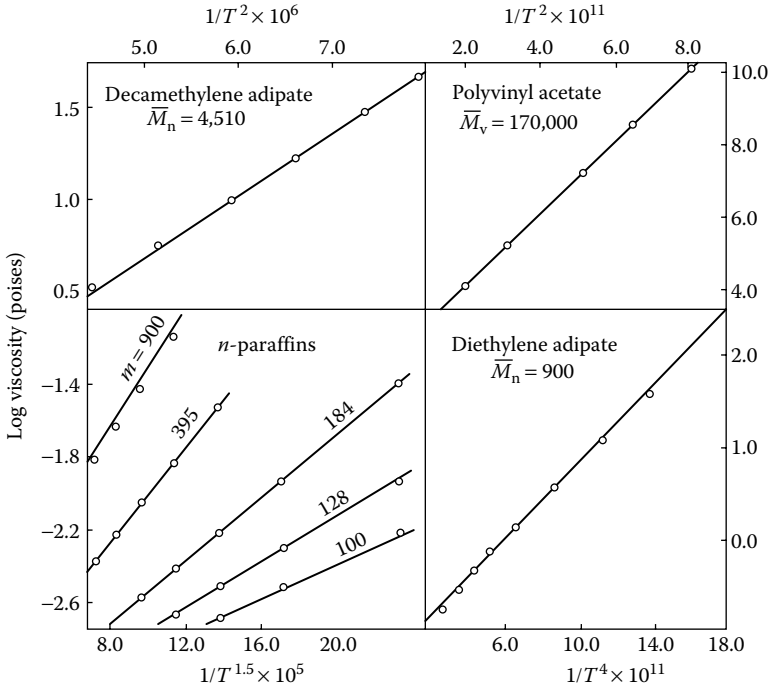


FIGURE 7.19 Viscosity–temperature curves according to Equation 7.65. (Data from Berry, G. C., and T. G. Fox, *Adv. Polym. Sci.*, 26, 359, 1955.)

7.7 ELONGATIONAL VISCOSITY

Despite their simplicity and relative ease of use, viscometers based on pressure driven or simple shear flows provide only limited information about the flow resistance of polymer materials. In many common polymer forming processes, such as fiber spinning, injection molding, and film blowing, polymers experience a combination of shear, compression, and extensional deformations that require different types of characterization to understand how the material will respond and how the process might be designed to accommodate this response [74]. This situation can be traced to the high degree of stretching or traction of microstructural units (e.g., molecules, domains, droplets) that occur when macroscopic polymer fibers are wound and stretched in a spinning process, inflated in a film blowing device, or when a fluid stream is injected against the immovable wall of a cold mold in an injection molding process. In these situations, the resistance to flow arising from relative motion of layers sliding by each other, as occurred in simple shear flow, is augmented by the resistance of molecular and structural elements to changes in size, shape, and orientation. Thus, important and relevant insights into polymer processing can be obtained by studying their rheological properties in **extensional flow**.

The simplest extensional flow that can be used to characterize the resistance of a polymer is **uniaxial elongation** [9]. In this flow, an element of fluid is stretched

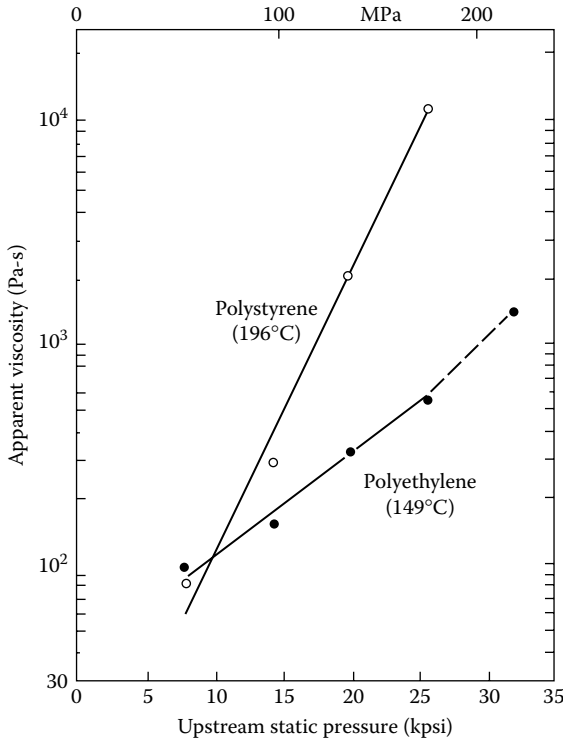


FIGURE 7.20 Apparent viscosity versus upstream pressure for polyethylene and polystyrene. (Data from Carley, J. E., *Mod. Plast.*, 39, 123, December 1961.)

along one axis and shrinks uniformly in the plane with surface normal parallel to this axis (Figure 7.21). If the resultant deformation produced in the test specimen is homogeneous in space, the rate of deformation can be described in terms of a single parameter termed the extension rate ($\dot{\epsilon}$) related to the rate of change of length by

$$\dot{\epsilon} = \frac{V}{L} = \frac{1}{L} \frac{\partial L}{\partial t} \tag{7.66}$$

Integrating this equation yields an expression for how the length of the material changes with time, $L(t) = L_0 \exp(\dot{\epsilon}t)$, whence it is seen that in the uniaxial extensional flow, material points separate as an exponential function of time. This can be contrasted with the case for simple shear flow depicted in Figure 7.1 for which $\dot{\gamma} = V/d = (1/d)(\partial L/\partial t)$ and $L = d\dot{\gamma}t$ (i.e., material points separate linearly with time). A fundamental consequence of this difference is that in an extensional flow material elements are strongly stretched in flow, which provides an additional source of resistance that can become quite large when polymers with long entangled side branches are involved. A practical consequence is that the physical space required to maintain a fixed extension rate over long enough time that the material response comes to a steady-state (i.e., ceases to depend on time) can be very large. A somewhat subtler but important feature apparent

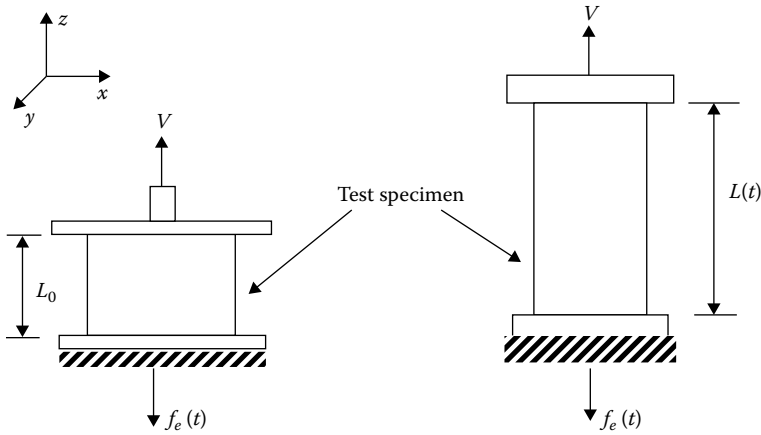


FIGURE 7.21 Configuration for imposing time-dependent uniaxial extensional deformation of a polymer specimen of initial length L_0 (left) and instantaneous stretch length L (right).

from Equation 7.66 is that the imposed speed must be decreased at an exponential rate with time to sustain a uniform rate, meaning that good feedback control of speed is required to achieve a constant $\dot{\epsilon}$ in uniaxial extension.

As in shear flow, one can define an **extensional stress** τ as the traction force in the direction of stretching divided by the specimen area normal to the direction of the stretching:

$$\tau(\dot{\epsilon}, t) = \frac{f_e(\dot{\epsilon}, t)}{A(\dot{\epsilon}, t)} \quad (7.67)$$

The ratio of the extension stress to the extension rate defines the apparent elongational viscosity of the material:

$$\bar{\eta}_E(\dot{\epsilon}, t) = \frac{\tau(\dot{\epsilon}, t)}{\dot{\epsilon}} \quad (7.68)$$

A significant impediment to measuring the elongational viscosity of polymers is that the idealized deformation depicted in Figure 7.21 is much more difficult to achieve in practice than in the corresponding case of a simple shear flow. A consequence is that the elongational viscosity in a material subject to a constant extension rate rarely, if ever, becomes independent of time, meaning that the measured elongational viscosity is almost never a **material property**. Additionally, the cross-sectional area of a uniaxially deformed specimen is a function of position along its length, which has led to the practice of using the smallest cross-sectional area, near the neck of the deformed material, in computing the extensional stress by Equation 7.67.

Notwithstanding these difficulties, numerous devices have been developed that approximate the uniaxial extension flow to some degree and which allow the elongational viscosity of polymers to be measured. Unfortunately, all have practical drawbacks that must be understood and taken into account in interpreting polymer elongational viscosity data. Figure 7.22, for instance, graphically illustrates the

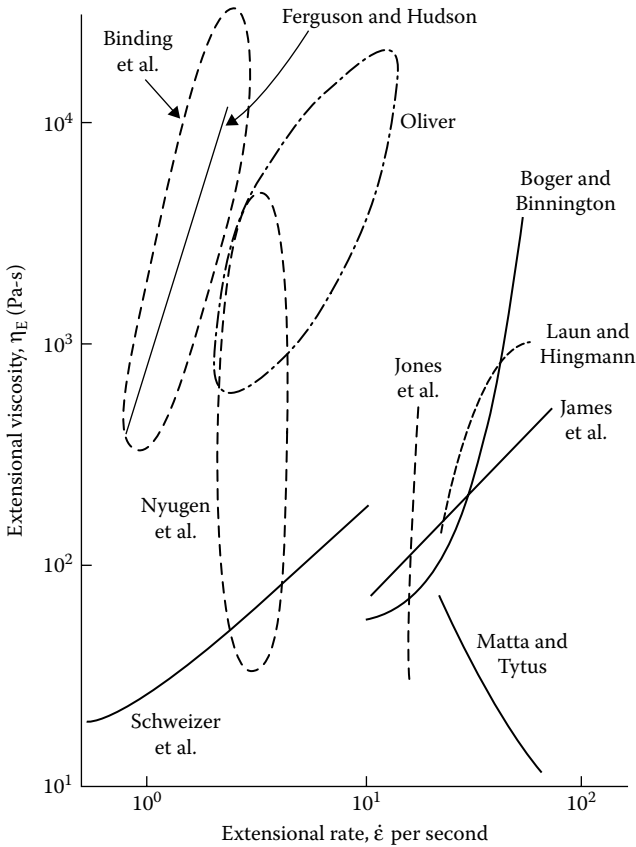


FIGURE 7.22 Elongational viscosity versus extension rate measured for a solution of a high-molecular-weight polybutadiene ($M_w = 4\text{--}6 \times 10^6$ g/mol) in a low-molecular-weight polybutene ($M_w = 650$ g/mol)/kerosene mixture. The plot reports data obtained by multiple researchers using different extensional flow measurement methods: Binding et al., spinline rheometer; Boger and Binnington, contraction flow; Ferguson and Hudson, spinline rheometer; James et al., converging flow rheometer; Jones et al., pendant drop (filament stretching); Laun and Hingmann, opposed jets; Matta and Tytus, falling weight (filament stretching); Nguyen et al., filament stretching; Oliver, horizontal jet (spinning); Schweizer et al., opposed jets (stagnation flow). (Data from James, D. F., and K. Walters, chap. 2 in A. A. Collyer, ed., *Techniques of Rheological Measurement*, Elsevier, New York, 33–53, 1994.)

difficulty of making elongational viscosity measurements. The figure shows that wild swings in viscosity can be obtained for the same material characterized by different researchers using different devices, all capable of approximating the uniaxial extension. Hopefully after consideration of this figure, the reader has developed a healthy sense of caution in drawing too strong conclusions from elongational viscosity data. The pessimistic outlook about the reliability of measured or published elongational viscosity data that naturally follows from consideration of Figure 7.22 is fortunately being eroded as more modern measurement devices become available. Some of these instruments are attractive because of their versatility or ability to

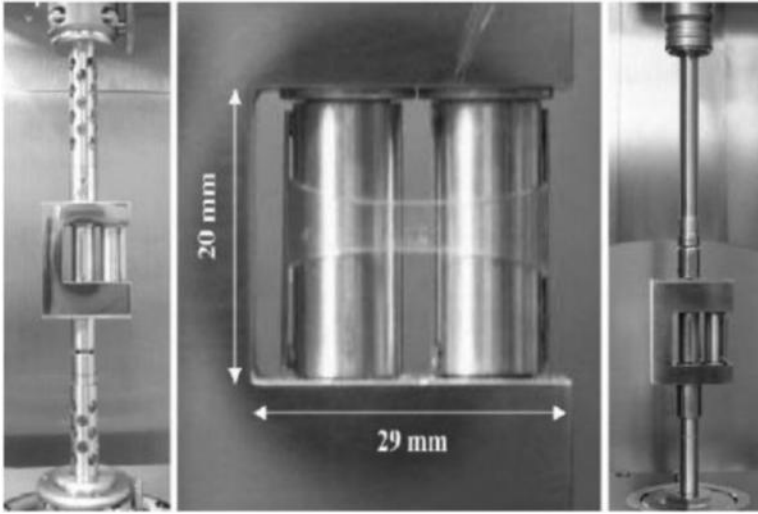


FIGURE 7.23 Photographs of a Sentmanat extensional rheometer (SER) illustrating the mode of operation (center) and mounting configurations for two commercial rotational rheometers (left: Rheometrics Scientific Ares; right: Anton Paar MCR). (Data from Sentmanat, M. et al., *J. Rheol.*, 49, 585, 2005.)

produce nearly homogeneous uniaxial elongation in molten polymers. The filament stretching apparatus depicted in Figure 7.23 is one such device. In this instrument, a rotational flow is employed to create an extension of a polymer filament anchored between two cylindrical rollers: one attached to a rotating shaft and the other permanently anchored to a rigid mechanical frame. Rotation of the shaft causes the movable roller to spin and the polymer to be wound up and stretched in the space between the two rollers. After correcting the measured extensional stress by removing the contribution due to surface tension, the fluid's time-dependent elongational viscosity $\eta_E(\dot{\epsilon}, t)$ can be determined from the following expressions [77]:

$$\tau_e(\dot{\epsilon}, t) = \frac{f_e(\dot{\epsilon}, t)}{A(\dot{\epsilon}, t)} - \frac{\gamma}{R} \quad (7.69)$$

$$\eta_E(\dot{\epsilon}, t) = \frac{\tau_e(\dot{\epsilon}, t)}{\dot{\epsilon}} \quad (7.70)$$

where:

γ is the coefficient of surface tension

R is the radius of curvature of the elongated specimen

For simple Newtonian liquids (and some complex fluids at low enough extension rates, $\dot{\epsilon} \ll \lambda_p^{-1}$, where λ_p is again the longest material relaxation time or terminal time), the viscosity of a material measured in uniaxial elongation becomes independent of time upon persistent stretching and can be related to its zero-shear viscosity by the

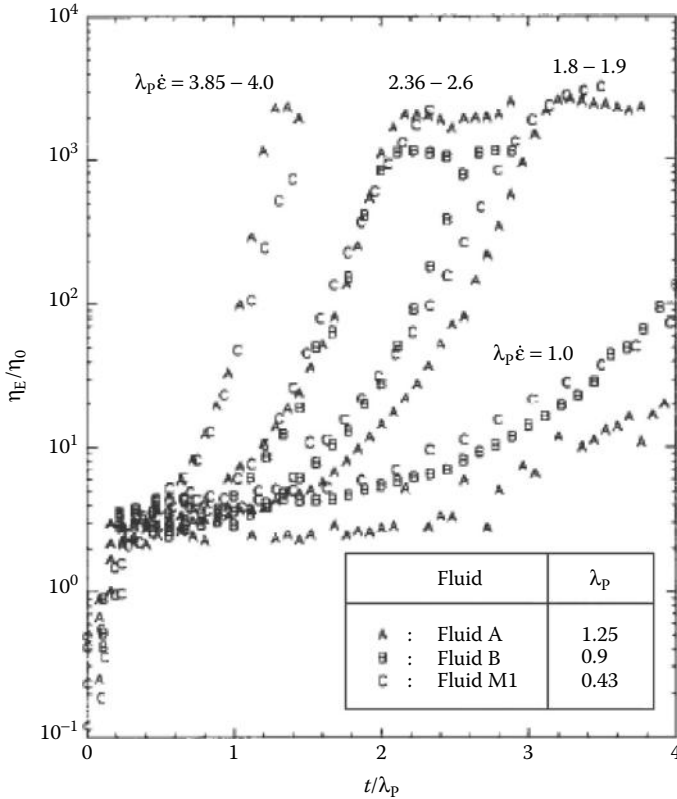


FIGURE 7.24 Trouton ratio (η_E/η_0) versus dimensionless time (t/λ_p) for three different polyisobutylene solutions in low-molecular-weight polybutene at different dimensionless extension rates ($\epsilon \lambda_p$). Both the time and the extension rate are made dimensionless using the longest relaxation times for the solutions provided in the inset. (Data from Tirtaatmadja, V., and T. Sridhar, *J. Rheol.*, 37, 1081, 1993.)

expression $\eta_E = 3\eta_0$ [78] known as **Trouton’s rule**. This means that even in the case where polymer molecules are able to relax to the equilibrium configurations faster than the rate of stretching, the extensional flow resistance is substantially larger than the resistance to shear. As the extension rate increases above the molecular relaxation rate, the time-dependent elongational flow viscosity is generally much higher than the shear viscosity (see Figure 7.24), underscoring the important role even a small amount of extensional flow can have on the fluid resistance in polymer processing.

7.8 DRAG REDUCTION IN TURBULENT FLOW

The friction coefficient of simple fluids in highly turbulent flows can be dramatically lowered by addition of rather small quantities of polymer. Fabula has shown, for example, that extremely small amounts of poly(ethylene oxide) in water reduce the pressure drop for a given flow rate to as little as one-fourth that

for water alone [80]. Drag reduction has been suggested as a means of extending the distance that water from fire hoses can be discharged. For a fixed pressure drop, a smaller diameter hose will transmit the same flow of water enabling firemen to drag less weight per unit length when pulling hoses into buildings. Storm sewer capacity during temporary overloads can be increased by injection of polymers. A ship's speed can be increased by injection of a polymer solution at the bow. Oil-soluble polymers have been used to assist the flow of crude oil in the *trans*-Alaska pipeline as well as in pipes carrying oil from offshore platforms to facilities on the shore. Friction reduction of 30%–50% is achieved using as little as 10 ppm polymer [81].

In the experiments summarized in Figure 7.25, it was found that the pressure drop, which is proportional to τ_R , during turbulent flow of water in tubes steadily decreased as a high-molecular-weight ($M_v = 5.8 \times 10^6$) poly(ethylene oxide) was added. The **Reynolds number** N_{Re} in a tube with diameter $D = 2R$ is given by

$$N_{Re} = \frac{D\bar{v}\rho}{\eta} \quad (7.71)$$

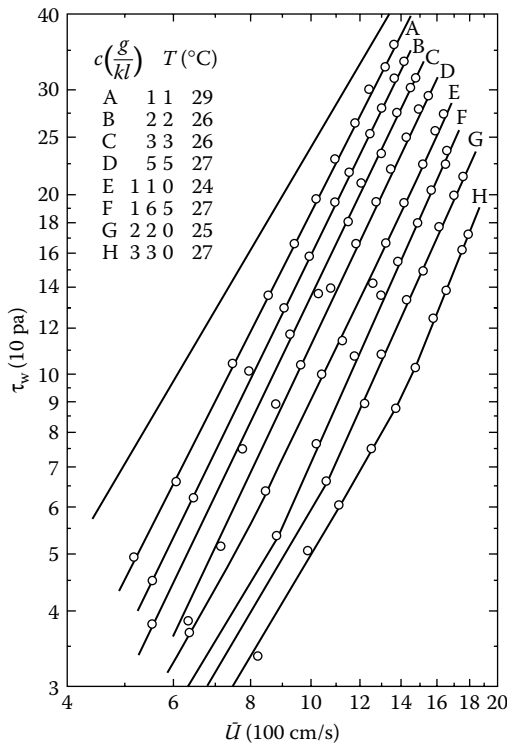


FIGURE 7.25 Decrease in stress (drag reduction) at constant average velocity \bar{U} by addition of small amounts of high-molecular-weight poly(ethylene oxide). (Data from Hoyt, J. W., Drag reduction, in *Encyclopedia of Polymer Science and Engineering*, vol. 5, 2nd edn., Wiley, New York, 129, 1986.)

where:

$\bar{v} = Q/(\pi R^2)$ is the average velocity of fluid in the tube

The viscosity η of water at the temperatures in Figure 7.26 is approximately $0.01 \text{ poise} = 0.01 \text{ g/(s}\cdot\text{cm)} = 0.001 \text{ Pa}\cdot\text{s}$ and its density $\rho = 1 \text{ g/cm}$. For water flowing in a 1-cm diameter tube, $D\rho/\eta \approx 100$ and the range of \bar{v} in Figure 7.25 correspond to N_{Re} between 40,000 and 200,000. At the polymer concentrations generally used for drag reduction, ordinary shear viscosity of the fluid is relatively unaffected by polymer. However, even at very low concentrations, **elongational viscosity** is increased dramatically. This can be demonstrated by the long, pituitous strings that can be drawn from dilute polymer solutions by dipping in an object and then withdrawing it rapidly. Other manifestations of the same phenomenon are the elastic recoil of stirred solutions when stopped suddenly and the inhibition of vortex formation in a draining vessel by adding polymer.

It is the high elongational viscosity of polymer solutions that is believed to change the rate of energy dissipation in turbulence. Turbulent flow dissipates energy because of the exchange of momentum between fluid domains. These domains, or eddies, can be characterized by measuring velocity fluctuations in a turbulent flow. In any system, there will be a spectrum of eddy sizes. Turbulence is sometimes pictured as “eddies within eddies within eddies.” The withdrawal of material from the viscous sublayer along the wall is decreased by high elongational viscosity. Also, the small eddies throughout the conduit are decreased in intensity as a result of viscous damping.

For a quantitative demonstration [82], a simple apparatus (Figure 7.26) consisting of a reservoir that holds about 2000 cm^3 of liquid and a flexible tube of 200 cm long with an inside diameter of about 1 cm. This in turn is connected to a horizontal precision bore tube. The efflux from the horizontal tube is allowed to fall freely a vertical distance of 19.6 cm into a trough and the horizontal jet distance x is measured. From simple mechanics, the average velocity in the tube u is related to x and the time t for liquid to fall a distance of 19.6 cm under the force due to gravity.

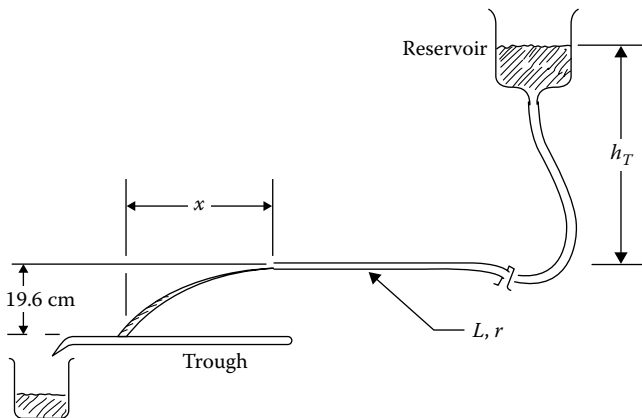


FIGURE 7.26 Apparatus for performing turbulent flow measurements using polymer solutions.

$$u = \frac{x}{t} = x \left(\frac{981}{39.2} \right)^{1/2} = 5.00x \tag{7.72}$$

If the total head is 150 cm, x will be around 30 cm at room temperature for water flowing through a tube with the dimensions listed in Table 7.9. When water is replaced by a dilute polymer solution, much larger values of x result. Typical results are shown in Figure 7.27 for polyacrylamide (Separan AP30, Dow Chemical Co, Midland, Michigan) solutions. In engineering calculations, the Reynolds number

TABLE 7.9
Parameters Used for Performing Turbulent Flow Measurements Using Apparatus Depicted in Figure 7.26

Apparatus	A 2000-cm³ Beaker + a Precision Bore Tube (Figure 7.28)	
Typical data (water, 25°C)	Tube length, $L = 91.3$ cm	Jet distance, $x = 30.0$ cm
	Tube radius, $r = 0.15$ cm	Jet height, $y = 19.6$ cm
	Head, $h_T = 150$ cm	$\eta/\rho = 0.0090$ cm ² /s (25°C)
Equations	Velocity, $u = 5.00x$	Reynolds number, $N_{Re} = 2rui(\eta/\rho)$
	Friction factor, $f = [(g/50)(h_T/x^2) - 0.35] (2r/L)$ (the second term is kinetic energy correction)	
Calculated result (water)	$u = 150$ cm/s	$N_{Re} = 5000$
	$f = 0.0096$ (compared to expected value of 0.0094)	

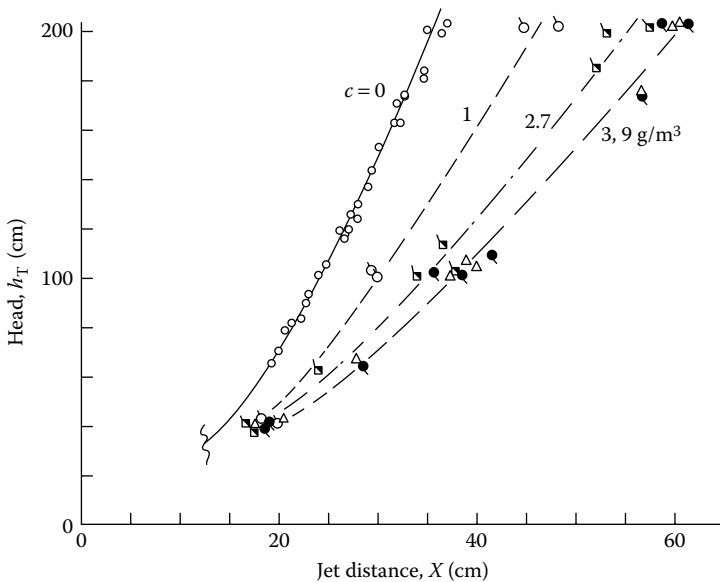


FIGURE 7.27 Typical flow data for dilute solutions of polyacrylamide in water. The plot shows results obtained by several groups of students. The concentration c of the solutions increase from left to right in the figure.

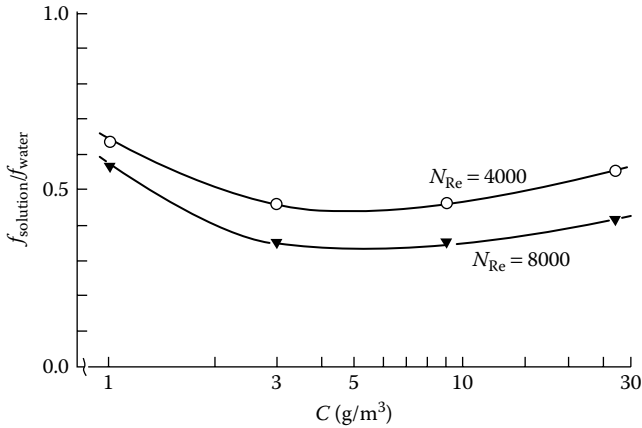


FIGURE 7.28 Data from Figure 7.27 presented as ratio of friction factors at constant Reynolds number. The open circles correspond to $N_{Re} = 4000$ and the filled triangles correspond to $N_{Re} = 8000$.

and the **friction factor** are of interest (Table 7.9). The reduction in friction by a polyacrylamide solution is seen in Figure 7.28. Poly(ethylene oxide) (Polyox WSR 308, Union Carbide Corporation, Bound Brook, NJ) are also found to be very effective.

KEYWORDS

Polymer forming processes
 3D printing
 Rheology
 Viscosity
 Planar Couette shear
 Laminar flow
 Shear flow
 Shear stress
 Shear rate
 Viscous drag
 Viscous dissipation
 Monomeric friction coefficient
 Free draining
 Hydrodynamic interaction
 Material property
 Newtonian and non-Newtonian liquids
 Apparent viscosity
 Flow curve
 Bingham plastic
 Shear thickening and dilatant
 Shear thinning and pseudoplastic

Zero-shear viscosity
Shear-thinning exponent
Upper and lower Newtonian
Random coil structure
Relaxation time
End-to-end distance
Deborah number
Weissenberg number
Constitutive equation
Power-law fluid
Ellis model
Cross model
Characteristic relaxation time
Carreau model
Kinematic viscosity
Ostwald viscometer
Ubbelohde viscometer
Differential viscometer
Melt index
End-to-end vector
Freely jointed chain
Random flight model
Root-mean-squared end-to-end distance
Freely rotating chain model
trans conformation
Gauche position
Symmetric restricted rotation model
Statistical segment length
C-infinity
Chain stiffness
Radius of gyration
Expansion coefficient
Excluded volume
Theta temperature
Flory temperature
Intrinsic viscosity
Specific viscosity
Inherent viscosity
Huggins equation
Kraemer equation
Flory–Fox parameter
Reduced viscosity
Relative viscosity
Mark–Houwink–Sakurada relationship
Zimm theory
Beads

Springs
 Nondraining
 Viscosity-averaged molecular weight
 Hydrodynamic volume
 Restricted rotation
 Steric factor
 Rouse chain motion
 Chain-end effect
 Overlap concentration
 Topological constraints
 Critical molecular weight
 Entanglements
 Tube diameter
 Contour length
 Entanglement spacing
 De Gennes tube
 Tube model
 Constraint-release time
 Reptation time
 Self-diffusion coefficient
 Unentangled and entangled polymers
 Drag-coupling model
 Slippage factor
 Friction coefficient
 Diffusion coefficient
 Tube length fluctuations
 Free volume
 WLF equation
 Extensional flow
 Uniaxial extension
 Elongational viscosity
 Trouton rule
 Chain stretching
 Turbulent flow
 Drag (friction) reduction

PROBLEMS

7.1 The following data are for a narrow molecular weight fraction of poly(methyl methacrylate) in acetone at 30°C (density = 0.780 g/cm³):

Concentration, c (g/100 ml)	Osmotic Pressure, π (h) cm Solvent	Relative Viscosity, η_r
0.275	0.457	1.170
0.338	0.592	—

(Continued)

Concentration, c (g/100 ml)	Osmotic Pressure, π (h) cm Solvent	Relative Viscosity, η_r
0.344	0.609	1.215
0.486	0.867	—
0.896	1.756	1.629
1.006	2.098	—
1.199	2.710	1.892
1.536	3.725	—
1.604	3.978	2.330
2.108	5.919	2.995
2.878	9.713	—

Plot appropriately and estimate $[\eta]$, k' (Huggins), M , and the second virial coefficient. Include dimensions for each. Knowing that $[\eta]\theta = 6.5 \times 10^{-4} M^{0.5}$ for this polymer in a theta solvent at 30°C, calculate from these data $(r_0^2)^{1/2}$, $(r^2)^{1/2}$, and α the expansion factor.

7.2 Two samples with narrow molecular weight distributions are prepared of a new polymer. Some measurements are made in acetone and hexane.

Medium	Parameter	Sample A	Sample B
Acetone, 25°C	M_n (osmotic pressure)	8.50×10^4	Not run
	Second virial coefficient	Zero	
	Intrinsic viscosity	0.87 dl/g	1.32 dl/g
Hexane, 25°C	Intrinsic viscosity	1.25 dl/g	2.05 dl/g

- (a) What is the M_n of sample B?
- (b) What are the Mark–Houwink–Sakurada parameters (K' and a) in acetone and hexane?
- 7.3** The system polyisobutylene–benzene has a theta temperature of 24°C. Describe how each of the quantities mentioned below would change for a given sample as the temperature is increased to 40°C from 24°C (increase, decrease, or no change). Explain why.
- (a) Molecular weight measured by osmotic pressure.
- (b) Osmotic pressure of a 1-g/dl solution.
- (c) Intrinsic viscosity.
- (d) Ratio of M_w (light scattering) to M_n (osmotic pressure).
- 7.4** A polymer based on isobutylene (FW = 56.0) has a steric factor of 1.93 at 24.0°C. What is the molecular weight of a sample that has an intrinsic viscosity of 0.780 dl/g in a good solvent at 24°C for which the expansion factor is 1.22?
- 7.5** A monodisperse polymer P is characterized in solvent S with the following results (all at 27°C):

Concentration (g/dl)	Osmotic Pressure (atm)	Viscosity (Pa·s)
0.000	–	0.00700
0.600	0.00500	0.00995
1.000	0.01125	0.01225

In theta solvent T, P has an intrinsic viscosity of 0.350 dl/g at 27°C.

- (a) What osmotic pressure (atm) will be exhibited by a 0.25-g/dl solution of P in T at 27°C?
- (b) What is the expansion factor in S for a new polymer sample P_{new} from the same monomer that exhibits a viscosity of 0.01225 Pa·s at a concentration of 0.600 g/dl at 27°C? The molecular weight of P_{new} is 100,000 (monodisperse).

7.6 For a certain monodisperse polymer in solution, the original concentration c_0 is unknown. At a series of dilutions, the osmotic pressure and viscosity are measured. Notice that the osmotic pressure is directly proportional to the concentration. Plot the data properly to obtain the absolute value of the hydrodynamic volume $[\eta]M$ in units of dl/mol.

Concentration	Osmotic Pressure at 27°C (atm)	Viscosity at 27°C (centipoise)
c_0 divided by 10.0	2.00×10^{-3}	4.60
12.5	1.60×10^{-3}	3.62
15.0	1.33×10^{-3}	3.04
20.0	1.00×10^{-3}	2.40
Solvent alone	0.00	1.00

7.7 For polymer X, the hydrodynamic volume in a theta solvent at 40°C is 6.0 times that calculated for a chain of constant tetrahedral bond angle ($\theta = 70.53^\circ$). If the repeat unit of four carbon chain atoms has a formula (molecular) weight of 115, what is the molecular weight of the monodisperse sample described by the following data (obtained in a theta solvent at 40°C)?

Concentration (g/dl)	Viscosity (mPa·s)
0.000	3.00
0.050	3.52
0.100	4.20
0.175	5.35
0.250	6.94

7.8 What is the rms end-to-end distance for a monodisperse polymer sample that is characterized by osmotic pressure measurements (π) and viscosity measurements (η).

Concentration, c (g/dl)	Osmotic Pressure, π (cm of Solvent)	Relative Viscosity, η_r
0.137	0.228	1.085
0.243	0.433	–
0.448	0.878	1.315
0.599	1.355	1.446

Solvent density = 0.780 g/cm³. $T = 27.0^\circ\text{C}$.

7.9 The following data are obtained for solutions of two samples of polymer P in two solvents, A and B, all at 30°C. Solvent B is a theta solvent. The repeat unit of the carbon chain making up the polymer has a formula weight of 152 atomic mass units per two chain atoms. The carbon–carbon bond has a length of 1.54Å and the usual tetrahedral bond angle.

Concentration (g/dl)	Viscosity (Pa·s)		
	0.000	1.200	1.200
0.100	1.757	1.338	1.136
0.200	2.467	1.487	1.384
Solvent	A	A	B
Molecular weight of polymer	1.00×10^6	2.00×10^5	1.00×10^6

Calculate the following:

- The rms end-to-end distance for the unperturbed chain of molecular weight of 1,000,000.
 - The value of the steric factor.
 - The value of the expansion factor in solvent A for the molecular weight of 1,000,000.
- 7.10** A sample of polyacrylamide forms solutions in water that can be fitted by a Huggins equation plot over the range of $1.0 < \eta_r < 1.5$ with a slope of 0.700 (g/dl)² and an intercept of 1.35 dl/g. If the data from the Huggins equation at relative viscosities of 1.0 and 1.5 are used to fit the Martin equation, specific viscosity can be predicted at a concentration of 5.0 g/dl?
- 7.11** The ratio of the intrinsic viscosity (dl/g) to the square root of weight for polystyrene in solvent K at 25°C is 0.00360. In solvent J at the same temperature, the ratio of the intrinsic viscosity to the square root of molecular weight for poly(vinyl acetate) is proportional to the one-fifth power of molecular weight. A polystyrene of molecular weight 1.85×10^5 has an intrinsic viscosity in K exactly 2.5 times that of a poly(vinyl acetate) sample of the same molecular

weight in J. What is the expected *relative viscosity* for a poly(vinyl acetate) sample with molecular weight 4.45×10^5 in solvent J at a concentration of 0.275 g/dl? The Huggins constant can be assumed to have a value of 0.400.

- 7.12 Three monodisperse samples of polystyrene are dissolved in the same solvent at 27°C. Relative viscosities are measured. Given the following information, calculate the rms end-to-end distance and the hydrodynamic volume, $[\eta]M$, for polymer sample C.

Polymer Sample	Relative Viscosity at c		
	1.0 g/dl	0.5 g/dl	Molecular Weight
A	–	5.572	710,000
B	3.086	1.872	500,000
C	–	1.250	–

- 7.13 The following data are obtained for a series of polymers all made from the same monomer ($\text{CH}_2=\text{CHX}$, formula weight = 92.0, $T_g = 25^\circ\text{C}$):

Sample	$[\eta]_q$ (dl/g)	Melt Viscosity at 175°C (poise)
A	0.21	3.6×10^2
B	0.25	5.0×10^2
C	0.32	8.1×10^2
D	0.50	33×10^2
E	0.85	0.14×10^6
F	1.13	1.0×10^6
G	1.37	3.9×10^6

The molecular weight of sample E measured by osmometry is 150,000. All samples are monodisperse.

- (a) What is the *chain entanglement point* in terms of the number of chain atoms?
- (b) At what intrinsic viscosity for sample E (in a good solvent) would the rms end-to-end distance be double the unperturbed length?
- 7.14 Three fractions are cut from a homopolymer. Each fraction has a very narrow molecular weight distribution. The following data are obtained. Fill in the missing data.

Fraction no.	Intrinsic Viscosity at 25°C (dl/g)		Melt Viscosity at 200°C (Pa-s)	Molecular Weight (g/mol)
	Solvent A	Solvent B		
1	1.2	2.0	?	1.3×10^5
2	1.8	3.6	4.0×10^5	?
3	2.5	?	?	5.6×10^5

? represents unknown variables.

- What is the actual radius of gyration (nm) of fraction 1 in solvent B at 25°C?
- 7.15** Assuming that the rms end-to-end distance is an approximation to the diameter of the spherical, coiled polymer in dilute solution, compare the volume occupied by one molecule of polyisobutylene (molecular weight = 10^6) (a) as a solid at 30°C ($\rho = 0.92 \text{ g/cm}^3$), (b) in a theta solvent at 24°C (see Table 7.6), and (c) in cyclohexane at 30°C (see Table 7.6).
- 7.16** From the information given below, calculate the ratio of the rms end-to-end distance in solvent A to that in solvent B for a polymer with a molecular weight of 1.00×10^7 .

Molecular Weight	$[\eta]$ in A (dl/g)	$[\eta]$ in B (dl/g)
1.0×10^6	4.0	2.0
0.2×10^6	1.1	0.9
5.0×10^4	0.36	0.44

- 7.17** For poly(amyl zolate), assume that the hydrodynamic volume in a theta solvent at 30°C is 7.5 times that calculated for a chain of constant tetrahedral bond angle. If the repeat unit of four chain atoms has a molecular weight of 90, what is the molecular weight of the sample described by these data?

Theta Solvent at 30°C	
c (g/dl)	Viscosity (mPa·s)
0.00	2.00
0.10	2.35
0.20	2.78
0.50	4.63
1.00	9.50

- 7.18** As a lecture demonstration, it is desired to drop a plastic sphere (radius R , density $\rho = 1.200 \text{ g/cm}^3$) into a graduated cylinder full of a Newtonian solution (viscosity η , density $\rho_0 = 1.050 \text{ g/cm}^3$). According to Stokes' law, the terminal velocity of the sphere \bar{u} is given by

$$\frac{2}{9} R^2 g (\rho - \rho_0) = \eta \bar{u}$$

What values of R and η are reasonable for an effective experiment? The equation is valid only when the Reynolds number $N_{\text{Re},\rho}$ is less than 0.1:

$$N_{\text{Re},\rho} = \frac{2\bar{u}\rho_0 R}{\eta}$$

- 7.19** An empirical equation relating stress τ to the rate of shear $\dot{\gamma}$ contains two constants, A and B.

$$\tau = \frac{A\dot{\gamma}}{1 + \sqrt{B\dot{\gamma}}}$$

Given that the zero-shear viscosity is 10 Pa·s for a certain sample and that the viscosity is 1.0 Pa·s at a stress of 10^3 Pa, calculate the viscosity at a rate of shear of 4×10^3 s⁻¹.

- 7.20** Three Ubbelohde viscometers are constructed and their parameters are identified by subscripts 1, 2, and 3, respectively. Construction is such that $h_1 = h_2 = h_3$, $L_2 = L_3 = 2L_1$, and $D_1 = D_2 = 0.5D_3$. The volume of a power-law liquid that flows through each in 100 s is measured (volumes V_1 , V_2 , and V_3). If $V_2/V_1 = 1/3$, what is V_3/V_2 ?

- 7.21** For some polymer melts, viscosity plotted against shear stress on semilog paper gives a straight line.

- (a) Write the corresponding equation for the rate of shear of a pseudoplastic melt in terms of the stress, the zero-shear viscosity, and the minimum number of remaining terms.
 (b) Derive an equation for z as a function of stress, where

$$z = \frac{d(\ln \dot{\gamma})}{d(\ln \tau)}$$

- 7.22** The Ellis model for a non-Newtonian fluid can be written as

$$\frac{\eta_0}{\eta} - 1 = \left(\frac{\tau}{\tau_c} \right)^m$$

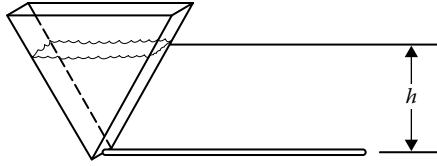
where:

η is the apparent viscosity at shear stress τ

Assuming that the shear rate can be given by $\dot{\gamma}_a = 4Q / \pi r^3$ and the stress by $\tau = \Delta Pr / 2L$, calculate the flow rate in m³/h through a long, vertical pipe draining under its own head with $\eta_0 = 10$ Pa·s, $\tau_c = 312$ Pa, $m = 0.75$, $\rho = 1.0$ g/cm³, and $r = 1.0$ cm. Calculate a Reynolds number using the apparent viscosity.

- 7.23** A certain polymer solution can be characterized as a power-law fluid. Solution issues from a cylindrical storage tank through a horizontal capillary of length $L = 10.0$ cm and $r = 0.025$ cm. The time is measured for the level in the cylinder to fall from 981.0 to 968.0 cm (40.0 s) and from 742.0 to 721.5 cm (90.0 s). Predict the time it will take for the level to fall from 550.0 to 540.0 cm.

- 7.24** Solve Problem 7.23, assuming that the reservoir has a rectangular cross section with two rectangular sides and two triangular sides. The apex of the triangles is at the entrance to the pipe.



7.25 The following mathematical model is proposed for non-Newtonian flow:

$$A\eta = \frac{1 + B\tau^z}{1 + C\tau^z}$$

- (a) Rewrite the equation in terms of $\dot{\gamma}$, τ , η_0 , η_∞ , C , and z .
 (b) If $C > B$, is the material dilatant or pseudoplastic? Why?

7.26 A polymer solution can be represented by the equation relating stress τ to the rate of shear $\dot{\gamma}$:

$$\tau = 2.70 \times 10^2 (\text{Pa})(s^{0.635})(\dot{\gamma}^{0.635})$$

What is the viscosity (mPa·s) at a stress of 1000 Pa?

7.27 For a sample of poly(vinyl alcohol) in water at 21°C, the following data are obtained:

Concentration (g/dl)	0	2.0	3.0	4.0	6.0	7.0	10.0
Viscosity (mPa·s)	1.00	10.0	28.0	58.0	240	550	4000

From a Martin's plot, estimate $[\eta]$.

7.28 Estimate the appropriate parameters for the power-law and Ellis models from the flow curve at 260°C (polystyrene) in Figure 7.4.

REFERENCES

1. Baird, D. G., and D. I. Collias: *Polymer Processing Principles and Design*, Wiley, New York, 1998.
2. Osswald, T. A.: *Understanding Polymer Processing*, Hanser Publishers, Cincinnati, OH, 2010.
3. Lipson, H., and M. Kurman: *Fabricated: The New World of 3D Printing*, Wiley, Indianapolis, IN, 2013.
4. Pezzin, G.: *Materie Plastiche ed Elastomerie*, Instron Corporation, Canton, MA, August, 1962 (English translation).
5. Ferry, J. D.: *Viscoelastic Properties of Polymers*, Wiley, New York, 1980, pp. 330–331.
6. Bird, R. B., R. C. Armstrong, and O. Hassager: *Dynamics of Polymeric Liquids: Vol. 1: Fluid Mechanics*, 2nd edn., Wiley, New York, 1987, p. 92.
7. Doi, M., and S. F. Edwards: *The Theory of Polymer Dynamics*, chaps. 6 and 7, Oxford, New York, 1980.
8. Bird, R. B., R. C. Armstrong, and O. Hassager: *Dynamics of Polymeric Liquids: Vol. 2: Kinetic Theory*, 2nd edn., Wiley, New York, 1987.
9. Larson, R. G.: *Constitutive Equations for Polymer Melts and Solutions*, Butterworth, Stoneham, MA, 1988.
10. Mead, D. W., R. G. Larson, and M. Doi: *Macromolecules*, 31:7895 (1998).

11. Islam, M. T., and L. A. Archer: *J. Polym. Sci. Part B: Polym. Phys.*, 39:2275 (2001).
12. Ianniruberto, G., and G. Marrucci: *J. Rheol.*, 45:1305 (2001).
13. Ostwald, W.: *Kolloid Z.*, 36:99 (1925); DeWaele, A.: *J. Oil Colloid. Chem. Assoc.*, 6:33 (1925).
14. Rodriguez, F., and L. A. Goettler: *Trans. Soc. Rheol.*, 8:3 (1964).
15. Rodriguez, F.: *Trans. Soc. Rheol.*, 10:169 (1966).
16. Fabula, A. G.: in E. H. Lee (ed.), *Proc. 4th Intern. Congr. Rheol.*, part 3, Wiley, New York, 1965, p. 455ff.
17. Ellis, S. B.: Thesis, Lafayette College, Easton, PA, quoted by M. Reiner, *J. Rheol.*, 1:14 (1929); also Gee, R. E., and J. B. Lyon, *Ind. Eng. Chem.*, 49:956 (1957).
18. Williamson, R. V.: *Ind. Eng. Chem.*, 21:1108 (1929).
19. Krieger, I. M., and J. T. Dougherty: *Trans. Soc. Rheol.*, 3:137 (1959).
20. Ree, F. H., T. Ree, and H. Eyring: *Ind. Eng. Chem.*, 50:1036 (1958).
21. Phillippoff, W.: *Kolloid Z.* 130:129 (1935); Bird, R. B., W. E. Stewart, and E. N. Lightfoot: *Transport Phenomena*, Wiley, New York, 1960, pp. 11–15.
22. Denny, D. A., and R. S. Brodkey: *J. Appl. Phys.*, 33:2269 (1962).
23. Cross, M. M.: *J. Coll. Sci.*, 20:417 (1965); *Rheol. Acta*, 18:609 (1979).
24. Carreau, P. J.: Ph.D. Thesis, University of Wisconsin, Madison, WI, 1968; Bird, R. B., R. C. Armstrong, and O. Hassager: *Dynamics of Polymeric Liquids: Vol. 1: Fluid Mechanics*, 1st edn., Wiley, New York, 1987, p. 172.
25. Rodriguez, F., and C. C. Winding: *Ind. Eng. Chem.*, 51:1281 (1959).
26. Carley, J. E.: *Mod. Plast.*, 39:123 (December 1961).
27. Tordella, J.: *Trans. Soc. Rheol.*, 1:203 (1957); *Rheol. Acta*, 1:216 (1958).
28. Kearsley, E. A.: *Trans. Soc. Rheol.*, 6:253 (1962).
29. Macosko, C. W.: *Rheology: Principles, Measurements and Applications*, VCH, New York, 1994.
30. Cannon, M. R., R. E. Manning, and J. D. Bell: *Anal. Chem.*, 32:355 (1960).
31. Hitchcock, C. D., H. K. Hammons, and W. W. Yau: *Am. Lab.*, 26(11):26 (1994).
32. Haney, M. A.: *J. Appl. Polym. Sci.*, 30:3023 (1985); *J. Appl. Polym. Sci.*, 30:3037 (1985).
33. Lew, R., D. Suwanda, S. T. Balke, and T. H. Moury: *J. Appl. Polym. Sci.: Appl. Polym. Symp.*, 52:125 (1993).
34. Flory, P. J.: *Principles of Polymer Chemistry*, chaps. 10 and 14, Cornell University Press, Ithaca, NY, 1953.
35. Morawetz, H. (ed.): *Macromolecules in Solution*, 2nd edn., Wiley, New York, 1975.
36. Flory, P. J.: *Principles of Polymer Chemistry*, Cornell University Press, Ithaca, NY, 1953, p. 618.
37. Brandrup, J., and E. H. Immergut (eds.): *Polymer Handbook*, 3rd edn., Wiley, New York, 1989.
38. Zimm, B. H., and W. H. Stockmayer: *J. Chem. Phys.*, 17:1301 (1949).
39. Berry, G. C., and T. A. Orofino: *J. Chem. Phys.*, 46:1614 (1964).
40. Hadjichristidis, N., M. Xenidou, H. Iatrou, M. Pitsikalis, Y. Poulos, A. Avgeropoulos, S. Sioula et al.: *Macromolecules*, 33:2424 (2000).
41. Kurata, M., and W. H. Stockmayer: *Fortschr. Hochpolymer. Forsch.*, 3(2):196 (1963).
42. Muthukumar, M., and B. G. Nickel: *J. Chem. Phys.*, 80:5839 (1984).
43. Huggins, M. L.: *J. Am. Chem. Soc.*, 64: 2716 (1942).
44. Kraemer, E. O.: *Ind. Eng. Chem.*, 30:1200 (1938).
45. Rodriguez, F.: Ph.D. Thesis, Cornell University Press, Ithaca, NY, 1958.
46. Staudinger, H.: *Die Hochmolekularen Organischer Verbindungen*, Springer, Berlin, Germany, 1932.
47. Kurata M., and Y. Tsunashima: in *Polymer Handbook*, 3rd edn., sec. VII, Wiley, New York, 1989.

48. Doi, M., and S. F. Edwards: *The Theory of Polymer Dynamics*, Oxford, New York, 1986, pp. 113–114.
49. Zimm, B. H.: *J. Chem. Phys.*, 24:269 (1956).
50. Haney, M. A., D. Gillespie, and W. W. Yau: *Today's Chem. Work*, 3(11):39 (1994).
51. Ott, E., H. Spurlin, and M. W. Grafflin (eds.): *Cellulose and Cellulose Derivatives*, part III, Wiley, New York, 1955, p. 1216.
52. Lyons, P. F., and A. V. Tobolsky: *Polym. Eng. Sci.*, 10:1 (1970).
53. Fujita, H., and A. Kishimoto: *J. Chem. Phys.*, 34:393 (1961).
54. Rodriguez, F.: *Polym. Lett.*, 10:455 (1972).
55. Rouse, P. E.: *J. Chem. Phys.*, 21:1272 (1953).
56. Doi, M., and S. F. Edwards: *The Theory of Polymer Dynamics*, chap. 4, Oxford, New York, 1986.
57. Fox, T. G., S. Gratch, and S. Loshaek: chap. 12 in F. R. Eirich (ed.), *Rheology*, vol. 1, Academic Press, New York, 1956.
58. Berry, G. C., and T. G. Fox: *Adv. Polym. Sci.*, 26:359 (1955).
59. Ferry, J. D.: *Viscoelastic Properties of Polymers*, chap. 10, Wiley, New York, 1980.
60. de Gennes, P. G.: *J. Chem. Phys.*, 55:572 (1971).
61. Fetters, L. J., D. J. Lohse, D. Richter, T. A. Witten, and A. Zirkel: *Macromolecules*, 27:4639 (1994).
62. Doi, M., and S. F. Edwards: *The Theory of Polymer Dynamics*, chaps. 6 and 7, Oxford, New York, 1986.
63. Larson, R. G.: *The Structure and Rheology of Complex Fluids*, sec. 3.7, Oxford, New York, 1999.
64. Watanabe, H.: *Prog. Polym. Sci.*, 24:1253 (1999).
65. Bueche, F.: *J. Chem. Phys.*, 20:1959 (1952); 25:599 (1956).
66. Mhetar, V. R., and L. A. Archer: *J. Polym. Sci.: Polym. Phys.*, 38:222 (2000).
67. Lee, J. H., and L. A. Archer: *J. Polym. Sci. Part B: Polym. Phys.*, 39:2501 (2001).
68. Doi, M.: *J. Polym. Sci. Polym. Phys. Ed.*, 21:667 (1983).
69. Rubinstein, M., and R. H. Colby: *Polymer Physics*, sec. 9.4.5, Oxford, New York, 2003.
70. Doolittle, A. K.: *J. Appl. Phys.*, 22:1471 (1951).
71. Williams, M. L., R. F. Landel, and J. D. Ferry: *J. Am. Chem. Soc.*, 77:3701 (1955).
72. Carley, J. E.: *Mod. Plast.*, 39:123 (December 1961).
73. Goldblatt, P. H., and R. S. Porter: *J. Appl. Polym. Sci.*, 20:1199 (1976).
74. Dealy, J. M., and K. F. Wissbrun: *Melt Rheology and Its Role in Plastics Processing—Theory and Applications*, Van Nostrand Reinhold, New York, 1990.
75. James, D. F., and K. Walters: chap. 2 in A. A. Collyer (ed.), *Techniques of Rheological Measurement*, Elsevier, New York, 1994, pp. 33–53.
76. Sentmanat, M., B. N. Wang, and G. H. McKinley: *J. Rheol.*, 49:585 (2005).
77. Petrie, C. J. S.: *J. Non-Newt. Fluid Mech.*, 137:15 (2006).
78. Trouton, F. T.: *Proc. Roy. Soc. A*, 77:426 (1906).
79. Tirtaatmadja, V., and T. Sridhar: *J. Rheol.*, 37:1081 (1993).
80. Hoyt, J. W.: Drag reduction, in *Encyclopedia of Polymer Science and Engineering*, vol. 5, 2nd edn., Wiley, New York, 1986, p. 129.
81. Rodriguez, F.: *Eng. Educ.*, 65:245 (1974).
82. Rodriguez, F.: *Trans. Soc. Rheol.*, 10:169 (1966).

8 Rheometry and Viscoelastic Fluid Flow

8.1 INTRODUCTION

In some situations, the viscosity of polymer liquids is too high to be characterized by gravity-driven flow in a viscometer. In many other situations treated in Chapter 7, the polymer viscosity is not a material property and may be a complex function of deformation rate, imposed stress, and time. In yet other circumstances, polymeric fluids exhibit solid-like elasticity and even in the simple shear flow device depicted in Figure 7.1 might manifest net forces in directions orthogonal to the direction of the applied deformation. These so-called **normal stress differences** are responsible for some of the most spectacular flow phenomena such as rod climbing, tubeless syphons, and turbulent drag reduction associated with high molar mass polymer solutions. Altogether these features imply that the response one obtains when a polymer melt or solution is subjected to an applied stress or flow field can be quite complex. Polymer liquids are for this reason given the collective designation **complex fluids**. The task of characterizing and understanding the flow properties of a complex fluid cannot be handled using viscometers. These tasks require, instead by sophisticated mechanically driven flow measurement devices, or **rheometers**, equipped with precise temperature measurement and control capabilities and specialized sensors for carrying out time-dependent measurements of shear rate, shear strain, shear stress, and normal stress differences.

The subject of **rheometry** is concerned with measurement principles, data analysis procedures, and sources of measurement artifacts in rheometers. In this chapter, we will analyze several widely used rheometer configurations in detail. Incorrect use of the governing equations, or use of incomplete equations, for extracting polymer flow property data from rheological measurements constitutes a serious source of experimental error. The reader is therefore encouraged to work through the derivations presented below. Because the principal task of a rheometer is to measure the properties of materials, the most useful configurations are ones in which the underlying flow is simple and its intensity may be characterized by a single parameter. A particular class of fluid flows termed **viscometric flows** has emerged as the most convenient for characterizing polymer properties using rheometry. In such flows, only one component of the velocity vector is non-zero and that velocity component varies only along one coordinate axis normal to the direction of the flow. The velocity gradient therefore comprises a single off-diagonal element, which is customarily designated as the shear rate $\dot{\gamma}$. Thus, for a simple unidirectional imposed flow, such as that considered in Figure 8.1, with velocity vector,

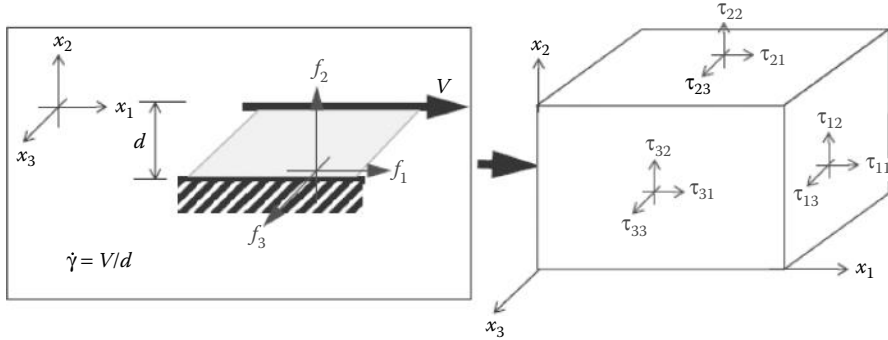


FIGURE 8.1 Forces and stresses developed in a polymer liquid sheared between parallel planes.

$$\mathbf{v} = v_1(x_2)e_1 \quad (8.1)$$

the three-dimensional **velocity gradient** and **rate of deformation** may be written in matrix form as

$$\nabla \mathbf{v} = \dot{\gamma} \begin{bmatrix} 0 & 1 & 0 \\ 0 & 0 & 0 \\ 0 & 0 & 0 \end{bmatrix}; D = \frac{\dot{\gamma}}{2} \begin{bmatrix} 0 & 1 & 0 \\ 1 & 0 & 0 \\ 0 & 0 & 0 \end{bmatrix} \quad (8.2)$$

where:

in this case the shear rate is given by $\dot{\gamma} = dv_1/dx_2$

The response of fluid in laminar flow is proportional to the driving force. Therefore, the expression for the velocity vector in Equation 8.1 implies that the velocity imposed on the fluid is in the “1” direction, varies in the “2” direction, and does not change in the “3” direction. In this type of flow, fluid planes will therefore slide past each other at different speeds, and the velocity gradient and rate of deformation described by Equation 8.2 correspond to a simple shear flow. The subscript 1 is therefore conventionally labeled the flow direction; 2, the flow-gradient direction; and 3, the neutral or vorticity direction in a cartesian reference frame. A variety of specific flow configurations capable of generating steady, viscometric flow have been developed and are widely used for characterizing the rheological properties of fluids; several will be analyzed in this chapter.

8.2 NORMAL STRESS DIFFERENCES IN SHEAR

Some of the most unusual manifestations of polymer elasticity arise from the existence of normal stress differences. For example, if a rod is immersed in a polymer solution contained in a stationary beaker and rotated, the solution is observed to climb the rod (Figure 8.2) [1]. This effect known as the **Weissenberg effect** is qualitatively very different from what is observed in a simple Newtonian fluid. In the

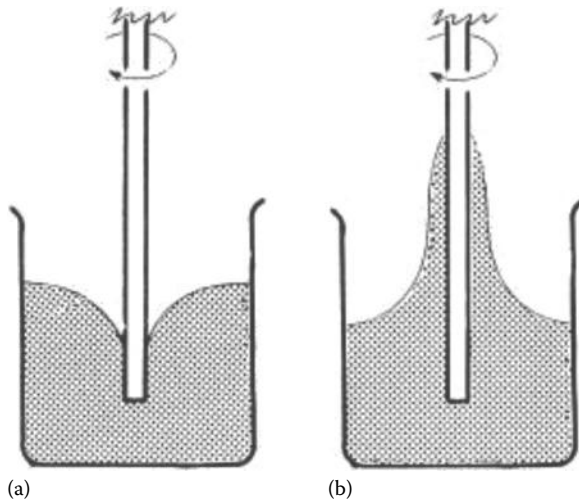


FIGURE 8.2 Rotating rod in a pool of liquid: (a) Newtonian fluid response; (b) elastic fluid response.

latter, centrifugal forces created by rotating the rod deplete fluid from the region immediately adjacent to it and create a vortex in the liquid near the rod. In another manifestation of normal stresses, when a polymer liquid is forced under pressure to flow through a capillary tube, the diameter of the polymer at the exit of the tube or **extrudate** can be many times larger than that of the tube (Figure 8.3). This effect known as **die swell** is again qualitatively different from what is observed with simple liquids, where the diameter of the extrudate is typically smaller than that of the capillary tube. Normal stress differences are also the source of secondary flows in polymer liquids subjected to simple shear flow. As discussed in Section 8.5 and in greater detail elsewhere [2,3], such flows complicate rheological characterization of

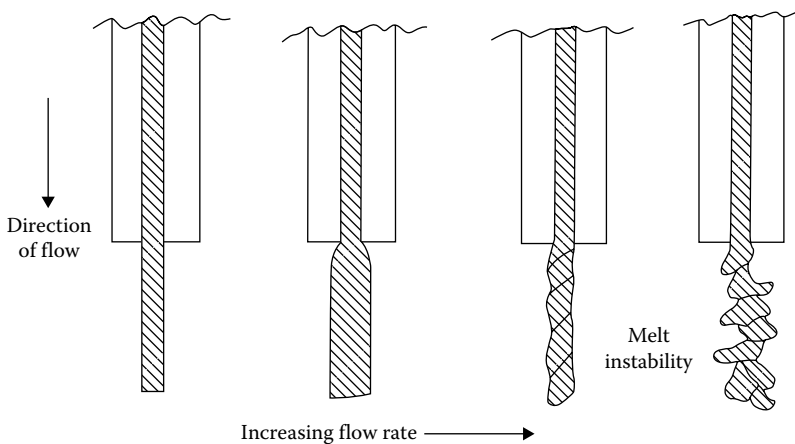


FIGURE 8.3 Typical stages in extrusion of polymer melt through the capillary of diameter D_c . The degree of die swell β is the ratio of the extrudate diameter to D_c .

polymers. Finally, normal stresses can also severely compromise control over shape and surface finish in polymer-forming processes. For example, in extrusion processes, molten polymer is forced under an external pressure, to flow through narrow channels or dies. Subsequent cooling of the molten extrudate produces polymer components with well-defined shapes. Die swell introduces obvious challenges for shape control in extruders. Large normal stress differences are also thought to cause solid-like fracture of molten polymers, **melt fracture**, that grossly roughens the surface of polymer extrudates (Figure 8.3) at high product throughput rates [3,4]. Changing the geometry of the extruder entrance to a more gradual constriction has been found to raise the maximum flow rate at which these irregularities appear; however, no reliable procedures are yet available for removing them altogether.

To determine the source of these and other normal stress-related phenomena, consider a polymer liquid subject to steady shear flow in the planar Couette flow arrangement depicted in Figure 8.1. In general, the liquid will resist flow by exerting a force f with nonzero components f_1 , f_2 , and f_3 along all three cartesian coordinate directions. The rheological response of the fluid is therefore best described in terms of a stress matrix or a stress tensor, with elements $\tau_{ij} = (n_i f_j)/A$, where n_i is the normal vector to the surface of area A on which the force f_j acts. In a cartesian coordinate frame, i and j can take independent values ranging from 1 to 3, so the stress tensor will generally have nine independent components and may be represented by a 3×3 matrix. For most liquids, $\tau_{ij} = \tau_{ji}$, and the stress tensor possesses only six independent components and is said to be symmetric,

$$[\tau] = \begin{bmatrix} \tau_{11} & \tau_{21} & \tau_{13} \\ \tau_{21} & \tau_{22} & \tau_{23} \\ \tau_{13} & \tau_{23} & \tau_{33} \end{bmatrix} = \begin{bmatrix} \tau_{xx} & \tau_{yx} & \tau_{zx} \\ \tau_{yx} & \tau_{yy} & \tau_{zy} \\ \tau_{zx} & \tau_{zy} & \tau_{zz} \end{bmatrix} \quad (8.3)$$

Off-diagonal components of the matrices in the above equation, for example, τ_{yx} and τ_{zy} , are termed shear stresses, whereas diagonal components, such as τ_{xx} and τ_{yy} , are termed normal stresses. Because forces produced by normal stresses are always parallel to the normal vectors of surfaces on which they act, these stresses are qualitatively similar to **hydrostatic pressures**. In fact for any fluid in its undeformed state, we can write $\tau_{xx} = \tau_{yy} = \tau_{zz} = p$.

That polymers exhibit normal stresses in excess of the mean hydrostatic pressure follows naturally from the discussion in Section 7.2.2. Specifically, imagine a polymer liquid composed of randomly oriented spherical coils at rest. If this liquid is subjected to a fast steady shear flow, that is one in which, $Wi \gg 1$, in the planar Couette flow apparatus depicted in Figure 8.1, molecules will uncoil and align parallel to the direction of shear. Molecular alignment is resisted by randomizing thermal forces that favor a random coil structure. Resisting forces are therefore felt on all planes of the shear cell. In this example, we anticipate that maximum alignment occurs in the **shear direction** $x_1 = x$, so resistance will be largest in this direction. Since no obvious driving force exists for an orientation bias in the shear gradient $x_2 = y$ and neutral $x_3 = z$ directions, we would also expect the resisting force to be nearly equal in these directions. The end result is that the molecular alignment produces normal stresses that are not only different from the hydrostatic pressure, but are also not the same in different directions, that is, they are **anisotropic**.

Because of their similarity to pressure, normal stresses developed by a fluid cannot be easily separated from the hydrostatic pressure. It is therefore more meaningful to speak of normal stress differences in the fluid since they directly report the extra, anisotropic normal stresses produced by fluid flow. By convention, the **first normal stress difference** N_1 is defined as the difference between the normal stresses on fluid planes with surface normals parallel to x and y , $N_1 = \tau_{xx} - \tau_{yy}$. The **second normal stress difference** N_2 is defined as, $N_2 = \tau_{yy} - \tau_{zz}$ whereas the **third normal stress difference** N_3 is given by $N_3 = N_1 + N_2 = \tau_{xx} - \tau_{zz}$. Based on the physical origins outlined in the last paragraph, we would anticipate $N_1 \approx N_3 > 0$ and $N_2 \approx 0$. As illustrated in Figure 8.4, this is in fact what is typically observed in polymer solutions, with N_2 small and negative [5,6].

At low shear rates, $Wi \ll 1$, all three normal stress differences are quadratic functions of shear rate (see Figure 8.4). It is therefore customary to define three **normal stress coefficients** $\Psi_1(\dot{\gamma}) \equiv N_1(\dot{\gamma})/\dot{\gamma}^2$, $\Psi_2(\dot{\gamma}) \equiv N_2(\dot{\gamma})/\dot{\gamma}^2$, and $\Psi_3(\dot{\gamma}) \equiv N_3(\dot{\gamma})/\dot{\gamma}^2$, which are independent of shear rate at low rates (Figure 8.5), as is also the case for the apparent viscosity. Generally, Ψ_1 , the first normal stress coefficient, is easiest to measure. Ψ_1 data at low shear rates, $\Psi_1(\dot{\gamma} \rightarrow 0) = \Psi_{10}$, are particularly useful because they can be used in conjunction with the zero shear viscosity η_0 to calculate the longest relaxation time $\lambda_1 = \Psi_{10}/2\eta_0$ of a polymer melt or solution. Typical values of the three normal stress coefficients and the apparent viscosity for a moderately entangled, $n/n_e = 6$, polystyrene/diethylphthalate solution are presented in Figure 8.5. These results show that the normal stress coefficients Ψ_i are very sensitive to shear

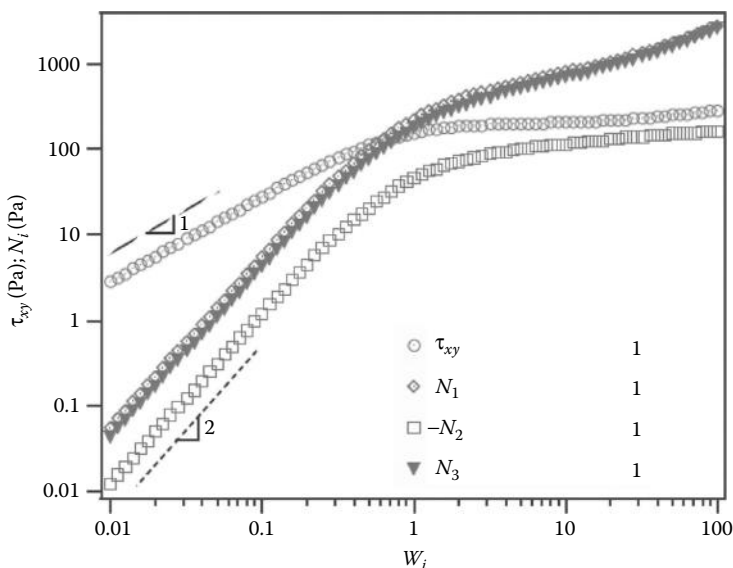


FIGURE 8.4 Steady-state shear stress τ_{xy} and normal stress differences N_i for a 6 vol% solution of high-molecular-weight polystyrene $M_w = 3.84 \times 10^6$ g/mol in diethyl phthalate sheared at variable W_i . Results shown are predicted using the theory of Islam and Archer. (Data from Islam, M. T., and L. A. Archer, *J. Polym. Sci. Part B: Polym. Phys.*, 39, 2275, 2001.)

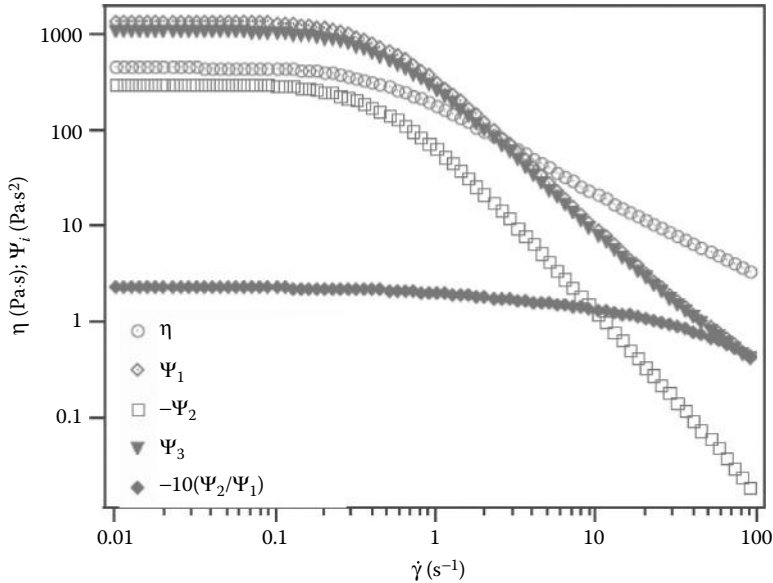


FIGURE 8.5 Apparent viscosity η and normal stress coefficients Ψ_i for a 6 vol% solution of polystyrene, $M_w = 3.84 \times 10^6$ g/mol, in diethyl phthalate at variable shear rates $\dot{\gamma}$. Results shown are predicted using the theory of Islam and Archer. (Data from Islam, M. T., and L. A. Archer, *J. Polym. Sci. Part B: Polym. Phys.*, 39, 2275, 2001.)

rate and that all normal stress coefficients are more shear thinning than η . Figure 8.5 also indicates that $-\Psi_2(\dot{\gamma})$ is not only smaller than Ψ_1 and Ψ_3 , but is even more shear thinning, particularly at high shear rates. Similar observations have been reported in the literature for all polymer liquids for which N_1 and N_2 data are available [5]. One practical consequence of the relatively small size and greater shear sensitivity of N_2 is that high-quality $\Psi_2(\dot{\gamma})$ data are extremely difficult to obtain for polymer melts and solutions. Furthermore, because one of the force components in N_3 acts parallel to the neutral direction, N_3 is also difficult to determine from force measurements. The best techniques for measuring N_3 in fact rely on anisotropic refraction of polarized light produced by shear-induced alignment of polymer molecules, which leads to **birefringence** in sheared polymer liquids [8,9].

8.3 POISEUILLE FLOW IN TUBES AND CAPILLARIES

One of the most widely used rheometer configurations is a simple variant of the capillary flow viscometer. In this device, a concentrated polymer solution or melt undergoes **Poiseuille flow** in a narrow capillary, length L and internal radius R , under the action of an external pressure P . The capillary exit is typically open to the atmosphere, such that a pressure difference $\Delta p = P - p_{\text{atm}}$ produces the driving force that leads to fluid flow (Figure 8.3). If the volumetric flow rate of fluid through the capillary Q is known (measured), Poiseuille's equation can be used to determine the fluid's viscosity if the fluid is Newtonian.

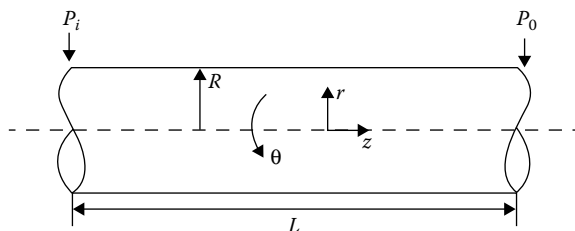


FIGURE 8.6 Pressure-driven flow in a capillary tube.

For non-Newtonian fluids, a more general analysis procedure is needed. We will consider only the simplest flow situation: fully developed flow in the capillary, steady-state conditions, negligible fluid inertia, and **no slip** at the fluid–solid interface. **Capillary flow** rheological measurements are typically carried out under conditions of low flow rates and using long metallic capillaries, where these assumptions hold, so the analysis is not as restrictive as one might at first infer from the number of assumptions. For these conditions and the capillary flow configuration in Figure 8.6, we can write $\mathbf{v} = v_z(r)\mathbf{e}_z$. The shear rate experienced by the fluid is then

$$\dot{\gamma}(r) = \frac{dv_z}{dr} \quad (8.4)$$

Furthermore, based on the axial symmetry of the tube, only derivatives of the stress tensor with respect to r are nonzero (Appendix 8.A). The **differential momentum balance** equations in cylindrical coordinates (Appendix 8.B) can be simplified as follows:

$$0 = -\frac{\partial p}{\partial r} + \frac{1}{r} \frac{\partial}{\partial r} r \tau_{rr} - \frac{\tau_{\theta\theta}}{r} \quad (8.5)$$

$$0 = -\frac{\partial p}{\partial \theta} \quad (8.6)$$

$$0 = -\frac{\partial p}{\partial z} + \frac{1}{r} \frac{\partial}{\partial r} r \tau_{rz} \quad (8.7)$$

Integrating Equations 8.4 and 8.7 yields

$$p = \tau_{rr}(r) + \int \frac{N_2(r)}{r} dr + f(z) \quad (8.8)$$

and

$$p = \int \frac{1}{r} \frac{\partial}{\partial r} r \tau_{rz}(r) dz + g(r) \quad (8.9)$$

where:

$f(z)$ and $g(r)$ are unknown functions of z and r , respectively
 $N_2 = \tau_{rr} - \tau_{\theta\theta}$ is the second normal stress difference

The dependencies on r arise from the structure of the velocity field, $\mathbf{v} = v_z(r)\mathbf{e}_z$. Since τ_{rz} is only a function of r , Equation 8.9 can be readily rearranged to give

$$\tau_{rz} = \frac{r}{2} \left(\frac{\partial p}{\partial z} \right) + \frac{c_2}{r} \quad (8.10)$$

We expect that τ_{rz} is finite along the tube center line ($r = 0$), so $c_2 = 0$. Hence, the shear stress at the wall $\tau_R = \tau_{rz}(r = R) = (R/2)(\partial p/\partial z)$ can be easily determined once the pressure gradient $\partial p/\partial z = \Delta p/L = (p_i - p_o)/L$ in the fluid is known.

The total volumetric flow rate in the capillary can be found:

$$Q = 2\pi \int_0^R v_z(r) r \, dr \quad (8.11)$$

which can be integrated by parts to give

$$Q = \pi r^2 v_z(r) \Big|_0^R - \pi \int_0^R r^2 \frac{dv_z}{dr} \, dr = -\pi \int_0^R r^2 \dot{\gamma} \, dr \quad (8.12)$$

$$Q = -\frac{\pi R^3}{\tau_R^3} \int_0^{\tau_R} \dot{\gamma} \tau_{rz}^2 \, d\tau_{rz} \quad (8.13)$$

where:

$$v_z(R) = v_z(0) = 0 \text{ by the no-slip condition}$$

The final integral in Equation 8.12 requires *a priori* knowledge of $\dot{\gamma}(r)$ to determine Q . However, to determine $\dot{\gamma}(r)$, we need to know $v_z(r)$, which in turn requires knowledge of the relationship between shear stress and shear rate for the material; the latter is precisely the objective of rheological measurements. This dilemma can be avoided by directly transforming Equation 8.12 to obtain an explicit relationship between Q and τ_R . To do this, we utilize the expression for τ_R and rewrite Equation 8.10 as $r = (R/\tau_R)\tau_{rz}$ and use the result to rewrite Equation 8.12 in terms of τ_{rz} .

Differentiating with respect to τ_R and using **Leibnitz's theorem** for differentiating an integral,

$$\frac{d}{d\chi} \int_{a(\chi)}^{b(\chi)} f(y, \chi) dy = \int_{a(\chi)}^{b(\chi)} \frac{df}{d\chi}(y, \chi) dy + f(b, \chi) \frac{db}{d\chi} - f(a, \chi) \frac{da}{d\chi} \quad (8.14)$$

yields

$$\frac{dQ}{d\tau_R} = -\frac{3}{\tau_R} Q - \frac{\pi R^3}{\tau_R} \dot{\gamma}_R \quad (8.15)$$

where:

$\dot{\gamma}_R = \dot{\gamma}(\tau_{rz} = \tau_R) = \dot{\gamma}(r = R)$ is the shear rate at the capillary wall

Rearrangement of Equation 8.15 finally yields

$$\dot{\gamma}_R = -\frac{1}{\pi R^3} \left(3Q + \tau_R \frac{dQ}{d\tau_R} \right) \tag{8.16}$$

This equation is the **Weissenberg–Rabinowitsch equation** [10,11]; it facilitates the measurement of the wall shear rate from Q versus Δp data for any fluid that satisfy the assumptions leading up to Equation 8.4.

The most severe source of measurement error in capillary tube rheometers comes from using tubes that are too short. In the case of Newtonian liquids, the largest measurement errors result from the absence of a fully developed flow near the entrance and exit of the capillary. Normal stresses in non-Newtonian polymer liquids cause additional errors due to **entrance and exit losses**. While all these sources of measurement error can be remedied by employing very long capillary tubes, typically $L/R > 100$, the size of the error depends on flow conditions and fluid properties. The **Bagley correction** provides a procedure for correcting entrance errors due to fluid elasticity in capillary flow [12]. Extrusion of a polymer melt or solution requires a differential pressure in excess of that predicted from Equation 8.10. This can be visualized as being due to a fictitious additional length corresponding to the **recoverable shear strain** (γ_{Rc}) stored elastically in the melt while it is in the capillary. Thus, the *true* stress at the wall, ($\tau_{R,t}$), is proportional to the slope of the Δp versus L/R plot (Figure 8.7) according to

$$\tau_{R,t} = \frac{\Delta p}{2(L/R + e)} \tag{8.17}$$

where:

e is the dimensionless end correction

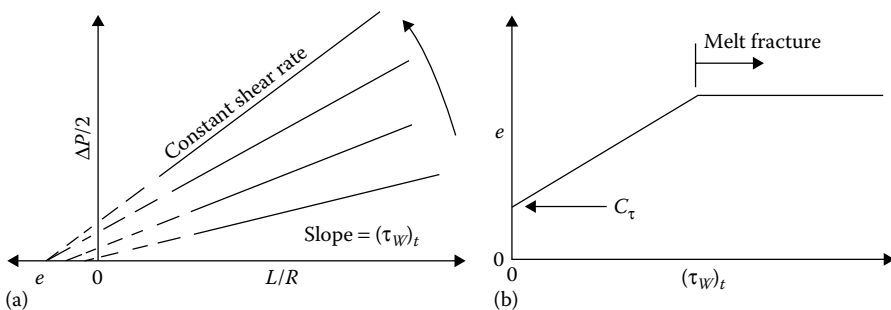


FIGURE 8.7 Plot of pressure drop versus length-to-radius ratio for flow in a capillary die. Extrapolation of measurements at a constant apparent shear rate $\dot{\gamma}_a = 4Q/\pi R^3$ in a set of dies with a range of values of L/R (a) yields values for the end correction e and the wall shear stress τ_R . A typical plot of e versus τ_R is presented in (b).

The correction term may also be divided up into a so-called *Couette* part, arising from deviations from fully developed flow at the tube entrance and exit, and an *elasticity* part, arising from normal stress effects:

$$e = \frac{C_t + \gamma_{Rc}}{2} \quad (8.18)$$

With various grades of polyethylene, Bagley found that e invariably reached a plateau value at the stress corresponding to melt fracture (Figure 8.7). This behavior is not always observed with other polymers, but the end correction method is widely used to reconcile melt flow behavior when results from capillary rheometers with variable L/R ratios must be compared.

A second and more serious source of error arises from violations of the no-slip boundary condition at the capillary walls. The no-slip condition states that the tangential velocity component of a fluid in contact with a solid substrate is equal to the velocity of the substrate. At least three different sources of slip violations have been reported: (1) depletion slip, (2) adhesive failure, and (3) cohesive failure [13,14]. Depletion slip can be traced to the lower number of conformations available to polymer segments near rigid substrates. As a result, polymer molecules in solution and high-molecular-weight polymer components in polydisperse melts possess lower configurational freedom near rigid substrates. A thermodynamic driving force therefore exists in both materials for diffusion of high-molecular-weight polymer molecules away from liquid/solid interfaces. The net effect is that the viscosity of the first layer (thickness of order of 0.5–10 nm) of a polymer liquid near a substrate is generally lower than that of the bulk fluid. Fluid in this layer therefore lubricates the bulk flow, enhancing the volumetric flow rate observed at any given pressure drop. Slip by the other two mechanisms require large enough shear stresses to break polymer/substrate bonds (adhesive slip) or to break down polymer/polymer entanglements (cohesive slip) near the substrate. In either event, the resistance to fluid motion provided by the capillary surface is reduced by slip and an enhanced volumetric flow rate or **spurt** of polymer is observed at wall shear stresses exceeding the respective critical values.

When wall slip of any kind is present, the boundary condition on the axial velocity component can be written as $v_z(R) = v_z(0) = v_s$, where v_s is the slip velocity. v_s is generally not a simple function of τ_R , particularly if slip occurs by mechanisms 2 and 3. Nonetheless, at any wall shear stress, Equation 8.13 can be written as

$$\frac{Q}{\pi R^3} = \frac{v_s}{R} - \frac{1}{\tau_R^3} \left(\int_0^{\tau_R} \dot{\gamma} \tau_{rz}^2 d\tau_z \right) \quad (8.19)$$

The above equation suggests a simple method for identifying and reducing slip errors. Specifically, this equation indicates that if the quantity $Q/(\pi R^3)$ is plotted against τ_R for several capillaries with variable R , but constant L , slip will be evidenced by an inverse relationship between $Q/(\pi R^3)$ and R at each τ_R . In fact, the slope of a plot of $Q/(\pi R^3)$ versus $1/R$ at a constant τ_R yields v_s at that value of τ_R , allowing the magnitude of slip to be quantified. It is likewise apparent that slip errors are amplified

in capillary flow rheological measurements when small tube diameters are used. Larger tube diameters are therefore advantageous for reducing measurement errors caused by slip. As discussed in Section 7.2.1, viscous flow generates heat, particularly at high shear rates and for highly viscous fluids. To maintain the temperature in a polymer liquid during capillary flow rheometry, heat produced by viscous dissipation must be removed. Low thermal conductivities of many polymers demand that small capillary tube diameters be used. Smaller diameters are also advantageous because smaller quantities of fluid are needed for rheological measurements. The actual diameter of the capillary tube chosen for capillary flow rheometry is therefore a compromise between the need to minimize wall slip errors, viscous heating, and sample volume.

8.4 COUETTE SHEAR FLOW BETWEEN COAXIAL CYLINDERS

The **cup-and-bob** or **Couette flow rheometer** (Figure 8.8) is a variant of the planar Couette flow device depicted in Figure 7.1. Its main advantage over the planar Couette apparatus is that low viscosity fluids can be studied without risk of the fluid flowing out of the gap during measurements. Because the travel distance of the cup-and-bob Couette device is in principle infinite, polymer properties at much higher shear strains and shear rates can also be studied. In a cup-and-bob Couette flow rheometer, fluid is sandwiched between coaxial cylinders, with radii $R_2 = \kappa R$ and $R_1 = R$, gap $d = R(\kappa - 1)$, length L , and $\kappa > 1$. Shear is generated by rotating the two cylinders at different angular speeds. Typically, the outer cylinder is rotated at an angular velocity Ω and the torque T required to hold the inner cylinder stationary measured. This approach is preferred (compared with the inner cylinder rotated and the outer one held stationary) because it produces stable flow over a wider range of rotation rates (Figure 8.9).

Again from the cylindrical symmetry of the flow geometry and the assumptions that: (1) the fluid is incompressible, (2) flow occurs under isothermal conditions, and (3) the flow in the gap is uniform (i.e., negligible disturbance from the ends or **end effects**), we conclude that only spatial derivatives with respect to the radial coordinates are nonzero. Thus, $v = v_\theta(r)e_\theta$ and the shear rate is given by

$$\dot{\gamma}(r) = r \frac{d}{dr} \left[\frac{v_\theta(r)}{r} \right] = \frac{d}{dr} \left[v_\theta(r) \right] - \frac{v_\theta(r)}{r} \quad (8.20)$$

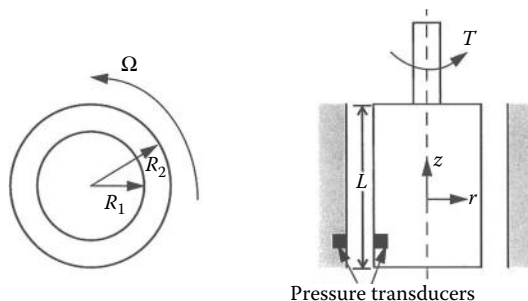


FIGURE 8.8 Schematic of a coaxial cylinder or Couette flow rheometer.

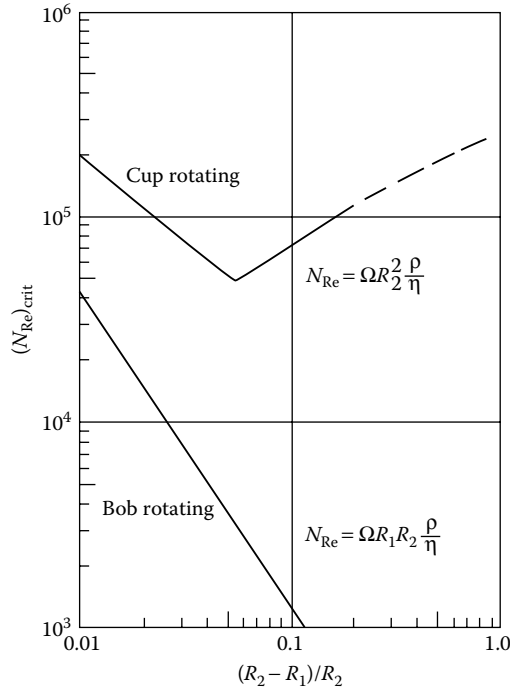


FIGURE 8.9 Onset of unstable flow in shear flow between concentric cylinders. (Data from Bird, R. B. et al., *Dynamics of Polymeric Liquids. Vol. 1: Fluid Mechanics*, 1st edn., Wiley, New York, 1987, pp. 521–523.)

It follows that only stress gradients with respect to r are nonzero. Neglecting inertia, the differential linear momentum conservation equations in cylindrical coordinates (Appendix 8.B) read

$$0 = \frac{\partial}{\partial r}(r^2 \tau_{r\theta}) \quad (8.21)$$

$$0 = \frac{\partial}{\partial r}(-p + \tau_{rr}) - \frac{N_1}{r} \quad (8.22)$$

$$\frac{\partial p}{\partial z} = 0 \quad (8.23)$$

where:

$$N_1 = \tau_{\theta\theta} - \tau_{rr}$$

Equation 8.21 can be integrated to yield $\tau_{r\theta} = A/r^2$, where A is an integration constant. To determine A , we balance the total torque exerted by the fluid on the inner cylinder

$$T = \int_0^L \int_0^{2\pi} r^2 \tau_{r\theta} d\theta dz = 2\pi L A \tag{8.24}$$

against the torque T required to prevent the inner cylinder from rotating. It therefore follows that $A = T/(2\pi L)$ and the shear stress

$$\tau_{r\theta} = \frac{T}{2\pi L r^2} = \tau_r \tag{8.25}$$

Provided that the constitutive relationship between the stress components and the velocity gradient is known, Equations 8.20 through 8.23 can be solved to determine $v_\theta(r)$ and $\dot{\gamma}(r)$. Unfortunately, this information is again precisely what is sought in a rheological experiment, so it is not known *a priori*. A more general procedure is therefore needed to relate the shear rate to experimentally measurable quantities, such as T and Ω . Our starting point is the no-slip condition at the fluid cylinder interfaces, $v_\theta(R) = 0$ and $v_\theta(\kappa R) = \kappa R \Omega$, which implies that

$$\Omega = \int_R^{\kappa R} d \left[\frac{v_\theta(r)}{r} \right] = \int_R^{\kappa R} \frac{\dot{\gamma}(r)}{r} dr \tag{8.26}$$

But, from Equation 8.25, we know $r = (A/\tau_r)^{1/2}$, which in turn implies that $dr = -(1/2)(A/\tau_r^3)^{1/2} d\tau_r$. Substituting for r in Equation 8.26 yields

$$\Omega = \int_{\tau_R/\kappa^2}^{\tau_R} \dot{\gamma}(\tau_r) \frac{d\tau_r}{2\tau_r} \tag{8.27}$$

where:

$$\tau_R = \tau_{R\theta} \ (r = R)$$

Now differentiating Equation 8.27 with respect to τ_R , utilizing Equation 8.14, we find

$$\dot{\gamma}(\tau_R) - \dot{\gamma} \left(\frac{\tau_R}{\kappa^2} \right) = 2\tau_R \frac{d\Omega}{d\tau_R} = 2 \frac{d\Omega}{d \ln \tau_R} \tag{8.28}$$

This equation is a simple difference equation, which can be solved to give

$$\dot{\gamma}(\tau_R) = 2 \sum_{i=0}^{\infty} \frac{d\Omega}{d \ln(\tau_R/\kappa^{2i})} \tag{8.29}$$

Therefore, in general, one needs quite a lot of Ω versus τ_R data to correctly determine the shear rate in a Couette flow experiment. Based on Equation 8.29, it may also appear that larger cylinder spacings, that is, larger κ , are advantageous because the right-hand side of the equation converges more quickly. Considering the limiting case of a bob rotating in an unbounded pool of fluid (i.e., $R_2 \rightarrow \infty$ and $\kappa \rightarrow \infty$),

Equation 7.28 yields $\dot{\gamma}(\tau_R) = 2(d\Omega/d\ln\tau_R)$, which does not require as much data of Ω versus τ_R to determine $\dot{\gamma}(\tau_R)$.

More careful scrutiny of Equation 8.26 reveals an even more useful simplification. Specifically, notice that if $(\kappa - 1) \ll 1$, the curvature becomes negligible and the shear rate will be essentially constant across the gap. In this case, the integral on the right-hand side of Equation 8.26 can be evaluated using a simple trapezoidal rule to give

$$\Omega = \frac{\dot{\gamma}}{2R} \left(\frac{\kappa+1}{\kappa} \right) d \approx \frac{\dot{\gamma}d}{R} \quad (8.30)$$

where:

$d = (\kappa - 1)R$ is the thickness of the polymer layer between the cylinders

We therefore conclude that for $(d/R) \ll 1$, $\dot{\gamma} \approx (R\Omega/d)$, a result we might have guessed from the similarity of Couette shear flow with $d/R \ll 1$ to planar Couette shear. Thus, Couette shear flow measurements performed using small cylinder spacings (typically $d/R < 1/15$) lend themselves to particularly straightforward interpretation in terms of standard rheological variables such as shear stress τ_R and shear rate $\dot{\gamma}$.

If the fluid satisfies the power-law model, an alternative, sometimes simpler procedure can be used for relating $\dot{\gamma}$ and Ω at an arbitrary gap. First, define the angular velocity of fluid at any radial location in the gap, $\omega_r = v_\theta(r)/r$, and substituting in Equation 8.20 yields

$$\dot{\gamma}(r) = \dot{\gamma}_r = \frac{r d \omega_r}{dr} \quad (8.31)$$

But if the fluid satisfies the power-law model, we have from Equation 7.12

$$\dot{\gamma}_r = \left(\frac{\tau_r}{K} \right)^q = \left(\frac{T}{2\pi L r^2 K} \right)^q = C_p r^{-2q} \quad (8.32)$$

where:

$$q = 1/n, \quad C_q = \left(\frac{T}{2\pi L K} \right)^q$$

Substituting in Equation 7.26 and integrating yield

$$\Omega = \frac{C_q}{2q} [R^{-2q} - (\kappa R)^{-2q}]$$

and

$$\dot{\gamma}_r = \frac{2q\Omega r^{-2q}}{R_1^{-2q} - R_2^{-2q}} = \frac{2q\Omega}{(1 - \kappa^{-2q})} \left(\frac{r}{R} \right)^{-2q} \quad (8.33)$$

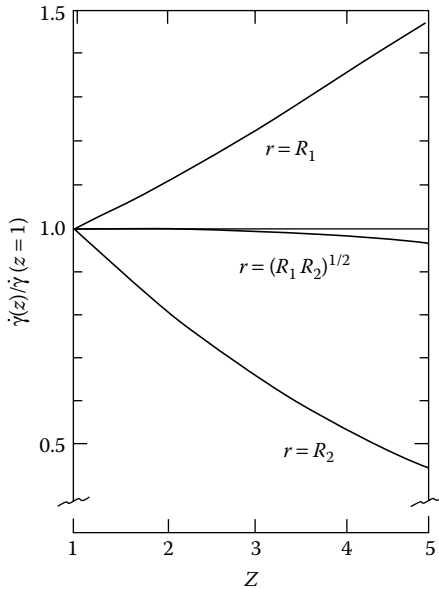


FIGURE 8.10 Relative change in shear rate $\dot{\gamma}$ with increasing shear-thinning behavior [increasing $n = d(\ln\dot{\gamma})/d(\ln\tau)$] for $R_1/R_2 = 0.9$.

Although the above equation can be applied to any r , if we choose $r = r_{gm} = (R_1 R_2)^{1/2} = R\kappa^{1/2}$, that is, r is located at the geometric mean radius r_{gm} of the two cylinders,

$$\dot{\gamma}_r = \dot{\gamma}_{gm} = 2q\Omega(\kappa^q - \kappa^{-q}) \tag{8.34}$$

and the precise value of the power-law exponent only has a weak effect on the shear rate (Figure 8.10).

Example 8.1

A coaxial cylinder rheometer is available with bob-and-cup radii R of 1.50 and 1.60 cm, respectively. The instrument is calibrated by measuring the torque needed to rotate the inner cylinder at 200 rpm in a Newtonian standard oil of viscosity of 12.5 Pa·s. The torque is read as 92.5% of full scale on a meter.

1. What are the power-law parameters for a polymer solution that gives readings of 40.0% and 72.0% of full scale at rotational rates of 50 and 200 rpm?
2. What is the rate of shear at the inner cylinder surface when the polymer solution is measured at 200 rpm? How does this compare with the geometric mean value?

Solution:

1. The rate of shear at the geometric mean radius $\dot{\gamma}_{\text{gm}}$ for $\Omega = 200$ rpm and $q = 1$ can be determined as follows:

$$\Omega = 200 \times \frac{2\pi}{60} = 20.9 \text{ s}^{-1}$$

$$\dot{\gamma}_{\text{gm}} = 2 \times 20.9 \left(\frac{1.6}{1.5} - \frac{1.5}{1.6} \right) = 324 \text{ s}^{-1}$$

For oil: $\tau_{\text{gm}} = 12.5 \times 324 = 4050 \text{ Pa}$

Therefore, the full-scale reading corresponds to

$$\frac{4050 \text{ Pa}}{0.925} = 4380 \text{ Pa}$$

For the polymer solution, ignoring the fact that $q \neq 1$, we get

$$\tau_{\text{gm}} = 0.4 \times 4380 = 1750 \text{ Pa} \quad \text{at } \dot{\gamma}_{\text{gm}} = 81 \text{ s}^{-1}$$

$$\tau_{\text{gm}} = 0.72 \times 4380 = 3160 \text{ Pa} \quad \text{at } \dot{\gamma}_{\text{gm}} = 324 \text{ s}^{-1}$$

This implies that $3160/1750 = (324/81)^{1/q} \Rightarrow q = 2.35$ and $p = 0.425$.
Substituting in the power-law model finally gives

$$K = \frac{1750 \text{ Pa}}{(0.81 \text{ s}^{-1})^{0.425}} = 270 \text{ Pa} \cdot \text{s}^{0.425}$$

Check: for $q = 2.35$, $\dot{\gamma}_{\text{gm}}$ can be more accurately calculated for $\Omega = 200$ rpm using Equation 8.34:

$$\dot{\gamma}_{\text{gm}} = 2 \times 2.35 \times 20.9 \left[\left(\frac{1.6}{1.5} \right)^{2.35} - \left(\frac{1.5}{1.6} \right)^{2.35} \right] = 323 \text{ s}^{-1}$$

We therefore conclude that for κ values in this range, q only has a minor effect on $\dot{\gamma}_{\text{gm}}$.

2. Using Equation 8.33, we obtain

$$\dot{\gamma}_R = \frac{2q\Omega}{1 - \kappa^{-2q}} = \frac{2 \times 2.35 \times 20.9}{[1 - (1.6/1.5)^{-4.7}]} = 375 \text{ s}^{-1}$$

This is 1.16 times the geometric mean value.

Because the fluids used for Couette flow rheometry are typically low viscosity polymer solutions, viscous heating and wall slip are normally negligible in this geometry. At high shear rates, the Weissenberg effect can be a significant source of error, particularly if large k and highly elastic polymeric fluids are used in the measurements [16]. If the spacing between the bob and the base of the cup is comparable to

the Couette cell gap, $d = R(\kappa - 1)$, and the bob is too short, the torque contribution from shear flow between the bases of the rotating bob and cup is not negligible and must be included in a complete analysis. Also, at high shear rates inertia cannot be neglected. Finally, even for the rotating bob–stationary cup configuration, Couette flow does eventually become unstable at very high shear rates.

8.5 TORSIONAL SHEAR BETWEEN PARALLEL PLATES

In a **parallel plate rheometer**, shear flow is generated in a layer of fluid (thickness d) sandwiched between parallel discs (Figure 8.11). The fluid is retained in the gap by surface tension. Shear is created by rotating one disc at an angular speed Ω , while the other is maintained stationary by applying a torque T . In this case, it does not matter which of the two discs is rotated, and in some designs both discs are rotated in opposite directions. Fluid elasticity creates a normal force F that attempts to separate the plates. T , Ω , and F are the experimental measurables in this flow configuration.

As stated earlier, our goal is to derive general equations that relate these quantities to rheological variables such as shear stress, shear rate, and normal stress differences. Based on the direction of the imposed velocity, the cylindrical symmetry of the flow geometry, and the assumptions that the fluid is incompressible and flow occurs under isothermal conditions, the equations of continuity (Appendix 8.A) yield $v = v_\theta(r,z)e_\theta$. Neglecting inertia, the differential linear momentum conservation equations (Appendix 8.B) can be simplified to give

$$0 = \frac{\partial}{\partial r}(\tau_{rr} - p) - \left(\frac{N_1 + N_2}{r}\right) \tag{8.35}$$

$$0 = \frac{\partial \tau_{\theta z}}{\partial z} \tag{8.36}$$

$$0 = \frac{\partial p}{\partial z} + \frac{\partial \tau_{zz}}{\partial z} \tag{8.37}$$

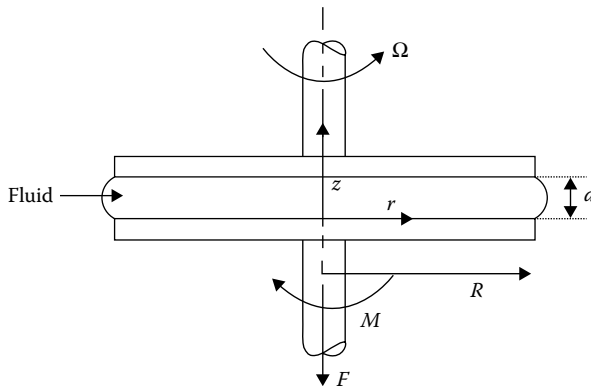


FIGURE 8.11 Torsional shear flow between parallel plates.

where:

$$\begin{aligned} N_1 &= \tau_{\theta\theta} - \tau_{zz} \\ N_2 &= \tau_{zz} - \tau_{rr} \end{aligned}$$

It is apparent from Equation 8.36 that the shear stress $\tau_{\theta z}$ can only be a function of r . Anticipating a relationship between $\tau_{\theta z}$ and the shear rate of the general form $\tau_{\theta z} = f(\dot{\gamma}) = f(\partial v_\theta / \partial z)$ leads to

$$v_\theta(r, z) = f(r)z + g(r) \quad (8.38)$$

For the flow configuration depicted in Figure 8.11, the no-slip boundary condition yields $v_\theta(z = 0) = 0$, all r , and $v_\theta(z = d) = \Omega r$. Applying these conditions to Equation 8.38, we find

$$v_\theta(r, z) = \frac{\Omega}{d} r z \quad (8.39)$$

The shear rate is therefore given by $\dot{\gamma} = (\Omega/d)r$. The shear stress $\tau_{\theta z}$ can be expressed in terms of the measured torque T by equating the torque exerted by the fluid on the lower plate with the external torque T required to prevent rotation:

$$2\pi \int_0^R \tau_{\theta z} r^2 dr = T \quad (8.40)$$

Therefore, the radial dependence of the shear stress must be known before the above equation can be exploited to relate the stress to the measured torque. This situation is analogous to the problem we encountered in Section 8.3; we will solve it using a similar approach. First, change variables in Equation 8.40 to introduce the shear rate:

$$\begin{aligned} r &= \frac{d}{\Omega} \dot{\gamma} = \frac{R}{\dot{\gamma}_R} \dot{\gamma}, \quad dr = \frac{R}{\dot{\gamma}_R} d\dot{\gamma} \\ T &= 2\pi \int_0^{\dot{\gamma}_R} \left(\frac{R}{\dot{\gamma}_R} \right)^3 \dot{\gamma}^2 \tau_{\theta z} d\dot{\gamma} \end{aligned} \quad (8.41)$$

where:

$$\dot{\gamma}_R = \dot{\gamma}(r=R)$$

Differentiating Equation 8.41 with respect to $\dot{\gamma}_R$ and applying Equation 8.14 yield $dT / d\dot{\gamma}_R = (2\pi R^3 / \dot{\gamma}_R) \tau_{\theta z} - (3 / \dot{\gamma}_R) T$, and finally,

$$\tau_{\theta z} = \frac{T}{2\pi R^3} \left[3 + \frac{d}{d \ln \dot{\gamma}_R} \ln T \right] \quad (8.42)$$

To determine the shear stress, a sufficiently large amount of $\ln T$ versus $\ln \dot{\gamma}_R$ data must be collected so that the derivative in Equation 8.42 can be accurately determined.

The total thrust force F produced during shear can be related to the normal stress difference in shear. Integrating Equation 8.37 yields $P_{zz}(r) = \tau_{zz}(r) - p(r)$, where $P_{zz}(r)$ is the integration constant and, physically, is the net pressure exerted by the sheared fluid on a surface with normal vector n_z . Substituting for p in Equation 8.35 and integrating the resulting equation from r to R yields

$$P_{zz}(R) - P_{zz}(r) = N_2(R) - N_2(r) + \int_r^R \left(\frac{N_1 + N_2}{\phi} \right) d\phi \tag{8.43}$$

where:

$P_{zz}(R) - N_2(R) = -p(R) + \tau_{rr}(R)$ is the total outward pressure exerted by the fluid on the meniscus and surrounding atmosphere

This pressure is balanced by surface tension and atmospheric pressure p_a acting inward on the meniscus. If the shape of the fluid's meniscus is allowed sufficient time to equilibrate, the surface tension can be neglected and $-p_a = -p(R) + \tau_{rr}(R)$. Substituting in Equation 8.43 then yields

$$P_{zz}(r) = N_2(r) - P_a - \int_r^R \left(\frac{N_1 + N_2}{\phi} \right) d\phi \tag{8.44}$$

The total thrust force F on the lower plate is therefore

$$F = -2\pi \int_0^R [P_{zz}(r) + P_a] r dr = -2\pi \int_0^R N_2 r dr + 2\pi \int_0^R \int_r^R \left(\frac{N_1 + N_2}{\phi} \right) d\phi r dr \tag{8.45}$$

This equation can be integrated by parts to give

$$F = \pi \int_0^R (N_1 - N_2) r dr \tag{8.46}$$

It is again evident that the radial dependence of the normal stresses must be known before Equation 8.46 can be exploited to relate the normal stress differences to the measured axial force F . To circumvent this difficulty, we use the same change of variable, as earlier, and Equation 8.14 to obtain

$$N_1 - N_2 = \frac{2F}{\pi R^2} \left[1 + \frac{1}{2} \frac{d}{d \ln \dot{\gamma}_R} \ln F \right] \tag{8.47}$$

It is then clear that measurements of F at multiple shear rates $\dot{\gamma}_R$ can be used to determine how $N_1 - N_2$ changes with shear rate. As discussed in Section 8.2, N_1 is typically much larger than N_2 for polymer liquids and increases more quickly with shear rate than $-N_2$ at high shear rates. Experimental measurements of $N_1 - N_2$ are therefore quite sensitive to the first normal stress difference N_1 , particularly at high shear rates.

The accuracy of rheological data obtained using parallel plate measurements depends on a variety of factors. First, it is essential that sufficient T versus Ω and F versus Ω data be collected to properly use Equations 8.42 and 8.47. Second, a good temperature control system must be in place to ensure uniform temperature throughout the gap. Finally, experimental conditions should be chosen to reduce errors from edge fracture, sample expulsion from the gap, wall slip, secondary flow effects due to fluid elasticity and/or misalignment of the plates, and viscous heating.

Edge fracture arises from an imbalance of stresses at the meniscus and is driven primarily by N_2 in the fluid [2,3]. It reduces the cross-sectional area of the fluid in contact with the plates, which causes the measured torque to decrease (usually in a time-dependent manner). A common remedy is to reduce d so that the shear rate at which edge fracture occurs is pushed outside the range of experimental interest. Sample expulsion usually occurs from the small centrifugal force term v^2_ϕ/r in Equation 8.35. This term cannot be neglected at high shear rates. Measurement errors due to sample expulsion are evidenced by a gradual but irreversible reduction in the total torque at high shear rates. The only true remedy is to first identify the shear rate where the effect is first observed for a material of interest and perform subsequent steady shear rheometric measurements at shear rates 2–5 times lower than this value. As was the case of Poiseuille flow, the wall slip can also compromise rheological data. A procedure first discussed by Yoshimura and Prud'homme [17] can be used to quantify and correct measurement errors caused by the wall slip. Again, because the slip velocity is generally a nonmonotonic function of shear stress, slip errors are difficult to correct after the fact. Large gaps and/or moderately roughened fixtures are therefore the most effective remedies. Secondary flow effects can be reduced by choosing narrow gaps, by carefully aligning the plates to achieve parallelism, and by ensuring that the center of rotation is the same for both plates, and that the center of rotation of the plates matches the center of rotation of the drive mechanism. Alignment problems can also lead to **apparent gap errors** [2], wherein the gap back-calculated from viscosity measurements using standard fluids appears smaller than the actual plate separation used for the measurements. These errors are amplified at lower d , so a compromise between the plate alignment and the onset of secondary flow must be reached in choosing the gap. **Viscous heating** is always present during shear of high-viscosity polymer liquids. It becomes a problem in rheometry when the rate of heat generation becomes so large that temperature gradients are created in the fluid. Experimental conditions that reduce the heat generation rate, for example, low shear rates, and enhance the heat dissipation rate, for example, small d and highly conducting metallic plates, are required to minimize measurement errors due to viscous heating.

8.6 SHEAR BETWEEN CONE-AND-PLATE FIXTURES

The cone-and-plate rheometer (Figure 8.12) is a simple variant of the parallel plate device considered in Section 8.5. In a **cone-and-plate rheometer**, polymer samples are sandwiched between a blunt cone and a flat plate. Shear is generated by rotating either the cone or the plate at an angular speed Ω , while the other fixture is maintained stationary. Typically, the cone angle α is maintained small $\alpha < 6^\circ$ to minimize measurement artifacts caused by secondary flow [18]. The main advantage of the cone-and-plate rheometer over the parallel plate device is the homogeneity of the shear field it creates

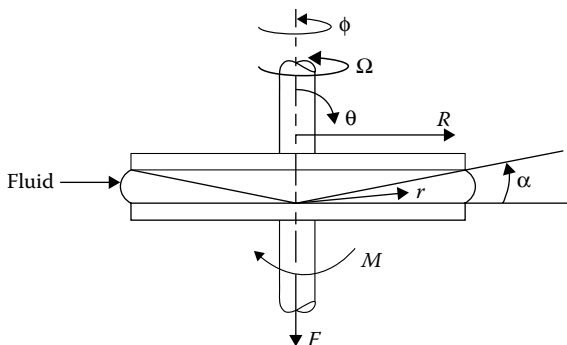


FIGURE 8.12 Torsional shear flow between cone-and-plate fixtures.

in a fluid. Stress components are therefore the same everywhere in the gap, allowing the experimental parameters, Ω , T , and F , to be easily related to rheological variables.

Based on the direction of the imposed velocity, and the assumptions that the fluid is incompressible and flow occurs under isothermal conditions, the equations of continuity in spherical coordinates (Appendix 8.A) yield $v = v_\phi(\theta, r)$. The shear rate is therefore given by

$$\dot{\gamma}(\theta) = \frac{\sin \theta}{r} \frac{\partial}{\partial \theta} \left(\frac{v_\phi}{\sin \theta} \right) = \frac{1}{r} \frac{\partial v_\phi}{\partial \theta} - \frac{v_\phi \cot \theta}{r} \tag{8.48}$$

Neglecting inertia, the differential linear momentum conservation equations in spherical coordinates (Appendix 8.B) can be written as

$$0 = r \frac{\partial}{\partial r} (\tau_{rr} - p) - (N_1 + 2N_2) \tag{8.49}$$

$$0 = \frac{1}{r \sin \theta} \frac{\partial}{\partial \theta} (\tau_{\theta\phi} \sin \theta) + \frac{\tau_{\theta\phi} \cot \theta}{r} \tag{8.50}$$

$$0 = \frac{1}{r \sin \theta} \tau_{\theta\theta} \sin \theta - \frac{\tau_{\phi\phi} \cot \theta}{r} - \frac{1}{r} \frac{\partial p}{\partial \theta} \tag{8.51}$$

where:

$\tau_{\theta\phi} = \tau$ is the shear stress

$N_1 = \tau_{\phi\phi} - \tau_{\theta\theta}$ is the first normal stress difference

$N_2 = \tau_{\theta\theta} - \tau_{rr}$ is the second normal stress difference

Equation 8.50 can be simplified to give $(\partial\tau_{\theta\phi}/\partial\theta) + 2\tau_{\theta\phi} \cot \theta = 0$, which can be integrated to yield

$$\tau_{\theta\phi} = \frac{A(r)}{(\sin \theta)^2} \tag{8.52}$$

where:

$A(r)$ is an integration constant for the θ integration

Notice from Figure 8.12 that θ varies from $\pi/2 - \alpha$ to α for the cone-and-plate geometry. The shear stress difference across the gap is therefore $\Delta\tau/A(r) = [\sin^2(\pi/2 - \alpha)]^{-1} - 1 \approx 0$ for small **cone angles** α . Therefore, provided that cones with small angles are used, the shear stress in a cone-and-plate shear flow is constant irrespective of location θ in the gap.

If the shear stress is independent of θ , then the shear rate must also be independent of θ for small α . Substituting $\dot{\gamma}(\theta) = \dot{\gamma}$ in Equation 8.48 yields $\dot{\gamma} = (1/r)(\partial v_\phi / \partial \theta) = \text{const}$, which can be integrated to give $v_\phi = \dot{\gamma}r\theta - g(r)$, where $g(r)$ is an integration constant. However, by the no-slip condition, we know $v_\phi(\pi/2, r) = 0$ and $v_\phi(\pi/2 - \alpha, r) = r\Omega$. This implies that $g(r) = -\dot{\gamma}r(\pi/2)$ and

$$|\dot{\gamma}| = \frac{\Omega}{\alpha} \quad (8.53)$$

If the shear rate is independent of the radial position in the gap, then the shear stress must also be independent of r , which implies that $A(r) = A$, where A is a constant. The torque required to maintain the plate stationary can be computed as earlier from a torque balance:

$$T = 2\pi \int_0^R \tau_{\theta\phi} r^2 dr = \frac{2}{3} \pi R^3 \tau_{\theta\phi} \quad (8.54)$$

Therefore, the shear stress can be quite easily obtained from the measured torque, $\tau = 3T/(2\pi R^3)$. Thus, both the shear stress τ and the shear rate $|\dot{\gamma}|$ are readily obtained from the measurements of T and Ω .

The axial force F can be used to determine the first normal stress difference N_1 . Again assuming small α , we conclude that if $\dot{\gamma}$ is a constant, then the normal stress differences must also be independent of r and θ . Therefore, for small cone angles, Equation 8.49 can be written as $r(\partial/\partial r)(\tau_{rr} - p) = N_1 + 2N_2 = \text{const}$. Integrating this equation yields

$$\tau_{rr} - p = (N_1 + 2N_2) \ln r + B \quad (8.55)$$

where:

B can be determined by enforcing the balance between the total radial pressure $\tau_{rr} - p = p_{rr}$ exerted by the fluid in the gap on the meniscus and the atmospheric pressure, which acts inward on the meniscus, $p_{rr}(R) = -p_a$. Substituting in Equation 8.55 gives $B = -(N_1 + 2N_2) \ln R - p_a$ and

$$\tau_{rr} - p = (N_1 + 2N_2) \ln \left(\frac{r}{R} \right) - p_a \quad (8.56)$$

But if $N_2 = \tau_{\theta\theta} - \tau_{rr}$ is constant,

$$\tau_{\theta\theta} - p = (N_1 + 2N_2) \ln \left(\frac{r}{R} \right) - p_a + N_2 = p_{\theta\theta} \quad (8.57)$$

where:

$p_{\theta\theta}$ is the total fluid pressure exerted in the gapwise direction

The axial force F balances $p_{\theta\theta}$ and the atmospheric pressure integrated over the plate:

$$F = -2\pi \int_0^R (p_{\theta\theta} + p_a) r dr = \frac{\pi R^2}{2} N_1 \tag{8.58}$$

Therefore, the first normal stress difference $N_1 = 2F/(\pi R^2)$ is also easily obtained from cone-and-plate shear measurements, again provided that α is small. Equation 8.57 also suggests a procedure for measuring N_2 . Specifically, if $p_{\theta\theta}$ is measured at several radial positions as illustrated in Figure 8.13, a plot of $p_{\theta\theta}$ versus $\ln(r/R)$ should yield a straight line with slope $N_1 + 2N_2$ and intercept $N_2 - p_a$, allowing N_1 and N_2 to be determined. Because N_2 is generally quite small, edge effects severely limit the accuracy of data obtained using this approach. Better quality N_2 data can be obtained if N_1 is measured separately from total thrust force measurements, and N_2 determined from the slope of a $p_{\theta\theta}$ versus $\ln(r/R)$ plot.

Measurement errors in this geometry arise from many of the same sources as in parallel plate shear. Since the gap is set by the cone angle, changes in α have a similar effect as changes in d . Equations 8.53, 8.54, and 8.58 have all been developed based on the assumption of small cone angles, with an upper limit of about 8° . Although lower α values are generally preferred, alignment problems and slip errors similar to those discussed in Section 8.5 become more severe at low cone angles. The spatially uniform shear rate achieved in the cone-and-plate fixture has inspired creative approaches for ameliorating measurement artifacts due to edge fracture. A **cone-segmented plate** design first described by Meissner and coworkers [19] and evaluated more recently by Snijkers and Vlassopoulos [20] presents a particularly convenient design that may extend, by as much as a decade, the shear rate range at which measurements uncontaminated by edge

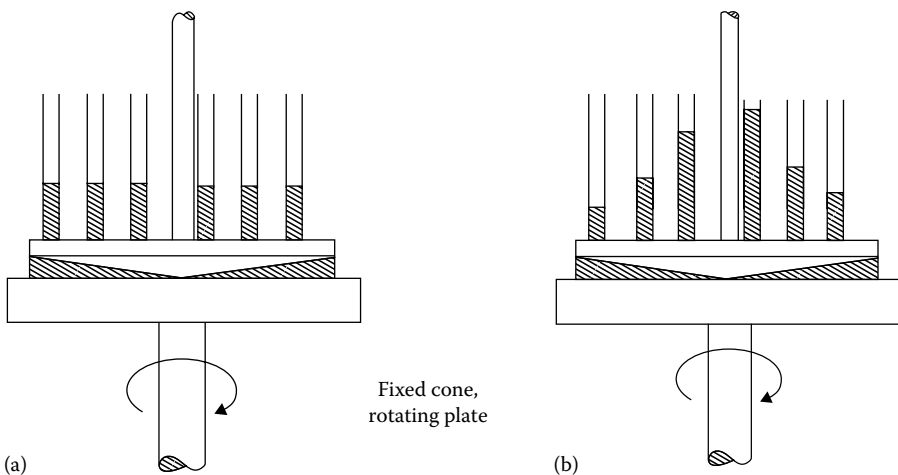


FIGURE 8.13 Relative normal pressures as shown by manometers inserted in stationary cone of a cone-and-plate rheometer: (a) purely viscous behavior; (b) viscoelastic behavior.

fracture can be carried out in entangled polymer melts and solutions prone to edge fracture in torsional shear flows.

Example 8.2

A power-law fluid is characterized in a cone–plate viscometer (cone angle = 0.50°). The measured viscosity is 0.200 Pa·s at 6 rpm and 0.080 Pa·s at 60 rpm. What value of $\Delta p/L$ is required to produce a volumetric flow rate of 1.00 liter/s of this same fluid in a horizontal pipeline with an inner diameter of 2.00 cm?

Solution: By Equation 8.53 we can directly compute the shear rate at each angular speed:

$$\dot{\gamma} (6 \text{ rpm}) = \frac{2\pi \times 6/60}{\pi \times 0.50/180} = 72.0 \text{ s}^{-1}$$

$$\dot{\gamma} (60 \text{ rpm}) = \frac{2\pi \times 60/60}{\pi \times 0.50/180} = 720 \text{ s}^{-1}$$

Applying the power-law fluid model (Equation 7.12) gives

$$\frac{0.08}{0.2} = 10^{n-1} \Rightarrow n = 0.602 \quad \text{and} \quad K = \frac{0.2}{72.0^{-0.398}} = 1.1 \text{ Pa} \cdot \text{s}^{0.4}$$

For a power-law fluid, Equation 8.16 can be simplified to give

$$\dot{\gamma}_R = \left(3 + \frac{1}{n}\right) \frac{Q}{\pi R^3}$$

Substituting for Q and n yields

$$\begin{aligned} \dot{\gamma}_R &= \left(3 + \frac{1}{0.602}\right) \frac{10^3}{\pi} = 1484 \text{ s}^{-1} \\ \Rightarrow \tau_R &= 1.1 \times (1484)^{0.602} = 89.24 \text{ Pa} \end{aligned}$$

Finally, substituting in Equation 8.10 gives

$$\frac{\Delta p}{L} = \frac{2}{R} \tau_R = \frac{2}{10^{-2}} \times 89.24 = 1.78 \times 10^4 \text{ Pa/m}$$

In order to characterize the rheological properties of a polymer melt over a very large range of shear rates, data obtained in multiple rheometer configurations are typically combined. Cone-and-plate and parallel plate shear measurements are, for example, the most accurate at low shear rates. However, the shear rates accessible in a capillary rheometer are well above those that can be achieved in any other configuration. Capillary rheometry, cone-and-plate shear, and parallel plate shear rheometry provide complementary information about polymer flow response. In the example shown in Figure 8.14, an uncross-linked silicone rubber was measured using three

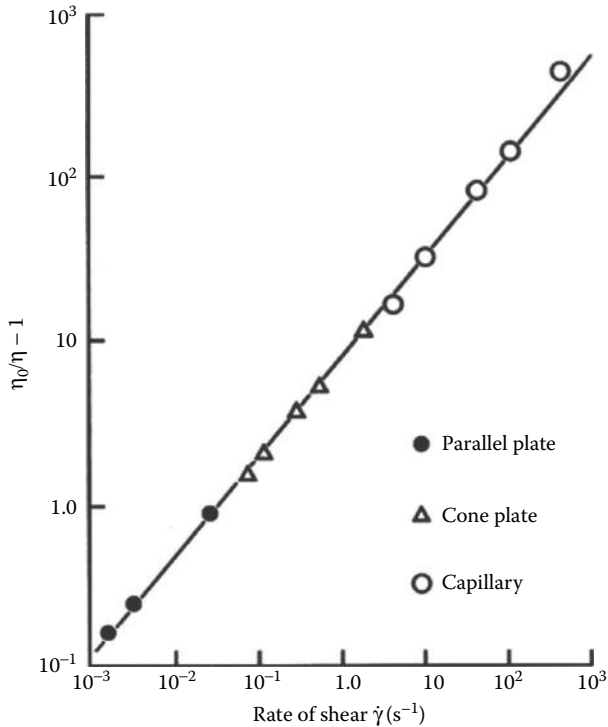


FIGURE 8.14 Comparison of Cross model prediction with experimental viscosity data for a high-molecular-weight poly(dimethylsiloxane) using parallel plate, cone-and-plate, and capillary flow rheometry at 23°C. The fitted parameters are $\lambda = 34.5$ s, $s = 0.604$, and $\eta_0 = 98.0$ kPa · s.

separate instruments covering nearly six decades of shear rate. The line through the data is the prediction of Cross model and illustrates the broad shear rate range over which the Cross model is applicable for this material.

APPENDIX 8.A EQUATIONS OF CONTINUITY FOR INCOMPRESSIBLE FLUIDS UNDER ISOTHERMAL FLOW CONDITIONS

Rectangular coordinates

$$\frac{\partial v_x}{\partial x} + \frac{\partial v_y}{\partial y} + \frac{\partial v_z}{\partial z} = 0 \tag{8.A.1}$$

Cylindrical coordinates

$$\frac{1}{r} \frac{\partial}{\partial r} (rv_r) + \frac{1}{r} \frac{\partial}{\partial \theta} (v_\theta) + \frac{\partial v_z}{\partial z} \tag{8.A.2}$$

Spherical coordinates

$$\frac{1}{r^2} \frac{\partial}{\partial r} (r^2 v_r) + \frac{1}{r \sin \theta} \frac{\partial}{\partial \theta} (v_\theta \sin \theta) + \frac{1}{r \sin \theta} \frac{\partial}{\partial \phi} (v_\phi) = 0 \quad (8.A.3)$$

APPENDIX 8.B DIFFERENTIAL EQUATIONS OF MOTION**Rectangular coordinates**

$$\left(\frac{\partial v_x}{\partial t} + v_x \frac{\partial v_x}{\partial x} + v_y \frac{\partial v_x}{\partial y} + v_z \frac{\partial v_x}{\partial z} \right) = g_x - \frac{1}{\rho} \frac{\partial p}{\partial x} - \frac{1}{\rho} \left(\frac{\partial \tau_{xx}}{\partial x} + \frac{\partial \tau_{yx}}{\partial y} + \frac{\partial \tau_{zx}}{\partial z} \right) \quad (8.B.1)$$

$$\left(\frac{\partial v_y}{\partial t} + v_x \frac{\partial v_y}{\partial x} + v_y \frac{\partial v_y}{\partial y} + v_z \frac{\partial v_y}{\partial z} \right) = g_y - \frac{1}{\rho} \frac{\partial p}{\partial y} - \frac{1}{\rho} \left(\frac{\partial \tau_{xy}}{\partial x} + \frac{\partial \tau_{yy}}{\partial y} + \frac{\partial \tau_{zy}}{\partial z} \right) \quad (8.B.2)$$

$$\left(\frac{\partial v_z}{\partial t} + v_x \frac{\partial v_z}{\partial x} + v_y \frac{\partial v_z}{\partial y} + v_z \frac{\partial v_z}{\partial z} \right) = g_z - \frac{1}{\rho} \frac{\partial p}{\partial z} - \frac{1}{\rho} \left(\frac{\partial \tau_{xz}}{\partial x} + \frac{\partial \tau_{yz}}{\partial y} + \frac{\partial \tau_{zz}}{\partial z} \right) \quad (8.B.3)$$

Cylindrical coordinates

$$\left(\frac{\partial v_r}{\partial t} + v_r \frac{\partial v_r}{\partial r} + \frac{v_\theta}{r} \frac{\partial v_r}{\partial \theta} - \frac{v_\theta^2}{r} + v_z \frac{\partial v_r}{\partial z} \right) = g_r - \frac{1}{\rho} \frac{\partial p}{\partial r} - \frac{1}{\rho} \left[\frac{1}{r} \frac{\partial}{\partial r} (r \tau_{rr}) + \frac{1}{r} \frac{\partial \tau_{\theta r}}{\partial \theta} - \frac{\tau_{\theta\theta}}{r} + \frac{\partial \tau_{zr}}{\partial z} \right] \quad (8.B.4)$$

$$\left(\frac{\partial v_\theta}{\partial t} + v_r \frac{\partial v_\theta}{\partial r} + \frac{v_\theta}{r} \frac{\partial v_\theta}{\partial \theta} - \frac{v_r v_\theta}{r} + v_z \frac{\partial v_\theta}{\partial z} \right) = g_\theta - \frac{1}{\rho r} \frac{\partial p}{\partial \theta} - \frac{1}{\rho} \left[\frac{1}{r^2} \frac{\partial}{\partial r} (r^2 \tau_{r\theta}) + \frac{1}{r} \frac{\partial \tau_{\theta\theta}}{\partial \theta} - \frac{\tau_{\theta r} - \tau_{r\theta}}{r} + \frac{\partial \tau_{z\theta}}{\partial z} \right] \quad (8.B.5)$$

$$\left(\frac{\partial v_z}{\partial t} + v_r \frac{\partial v_z}{\partial r} + \frac{v_\theta}{r} \frac{\partial v_z}{\partial \theta} + v_z \frac{\partial v_z}{\partial z} \right) = g_z - \frac{1}{\rho} \frac{\partial p}{\partial z} - \frac{1}{\rho} \left[\frac{1}{r} \frac{\partial}{\partial r} (r \tau_{rz}) + \frac{1}{r} \frac{\partial \tau_{\theta z}}{\partial \theta} + \frac{\partial \tau_{zz}}{\partial z} \right] \quad (8.B.6)$$

Spherical coordinates

$$\left(\frac{\partial v_r}{\partial t} + v_r \frac{\partial v_r}{\partial r} + \frac{v_\theta}{r} \frac{\partial v_r}{\partial \theta} - \frac{(v_\theta^2 + v_\phi^2)}{r} + \frac{v_\phi}{r s_\theta} \frac{\partial v_r}{\partial \phi} \right) = g_r - \frac{1}{\rho} \frac{\partial p}{\partial r} - \frac{1}{\rho} \left[\frac{1}{r^2} \frac{\partial}{\partial r} (r^2 \tau_{rr}) + \frac{1}{r s_\theta} \frac{\partial}{\partial \theta} (\tau_{\theta r} s_\theta) - \frac{\tau_{\theta\theta} + \tau_{\phi\phi}}{r} + \frac{1}{r s_\theta} \frac{\partial \tau_{\phi r}}{\partial \phi} \right] \quad (8.B.7)$$

$$\left(\frac{\partial v_\theta}{\partial t} + v_r \frac{\partial v_\theta}{\partial r} + \frac{v_\theta}{r} \frac{\partial v_\theta}{\partial \theta} + \frac{v_\phi}{rs_\theta} \frac{\partial v_\theta}{\partial \phi} - \frac{(v_r v_\theta + v_\phi^2 c_\theta)}{r} \right)$$

$$= g_\theta - \frac{1}{\rho r} \frac{\partial p}{\partial \theta} - \frac{1}{\rho} \left[\frac{1}{r^3} \frac{\partial}{\partial r} (r^3 \tau_{r\theta}) + \frac{1}{rs_\theta} \frac{\partial}{\partial \theta} (\tau_{\theta\theta} s_\theta) + \frac{1}{rs_\theta} \frac{\partial \tau_{\phi\theta}}{\partial \phi} - \frac{(\tau_{r\theta} - \tau_{\theta r} + \tau_{\phi\theta} c_\theta)}{r} \right] \tag{8.B.8}$$

$$\left(\frac{\partial v_\phi}{\partial t} + v_r \frac{\partial v_\phi}{\partial r} + \frac{v_\theta}{r} \frac{\partial v_\phi}{\partial \theta} + \frac{v_\phi}{rs_\theta} \frac{\partial v_\phi}{\partial \phi} - \frac{(v_\phi v_r - v_\theta v_\phi c_\theta)}{r} \right)$$

$$= g_\phi - \frac{1}{\rho r s_\theta} \frac{\partial p}{\partial \phi} - \frac{1}{\rho} \left[\frac{1}{r^3} \frac{\partial}{\partial r} (r^3 \tau_{r\phi}) + \frac{1}{rs_\theta} \frac{\partial}{\partial \theta} (\tau_{\theta\phi} s_\theta) + \frac{1}{rs_\theta} \frac{\partial \tau_{\phi\phi}}{\partial \phi} - \frac{(\tau_{r\phi} + \tau_{\phi r} - \tau_{\phi\theta} c_\theta)}{r} \right] \tag{8.B.9}$$

where:

$$s_\theta = \sin\theta$$

$$c_\theta = \cot\theta$$

KEYWORDS

- Normal stress difference
- Complex fluid
- Rheometers
- Rheometry
- Viscometric flows
- Velocity gradient
- Rate of deformation
- Weissenberg effect
- Extrudate
- Die swell
- Melt fracture
- Hydrostatic pressure
- Shear direction
- Anisotropic
- First normal stress difference
- Second normal stress difference
- Third normal stress difference
- Normal stress coefficient
- Birefringence
- Poiseuille flow
- No-slip condition
- Capillary flow
- Differential momentum balance

Leibnitz theorem
 Weissenberg–Rabinowitsch equation
 Entrance and exit losses
 Recoverable shear strain
 Bagley correction
 Recoverable shear strain
 Spurt
 Cup-and-bob rheometer
 Couette flow
 End effects
 Parallel plate rheometer
 Edge fracture
 Apparent gap error
 Viscous heating
 Cone-and-plate rheometer
 Apparent gap error
 Viscous heating
 Cone angle
 Cone-segmented plate

PROBLEMS

- 8.1 A coaxial viscometer with $R_2/R_1 = 1.10$, $R_1 = 2$ cm, and $L = 5$ cm is used to measure the viscosity of a fluid that follows the equation:

$$A\dot{\gamma} = \tau \left[1 + \left(\frac{\tau}{B} \right)^{1.5} \right]$$

where:

$$A = 100 \text{ Pa}\cdot\text{s}$$

$$B = 1000 \text{ Pa}$$

When $\tau = 800$ Pa at the geometric mean radius, what is (a) the steady-state torque (N·m), (b) the rotational speed of the cup (rpm), and (c) the ratio of the rate of shear at the bob to that at the cup?

- 8.2 A power-law polymer solution (S) is characterized in a Brookfield viscometer, which consists of a vertical cylinder rotating in an *infinite* amount of liquid. Data are obtained as follows:

Liquid Being Tested	Rate of Rotation (rpm)	Scale Reading
Newtonian standard, $\eta = 0.200$ Pa·s	6	175
S	6	200
S	60	400

Now S is pumped first through cylindrical pipe A and then splits into two flows through pipes B and C . Pipe A has a diameter twice that of B or C and a length that is 10 times that of B or C . What is the expected ratio of pressure drop over pipe A to that over pipe B ? Neglect end effects.

- 8.3** A fluid is forced by a pressure drop $P_2 - P_1$ to flow through two filters F_1 and F_2 . The filters have the same thickness and the same total open area, but the pores of F_2 are half the diameter of those of F_1 . If the fluid is Newtonian, what is the ratio of the flows Q_1/Q_2 through F_1 and F_2 ? What is the ratio if the fluid follows a power law?

If the fluid is non-Newtonian, is there a possibility of the ratio Q_1/Q_2 being less than 1? Assume that each filter is made up of a number of tubes of uniform length with no end effects. Assume that all tubes of F_1 have the same diameter and so on.

- 8.4** Given the equation

$$\dot{\gamma} = A\tau + B\tau^2 + C\tau^3$$

where:

$$A = 1.0 \times 10^{-3}$$

$$B = 2.0 \times 10^{-6}$$

$$C = 3.0 \times 10^{-9}$$

- (a) What is the zero-shear viscosity in Pa-s? ($\dot{\gamma}$ in s^{-1} ; τ in Pa)
 (b) Calculate the ratio of flow rate (cm^3/s) in a capillary viscometer at a stress of $\tau = 1000$ Pa compared to that at $\tau = 10$ Pa.

For the capillary: $r = 0.05$ cm, $L = 10.0$ cm.

- 8.5** If 0.500 cm^3 of polymer described by the following model is placed in a parallel plate viscometer with a plate separation of 0.0100 cm and a weight of 0.500 g is applied to the movable plate by appropriate pulleys, how far will the plate move in 10 s? (τ in Pa).

$$\text{Model: } \dot{\gamma} = 2.00 \times 10^{-2} \tau^2$$

- 8.6** A typical laboratory capillary viscometer has a flow time t of water at $30^\circ C$ of 200.0 s. The flow volume V is 5.0 cm^3 , the capillary length L is 15 cm, and the average head h is $1.10L$. Estimate the diameter of the capillary disregarding end effects.

- 8.7** In order to simplify end corrections in a cup-and-bob viscometer, the ends can be conical. If each end of the bob is the cone of a cone-plate viscometer, what is the ratio of the torque due to the ends of the bob to the torque due to flow in the annulus in the cylindrical part? Assume a bob of length L and radius KR , a cup of radius R , and a cone angle of $1 - K$. Assume a Newtonian fluid and refer torque in the annulus to the geometric mean radius.

- 8.8** For a Bingham plastic, qualitatively, what unusual feature must a velocity profile in pipe flow exhibit? In a cup-and-bob viscometer, what discontinuity might be expected in the flow field for the same model? In a cone–plate viscometer, would any discontinuities be expected?
- 8.9** What is the maximum shear rate that one could use in a cone–plate viscometer with a Newtonian liquid of 100 Pa·s if the adiabatic heating rate is to be kept below 0.01°C/min? Assume a density of 0.95 g/cm³ and a specific heat of 2.5 J/g·°C.

REFERENCES

1. Lodge, A. S.: *Elastic Liquids*, Academic Press, New York, 1964, p. 192.
2. Macosko, C. W.: *Rheology: Principles, Measurements and Applications*, VCH, New York, 1994.
3. Larson, R. G.: *Rheol. Acta*, 31:213 (1992).
4. El Kissi, N., L. Leger, J.-M. Piau, and A. Mezghani: *J. Non-Newt. Fluid Mech.*, 52:249 (1994).
5. Larson, R. G.: *Constitutive Equations for Polymer Melts and Solutions*, Butterworth, Stoneham, MA, 1988.
6. Bird, R. B., R. C. Armstrong, and O. Hassager: *Dynamics of Polymeric Liquids. Vol. 1: Fluid Mechanics*, 1st edn., chap. 3, Wiley, New York, 1987.
7. Islam, M. T., and L. A. Archer: *J. Polym. Sci. Part B: Polym. Phys.*, 39:2275 (2001).
8. Fuller, G. G.: *Optical Rheometry of Complex Fluids*, Oxford, New York, 1995.
9. Janeschitz-Kriegl, H.: *Polymer Melt Rheology and Flow Birefringence*, Springer-Verlag, Berlin, Germany, 1983.
10. Rabinowitsch, B.: *Z. Physik. Chem.*, A145:1 (1929).
11. Darby, R.: *Viscoelastic Fluids*, chap. 5, Dekker, New York, 1976.
12. Bagley, E. B.: *J. Appl. Phys.*, 28:624 (1957); 31:1126 (1960).
13. Denn, M. M.: *Annu. Rev. Fluid. Mech.*, 22:13 (1990); 33:265 (2001).
14. Archer, L. A.: Wall-Slip Measurement and Modeling Issues, in K. Migler and S. Hatzikiriakos (eds.), *Polymer Processing Instabilities*, Dekker, New York, 2004, pp. 73–120.
15. Bird, R. B., W. E. Stewart, and E. N. Lightfoot: *Transport Phenomena*, Wiley, New York, 1960, p. 96.
16. Dealy, J. M., and K. F. Wissbrun: *Melt Rheology and Its Role in Plastics Processing—Theory and Applications*, Van Nostrand Reinhold, New York, 1990.
17. Yoshimura, A., and R. K. Prud'homme: *J. Rheol.*, 32:53 (1988).
18. Bird, R. B., R. C. Armstrong, and O. Hassager: *Dynamics of Polymeric Liquids. Vol. 1: Fluid Mechanics*, 1st edn., Wiley, New York, 1987, pp. 521–523.
19. Meissner, J., R. W. Garbella, and J. Hostettler: *J. Rheol.*, 33:843 (1989).
20. Snijkers, F. and D. Vlassopoulos: *J. Rheol.*, 55:1167 (2011).

9 Mechanical Properties at Small Deformations

9.1 INTRODUCTION

The study of mechanical properties of amorphous polymers at small deformations has been one of the most fruitful areas in polymer science. For uncross-linked polymer melts, experimental results from measurements in the linear **viscoelasticity** regime are accurately described by theoretical models and empirical generalizations. For cross-linked amorphous networks, the equation for equilibrium elasticity is broadly considered as of the successes of statistical mechanics. However, even at small deformations, partly crystalline and heterogeneous, reinforced materials continue to present insurmountable challenges for mechanical modeling at all length scales. The situation regarding the ultimate properties of all materials (tensile strength, fatigue strength, impact strength, burst strength) is even more nebulous, although there is a vast store of empirical knowledge.

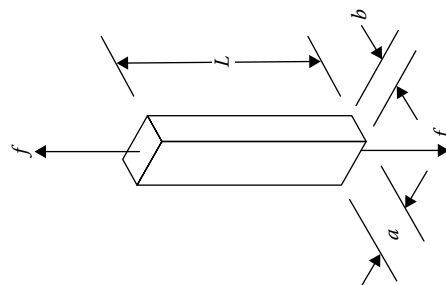
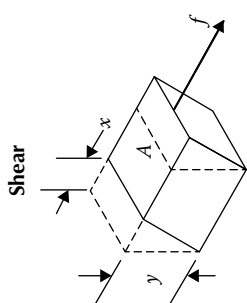
9.2 POLYMER ELASTICITY IN VARIOUS DEFORMATIONS

In Chapter 7, we studied polymer melts and solutions as viscous liquids, and in Chapter 8, we introduced the idea of viscoelasticity to describe both the viscous and elastic properties of polymeric liquids. For the case of cross-linked polymers, amorphous glassy materials, and materials that exhibit flow under stress, it is easier and profitable to describe their mechanical properties as elastic solids whose characteristic parameters are somewhat time dependent. Some familiar mechanical properties are summarized in Table 9.1.

Other quantities are also used. For example, *true* stress is sometimes used as force/(actual area) rather than the more conventional definition of force/(original area). In ordinary calculations for steel, wood, and other materials of construction, the materials are regarded as linearly elastic and the modulus is a **material property**. In the case of polymers subject to larger deformations, the modulus is a function of deformation, deformation rate, and time. It is therefore no longer a material property and various formulas from theory or empirical practice are required to describe polymer elasticity.

From the definition of **Poisson's ratio**, in Table 9.1, it is easily seen that when the volume of a material ($V = abL$) does not change on stretching, $\nu = 0.5$.

TABLE 9.1
Mechanical Deformation—Terminology and Formulas

<p>Tension</p> 	<p>Original dimensions L_0, a_0, b_0</p> <p>$\sigma = \text{tensile stress} = \frac{f}{ab} = \text{force/area}$</p> <p>$\epsilon = \text{elongation} = \frac{\Delta L}{L_0} = \alpha - 1$</p> <p>$E = \text{Young's modulus} = \frac{\sigma}{\epsilon}$</p> <p>$J = \text{compliance} = \frac{\epsilon}{\sigma}$</p> <p>$\nu = \text{Poisson's ratio} = \frac{-d(\ln a)}{d(\ln L)} = \frac{-d(\ln b)}{d(\ln L)}$</p>
<p>Shear</p> 	<p>$\tau = \text{shear stress} = \frac{f}{A}$</p> <p>$\gamma = \text{shear strain} = \frac{x}{y}$</p> <p>$G = \text{storage (shear) modulus} = \frac{\tau}{\gamma}$</p>

Bulk

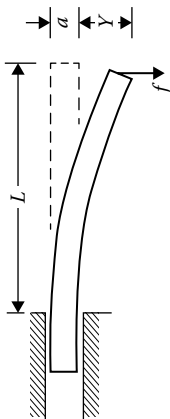
P = hydrostatic pressure, V = volume

$$B = \text{bulk modulus} = \frac{\Delta P}{\Delta V/V_0} = \text{compressibility}^{-1}$$

$$E = 2G(1 + \nu) = 3B(1 - 2\nu)$$

$\nu = 0.5$ for incompressible liquids, most rubbers

Cantilever beam, end-loaded (b = width):

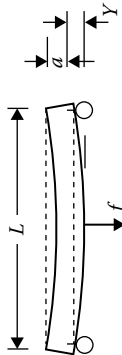


$$(9.1)$$

$$y = \frac{4fL^3}{ba^3 E}$$

$$(9.2)$$

Simple beam, center-loaded (b = width):



$$(9.3)$$

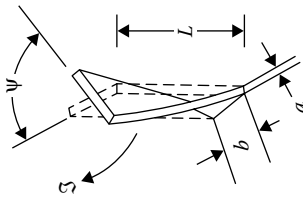
$$y = \frac{fL^3}{4ba^3 E}$$

(Continued)

Isotropic materials

TABLE 9.1
(Continued) Mechanical Deformation—Terminology and Formulas

Beam in torsion [torque \mathfrak{T} ; angle of twist, ψ' (rad)]:



$$\frac{\psi'}{\mathfrak{T}} = \frac{16L}{ba^3G\mu} \quad (9.4)$$

$$\mu = 5.333 - 3.36 \frac{a}{b}, \quad 0 < \frac{a}{b} < 0.5$$

$$V = abL \tag{9.5}$$

$$\frac{d(\ln V)}{d(\ln L)} = \frac{d(\ln a)}{d(\ln L)} + \frac{d(\ln b)}{d(\ln L)} + 1 \tag{9.6}$$

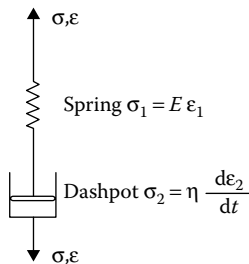
If the changes in a and b with L are proportionately the same and V does not change with L ,

$$2 \frac{d(\ln a)}{d(\ln L)} + 1 = 0 \quad \nu = 0.5 \tag{9.7}$$

Hooke’s law, the direct proportionality between stress and strain in tension or shear, is often assumed such that the constitutive equations for a purely elastic solid are $\sigma = \bar{\eta}\dot{\epsilon}$ for unidirectional extension and $\tau = \eta\dot{\gamma}$ in simple shear flow. The latter expression is recognized from Chapter 7 as the constitutive relationship for a Newtonian fluid and, in analogy to Hooke’s law for elastic solids, is sometimes termed **Newton’s law of viscosity**. For cross-linked, amorphous polymers above T_g , a nonlinear relationship can be derived theoretically. For such materials $\nu = 0.5$. When ν is not 0.5, it is an indication that voids are forming in the sample or that crystallization is taking place. In either case, neither the theoretical equation nor Hooke’s law generally applies. Before turning to one of the simplest mathematical models of viscoelasticity, it is important to recall that the constitutive equations of a purely viscous fluid are $\sigma = \bar{\eta}\dot{\epsilon}$ for elongational flow and $\tau = \eta\dot{\gamma}$ for shear flow.

9.3 VISCOELASTICITY—MAXWELL MODEL

A simple way to illustrate the viscoelastic properties of materials subjected to small deformations is to evaluate the stress that results from combining a linear spring that obeys Hooke’s law and a simple fluid that obeys Newton’s law of viscosity. An example of such combination is the mathematical representation of the **Maxwell element**. Even though this model is inadequate for quantitative correlation of polymer properties, it illustrates the qualitative nature of real behavior. Furthermore, it can be generalized by the concept of a distribution of relaxation times so that it becomes adequate for quantitative evaluation. Maxwell’s element is a simple one combining one viscous parameter and one elastic parameter. Mechanically, it can be visualized as a Hookean spring and a Newtonian dashpot in series:



In the above diagram, σ is the stress, ϵ is the elongation, $d\epsilon/dt$ is the rate of elongation with time, E is the **Hooke’s law constant** or **Young’s modulus**, and η is the apparent viscosity.

From the diagram, it is apparent that

$$\sigma = \sigma_1 = \sigma_2 \quad \varepsilon = \varepsilon_1 + \varepsilon_2$$

and

$$\frac{d\varepsilon}{dt} = \frac{d\varepsilon_1}{dt} + \frac{d\varepsilon_2}{dt} = \frac{1}{E} \frac{d\sigma}{dt} + \frac{\sigma}{\eta} \tag{9.8}$$

The behavior of this simple differential equation for a material's viscoelastic response in four experiments frequently used to characterize the behavior of polymers subjected to the mechanical deformations in these experiments is considered now.

9.3.1 CREEP

In a Creep experiment a fixed stress σ_0 is applied to the sample at time $t = 0$ (Figure 9.1a). This will cause a time-dependent elongation $\varepsilon(t)$, which we want to determine. With stress constant in the spring, ε_1 is a constant and $d\varepsilon_1/dt = 0$.

$$\frac{d\varepsilon}{dt} = \frac{d\varepsilon_1}{dt} + \frac{d\varepsilon_2}{dt} = \frac{\sigma_0}{\eta} \tag{9.9}$$

$$\int_{\varepsilon_0}^{\varepsilon(t)} d\varepsilon = \frac{\sigma_0}{\eta} \int_0^t dt \tag{9.10}$$

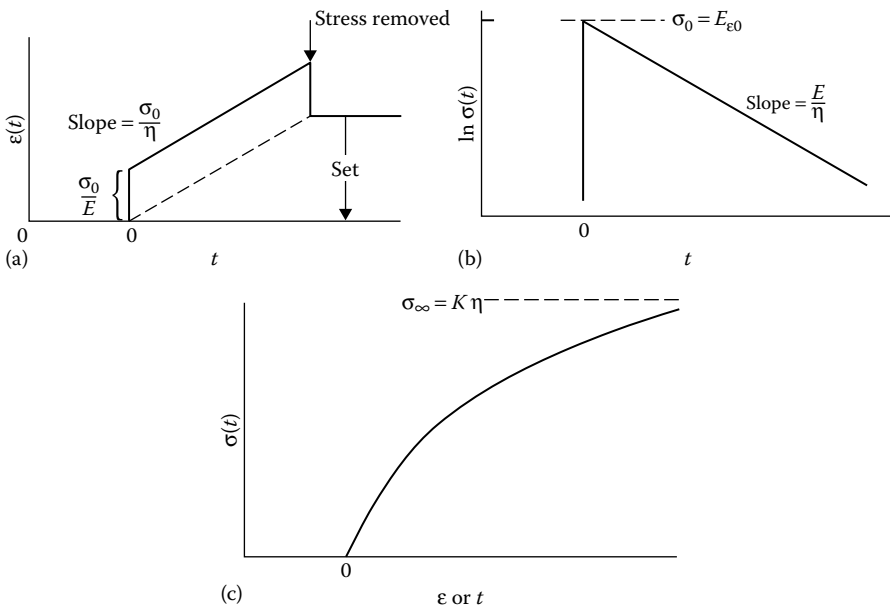


FIGURE 9.1 The Maxwell model in creep (a), stress relaxation (b), and constant rate of extension (c).

$$\varepsilon(t) = \varepsilon_0 + \frac{\sigma_0 t}{\eta} = \sigma_0 \left(E^{-1} + \frac{t}{\eta} \right) \tag{9.11}$$

Often, it is useful to express the results as a time-dependent **compliance** $J(t)$, where

$$J(t) = \frac{\varepsilon(t)}{\sigma_0} = E^{-1} + \frac{t}{\eta} \tag{9.12}$$

The **linear viscoelastic region** is the region where $J(t)$ is independent of σ_0 or, more generally, where the dependence is expressible by an exact relationship like Equation 9.12. For polymers, this condition holds in general at small stresses. It can be seen from the diagram that when the stress is removed, only the deformation of the spring is recovered. The flow of the dashpot is retained as a permanent *set*. It is remarkable that these predicted behaviors are observed for many uncross-linked polymers.

Another popular method of presenting experimental creep data is to plot the elongation versus time on a log-log graph. A straight line on this kind of plot gives the Nutting equation [1]:

$$\log \varepsilon(t) = \log A + s \log t \tag{9.13}$$

where:

log A and s are the intercept and the slope of the plot, respectively

9.3.2 STRESS RELAXATION

In a stress relaxation measurement a fixed elongation ε_0 is applied at time $t = 0$ and held (Figure 9.1b). A time dependent stress $\sigma(t)$ develops in the material, which we will determine.

$$\frac{d\varepsilon}{dt} = \frac{d\varepsilon_1}{dt} + \frac{d\varepsilon_2}{dt} = 0 \tag{9.14}$$

$$E^{-1} \frac{d\sigma}{dt} + \frac{\sigma}{\eta} = 0 \tag{9.15}$$

$$\int_{\sigma_0}^{\sigma(t)} \frac{d\sigma}{\sigma} = -\frac{E}{\eta} \int_0^t dt \tag{9.16}$$

$$\ln \left[\frac{\sigma(t)}{\sigma_0} \right] = -\frac{Et}{\eta} \tag{9.17}$$

A time-dependent modulus $E(t)$ can be defined as

$$E(t) = \frac{\sigma(t)}{\varepsilon_0} = E \exp \left(-\frac{Et}{\eta} \right) \tag{9.18}$$

The term η/E , the **relaxation time**, is the reciprocal of the rate at which stress decays.

The linear viscoelastic region, of course, corresponds to $E(t)$ being independent of ε_0 .

9.3.3 CONSTANT RATE OF STRAIN

Many commercial testing machines operate under conditions in which the strain rate $d\varepsilon/dt$ is approximately constant (i.e., $\varepsilon = K_0 t$, Figure 9.1c). The stress in such a deformation is a function of time $\sigma(t)$, which we will now determine.

$$\frac{d\varepsilon_1}{dt} + \frac{d\varepsilon_2}{dt} = K_0 \quad (9.19)$$

$$E^{-1} \frac{d\sigma}{dt} + \frac{\sigma}{\eta} = K_0 \quad (9.20)$$

$$\int_0^{\sigma(t)} \frac{d\sigma}{K_0 \eta - \sigma} = \frac{E}{\eta} \int_0^t dt \quad (9.21)$$

$$\sigma(t) = K_0 \eta \left[1 - \exp\left(-\frac{Et}{\eta}\right) \right] = K_0 \eta \left[1 - \exp\left(-\frac{E\varepsilon}{K_0 \eta}\right) \right] \quad (9.22)$$

Example 9.1

When a 10.0-cm-long polymer sample is subjected to a constant tensile load of 15.0 kPa, it stretches to a total length of 12.5 cm in 1200 s. Upon removal of the load, the sample recovers only to 10.85 cm. Representing the polymer as a Maxwell element, estimate the time it would take for an identical (untested) sample to relax to 0.850 its original stress when a constant elongation of 85% is applied.

Solution: In creep, the set (permanent deformation) represents the deformation of the dashpot only, since the spring returns to its original length upon removal of the load.

$$\text{Set} = \frac{10.85 - 10.00}{10.00} = 0.085 \text{ (dimensionless)}$$

The recoverable strain is due to deformation of the spring:

$$\text{Spring deformation} = \frac{12.50 - 10.85}{10.0} = 0.165$$

At time = 0 (after loading),

$$\varepsilon(0) = 15.0 \text{ kPa} \times E^{-1} = 0.165, \text{ and } E = 90.9 \times 10^3 \text{ Pa}$$

After 1200 s,

$$\varepsilon(1200) = \frac{12.50 - 10.00}{10.00} = 0.250$$

$$15.0 \times 10^3 \left(E^{-1} + \frac{1200}{\eta} \right) = 0.250$$

$$\eta = 212 \times 10^6 \text{ Pa} \cdot \text{s}$$

$$\text{Relaxation time} = \frac{\eta}{E} = \lambda = 2.33 \times 10^3 \text{ s}$$

In stress relaxation,

$$\ln \left[\frac{\sigma(t)}{\sigma_0} \right] = \ln 0.85 = \frac{-t}{2.33 \times 10^3}$$

$$t = 379 \text{ s}$$

Example 9.2

If the sample of the preceding example is stretched at a constant rate of 0.60 cm/min, what will be the stress at (a) 1 min and (b) 100 min?

Solution:

$$K_0 = \frac{0.60}{10 \times 60} = 0.0010 \text{ s}^{-1}$$

$$(a) \quad \sigma(60 \text{ s}) = 0.0010 \times 212 \times 10^6 \left[1 - \exp \left(\frac{-60}{2.33 \times 10^3} \right) \right] = 5.39 \text{ kPa}$$

$$(b) \quad \sigma(6000 \text{ s}) = 0.0010 \times 212 \times 10^6 \left[1 - \exp \left(\frac{-6000}{2.33 \times 10^3} \right) \right] = 196 \text{ kPa}$$

9.3.4 HARMONIC MOTION

If a sinusoidal force acts on a Maxwell element, the resulting strain will be sinusoidal at the same frequency, but out of phase. The same holds true if the strain is the input and the stress is the output. For example, let the strain be a sinusoidal function of time with frequency ω (rad/s),

$$\varepsilon = \varepsilon_m \cos \omega t \quad (9.23)$$

The motion of the Maxwell element (with modulus E and relaxation time $\lambda = \eta/E$) is given by

$$\frac{d\varepsilon}{dt} = \frac{1}{E} \frac{d\sigma}{dt} + \frac{\sigma}{\lambda E} \quad (9.24)$$

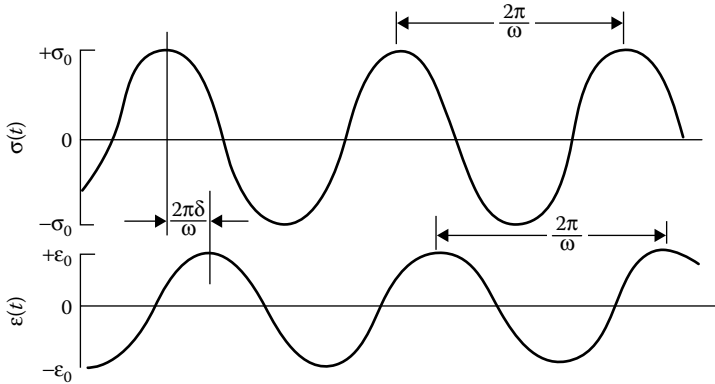


FIGURE 9.2 The Maxwell element in harmonic oscillation.

The resulting stress (see Appendix 9.A) is therefore proportional to E . Also, the magnitude will be affected by the product $\omega\lambda$ and will *lead* the strain by an angle $\delta = \cot^{-1}\omega\lambda$:

$$\sigma = \varepsilon_m E \frac{\omega\lambda}{(1 + \omega^2\lambda^2)^{1/2}} \cos(\omega t + \delta) \quad (9.25)$$

The situation is shown in Figure 9.2. A more common notation for sinusoidal tests is the complex dynamic modulus E^* , which is made up of a dynamic modulus E' and a loss modulus E'' :

$$E^* = E' + iE'' = \frac{\sigma^*}{\varepsilon^*} \quad (9.26)$$

Let the strain be a complex oscillating function of time with maximum amplitude ε_m , and frequency ω :

$$\varepsilon^* = \varepsilon_m \exp(i\omega t) \quad (9.27)$$

The real strain is the real part of the complex strain ε^* . The resulting ratio of stress to strain can be written (Appendix 9.A) as

$$\frac{\sigma^*}{\varepsilon^*} = \frac{E\omega^2\lambda^2}{(1 + \omega^2\lambda^2)} + \frac{iE\omega\lambda}{(1 + \omega^2\lambda^2)} \quad (9.28)$$

or

$$\sigma^* = \sigma_m \exp(i\omega t + \delta)$$

that is, σ^* leads ε^* by a loss angle δ . Once again, the actual stress is the real part of the complex stress σ^* . Identification with Equation 9.26 leads to

$$E' = \frac{E\omega^2\lambda^2}{(1 + \omega^2\lambda^2)} \quad E'' = \frac{E\omega\lambda}{(1 + \omega^2\lambda^2)} \quad (9.29)$$

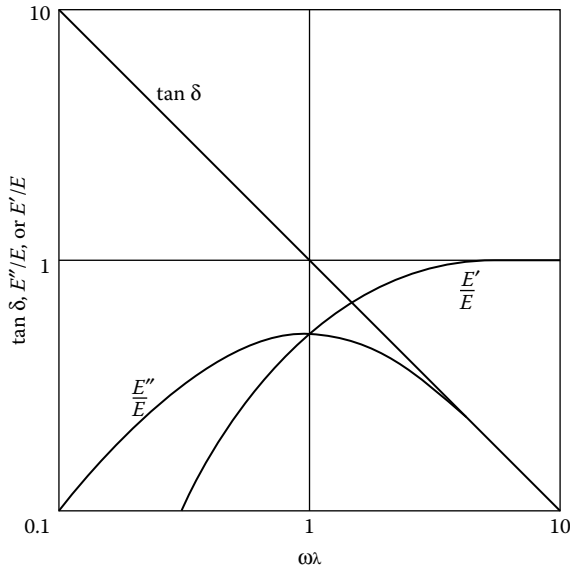


FIGURE 9.3 The quantities E' , E'' , and $\tan \delta$ as functions of E and λ for the Maxwell element.

$$\tan \delta = \frac{1}{\omega\lambda} = \frac{E''}{E'} \tag{9.30}$$

Another term sometimes used is the **dynamic tensile viscosity** η'_T :

$$\eta'_T = \frac{E''}{\omega} \tag{9.31}$$

The variations of E' , E'' , and $\tan \delta$ with λ are shown in Figure 9.3. E'' also is a measure of energy lost per cycle per unit volume (u_e), since

$$u_e = \pi E'' \epsilon_{\max}^2 \tag{9.32}$$

where:

ϵ_{\max} is the maximum amplitude of strain

The dissipation of energy in a cyclic process is sometimes known as **hysteresis**.

It is noteworthy that in an oscillatory experiment we can detect a peak in loss angle or loss modulus at a transition point such as T_g or T_m (where $\omega = 1/\lambda$), whereas creep, stress relaxation, and constant rate of strain give only changes in level of modulus.

9.4 DYNAMIC MEASUREMENTS

A number of commercial instruments are made that apply a harmonic stress or strain to a sample and measure the response [2,3]. In a **dynamic mechanical (thermal) analyzer**, often abbreviated as **DMA** or **DMTA**, modulus and loss can be measured as a function of controlled frequency, amplitude, and temperature. Commercial machines may include provisions for testing materials in tension, bending, or

compression [4–6]. Such devices have the advantage that the cycles are repeated many times and the sample can come to a steady state. Analysis of in-phase and out-of-phase responses follows along the lines of the Maxwell model discussed in Section 9.2. Variations in geometry and frequency can permit the examination of many materials. A disadvantage of the technique is that the energy dissipated within the sample may cause the temperature to increase. One way to minimize the effect is to store only a small amount of energy in the sample initially and then to measure the rate of dissipation without any additional inputs of energy. This is done in stress relaxation. A dynamic mechanical analog is the pendulum. In the common pendulum, a mass on the end of a string is given an initial input of energy (by raising it above its resting place). Potential energy is converted to kinetic energy as the mass returns to its rest position and again to potential energy as it rises. The frequency of oscillation of the mass is independent of the amplitude.

A **torsion pendulum** is a particular useful device for examining the modulus and internal friction of polymers. When the sample geometry is in the form of a cone-and-plate or concentric cylinders, the pendulum can be used for very weak gels, which are hard to characterize in conventional testing machines. Commercial models are available which give a complete record of amplitude versus time. However, even manual estimation of the frequency of oscillation and the number of cycles to decrease the amplitude by some factor can be quite useful.

In any torsion pendulum, the sample is the energy-storing and energy-dissipating element (*S* in Figure 9.4), and the external masses (*m*) can be used to regulate the frequency of oscillation ω . The stiffness of the sample (torque per unit twist \mathfrak{T}/ψ') depends on the shear modulus *G* and a geometric factor *K''*. Formulas for *K''* are tabulated (Table 9.2) for various sample geometries. The overall equation is

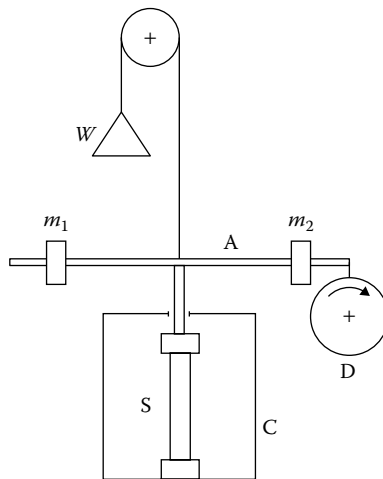


FIGURE 9.4 Torsion pendulum. Sample *S* in conditioning chamber *C* acts as the restoring element. The moment arm *A* with masses m_1 and m_2 is counterbalanced by weight *W*. Amplitude of oscillation can be recorded on drum *D* using thermal or light-sensitive papers or stored and plotted on a computer.

TABLE 9.2
Geometric Factor K'' for Torque Per Unit Twist

1. Sample geometry	Geometric factor, K''
a. Beam in torsion	See Table 9.1
b. Thin-walled tube	
D = average diameter	$\left(\frac{t\pi D^3}{4L} \right) \quad (9.37)$
t = wall thickness	
L = length	
2. Sample between concentric cylinders	$\left(\frac{4\pi L}{R_1^2 - R_2^2} \right) \quad (9.38)$
R_1, R_2 = radii of inner and outer cylinders, respectively	
L = length of sample	
3. Sample between a cone and a plate	$\left(\frac{2\pi R^3}{3\psi} \right) \quad (9.39)$
R = radius of cone	
ψ = angle between cone and plate	

$$\frac{\mathfrak{J}}{\psi'} = GK'' = \omega^2 I \left[1 + \left(\frac{\Delta}{2\pi} \right)^2 \right] \quad (9.33)$$

where:

I is the moment of inertia

The last term contains the **logarithmic decrement** Δ , which is the logarithm of the ratio of amplitudes A for successive cycles n

$$\Delta = \ln \left(\frac{A_n}{A_{n+1}} \right) \quad (9.34)$$

It represents the fraction of stored energy lost per cycle. The moment of inertia of the moving part of the system usually is due mainly to external masses and can be calculated from

$$I_r = \frac{m'L^2}{12} \quad (9.35)$$

for a transverse rod of total mass m' and length L rotating about its center, and

$$I_m = mr^2 \quad (9.36)$$

for a mass m at a distance r from the center of rotation.

Example 9.3

The restoring element for a torsion pendulum is a piece of plasticized vinyl laboratory tubing, and the formula for a thin-walled tube can be used (Table 9.2). The apparatus outlined in Figure 9.4 is used with $I = 7.4 \times 10^3 \text{ g}\cdot\text{cm}^2$, $L = 10 \text{ cm}$, $t = 0.15 \text{ cm}$, and $D = 0.85 \text{ cm}$. Using the period of 1.67 s and $\Delta = 0.23$ (Figure 9.5), calculate G and the modulus G'' , which is the product of G and Δ . It should be

noted that with the units employed above, G will have the units of $\text{g/cm}\cdot\text{s}^2$, which is equivalent to dyne/cm^2 .

Solution:

$$K'' \text{ (Equation 9.37)} = \frac{0.15 \times \pi \times 0.85^3}{4 \times 10} = 7.2 \times 10^{-3} \text{ cm}^3$$

$$\omega = \frac{2\pi}{\text{period}} = \frac{2\pi}{1.67} = 3.76 \text{ rad/s}$$

Using Equation 9.33,

$$G(7.2 \times 10^{-3}) = (3.76)^2 (7.4 \times 10^3) \left(\frac{1+0.23}{2\pi} \right)$$

$$G = 14 \times 10^6 \text{ dyne/cm}^2 = 1.4 \text{ MPa}$$

$$G'' = 0.23 \times 1.4 \text{ MPa} = 0.32 \text{ MPa}$$

When oscillations are slow, as in this example, manual measurement of successive amplitudes is as simple as making marks with a pencil at the extreme position of the moment arm for each cycle. Faster oscillations require some mechanical or electronic recording device, especially when the amplitudes are very small. Figure 9.16 (Section 9.7) illustrates the use of the torsion pendulum for multiple transitions.

In one modification, the restoring element is not simply the polymer sample, but some semirigid substrate in or on which the polymer is mounted. If a blotting paper is impregnated with polymer, the restoring element does not change in rigidity very much at transitions, but the loss peaks are quite easily detected [7]. In the **torsional braid** pendulum, a glass braid is impregnated with polymer. Because of the inert nature of the glass, the torsion pendulum will respond with changes in damping and stiffness, not only for transitions but also for chemical reactions such as oxidation, polymerization, and condensation [8,9].

9.5 POLYMERS—FIVE REGIONS OF VISCOELASTICITY

The time-dependent modulus for a typical amorphous polymer, poly(methyl methacrylate) (PMMA), measured by stress relaxation at various temperatures is shown in Figure 9.6. One way to define the five regions of viscoelasticity [10] is to take a cross section of the modulus–time curve at some fixed relaxation time—say 100, 1, or 0.001 h (Figure 9.7). In each of these, there are two reasonably well-defined plateaus. The first, at $E = 10^9$ or 10^{10} Pa, is the region of **glassy behavior**; the second is the region of **rubbery behavior**. Between the two plateaus, we have the main **glass transition**. Figure 9.7 illustrates the rate dependence of this important temperature. Finally, at high temperatures, **rubbery flow** marks the transition to the **liquid flow** region.

Horizontal shifting of stress–relaxation curves from Figure 9.6 to correspond with that at some reference temperature T_R gives the composite curve in Figure 9.8. This would be an academic exercise except that this **time–temperature superposition** is

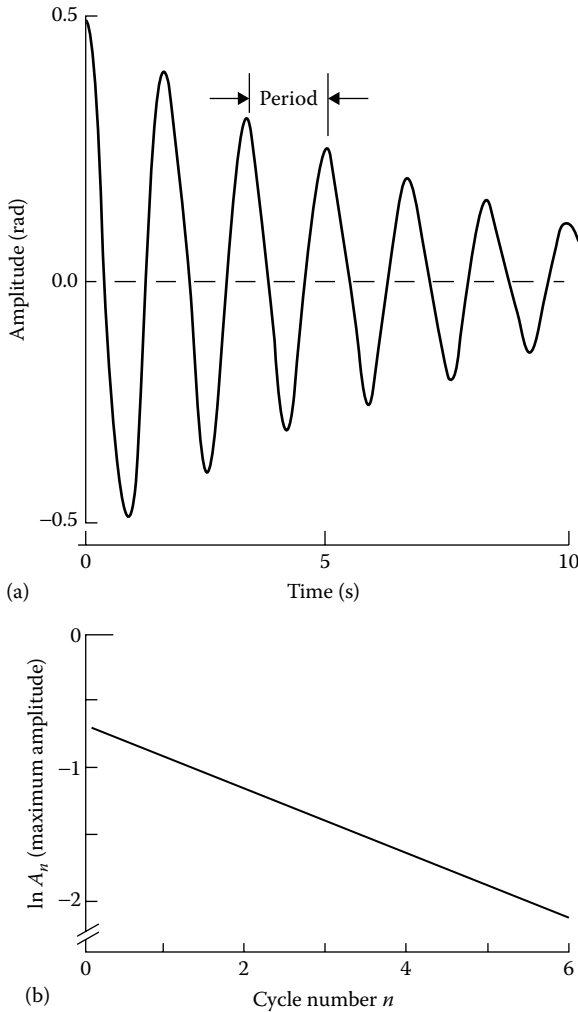


FIGURE 9.5 Typical analysis of torsion pendulum. (a) Oscillating trace made by the tip of moment arm gives a period of 1.67 s corresponding to a frequency of 0.600 Hz or 1.20π rad/s. (b) Plot according to Equation 9.34 gives a logarithmic decrement of 0.23.

real and has been confirmed by experiments covering the extremes of timescales at the same temperature. The horizontal shifts $[\log t(T) - \log t(T_g)]$ along the time axis in the vicinity of T_g are correlated by the Williams–Landel–Ferry (WLF) equation (Equation 7.62).

$$\log a_T = \log \frac{t(T)}{t(T_g)} = \frac{-17.44(T - T_g)}{51.6 + (T - T_g)} \quad (9.40)$$

Obviously, the curves could be shifted to any temperature other than T_g also by the same equation ($T_R = 115^\circ\text{C}$, while $T_g = 105^\circ\text{C}$ in Figure 9.8).

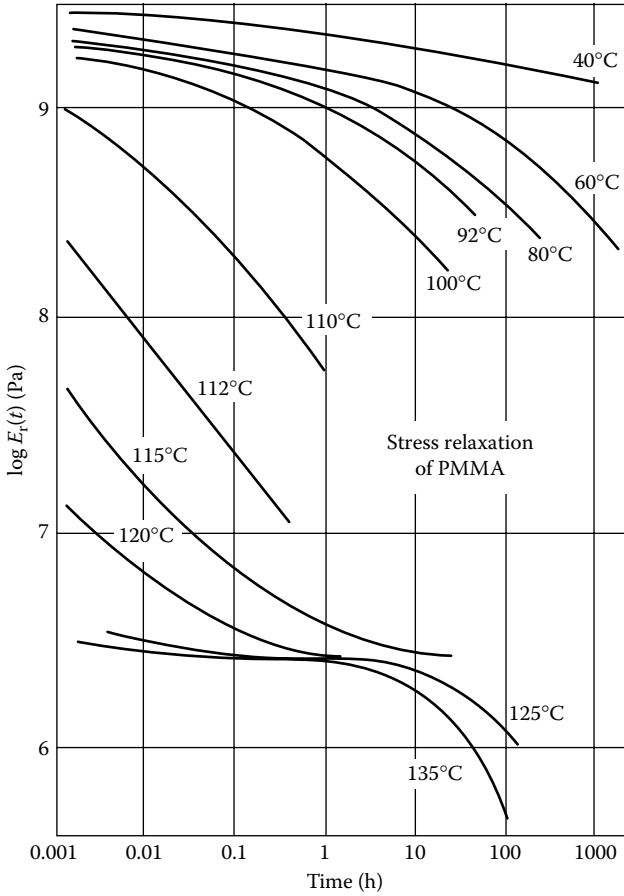


FIGURE 9.6 Log $E_r(t)$ versus log t for unfractionated PMMA of $M_v = 3.6 \times 10^6$. (Data from McLoughlin, J. R., and A. V. Tobolsky, *J. Colloid Sci.*, 7, 555, 1952.)

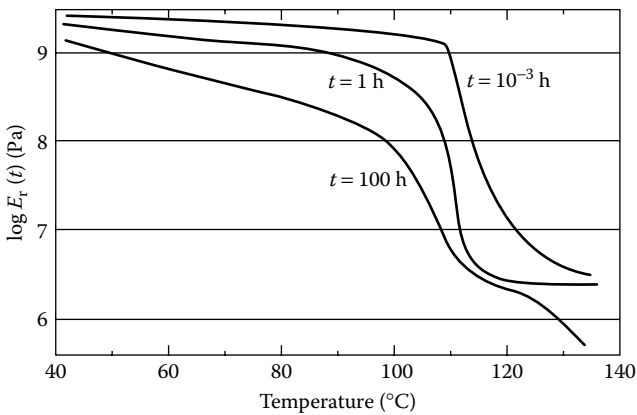


FIGURE 9.7 Modulus-temperature master curve based on cross sections of Figure 9.6.

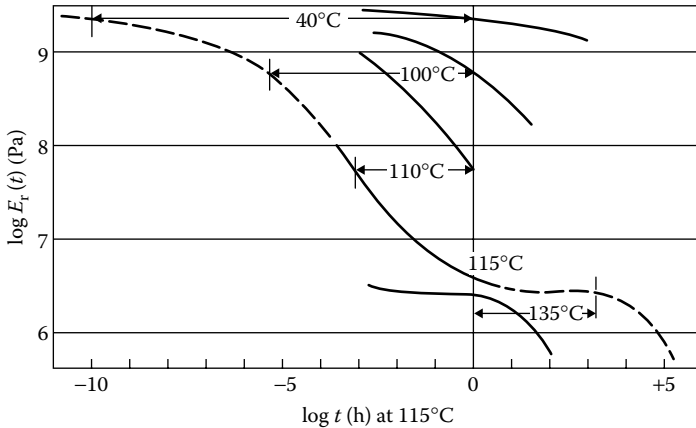


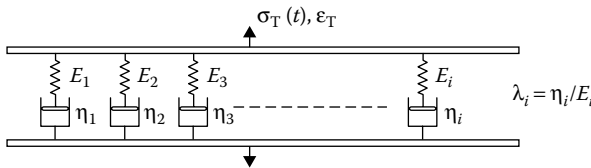
FIGURE 9.8 Modulus–time master curve based on time–temperature superposition of data in Figure 9.6. Times are referred to the temperature of 115°C.

The significance of this generalization cannot be overstated for materials such as polymers, which manifest time-dependent behavior. Again and again, we find in the literature the methods of superposing time and temperature for mechanical and other properties in amorphous and partially amorphous materials. Remarkably, whatever modifications are introduced usually reduce the behavior back in the direction of Equation 9.40.

9.6 GENERALIZED MAXWELL MODEL

In Figure 9.9, we compare stress–relaxation curves for a single Maxwell element with the same glassy modulus as the *master curve* but with various values of η [12]. Obviously, this simple model does not capture the behavior of the real system.

But suppose we used a model made up of multiple Maxwell elements in parallel held at fixed elongation ϵ_T , which is the same for all elements:



The total time-dependent force $\sigma_T(t)$ is the sum of the forces acting on the individual elements σ_i :

$$\sigma(t) = \sum \sigma_i = \sum \epsilon_T E_i \exp\left(-\frac{t}{\lambda_i}\right) \tag{9.41}$$

The overall time-dependent modulus $E_T(t)$ is also definable:

$$E_T(t) = \frac{\sigma_T(t)}{\epsilon_T} = \sum E_i \exp\left(-\frac{t}{\lambda_i}\right) \tag{9.42}$$

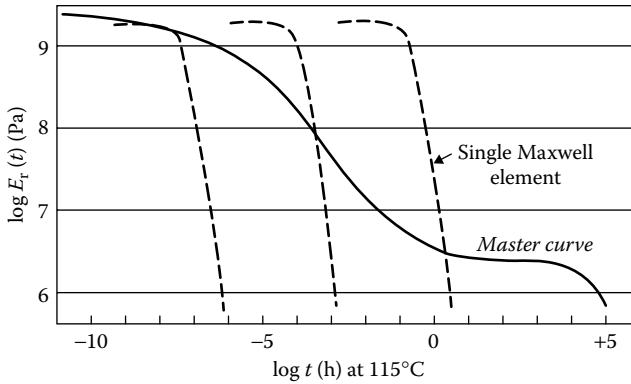


FIGURE 9.9 Master curve for PMMA compared with single Maxwell elements.

The synthesis of $E_T(t)$ from the known values of E_i and λ_i is simplified by the use of semilog paper.

For example, one can derive $E_T(t)$ for $0 < t < 200$ s using the data in the following table.

i	E_0 (dyne/cm ² × 10 ⁻⁹)	E_0 (MPa)	λ (s)
1	1.000	10.0	100
2	0.667	6.67	50
3	0.333	3.33	25

For each element, $E_i(t)$ is given by a straight line on the semilog paper with an intercept $(E_i)_0$ and a negative slope of $(\lambda_i)^{-1}$ (each divided by 2.303, since we are using paper based on logarithms to the base 10) (Figure 9.10). Adding the curves arithmetically gives $E_T(t)$ directly:

$$E_i(t) = (E_i)_0 \exp\left(-\frac{t}{\lambda}\right) \quad (9.43)$$

$$E_T(t) = \sum_{i=1}^3 E_i(t) \quad (9.44)$$

Note that $E_T(t)$ is not a straight line in Figure 9.10.

Example 9.4

A cross-linked polymer can be represented by three Maxwell elements in parallel with constants:

$$E_1 = E_2 = E_3 = 100 \text{ kPa}$$

$$\lambda_1 = 10 \text{ s}; \lambda_2 = 100 \text{ s}; \lambda_3 = \text{infinity}$$

1. What stress is required for a sudden elongation to 3 times the original length?
2. What will be the stress after being held at 3 times the original length for 100 s?
3. What will be the stress after being held at 3 times the original length for 100,000 s?

Solution:

1. At $t = 0$ and $\epsilon_T = 2.00$ (Equation 9.41),

$$\sigma(0) = 2.00 (3 \times 100 \text{ kPa}) = 600 \text{ kPa}$$
2. $\sigma(100 \text{ s}) = 200 \text{ kPa} [\exp(-10) + \exp(-1) + \exp(0)] = 274 \text{ kPa}$
3. $\sigma(100,000 \text{ s}) = 200 \text{ kPa} (0 + 0 + 1) = 200 \text{ kPa}$

For an infinite number of elements, the continuous analog of equation 9.44 is

$$E_T(t) = \int_0^\infty E(\lambda) \exp\left(-\frac{t}{\lambda}\right) d\lambda \tag{9.45}$$

or

$$E_T(t) = \int_{-\infty}^\infty \bar{H}(\log \lambda) \exp\left(-\frac{t}{\lambda}\right) d(\log \lambda) \tag{9.46}$$

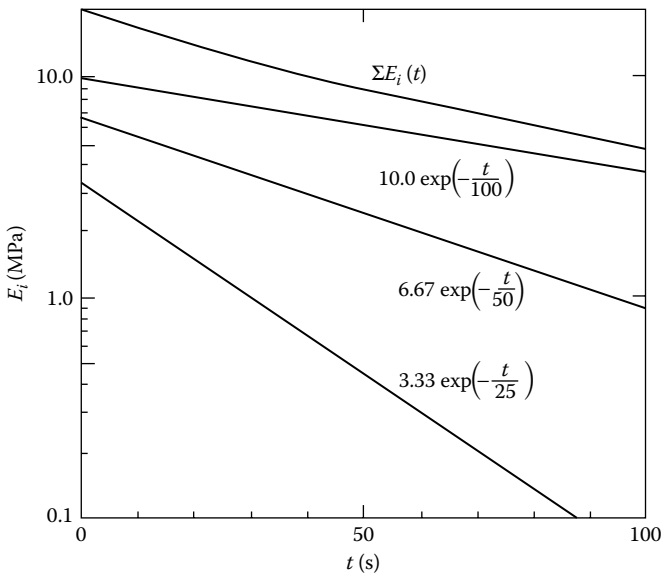


FIGURE 9.10 Time-dependent modulus for individual Maxwell elements and the sum of three elements in parallel $\Sigma E_i(t)$.

where:

$$\bar{H}(\log \lambda) = 2.303 \lambda E(\lambda)$$

Both $E(\lambda)$ and $\bar{H}(\log \lambda)$ are referred to as the **distribution of relaxation times**. A number of mathematical models have been proposed for the relationship between \bar{H} and λ . When these are inserted in Equation 9.46, the infinite array is reduced to something represented by a few parameters. Two elementary models are the box and the wedge:

Box:

$$\bar{H} = E_m \quad \text{for } \lambda_3 < \lambda < \lambda_m \quad \text{and} \quad \bar{H} = 0 \quad \text{for } \lambda < \lambda_3 \quad \text{or} \quad \lambda > \lambda_m \quad (9.47)$$

Wedge:

$$\bar{H} = \frac{M_0}{(\lambda)^{1/2}} \quad \text{for } \lambda_1 < \lambda < \lambda_2 \quad \text{and} \quad \bar{H} = 0 \quad \text{for } \lambda < \lambda_1 \quad \text{or} \quad \lambda > \lambda_2 \quad (9.48)$$

The functions that result when these distributions are inserted into Equation 9.46 are the incomplete gamma function (for the wedge) and the exponential integral function (for the box), each evaluated between limits of λ (Figure 9.11). A comparison of $E_T(t)$ for polyisobutylene with the fit based on a box and a wedge shows the degree of approximation of the wedge to the glass transition region and the box to the rubbery flow region (Figure 9.11).

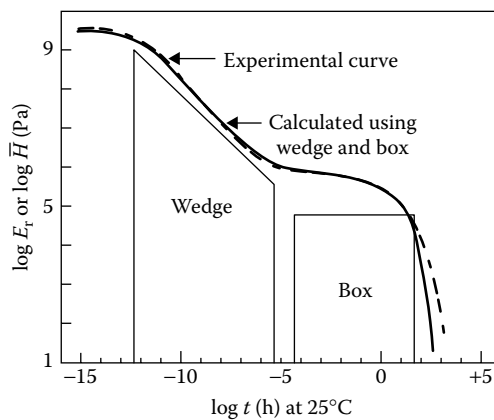


FIGURE 9.11 Master curve for polyisobutylene as determined by superposition of experimental stress relaxation data (dashed line) and from the insertion of the wedge and box models in Equation 9.46. (Data from Tobolsky, A. V., *Properties and Structure of Polymers*, chap. 3, Wiley, New York, 1960.)

9.7 COARSE-GRAINED MOLECULAR MODELS AND EFFECT OF MOLECULAR WEIGHT

The type of **coarse-grained molecular model** of a polymer molecule used by Flory and Huggins to develop the statistical thermodynamic properties of polymer solutions can also be used to develop dynamic (or mechanical) properties of polymers. The dynamic models consider the linear macromolecular chain as consisting of N subsegments whose mass is represented by equal size beads connected by massless Hookean springs as illustrated in Figure 9.12. This **bead-spring model** of the chain obeys Gaussian statistics and is placed in a continuum viscous fluid. The beads are subjected to identical elastic forces (from the springs) and friction forces (from the surrounding fluid). These types of models lead to a series of relaxation times similar to the relaxation times of a **generalized Maxwell model** but with the advantage of describing molecular effects such as the effect of the molecular weight of the polymer. Because it ignores the effect of interaction between polymer molecules (e.g., entanglements and hydrodynamic interactions), the Rouse model [13] should be applicable only to melts of molar mass lower than the critical molecular weight M_c and to dilute polymer solutions. The model predictions for the elastic and loss modulus in an oscillating shear flow are as follows [14]:

$$G'(\omega) = nkT \sum_{i=1}^N \frac{\omega^2 \lambda_i^2}{1 + \omega^2 \lambda_i^2} \quad \text{and} \quad G''(\omega) = \omega \eta_s + nkT \sum_{i=1}^N \frac{\omega \lambda_i}{1 + \omega^2 \lambda_i^2} \quad (9.49)$$

where:

n is the number density of polymer molecules

λ_i 's are the relaxation times of the various relaxation modes

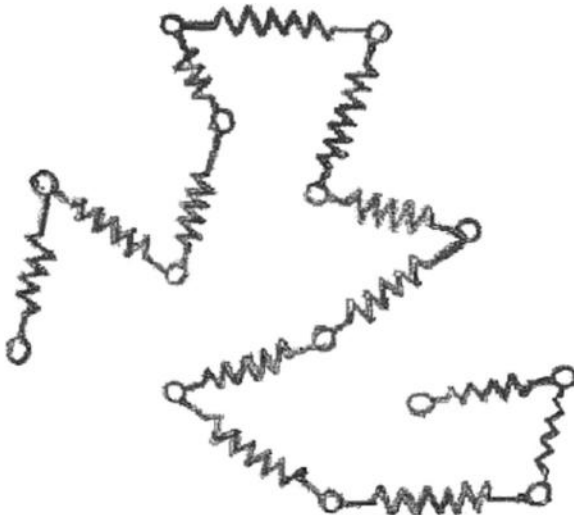


FIGURE 9.12 Schematic representation of the Rouse–Zimm bead-spring model.

η_s is the solvent viscosity (if present)
 k and T have their usual meaning

The characteristic relaxation times for each of the spectrum of relaxation modes are given by

$$\lambda_i = \frac{a^2 N^2 \zeta}{6\pi^2 i^2 kT} \quad (9.50)$$

where:

a is the equilibrium spring length
 ζ is the bead friction coefficient

Figure 9.13 shows the reasonable agreement that this model gives to experimental data on two polystyrene (PS) melt of low molecular weights. The moduli in this figure are normalized with $\rho RT/M_w$, where ρ is the polymer mass concentration and the frequency is normalized with the **terminal** (i.e., longest) **relaxation** time, λ_1 . Note that the numerator in Equation 9.50 can be expressed as the product of Na^2 that represents the mean-squared end-to-end distance of the molecule and $N\zeta$ that repre-

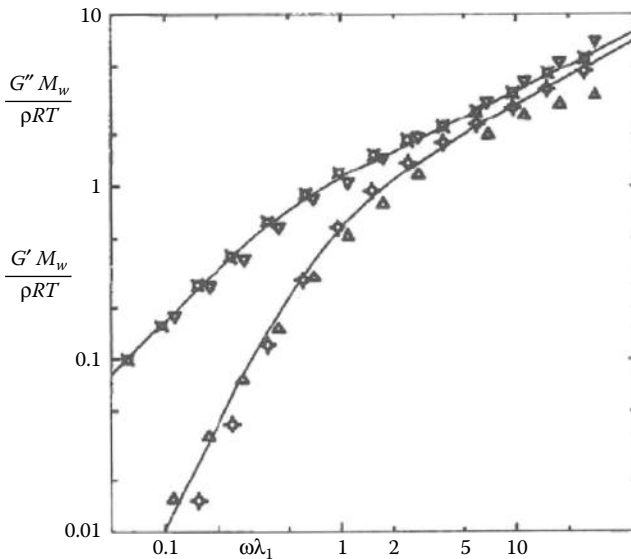


FIGURE 9.13 Plots of normalized shear elastic and loss moduli versus frequency normalized with the longest relaxation time, represented here by λ_1 . The data are for two PS samples of molecular weight of 2×10^4 and 3×10^4 . The lines are the best-fit Rouse model results with the upper and lower curves representing G'' and G' , respectively. (Data from Mills, N. J., and A. Niven, *J. Polym. Sci. Part A-2*, 9, 267, 1971. Reproduced with permission.)

sents the friction coefficient of the entire molecule, both of which can be determined experimentally.

One would have expected, at first, that the Rouse model would also predict the dynamic behavior of a very dilute noninteracting polymer molecules in solutions. The model ignores, however, the perturbing effect the motion of one bead has on its surrounding fluid, which in turn affects the motion of nearby beads. This effect, known as **hydrodynamic interaction (HI)**, was introduced a few years later by Zimm [16] through an adjustable HI parameter (see also Section 7.4.2). The Rouse–Zimm model was shown to be quite successful in fitting experimental oscillatory data of high-molecular-weight polymer in dilute solution [17]. The model fares poorly, however, compared to steady-state shear data as it does not predict any shear-thinning behavior. This discrepancy can be removed (at least qualitatively) by introducing a nonlinear spring force in the model. A useful model often utilized in computer simulation is the finitely extensible nonlinear elastic spring [18].

Note that G'' from Equations 9.49 and 9.50 goes like M such that the viscosity given by $\eta' = G''/\omega$ in the limit of $\omega \rightarrow 0$ (steady-state shear) for nonentangled polymer melt (absence of solvent) will be proportional to the molecular weight (M) as observed experimentally in Figures 7.18 and 9.13 for low molecular weights. Once M (or the number of chain atoms along the chain) goes beyond a critical value, the viscosity scales approximately as $M^{3.4-3.5}$. Models were developed in the late 1970s and 1980s to predict this dependence. The initial reptation hypothesis advanced by de Gennes and used in the development of the tube model of Doi and Edwards described in Section 7.5 predicts an exponent of 3 for the molecular weight dependence of the viscosity of entangled melts. As presented in this section, further refinements of the theory introducing additional modes of relaxations have generated exponents close to the experimental values.

Another result of the Doi–Edwards model is that the rubbery plateau shear modulus is related to the molecular weight between entanglements (M_e) by

$$G_N^0 = \frac{4\rho k N_{AV} T}{5M_e} = \frac{4}{5} NRT \quad (9.51)$$

where:

ρ is the mass density

k is the Boltzmann constant

N_{AV} is Avogadro's number

N is the molar density of *effective* elastic chains, that is, chains between entanglements

Equation 9.51 differs from the result of **ideal rubber elasticity** presented below by a factor of 4/5. The reasons for this factor are complexities in the model [19] that are beyond the scope of this text, but one would expect a factor of less than unity because of chain ends that do not contribute to the elasticity of the entangled polymer network. Given that the plateau modulus is independent of molecular weights, M , for $M > M_e$, the value of M_e in Equation 9.51 is a constant for a given melt but will vary from polymer to polymer depending on the structural properties of the polymer such

as the stiffness of the chain. The relation between M_c and M_e is also dependent on the chemical structure of the polymer and varies from a factor of 2 to a factor of 5. For PS, for example, $M_c \approx 3M_e$. It turns out that the value of M_e can be predicted fairly accurately from the molecular properties of the chain in the melt or in Flory theta condition. Using a parameter called **packing length** (p_c) defined below, Fetters showed empirically that M_e is given by [20]

$$M_e = B^{-2} p_c^3 (\rho N_{AV}) \quad (9.52)$$

where:

B is a dimensionless factor equal to about 0.051 at 140°C

p_c is related to the unperturbed chain dimension (Section 7.4) given by

$$\frac{1}{p_c} = \left(\frac{\overline{r_0^2}}{M} \right) \rho N_{AV} \quad (9.53)$$

where:

M is the molecular weight

It will be recalled that $(\overline{r_0^2}/M)$ is nearly constant for each homopolymer at a given temperature. Thus, by combining equations, the modulus can be estimated from a measurement of the unperturbed dimension:

$$G_N^0 = \frac{(4/5)B^2 kT}{(p_c)^3} \quad (9.54)$$

As an example, the values for PMMA used by Fetters et al. [20] are $(\overline{r_0^2}/M) = 0.425 \text{ \AA}^2 \cdot \text{mol/g}$ and $\rho = 1.13 \text{ g/cm}^3$ at 140°C.

The calculated values are as follows:

$$p_c = 3.46 \text{ \AA} \quad (\text{from Equation 9.53})$$

$$M_e = 10.5 \times 10^3 \text{ g/mol}$$

$$G_N^0 = 0.29 \text{ MPa} \quad (\text{from Equation 9.54})$$

This is very close to an experimentally measured value of $G_N^0 = 0.31 \text{ MPa}$. A few other examples illustrating the accuracy of the Fetters packing-length method are listed in Table 9.3.

Measured values of the plateau modulus range from 0.18 MPa for poly(dimethyl siloxane) (PDMS) to 2.50 MPa for polyethylene [24]. However, it can be seen that the level of the rubbery modulus in Figure 9.14 is not affected by molecular weight, since the packing length depends on the ratio of unperturbed end-to-end distance to molecular weight, a relatively constant number for any specified homopolymer. Note that it is the elongational modulus that is plotted in Figure 9.14. However, for

TABLE 9.3
Unperturbed Molecular Characteristics and Plateau Values for Selected
Polymers at 413 K

Polymer	$\overline{(r_0^2/M)}$ ($\text{\AA}^2 \text{ mol g}^{-1}$)	ρ (g cm^{-3})	ρ_c (\AA)	G (Measured/ Calculated) (MPa)	M_e (Measured/ Calculated)
PE	1.25	0.784	1.6942	2.60/2.50	828/861
PEO	0.805	1.064	1.9384	1.80/1.67	1624/1751
1,4-PBd	0.876	0.826	2.2946	1.25/1.01	1815/2254
a-PP	0.670	0.791	3.1328	0.47/0.40	4623/5494
1,4-PI	0.625	0.830	3.2006	0.42/0.37	5429/6147
PIB	0.570	0.849	3.4309	0.32/0.30	7288/7745
PMMA	0.425	1.13	3.4572	0.31/0.29	10013/10547
PS	0.434	0.969	3.9480	0.20/0.20	13309/13469
PDMS	0.457	0.895	4.0593	0.20/0.18	12293/13522

Source: Fetters, L. J. et al., *Macromolecules*, 27, 4639, 1994.

a-PP, atactic polypropylene; PBd, polybutadiene; PDMS, poly(dimethyl siloxane); PE, polyethylene; PEO, poly(ethylene oxide); PI, polyisoprene; PIB, polyisobutylene; PMMA, poly(methyl methacrylate); PS, polystyrene.

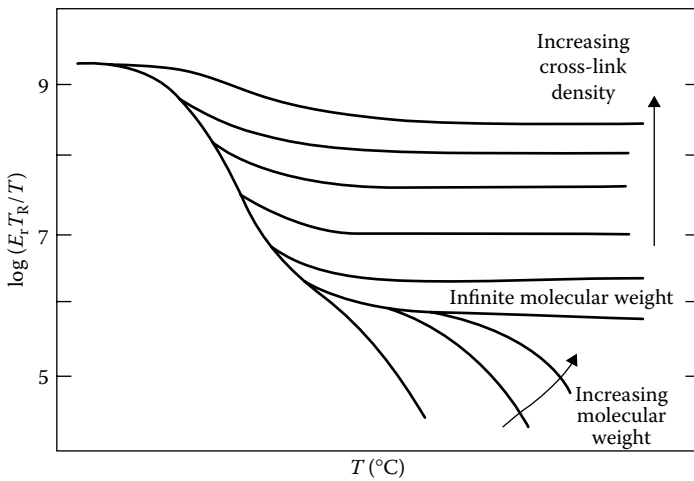


FIGURE 9.14 Qualitative effects of increasing molecular weight and cross-linking on the master curve.

most incompressible materials including most rubbery materials, Poisson’s ratio is 1/2 and $E = 3G$ (see Table 9.1). We expect E to increase linearly with absolute temperature and cross-link density in the case of cross-linked networks. The effect of T on E is corrected in the ordinate (T_R is any reference temperature). The effect of molecular weight for polymer melts on the curves is also shown (Figure 9.14). At a

low enough molecular weight (below M_c) there is no rubbery plateau and a polymer glass transitions directly to a melt. However, the number of entanglements along a chain increases with molecular weights above M_c requiring more time or higher temperature for the chains to diffuse (flow).

As long as the molecular weight is appreciably larger than that of a polymer segment, glassy behavior and T_g should be relatively insensitive to further increases in molecular weight. For our purposes here, this can be taken as 50–100 chain atoms, although there is no clear-cut definition of a segment for all situations. For entangled melts, Rouse relaxations occur for portions of the chains between entanglements (length scale of 50–100Å), whereas flow requires reptation of the contour length of the chain. As illustrated in Figure 9.14, very high cross-link densities in a network preserve a pseudo-glassy behavior to high temperatures. A thermoset such as a phenol formaldehyde resin remains glassy with no measurable mechanical transition in the absence of chemical change. Only vibrations and short-range rotations between atoms occur within the segment.

9.8 EFFECT OF CRYSTALLINITY

The main response of a partially crystalline material to an external stress is borne by the amorphous fraction. In materials of low crystallinity, say, less than 30% crystallinity, the crystallites function as temperature-dependent cross-links. We expect the glassy and rubbery plateaus to exist as earlier, but we expect the rubbery region to undergo a time-independent, fairly sharp transition at the melting temperature T_m . Of course, smaller crystallites and those formed at lower temperatures have lower T_m s than others. This blurs the transition.

With highly crystalline materials, the glass transition may become less pronounced. The behavior of nylon 6,6 is illustrative (Figure 9.15). The glass transition is quite

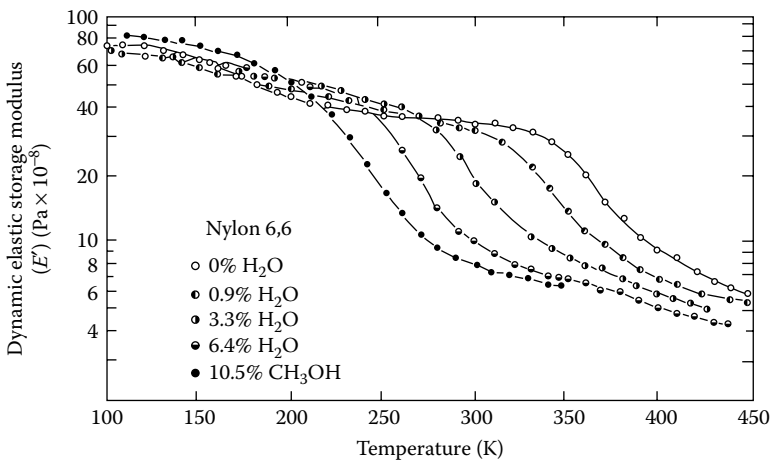


FIGURE 9.15 Dynamic modulus versus temperature for nylon 6,6 containing various amounts of water or methanol. (Data from Sauer, J. A., *SPE Trans.*, 2, 57, 1962.)

sensitive to moisture but involves a modulus change of only about 10-fold compared to 1000-fold for a completely amorphous material (Figure 9.8). However, both above and below T_g there is a continuous loss in stiffness due to decrease in crystalline content. When an oscillating stress is imposed on the material, the fraction of energy dissipated per cycle (logarithmic decrement) is a sensitive measure of transitions. The data for partially crystalline tetrafluoroethylene (Figure 9.16) show four transitions below the melting temperature, which is about 600 K. At 176 K, the transition is thought to be the hindered rotation of small segments of the polymer chains. The transition of 292 K marks changes in crystalline morphology from triclinic to disordered hexagonal and a change in the helical repeating unit of 13–15 chain atoms. At 303 K there is further disordering of the hexagonal lattice to an irregular repeating unit. At 400 K we have the main glass transition T_g .

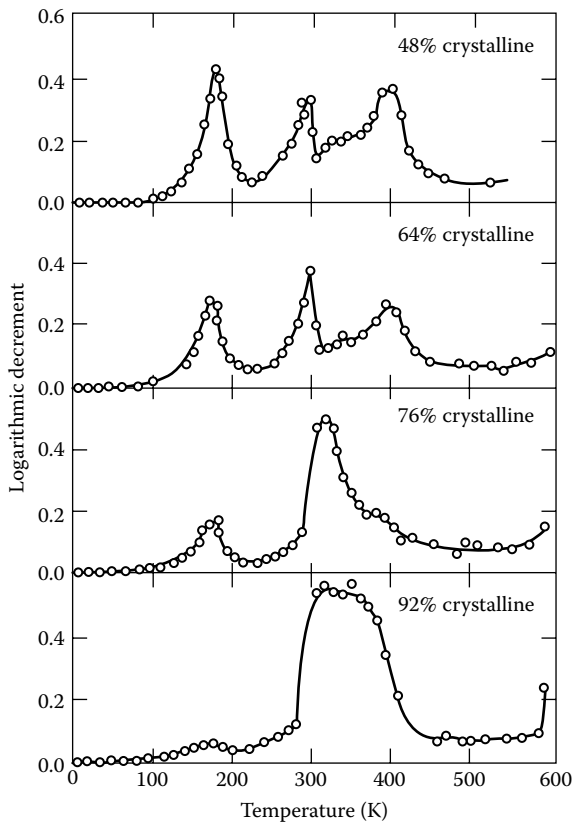


FIGURE 9.16 Variation with temperature of the logarithmic decrement for samples of poly(tetrafluoroethylene) of various degrees of crystallinity. (Data from Sinnott, K. M., *SPE Trans.*, 2, 65, 1962.)

9.9 RUBBER ELASTICITY

9.9.1 IDEAL RUBBER ELASTICITY

The first law of thermodynamics states that the change in internal energy of an isolated system ΔE is equal to the difference of the heat added to the system Q and the work done by the system W [23]:

$$\Delta E = Q - W \quad (9.55)$$

From the second law, we know that an increment of entropy dS is equal to an increment of heat dQ added reversibly at temperature T :

$$dS = \frac{dQ_{\text{rev}}}{T} \quad (9.56)$$

If we stretch a piece of rubber with force f a distance (dL) we also do work involving pressure and volume:

$$dW = PdV - fdL \quad (9.57)$$

Combining all these contributions, we have (differentiating Equation 9.55)

$$dE = TdS - PdV + fdL \quad (9.58)$$

With the introduction of several assumptions, the chief one being that V does not change greatly on stretching (a good assumption for rubber), the **thermodynamic equation of state** for rubber is

$$f = \left(\frac{\partial E}{\partial L} \right)_{T,V} + T \left(\frac{\partial f}{\partial T} \right)_{P,\alpha} \quad (9.59)$$

and

$$\left(\frac{\partial f}{\partial T} \right)_{P,\alpha} = - \left(\frac{\partial S}{\partial L} \right)_{T,V} \quad (9.60)$$

where:

$\alpha = L/L_u$ is the ratio of length to unstretched length at T

Changes in ΔE for a system are identified with changes in temperature and with energy stored by bond bending and stretching. Changes in ΔS are changes due to differences in conformation. In this respect, the concept of entropy as a measure of probability is useful. If a string is stretched tightly between two points, there is only one arrangement for the string in space to satisfy the condition. If the two points are

moved closer to each other, the rest of the string can accommodate the change by numerous conformations in space. In other words, if all conformations in space are equally likely, the stretched condition is the least probable (only one way of being achieved, lowest entropy), and the two ends together are the most probable (many ways of being achieved, highest entropy).

The *ideal* rubber should respond to an external stress only by uncoiling, that is, $\partial E/\partial L = 0$. Experiments in which f , L , and T are varied confirm that for many amorphous, cross-linked materials above T_g , $\partial E/\partial L$ is very small (Figure 9.17). Below T_g we have said that polymer segments cannot deform in the timescale in which T_g was measured, so $\partial S/\partial L = 0$. In a glass we expect external stresses to be countered by bond bending and stretching.

Now, for an ideal rubber, we have

$$f = -T \left(\frac{\partial S}{\partial L} \right)_{T,V} \tag{9.61}$$

According to Boltzmann, the entropy of a system in a given state with respect to a reference state entropy is related to the ratio of the probability of that state, Ω_2 , to that of the reference state, Ω_1 , by the equation:

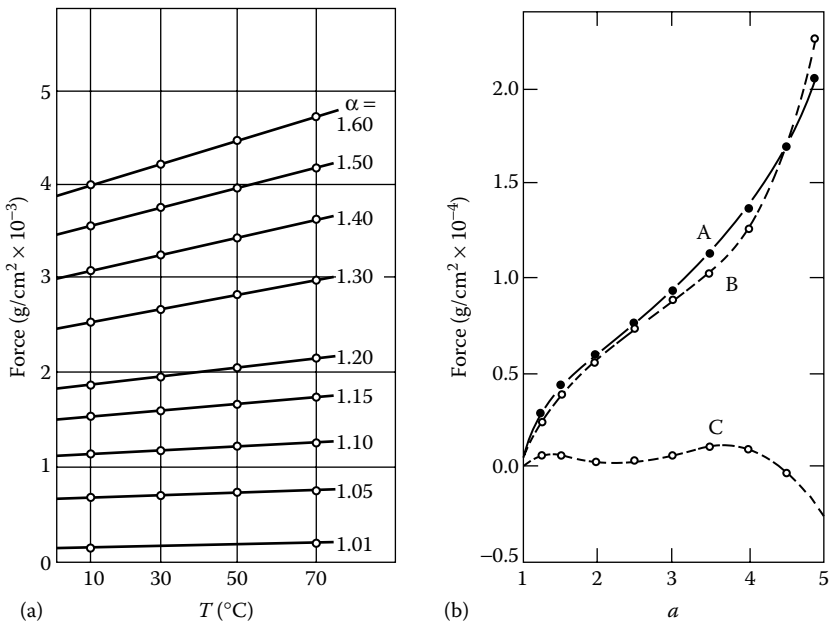


FIGURE 9.17 (a) Force versus temperature at constant values of α for sulfur-cross-linked natural rubber (b) Force of retraction (A), $T(\partial S/\partial L)_{T,V}$ (B), $(\partial E/\partial L)_{T,V}$ (C) obtained by using Equations 9.59 and 9.60. (Reproduced by permission from Anthony, R. L. et al., *J Phys. Chem.*, 46, 826, Copyright 1942 the Williams & Wilkins Company, Baltimore, MD.)

$$\Delta S = k \ln \left(\frac{\Omega_2}{\Omega_1} \right) \quad (9.62)$$

where:

k is the **Boltzmann constant**, the gas constant per molecule

What we need to know, then, is how does the probability of a polymer segment quantitatively decrease when it goes from a more probable state to a less probable state? The picture we have is a polymer segment that is part of a loose network. When we stretch the whole piece of rubber, we may assume that we move the ends of an elastic strand (chain between cross-links) to new positions in the same proportion as we do the whole piece (an **affine deformation**). Because these chains are part of a network, the chain ends cannot diffuse to their original positions governed by the most probable distribution of chain segments, that is, the rubber cannot *relax*. Only removal of the external stress will allow the chain ends to return to their original average position. The derivation of a distribution of chain lengths follows the same pattern as the random flight problem. Consider the probability $\Omega(x, y, z)$ that a polymer segment has one end fixed at the origin of a coordinate system (Figure 9.18) and the other end at (x, y, z) . A simple model for this probability is one in which Ω decays exponentially with the square of the distance from the origin.

$$\Omega(x, y, z) = \left(\frac{\beta^2}{\pi} \right)^{3/2} \exp \left[-\beta^2 (x^2 + y^2 + z^2) \right] \quad (9.63)$$

This is a **Gaussian distribution**. Here, $\beta = (3/2)^{1/2} n^{-1/2} a^{-1}$ and n is the number of bonds each of length a . Of course, this will apply only at small deformations. After all, the polymer can be elongated only to its length of n bonds, whereas this model predicts a small but real probability of chain lengths increasing without limit. The most probable value of r^2 can be obtained from Equation 9.63 to be $r_0^2 = na^2$, where

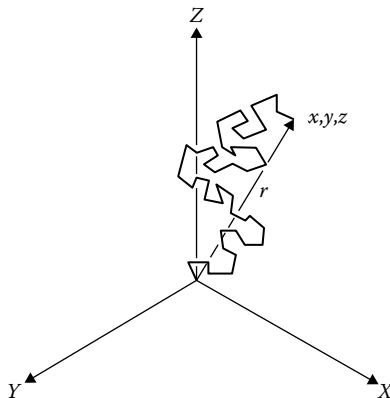


FIGURE 9.18 Random flight in three dimensions with a resultant distance traveled equal to r .

from geometry $r^2 = x^2 + y^2 + z^2$. The most probable value of r , as well as for x , y , and z , however, is 0. In Equation 7.21, we saw a generalization of the above result, where n is replaced by the degree of polymerization and a represented the size of the repeat unit.

If we change the overall dimensions of the sample so that now $x_2 = \alpha_x x$, $y_2 = \alpha_y y$, and $z_2 = \alpha_z z$, the ratio of the probability in perturbed state 2 to that in unperturbed state 1 can be expressed as

$$\ln\left(\frac{\Omega_2}{\Omega_1}\right) = -\beta^2 \left[(\alpha_x^2 - 1)x^2 + (\alpha_y^2 - 1)y^2 + (\alpha_z^2 - 1)z^2 \right] \quad (9.64)$$

But initially in our sample, chain ends were randomly oriented in all directions, so we can replace x^2 , y^2 , and z^2 each by their average value, $r_0^2/3$, giving for each chain (Equations 9.62 and 9.64):

$$\Delta S = S_2 - S_1 = k \ln\left(\frac{\Omega_2}{\Omega_1}\right) = -k \frac{3}{2na^2} \frac{r_0^2}{3} (\alpha_x^2 + \alpha_y^2 + \alpha_z^2 - 3) \quad (9.65)$$

or

$$\Delta S = -\frac{k}{2} (\alpha_x^2 + \alpha_y^2 + \alpha_z^2 - 3)$$

Let us say that we have ζ moles of effective chains in our system, that is, ζ moles of elastic strands that cannot move freely because their ends are tied in junctions (cross-links). Then for the entire system,

$$\Delta S = -\frac{R\zeta}{2} (\alpha_x^2 + \alpha_y^2 + \alpha_z^2 - 3) \quad (9.66)$$

We also have

$$f = -T \left(\frac{\partial \Delta S}{\partial L} \right)_{T,V} = -\left(\frac{T}{L_u} \right) \left(\frac{\partial \Delta S}{\partial \alpha_x} \right)_{T,V} \quad (9.67)$$

Consider now two cases:

1. When a rubber sample is stretched in the x -direction and its total volume remains constant,

$$\alpha_x \alpha_y \alpha_z = 1 \quad \text{and} \quad \alpha_y^2 = \alpha_z^2 = \frac{1}{\alpha_x} \quad (9.68)$$

Using Equations 9.66 and 9.67, one finds

$$f = \frac{RT\zeta}{L_u} \left[\alpha_x - \left(\frac{1}{\alpha_x} \right)^2 \right] \quad (9.69)$$

If a retractive force per unit area $\sigma = f/A_u$, where A_u is the original cross-sectional area, and an original volume $V_u = L_u A_u$, then

$$\sigma = RT \frac{\zeta}{V_u} \left[\alpha_x - \left(\frac{1}{\alpha_x} \right)^2 \right] = RTN \left(\alpha - \frac{1}{\alpha^2} \right) \quad (9.70)$$

where:

R is the gas constant per mole

N is the moles of elastic polymer strands per unit volume

The combination of parameters RTN in front of $(\alpha - \alpha^{-2})$ represents the storage (or elastic) modulus G of the rubber. One of the great successes of the theory of rubber elasticity is the prediction that the modulus *increases* linearly with temperature, meaning that at higher temperature, a greater force is needed to accomplish the same deformation. This result is clearly supported by experimental results (Figure 9.17a).

2. When a rubber sample is swollen isotropically in a solvent,

$$\alpha_x = \alpha_y = \alpha_z \quad (9.71)$$

The elastic entropy change due to swelling can be obtained from Equation 9.66 as

$$\Delta S_{el} = -\frac{3R\zeta}{2}(\alpha^2 - 1) \quad (9.72)$$

The contribution to the free energy of swelling due to the elasticity of the network is then

$$\Delta G_{el} = \frac{3RT\zeta}{2}(\alpha^2 - 1) \quad (9.73)$$

which was presented earlier as Equation 2.15 in the treatment of the swelling of networks.

Example 9.5

A cross-linked rubber with a density of 1.00 g/cm³ is composed of segments with a molecular weight of 10,000. What is the tensile stress at 100% elongation ($\alpha = 2.00$) at 25°C?

Solution:

$$N = (1.00 \text{ g/cm}^3)(\text{mol}/10,000 \text{ g}) = 1.00 \times 10^{-4} \text{ mol/cm}^3$$

$$R = 8.3145 \text{ J/mol} \cdot \text{K}$$

$$\sigma = 8.3145 \times 298 \times 1.00 \times 10^{-4} (2.00 - 0.25) = 0.434 \text{ J/cm}^3$$

Since $\text{Pa} = \text{J}/\text{m}^3$,

$$\sigma = 434 \text{ kPa (or 62.8 psi)}$$

Example 9.6

The area under a reversible stress–strain diagram represents the energy stored per unit volume. How much work is done on an ideal rubber band that is slowly and reversibly stretched to $\alpha = 2.00$? The initial slope of the stress–strain curve is known to be 2 MPa, and the volume of the rubber band is 4.0 cm^3 .

Solution:

$$\text{Work} = \int f dL \quad \sigma = \frac{f}{A_0} \quad \alpha = \frac{L}{L_0}$$

$$\frac{\text{Work}}{\text{Volume}} = \frac{\text{Work}}{A_0 L_0} = \int \sigma d\alpha = NRT \int (\alpha - \alpha^{-2}) d\alpha$$

Integration from $\alpha = 1$ gives $NRT/(\alpha^2/2 + \alpha^{-1} - 3/2)$. The initial slope (at $\alpha = 1$) = $(d\sigma/d\alpha) = 3NRT$ from differentiation of Equation 9.70 and substituting $\alpha = 1$. Then

$$3NRT = 2 \text{ MPa}$$

Thus, at $\alpha = 2$,

$$\frac{\text{Work}}{\text{Volume}} = \left(\frac{2}{3}\right) \text{MPa} \left(\frac{2^2}{2} + \frac{1}{2} - \frac{3}{2}\right) = 0.667 \text{ MJ}/\text{m}^3$$

$$\text{Volume} = 4.0 \times 10^{-6} \text{ m}^3$$

$$\text{Work} = 0.667 \times 4.0 = 2.67 \text{ J}$$

9.9.2 MODIFICATIONS OF THE IDEAL RUBBER MODEL

Besides the assumption of ideality inherent in Equation 9.61, several approximations were made in obtaining the force–extension relation of Equation 9.70. These assumptions are as follows:

1. All chains are elastic and end at cross-links.
2. Individual chains between cross-links (strands) obey Gaussian statistics.
3. The cross-links are fixed in space and deform affinely.
4. The chains are all independent and do not interact with one another (**phantom chain approximation**).

Several theoretical and empirical modifications of Equation 9.70 have been developed to improve the agreement between predictions and experimental results [24–26]. Some of these modifications will now be discussed:

1. Flory, who developed the theory of ideal rubber elasticity presented above, introduced early on a correction to account for the fact that in the random cross-linking of a melt of polymer chains with a number-average molecular weight M_n , there will be pendant inelastic strands at the ends of the original uncross-linked chains [23]. The number of moles of original chains is given by

$$\frac{\text{Mass of sample}}{M_n} = V_0 \frac{\rho}{M_n}$$

where:

V_0 is the volume of the sample

ρ is the density of the polymer

The molar density of dangling chain ends is then given by $2\rho/M_n$. The molar density of elastic strands N in the rubber elasticity formula in Equation 9.70 has then to be replaced by $N - 2\rho/M_n$ and the rubber elasticity expression becomes

$$\sigma = RT \left(N - \frac{2\rho}{M_n} \right) \left(\alpha - \frac{1}{\alpha^2} \right) \quad (9.74)$$

Although still occasionally used, the above correction to the elastic modulus due to chain ends is of no practical relevance because of the effect of entanglements on the modulus that is ignored by assumption 4. Because of the structural complexities of cross-linked polymers, their equilibrium modulus obtained at small deformations cannot yet be predicted theoretically and is a fitted parameter in comparisons between theories and experiments.

2. At large deformation, the assumption of Gaussian chain statistics represented by Equation 9.63 breaks down. It can be shown that these statistics are a consequence of a Hookean force $F_1(r)$ between the chain ends when chain ends are disturbed from their most probable positions. This force is expressed in terms of a linear relation between the force and the distance r between the ends:

$$F_1(r) = \frac{3kT}{(n-1)a^2} r \quad (9.75)$$

A more accurate representation of this force at large deformation is the inverse Langevin force law given by [25]

$$F_2(r) = \frac{kT}{a} \mathcal{L}^{-1} \left[\frac{r}{(n-1)a} \right] \quad (9.76)$$

where:

$\mathfrak{L}^{-1}[z]$ is the inverse Langevin function that can be expressed as the following series:

$$\mathfrak{L}^{-1}[z] = 3z + 9/5 z^3 + 297/175 z^5 + \dots \quad (9.77)$$

Use of this force in the case of a unidirectional strain yields the more general result:

$$\sigma = \frac{NRT}{3} n^{1/2} \left[\mathfrak{L}^{-1}\left(\frac{\alpha}{n^{1/2}}\right) - \alpha^{-3/2} \mathfrak{L}^{-1}\left(\frac{1}{\alpha^{1/2} n^{1/2}}\right) \right] \quad (9.78)$$

For small deformations, $\alpha/n^{1/2} \ll 1$, the above equation reduces to the ideal rubber elasticity formula of Equation 9.70 when one keeps only the lowest term in Equation 9.77. For higher deformations, Equation 9.78 gives much better agreement with experimental results as it has the additional parameter $n^{1/2}$ [25].

4. Rather than assuming that the cross-links are fixed in space in a network at rest, James and Guth [27] proposed an analogous theory to that of Flory, but one where the cross-links fluctuate in space around a mean position and that the mean positions deform affinely. These fluctuations reduce the force needed for a given deformation by the following relation:

$$\frac{\sigma \text{ (for fluctuating cross-links)}}{\sigma \text{ (for fixed cross-links)}} = 1 - \frac{2}{f} \quad (9.79)$$

where:

f is the functionality of the cross-links

For a functionality of four, the force and therefore the elastic modulus are then reduced by a factor of 2 compared to the fixed cross-links hypothesis. It is now accepted that the cross-links of an elastomer fluctuate in the sample volume and that the postulate of this theory is the more appropriate one.

4. The consequences of chain interactions upon deformation of a network are the most difficult to ascertain and are still the subject of research. In the original model where polymer chains are assumed not to interact and are therefore able to cross one another as though they were not present, the term **phantom model** network has been used. Molecular models and computer simulation models, the details of which are beyond the scope of this textbook, have been developed to ascertain the effects of these interactions. One of the earlier models is the **constrained fluctuation model** that imposes additional interactions between the chains by constraining the motion of the cross-links [28,29] and subsequently extends to constrain the motion of the segments along the elastic strand [30]. More recently, the **slip-link model** of Edwards and Vilgis [31] uses the tube model of polymer melts to predict that entanglements will increase the value of the modulus

of an elastomer over that predicted by a phantom model. Their prediction for the modulus takes the form:

$$G = G_{\text{ph}} + F(N_e, \beta) \quad (9.80)$$

where:

G_{ph} is the phantom model prediction

F is a function of the density of trapped entanglements (N_e) and an entanglement slip coefficient (β) between 0 and 1

Equation 9.80 is consistent with experimental results and empirical fits to these results represented by

$$G = G_{\text{ph}} + G_N^0 T_e \quad (9.81)$$

where:

G_N^0 represents the plateau modulus of the polymer melt (see Section 9.6)

T_e is an entanglement effectiveness factor less or equal to unity [32]

Because G_{ph} is proportional to NRT , a plot of G/T_e versus NRT/T_e for elastomers of a given homopolymer should be linear as shown in Figure 9.19. In this figure, G is represented as G_0 to indicate the equilibrium modulus

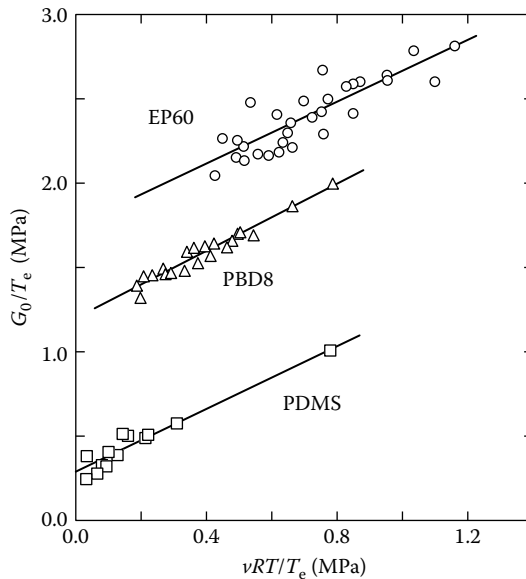


FIGURE 9.19 Plots of equilibrium modulus data for cross-linked ethylene-propylene (EP60), 1,4-polybutadiene (PBDB), and PDMS from various sources. The density of elastic chains N is represented by the symbol ν . (Reprinted with permission from Graessley, W. W., *Polymeric Liquids & Networks: Structure and Properties*, Garland Science, chap. 9, New York, 2004.)

and N is denoted as ν and estimated from a statistical theory [34]. The y -intercepts in these plots do indeed correspond to the plateau moduli of the respective homopolymer melt [33].

The most recent model is due to Rubinstein and Panyukov [35] and is known as the **nonaffine slip tube (NAST) model**. The stress–strain relation for uniaxial deformation in this model is given by the result:

$$\sigma^* = \frac{\sigma}{\alpha - \alpha^{-2}} = G_c + \frac{G_e}{0.74\alpha + 0.61\alpha^{-1/2} - 0.35} \tag{9.82}$$

where:

G_c and G_e represent the cross-links and the entanglements contribution to the modulus, respectively

Note that the equilibrium modulus, $G(\alpha \rightarrow 1)$, is given by the sum $G_c + G_e$. The advantage of this model is that it gives a reasonable fit to experimental data in both uniaxial extension and compression. Figure 9.20 shows the adequacy of the model for a PDMS network prepared in solution at $\nu_2 = 0.7$ and measured in the prepared swollen state. Similar agreement is obtained for networks synthesized under many different preparation conditions and having very different values of G_c and G_e [36]. Despite some deviations at high compression, the results of the model are quite satisfactory and allow the determination of how the sample preparation conditions affect the two contributions to the modulus. The deviations around $\alpha = 1$ are known to be due to large experimental errors.

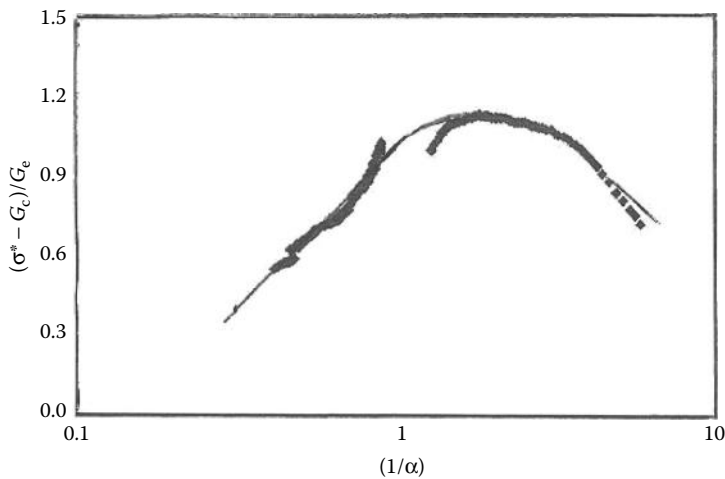


FIGURE 9.20 Equilibrium modulus data under uniaxial extension and compression of a PDMS network prepared in an inert solvent at $\nu_2 = 0.7$ and tested in the preparation state. The curve represents the result of the NAST model given by Equation 9.82. There are large experimental errors around $\alpha = 1$.

9.9.3 CONTINUUM MECHANICS AND EMPIRICAL MODELS OF RUBBER ELASTICITY

An earlier and different approach from the molecular models of rubber elasticity presented so far is based on a phenomenological model and continuum mechanics. It considers the elastic energy stored in the system. The work done on the system must be stored as elastic energy W and given by

$$W(\alpha_i) = \sum_i \int_{\alpha_i=1}^{\alpha_i} \sigma_i d\alpha_i \quad (9.83)$$

where:

$$i = 1, 2, \text{ and } 3$$

α_i 's are the principal deformation ratios

The argument that continuum mechanics makes is that for an isotropic system, the scalar variable W must depend on scalar variables only (unlike the α_i 's that depend on directions). The scalar variables are called strain invariants and denoted by I_i 's. The strain energy is then written in terms of three invariants as

$$W = W(I_1, I_2, I_3) \quad (9.84)$$

where:

$$I_1 = \alpha_1^2 + \alpha_2^2 + \alpha_3^2$$

$$I_2 = \alpha_1^2\alpha_2^2 + \alpha_2^2\alpha_3^2 + \alpha_3^2\alpha_1^2$$

$$I_3 = \alpha_1^2\alpha_2^2\alpha_3^2$$

However, $I_3 = (V/V_u)^2 = 1$ for incompressible materials and is not a variable. A general expression that one can then write for W in terms of I_1 and I_2 can take the form of a power series:

$$W = \sum_{i,j=0}^{\infty} C_{ij} (I_1 - 3)^i (I_2 - 3)^j \quad (9.85)$$

When all α_i 's are equal to unity, $W = 0$ as it should. For $i = 1$ and $j = 0$, we get

$$W = C_{10}(I_1 - 3) = C_1(\alpha_1^2 + \alpha_2^2 + \alpha_3^2 - 3) \quad (9.86)$$

where:

$$C_{10} = C_1$$

The force is the derivative of the energy, and for the simple case of uniaxial extension where only σ_1 is nonzero and $\alpha_2^2 = \alpha_3^2 = 1/\alpha_1$, from symmetry and volume conservation, one obtains

$$\sigma = \frac{\partial W}{\partial \alpha_1} = C_1 \frac{\partial(\alpha_1^2 + 2/\alpha_1 - 3)}{\partial \alpha_1} = 2C_1 \left(\alpha_1 - \frac{1}{\alpha_1^2} \right) \quad (9.87)$$

Note the analogy to Equation 9.70 where the phenomenological coefficient $2C_1$ can be equated to RTN , the elastic modulus of the ideal rubber elasticity model. If we also keep the next term in the series in Equation 9.85, for $i = 0$ and $j = 1$, we get

$$W = C_1(\alpha_1^2 + \alpha_2^2 + \alpha_3^2 - 3) + C_2(\alpha_1^2 \cdot \alpha_2^2 + \alpha_2^2 \cdot \alpha_3^2 + \alpha_3^2 \cdot \alpha_1^2 - 3) \quad (9.88)$$

where:

$$\begin{aligned} C_1 &= C_{10} \\ C_2 &= C_{20} \end{aligned}$$

For a unidirectional strain, assuming incompressibility, Equation 9.88 reduces to

$$W = C_1[\alpha_1^2 + (2/\alpha_1) - 3] + C_2[2\alpha_1 + (1/\alpha_1^2) - 3] \quad (9.89)$$

and

$$\sigma = \frac{\partial W}{\partial \alpha_1} = 2C_1[\alpha_1 - (1/\alpha_1^2)] + 2C_2\left(1 - \frac{1}{\alpha_1^3}\right) \quad (9.90)$$

This relation can be rewritten as

$$\sigma = 2 [C_1 + C_2/\alpha_1][\alpha_1 - (1/\alpha_1^2)] \quad (9.91)$$

This equation is known as the **Mooney–Rivlin equation**. It has been modified for the case of networks swollen with a solvent to read [37]

$$\sigma = 2 [C_1 + C_2/\alpha_1] \left(\alpha_1 - \frac{1}{\alpha_1^2} \right) \left(\frac{1}{v_2} \right)^{1/3} \quad (9.92)$$

where:

- σ is based on the original, *unswollen* cross section
- α is the ratio of the length to the swollen, unstretched length
- $v_2 = V_u/V_s$, the polymer volume fraction of the swollen network

An example of natural rubber swollen in benzene (Figure 9.21) gives a value for C_1 that is relatively constant and values of C_2 that decrease as v_2 decreases. The parameter $2C_1$ can then be considered to be the contribution to the modulus from cross-links that is not affected by the solvent, whereas $2C_2$ is the contribution to the modulus from entanglements (interactions) that is reduced by the presence of the solvent.

Comparison with values of G_c and G_e of the NAST model described earlier supports this hypothesis [36]. However, unlike the NAST model, the Mooney–Rivlin model fails to predict compression data as the linearity shown in Figure 9.21 continues for $\alpha^{-1} > 1$, whereas the experimental data show a maximum and a decrease in the function plotted in Figure 9.21. There have been many other constitutive relations for rubbers based on different representation of the strain energy function

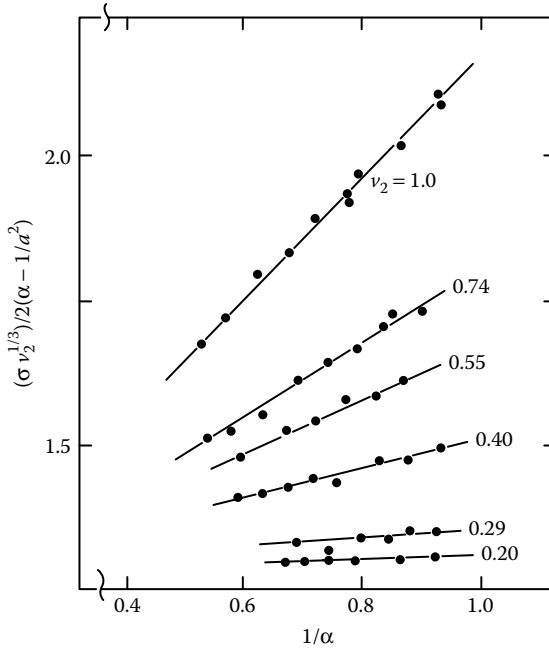


FIGURE 9.21 Stress–strain data for cross-linked natural rubber swollen to various degrees in benzene plotted according to Equation 9.92. (Data from Gumbrell, S. et al., *Trans. Faraday Soc.*, 49, 1945, 1953.)

in order to improve agreement with experimental results obtained under different mechanical deformations [38]. Many unswollen, homogeneous rubbers (gum or unfilled materials) are represented by the empirical equation of Martin, Roth, and Stiehler (MRS) [39]:

$$\ln \left(\frac{\sigma \alpha^2}{\alpha - 1} \right) = \ln \Lambda + \lambda \left(\frac{\alpha^2 - 1}{\alpha} \right) \quad (9.93)$$

where:

the constant λ normally has a value of 0.38 ± 0.02

At small elongations (as α approaches unity), the modulus (E) approaches its constant equilibrium value:

$$E(\alpha \rightarrow 1) = \frac{\sigma}{\alpha - 1} = \Lambda \quad (9.94)$$

The results for two samples of rubber (Figure 9.22) show that this equation applies in compression as well as tension. More extensive discussion of the validity of the MRS equation can be found in Reference 41.

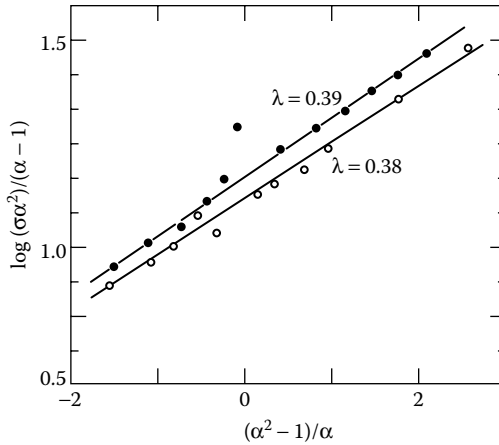


FIGURE 9.22 Plots for two samples of cross-linked natural rubber according to Equation 9.93. Stress is in kg/cm². (Data from Wood, L. A., *Rubber Chem. Technol.*, 32, 1, 1959.)

9.9.4 VISCOELASTICITY OF ELASTOMERS

Elastomer is a general term used for cross-linked polymeric materials such as rubber with elastic properties described above. However, elastomers are not purely elastic materials and they exhibit damping, that is, fractional energy loss per cycle in, say, an oscillatory experiment. The energy loss is due primarily to stress relaxation (viscous dissipation) of inelastic pendant chains and unentangled loops in the network. In the case of a prescribed stress sinusoidal deformation, the applied stress is expressed as

$$\sigma_{21}(t) = \sigma_0 \sin \omega t \tag{9.95}$$

The strain is then represented by two components: one in phase and the other 90° out of phase with the stress. The compliance J of a viscoelastic material subjected to a small shear stress deformation is expressed as

$$\gamma(t) = \sigma_0 [J'(\omega) \sin \omega t - J''(\omega) \cos \omega t] \tag{9.96}$$

where:

$J'(\omega)$ and $J''(\omega)$ represent the storage and loss compliances, respectively

In the linear viscoelasticity regime, the principle of time-temperature superposition that was developed for polymer melts seems to work equally well for unfilled elastomers. Data of $J'(\omega)$, $J''(\omega)$, and values of $\tan \delta = J''(\omega)/J'(\omega)$ versus ω for butyl rubber vulcanized with sulfur to various extents over a wide range of temperature (from -25°C to 50°C) were shown separately to collapse on master curves with a temperature shift factor a_T obeying the general form of the WLF equation. Figure 9.23 shows the results for $\tan \delta$ [42]. Each curve represents the master curve for data of a given

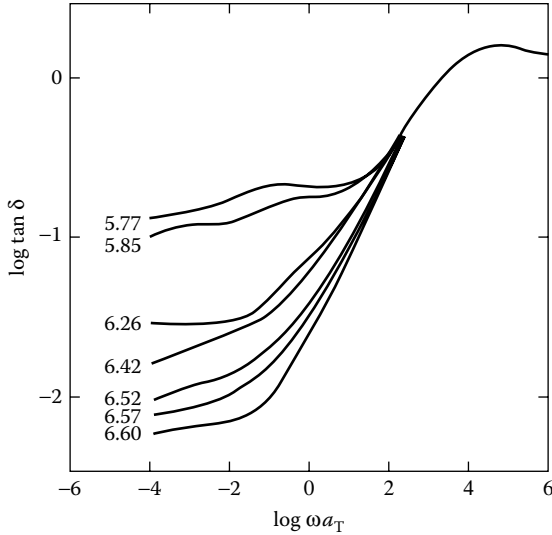


FIGURE 9.23 Loss tangent (J''/J') of butyl rubber samples cross-linked to different extent by sulfur. The data for each sample were collected over a range of temperatures and shifted to a reference temperature of 25°C. Values indicated are the values of $-\log J_e$ (the equilibrium compliance). (Reprinted with permission from Sanders, J. F., and J. D. Ferry, *Macromolecules*, 7, 1974, 681. Copyright 1974 American Chemical Society.)

sample over the examined temperature range. At high frequencies, where the local (small length-scale) dynamics are unaffected by the extent of cross-linking, the $\tan \delta$ results of all the samples merge. At low frequencies, $\tan \delta$ levels off at lower values with increasing extent of cross-linking as expected.

In a shear stress relaxation experiment, an elastomer can be cured between a cone-and-plate or a parallel-plate fixture of a rheometer, which is subjected to a step strain γ that is held constant for times $t \geq 0$. The stress $\sigma(t)$ is monitored and reported in terms of a time-dependent modulus $G(t)$ defined by

$$G(t) = \frac{\sigma(t)}{\gamma} \quad (9.97)$$

The simplest form of $G(t)$ is an exponential decay:

$$G(t) = G_0 \exp\left(\frac{-t}{\lambda}\right) \quad (9.98)$$

where:

G_0 is the initial modulus related to the initial value of the stress

λ is the relaxation time as exhibited by the single Maxwell element

The earliest published analysis of stress relaxation in cross-linked rubbers was performed by Chasset and Thirion [43]. They established the following empirical equation:

$$G(t) = G_e \left[1 + \left(\frac{t}{\tau_e} \right)^{-m} \right] \quad (9.99)$$

where:

- $G(t)$ is the stress relaxation modulus
- G_e is the equilibrium elastic shear modulus
- m and τ_e are material parameters

The term τ_e^m represents the relative unrelaxed stress in excess of the equilibrium stress at $t = 1$ s. Equation 9.99 has been widely used in the stress analysis of stress relaxation data from elastomers even though it is applicable only to data in an intermediate range of relaxation times. Several molecular models have been proposed in support of the form of Equation 9.99, but the molecular mechanisms of relaxation differ in these proposed models [44] so that complete understanding at the molecular level of viscoelastic relaxation in elastomers has not yet been achieved.

9.10 EFFECT OF FILLERS

In the region of small deformations, fillers have much the same role as crystallites, especially if the filler surface is wetted by the polymer. The behavior of carbon black in a cross-linked natural rubber is typified by Figure 9.24 showing an increase in stiffness (spring constant) with loading and a moderate increase in damping, that is, fractional energy loss per cycle. Note that the stiffness increases with temperature as is expected from Equation 9.70 when no filler is added. The situation is more complex when filler is present. Filled elastomers typically exhibit nonlinear viscoelasticity even at very small strain, a behavior known as the Payne effect [45]. They also exhibit strong hysteresis and stress softening in their stress-strain behavior at large strains (Mullins effect) [46]. Recently, efforts and progress toward developing constitutive modeling of time-dependent nonlinear viscoelasticity of heterogeneous filled elastomers and Thermoplastic elastomers (TPEs) have been made [47]. This continues to be an active research area. For glassy polymers, the modulus is increased by fillers, and T_g may be increased somewhat also (Figure 9.25).

9.11 OTHER TRANSITIONS

There are other transitions in molecular conformations that give rise to loss peaks in oscillatory experiments such as the torsion pendulum. Often the modulus changes by such a small amount at a minor transition that performance properties are not noticeably affected. It has been pointed out that an additional amorphous change occurs well below the main glass transition temperature of poly(tetrafluoroethylene) (Figure 9.16). In the dielectric relaxation literature

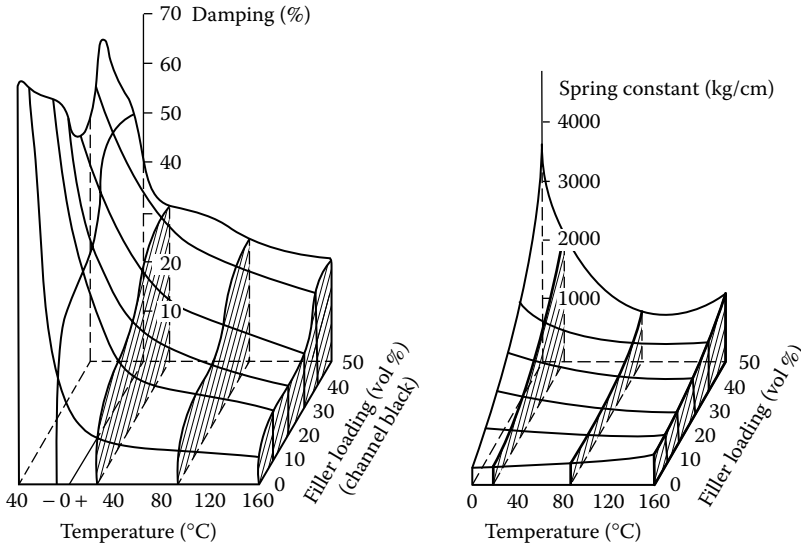


FIGURE 9.24 Contour representation of dependence of dynamic properties of natural rubber on filler loading and temperature. (Data from Gehman, S. D., *Rubber Chem. Technol.*, 30, 1202, 1957.)

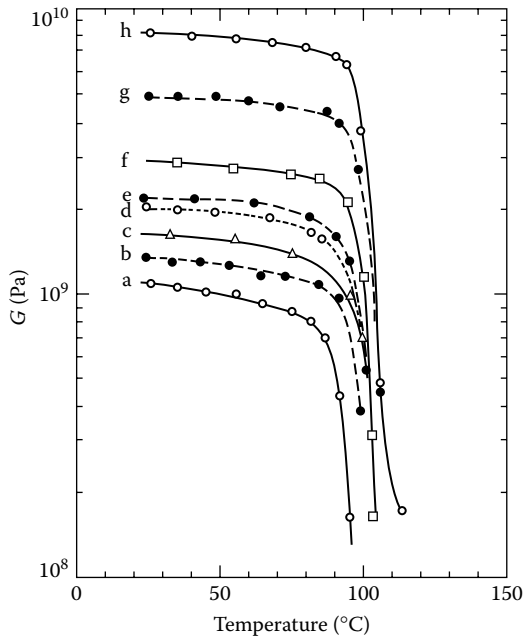


FIGURE 9.25 (a) Shear modulus versus temperature for PS and (b) PS containing 20% calcium carbonate, (c) 20% asbestos, (d) 20% mica, (e) 40% asbestos, (f) 60% asbestos, (g) 40% mica, and (h) 60% mica. (Data from Nielsen, L. E., R. A. Wall, and P. G. Richmond, *SPE J.*, 11, 22, 1955.)

(Chapter 18), the main T_g is designated as the **alpha** transition, and transitions at successively lower temperatures are termed **beta** and **gamma**. For nylon 66, loss peaks identified in the amorphous region are seen at 200 K (beta transition) and 135 K (gamma transition) [50]. The **storage modulus** (Figure 9.15) scarcely changes at those temperatures.

More controversial is the observation of a loss peak above T_g in the amorphous melt. This $T_{l,l}$ transition temperature represents a change from one liquid state to another [51,52]. For PS $T_{l,l}$ is about 70°C higher than T_g , and for polyisobutylene it is about 105°C higher than the T_g measured by the same method.

APPENDIX 9.A HARMONIC DEFORMATION OF A MAXWELL ELEMENT

9.A.1 TRIGONOMETRIC NOTATION

Starting with a sinusoidal input of strain in a Maxwell element (Section 9.2), we derive the resulting sinusoidal stress. First, we let the strain ε be a function of a maximum strain ε_m and time t with a frequency ω :

$$\varepsilon = \varepsilon_m \cos \omega t \quad (9.A.1)$$

For a Maxwell element, we have from Equation 9.24:

$$\frac{d\varepsilon}{dt} = \frac{1}{E} \frac{d\sigma}{dt} + \frac{\sigma}{E\lambda} \quad (9.A.2)$$

so that

$$\frac{d\sigma}{dt} + \frac{\sigma}{\lambda} = E \frac{d\varepsilon}{dt} \quad (9.A.3)$$

Differentiating Equation 9.A.1 and substituting in Equation 9.A.3,

$$\frac{d\sigma}{dt} + \frac{\sigma}{\lambda} = -\omega \varepsilon_m E \sin \omega t \quad (9.A.4)$$

This is a simple linear differential equation of the form:

$$\frac{dy}{dx} + Py = Q$$

When P and Q are functions of x only, the general solution of such an equation is

$$y \exp(\psi) = \int \exp(\psi) Q dx + C$$

where:

$$\psi = \int P dx \quad (9.A.5)$$

Applying the above equation to Equation 9.A.4, one obtains

$$\Psi = \frac{t}{\lambda} \quad (9.A.6)$$

and

$$\sigma \exp\left(\frac{t}{\lambda}\right) = -\omega \varepsilon_m E \int \exp\left(\frac{t}{\lambda}\right) \sin \omega t dt + C \quad (9.A.7)$$

The last equation gives

$$\sigma \exp\left(\frac{t}{\lambda}\right) = -\frac{\omega \lambda}{1 + \omega^2 \lambda^2} \varepsilon_m E (\sin \omega t - \omega \lambda \cos \omega t) \exp\left(\frac{t}{\lambda}\right) + C \quad (9.A.8)$$

or

$$\sigma = -\frac{\omega \lambda}{1 + \omega^2 \lambda^2} \varepsilon_m E (\sin \omega t - \omega \lambda \cos \omega t) + C \exp\left(\frac{-t}{\lambda}\right) \quad (9.A.9)$$

Under steady-state conditions for which $t/\lambda \gg 1$, the second term on the right-hand side of the above equation drops out leaving

$$\sigma = -\frac{\omega \lambda}{1 + \omega^2 \lambda^2} \varepsilon_m E (\sin \omega t - \omega \lambda \cos \omega t) \quad (9.A.10)$$

We can define an angle δ by

$$\tan \delta = \frac{1}{\omega \lambda} = \frac{\sin \delta}{\cos \delta} \quad \text{and} \quad \sin \delta = (1 + \omega^2 \lambda^2)^{-1/2} \quad (9.A.11)$$

Then, making use of trigonometric identities, we can write

$$\begin{aligned} \sin \omega t - \omega \lambda \cos \omega t &= \frac{(\sin \omega t)(\sin \delta)}{\sin \delta} - \frac{(\cos \omega t)(\cos \delta)}{\sin \delta} \\ &= -\frac{\cos(\omega t + \delta)}{\sin \delta} \\ &= -(1 + \omega^2 \lambda^2)^{1/2} \cos(\omega t + \delta) \end{aligned} \quad (9.A.12)$$

Substituting the above equation into Equation 9.A.10, we arrive at

$$\sigma = \frac{\omega \lambda}{(1 + \omega^2 \lambda^2)^{1/2}} \varepsilon_m E \cos(\omega t + \delta) \quad (9.A.13)$$

The maximum value of the stress occurs at $\omega t + \delta = 0$ and is given by

$$\sigma_m = \frac{E \omega \lambda \varepsilon_m}{(1 + \omega^2 \lambda^2)^{1/2}} \quad (9.A.14)$$

Equation 9.A.10 implies that the stress of the Maxwell element can be decomposed into an elastic component term (the cosine term) that is in phase with the applied strain and a viscous component term (the sine term) that is exactly 90° out of phase of the applied strain. This result can also be seen by using Equation 9.A.1 and by writing Equation 9.A.10 in the form:

$$\sigma = \frac{E\omega^2\lambda^2}{1+\omega^2\lambda^2}\varepsilon + \frac{E\omega\lambda}{1+\omega^2\lambda^2}\frac{d\varepsilon}{dt} = E'\varepsilon + E''\frac{d\varepsilon}{dt} \quad (9.A.15)$$

where:

$E' = E\omega^2\lambda^2/1 + \omega^2\lambda^2$ is known as the elastic modulus

$E'' = E\omega\lambda/1 + \omega^2\lambda^2$ is known as the loss modulus

Note that

$$\frac{E''}{E'} = \frac{1}{\omega\lambda} = \tan \delta \quad (9.A.16)$$

It is conventional to call δ the loss angle.

9.A.2 COMPLEX NOTATION

The above results can be obtained by using complex notation and expressing the actual strain as the real part of a complex strain defined by

$$\varepsilon^* = \varepsilon_m \exp(i\omega t) \quad (9.A.17)$$

The constitutive equation for a Maxwell element in terms of a complex strain is:

$$\frac{d\varepsilon^*}{dt} = \frac{1}{E} \frac{d\sigma^*}{dt} + \frac{\sigma^*}{E\lambda} \quad (9.A.18)$$

Using Equation 9.A.17, this can be rewritten as

$$\frac{d\sigma^*}{dt} + \frac{\sigma^*}{\lambda} = E \frac{d\varepsilon^*}{dt} = i\omega\varepsilon_m E \exp(i\omega t) = Q \quad (9.A.19)$$

As in Section 9.A.1, the general solution is

$$\sigma^* \exp\left(\frac{t}{\lambda}\right) = \int \exp\left(\frac{t}{\lambda}\right) Q dt + C \quad (9.A.20)$$

But

$$\int \exp\left(\frac{t}{\lambda}\right) Q dt = i\omega\varepsilon_m E \int \exp\left(i\omega t + \frac{t}{\lambda}\right) dt = \frac{i\omega\varepsilon_m E \exp(i\omega t + t/\lambda)}{i\omega + 1/\lambda} \quad (9.A.21)$$

Substitution in Equation 9.A.20 and rearrangement yield

$$\sigma^* = \frac{i\omega\varepsilon_m\lambda E \exp(i\omega t)}{i\omega\lambda + 1} + C \exp\left(\frac{-t}{\lambda}\right) \quad (9.A.22)$$

Once again, the second term on the right-hand side drops out at steady state when $t/\lambda \gg 1$. Multiplying both the numerator and the denominator of the first term by $(1 - i\omega\lambda)$, we get

$$\sigma^* = \frac{E\omega^2\lambda^2\varepsilon_m \exp(i\omega t) + Ei\omega\lambda\varepsilon_m \exp(i\omega t)}{1 + \omega^2\lambda^2} \quad (9.A.23)$$

The actual stress σ is the real part of σ^* and is therefore given by

$$\sigma = \frac{E\omega^2\lambda^2}{1 + \omega^2\lambda^2} \varepsilon_m \cos \omega t - \frac{E\omega\lambda}{1 + \omega^2\lambda^2} \varepsilon_m \sin \omega t \quad (9.A.24)$$

This is the same as Equation 9.A.10 and can also be written in terms of the elastic and loss moduli as

$$\sigma = E'\varepsilon_m \cos \omega t - E''\varepsilon_m \sin \omega t = E'\varepsilon + E'' \frac{d\varepsilon}{dt} \quad (9.A.25)$$

KEYWORDS

Viscoelasticity
 Poisson's ratio
 Hooke's law
 Maxwell element
 Young's modulus
 Compliance
 Maxwell model
 Creep
 Linear viscoelastic region
 Stress relaxation
 Harmonic motion
 Dynamic mechanical analyzer
 Torsion pendulum
 Logarithmic decrement
 Torsional braid
 Glassy behavior
 Rubbery behavior
 Glass transition
 Rubbery flow
 Liquid flow
 Time-temperature superposition
 Distribution of relaxation times

Coarse-grained molecular models
Bead-spring model
Generalized Maxwell model
Terminal relaxation
Hydrodynamic interaction
Ideal rubber elasticity
Packing length
Thermodynamic equation of state
Boltzmann constant
Affine deformation
Gaussian distribution
Phantom chain approximation
Phantom model
Constrained fluctuation model
Slip-link model
Nonaffine slip tube model
Mooney–Rivlin equation
Visoelasticity of elastomers
Alpha transition
Beta transition
Gamma transition
Storage modulus

PROBLEMS

- 9.1** A polymer can be represented by two Maxwell elements connected in parallel, each with the same spring modulus. In a stress relaxation experiment, the stress decreases to 23.7% of its initial value after 10 min. If the relaxation time of the first element is 10 min, what is the relaxation time of the second element?
- 9.2** A certain polymer sample can be represented by a single Maxwell element. When a tensile stress of 10^3 Pa is applied for 10 s, the maximum length attained by the sample is 1.15 times the original length. After removal of the stress (at 10 s), the length is only 1.10 times the original length. What is the relaxation time of the element?
- 9.3** A Maxwell element is placed in parallel with an ideal rubber band. In a stress relaxation experiment, the initial stress supported at a fixed elongation (stretched length = $1.5 \times$ unstretched length) is 145,000 Pa. After 250 s, the stress decays to 120,000 Pa. However, if the fixed elongation corresponds to $2.5 \times$ unstretched length, the initial stress is 367,000 Pa. Going back to the first experiment (with fixed elongation = $1.5 \times$ unstretched length), what stress should be expected after 500 s?
- 9.4** A Maxwell-type element is constructed of the usual viscous dashpot but with an *ideal rubber* band in place of the usual Hookean spring. In a creep experiment with a constant load of 1000 Pa, and at a temperature of 27°C, the total deformation in tensile strain units after 3 h is $\epsilon = 2.00$. When the

load is removed (at 3 h), the resulting permanent set is 0.750 units. Now the same element (with no starting deformation) is made to undergo stress relaxation at 127°C with a fixed elongation of 1.5 strain units. What is the stress at time zero in the stress relaxation experiment?

- 9.5** Maxwell element A in creep at a constant stress of 10,000 Pa exhibits a total elongation of 0.65 strain units after 100 h and a permanent set of 1.00 unit on removal of the load after a total of 250 h. Now a generalized Maxwell model made up of elements A, B, and C is constructed. B has twice the spring modulus and one-half the relaxation time of A, whereas C has one-half the spring modulus and twice the relaxation time of A. If a sudden elongation of 1.80 units is applied and held constant on the generalized Maxwell model, what stress will be exerted by it after 100 h?
- 9.6** Assume that a polymer can be approximated by three Maxwell elements in parallel each having the same modulus but with viscosities for elements 1, 2, and 3 having the relationship $\eta_1 = 4\eta_2 = 9\eta_3$. Plot $\log(\sigma/\sigma_0)$ versus t/λ_1 and versus $\log(t/\lambda_1)$ for the overall assembly between $t/\lambda_1 = 0.01$ and $t/\lambda_1 = 2$, where λ_1 is the relaxation time for element 1. What is the relaxation time [t for $\log(\sigma/\sigma_0) = -1$] for the assembly?
- 9.7** Two Maxwell elements are tested separately in creep experiments in which the stress is equal to σ_0 . The time to reach an elongation ϵ of 150% is measured. At that exact time, the stress is removed and the permanent set is measured. Next, the two elements are combined in parallel (a generalized Maxwell model) and subjected to a stress relaxation experiment with a total elongation of ϵ_0 . What is the ratio of the stress at 250.0 s compared to that at 50.0 s?

	Creep Data	
	Time to Reach 150% Elongation (s)	Permanent Set (%)
	Element 1	120
Element 2	186	55.0

- 9.8** At times such that t is much less than λ_1 , a polymer has a glassy modulus of E_g . At times greater than $t = \lambda_2$, it exhibits liquid flow. Between λ_1 and λ_2 , the transition can be described by a continuous distribution of relaxation times, $E(\lambda) = Y/\lambda^2$. Derive an equation for the time-dependent modulus $E(t)$ as a function of t , Y , λ_1 , and λ_2 . Also, express E_g in terms of Y , λ_1 , and λ_2 . Plot the curve of $\log E(t)$ versus $\log t$ from $t = 0.01$ to $t = 100$ s for the following set of constants: $E_g = 10^9$ Pa; $\lambda_1 = 0.1$ s; $\lambda_2 = 10$ s. How does the result compare with the relaxation of a single Maxwell element?
- 9.9** A generalized Maxwell model has a distribution of relaxation times, $E_i(\lambda)$, given by $E_i(\lambda) = k_1\lambda^{-2} + k_2$ and $\lambda = 1, 2,$ and 3 min only.

In a stress relaxation experiment, the initial stress of 2.50×10^8 dyn/cm² decays to 1.00×10^8 dyn/cm² after 1.50 min. What is the expected value of stress 3.75 min after the initial stress is applied?

9.10 Samples of polymers X and Y behave like perfect Maxwell elements with the same spring modulus and the same initial length (20.0 cm). When the two samples are connected in series with a constant force of 2.00 kPa, the assembly stretches to a total length of 90.0 cm in 120 s. At that time, the force is removed and the assembly contracts to a length of 60.0 cm. Sample X now is 25.0 cm long and sample Y is 35.0 cm long.

If two new samples of X and Y (each 20.0 cm long) are connected in parallel and subjected to an instantaneous stretching to 30.0 cm, what fraction of the initial stress will remain after 5.00 min? (The assembly is held at a total length of 30.0 cm throughout this period.)

9.11 A minimum of two Maxwell elements in parallel is required to represent the *master curve* of (log) modulus versus (log) time for a real polymer. In a hypothetical case, the glassy plateau modulus (extending to time = 0) is 1.20×10^9 Pa and the rubbery plateau modulus (extending to time = ∞) is 0.300×10^7 Pa. If the time corresponding to a modulus of 2.00×10^8 Pa is 150 s, what are the appropriate values of the spring constants and relaxation times for the two elements?

9.12 (a) Based on Equation 9.29 for E' and E'' of the Maxwell model, write down what you expect for G' and G'' for a generalized Maxwell model.

(b) Compare your results of (a) with the results of the Rouse Model in Equation 9.49. Comment on your observations: Any similarities between the two results?

(c) Consider the physical basis of the two (*apparently* different) models. Can this help explain your observations?

9.13 The Voigt (or Kelvin) element resembles the Maxwell element except that the spring and dashpot are in parallel rather than in series. Show that the creep compliance of such an element is

$$J(t) = (E)^{-1} \left[1 - \exp\left(-\frac{tE}{\eta}\right) \right]$$

9.14 For four Voigt elements (see Problem 9.13) in series for a creep experiment, plot compliance versus time on log–log paper for each element and add them to get the total compliance. What constants do you obtain for a Nutting equation fitted between the times $t = 10$ and $t = 1000$ s?

	Element Number			
	1	2	3	4
E_i (Pa)	0	1.0×10^4	1.333×10^4	2.0×10^4
η_i (Pa·s)	2.0×10^6	5.0×10^5	1.333×10^5	4.0×10^4

9.15 An amorphous polymer in a creep experiment behaves like a Maxwell element joined in series with a Voigt element. A constant load of 10^4 Pa is

applied to a tensile specimen at time $t = 0$. After 10 h the strain is 0.05 cm/cm. The load is removed. The strain can be described thereafter by

$$\text{Strain} = \frac{3 + e^{-t'}}{100}$$

where:

$$t' = t - 10 \text{ (h)}$$

Identify and evaluate the four-model parameters. Use proper units.

- 9.16** An ideal rubber has a density of 0.93 g/cm^3 and an average molecular weight between cross-links of 1250 g/mol . It is placed in a torsion pendulum (rectangular specimen) and cooled to 100 K , which is 80°C below the glass transition temperature. In the pendulum it exhibits a frequency of 55 cycles/s . What frequency do we expect to observe at 27°C ? Assume that changes in dimensions of the sample are negligible between the extremes of temperature. In the glassy state, it resembles room-temperature PS, that is, it has a shear modulus of 3.0 GPa .
- 9.17** Samples of a given amorphous polymer are strained 1% at a variety of temperatures. Draw a typical diagram for stress (measured after 10 s) versus temperature for the polymer. Identify on the diagram T_g (a) and the rubbery plateau (b). How would the diagram be changed if: (c) The material were to be degraded to 10% of the original molecular weight? (d) The material were to be loosely cross-linked? (e) It were to be plotted using stress measured after 10 h?
- 9.18** (a) Use Figure 9.8 to determine the values of the shift factor a_T as a function of T for PMMA using the reference temperature of 115°C and plot the date of $\log a_T$ versus $(T - T_{\text{ref}})$.
 (b) Fit the data of (a) to an equation of the form of the WLF equation and determine the coefficients C_1 and C_2 of such an equation for this case.
 (c) Estimate the value of the molecular weight (MW) between entanglements for PMMA from the value of the rubbery plateau.
- 9.19** How much of a shift in T_d (temperature at peak in mechanical loss) do you expect from the WLF equation when the timescale of the test is decreased by a factor of 10^2 ?
- 9.20** Creep data for a sample of plasticized poly(vinyl chloride) at six temperatures can be represented by the Nutting equation with constants as follows:

$$J(t) = A't^n \text{ and } 10\text{s} < t < 1000\text{s}$$

Temperature T ($^\circ\text{C}$)	A' (s^n/Pa)	n
37	9.5×10^{-10}	0.08
44	1.3×10^{-9}	0.19
50	1.3×10^{-9}	0.68
53	2.2×10^{-8}	0.37
63	2.2×10^{-7}	0.18
72	5.2×10^{-7}	0.10

Assuming $T_g = 50^\circ\text{C}$, construct a plot of $J(t)$ versus $\log t$ at 50°C over the range of t from 10^{-3} to 10^7 s by choosing shift factors according to the WLF equation. If a sample has a strain of 0.0005 units after 5 s of creep at constant stress at 50°C , how long will it take (in seconds) to grow to a strain of 0.050 unit?

- 9.21** An unstressed rubber band becomes longer when heated. A stretched rubber band with constant load becomes shorter when heated. Is this behavior consistent with Equation 8.23? Explain.
- 9.22** An ideal rubber is stretched to 1.10 times its unstretched length at 27°C (300 K) supporting a stress of 150 psi. After aging 10 days in air at 127°C , the stress at 1.10 times its unstretched length is only 100 psi (measured at 127°C). If the original polymer contained 0.015 mol of cross-links per unit volume originally, how many moles of cross-links per unit volume were lost or gained on aging?
- 9.23** The following data are obtained on a sample of natural rubber. Calculate the stress to be expected at 100% elongation for the dry rubber (in Pa) at 27°C .
Swelling in benzene at 27°C :
 $\chi = 0.44$
 $v_2 = 0.20$
 $V_1 = 100 \text{ cm}^3/\text{mol}$
 $R = 8.31 \text{ J/mol}\cdot\text{K}$
- 9.24** An ideal rubber has a nonlinear stress–strain curve. If a 1.00-cm cube of such a rubber is compressed to 0.98 cm by a mass of 3 kg, what stress is going to be required to stretch a 5-cm strip of the same rubber to a length of 7.5 cm?
- 9.25** An ideal rubber band is stretched to a length of 15.0 cm from its original length of 6.00 cm. It is found that the stress at this length increases by an increment of 1.5×10^5 Pa when the temperature is raised 5°C (from 27°C up to 32°C). What modulus ($E = \sigma/\epsilon$) should we expect to measure at 1% elongation at 27°C ? Neglect any changes in volume with temperature.
- 9.26** The area under a reversible stress–strain curve represents the energy stored per unit volume. For an ideal rubber strip, 40.0 J of work is expended in extending it to an elongation of 100% at 27.0°C . If the rubber strip is 30.0 cm long, 1.25 cm thick, and 2.50 cm wide, what is the chain density in mol/cm^3 ?
- 9.27** Blocks A and B are connected by three ideal, flexible rubber cables. The cables are as follows:

Cable	Diameter (cm)	Length (ft)
1. Neoprene	0.250	2.00
2. Styrene–butadiene rubber	0.500	2.50
3. Silicone	0.350	3.00

The force needed to separate block A from B is as follows:

Distance between Blocks (ft)	Force (N)
2.00	0.0
2.35	100.0
3.55	485.0
4.00	625.0

What force is required to separate the blocks a distance of 5.00 ft if cable 3 is cut so that only cables 1 and 2 connect A with B?

- 9.28** An ideal rubber band is stretched to 1.20 times its unstretched length (20% elongation) at room temperature (27°C). The force required is 2.00 N. The sample is allowed to relax to its original length. Now the temperature of the relaxed sample is raised to 127°C and it is aged there for 1 week. At the end of the week, the force required to stretch the sample to 1.30 times its unstretched length (measured at 127°C) is 2.25 N. Assume that the overall dimensions of the rubber band are not changed significantly by temperature or aging. If the original sample contained 0.020 mol of cross-links per unit volume, how many moles of cross-links per unit volume were lost or gained upon aging?
- 9.29** (a) Consider an ideal rubber subjected to a shear deformation (depicted in Table 9.1). Show that for a shear stress σ_{xy} , one has the product $\alpha_x \alpha_y = 1$ and $\alpha_z = 1$. Hint: Consider a unit circle in the x - y plane being deformed into an ellipse with axes α_x and α_y .
 (b) Show that in this case $\sigma_{xy} = G\gamma$, where G is the elastic shear modulus and γ is the strain given by $\alpha_x - \alpha_y$.
- 9.30** In a certain test, a constant stress is instantly applied to a dumbbell sample (in tension). Three materials are tested. A rubber reacts by deforming rather rapidly to start and then more and more slowly until it reaches an equilibrium extension. A thermoplast reacts by deforming almost instantly to some substantial extension and then deforming further linearly with time. A thermoset reacts by deforming almost instantly to an equilibrium extension.
 (a) Describe the behavior of each material with an appropriate combination of dashpots and springs.
 (b) Describe what happens to each model when the stress is removed instantaneously.
- 9.31** Telechelic PDMS chains of MW = 20,000 g/mol are end-linked (cross-linked at their reactive ends) in the melt to form an elastomeric network. The network is found to have a shear modulus of 0.27 MPa.
 (a) Assuming that the elastomer formed is a perfect network with elastic strands of 20,000 g/mol, what would be its expected shear modulus based on ideal rubber elasticity?
 (b) What is the average MW between *effective* cross-links based on the experimental value of the shear modulus and what is the cause of the discrepancy between the calculated value in (a) and the experimental values of G ?

- 9.32** The transparent polymer thin sheet used in see-through envelope that allows the addressee's name and address to be seen is made from biaxially stretched PS. The PS film is stretched above its T_g with equal forces in two directions (say x and y).
- (a) Assume that PS behaves as an ideal rubber just above its glass transition. Use the statistical mechanical result of the entropy change upon deformation to obtain the relation between stress and extension ratio (i.e., the function $\sigma(\alpha)$, where $\alpha = \alpha_x = \alpha_y$) for the case of equal biaxial extension.
- (b) Given that the rubbery plateau modulus of PS has a value of 0.2 MPa, estimate the stress to be imposed on each side of the film to double its original length, that is, to achieve $\alpha = 2$.
- 9.33** (a) Using the entropy change upon deformation of an ideal rubber, show that the stored elastic energy per unit volume (ΔE) can be expressed as

$$\Delta E = \left(\frac{G}{2} \right) (\alpha_x^2 + \alpha_y^2 + \alpha_z^2 - 3)$$

where:

G is the shear elastic modulus

α_i is the extension ratio in the i -direction

G is given by RTN , where N is the density of elastic strands, and R and T have their usual meaning. Hint: Start from the expression of ΔS in the Equation 9.66

- (b) Calculate the value of this energy in units of G for a uniaxial extension at an extension ratio of 4.
- (c) Obtain an expression for this energy for a uniaxial compression and calculate the value of the uniaxial compression ratio, that is, value of α along the compression axis ($\alpha_{\text{compression}}$), which leads to the same stored energy as for $\alpha_{\text{extension}} = 4$.
- (d) Finally, demonstrate that for a flat sample (i.e., in Cartesian coordinates), uniaxial compression corresponds to biaxial extension. To do this, obtain the expression for ΔE in equal biaxial extension and show that the value of α_{biaxial} that corresponds to the value $\alpha_{\text{compression}}$ obtained in (c) gives the same value of ΔE .

REFERENCES

- Nielsen, L. E.: *The Mechanical Properties of Polymers*. Reinhold, New York, 1962, p. 55.
- Nielsen, L. E.: *Mechanical Properties of Polymers and Composites*, vol. 1, chap. 4, Dekker, New York, 1974.
- Whorlow, R. W.: *Rheological Techniques*, chap. 5, Wiley, New York, 1980.
- Wetton, R. E.: chap. 5 in J. Dawkins (ed.), *Developments in Polymer Characterization*, Applied Science, New York, 1984.
- Xue, G., J. Dong, and J. Ding: chap. 40 in N. P. Cheremisinoff, and P. N. Cheremisinoff (eds.), *Handbook of Advanced Materials Testing*, Dekker, New York, 1995.

6. Grubb, D. T.: chap. 40 in R. W. Cahn, P. Haasen, and E. J. Kramer (eds.), *Materials Science and Technology: Structure and Properties of Polymers*, VCH, New York, 1993.
7. Koleske, J. V., and J. A. Faucher: *Polym. Eng. Sci.*, 19:716 (1979).
8. Kiran, E., and J. K. Gillham: *Polym. Eng. Sci.*, 19:699 (1979).
9. Gillham, J. K.: *Polym. Eng. Sci.*, 19:676 (1979).
10. Tobolsky, A. V.: *Properties and Structure of Polymers*, Wiley, New York, 1960.
11. McLoughlin, J. R., and A. V. Tobolsky: *J. Colloid Sci.*, 7:555 (1952).
12. Tobolsky, A. V.: *Properties and Structure of Polymers*, chap. 3, Wiley, New York, 1960.
13. Rouse, P. E., Jr.: *Chem. Phys.*, 21:1272 (1953).
14. Ferry, J. D.: *Viscoelastic Properties of Polymers*, 3rd edn., Wiley, New York, 1980.
15. Mills, N. J., and A. Niven: *J. Polym. Sci. Part A-2*, 9:267 (1971).
16. Zimm, B. H.: *J. Chem. Phys.*, 24:269 (1956).
17. Johnson, R. M., J. L. Schrag, and J. D. Ferry: *Polym. J.*, 1:742 (1970).
18. Bird, R. B., C. F. Curtiss, R. C. Armstrong, and O. Hassager: *Dynamics of Polymeric Liquids*, 2nd edn., chap.13, Wiley, New York, 1987.
19. Larson, R. G.: *The Structure and Rheology of Complex Fluids*, chap. 3, Oxford University Press, Oxford, 1999.
20. Fetters, L. J., D. J. Lohse, D. Richter, T. A. Witten, and A. Zirkel: *Macromolecules*, 27:4639 (1994).
21. Sauer, J. A.: *SPE Trans.*, 2:57 (1962).
22. Sinnot, K. M.: *SPE Trans.*, 2:65 (1962).
23. Flory, P. J.: *Principles of Polymer Chemistry*, chap. 11, Cornell University Press, Ithaca, NY, 1953.
24. Anthony, R. L., R. H. Caston, and E. Guth: *J. Phys. Chem.*, 46:826 (1942).
25. Eisele, U.: *Introduction to Polymer Physics*, chap. 10, Springer-Verlag, New York, 1990.
26. Erman, B., and J. E. Mark: *Structures and Properties of Rubberlike Networks*, Oxford University Press, New York, 1997.
27. James, H. M., and E. Guth: *J. Chem. Phys.*, 15:669 (1947).
28. Flory, P. J., and B. Erman: *Macromolecules*, 15:800 (1982).
29. Ronca, G., and G. Allegra: *J. Chem. Phys.*, 63:4990 (1975).
30. Kloczkowski, A., J. E. Mark, and B. Erman: *Macromolecules*, 28:5089 (1995).
31. Edwards, S. F., and T. A. Vilgis: *Polymer*, 27:483 (1986).
32. Dossin, L. M., and W. W. Graessley: *Macromolecules*, 12:123 (1979).
33. Graessley, W. W.: *Polymeric Liquids & Networks: Structure and Properties*, Garland Science, New York, 2004, chap.9.
34. Miller, R. D., and C. W. Macosko: *J. Polym. Sci., Part B: Polym. Phys.*, 26:1 (1988).
35. Rubinstein, M., and S. Panyukov: *Macromolecules*, 35:6670 (2002).
36. Yoo, S. H., L. Yee, and C. Cohen: *Polymer*, 51:1608 (2010).
37. Gumbrell, S., L. Mullins, and R. S. Rivlin: *Trans. Faraday Soc.*, 49:1945 (1953).
38. Martin, G. M., F. L. Roth, and R. D. Stiehler: *Trans. Inst. Rubber Ind.*, 32:189 (1956); *Rubber Chem. Technol.*, 30:876 (1957).
39. Ogden, R. W.: *Rubber Chem. Technol.*, 59:361 (1986).
40. Wood, L. A.: *Rubber Chem. Technol.*, 32:1 (1959).
41. Wood, L. A.: *Rubber Chem. Technol.*, 51:840 (1978).
42. Sanders, J. F., and J. D. Ferry: *Macromolecules*, 7:681 (1974).
43. Chasset, R., and P. Thirion: Viscoelastic relaxation of rubber vulcanizates between the glass transition and equilibrium in J. A. Prins (ed.), *Proceedings of the Conference on Physics of Non-Crystalline Solids*, North-Holland Publishing Co., Amsterdam, The Netherlands, 1965, p. 345.
44. McKenna, G. B., and Gaylord R. J.: *Polymer*, 29:2027 (1988).
45. Payne, A. R.: *J. Appl. Polym. Sci.*, 6:57 (1962).

46. Mullins, L.: *Rubber Chem. Technol.*, 42:339 (1969).
47. Dorfmann, A., and R. W. Ogden: *Int. J. Solids Struct.*, 41:1855 (2004).
48. Gehman, S. D.: *Rubber Chem. Technol.*, 30:1202 (1957).
49. Nielsen, L. E., R. A. Wall, and P. G. Richmond: *SPE J.*, 11:22 (1955).
50. Murayama, T.: *Dynamic Mechanical Analysis of Polymeric Material*, Elsevier, New York, 1978, p. 65.
51. Boyer, R. F.: *Polym. Eng. Sci.*, 19:732 (1979).
52. Gillham, J. K.: *Polym. Eng. Sci.*, 19:749 (1979).

GENERAL REFERENCES

- Aklonis, J. J., and W. J. MacKnight: *Introduction to Polymer Viscoelasticity*, 2nd edn., Wiley, New York, 1983.
- Aragon, A.: *The Physics of Deformation and Fracture of Polymers*, Cambridge University Press, Cambridge, 2013.
- Arridge, R. G. C.: *An Introduction to Polymer Mechanics*, Taylor & Francis, Philadelphia, PA, 1985.
- Boyer, R. F. (ed.): *Technological Aspects of the Mechanical Behavior of Polymers*, Wiley, New York, 1975.
- Boyer, R. F., and S. Keinath (eds.): *Molecular Motion in Polymers by ESR*, Harwood Academic, New York, 1980.
- Brown, R. P. (ed.): *Physical Testing of Rubber*, 2nd edn., Elsevier, New York, 1986.
- Brown, R. P., and B. E. Read (eds.): *Measurement Techniques for Polymeric Solids*, Elsevier Applied Science, New York, 1984.
- Clegg, D. W., and A. A. Collyer (eds.): *Mechanical Properties of Reinforced Thermoplastics*, Elsevier Applied Science, New York, 1986.
- Collyer, A. A., and D. W. Clegg (eds.): *Rheological Measurement*, Elsevier, New York, 1988.
- Collyer, A. A., and L. A. Utracki (eds.): *Polymer Rheology and Processing*, Elsevier, New York, 1990.
- Craver, C. D., and T. Provder (eds.): *Polymer Characterization: Physical Property, Spectroscopic, and Chromatographic Methods*, ACS, Washington, DC, 1990.
- Enikoloyan, N. S. (ed.): *Filled Polymers I. Science and Technology*, Springer, Secaucus, NJ, 1990.
- Ferry, J. D.: *Viscoelastic Properties of Polymers*, 3rd edn., Wiley, New York, 1980.
- Flory, P. J.: *Principles of Polymer Chemistry*, Cornell University Press, Ithaca, NY, 1953.
- Flory, P. J.: *Statistical Mechanics of Chain Molecules (Revised)*, Hanser-Gardner, Cincinnati, OH, 1991.
- Goldman, A. Y.: *Prediction of the Deformation Properties of Polymeric and Composite Materials*, ACS, Washington, DC, 1993.
- Krishnamachari, S. I., and L. J. Broutman: *Applied Stress Analysis of Plastics*, Chapman & Hall, New York, 1993.
- Lal, J., and J. E. Mark: *Advances in Elastomers and Rubber Elasticity*, Plenum Press, New York, 1986.
- Macosko, C. W.: *Rheology: Principles, Measurements and Applications*, VCH, New York, 1994.
- Mark, J. E., A. Eisenberg, W. W. Graessley, L. Mandelkern, E. T. Samulski, J. L. Koenig, and G. D. Wignall: *Physical Properties of Polymers*, 2nd edn., ACS, Washington, DC, 1993.
- Matsuoka, S.: *Relaxation Phenomena in Polymers*, Hanser-Gardner, Cincinnati, OH, 1992.
- McCauley, J. W., and V. Weiss (eds.): *Materials Characterization for Systems Performance and Reliability*, Plenum Press, New York, 1986.
- McCrum, N. G., C. P. Buckley, and C. B. Bucknall: *Principles of Polymer Engineering*, Oxford University Press, New York, 1988.

- Meier, D. J. (ed.): *Molecular Basis of Transitions and Relaxations*, Gordon & Breach, New York, 1978.
- Mitchell, J., Jr. (ed.): *Applied Polymer Analysis and Characterization*, Hanser-Gardner, Cincinnati, OH, 1992.
- Murayama, T.: *Dynamic Mechanical Analysis of Polymer Material*, 2nd edn., Elsevier, Amsterdam, The Netherlands, 1982.
- Nielsen, L. E., and R. F. Landel: *Mechanical Properties of Polymers and Composites*, 2nd edn., Dekker, New York, 1993.
- Proc. Roy. Soc. London Ser. A*, No. 1666 (November 19, 1976). This issue has five papers on rubber elasticity, pp. 297–406.
- Rubinstein, M., and R. H. Colby: *Polymer Physics*, Oxford University Press, Oxford, 2003.
- Schultz, J., and S. Fakirov: *Solid State Behavior of Linear Polyesters and Polyamides*, Prentice Hall, Englewood Cliffs, NJ, 1990.
- Shah, V.: *Handbook of Plastics Testing Technology*, Wiley, New York, 1984.
- Skrzypek, J. J., and R. B. Hetnarski: *Plasticity and Creep*, CRC Press, Boca Raton, FL, 1993.
- Spells, S. J. (ed.): *Characterization of Solid Polymers: New Techniques and Developments*, Chapman & Hall, New York, 1994.
- Struik, L. C. E.: *Internal Stresses, Dimensional Instabilities and Molecular Orientations in Plastics*, Wiley, New York, 1990.
- Thomas, E. L. (ed.): *Materials Science and Technology. Structure and Properties of Polymers*, vol. 12, VCH, New York, 1993.
- Tobolsky, A. V.: *Properties and Structure of Polymers*, Wiley, New York, 1960.
- Treloar, L. R. G.: *Reports Prog. Phys.*, 36:755 (1973); also reprinted as *Rubber Chem. Tech.*, 47:625 (1974).
- Treloar, L. R. G.: *The Physics of Rubber Elasticity*, 3rd edn., Oxford University Press, New York, 1975.
- Turner, S.: *Mechanical Testing of Plastics*, Wiley, New York, 1986.
- Van Krevelen, D. W.: *Properties of Polymers: Their Correlation with Chemical Structure, Their Numerical Estimation and Prediction from Additive Group Contributions*, 3rd edn., Elsevier, New York, 1990.
- Ward, I. M., and D. W. Hadley: *An Introduction to the Mechanical Properties of Solid Polymers*, Wiley, New York, 1993.
- Williams, J. G.: *Stress Analysis of Polymers*, 2nd edn., Halsted-Wiley, New York, 1980.
- Wunderlich, B.: *Macromolecular Physics*, 3 vols., Academic Press, New York, 1976–1980.
- Zachariades, A. E., and R. S. Porter (eds.): *High Modulus Polymers*, Dekker, New York, 1987.

10 Ultimate Properties

10.1 FAILURE TESTS

Most industrial tests of polymer systems are carried to failure with some degree of simulation between test and end use. A manufacturer of plastic cups is more interested in a fast breaking test that simulates dropping a cup than in a slow, steady deformation. The compromise that is reached is between a specific test (dropping a cup, wearing out a tire on the road, parachuting greater weights until the cords on the chute break) and a more general one (impact strength, sandpaper abrasion, high-speed tensile strength).

Usually, the **ultimate strength** of a material is the stress at or near failure. For most materials, failure is catastrophic and results in a complete break of the test specimen. However, some materials, especially spherulitic crystalline polymers, reach a point where a large inelastic deformation starts (**yielding**) but then continue as the material continues to deform and absorb energy long beyond that point. Even when strength is defined unequivocally and measured with care and statistical confidence, it can be a misleading criterion for the unwary designer. Although it is one of the most widely specified parameters, tensile strength is almost never the limiting factor in a practical application. Seldom, if ever, is a polymer subjected in an end use to a single, steady deformation in the absence of aggressive environments or stress concentrators. In garments, rugs, instrument cases, tires, book covers, and upholstery, polymers fail from repeated stresses, impact, penetration by sharp objects, or propagation of a tear. It is only insofar as the tensile strength correlates with toughness, tear resistance, and fatigue strength that it has real merit.

Toughness can be defined as the energy that has been absorbed before reaching failure. The area under the stress–strain curve has the units of joules per cubic meter when stress is in pascals and strain is in meters per meter. If stress is in pounds per square inch and strain is expressed as inches per inch, the area under the curve has the units of inch-pounds per cubic inch, which also represents energy per unit volume. The energy may be stored elastically as in unfilled rubber, or it may be dissipated as heat as in the permanent deformation of a crystalline material. A rod made from a glass with a strength of 100 MPa can be used to suspend 10 times the weight that a rubber rod with a strength of 10 MPa can withstand. But because the rubber may have an elongation at break that is a thousand times larger than that of the glass, the energy that the rubber rod can absorb before breaking may be many times that of the glass rod.

There is an important qualitative difference between the mechanical properties at small deformations and those at large deformations. The modulus, for example, truly is a material property. However, most ultimate properties are functions of the measurement conditions, including sample orientation and preparation, and as such are very much sample specific. Failure invariably takes place at a defect or stress concentrator. Every value reported must be regarded as an average that is meaningless

unless a sufficiently large number of measurements are made to characterize the distribution. A typical distribution found useful for rubber testing is the double exponential [1], which can be represented in integral form by

$$\sigma_b(n) = \bar{\sigma}_b + s \ln \left[-\ln \left(\frac{n-0.5}{N} \right) \right] \quad (10.1)$$

where:

$\sigma_b(n)$ is the strength of the n th sample when all N samples of a population are ranked in order of decreasing strength. The mode of the distribution is $\bar{\sigma}_b$ and the standard deviation is s . An analysis of 24 tests shows values for tensile strength that vary from 25 to 29 MPa (3500–4100 psi) (Figure 10.1). All points are equally valid, since all are part of the expected distribution. If the 24 point had a tensile strength of 20 MPa (3000 psi), one would be justified in discarding it as being atypical of the distribution. In making plots for this purpose, one arranges the samples in order of decreasing tensile strength.

In presenting the strength data for fibers, a very similar distribution first proposed by **Weibull** (originally in 1939) has become popular [2]. When the stress at break covers a wide range, the logarithm scale for the stress may be used in place of the arithmetic scale of Figure 10.1. Also, the length of the fiber tested may be taken into account. A long fiber is more likely than a short fiber to contain a flaw that limits stress. In a typical application, both the average strength and the slope of the probability curve were found to vary with strain rate and sample length for ultrahigh-strength polyethylene fibers [3]. In testing plastics and rubber, the use of dumbbell-shaped specimens

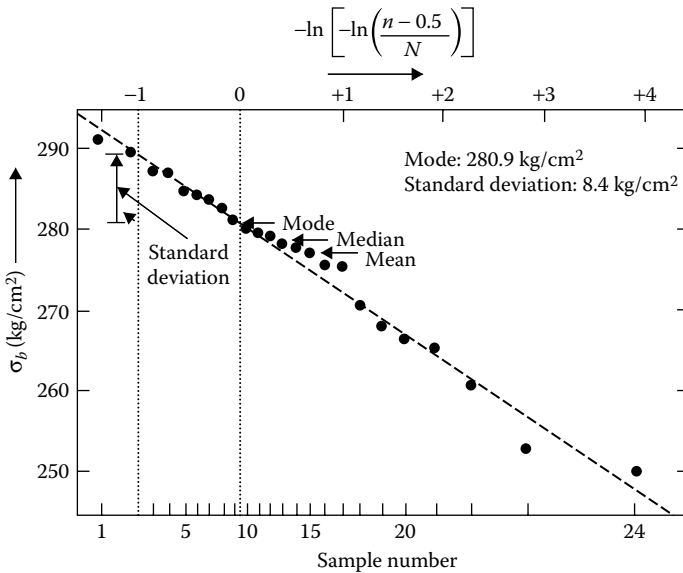


FIGURE 10.1 Stress at break plotted according to Equation 10.1. All points are typical. (Data from May, W., *Trans. Inst. Rubber Ind.*, 40, T109, 1964; *Rubber Chem. Technol.*, 37, 826, 1964.)

is standard, although a longer straight length in the narrow section of the specimen could have the same effect as the length of a fiber.

10.2 CONSTANT-RATE-OF-STRAIN TESTS

A common tensile test involves elongating a dumbbell-shaped sample held in jaws that separate at a constant rate (Figure 10.2). The stress is measured as a function of time. Because the section of uniform cross section of the sample does not elongate at a constant rate, an independent measure of elongation is required if a stress–strain curve is to be constructed from the experiment. The true rate of extension in the center portion can be estimated by measuring the separation of two benchmarks that were originally inscribed in the measurement specimen a convenient distance apart, say 1 in (2.5 cm). At each half-inch or inch interval, a pip may be placed on the record of stress to indicate increments of strain. An extensometer (extension-measuring

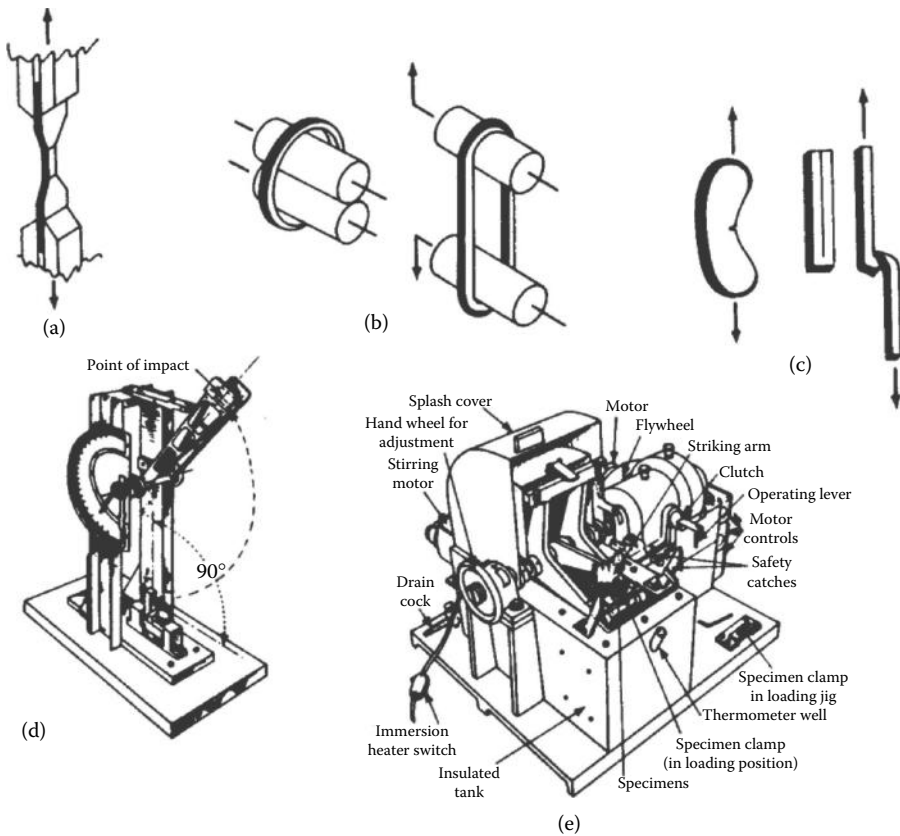


FIGURE 10.2 Mechanical failure tests: (a) tensile test on dumbbell specimen; (b) tensile test on ring specimen; (c) notched crescent and trousers tear specimens; (d) Izod impact test machine (Data from Hallinan, A. J., Jr., *J. Qual. Tech.*, 25, 85, 1993); (e) motor-driven brittleness temperature tester. (Data from *Book of Standards*, ASTM, Baltimore, MD, 1958, 286, 356.)

device) for materials that elongate between 2 and 10 times before breaking can be a pair of clamps that are connected by a tape. As the clamps separate, the tape moves with one and is pulled through the other. If the tape has a pattern that generates a signal at equal intervals, pips can be put on the stress record automatically. When the extension at break is very small, as with glassy materials, an elaborate means of monitoring extension is to follow and record the position of several luminescent benchmarks by means of photocells and a servomotor. Despite the difficulty of measuring strain accurately, the dumbbell samples have the great advantage that ultimate failure will take place in the center of the sample and will not be affected by **stress concentration** at the jaws.

Molded, die-cut, or lathe-cut rings can be used for rubbery samples. The rate of strain is uniform, so that the stress–time record is also a stress–strain record. With care the strength measured on ring samples is the same as that on dumbbells. However, stress concentration at the holder is difficult to avoid even when the holder is lubricated or rotated. Also, the initial portion of the stress–strain curve may be distorted because the stress needed to deform the ring into an oval may mask the stress due to uniform elongation.

Tests with fibers offer another complication. With the uniform cross section, any local yielding or necking is likely to start at the holders and the effective length of the sample may be increased by **jaw penetration**. Long samples or multiple samples wound around spools at either end will minimize the uncertainty in length.

Anyone who has tried to open a plastic-wrapped article has a real appreciation for the difference between the stress needed to rupture a smooth-edged film and the stress needed to propagate a tear. An ordinary piece of cellophane tape with a cross section of a thousandth of a square inch will support a load of many pounds. The slightest notch with a razor on one edge will reduce the supportable load to several ounces. Although there are a number of tear-testing geometries to choose from, the trouser tear test has the merit that the stress to propagate the tear often stays at a constant value, making it easier to estimate than some others where the tear propagates so rapidly that only a peak stress can be read (Figures 10.2 and 10.3).

We have pointed out that the extension at break for a glassy sample often is so small that it becomes hard to measure. In a flexural test, elongation occurs on one side of the sample and compression on the other. A small elongation at break corresponds to a large flexural deflection, which is easily measured. The simple beam with sliding supports is used most often.

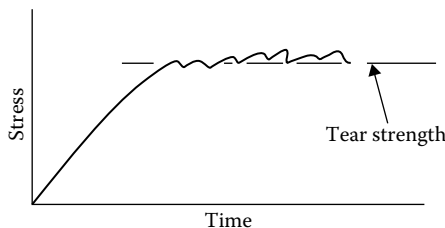


FIGURE 10.3 Typical trouser tear test diagram.

For an adhesive bond, the peel strength (normal to the bonded surface) or the shear strength (in the plane of the bonded surface) may be measured. For another application, the stress supportable in compression before yielding may be the most important parameter. This would be true for a rigid foam, for example.

10.3 BREAKING ENERGY

If more than enough energy is applied to rupture the sample, we can measure directly the total **energy to cause rupture**, or **toughness**, which is the area under the stress–strain curve. The **impact tester** is a simple device used for characterizing the toughness of materials. In this device a hammer with a potential energy, wh_1 , is made to impact and break the sample specimen. The potential energy of the hammer, wh_2 , measured after the break is used to compute the work of fracture and thereby quantify the toughness. The energy used in breaking the sample is proportional to the difference in height before and after the break. The total fracture work W is given by

$$W = (h_1 - h_2)w \text{ in units of ft}\cdot\text{lb}_f \text{ or J}$$

The **Izod** test uses a cantilever beam (Figures 10.2 and 10.4), whereas the **Charpy** test uses a simple beam. In practice, to account for friction in the apparatus, h_0 is

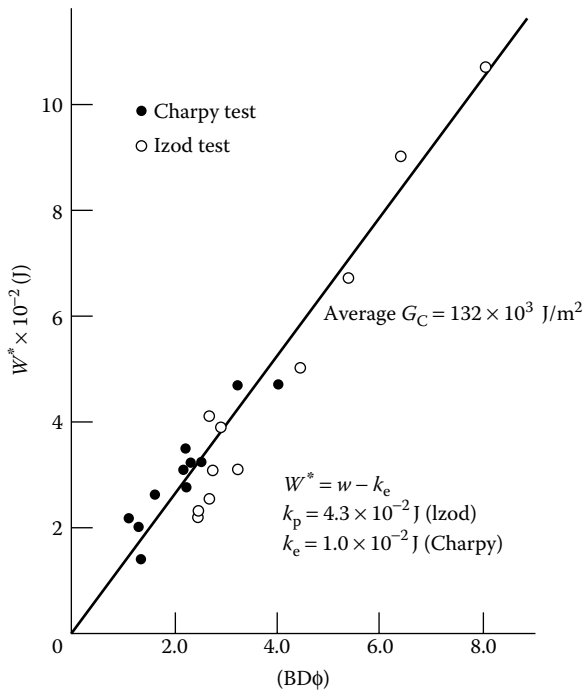


FIGURE 10.4 Impact energy as a function of cross-sectional dimensions from Charpy and Izod tests on PMMA bars. (Reproduced with permission from Patti, E., and J. G. Williams, *Polym. Eng. Sci.*, 15, 470, 1975.)

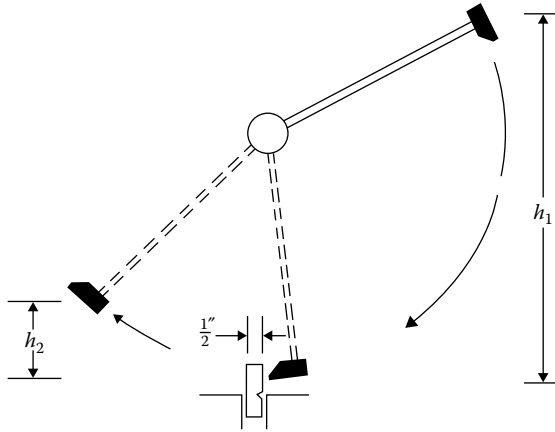


FIGURE 10.5 Impact testing (notched Izod). Original and final heights h_1 and h_2 of hammer determine the strength of sample of thickness d held in vise.

used rather than h_1 , where h_0 is the final height with no sample. Some energy k_c goes into accelerating the broken piece of sample. This can be subtracted from W . Also, calibration factors for both the Izod and Charpy tests based on the specimen dimensions and the compliance of the cantilever are needed to get agreement between the two tests [5]. Figure 10.5 shows such an agreement for poly(methyl methacrylate) (PMMA) samples based on the expression:

$$W^* = W - k_c = G_c B D j \left(\frac{a}{D} \right)$$

where:

- G_c is the specific fracture work (per unit cross-sectional area) expressed in J/m^2
- B is the specimen thickness
- D is the specimen depth
- $j(a/D)$ is the calibration factor with a being the notch depth

Reported values of G_c vary from $1.28 \times 10^3 \text{ J/m}^2$ for PMMA to $15.8 \times 10^3 \text{ J/m}^2$ for high impact polystyrene (HIPS) [5]. The impact strength of a bar sample is measured only on glassy or crystalline materials, since most rubbers will not fracture in this test (see Section 10.8 for breaking energy in elastomers). A pendulum arm is used to break rubber and soft plastics in the **brittleness temperature** test (Figure 10.2). The energy to break is not measured, but the temperature is progressively lowered until the samples do fracture. The brittleness temperature so established often corresponds to T_g or T_m .

10.4 CREEP FAILURE

A single **creep test** in tension or flexure gives information on long-term dimensional stability of a load-bearing element. When combined with a variable temperature, the test provides a simple means of measuring the heat deflection temperature,

where creep rate changes rapidly. Once again, this is close to T_g . The load at which deflection took place also must be specified. A more specific test uses a tube-shape sample specimen that contains a fluid at a specified pressure. Creep failure is determined by measuring the time at which the specimen ruptures. Conducted in an aggressive environment such as soapy water or organic solvents, failure will typically occur earlier as the sample develops cracks and fissures at its surface by a process known as **environmental stress cracking**. Although such tests are useful in predicting the service life of a product, they are even more useful when run at different temperatures and then combined by time–temperature superposition (Section 9.4) in order to estimate the service life at the temperature expected to be encountered in actual use.

10.5 FATIGUE

Most materials subjected to a stress repeatedly will fail even when that stress is well below the ultimate stress measured in a single deformation. When a stress is applied in an alternating fashion, as in a flexing test, the sample usually fails after a certain number of cycles. The lower the applied stress, the more cycles are needed to cause failure. For some materials, the stress reaches a limit below which failure does not occur in a measurable number of cycles. Poly(tetrafluoroethylene) and PMMA in Figure 10.6 exhibit such an **endurance limit** or **fatigue strength**, whereas nylon 6 does not. Rigid plastics such as the crystalline and glassy thermoplastics fail catastrophically, often with a sharp increase in temperature at the time of failing. A rubber being flex-tested may fail more gradually by the development of cracks or by the growth of a cut artificially introduced before testing. Also, in a rubber, the temperature rise due to mechanical hysteresis may be great enough to accelerate oxidative degradation.

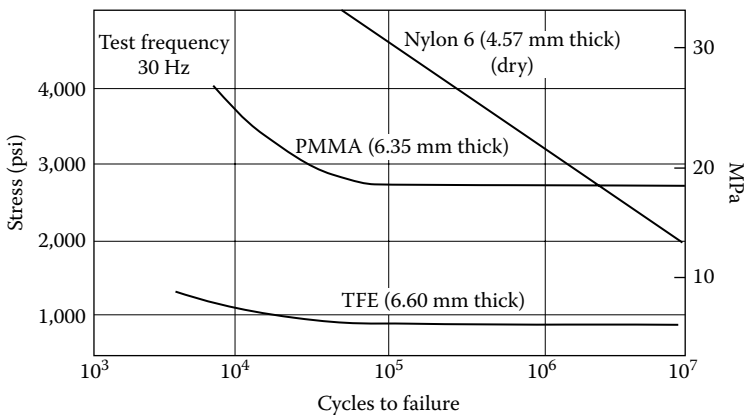


FIGURE 10.6 Fatigue life curves for nylon 6, PMMA, and poly(tetrafluoroethylene) (PTFE). (Data from Riddell, M. N., G. P. Koo, and J. L. O’Toole: *Polym. Sci. Eng.*, 6, 363, 1966.)

10.6 REDUCED-VARIABLE FAILURE CORRELATIONS

The relationship between stress and strain at large values of strain follows the same pattern discussed in Chapter 9. We expect typical glasses (and highly cross-linked networks) to be brittle, rubbers to have high elongations before breaking, and crystalline materials to be strong and tough if oriented and to *neck* and yield if not oriented (Figure 10.7). However, all of these types of behavior depend on the timescale of the test, the temperature at which it is run, the presence of fillers or other polymers, and even sample geometry and history.

Any amorphous polymer at a temperature above T_g that is stretched undergoes some orientation of chain segments. In this oriented state, crystallization may occur, which will increase the effective number of cross-links (see Section 3.4). If crystallization does not occur, the behavior of the sample to rupture is similar at large and small deformations. Figure 10.8 shows that the stress–strain curves for some elastic fibers correlate well (give a linear plot) with Equation 9.93 up to the rupture point (about 600% elongation). The most often used mechanical test is one that measures stress at a constant strain rate. The ultimate tensile stress and strain at rupture vary with temperature and rate of strain.

Working with a cross-linked, unfilled rubber, Smith [7] found that stress–strain data obtained over a range of elongation rates and temperatures could be brought together using a form of the Williams–Landel–Ferry (WLF) equation to bring about time–temperature superposition. The general form of behavior for a number of materials could be represented as a **failure envelope** as shown in Figure 10.9. Lines *OA*, *OB*, and *OC* are typical for constant-rate-of-strain experiments at decreasing temperatures or increasing strain rates, respectively. In the case of strain rates at constant

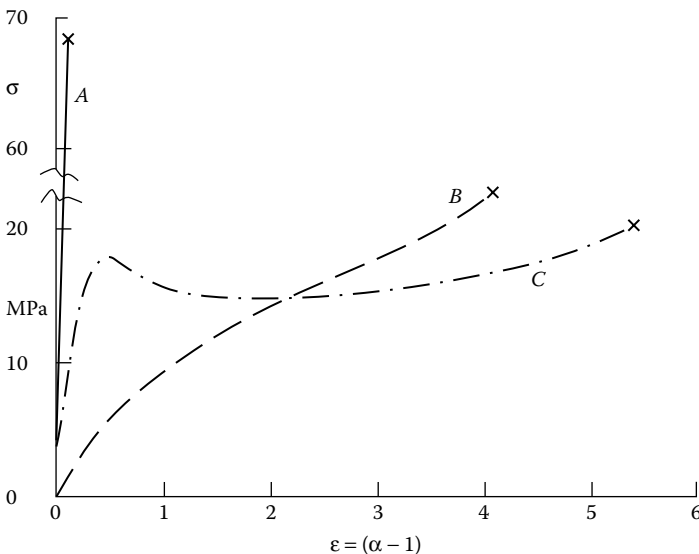


FIGURE 10.7 Typical stress–strain diagrams for brittle glass (*A*), resilient rubber (*B*), and ductile plastic (*C*).

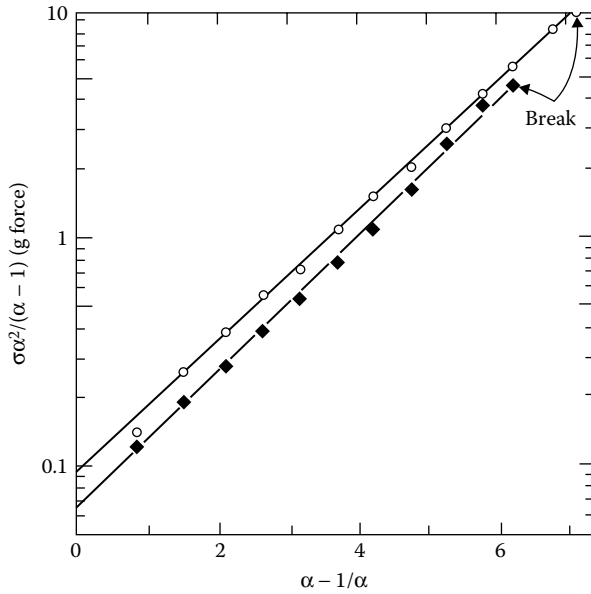


FIGURE 10.8 Stress–strain data to break for two spandex fibers plotted according to Equation 9.93. Here α and σ are the tensile extension ratio and stress, respectively. (Data from Higgins, T. D., Union Carbide Corporation, S. Charleston, private communication, 1969.)

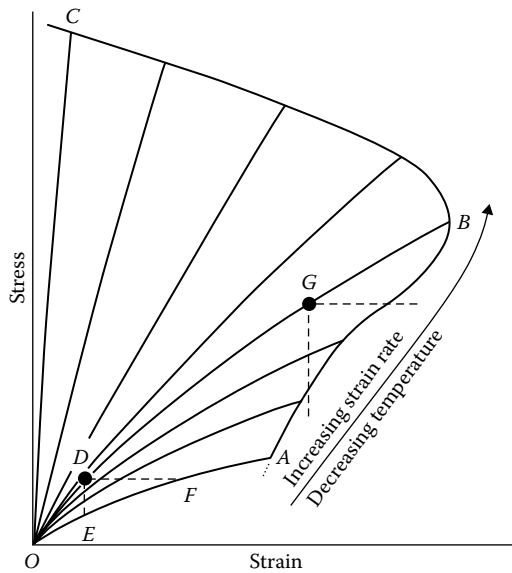


FIGURE 10.9 Schematic representation of failure envelope enclosing curves at constant strain rate. Dashed lines illustrate stress relaxation and creep under different conditions. (Data from Smith, T. L., *J. App. Phys.*, 35, 27, 1964.)

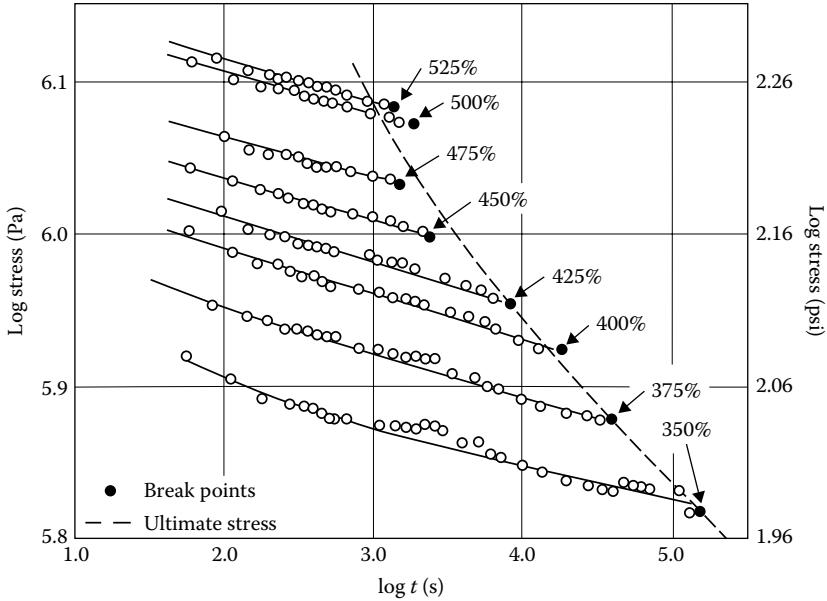


FIGURE 10.10 Stress relaxation of a cross-linked styrene-butadiene rubber at 1.7°C at elongations from 350% to 525%. Solid points indicate rupture. (Data from Smith, T. L., *J. App. Phys.*, 35, 27, 1964.)

temperature, we can superpose a time grid on the diagram, since each strain on each line corresponds to a value of elapsed time.

The lowest line, *OA*, is the **equilibrium elastic line** for a cross-linked material. Its position is subject to the cross-link density and temperature but independent of time. All the constant-rate-of-strain lines exhibit higher stresses at the same strain, because part of the stress is used to dissipate viscous energy in the sample. Several other cases are illustrated in Figure 10.9. For example, let us stretch a sample from 0 to point *D* and then hold it at constant stress. This becomes a creep experiment. By following the isochronal lines, we can depict the time-dependent strain that culminates when the point *F* on the equilibrium curve is reached. If at point *D* we held the strain constant, we would have a stress relaxation experiment culminating in point *E*. However, if we extended the sample to point *G* and held it at constant stress or strain, the diagram predicts eventual failure. Experimental curves showing the stress relaxation culminating in failure for a synthetic rubber are shown in Figure 10.10.

Failure envelopes for real polymers have been most successful for nonfilled, non-crystallizing rubbers. Efforts to find ways of generalizing the principles of superposition to a wider range of commercial rubber compounds continue [8].

10.7 FRACTURE OF GLASSY POLYMERS

There are two major mechanisms by which glassy polymers yield in response to stress. Shear deformation is a localized phenomenon that may appear as **shear bands**. When a polystyrene cube is uniaxially compressed, the bands appear at a

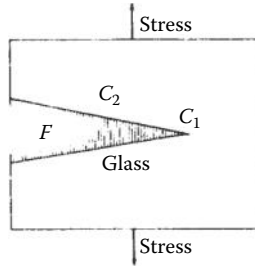


FIGURE 10.11 In response to a stress, the unoriented glassy polymer is pulled into fibrils at the craze tip C_1 . At the crack tip C_2 , the fibrils rupture leaving a layer (typically about 500 nm thick) of craze material on the fracture surface F .

large angle (about 38°) to the compression direction. The bands can be about $1\ \mu\text{m}$ thick and are made up of oriented polymers.

A second mechanism is **crazing**. Crazes are typically seen in a tensile test on a thin sample. What appear to be fine cracks at right angles to the applied stress are not cracks but crazes—“narrow zones of highly deformed and voided polymer” [9]. The typical craze contains 20%–90% voids and the rest fibrils of molecules oriented in the direction of the applied stress (Figure 10.11). The shear bands, by contrast, have very little void volume. Unlike actual cracks, both crazes and shear bands are capable of supporting stresses because of the oriented polymers involved. The failure of a glassy polymer in tension may involve both mechanisms [10–14]. The structure and role of the crazes in the fracture of amorphous polystyrene were thoroughly investigated by Kramer and coworkers [14,15]. Transmission electron micrographs show that a developed craze is made up of fibrils of diameter 6 nm composed of extended polystyrene molecules with 755 voids. Chain scission of the molecules being pulled out of the bulk to be incorporated into the fibrils weakens the craze resistance to an increased stress. In general, fracture starts with the inability of the craze matter to sustain the imposed stress. When a crack propagates, a plastically deformed zone usually precedes the crack. To quote Kambour [11], “Optimists concentrate on plastic deformation in crazes as a source of toughness or stress relief on polymers, while pessimists focus on crazing as the beginning of brittle fracture.” The surfaces left on the crack retain a layer of craze material. The dimensions of a craze that have not yet developed into a crack are shown in the profile obtained for a craze in a thin film of polystyrene (Figure 10.12). The total length of this craze was $189\ \mu\text{m}$. The individual fibrils connecting the two sides were about 15 nm in diameter [15]. Fibrils are an essential feature of crazes. The energy absorbed in their orientation process contributes to polymer toughness.

If crack propagation is carried out in the presence of a liquid that can act as a plasticizer, the stress needed to cause crazing may be decreased substantially by the greater ability of the polymer to form fibrils [10,14]. **Environmental stress cracking** of polymers is studied as a practical test of performance for pipes and other load-bearing components where the polymer will be exposed to an aggressive environment. The effects are seen not only in glassy polymers, but also in semicrystalline materials such as polyethylene.

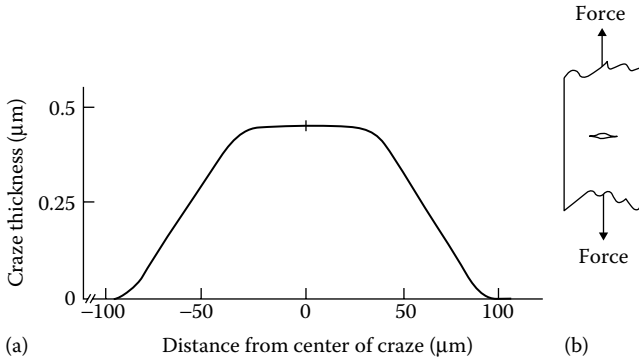


FIGURE 10.12 (a) Thickness profile for an isolated air craze in a thin polystyrene film. (Data from Lauterwasser, B. D., and E. J. Kramer, *Phil. Mag. A*, 39, 469, 1979.) (b) Thickness is measured in the direction of the applied force and is a measure of fibril length in the craze.

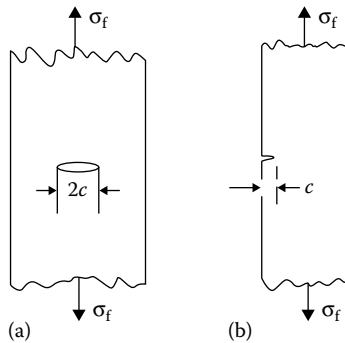


FIGURE 10.13 (a) A model system for crack propagation is an elliptical hole of length $2c$ in a large sheet of material subjected to a tensile stress σ_f . (b) It is often convenient to introduce the crack as a notch in a single edge of a sheet.

To quantify the processes occurring when a crack propagates, a model system comprised of an elliptical hole of length $2c$ in a large sheet of material (Figure 10.13). The stress at fracture σ_f should be related to the modulus of the material E (since E represents energy storage capability) and the energy γ expended to create the new surface area in the crack.

Another approach relates the strain energy released per unit area of crack growth. When the **strain energy release rate** \hat{g}_{1c} exceeds 2γ , fracture will result. For the model system, the latter approach gives

$$\hat{g}_{1c} = \frac{\sigma_f^2 \pi c}{E} \quad (10.2)$$

Unfortunately, various groups who study brittle fracture of polymers throughout the world choose to express their results in different ways. A related parameter used by some groups to describe the dependence of stress at fracture to crack size is the **critical stress intensity factor** K_{1c} :

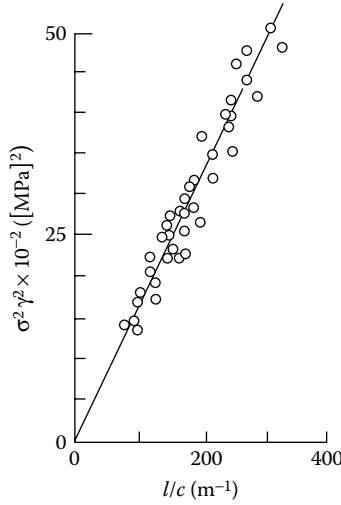


FIGURE 10.14 Brittle fracture data for polycarbonate. Points were obtained at various rates of crack growth and various forms of crack initiation. (Data from Williams, J. G., *Polym. Eng. Sci.*, 17, 144, 1977.)

$$K_{Ic} = 2E\gamma = \hat{g}_{Ic}E \tag{10.3}$$

Some authors refer to K_{Ic} as the **fracture toughness**.

In an experiment corresponding to Figure 10.13b, the specific geometry is accommodated in a constant Y so that

$$\sigma_f^2 Y^2 = \frac{K_{Ic}^2}{c} \tag{10.4}$$

Values of Y are tabulated for many geometries [12,16]. For the sample of polycarbonate (Figure 10.14), the value of K_{Ic} is 4.0 MPa·m^{1/2}, with little dependence on the manner in which the notch was introduced or on the rate of crack propagation (within limits). For many glassy materials, including polystyrene and PMMA, K_{Ic} is relatively independent of thickness. The failure process in polycarbonate is somewhat more complex. In a thin sheet, the plate surfaces can contract laterally and the plastic zone extends from one surface to the other. In a thick sheet, lateral contraction is constrained and part of the crack tip is put in triaxial tension, greatly reducing the overall stress needed for failure. Sheets of polycarbonate less than 3 mm thick may have a K_{Ic} of about 5.5 MPa·m^{1/2}. The sample of Figure 10.14 was about 5 mm thick. Very thick sheets approach a K_{Ic} of about 2.2 MPa·m^{1/2}. The two extreme values reflect the two different failure mechanisms that predominate at the extremes in thickness. A list of fracture toughness values for a selection of different polymeric materials is shown in Table 10.1.

The impact *strength* (Section 10.3) is the most often reported measure of toughness for brittle materials. The equipment is inexpensive, the test is fast, and the results for notched samples of specified dimensions are satisfactorily reproducible.

TABLE 10.1
Fracture Toughness K_{Ic} for a Selection
of Some Common Polymers

	K_{Ic} (MPa m ^{1/2})
PMMA	0.7–1.6
PS	0.7–1.1
PC	2.2
HIPS	1.0–2.0
ABS	2.0
PVC	2.0–4.0
PP	3.0–4.5
HDPE	1.0–6.0
Nylon 6	2.5–3.0
PET	5.0

Source: Williams, J. G.: *Fracture Mechanics of Polymers*, Wiley, New York, 1984. Copyright Wiley-VCH Verlag GmbH & Co. KGaA. Reproduced with permission.

ABS, acrylonitrile–butadiene–styrene; HDPE, high-density polyethylene; PC, polycarbonate; PET, poly(ethylene terephthalate); PP, polypropylene; PS, polystyrene; PVC, poly(vinyl chloride).

However, even in a notched sample, much energy is used in initiating the actual crack and the propagation energy is not clearly distinguishable.

Fracture toughness (and impact strength) is higher in polymers that contain various inclusions. Rigid fibers or particles that adhere well to a glassy polymer matrix can spread the applied force over a larger zone, thus decreasing local stress concentration. Inclusion of amorphous particles in polymers studied at temperatures above their T_g increases energy dissipation by viscous deformation. Cross-linking a glassy polymer inhibits the orientation processes and usually decreases the impact strength. In a typical thermoset glass such as a phenolic resin, cross-linking contributes high-temperature stability. Fiber or particulate reinforcement is used to keep up the impact strength. Heterophase systems (see Section 10.8) are commonly employed when toughness is a major criterion. Despite what has been said about the obvious differences in fracture mechanisms for glasses and rubbers, some generalizations remain. For example, the stress at failure is linear in the logarithm of time to fail (Figure 10.15) for virtually all materials when one ignores minor variations [18].

10.8 FRACTURE OF ELASTOMERS

The standard methods of measuring the strength of elastomers are tensile tests and tear measurements. Uniaxial extension tests give ultimate stress values and the area under the stress–strain curve represents the toughness or elastic energy per unit

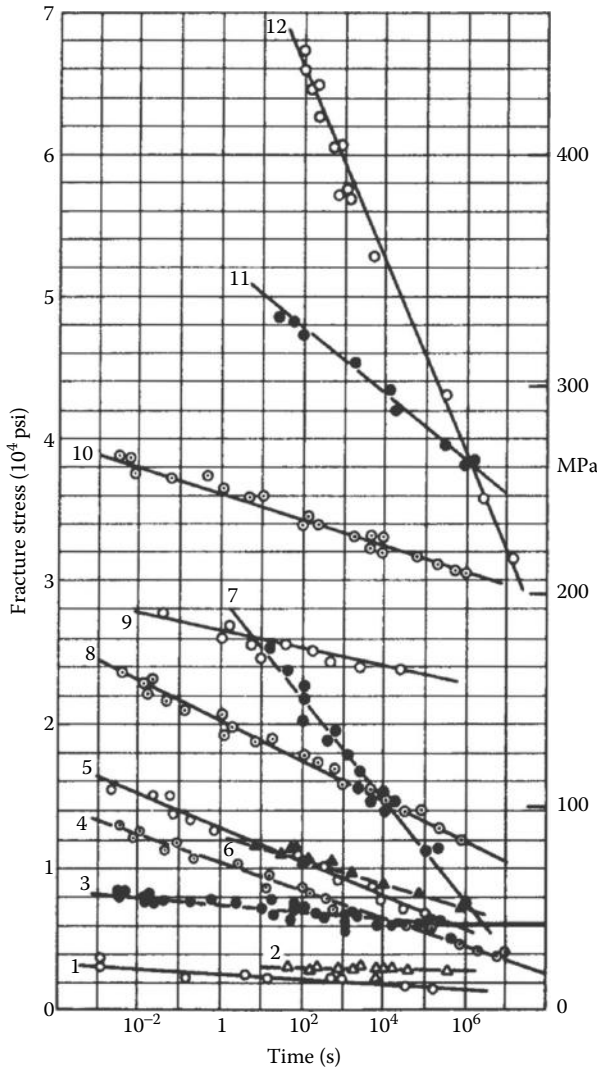


FIGURE 10.15 Time-dependent strength for polymeric and nonpolymeric materials: 1, silver chloride; 2, poly(vinyl chloride); 3, aluminum; 4, PMMA; 5, zinc; 6, celluloid; 7, rubber; 8, nitrocelluloid; 9, platinum; 10, silver; 11, phosphoric bronze; 12, nylon 6 (oriented). (Data from Hsaio, C. C., *Phys. Today*, 19, 49, March 1966.)

volume stored at break. Tensile test results tend to be highly dependent on natural flaws in the material. Tear test measurements, however, are often preferred because the failure point is controlled by introducing a long precut in the sample such as in the trouser test (Figure 10.2c) or simple shear test [19].

A classic theory by Lake and Thomas [20] has guided many of the analysis of correlating the **threshold fracture energy** G_c of an elastomer with the length of the

elastic strands making up the elastomers and the dissociation energy of the chemical bonds of these strands. According to this simple theory,

$$G_c = KM^{1/2} \quad (10.5)$$

where:

M is the molar mass of the elastic strand

K is a prefactor that depends on the polymer properties and is given by [20]

$$K = C\rho N_{AV}Uq^{1/2}l/M_0^{3/2}$$

where:

ρ is the density of the polymer

N_{AV} is Avogadro's number

U is the dissociation energy of a bond along the polymer chain

q is the chain stiffness

l is the bond length

M_0 is the molar mass of the repeat unit

The constant C is a numerical factor of order unity that depends on the shape and size of the crack tip

Using trouser tear tests, Gent and Tobias [21] showed that the Lake–Thomas model held reasonably well for a number of elastomers. In their analysis, they took the molecular mass of a strand as that extracted from the elastic modulus and thereby incorporated the effect of entanglements (Section 9.8.2). More recent results on poly(dimethyl siloxane) (PDMS) elastomers using simple shear tests [22,23] over a wide range of structure (extent of cross-links and trapped entanglements) indicate that the role of entanglements in elastomer fracture needs to be elucidated further.

10.9 HETEROPHASE SYSTEMS

10.9.1 PARTLY CRYSTALLINE MATERIALS

The stress–strain behavior exhibited by partially crystalline polymers are a function of both the deformation rate and temperature. Some three-dimensional representations for commercial polyethylene show the behavior of yield point and elongation with test conditions [24]. **Yielding** often coincides with the onset of **necking** (Section 3.4) and marks the limit of rubbery behavior in the amorphous portion and bond bending and stretching in the crystalline portion that can be borne before spherulites become unstable (Figure 10.16). Once a crystalline polymer is oriented, as in typical drawn fibers, the ultimate elongations are much lower. The ultimate tensile strengths are higher mainly because they are now based on the cross section of the drawn fiber rather than on an originally spherulitic sample. Undrawn nylon 6,6 might typically have an ultimate tensile strength of 50 MPa at a breaking elongation of 200%. Based on the cross section of a drawn fiber, the tensile strength (tenacity) may be over 500 MPa. When a spherulitic material is

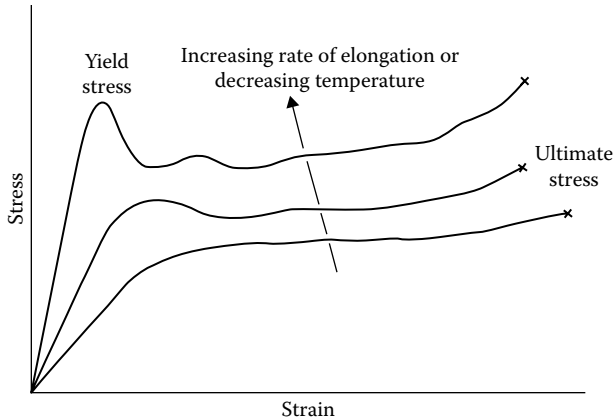


FIGURE 10.16 Typical stress–strain curves for polyethylene.

stressed below T_g , the rearrangement to oriented crystallites becomes very difficult. Reding and Brown [25] found that in poly(chlorotrifluoroethylene) cracks tend to propagate along the radii of spherulites and sometimes between two spherulites. For this reason, large, well-formed spherulites usually are avoided. Long-term creep tests leading to stress cracking in polyethylene that is above its T_g may involve spherulite growth also. These spherulites eventually reach the size of macroscopic flaws and can act as stress concentrators.

10.9.2 FIBERS

Since fibers consist primarily of oriented crystallites, it is unfair to classify them as heterophase. However, the generalizations of time–temperature superposition that work so well with amorphous polymers do not apply to fibers. Fibers do exhibit viscoelasticity qualitatively like the amorphous polymers. It comes as a surprise to some that J. C. Maxwell, who is best known for his work in electricity and magnetism, should have contributed to the mathematics of viscoelasticity. The story goes that while using a silk thread as the restoring element in a charge-measuring device, Maxwell noticed that the material was not perfectly elastic and exhibited time-dependent effects. He noticed that the material was not perfectly elastic and showed time effects. The model that bears his name was propounded to correlate the real behavior of a fiber.

The high melting temperature desirable in a crystalline fiber can be achieved by using a polar structure. Rayon, nylon, the polyesters, the acrylics, cotton, wool, and silk all contain ester, amide, or hydroxyl groups that can form strong hydrogen bonds. A corollary is that moisture and heat will almost always have a large effect on the physical properties of fibers that is magnified by the large exposed surface area. The terms used in the fiber industry for strength and diameter differ from those in other polymer industries. When one considers a typical fiber or yarn, the actual cross section may be very difficult to describe (see Figure 14.14). However, it is a

very simple exercise to obtain a measure of linear density by weighing a strand of measured length. Also, when a given strand is stretched to the breaking point in tension, the actual force, rather than the force per unit area, is easily measured. A measure of linear density is the **tex** of a fiber, defined as the weight per unit length, in grams per kilometer. The strength is expressed as the **tenacity** defined as stress per unit of linear density, usually Newtons per tex (**N/tex**). The older terms still often encountered are **denier** (grams per 9000 m) and grams (force) per denier. It can be seen that $1 \text{ g/denier} = 0.0883 \text{ N/tex}$. Some authors favor the usage of decinewton/tex, abbreviated as dN/tex, because the figures that result are close to those from the older form ($1 \text{ dN/tex} = 1.13 \text{ g/denier}$).

Example 10.1

The relationship between density, linear density, tenacity, and strength for a round fiber of diameter D can be illustrated. An ordinary nylon fishing line of density 1.14 g/cm^3 with a diameter of 0.850 mm has a rating of 60.0 lb (force) at break.

$$\text{Cross-sectional area} = A = \frac{\pi D^2}{4} = \frac{\pi (0.0850)^2 \text{ cm}^2}{4} = 5.67 \times 10^{-3} \text{ cm}^2$$

$$\begin{aligned} \text{Linear density} &= \rho A 10^5 = (1.14 \text{ g/cm}^3)(5.67 \times 10^{-3} \text{ cm}^2) 10^5 \\ &= 647 \text{ tex (or 5822 denier)} \end{aligned}$$

$$\text{Stress at break} = 60.0 \text{ lb (force)} = 27.2 \text{ kg(force)} = 267 \text{ N}$$

$$\text{Tenacity} = 267/647 = 0.413 \text{ N/tex} = 4.13 \text{ dN/tex} = 4.67 \text{ g/denier}$$

In conventional engineering units, the strength is also given by

$$\text{Strength} = \text{force/area} = 60.0 \text{ lb}/87.9 \times 10^{-5} \text{ in}^2 = 68.3 \times 10^3 \text{ psi} = 471 \text{ MPa}$$

Nylon and silk show a uniform decrease in tenacity with increasing humidity, which is understandable in terms of a weaker crystal lattice with as much as 8% sorbed water competing for the hydrogen bonds (Figure 10.17). Cotton, conversely, increases in tenacity as it sorbs up to 25% moisture, presumably because its cellular structure is then able to distort and allow more molecular chains to support stress along the major axis. Rayon, which is the same as cotton chemically but differs crystallographically, shows the more normal decrease with moisture at high humidities. The strengths indicated are for high-tenacity nylon and rayon. The overall balance of properties does not always make the strongest fiber the best for a particular application. The effect of temperature on rayon and nylon also reflects the relative stability of the hydrogen-bonded structure in each (Figure 10.18).

Fracture studies of highly oriented nylon 6 fibers were performed by Zhurkov and coworkers [27–29]. They found that the stress dependence of the fracture time exhibits characteristics of a kinetic process. The extrapolated stress data at different

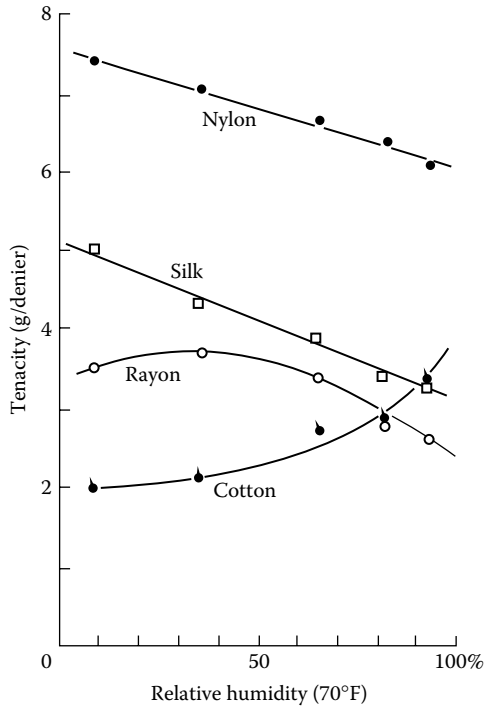


FIGURE 10.17 Strength versus humidity for common fibers. (Data from Zurkhov, S. N., and E. E. Tomashevskii, in A. C. Strickland and R. A. Cook, eds., *Proceedings of Conference on the Physical Basis of Yield and Fracture*, Physical Society, London, 1966, 200.)

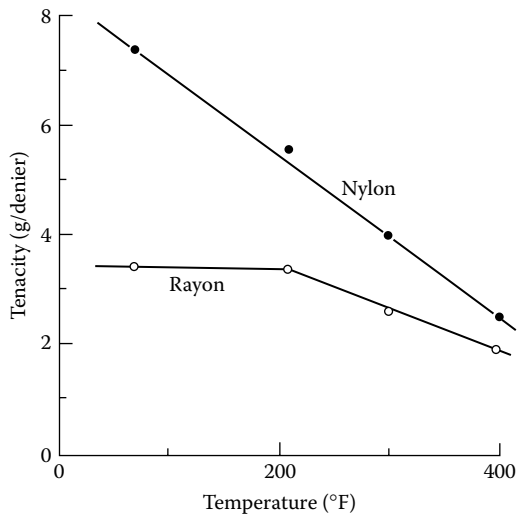


FIGURE 10.18 Strength versus temperature for nylon 6,6 and rayon. (Data from Zurkhov, S. N., and E. E. Tomashevskii, in A. C. Strickland and R. A. Cook, eds., *Proceedings of Conference on the Physical Basis of Yield and Fracture*, Physical Society, London, 1966, 200.)

temperatures all converged to the same maximum stress of 1.67 GPa that would occur at the shortest fracture time of around 10^{-12} s (timescale of bond vibration). This result implies that the fracture process occurs as a consequence of chain scissions and was observed in many highly oriented polymers. It is surmised that nanovoid concentration increases as a function of chain scissions and reaches a critical concentration at the final fracture.

10.9.3 RUBBER

Almost all applications of rubber make use of particulate fillers. Because automotive tires utilize about 70% of all the rubber consumed in the United States and because all tires are reinforced with carbon black, the economic importance of this one class of fillers is large. The term *reinforcement* implies an increase in the magnitude of some ultimate property. However, tensile strength is not the only property that may be reinforced. An improvement in tear strength, abrasion resistance, or fatigue may also justify the use of the term. The typical effect of carbon blacks on the ultimate tensile strength of natural rubber and a styrene-butadiene copolymer is found to be quite different [30]. Natural rubber crystallizes on stretching even though it may be well above its normal melting temperature (see Section 3.4). This is a reversible process in that the crystallites melt on release of the stress. The crystallites act as massive cross-links that spread the concentration of stress that would otherwise be located in a few bonds over a much wider area. Such a material is **self-reinforcing** in that it is stronger at a highly stressed point than elsewhere. At ordinary temperatures, polychloroprene, some polyurethanes, polyisobutylene, and poly(propylene oxide) rubbers also are self-reinforcing, as evidenced by the fact that unfilled, cross-linked polymers of each can be made with tensile strengths of over 20 MPa (2900 psi) with high elongations. Addition of fillers such as carbon black increases tensile strength only slightly for this class of polymers, although tear strength may be improved greatly, and abrasion resistance may be very much improved.

Rubbers that do not crystallize on stretching must be compounded with fillers to attain a tensile strength of more than a few megapascals. The styrene-butadiene rubber typifies this class, which includes PDMS, ethylene-propylene copolymers, and butadiene-acrylonitrile copolymers. It must be emphasized that we are speaking of typical behavior and relative changes in properties. Tensile strength and other properties are affected by cross-link density, temperature, rate of testing, and other compounding ingredients (Section 11.2).

Ultimate properties are sample-dependent properties, so the skill of the person making and testing the sample also becomes a consideration. Despite the many standardized procedures promulgated by the American Society for Testing and Materials (ASTM), among others, it is an incontrovertible fact that an experienced laboratory worker can always produce samples that outperform those put together by a neophyte using the same raw materials and equipment. The importance of the laboratory technician in providing reliable and reproducible characterizations should never be underestimated.

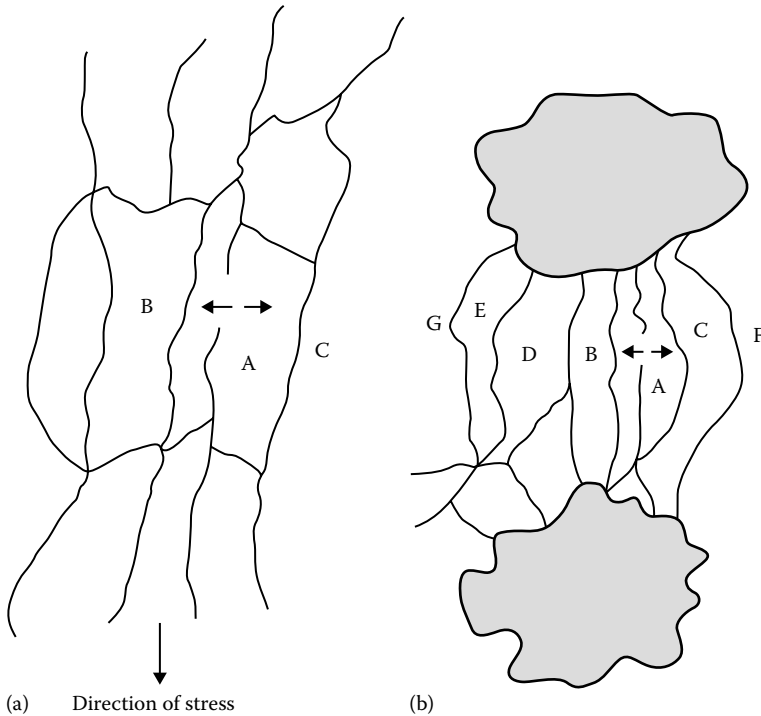


FIGURE 10.19 Stress-sharing mechanism for filler or crystallite reinforcement: (a) polymer under stress without filler particles; (b) with filler particles or crystallites about 10–50 nm in diameter.

An unsophisticated rationalization of the fact that fillers (or crystallites) often increase tensile strength was given by Bueche [31]. In a simple network (Figure 10.19), the breaking of highly oriented strand A shifts the entire stress formerly borne by that strand to its few immediate neighbors. If they are near the stress to rupture themselves already, they may break under the new added load and the flaw will propagate catastrophically. However, with a particle anchoring many strands, the load formerly borne by A can be shared among many strands rather than just the immediate neighbors (Figure 10.19). The filler particle, in addition to acting as a cross-link, has the virtue of extremely high functionality, binding many chains to a rigid surface.

It is important that the filler be bonded to the polymer for this theory to apply. A test case is where polymer and filler are not similar chemically and thus have poor adhesion. Ethylene–propylene terpolymer and finely divided silica make such a system. Under the same conditions of mixing and cross-linking, a gum (unfilled) compound has a tensile strength of less than 1 MPa. A loading of 100 g of silica for 100 g of polymer raises this to 3.6 MPa. However, when the system is stressed, the polymer pulls away from the filler surface, forming **vacuoles**. Such vacuoles have been observed in carbon black-filled systems under the electron microscope. An indirect effect that they have is to cause opacity, a whitening at the stressed point,

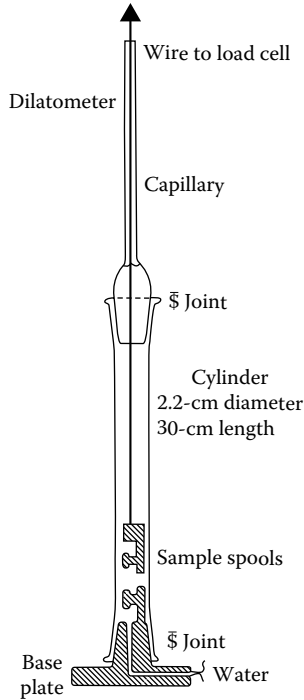
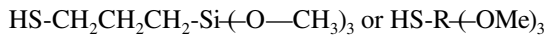


FIGURE 10.20 Dilatometer for measurement of volume during stretching of rubber. (Data from Schwaber, D. M., and F. Rodriguez, *Rubber Plast. Age*, 48, 1081, 1967.)

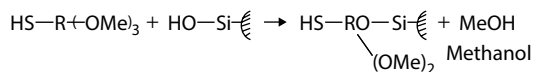
due to the light scattered at the additional interface formed. The net volume of the system must also increase as a result of vacuole formation. By placing a rubber band of the material in a dilatometer filled with water and stretching the band by means of a wire that issues through the capillary, one can measure the stress-strain behavior and the volume change as seen in the capillary section simultaneously (Figure 10.20).

When the polymer-silica band is extended, the volume does increase by a substantial amount (Figure 10.21). However, incorporation of a coupling agent that can react with the filler surface and with the polymer can be used to prevent the vacuole formation. Such a compound is a mercaptosilane:



3-Mercaptopropyltrimethoxysilane

A SiO_2 filler presents between 3 and 5 reactive Si-OH group per square nm of surface, which react with the alkoxy portion of the coupling agent:



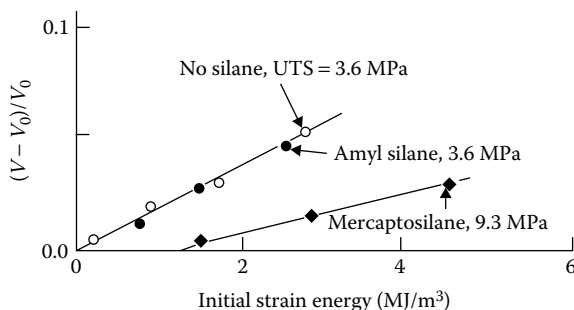
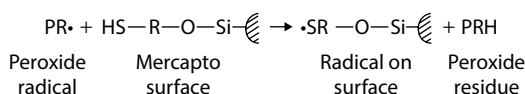


FIGURE 10.21 Change in volume on stretching for silica-filled, peroxide-cross-linked ethylene-propylene terpolymer. UTS, ultimate tensile strength. (Data from Schwaber, D. M., and F. Rodriguez, *Rubber Plast. Age*, 48, 1081, 1967.)

The mercapto portion can be expected to react during cross-linking:



The surface radical may add to a double bond of the polymer as in initiation of polymerization. If the mercapto functionality is absent, as in an amyl silane, no reaction with polymer should occur. It is obvious (Figure 10.21) that the mercaptosilane has increased tensile strength and prevented the filler and polymer from parting at substantial energy inputs (area under the stress-strain curve). The amyl silane has no such effect.

In the carbon black reinforcement of rubber, the chemistry of the carbon black surface is important. The amount and functionality of oxygen, nitrogen, and hydrogen on the surface varies with the method of preparation. Particle size itself is important, the generalization being that the finer the particle size the greater the reinforcement. Matters of ease of incorporation and fabrication as well as cost and other properties enter in to complicate the choice for any one application.

10.9.4 COMPOSITES

Particulate fillers are used also in adhesives and protective coatings. The function in the latter generally is pigmentation rather than reinforcement. Thermoset resins may also be filled, but the most common additive would be fibrous. The term **composites** has been applied to heterophase materials when the dimensions involved approach the macroscopic. Plywood and corrugated paper are two familiar examples. Fibrous glass is used in several forms with polymers. As in the case of silica-reinforced rubber discussed earlier, coupling agents are useful to promote adhesion between the polymer and glass fiber, which is about 50% SiO₂ and 50% oxides of aluminum, calcium, and other cations. The surface contains hydroxyl groups that can react with

alkoxy silanes. The organofunctional alkyl group on the silane is tailored to react with the particular polymer.

Chopped strands of glass of 1–10 mm in length can be incorporated in thermoset or thermoplastic materials about as easily as the particulate fillers. Each strand may be made up of hundreds of individual filaments whose diameter is 5–20 μm . Since the modulus and tensile strength of the glass (Table 10.2) both are much higher than those of the typical plastic, it is not surprising that the stiffness and strength of most plastics can be increased by compounding with glass. In looking at the effect of glass on tensile and flexural strength of nylon 6,6 (Table 10.3), the sacrifice in elongation should not be ignored. The total energy that can be absorbed by the system before failing is much smaller for nylon 6,6 with glass, for example, than without, as indicated by the product of stress and elongation at break. However, the designer of a

TABLE 10.2
Properties of Some Reinforcing Fibers

Reinforcing Fibers	Density (g/cm^3)	Tensile Strength (GPa)	Tensile Modulus (GPa)
Glass (E-glass)	2.5	3.4–4.5	70–85
Carbon from			
Polyacrylmitie	1.7–1.9	2.3–7.1	230–490
Pitch	1.6–2.2	0.8–2.3	38–820
Rayon	1.4–1.5	0.7–1.2	34–55
Aramid (Kevlar)	1.4	2.4–2.8	60–200

Source: Matsuda, H. S., *Chem. Tech.*, 18(5), 310, 1988.

TABLE 10.3
Typical Mechanical Properties of Some Glass-Reinforced Thermoplastics

Polymer	Glass Fiber (% by Weight)	Specific Gravity	Tensile Strength (MPa)	Elongation (%)	Flexural Modulus (GPa)	Impact Strength (J/cm)
Acetal	0	1.41	60	40	2.6	5.0
Acetal	25	1.61	130	3	7.6	9.5
Nylon 6,6	0	1.13	80	60	2.9	4.5
Nylon 6,6	30	1.48	160	2	5.5	12
Polypropylene	0	0.89	35	200	0.9–1.4	6.5
Polypropylene	20	1.04	45	3	3.6	6.0
Poly(ethylene terephthalate)	0	1.34	60	50	2.4–3.1	1.5–3.5
Poly(ethylene terephthalate)	30	1.56	145	6.5	8.6	9.5

Source: Owens-Corning Fiberglass Corporation, Toledo, Ohio.

nylon gear or wheel has no need for high elongation, so that the higher modulus and added strength are obtained at the loss of a property he or she did not particularly cherish from the beginning.

Chopped strands of glass or other rigid fibers several centimeters long can be loosely bound as a mat which is porous and in which the strands are randomly oriented in two dimensions. This form is suitable for impregnation by a liquid **prepolymer**. After polymerization or cross-linking (curing) under pressure, the composite will comprise a network–polymer matrix in which the individual strands are embedded. A woven glass cloth might be used in place of the mat or in combination with it. In this case, there will be a variation in strength with the angle between the axis of the fibers and the direction of stress (Figure 10.22). The **filament-wound structure** represents the ultimate in directional strength (Figure 10.23). With careful fabrication and with the aid of coupling agents, the tensile strength of the glass is approached. In one glass-reinforced, unsaturated polyester–styrene system, the ultimate flexural strength varied with treatment. The resin itself had a strength of only 115 MPa (16.7×10^3 psi) compared to 924 MPa (134×10^3 psi) for an untreated glass–resin filament-wound ring. With proper sizing and with application of a vinyl silane coupling agent, the strength rose to 1.17 GPa (170×10^3 psi). In this last condition, the system was 87% glass by weight

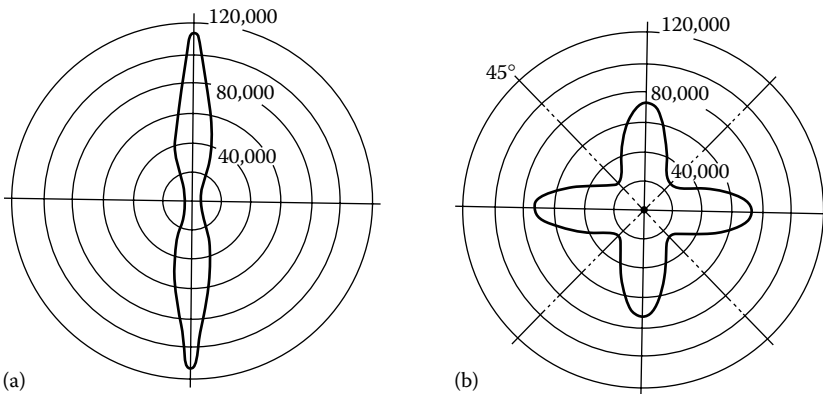


FIGURE 10.22 Tensile strength as a function of direction for fiber-reinforced plastics: (a) unidirectional fibers; (b) cross-ply fibers. 1000 psi = 6.895 MPa. (Data from Liu, X., and Q. Wu, *Macromol. Mater. Eng.*, 287, 180, 2002.)

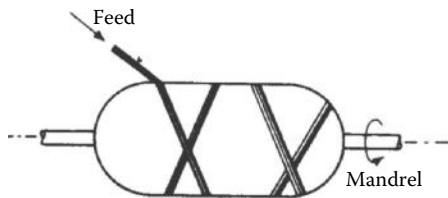


FIGURE 10.23 A cylindrical pressure vessel being fabricated by winding glass filaments over a mandrel.

(75% by volume). In some applications where weight is important, the ratio of the strength to the density of a material becomes a dominant factor. The ratio of strength to density, the **specific strength**, is often expressed in inches when the engineering system of units is used. For the composite just described, a strength of 170×10^3 psi divided by a density of 0.077 lb/in³ yields a specific strength of 2.2×10^6 in. The *cancellation* of pounds mass by pounds force is a delightful peculiarity of the older system of units. In SI units, the specific strength for the same material is 550 kJ/kg. A high-strength steel alloy would have a specific strength about one-third that of the composite [34].

The properties of several other reinforcing fibers are listed in Table 10.2. Carbon fibers are made by pyrolysis of precursor fibers, and their properties differ according to the source. Glass, carbon, and aramid fibers have also been used in composite for applications ranging from golf clubs to automobile transmission shafts. Probably the most often used matrix is some form of epoxy resin. Another kind of composite is the polymer **alloy**. Two polymers of marginal compatibility and widely differing moduli will act somewhat like the glass and polymer, having a rigid, load-bearing element and at the same time a softer, energy-absorbing element. Styrene–butadiene copolymer ($T_g = -50^\circ\text{C}$) is combined with polystyrene ($T_g = 100^\circ\text{C}$) to give a *rubber-reinforced* plastic. In long timescale tests such as ordinary tensile testing, the rigidity and strength of pure polystyrene are approached. However, in a rapid test, such as the Izod impact test, the rubbery portion will deform, absorbing much more energy than the brittle polystyrene would have. The toughness of alloys together with their dimensional stability makes them quite versatile. Some other examples are butadiene–acrylonitrile copolymer in poly(vinyl chloride) and acrylonitrile–butadiene–styrene terpolymer with polycarbonates. Applications include refrigerator door liners, radio and television cabinets, pipe and fittings, and women's shoe heels.

The term **nanocomposite** was originally attached to the class of materials that are characterized by the interaction of polymers with layered silicates. **Polymer–clay nanocomposites** (PCNs) were first introduced by Toyota in 1985 and a nylon 6–PCN was used in auto parts in 1989 [35]. Although minerals such as talc, mica, and nanoparticle carbon black have been used extensively for many years as conventional fillers in plastics and rubber, they were added in high loadings to achieve reinforcement. The advantage of the PCNs is that only a few weight percentage of silicate achieved similar or better property enhancement. The replacement of inorganic cations in the mineral lattice of the colloidal clay bentonite by organic cations had previously been used to convert the hydrophilic minerals into highly efficient organophilic thickeners for paints and similar products [36]. These **organically modified layered silicates** have been shown more recently to improve some mechanical properties of common polymers even when present in very small amounts.

To make a typical nanocomposite, Liu and Wu [37] combined 100 g of a sodium-montmorillonite clay with 30 g of hexadecyltrimethylammonium bromide in 5000 ml of hot water using a homogenizer. After drying and grinding, the treated clay was combined with 20 g of a bisphenol-based epoxy resin (MW = 360) in a dough mixer. The product is termed a co-intercalated clay since the organic moieties now have

replaced the inorganic ions that originally occupied the spaces between the silicate layers. To demonstrate the value of this preparation, the surface-functionalized particles were combined with nylon 6,6 in various proportions using a conventional twin-screw extruder at temperatures ranging from 270°C to 290°C. The final product containing 5% clay (by weight) had a tensile strength of 98 MPa compared to 78 MPa for the polymer with no clay. Likewise, the tensile modulus was 4.7 GPa with the additive compared to 3.0 GPa without it. Other properties improved were impact strength (145 vs. 95 J/m) and heat distortion temperature (140°C vs. 75°C). Clay nanocomposites also can be made by intercalating a monomer followed by polymerization and simple precipitation of polymer and silicate from a suitable solvent. Vaia and Giannelis have taken entropic and energetic factors into account in order to derive a theoretical lattice model for the more versatile melt intercalation process [38]. Although it appears that, so far, only nylon–clay nanocomposites are used in practice, efforts in both academia and industry with carbon nanofibers and other nanofillers are being extensively pursued [39,40].

KEYWORDS

Ultimate strength
Yielding
Toughness
Weibull distribution
Stress concentration
Trousers tear
Simple shear test
Energy to cause rupture
Impact tester
Izod test
Charpy test
Brittleness temperature test
Creep test
Deflection temperature
Environmental stress cracking
Fatigue strength
Equilibrium elastic line
Shear bands
Failure envelope
Crazing
Fracture toughness
Tenacity
Denier
Tex
Reinforcement
Vacuoles
Coupling agent
Composites

Prepolymer
 Filament-wound structure
 Specific strength
 Alloy
 Nanocomposite
 Organically modified layered silicates

PROBLEMS

10.1 Three different rubber compositions give the following strengths in a standard tensile test:

Strength for Compositions (psi)			
Sample	A	B	C
1	3300	2310	1660
2	3250	2310	1600
3	3125	2200	1600
4	3000	2150	1510
5	2850	1990	1325

Are any samples atypical? If a fourth composition were run and gave a value of 2000 psi for a single sample, how confident would you be that this was the average strength?

10.2 For a very large population of samples ($N = 10^4$), what fraction of the population will have a tensile strength greater than $\sigma_b + s$? What fraction will have a tensile strength greater than $\sigma_b - s$ and $\sigma_b - 2s$?

10.3 An amorphous polymer can be approximated by a Maxwell element in which a spring flies apart when it reaches some maximum elongation ϵ_{sb} . Show how this model leads to a typical failure envelope. Why is this model inadequate for a cross-linked styrene-butadiene rubber?

REFERENCES

1. May, W.: *Trans. Inst. Rubber Ind.*, 40:T109 (1964); *Rubber Chem. Technol.*, 37:826 (1964).
2. Hallinan, A. J., Jr.: *J. Qual. Tech.*, 25:85 (1993).
3. Schwartz, P., A. Netravali, and S. Sembach: *Text. Res. J.*, 56:502 (1986).
4. *Book of Standards*, ASTM, Baltimore, MD, 1958, pp. 286, 356.
5. Patti, E., and J. G. Williams: *Polym. Eng. Sci.*, 15:470 (1975).
6. Riddell, M. N., G. P. Koo, and J. L. O'Toole: *Polym. Sci. Eng.*, 6:363 (1966).
7. Smith, T. L.: *J. App. Phys.*, 35:27 (1964).
8. Gent, A.: Strength of elastomers, in J. E. Mark, B. Erman, and F. R. Eirich (eds.), *Science and Technology of Rubber*, 2nd edn., Academic Press, New York, 1994.
9. Andrews, E. H.: chap. 7 in R. N. Haward (ed.): *The Physics of Glassy Polymers*, Wiley, New York, 1973.

10. Kramer, E. J.: chap. 3 in E. H. Andrews (ed.), *Developments in Polymer Fracture—I*, Applied Science Publishers, London, 1979.
11. Kambour, R. P.: *J. Polym. Sci. D*, 7:1 (1973).
12. Williams, J. G.: *Polym. Eng. Sci.*, 17:144 (1977).
13. Sauer, J. A., and K. D. Pae: chap. 7 in H. S. Kaufman and J. J. Falchetta (eds.), *Introduction to Polymer Sciences and Technology*, Wiley, New York, 1977.
14. Lauterwasser, B. D., and E. J. Kramer: *Phil. Mag. A*, 39:469 (1979).
15. Kramer, E. J., and L. L. Berger: in H. H. Kausch (ed.), *Crazing in Polymers*, vol. 2, *Advances in Polymer Science*, vols. 91/92, Springer-Verlag, Berlin, Germany, 1990, p. 1.
16. Brown, H. F., and J. E. Srawley: *ASTM*, STP 410 (1966).
17. Williams, J. G.: *Fracture Mechanics of Polymers*, Wiley, New York, 1984.
18. Hsaio, C. C.: *Phys. Today*, 19:49 (March 1966).
19. Rivlin, R. S., and A. G. Thomas: *J. Polym. Sci.* 10(3):291 (1953).
20. Lake, G. J., and A. G. Thomas: *Proc. Roy. Soc. London, Ser. A*, 300:108 (1967).
21. Gent, A. N., and R. H. Tobias: *J. Polym. Sci. Polym. Phys. Ed.*, 20:2051 (1982).
22. Mazich, K. A., M. A. Samus, C. A. Smith, and G. Rossi: *Macromolecules*, 24:2766 (1991).
23. Genesky, G., and C. Cohen: *Polymer*, 51:4152 (2010).
24. Pritchard, J. E., R. L. McGlamery, and P. J. Boeke: *Mod. Plast.*, 37(2):132 (October 1959).
25. Reding, F. P., and A. Brown: *Ind. Eng. Chem.*, 46:1962 (1954).
26. Zurkhov, S. N., and E. E. Tomashevskii: in A. C. Strickland and R. A. Cook (eds.), *Proceedings of Conference on the Physical Basis of Yield and Fracture*, Physical Society, London, 1966, p. 200.
27. Zurkhov, S. N., V. S. Kukshenko, and A. Slutsker: in P. L. Pratt (ed.), *Fracture*, Chapman & Hall, London, 1969, p. 531.
28. Zurkhov, S. N., and V. E. Korsukov: *J. Polym. Sci. Polym. Phys. Ed.*, 12:385 (1974).
29. *Tensile Stress–Strain Properties of Fibers*, Reprint T-1, Instron Corporation, Canton, MA, 1958.
30. Studebaker, M. L.: chap. 12 in G. Kraus (ed.), *Reinforcement of Elastomers*, Wiley, New York, 1965, pp. 356, 357, 362.
31. Bueche, F.: *Rubber Chem. Technol.*, 32:1269 (1959).
32. Schwaber, D. M., and F. Rodriguez: *Rubber Plast. Age (London)*, 48:1081 (1967).
33. Matsuda, H. S.: *Chem. Tech.*, 18(5):310 (1988).
34. Throckmorton, P. E., H. M. Hickman, and M. F. Browne: *Mod. Plast.*, 41:140 (November 1963).
35. Okada, A., and A. Usuki: *SAE Technical Paper 2007-01-1017*, 2007.
36. Bentone™ Gellants, National Lead Company, 1960.
37. Liu, X., and Q. Wu: *Macromol. Mater. Eng.*, 287:180 (2002).
38. Vaia, R. A., and E. P. Giannelis: *Macromolecules*, 30:1990 (1997).
39. Thomas, S.: *Polymer Composites*, Wiley-VCH Verlag, Somerset, NJ, 2013.
40. Mai, Y. W., and Z.-Z. Yu: *Polymer Nanocomposites*, CRC Press, Boca Raton, FL, 2006.

GENERAL REFERENCES

- Andrews, E. H. (ed.): *Developments in Polymer Fracture—I*, Applied Science Publishers, London, 1979.
- Argon, A. S.: *The Physics of Deformation and Failure of Polymers*, Cambridge University Press, Cambridge, 2013.
- Baumont, P. W. R., J. M. Schultz, and K. Friedrich: *Failure Analysis of Composite Materials*, Technomic, Lancaster, PA, 1990.

- Brostow, W., and R. Corneliussen (eds.): *Failure of Plastics*, Macmillan, New York, 1986.
- Cheremisinoff, N. P. (ed.): *Product Design and Testing of Polymeric Materials*, Dekker, New York, 1990.
- Clegg, D. W., and A. A. Collyer (eds.): *Mechanical Properties of Reinforced Thermoplastics*, Elsevier Applied Science, New York, 1986.
- Enikoloyan, N. S. (ed.): *Filled Polymers I: Science and Technology*, Springer, Secaucus, NJ, 1990.
- Harper, C. A. (ed.): *Handbook of Plastics, Elastomers, and Composites*, 2nd edn., McGraw-Hill, New York, 1992.
- Hertzberg, R. W., and J. A. Manson: *Fatigue of Engineering Plastics*, Academic Press, New York, 1980.
- Kausch, H. H.: *Polymer Fracture*, Springer-Verlag, New York, 1979.
- Kausch, H. H. (ed.): *Crazing in Polymers*, vol. 2, Springer, Secaucus, NJ, 1990.
- Kessler, S. L. (ed.): *Instrumented Impact Testing of Plastics and Composite Materials*, American Society for Testing and Materials, Philadelphia, PA, 1987.
- Kinloch, A. J., and R. J. Young: *Fracture Behaviour of Polymers*, Elsevier Applied Science, New York, 1983.
- Lake, G. J., and A. G. Thomas: chap. 5 in A. N. Gent (ed.), *Engineering with Rubber: How to Design Rubber Component*, 2nd edn., Hanser, Cincinnati, OH, 2001.
- Lipatov, Y.: *Polymer Reinforcement*, ChemTec, Toronto, ON, 1995.
- Mark, J. E., A. Eisenberg, W. W. Graessley, L. Mandelkern, E. T. Samulski, J. L. Koenig, and G. D. Wignall: *Physical Properties of Polymers*, 2nd edn., ACS, Washington, DC, 1993.
- Mark, J. E., B. Erman, and F. R. Eirich (eds.): *Science and Technology of Rubber*, 2nd edn., Academic Press, New York, 1994.
- McCauley, J. W, and V. Weiss (eds.): *Materials Characterization for Systems Performance and Reliability*, Plenum Press, New York, 1986.
- Milewski, J. V., and H. S. Katz (eds.): *Handbook of Reinforcements for Plastics*, Van Nostrand Reinhold, New York, 1987.
- Nielsen, L. E., and R. F Landel: *Mechanical Properties of Polymers and Composites*, 2nd edn., Dekker, New York, 1993.
- Plueddemann, E. P.: *Silane Coupling Agents*, 2nd edn., Plenum Press, New York, 1990.
- Roulin-Moloney, A. C.: *Fractography and Failure Mechanisms of Polymers and Composites*, Elsevier, New York, 1989.
- Schultz, J., and S. Fakirov: *Solid State Behavior of Linear Polyesters and Polyamides*, Prentice Hall, Englewood Cliffs, NJ, 1990.
- Shah, V.: *Handbook of Plastics Testing Technology*, Wiley, New York, 1984.
- Spells, S. J. (ed.): *Characterization of Solid Polymers: New Techniques and Developments*, Chapman & Hall, New York, 1994.
- Turner, S.: *Mechanical Testing of Plastics*, Wiley, New York, 1986.
- Ward, I. M., and D. W. Hadley: *An Introduction to the Mechanical Properties of Solid Polymers*, Wiley, New York, 1993.
- Williams, J. G.: *Stress Analysis of Polymers*, 2nd edn., Halsted-Wiley, New York, 1980.
- Williams, J. G.: *Fracture Mechanics of Polymers*, Wiley, New York, 1984.
- Zachariades, A. E., and R. S. Porter (eds.): *The Strength and Stiffness of Polymers*, Dekker, New York, 1983.

11 Some General Properties of Polymer Systems

11.1 DESIGN CRITERIA

The final judgment on the suitability of a polymer for a given application usually involves a complex combination of properties. Some of these properties are inherent in the physical state of the polymer. A glassy material will not stretch, nor will an uncross-linked, amorphous polymer support a stress indefinitely when it is above its T_g . Some properties are inherent in the chemical structure of the polymer. Hydrolysis, thermal dissociation, and toxicity may be fixed by the reactivity of certain groups within the polymer structure.

In any application, cost is an important factor. The price of the polymer in the form of a powder, latex, solution, or bale is just part of the economic picture. The cost of other ingredients, equipment for fabrication, labor, power, and all the indirect costs, may well overshadow the polymer's share. A first-line tire containing the best rubber sells for 10–20 times the cost of the raw rubber it contains. Even in a much less complicated structure, such as plasticized poly(vinyl chloride) laboratory tubing, the raw material cost may be less than one-tenth of the selling price. Some properties that might be considered for a single application are as follows:

Appearance

Density

Mechanical properties

Durability

Thermal properties

Flammability

Electrical properties

Chemical resistance to acids, bases, solvents, and oils

11.2 COMPOUNDING

The polymer characteristics we have discussed so far are useful guideposts in predicting the behavior of polymers in real applications. However, a lacquer is not an *infinitely dilute* solution, nor is a tire composed of *ideal* rubber. In many useful systems, the polymer is one of several constituents, and perhaps not the most important one.

The largest volume synthetic rubber today, styrene–butadiene rubber (SBR), is a prime example of the complexities of polymer compounding for real life. By **compounding**, we mean the mixing of polymer with other ingredients. In SBR these can be the following:

1. *Reinforcing fillers*. These improve tensile or tear strength. Carbon black and silica are typical.
2. *Inert fillers and pigments*. These may not change the final properties in a desirable direction, but they may make the polymer easier to mold or extrude and also lower in cost. Clay, talc, and calcium carbonate are used.
3. *Plasticizers and lubricants*. Petroleum-based oils, fatty acids, and esters are most often used.
4. *Antioxidants*. These generally act as free-radical *sinks* and thus stop the chain reactions in oxidation.
5. *Curatives*. These are essential to form the network of cross-links that guarantee elasticity rather than flow. Sulfur for unsaturated and peroxides for saturated polymers are used with auxiliaries to control the reaction rate.

One may ask why all this is necessary, since SBR (cross-linked) is almost an ideal rubber as defined earlier. The trouble with this ideal material is that it does not extrude smoothly, it degrades rapidly on exposure to warm air, and it has a tensile strength of about 500 psi (3.5 MPa). Proper compounding changes SBR to a smooth-processing, heat-stable rubber with a tensile strength of over 3000 psi (20 MPa)! However, theoretical equations no longer describe its mechanical behavior. The compounder then must be part scientist, part artist, and part statistician if he or she is to develop optimum properties in a material. It is virtually impossible to optimize all properties at once, so compounders have developed specialized *recipes* for swimsuits, tires, fan belts, tarpaulins, electrical insulation, and so on. Over 9000 such recipes were published between 1948 and 1957 alone!

Figure 11.1 illustrates the means by which compounders have attempted to shorten the work of formulation. A grid of data points is determined experimentally and a *contour map* is prepared. A mathematical counterpart can be obtained with the help of a computer [1]. While such techniques are helpful, the experience of the compounder and his or her willingness to innovate usually determine the effectiveness.

Mixing machines for polymers vary from ball-and-pebble mills that disperse pigments in low-viscosity paints over periods of hours and days to heavy *internal mixers* (see Section 13.3) that may use 1500 hp (about 1100 kW) to disperse 100 kg of carbon black in 200 kg of rubber in about 10 min.

One might divide polymer applications into those that involve extensive compounding and those that do not. Of course, there are many exceptions.

- *Generally compounded extensively*: Rubber, thermosets, adhesives, protective and decorative coatings, and poly(vinyl alcohol) (PVC)
- *Generally not compounded except for minor additives*: Fibers and thermoplastics (PVC is an exception)

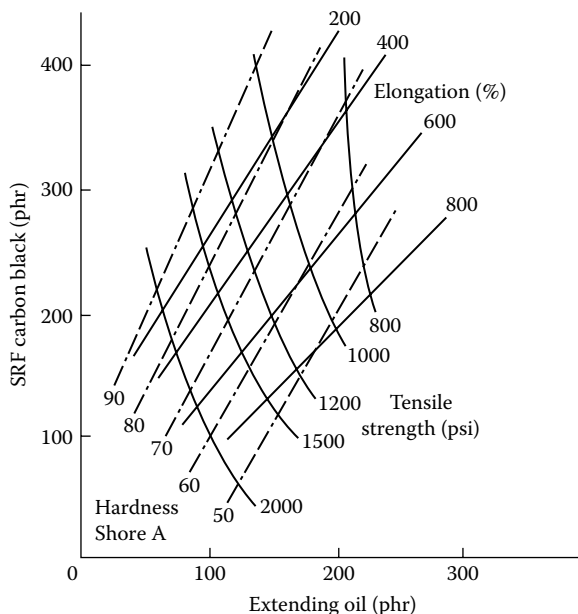


FIGURE 11.1 Typical contour plot to abbreviate compounding data (Vistalon 3708/Ethylene-Propylene Terpolymer, Enjay Chemical Company, 1968). Note that a compound with 200 parts each of oil and filler per 100 parts of rubber by weight (phr) still has a strength of about 1000 psi (7 MPa), quite acceptable for many mechanical applications. The compound, based on a high-molecular-weight ethylene-propylene terpolymer, also contains 5 parts zinc oxide, 1 part stearic acid, 1.5 parts sulfur, 1.5 parts tetramethylthiuram disulfide, and 0.5 parts of benzothiazyl disulfide. Cross-linking takes place at 160°C for 20 min. SRF, Semi-reinforcing furnace.

In the case of fibers, the art of compounding is of less importance than the art of **aftertreatment**. Dyeing, texturing, and fabrication of textiles are complex processes that can obscure the ideal properties of polymers in the final product.

11.3 HARDNESS

The most common measure of **hardness** is the distance a steel ball penetrates into the material under a specified load. A spring-loaded, ball-tipped indenter may be used so that the stress is not a linear function of penetration. Since the measurement is basically a compressive modulus, one expects stiff materials to be hard and flexible materials to be soft. In choosing a material for a gasket, hardness often is the only specification listed.

Surface hardness of coatings and molded objects is also measured by scratch and abrasion resistance. In one simple test for painted surfaces, the hardness can be quantified in terms of the pencil hardness (HB, 4H, etc.) that leaves an indentation. As a rule, polymer systems cannot approach the surface hardness of silica glass, which is itself a highly cross-linked structure. Some highly cross-linked laminates do have scratch resistance nearly like that of glass.

11.4 DENSITY

Polymers and other ingredients of polymer systems are sold on a weight basis. However, in most applications they compete on a volume or strength basis. On a strength–volume basis, a reinforced plastic sheet may prove much more economical for an aircraft seat shell than a metal sheet that sells for a hundred times as much on a pound basis. Several factors that affect density include pressure, temperature, and crystallinity.

Specific volume increases with temperature for polymers, especially where melting occurs. Since a crystal requires a closer packing of molecules than an amorphous glass, density has been used to measure crystallinity. The specific gravity of polyethylene, for example, varies from 0.86 (extrapolated from the melt) when amorphous to 0.98 when highly crystalline at 25°C (see Chapter 3). The effect of pressure is important in molding processes, where the high molding pressures alter the dimensions of a piece from what they will be at 1 atm. High pressures that increase density also increase viscosity, because less *free volume* is available for segmental motion (see Section 7.6). In a molding operation just above the normal melting temperature, a high pressure may induce crystallization, which stops flow altogether [3]. The temperature at which crystallization of high-density polyethylene occurs can be raised by 20°C or more when pressure is raised by about 5000 atm. Polystyrene in the glassy state (35°C) can be compressed less than 0.5% by a pressure of 5000 atm. In the melt state (170°C), the same pressure will compress the polymer about 5%. The compression is time dependent, which is a factor in molding operations where the weight of polymer injected into a mold of fixed volume can be increased by a slower molding cycle. This is important when polypropylene is molded. The additional material introduced after maximum pressure has been reached (a process called **packing**) compensates for the decrease in volume on subsequent cooling and crystallization (see Chapter 14).

The atomic makeup of polymers affects density in much the same way it does for low-molecular-weight compounds (Table 11.1). It should be remembered that a typical linear polymer is 15%–30% more dense than the corresponding monomer.

TABLE 11.1
Specific Gravity of Polymers

Chemical Composition of Polymer	Typical Specific Gravity of Pure Polymer Near Room Temperature
Aliphatic hydrocarbons (polyethylene, polyisoprene)	0.8–1.0
Aromatic hydrocarbons and silicones (polystyrene)	1.0–1.1
Oxygen- and nitrogen-containing polymers (cellulosics, polyesters, polyamides)	1.1–1.4
Chlorinated polymers	1.2–1.8
Fluorinated polymers	1.8–2.2

TABLE 11.2
Specific Gravity of Filled Polymers

Parts by Weight	Polymer	Specific Gravity	Parts by Weight	Filler	Specific Gravity	Final Specific Gravity
100	Natural rubber	0.93	50	Carbon black	1.8	1.1
100	Natural rubber	0.93	100	Calcined clay	2.6	1.4
100	Epoxy resin	1.2	200	Glass fibers	2.5	1.8
100	Phenolic resin	1.3	100	Wood flour	0.9	1.1
100	Polyurethane	1.2	900	Nitrogen		0.12

(parts by volume)

The density of final compounded products usually is the weighted average of the ingredients (provided none are volatilized during fabrication). Some examples are given in Table 11.2.

11.5 THERMAL PROPERTIES

Many polymers have a coefficient of linear thermal expansion α_e in the range of $2\text{--}20 \times 10^{-5} \text{ K}^{-1}$, compared to that for steel which is about 1×10^{-5} . This complicates the design of molds for precision parts and the design of metal inserts in polymer parts. Of course, α_e varies with the state of the polymer, as indicated earlier in comments on the variations of specific volume at T_g and T_m (Section 3.4). Replacement of polymer by less expansile fillers lowers the overall expansion.

Thermal conductivity (k_c) of polymers is uniformly low. Values of $k_c = 0.05\text{--}0.20 \text{ Btu/ft}\cdot\text{h}\cdot^\circ\text{F}$ are common.

$$\frac{242 \text{ Btu}}{\text{ft}\cdot\text{h}\cdot^\circ\text{F}} = \frac{1 \text{ cal}}{\text{cm}\cdot\text{s}\cdot^\circ\text{C}} = \frac{419 \text{ watt}}{\text{m}\cdot^\circ\text{C}}$$

Conductivity is not easily increased. A high concentration of a metal in powder or fiber form can raise it perhaps tenfold. The thermal conductivity of the base resins in Table 11.3 can be increased by aluminum or copper metal. These also increase the electrical conductivity. If low electrical conductivity, of the order of $10^{-16} \text{ (ohm}\cdot\text{cm)}^{-1}$, must be combined with high thermal conductivity, the mixture of aluminas (Table 11.3) will increase the former by a factor of only 1.5 over that of the base epoxy resin, whereas the latter is increased by a factor of 12. Foaming with air or some other gas is used to decrease the thermal conductivity. A foamed polystyrene with a density of 15 kg/m^3 and $k_c = 0.040 \text{ W/m}\cdot^\circ\text{C}$ is useful as insulation for a variety of applications, from picnic baskets to boxcars.

TABLE 11.3
Thermal Conductivity of Various Filled Epoxy Resins

Filler	Volume Percentage of Filler in Compound	Thermal Conductivity (cal/cm·s·°C) × 10 ⁴		
		Filler	Base Resin	Filled Compound
Aluminum, 30 mesh	63	4970	4.7	60.4
Sand, coarse grain	64	28	4.7	23.6
Mica, 325 mesh	24	16	4.7	12.2
Alumina, tabular	53	723	4.7	24.5
Alumina, 325 mesh	53	723	5.4	34.0
Copper powder	60	9180	5.4	39.0
Silica, 325 mesh	39	28	5.4	18.3
Mixture of				
Alumina, tabular (20–30 mesh)	45	723	4.7	58.8
Alumina, 325 mesh	20			

Source: Colleti, W., and L. Rebori, *Insulation*, 11, 27, January 1965.

A **specific heat** of 0.4 ± 0.1 cal/g·°C is typical for unfilled polymers. Composites generally have the average specific heat of the components. This is another property that varies with the physical state of the polymer in relation to T_g and T_m .

The yielding of a polymer under load or its own weight usually occurs at a **deflection temperature** that is in the vicinity of T_g or T_m . The older term, **heat distortion temperature**, is still used in many places.

Flammability is a function of physical form and chemical composition. An air-foamed material or a thin film presents extensive surface for burning compared to a heavy solid section. Chemical composition has the same effect that it has with lower molecular-weight compounds. In general, we can rank uncompounded polymers from most to least flammable as follows:

- Nitrated polymers
- Oxygen-containing polymers
- Hydrocarbon polymers
- Polyamides
- Halogenated polymers
- Phosphorous-containing polymers

Flammability of polymers can be measured objectively by tests that present varying degrees of simulation of real-life situations. For many plastics, the oxygen index method is used, since it requires rather small amounts of material (ASTM D2863). The minimum concentration of oxygen in an oxygen–nitrogen mixture that will just support combustion after the sample is ignited is termed the **oxygen index**, often

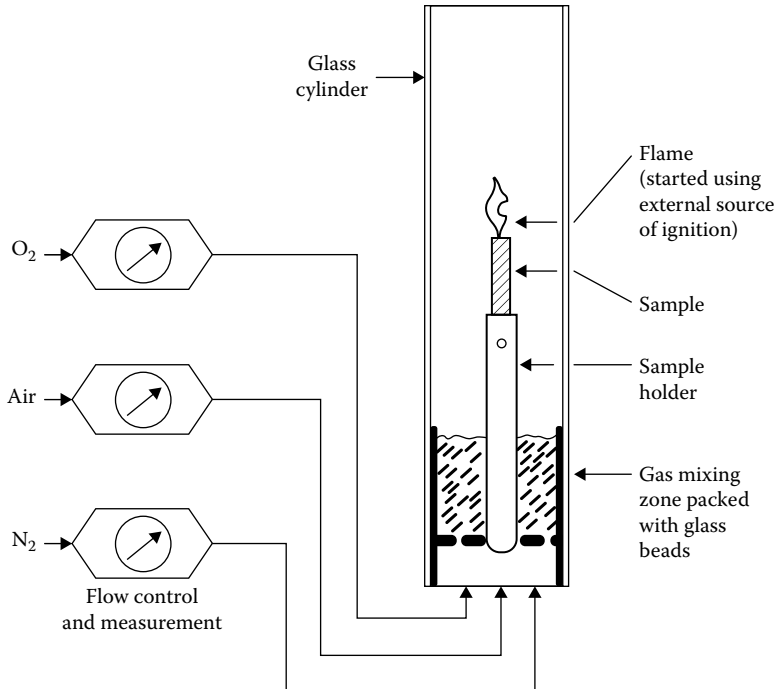


FIGURE 11.2 To measure the flammability, a sample about the size of a birthday cake candle is ignited by an external source such as a propane torch. The percentage of oxygen in a mixture of air with either oxygen or nitrogen that is barely able to sustain burning is called the oxygen index (ASTM D2863). A sample size of $6 \times 3 \times 100$ mm is typical.

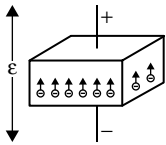
called the **limiting oxygen index (LOI)** (Figure 11.2). Some typical LOI values for pure polymers are 17.4% for polyethylene, 21.5% for nylon 6,6, 29.4% for polycarbonate, 47.0% for poly(vinyl chloride), and 95.0% for poly(tetrafluoroethylene) [5]. Certain plasticizers (phosphate ester and halogenated waxes) and fillers (antimony trioxide combined with chlorinated hydrocarbons) can contribute flame resistance. However, nitroglycerine is an ideal plasticizer for nitrocellulose when the objective is to maintain the flammability of a rocket propellant [6].

11.6 ELECTRICAL PROPERTIES

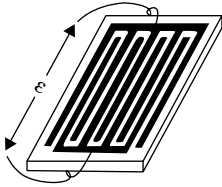
Resistance is a familiar electrical property. The **volume resistivity** ρ_r is the resistance in ohms of a material 1 cm thick, t , and 1 cm² in area, A (Table 11.4). The resistance R of any other configuration is given by

$$R = \frac{\rho_r t}{A} \quad (11.1)$$

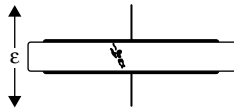
TABLE 11.4
Electrical Properties



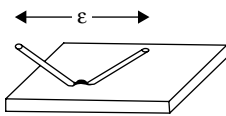
Volume resistivity is the ohmic resistance of the bulk dielectric material measured as though the material were a conductor. The resistance is expressed as the resistance of a cube 1 cm on a side measured between faces. This value is measured according to ASTM D257. It is dependent on temperature, frequency, and voltage, and will vary with the conditioning of the material.



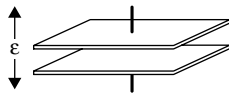
Surface resistivity is defined as the resistance between two electrodes on the surface of an insulating material. It obviously can be measured only on materials having high intrinsic volume resistivity as a reduction of resistance. The units are ohms per square centimeter, and the test method is ASTM D257. The value is dependent on temperature, frequency, and voltage, but is most affected by the humidity- and moisture-conditioning cycles to which it has been subjected, all of which must be given with the value.



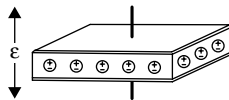
Dielectric strength is defined as the potential per unit of thickness that will cause catastrophic failure of a dielectric material. This value is measured according to ASTM D149. The value is dependent on the method of application of potential the nature of the potential dc or frequency of ac, and the temperature, and it varies with the conditioning of the specimen, all of which must be specified with the value.



Arc resistance is the time in seconds that an arc may play across the surface of a material without rendering it conductive. The property is measured according to ASTM D495 with the low-current, high-voltage arc. The failure may occur by carbonization, heating, and other means, and it is dependent on temperature, frequency, and conditioning, which, as well as the type of failure, must be specified.

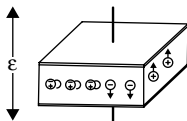


Dielectric constant is defined as the ratio of the capacity of a condenser made with a particular dielectric to the capacity of the same condenser with air as the dielectric. The test method for plastics is ASTM DC150. The value is frequency and temperature dependent, and varies with conditioning, all of which must be specified with the value.



Dissipation factor is the ratio of the real power (in-phase power) to the reactive power (power 90° out of phase). It is related to the power factor, which is the ratio of the real power to the voltage-ampere product by the relation:

$$\text{Dissipation factor} = \frac{\text{power factor}}{\sqrt{1 - \text{power factor}^2}}$$



Loss factor is the product of the dielectric constant and the power factor, and is a measure of signal absorption. The dissipation factor is a measure of the conversion of the reactive power to real power, showing as heat. The mode of heating can be by electron or ion flow and by dipole rotation. It is variable with frequency, temperature, conditioning, and potential. The test method is ASTM D150, and the conditions of the test and frequency must be specified.

Source: Levy, S., *Mod. Plast. Encycl.*, 39(1A), 28, 1961.

In the case of an insulated cable with inside radius R_1 , outside radius R_2 , and length L ,

$$R = \frac{\rho_r}{2\pi L} \ln\left(\frac{R_2}{R_1}\right) \quad (11.2)$$

High values of resistivity are common for organic polymers, 10^{12} – 10^{18} ohm-cm being typical. The reciprocal of the ohm is the siemens, abbreviated as S. Formerly the term mho was used. **Conductivity**, the reciprocal of resistivity, most often is expressed in terms of S/cm. The actual value of resistivity depends on frequency and voltage. It decreases with increasing temperature (Figure 11.3). In any polymer system, fillers or absorbed water may provide conductive paths.

Electrical resistance can be lowered markedly by the addition of conductive fillers. A novel application involves the use of a conductive, elastic silicone rubber, as a metal-free ignition wire in automobiles. Certain carbon blacks impart conductivity:

Carbon Black (Vulcan XC-72, Cabot Corporation, Billerica, MA), Parts by Weight/100 Parts of Rubber	Volume Resistivity (ohm-cm)
0	10^{14}
15	10^4
60	10

For getting a good thermal and electrical contact between a computer chip and its ceramic support plate, a **die attach adhesive** can be used. Silver- or gold-filled epoxy resins are available with conductivities on the order of 10^4 S/cm. A high conductivity (low resistivity) often is desirable to prevent the accumulation of static charges, which can be merely annoying in clothing or carpeting but very dangerous in the presence of a combustible gas. Plastic tile floors for special rooms such as places where computer chips are handled may be compounded with conductive fillers. The reciprocal of resistivity is the conductivity.

An important use for conducting polymers is as shielding against **electromagnetic interference (EMI)**. Almost all devices that use electricity generate some electromagnetic radiation, which include motors, television sets, radios, computers, and light switches. Additionally, some sources of EMI occur naturally as in lightning, static buildup, and discharge from belts, carpets, and clothing. Conductive housings around computers have become necessary because of their particular vulnerability to chance signals that can disrupt stored information. **EMI shielding** can be achieved by coating an appliance housing with a conductive layer of metal or by making the entire housing from a plastic that has had its conductivity increased by a metallic filler.

Several classes of polymers span the range from insulator to conductor [10]. **Polyacetylene** (see also Chapter 16) by itself has a conductivity of about 10^{-8} S/cm, which makes it, classically speaking, an insulator. However, **doping** (complexing) with large amounts of AsF_5 can increase the conductivity to as much as 1000 S/cm. This is still about 1000 times less than the conductivity of copper, silver, or gold. The

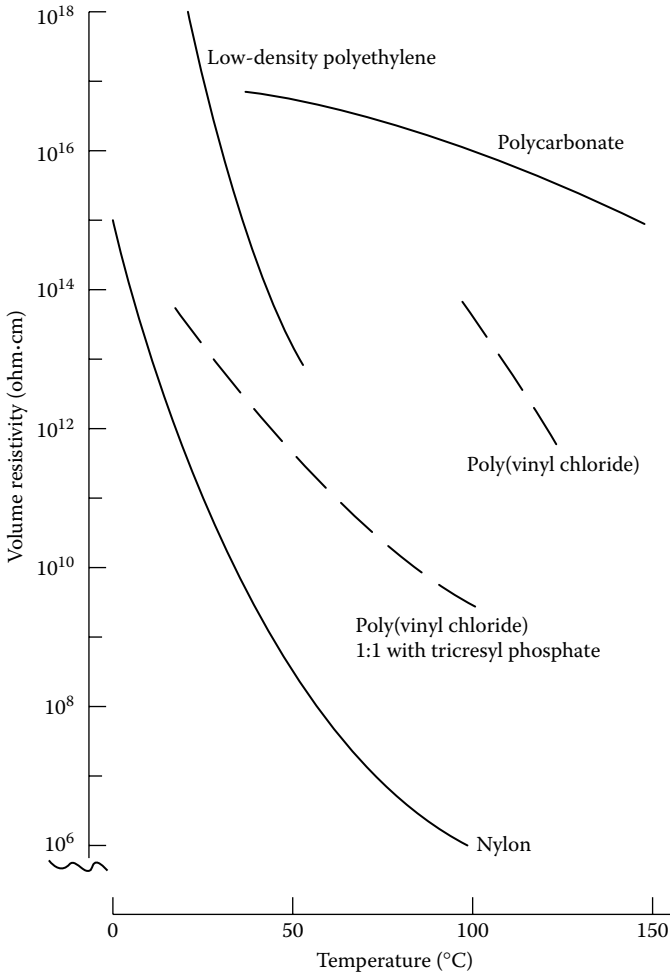


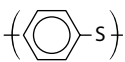
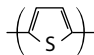


FIGURE 11.3 Most polymers decrease in resistivity as the temperature is raised. (Data from Ball, A. M., *Chem. Eng. Progr.*, 57, 80, 1961; Levy, S., *Mod. Plast. Encycl.*, 39, 28, 1961.)

role of the dopant is either to remove or to add electrons to a conjugated polymer. When an electron is removed, a radical cation (also called **polaron**) is created. Almost all the common polymers being investigated (Table 11.5) are characterized by delocalized electron structures [11]. A. J. Heeger, A. G. MacDiarmid, and H. Shirakawa shared the Nobel Prize in 2000 for their pioneering work on doped polyacetylene. Since polyacetylene itself is not very resistant to oxidation, aromatic polymers with somewhat lesser conducting possibilities can become attractive because of their chemical stability.

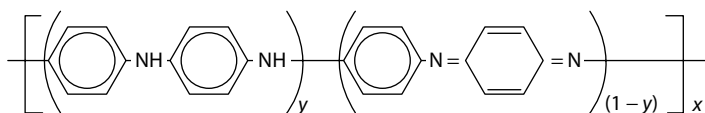
One conductive polymer that has received much attention is **polyaniline** [13]. The popularity of the material can be judged from the fact that, in the four-year period of 1986–1989, almost 1000 papers and patents were published dealing with

TABLE 11.5
Some Typical Organic Polymers That Can Be Doped to Become Electrical Conductors

Polymer Repeat (Monomer) Unit		Dopant		
Name	Structure	Formula	Concentration Equivalents per Double Bond	Conductivity at 25°C (s/cm)
Acetylene (<i>cis</i>)		None	–	1.7×10^{-9}
		AsF ₅	0.28	560
		Na	0.42	25
		Iodine	0.50	360
Phenylene		AsF ₅	0.13	500
		Na	0.19	3000
Phenylene sulfide		AsF ₅	0.33	1
Thiophene		Iodine	0.15	0.1

Source: Cowan, D. O., and F. M. Wiygul, *Chem. Eng. News*, 64(29), 28, 1986, Copyright 1986 American Chemical Society; Gibson, H. W., *Polymer*, 25, 3, 1984.

polyanilines. The average oxidation state of the polymer is characterized by the term $(1 - y)$.



[Polyaniline with reduced y portion and oxidized $(1 - y)$ portion]

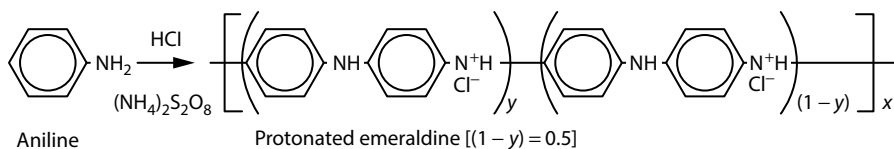
There are three neutral states for polyaniline, which are as follows:

Leucoemeraldine, which is completely reduced, $(1 - y) = 0$

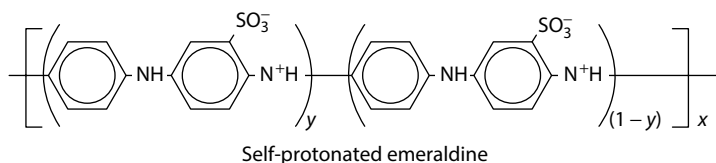
Emeraldine, with $(1 - y) = 0.5$

Pernigraniline, which is completely oxidized, $(1 - y) = 1$

When a compressed powder pellet of the emeraldine form ($M_w = 211,000$) is protonated using 1 M aqueous HCl, a conductivity of 15 S/cm is achieved. This represents an increase in conductivity of about 10^{10} times over the unprotonated polymer. Oxidation of aniline using ammonium persulfate in aqueous HCl gives directly the crystalline, black-green precipitate appropriately called *emeraldine*. The protonated polymer is believed to have a polysemiquinone radical cation structure.



Both fibers and films of the conductive polymer have been made. Self-protonation results from the reaction of fuming sulfuric acid on emeraldine. Unlike the *externally* protonated chain, the conductivity of *self-protonated* emeraldine (in pellet form) remains constant at about 0.1 S/cm over the pH range of 0–7.



Also, this latter polymer dissolves in aqueous sodium hydroxide without decomposition.

Conducting polymers that can be molded by conventional melt processes have been made by attaching side groups to the conjugated polymers of Table 11.5. For example, poly(3-octylthiophene) in the undoped state can be molded by compression or injection just like other thermoplastics [14]. When films of this polymer are doped with FeCl_3 , conductivities of over 10 S/cm are measured. Even a blend of 20 parts of the polymer with 80 parts of an ethylene–vinyl acetate copolymer can be doped with iodine to a conductivity of about 1 S/cm.

Some polymers increase in conductivity on exposure to light (**photoconductive polymers**). Poly(vinyl carbazole) that has been dyed (chemically reacted) with methylene blue is an example [12]. Others, such as poly(vinylidene fluoride), change conductivity in response to pressure (**piezoelectric polymers**). Both of these polymers have obvious applications as sensors in various devices. Other applications for conductive polymers include electrical wiring, switches, and lightweight batteries. A most intriguing possibility is that of molecule-sized components in an integrated circuit. The idea of replacing silicon or gallium arsenide in computer chips by organic semiconductors conjures up the image of a synthetic brain. While a great deal of progress has been made in recent years, much more must be learned about controlling conductivity in polymers before such molecular electronics become reality [15].

Surface resistivity (Table 11.3) is especially important when the fabricated article may be subjected to a high humidity, which can alter the surface physically or chemically to give a lower resistance than the bulk of the material. Circuit boards require a high surface resistivity. Containers for transporting charge-sensitive materials such as computer chips require high surface conductivity.

Dielectric strength (Table 11.3) is analogous to tensile strength. The voltage on a thin slab of material held between two electrodes is increased until catastrophic failure occurs, usually burning a hole completely through the slab. The shape of the

electrodes, the rate of increase of voltage, and the thickness of the slab all affect the dielectric strength. Values of several hundred volts for a thickness of 25 μm are not uncommon.

Arc resistance (Table 11.3) of a polymer that decomposes to volatile products in the presence of an arc usually is better than that of a polymer that is reduced by the arc to conductive carbon. For example, poly(methyl methacrylate) is *nontracking* because it depolymerizes to monomer (see Section 11.3).

Dielectric constant (K_c) has its mechanical analog in the stiffness modulus. Most often it is measured as the ratio of the capacitance of a parallel-plate capacitor with the material as the dielectric to the capacitance of the same capacitor in a vacuum (or air, which is about the same). The **capacitance** C_f in farads for a given plate spacing d in centimeters and plate area A in square centimeters is

$$C_f = \frac{K_c A}{d(3.6\pi 10^{-12})} \quad (11.3)$$

The capacitance is expressed in nanofarads (10^{-9}) or picofarads (10^{-12}). Often the dielectric constant is measured in an alternating field. The reason more electrons can be stored on one plate of the capacitor at a given voltage with a solid dielectric is that electron fields in the material are distorted and counteract the impressed stress. Even a nonpolar polymer such as polyethylene can have valence electrons displaced to give an electronic displacement with a corresponding component of dielectric constant of about 2.0–2.5. A polar polymer such as poly(vinyl chloride) also can respond to an imposed field by actual orientation of molecular segments, provided it is above T_g .

Dissipation factor, $\tan \delta$, is a measure of the hysteresis in charging and discharging a dielectric. One method of measuring it is in a **Schering bridge circuit** (Figure 11.4) [16]. When resistance R_3 and capacitance C_{f4} are adjusted to give a null at the galvanometer, the equivalent series capacitance of the specimen C_{f1} is

$$C_{f1} = C_{f2} \frac{R_4}{R_3} \quad (11.4)$$

and

$$\tan \delta = 2\pi\omega_c C_{f4} R_4 \quad (11.5)$$

where:

- ω_c is the frequency
- C_{f4} is in farads
- R_4 is in ohms

Because C_{f2} and R_4 are usually fixed, adjustment of two dials gives a null and the dial for R_3 can be calibrated directly in capacitance, whereas that for C_{f4} can be calibrated

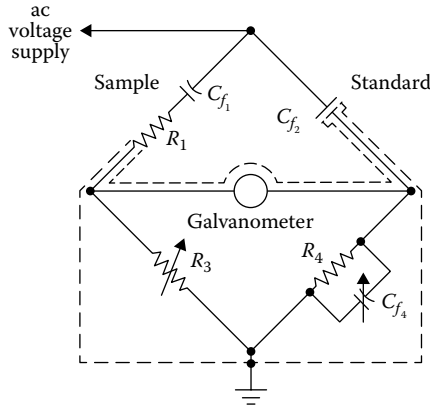


FIGURE 11.4 Simplified Schering bridge. (Data from Botts, S. C., and G. L. Moses, *Insulation*, 7, 19, December 1961.)

directly in dissipation factor. The **power factor**, $\sin \delta$, is sometimes specified, as is the **loss factor**, $K_c \tan \delta$. The power factor is the ratio of the energy loss in a dielectric to the volt-ampere input.

Since the energy loss in a dielectric appears as heat, placing the material in a high-frequency field represents a method of heating a thick section uniformly. This is especially useful because heat conduction often is so poor that bringing a thick piece to a high temperature in an oven might take hours. The relationship between material properties, sample dimensions, and heating source parameters is [17]

$$U_p = 1.77 \times 10^{-13} \pi \omega_c K_c \varepsilon^2 A (\tan \delta) d^{-1} = 10^3 M c_p \frac{dT}{dt} \quad (11.6)$$

where:

- U_p is the power (W)
- ω_c is the frequency (Hz [cycles/s])
- A is the area (cm^2)
- K_c is the dielectric constant
- ε is the voltage (V rms)
- $\tan \delta$ is the dissipation factor
- d is the sample thickness (cm)
- M is the sample mass (kg)
- c_p is the specific heat ($\text{J/g}\cdot^\circ\text{C}$)
- dT/dt is the rate of heating ($^\circ\text{C/s}$)

Example 11.1

Given the following information for a slab of rubber that is to be heated, find dT/dt and U_p .

Source parameters: 10 kV at 1 MHz

Sample properties: $K_c = 3.0$, $\tan \delta = 0.035$, $c_p = 1.67 \text{ J/g}^\circ\text{C}$, density = 0.96 g/cm^3

Sample dimensions: $A = 1610 \text{ cm}^2$, thickness = 2.54 cm

Mass = $1610 \times 2.54 \times 0.96 = 3926 \text{ g} = 3.93 \text{ kg}$

Solution:

$$U_p = \frac{1.77 \times 10^{-13} \pi \times 10^6 \times 3.0 (10^4)^2 (1610) 0.035}{2.54} = 3.7 \times 10^3 \text{ J/s} = 3.7 \text{ kW}$$

$$\frac{dT}{dt} = \frac{3.7 \times 10^3}{10^3 \times 3.93 \times 1.67} = 0.56^\circ\text{C/s}$$

(The actual expected dT/dt would be more like 0.40°C/s after accounting for heat losses at the surfaces.)

Dielectric heating is used for preheating plastics before molding, for welding and sealing plastic film and sheeting, and in woodworking for heating joints. In general, industrial dielectric heating uses frequencies in the range of 1–100 MHz [18]. The common microwave kitchen oven uses frequencies in the range of 915–2450 MHz.

Radio-frequency energy has been used to heat the adhesive between two polymers. In order to fasten a PVC skin to a polypropylene panel for an automobile interior, a water-based adhesive was used that had to be heated to 90°C to be activated [19]. Five seconds of exposure to a 10- to 100-MHz source at 0.03 kW/cm was sufficient to heat the adhesive, which has a high dielectric loss compared to the skin and panel materials. Neither the PVC nor the polypropylene was heated measurably. The radio-frequency heating was 10 times faster than the conductive heating, which would have distorted the plastic skin and panel.

When a signal in the radio-frequency range is to be transmitted over long distances in coaxial cables, the dielectric loss becomes particularly objectionable. The maxima in dielectric loss often parallel the maxima in mechanical loss for the same material. We expect maximum losses at transition temperatures (Figure 11.5) for both electrical and mechanical deformations. In Figure 11.6, we can see the increase in apparent main T_g (about 120°C) with increased frequency in the behavior of $\tan \delta$ for a partly crystalline material.

Just as mechanical fatigue after many alternating cycles causes a polymer to fail at a lower stress than in a rapid single test, so insulation can fatigue under electrical stresses. **Treeing** is a poorly understood phenomenon in which conductive paths extend themselves even at rather low overall voltages because the stress at the needlelike end of the tree is so high (Figure 11.7).

11.7 OPTICAL PROPERTIES

The **transparency** of most unfilled plastics is obvious in thin-film applications such as packaging. However, the number of polymers that are very transparent in thick sections (greater than 0.5 cm thick) is limited. Applications such as eyeglass lenses,

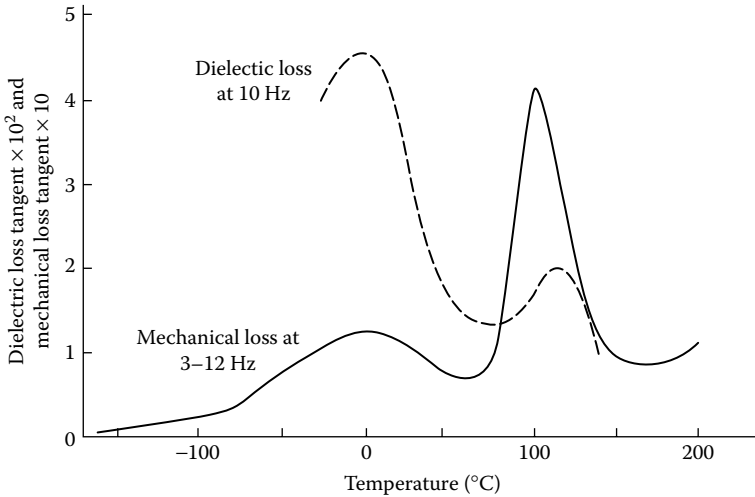


FIGURE 11.5 Mechanical and dielectric loss tangents for poly(chlorotrifluoroethylene). (After Saito, N. et al., in F. Seitz and D. Turnbull, eds., *Solid State Physics*, vol. 14, Academic Press, New York, 1963, p. 420.)

contact lenses, and precision optics all place special demands on the mechanical and optical properties of the materials.

Transparency can be measured as the light intensity transmitted through a given thickness of material using the light of a specified wavelength. Some relative values for useful optical polymers are shown in Table 11.6 along with other properties. The **index of refraction** (n) is the ratio of the velocity of light of a specific wavelength in a vacuum to the velocity of the same light in the material. The common wavelengths used are 486 nm (F line), 589 nm (D *sodium* line), and 651 nm (C line). The change in n with wavelength is summarized by the **dispersion** (D_s) or the **Abbé value**, defined as

$$D_s = \frac{n_F - n_C}{n_D - 1} = \frac{100}{\text{Abbé value}} \quad (11.7)$$

The first three materials listed in Table 11.6 are amorphous thermoplastics. CR-39 is a cross-linked, amorphous network (see Section 17.2). Most highly crystalline polymers are hazy because the crystals and the amorphous phases do not have the same index of refraction and light is scattered at the interfaces. Poly(4-methyl-1-pentene) is unusual in that the two phases have nearly the same index of refraction. The haze in crystalline polymers can be reduced if the crystallite size is very small. A sorbitol-based **clarifier** for polypropylene is bis(3,4-dimethyldibenzylidene) [25]. It acts as a **nucleating agent** and makes it possible to produce a water bottle with *PET-like clarity*.

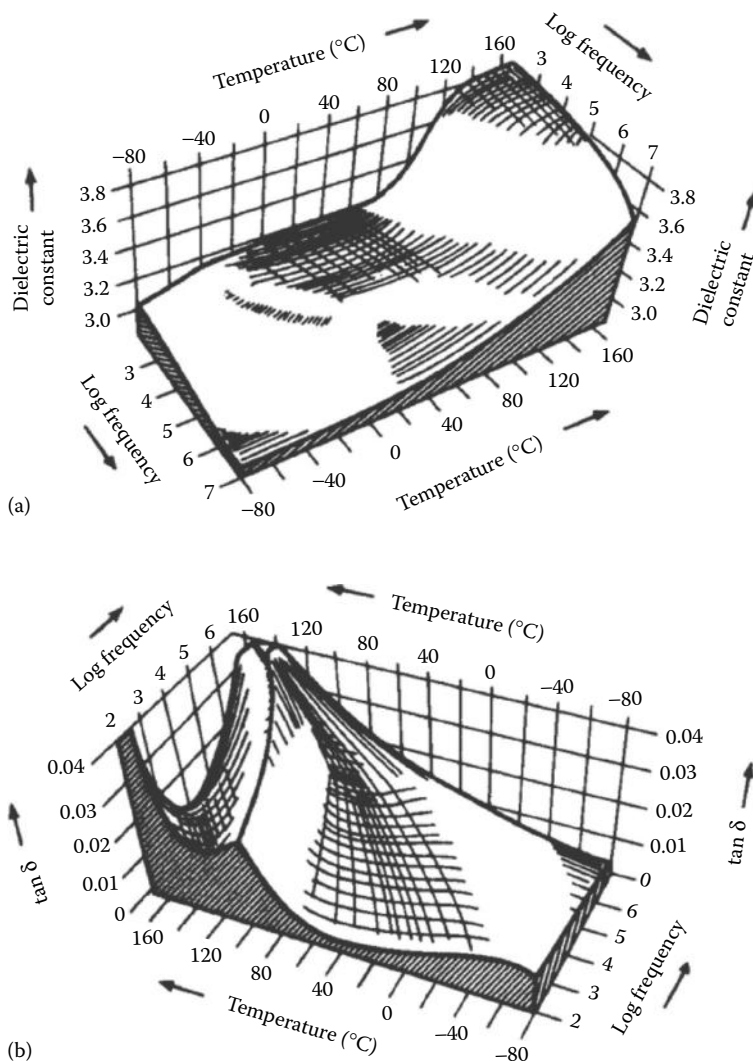


FIGURE 11.6 (a) Dielectric constant and (b) loss tangent as functions of frequency and temperature for poly(ethylene terephthalate). (Data from Reddish, W., *Trans. Faraday Soc.*, 46, 459, 1950; redrawn by A. J. Curtis in J. B. Birks and J. H. Schulman, eds., *Progress in Dielectrics*, vol. 2, Wiley, New York, 1960, p. 37.)

The comparison of densities of various plastics with crown glass shows why eye-glass lenses of plastic are popular despite their generally lower scratch resistance. Contact lenses that are hydrophilic may be made from copolymers of hydroxyethyl methacrylate (see Section 16.6). Transparency is high since the lenses are essentially cross-linked gels containing 40%–70% water.

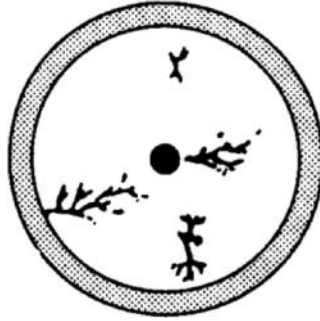


FIGURE 11.7 Treeing in high-voltage cable. (Data from Olyphant, M., Jr., *Insulation*, 9, 23, March 1963; 9, 33, November 1963.)

TABLE 11.6
Selected Optical Properties

Material	Index of Refraction			Abbé Value	Density (g/cm ³)	Transparency (%)	Linear Expansion Coefficient (°C) ⁻¹
	n_F	n_D	n_C				
Poly(methyl methacrylate)	1.497	1.491	1.489	57.2	1.19	92	65×10^{-6}
Polystyrene	1.604	1.590	1.584	30.8	1.10	88	63×10^{-6}
Polycarbonate	1.593	1.586	1.576	34.0	1.20	89	68×10^{-6}
Poly(4-methyl-1-pentene)	–	1.466	–	56.4	0.83	–	117×10^{-6}
Allyl diglycol carbonate (CR-39™)	–	1.499	–	57.8	1.32	–	120×10^{-6}
Crown glass	–	1.525	–	–	2.53	–	–

Source: Mills, N. J., *Enc. Polym. Sci. & Eng.*, 10, 496, 1987; Teyssier, C., and C. Tribastone, *Lasers Optronics*, 12, 50, 1990.

11.8 DIFFUSION IN POLYMERS

Diffusion of small molecules in or out of polymers plays important roles in many processes and applications of polymers. A few examples encountered in various chapters include membrane and fiber formation processes, paints, coatings, diffusion of plasticizers and additives, and environmental crazing.

The simplest law of diffusion in one dimension of a gas or liquid (denoted as species 1) in a polymer (species 2) is the empirical **Fick's law** of diffusion given by

$$J_1 = -D_{12} \frac{dc_1}{dx} \quad (11.8)$$

where:

J_1 is the flux of 1 (mol/cm².s or g/cm².s)

D_{12} is called the **binary diffusion** coefficient of the 1–2 binary mixture (cm²/s)

c_1 is the concentration of 1 in 2 (mol/cm³ or in g/cm³)

In the simple form of Equation 11.8, c_1 varies only in the x -direction. Unless one is in very dilute conditions, D_{12} is not a constant because Equation 1.8 is a simplification of the more accurate representation of the flux that should be written as [26]

$$J_1 = -L_1 \frac{d\mu_1}{dx} \quad (11.9)$$

where:

L_1 is a transport coefficient

μ_1 is the chemical potential of species 1 in 2

The above equation correctly implies that the driving force of a flux is the gradient of chemical potential that represent the gradient of the Gibbs free energy of 1 and not just the gradient in concentration. Both L_1 and μ_1 depend on c_1 , temperature, and pressure (or stress). At constant T and p , one can express Equation 11.9 as

$$J_1 = -L_1 \left(\frac{\partial \mu_1}{\partial c_1} \right)_{T,p} \frac{dc_1}{dx} = -D_{12}(c_1) \frac{dc_1}{dx} \quad (11.10)$$

such that one recovers Fick's law with a concentration-dependent diffusion coefficient. The dependence of μ_1 on c_1 can be obtained, for example, from the Flory–Huggins theory (Equation 3.6).

For gas diffusion in polymers such as in the application of polymeric membranes for gas separation, the concentrations of the gases in the polymer are usually quite small and the simple Fick's law (Equation 11.8) is applicable. In that case, the concentration c_1 can be expressed as

$$c_1 = Sp \quad (11.11)$$

where:

S is the equilibrium solubility of the gas in the polymer

p is the partial pressure of the gas

Equation 11.8 can now be written as

$$J_1 = -D_{12}S \frac{dp}{dx} = -P_{12} \frac{dp}{dx} \quad (11.12)$$

where:

$P_{12} = D_{12}S$ represents the **permeability coefficient** of gas 1 in polymer 2

Because of the practical importance of this parameter, an extensive list of references for values of P_{12} of many polymer–gas systems has been compiled [27]. The ratio of permeabilities of two gases in a membrane defines the **selectivity** of the membrane.

For a liquid solvent diffusing in a polymer melt or an elastomer, the concentration of the solvent in the polymer can vary greatly such that the binary diffusion coefficient is often observed to increase exponentially with solvent concentration [28]. One also needs to be careful in distinguishing the binary diffusion coefficient in the generalized Fick's law of Equation 11.10 with **tracer diffusion** of tagged molecules [29].

It was found in several glassy polymers that a gas permeability depended on p and that sorption must be interpreted as occurring by two mechanisms: the usual Fickian mechanism described above and a second mechanism resembling a Langmuir-type isotherm. The total concentration in the polymer in this **dual-sorption model** was then expressed as [30]

$$c_1 = c_{1a} + c_{1b} = Sp + c'_b \frac{bp}{1 + bp} \quad (11.13)$$

where:

c'_b is an additional sorption capacity possibly caused by nanovoids in the glassy polymer
 b is a constant

In the permeation of a pure gas across a thin film with an upstream pressure p , a zero downstream pressure, and assuming a simplified flux expression of the form:

$$J_1 = -D_{1a}S \frac{dc_{1a}}{dx} - D_{1b} \frac{dc_{1b}}{dx} \quad (11.14)$$

it was shown that the permeability coefficient is expressed as [30]

$$P = D_{1a}S \left[1 + \frac{FK}{1 + bp} \right] \quad (11.15)$$

where:

$$F = D_{1b}/D_{1a}$$

$$K = c'_b b / s$$

Equation 11.15 can account for the observed pressure dependence of P of several gas–polymer systems. Other models for the interpretation of the pressure dependence of P have also been formulated. It is easy to realize that the empirical second term on the right-hand side of Equation 11.14 must arise from a fundamental dependence of the chemical potential on inherent stresses in the glassy polymer and lead to a new contribution to the flux in addition to that due to the concentration dependence of the chemical potential.

The above case of dual-sorption model can be considered a special case of what has been termed **anomalous diffusion** in polymers. Because organic vapors or liquids can interact strongly with a polymer and cause it to swell, an extreme case of anomalous diffusion occurs when the mass uptake (time-integrated flux) into the polymer is totally controlled by the stress gradient between the swollen and unswollen regions rather than by the concentration gradient. This was first characterized by Alfrey and coworkers [31] and referred to as **case II diffusion**. Fickian diffusion leads to an initial mass uptake of a polymer film or sheet exposed to a swelling solvent that follows the expression [32]:

$$M(t) = \text{const} \times t^{1/2} \quad (11.16)$$

where:

t is the time

A solvent diffusion is defined anomalous whenever the exponent of t in Equation 11.16 is greater than $1/2$, and in the case where the exponent is unity, it is considered a case II diffusion. For that latter case, a sharp concentration front separates the equilibrium swollen region from the glassy inner core and advances at a constant velocity where the flux is controlled by the stress gradient [33].

KEYWORDS

Compounding
Posttreatment
Aftertreatment
Hardness
Packing
Thermal conductivity
Specific heat
Deflection temperature
Heat distortion temperature
Flammability
Oxygen index
Limiting oxygen index
Resistance
Volume resistivity
Conductivity
Die attach adhesive
Electromagnetic interference (EMI)
EMI shielding
Polyacetylene
Doping
Polaron
Polyaniline

Leucoemeraldine
Emeraldine
Pernigraniline
Photoconductive polymer
Piezoelectric polymer
Surface resistivity
Dielectric strength
Arc resistance
Dielectric constant
Capacitance
Dissipation factor
Schering bridge circuit
Power factor
Loss factor
Dielectric heating
Treeing
Transparency
Index of refraction
Dispersion
Abbé value
Clarifier
Nucleating agent
Fick's law
Binary diffusion
Permeability coefficient
Membrane selectivity
Dual-sorption mode
Tracer diffusion
Anomalous diffusion
Case II diffusion

PROBLEMS

- 11.1** A major concern of civic organizations and local governments has been the disposal of plastic containers. Bleach bottles and other blow-molded containers from polyolefins are lighter than water and litter the shores of our lakes and streams. What are some ways in which the problem might be attacked?
- 11.2** What loading of wood flour (Table 11.2) in parts by weight is needed to make a polystyrene (density of 1.043 g/cm^3) composite with the same density as water at 20°C (0.997 g/cm^3)? What loading of clay (Table 11.2) in polyisobutylene (density of 0.859 g/cm^3) would give the same resulting density?
- 11.3** A silicone rubber cable is made with a conductive carbon-loaded core and an unfilled layer of insulation. If the resistivities are 10 and 10^{14} ohm-cm, respectively, and the outer and inner diameters of the insulation are 0.3 and 0.1 cm, respectively, how fast will the cable heat up when a potential of 100 V dc is impressed on a cable of 10 m long? Assume the heat capacity of

both filled and unfilled rubber to be $0.5 \text{ cal/cm}^3\cdot^\circ\text{C}$ and the cable to behave adiabatically.

- 11.4** If carbon black costs \$0.30/lb, oil \$0.15/lb, and EPDM rubber \$0.95/lb, what is the most economical composition (based on Figure 11.1) that will yield a tensile strength of 1500 psi with a hardness of at least 50 (shore A)? The carbon black has a density of 1.80 g/cm^3 , the oil of 0.92 g/cm^3 , and the rubber of 0.86 g/cm^3 .
- 11.5** A wheel is cast from low-molecular-weight polystyrene in a stainless-steel mold at 300°F . If the mold is 5 in in diameter at 75°F , what is the diameter of the plastic wheel at 75°F ? Linear coefficients of thermal expansion are $1 \times 10^{-5} (\text{ }^\circ\text{F})^{-1}$ for steel and $1.5 \times 10^{-4} (\text{ }^\circ\text{F})^{-1}$ for the polymer.
- 11.6** A cubic container with a volume of 1.00 m^3 is to be insulated so that a charge of 100 kg of ice will take at least 20 h to melt completely. What thickness of insulation is required? Urethane foam insulation k is $0.050 \text{ W/m}\cdot^\circ\text{C}$; heat of fusion for water is 79.7 cal/g (334 kJ/kg); average outside temperature is 40°C .
- 11.7** The thermal resistance of pipe insulation can be calculated from Equation 11.2 if the reciprocal of the thermal conductivity of the insulation is taken as the equivalent of the electrical resistance. The rate of energy loss from the pipe then is directly proportional to the temperature difference and inversely proportional to the thermal *resistance*. If a 6.0-cm-diameter pipe carries chilled water at an average velocity of 3.0 m/s over a distance of 1.50 km, what thickness of insulation (same k as in Problem 11.6) is needed to keep the temperature from rising more than 2.0°C when the inside temperature is 10°C and the outside is 65°C ? Neglect all resistance except that of the insulation.
- 11.8** (a) Use the concentration and flux expressions of the dual-sorption model to derive Equation 11.15 for the permeability coefficient for the case of zero gas pressure downstream.
 (b) The following parameters have been used to fit the absorption data for CO_2 and CH_4 in a polysulfone membrane:

	$S_a (\text{cm}^3[\text{STP}]/\text{cm}^3\cdot\text{atm})$	$D_a (10^8 \text{ cm}^2/\text{s})$	$C'_c (\text{cm}^3[\text{STP}]/\text{cm}^3)$	$b (\text{atm}^{-1})$	f
CO_2	0.664	4.40	17.90	0.326	0.105
CH_4	0.161	0.44	9.86	0.070	0.349

Note: STP, Standard Temperature and Pressure.

Calculate the permeabilities of the pure components in the membrane, taking $P = 10 \text{ atm}$.

- (c) For a gas mixture, account must be taken that some fraction of the sorption capacity in the *nanovoids* is occupied by each solute such that

$$c_i = S_i p + c'_b b_i p / (1 + \sum b_j p)$$

and

$$Q_i = S_i D_{i,a} \{1 + F_i K_i / (1 + \sum b_j p)\}$$

What are the permeabilities of the CO₂ and CH₄ in the membrane for the gas mixture where each component partial pressure is 10 atm and what is the selectivity of the membrane? Compare with the ideal selectivity obtained based on the permeabilities of the pure gases in (b). Discuss the results.

REFERENCES

- Bertsch, P. F.: Graphical Analysis of Compounding Data, BL-355, Elastomer Chemical Department, E. I. du Pont de Nemours and Co., June 1959.
- Vistalon 3708/Ethylene-Propylene Terpolymer, Enjay Chemical Company, 1968.
- Matsuoka, S., and B. Maxwell: *J. Polym. Sci.*, 32:131 (1958).
- Colleti, W., and L. Rebori: *Insulation*, 11:27 (1965).
- Khanna, Y. P., and E. M. Pearce: Flammability of polymers, in R. W. Tess and G. W. Poehlein (eds.), *Applied Polymer Science*, 2nd edn., ACS, Washington, DC, 1985.
- Ball, A. M.: *Chem. Eng. Progr.*, 57(9):80 (1961).
- Levy, S.: *Mod. Plast. Encycl.*, 39(1A):28 (1961).
- Mathes, K. N.: chap. 7 in E. Baer (ed.), *Engineering Design for Plastics*, Reinhold, New York, 1964.
- Davies, J., R. Miller, and W. Busse: *J. Am. Chem. Soc.*, 63:361 (1941).
- Seanor, D. A. (ed.): *Electrical Properties of Polymers*, Academic Press, New York, 1982.
- Cowan, D. O., and F. M. Wiygul: *Chem. Eng. News*, 64(29):28 (1986).
- Gibson, H. W.: *Polymer*, 25:3 (1984).
- MacDiarmid, A. G., and A. J. Epstein: chap. 5 in W. R. Salaneck, D. T. Clark, and E. J. Samuelson (eds.), *Science and Applications of Conducting Polymers*, A. Hilger, Philadelphia, PA, 1991, p. 117.
- Osterholm, J. E., J. Laakso, and P. Nyholm: *Polym. Preprints*, 30(1):145 (1989).
- Carter, F. L. (ed.): *Molecular Electronic Devices II*, Dekker, New York, 1987.
- Botts, S. C., and G. L. Moses: *Insulation*, 7:19 (1961).
- Kloeffler, R. G.: *Industrial Electronics and Control*, Wiley, New York, 1949, pp. 318, 326.
- Wilson, J. L.: chap. 1 in J. I. Kroschwitz (ed.), *Encyclopedia of Polymer Science and Engineering*, 2nd edn., vol. 5, 1987.
- Li, C., K. A. Chaffin, and A. Thakore: *Adhesives Age*, 37(7):18 (1994).
- Saito, N., K. Okano, S Iwayanagi, and T. Hideshima: in F. Seitz and D. Turnbull (eds.), *Solid State Physics*, vol. 14, Academic Press, New York, 1963, p. 420.
- Reddish, W.: *Trans. Faraday Soc.*, 46:459 (1950); redrawn by A. J. Curtis in J. B. Birks and J. H. Schulman (eds.): *Progress in Dielectrics*, vol. 2, Wiley, New York, 1960, p. 37.
- Olyphant, M., Jr.: *Insulation*, 9:23 (March 1963); 9:33 (November 1963).
- Mills, N. J.: *Enc. Polym. Sci. and Eng.*, 10:496 (1987).
- Teyssier, C., and C. Tribastone: *Lasers Optronics*, 12:50 (1990).
- Leaversuch, R. D.: *Mod. Plast.*, 75(8):50 (August 1998).
- Fitts, D. D.: *Non-Equilibrium Thermodynamics*, chap. 1, McGraw-Hill, New York, 1962.
- Stern, S. A., B. Krishnakumar, and S. M. Nadakatti: chap. 50 in J. E. Mark (ed.), *Physical Properties of Polymer Handbook*, American Institute of Physics Press, Woodbury, NY, 1996.
- Fujita, H.: chap. 3 in J. Crank and G. S. Park (eds.), *Diffusion in Polymers*, Academic Press, London, 1968.
- Cussler, E. L.: *Diffusion: Mass Transfer in Fluid Systems*, chap. 7, Cambridge University Press, New York, 2009.

30. Paul, D. R., and W. J. Koros: *J. Polym. Sci. Phys. Ed.* 14:675 (1976).
31. Alfrey, Jr., T. E., E. F. Gurnee, and W. G. Lloyd: *J. Polym. Sci. Part C: Polymer Symposia*, 12:249 (1966).
32. Crank, J.: *The Mathematics of Diffusion*, chap. 3, 2nd edn., Oxford University Press, London, 1975.
33. Thomas, N. L., and A. H. Windle: *Polymer*, 19:255 (1978).

GENERAL REFERENCES

- Andrade, J. D. (ed.): *Polymer Surface Dynamics*, Plenum Press, New York, 1988.
- Aseeva, R. M., and G. E. Zaikov: *Combustion of Polymer Materials*, Macmillan, New York, 1986.
- Baijal, M. D. (ed.): *Plastics Polymer Science and Technology*, Wiley, New York, 1982.
- Bakshi, A. K.: *Electronic Structure of Biopolymers and Highly Conducting Polymers*, Wiley, New York, 1993.
- Barlow, F. W.: *Rubber Compounding*, Dekker, New York, 1988.
- Bhattacharya, S. K. (ed.): *Metal-Filled Polymers*, Dekker, New York, 1986.
- Bhowmick, A. K., and H. L. Stephens (eds.): *Handbook of Elastomers*, Dekker, New York, 1988.
- Birley, A. W., and M. J. Scott: *Plastics Materials Properties and Applications*, 2nd edn., Chapman & Hall, New York, 1988.
- Bloor, D., and R. R. Chance (eds.): *Polydiacetylenes: Synthesis, Structure, and Electronic Properties*, Martinus Nijhoff, Leiden, The Netherlands, 1985.
- Blythe, A. R.: *Electrical Properties of Polymers*, Cambridge University Press, Cambridge, 1979.
- Brostow, W., and A.A. Collyer (eds.): *Electrical, Magnetic and Optical Effects on Polymer Liquid Crystals and Their Use in Optoelectronics*, Chapman & Hall, New York, 1997.
- Chan, C.-M.: *Polymer Surface Modification and Characterization*, Hanser Gardner, Cincinnati, OH, 1993.
- Comyn, J. (ed.): *Polymer Permeability*, Elsevier Applied Science, New York, 1985.
- Cotts, D. B., and Z. Reyes: *Electrically Conductive Organic Polymers for Advanced Applications*, Noyes Data, Park Ridge, NJ, 1986.
- Farges, J.-P. (ed): *Organic Conductors: Fundamentals and Applications*, Dekker, New York, 1994.
- National Research Council. Fire Safety Aspects of Polymeric Materials, 10 vols., Technomic, Lancaster, PA, 1977–1981.
- Ford, W. I. (ed.): *Polymeric Reagents and Catalysts*, ACS, Washington, DC, 1986.
- Goosey, M. I.: *Plastics for Electronics*, Elsevier Applied Science, New York, 1985.
- Grand, A. F., and C. A. Wilkie (eds.): *Fire Retardancy of Polymeric Materials*, Dekker, New York, 2000.
- Hall, C.: *Polymer Materials*, Halsted-Wiley, New York, 1981.
- Hartwig, G.: *Polymer Properties at Room and Cryogenic Temperatures*, Plenum Press, New York, 1995.
- Hilado, C. J.: *Flammability Handbook for Plastics*, 5th edn., Technomic, Lancaster, PA, 1998.
- Hornak, L. A. (ed.): *Polymers for Lightwave and Integrated Optics*, Dekker, New York, 1995.
- Hunter, R. S.: *The Measurement of Appearance*, Wiley, New York, 1975.
- Ikada, Y., and Y. Uyama: *Lubricating Polymer Surfaces*, Technomic, Lancaster, PA, 1993.
- Ishida, H., and J. L. Koenig (eds.): *Composite Interfaces*, Elsevier Applied Science, New York, 1986.
- Ishida, H., and G. Kumar (eds.): *Molecular Characterization of Composite Interfaces*, Plenum Press, New York, 1985.

- Kitihara, A., and A. Watanabe (eds.): *Electrical Phenomena at Interfaces*, Dekker, New York, 1984.
- Kovarskii, A. L. (ed.): *High-Pressure Chemistry and Physics of Polymers*, CRC Press, Boca Raton, FL, 1994.
- Kroschwitz, I. I. (ed.): *Electrical and Electronic Properties of Polymers: A State-of-the-Art Compendium*, Wiley, New York, 1988.
- Ku, C. C., and R. Liepins: *Electrical Properties of Polymers*, Macmillan, New York, 1987.
- Kuryla, W. C., and A. J. Papa: *Flame Retardancy of Polymeric Materials*, 5 vols., Dekker, New York, 1973–1979.
- Kuzmany, H., M. Mehring, and S. Roth (eds.): *Electronic Properties of Polymers and Related Compounds*, Springer-Verlag, New York, 1985.
- Labana, S. S., and R. A. Dickie (eds.): *Characterization of Highly Cross-linked Polymers*, ACS, Washington, DC, 1984.
- Ladik, J. J.: *Quantum Theory of Polymers as Solids: Part 1, Quantum Theory of Polymeric Electronic Structure*, Plenum Press, New York, 1987.
- Landrock, A. H.: *Handbook of Plastics Flammability and Combustion Technology*, Noyes Data, Park Ridge, NJ, 1983.
- Linford, R. G. (ed.): *Electrochemical Science and Technology of Polymers*, Elsevier Applied Science, New York, 1987.
- Lutz, J. T. (ed.): *Thermoplastic Polymer Additives*, Dekker, New York, 1988.
- Lyons, M.: *Electroactive Polymer Electrochemistry, Part 1: Fundamentals*, Plenum Press, New York, 1994.
- Margolis, J. M.: *Conductive Polymers and Plastics*, Chapman & Hall, New York, 1989.
- Mark, J. E., A. Eisenberg, W. W. Graessley, L. Mandelkern, E. T. Samulski, I. L. Koenig, and G. D. Wignall: *Physical Properties of Polymers*, 2nd edn., ACS, Washington, DC, 1993.
- McCauley, J. W., and V. Weiss (eds.): *Materials Characterization for Systems Performance and Reliability*, Plenum Press, New York, 1986.
- Meeten, G. H. (ed.): *Optimal Properties of Polymers*, Elsevier Applied Science, New York, 1986.
- Moiseev, Y. V., and G. E. Zaikov: *Chemical Resistance of Polymers in Aggressive Media*, Plenum Press, New York, 1987.
- Mort, J., and G. Pfister (eds.): *Electronic Properties of Polymers*, Wiley, New York, 1982.
- Nalwa, H. S. (ed.): *Handbook of Organic Conductive Molecules and Polymers*, 4 vols., Wiley, New York, 1997.
- Nelson, G. L. (ed.): *Fire and Polymers: Hazards Identification and Prevention*, ACS, Washington, DC, 1990.
- Nielsen, L. E., and R. F. Landel: *Mechanical Properties of Polymers and Composites*, 2nd edn., Dekker, New York, 1993.
- Ohm, R. F. (ed.): *The Vanderbilt Rubber Handbook*, 13th edn., R. T. Vanderbilt Co., Norwalk, CT, 1990.
- Prasad, P. N., and D. R. Ulrich (eds.): *Nonlinear Optical and Electroactive Polymers*, Plenum Press, New York, 1988.
- Scrosati, B. (ed.): *Applications of Electroactive Polymers*, Chapman & Hall, New York, 1993.
- Seanor, D. A. (ed.): *Electrical Properties of Polymers*, Academic Press, New York, 1982.
- Schopf, G., and G. Kossmehl: *Polythiophenes—Electrically Conductive Polymers*, Springer, New York, 1997.
- Schweitzer, P. A.: *Mechanical and Corrosion-Resistant Properties of Plastics and Elastomers*, Dekker, New York, 2000.
- Sichel, E. K. (ed.): *Carbon-Black Polymer Composites: The Physics of Electrically Conducting Composites*, Dekker, New York, 1982.
- Simpson, W. G. G. (ed.): *Plastics Surface and Finish*, CRC Press, Boca Raton, FL, 1994.

- Skotheim, T. A. (ed.): *Electroresponsive Molecular and Polymeric Systems*, Vol. II, Dekker, New York, 1991.
- Skotheim, T. A., R. L. Elsenbaumer, and J. R. Reynolds (eds.): *Handbook of Conducting Polymers*, Dekker, New York, 1997.
- Thomas, E. L. (ed.): *Materials Science and Technology. Structure and Properties of Polymers*, VCH, New York, 1993.
- Troitzsch, J.: *International Plastics Flammability Handbook*, Macmillan, New York, 1983.
- Urban, M. W., and C. D. Craver (eds.): *Structure–Property Relations in Polymers: Spectroscopy and Performance*, ACS, Washington, DC, 1993.
- van Krevelen, D. W.: *Properties of Polymers*, Elsevier, Amsterdam, The Netherlands, 1990.
- Vieth, W. R.: *Diffusion in and Through Polymers*, Hanser Gardner, Cincinnati, OH, 1991.
- Wallace, G. G., G. M. Spinks, and P. R. Teasdale: *Conductive Electroactive Polymers—Intelligent Materials Systems*, Technomic, Lancaster, PA, 1996.
- Wise, D. L., G. E. Wnek, D. J. Trantolo, T. M. Cooper, and J. D. Gresser (eds.): *Electrical and Optical Polymer Systems—Fundamentals, Methods, and Applications*, Dekker, New York, 1998.
- Zoller, P., and D. J. Walsh: *Standard Pressure–Volume–Temperature Data for Polymers*, Technomic, Lancaster, PA, 1995.

12 Degradation and Stabilization of Polymer Systems

12.1 INTRODUCTION

Degradation of a polymer may occur during synthesis or in the fabrication process. For example, high-speed stirring, turbulent flow, and ultrasonic irradiation of polymer solutions can cause changes in polymer structure. The predominant response is a decrease in molecular weight, because recombination of radicals is not favored in solution. Similarly, when a melt is masticated at high shear rates, a great deal of mechanical energy is dissipated in the system. Recombination of radicals can take place, as well as some other reactions depending on circumstances.

This chapter focuses on degradation as any undesirable change in properties that occurs after a material has been put into service. We can categorize degradation as affecting the polymer alone chemically or the polymer system physically or chemically. Examples of the latter include the wearing of tires, the loss of plasticizer from a polymer system by evaporation or migration, or the separation of polymer from rigid fillers leaving voids at the interface. To counteract the degradation of systems by various agencies, certain stabilizers can be added that interfere with specific reactions. In this chapter, we shall consider the agencies that produce degradation, the physical and chemical consequences of degradation, and some of the preventative measures that can be taken to diminish degradation.

12.2 DEGRADING AGENCIES

The agencies that bring about changes in polymers seldom act individually except in the laboratory. We can speak about the separate effects of heat, radiation, chemicals, and mechanical energy, but in practice, all four may be present to some degree. **Weathering** is a term used for outdoor exposure. During weathering, sunlight causes damage by ultraviolet (UV) radiation absorption as well as by heat built up by infrared absorption. Atmospheric oxygen and moisture provide the most common chemical attacks. And, of course, a sample may be mounted in a strained condition to approximate a real application.

In the laboratory, the degrading agencies are usually separated. However, in some accelerated weathering tests, a high-intensity mercury or xenon arc, water spray, and temperature and humidity control may be used. Outdoor exposure itself

varies considerably from one location to another. Samples may be sent to Florida for sunlight and salt spray exposure and to Los Angeles for the effects of smog and ozone.

12.2.1 ELECTROMAGNETIC WAVES

The **spectrum of electromagnetic waves** ranges from radio waves of long wavelength λ and low frequency ω_c to gamma rays (and cosmic rays) of short wavelength (Figure 12.1). Certain radio bands are familiar because of specific applications. Almost all uses are regulated by government agencies. Industrial dielectric heating uses 1–100 MHz, microwave ovens use 915–2450 MHz, and television and frequency

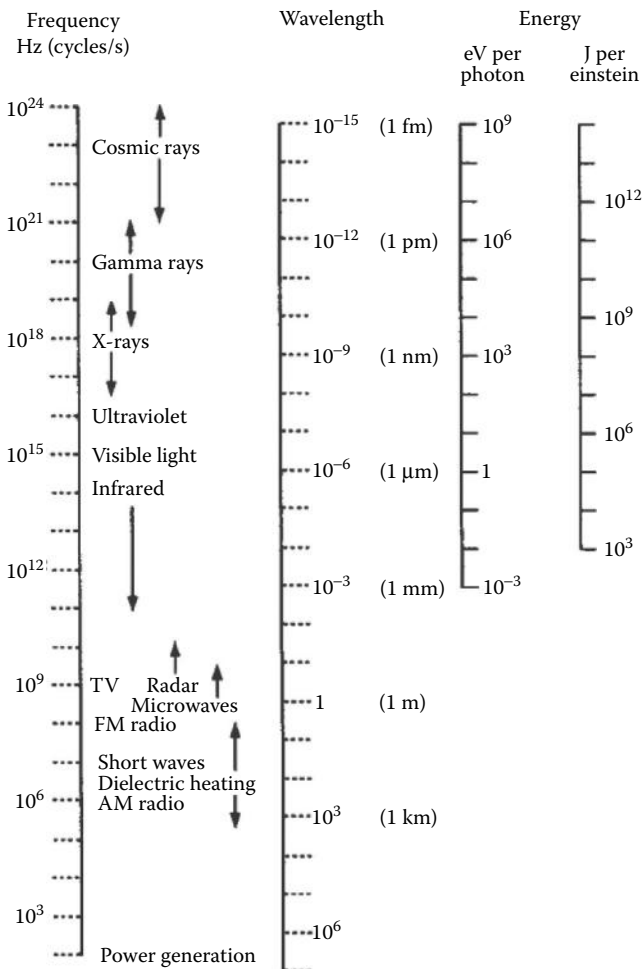


FIGURE 12.1 The electromagnetic spectrum. The positions of various applications are approximate, since definitions of the various bands are not exact. AM, amplitude modulation; FM, frequency modulation.

amplitude (FM) broadcasting bands generally fall between 100 and 915 MHz. Radars can use a wide range of frequencies, with most applications between 200 and 35,000 MHz [1].

The energy associated with a quantum or photon (the smallest unit of radiant energy) is simply related to the wavelength or frequency through Planck's constant h and the velocity of light c . Some interrelations are

$$\lambda\omega_c = c = 3.00 \times 10^8 \text{ m/s} \quad (12.1)$$

$$\frac{\text{Energy}}{\omega_c} = h = 6.62 \times 10^{-34} \text{ J} \cdot \text{s} \quad (12.2)$$

For example, light with a wavelength of 100 nm has a frequency of 3.0×10^{15} Hz. A commonly used mercury germicidal lamp has a strong UV emission at 254 nm, corresponding to a frequency of 1.18×10^{15} Hz. The energy associated with 6.02×10^{23} (Avogadro's number) photons is called an **einstein**. Thus, the energy in each einstein of 254-nm radiation is 470 kJ or 11 kcal. Since the average bond energy of the carbon-carbon bond is 83 kcal/mol, it is apparent that absorption of UV light is more likely to cause chemical reactions in polymers than visible light (400–700 nm).

It can be seen from the distribution curve for the spectral energy of sunlight (Figure 12.2) that most of the energy is in the visible region of 380–800 nm. At the high-energy end, about $\lambda = 350$ nm, the energy per einstein approaches or exceeds the dissociation energy of a number of covalent bonds found in polymers (see Section 2.1). Of course, the incident light may be transmitted, refracted, or scattered. However, if it is absorbed locally in a polymer, dissociation may result, most commonly with the loss of a hydrogen atom, leaving a free radical on the chain. When UV light or gamma radiation is used, such dissociations become much more probable.

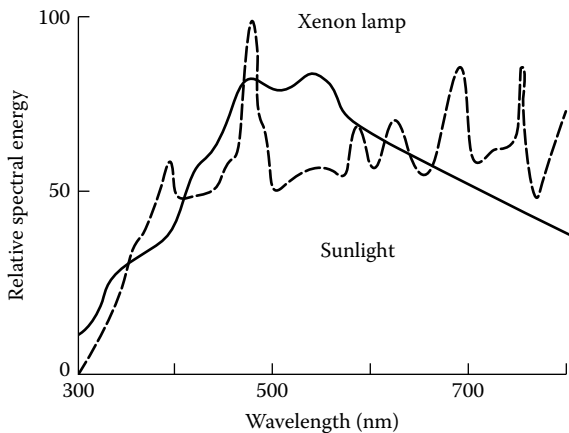


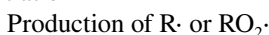
FIGURE 12.2 Spectral energy distribution. (Data from Brighton, C. A., in S. H. Pinner (ed.), *Weathering and Degradation of Plastics*, Columbine, London, 1966, p. 51.)

The penetrating depth also increases with increasing frequency. At the other end of the sun's spectrum, the infrared rays may be absorbed with no great localized energy but with a general increase in temperature. In the laboratory, sunlight may be simulated by a xenon lamp having the spectrum shown in Figure 12.2.

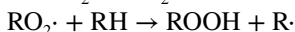
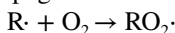
12.2.2 OXIDATION

Almost all materials are subject to attack by oxygen and water when they are put into use. The process of **oxidation** is so important that it is worth noting a few generalizations that have been made concerning it. Oxidation typically is a chain process [3]:

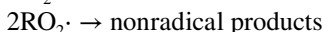
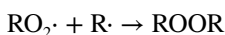
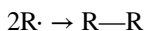
Initiation



Propagation



Termination



The end products are seen to consist of covalent carbon-carbon bonds, peroxide bonds, and perhaps hydroperoxides. Although any carbon-hydrogen bond might be attacked, positions that are especially vulnerable are those adjacent to a double bond, adjacent to an ether linkage, or on a tertiary carbon (indicated by arrows in Table 12.1).

In the laboratory, the effects of oxidation are measured by several kinds of tests. Most commonly, samples of a polymer system are aged at an elevated temperature in nitrogen, air, or oxygen. For air, a circulating air oven is used. Exposure to atmospheres of pure nitrogen or oxygen is usually carried out in sealed tubes (bombs). Changes in structure may be inferred from changes in physical properties such as tensile modulus or elongation at break on aging. A more sophisticated measure of change is found in infrared spectral analysis. An actual measurement of the amount of oxygen absorbed is useful in studying the mechanism of oxidation. The four stages of oxidation found by Shelton and coworkers are shown in Figure 12.3 [4]. The first two stages may not always be discernible in uninhibited polymers. In addition, one can measure the concentration of specific groups as a function of time or oxygen content (Figure 12.4).

12.2.3 MOISTURE AND SOLVENTS

Moisture can be important by acting as a plasticizer or by acting as a solvent for some catalytic species. UV light and oxygen usually will have different effects on a polymer depending on the humidity. This is especially true when the polymer has a

TABLE 12.1
Relative Rates of Oxidation versus Structure

Structure	Relative Rate of Oxidation
$\begin{array}{c} \text{CH}_3 \\ \\ (-\text{CH}_2-\text{C}=\text{CH}-\text{CH}_2-) \\ \uparrow \qquad \qquad \uparrow \end{array}$	10
$\begin{array}{c} \text{CH}_3 \\ \\ (-\text{CH}_2-\text{CH}-\text{O}-) \\ \uparrow \end{array}$	9
$\begin{array}{c} \text{CH}_3 \\ \\ (-\text{CH}_2-\text{CH}-) \\ \uparrow \end{array}$	6.5
$\begin{array}{c} \text{CH}_3 \\ \\ \text{O} \\ \\ (-\text{CH}_2-\text{CH}-) \\ \uparrow \end{array}$	2.8
$\begin{array}{c} \text{CH}_3\text{CH}_2-\text{O} \\ \\ \text{C}=\text{O} \\ \\ -\text{CH}_2-\text{CH}- \\ \uparrow \end{array}$	1.4

Source: Norling, P. M. et al., *Rubber Chem. Technol.*, 38, 1298, 1965.

substantial equilibrium moisture content. Nylon, for example, may vary in moisture content from 0% to over 5% depending on the humidity. Polyethylene has almost no moisture content. Water penetration at the interface between two phases can cause delamination. The hydroxyl-rich surface of glass has a great affinity for water, so that a layer of organic polymer on the glass may be displaced by water at high humidities. Another reaction with water is **hydrolysis**. In some of the first commercial urethane foams (1950s), it was found that the urea, urethane, and aliphatic ester groups were rather easily hydrolyzed, the rate increasing with pH above 7. Present-day formulations are much less sensitive, but water remains a factor to be considered whenever hydrolyzable groups are part of the polymeric structure.

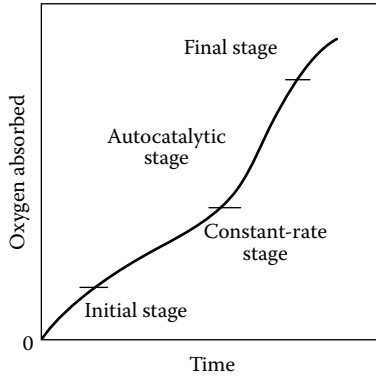


FIGURE 12.3 Four stages observed in oxygen absorption measurements on elastomers. (Data from Shelton, J. R., *Rubber Chem. Technol.* 30, 1251, 1957.)

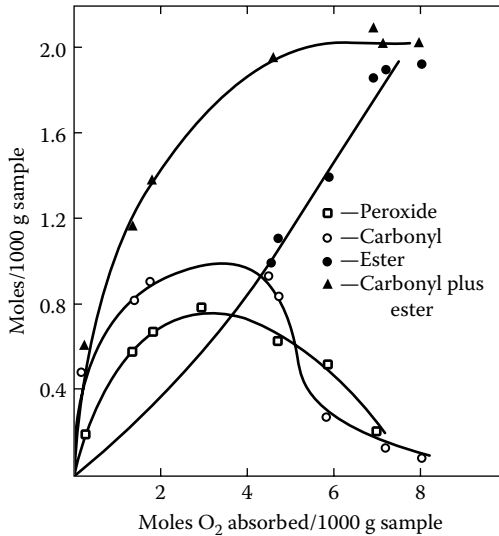


FIGURE 12.4 Concentration of peroxide, carbonyl, and ester groups as a function of oxygen absorbed in oxidation of 5-phenyl-2-pentene at 80°C. (Data from Shelton, J. R., *Rubber Chem. Technol.* 30, 1251, 1957.)

The overall view of chemical attack is impossible to condense because of the wide variety of chemical species and polymeric substrates. Whenever a polymer is suggested as a material of construction in a chemical plant, a thorough consideration of resistance to specific chemicals is desirable. Polymeric pipes and tank liners are used for acids and alkalis, oxidizing and reducing agents, and all kinds of organic reactants. In each case the most economical solution will be specific, because factors of initial cost, versatility, and maintenance may enter in.

Swelling of rubbers and polymers was mentioned in Section 2.6 in connection with cohesive energy density. Solvents may extract portions of polymer systems, for example, the plasticizer from a poly(vinyl chloride)-based system. Swelling at a surface may set up a stress that is relieved by crazing. Craze lines consist of oriented polymers. They become evident by their opacity in glassy polymers stressed by a purely mechanical couple or by surface absorption of a liquid (see Section 10.7).

12.2.4 BIOLOGICAL DEGRADATION

Biological attack includes alteration of polymer systems by fungi, bacteria, and larger species such as insects and animals [5–7]. Most naturally occurring polymers are biodegradable in their native state. Cellulose and natural rubber can be digested by a variety of microorganisms. Modified natural materials such as acetylated cellulose or sulfur-cross-linked rubber are quite resistant. Totally synthetic polymers, by and large, are resistant to attack when the molecular weight exceeds about 5000. Some heterochain polymers, including polyesters, polyamides, and polyurethanes, may degrade in the presence of some microorganisms [5,8]. In this degradation, the microorganisms are using the material as a source of nutriment, with enzymes generated by the organism acting as catalysts. For many years the polymer industries emphasized the development of bioresistant materials. The treatment of cellulose to prevent deterioration of cotton and linen in tropical climates has long been a major effort of military suppliers. Since the early 1970s, public concern for the problem of litter as part of the overall problem of waste disposal has led to the development of polymers that are biodegradable (see Chapter 15). However, with the exception of a few applications, the ability and cost of marketing polymer containers that are truly biodegradable remain a challenge. Waste disposal is also discussed in Chapter 15.

12.3 PHASE SEPARATION AND INTERFACIAL FAILURE

The degradation of a polymer system can take place without changing the structure of the whole polymer. The two common cases are where one component of a homogeneous mixture is extracted and where components of a heterogeneous assembly delaminate.

The extraction of plasticizer from a poly(vinyl chloride) composition does not always require organic solvents. Soapy water in contact long enough with a vinyl foam or film can extract low-molecular-weight plasticizers. A plasticized vinyl shower curtain has the added hazard of relatively high temperatures and humidities to contend with. When a plasticized system is put in physical contact with an unplasticized polymer, the plasticizer may migrate from one to the other. In designing a vinyl coaster, for example, the compounder must take into account the possibility that the item may be placed on a lacquered surface. **Plasticizer migration** of dioctyl phthalate from the poly(vinyl chloride) coaster to a cellulose acetate surface will result in a softened, marred appearance.

Delamination is most easily illustrated by interior plywood soaked in water. The layers may come apart as the wood swells and the phenolic adhesive is displaced. The same sort of failure can occur in a glass fiber-reinforced thermoset. Coupling agents that tie glass and polymer together can decrease this tendency (see Section 10.9). Systems that delaminate are not always so obviously heterogeneous to start. It is common for large injection-molded polyethylene objects to develop a layer that peels off in the vicinity of the injection point on aging. Apparently the crystal structure of the polymer layer that is adjacent to the wall is different from the structure developed in the polymer that cools more slowly away from the wall. The interface between the two represents a plane of weakness that is aggravated by warm water and detergent. A continued change in crystalline structure at the interface may be taking place.

Mechanical stresses often induce delamination. A tensile stress in loaded rubber may tear polymer from filler, leaving vacuoles (Section 10.9). Constant flexing of a conveyor belt or a tire may pull rubber from the fibrous reinforcement.

12.4 POLYMER DEGRADATION

As far as the polymers themselves are concerned, many types of *degradation* can be predicted from the reactions of low-molecular-weight analogs. Oxidation of hydrocarbons and hydrolysis of esters are often more easily studied in such analogs. However, as we consider the response of polymers that are predominantly linear, we can categorize degradation as affecting the backbone of the polymer or the side chains on the polymer. Some degradative effects are scission, depolymerization, cross-linking, bond changes, and side-group changes. All except the last one can affect the backbone of the polymer.

12.4.1 CHAIN SCISSION

In **chain scission** we have bonds broken at random within the polymer molecules. Each breaking bond creates another molecule and lowers the average molecular weight. Hydrolysis of a polyester is a good example of a **random scission** process, since the susceptibility of a bond does not depend greatly on molecular size. If we take a polyester of number-average degree of polymerization x_n in a dilute solution of concentration c (g/dl), we can calculate the concentration of ester bonds in the system $[\phi]$:

$$[\phi] = N - m \quad (12.3)$$

where:

N is the concentration of monomer units in solution

m is the concentration of polymer molecules

Such that

$$N = \frac{c}{M_0} \quad (12.4)$$

and

$$m = \frac{N}{x_n} \quad (12.5)$$

where:

M_0 is the molecular weight of a monomer unit

If we postulate that the rate of bond disappearance (hydrolysis) with time $(-d[\phi]/dt)$ will be proportional to the bond concentration $[\phi]$, we have a first-order expression:

$$-\frac{d[\phi]}{dt} = k[\phi] = k(N - m) = \frac{kc(1 - 1/x_n)}{M_0} \quad (12.6)$$

Also, differentiating the second and fourth expressions of the above equation yields

$$-k \frac{d[\phi]}{dt} = \frac{kc}{M_0} \frac{d(1/x_n)}{dt} \quad (12.7)$$

But in Equation 12.6, $1/x_n$ is much less than 1; therefore, the reaction is *pseudo-zero-order* and

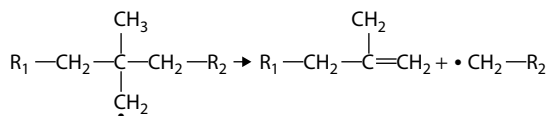
$$\frac{c}{M_0} \frac{d(1/x_n)}{dt} = \frac{kc(1 - 1/x_n)}{M_0} = \frac{kc}{M_0} \quad (12.8)$$

If we start at time $t = 0$ and $x_n = (x_n)_0$, we get the change in number-average degree of polymerization as a function of time:

$$\frac{1}{x_n} - \left(\frac{1}{x_n} \right)_0 = kt \quad (12.9)$$

It should be emphasized that this relationship holds only when x is much greater than 1. When $(x_n)_0 = 1000$, for example, breaking one bond in each molecule cuts x_n to 500. However, the available number of hydrolyzable bonds has been decreased by only 0.10%.

Polymers containing a completely substituted carbon in the chain often undergo chain scission on oxidation or exposure to UV or gamma radiation. This is because rearrangements are formed when an unpaired electron is left on a structure as in polyisobutylene:



Some other structures that favor chain scission are polypropylenes, polyacrylates, and polymethacrylates.

In contrast to the absorption of energy from UV and visible light, **high-energy radiation** usually is absorbed nonspecifically rather than by specific absorbing

chemical groups (chromophores). With most polymers, a free-radical site results with consequent reaction leading either to chain scission or to cross-linking. Some representative fields of study include the following:

1. Stability of materials used in nuclear reactors and related installations; often the mechanical properties are the focus of attention
2. Stability of materials used in connection with radiation sterilization of medical products or foods
3. Cross-linking of polymers such as polyethylene used in electrical insulation
4. Selective chain scissioning to make patterns in thin films (microlithography)

Polymers can be characterized by the yield of scissions (G_s) or cross-links (G_x) in units of events/100 eV of energy absorbed. Some examples are shown below:

	G_s	G_x
Polyethylene	–	2.0
Polystyrene	0.02	0.03
Poly(methyl methacrylate)	1.2–2.6	–
Poly(butene sulfone)	12.2	–

It can be seen that polyethylene and polystyrene mainly cross-link, whereas the other two polymers undergo chain scissioning. The measurement of the yield of scissions follows from Equation 12.9 replacing time by the dose, usually administered at a uniform rate.

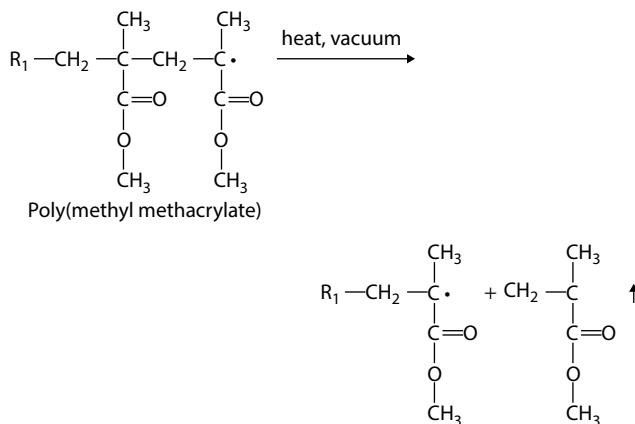
Three forms of radiation commonly used are soft X-rays (from synchrotrons), electron beams, and gamma radiation, say from Co^{60} . The first two can be used to make patterns in thin films since they are unidirectional. An electron beam of, say, 50 keV can be directed in much the same manner of operating a scanning electron microscope. Poly(methyl methacrylate) has been used as a thin film on silicon in order to produce patterns with line widths in the tens of nanometers (see Section 13.5). The scissioned (low-molecular-weight) polymer dissolves so much faster than the original material that the final pattern is relatively undistorted. The production of a pattern using unidirectional X-rays requires exposure of a similar film through a mask with opaque lines.

Because the industrially important process of cross-linking rubber often is carried out under oxidative conditions, and because chain scission generally is undesirable, other agencies must be employed for cross-linking when the chain contains such unstable groups. A case in point is polyisobutylene that is easily scissioned by peroxides. However, the corresponding commercial rubber is a copolymer with a small amount of isoprene so that sulfur can be used to cross-link via the resulting residual unsaturation in the main chain.

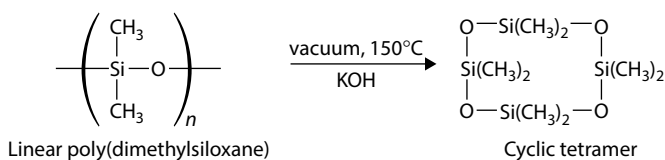
12.4.2 DEPOLYMERIZATION

Depolymerization also decreases molecular weight. Some common examples are merely the polymerization reactions previously considered taken in reverse. With

some systems, almost quantitative regeneration of monomer is possible. In fact, depolymerization is used to recover monomers from scrap polymer when economics permit. For example, methyl methacrylate can be recovered in good yield and high purity from the polymer by using low pressures, high temperatures, and a source of free radicals:



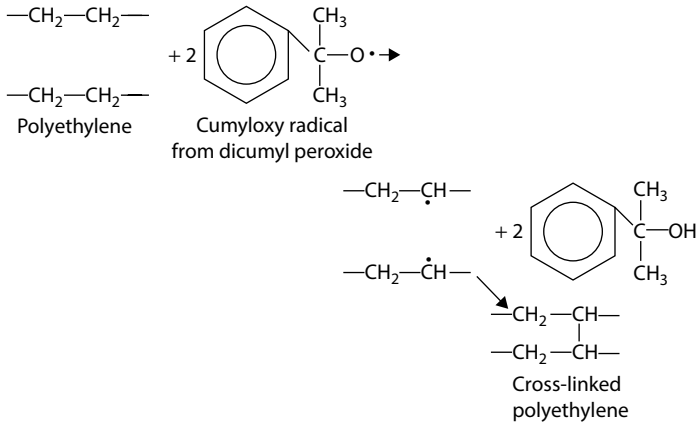
Polystyrene also depolymerizes to a large extent under these conditions, but the original monomer is not expensive enough to warrant commercial regeneration from scrap polymer. Ionic reactions also may lead to depolymerization. Heating almost any polysiloxane with potassium hydroxide in a vacuum eventually will convert the entire system to volatile cyclic material, predominantly the eight-membered ring of the tetramer:



12.4.3 CROSS-LINKING

Although **cross-linking** is a useful reaction in making a rubbery material that is dimensionally stable at high temperatures, there may be undesirable consequences when it occurs after a material is in service. The modulus increases with cross-linking, but the energy-absorbing capacity goes through a maximum and decreases thereafter. A rubbery polymer system generally becomes brittle as a result. Another typical pattern accompanying cross-linking is a decrease in compatibility, so that as plasticizers exude, systems shrink and delamination occurs. Polyethylene affords a primitive example of desirable and undesirable cross-linking. Molten polymer (150°C) may be mixed with a peroxide that does not decompose until an even higher *curing* temperature (205°C) is reached.

The finished product is a cross-linked polymer very useful as high-temperature electrical insulation. Cross-linking can also be induced by gamma radiation or high-energy electron beams:



However, the same polyethylene in film form that is kept outdoors may undergo slow attack from atmospheric oxygen in the presence of sunlight. Although cross-linking does take place, it is accompanied now by incorporation of oxygen to give polar groups and by chain scission. The end result is a brittle, easily ripped film with poor optical and electrical properties.

Accelerated aging tests have been mentioned in an earlier discussion of oxidation. It is desirable in analyzing such tests to be able to measure cross-linking and chain scission. For rubbery polymers this can be done by making two kinds of measurements [9]. Both depend on the proportionality of cross-link density with modulus (see Section 9.8). It should be obvious that if a tensile modulus E is measured intermittently on an aging sample, any cross-link that is formed will be reflected in an increased modulus. Chain scission, however, will decrease this modulus. In other words, the rate of change of E_t is the difference in the rates of cross-linking (dN_c/dt) and chain breaking (dN_s/dt):

$$\frac{dE_t}{dt} = K \left(\frac{dN_c}{dt} - \frac{dN_s}{dt} \right) \quad (12.10)$$

where:

K is a proportionality constant

Now in a separate test we can measure the relaxation of stress in a sample held at constant elongation. Any chain scission that occurs also decreases this relaxation modulus E_r . However, cross-linking of the strained sample does not increase the modulus, because only the cross-links that were put in the relaxed sample and were

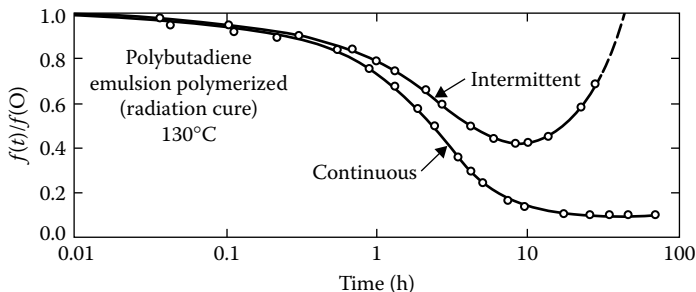


FIGURE 12.5 Continuous stress relaxation and intermittent stress measurements at 130°C. (Data from Tobolsky, A. V., *Properties and Structure of Polymers*, Wiley, New York, 1960, chap. V.)

distorted from their equilibrium, random positions will contribute. For this case, we measure only the rate of chain breaking:

$$\frac{dE_r}{dt} = -K \frac{dN_s}{dt} \quad (12.11)$$

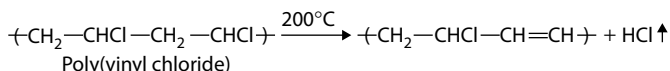
where:

K is the same constant as in Equation 12.10

The simultaneous measurement of E_t and E_r for polybutadiene aged in air at 130°C can be interpreted as showing that much scission and limited cross-linking occur up to 1 h (Figure 12.5). After 10 h the main reaction is cross-linking, and chain scission almost ceases.

12.4.4 BOND CHANGES

Changes can be brought about in the polymer backbone without scission or cross-linking. When poly(vinyl chloride) is heated above 200°C in the absence of stabilizing materials, copious quantities of HCl are evolved after a few minutes. Although scission and cross-linking ensue, the primary effect of heating this polymer is **dehydrohalogenation**, which changes the backbone structure.



The allyl chloride structure that is left after a single abstraction of HCl is more susceptible to free-radical attack than the fully saturated material. A **zippering** occurs, leaving behind successive conjugated double bonds. This remaining structure is chromophoric and highly reactive with metal salts and oxygen. Since the chain cannot rotate around double bonds, it is stiffened even in the absence of cross-linking. The proclivity of poly(vinyl chloride) toward dehydrohalogenation is shared to some extent by other chlorinated aliphatic materials including poly(vinylidene chloride),

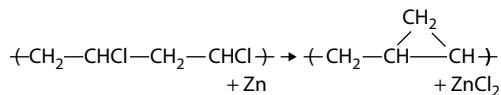
chlorinated waxes, and chlorosulfonated polyethylene. Since worldwide production of poly(vinyl chloride) exceeds 10×10^9 kg/year, the production of stabilizers to retard dehydrohalogenation is itself a multimillion-dollar business. The degradation reaction is not completely understood, although it has been studied extensively for many years [16]. On a practical level, however, the species effective in stabilizing poly(vinyl chloride) typically are found to

1. Absorb or neutralize HCl.
2. Displace *active* chlorine atoms such as those on tertiary carbons.
3. React with double bonds.
4. React with free radicals.
5. Neutralize other species that might accelerate degradation.

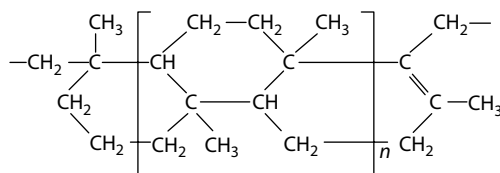
Metal soaps of barium, cadmium, lead, zinc, and calcium obviously can react with HCl. The addition of a zinc soap (or zinc oxide) to poly(vinyl chloride) gives a material that can be heated at 175°C for 10 or 15 min with scarcely any discoloration, as opposed to a control with no zinc that turns yellow or brown as a result of the conjugated unsaturations and oxidized structures. However, once the zinc is converted in large measure to zinc chloride, there is a very rapid and copious evolution of HCl and the remaining material is blue-black and brittle. The zinc soap, which was a stabilizer, is converted to zinc chloride, a rapid and efficient degradation catalyst.

Besides the metal soaps and general antioxidants, some species used to stabilize poly(vinyl chloride) are organotin compounds, epoxy compounds, phosphites, and phenols.

Other reactions can take place that alter the backbone stiffness. When heated in zinc metal powder, poly(vinyl chloride) can be cyclicized to a large extent:

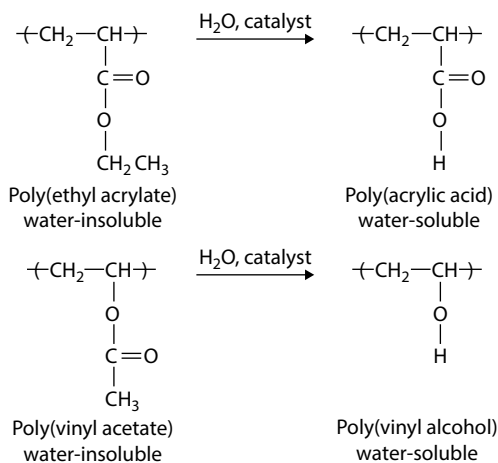


The oxidation of polyacrylonitrile to give a heat-stable, ladder polymer was mentioned in Section 3.5. Natural rubber is cyclicized in order to give abrasion-resistant inks and paint resins. In the presence of chlorostannic acid ($\text{H}_2\text{SnCl}_6 \cdot 6\text{H}_2\text{O}$), *cis*-polyisoprene is cyclicized by refluxing in benzene [10]. The new material can be reduced to a powder at room temperature, indicating that its T_g has been raised considerably over the original -70°C . Cross-linking and chain scissions have not taken place to any large extent, because the product redissolves completely to give solutions of high viscosity. The probable structure is [11]



12.4.5 SIDE-GROUP CHANGES

Of course, reactions of the *foliage*, the side chains on polymers, can take place without altering the molecular weight or the chain stiffness. Changes in solubility, compatibility, color, and mechanical and electrical properties may result. The main chains of poly(ethyl acrylate) or poly(vinyl acetate), for example, are not affected by hydrolysis. But in either case, hydrolysis changes water-insoluble precursors into water-soluble resins:



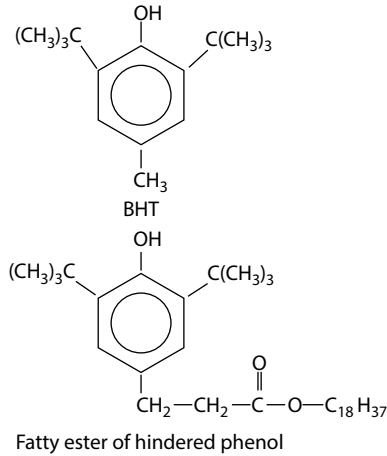
In the case of poly(vinyl alcohol), the reaction is a commercially useful one. But in either case, a drastic change in solubility has been made. It is clearly an undesirable change if the precursors are being used as water-insoluble protective coatings.

12.5 ANTIOXIDANTS AND RELATED COMPOUNDS

The most frequently employed stabilizing ingredient in plastics, fibers, rubbers, and adhesives is the **antioxidant**. Since oxidation is a free-radical, chain process, it is to be expected that useful molecules will be those that combine with free radicals to give stable species incapable of further reaction.

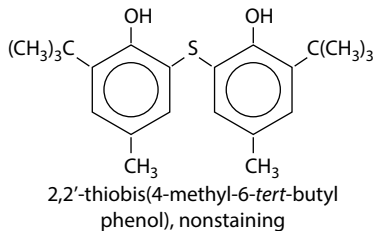
Quinones may act as free-radical stoppers by adding the radical to the ring or the carbonyl oxygen. The most widely used classes of antioxidants are the hindered phenols and diaryl amines. Presumably these react with RO_2 radicals by giving up a hydrogen and forming a rather stable radical, which also might stop a second radical by combining with RO_2 . Electron transfer and ring-addition reactions may also take place. It will be recalled that such action may be thought of as degradative chain transfer and that it is the principle by which inhibitors of free-radical polymerization function (see Section 4.4). Two important considerations in selecting antioxidants can be toxicity and color formation. The use of any chemical additive in food wrapping must be approved by the appropriate federal agency (Food and Drug Administration). Usually, only specific formulations and not general classes of materials are approved.

A widely used antioxidant in food products is butylated hydroxytoluene (BHT):



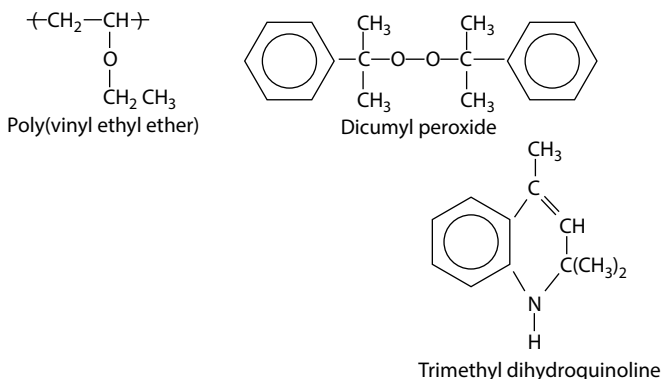
It is added to a variety of consumer items ranging from chewing gum and potato chips to bread wrapping and vitamin A. When modified as in the fatty derivative, an antioxidant of lower volatility and better compatibility with polyethylene is formed.

Antioxidants used in rubber compounds often are classified as *staining* or *non-staining* depending on whether or not they develop color in use. In a carbon black-loaded tire tread, a staining material has no drawback. But in the white sidewalls, it is important to use additives that are colorless to start with and stay colorless as they protect against oxidation. Phenylenediamine derivatives are very effective antioxidants but discolor (stain) severely. Where light colors must be preserved, a sulfur-cross-linked, hindered phenol that does not discolor is preferable:



Most unsaturated raw rubber has a small amount of antioxidant added before shipping to protect it during storage. Butyl rubber may have only four double bonds for each 1000 single bonds in the main chain, but it is usually supplied with BHT (about 0.1%). Ethylene-propylene terpolymer has a higher level of unsaturation, but it is confined to pendant groups of somewhat lower reactivity. About 0.25% of BHT is added by one manufacturer.

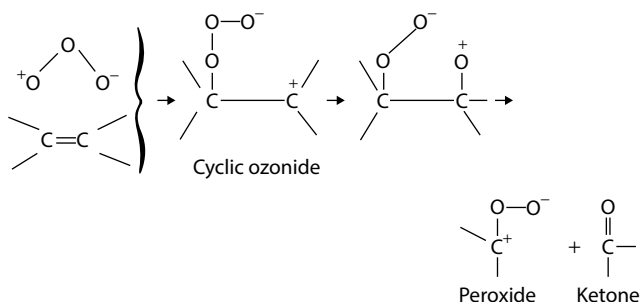
In contrast to the small amounts of antioxidant in raw rubber, compounded rubber often contains several percentages of protective material. It seems contradictory at first that antioxidants can continue to be very effective even after the polymer system has undergone a high-temperature, oxidative cross-linking. A case in point is poly(vinyl ethyl ether) cross-linked by dicumyl peroxide:



In a primitive formulation, the only ingredients besides the polymer are a reinforcing filler, a lubricant, and a cross-linking agent (Table 12.2). The cross-linking reaction takes 30 min at 150°C.

Adding as much as two parts of an antioxidant, Agerite Resin D, a polymerized trimethyl dihydroquinoline [13], does not degrade the original tensile strength of elongation. And yet the antioxidant is quite effective in preventing degradation for a period of a week in air at 120°C (Figures 12.6 and 12.7).

Ozone (O_3) also attacks polymers. Unlike molecular oxygen (O_2), ozone appears to add directly to a double bond [14,15]. Subsequently, chain scission often occurs.



The circumstances generally calling for stabilization against ozone are the combination of a highly unsaturated material, such as diene rubber (polyisoprene, styrene-butadiene

TABLE 12.2
Poly(Vinyl Ether) Rubber

Ingredient	Formulation (Parts by Weight)
Polymer (Bakelite EDBM, Union Carbide, Bound Brook, NJ)	100
Carbon black (Wyex, channel black, Huber, Edison, NJ)	50
Stearic acid	2
Dicumyl peroxide	4

Source: Rodriguez, F., and S. R. Lynch, *Ind. Eng. Chem. Prod. Res. Develop.*, 1, 206, 1962.

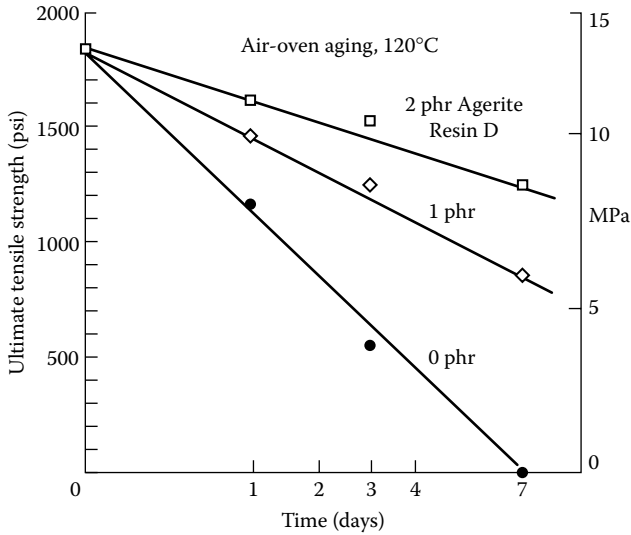


FIGURE 12.6 Effect of antioxidant (polymerized trimethyldihydroquinoline) on tensile strength of poly(vinyl ethyl ether). Abscissa is square root of time. (Data from Rodriguez, F., and S. R. Lynch, *Ind. Eng. Chem. Prod. Res. Develop.*, 1, 206, 1962.)

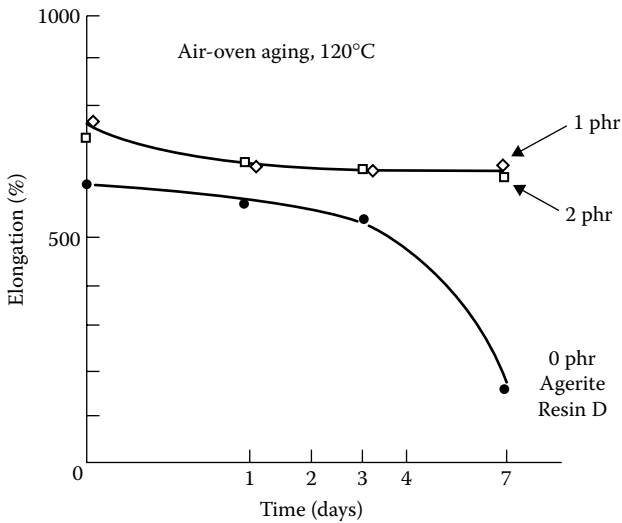


FIGURE 12.7 Effect of antioxidant on elongation at break for polymer of Figure 12.6 and Table 12.2. (Data from Rodriguez, F., and S. R. Lynch, *Ind. Eng. Chem. Prod. Res. Develop.*, 1, 206, 1962.)

rubber), some stress, and, of course, ozone. The automobile tire, especially in some urban locations, combines these features. Although the usual concentration of ozone in the atmosphere is only 0–20 parts/100 million, in the Los Angeles area it may run to about 25 parts/100 million (and can reach concentrations of 80 parts in heavy smog). An even higher concentration is encountered on the surface of high-voltage insulators.

Corona discharge is the flow of electric energy from a high-voltage conductor through ionized air on the surface or in voids or air spaces between conductor and insulation. Although most corona testing is done at voltages of over 10,000 V, the discharge may commence at less than 1000 V. The discharge is accompanied by a faint glow (hence the name *corona*) and a crackling sound indicating the pulsating character of the conduction. Oxygen is converted to ozone (ozone generators are built on the principle of corona discharge) so that an insulator may be subjected to very high concentrations.

In insulators the physical changes that are noted are pitting, erosion, and discoloration, and the chemical changes are chain scission and oxidation. In rubber for tires, most tests are run on static specimens at various strains. A sample elongated 20% cracks much more rapidly than an unstrained sample. The sensitivity does not continue to increase with elongation but may go through a maximum. The particular manifestation usually studied is crack growth. Under a given set of conditions, a crack started by a razor blade will grow in a linear fashion perpendicular to the direction of mechanical strain.

Some **antiozonants** are effective just by forming a surface barrier to diffusion of O_3 . Waxes can be added that **bloom**, that is, that exude to the surface, and form a sacrificial layer of hydrocarbon. Dialkyl-*p*-phenylenediamines (the largest chemical class) may react directly with ozone or the ozone-olefin reaction products in such a way as to interfere with chain scission. Even the reaction products of this latter class may form an additional barrier to O_3 diffusion, since they react at the surface initially. It can be seen that addition of such an amine increases the rate of ozone absorption initially but affords protection after a short time (Figure 12.8).

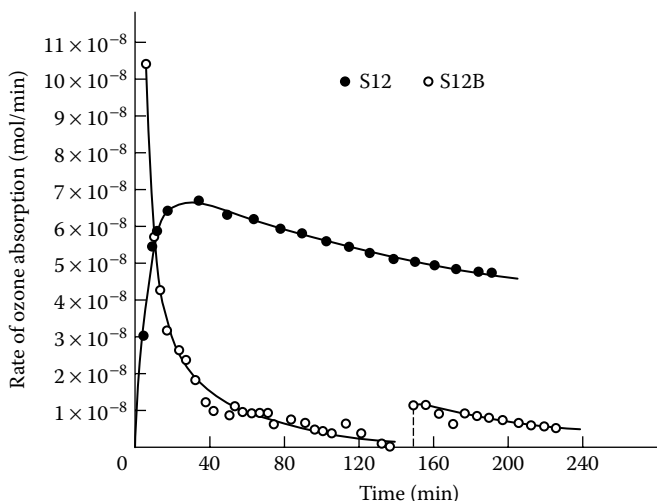


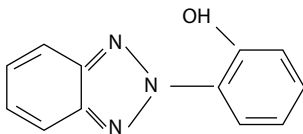
FIGURE 12.8 Rate of ozone absorption versus time for a specimen under 20% elongation. Ozone flow rate = 1.05×10^{-7} mol/min. S12 is unprotected elastomer. S12B contains 2 phr of *N,N'*-di-*sec*-butyl-*p*-phenylenediamine. The discontinuity in the curve for S12B resulted from an interruption in the test that allowed more ozone-sensitive material to diffuse to the surface. (Data from Ambelang, J. C. et al., *Rubber Chem. Technol.*, 36, 1497, 1963; Erickson, E. R. et al., *Rubber Chem. Technol.*, 32, 1062, 1959.)

12.6 STABILIZERS FOR IRRADIATED SYSTEMS

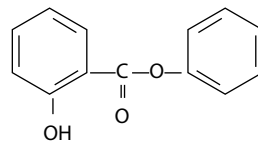
Most **UV absorbers** protect the substrate by preferentially absorbing the harmful portion of the sun's spectrum between 300 and 400 nm. The earth's atmosphere filters out most of the shorter wavelengths. To be effective, the UV absorber should dissipate the absorbed energy by transferring it to its surroundings as heat or by reemitting it at longer wavelengths through phosphorescence, fluorescence, or infrared radiation. Some other desirable properties of a UV absorber are compatibility with the substrate, lack of visible color, low vapor pressure, low reactivity with other materials in the system, and low toxicity.

Carbon black can be tolerated in a limited number of formulations where color is not a criterion. The pigment not only absorbs light, but is also reactive with those free-radical species that might be formed. Wire and cable insulation and pipe for outdoor applications can be protected this way. Films for mulching and water containment in ponds may be made from polyethylene containing carbon black. Five UV absorbers and their corresponding transmission curves are shown in Table 12.3 and

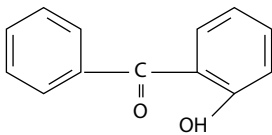
TABLE 12.3
Structures of Five Different UV absorbers



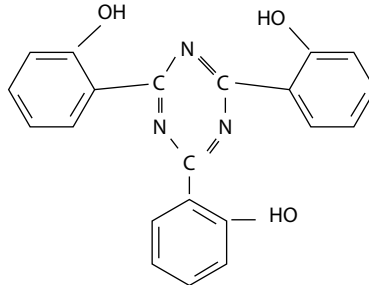
2-(Hydroxyphenyl)benzotriazole



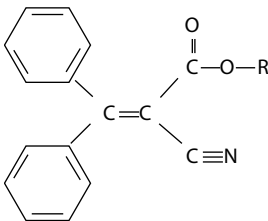
Phenyl salicylate



2-Hydroxybenzophenone



1,3,5-Tris(2'-hydroxyphenyl)triazine



Alkyl-2-cyano-3-phenyl cinnamate
(substituted acrylonitrile)

Source: Cipriani, L. P., and J. F. Hosler, *Mod. Plast.*, 45(1A, Encycl. Issue), 406, September 1967.

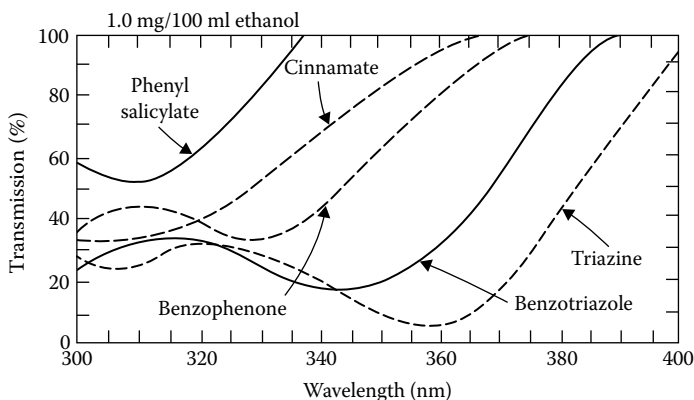
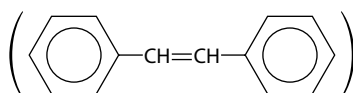


FIGURE 12.9 Transmission of UV light by absorbers listed in Table 12.3. (Data from Cipriani, L. P., and J. F. Hosler, *Mod. Plast.*, 45, Encycl. Issue, 406, September 1967.)

Figure 12.9. The common feature of these UV absorbers is conjugated unsaturation enhanced by stable aryl groups. A variety of groups may be substituted on these basic structures in order to decrease solubility in water and volatility or to increase compatibility [18,19].

Phenyl salicylate has the common name **salol**. In addition to its use as a stabilizer in polymers, salol is used at concentrations of about 1%–10% in suntan oils and ointments, as are other absorbers. The function of the stabilizer in such a situation is the same as in the polymer, to decrease the concentration of skin-damaging radiation. Toxicity and reactivity take on a personal and obvious importance for this application. Suntan oils illustrate one way in which stabilizers can be used. If the UV absorber is in a thin layer on the surface, the article is protected to a greater extent than if it is dispersed throughout. Occasionally this can be done, as when multiple coats of lacquer are applied to furniture. All the UV absorbers can be put in the top coat. When articles are to be molded, however, it is not economical to coat separately, so the UV absorber is mixed in with the other ingredients.

Despite the addition of stabilizers, many polymer systems reflect less visible light at short wavelengths (400 nm) than at long ones (700 nm). To compensate for this nonuniformity, a blue dye can be added that absorbs at long wavelengths but not at short ones. For years **laundry bluing** has been added to fabrics to give an overall whiteness. In doing this the total reflectance is decreased. **Brighteners**, also called **optical bleaches**, operate by absorbing invisible light below 400 nm and then fluorescing (reradiating) in the visible wavelengths [20]. The effect is seen in Figure 12.10. A violet dye decreases the total reflectance in a poly(vinyl chloride) plaque. The fluorescent whitening agent absorbs light at less than 400 nm and reemits it between 400 and 500 nm. Some typical structures (Table 12.4) incorporate the stilbene group:



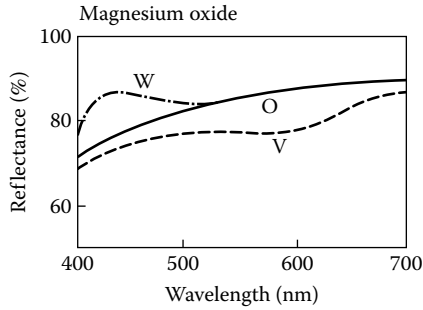
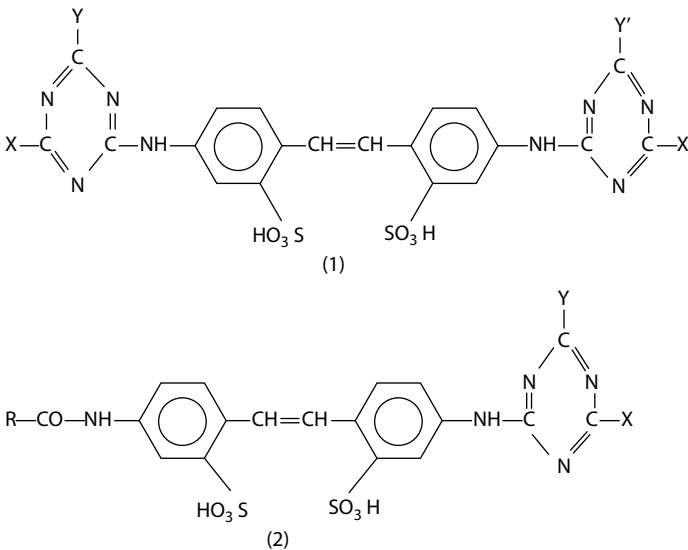


FIGURE 12.10 Reflectance curves of poly(vinyl chloride) alone (O), with violet dye (V), and with brightener (W). (Data from Villanne, F. G., *Mod. Plast.*, 41, Encycl. Issue, 428, September 1963.)

In Figure 12.11, the absorption and emission spectra for structure 1 of Table 12.4 have been superimposed. Brighteners have been used in soaps and detergents extensively since 1948 and undoubtedly gave rise to the various extravagant advertising claims for whiteness with which the soap-consuming public has been bombarded ever since. Textile and paper usage of brighteners followed. Typical concentrations in plastics are of the order of 0.001% and 0.05%. Because the brighteners *feed* on UV light, their effect is most noticeable by sunlight and hardly perceptible by incandescent light. Fluorescent lights give an intermediate effect. Also, more brightener has

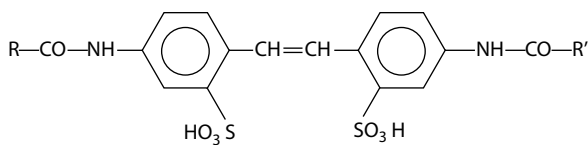
TABLE 12.4

Derivatives of (Di)aminostilbene(di)sulfonic Acid

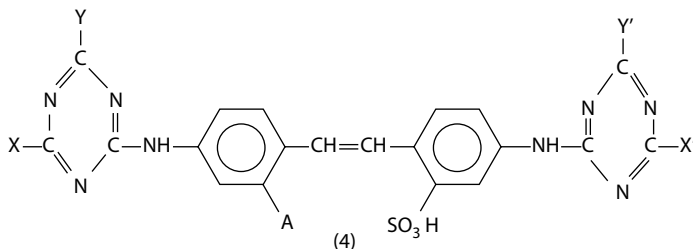


(Continued)

TABLE 12.4
(Continued) Derivatives of (Di)aminostilbene(di)sulfonic Acid

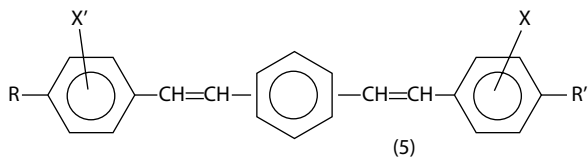


(3)



(4)

A = alkyl, aryl groups, etc.



(5)

R, R' = substituted
 amino,
 carboxyl,
 acetylamino
 groups, etc.

X, X' = -H, -SO₃H

Source: Zweidler, R., and H. Hausermann: in *Encyclopedia of Chemical Technology*, 2nd edn., vol. 3, Wiley, New York, 1964, p. 738.

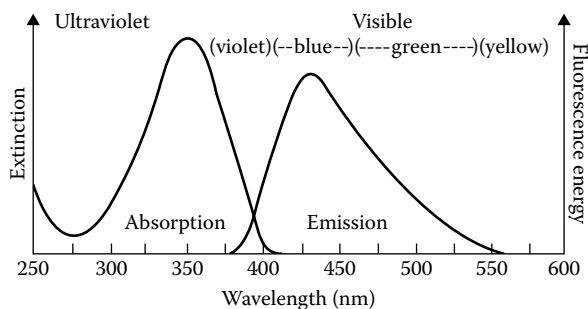


FIGURE 12.11 Absorption and emission spectra in solution for a compound of structure 1 in Table 12.4. (Data from Zweidler, R., and H. Hausermann, in *Encyclopedia of Chemical Technology*, 2nd edn., vol. 3, Wiley, New York, 1964, 738.)

to be added if a UV absorber is incorporated in the same system to maintain a given intensity of whiteness.

As work with ionizing radiation (X-rays, gamma rays, electron beams) has increased, some means of protecting systems has been sought to interfere with degradation by radiation. In some polymers, the aromatic amines and phenolic compounds similar to the antioxidants and antiozonants already described are effective in decreasing the production of cross-links during gamma radiation [22,23]. In aqueous poly(acrylic acid) solutions, Sakurada [24] reports that as little as one molecule of thiourea per three molecules of polymer will increase the dose of gamma radiation needed for gelation to occur by a factor of 5.

12.7 ABLATION

When a space vehicle reenters the earth's atmosphere (or any other planet's atmosphere), it adiabatically compresses the air in front of it. Aerodynamic heating also results from the viscous dissipation of energy in the layer of air around the vehicle. Using a reentering satellite as a frame of reference, the situation is the same as if air at a velocity $u = 6$ km/s encountering the nose of the satellite suddenly had its kinetic energy entirely converted to enthalpy (J/g of air). With an appropriate conversion of units, the result is a change in enthalpy of about 18 kJ/g air (8×10^3 Btu/lb). To interpret this in terms of temperature is rather difficult. It can be appreciated that measures must be taken to protect the contents of a space vehicle from the heat. The actual heat load will vary with vehicle geometry, entry and flight path angles, velocity, and altitude. Some typical trajectories with their corresponding **stagnation enthalpies** are shown in Figure 12.12. The heat load may be handled by heating up a large mass acting as a **heat sink**, energy transfer by radiation, and **transpiration**, where a coolant is pumped to the surface and evaporated such as the body is cooled

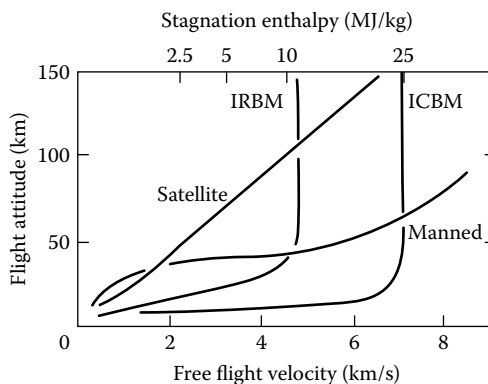


FIGURE 12.12 Representative reentry trajectories for various flight vehicles. ICBM, intercontinental ballistic missile; IRBM, intermediate-range ballistic missile. (Data from Schmidt, D. L., *Mod. Plast.*, 37, 131, November 1960; 147, December 1960.)

by perspiration. In terms of cooling capacity and reliability a fourth method has been favored. **Ablation** can be defined as a sacrificial loss of material accompanied by transfer of energy.

Polymers have been used in ablative systems for a combination of reasons. These have been summarized by Schmidt [25] as follows:

1. High heat absorption and dissipation per unit mass expended, which ranges from several hundred to several thousand Btu/lb of ablative material
2. Excellent thermal insulation, which eliminates or reduces the need for an additional internal cooling system
3. Useful performance in a wide variety of hyperthermal environments
4. Automatic temperature control of surface by self-regulating ablative degradation
5. Light weight
6. Increase in efficiency with the severity of the thermal environment
7. Tailored performance by varying the individual material components and construction
8. Design simplicity and ease of fabrication
9. Low cost and nonstrategic

Schmidt also lists the limitations of polymers:

1. The loss of surface material and attendant dimensional changes during ablation must be predicted and incorporated into the design.
2. Service life is greatly time dependent. Present uses are for transitory periods of several minutes or less at very high temperatures and heating rates.
3. Thermal efficiency and insulative value are generally lowered by combined conditions of low incident flux and long-time heating.

The **heat of ablation** (the ability of the material to absorb and dissipate energy per unit mass) can be measured in various ways. In general it will be made up of the energy to heat the material up to a reaction temperature, the energy to decompose or depolymerize, the energy to vaporize, and the energy to heat the gases. Any exothermic reactions such as oxidation of hydrocarbons work in the opposite direction and lower the heat of ablation.

In addition to a high heat of ablation, it is desirable that the materials possess good strength even after charring. Any sloughing off of chunks of material represents poor usage, because the pieces have absorbed only enough heat to come to temperature and have not decomposed or vaporized. The various stages of heating, charring, and melting are profiled in Figure 12.13 for two composites. It can be noted that the glass-reinforced system produces a molten glass surface, which can be an advantage mechanically. However, the nylon-reinforced system may have the higher thermal efficiency.

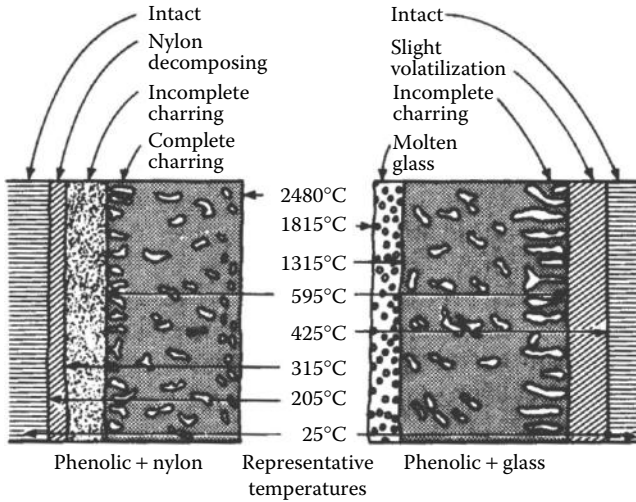


FIGURE 12.13 Temperature distribution in two plastics during steady-state ablation. (Data from Schmidt, D. L., *Mod. Plast.*, 37, 131, November 1960; 147, December 1960.)

KEYWORDS

Degradation
 Weathering
 Electromagnetic waves
 Einstein
 Oxidation
 Plasticizer migration
 Delamination
 Chain scission
 Random scission
 High energy radiation
 Depolymerization
 Cross-linking
 Dehydrohalogenation
 Zippering
 Antioxidant
 Corona discharge
 Ozone
 Antiozonant
 Bloom
 UV absorber
 Laundry bluing
 Brightener
 Optical bleach
 Ablation

Stagnation enthalpy
Heat sink
Transpiration

PROBLEMS

- 12.1** Why does a suspension of poly(vinyl chloride) powder in dioctyl phthalate on heating first become clear and then start to turn yellow?
- 12.2** In mechanical degradation of a polymer in solution, the rate of chain scission may be faster for higher molecular-weight chains. If in Equation 12.6 we have $k = k'x_n^a$, where a is a power greater than 0, derive an expression for x_n as a function of time.
- 12.3** Cite instances in which each of these *degradation* reactions is desirable: (a) hydrolysis, (b) cross-linking, and (c) depolymerization.
- 12.4** If a heat shield of 5 ft in diameter is to be made from glass-reinforced polystyrene, how much heat can be removed by the depolymerization of a layer of 1 in (2.54 cm) thick of composite which is 70 vol% polymer and 30 vol% glass? $\Delta H_{\text{vap}} = 153 \text{ Btu/lb}$ (356 J/g) for monomer. See Table 5.1 for heat of polymerization.

REFERENCES

- Fink, D. G., and D. Christiansen (eds.): *Electronics Engineers Handbook*, 3rd edn., sec. 1, McGraw-Hill, New York, 1989.
- Brighton, C. A.: in S. H. Pinner (ed.), *Weathering and Degradation of Plastics*, Columbine, London, 1966, p. 51.
- Norling, P. M., T. C. P. Lee, and A. V. Tobolsky: *Rubber Chem. Technol.*, 38:1298 (1965).
- Shelton, J. R.: *Rubber Chem. Technol.*, 30:1251 (1957).
- Rodriguez, F.: *Chem. Tech.*, 1:409 (1971).
- Sharpley, J. M., and A. M. Kaplan (eds.): *Proceedings of the 3rd International Biodegradation Symposium*, Applied Science Publishers, London, 1976.
- Plastics Institute, *Degradability of Polymers and Plastics* (Conference Reprints), London, 1973.
- Fields, R. D., F. Rodriguez, and R. K. Finn: *J. Appl. Polym. Sci.*, 18:3571 (1974).
- Tobolsky, A. V.: *Properties and Structure of Polymers*, chap. V., Wiley, New York, 1960.
- Baker, C. S. L.: chap. 2 in A. K. Bhowmick and H. L. Stephens (eds.), *Handbook of Elastomers*, Dekker, New York, 1988, p. 35.
- Stern, H. J.: *Rubber: Natural and Synthetic*, 2nd edn., Palmerton, New York, 1967, p. 49.
- Rodriguez, F., and S. R. Lynch: *Ind. Eng. Chem. Prod. Res. Develop.*, 1:206 (1962).
- Ohm, R. F. (ed.): chap. 1 in R. T. Vanderbilt (ed.), *Vanderbilt Rubber Handbook*, 13th edn., New York, 1990, p. 357.
- Bateman, L. (ed.): *The Chemistry and Physics of Rubber-Like Substances*, chap. 12, Wiley, New York, 1963; A. F. Halasa, J. M. Massie, and R. J. Ceresa: in *Science and Technology of Rubber*, 2nd edn., Academic Press, New York, 1994, p. 535.
- Ambelang, J. C., R. H. Kline, O. M. Lorenz, C. R. Parks, and J. R. Shelton: *Rubber Chem. Technol.*, 36:1497 (1963); Erickson, E. R. et al.: *Rubber Chem. Technol.*, 32:1062 (1959).
- Koleske, J. V., and L. H. Wartman: *Poly(Vinyl Chloride)*, Gordon & Breach, New York, 1969.

17. Cipriani, L. P., and J. F. Hosler: *Mod. Plast.*, 45(1A, Encycl. Issue):406 (September 1967).
18. Wypych, G.: *Handbook of Material Weathering*, 4th edn., ChemTech Publications, Toronto, ON, 2008, chap. 17.
19. Pritchard, G.: *Plastic Additives: An A-Z Reference*, Chapman & Hall, London, 1998, p. 427.
20. Zweidler, R., and H. Hausermann: in *Encyclopedia of Chemical Technology*, 2nd edn., vol. 3, Wiley, New York, 1964, p. 738.
21. Villanne, F. G.: *Mod. Plast.*, 41(1A, Encycl. Issue):428 (September 1963).
22. Clough, R.: *Enc. Polym. Sci. Eng.*, 13:667 (1988).
23. Sinco, P.: *Nuclear News*, 42(6):92 (May 1999).
24. Sakurada, I., and Y. Ikada: *Bull. Inst. Chem. Res. Kyoto Univ.*, 41:123 (1963).
25. Schmidt, D. L.: *Mod. Plast.*, 37:131 (November 1960); 147 (December 1960).

GENERAL REFERENCES

- Albertsson, A.-C., and S. J. Huang (eds.): *Degradable Polymers, Recycling, and Plastics Waste Management*, Dekker, New York, 1995.
- Allen, N. S., and M. Edge: *Fundamentals of Polymer Degradation and Stabilization*, Chapman & Hall, New York, 1993.
- Allen, N. S., and J. F. Rabek (eds.): *New Trends in the Photochemistry of Polymers*, Elsevier Applied Science, New York, 1985.
- Allen, N. S., and W. Schnabel (eds.): *Photochemistry and Photophysics in Polymers*, Elsevier Applied Science, New York, 1984.
- Billingham, N. C., and D. M. Wiles (eds.): *Polymer Stabilization Mechanisms and Applications*, Elsevier, New York, 1991.
- Casale, A., and R. S. Porter: *Polymer Stress Reactions*, Academic Press, New York, vol. 1, 1978; vol. 2, 1979.
- Davis, A., and D. Sims: *Weathering of Polymers*, Elsevier Applied Science, New York, 1983.
- El-Nokaly, M. A., D. M. Piatt, and B. A. Charpentier (eds.): *Polymeric Delivery Systems: Properties and Applications*, ACS, Washington, DC, 1993.
- Emanuel, N. M., and A. L. Buchachenko: *Chemical Physics of Polymer Degradation and Stabilization*, VNU Science, Utrecht, The Netherlands, 1987.
- Fouassier, J. P., and J. F. Rabek (eds.): *Radiation Curing in Polymer Science and Technology*, 4 vols., Chapman & Hall, New York, 1994.
- Gächter, R., and H. Muller (eds.): *Plastics Additives Handbook*, 4th edn., Hanser Gardner, Cincinnati, OH, 1993.
- Grassie, N. (ed.): *Developments in Polymer Degradation—1 to 6*, Elsevier Applied Science, New York, 1977–1985.
- Griffin, G.: *Chemistry and Technology of Biodegradable Polymers*, Chapman & Hall, New York, 1993.
- Guillet, J.: *Polymer Photophysics and Photochemistry*, Cambridge University Press, Cambridge, 1986.
- Hamid, S. H. (ed.): *Handbook of Polymer Degradation*, 2nd edn., Dekker, New York, 2000.
- Hoyle, C. E., and J. F. Kinstle (eds.): *Radiation Curing of Polymeric Materials*, ACS, Washington, DC, 1990.
- Hoyle, C. E., and J. M. Torkelson (eds.): *Photophysics of Polymers*, ACS, Washington, DC, 1987.
- Ivanov, V. S.: *Radiation Chemistry of Polymers*, VSP, Zeist, The Netherlands, 1992.
- Jellinek, H. H. G.: *Aspects of Degradation and Stabilization of Polymers*, Elsevier, New York, 1978.

- Jellinek, H. H. G., and H. Kaachi (eds.): *Degradation and Stabilization of Polymers: A Series of Comprehensive Reviews*, vol. 2, Elsevier, New York, 1989.
- Kaplan, D. L., E. L. Thomas, and C. Ching (eds.): *Biodegradable Polymers and Packaging*, Technomic, Lancaster, PA, 1993.
- Kelly, J. M., C. B. McArdle, and M. J. F. Maunder (eds.): *Photochemistry and Polymeric Systems*, CRC Press, Boca Raton, FL, 1993.
- Krongauz, V. V., and A. D. Trifunac (eds.): *Processes in Photoreactive Polymers*, Chapman & Hall, New York, 1994.
- Minsker, K. S., S. K. Kolesov, and G. E. Zaikov (eds.): *Degradation and Stabilization of Vinyl Chloride-Based Polymers*, Pergamon Press, New York, 1988.
- Mobley, D. P. (ed.): *Plastics from Microbes*, Hanser-Gardner, Cincinnati, OH, 1994.
- Murphy, J.: *Additives for Plastics Handbook*, Elsevier Advanced Technology, New York, 2001.
- Popov, A., N. Rapoport, and G. Zaikov: *Oxidation of Stressed Polymers*, Gordon & Breach, New York, 1991.
- Rabek, J. F.: *Polymer Photodegradation: Mechanisms and Experimental Methods*, Chapman & Hall, New York, 1994.
- Rabek, J. F.: *Photodegradation of Polymers*, Springer, New York, 1996.
- Randell, D. R.: *Radiation Curing of Polymers II*, CRC Press, Boca Raton, FL, 1992.
- Reichmanis, E., and J. H. O'Donnell (eds.): *The Effects of Radiation on High-Technology Polymers*, ACS, Washington, DC, 1989.
- Reichmanis, E., C. W. Frank, and J. H. O'Donnell (eds.): *Irradiation of Polymeric Materials: Processes, Mechanisms, and Applications*, ACS, Washington, DC, 1993.
- Schweitzer, P.: *Corrosion Resistance of Elastomers*, Dekker, New York, 1990.
- Scott, G. (ed.): *Mechanisms of Polymer Degradation and Stabilization*, Elsevier, New York, 1990.
- Shlyapmtokh, V. Y.: *Photochemical Conversion and Stabilization of Polymers*, Macmillan, New York, 1984.
- Singh, A., and J. Silverman (eds.): *Radiation Processing of Polymers*, Hanser-Gardner, Cincinnati, OH, 1992.
- Struik, L. C. F.: *Internal Stresses, Dimensional Instabilities and Molecular Orientations in Plastics*, Wiley, New York, 1990.
- Tötsch, W., and H. Gaensslen: *Polyvinylchloride: Environmental Aspects of a Common Plastic*, Elsevier, New York, 1992.
- Troitzsch, J. (ed.): *International Plastics Flammability Handbook*, 2nd edn., Hanser-Gardner, Cincinnati, OH, 1990.
- Vert, M., J. Feijen, A.-C. Albertsson, G. Scott, and E. Chiellini: *Biodegradable Polymers and Plastics*, CRC Press, Boca Raton, FL, 1992.
- Volynskii, A. L., and N. F. Bakeev: *Solvent Crazing of Polymers*, Elsevier, Amsterdam, The Netherlands, 1995.
- Voyiadjis, G. Z., and D. H. Allen (eds.): *Damage and Interfacial Debonding in Composites*, Elsevier, Amsterdam, The Netherlands, 1996.
- Wypych, G.: *PVC Degradation and Stabilization*, ChemTech Publications, Toronto, ON, 2008.
- Wypych, G.: *Handbook of Material Weathering*, 5th edn., ChemTech Publications, Toronto, ON, 2013.
- Zweifel, H.: *Stabilization of Polymeric Materials*, Springer, New York, 1998 (reprinted in soft-cover 2011).

13 Fabrication Processes

13.1 FABRICATION

It is only in general terms that we can differentiate fabrication from other processes that carry out the steps that change a fraction of natural gas into a sweater, a petroleum fraction into a garbage can, or linseed oil into a bucket of paint. The fabricator sometimes starts with monomers or prepolymers, but more often with polymers. A customer may change the ingredients physically and perhaps chemically. He or she may be the ultimate user, as with the garbage can or paint, or may be someone who changes the physical form again, as with the fiber for the apparel manufacturer. Several fabricators may add to the value of materials they process in sequence. One company may produce a rubbery polymer, a second may compound it, a third may convert it into a sheet, and a fourth finally may form the sheet into a gasket. Liaison between the polymer producer and the ultimate user is a difficult and demanding facet of polymer technology. Because the ultimate user often has limited technical resources and is preoccupied with immediate problems, most polymer and monomer producers have built up substantial technical service organizations to generate techniques and materials (together with immense quantities of data) that guide fabricators and provide a basis for selecting the best polymers and fabrication conditions for a given application. Rather than covering all of fabrication processes in one very large chapter, this topic is presented in two chapters. This chapter provides a description of raw materials used in fabrications, mixing and compounding, fabrication of coatings and adhesives, application of polymers to microelectronics, polymeric membranes for separation processes, and finally applications of polymers in medicine. Extrusion and molding in their various forms are discussed in Chapter 14 as these processes are the workhorses of the plastic industry and use up the majority (about 80%) of all the polymers consumed.

13.2 RAW MATERIAL FORMS

Liquid raw materials may be received in 55-gal drums or 8000-gal (30-m³) tank cars. Smaller units such as carboys and cans may be used. Individual tank trucks and tank cars vary in capacity from one to another. Monomers and prepolymers often come as liquids. The large-scale producer of urethane foams receives polyols and diisocyanates in tank cars and uses them directly from the siding or perhaps transfers them to storage tanks. On a different scale, the familiar two-part epoxy adhesive can be bought as a pair of tubes in most hardware stores. Once again, the two liquids represent a liquid prepolymer and another reactive ingredient, in this case an amine hardener. Both epoxy systems and solutions of unsaturated polyesters in styrene monomer are used as liquids by fabricators of glass-reinforced structures, among which are auto bodies, boat hulls, and filament-wound rocket casings or storage tanks.

Most latexes are the result of emulsion polymerization processes. For the coatings industry no chemical change is necessary, and the compounder adds value to the product by mixing the latex with a stable dispersion of pigments, stabilizers, and other ingredients to make a protective or decorative coating. However, the latex may be coagulated and cross-linked in the process of making a foam or a dipped glove. It is important that the polymerization process leave no objectionable residues in the latex, because only very volatile ingredients can be removed economically. Not all latexes come from emulsion polymerization. Natural rubber latex is recovered from the tree. Polymers that are best produced by bulk or solution techniques can be converted into latexes by **postemulsification**. In a typical process a polymer solution is emulsified in water with a surfactant, and then the solvent is evaporated. Latexes of butyl rubber and polyethylene are available, even though neither is usually polymerized in emulsion.

Massive solid forms are common in the rubber industry. Bales of natural rubber may weigh 100 kg. Synthetic rubber is often sold in bales (blocks) that are wrapped in polyethylene or dusted with talc and weigh 20–50 kg. Polychloroprene is available in batons or smaller pieces that weigh less than a pound and are packaged in bags. For ease in dissolving rubber in solvents for coatings and adhesives applications, both natural and synthetic rubbers have been put in crumb form. The porous particles have a much greater surface area for solvent attack. Most thermoplastics for molding and extrusion applications are sold as pellets (often called *powder*), which are cylinders about 3 mm in diameter and length. In this form the polymer flows freely in automatic dispensing devices and in bins and hoppers. Thermoplastics are used as fine powders in rotational and fluidized bed coating systems (Section 13.4). Most thermoset resins are supplied as powders that can be compressed at room temperature into cakes or *preforms*. Poly(vinyl chloride) from suspension or emulsion polymerization is supplied as a powder. Suspension polymer particles range from 50 μm to a few hundred micrometers in diameter and are quite porous. They are dry-blended with plasticizers, yielding a dry, flowing, plasticized power. The emulsion-polymerized resin is smaller in particle diameter and denser so as to be suitable for dispersion in plasticizers that are mobile liquids.

For many fabricators the raw form of the polymers they use is the result of a previous fabrication step. This is true of the sheet formers, since the molder of blister packages or refrigerator door liners seldom makes the original flat sheet but buys it from a separate converter. Builders of ductwork, storage tanks, and luggage commonly buy their raw materials as sheets, tubes, or other extruded shapes.

13.3 MIXING

Mixing low-viscosity liquids or blending dry powders can be accomplished with conventional equipment. Turbine and propeller agitators are used to mix low-viscosity liquids, and twin-cone blenders or tumblers are used for dry powders. These devices have low power requirements and rather low residence times. At the other extreme, the dispersion of a finely divided solid such as carbon black in a rubber with viscosity of about a million poises presents a situation requiring more power.

The degree of mixing, the uniformity of dispersion of one phase in another, can be measured in several ways. One could take a series of samples of uniform size

from a large batch and determine in each the concentrations of various ingredients. A statistical analysis coupled with a mathematical model can yield a number that can be fitted into a scale of uniformity or a degree of mixedness. It is more common to judge the uniformity by some performance test. Mechanical failure tests such as tensile, tear, and impact strength are used. Optical tests are conventional for judging pigment dispersion. When an entire cable is tested for electrical strength through the insulation, a very sensitive measure of uniformity is obtained, since it takes only one pinpoint of poorly dispersed filler to bring about failure at a low-impressed voltage.

For mixing liquids with viscosities less than about 10 poise (1 Pa·s), paddles, turbines, and propellers are suitable. Power requirements vary from 0.5 to 15 hp/1000 gal (0.1–3 kW/m³). If a solid polymer is to be dissolved in a solvent, a mixing impeller with a saw-toothed edge is available that can cut the swollen solid ribbons in addition to circulating the contents of the tank (Figure 13.1). However, the high speeds characteristic of some agitators can decrease the molecular weight of the polymer by a mechanical shearing action.

Mixing viscoelastic materials involves techniques different from those used with low-viscosity fluids. In the latter case, the normal procedure is to induce turbulence to a degree such that molecular diffusion can proceed rapidly to establish a uniform concentration of ingredients. With polymers it is necessary to use high local shear rates and rather gross mechanical *folding* to get the same result. A simple analogy to the two processes is the comparison between mixing cream in coffee and dispersing a spoonful of caraway seeds in a batch of bread dough. The power and time requirements are much more stringent for the dough, of course.

Pastes and liquids with viscosities higher than 100 poise (10 Pa·s) are handled in machinery, resembling that familiar in the baking industry. Kneaders and dough mixers are used to mix pigments in printing inks, to disperse poly(vinyl chloride) in plastisols, and to blend together the more viscous prepolymers and other ingredients for

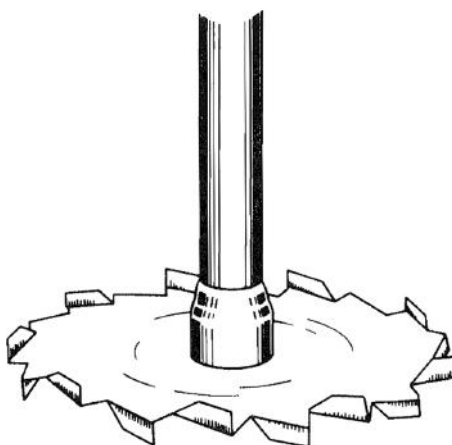


FIGURE 13.1 The impeller of the Cowles dissolver. (Data from Nylen, P., and E. Sunderland: *Modern Surface Coatings*, Wiley, New York, 534, 543, 1965. Copyright Wiley-VCH Verlag GmbH & Co. KGaA. Reproduced with permission.)

urethane foams. The agitator speeds are lower and the power requirements are higher (10–1000 hp/1000 gal or 2.5–250 kW/m³) than those for turbines and propellers.

Amorphous polymers that are 50°C–200°C above T_g and have molecular weights in the range of 10^4 – 10^6 are most often mixed with solids or other polymers in intensive mixers or on mixing rolls. The **intensive mixer** is distinguishable from the dough mixers and kneaders by two features. One is the sturdier construction, which allows a higher power input per unit volume. The second is pressurized mixing, usually with temperature control. In the **Banbury mixer**, two interrupted spirals (Figure 13.2a) rotate in opposite directions at 30–40 rpm. Polymers, fillers, and other ingredients are charged through the feed hopper (Figure 13.2b) and then held in the mixing chamber under the pressure of the hydraulic ram. Both the rotors and the walls of the mixing chamber can be cooled or heated by circulating fluid.

The mainstays of the rubber industry for over 60 years have been the **two-roll mill** and the Banbury mixer. Roll mills were first used for rubber mixing over 100 years ago! The plastics and adhesives industries adopted these tools later on. The Banbury is often termed an **internal mixer** since the contents are under pressure as opposed to the roll mills that are open to the atmosphere.

The two-roll mill shears the material in the nip between the rolls, one of which is rotating faster than the other. Mixing is a function of the following:

1. Roll speeds
2. Amount of turnover (folding) between passes
3. Number of passes
4. Gap between rolls

The value of roll speeds may be fixed in any machine; amount of turnover (folding) between passes and number of passes are functions of the amount of material in a batch and time of milling. They are also functions of the viscoelastic properties of the material being mixed, since multiple passes often depend on the material adhering to the roll and being carried around back to the nip. The value of gap between rolls is usually changed fairly easily on most machines and is often decreased during the course of a single mixing operation.

In the Banbury mixer, the material is subjected to less shearing than in roll mills, since the gap between scroll and wall is not adjustable. Also, heat transfer is more difficult, so that a temperature rise invariably is produced. However, incorporation of solids is more rapid because the mixing is done under the pressure of a hydraulic (or manual) ram. Also, the mixing depends much less on the viscoelastic properties of the material than does the mixing on a roll mill. White has reviewed the history of internal mixers in fascinating detail [3].

Powders can be blended together by a simple tumbling action. In the **ribbon blender**, **double-cone mixer**, or **twin-shell blender** (Figures 13.3 and 13.4), a simple rotational motion causes particles to be raised together and then to fall, splitting into small domains that are rejoined at random in the next cycle. Rolling and folding of the charge also occur. The same apparatus is used to blend porous poly(vinyl chloride) with plasticizers. Liquid plasticizer is poured or sprayed onto the powdered resin. During the tumbling, capillary action draws the liquid into the pores

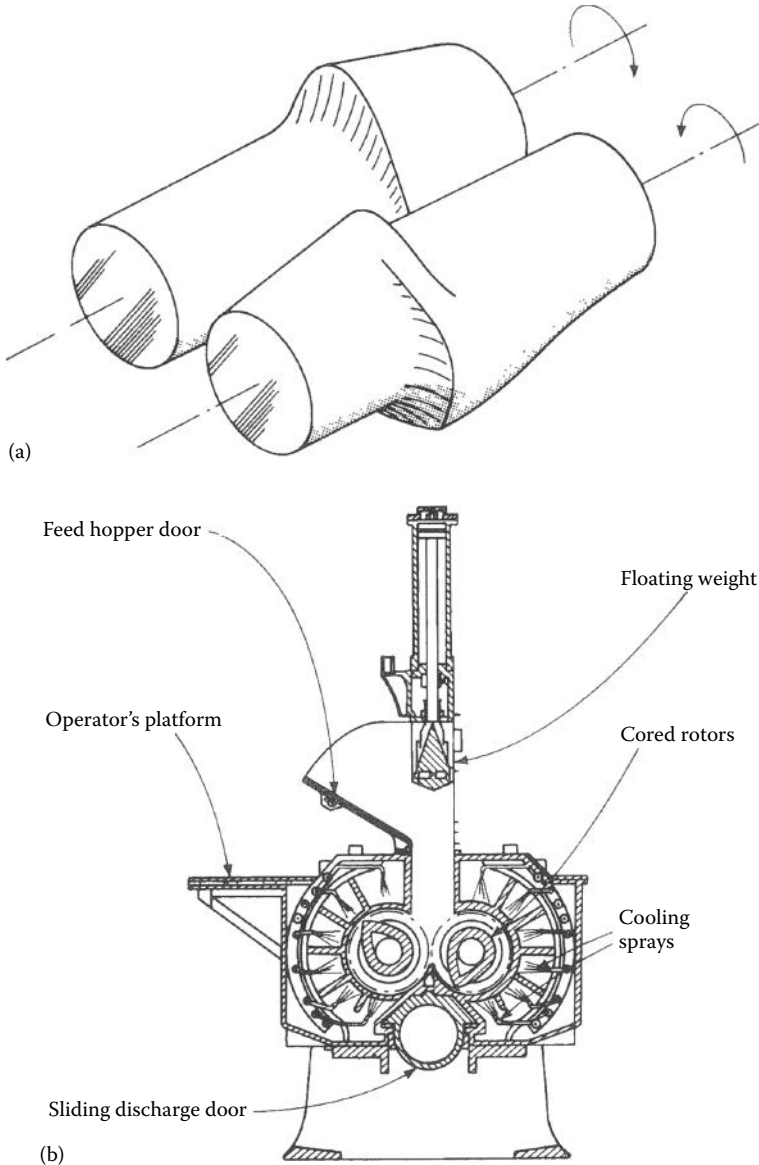


FIGURE 13.2 (a) Roll mixing blades in the Banbury mixer. (b) Cross section of Banbury mixer (registered trademark of Farrel Co., Ansonia, CT). (Data from McCabe, W., and J. C. Smith, *Unit Operations of Chemical Engineering*, 2nd edn., McGraw-Hill, New York, 851–859, 1967.)

of the resin, so that in a few minutes the dry, powdery character is restored and the resin–plasticizer combination can be charged to some other equipment (extruder or calendar) in which it will be fused into a continuous product. Roll mills have been mentioned as functioning to mix polymers with fillers. The same equipment can be used not only to disperse a solid but also to attrite it. Roll mills with up to five rolls,

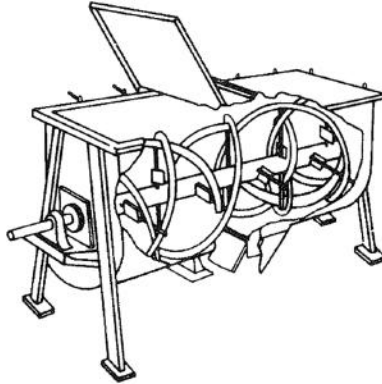


FIGURE 13.3 Ribbon blender. (Data from McCabe, W., and J. C. Smith, *Unit Operations of Chemical Engineering*, 2nd edn., McGraw-Hill, New York, 851–859, 1967.)

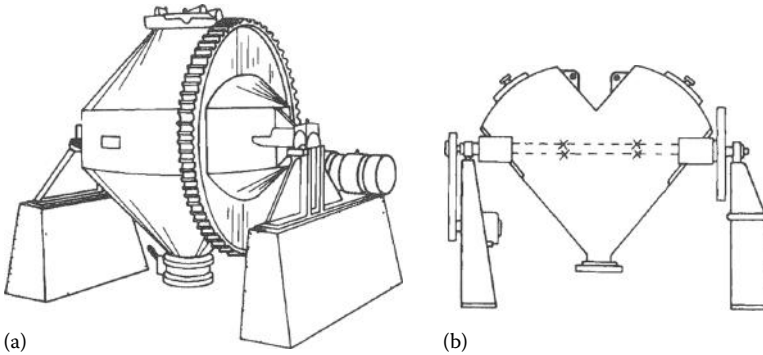


FIGURE 13.4 Tumbler mixers: (a) double-cone mixer; (b) twin-shell blender. (Data from McCabe, W., and J. C. Smith, *Unit Operations of Chemical Engineering*, 2nd edn., McGraw-Hill, New York, 1967, 851–859.)

each rotating faster than the preceding one, are used to disperse pigments rapidly in paint master batches. A slowly rotating cylinder half-filled with ceramic balls can also be used to disperse pigments. As opposed to the roll mills, which disperse the pigment in a few passes with an elapsed machine time of a minute or so, the ball mills usually operate on a cycle of hours or days.

It is obvious that less energy (and expense) is required to disperse solids in low-viscosity media than in rubbery polymer melts. In applications where a standard filler and a plasticizer are being used in large amounts, the producer of a rubber may find it expedient to add the carbon black and oil to the latex before coagulating and baling it. About half the styrene-butadiene rubber supplied in recent years has had oil added to it before coagulation (about a gram of oil for each 3 g of rubber in a typical formulation). Half of the oil-extended rubber has also had carbon black added (see Section 16.3). Master batching undoubtedly will continue to grow in popularity whenever a market justifies it to the polymer producer.

13.4 COATINGS AND ADHESIVES

Unlike most of the processes considered in Chapter 14, extrusion and molding, the only important dimension usually controlled in the application of coatings and adhesives is the thickness. There are many other parameters to be considered, of course. Adhesion is of overwhelming concern. In coatings, adhesion to one surface must be controlled. Adhesives often represent a more complicated situation because two unlike surfaces may be involved. However, the coating must face the challenge of its environment with its hazards of chemical, bacteriological, and mechanically abrasive attack over a high surface area. The adhesive seldom has to contend with these to the same extent.

13.4.1 COATINGS

A **coating** is a thin layer of material intended to protect or decorate a substrate. Most often it is expected to remain bonded to the surface permanently, although there are strippable coatings that afford a temporary protection. We can subdivide coatings by considering whether or not they contain a volatile solvent and whether or not a chemical reaction is involved in film formation (Table 13.1).

13.4.1.1 Nondiluent, Nonreactive

The oldest recorded use of polymers was for a coating of this type. The Lord told Noah, “Make yourself an ark of gopher wood; make rooms in the ark, and cover it inside and out with pitch” (Genesis 6:14). The pitch may have been a naturally occurring bitumen or wood rosin applied as a **hot melt**. A more recent application in which moisture impermeability is sought is the wax or polyethylene-coated milk container now so familiar. The hot melt can be applied from a roll on a continuous basis. More commonly, the polyethylene might be extruded through a slot (Section 14.1) as a film layer and laminated with the cardboard. The formulation of a strippable hot-melt coating with ethyl cellulose as the binder is given in Table 13.2. The ingredients are melted together at about 190°C. Metal pieces such as drill bits or other tools and gears can be dipped in the molten mass and cooled in air with a thick (2-mm) coating. Castor oil is used as a plasticizer. Mineral oil and wax are less compatible than the castor oil, but they serve as lubricants as well as plasticizers. Exuding to the metal surface, they can

TABLE 13.1
Coatings

Examples of Coatings			
Nondiluent		Diluent	
Nonreactive	Reactive	Nonreactive	Reactive
Natural pitch	Fluidized bed with epoxy + anhydride	Polymer solution (lacquer, dope)	Paint (drying oil, pigment, driers)
Polyethylene on paper	Paraxylene	Nail polish	Alkyd resins
Fluidized bed	Photoresists	Latex <i>paints</i>	Oleoresinous varnish

TABLE 13.2
Peelable Hot-Melt Coating

Material	Parts by Weight
Ethyl cellulose (50 cps grade)	25
Castor oil	10
Mineral oil	61
Paraffin wax	3
Stabilizer (antioxidant)	1

Source: Parker, D. H.: *Principles of Surface Coating Technology*, Wiley, New York, 1965, p. 762.
cps, centipoises.

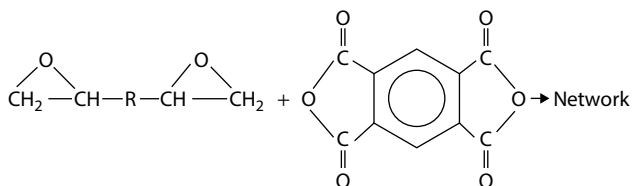
function to prevent corrosion as well as mechanical abrasion during shipping and handling. The coating is easily stripped when the tool or other article is to be put into use.

Another application of nonreactive melt coating is **fluidized-bed coating**. In a typical setup (Figure 13.5), a bed of powdered polyethylene in the range of 200 mesh (75 μm in diameter) is fluidized by the passage of air through a porous plate. A metal object to be coated is heated to well above the fusion point of the resin. When it is dipped into the bed and moved laterally as well, a layer of powder adheres to its surface and melts to form a continuous coating. The process is self-limiting because the metal cools as the polymer melts, and the layer of polymer is a poor conductor of heat. After being removed from the bed, the object may further be heated to ensure the integrity of the film. There is nothing in the technique that limits it to thermoplastic coatings. The bed is not heated; only the surface of the object to be coated is hot.

The powder can also be applied to a hot surface as a charged spray. In **electrostatic spray coating**, a powder is carried by an air stream from a fluidized reservoir and through an orifice, where it is charged by a high-voltage power supply (Figure 13.6). The parts to be coated are grounded, so the charged powder is applied very efficiently to the desired locations. The part may be hot when it is coated, or it can be heated subsequent to coating. Some applications of the electrostatic spray process are automobiles, appliances, metal furniture, luggage hardware, and even glass bottles [7].

13.4.1.2 Nondiluent, Reactive

The fluidized-bed method can be used when the polymer is a reactive powder. A mixture of an epoxy resin and an acid *hardener* can be fluidized and deposited simultaneously. Reaction occurs only on the hot surface.



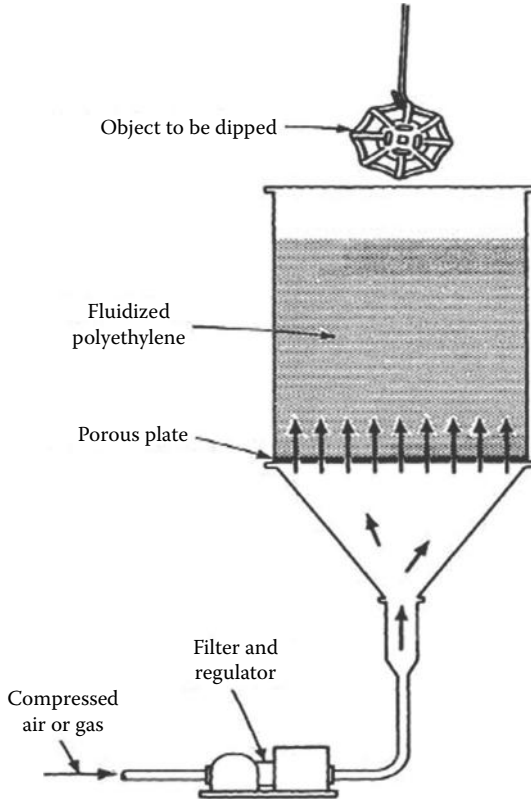


FIGURE 13.5 Fluidized-bed coating with powdered polyethylene. (Data from *Coating Metals and Other Rigid Materials with Microthene Polyethylene Powder*, 2nd edn., U.S.I. Chemicals, New York, 1965.)

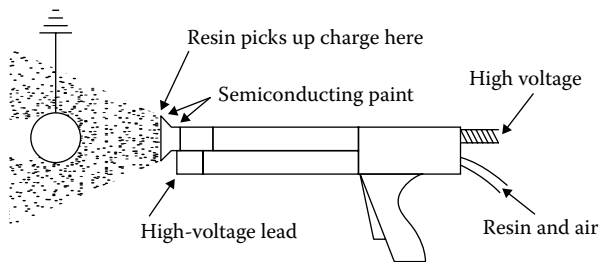
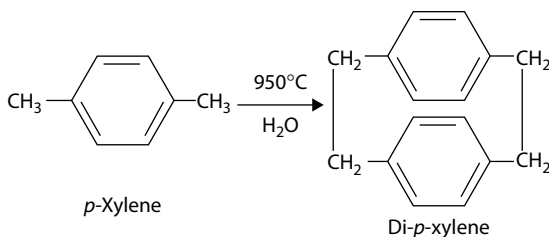
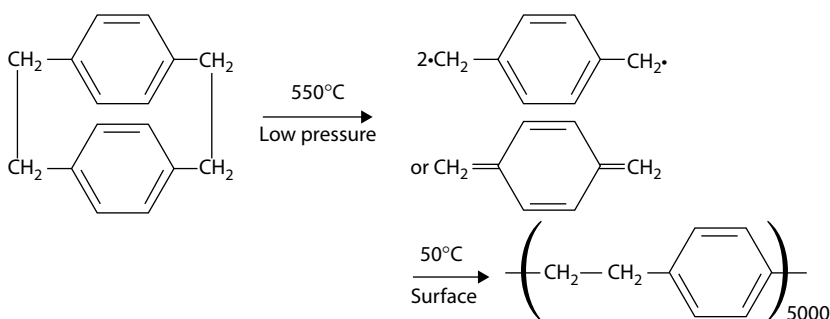


FIGURE 13.6 Electrostatic powder spray gun. (Data from *Microthene, F. Microfine Polyolefin Powders*, U.S.I. Chemicals, New York, 1976.)

A general technique has been developed whereby a reactive monomer is sprayed on a surface and forms a polymer immediately. In one application, the monomer is di-*p*-xylene formed by the pyrolysis of *p*-xylene at 950°C in the presence of steam [8]:



When the purified monomer is heated to about 550°C at a reduced pressure, a diradical results in the vapor phase, which when deposited on a surface below 50°C polymerizes instantaneously to a molecular weight of about 500,000:



The process of producing polymers on a surface through the use of ionized, gaseous plasmas has been used with hydrocarbons, fluorocarbons, and other systems [9,10]. In **glow-discharge polymerization**, the surface to be coated can be made the anode for an electrical discharge over a potential of several thousand volts. Monomers adsorbed on the surface can form highly adherent, and often cross-linked, films. Another technique that makes use of plasma technology uses polymer powders rather than monomers. The plasma in this case consists of an inert gas such as argon passed through an electric arc so that its temperature is raised to 5000°C – 8000°C . Poly(tetrafluoroethylene) powder is blown at high velocity through the plasma jet and onto the surface to be coated. As the polymer impinges on the surface, it is sintered to a continuous coating.

In a special class of nondiluent, reactive systems are those that react because of high-energy radiation. A **photocurable printing ink** is such an example. It might include an acrylated urethane polymer (containing pendant unsaturation), several monomers such as neopentyl glycol diacrylate and *N*-vinyl pyrrolidone, a sensitizer such as a benzoin ether or benzoquinone, and various pigments. The ink is transferred to a surface by conventional printing press processes. A dry, smudge-proof film can take place in seconds under a strong ultraviolet (UV) lamp rather than by evaporation of a solvent or oxidation of a drying oil, which would take much longer. The monomers act as diluents in the system, but they react to become part of the film and are not evaporated.

TABLE 13.3
White Vinyl Topcoat

Material	Pounds
Titanium dioxide	100.0
Vinyl resin (VAGH)	66.7
Vinyl resin (VMCH)	66.7
Tricresyl phosphate	25.0
Methyl isobutyl ketone	288.0
Toluene	288.0
Total	834.4
Weight per gallon: 8.34 lb	

Source: Parker, D. H.: *Principles of Surface Coating Technology*, Wiley, New York, 1965, pp. 563 and 752.

Vinyl chloride polymers, cellulose derivatives (acetate and nitrate), and acrylic copolymers can be formulated to remain tough over a wider range of temperatures than most homopolymers, so they have been favored for lacquers.

Some homely examples of lacquers include the spray cans of *touch-up paint* sold to the auto owner. Most of these are pigmented acrylic resins in solvents together with a very volatile solvent that acts as a propellant (usually a low-molecular-weight hydrocarbon). Model airplane dope may be a solution of cellulose acetate butyrate in a mixture of ketones and aromatic solvents.

The latex paints are another class of coatings that form films by loss of a liquid and deposition of a polymer layer. During World War II, latexes resulting from emulsion polymerization of styrene and butadiene similar to those made for rubber were found to be well suited to film formation. The fast drying, low odor, and, above all, ease of cleaning up spots and applicators when water is the diluent contributed to a do-it-yourself movement of tremendous proportions. Some ingredients for an exterior, light-toned paint based on an acrylic–vinyl copolymer include pigments (TiO_2 , mica, and talc), surfactants for dispersing the pigment in addition to the surfactant remaining in the latex from polymerization, an organotin polymer or cuprous oxide as a mildew preventative, a defoamer (needed during mixing and during application to decrease trapped air bubbles), and plasticizers. The ethylene glycol also functions as an anti-freeze, since freezing and thawing can break suspension and bring about coagulation.

As in the case of lacquers, the T_g of a latex paint polymer usually is adjusted by copolymerization or plasticization to the range of 30°C – 50°C . Film formation proceeds differently, however. One can picture the latex particles as so many marbles being deposited on a surface. As the water evaporates or, on wood and plaster surfaces, diffuses into the substrate, the spherical particles approach each other more and more closely. The minimum temperature at which the particles will coalesce to form a continuous layer depends mainly on the T_g . The water may have some plasticizing action, so the actual T_g may be slightly lower than one that might be measured

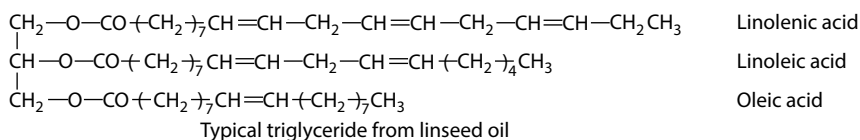
in dry test. The driving force tending to push the particles together is related to the capillary pressure of water in the system. Smaller particles and higher surface tensions should result in lower film-forming temperatures. In practice, it is found that the ratio of monomers or addition of plasticizers is a better control for film formation than the particle size or surface tension [12].

While most latex house paints fall in the nonreactive class, many applications use a subsequent cross-linking reaction to enhance durability. In a simple example, pendant hydroxyl and carboxyl groups on a polymer chain may not react with each other, while the polymer is suspended as a latex. But when the film is dried and heated, esterification can take place. It may be possible to wash off a fresh film with soap and water, but not one that has aged and become cross-linked. The advantages in an exterior house paint are obvious because cleaning up is easy but permanence (water resistance) increases with time.

Another broad application of latex films involving very low pigment volumes is the whole field of water-based polishes for industrial and home-use coatings. Latexes have also been used as paper coatings, wet strength promoters in paper, and asphalt dispersions, and in concrete. In each case it is the binding action of the continuous film formed when the water is gone that is sought.

13.4.1.4 Diluent, Reactive

Although the term **paint** is used for latex-based as well as many other systems, some favor its use to describe one of the oldest coating systems known—that of a pigment combined with a drying oil and a solvent [11]. Linseed oil is a **drying oil** by virtue of its multiple unsaturation. In effect, the oil is a polyfunctional monomer that can polymerize (*dry*) by a combination of oxidation and free-radical propagation. Modern methods of recovery by pressing and extraction remove almost all of the oil content (about 40%) of the flax seeds. The oil is a triglyceride of a mixture of fatty acids. About half the fatty acid content is linolenic acid, another 20% is linoleic, and another 20% is oleic:



One can distinguish three stages in the film formation of a drying oil by oxidation. In the first stage, **autoxidation**, the oil reacts with oxygen to form peroxy compounds. In the second stage, network formation, the peroxy compounds react to create covalent bonds between the original drying oil molecules. In the third, much slower, stage, aging, the polymer film continues to react with oxygen, forming additional cross-links and also some volatile products.

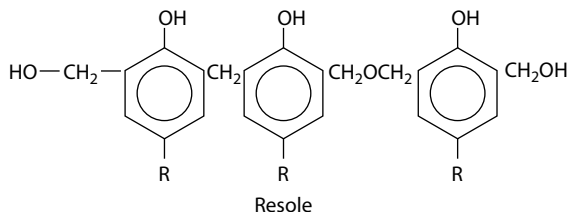
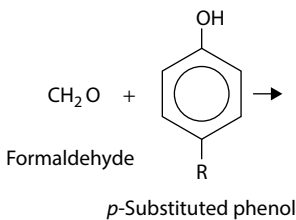
Oil-soluble metallic soaps called **driers** are used to catalyze the oxidation process. The time necessary to change a film of linseed oil to an insoluble network is decreased from days to hours by the addition of 0.05% cobalt metal in soluble form. Cobalt and manganese are commonly used as salts (soaps or driers) of naphthenic acid. Previously used lead is no longer permitted in consumer products. The acid,

a by-product of naphthenic lubricating oil refining, is predominantly composed of saturated, cyclic, monocarboxylic species. With a typical molecular weight of 150–250, the acid yields soaps with excellent solubility in aliphatic solvents and good drying activity. The metallic soaps accelerate the rate of oxygen uptake and network formation and may also alter the details of the mechanism [13].

Pigments include calcium carbonate and zinc oxide, which would give a white appearance of moderate hiding power. The iron oxide gives a durable brown color, which is stable over a long period of time. The soya lecithin is a substituted phosphoric acid ester of a diglyceride that acts as a dispersing and stabilizing agent for the pigments.

In the slow process of aging or weathering, the gradual erosion of the surface that accompanies further oxidation is not always undesirable. A **chalking** paint, which erodes at the surface, is self-cleaning. In a house paint, this means that atmospheric dirt will be removed from the surface along with some of the film by ordinary wind and rain or by deliberate washing.

Oleoresinous varnishes, as the name implies, are combinations of resins and drying oils. Prior to the introduction of alkyd resins in the 1920s (discussed below), the term *varnish* usually denoted the reaction product of a heat-treated natural resin with drying oil. The product often was dissolved in a solvent called a thinner because it decreased the viscosity of the varnish, together with appropriate driers. Addition of a pigment to a varnish yields an enamel, although the terminology is far from standardized. The natural resins are not widely used any longer. The synthetic resins that are used often are somewhat complex. A simple example is a phenolic resole, a reactive, soluble material. Reaction of formaldehyde with a *para*-substituted phenol under alkaline conditions yields the resin, which can be further reacted with an oil to form an air-drying coating.



Reaction at 200°C–250°C with a triglyceride such as tung oil is accompanied by the evolution of water, so presumably the resole reacts with free acid groups from oxidation of tung oil, as well as by ester interchange with the terminal hydroxyls of the resole. Other reactions involving the phenolic hydroxyl are also probable.

The combination of hard, wear-resistant resin with softer, energy-absorbing drying oil films can be designed to give products with a wide range of gloss and durability. The terms *long oil* and *short oil* are used to denote varnishes that are higher and lower, respectively, in the ratio of drying oil to resin.

Another route to balancing drying properties, durability, gloss, and hardness is via **alkyd resins**. These esters are formed from alcohols and acids, hence the coined name *alkyd*. A common mode of operation is to start with the free fatty acids from the drying oil rather than with the triglycerides. The drying mechanism for alkyd resins resembles that described for linseed oil. Some applications do not use driers but react in a short time at an elevated temperature.

The legislation enacted over the past several decades limiting the discharge of solvents into the atmosphere has had a major influence on the coating industry. With the limitation on solvent vapor discharges of all kinds, there has been a trend toward water-borne coatings, powder coatings, and UV-curable (100% reactive) coatings [14].

13.4.2 ADHESIVES

In the broad sense of the word, adhesion is important in every heterophase system including the coatings just described. However, we can look at the process more narrowly as involving a layer of material (**adhesive**) between two surfaces (**adherends** or substrates). **Mechanical adhesion** is easy to visualize. When two porous surfaces such as paper are glued together with a liquid adhesive, the interlocking action of the liquid that penetrates the pores acts as a mechanical fastener. However, gluing together two smooth, impervious surfaces must involve other forces. In **specific adhesion** the secondary forces between the adhesive and the surface bond the two. Actual covalent bonds may be formed, but this is hard to demonstrate in most cases. In any kind of adhesion, **wetting** of the surface by the adhesive is important. One way of characterizing a surface is to measure the **contact angle** θ_c made by a drop of liquid on the surface at the point where the two phases meet (Figure 13.7). Perfect wetting occurs when $\cos \theta_c = 1$, that is, when $\theta_c = 0$. When $\cos \theta_c$ is plotted for a series of liquids on a single surface, the intercept at $\cos \theta_c = 1$ is γ_c , the **critical surface tension** of that surface [15]. The values obtained for some common polymers are summarized in Table 13.4. In general, liquids will spread when the surface tension of the liquid is lower than the critical surface tension of the surface. Thus, glass and metals are easily wetted by organic materials when they are clean.

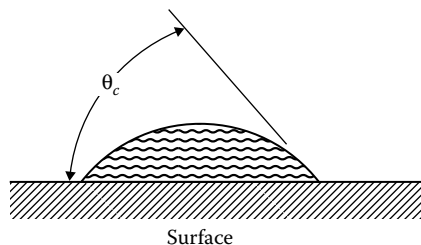


FIGURE 13.7 Definition of contact angle (θ_c) for liquid droplet on a surface.

TABLE 13.4
Critical Surface Tensions of Polymeric Solids at 20°C

Polymeric Solid	γ_c dyne/cm (mN/m)
Polymethacrylic ester of Φ' -octanol ^a	10.6
Poly(hexafluoropropylene)	16.2
Poly(tetrafluoroethylene)	18.5
Poly(trifluoroethylene)	22
Poly(vinylidene fluoride)	25
Poly(vinyl fluoride)	28
Polyethylene	31
Poly(trifluorochloroethylene)	31
Polystyrene	33
Poly(vinyl alcohol)	37
Poly(methyl methacrylate)	39
Poly(vinyl chloride)	40
Poly(vinylidene chloride)	40
Poly(ethylene terephthalate)	43
Poly(hexamethylene adipamide)	46

Source: Zisman, W. A., *Ind. Eng. Chem.* 55, 18, 1963.

^a Φ' -octanol is $\text{CF}_3(\text{C}_2\text{F})_3\text{CH}_2\text{OH}$.

However, some liquids, upon contacting surface, orient in such a way that the surface is converted to one more or less easily wetted than the original.

Poly(dimethylsiloxane) liquids have a surface tension of 19–20 dyne/cm (mN/m). However, a closely packed, adsorbed monolayer of the same polymer exhibits a surface of methyl groups with a critical surface tension of about 24 dyne/cm. Thus, silicones spread on almost all surfaces, since each surface, once wetted, is converted to one of higher surface tension than that of the liquid itself. Normal octyl alcohol also orients at a high-energy surface to convert it to a methyl surface. But now the surface tension of the alcohol (25 dyne/cm) is higher than that of the layer on the surface. Such a system is **autophobic**, that is, spreading does not occur because the first molecules antagonize the surface. If surfaces were perfectly smooth and clean, no adhesive would be needed. Almost any material cleaved in a high vacuum can be fused back together without an adhesive or high temperature. However, surfaces are rough on an atomic scale, and one of the functions of an adhesive is to fill in the asperities. Therefore, all adhesives are applied as liquids.

Most adhesives are counterparts of the coating systems we have already discussed (Table 13.5). A plasticized rubbery polymer has low volatility, high viscosity, and low surface tension, and makes a good adhesive. Cellophane tapes and *self-stick* postage stamps are typical applications of such a pressure-sensitive adhesive. The material remains permanently liquid but forms a strong bond between the surface and the cellophane backing when slight pressure is applied to cause flow. When the surface is paper, presumably both specific and mechanical adhesion may be involved. Water

TABLE 13.5
Adhesives

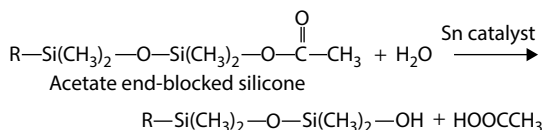
Examples of Adhesives			
Nondiluent		Diluent	
Nonreactive	Reactive	Nonreactive	Reactive
Permanent liquid (cellophane tape, labels, stamps)	RTV silicone	Rubber cement	Phenol–formaldehyde for plywood
Water	Epoxy + amine <i>hardener</i>	Cellulose nitrate in ketone (model cement)	Alkyd resins
Hot melt	Cyanoacrylate	Poly(vinyl acetate) latex (<i>white glue</i>)	Oleoresinous varnish

RTV, room-temperature vulcanization.

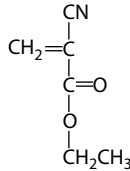
is a good example of a liquid adhesive for almost any two surfaces. Its volatility, low viscosity, and high surface tension make it a poor adhesive; although when it freezes, it can be a very strong adhesive, as someone who has put his or her tongue on a frozen sled runner can attest. Tar and sealing wax are examples of hot melt adhesives that solidify by cooling after being applied as hot liquids. Some animal glues and thermoplastic resins are applied similarly.

In the category of diluent, nonreactive adhesives, one example is model airplane cement (often cellulose nitrate in a mixture of ketones and aromatic solvents). As a coating we would call it a lacquer. Aqueous solutions of natural and synthetic gums are used in library paste. Some of the popular white glues for paper and wood are simply poly(vinyl acetate) emulsions with a small amount of plasticizer. All of these materials solidify after contacting the surface as a liquid by loss of solvent or diluent. Evaporation or diffusion into a porous substrate may be involved.

The stronger adhesives generally are those that are thermosetting. They are applied as liquids but form network polymers by chemical reaction. It may be necessary to heat the liquid to cause the reaction to occur. A common system involves mixing two ingredients that will react after an induction period. The **pot life** of such a system is the time between mixing and conversion to a high viscosity unsuitable for spreading. Epoxy resins can be formulated so that the reaction between the epoxy prepolymer and the amine *hardener* (both polyfunctional) takes place 15–30 min after the mixing. Not every reactive adhesive is made by mixing two ingredients. The room-temperature-vulcanizing silicones are stable pastes for months as long as they are protected from the atmosphere. Exposure to a humid atmosphere brings about hydrolysis of acetate ester end groups. In the presence of certain catalysts (especially tin soaps), the SiOH groups condense to form Si—O—Si bonds.



The **cyanoacrylate adhesives** were introduced in the late 1950s. Unlike the epoxy or silicone adhesives, these materials contain a monomer that undergoes rapid polymerization at room temperature. The monomer ethyl cyanoacrylate is stable with trace amounts of an acid inhibitor such as polyphosphoric acid. The commercial formulations may contain methyl and higher cyanoacrylate esters, thickeners such as organic polymers, and plasticizers for increased final film toughness. A slightly basic surface is needed for ionic polymerization to occur. Even the surface moisture of an ostensibly *dry* metal or ceramic surface is sufficiently basic.



Ethyl cyanoacrylate

A really acid surface does require an alkaline pretreatment. The reaction time for polymerization is less than 10 s when a thin layer of monomer is applied to a clean, dry, smooth surface. A variety of cyanoacrylate adhesives are on the market with numerous brand names that convey the rapidity of bonding, the *super strength* of the bond, or merely the imagination of a sales organization. Repairs of china, glass, plastics, and metals all can be quite dramatic, as demonstrated in television ads. However, the cyanoacrylates have also been used as sutures to glue together skin or other body tissues, as dental adhesives, and in industrial applications such as attaching ornaments in automobiles and in assembling electronic devices.

Other commercially successful reactive acrylic-based adhesives are mixtures of methacrylate polymers dissolved in methyl methacrylate (MMA) monomers. Extensive research and development of these adhesives first introduced in the 1960s have led to what is termed *high-performance acrylic adhesives*. These products are supplied as two separate components to be mixed prior to an application. A peroxide in one component and an amine or metal salt (reducing agent) in the other initiate a free-radical polymerization of the MMA upon mixing [16].

Some reactive adhesives are applied with the aid of a volatile diluent. When a phenol-formaldehyde resin is used to impregnate and glue together the layers of wood that make up plywood, water is evaporated from the system. Alkyd resins and oleoresinous varnishes with a volatile diluent can be applied to a surface that is glued to another surface after the diluent is evaporated.

13.5 PHOTORESISTS: AN APPLICATION OF POLYMERS TO MICROELECTRONICS

Photoresists have been used for many years in lithography for the production of printing plates. Strictly speaking, these generally are applied from a solution.

Chromated gelatin is one classical example that still finds some use in making masks for silk screens. Somewhat newer are films made from poly(vinyl alcohol)

containing bichromate. For a printing process, the film might be deposited on a metal surface from an aqueous solution. The dry film on exposure to UV light through a mask is insolubilized by oxidative cross-linking. Patient washing with warm water removes the unexposed portions of the film. Next the film is baked to increase adherence of the cross-linked portions. Then an etchant is applied to attack the metal and to leave a raised pattern where the polymer was irradiated. The polymer *resists* the etching of the metal. In some applications, etching is not needed, as when ink receptivity is different for bare metal compared to a polymer surface. Another application of the poly(vinyl alcohol)-bichromate system has been in the production of color television tubes. The screen of the tube requires a pattern of three types of phosphor dots. Each of the three phosphors can be applied in separate stages by exposure through a carefully registered set of masks. In each of three stages, a single phosphor is suspended in the polymer film and the dots are insolubilized. The uncross-linked polymer with its phosphor content is washed away. Etching is not required. The screen is baked between stages to oxidize the polymer film and to leave the phosphor firmly attached to the glass. The glass screen is fused onto the front of the television tube with the phosphors on the inside surface. Because of environmental concerns, chromate-based systems are no longer recommended.

The microelectronics industry is built around the ability to assemble transistors that have dimensions on the order of 100 nm or less. Almost all lithography involves the creation of patterns in photopolymers made possible by a radiation-induced solubility change in the polymer. A photoresist needs to adhere to a substrate, undergo a radiation-induced solubility change, possess etch resistance, be developable in aqueous base (or other solvent), and disappear when not wanted. Photoresists are classified as positive tone if they become more soluble in the exposed region and negative tone if they are less soluble in the exposed area.

Photoresists depend on one of several mechanisms for their needed solubility change including cross-linking, chain scission, and a polarity change. The former two mechanisms are less widely practiced for high-resolution resists as they can swell in solvents and this leads to destruction of the pattern. However, a polarity change can produce fine, small-scale images because the solvent (typically water) cannot swell the unexposed regions.

The production of semiconductor devices, especially integrated circuits, represents the most demanding set of conditions for polymeric resists. This operation still is a form of lithography (litho = stone, graph = image), although it is more often termed **microlithography**. The *image* being created is the circuit, and the silicon (or its surface layer of silicon oxide) is the *stone*. Many silicon chips used in calculators and computers are produced by some variation of the following sequence of operations (Figure 13.8):

1. A silicon wafer as much as 300 mm in diameter has one surface oxidized to a controlled depth.
2. Polymer is applied by placing a few drops of solution at the center of the oxide side of the wafer and then spinning the wafer to obtain a thin, uniform coating that when dry is about 1 μm thick. The polymers used are those that will change in solubility upon irradiation. Polymers such as poly(vinyl cinnamate)

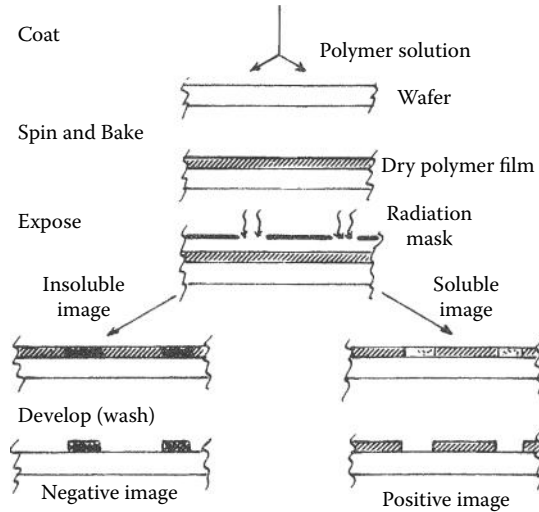


FIGURE 13.8 The silicon single-crystal wafer (with oxidized surface) is coated with a polymer film by spinning and baking and then selectively exposed to UV light or X-rays, or to an electron beam. The latent image is developed into a positive or negative pattern on the wafer by dissolution of the appropriate areas of the polymer *resist* film.

- (see Section 16.5) and cyclized rubber (see Section 12.3) cross-link on exposure to UV light and are termed **negative resists** (Figure 13.8). Others, such as the novolak–diazoketone mixtures (see below), change from oil soluble to base soluble as a result of irradiation and are termed **positive resists**.
3. In either case, exposure to UV light via a mask (in contact or with a projected image) changes the solubility of exposed polymer film.
 4. In the case of negative resists, the uncross-linked polymer is washed off, leaving the cross-linked image behind. For positive resists, it is the exposed film that is washed off.
 5. The bare substrate parts are etched through the oxide layer down to the silicon layer by a fluoride solution in water or by a plasma containing reactive ions.
 6. The chemical compositions of the etched regions are altered. Ion implantation can be used to introduce *dopants*, that is, impurities that make semiconductors of the diffused-base transistor type. Other operations can include depositing a layer of aluminum to act as a conductor or other materials to act as insulators.
 7. All polymer is removed by solvents, plasmas, or baking.
 8. The wafer is recoated and a new pattern imposed and processed. This entire sequence may be repeated a number of times to give integrated circuits with many layers and amazing complexity.

The minimum line width on chips produced by photolithography has decreased steadily from year to year. As a rule of thumb, the minimum feature size on a dynamic random access memory (DRAM) silicon chip has decreased by a factor of

2 about every 6 years. For example, from 1985 to 1995, many commercial DRAM chips went from minimum line widths of 1 μm down to 0.35 μm . As dimensions shrink in microelectronic circuits so too must the exposing radiation. Only a few years ago most resists were processed using 365 nm radiation, but over the last decade new steppers (the tools used to image microelectronic circuits) have been introduced that operate at 248 nm and more recently 193 nm with a near-term goal of resists that operate at 157 nm. For example, an F_2 excimer laser operating at 157 nm has been used to achieve resolution better than 80 nm and should be capable of 50 nm [17].

A single wafer is processed as a unit but then is cut up into individual chips. Wafers in use in 1995 typically were 100–200 mm in diameter, but 300-mm wafers were already being tested. The chips themselves range from several centimeters on a side (for a complex chip such as Intel’s Pentium) to a few millimeters on a side (for a wristwatch chip). Attaching electrical leads to the tiny conducting spots on the chip is a separate, demanding task.

In terms of volume used, the most popular photoresist type has been a physical combination of a phenol–formaldehyde **novolak resin** with a diazoquinone. The novolak (molecular weight of about 500–2000) does not dissolve in dilute alkali when 20%–50% of a diazoketone is present in the dry film. However, UV light converts the alkali-insoluble diazoquinone into the hydrophilic carboxylate form via the **Wolff rearrangement** (Figure 13.9). Without the diazoquinone *dissolution inhibitor* in the exposed areas, the novolak now dissolves in dilute alkali.

In 1980, researchers at IBM Almaden Research Center became concerned that the then present light sources would not be able to provide enough radiation to trigger the photoimaging process. To overcome this problem, the researchers used **chemical amplification**, a method that permits a single photon of light to carry out many hundreds of photochemical events. A very small amount of acid produced by a light-sensitive compound known as a **photoacid generator (PAG)** becomes the catalyst for a subsequent chemical reaction that causes the change in resist solubility [18]. For example, a diaryl iodonium salt can act as the PAG in a matrix

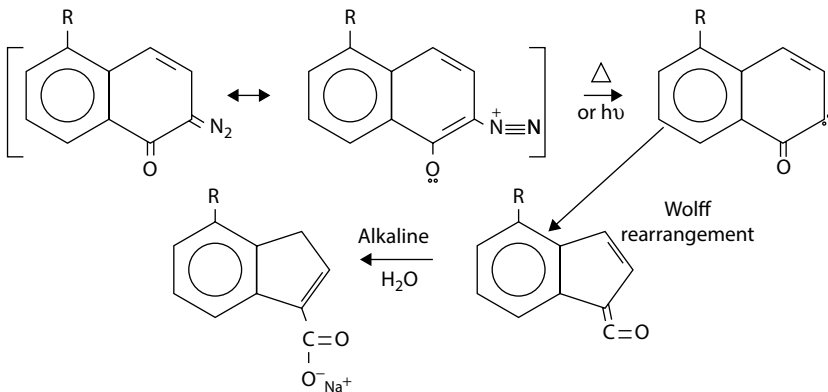


FIGURE 13.9 Photochemistry of diazoquinone including subsequent Wolff rearrangement to carboxyl.

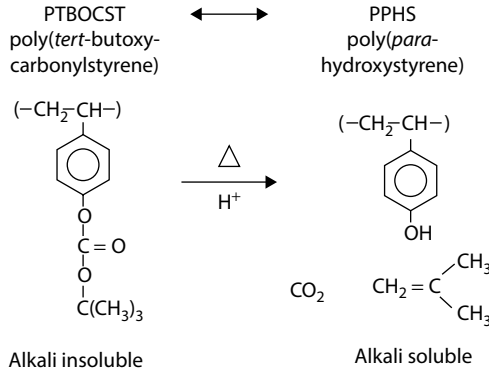


FIGURE 13.10 In a CA resist, the acid generated by exposure to light is used to catalyze the thermal deprotection of the alkali-insoluble polymer, rendering it soluble in alkali.

of an acid-sensitive polymer such as the *protected* form of poly(*p*-hydroxystyrene). Following exposure, heating the mixture causes loss of the *tert*-butoxycarbonyl protecting group to occur in the exposed regions (Figure 13.10). Now the film is soluble in alkali where it has been exposed, but insoluble where it is still protected. Each PAG can induce as many as a thousand reactions. In this way, the small amount of energy used in exposure is amplified by the subsequent chemical reaction. Another important aspect of chemically amplified (CA) resists is the large difference in solubility of the exposed and unexposed regions. This means that CA resists can reliably form images that are smaller than the wavelength of the imaging radiation. This process has become very successful even though laser sources for UV light have since been invented and the prior concern that light intensity will be too low now no longer exists.

For each generation of resist, new polymer structures are needed. Until recently, resists containing aromatic groups were produced because of the greater etch resistance of these polymers. The current 193-nm resists have no aromatic groups because of their strong absorption at 193 nm. For the next generation of 157-nm resists, the situation becomes still more complicated since even carbonyl groups absorb strongly and only fluorinated and silicone polymers are highly transparent.

Electron beam lithography is used to produce masks for UV photolithography and, in some places, to produce the chips themselves. A scanning electron beam similar to a scanning electron microscope can be programmed to produce patterns on a very thin polymer layer (less than 1 μm thick). The electron beam may cause cross-linking or may solubilize the polymer. Both poly(methyl methacrylate) and poly(butene-1-sulfone) respond to electrons by chain scission. The lower molecular-weight polymer produced is more soluble than the original. In order to enhance the solubility difference, often very high-molecular-weight polymers are used on the order of 500,000 g/mol. By contrast, most base-soluble resists are of very modest molecular weight. Another type of radiation that has been used for lithography is high-energy X-rays, known as extreme UV (EUV) radiation, with a wavelength

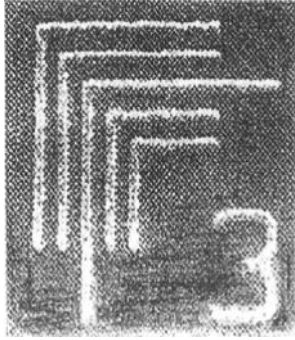


FIGURE 13.11 Electron micrograph of a fluorinated, CA photoresist developed in sc CO_2 . Each line in the pattern is only 300 nm wide.

of 13 nm. These polymers will have very different compositions from those previously produced, since they may contain elements such as silicon or boron in order to produce a resist with greater transparency. Research is currently under way to perfect photoresists for this next-generation lithography.

The semiconductor industry is becoming increasingly concerned about environmental aspects of the manufacture of microelectronics. Note that most of the development processes involving resist processing are now carried out using aqueous systems, making the process environmentally friendly. Nevertheless, many semiconductor *fabs* are located in areas where water is difficult to come by. As a result, new processes are being investigated, one such being the use of **supercritical** (sc) CO_2 as a developer solvent. Sc CO_2 is a nonpolar solvent with low viscosity and no surface tension, since there is no distinction between the gas phase and the liquid state. The lack of surface tension means that the capillary forces present during aqueous development that can destroy detailed patterns created in the resist are entirely absent in sc CO_2 . A particular advantage of this solvent is that a reduction of pressure will convert it to the gas phase making disposal of waste very easy. Current water-developable resists cannot be used because of the very nonpolar nature of sc CO_2 . To overcome this problem, fluorinated polymers have been used that can undergo CA solubility change. Figure 13.11 shows a 300-nm test pattern that was developed in sc CO_2 . Please note that these patterns are so small that each line is only a few hundred polymer chains wide. Since the average human hair is on the order of 100 μm in diameter, it can be seen that the lines in this pattern are 300 times smaller than a human hair.

13.6 POLYMERIC MEMBRANES

The use of synthetic polymeric membranes in separation processes [19,20] took off with the breakthrough of **asymmetric membrane** formation first developed by Loeb and Sourirajan [21]. These membranes have a thin dense polymer layer that governs the separation on top of a much thicker porous layer that provides mechanical support. They were first produced in the laboratory by spreading

uniform thickness films of polymer solutions on glass plates using a hand-casting knife (called a doctor's blade). The film and glass plate were then immersed in a nonsolvent bath to precipitate the polymer. Because the flux through a membrane is inversely proportional to its thickness, it was not previously possible to use dense (nonporous) membranes that could withstand the needed pressures across the membranes to achieve practical permeation rates. The separation process in asymmetric membrane is not based on filtration (i.e., size separation), but rather on a solution-diffusion model where the different solubility of the various components permeating through the polymer plays a crucial role in the efficiency of the separation.

The **wet casting process** developed by Loeb and Sourirajan is illustrated in Figure 13.12 for a small scale-up production [19]. Three possible outcomes of membrane structures can be obtained via this process: a dense membrane, an asymmetric membrane, or a porous membrane. The thermodynamic properties of the polymer/solvent/nonsolvent ternary system, the flux of the solvent out of the polymer solution, and the flux of the nonsolvent into the polymer film will govern the structure of the ensuing membrane. This is illustrated in Figure 13.13 for one of the earliest successful asymmetric membranes based on cellulose acetate (component 3) in acetone (component 2) using water (component 3) as the standard nonsolvent medium. The triangular diagram shows the phase equilibrium of this ternary system. The stars and tie-lines between them are experimental data of coexisting phases. The spinodal and bimodal

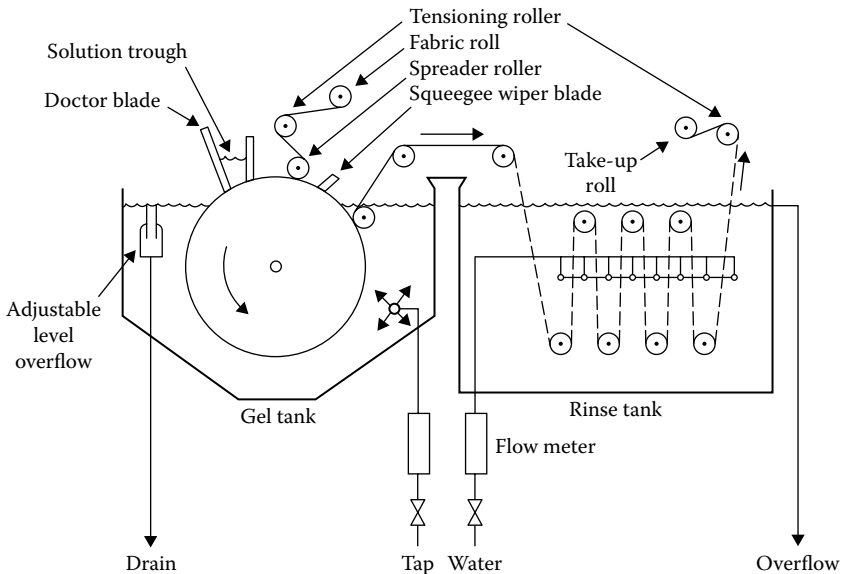


FIGURE 13.12 Machine used to prepare polymeric membranes by the Loeb–Sourirajan wet casting process. (Data from Baker, R. W.: *Membrane Technology and Applications*, 2nd edn., Wiley, Hoboken, NJ, 2004. Copyright Wiley-VCH Verlag GmbH & Co. KGaA. Reproduced with permission.)

curves are best-fit results based on the Flory–Huggins thermodynamic model [22,23] generalized to a three-component system:

$$\mu_1 - \mu_1^0 = RT \left[\ln v_1 + (1 - v_1)(1 + \chi_{12}v_2 + \chi_{13}v_3) - \frac{v_2(1 + \chi_{23}v_3)V_1}{V_2} - \frac{v_3V_1}{V_3} \right]$$

$$\mu_2 - \mu_2^0 = RT \left[\ln v_2 + (1 - v_2) \left(1 + \frac{\chi_{12}v_1V_2}{V_1} + \chi_{23}v_3 \right) - \frac{v_1(1 + \chi_{13}v_3)V_2}{V_1} - \frac{v_3V_2}{V_3} \right]$$

The variables in the above equations have the same definitions as in Section 3.3, and the Flory–Huggins assumption of no volume change upon mixing, $v_1 + v_2 + v_3 = 1$, has been used. When these thermodynamic properties are combined with the diffusion of nonsolvent and solvent in and out of the cast polymer solution, the concentration profile that develops in the diffusion layer inside the polymer film can be calculated [22,23]. Figure 13.13 shows the dependence of such profiles on the ratio of the fluxes of non-solvent to solvent, $\sigma = J_1/J_2$. These profiles were computed based on some simplifying assumptions for a casting polymer composition of $v_1 = 0$, $v_2 = 0.85$, and $v_3 = 0.15$ [22]. In a narrow range of values of σ between -0.97 and -0.95 , a polymer concentration path between the casting polymer composition and a surface: layer of a one-phase high

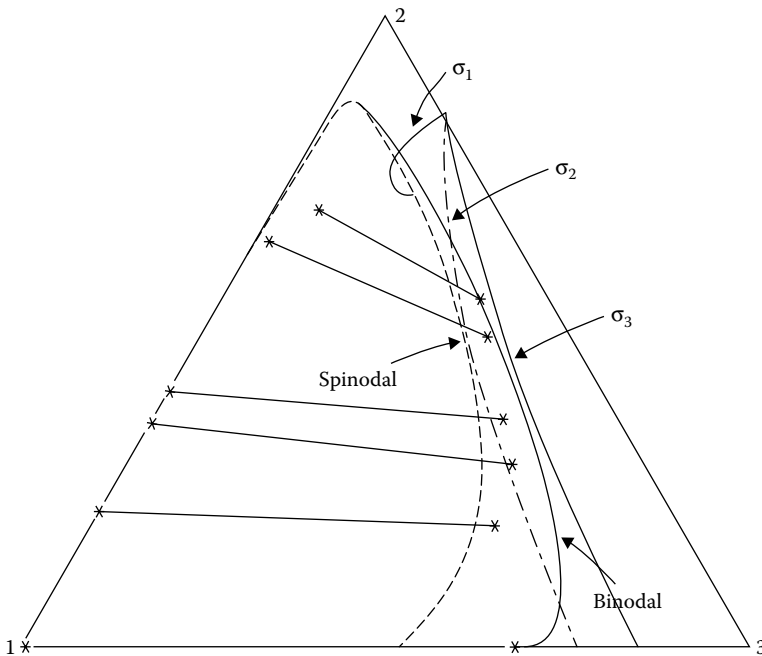


FIGURE 13.13 Ternary phase diagram of cellulose acetate (component 3), acetone (component 2), and water (component 3). The $\sigma = J_1/J_2$ curves represent concentration paths that develop in the diffusion layer of the cast film for different values of the ratio of the fluxes, $\sigma_1 = -0.97$, $\sigma_2 = -0.96$, and $\sigma_3 = -0.95$.

polymer concentration in contact with the nonsolvent bath enters the two-phase region. This path would lead to an asymmetric membrane where a dense surface layer has developed over a microphase-separated layer in the polymer film. One of the microseparated phases is polymer rich and the other is a mixture of solvent and nonsolvent that produces the underlying porous layer after washing and drying. According to these predictions, concentration paths with σ greater than -0.95 and those with σ less than -0.97 will lead to totally dense membranes and totally porous membranes, respectively. Both the thermodynamics of the ternary system and the kinetics of mass transfer play an important role in the structure formation of the membrane such that only certain polymers can lead to asymmetric membranes via this process. The success of asymmetric cellulose acetate membranes in water desalination by reverse osmosis led the way for the development of other asymmetric membranes based on polysulfones and polyimides in the 1980s and 1990s for gas separations. Polymeric membranes were also developed for liquid–liquid separations by pervaporation and totally porous membranes from a variety of polymers are used in filtration processes in the whole range from ultrafiltration to conventional filtration depending on their average pore size. The selectivity in porous membranes is based on the size exclusion of solute particles. Many different versions of the wet casting process as well as other fabrication processes are now used in the preparation of polymeric membranes [19].

13.7 APPLICATIONS OF POLYMERS IN MEDICINE

For medical purposes, fabrication takes on a special meaning, since the conversion of polymers into useful artifacts that will impact the human body externally or internally is a topic that affects us all on a very personal level. Gathered together in this section are just a few examples of the many and varied applications of synthetic polymers in medicine. Anyone who has had a hospital experience is aware of the multiplicity of plastics, elastomers, and fibers used in sterile items such as gloves, tubing, bags, syringes, towels, and the like. The disposable nature of many such items has the advantage of eliminating resterilization, thus reducing the hazards of cross-contamination. A major requirement, of course, is that these articles do not introduce even traces of adventitious impurities. Contact lenses, dentures, and dental fillings are of even greater concern since they entail intimate contact with the body. The issue of **biocompatibility** becomes paramount when the polymer remains in contact with the body over long periods of time as in the case of hip and other bone prostheses, sutures, vascular grafts, soft tissue replacements (facial tissues, breast implants), implantable drug delivery systems, and semiexternal devices such as dialysis (*artificial kidney*) and blood processing devices [24,25].

An abbreviated list of medical applications for *commodity* polymers (Table 13.6) is an indication of the wide scope of both materials and their uses. Since many of these uses require small volumes of premium materials, it is often feasible to supplement commodity plastics by developing specialty polymers that would not otherwise be justified on an economic basis. In the examples that follow, one encounters both *commodity* polymers such as ultrahigh-molecular-weight polyethylene (UHMWPE) and poly(tetrafluoroethylene) (PTFE), and specialty polymers such as the polyanhydrides and poly(glycolic acid).

TABLE 13.6
Some Medical Applications of Common Polymers

Application	Typical Polymers
Sterile packaging	LDPE, HDPE, PVC, polystyrene, polycarbonate, polyester
Syringes	Polypropylene, polystyrene
Tubing and bags for blood, urine, and infusion solutions	PVC, LDPE, polyurethanes
Contact lenses	PMMA (hard), poly(hydroxyethyl acrylate) (soft)
Denture materials and fillings	PMMA (cross-linked)
Dialysis tubing	Regenerated cellulose, cellulose acetate, polyacrylonitrile, polysulfone
Sutures	Nylon, polyester, silk
Sutures (absorbable)	Aliphatic polyesters, regenerated collagen
Hip joint prostheses	PMMA, UHMWPE
Vascular grafts (blood vessel)	Polyester, PTFE
Soft tissue replacement	Silicones, polyurethanes
Breast implants	Silicones
Burn treatment and skin grafts	Composites containing polyesters or nylons together with natural materials.
Implantable drug delivery systems	Various natural polymers as well as aliphatic polyesters and poly amides

Source: Halpern, B. D., and Y.-C. Tong: Medical applications, in H. F. Mark, N. M. Bikales, C. G. Overberger, and G. Menges (eds.), *Encyclopedia of Polymer Science and Engineering*, 2nd edn., vol. 9, 1987, 486. Copyright Wiley-VCH Verlag GmbH & Co. KGaA; Bronzino, J. D. (ed.), *The Biomedical Engineering Handbook*, 2nd edn., CRC Press, Boca Raton, FL, 2000.

HDPE, high-density polyethylene; LDPE, low-density polyethylene; PMMA, poly(methyl methacrylate); PTFE, poly(tetrafluoroethylene); PVC, poly(vinyl chloride); UHMWPE, ultrahigh-molecular-weight polyethylene.

13.7.1 HIP PROSTHESIS

In the United States alone, over 100,000 hips are replaced each year [26]. There are a number of reasons causing the hip joint to deteriorate. A gradual wearing away of the cartilage between the thighbone and the pelvis (**osteoarthritis**) is the most common. It is not unusual for replacement of the joint to allow wheelchair-ridden patients to walk again and to alleviate much of the pain. There are a variety of designs, but almost all involve a metal rod that is placed into a hollow shaft drilled into the top of the femur (thighbone) (Figure 13.14). The top of the rod terminates in a metal or ceramic ball. The ball, in turn, fits into a cup-shaped plastic socket (the acetabular cup) sometimes encased in metal. UHMWPE is the polymer of choice for most sockets. A kind of powder compression molding is needed to produce the socket because the polymer does not flow readily. After molding, the socket must be packaged and sterilized, often using gamma radiation. Securing the socket and rod into the femur and pelvis requires the use of an adhesive. A partially polymerized MMA syrup, similar to that used in the production of sheet (Chapter 5), has been widely used. A cross-linking agent may

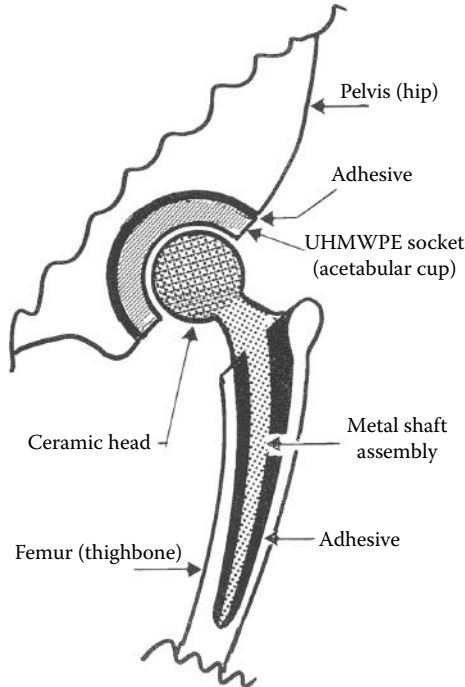


FIGURE 13.14 Typical hip replacement.

be present. Some hip implants are *cementless* in that a porous surface on the metal allows bone to grow in and around the prosthesis. As a rule, cementless implants are more successful with younger patients than with those who are over, say, 60. With both types of replacements, wear and tear on the surfaces can create debris leading to irritation and loosening of the joint. However, after almost 40 years of experience with this prosthesis (over a million hips), it can be said that “85% of people can still walk and move comfortably 15 years after surgery” [26].

Since reducing friction is paramount in the choice of socket material, a logical first choice (and one that was made 40 years ago) would be PTFE. However, the cold flow of the polymer near body temperature (see Section 9.7) is undesirable. UHMWPE has a good combination of lubricity and mechanical stability. There are still problems of degradation, especially along grain boundaries that may remain from the compression molding process as well as persistent by-products from the sterilization step.

Other adhesives such as the epoxies have been used, particularly in the rod–femur area. The major problem is mechanical loosening. Many variations are employed, but the thermosetting methacrylates are still favored.

Replacement of other joints uses many of the same materials as have been found useful in hips. However, the knee joint has the complication of a more complicated geometry and smaller load-bearing surfaces. Shoulder, elbow, and finger joints have also been replaced.

13.7.2 VASCULAR GRAFTS

When it is necessary to replace part of a blood vessel, a vein taken from another location in the same person may be used (an **autogenous graft**). This is the most common method used for small diameter (less than 6 mm) vessels. A wide variety of other materials have been used. For larger blood vessels, knitted or woven tubes of poly(ethylene terephthalate) (PET) or expanded poly(tetrafluoroethylene) (ePTFE) have been used for many years. PET may be woven to give a tube with little stretch or knitted to make a tube that is porous and can stretch. The knitted tube can be coated with a combination of albumin and collagen to make it impervious. Tubes of ePTFE are actually made from an expanded form of the polymer made by stretching (GoreTex™). In most cases, some sort of coating is applied before the tube is implanted. With all blood vessel replacements, the two terms that one encounters frequently are **thrombosis** and **patency**. Thrombosis is the formation of a blood clot in the vein or artery. The clot is initiated by platelet aggregates followed by deposition of fibrin and thrombin (two proteins). It can happen even in an otherwise healthy body, but it is the natural reaction of blood to any foreign surface it sees. Patency is the technical term used to denote openness. Thus, thrombosis leads to a loss of patency.

The ideal vascular graft should be the following [27]:

1. Biocompatible
2. Nonthrombogenic (having long-term patency)
3. Durable but compliant
4. Infection resistant
5. Easy to install

Although many synthetic polymers have been used, none, including PET and ePTFE, are ideal. Much of current research focuses on coatings for improving compatibility, especially for small diameter grafts.

13.7.3 SUTURES

Sutures are fiber assemblies used to sew wounds closed or surgical incisions (Table 13.7). External wounds often are sewn using relatively permanent polymers such as polypropylene, PET, and silk. Internal (as well as some external) stitching may make use of a polymer that gradually disintegrates. An absorbable (degradable) suture should have high strength initially and should not cause an inflammatory reaction. However, with time it should be converted to products that can be metabolized in the body. Designing a material that will have the right combination of initial and long-term properties is a challenging problem. Most often the polymer contains hydrolyzable linkages in the main chain. So-called catgut is actually a proteinaceous polymer high in collagen usually recovered from sheep intestines or various animal hides. **Chromated catgut** that has been cross-linked and toughened is a generic term that covers a multitude of products. The packaged item may also contain liquid to prevent the catgut from being too stiff to manipulate. **Poly(glycolic acid) (PGA)** is a

TABLE 13.7
Suture Materials

Polymer	Breaking Stress (grams/denier)	Yield Stress (grams/denier)	Yield Strain (%)
Nonabsorbable			
Silk	3.4	1.3	2
Polypropylene	5.1	0.5	1
PET	4.2	1.2	3
Absorbable			
Poly(glycolic acid)	6.3	0.8	2
Polyglactin 910	6.5	1.0	2

Source: Ambrosio, L. et al., Composite materials, in J. Black and G. Hastings (eds.), *Handbook of Biomaterial Properties*, Chapman & Hall, New York, 1998.

simple polyester introduced in the 1970s and has been widely used since then. The copolyester of 9 moles of glycolic acid with one of lactic acids [**polyglactin 910**, poly(lactic-*co*-glycolic acid) **PLGA**] is another popular entry (see Section 15.4). It hydrolyzes more slowly than PGA. However, numerous variations are available commercially. Like catgut, these polyesters are biodegraded with time and the products of degradation are eliminated. PGA and PLGA probably degrade in stages mainly through hydrolysis [29]. Products of degradation are eliminated through the kidney or as CO₂.

It is obvious that fibers to be useful as sutures should be strong and have good knot-tying ability; that is, the knot should be easy to tie and not come easily untied. Sutures have to be sterilized, usually after being sealed in a package. Whether they are in the body for a short or long time, biocompatibility is vital. This means that even traces of compounds that might be used in coating the fibers for ease of spinning, packaging, or sterilizing the product must be chosen with great care.

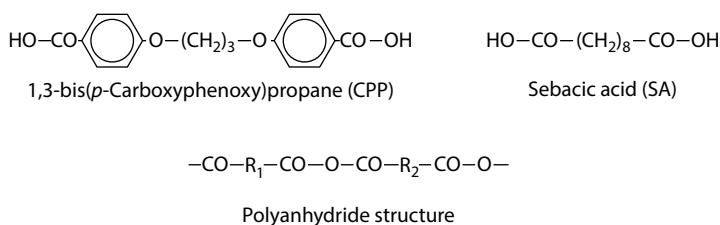
13.7.4 CONTROLLED DRUG DELIVERY SYSTEMS

In general, drugs that are delivered into the body in discrete doses by injection or ingestion are present at concentrations that vary widely with time. The more time that elapses between doses, the greater is the danger that the concentration in the body will go from being too concentrated (or nearly toxic) initially to being too dilute (ineffective) just before the next dose. There are various ways in which a relatively constant flow of medicine can be introduced into the body [30]. **Skin patches** have been used in which a low-molecular-weight material diffuses through a membrane at a controlled rate. Scopolamine patches for control of motion sickness can be effective for up to 3 days. Another familiar example is a skin patch for overcoming nicotine addiction.

Both PLA and PLGA have been approved by the Food and Drug Administration (FDA) for drug delivery devices. In one example, a dispersion of polymer and drug is made using surfactants in a homogenizer. The drug is thus encapsulated within nanoparticles of PLGA. The emulsion can be administered intravenously through a conventional syringe [31]. Drug release is regulated by diffusion and erosion of the polymer matrix. Other techniques for making micro- or nanoparticles include phase separation by addition of a nonsolvent or spray drying. Some PLGA–drug combinations have been implanted in the form of beads, discs, and cylinders.

In contrast to the bulk disintegration of PLGA, a novel **controlled polymer degradation** has been used to make a drug delivery system. With a high-molecular-weight drug, diffusion may be too slow through any practical membrane. However, if such a drug can be mixed with a **surface-degradable** polymer, the drug can be made available at the same rate as the polymer erodes. Langer [32–34] has described the design of various systems. One such system is used for the delivery of a powerful **chemotherapy** agent for brain cancer [30]. The agent, [1,3-bis-(2-chloroethyl)-1-nitrosourea] (BCNU), has a systemic half-life of only 15 min when it is introduced into the body. Moreover, the agent has various deleterious side effects. However, when the drug is incorporated into a proper polymer matrix, release can be controlled so that a wafer implanted into the site of an excised tumor will release an effective flow of BCNU over a period of days or even weeks.

Proper design calls for a polymer that will degrade by **surface erosion** much as a bar of soap wears away. Unfortunately, most polymers decompose by penetration of solvent into the interior of a wafer, resulting in **bulk erosion**. Also, the rate should be linear and predictable. The **polyanhydrides** form a class that degrades by hydrolysis and that can be tailored accurately to rigid specifications. For the BCNU delivery system, Langer and his collaborators chose a polyanhydride copolymer (20:80) of 1,3-bis(*p*-carboxyphenoxy)propane:sebacic acid (CPP:SA).



In order to produce wafers, a cosolution of BCNU with the copolymer was spray dried to make uniform spheres that could be compressed into wafers about 1.4 cm in diameter and 1.0 mm thick. They were sterilized by gamma radiation before implantation. The properties of this system include the desired rate of surface erosion, proper release of the BCNU, and no ill effects from the products of hydrolysis (the mechanism for degradation). Of course, the tests for safety and efficacy went through many stages before human patients received treatment. Other diseases that can benefit from implanted degradable systems include Alzheimer's disease, osteomyelitis, and diabetes.

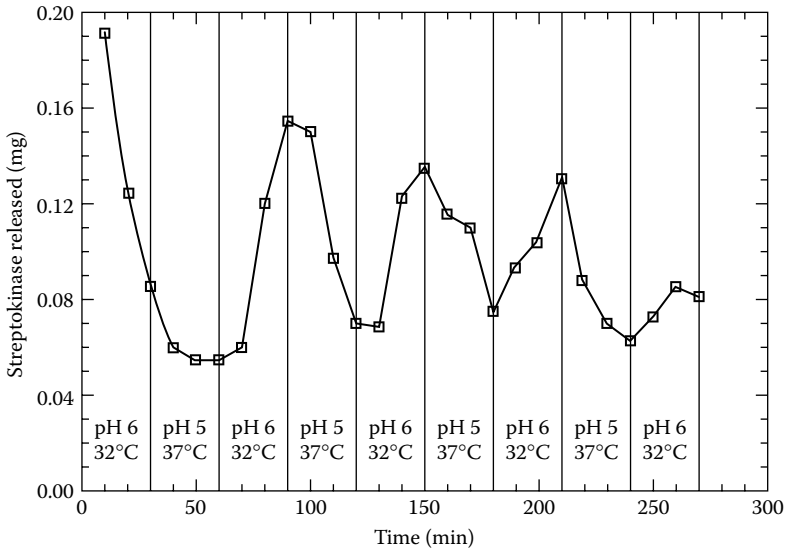


FIGURE 13.15 Drug release over 10-min intervals from a hydrogel subjected to oscillatory changes of pH and temperature from pH 6 and 32°C to pH 5 and 37°C in 30-min intervals. (Reprinted with permission from Peppas, N. A. et al., *Ann. Rev. Biomed. Eng.*, 2, 9, 2000. Copyright 2000 American Chemical Society.)

The use of hydrogels (Section 3.15) as vehicles for drug delivery has been extensively researched. The swollen state of a hydrogel controls the diffusion of solutes through the gel and is the basis of some controlled drug delivery applications. Besides the water content and the physical structure of the gel, the chemical composition of its polymer and its ionic charges will affect the diffusion of a given solute. Because charged hydrogels are able to change their swollen state in response to external stimuli such as changes in temperature, pH, ionic strength, solvent composition, and electric field, they can control the rate of diffusion of a solute (drug) through the gel. The largest changes in diffusion rates are associated with the transition from highly swollen to collapsed state of the hydrogel (see Figure 3.29). These changes are reversible as demonstrated in Figure 13.15. The hydrogel in this case is a random terpolymer synthesized from the monomers *N*-isopropylacrylamide (NIPAAm), acrylic acid (AA), and 2-hydroxyethyl methacrylate (HEMA) in the molar ratio of 10:10:80. The gel was loaded with the drug streptokinase during the synthesis. When subjected to oscillatory changes of pH and temperature over 30-min intervals, the monitored release of the drug over 10-min intervals is observed to oscillate accordingly with the highest drug release rate occurring from the most swollen state [35]. More recent works are focusing on conjugation of drugs to biodegradable polymer carriers to improve the pharmacokinetics of the drug release. Polyethylene glycol is often the polymer of choice to which the drug is attached through a linker that self-cleaves to release the drug under appropriate conditions [36,37]. Advances in hydrogel-based drug delivery for the human body and the progress in clinical applications made over the past decades have been recently reviewed [38].

13.7.5 TISSUE ENGINEERING

Another medical application that uses biodegradable polymers such as collagen and PLGA is in the generation of body tissues. Autogenous transplantation of cells does away with the need for a donor with the accompanying problems of immune response and rejection. The general principle behind **tissue engineering** is the growth of tissue from cell cultures taken from the body into which the new tissue will be placed. The cells are seeded into a temporary **scaffold** composed of the biodegradable polymer. The scaffold acts as a support and also serves as a template to define the three-dimensional structure of the growing assembly whether *in vivo* or *in vitro* [39].

Fabrics of biodegradable polymers have been made in the shape of a missing organ and then seeded with cells. Both bone and cartilage have been successfully grown in this fashion with the polymer gradually being degraded and replaced. Other examples of successful growth include liver tissues and ligaments. Tubular structures have been used to reconnect nerves.

KEYWORDS

Fabrication
Roll mill
Internal mixer
Blender
Fluidized-bed coating
Electrostatic spray coating
Photocurable coating
Lacquer
Dope
Blushing
Hiding power
Paint
Drying oil
Autoxidation
Drier
Varnish (oleoresinous)
Enamel
Thinner, diluent
Alkyd
Adhesive
Adherend
Mechanical adhesion
Specific adhesion
Contact angle
Critical surface tension
Photoresists
Microlithography
Negative and positive resists

Wolff rearrangement
 Chemical amplification
 Asymmetric membranes
 Wet casting process
 Ternary system
 Microphase separated layer
 Biocompatibility
 Osteoarthritis
 Autogenous graft
 Thrombosis
 Patency
 Suture
 Catgut
 Polyglycolic acid
 Polyglactin 910
 Controlled drug delivery
 Skin patch
 Controlled polymer degradation
 Surface degradable polymer
 Chemotherapy
 Surface and bulk erosion
 Polyamides
 Drug delivery
 Tissue engineering
 Scaffold

PROBLEMS

- 13.1** How might you expect the critical surface tension of a polymer to vary with the cohesive energy density? What factor could change the expected correlation? Compare the values of γ_c (Table 13.6) with values of δ_2 and δ_H (Table 2.5).
- 13.2** The statement is often made that one cannot glue anything to polyethylene. Show that this is incorrect by applying a strip of cellophane tape to a film of polyethylene (a bread wrapper or a freezer bag will do). From the force necessary to pull the tape off in shear, estimate the shear strength of the bond. Is the strength dependent on the timescale of the test? How?
- 13.3** A 60:40 emulsion copolymer of styrene and ethyl acrylate is proposed as a coating material (a latex paint). What difficulty is likely to be encountered? How might it be overcome?
- 13.4** Describe the role of each of these ingredients within each system and classify each system as a paint, an enamel, a varnish, a lacquer, or a putty.
- System A
- Linseed oil
 - Mineral spirits
 - Cobalt naphthenate

- Calcium carbonate
- System B
 - Cellulose nitrate
 - Methyl ethyl ketone
 - Titanium dioxide
- System C (first four ingredients are cooked together but describe them separately)
 - Tall oil fatty acids
 - Ethylene glycol
 - Glycerol
 - Phthalic anhydride
 - Mineral spirits
 - Cobalt naphthenate
- System D
 - Shellac
 - Ethyl alcohol

REFERENCES

1. Nylen, P., and E. Sunderland: *Modern Surface Coatings*, Wiley, New York, 1965, pp. 534, 543.
2. McCabe, W., and J. C. Smith: *Unit Operations of Chemical Engineering*, 2nd edn., McGraw-Hill, New York, 1967, pp. 851–859.
3. White, J. L.: *Rubber Chem. Technol.*, 65:527 (1992).
4. Parker, D. H.: *Principles of Surface Coating Technology*, Wiley, New York, 1965, p. 762.
5. *Coating Metals and Other Rigid Materials with Microthene Polyethylene Powder*, 2nd edn., U.S.I. Chemicals, New York, 1965.
6. Microthene F Microfine Polyolefin Powders, U.S.I. Chemicals, New York, 1976.
7. Glover, E.: *Mod. Plast. Encycl.*, 56:250 (1979).
8. Gorham, W. F.: *Mod. Plast.*, 45(1A, Encycl. Issue):173 (1967).
9. Shen, M., and A. T. Bell (eds.): *Plasma Polymerization*, ACS, Washington, DC, 1979.
10. Inagaki, N.: *Plasma Surface Modification and Plasma Polymerization*, Technomic, Lancaster, PA, 1996.
11. Parker, D. H.: *Principles of Surface Coating Technology*, Wiley, New York, 1965, pp. 563, 752.
12. Brodnyan, J. G., and T. Konen: *J. Appl. Polym. Sci.*, 8:687 (1964).
13. Nylen, P., and E. Sunderland: *Modern Surface Coatings*, Wiley-Interscience, New York, 1965, p. 123.
14. Wicks, Z. W., Jr., F. N. Jones, and S. P. Pappas: *Organic Coatings Science and Technology*, 2nd edn., Wiley, New York, 1999.
15. Zisman, W. A.: *Ind. Eng. Chem.*, 55:18 (1963).
16. Damico, D. J.: chap. 38 in A. Pizzi and K. L. Mittal (eds.), *Handbook of Adhesive Technology*, Revised and Expanded, CRC Press, Boca Raton, FL, 2003.
17. Selective Oxidation in Heterostructures Improves VCSEL Efficiency, *Laser Focus World*, 31(3):9 (1995).
18. Reichmanis, E., F. M. Houlihan, O. Nalamasu, and T. X. Neenan: chap. 1 in L. F. Thompson, C. G. Willson, and S. Tagawa (eds.), *Polymers for Microelectronics*, ACS, Washington, DC, 1994.
19. Baker, R. W.: *Membrane Technology and Applications*, 2nd edn., Wiley, Hoboken, NJ, 2004.

20. Li, N. N., A. G. Fane, W. S. W. HO, and T. Matsuura: *Advanced Membrane Technology and Applications*, Wiley, Hoboken, NJ, 2008.
21. Loeb, S., and S. Sourirajan: *Adv. Chem. Ser.*, 38:117 (1963).
22. Cohen, C., G. B. Tanny, and S. Prager: *J. Polym. Sci.*, Part A-2, 17:477 (1979).
23. Yilmaz, L., and A. J. McHugh: *J. Memb. Sci.*, 28:287 (1986).
24. Halpern, B. D., and Y.-C. Tong: Medical applications, in H. F. Mark, N. M. Bikales, C. G. Overberger, and G. Menges (eds.), *Encyclopedia of Polymer Science and Engineering*, 2nd edn., vol. 9, Wiley, New York, 1987, p. 486.
25. Bronzino, J. D. (ed.): *The Biomedical Engineering Handbook*, 2nd edn., CRC Press, Boca Raton, FL, 2000.
26. *Mayo Clinic Health Letter*, 12(8):1 (1994).
27. Ku, D. N., and R. C. Allen: Vascular grafts, in J. D. Bronzino (ed.), *The Biomedical Engineering Handbook*, 1st edn., CRC Press, Boca Raton, FL, 1996, p. 1871.
28. Ambrosio, L., G. Carotenuto, and L. Nicolais: Composite materials, in J. Black and G. Hastings (eds.), *Handbook of Biomaterial Properties*, Chapman & Hall, New York, 1998.
29. An, Y. H., S. K. Woolf, and R. J. Friedman: *Biomaterials*, 21:2635 (2000).
30. Saltzman, M.: *Drug Delivery*, Oxford, New York, 2001.
31. Jain, R. A.: *Biomaterials*, 21:2475 (2000).
32. Langer, R.: *Science*, 249:1527 (1990).
33. Tamada, J., and R. Langer: *J. Biomater. Sci. Polym. Ed.*, 3:315 (1992).
34. Tamada, J., and R. Langer: *Proc. Natl. Acad. Sci. USA*, 90:552 (1993).
35. Peppas, N. A., Y. Huang, M. Torres-Lugo, J. H. Ward, and J. Zhang: *Ann. Rev. Biomed. Eng.*, 2:9 (2000).
36. Metters, A., and J. Hubbell: *Biomacromolecules*, 6:290 (2005).
37. Ashley, G. W., J. Henise, R. Reid, and D. V. Santi: *Proc. Natl. Acad. Sci. USA*, 110:2318 (2013).
38. Vashist, A., A. Vashist, Y. K. Gupta, and S. Ahmad: *J. Matr. Chem. B*, 2:147 (2014).
39. Mooney, D. J., and R. S. Langer: Engineering biomaterials for tissue engineering, in J. Black and G. Hastings (eds.), *Handbook of Biomaterial Properties*, Chapman & Hall, New York, 1998.

GENERAL REFERENCES

(The entries under each heading often are not exclusively on one subject, but they are grouped for convenience according to major emphasis.)

Compounding

- Agassant, J. F., P. Avenas, J. Sergent, and P. J. Carreau: *Polymer Processing: Principles and Modeling*, Hanser-Gardner, Cincinnati, OH, 1991.
- Baird, D. G., and D. M. Collias: *Polymer Processing: Principles and Design*, Butterworth-Heinemann, Newton, MA, 1995.
- Belofsky, H.: *Plastics: Product Design and Process Engineering*, Hanser-Gardner, Cincinnati, OH, 1995.
- Birley, A. W., B. Haworth, and J. Batchelor: *Physics of Plastics: Processing, Properties and Materials Engineering*, Hanser-Gardner, Cincinnati, OH, 1992.
- Chandra, M., and S. K. Roy: *Plastics Technology Handbook*, 3rd edn., Dekker, New York, 1999.
- Cheremisinoff, N. P.: *Polymer Mixing and Extrusion Technology*, Dekker, New York, 1987.
- Cheremisinoff, N. P. (ed.): *Product Design and Testing of Polymeric Materials*, Dekker, New York, 1990.

- Cheremisinoff, N. P., and P. N. Cheremisinoff (eds.): *Handbook of Applied Polymer Processing Technology*, Dekker, New York, 1996.
- Collyer, A. A. (ed.): *Rubber Toughened Engineering Plastics*, Chapman & Hall, New York, 1994.
- Corish, P. J. (ed.): *Concise Encyclopedia of Polymer Processing and Applications*, Pergamon Press, New York, 1991.
- Cracknell, P. S., and R. W. Dyson: *Handbook of Thermoplastics Injection Mould Design*, Chapman & Hall, New York, 1993.
- Enikoloyan, N. S. (ed.): *Filled Polymers I. Science and Technology*, Springer, Secaucus, NJ, 1990.
- Flick, E. W.: *Industrial Synthetic Resins Handbook*, Noyes, Park Ridge, NJ, 1985.
- Flick, E. W.: *Plastics Additives: An Industrial Guide*, Noyes, Park Ridge, NJ, 1986.
- Flick, E. W.: *Epoxy Resins Curing Agents, Compounds, and Modifiers: An Industrial Guide*, Noyes, Park Ridge, NJ, 1987.
- Florian, J.: *Practical Thermoforming*, Dekker, New York, 1987.
- Fouassier, J. P., and J. F. Rabek (eds.): *Radiation Curing in Polymer Science and Technology*, 4 vols., Chapman & Hall, New York, 1994.
- Gächter, R., and H. Muller (eds.): *Plastics Additives Handbook*, 4th edn., Hanser-Gardner, Cincinnati, OH, 1993.
- Gomez, I. L.: *High Nitrile Polymers for Beverage Container Applications*, Technomic, Lancaster, PA, 1990.
- Goodman, I. (ed.): *Developments in Block Copolymers—1*, Elsevier Applied Science, New York, 1982.
- Griskey, R. G.: *Polymer Process Engineering*, Chapman & Hall, New York, 1994.
- Gruenwald, G.: *Thermoforming—A Plastics Processing Guide*, 2nd edn., Technomic, Lancaster, PA, 1998.
- Harper, C. A. (ed): *Handbook of Plastics, Elastomers, and Composites*, 2nd edn., McGraw-Hill, New York, 1992.
- Hermansen, R. D.: *Formulating Plastics and Elastomers by Computer*, Noyes, Park Ridge, NJ, 1991.
- Hoyle, C. E., and J. F. Kinstle (eds.): *Radiation Curing of Polymeric Materials*, ACS, Washington, DC, 1990.
- Ivanov, V. S.: *Radiation Chemistry of Polymers*, VSP, Zeist, The Netherlands, 1992.
- Lin, S.-C.: *High-Performance Thermosets*, Hanser-Gardner, Cincinnati, OH, 1993.
- Manas-Zloczower, I., and Z. Tadmor (eds.): *Mixing and Compounding of Polymers*, Hanser-Gardner, Cincinnati, OH, 1994.
- Meyer, R. W.: *Handbook of Pultrusion Technology*, Chapman & Hall (Methuen), New York, 1985.
- Meyer, R. W.: *Handbook of Polyester Molding Compounds and Molding Technology*, Chapman & Hall (Methuen), New York, 1987.
- Michaeli, W.: *Plastics Processing: An Introduction*, Hanser-Gardner, Cincinnati, OH, 1995.
- Middleman, S.: *Fundamentals of Polymer Processing*, McGraw-Hill, New York, 1977.
- Narkis, M., and N. Rosenzweig (eds.): *Polymer Powder Technology*, Wiley, New York, 1995.
- O'Brien, K. T. (ed.): *Applications of Computer Modeling for Extrusion and Other Continuous Polymer Processes*, Hanser-Gardner, Cincinnati, OH, 1992.
- Olabisi, O. (ed.): *Handbook of Thermoplastics*, Dekker, New York, 1998.
- Plueddemann, E. P.: *Silane Coupling Agents*, 2nd edn., Plenum, New York, 1990.
- Progelhof, R. C., and J. L. Throne: *Polymer Engineering Principles: Properties, Processes, and Tests for Design*, Hanser-Gardner, Cincinnati, OH, 1993.
- Provder, T. (ed.): *Computer Applications in the Polymer Laboratory*, ACS, Washington, DC, 1986.
- Radian Corporation: Chemical additives for the plastics industry, properties, applications, toxicologies, Noyes, Park Ridge, NJ, 1987.

- Randell, D. R. (ed.): *Radiation Curing of Polymers*, CRC Press, Boca Raton, FL, 1987.
- Randell, D. R.: *Radiation Curing of Polymers, II*, CRC Press, Boca Raton, FL, 1992.
- Rauwendaal, C. J. (ed.): *Mixing in Polymer Processing*, Dekker, New York, 1991.
- Reichmanis, E., C. W. Frank, and J. H. O'Donnell (eds.): *Irradiation of Polymeric Materials: Processes, Mechanisms, and Applications*, ACS, Washington, DC, 1993.
- Whelan, T.: *Polymer Technology Dictionary*, Chapman & Hall, New York, 1994.
- Wickson, E. J. (ed.): *Handbook of PVC Formulating*, Wiley, New York, 1993.

Coatings

- Athey, R. D., Jr.: *Emulsion Polymer Technology*, Dekker, New York, 1991.
- Benkreira, H. (ed.): *Thin Film Coating*, CRC Press, Boca Raton, FL, 1993.
- Bentley, J., and G. P. A. Turner: *Introduction to Paint Chemistry and Principles of Paint Technology*, 4th edn., Chapman & Hall, New York, 1997.
- Biederman, H., and Y. Osada: *Plasma Polymerization Processes*, Elsevier, New York, 1992.
- Calbo, L. J. (Ed.): *Handbook of Coatings Additives*, vol. 2, Dekker, New York, 1992.
- Daniels, E. S., E. D. Sudol, and M. S. El-Aasser (eds.): *Polymer Latexes: Preparation, Characterization, and Applications*, ACS, Washington, DC, 1992.
- Dören, K., W. Freitag, and D. Stoye: *Water-Borne Coatings*, Hanser-Gardner, Cincinnati, OH, 1994.
- Flick, E. W.: *Water-Based Trade Paint Formulations*, Noyes, Park Ridge, NJ, 1975.
- Flick, E. W.: *Solvent-Based Paint Formulations*, Noyes, Park Ridge, NJ, 1977.
- Flick, E. W.: *Contemporary Industrial Coatings*, Noyes, Park Ridge, NJ, 1985.
- Flick, E. W.: *Printing Ink Formulations*, Noyes, Park Ridge, NJ, 1985.
- Gutoff, E. B., and E. D. Cohen: *Coating & Drying Defects*, Wiley, New York, 1995.
- Kelly, J. M., C. B. McArdle, and M. J. F. Maunder (eds.): *Photochemistry and Polymeric Systems*, CRC Press, Boca Raton, FL, 1993.
- Koleske, J. (ed.): *Paint and Coating Testing Manual*, 14th edn., ASTM, Philadelphia, PA, 1995.
- Krongauz, V. V., and A. D. Trifunac (eds.): *Processes in Photoreactive Polymers*, Chapman & Hall, New York, 1994.
- Marrion, A. R. (ed.): *The Chemistry and Physics of Coatings*, 2nd edn., Royal Society of Chemistry, London, 2004.
- Provder, T., M. A. Winnik, and M. W. Urban (eds.): *Film Formation in Waterborne Coatings*, ACS, Washington, DC, 1996.
- Seymour, R. B., and H. F. Mark (eds.): *Organic Coatings: Their Origin and Development*, Elsevier, Amsterdam, The Netherlands, 1989.
- Solomon, D. H., and D. G. Hawthorne: *Chemistry of Pigments and Fillers*, Krieger Publishing, Malabar, FL, 1991.
- Surface Coating Technology Handbook*, Asia Pacific Business Press, Delhi, India, 2009.
- Wicks, Z. W., Jr., F. N. Jones, S. P. Pappas, and D. A. Wicks: *Organic Coatings, Science and Technology*, 3rd edn., Wiley, New York, 2007.

Adhesives

- Adams, R. D., and W. C. Wake: *Structural Adhesive Joints in Engineering*, Elsevier, Amsterdam, The Netherlands.
- Benedek, I., and L. J. Heymans: *Pressure-Sensitive Adhesives Technology*, Dekker, New York, 1996.
- Evans, R. M.: *Polyurethane Sealants—Technology and Applications*, Technomic, Lancaster, PA, 1993.
- Minford, J. D. (ed.): *Treatise on Adhesion and Adhesives*, vol. 7, CRC Press, Boca Raton, FL, 1991.

- Patrick, R. L., K. L. DeVries, and G. P. Anderson (eds.): *Treatise on Adhesion and Adhesives*, vol. 6, Dekker, New York, 1988.
- Patsis, A. V. (ed.): *Advances in Organic Coatings Science and Technology*, vol. 12, Technomic, Lancaster, PA, 1990.
- Pizzi, A., and K. L. Mittal (eds.): *Wood Adhesives, Chemistry and Technology*, CRC Press, Boca Raton, FL, 2011.
- Pizzi, A., and K. L. Mittal (eds.): *Handbook of Adhesive Technology*, CRC Press, Boca Raton, FL, 2003.
- Pocius, A.: *Adhesion and Adhesive Technology*, 3rd edn., Hanser Publishers, New York, 2013.
- Sanchez, I. C. (ed.): *Physics of Polymer Surfaces and Interfaces*, Butterworth, Oxford, 1992.
- Sellers, T., Jr.: *Plywood and Adhesive Technology*, Dekker, New York, 1985.
- Vacula, V. L., and L. M. Pritykin: *Physical Chemistry of Polymer Adhesion*, Prentice Hall, Englewood Cliffs, NJ, 1991.
- Wegman, R. F., and T. R. Tullos: *Handbook of Adhesive Bonded Structural Repair*, Noyes, Park Ridge, NJ, 1992.
- Wool, R. P.: *Polymer Interfaces Structure and Strength*, Hanser-Gardner, Cincinnati, OH, 1995.

Electronics

- Chilton, J. A., and M. Goosey (eds.): *Special Polymers for Electronics and Optoelectronics*, Chapman & Hall, New York, 1995.
- Feit, E. D., and C. Wilkins, Jr. (eds.): *Polymer Materials for Electronic Applications*, ACS, Washington, DC, 1982.
- Flick, E. W.: *Adhesives, Sealants, and Coatings for the Electronics Industry*, 2nd edn., Noyes, Park Ridge, NJ, 1992.
- Ito, H., S. Tagawa, and K. Hone (eds.): *Polymeric Materials for Microelectronic Applications: Science and Technology*, ACS, Washington, DC, 1995.
- McArdle, C. B.: *Applied Photochromic Polymer Systems*, Chapman & Hall, New York, 1991.
- Moreau, W. M.: *Semiconductor Lithography*, Plenum Press, New York, 1988.
- Prasad, P. N., and D. R. Ulrich (eds.): *Nonlinear Optical and Electroactive Polymers*, Plenum Press, New York, 1988.
- Soane, D. S., and Z. Martynenko: *Polymers in Electronics: Fundamentals and Applications*, Elsevier, New York, 1989.
- Thompson, L. F., C. G. Willson, and M. J. Bowden (eds.): *Introduction to Microlithography*, 2nd edn., ACS, Washington, DC, 1994.
- Thompson, L. F., C. G. Willson, and S. Tagawa (eds.): *Polymers for Microelectronics: Resists and Dielectrics*, ACS, Washington, DC, 1994.
- Wong, C. P. (ed.): *Polymers for Electronic and Photonic Applications*, Academic Press, San Diego, CA, 1992.

Biomedical applications

- DeRossi, D., K. Kajiwara, Y. Osada, and A. Yamauchi (eds.): *Polymer Gels: Fundamentals and Biomedical Applications*, Plenum Press, New York, 1991.
- Dunn, R. L., and R. M. Ottenbrite (eds.): *Polymeric Drugs and Drug Delivery Systems*, ACS, Washington, DC, 1991.
- El-Nokaly, M. A., D. M. Piatt, and B. A. Charpentier (eds.): *Polymeric Delivery Systems: Properties and Applications*, ACS, Washington, DC, 1993.
- Gebelein, C. G.: *Biotechnology Polymers—Medical, Pharmaceutical and Industrial Applications*, Technomic, Lancaster, PA, 1993.
- Gebelein, C. G., and C. E. Carraher, Jr. (eds.): *Biotechnology and Bioactive Polymers*, Plenum Press, New York, 1994.

- Gebelein, C. G., and R. L. Dunn (eds.): *Progress in Biomedical Polymers*, Plenum Press, New York, 1990.
- Ikano, T.: *Biorelated Polymers and Gels*, Academic Press, New York, 1998.
- Lee, K.-S. (ed.): *Filled Elastomers Drug Delivery Systems*, vol. 160, Springer, Berlin, Germany, 2002.
- McCulloch, I., and S. W. Shalaby (eds.): *Tailored Polymeric Materials for Controlled Degradation Systems*, ACS, Washington, DC, 1998.
- Ottenbrite, R. M. (ed.): *Polymeric Drugs and Drug Administration*, ACS, Washington, DC, 1994.
- Ottenbrite, R. M. (ed.): *Frontiers in Biomedical Polymer Applications*, 2 vols., Technomic, Lancaster, PA, 1998–1999.
- Ottenbrite, R. M., and E. Chiellini (eds.): *Polymers in Medicine: Biomedical and Pharmaceutical Applications*, Technomic, Lancaster, PA, 1992.
- Park, K., S. W. Shalaby, and H. Park: *Biodegradable Hydrogels for Drug Delivery*, Technomic, Lancaster, PA, 1993.
- Peppas, N. K. (ed.): *Hydrogels in Medicine and Pharmacy*, CRC Press, Boca Raton, FL, vol. 1, Fundamentals, 1986; vol. 2, Polymers, 1987; vol. 3, Properties and Applications, 1987.
- Saltzman, M.: *Drug Delivery*, Oxford, New York, 2001.
- Shalaby, S. W. (ed.): *Biomedical Polymers: Designed-to-Degrade Systems*, Hanser Publishers, New York, 1994.
- Shalaby, S. W., Y. Ikada, R. Langer, and J. Williams (eds.): *Polymers of Biological and Biomedical Significance*, ACS, Washington, DC, 1994.
- Shoichet, M. S., and J. A. Hubbell (eds.): *Polymers for Tissue Engineering*, VSP, Utrecht, The Netherlands, 1998.
- Stoy, V. A., and C. K. Kliment: *Hydrogels: Specialty Plastics for Biomedical, Pharmaceutical and Industrial Applications*, Technomic, Lancaster, PA, 1990.
- Tarcha, P. J. (ed.): *Polymers for Controlled Drug Delivery*, CRC Press, Boca Raton, FL, 1990.
- Van Bitterswijk, C., P. Thomsen, J. Hubbell, and R. Cancedda.: *Tissue Engineering*, Academic Press, New York, 2008.
- Wise, D. (ed.): *Biomaterials and Bioengineering Handbook*, Dekker, New York, 2000.

14 Fabrication Processes

Extrusion and Molding

14.1 EXTRUSION IN GENERAL

In **extrusion** a material is forced through a **die** that shapes the profile. Continuous flow of material results in a long shape of constant cross section. Unlike the extrudate from a toothpaste tube or a meat grinder, plastic extrudates generally approach truly continuous formation. They may attain dimensional stability in various ways. Like the usual meat grinder, the extruder (Figure 14.1) is essentially a screw conveyor carrying cold plastic pellets forward and compacting them in the compression section with heat from external heaters and the friction of viscous flow. The pressure is highest right before the plastic enters the die that shapes the extrudate. The **screen pack** and **breaker plate** between the screw and the die filter out dirt and unfused polymer lumps. When thermoplastics are extruded, it is necessary to cool the extrudate below T_m or T_g in order to gain dimensional stability. In some cases this can be done by simply running the product through a tank of water or, even more simply, by air cooling. When rubber is extruded, dimensional stability comes about by cross-linking (vulcanization). Special attachments for continuous vulcanization are described later. Actually, rubber extrusion for wire coating was the first application of the screw extruder in the 1880s. Standard sizes of single-screw extruders (specified by the inside diameter of the barrel) are 1.5, 2, 2.5, 3, 3.5, 4.5, 6, and 8 in. Smaller sizes are available for laboratory evaluations.

An analysis of the polymer flow along the screw is divided into three parts corresponding to the three sections described in Figure 14.1: The feed section (solid conveying zone), the compression section (plasticating or melting zone), and the metering section (melt flow). Model equations for the polymer convection have been developed for each zone [2]. In the feed zone, the resin transport is described by a *stick-slip* flow used for granular material that leads to plug flow in the channel between the flights. This flow is enhanced by increasing the friction coefficient between the resin and the barrel compared to that between the resin and the screw. The barrel is often grooved to increase the difference [3]. Assuming a constant screw diameter D , constant pitch between the flights and neglecting flight thickness, a simplified analysis predicts the following dependence for the flow rate [2]:

$$Q = KN\rho D_b (D_b^2 - D^2) \quad (14.1)$$

where:

K is a geometric factor that includes parameters such as helix angle (tilt of the flights) and the angle formed between the velocity of the solids and the barrel surface
 D_b is the barrel diameter

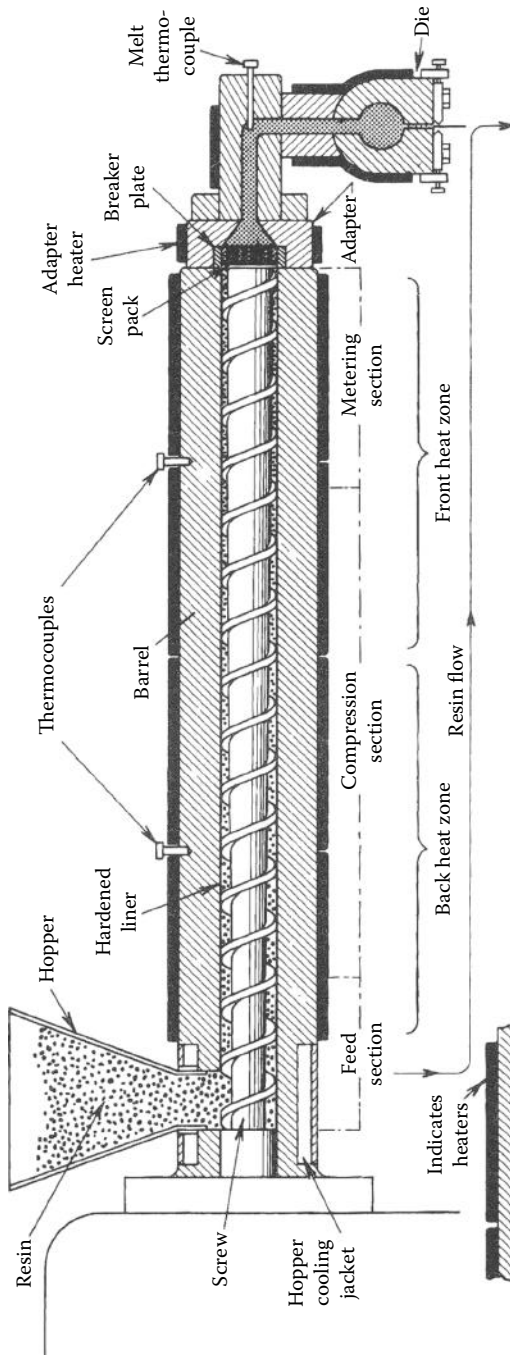


FIGURE 14.1 Cross section of a typical extruder. (Data from U. S. I. Chemicals/Quantum, *Petrothene Polyolefins: A Processing Guide*, 5th edn., National Distillers and Chemical Corporation.)

N is the rotation rate of the screw
 ρ is the resin bulk density

For grooved barrels, the predicted proportionality between Q and N seems to hold reasonably well for extruded low-density polyethylene [3]. However, an empirical rough guide has suggested a power of 2.2 for the dependence of Q on D_b [4].

Another guide to extruder capacity stems from the fact that most of the energy that melts the thermoplastic results from mechanical work. The barrel heaters serve mainly to insulate the material. Allowing for an efficiency from drive to screw of about 75%, the capacity then depends on the power supplied H_p (horsepower), the heat capacity of the material c_p (Btu/lb·°F), and the temperature change from feed to extrudate ΔT (°F):

$$H_p = 5.3 \times 10^{-4} Q_c c_p \Delta T \quad (14.2)$$

For example, a 10-hp motor on a 2-in extruder might be used for poly(methyl methacrylate), for which c_p is about 0.6 Btu/lb·°F, giving an estimate of $Q_c = 74$ lb/h [4]. Equation 14.2 indicates that ΔT_{\max} would be 430°F (221°C). In actual practice, a ΔT of 350°F (177°C) would usually be adequate for this polymer. The same calculation is, of course, much simpler in SI units. For example, if a 10-kW motor delivers 75% of its energy to a throughput of 10 g/s of polymer with a heat capacity of 2.5 J/g·°C, the temperature change is

$$\Delta T = \frac{7500 \text{ J/s}}{(10 \text{ g/s})(2.5 \text{ J/s} \cdot \text{°C})} = 300^\circ\text{C}$$

Obviously, these are very rough guides, since both polymers and machines are variable. Also, we have ignored the heat of melting and other thermal effects.

During the compression zone, the melting of the resin takes place over a significant portion of the screw length. Besides the viscous heating due to compression and shear mentioned above, resin heating and melting occur at the barrel wall from heaters within the barrel wall. An analysis based on experimental data of the melting process predicts that the length of the compression section scales like the length of the lead (pitch) to the power of 1/2 [2]. Doubling the pitch would square the length of the compression zone.

In the metering zone, the molten polymer is pressurized because the flow at the end of the barrel is partially blocked by the breaker plate. In the feed and compaction zones, there is little pressure buildup as air in these zones escapes through the porous solid granules and back through the hopper [3]. The net flow in the metering section consists of the drag flow by the screw advancing the fluid forward minus a backflow caused by the pressure build up at the breaker plate and a leakage flow between the tip of the flights and the barrel wall [2,3]. After the breaker plate, the pressure decreases and eventually returns to atmospheric pressure at the exit of the die.

Besides the barrel diameter, the **length-to-diameter ratio (L/D)** of an extruder is most often specified. Ratios of 20:1 and 24:1 are common for thermoplastics. Lower values are used for rubber. A long barrel gives a more homogeneous extrudate, which

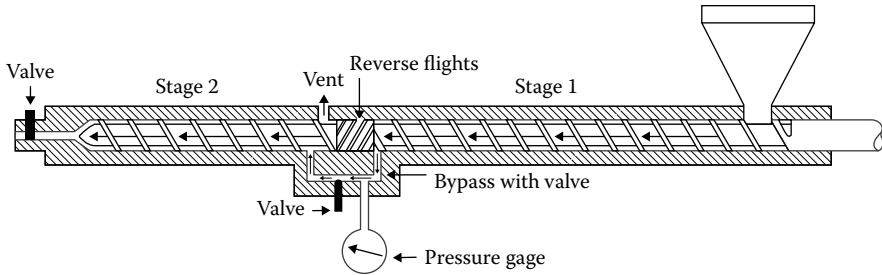


FIGURE 14.2 A two-stage vented extruder in which a valved bypass section steps down the pressure developed in the first stage to atmospheric pressure for venting; valve is for adjustment. (Data from Van Ness, R. I. et al., *Mod. Plast.*, 45, 672, October 1968.)

is especially important when pigmented materials are handled. A popular variant of the standard single-screw extruder is the **vented** model. Even when polymer pellets are pre-dried, the compacting process may trap air bubbles in the melt. By placing an obstruction in the barrel (the reverse flights in Figure 14.2), the pressure on the melt can be reduced suddenly to that of the atmosphere. Since the polymer does not have to be remelted, the feed section does not have to be replicated in the remainder of the screw. Valves can be used to adjust the pressure in various sections of the barrel. Although many screw designs are available, most have three zones, which differ in channel depth but not in pitch (which is synonymous with lead, since we are dealing with a single thread) (Figure 14.3). The ratio of channel depth in the feed section to that in the metering section, the **compression ratio**, probably would best be adjusted to each polymer and each temperature used in a given machine. However, it is seldom feasible to stock more than two or three screws for a single extruder, so a compromise is made. Some considerations would be (1) the form in which polymer is to be fed to the machine, that is, pellets, powder, and continuous ribbon; (2) the melt viscosity; and (3) thermal degradation. One screw might be suitable for polyethylene and **acrylonitrile butadiene styrene (ABS)** polymers, another for polyamides with their characteristic low melt viscosities, and another for poly(vinyl chloride) or poly(vinylidene chloride), each of which degrades easily at elevated temperatures. In laboratory-sized equipment, one might extrude a filled rubber by using still another screw. However, since rubber usually is fed as a warm ribbon, it has to be cooled to prevent cross-linking in the barrel, and then must be heated to cross-link subsequent to extrusion; it becomes apparent that production machinery that attempts to do all this and still be versatile enough to handle thermoplastics probably will be inefficient for both.

Twin-screw extruders may have the two parallel screws rotating in the same direction. Another form has counterrotating screws with some meshing to give a conveying action similar to a positive displacement pump. Some advantages generally claimed for twin-screw over single-screw extruders are better control, lower possible melt temperatures, and better mixing. These advantages must be weighed against a higher initial cost. Some other features of extruders are best described in terms of specific shapes.

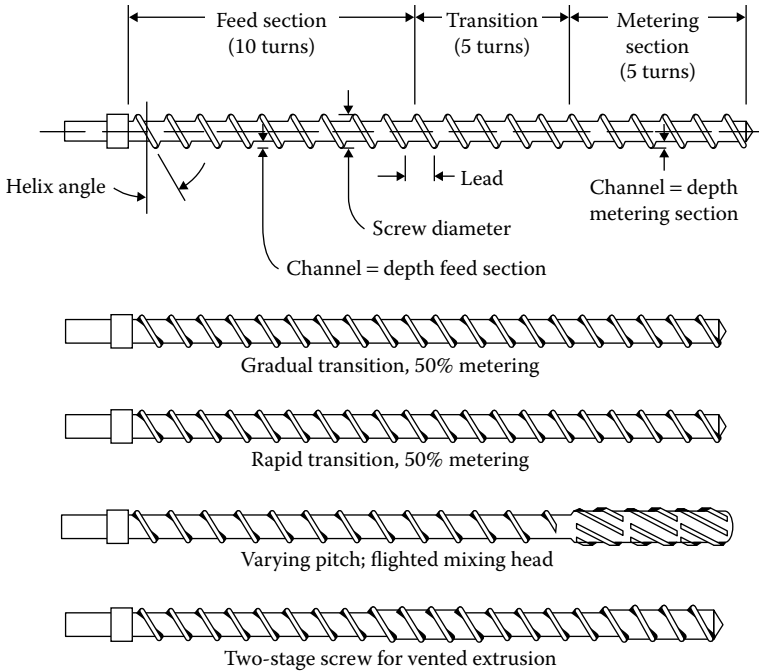


FIGURE 14.3 The various zones or sections of a standard constant-pitch, rapid-transition, metering extruder screw are labeled. (Data from Van Ness, R. I. et al., *Mod. Plast.*, 45, 672, October 1968.) Some other designs are also shown.

14.2 EXTRUSION OF FLAT FILM, SHEET, AND TUBING

In common usage, the term **film** is used for material less than 0.010 in (0.25 mm) thick and **sheet** for material that is thicker. Since the material will issue from the extruder as a thin, unsupported web of molten polymer, it is obvious that a high melt viscosity and some elasticity are desirable. The most direct control for these parameters is the molecular weight distribution. Often a polymer blend of different average molecular weight will perform better than a single component. **Flat-film extrusion** uses a T-shaped die (Figure 14.4). The die opening for polyethylene may be 0.015–0.030 in, even for films that are less than 0.003 in thick. The speed of taking up the film (various driven rolls) is high enough to draw down the film with a concurrent thinning. Dies may be as wide as 10 ft. On leaving the extruder, the film may be chilled below T_m or T_g by passing through a water bath or contacting a water-cooled roll. A schematic drawing of a **chill-roll** (also called **cast-film**) operation (Figure 14.5) shows how the hot web is made dimensionally stable by contacting several chrome-plated chill rolls before being pulled by the driven carrier rolls and wound up. The edges of the sheet may be trimmed off, since some curling occurs there. The **draw-down** process (followed by cooling before relaxation can occur) results in an oriented film, whether the polymer is glassy or crystalline.

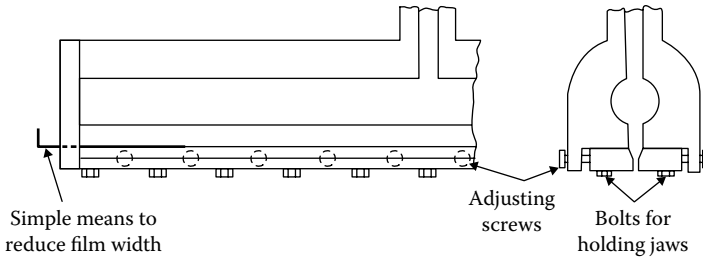


FIGURE 14.4 Schematic drawing of a manifold-type flat-film die with adjustable jaws. (Data from U. S. I. Chemicals/Quantum, *Petrothene Polyolefins: A Processing Guide*, 5th edn., National Distillers and Chemical Corporation.)

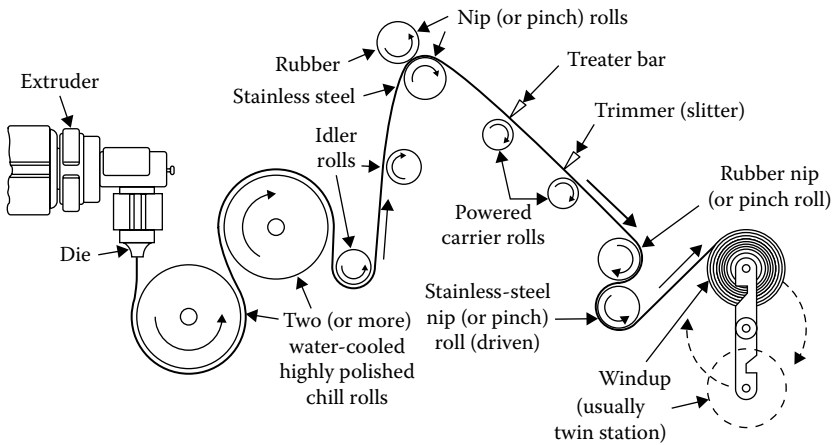


FIGURE 14.5 Schematic drawing of chill-roll film extrusion equipment. (Data from U. S. I. Chemicals/Quantum, *Petrothene Polyolefins: A Processing Guide*, 5th edn., National Distillers and Chemical Corporation.)

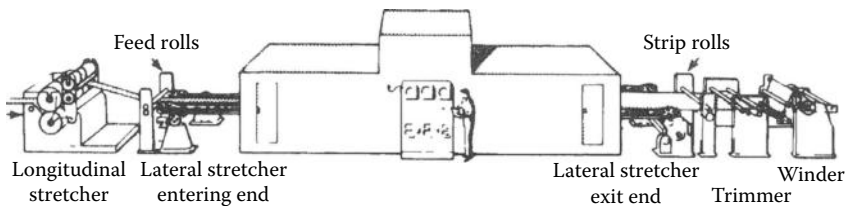


FIGURE 14.6 Biaxial orientation (tentering) of flat sheet in housing with programmed temperature. (Data from Plastic Film Orienting, Bull. 1-6, Marshall and Williams, Providence, RI, 1967.)

Thicker sheets generally are not drawn down as much and exhibit much less residual orientation. **Biaxially oriented film** can be produced from a flat web by using a **tenter** (Figure 14.6). Polypropylene, for example, might be extruded as a web about 0.005 in thick from a slot die. Inside a temperature-controlled box, the web is grasped on either side by **tenterhooks** that can exert a drawing tension as well as a widening tension. Where hooks disengage, the final sheet might be 2 or 3 times as

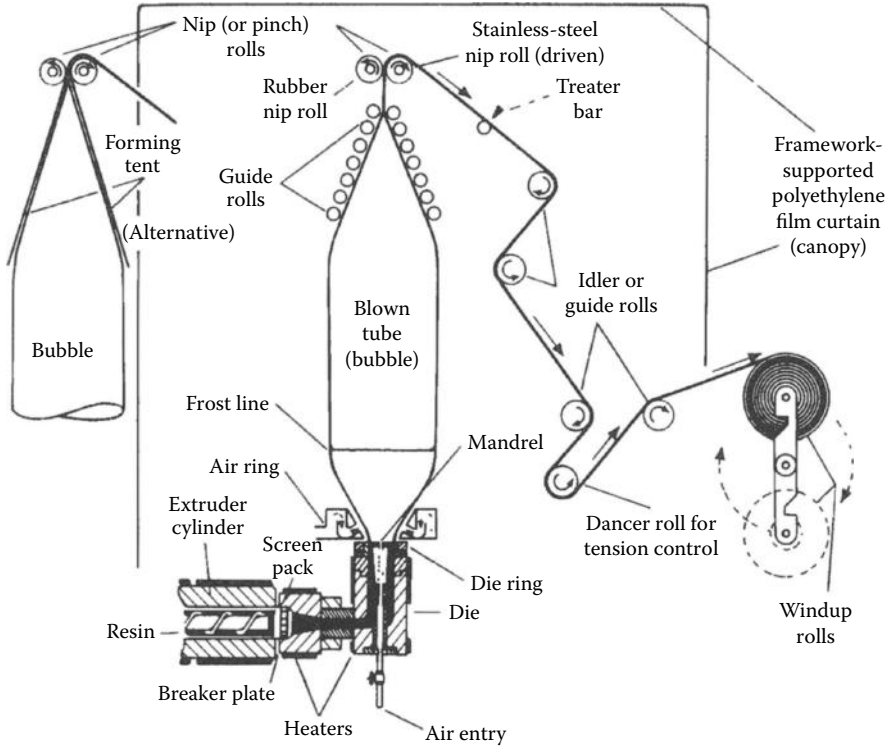


FIGURE 14.7 Schematic drawing of the blown-film extrusion process. (Data from U. S. I. Chemicals/Quantum, *Petrothene Polyolefins: A Processing Guide*, 5th edn., National Distillers and Chemical Corporation.)

wide as it was originally and, of course, considerably thinner. Biaxial orientation can be equal in two directions or unbalanced. In either case, molecules are now randomly oriented in two dimensions, just as fibers would be in a random mat. With polyethylene, biaxial orientation often can be achieved in **blown-film extrusion**. The molten polymer (Figure 14.7) is extruded through a ring-shaped die around a mandrel. The tube or sleeve so formed is expanded around an air bubble, cooled to below T_m , and then rolled into a flattened tube and wound up. Since the bubble is sealed at one end by the mandrel and at the other by the nip where the tube is flattened, air cannot escape and the bubble acts like a permanent shaping mandrel once it has been injected. Cooling of the film is controlled by an air ring below the bubble. When polyethylene cools, the crystalline material is cloudy compared to the clear amorphous melt, so the transition line, which coincides with dimensional stabilization, is called the **frost line**. The **blowup ratio** (bubble diameter/die diameter) may range as high as 4 or 5, although 2.5 is a more typical figure. Orientation occurs in the hoop direction during blowup. Orientation in the machine direction (in the direction of extrudate flow from the die) can be induced by tension from the nip roll. The method produces wide films used in construction trades as wind or moisture barriers. One example is reported as involving a 10-in extruder, a 5-ft-diameter die,

and a blowup ratio of 2.5 to give 1100 lb/h of polyethylene film, which when slit is 40 ft wide [5]. Such films in thicknesses of 0.004–0.008 in are readily available from hardware firms and mail-order companies for farm and construction applications. Nylon and poly(vinylidene chloride) are also produced by blow extrusion.

For some applications, more than one polymer layer is desirable. For example, a food tray might need a strong, abrasion-resistant surface layer such as polypropylene combined with an inner layer such as poly(vinylidene chloride) to contribute low oxygen permeability. House siding of poly(vinyl chloride) can benefit from a surface layer of an ABS-type polymer with superior weathering properties. In order to produce laminated, multilayer film by **coextrusion**, several extruders can be coupled. Each will contribute a separate stream of polymer melt to be combined without mixing in a feed block from which a layered melt issues. Much better adhesion between film layers often can be achieved in this way than could be attained by coating one melt onto a previously extruded and cooled second film.

Pipe or tubing is extruded through a ring-shaped die around a **mandrel**. Because heavier walls are involved than in blown-film extrusion, it is advantageous to cool by circulating water through the mandrel as well as by running the extrudate through a water bath. The extrusion of rubber tubing differs from thermoplastic tubing, since dimensional stability results from a cross-linking reaction at a temperature above that in the extruder rather than by cooling below T_g or T_m . The high melt viscosity needed to ensure a constant shape during the cross-linking may be an inherent property of the rubber being extruded. More often, however, the addition of a filler will induce the same behavior. For example, 20 parts of finely divided silica added to 100 parts of a poly(dimethyl siloxane) will increase the apparent viscosity only about twofold at a rate of shear equal to 100 s^{-1} . The viscosity at a stress corresponding to the unsupported polymer is measurable for the unfilled material but essentially infinite for the filled polymer. It is possible to extrude a filled rubber through a ring die to give a tube with an outside diameter of 12 mm and a wall thickness of 3 mm. The emerging rubber is cross-linked continuously by carrying it through a radiant-heated tunnel on a steel conveyor belt. With a residence time of 10 s in a 6-m-long tunnel, the tubing emerges with very little sagging of the original circular cross section.

Almost any cross section can be extruded. A complication is the swelling of the polymer when the elastic energy stored in capillary flow is relaxed on leaving the die. The flat sheet or circular cross sections discussed so far are not sensitive to this die swell (Section 8.2), since the shape remains symmetrical even though the extrudate dimensions differ from those of the die. Also, the tension exerted on the extrudate can be used to counteract the swelling. Unsymmetrical cross sections may be distorted as a result of die swell. A standard test in the rubber industry gives a qualitative answer to the question of suitability for a given compound and machine setting. Extrusion through the peculiarly shaped **Garvey die** (Figure 14.8) is sensitive to both die swell (shown by rounded corners and convex surfaces) and other irregularities that may occur because of poor cohesion and poor surface lubricity [6]. The maximum rate at which even a symmetrical cross section can be extruded generally will correspond to the flow rate region of *melt fracture* or some other kind of periodic flow distortion. Die entrance geometry and temperature control may affect the extrudate as well as the usual variables of composition.

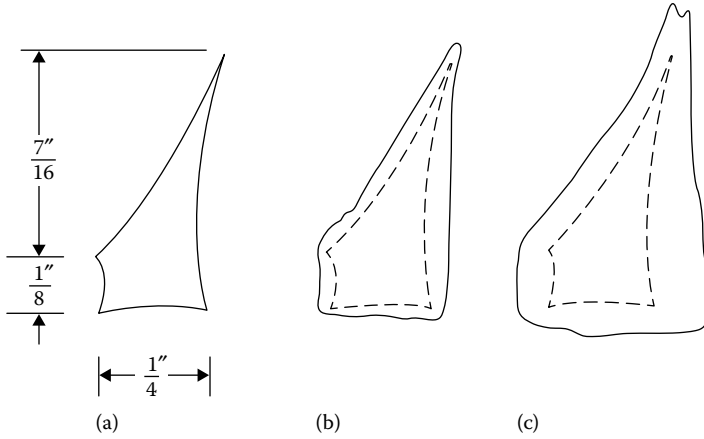


FIGURE 14.8 Garvey die for judging extrudate quality: (a) die dimensions (and dimensions of ideal extrudate); (b) marginal extrudate showing swelling and some distortion; (c) badly distorted extrudate.

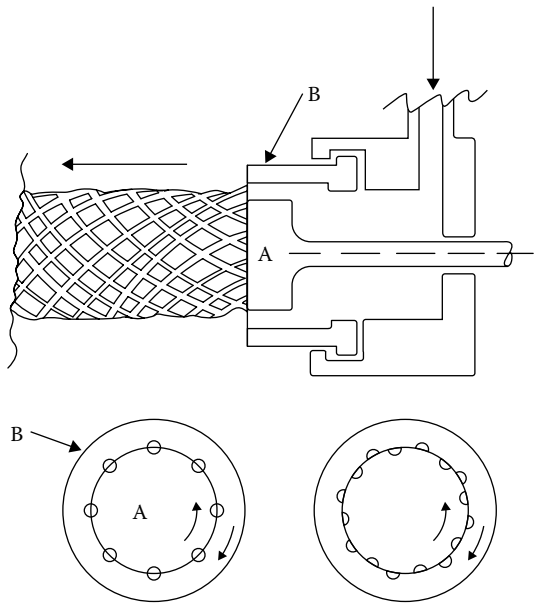


FIGURE 14.9 Rotating dies for extrusion of net material. (Data from Schenkel, G.: *Plastics Extrusion Technology and Theory*, Elsevier, New York, 383–385, 1966.)

A particularly clever mechanical arrangement permits the extrusion of a continuous sleeve of loosely knitted fibers suitable for being made into bags of the sort used for onions and potatoes. Two elements that rotate concentrically (Figure 14.9) bear hemicylindrical slots through which the polymer melt is pumped. When the slots coincide, the filaments being extruded converge and are welded together. With a

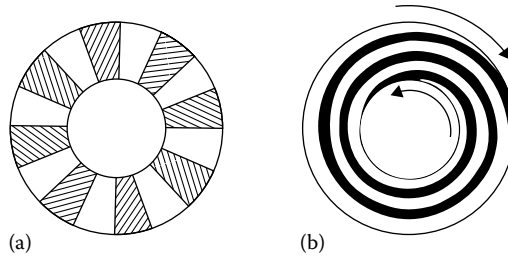


FIGURE 14.10 Production of multilayered sheet by extrusion: (a) head-on view of two polymers entering an annular die like spokes on a wheel; (b) spiral formation of multiple layers by a single spoke between counterrotating dies.

die like that in Figure 14.9, 16 threads are extruded, 8 of which convex outward and 8 toward the axis about which the elements rotate.

Another intriguing process also uses counterrotating dies. Two polymers are fed between the dies in the manner suggested by Figure 14.10. As the dies rotate, the two polymers are stretched out laterally into a multiplicity of layers. In one example [9], poly(methyl methacrylate) and polystyrene are made into a tube with over 100 layers. Combined with blown-film extrusion, a film only 25 μm thick can be made with individual layers having thicknesses near the wavelength of visible light. Very attractive diffraction patterns are produced, which suggest the use of the film in decorative applications. An iridescent film based on polypropylene and polystyrene has been available commercially since 1976 [10]. Some of its uses include overwraps for cosmetics and toiletries, gift wrapping, and wall coverings.

The application of insulation to a continuous length of conductor represented one of the first uses of extruders for rubber about 100 years ago and also one of the first uses with thermoplastics in the 1930s. The process resembles that used for pipe with extrusion around a mandrel except for the drawing of the conductor through the mandrel on a continuous basis. For thermoplastics such as polyethylene, nylon, and plasticized poly(vinyl chloride), a slight downward pitch from the extruder into a water trough is enough to cool the insulation below T_m or T_g . At the far end of the trough, the wire or cable with its hardened insulation can be withdrawn under tension around a pulley or drum, dried, and wound up. The conductor is not always a single metal strand. It can be a multiple strand or even a bundle of previously individually insulated wires. Cloth or paper may have been wrapped around the bundle in a previous stage also. With rubbers that have to be cross-linked by heating subsequent to extrusion, several routes are available. If the insulation has high dimensional stability, the uncross-linked extrudate may be coiled up and the entire assembly heated in a pressurized, steam-heated tank. The hot-air vulcanization mentioned previously for silicone tubing is feasible. Higher heat transfer rates and less porosity than the hot-air tunnel are obtained by vulcanizing in high-pressure steam. The **continuous vulcanizing process** puts the coated conductor through as much as several hundred feet of pipe containing steam at up to 250 psig (1.7 MPa). By extruding vertically downward, the sagging of the insulated wire is avoided [11].

Pultrusion is a continuous molding process resembling the application of insulation to wire and cable (Figure 14.11). Typically, a glass fiber or fabric reinforcement is fed

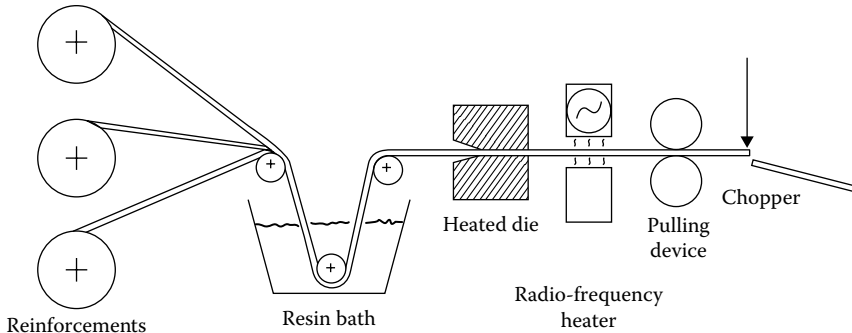


FIGURE 14.11 Pultrusion.

continuously from a spool through a resin bath. The resin-impregnated reinforcement is then pulled through a die that forms the desired cross section and heats the material to start a *curing* reaction. If the resin is a mixture of styrene monomer and unsaturated polyester with a peroxide initiator, heating causes a free-radical copolymerization to occur. After emerging from the die, the pultruded shape may be further heated by radio-frequency energy (see Section 11.6). Some standard shapes produced by this process are angles, channels, I-beams, and tubes, as well as table legs and platforms [12].

Extruders are used as auxiliary equipment in many other kinds of forming operations. Pellets for thermoplastic molding are made by chopping the cylindrical *spaghetti* extruded through a multidie extruder head. The feed for a calender (see below) may come from an extruder. The thin film for a flat-film extruder may be laminated directly onto the cardboard or another polymer film. Finally, a vented extruder can be used to dry a product or remove residual monomer from a polymer in an intermediate stage of production.

Two methods of producing flat films that do not involve extrusion should be mentioned. **Dry casting** is similar to the wet casting process described in Section 13.6 for membrane formation except that the solvent is allowed to evaporate rather than being extracted in a nonsolvent water bath. It is the oldest technology in thin polymer film technology, and over the years it has developed into a high-precision technique [13]. Most cellulose triacetate, diacetate, and acetate–butyrate are produced by this process. The triacetate films are used as protective layers in the production of polarized poly(vinyl alcohol) films for liquid crystal displays (LCDs). Demand for these films increased substantially with the popularity of large flat screens. The diacetate and acetate–butyrate films are predominantly used for photographic purposes after being coated with a gelatin emulsion. The dry casting process that is also used for membrane formation consists of depositing a polymer solution (dope, lacquer) on a large drum and evaporating the solvent. In a typical installation, the drum might be 1.20–1.50 m wide and 4–8 m in diameter and is tightly sealed to prevent vapor emissions [14]. The solution is introduced at the top from a flow box, and by the time the wheel has turned about 300° (say 15 or 20 s), enough solvent has evaporated, which the web is self-supporting and can be carried on to further drying and conditioning. The drum surface is usually made of polished stainless steel or chromium plated steel. The alignment and polishing of the drum are very critical for many film applications.

For example, the thickness of the emulsion to be added later on for photographic applications will reflect any variations in the film base material. Continuous steel belts also have been used. Associated with this kind of operation is an elaborate solvent-recovery system [14], without which it is uneconomical.

Calenders resemble the two-roll mill (Section 13.3), except that three to five rolls may be used and they all rotate at the same speed. The action is essentially that of a rolling pin or washer wringer. The material fed to the calender is usually preheated and may come directly from an internal mixer or an extruder. The calendar squeezes the mass into a film or sheet, usually at an elevated temperature, and imparts a surface gloss or texture. Embossed or printed patterns are added on subsequent rolls. Some variations are shown in Figure 14.12. Thick sections of rubber can be made by applying one layer of polymer upon a previous layer (double plying) or onto cloth fabric. Most plasticized poly(vinyl chloride) film and sheet from the 0.1-mm film for baby pants to the 2.5-mm *vinyl* tile for floor coverings is calendered. With thermoplastics the cooling below T_g or T_m can be accomplished on the rolls with good control over dimensions. With rubber, cross-linking can be carried out with the support of the rolls, once again with good control. It is only fair to point out that despite the simple appearance of the calender compared to the extruder, the close tolerances involved and other mechanical problems bring the cost of a calendering line to millions of dollars.

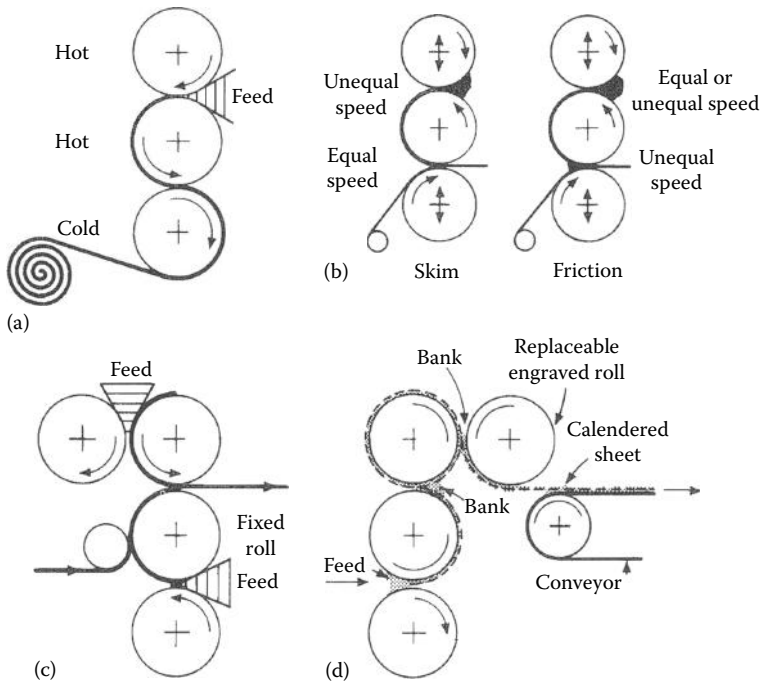


FIGURE 14.12 Calendering of rubber and plastics (Data from Winspear, G. G. ed., *Vanderbilt Rubber Handbook*, R. T. Vanderbilt Co., New York, 392, 1958.): (a) single-ply sheeting; (b) applying rubber to fabrics; (c) double-ply sheeting; (d) profiling—four-roll engraving calendar.

14.3 FIBERS

The term **spinning** as used with the natural fibers (and with the spinning wheel of colonial days) refers to the twisting of short fibers into continuous lengths. In the modern synthetic fiber industry, the term is used to denote the process of producing continuous lengths by any means. First, we should define several other terms. A **fiber** is the fundamental unit of textiles and fabrics and can be defined as a unit of matter having a length at least 100 times its width or diameter. A **filament** is an individual strand of continuous length. **Yarn** may be formed by several processes. **Continuous filament yarn**, as the name implies, is made by twisting together filaments into a strand. If the filaments are assembled in a loose bundle, we have **tow** or **roving**, which can be chopped into lengths of **staple** (an inch to several inches long). **Spun yarn** is made by twisting (**plying**) the lengths of staple into a single continuous strand. Sewing **thread** is a variety of yarn that is plied and then finished to give a smooth, compact strand. **Cord** is formed by twisting together two or more yarns. In the production of synthetic fibers, the primary fabrication process of interest is the formation, *spinning*, of filaments. In every case a polymer melt or solution is put in filament form by extrusion through a die. Usually the **spinneret**, the element through which the polymer is extruded, has a multiplicity of holes. Some rayon spinnerets have as many as 10,000 holes in a 15-cm-diameter platinum disc. Textile yarns might be spun from spinnerets with 10–120 holes and industrial yarns such as tire cord from spinnerets with up to 720 holes. Very soft fabrics for apparel are produced from various polymers by using small-diameter fibers. The term **microfiber** is used to denote fibers with a denier less than unity [16]. Three major categories of spinning processes are used: melt, dry, and wet spinning.

Melt spinning of fibers is fundamentally the same as melt extrusion of gaskets and tubing. However, the actual machinery for carrying out the processing steps may differ greatly. Polypropylene may require an extruder together with a gear pump, whereas nylon, which has a lower melt viscosity, may require only the gear pump (Figure 14.13). For producing fully oriented polypropylene yarn, a compact melt extrusion apparatus combines a screw extruder with gear (metering) pumps. The polymer chips fed to the extruder are melted, mixed, and pressurized. A color concentrate can be added to the extruder feed. After filtration, the melt goes to a *spin beam* containing four metering pumps. Each pump controls the flow of melt through spinnerets (76 holes per spinneret) to as many as four **threadlines** (individually wound spools of product) per pump. Thus, one extruder and four pumps can combine to feed 16 take-up stations. When producing 400-denier yarn, such an apparatus can handle 84 kg/h with final yarn take-up speeds of 2000 m/min [17].

Dry spinning usually uses a pump to feed a polymer solution to a spinneret. Dimensional stability now involves evaporation of solvent as in the film-casting process. Even when dried under some tension, the diffusion of solvent out of the partly dried fiber results in an uneven fiber formation. The skin that forms first on the fiber gradually collapses and wrinkles as more solvent diffuses out and decreases the diameter. The cross section of a dry-spun fiber characteristically has an irregularly lobed appearance (Figure 14.14). Solvent recovery is important to the economics of the process. Cellulose diacetate dissolved in acetone and polyacrylonitrile in dimethyl formamide are two current examples.

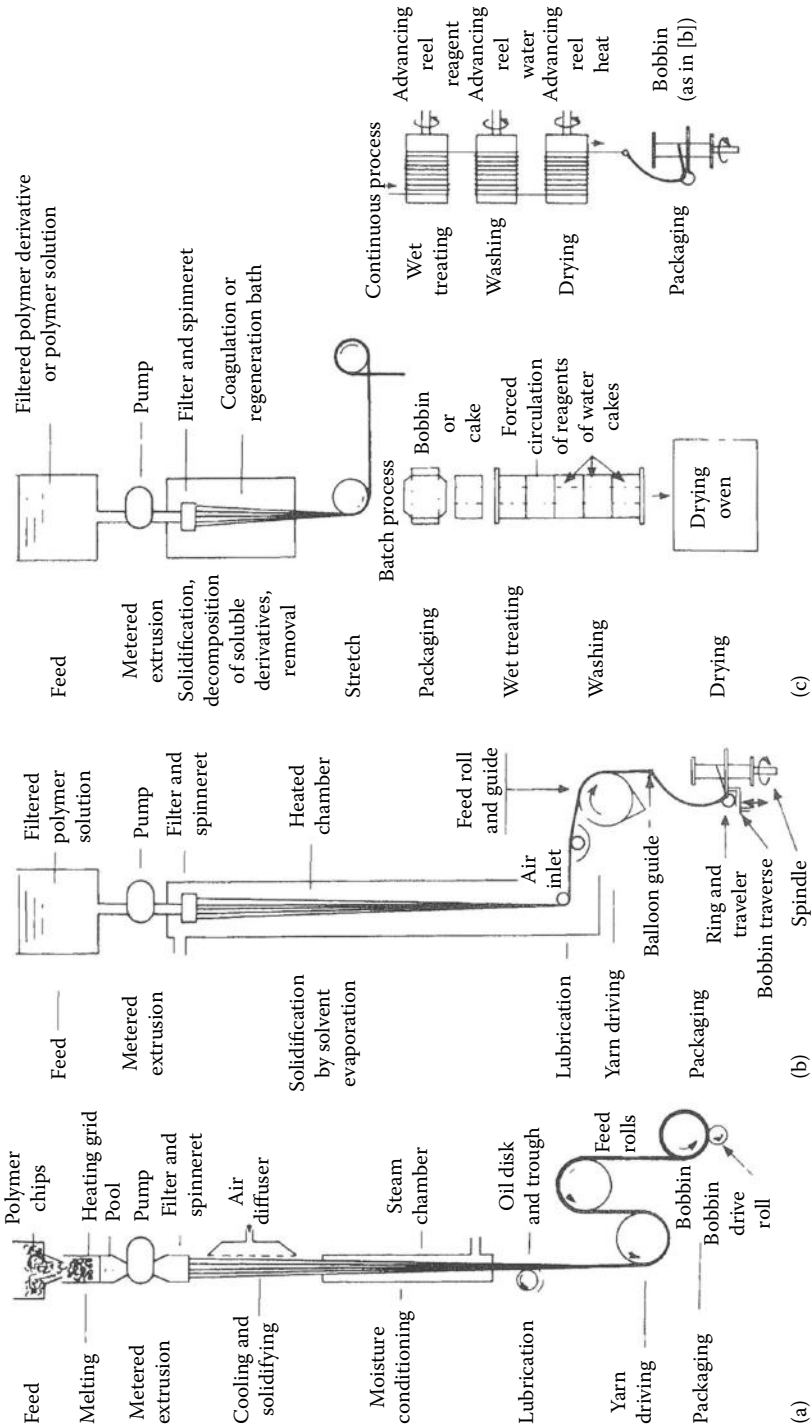


FIGURE 14.13 Features of the three principal types of fiber spinning (Courtesy of Celanese Corporation; Riley, J. L., chap.18 in C. E. Schildknecht, ed., *Polymer Processes*, Wiley, New York, 1956): (a) melt spinning, (b) dry spinning, (c) wet spinning.

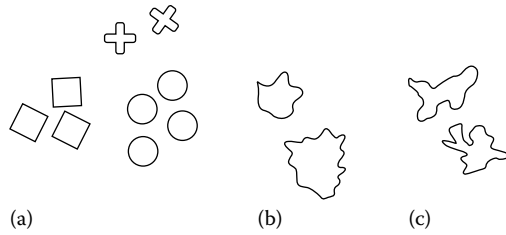
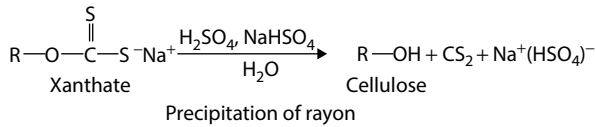


FIGURE 14.14 Typical cross sections of (a) melt-spun nylon from various shaped orifices, (b) dry-spun cellulose acetate from round orifice, and (c) wet-spun viscose rayon from round orifice.

Wet spinning also involves pumping a solution to the spinneret. Now, however, the polymer is precipitated in an immiscible liquid. Polyacrylonitrile in dimethyl formamide, for example, can be precipitated by passing a jet of the solution through a bath of water, which is miscible with the solvent but causes the polymer to coagulate. Cellulose triacetate can be wet-spun from a methylene chloride–alcohol mixture into a toluene bath, where it precipitates. In other fibers, the precipitation can involve a chemical reaction. **Viscose rayon** is made by regenerating cellulose from a solution of cellulose xanthate.



This process could be carried out with a slot die rather than a spinneret, in which case cellophane film would be produced. A ring die would give a continuous tube used as a sausage casing for the ubiquitous American hot dog. The casing is removed before final packaging of the *skinless* frankfurter.

When *liquid crystal* polymers are spun, the molecules are highly oriented. Some, such as copolyarylestere of 4-hydroxybenzoic acid, are melt-spun. The polyarylamide based on *p*-phenylene terephthalamide, is wet-spun from a solution in concentrated sulfuric acid. In either case, the tensile strength can exceed that of steel (Table 14.1). A flexible polymer such as ultrahigh-molecular-weight, linear polyethylene (UHMWPE) can also be drawn into an extended-chain configuration when fibers are formed by **gel spinning**. In one example [18], a hot, dilute (5%–15%) solution of the polymer (molecular weight exceeding 1 million) in a solvent such as decalin is extruded through a spinneret and immediately cooled to form a gel. The extrudate is quenched and extracted in a hydrocarbon liquid bath and dried under vacuum. Then the fiber, retaining the conformation it had in the gel, is drawn 30–100 times its original length at a controlled temperature of 100°C–150°C. The highly oriented structure that results gives the fibers a modulus and strength in tension much higher than that of the ordinary nylon and poly(ethylene terephthalate) used in textiles (Table 14.1). Both the polyarylamides and the UHMWPE fibers have found many uses. Probably the most exotic application is in the manufacture of lightweight, bullet-proof clothing for police protection.

TABLE 14.1
Comparative Properties of Selected Fibers

Material (Fiber)	Tensile Modulus (GPa)	Tensile Strength (GPa)	Compressive Strength (GPa)	Density (g/cm ³)
Steel	200	2.8		7.8
Carbon	585	3.8	1.67	1.94
Polyarylamide ^a	185	3.4	0.39	1.47
Polyarylester ^b	65	2.9	—	1.4
UHMWPE ^c	172	3	0.17	1
Nylon	6	1	0.1	1.14
Polyester	12	1.2	0.09	1.39

Source: Jiang, H., W. W. Adams, and R. K. Eby: chap. 13 in R. W. Cahn, P. Haasen, and E. J. Kramer (eds.), *Materials Science and Technology: Structure and Properties of Polymers*, VCH, New York, 1993.

Note: These values are only typical; actual values vary.

^a Polyarylamide = Kevlar.

^b Polyarylester = Vectra.

^c UHMWPE = Spectra.

Almost all synthetic yarns are **drawn** (stretched) so that the crystalline structure is oriented in the direction of the fiber axis. Very large draw ratios are used to decrease the diameter of the fibers to well below the spinneret dimensions. Usually yarns are drawn at a temperature between T_g and T_m . The T_g may be depressed by the presence of a plasticizer, particularly water (Sections 3.3 and 3.6). Some mechanical arrangements for continuously drawing yarn are shown in Figure 14.15. In each case the drawing is accomplished by winding the yarn around a drum or wheel driven at a faster surface velocity than a preceding one. Polyethylene could be drawn, as indicated in Figure 14.15a, at room temperature, but nylon 6,6 would have to be heated or humidified to be drawn. Fluted glass feed rolls called **godets** are used (see Figure 14.15b and c) to control the speed of yarn. Many fibers are drawn as an integral part of the spinning process. In some cases, it is preferable to store the fibers or carry out some other operation first, such as dyeing or twisting, and then to draw, in which case a plasticizing bath may be used to facilitate the process. In any case, the drawing does orient crystallites in the direction of the applied strain so that the modulus in that direction is increased and elongation at break is decreased.

The smooth cylindrical shape may not be the optimum one for apparel use. The seeming futility of chopping tow or roving into staple, only to respin the staple into a yarn, makes more sense when one sees the difference the operation makes in the apparent bulkiness of fibers in a sweater or blouse. Another means of increasing the bulkiness of yarn is to crimp the fibers by mechanical or other means. A primitive means of inducing **crimp** (waviness) is to pass the fiber between two heated, fluted rolls or between two meshing gears (Figure 14.16). More elaborate means of **texturing** yarns include twisting and untwisting, knitting and deknitting, and chemical treatments. Staple fibers often are textured before being chopped into staple.

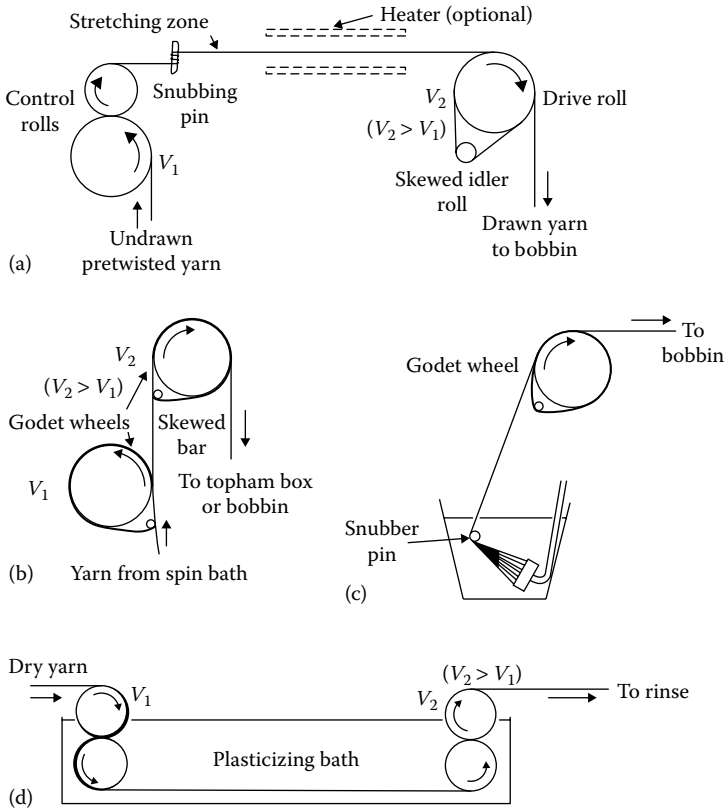


FIGURE 14.15 Four types of drawing processes used for synthetic fibers. V_1 and V_2 indicate the relative velocities of take-up rolls. (Courtesy of Celanese Corporation; Riley, J. L., chap.18 in C. E. Schildknecht, ed., *Polymer Processes*, Wiley, New York, 1956.) The processes involve (a) cold (or hot) draw, (b) godet-controlled wet stretch of nascent yarn, (c) snubber-controlled wet stretch of nascent yarn, and (d) roll-controlled wet stretch of replasticized yarn.

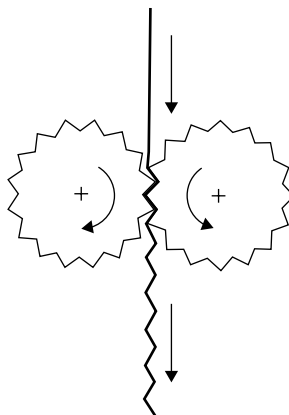


FIGURE 14.16 Mechanical crimping.

Some applications require individual fibers that are very stiff. A column with a cruciform cross section is stiffer than one with a circular cross section (Figure 14.14), and it is quite feasible to melt-extrude such shapes in polypropylene for rugs, for example. Hollow fibers can be produced in various ways. Discontinuous air cells increase the bulk of the fiber and can give some interesting handling properties, causing some synthetics to resemble fine wool. By extruding around a mandrel, a continuous void can be formed inside a fiber. So-called hollow fibers are really small-size tubes. Bundles of such fibers are assembled into separators that resemble shell-and-tube heat exchangers. The tubes act as semipermeable membranes. Such devices have been used for water desalination and as artificial kidneys. For separating hydrogen from gas streams, over 10,000 fibers (0.8-mm outer diameter, 0.4-mm inner diameter) may be packed into a shell that is 20 cm in diameter and 3 m long [19].

In most mechanical operations with fibers such as knitting and spinning, lubricants or other agents may be needed to prevent fouling of machinery. Printing and dyeing of textile fabrics is another large field in itself.

For many years the application of thermosetting resins to fibers as wash-and-wear treatments has been a major industrial process. The general idea is to enhance the *memory* of the fabric for creases put in before setting the resin and to minimize subsequent wrinkling. Melamine and urea resins applied to cotton comprise one large class of such materials. Due to their comparatively hydrophobic nature, nylon and poly(ethylene terephthalate) fibers do not require such treatment. While low-moisture absorption is good for dimensional stability, it is often accompanied by low electrical conductivity. This brings on a second problem, that of static electricity. The charges on hydrophobic fibers do not leak off, and they cause apparel to cling uncomfortably. Also, most people have had the experience of walking across a deep pile rug on a low-humidity, winter day and finding on reaching for the doorknob that a substantial difference in electrical potential has been induced between themselves and the knob. Finishes are available to counteract that static buildup too. In apparel the solution most often is to blend the nonconducting synthetics with the more conductive cotton or wool.

14.4 LAMINATES

In industrial terminology, **laminates** include many types of heterogeneous materials whether in layers or not. Here we shall restrict the term to standard shapes that are made in flat sheets of the same or different materials. A familiar example that illustrates the method and the advantages of lamination is **plywood**. Thin sheets of **veneer** are cut by knives whose blades stretch the length of a log and cut at an angle almost tangential to the curvature of the log surface. Such sheets are very strong in the direction of the tree axis and comparatively weak at 90° to that axis in the plane of the veneer. By plying the layers of veneer at right angles (usually with an odd number of layers), the strength can be made nearly equal in both directions. This makes the plywood superior to a board cut from the same wood, provided the plies can be held together strongly. Phenol-formaldehyde resins are often used to bond and, to a certain extent, impregnate the veneers. The conversion of the pre-polymers to

the final thermosetting form takes place when the assembly is in a press under high pressure. There are several other advantages of plywood over single boards besides equalizing the directional strength. The impregnation decreases the moisture pickup of the wood, so that there is less swelling in humid atmospheres. For decorative purposes, plywood paneling can be made from inexpensive wood such as fir except for the top layer on one side, which might be a specially decorated material or an expensive, rather rare wood. It is also possible to build moisture barriers, flame-retardant materials, or insulating layers into such panels by modifying the inner layers.

Paper layers are laminated with various resins to make materials useful in electrical applications as well as the **decorative laminates** that are best known by their trade names such as Formica and Micarta. Kraft paper, about the weight used in shopping bags, is taken directly from rolls and run through a solution of melamine-formaldehyde pre-polymer in a typical application. Driving off the solvent or drying out water leaves an impregnated sheet that can be handled easily, since the brittle pre-polymer does not leave the surface sticky. As many as a dozen or more layers of impregnated paper are laid up. The entire assembly is heated between smooth plates in a high-pressure press to carry out the thermosetting reaction that binds the sheets together into a strong, solvent-resistant, heat-resistant surfacing material. For use in tabletops, countertops, and so on, the laminate, which is only about 1.5 mm thick, can be glued to a plywood or fiberboard base.

The impregnated sheet materials can be wound on themselves or on a mandrel and heated in a press with curved surfaces to make rods or tubes. In any case, the ultimate use of the laminates often involves machining operations. For this reason, the ease with which a particular laminate can be sawed, drilled, or punched often has a bearing on its suitability for a given application.

Sandwich construction usually connotes assembly with one material for both surfaces and a second material in between. A core of foamed polymer covered by plywood or metal layers is very stiff without being very heavy and is a good insulator. Plywood surface with a foamed polystyrene core is available in 4-by-8- and 4-by-10-ft panels for quick assembly into small housing units. Surface and core can be varied to impart abrasion resistance, weathering resistance, flame resistance, or radiation resistance for particular applications.

Laminates can be produced during extrusion. A multilayered laminate made using rotating dies has already been mentioned. **Coextruded film and sheet** may combine two or three different polymers in a single product. Adhesion is enhanced by cooling the laminate directly from the melt rather than in a separate operation after the film components have been formed and cooled separately. In one form, flows from individual extruders are combined in a **flow block** and then conveyed to a single manifold die. Because laminar flow must be maintained, all the polymer streams have to have about the same viscosity. Systems with up to seven layers are reported to be in operation [20]. There are various reasons for wanting **multilayer films and sheets**. A chemically resistant sheet can be combined with a good barrier to oxygen or water diffusion. A decorative, glossy sheet can be placed over a tough, strong material. Not all combinations adhere equally well, so there are limits to the design of such structures. One commercial example is a four-layered sheet (ABS, polyethylene, polystyrene, and rubber-modified polystyrene) for butter and

margarine packages. Another is an ABS, high-impact-polystyrene sheet, which can be thermoformed (see Section 14.10) to make the inside door and food compartment of a refrigerator [20].

14.5 COMPRESSION MOLDING

In almost all molding operations, heat and pressure are applied to make the polymer flow into a preferred form. Dimensional stability then is conferred by cooling or further heating. Thermoplastic materials have to be cooled below T_m or T_g before being removed from the mold. This means a sequence of heating, pressurized flow, and pressurized cooling. Thermoset materials and rubbers have to be heated long enough for some chemical reaction to occur that brings about a stable, network structure. The sequence here is heating, pressurized flow, and pressurized reaction. Although some thermosets are cooled before ejection from the mold, most can be ejected hot.

Compression molding of combinations of shellac, straw, and various waxes and pitches goes back at least to the 1860s. The simplest compression mold is the **flash mold**. The only pressure on the material remaining in the mold when it is closed (Figure 14.17) results from the high viscosity of the melt, which does not allow it to escape. Since most rubbers have high melt viscosities, especially when filled, the flash mold is widely used for mechanical goods such as gaskets and grommets and also for shoe heels, tub and flask stoppers, doormats, and other familiar items. Most thermoset prepolymers (e.g., phenolic and melamine) are brittle and powdery at room temperature but have low viscosity when heated, although the viscosity rapidly increases as cross-linking occurs. A primitive **positive pressure mold** can be made from a ring and two plates (Figure 14.18). The final thickness of the molded disc varies with the amount of polymer charged initially. An internally landed **semipositive mold** (Figure 14.19) exerts more pressure on the melt than the flash mold, but the final dimensions are controlled by the meeting of the plunger and a land, or shelf, on the cavity.

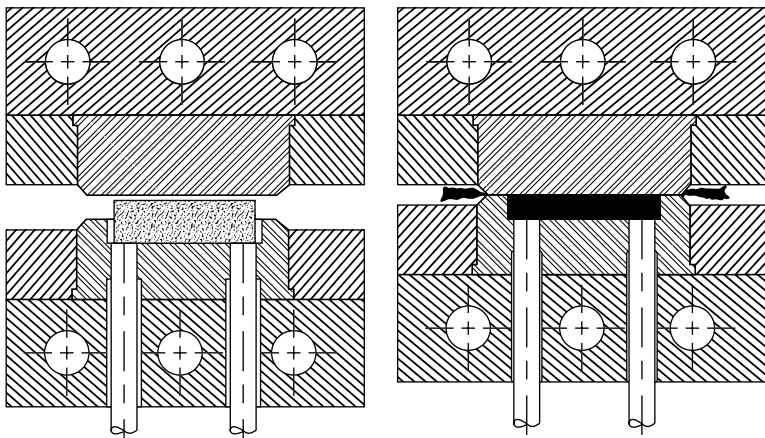


FIGURE 14.17 Flash mold: open, with preform in place, and closed, with flash forced out between mold halves. (Data from Vaill, E. W., *Mod. Plast.*, 40, 767, September 1962.)

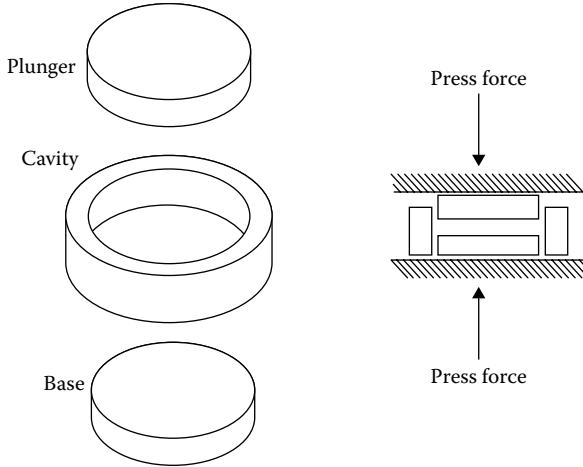


FIGURE 14.18 Elementary positive-pressure mold.

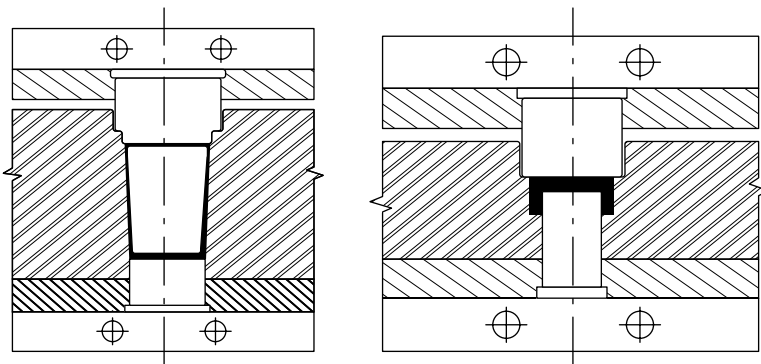


FIGURE 14.19 Internally landed positive and semipositive molds (both shown in closed position). (Data from Vaill, E. W., *Mod. Plast.*, 40, 767, September 1962.)

In either of the compression molds, the prepolymer (molding powder) is melted and forced into the cavity simultaneously. If the polymer is being molded around a metal insert such as an electrical lug, the prepolymer may resist flow initially and exert a high force on the insert. In such a case, it is desirable to melt the polymer in a separate operation and then inject it into the cavity. Because only seconds are available, both operations are carried out in the same equipment by **transfer molding**. The prepolymer is put into a pot in the mold (Figure 14.20), from which it flows under the force of the plunger only after it has become hot enough to be rather low in viscosity. The material then is pushed into the cavity where it is held for the thermosetting reaction. When the mold is disassembled, note that the part is pushed out of the mold by **ejector pins** that operate automatically. The **sprue** is withdrawn, because of a slight undercut section, along with the **cull**, the uninjected remainder. The **gate** is the point where the sprue meets the **runners** that carry resin from the sprue bushing to the individual cavities.

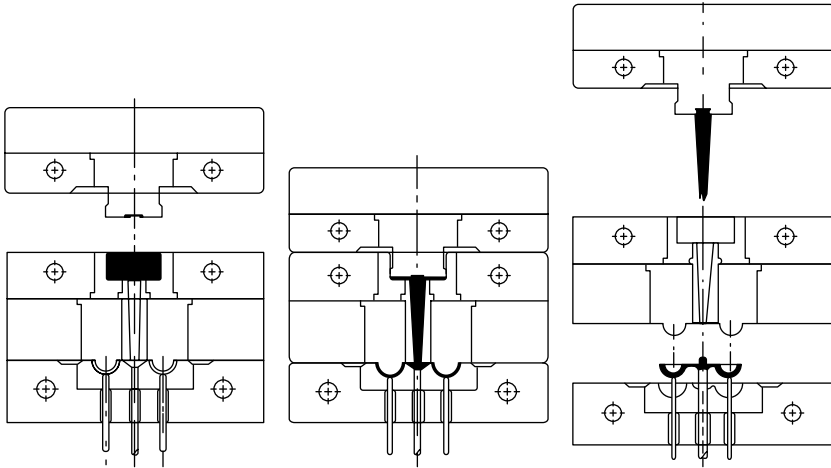


FIGURE 14.20 Typical transfer-mold operation. Material is fed into the pot of the transfer mold and then forced under pressure when hot through an orifice and into a closed mold. After the polymer has formed, the part is lifted by ejector pins. The sprue remains with the cull in the pot. (Data from Vaill, E. W., *Mod. Plast.*, 40, 767, September 1962.)

Compression molding is used predominantly for large flat or curved auto parts such as hoods and fenders and with thermosetting resins. Because compression molding of a thermoplastic resin involves heating and then cooling the mold, most such materials are more efficiently molded in the injection machines described in Section 14.6.

14.6 INJECTION MOLDING

Injection molding accomplishes the cyclic operation by carrying out each step of the process in a separate zone of the same apparatus. The mold cavity is again formed from two steel parts (at least): one of which is movable so that it can open and close during different parts of the molding cycle. The entire mold is cooled to temperatures below T_g or T_m , usually by using circulating water through channels cut out into the mold. The polymer melt from the nozzle of the injection unit flows through the **sprue**, the **runner system**, and the **gate** before it enters into the actual part cavity. A **plunger** (also called a ram or piston) pushes pellets, which fall from the hopper into the barrel when the plunger is withdrawn (Figure 14.21) into a heated zone. By spreading the polymer around a **torpedo** into a thin film, a rapid heating is possible. The already molten polymer displaced by this new material is pushed forward through the **nozzle** and the sprue bushing, down the runner, and past the gate into a cooled cavity. The thermoplastic must be cooled under pressure below T_m or T_g before the mold is opened and the part is ejected. The plunger is withdrawn, new pellets drop down, the mold is clamped shut, and the entire cycle is repeated. Mold pressures of 8,000–40,000 psi (55–275 MPa) and cycles as low as 15 s are achieved on some machines. Injection-molding machines are rated by their capacity to mold polystyrene in a single shot.

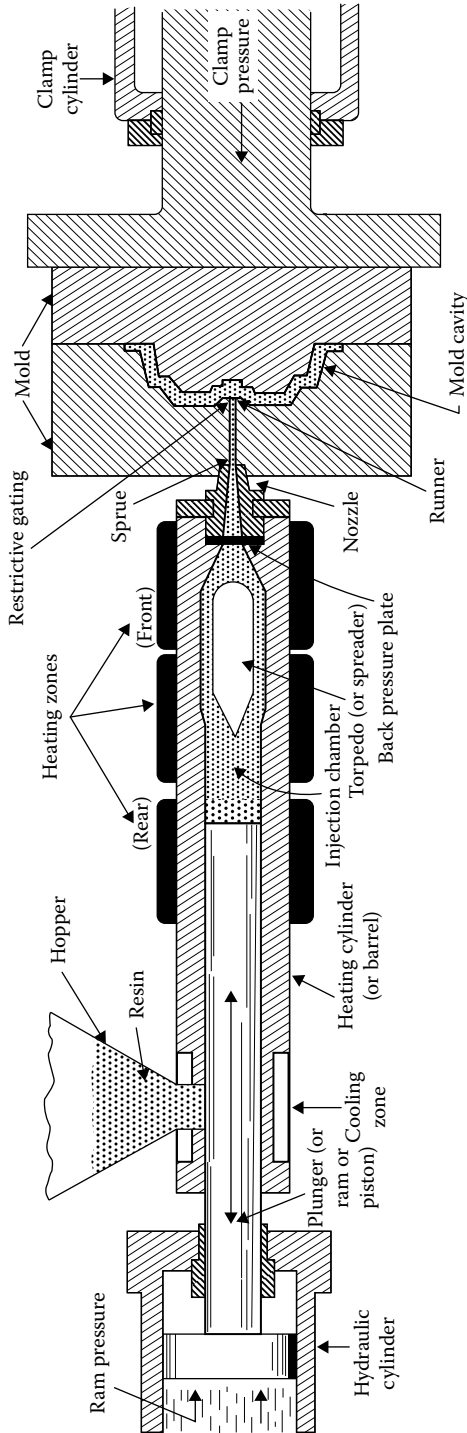


FIGURE 14.21 Schematic cross section of typical plunger (or ram or piston) injection-molding machine. (Data from U. S. I. Chemicals/Quantum, *Petrothene Polyolefins: A Processing Guide*, 5th edn., National Distillers and Chemical Corporation, New York, 1986.)

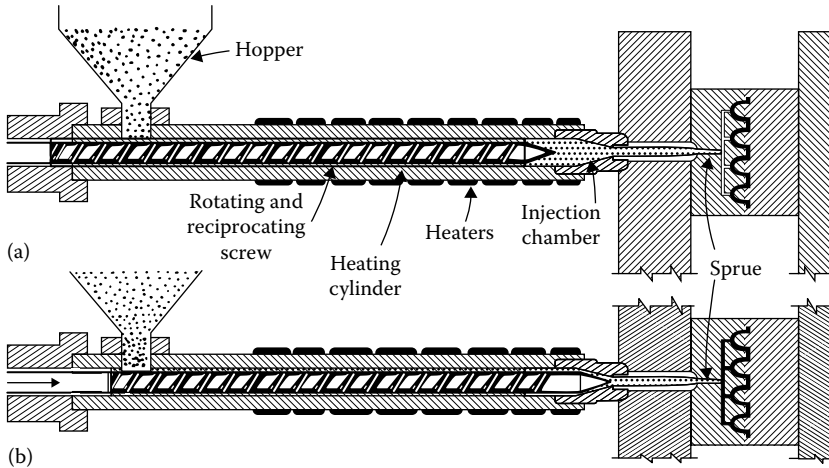


FIGURE 14.22 Cross section of a typical screw injection-molding machine, showing the screw in the (a) retracted and (b) forward positions. (Data from U. S. I. Chemicals/Quantum, *Petrothene Polyolefins: A Processing Guide*, 5th edn., National Distillers and Chemical Corporation, New York, 1986.)

A 2-oz machine can heat and push 2 oz of general-purpose polystyrene into a mold. Plunger diameter, plunger travel, and heating capacity all are involved. Although the plunger-type machines are inherently simple, the limited heating rate has caused a decline in popularity, so that most machines in use today in the United States are of the **reciprocating-screw** type.

By virtue of a check valve on the forward end of the screw (Figure 14.22), the reciprocating screw can push forward without rotation and act just as the plunger in an ordinary injection-molding machine. The screw may remain forward, whereas the melt cools or, in the case of rubber, the polymer in a hot mold cross-links. The steps of the cycle in a reciprocating-screw injection-molding machine consist of the following:

1. The mold is closed and clamp pressure is applied to keep the mold closed during injection.
2. The screw acts as a plunger and the molten polymer flows into the cavity (**filling stage**).
3. When the cavity is full, the pressure on the molten plastic is increased to add more material into the cavity in compensation for the shrinkage caused by cooling (**packing stage**).
4. The cavity is cooled to bring the polymer below T_g or T_m (**cooling stage**).
5. During the cooling stage, the screw starts to turn to melt more material for the next part.
6. Once the part is cooled, the mold opens and the part is ejected.
7. The mold closes and the cycle is repeated.

The whole cycle takes less than a minute for small parts and several minutes for large parts. In step 5, the check valve is open during rotation, allowing the molten polymer

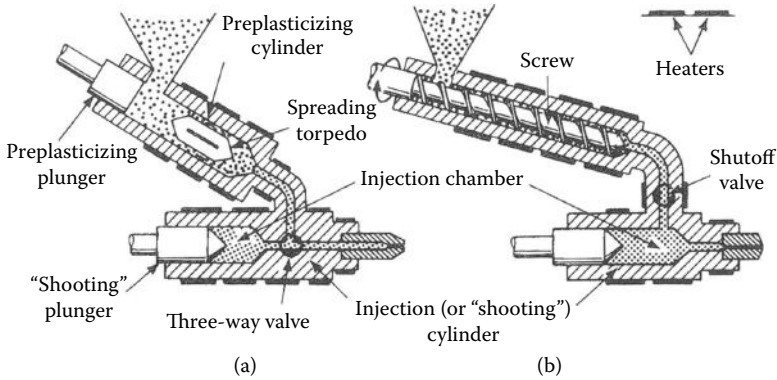


FIGURE 14.23 Drawings of (a) a plunger-type and (b) a screw-type preplasticizer atop plunger-type injection-molding machines. (Data from U. S. I. Chemicals/Quantum, *Petrothene Polyolefins: A Processing Guide*, 5th edn., National Distillers and Chemical Corporation, New York, 1986.)

to flow around the screw. It is in this part of the cycle that the screw is valuable, because it increases heat transfer at the walls and also does considerable heating by the conversion of mechanical energy into heat in an adiabatic system. Another advantage of the screw machine is its mixing and homogenizing action. Another way of taking advantage of the screw feature is by pre-plasticizing the melt with a screw arrangement, which then feeds to a barrel from which the molten polymer can be injected by a ram (Figure 14.23).

During the filling stage, as the polymer melt enters the sprue, the runner system, and the part cavity, it is encountering more and more resistance due to the friction with the walls. Most injection-molded parts are thin and can be quite large and thus require very large pressures to insure their filling. If one operates at a constant high pressure, two problems may be encountered: (1) instead of a uniform flow progression inside the cavity, jetting may occur and produce a poor product; and (2) if the pressure is not high enough, the flow rate will continue to decrease and a **short shot** is likely to occur. A short shot is the name given to an incomplete part due to premature solidification inside the cavity. A simple analysis of isothermal filling in an idealized runner system modeled as a straight cylindrical runner of radius R can demonstrate this point: Assume an incompressible, isothermal, fully developed (steady-state) power-law fluid. We can calculate the position $z(t)$ of the melt front and the instantaneous flow rate $Q(t)$ in terms of P_0 , the pressure at the inlet of the runner. The position $z(t)$ is obtained from a mass balance:

$$z(t) = \frac{1}{\pi R^2} \int_0^t Q(t) dt \tag{14.3}$$

which gives upon differentiation with respect to t :

$$\frac{dz(t)}{dt} = \frac{Q(t)}{\pi R^2} \tag{14.4}$$

For a general power-law flow in a cylindrical pipe, $Q(t)$ is given by [22]

$$Q(t) = \frac{\pi R^3}{1/n + 3} \left[\frac{RP_0}{2Kz(t)} \right]^{1/n} \quad (14.5)$$

where:

n and K are the power-law index and the fluid consistency, respectively (see Section 7.2)

One then finds by combining Equations 14.4 and 14.5:

$$z(t) = \left(\frac{1+n}{1+3n} \right)^{n/1+n} R \left(\frac{P_0}{2K} \right)^{1/1+n} t^{n/1+n} \quad (14.6)$$

and the flow rate is

$$Q(t) = \pi R^3 \left(\frac{1+n}{1+3n} \right)^{n/1+n} \left(\frac{n}{1+n} \right) \left(\frac{P_0}{2K} \right)^{1/1+n} \left(\frac{1}{t^{n/1+n}} \right) \quad (14.7)$$

Although it is for a very simple case, the result of the above equation is revealing because

1. It indicates that for a constant pressure injection, we should expect a high flow rate and quick filling initially (at short times), followed by a rapid drop in Q . Because of the assumption of fully developed quasi-steady-state, we cannot take $t \rightarrow 0$ in Equation 14.7. For experimental values of K and n of polymer melts, one can show that a constant P_0 is impractical in the real nonisothermal situation where the viscosity increases exponentially as the polymer melt cools and the flow stops completely leading to a short shot.
2. From Equation 14.7, it is seen that for a constant flow rate, the applied pressure at the gate must increase with time to a certain power. In practice, the initial part of the mold-filling cycle is one of increasing applied pressures to maintain a constant flow rate.
3. For better control of production parts, constant Q is most desirable until the mold-filling stage is completed. However, for large (and thin) parts that offer high resistance to melt flow, the pressure will reach the maximum achievable by the machine and then remain constant while the flow rate is decreasing with time (with higher risks of short shots).

Because of the complexities of the process described above, there is no simple way to optimize the molding conditions (melt temperature, mold temperature, pressure or flow rate, etc.) for a given polymer and a given mold cavity. Before the advent of computer simulations (Section 14.7), empirical *molding area* diagrams (Figure 14.24) were developed for different polymers and different molds, and the process was one of trial and error.

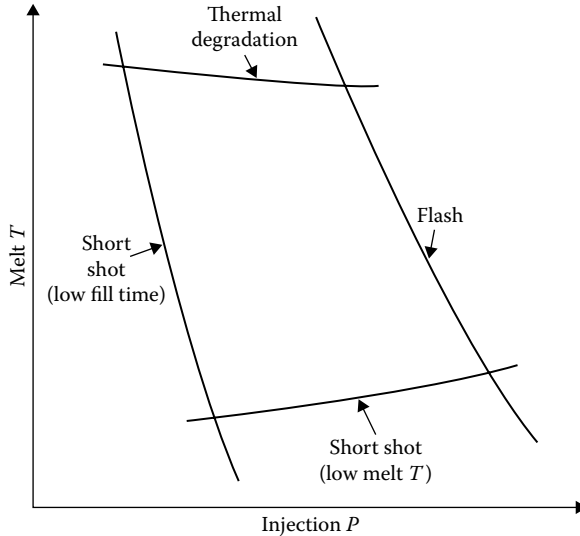


FIGURE 14.24 Schematic representation of a window of moldability of a thermoplastic.

As with extrusion, injection molding of thermoset resins is difficult but possible. In effect, a kind of automated transfer molding is used. Injection molding of rubber (with a heated mold and ejection of hot parts) gives faster cycles and pieces with less porosity than flash compression molding. A side benefit is that rubber molded and cross-linked at a high pressure has built in residual stresses that increase resilience. A cross-linked polybutadiene rubber ball will bounce back up to about 85% of its original height when molded at pressures of less than 1000 psi (7 MPa). However, molding at about 10 times that pressure can increase the bounce to as much as 92%. Since this particular property is not of great importance except to toy manufacturers, the more often cited benefits of injection molding for rubber are the faster cycle time and the lower scrap level (less flash, sprues, etc.) compared to compression molding.

14.7 INJECTION-MOLDING SIMULATIONS

14.7.1 FILLING STAGE

A complete mold-filling computer simulations requires the calculations of the velocity and temperature profiles throughout the flow region, including the position and shape of the advancing melt front in the cavity.

The complete problem is very complex even for simple molds. The problem has been divided into smaller isolated problems representing each different flow regions in the mold and the solutions combined together. Each of these regions requires different approaches and simulation tools that are beyond the scope of this textbook. The basis of these approaches is nonetheless illustrated below for the case of one-dimensional flow filling of cavities of simple geometries. Over the past 30 years, a great deal of information and insight has been provided by these simulations.

Computer simulation packages for injection molding are now available commercially and have transformed the art of injection molding into a science-based process.

The analysis of mold filling has been divided into the following three regions:

1. *The fully developed region.* The majority of the filling process involves the flow of the melt in a narrow gap configuration between cold walls in an almost fully developed manner. The nature of the flow determines the filling time, the part core molecular orientation and stresses, as well as the occurrence of short shot and the location of **weld lines** where two melt fronts meet inside a cavity. If we consider simulating the filling of a center-gated circular disk (e.g., compact disk) or the filling of an end-gated rectangular strip (e.g., ruler), we would use the appropriate equations of motion (Appendix 8.B) and an equation for the conservation of energy. If we denote the direction of flow by x , and the gap-wise direction by z , the approximate governing equations for our simple geometries reduce to

$$0 = \frac{\partial}{\partial z} \left(\eta \frac{\partial u}{\partial z} \right) - \frac{\partial p}{\partial z} \quad (14.8)$$

$$\rho C_p \left(\frac{\partial T}{\partial t} + u \frac{\partial T}{\partial x} \right) = k \frac{\partial^2 T}{\partial z^2} + \eta \left(\frac{\partial u}{\partial z} \right)^2 \quad (14.9)$$

where:

u is the x -component velocity

T is the melt temperature

p is the melt pressure

The viscosity, density, heat capacity, and thermal conductivity of the polymer are denoted by η , ρ , C_p , and k , respectively. In writing the above governing equations, one assumes that inertia, stream-wise conduction, gap-wise convection, and elastic effects are negligible. Average values of ρ , C_p , and k are often used, but the temperature and shear-rate dependence of the viscosity need to be taken explicitly in order to make reasonable predictions. A modified Cross model with an Arrhenius dependence of the zero-shear rate viscosity usually fits the rheological viscosity master curve quite well [23]. During filling, the cooling creates a frozen layer in the cavity that affects the flow. This layer creates a different molecular and fiber (in the case of short-fiber-filled polymer) orientation in the different sections of the molded part. Therefore, the energy equation and the momentum equations (flow equations) are always coupled and have to be solved simultaneously. Finite-element and finite-difference methods were used for the first time with appropriate initial and boundary conditions in the work of Hieber and Shen [24] to solve these equations as a function of time and predict local pressure, temperature, and the advancement of the melt front. The above equations were also generalized to two-dimensional flows and compared to experimental

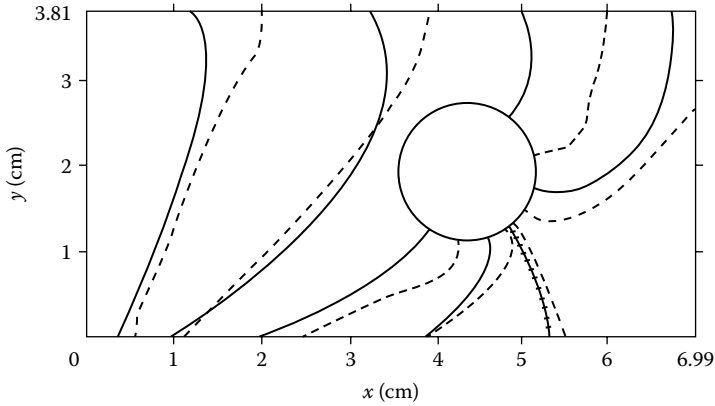


FIGURE 14.25 Comparison between predicted melt fronts (dashed lines) and experimental short shots (solid lines) for the filling of a variable thickness rectangular cavity with a cylindrical insert. The polymer used was polypropylene, the injection temperature was 197°C, and the cavity wall temperature was 27°C. Predicted weld line is denoted by +++. (Data from Hieber, C. A. et al., *Polym. Eng. Sci.*, 23, 20, 1983. Reprinted by permission of the Society of Plastics Engineers.)

results [25]. The comparison between the predictions of pressure, melt front advancement, and weld lines inside the cavity with the experimental results are fairly satisfactory (see example in Figure 14.25) and indicate that in the filling stage, the various approximations made are quite reasonable even in complex geometries. The melt front advancement is obtained experimentally by producing short shots achieved by having the amount of the polymer that is molten and injected in the cavity less than the total amount needed to fill the cavity.

2. *The flow front region.* This region turns out to play an important role in the surface properties such as orientation and stresses in skin formation. The flow in this region is more complex as it involves both shear and elongational flow. Figure 14.26 illustrates the flow of tracers in this region [26]. The shape of the streamlines in this region resembles the streams flowing out of a fountain and the flow in this region has been described as a **fountain flow** [22].

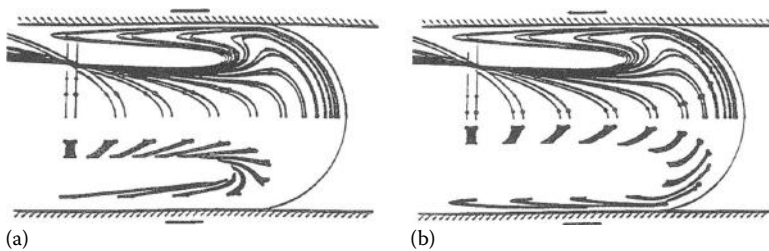


FIGURE 14.26 Tracer patterns near the advancing melt front showing the fountain effect for two different initial tracer locations. The rectangular element at the initial melt front gets sheared and extended and reverses direction as material on the flow front gets deposited near the wall. (Data from Coyle, D. J. et al., *AIChE J.*, 33, 1168, 1987. Reprinted by permission of the American Institute of Chemical Engineers.)

3. *The gate region.* Because of high shear and often strong elongational component of the flow in this region, viscoelastic effects of the polymer are important and need to be taken into account for the predictions of the overall simulation of the filling process. At this time, this can be done only approximately.

14.7.2 PACKING STAGE

Once the mold is filled, there is no more free surface flow, but melt still enters the cavity to compensate for shrinkage caused by cooling. The control of the machine would typically shift from a constant Q to a constant P . Because the change in density is the major phenomenon taking place during packing, the assumption of incompressibility that is adequate for simulating the filling stage is no longer acceptable. The dependence of the polymer density on temperature and pressure is required [3,27]. The analysis of this phase will therefore also include the conservation of mass (continuity equation for compressible liquids) along with the momentum (flow) equations and the energy equation (temperature) used in the filling stage. Figure 14.27 shows a comparison between the simulation predictions and the experimental results of pressure traces obtained from flush-mounted transducers inside

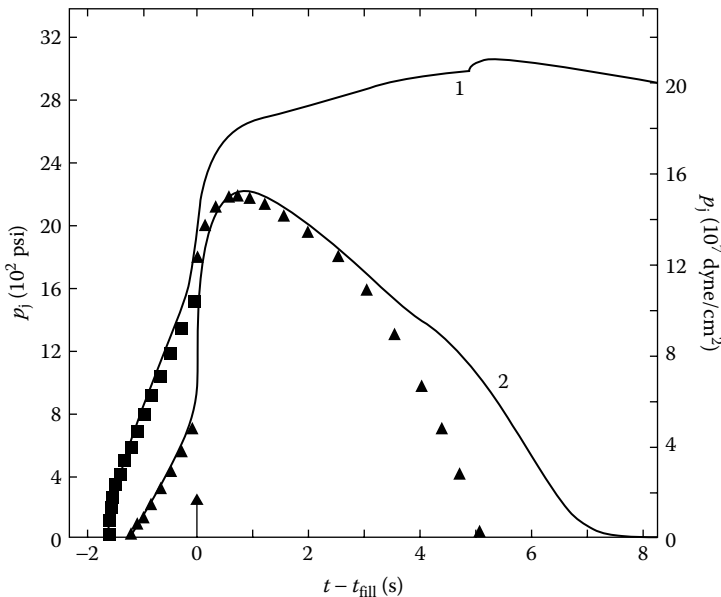


FIGURE 14.27 Comparison between pressure traces from flush-mounted transducers (curves) and corresponding simulated data (squares and triangles) for a center-gated disk with a half-gap thickness of 0.98 mm and an outer radius of 7.62 cm. The injected polymer is polystyrene at 225°C with a volumetric flow rate of 23.8 cm³/s and a cavity wall temperature of 40°C. Locations of the transducers are under the sprue ($x = 0$) for curve 1 and midway to outer radius ($x = 3.80$ cm) for curve 2. (Data from Wang, K. K., *Cornell Injection Molding Program, Progress Report 16*, Cornell University, Ithaca, NY, December 1991.)

the cavity for a center-gated disk [27]. The zero time on the abscissa corresponds to the time of fill. Note the increased pressure at packing and the subsequent decrease of pressure inside the cavity (curve 2) as cooling and solidification take place. The simulations here were performed using a modified Cross model for the viscosity (see Section 7.2.3); better agreement with the experimental results is achieved when a viscoelastic model is used [27].

14.7.3 COOLING STAGE

Once the gate freezes, the cavity is disconnected from the applied pressure of the extruder, the pressure inside the cavity drops and final cooling of the part takes place. This is the final step of the process before part ejection. However, cooling occurs from the beginning during the filling and packing stages, and continues afterward until the part is solidified. The major effect of polymer cooling is that it retards stress relaxation and some of the stresses remain frozen-in after solidification. These stresses often create shrinkage and warpage problems. To predict these stresses, a viscoelastic constitutive model is needed. Much effort has been spent studying ways to reduce (or eliminate) such stresses in optical and electronics parts such as compact discs and lenses for cameras and overhead projectors. Computer simulations have been of great help in this regard for noncrystallizable polymers [28].

14.8 OTHER MOLDING PROCESSES

14.8.1 REACTION INJECTION MOLDING

The rapidity with which isocyanate–polyol reactions take place has been used to advantage in **reaction injection molding (RIM)**. In the typical process (Figure 14.28), two components are mixed by high-pressure injection into a special chamber and injected almost immediately into a closed, low-pressure mold. The finished parts can be cellular or solid depending on the amount of material injected

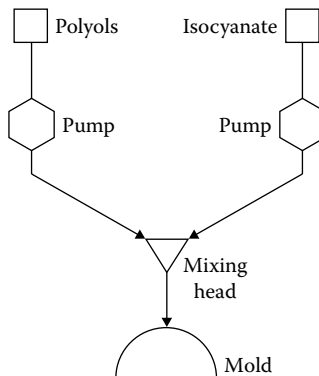


FIGURE 14.28 Reaction injection molding. Polyols and isocyanates are pumped at high pressure from storage reservoirs into the mixing head. The mixed streams are then injected into the mold at a much lower pressure.

and the formulation used. In the automobile industry, the need for lightweight, cushioning parts has been met by RIM. Front and rear bumpers and the **fascia** (face part, which can include grill and headlight housings) are made as single units. The mixing head is the critical point in the system. Volume in the mixing chamber is kept small (1–5 cm³), and impingement pressures for mixing are 100–200 atm. There is a self-cleaning feature so that when one mold is filled, the head will remain clear until another mold is ready. Mold filling may take 2–3 s at mold pressures of only 3–4 atm. A single metering pump may feed up to 12 mixing heads. In another modification called **liquid injection molding**, the entire shot for a mold is mixed in a chamber before injection so that it resembles transfer molding [29].

The RIM process has been used to make **rigid structural foams** with densities of about 0.5 g/cm³. These have been used as housings for electronic equipment and the rigid members of various pieces of furniture. A wide variety of densities and flexibilities can be made using the same basic system. Low-modulus elastomers have been used for bumpers. With two mixing machines and eight molds, a production rate can be maintained of 1400 6-kg bumpers per day. Each cycle involves a 3-s injection time and a 2-min demolding time [30]. The addition of milled glass or mineral fillers to RIM formulations has led to high-modulus materials that may find their use as automobile fenders.

14.8.2 CASTING

Molding with little or no pressure is practical if the melt viscosity is very low so that the polymer can be cast (poured) into a mold and allowed to set by reaction or cooling. Most polymers with molecular weights low enough to be pourable have poor physical strength. Paraffin wax is a good example of a kind of polyethylene with low enough melt viscosity to be poured into a mold. When a cotton string insert is included, such a casting operation produces a candle. Since mold casting of candles goes back at least to colonial times, it ranks as one of the more antique fabricating methods still in use. Casting a monomer in a mold to make a sheet of acrylic plastic was described in Section 5.2. Some other polymers that are cast are the epoxies and the silicones. A highly filled epoxy resin with good cured strength and abrasion resistance can be cast inexpensively to make a metal stamping die. One takes a pattern (same dimensions as final piece), places it in a box, and pours in the resin–hardener mixture (usually with a filler), which sets to a network polymer on heating (Figure 14.29). After a mold release compound is sprayed on the surface, another layer is poured and set. The two pourings are attached to opposite platens of a stamping press and form a matched mold for the forming of metal sheets. Compression and injection molds can be made in the same manner.

It is possible to produce three-dimensional prototype parts using **photopolymerization**. In one system [31], a ultraviolet laser light source is moved in two dimensions (x and y) over a pool of photosensitive pre-polymer in a programmed fashion, producing a thin film of cross-linked polymer on the surface wherever the light strikes. A fresh layer of pre-polymer is added and the next *slice* of the part is cross-linked selectively. By repeating this operation a number of times with increasing amounts of pre-polymer, and with careful control of the cross-linking in a thin

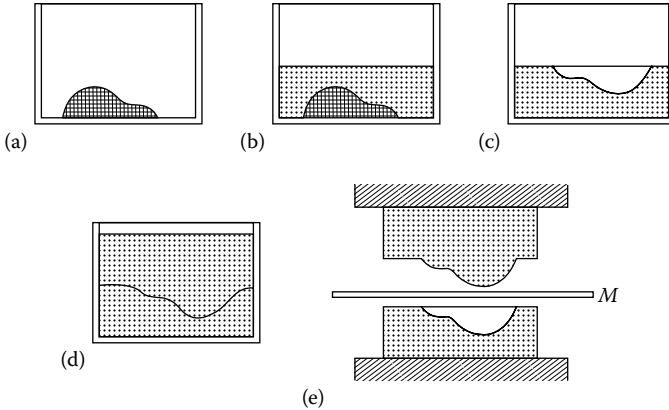


FIGURE 14.29 Making a stamping die from a filled epoxy resin: (a) pattern placed in box; (b) resin added and hardened to make lower half of die; (c) pattern removed and lower half of die inverted and coated with release agent; (d) resin added and hardened to make upper half of die; (e) two halves of die mounted in press to form metal sheet, *M*.

surface layer each time (by limiting the amount of transmitted light through the top layer), a final part can be made with a thickness (*z*-axis) of 10–20 cm. Pouring off the uncross-linked polymer leaves a part that can be quite complex. This **prototyping process** has been used in automotive, electronics, aerospace, medical, and consumer product companies.

Plastisols represent a special heat-convertible liquid category that is made possible by the unique properties of poly(vinyl chloride). The polymer is quite insoluble in a large class of high-boiling liquids including di-2-ethylhexylphthalate. It is possible to disperse finely divided polymer particles in this liquid and have a stable, free-flowing suspension (a plastisol) at a weight ratio of 3:5 or higher (liquid to polymer). The polymer particles preferably have been recovered from an emulsion polymerization to aid in the plastisol formation. Such polymers are sometimes called **plastisol, dispersion, paste, or stir-in resins**. When the plastisol is heated to about 175°C (the temperature varies with resin and plasticizer), the resin rapidly dissolves in the plasticizer. Only a small amount of plasticizer is volatilized at this temperature. On cooling, the solution of resin in plasticizer remains stable indefinitely. It will be recalled that the major effect of a plasticizer is to change the T_g of a system. Examples were given in Section 3.6. The utility of such a liquid, castable, heat-convertible system is obvious. Although other polymers have been proposed as plastisol resins, only polymers and copolymers of vinyl chloride seem to have the combination of low-temperature insolubility, high-temperature solubility, and high tensile strength when plasticized that is needed [32,33]. While hundreds of liquids are sold as plasticizers, esters of phthalic and adipic acid, along with epoxidized drying oils, chlorinated waxes, and esters of phosphoric acid, dominate the market. Primary consideration may be given to the final properties of the system such as T_g , modulus, strength, stability, and odor. However, the viscosity of the plastisol initially and on aging often becomes a controlling factor in plasticizer selection. The problems of physical and

chemical stability (plasticizer migration and thermal breakdown) are discussed in Chapter 12.

Some articles, such as fishing lures, washers, overshoes, and plastic gloves, are made by casting in open molds. **Slush molding** and **dipping** are two techniques with great resemblance to fluidized bed coating (Section 13.4). A preheated, hollow metal mold is filled with plastisol and then inverted. The hot wall solvates some resin so that on inversion of the mold the core flows out but the skin remains. Further heating completes the fusion process. Some cooling is necessary before the boot can be stripped from the mold. The mold might be split to facilitate removal of the molded object, which now bears on its outer side the pattern from the inner side of the metal mold. Squeezable dolls or parts of dolls are most often made by slush molding.

Wire dish drainers, coat hangers, and other industrial and household metal items can be coated with a thick layer of flexible vinyl plastic by the simple process of dipping and fusion. A more elaborate artifact is a plastic glove, which could be produced either by dipping a hand-shaped mandrel or by slush molding in a hollow mold for the same shape. Several variations of plastisols have been developed to alter the properties of the liquid as well as the final solid.

The viscosity of the plastisol increases as the ratio of resin to plasticizer increases. Where a thin coating of rigid product is required and the plasticizer content is so low that the plastisol will not flow easily, a nonsolvating diluent can be added. The process of solidification is more complex now, since the diluent (usually an aliphatic or naphthenic liquid in the mineral spirits range) must evaporate before the fusion is attempted. **Organosols**, as these diluted plastisols are termed, are used to advantage in dipping processes as well as in impregnating cloth or rope with vinyl polymer. There are some applications where it is desirable to have an infinite viscosity at low shear stresses. **Plastigels** are made by adding a metallic soap or finely divided filler as a gelling agent to the resin-plasticizer suspension. Aluminum stearate is an effective gelling agent, especially if a petroleum oil is being used as a secondary (extending) plasticizer. The suspension of resin in gelled plasticizer can be cold-molded, placed on a pan, and heated to fusion without discernible flow. The whole operation resembles baking cookies, with molding and baking being done in two separate steps.

Rotational molding can be used with plastisols, but it can also be used with finely divided powders of polyethylene and other polymers [3]. In this case the hollow, split mold is charged only with enough material to make the final object. The mold is closed and heated while being rotated in an eccentric manner so that all surfaces on the inside of the mold become coated with a fused material. Cooling, opening the mold, and removing the hollow object go rather rapidly, since heat transfer is to a thin skin through a metal wall. Large containers, suitcases, and display novelties are inexpensively produced from a lightweight mold that undergoes no great stress during the process [3].

14.8.3 BLOW MOLDING AND SHEET MOLDING

The need for a rapid production of bottles with uniform thickness for soft drinks, milk, and myriad household products is best met by **blow molding**. A tube of molten polymer, the **parison**, is sealed at both ends and held in place, whereas two halves

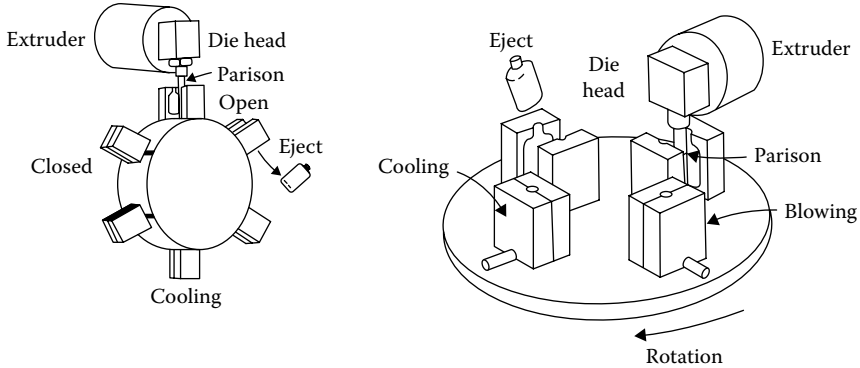


FIGURE 14.30 Vertical wheel type of continuous extrusion blow molding machine; molds are carried to the die head by rotation of the wheel. In a horizontal table type, all steps of the process are carried out simultaneously also. (Data from Morgan, B. T. et al., *Mod. Plast.*, 45, 797, September 1967.)

of a hollow mold surround it. Air is injected into the parison, which blows up as if it were a rubber balloon. When the polymer surface meets the cold metal wall of the mold, it is cooled rapidly below T_g or T_m . Once the product is dimensionally stable, the mold is opened, the bottle is ejected, a new parison is introduced, the mold is closed, and so on. The parison can be produced continuously from a screw extruder and converted to a bottle on a rotating platform (Figure 14.30). In the ram extrusion method, the parison is formed in a cyclic manner by a plunger forcing a charge out from an accumulated molten mass as in the pre-plasticizer injection-molding machine (Figure 14.31). In the production of large bottles, efficiency demands a rather uniform wall thickness and no dangerous thin spots. Inherently, the weight of the bottom of a parison that is suspended vertically from a machine will cause the wall to be thinner toward the top. Unless corrected, a long parison may give a bottle with a wall thickness near the bottom twice that near the top.

One way to correct the situation is to **program** the position of a mandrel around which the parison is being extruded so that the die opening increases during a shot (Figure 14.32). The parison now has a thicker wall toward the top, which will be evened out as it hangs waiting a second or two to be molded. Cycles are fast. Small plastic vials can be molded 10 vials at a time from one machine with multiple cavities using a cycle time of 10 s. For many food-packaging applications, multilayered parisons are coextruded in order to produce multilayered bottles. As many as seven layers may be sandwiched together to get the proper combination of appearance, strength, and barrier properties for foods such as ketchup or salad dressings. Even fuel tanks for automobiles are blow-molded from high-density polyethylene. The inner layer of the tank may be treated with SO_3 in order to enhance barrier properties. In **stretch blow molding**, biaxial orientation in the bottle is increased by longitudinal stretching during radial blowing. This is accomplished by an internal rod (Figure 14.33). Better clarity, increased impact strength, and improved barrier properties (water and gas diffusion) are claimed. Beverage bottles made from poly(ethylene terephthalate) have used the technique.

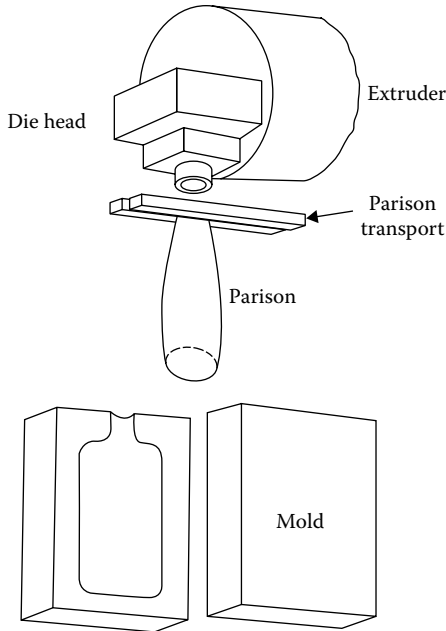


FIGURE 14.31 In this continuous extrusion blow molding system, a parison transfer device is used to lower the extruded parison from the die head into the waiting mold. The transport arm cuts and holds the parison during the transfer operation. (Data from Morgan, B. T. et al., *Mod. Plast.*, 45, 797, September 1967.)

Large moldings of glass fiber-reinforced polyester often are made using low pressures. A number of variations exist. A typical resin formulation might contain 30%–40% styrene monomer, with the balance being an unsaturated polyester (based on maleic anhydride, for example). The glass reinforcement can be in chopped strands, mats of strands, woven cloth, or continuous filaments.

For the production of a boat hull or an automobile body, layers of glass cloth or mat can be placed on a form and then impregnated by pouring *activated* resin from a pail. The activation usually consists of a peroxide initiator with an accelerator such as cobalt naphthenate. The resin is spread out with rollers and polymerization takes place after an induction period (*pot life*) of an hour or so at room temperature. If production volume justifies the added cost, a matched metal compression mold can be used to give a denser, stronger finished product. The hand layup may still be used. A more uniform product is obtained if the glass fibers are sprayed onto the form or if resin and glass are sprayed on simultaneously.

Another means of enhancing uniformity is to combine glass and resin beforehand. **Sheet molding compound (SMC)** is one approach [37]. When the liquid polyester (actually polyester and styrene) is thickened by less than 1% of calcium or magnesium oxide, the gel has a yield stress and can be handled without dripping. SMC is made by combining thickened polyester, fillers, peroxides, and chopped glass fiber between layers of polyethylene. The mat can be produced continuously

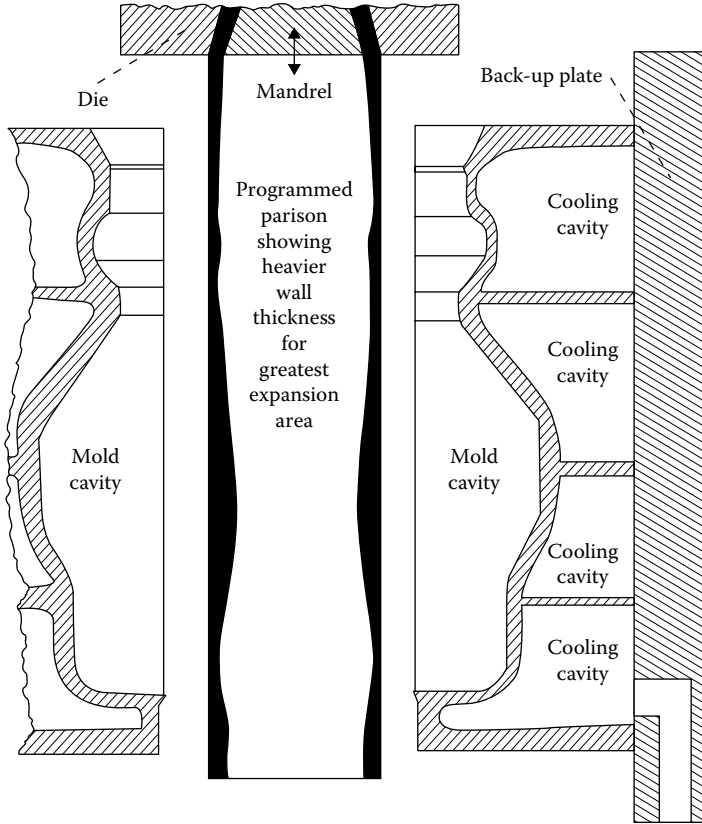


FIGURE 14.32 A programmed parison designed to fit a particular mold configuration. (Data from Polyethylene Blow Molding, U.S.I. Chemicals, New York, 1970.)

and uniformly. Molding requires stripping off the polyethylene film. The amount of SMC can be tailored to the requirements of the piece being molded. It is usually molded under some pressure and with heating.

Bulk molding compound is a puttylike mixture of polyester and chopped fiber glass strands [38]. Fillers such as calcium carbonate are the factor that changes the liquid polyester to a putty that can be applied with a trowel.

14.9 FOAMS

Foamed polymeric materials have several inherent features that combine to make them economically important. Any foamed material is a good heat insulator by virtue of the low conductivity of the gas, usually air, contained in the system. In a rigid foam, the gas contained in the cells may not be exchanged with air for a long time. The thermal conductivities of some common gases in $W/m \cdot ^\circ C$ at $27^\circ C$ are as follows: air, 0.0262; *n*-pentane, 0.0144; nitrogen, 0.024; and carbon dioxide, 0.0146. Despite the low conductivity of many chlorofluorocarbons at around $0.012 W/m \cdot ^\circ C$,

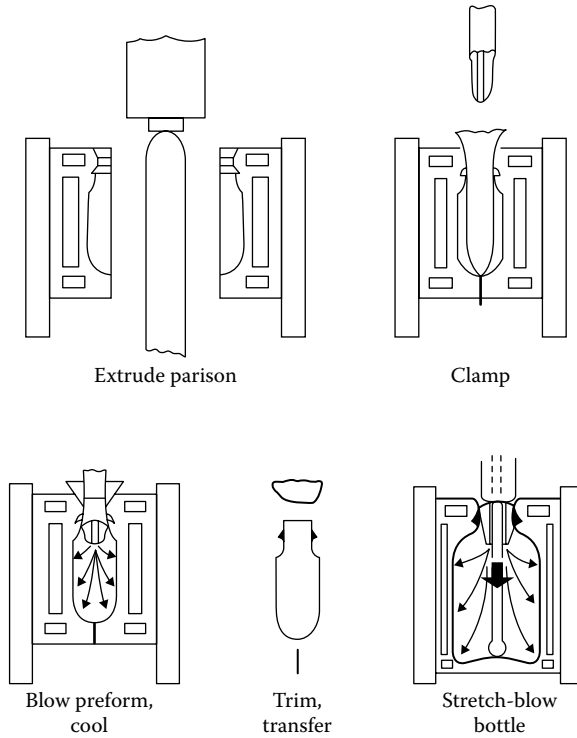


FIGURE 14.33 Stretch-blow molding. (Data from *Mod. Plast.*, 53, 36, February 1976.)

they have been banned because of their ozone depletion and global warming potentials. As an alternative, hydrocarbons and inert gases are being used. Because of their inertness, low thermal conductivity, and high solubility in polymers compared to N_2 , extensive efforts were made over the past decade to use high-pressure CO_2 as the foaming agent of choice in the foaming process of many thermoplastics [39].

A glassy polymer, when foamed, will have a much higher ratio of flexural modulus to density than when unfoamed. A beam of foam deflects less than an unfoamed beam of the same length, width, and weight under the same load. Finally, any foam will have energy-storing or energy-dissipating capacity operating through a greater distance than the unfoamed material. The resilient foam made when the polymer is rubbery can store most of the energy reversibly and makes a good cushion for upholstery and packaging applications. A compressible foam that breaks down on impact can absorb a great deal of energy and is widely used for packaging. The mere bulk of highly foamed polymers, along with good machinability, makes them economical for some decorative purposes where massiveness without great weight is demanded. One example is foamed polystyrene used as an artistic medium. A block of foam can be sculptured much as the artist might use clay for three-dimensional figures.

Foams can be classified according to several schemes. The structure of the cells is one scheme. Each cell may be completely enclosed by a membrane, or it may

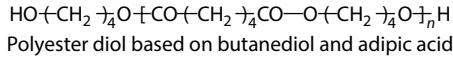
be interconnected with its neighbors. **Closed-cell foams** typically are produced in processes where some pressure is maintained during the cell formation process. **Open-cell foams** often are made during a free expansion. Most processes produce both kinds. In some applications there is an advantage to converting all cells to the open variety. A closed cell tends to store energy reversibly, as if it were a small rubber balloon. In cushioning applications, it is desirable to have compression cause the flow of air from cell to cell as if they were a series of orifices. This dissipates energy that is not entirely regained on unloading. An open-cell foam acts as a sponge, soaking up liquid by capillary action. A closed-cell foam makes a better buoy or life jacket because the cells do not fill with liquid.

Foams differ in the process conditions under which they are generated. A material that requires a high temperature or an external pressure for foam formation cannot be easily foamed in place, as could a system that can be mixed and poured at room temperature. And, of course, the polymer from which the foam is derived can be a thermoplastic or a thermoset, rubbery, or glassy.

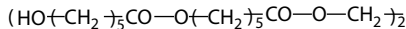
14.9.1 POLYURETHANE FOAMS

Foamed polyurethanes, rubber, and poly(vinyl chloride) dominate the upholstery market, so it is convenient to consider the rather different processes that are used for each. The earlier consideration of polyurethane foams (Section 4.7) showed only diisocyanate, water, and polyhydroxy compound as the ingredients. An actual foam formulation is more complex. A combination of a diol and a triol is used to give a partially cross-linked structure in the final form. The diisocyanate is a mixture of two isomers that differ slightly in reaction rate. The mixture is less expensive than either pure compound. The isocyanate group reacts slowly with the secondary hydroxyl groups that these polymers have on one end. A tin compound catalyzes the reaction, especially in the presence of a small amount of tertiary amine. A silicone surfactant is an essential ingredient that regulates the cell size, uniformity, and nature to a large extent, controlling the viscosity and surface tension of the cell membranes as they are stretched during foaming. A **blowing agent** that consists of a low-boiling liquid (such as pentane with boiling point of 36.1°C) that volatilizes when the urethane reaction starts or an expandable compressed gas is used to create the foam cells. The blowing agent increases the total volume without itself participating in the chemical reactions that are occurring.

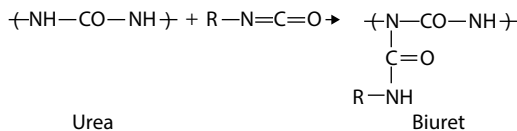
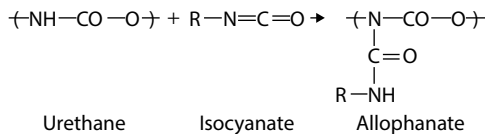
The urethane foam is a typical polymer system in that the number of variables that can significantly affect the important properties is very large. The optimization of the relative quantities of only the specific ingredients is in itself a time-consuming, expensive exercise, even with the aid of a computer and multiple regression analysis. We must add to that problem the possibilities of varying each ingredient chemically. The polyol can vary in functionality, with as many as five or six hydroxyls per molecule. Although polyols based on propylene oxide dominate the field, other polyethers are used based on tetrahydrofuran, ethylene oxide, or styrene oxide. Polyesters are widely used in rigid foams and, to a certain extent, in flexible foams. Such polyesters may be made with an excess of diol or by growth of a hydroxy acid on a diol.



Polyester diol based on butanediol and adipic acid

Polyester diol based on caprolactone *grown* on ethylene glycol

The diisocyanate most often used in foams is the toluene derivative, but the ratio of isomers can be changed. The remaining ingredients present similar opportunities for exploration. Even a single company may offer a line of a half-dozen to a dozen surfactants, catalysts, blowing agents, or auxiliary materials. Water is not an essential ingredient. Some urethane foams are made with only the blowing agent. Another parameter that affects foam properties is the manner in which mixing takes place and the timescale of the process. All these things not only can change the physical appearance of the foam, cell size, size distribution, openness, and strength but also can encourage or diminish subsidiary chemical reactions depending on the concentration of reactants, the temperature, and the viscosity of the system. Such reactions affect the extent of cross-links and make a definite contribution to modulus and permanent set. One of the largest markets for flexible urethane foams is in upholstery. The foam can be made in continuous loaves several feet in width and height and then sliced into slabs of the required thickness for pillows and mattresses.



14.9.2 RUBBER AND POLY(VINYL CHLORIDE) FOAMS

Although foamed rubber has many of the same properties as foamed urethanes, the foaming and the cross-linking of the polymer are accomplished in a radically different manner. To natural rubber latex is added a solution of a soap that yields a froth on beating. In addition, antioxidants, cross-linking agents, and a foam stabilizer are added as aqueous dispersions. Foaming can be done with an eggbeater type of wire whip, but most processes today use automatic mixing and foaming machines that combine agitation and aeration. The foam would collapse rapidly if it were not for the stabilizer, which usually is sodium silicofluoride (Na_2SiF_6). The hydrolysis of this salt yields a silica gel that increases the viscosity of (gels) the aqueous phase and prevents the foam from collapsing. The cross-linking agent has to act at 100°C or lower in order to react before the water is removed from the foam. Cross-linking (curing or vulcanization) takes place in 30 min at 100°C . In a large article such as a mattress, a metal mold is filled with the foam during the few minutes between the time foaming

TABLE 14.2
Foamed Rubber Formulation

Ingredient	Parts by Weight
Styrene-butadiene latex (65% solids)	123
Potassium oleate	0.75
Natural rubber latex (60% solids)	33
Sulfur	2.25
Accelerators	
Zinc diethyl dithiocarbamate	0.75
Zinc salt of mercaptobenzothiazole	1.0
Reaction product of ethyl chloride, formaldehyde, and ammonia (Trimene Base)	0.8
Antioxidant (phenolic)	0.75
Zinc oxide	3.0
Na_2SIF_6	2.5

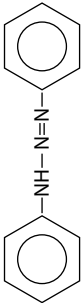
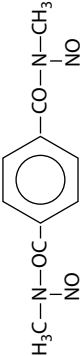
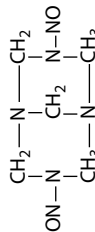
Source: Stern, H. J., *Rubber: Natural and Synthetic*, Palmerton, New York, 450, 1967.

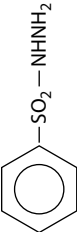
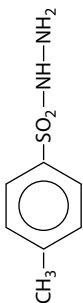
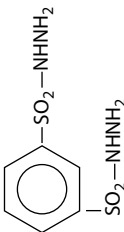
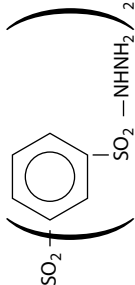
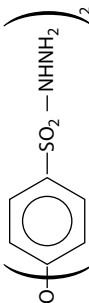
is complete and the silica gel has formed. The entire mold is then heated by steam at atmospheric pressure. After being removed from the mold, the foam may be dewatered by compression between rolls or centrifuging followed by drying with hot air in a tunnel dryer. Part of the natural latex can be replaced by a synthetic rubber such as the latex from emulsion copolymerization of styrene and butadiene. The overall composition of such a combination listed in Table 14.2 illustrates again the complexity of simple *model* systems in the real world.

Although poly(vinyl chloride) foams cannot be made as inexpensively as those from rubber or urethanes, their mechanical properties can sometimes be of value.

Most vinyl foams are stronger, torn less easily than rubber or urethane foams of comparable density, and less flammable. Two processes for making foamed poly(vinyl chloride) use plastisols (see Section 14.8). The first is a very generally applicable method that can be used whenever a system can be mixed at a lower temperature than the decomposition temperature of a **blowing agent**. Three important characteristics of a blowing agent are the decomposition temperature, the volume of gas generated per unit weight, and the nature of the decomposed residue. Several examples (Table 14.3) are especially recommended for vinyl plastisols [41]; in each case, the gas generated is nitrogen. Carbon dioxide can be generated by heating some inorganic carbonates. To produce uniform cells, the blowing agent must be uniformly dispersed or dissolved, uniformly nucleated, and rapidly, smoothly decomposed over a narrow temperature range, which is matched to the attainment of a high viscosity or gelation of the polymer system. In plastisols, gelation involves the solvation of resin in plasticizer at 150°C–200°C, depending on the particular ingredients employed. If gelation occurs before gas release, large fissures or holes may form. Cells formed too soon before gelation may collapse and give a coarse,

TABLE 14.3
Commercial Foaming (Blowing) Agents

Chemical Description	Structure	Decomposition Temperature in Air (°C)	Decomposition Range in Plastics (°C)	Gas Yield (ml [STP]/g)	Literature Reference
A. Azo compounds Azobisformamide (Azodicarbonamide)	$\text{H}_2\text{N}-\text{CO}-\text{N}=\text{N}-\text{CO}-\text{NH}_2$	195–200	160–200	220	BIOS Final Report 1150, 23 German Patent 871,835
Azobisisobutyronitrile	$\begin{array}{c} \text{CH}_3 \\ \\ \text{NC}-\text{C}-\text{N}=\text{N}-\text{C}-\text{CN} \\ \quad \\ \text{CH}_3 \quad \text{CH}_3 \end{array}$	115	90–115	130	German Plastics Practice, DeBell-Richardson p. 456 (1946) German Patent 899, 414
Diazoaminobenzene		103	95–100	115	US Patent 2,299,593
B. <i>N</i> -Nitrosocompounds <i>N</i> , <i>N'</i> -dimethyl- <i>N</i> , <i>N'</i> -dinitrosoterephthalamide		105	90–105	126 ^a	US Patent 2,754,326
<i>N</i> , <i>N'</i> -Dinitrosopentamethylenetetramine		195	130–190	265 ^b	US Patent 2,491,709

C. Sulfonyl hydrazides						
Benzenesulfonyl hydrazide		>95	95-100	130	} German Patent 821,423; US Patent 2,626,933	
Toluene-(4)-sulfonyl hydrazide		103	100-106	120		
Benzene-1,3-disulfonyl hydrazide		146	115-130	85 ^c		
Diphenylsulfon-3,3'-disulfonyl hydrazide		148	120-130	110	Same as above	
4,4'-Oxybis (benzenesulfonyl hydrazide)		150	120-140	125	Same as above; US Patent 2,552,065	

Source: Lasman, H. R.: *Mod. Plast.* 45(1A, En cycl. Issue):368 (September 1967).

^a 70% active.

^b 100% active.

^c 50% active.

weak, spongy material. Closed cells result when the decomposition and gelation are carried out in a closed mold almost filled with plastisol. After the heating cycle, the article is cooled in the mold still under pressure until it is dimensionally stable (about 50°C). It expands slightly on removal from the mold because of the compressed gas it now contains. Final expansion is accomplished by heating the free article somewhat below the previous molding temperature. Buoys, life jackets, floats, and protective padding are some items made by this process.

The same blowing agents can be used in making foamed rubber. The step corresponding to fusion of plastisols is the cross-linking reaction to give a stable network (vulcanization). Some thermoplastics such as polyethylene and cellulose derivatives can also be foamed by blowing agents even though they do not undergo an increase in dimensional stability at an elevated temperature. As long as the polymer melt is viscous enough to slow down the collapse of the cells and the system is cooled below its T_m or T_g , a reasonably uniform cell structure can be built in. When the plastisol containing a blowing agent is spread on a substrate and fused without a second confining surface, the cell structure is usually open. Fabrics with a bonded layer of insulation are made this way. Extrusion can also be used with a variety of thermoplastic and rubber compounds. Foamed gaskets and weather stripping are made by decomposing the agent in the barrel of the extruder and allowing the extrudate to expand freely. The product is predominantly open-celled.

14.9.3 RIGID FOAMS

Increasing the degree of cross-linking will make any flexible foam more rigid. Of the three flexible foams described above, only the urethanes are important in the commercial applications of rigid foams. Rigid foams result when the polyol is short chained and highly functional so that the distance between cross-links is small or when the polyol backbone contains bulky groups that raise the glass transition temperature. Fillers such as fibers or finely divided silica can be used to stiffen a foam, but they are seldom used because they increase the density of the system. Polyisocyanates of high functionality can be employed to increase the cross-link density. Some of these are condensation products of the commonly used toluene diisocyanate.

Rigid urethane foam can be foamed in place. One of the early commercial applications (1940s) was the filling of certain aircraft components with rigid foam. The advantages of the urethane foam are that it can be foamed in place, say in the rudder or aileron; adheres well to metal surfaces (as a rule); adds little weight; and greatly reduces the flexing of the element on stressing. Hollow walls in chambers such as boxcars can be filled with foam to provide strength and good thermal insulation. Some other products are crash pads for automobiles and packaging. Weather stripping is made from a thin tape of foam about 6×3 mm that is attached to a door frame by means of paper tape that has adhesive on both surfaces. Completely open-cell foams can be produced directly in the foaming process or by chemical or mechanical treatment of a previously formed material. These **reticulated foams** are widely used as air filters.

Another way to achieve rigidity is to use a polymer that is below T_g at normal use temperatures. The various forms of polystyrene foams illustrate techniques that can be applied to other thermoplastic polymers. A solution of polystyrene in methyl chloride can be heated well above the normal boiling point as long as the system is kept under pressure as in the barrel of an extruder [42]. Upon issuing from the extruder, the solvent evaporates, simultaneously foaming the plastic and cooling it below the T_g . Foaming and dimensional stabilization thus are carried out in one step. Rather extensive facilities are required to mix and convey the concentrated solution and to extrude the foamed logs. Because it is uneconomical to ship low-density foams a great distance, a modification of the solution process has been introduced [43]. Pellets chopped from an ordinary melt extruder or beads from a suspension polymerization are impregnated with a hydrocarbon such as pentane. As long as the beads or pellets are stored below 20°C, the vapor pressure of the pentane dissolved in the polymer is low enough that pressures of less than 1 atm build up in a closed container. Even so, manufacturers do not recommend storing the impregnated material more than a few months. The pellets may be used in an extrusion process to give logs or thin sheets. Usually a nucleating agent is added, such as citric acid or sodium bicarbonate [44], to control the cell size. This process has been especially successful in producing thin sheet that can subsequently be formed into containers. Tubular blow extrusion is used (Figure 14.34). Egg cartons and cold drink cups can be made by the thermoforming techniques mentioned in Section 14.10 starting with foamed sheet.

The beads often are molded in a two-step process. Prefoaming almost to the density that will be required in the final object is similar to corn popping. Steam heat is used in an agitated drum (Figure 14.35) with a residence time of a few minutes. The expanded beads can be stored for as long as a few weeks before final molding. In a typical mold (Figure 14.36), prefoamed beads are loaded into the mold cavity. After the mold is closed, steam is injected. The prefoamed beads expand further and fuse

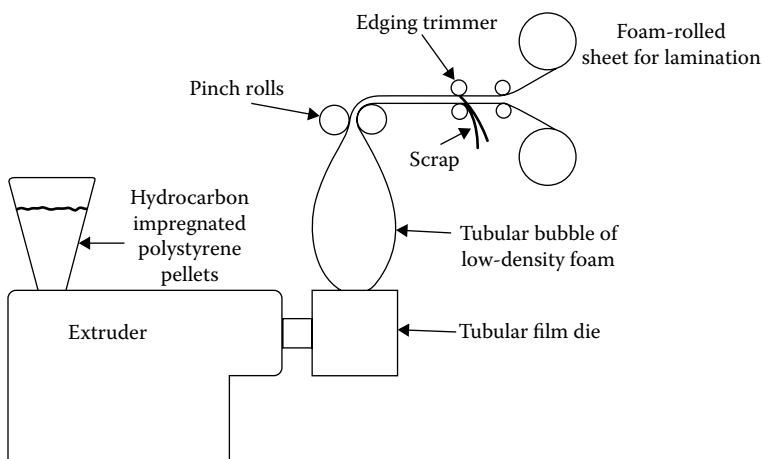


FIGURE 14.34 Production of low-density polystyrene foam sheet from tubular film die. (Data from Collins, F. H., *SPE J.*, 16, 705, July 1960.)

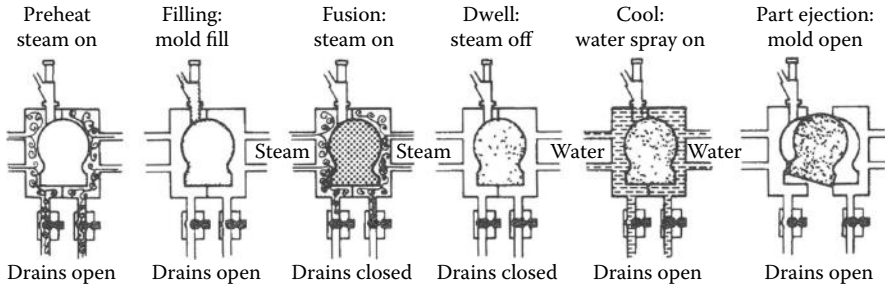


FIGURE 14.35 Molding polystyrene beads. (Reproduced by permission from PELASPAN Expandable Polystyrene, Form 171-414, Dow Chemical Co., 1966. Copyright 1966 Dow Chemical Co.)

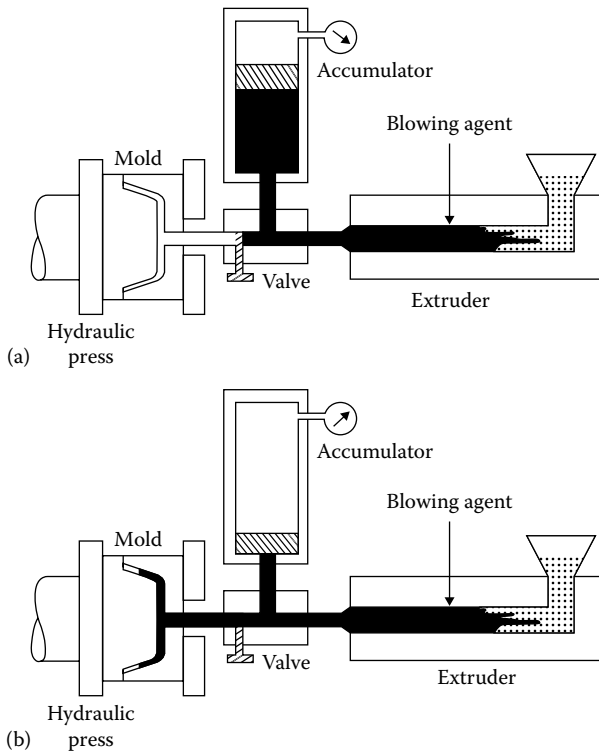


FIGURE 14.36 Structural foam process. (a) Filling the accumulator. The blowing agent—usually nitrogen—is injected into the melt in the extruder. The melt is passed into the accumulator, where it is maintained at a pressure and temperature high enough to prevent foaming until the predetermined charge is collected. (b) Filling the mold. The accumulator ram then injects the charge into the mold, where the reduced pressure allows the gas to foam the resin and drive it throughout the mold.

together as the temperature exceeds T_g . The article must be cooled in the mold to a temperature below T_g before removal. Packages shaped to fit their contents, picnic coolers, drinking cups, toys, and small sailboats are common consumer items fabricated from beads. The thin-walled cups demand a small bead for easy flow into the molding cavity.

Foams of phenol formaldehyde resins can be made from a dispersion of a volatile diluent (isopropyl ether dispersed with the aid of a surfactant) in an aqueous solution of an incomplete phenol–formaldehyde reaction product [46]. Addition of an acid catalyst such as hydrochloric or sulfuric acid causes further condensation of phenol and formaldehyde to give a dimensionally stable, network structure. At the same time the heat of reaction volatilizes the diluent, yielding a foam. The foaming can be done in place. Phenolic foams are used as heat-stable, flame-retardant, thermal insulation.

Another way to make a foam is to embed hollow spheres of glass or phenolic resin in another polymer. Usually the spheres are mixed with low-viscosity liquids that can be converted to solids. The spheres are not easily dispersed without breaking when extremely viscous rubbers and melts are used.

The **structural foam process** gets its name from the application for its product rather than the mechanics of the process itself [47]. In a manner directly opposite to the vented extruder (Figure 14.2), a blowing agent, nitrogen or carbon dioxide, is injected into the melt in the extruder (Figure 14.36). Polymer melt that has already been injected with gas goes to the accumulator. When a sufficient charge has accumulated, it is transferred into the mold. The melt foams and fills the mold at a relatively low pressure (200–400 psi, i.e., 1.3–2.6 MPa) compared to the much higher pressure in the accumulator. The lower pressures in the molds make the molds cheaper than those used for conventional injection molding. However, the cycle times are longer because the foam, being a good insulator, takes longer to cool. A major market for structural foams is in furniture. ABS and high-impact polystyrene are used to replace wood in seat panels, legs, chairs, and even some exterior panels for pianos. A wide variety of thermoplastics can be used. The trade-offs in deflection versus strength are illustrated in Table 14.4. Structural foams can also be made using a chemical blowing agent like those listed in Table 14.3 rather than an inert gas. A change in pressure or temperature on entering the mold triggers gas formation.

14.10 SHEET FORMING

Often it is more economical to fabricate an article from a previously formed sheet than to start from raw pellets or slabs. In the case of thermoplastic materials, the sheet is heated to a temperature at which it will deform under stress but not flow easily. This corresponds to the rubbery plateau region above T_g (and above T_m for a predominantly crystalline material). In this state the sheet readily deforms elastically. However, if the sheet is cooled below T_g (or T_m) in the deformed condition, it will remain there permanently. The process has many variations, as seen in Figure 14.37. In each case the sheet is first heated to a rubbery condition while firmly held in a frame. With thin sheets a few seconds of exposure to a radiant heating panel may

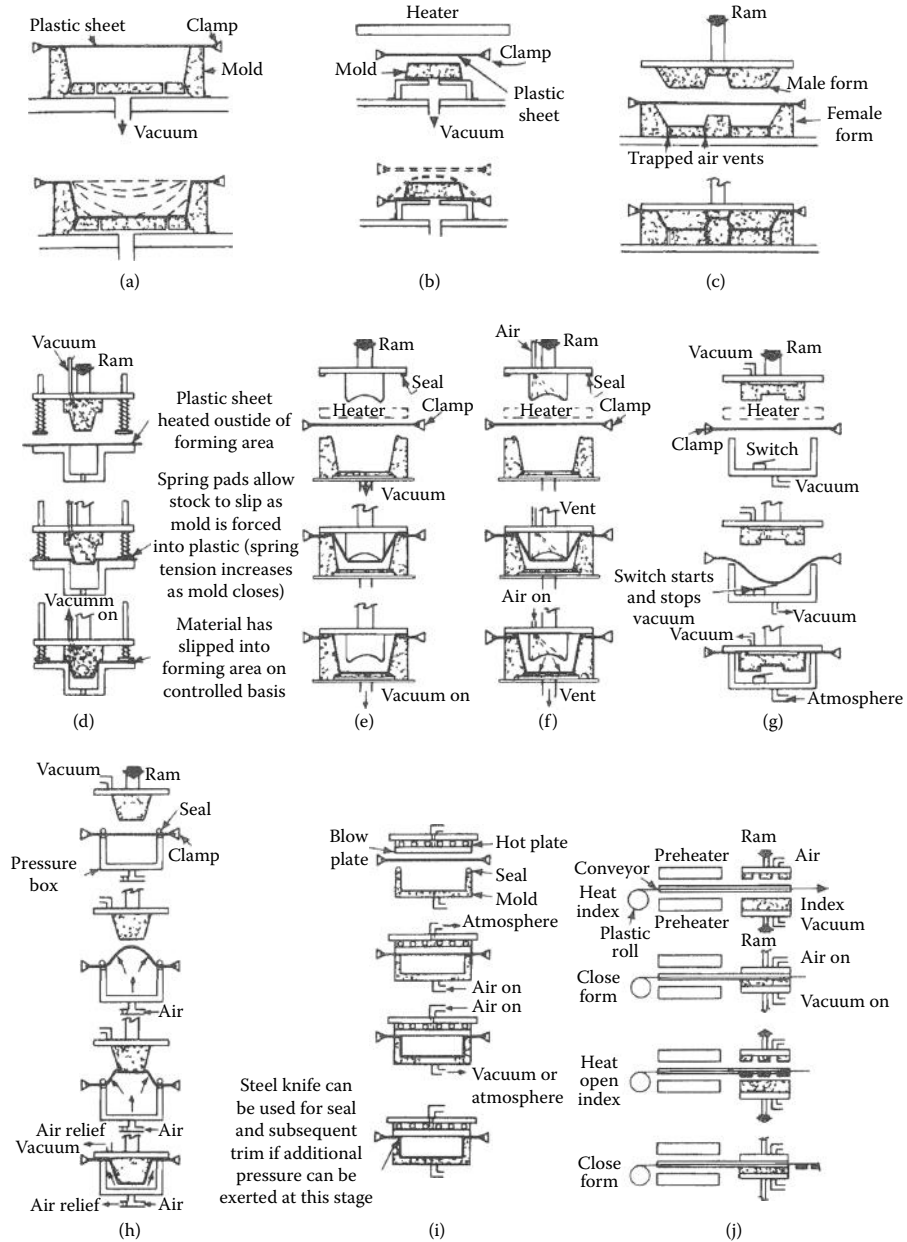


FIGURE 14.37 Ten methods of thermoforming: (a) straight vacuum; (b) drape; (c) match-mold; (d) slip-ring; (e) plug-assist, vacuum; (f) plug-assist, pressure; (g) snap-back, vacuum; (h) pillow; (i) trapped-sheet, contact-heat, pressure; (j) preheat, plug-assist, pressure forming. (Data from Zelnick, D., *Plast. Des. Proces.*, 8, 12, May 1968.)

TABLE 14.4
Typical Properties of Three Plastics for Structural Foam

Property	General-Purpose Polypropylene		High-Density Polyethylene		High-Impact Polystyrene	
	Solid	Foam	Solid	Foam	Solid	Foam
Sample thickness (cm)	0.38	0.635	0.38	0.635	0.44	0.635
Sample density (g/cm ³)	0.902	0.6	0.962	0.6	1.04	0.7
Flexural strength (MPa)	45	22	34	19	50	31
Flexural modulus (GPa)	1.30	0.83	1.10	0.83	1.86	1.45
Deflection of simple beam with 10-ctn span loaded with 2.3 kg·cm	0.36	0.23	0.50	0.32	0.20	0.11
Tensile strength (MPa)	33	14	28	9.0	24	12
Coefficient of linear expansion (cm/cm·°C × 10 ⁴)	9.4	9.4	12.1	12.1	9.0	9.0
Heat distortion temperature at 1.8 MPa load (°C)	56	55	45	34	76	80
Mold shrinkage (%)	0.018	0.015	0.020	0.018	0.010	0.008
Skin thickness (cm)	0.38	0.080	0.38	0.080	0.44	0.080

suffice. Vacuum forming can be used for making something like a contour map. The heated sheet is held above a plaster mold and sealed around the edges by a gasket. When a vacuum is applied through small holes in the mold, the sheet conforms to the mold and quickly cools to a temperature below T_g , since the mold surface, even of a poor conductor, has a heat capacity much greater than that of the thin sheet of plastic. The other methods illustrated use various combinations of pressure and vacuum as well as plugs and pads.

If the sheet has been subjected to biaxial orientation during extrusion (see Section 14.2), heating above the deformation temperature will cause the sheet to shrink. A tight package can be made by wrapping an article in a biaxially oriented sheet followed by a brief heat treatment. Such **shrink packaging** with polypropylene film is widely used for everything from lettuce and meats to books and video tapes.

Postforming of thermoset sheets resembles metal forming. As opposed to the various sheet-forming methods, the dies are rugged, the stresses are high, and the temperature often is fairly high. Because thermoset materials already possess a dimensionally stable structure, it is necessary actually to break some covalent bonds and to form some new ones during postforming. The curvature is limited, since a sharp bend may crack the sheet. Paper laminates are sometimes shaped by this method. Some common examples are trays, tote boxes, and countertops.

Some thermoplastic sheets can be cold formed. It is possible to form sheets of some ABS polymers into dishes, louvers, and housings by application of sufficient pressure.

KEYWORDS

Extrusion
Compression ratio
Twin-screw extruders
Film
Sheet
Biaxial orientation
Blown-film extrusion
Frost line
Coextrusion
Continuous vulcanization
Pultrusion
Calender
Spinning
Spinneret
Fiber
Melt spinning
Dry spinning
Wet spinning
Crimp
Laminate
Sandwich construction
Compression mold
Flash mold
Positive-pressure mold
Transfer molding
Injection (screw) molding
Filling stage
Packing stage
Cooling stage
Short shot
Weld line
Fountain flow
Reaction injection molding
Liquid injection molding
Casting
Plastisol
Slush molding
Dip molding
Rotational molding
Blow molding
Parison
Stretch blow molding
Foam
Expanded plastic

Closed-cell foam
Open-cell foam
Blowing agent
Expanded-bead foam
Structural foam
Sheet forming
Vacuum forming

PROBLEMS

- 14.1** A method for making rubber *thread* is to extrude and continuously vulcanize a flat sheet of rubber. The flat sheet is cut into individual strands with a rectangular cross section. For a sheet 0.030 in thick, strands are cut 0.060 in wide. Calculate the denier and the strength in grams per denier if the rubber compound has a density of 0.85 g/cm^3 and a tensile strength of 3500 psi.
- 14.2** What are the similarities between transfer and injection molding? What are the differences? Injection molding has been used for rubber and thermosets. What major problems must be overcome? What relationship between flow temperature and cross-linking or polymerization temperature is desirable?
- 14.3** A candlemaker has decided to automate production of small wax candles by using a continuous extrusion-coating process such as that used to insulate wire. Cotton string will be used instead of wire, and the extrudate will be chopped into candles 6 in long and 1/2 in in diameter. What problems might she expect? How might they be overcome? Should she hire a butcher and a baker as consultants? What experience have they had with extrusion?
- 14.4** Obtain a plastic bottle (an old bleach, shampoo, or beverage bottle will do). Using a razor blade, cut two cross sections through the length of the bottle at right angles to each other (one down the front, one down the side). Observe and explain any variation in thickness.
- 14.5** Obtain a foamed polystyrene article made from expanded beads. Consider an industrial packaging or a picnic hot-drink cup. From the weight and dimensions of a large piece, estimate the density. Break off some of the individual beads and estimate what the original bead diameter must have been before foaming.
- 14.6** How would you go about making rubber bands from vulcanized rubber?
- 14.7** Outline a suitable method of manufacture for (a) 100,000 ft of garden hose from plasticized poly(vinyl chloride); (b) 50,000 pocket combs from polystyrene; and (c) two boat hulls, each 15 ft long, from glass cloth and a solution of an unsaturated polyester in styrene monomer.

REFERENCES

1. U. S. I. Chemicals/Quantum: *Petrothene Polyolefins: A Processing Guide*, 5th edn., National Distillers and Chemical Corporation, New York, 1986.
2. Tadmor, Z., and C. G. Gogos: *Principles of Polymer Processing*, Wiley, New York, 1979, p. 487.

3. Ooswald, T. A.: *Polymer Processing Fundamentals*, Hanser-Gardner, Cincinnati, OH, 1998.
4. Van Ness, R. I., G. R. De Hoff, and R. M. Bonner: *Mod. Plast.*, 45(14A, Encycl. Issue):672 (October 1968).
5. Plastic Film Orienting, Bull. 1-6, Marshall and Williams, Providence, RI, 1967.
6. Schenkel, G.: *Plastics Extrusion Technology and Theory*, American Elsevier, New York, 1966, p. 323.
7. Garvey, B. S., Jr., M. H. Whitlock, and J. A. Freese, Jr.: *Ind. Eng. Chem.*, 34:1309 (1942).
8. Schenkel, G.: *Plastics Extrusion Technology and Theory*, Elsevier, New York, 1966, pp. 383–385.
9. Schrenk, W. J., and T. Alfrey, Jr.: *Polym. Eng. Sci.*, 9:393 (1969).
10. Mearl Iridescent Film, The Mearl Corporation, Peekskill, NY, 1976.
11. Stern, H. J.: *Rubber: Natural and Synthetic*, 2nd edn., Palmerton, New York, 1967, p. 388.
12. Ewald, G. W.: *Mod. Plast. Encycl.*, 56:379 (October 1979).
13. Sata, H., M. Murayama, and S. Shimamoto: *Macromol. Symp.*, 208:323 (2004).
14. Siemann, U.: *Progr. Colloid. Polym. Sci.*, 130:1 (2005).
15. Winspear, G. G. (ed.): *Vanderbilt Rubber Handbook*, R. T. Vanderbilt Co., New York, 1958, p. 392.
16. Riley, J. L.: chap. 18 in C. E. Schildknecht (ed.), *Polymer Processes*, Wiley, New York, 1956.
17. Fredericks, S. D.: “Melt Spinning of Polypropylene Fibers.” *Paper Presented at the Polypropylene Technology Conference*, Clemson University, Clemson, SC, September 1987.
18. Jiang, H., W. W. Adams, and R. K. Eby: chap. 13 in R. W. Cahn, P. Haasen, and E. J. Kramer (eds.), *Materials Science and Technology: Structure and Properties of Polymers*, VCH, New York, 1993.
19. MacLean, D. L., and T. E. Graham: *Chem. Eng.*, 87:54 (February 25, 1980).
20. Johnson, J. E.: *Mod. Plast. Encycl.*, 56:256 (October 1979).
21. Vaill, E. W.: *Mod. Plast.*, 40(1A, Encycl. Issue):767 (September 1962).
22. Tadmor, Z., and C. G. Gogos: *Principles of Polymer Processing*, Wiley, New York, 1979, p. 587.
23. Sanou, M., B. Chung, and C. Cohen: *Polym. Eng. Sci.*, 25:1008 (1985).
24. Hieber, C. A., and S. F. Shen: *J. Non-Newt. Fluid Mech.*, 7:1 (1980).
25. Hieber, C. A., L. S. Socha, S. F. Shen, K. K. Wang, and A. I. Isayev: *Polym. Eng. Sci.*, 23:20 (1983).
26. Coyle, D. J., J. J. Blake, and C. W. Macosko: *AIChE J.*, 33(7):1168 (1987).
27. Wang, K. K.: *Cornell Injection Molding Program, Progress Report 16*, Cornell University, Ithaca, NY, December 1991.
28. Liu, F., L. Deng, and H. Zhou: Residual stress and warpage simulations. in H. Zhou (ed.), *Computer Modeling for Injection Molding: Simulation, Optimization, and Control*, Wiley, New York, 2014.
29. Ooswald, T. A., E. Baur, S. Brinkmann, K. Oberbach, and E. Schmachtenberg: *International Plastics Handbook*, Hanser-Gardner, Cincinnati, OH, 2006.
30. Bonk, H. W.: *Mod. Plast. Encycl.*, 56:368 (October 1975).
31. Belforte, D. A.: *Laser Focus World*, 29(6):126 (1993).
32. Todd, W. D.: chap. 14 in C. E. Schildknecht (ed.): *Polymer Processes*, Wiley, New York, 1956.
33. Randolph, A. F. (ed.): *Plastics Engineering Handbook*, chap. 16, 3rd edn., Reinhold, New York, 1960.
34. Morgan, B. T., D. L. Peters, and N. R. Wilson: *Mod. Plast.*, 45(1A, Encycl. Issue):797 (September 1967).

35. Polyethylene Blow Molding, U.S.I. Chemicals, New York, 1970.
36. *Mod. Plast.*, 53:36 (February 1976).
37. Wood, A. S.: *Mod. Plast.*, 57:56 (January 1980).
38. Lichtenberg, D. W.: *Mod. Plast. Encycl.*, 56:147 (October 1979).
39. Eldib, I. A.: *Hydrocarbon Process. Petrol. Refiner*, 42(12):121 (December 19, 1963).
40. Stern, H. J.: *Rubber: Natural and Synthetic*, Palmerton, New York, 1967, p. 450.
41. Lasman, H. R.: *Mod. Plast.*, 45(1A, Encycl. Issue):368 (September 1967).
42. McIntire, O. R.: (Dow Chemical), U.S. Patent 2,515,250 (1950).
43. Collins, F. H.: *SPE J.*, 16:705 (July 1960).
44. Miles, D. C., and J. H. Briston: *Polymer Technology*, Chemical Publishing, New York, 1965, p. 187.
45. PELASPAN Expandable Polystyrene, Form 171-414, Dow Chemical Co., Midland, MI, 1966.
46. Randolph, A. F. (ed.): *Plastics Engineering Handbook*, chap. 12, 3rd edn., Reinhold, New York, 1960.
47. Cargile, H. M.: *Mod. Plast. Encycl.*, 56:296 (October 1979).
48. Zelnick, D.: *Plast. Des. Proces.*, 8(5):12 (May 1968).

GENERAL REFERENCES

Extrusion and Molding

- Belcher, S. L. (ed.): *Practical Extrusion Blow Molding*, Dekker, New York, 1999.
- Isayev, A. I. (ed.): *Injection and Compression Molding Fundamentals*, Dekker, New York, 1987.
- Isayev, A. I. (ed.): *Modeling of Polymer Processing*, Hanser-Gardner, Cincinnati, OH, 1991.
- Kennedy, P.: *Flow Analysis of Injection Molds*, Hanser Publishers, Munich, Germany, 1995.
- Kia, H. G. (ed.): *Sheet Molding Compounds*, Hanser-Gardner, Cincinnati, OH, 1993.
- Kircher, K.: *Chemical Reactions in Plastics Processing*, Macmillan, New York, 1987.
- Macosko, C.: *Fundamentals of Reaction Injection Molding*, Hanser (Oxford University Press), New York, 1988.
- Meyer, R. W.: *Handbook of Pultrusion Technology*, Chapman & Hall (Methuen), New York, 1985.
- Meyer, R. W.: *Handbook of Polyester Molding Compounds and Molding Technology*, Chapman & Hall (Methuen), New York, 1987.
- Michaeli, W.: *Plastics Processing: An Introduction*, Hanser-Gardner, Cincinnati, OH, 1995.
- Middleman, S.: *Fundamentals of Polymer Processing*, McGraw-Hill, New York, 1977.
- O'Brien, K. T. (ed.): *Applications of Computer Modeling for Extrusion and Other Continuous Polymer Processes*, Hanser-Gardner, Cincinnati, OH, 1992.
- Olabisi, O. (ed.): *Handbook of Thermoplastics*, Dekker, New York, 1998.
- Pearson, J. R. A.: *Mechanics of Polymer Processing*, Elsevier Applied Science, New York, 1985.
- Pearson, J. R. A., and S. M. Richardson (eds.): *Computational Analysis of Polymer Processing*, Elsevier Applied Science, New York, 1983.
- Pötsch, G., and W. Michaeli: *Injection Molding: An Introduction*, Hanser Publishers, Munich, Germany, 1995.
- Rauwendaal, C.: *Polymer Extrusion*, 3rd edn., Hanser-Gardner, Cincinnati, OH, 1995.
- Rees, H.: *Understanding Injection Molding Technology*, Hanser-Gardner, Cincinnati, OH, 1994.
- Rosato, D. V.: *Rosato's Plastics Encyclopedia and Dictionary*, Hanser-Gardner, Cincinnati, OH, 1993.
- Rosato, D. V., and D. V. Rosato (eds.): *Blow Molding Handbook*, Hanser-Gardner, Cincinnati, OH, 1989.

- Rosato, D. V., and D. V. Rosato: *Injection Molding Handbook*, 2nd edn., Chapman & Hall, New York, 1994.
- Shenoy, A. V., and D. R. Saini: *Thermoplastic Melt Rheology and Processing*, Dekker, New York, 1996.
- Starr, T. F. (ed.): *Databook of Thermoset Resins for Composites*, Elsevier, New York, 1993.
- Tadmor, Z., and C. G. Gogos: *Principles of Polymer Processing*, 2nd edn., Wiley, New York, 2006.
- Throne, J. L.: *Technology of Thermoforming*, Hanser Publishers, Munich, Germany, 1996.
- Tucker, C. L., III, and E. C. Bernhardt (eds.): *Fundamentals of Computer Modeling for Polymer Processing*, Hanser-Gardner, Cincinnati, OH, 1989.
- White, J. L.: *Twin-Screw Extrusion*, Hanser-Gardner, Cincinnati, OH, 1990.
- White, J. L.: *Rubber Processing*, Hanser-Gardner, Cincinnati, OH, 1995.
- Wright, R. E.: *Molded Thermosets: A Handbook for Plastics Engineers, Molders, and Designers*, Hanser-Gardner, Cincinnati, OH, 1991.
- Wright, R. E.: *Injection Transfer Molding of Thermosets*, Hanser-Gardner, Cincinnati, OH, 1995.
- Xanthos, M. (ed.): *Reactive Extrusion Principles and Practice*, Hanser-Gardner, Cincinnati, OH, 1992.
- Zhou, H. (ed.): *Computer Modeling for Injection Molding: Simulation, Optimization, and Control*, Wiley, New York, 2014.

Fibers

- Hongu, T., and G. O. Phillips: *New Fibers*, Prentice Hall, Englewood Cliffs, NJ, 1990.
- Lewin, M.: *Handbook of Fiber Chemistry*, 3rd edn., CRC Press, Boca Raton, FL, 2006.
- Lewin, M., and J. Preston (eds.): *Handbook of Fiber Science and Technology, High Technology Fibers, Part A*, Dekker, New York, 1984.
- Lewin, M., and J. Preston (eds.): *Handbook of Fiber Science and Technology, vol. III, High Technology Fibers, Part C*, Dekker, New York, 1993.
- Lewin, M., and S. B. Sello (eds.): *Handbook of Fiber Science and Technology, Functional Finishes, Part A*, Dekker, New York, 1983.
- Lewin, M., and S. B. Sello (eds.): *Handbook of Fiber Science and Technology, Chemical Processing: Fundamentals and Preparation, Part A*, Dekker, New York, 1983.
- Lewin, M., and S. B. Sello (eds.): *Handbook of Fiber Science and Technology, Functional Finishes, Part B*, Dekker, New York, 1984.
- Lewin, M., and S. B. Sello (eds.): *Handbook of Fiber Science and Technology, Chemical Processing: Fundamentals and Preparation, Part B*, Dekker, New York, 1984.
- Masson, J. C. (ed.): *Acrylic Fiber Technology and Applications*, Dekker, New York, 1995.
- Militky, J., V. Vanicek, J. Krystufek, and V. Hartych: *Modified Polyester Fibres*, Elsevier, Amsterdam, The Netherlands, 1991.
- Robinson, J. S. (ed.): *Fiber-Forming Polymers*, Noyes, Park Ridge, NJ, 1980.
- Schwartz, P., T. Rhodes, and M. Mohamed: *Fabric Forming Systems*, Noyes, Park Ridge, NJ, 1982.
- Warner, S. B.: *Fiber Science*, Prentice Hall, Englewood Cliffs, NJ, 1995.

Composites

- Ashbee, K. H. G.: *Fundamental Principles of Fiber Reinforced Composites*, 2nd edn., Technomic, Lancaster, PA, 1993.
- Bucinell, R. B. (ed.): *Composite Materials: Fatigue and Fracture*, vol. 7, ASTM, Philadelphia, PA, 1998.
- The Composite Materials Handbook—MTL 17*, 3 vols., U.S. Department of Defense, Technomic, Lancaster, PA, 1999.
- DiBenedetto, A. T., I. Nicolais, and R. Watanabe (eds.): *Composite Materials*, Elsevier, New York, 1992.
- Finlayson, K. M. (ed.): *Carbon Reinforced Epoxy Systems, Parts VI and VII*, Technomic, Lancaster, PA, 1989.

- Garbo, S. P. (ed.): *Composite Materials: Testing and Design*, ASTM, Philadelphia, PA, 1990.
- Grayson, M. (ed.): *Encyclopedia of Composite Materials and Components*, Chemical Publishing, New York, 1983.
- Halpin, J. C.: *Primer on Composite Materials Analysis*, 2nd edn., Technomic, Lancaster, PA, 1992.
- Hoa, S. V., and H. Hamada (eds.): *Design and Manufacturing of Composites*, Technomic, Lancaster, PA, 1997.
- Hooper, S. J. (ed.): *Composite Materials: Testing and Design*, vol. 13, ASTM, Philadelphia, PA, 1997.
- Karian, H. G. (ed.): *Handbook of Polypropylene and Polypropylene Composites*, Dekker, New York, 1999.
- Kausch, H.-H. (ed.): *Advanced Thermoplastic Composites*, Hanser-Gardner, Cincinnati, OH, 1992.
- Kelly, A. (ed.): *Concise Encyclopedia of Composite Materials*, Pergamon Press, New York, 1994.
- Mallick, P. K. (ed.): *Composites Engineering Handbook*, Dekker, New York, 1997.
- Matthews, F. L., and R. D. Rawlings: *Composite Materials: Engineering and Science*, Chapman & Hall, New York, 1994.
- Mayer, R.: *Design with Reinforced Plastics: A Guide for Engineers and Designers*, Chapman & Hall, New York, 1993.
- Mayer, R., and N. Hancox: *Design Data for Reinforced Plastics: A Guide for Engineers and Designers*, Chapman & Hall, New York, 1993.
- Murphy, J.: *Reinforced Plastics Handbook*, Elsevier, Cambridge, MA, 1994.
- Murphy, J.: *Reinforced Plastics Handbook*, 2nd edn., Elsevier, Amsterdam, The Netherlands, 1998.
- Powell, P. C.: *Engineering with Fibre-Polymer Laminates*, Chapman & Hall, New York, 1993.
- Quinn, J. A.: *Composites—Design Manual*, Technomic, Lancaster, PA, 1999.
- Staab, G. H.: *Laminar Composites*, Butterworth-Heinemann, Oxford, 1999.
- Strong, A. B.: *High Performance and Engineering Thermoplastic Composites*, Technomic, Lancaster, PA, 1993.
- Vigo, T. L., and B. J. Kinzig (eds.): *Composite Applications. The Role of Matrix, Fiber, and Interface*, VCH, New York, 1992.
- Yosomiya, R., K. Morimoto, A. Nakajima, Y. Ikada, and I. Suzuki: *Adhesion and Bonding in Composites*, Dekker, New York, 1989.
- Zinoviev, P., and Y. N. Ermakov: *Energy Dissipation in Composite Materials*, Technomic, Lancaster, PA, 1994.

Foams

- Defonsika, C.: *Practical Guide to Flexible Polyurethane Foams*, Smithers Rapra, Shrewsbury, 2013.
- Eaves, D.: *Handbook of Polymer Foams*, Rapra Technology Limited, Shrewsbury, 2004.
- Klempner, D., and K. C. Frisch (eds.): *Handbook of Polymeric Foams and Foam Technology*, Hanser-Gardner, Cincinnati, OH, 1992.
- McBrayer, R. L., and D. C. Wsocki (eds.): *Advances in Polyurethane Foams Formulations*, Technomic, Lancaster, PA, 1994.
- Meltzer, Y. L.: *Expanded Plastics and Related Products (Developments since 1978)*, Noyes, Park Ridge, NJ, 1983.
- Wendle, B. C.: *Structural Foam*, Dekker, New York, 1985.
- Woods, G.: *Flexible Polyurethane Foams*, Elsevier Applied Science, New York, 1982.

15 Polymers from Renewable Resources and Recycling of Polymers

15.1 INTRODUCTION

The past couple of decades has seen major efforts to produce more commercial polymers based partially or entirely on renewable resources. The driving forces are both the eventual depletion of the petrochemical feedstock as the source for raw materials in polymer synthesis (Section 1.4) and environmental concerns. The plastic industry is often considered to have started in the 1860s with the plasticization of cellulose nitrate (a modified natural polymer) by camphor to allow the molding of simple objects. Regenerated cellulose in the 1900s and cellulose acetate in the 1920s essentially displaced the nitrate from all markets except lacquers and explosives. The recent strive in developing polymers from renewable resources is in some sense a return of the industry back toward its origin. This chapter covers two separate themes. The first is natural polymers and polymer from renewable resources, and the second deals with the recycling and resource recovery of synthetic polymers.

15.2 POLYSACCHARIDES

Of the polysaccharides, **cellulose** receives the most attention from polymer chemists, since it is the basic polymer contained in cotton and wood. Cotton may have a cellulose content as high as 90% when dry, whereas wood contains about 50% of other compounds, notably lignin (about 30%), a natural phenolic polymer that is the binder in wood, and smaller amounts of sugars and salts. What appear to be minor structural changes in cellulose-related polymers lead to major differences in properties. The water solubility of some starch components and the well-known gelling action of pectin and agar in water are due primarily to differences in the stereoconfiguration. In addition to the hydroxyl groups of cellulose, polysaccharides may contain carboxyl groups (**pectin**), sulfate groups (**carrageenan** from Irish Moss and agar), or amide groups (**chitin**) [1,2]. Typical structures are shown in Figure 15.1. The half-ester sulfate group in agar is not shown, since it occurs only once every tenth repeat unit on the average.

At first glance there would seem to be little incentive for regenerating cellulose. However, wood pulp or the short fibers left from cotton recovery (linters) cannot be molded or spun into useful forms unless they are changed chemically. In the

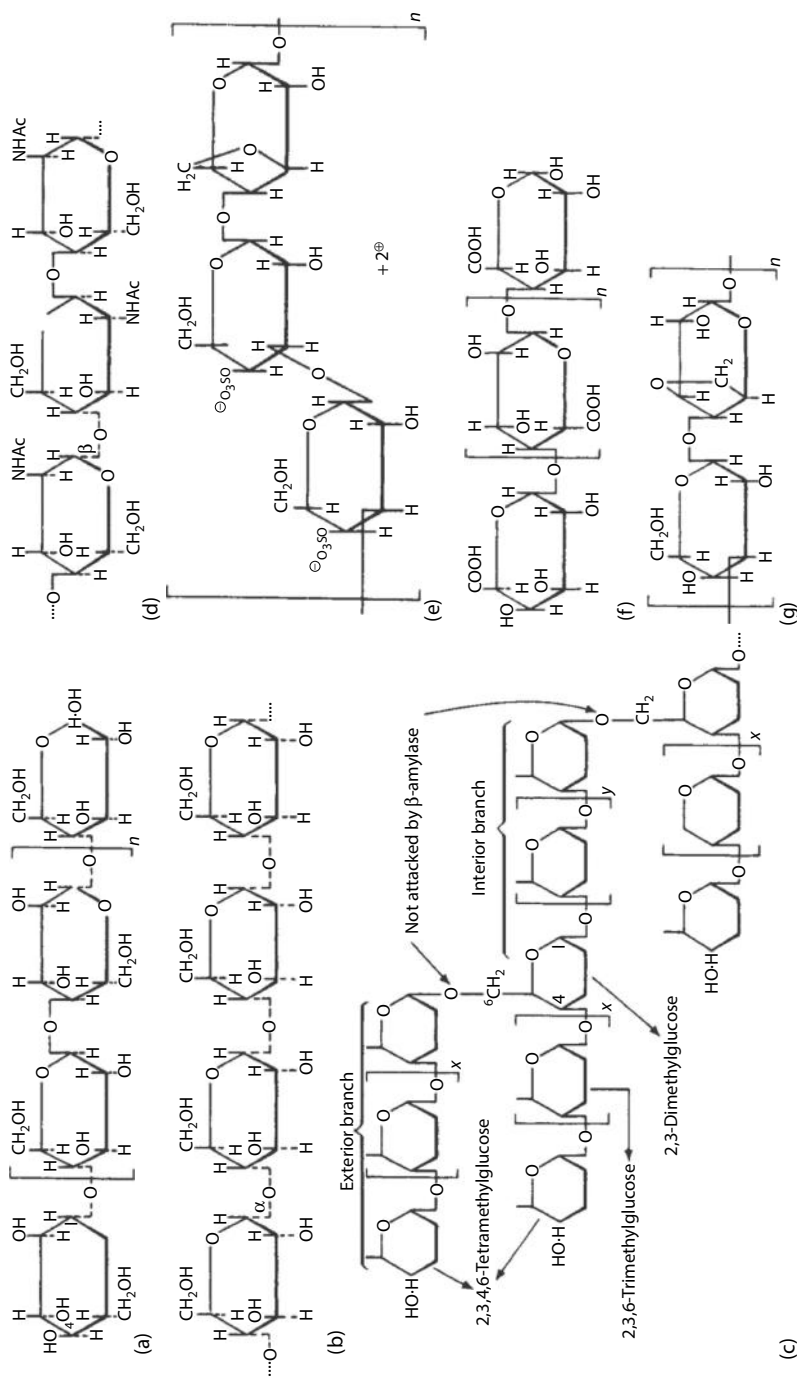


FIGURE 15.1 Polysaccharide structures: (a) cellulose; (b) starch; (c) amylopectin and glycogen; (d) chitin; (e) carrageenan; (f) pectic acid; (g) agar. (Data from Whistler, R. L., and J. N. BeMiller, eds., *Industrial Gums*, Academic Press, New York, 1959; Fieser, L. F., and M. Fieser, *Organic Chemistry*, 3rd edn., Heath, Boston, MA, 1963.)

viscose process (Table 15.1, III), cellulose in sheet form resembling blotter paper is steeped in aqueous alkali for 2–4 h in a rack in which it can then be pressed to squeeze out excess liquid. After the alkali cellulose is shredded, it is aged 2 or 3 days, during which the crystalline structure is disrupted and the molecular weight may be decreased. With carbon disulfide added in a rotating drum called a **barratte**, the **xanthate** is formed, which dissolves in alkali. The orange, unpleasant-smelling solution (7%–8% cellulose, 6.5%–7% NaOH) is ripened for 4–5 days, during which time

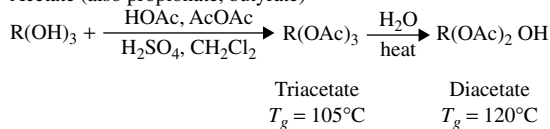
TABLE 15.1
Cellulose Derivatives

I. Esters

A. Nitrate

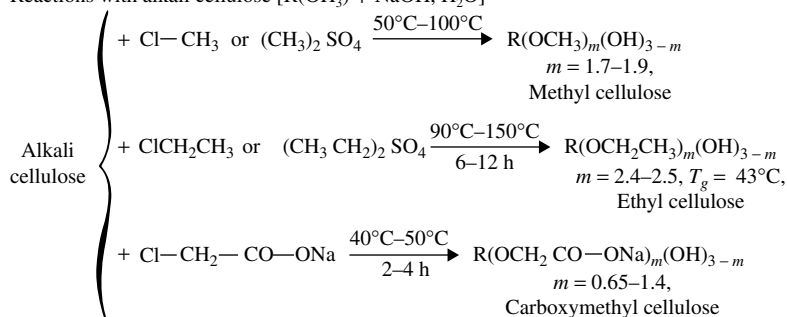


B. Acetate (also propionate, butyrate)

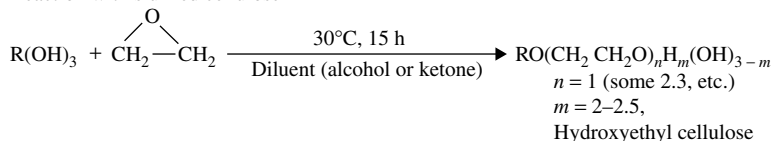


II. Ethers

A. Reactions with alkali cellulose [R(OH)₃ + NaOH, H₂O]

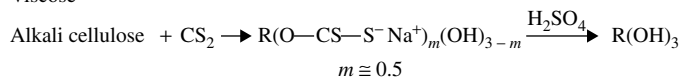


B. Reaction with slurried cellulose

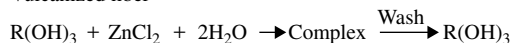


III. Regenerated cellulose

A. Viscose



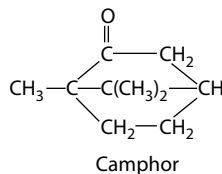
B. Vulcanized fiber



Note: Cellulose = R(OH)₃.

the distribution of xanthate groups presumably becomes more uniform. For rayon fibers the solution is spun through spinnerets with many small holes into a salt–acid bath. A number of operations may be carried out on the fibers, including washing, bleaching, drawing, and twisting and crimping. For **cellophane** a slot orifice is substituted for the spinneret, and after treatment may include plasticization by glycerol or coating by a moisture barrier such as cellulose nitrate. Although rayon is still a widely used fiber around the world, rayon and cellophane production in the United States has almost disappeared. Sausage casing for *skinless* hot dogs has been made by the same cellulose regeneration process using a tubular die. An important reason for decreased interest in rayon is the problem of waste disposal from the production process. In the past, sulfur compounds were not recovered and were the cause of air and water pollution. The search for an alternative process that would not involve disposal of by-products has not yet yielded a large-scale solution. However, one plant has been built that produces regenerated cellulose fiber by wet or dry spinning from a solution of cellulose in *N*-methyl morpholine (or similar solvents) [3].

The flammability of **cellulose nitrate** and the necessity of having a solvent present during forming operations have pretty much eliminated it as a molding plastic. Popular household cements for paper and wood may be solutions of the nitrate in ketones and esters. Lacquers for wood and metal also do not suffer from the limitations mentioned. One molded product that is slow to yield to the use of other polymers is the Ping–Pong ball with its peculiar requirements of resilience and toughness. The preferred plasticizer is still camphor:



The production of **cellulose diacetate** requires three steps. A preliminary treatment of cellulose with glacial acetic acid for 1 or 2 h is followed by reaction with acetic anhydride with a trace of sulfuric acid as a catalyst. In order to keep the temperature of the reaction at about 50°C, methylene chloride is refluxed. A typical charge would be the following [4]:

Step 1: Pretreatment

Cellulose	100 parts
Glacial acetic acid	35 parts

Step 2: Acetylation

Acetic anhydride	300 parts
Methylene chloride	400 parts
Sulfuric acid	1 part

The reaction product is the triacetate, from which some film and fiber are produced. Most of the triacetate is hydrolyzed in a third step to diacetate by adding water to the reaction product and ripening the mixture for several days. The diacetate is soluble in acetone or halogenated solvents, whereas the triacetate is soluble in fewer, more

expensive solvents such as chloroform. The diacetate is used in films, fibers, and coatings. Like vinyl chloride polymers, the acetate usually is plasticized, dimethyl phthalate being more suitable than the higher esters favored for vinyls. Cellulose propionate, butyrate, and a mixed acetate–butyrate are marketed for photographic film base, molding, and coating applications.

Ethyl cellulose resembles cellulose acetate in many of its qualities (toughness, transparency) and applications (films, coatings). The other common cellulose ethers are water soluble and have the usual string of applications such as thickening agents, textile and paper sizes, cosmetic and pharmaceutical suspending agents, and water-based paint additives. Except for the **hydroxyethyl cellulose**, the ethers are made by condensation of alkali cellulose with a chlorinated or sulfated compound. An acid, HCl or H₂SO₄, is eliminated in the reaction. Where low degrees of substitution are encountered, the ether groups may not be evenly distributed but may be clustered toward the outside of the original cellulose fiber structure. In this respect they differ from viscose rayon and cellulose acetate, where ripening or aging steps are included to increase uniformity.

15.2.1 SELECTED USES

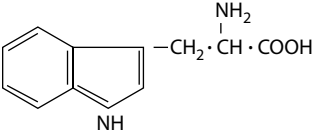
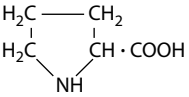
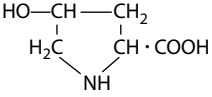
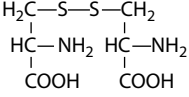
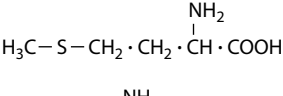
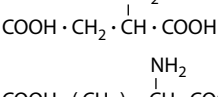
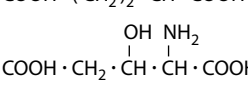
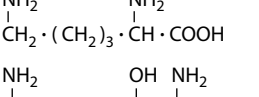
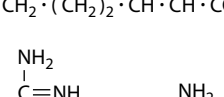
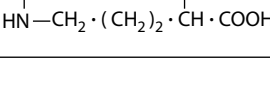

As befits a senior citizen of the polymer industry, the polysaccharide group is stable but rather sedate. The imminent demise of cotton, rayon, and cellophane at the hands of new synthetics has been predicted often but has not materialized. When cotton was attacked by nylon and polyesters for use in apparel, wash-and-wear finishes based on melamine and urea resins gave it new life. Polypropylene (PP) film has indeed taken over most cellophane–packaging markets. Cellophane for packaging usually is coated to lower the moisture sensitivity and permeability, and to provide a plastic surface that can be heat sealed. Vinylidene chloride–vinyl chloride copolymers, cellulose nitrate, poly(vinyl acetate), and other ethenic polymers are used as coatings. Some candy products such as caramels continue to be packaged in cellophane. Uncoated cellophane is sold by laboratory supply houses for membrane dialysis. A significant application for cellulose acetate film has been found in seawater desalination by reverse osmosis. The film is strong enough to resist the high pressures involved, and it has a good permeability to water and a low permeability to salt. Most cigarette filters are made of cellulose acetate fibers. Cellulose acetate–butyrate still is the most common material used for 35-mm photographic film base.

15.3 BIOLOGICAL POLYAMIDES

Naturally occurring **proteins** are polyamides. They are found in all living cells such as our own bodies or in the silkworm that produces **silk**, a protein fiber recovered from the worm cocoons. Simple proteins yield only α -amino acids upon hydrolysis. Proteins can be divided into two major classes: the fibrous and the globular proteins. The **fibrous proteins** act as structural materials in animals in much the same way that cellulose acts for plants. **Keratin** (the protein of hair, horn, feathers, and fingernails), **fibroin** (the protein of silk), and **collagen** (the protein of connective tissues) are all fibrous proteins with the common property of water insolubility. Collagen yields gelatin when boiled in water. **Globular proteins** are soluble in water or

aqueous solutions of acids or bases. **Albumin** (eggs), **casein** (milk), and **zein** (corn) are examples of globular proteins. The common amino acids and representative analyses of some proteins are shown in Tables 15.2 and 15.3. Because of advances in genetic engineering and interest in biodegradable materials based on renewable resources, proteins have attracted attention as potential sources of polymeric materials [6].

TABLE 15.2
Some Amino Acids Isolated from Proteins

Common Name	Systematic Name	Structural Formula	Discoverer (Date)
Tryptophan	α -Amino- β -indolpropionic acid		Hopkins and Cole (1901)
Proline	Pyrrolidine- α -carboxylic acid		E. Fischer (1901)
Hydroxyproline	γ -Hydroxypyrrolidine- α -carboxylic acid		E. Fischer (1901)
Cystine	Di-(α -amino- β -thiopropionic acid		Wollaston (1810)
Methionine	α -Amino- γ -methylthiol- <i>n</i> -butyric acid		Mueller (1922)
Aspartic acid	Aminosuccinic acid		Plisson (1827)
Glutamic acid	α -Aminoglutaric acid		Ritthausen (1866)
Hydroxy-glutamic acid	α -Amino- β -hydroxyglutaric acid		Dakin (1918)
Lysine	α - ϵ -Diaminocaproic acid		Drechsel (1889)
Hydroxylysine	α - ϵ -Diamino- β -hydroxy- <i>n</i> -caproic acid		Schryver et al. (1925)
Arginine	α -Amino- γ -guanidine- <i>n</i> -valeric acid		Schulze and Steiger (1886)

(Continued)

TABLE 15.2
(Continued) Some Amino Acids Isolated from Proteins

Common Name	Systematic Name	Structural Formula	Discoverer (Date)
Histidine	α -Amino- β -imidazol-propionic acid		Kossel (1896) Hedin (1896)
Glycine (glycocol)	Aminoacetic acid		Braconnot (1820)
Alanine	α -Aminopropionic acid		Strecker (1850)
Valine	α -Aminoisovaleric acid		Gorup-Besanez (1856)
Leucine	α -Aminoisocaproic acid		Proust (1819)
Isoleucine	α -Amino- β -ethyl- β -methyl-propionic acid		F. Ehrlich (1903)
Serine	α -Amino- β -hydroxy-propionic acid		Cramer (1865)
Threonine	α -Amino- β -hydroxy- <i>n</i> -butyric acid		Schryver and Buston (1925) Rose et al. (1935)
Phenylalanine	α -Amino- β -phenyl-propionic acid		Schulze and Barbieri (1879)
Tyrosine	α -Amino- β -(<i>p</i> -hydroxyphenyl) propionic acid		Liebig (1846)
Iodogorgoic acid	3,5-Diiidotyrosine		Drechsel (1896)
Thyroxine	β -3,5-Diiido-4-(3',5'-diiido-4-hydroxy) phenyl- α -aminopropionic acid		Kendall (1915)

Source: Mitchell, P. H.: *A Textbook of Biochemistry*, 2nd edn., McGraw-Hill, New York, 1950, 97, 98, 106.

TABLE 15.3
Partial Analysis of Some Proteins

	Egg Albumin	Lactalbumin	Serum Albumin	Serum Globulin	Edestin (Hemp)	Glutenin (Wheat)	Gliadin (Wheat)	Zein (Maize)	Keratin (Wool)	Fibroin (Silk)	Gelatin	Salmine (Salmon Sperm)	Casein (Cow's Milk)	Vitellin (Egg Yolk)	Insulin (Crystal)	Pepsin (Crystal)
Glycine	0.0	0.4	0.0	3.5	3.8	0.9	0.0	0.0	0.6	40.5	25.5	—	0.5	1.1	—	—
Alanine	2.2	2.4	2.7	2.2	3.6	4.7	2.0	9.8	4.4	25.0	8.7	—	1.9	0.2	—	—
Valine	2.5	3.3	—	—	6.3	0.2	3.4	1.9	2.8	—	0.0	4.3	7.9	2.4	—	—
Leucine and isoleucine	10.7	14.0	20.0	18.7	14.5	6.0	6.6	25.0	11.5	2.5	7.1	—	9.7	11.0	30.0	—
Phenylalanine	5.1	1.3	3.1	3.8	3.1	2.0	2.4	7.6	—	11.5	1.4	—	3.9	2.8	—	—
Tyrosine	4.2	2.0	4.7	6.7	4.6	4.5	3.4	5.9	4.8	11.0	0.0	—	6.6	5.0	12.2	10.3
Tryptophan	1.3	2.7	0.5	2.3	2.5	1.7	1.1	0.2	1.8	—	0.0	—	2.2	2.5	—	2.2
Threonine	—	—	—	—	—	—	—	—	—	1.5	—	—	3.6	—	2.7	—
Glutamic acid	14.0	12.9	7.7	8.2	19.2	25.7	43.7	31.3	12.9	—	5.8	—	21.8	12.2	30.0	18.6
Hydroxyglutamic acid	1.4	10.0	—	—	—	1.8	2.4	2.5	—	—	0.0	—	10.5	—	—	—
Aspartic acid	6.1	9.3	3.1	2.5	10.2	2.0	0.8	1.8	2.3	—	3.4	—	4.1	0.5	—	6.8
Proline	4.2	3.8	1.0	2.8	4.1	4.2	13.2	9.0	4.4	1.0	9.5	1.0	9.0	4.0	—	—
Hydroxyproline	—	—	—	—	—	—	—	—	—	—	14.1	—	0.2	—	—	—
Serine	—	1.8	0.6	—	0.3	0.7	—	1.0	2.9	13.6	0.4	7.8	5.0	—	3.6	—
Cystine	1.3	4.3	6.1	1.0	1.0	1.8	—	0.8	13.1	—	0.2	—	0.3	1.2	12.2	1.4
Methionine	4.6	2.6	—	—	2.1	—	2.1	2.3	—	—	—	—	3.4	—	0.0(?)	—
Arginine	5.2	3.0	4.8	5.2	15.8	4.7	2.9	1.8	7.8	0.7	8.2	87.4	3.8	7.8	3.2	2.7
Histidine	1.4	2.1	1.2	0.9	2.2	1.8	1.5	0.8	0.7	0.1	1.0	—	2.5	1.2	8.0	0.1
Lysine	6.4	8.8	6.9	6.2	2.2	1.9	0.6	0.0	2.3	0.3	5.9	—	6.0	5.4	2.2	2.1
Ammonia	1.4	1.3	—	—	2.3	4.0	5.2	3.6	—	—	0.4	—	2.3	—	1.7	8.8

Source: Mitchell, P. H.: *A Textbook of Biochemistry*, 2nd edn., McGraw-Hill, New York, 1950, 97, 98, 106.

Note: 1. “+” implies “some.”

2. “—” implies undetermined.

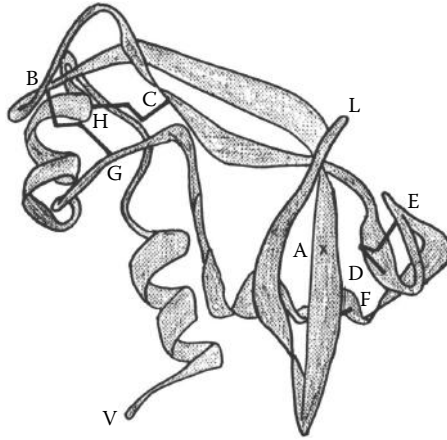


FIGURE 15.3 Three-dimensional representation of ribonuclease A. The valine (V) and leucine (L) ends are shown together with disulfide linkages labeled A–F, B–G, C–H, and D–E. Both sheet and helical forms are apparent.

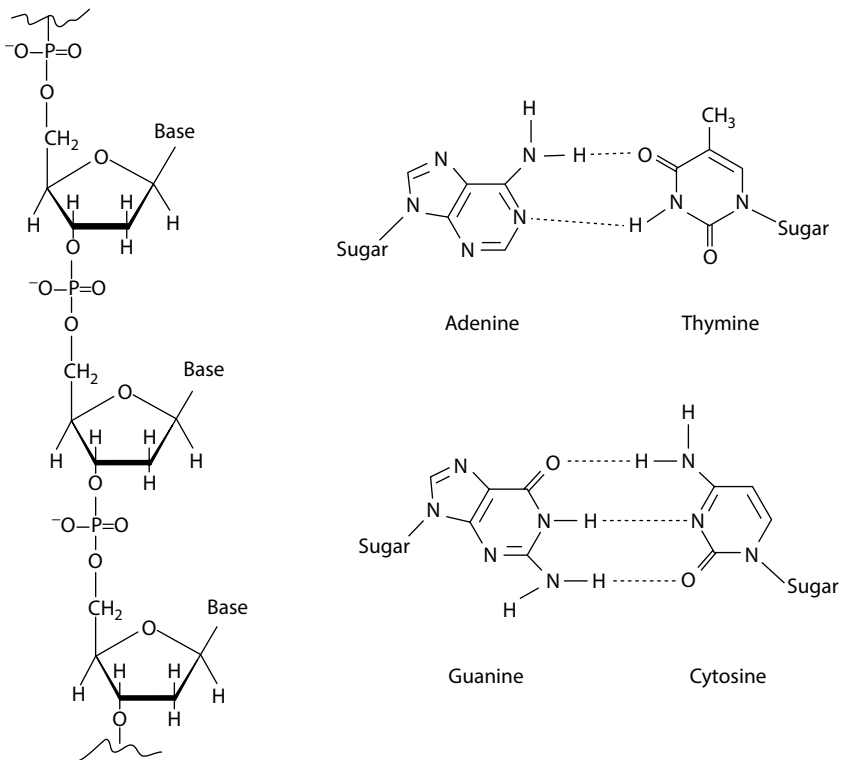


FIGURE 15.4 The polyester chain of DNA consists of phosphate and sugar groups. Each sugar, in turn, is associated with one of the four amines shown on the right. The entire double helix (not shown) is stabilized by hydrogen bonds between amines (base pairs). (Data from Sryer, L., *Biochemistry*, chap. 4, 4th edn., Freeman, New York, 1995; *Nature*, 421,396, 2003.)

bases to form a **nucleotide**. **Deoxyribonucleic acid (DNA)** is a **polynucleotide** made up of two high-molecular-weight strands coiled into a double helix, the strands being held together by hydrogen bonds between base pairs. The sequence of nucleotides in the polymer is what carries genetic information in living cells. A **chromosome** consists of several thousand DNA segments called genes. In the nucleus of the human cell, there are 23 pairs of chromosomes, each of which is very large (over 100 million pairs of base pairs). The sum of all the genes in a cell is termed a **genome**.

15.5 POLYMERS FROM RENEWABLE RESOURCES

15.5.1 POLYESTERS

Several commercially important polyesters are produced directly by plants and animals or synthesized from monomers obtained from renewable resources. The best known examples are **poly(lactic acid)** or polylactide (**PLA**), **poly(glycolic acid)** or polyglycolide (**PGA**), and **polyhydroxyalkanoates (PHAs)**.

Bacterial fermentation of starch or other polysaccharides is the major process used for the production of lactic acid (LA) that exists in the two enantiomeric structures, D and L forms. Modified strains of the responsible microorganisms produce stereoregular LA, whereas the chemical process produces a racemic mixture of the two forms. There are several methods used to synthesize PLA that are illustrated in Figure 15.5. A variety of structures and molecular weights can be synthesized. This

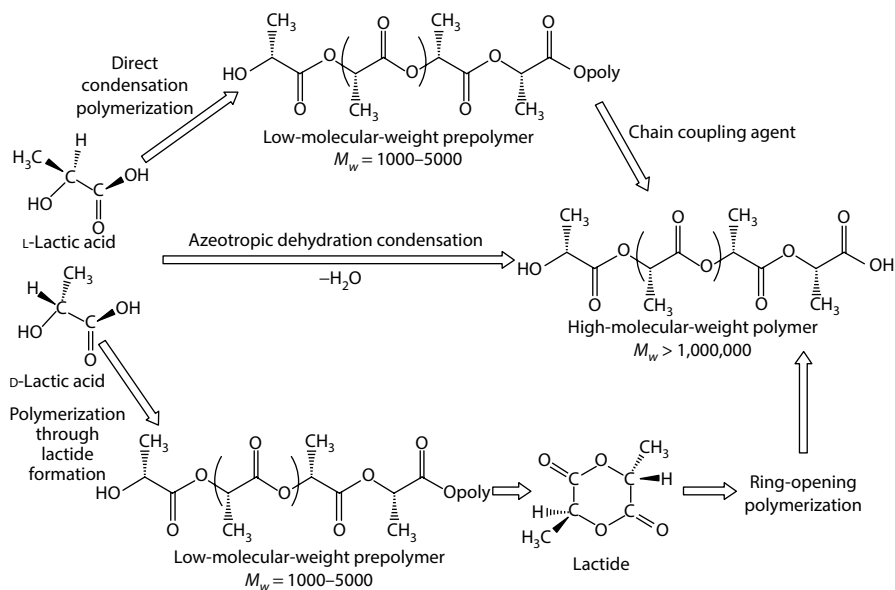


FIGURE 15.5 Synthesis methods of PLA. (Data from Averous, L., chap. 21 in M. N. Belgacem and A. Gandini, eds., *Monomers, Polymers and Composites from Renewable Resources*, Elsevier, Amsterdam, The Netherlands, 2008; With kind permission from Springer Science+Business Media: *Biopolymers from Renewable Resource*, chap. 15, 1998, D. L. Kaplan.)

leads to different physical, mechanical, and degradation properties that vary over a wide range. Poly(L-lactic acid) (PLLA) is crystalline and has better mechanical properties than poly(DL-lactic acid) (PLDLA) that is completely amorphous. Although the T_g ($\sim 60^\circ\text{C}$) and density ($\sim 1.27\text{g/cm}^3$) of these two forms of PLA do not differ much, the presence of crystallinity in high-molecular-weight PLLA ($T_m \sim 175^\circ\text{C}$) improves its flexural and tensile strength over PLDLA [10]. Articles of PLA are processed by the conventional method of melt spinning, film extrusion, and molding. They become relatively brittle over time due to physical aging and degradation under ambient conditions. This advantage of biodegradability induced by hydrolysis allowed PLA to find a niche of applications in food packaging, food containers, agricultural mulch films, and biomedical applications such as absorbable stents. Annual production of PLA is steadily increasing. A plant to produce PLA from corn was put into operation in 2002 by Cargill Dow LLC. This joint venture became wholly owned by Cargill and renamed Nature Works LLC in 2005 and is targeting a production of 300 million lb/year of PLA in the United States in 2014. Several other US, European, and Asian companies are also producers of PLA [10].

Glycolic acid (GA) is another monomer that is synthesized using an enzymatic biochemical process and is often used as a comonomer with LA. The homopolymer PGA is synthesized by methods similar to those used for PLA. Its glass transition temperature is around 35°C – 40°C and it is highly crystalline. Because of its degradability in hydrolytic conditions and the nontoxicity of the degradation product (GA), it was first used in synthetic absorbable sutures. Copolymers of LA and GA of different compositions, PLGAs, provide advantages over the pure homopolymers in terms of reduced crystallinity and better control of the mechanical properties and degradation time. They are used in drug delivery such as for growth deficiency treatment and pancreatic cancer therapy. They are also being studied for use as tissue engineering scaffolds and other biomedical applications [11–13].

A number of partially bio-based polyesters are also commercially available. Among the first introduced to the market in 2001 is poly(trimethylene terephthalate) (PTT) synthesized by DuPont under the trademark Sorona[®]. This polymer contains 37% renewable 1,3-propanediol made from glycerol produced from corn sugar via fermentation. The propanediol is polycondensed with fossil-derived terephthalic acid (TPA). Although PTT has a T_g of 45°C – 55°C and a T_m of 230°C , values that are lower than PET (see Table 3.1), it possesses, under appropriate processing conditions, mechanical properties that are comparable to PET [15]. The Coca-Cola Company has been using partially bio-based PET since 2009 using ethylene glycol produced from Brazilian sugar and molasses and polymerized with TPA making it 30% renewable. TPA or its precursor, *p*-xylene, is more difficult to produce biologically from renewable resources than the aliphatic acids (LA and GA). Nonetheless, the push to develop a 100% bio-based PET is under way [16].

PHAs are aliphatic biopolyesters produced by numerous bacteria. The most commonly found and best studied PHA is poly- β -hydroxybutyrolactone (**PHB**) made in high yield by fermentation of glucose [14,17,18]. A copolymer with hydroxyvalerolactone (**PHBV**) results when the fermentation is carried out in the presence of some propionic acid. The properties of PHB are often compared with PP and poly(ethylene terephthalate) (PET) (Table 15.4). PHBV is more easily processed than PHB, but

TABLE 15.4
Typical Properties of PHB Compared with Those of a Copolymer
(15% Hydroxyvalerolactone), PP, and PET

Polymer	PHB	PHB/HV*	PP	PET
$M_w \times 10^{-3}$	292	258	–	–
M_w/M_n	2.75	3.5	–	–
T_g (°C)	6	2	–18	80
T_m (°C)	191	177	176	265
Heat of cryst. (J/g)	127	45	–	–
Density (g/cm ³)	1.256	1.2	0.905	1.35
Modulus (GPa)	3.25	1.47	1.4	2.5
Tensile strength (MPa)	40	25	40	55
Impact strength, notched (J/m)	66	65	20–75	35–55
Impact strength, unnotched (J/m)	115	463	–	–

Source: Mitchell, P. H.: *A Textbook of Biochemistry*, 2nd edn., McGraw-Hill, New York, 1950, 97, 98, 106; Holmes, P. A., *Phys. Tech.*, 16, 32, 1985.

*Mechanical properties of PHB/HV are for 18 mol% copolymer.

has a lower melting temperature. The lower crystallinity of the PHBV copolymer is reflected in the lower energy of melting. The unnotched impact strength of the copolymer is much higher than that of the homopolymer. Uses for PHBV have included blow-molded bottles and packaging film.

Yields of 1 kg of polymer for 3 or 4 kg of glucose and fermentation times of 4–5 days have made the production of PHAs expensive. Alternative synthetic methods are being considered but commodity applications appear to be distant. A number of novel polyesters based on the polycondensation of hydroxydecanoic acids that are isolated from the hydrolysis of **suberin** are also being considered [19]. Suberin is an abundant component of the bark cell walls of higher plants and a major component of cork [20].

15.5.2 POLYOLS

Vegetable oils extracted from the seeds of plants such as soybean, flax, and rapeseed are oligomers that are used in numerous applications such as lubricants, cosmetics, and pharmaceuticals. One of the early applications of linseed oil is its use in paints (see Section 13.4.1.4). The major components of vegetable oils are **triglyceride** macromonomers consisting of different fatty acids. These monomers are attractive because of the olefin functionalities of unsaturated fatty acids that provide routes for functionalization and cross-linking. The network formation and drying of linseed oil paint, for example, is based on cross-linking of triglycerides via oxidation and free-radical propagation. Most olefin functionalization reactions such as epoxidation, hydrofomylation, and reduction can be used with triglycerides. A commercial application [21] is the production of polyols for the production of flexible polyurethane foams where natural oil-based polyols made from soybean oil substitute for petroleum-based

polyether-based polyols (see Section 14.9.1). Soybean oil contains an average of five unsaturations per molecule that can be functionalized to alcohol sites, typically via epoxidation of the olefin sites. Genetic engineering plays an important role in enhancing the structure and amount of triglycerides in plants [22]. The preparation of polyols from different vegetable oils and via different routes has been recently summarized [23]. The structures and properties of polyurethanes produced with renewable polyols are affected by the type of triglyceride used, the selection of the isocyanate moiety, and the degree of cross-linking. Particular interest has focused on the degradability and biocompatibility of these partially bio-based polyurethanes.

15.5.3 USE OF CO₂ AS FEEDSTOCK

Carbon dioxide is a sustainable resource even though it is not often thought of as a renewable raw material. Because CO₂ is more abundant than environmentally safe, several approaches to its sequestration are being developed. The fixation of CO₂ into polymer structures will not really affect its environmental level because all of polymers used represent only a minuscule amount compared to the fossil-based materials used in energy consumption that generates CO₂. The advantages of using CO₂ as a feedstock lie in its sustainability, biocompatibility, and the potential of biodegradability of the products. One of the first CO₂-based polymers to be synthesized is **poly(propylene) carbonate** (PPC) based on the copolymerization of CO₂ with fossil-derived propylene oxide (Figure 15.6). The role of the catalyst in this reaction is critical and has been reviewed recently [24].

The commercial production of PPC is still quite modest at several kilotons annually and its use is limited primarily to binder applications in ceramic sintering processes where it benefits from a lower decomposition temperature compared to other binders [25]. More recently developed cobalt salem catalysts [26] and proprietary catalysts with improved activity and selectivity are able to produce tailored PPC polyols with specific molecular weights and hydroxyl group functionalities [27,28]. The polyurethanes synthesized from these polyols are reported to exhibit increased strength and durability caused by the polycarbonate backbone [29]. Besides CO₂-based PPC, other poly(alkylene carbonate)s are produced in pilot-scale processes [27].

15.5.4 METABOLIC ENGINEERING PRODUCTION OF RAW MATERIALS

A very active area of research in both academia and industry is the use of genetic engineering to modify the existing metabolic pathways (or designing new ones) in plants and microbes to optimize the production of certain chemicals. Metabolic

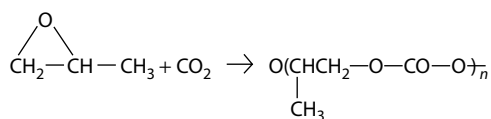


FIGURE 15.6 PPC synthesis using propylene and CO₂ in the presence of an appropriate catalyst.

engineering is successfully applied to the production of numerous pharmaceuticals, insulin being the most notable. In recent years, this approach has been applied to the production of biofuels (e.g., ethanol and other alcohols) from biomass and provides optimism for higher productivity and efficiency in the near future [30]. With the emergence of commercially viable routes to raw materials from renewable resources, it is normal that efforts be directed toward the optimization of these processes. Various approaches to the use of metabolic engineering in optimizing LA production, fatty acids, and triglycerides [22,31] used in the production of PLAs and polyols have been reported. This approach is being aggressively pursued for the production of a number of biomonomers. Recently, the production of 3-hydroxypropionic acid (3-HP) from renewable resources in pilot-scale quantities has been demonstrated [32]. This monomer is a precursor to acrylic acid used in the manufacture of **poly(acrylic acid)**, a superabsorbent polymer. Bio-based isoprene is another example [33] that led to the formation of joint ventures between chemical companies and tire companies [34,35] to produce prototype rubber tires. Companies are also looking at scale-up of biobutadiene and bio-isobutene.

Commercial polymers generated totally or partially from renewable resources will remain a very small component in the production of plastics, rubbers, and fibers, in the near future. However, their importance and marketability will continue to grow. They provide environmental and potentially economic advantages over their counterpart generated entirely from fossil raw materials. In addition, they offer more readily desirable properties such as biodegradability and biocompatibility that are more difficult to achieve with synthetic polymers. With extensive ongoing research and development pertaining to new catalysts that will enable the incorporation/modification of renewable monomers into feedstocks as well as the development of new metabolic microbial pathways for the bio-production of monomers, the field will continue to advance to achieve production costs of polymers from renewable resources that are reasonably competitive.

15.6 WASTE GENERATION AND DISPOSAL

For several decades since the 1960s, **the municipal solid waste (MSW)** in the United States has increased at a faster rate than the total population before leveling off in the last decade [36]. The per capita generation of waste reached a maximum of 4.7 lb/day/person in 2007. The trend has finally reversed in the past few years with a reported 4.3 lb/day/person of MSW in 2009 [37]. MSW includes material from commercial, industrial, and institutional sources as well as residences. Construction and demolition wastes are not included; neither is sludge from sewage treatment.

15.6.1 DISPOSAL

Until 1960 almost all solid waste had been dumped or buried in landfills or incinerated. These dumps have been largely replaced by **sanitary landfills**, in which layers of refuse are covered at regular intervals by layers of soil. Many communities have run out of space for landfills and are seeking alternatives. One of the largest landfills is the Fresh Kills landfill on Staten Island, New York. Originally a marshland, the

volume of material deposited there since it opened in the 1950s has been over 25 times the volume of the Great Pyramid of Khufu at Giza [38]. Although it ceased receiving MSW in 2000, the site was temporarily reactivated in order to accommodate debris from the World Trade Center disaster of 2001.

Much of the focus on waste has concentrated on the disposal of packaging. Unlike many other applications, packaging represents a short-term usage. Long-term usage also feeds products into the waste stream, but in a less obvious manner. Construction materials, clothing, automobiles, tires, batteries, and appliances all appear in the waste stream eventually, but in a whole spectrum of shapes, sizes, and conditions. For many concerned groups, waste has become almost synonymous with packaging made of paper, glass, aluminum, and plastics.

There is an ongoing controversy over the merits of paper packaging versus plastics. A rather elegant comparison of paper cups versus foamed polystyrene (PS) cups [39] showed that the choice between the two is complex and depends on various subjective criteria. A similar analysis compared grocery bags of paper and polyethylene [40]. Neither case demonstrated a clear-cut superiority for one material over the other for a container of the same capacity. The analyses included the costs of material and energy for production and ultimate disposal of each alternative.

Several terms should be distinguished. **Postconsumer waste** includes materials that have been gathered from a multiplicity of sources, often by a community recycling program. A somewhat more restrictive term often used to describe recovered materials that may potentially be recycled is **postconsumer recycle**. **Postindustrial waste** includes materials that have not gone into consumer products. The trimmings from edges of sheet materials and returned bulk containers are often easier to handle, since they are not geographically scattered. The explanatory legends on most packaging that makes use of recycled materials (cereal boxes, for example) usually distinguish between the two major categories of recycled waste.

Some governments have passed laws specifying minimum standards for recycling or have issued outright bans on certain products. Most of these have been at the local level, but national governments have also set specific targets. In Germany, for example, a law was passed to the effect that 64% of all plastics packaging was to be recycled by 1995 [41]. Similar laws have set goals for recycling of entire automobiles in some countries [42]. A US Highway Bill passed in 1991 mandated the use of *rubberized asphalt* for paving 5% of all new roads starting in 1994 [43]. **Rubberized asphalt** contains 1% by weight of crumb rubber, mainly from ground-up, discarded tires. However, of the 281 million tires discarded in 2001 (the United States only), only 12% were made into crumb rubber. Another 14% went into such engineering applications as side-slope stabilization and beach erosion control. About 41% were used for fuel [44].

An obvious way to minimize waste is to reduce the sources of waste. The **downsizing** of the polyethylene grocery bag provides a successful example. The grocery bag in current use is capable of containing a volume of about 15 l. The wall thickness is less than 0.013 mm (0.0005 in). Not so very long ago, a plastic bag of the same capacity required a wall thickness at least 5 times greater. The increased yield strength of the newer bag material has been brought about by changes in polymer structure and by improvements in the fabrication process.

15.6.2 RECYCLING OF PAPER, GLASS, AND ALUMINUM

The recycling of all materials has increased dramatically in recent years (Table 15.5). Much of this is due to community-based recycling programs that mandate collection of certain classes of material. Paper products, which are a large fraction of the waste stream, are successfully recycled, although the supply of recycled paper appears to exceed the demand. Consumer products containing recycled paper often sell at a

TABLE 15.5
Selected Data on Waste Generation and Disposal (Millions of Tons)

	1980	1990	2000	2005	2009
MSW Generation					
Item					
Waste, total	151.6	208.3	242.5	252.4	243.0
Per person per day (lb)	3.7	4.6	4.7	4.7	4.3
Paper products	55.2	72.7	87.7	84.8	68.4
Ferrous metals	12.6	12.6	14.1	15.0	15.6
Aluminum	1.7	2.8	3.2	3.3	3.4
Other nonferrous metals	1.2	1.1	1.6	1.9	1.9
Glass	15.1	13.1	12.8	12.5	11.8
Plastics	6.8	17.1	25.5	29.3	29.8
Rubber and leather	4.2	5.8	6.8	7.3	7.5
Textiles	2.6	5.8	9.4	11.4	12.6
Wood	7.0	12.3	13.6	14.9	15.8
Food wastes	13.0	20.8	26.8	32.0	34.3
Yard wastes	27.5	35.0	30.5	32.1	33.2
Other wastes	1.0	4.6	5.8	3.2	4.4
MSW Disposal					
Method					
Landfill	134.4	145.3	139.4	140.9	131.9
Combustion with energy recovery	2.7	29.7	33.7	31.6	29.0
Recovered materials, total	14.5	33.2	69.4	79.9	82.0
Paper products	11.7	20.2	37.6	42.0	42.5
Ferrous metals	0.4	2.2	4.7	5.0	5.2
Aluminum	0.3	1.0	0.9	0.7	0.7
Other nonferrous metals	0.5	0.7	1.1	1.3	1.3
Glass	0.8	2.6	2.9	2.6	3.0
Plastics	0.2	0.4	1.5	1.8	2.1
Yard trimmings	–	4.2	15.8	19.9	19.9
Other	0.6	1.9	4.9	6.6	7.3

Source: Characterization of Municipal Solid Waste in the United States: 2011 Facts and Figures Fact Sheet, U.S. Environmental Protection Agency, <http://www.epa.gov/osw/nonhaz/municipal/msw99.htm>; Statistical Abstract of the United States, Tables 377 and 378, U.S. Census Bureau, Washington, DC, 2012; Holmes, P. A.: *Phys. Tech.*, 16, (1985):32.

premium over the same products with nonrecycled material. There are lessons that polymer recyclers can learn from older programs. Recycling of aluminum beverage cans is a true success. The introduction of the 5-cent deposit per can in many states has greatly increased the rate of can recycling, mostly back to the original application [38]. Several other factors leading to this situation are worth considering for polymers:

1. The cans are all aluminum.
2. All vendors use the same material. If one used a modified alloy that was not compatible with that used by the others, the cans would have to be segregated before recycling.
3. The value of scrap aluminum is high (approximately \$0.70/lb).

The replacement of glass containers by aluminum and plastics is apparent in the statistics from 1970 to 1990. Glass is easily distinguished from other containers, which makes recycling easier. About 25% of glass containers used in 1993 were recycled [37]. Since less than one-fourth of all silica-based glass goes into other products (flat glass, fiberglass, etc.), the 25% figure is rather impressive.

Paper, particularly newspapers and office paper, was recycled at a rate of 42% in 1999 [36]. Newsprint itself does not make large use of reclaimed paper because fibers are degraded in structure and length during processing, giving rise to problems in high-speed printing [45]. The use of recycled newsprint in cardboard and building applications goes back many years. The degradation of properties and the use in downgraded products also are factors in polymer use. The separation problems with paper are simpler than those with polymers, since ink and adhesives are not very much like paper pulp. However, polyethylene and PS have much more in common. Separation of fillers (kaolin and other inorganic materials) from glossy papers is unattractive economically and generally avoided.







15.7 IDENTIFICATION AND SEPARATION

Gathering individual components from the waste stream into well-labeled and economically viable masses is the most difficult part of the recycling process. In many communities, some form of recycling is mandated by law. Residents may be required to separate their trash into separate containers, or they may be allowed to commingle (mix) all the *recyclables*. In some places, bottle deposit laws encourage consumers to return beverage containers to the place of purchase. Aluminum, glass, and polyester soft drink and beer containers are collected in stores and shipped to collection centers where they can be compacted. High-density polyethylene milk containers also are easily identified and collected.

15.7.1 IDENTIFICATION

In order to facilitate identification of containers, the Society of Plastics Industries introduced a code that has been used by most manufacturers since the 1990s. At or near the bottom of almost all plastic containers sold in the United States appears a triangular symbol with a number and an abbreviated name (Table 15.6) [47]. While

TABLE 15.6
Plastics Identification Code

Number and Letters (Polymer Type)	US Sales (1993) (billions of kg)			Typical Uses	Density (g/cm ³)
	Total	Containers	Film		
 PETE	1.2	0.8	0.4	Beverages	1.35
 HDPE	4.8	1.8	0.5	Milk, bags	0.95
 PVC	4.7	0.1	0.1	Oil, shampoos	1.32–1.38
 LDPE	5.9	0.2	1.9	Bags	0.93
 PP	4.1	0.2	0.3	Foods	0.90
 PS	3.1	0.5	0.1	Foam	1.08
7 Other	7.5	0.3	0.1		
Total	31.3	3.8	3.4		

Source: Plastic Container Code System, The Plastic Bottle Information Bureau, Washington, DC; *Mod. Plast.*, 70, 73, 1994.

this is a help when consumers participate in a recycling program, the symbols are not very visible and do not enhance automatic sorting. Most containers and almost all film materials are potentially included in the six categories. There are several cautionary points to be observed. Except for **PET**, containers are not the predominant use for any one polymer. For poly(vinyl chloride) (**PVC**), consumer-identifiable containers are less than 10% of the total. The identification on products is not always very prominently displayed. It can take some effort to ascertain that a given grocery bag is either number 2 (high-density polyethylene [**HDPE**]) or number 4 (low-density polyethylene [**LDPE**]). And there is a problem with composite products. Even the symbol on the base of a 2-liter soda bottle is somewhat ambiguous. The symbol is number 1 (**PETE**). While it is true that the clear bottle is, indeed, PET, often a base made of number 2 (HDPE) is placed over the round bottom of the bottle. Also, the bottle usually will contain small amounts of paper (label) and poly(vinyl acetate) (adhesive) in addition to a metal or **PP** cap with a copolymer liner.

There are other limitations on the system. PET from bottles is of a higher molecular weight than that used for fibers, so PET mixtures will not always be the same on recycling. It remains to be seen whether or not the identification code will be applicable for consumer sorting of more long-lived products such as garden hose (PVC) and pantyhose (nylon). Multicomponent products that do not come apart easily (laminated food trays, some food product bottles) were previously lumped in the “Other” category, number 7. More recently, this number has also been assigned to PLA.

On the whole, consumer sorting is a real step forward and greatly simplifies fuller treatment of any type. The environmentally aware consumer is able to take an active part in a process of great symbolic and some real significance. Because they are such

bulky items, removal of aluminum, glass, and plastic containers from the municipal waste stream has a very perceptible impact on any disposal system. The recycling of PET bottles reached over 41% in 1993 [49]. Bottle deposit laws are especially effective in gathering the bottles into central depots.

The ease with which materials can be identified and separated varies with the source of supply. Most automobile (lead–acid) batteries are made with PP casings. Since the metal in the batteries is reclaimed (97% recovery in 1999), the casings represent a centralized and relatively homogeneous source of one polymer. In 1990 it was reported that almost 150 million pounds of PP were recovered annually in the United States, representing as much as 95% of all discarded batteries. About 40% of the recovered PP went into the next generation of batteries, with the balance going into other automotive products and miscellaneous consumer products [50]. Automobile tires, however, contain several different polymers in addition to the metal bead and fabric reinforcement. The reuse of tires by separating all the components is economically unsound.

It has been suggested that automobiles, along with many other consumer products, should be designed for easy disassembly so that components can be separated and identified more easily. A drawback of the plan is the possibility of encouraging theft and vandalism. Nonetheless, manufacturers in Europe and the United States appear to be investigating the idea. Automatic methods of separating commingled plastics into homogeneous streams have been suggested. Manual sorting of recovered containers is still the rule for most processors.

15.7.2 SIZE REDUCTION

After any presorting, the scrap must be reduced to a manageable processing size. Shredders and granulators are employed to do this. The standard chip size is 0.25 in (~0.6 cm). Chips larger than this size have been determined to cause bridging and plugging within the process. The price for the smaller particle size is a decreasing granulator capacity. If shredded bottles are purchased from a supplier, as sometimes happens, only the granulation step is needed. These steps are industry standard.

The granulation of bottles and other scrap can be responsible for loss of physical strength. The application of mechanical shear in shredders and granulators breaks the polymer chains into smaller fragments. The decrease in chain size, and thus the molecular weight, can cause a corresponding degradation of the mechanical properties of the polymer. Mechanical properties are responsible for a substantial part of value of most plastics used in films and containers. As long as mechanical reduction of particle size is employed, this is a consideration.

15.7.3 DIRECT FLOTATION

Once a mixture of plastics is reduced to chips on the order of 0.6 cm in diameter, liquids with intermediate densities can be used to differentiate polymers, assuming that the polymers do not contain fillers that alter their density. A mixture of the six plastics listed in Table 15.6 can be separated into two groups using water. The polyolefins (numbers 2, 4, and 5) will float and the others (numbers 1, 3, and 6) will sink.

Further differentiation of the polyolefins requires liquids that are lighter than water and that do not swell the polymers. Aqueous solutions of methyl or ethyl alcohol are applicable. A solution of sodium chloride in water can be used to separate PS from the two denser polymers. However, separation of polyester (PET) from PVC is complicated by the fact that many variations in compounding PVC result in densities that can be greater or less than that of PET.

There are other complications in using float–sink separations. The adhesion of a small bit of label made of a different material alters the apparent density of a chip. Fillers and dirt may increase the apparent density. The method is obviously of greatest use when the overall composition of the mixed plastic stream remains relatively uniform.

15.7.4 FROTH FLOTATION

A variation of direct flotation is **froth flotation**. In this process, a stirred tank is generally employed, with air sparged in from the bottom. The feed also enters from the bottom. Originally a tool of the mining industry, it operates on the principle of the affinity of different materials for air bubbles. Materials with lower wettabilities will cling to air bubbles and rise to the surface. Frothing agents provide a stable froth in which floated materials remain suspended [51]. In the case of PET recycling, though, the wettabilities of the HDPE and PET would be too close for effective separation. Indeed, surfactants are usually added to the direct flotation column to ensure that froth flotation does not occur. Disposal of these chemicals is a problem. At present, direct flotation is the preferred approach to HDPE removal.

15.7.5 WATER REMOVAL

The presence of water will not only impair the electrostatic separation of plastics and aluminum but also severely interfere with any extrusion operations downstream. The maximum water level for extrusion is about 1 ppm [52]. Water levels of less than 0.5% must exist for effective electrostatic separation. As washing, rinsing, and flotation are key steps in recovery processes, some mechanism for water removal must be present.

One process uses *spin-drying* followed by a desiccant bed to achieve drying [53]. Spin-drying presumably refers to centrifugal drying, as is employed by a household washer. It could also be combined sequentially with heat drying methods. A countercurrent direct-heat rotary dryer is a possibility. In this device, the feed enters the top of a rotating drum that is tilted at an angle. Hot gases pass up the drum, drying the feed. This is the most thermally efficient of the rotary dryers [54]. Centrifugal drying by itself is more efficient in terms of energy but cannot remove as much water as hot air dryers.

15.7.6 PAPER REMOVAL

Paper labels often are attached to plastic products. The paper is generally removed first. Two approaches are currently practiced. One uses a fluidized bed and the other uses a cyclone. Both of these approaches are gravimetric. Thus, it should be kept in mind

that product loss is possible if polymer particles are of the same mass as the paper. Grinding to too fine a size must be avoided if a clean separation is to be achieved.

In the **fluidized bed**, air is fed into the bottom and the feed enters near the middle of the bed. When the lifting force of the air overcomes the force of gravity, the particles rise. The lightest particles are pushed out the top and the heaviest sink to the bottom, where they are removed. The particles exist in a gradient throughout the column. Several cuts can be taken from the bed.

A **cyclone** is generally conical in shape, with the feed entering tangentially at the top, the widest part. The outlets are at the bottom and through a pipe whose mouth is lower than the feed entry point. Having the feed enter off-center causes the linear velocity of the stream to be translated into angular velocity. Acceleration rates of several hundred gravities may be easily achieved this way. A vortex is formed, with the lightest material in the center and the heaviest toward the outside. Due to the nature of the vortex formed, material inside the vortex moves upward and out the top of the device. Material outside the vortex moves downward. In this way separation is simply and effectively accomplished. The cyclone offers simplicity to the process and thus lower capital costs and easier operation.

Fluidized beds offer more flexibility than cyclones in that more than one cut of material may be taken. This is valuable if partial recycling of the product stream is necessary. However, a second cyclone may be used if the first is not effective enough. Indeed, the use of a sequence of cyclones is a standard approach to many separation operations. Being more complex, fluidized beds are more expensive. There is a trade-off between price and efficiency

15.7.7 METAL REMOVAL

Two cases must be considered in metal removal: One may assume that aluminum is the only metal present or that some ferrous contaminants are present as well. If ferrous components are assumed to be present, magnetic separation must be employed [55]. This is generally performed in a drum separator. This would be the case only if very impure feedstocks were being used.

To separate aluminum from plastics, gravimetric, densimetric, or electrostatic means can be employed. Gravimetric methods have been less favored, mainly because separation depends on the particle size as well as the density. It is quite likely that some metal particles will settle more slowly than the plastic, if only because of their small size. However, metal particles will always be denser. One firm that has used this approach uses an *eddy current* separator combined with a fluidized bed to effect removal [56].

Electrostatic separation takes advantage of the difference in the conductivities of materials to sort them. Conducting materials will lose a charge more quickly than insulators. If charged pieces of both materials pass over a grounded drum and then fall past a rotating charged object, the weaker conductor will be more strongly attracted because it will retain more of its original charge. Thus, separation is achieved by the deflection of the insulating fraction away from the conducting fraction. The typical electrostatic separator is based on ion bombardment. An electric discharge forms a corona in which air is ionized. These ions contact the surface of the particles, transferring their charge [57].

15.7.8 DISSOLUTION

A second general method of separation is by **selective dissolution** and **precipitation**. In principle, this method is capable of purifying bonded, blended, and filled plastics. Dissolution of the polymer releases the impurities, which can be removed by filtration, adsorption, or flotation/sedimentation [58,59]. This is capable of yielding a polymer of high purity. The major drawback of a solvent system is the increased expense due to the complexity of equipment and the higher energy requirements.

Research on solvent-based polymer separation processes is by no means in its infancy. One of the first studies on mixed plastics was conducted by Sperber and Rosen [60,61] in the mid-1970s. These investigators used a blend of xylene and cyclohexanone to separate a mixture of PS, PVC, HDPE, LDPE, and PP into three separate phases. In addition, many US and foreign patents dating from the 1970s were granted for the solvent recovery of thermoplastic polymers. The interest in solvent processes waned in the late 1970s as the oil crisis eased, but the growing need to develop solutions to the solid waste problem has renewed the research effort.

Early investigators of solvent processes for mixed plastics [60,61] could not foresee the penetration of PET into the packaging industry, so their processes did not address the separation of PET from mixtures. The **Rensselaer Polytechnic Institute (RPI) process** [62], a much later research project on mixed plastics, did include the separation of PET. This process utilizes a single solvent (either tetrahydrofuran or xylene) to separate the polymers in batch mode based on the temperature-dependent dissolution rates of each resin. The polymer solution is then exposed to elevated temperatures and pressures before the flash-devolatilization of the solution. In addition to the high pressures required in the feed to the flash stage, elevated pressures are required in the dissolution stage of the RPI process because the normal boiling point of the solvent is below the temperature required to achieve PET dissolution. The use of elevated temperatures increases the risk of thermally degrading the polymers, while the elevated pressures translate into higher energy and equipment costs. An additional limitation of the RPI process lies in the use of a single solvent capable of dissolving all of the polymers. This reduces the purity of the final polymer streams due to the partial dissolution of polymers that were intended to be dissolved at a higher temperature and the carryover of undissolved polymers to a higher temperature-dissolving fraction. These limitations can be overcome by using multiple solvents, with each solvent being compatible with only a limited number of polymers at reasonable temperatures, and by incorporating a less energy-intensive recovery stage. In addition, lower cost processes could be employed to make initial separations.

15.7.9 COMBINED TECHNOLOGY

Each separation process has its merits and limitations. It would seem logical that a process combining various separation technologies could take advantage of the inherent strengths of an individual process while attenuating the limitations. For example, a combined technology process could utilize a flotation system to produce segregated polymer streams that could then be further purified in solvent-processing

trains. The strength of the flotation system is cost-effectiveness, but it is limited by the relatively low purity of the final products, as is true of all compositionally blind separators. Selective dissolution processes, however, can yield polymers of high purity but at an increased cost.

15.8 DOWN-CYCLING

The recycling of polymers is generally considered to be the most environment-friendly alternative for dealing with the disposal problem. Even if consumers can be persuaded to segregate polymer products before putting them into the municipal waste stream, there will always be the matter of separating (1) inadvertent mixtures and (2) multi-component products. One process that seems economically attractive in the current market is to separate *impurities* from a stream that is predominantly one polymer by using differences in density. The older PET beverage bottle with a polyethylene base is a case in point. Of course, there is the alternative of not separating the components of a waste stream, but to make a *plastic lumber* out of a mechanical mixture of polymers.

In general, a polymer recovered from a waste stream will have inferior physical properties compared to the original material. The exception to this rule is polymers produced by repolymerization of monomers recovered from waste. Virtually all polymers deteriorate after undergoing production processes involving heating and shearing, and weathering processes including oxidation, hydrolysis, or exposure to sunlight. Moreover, almost all commodity polymers are mutually immiscible. This means that any mixture of polymers will be likely to fail mechanically under less stress than pure materials. For this reason, recycling often takes the form of **down-cycling**; that is, the polymer is put into a less demanding application than the one from which it was derived. For example, 60%–70% of the 400 million pounds of PET recovered from beverage bottles in 1992 was used to make fibers for carpet yarn and the fibrous packing (fiberfill) that goes into pillows and bedding [63]. Another characteristic of down-cycling shown by this example is that it converts a material from a short-term usage (typically packaging) into a long-term usage such as construction, furniture, or decorative items.

Nonetheless, a great deal of work has been done to devise consumer products that can be made from mixtures. **Plastic lumber** is a term often used to describe forms that can be converted into park benches, shipping pallets, and flooring. Even when a single source of plastic is used, a mixture may be economically attractive. One plastics producer combines recovered HDPE from grocery sacks and stretch wrapping with an equal weight of sawdust (from discarded wooden shipping lumber) to make a product said to compete with top-grade treated marine lumber and clear cedar [64]. Factory floors are a suggested use. Some ways in which mixtures can be modified is by the addition of compatibilizing resins (often block copolymers) and by fillers.

Some pros and cons for plastic lumber in comparison with wood for outdoor furniture and decking have been enumerated by Scheirs [65]:

Pros

- Grain free
- Graffiti resistant (smooth surface)
- Low in moisture absorption

Cons

- More flexible than wood (4–5 times)
- Heavier than wood
- More tendency to creep
- May require special fasteners (to prevent loosening)
- Often more expensive

A general approach to using unsorted plastic mixtures involves granulation, mastication, heating, and molding. Dark colors usually are chosen in order to minimize the nonuniform appearance. In a lumber process developed at the Center for Plastics Recycling Research at Rutgers University, New Brunswick, New Jersey, the lower melting plastics in a mixture act as a flowable matrix in which as much as 40% of nonflowing materials such as paper, metal, glass, dirt, and cross-linked plastics can be accommodated [66].

15.8.1 FILM RECLAMATION PROCESS

In any reclamation process, certain steps are essential. For example, recovery of polyethylene from soiled agricultural film involves size reduction, washing, drying, and regranulating [67]. Agricultural film from mulch and packaging may be 25–150 μm thick and may contain as much as an equal weight of soil. Similar materials may be recovered from construction operations. A schematic flow sheet for a process owned by Herbold, a German machinery supplier (Figure 15.7), starts with bales of the soiled film being fed to a shredder that operates at a slow speed and has specially toughened, blunt blades that will not be worn rapidly by the soil particles. The coarse pieces of film are conveyed to an air separator followed by a grinding and washing tank. Most of the water and dirt is removed in the dewatering screw and is filtered or centrifuged to yield a sludge (*schlamm*) and a stream that goes to a water treatment plant. The washed product goes to a mechanical dryer followed by a cyclone separator to recover fines and, finally, a hot-air drying section leading to storage. Not shown are an extruder and pelletizer for converting the polymer into a form suitable for return to a film production line. It is obvious that even a relatively homogeneous entering stream involves a sizable capital investment and running costs for water and power. For a plant with

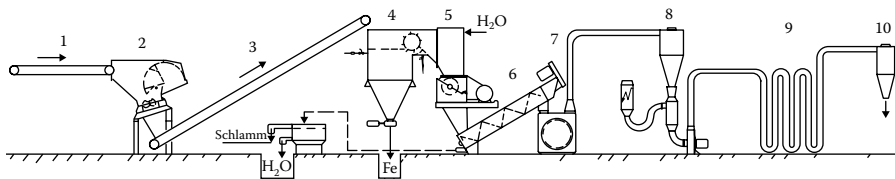


FIGURE 15.7 Facility for washing and size reduction of plastic scrap: 1, base material feeder; 2, shredder; 3, conveyor belt to preliminary size reduction; 4, separation of coarse matter; 5, wet grinder; 6, dewatering screw; 7, mechanical drier; 8, cyclone separator; 9, hot-air dryer; 10, cyclone separator (to storage). (Data from Herbold, K., *Kunststoffe: German Plastics*, 1989.)

a throughput of 500 kg/h (4 million kg/yr), the energy needed for size reduction, washing, and drying is about 0.3 kW·h/kg. Additional energy would be required for the pelletizer.

15.9 MONOMER RECOVERY

In principle, recovery of monomers and **repolymerization** should result in a product that is indistinguishable from the original polymer. PS and poly(methyl methacrylate), when heated with a free-radical source under vacuum, give high yields of the respective monomers (see Section 11.3). Poly(dimethyl siloxane) heated with KOH in a vacuum also produces a cyclic monomer. All of these processes are used for in-plant scrap treatment, but economics do not yet favor applying them to postconsumer plastic waste.

When PET is heated with an excess of methanol, a mixture of dimethyl terephthalate and ethylene glycol is produced [68]. In one example, a 1:4 mixture of polymer and methanol is said to produce a 99% yield of monomers after 1 h at 160°C–240°C and 20–70 atm. The process is somewhat sensitive to contaminants such as some of the dyes used in beverage bottles. Since polyester bottles are very difficult to distinguish from PVC, chlorine contamination at a low level is hard to avoid. The chlorine can interfere with subsequent repolymerization. A number of variants on the methanolysis route have been described. A second route [68] to depolymerization is **glycolysis**. Transesterification of PET with an excess of propylene glycol in the presence of a catalyst such as an amine, alkoxide, or metal acetate is used to obtain low-molecular-weight fragments with hydroxyl end groups. Glycolysis for 8 h at reflux (200°C) with a 1.5:1 ratio of glycol to PET results in a polyol with a number-average molecular weight of 480. The polyols are recommended for use in making polyurethanes (by reaction with isocyanates; see Sections 4.7 and 17.5).

Polyurethane scrap from industrial processes such as reaction injection molding, foam production, and recovered auto parts can also be treated with steam or glycols [69]. Yields of 60%–80% of polyols and diamines have been reported from polyurethane foam scrap using steam under pressure at 288°C in a continuous vertical reactor with a residence time of 10–28 min. Glycolysis as an alternative to steam hydrolysis produces a mixture of polyols. Digesting ground-up polyurethanes in a 90:10 mixture of di(alkylene)glycol/diethanolamine for several hours at 190°C–210°C gives a mixture which, after treatment with propylene oxide, can be used as part of the polyol charge in making rigid polyurethane foam.

Somewhat similar is the **devulcanization** of rubber, in which a sulfur cross-linked network is converted to a system of more-or-less thermoplastic components. Rubber reclaiming has fallen on hard times for various reasons, including the difficulty of making an environmentally attractive process.

15.10 HYDROGENATION, PYROLYSIS, AND GASIFICATION

Straightforward reversion to monomers is not convenient with some of the commodity polymers, namely, polyethylene, PP, and PVC. An omnibus solution is to use some sort of nonoxidizing thermal treatment that will produce a low-molecular-weight product. The terms **chemical recycling** and **plastics-to-chemicals** are used for such processes.

15.10.1 HYDROGENATION (LIQUID PRODUCT AND HYDROGEN ATMOSPHERE)

A plant in Germany was modified to accept ground-up plastic wastes as a partial feed. The plant, originally built to process coal to synthetic fuel, had been converted to oil sludge upgrading. The process has been described as follows [42]:

The unit recycles up to 40,000 metric tons per year of mixed plastic containing up to 10% PVC. Up to 20% of its feed will be milled plastic particles less than 8 mm in diameter. [The] unit operates at 150–300 bars and about 470°C in a hydrogen atmosphere, producing a **syncrude** containing 60% paraffins, 30% naphtha, 9% aromatics and 1% olefins. Chlorine... is converted to HCl in the reactor, then neutralized with calcium carbonate.

15.10.2 PYROLYSIS (GASEOUS PRODUCT AND INERT ATMOSPHERE)

In a **pyrolysis** plant tested in Great Britain, a sand bed is fluidized using some of the cracked gases produced by thermal cracking of plastics introduced as chips or strips. A mixture of polyolefins and up to 10% PVC is cracked at 600°C in an inert atmosphere to yield a naphtha-type gas. Mass yields are about 90%, and 10% of the gas is used to heat the bed. Chlorine is adsorbed within the bed by calcium oxide. Sand beds can be quite insensitive to the size of material fed. Kaminsky graphically describes one reactor that produced a mixture of gas, liquid, and carbon black from scrap tires [70]:

The whole tires roll through a gas tight lock into the reactor. The tire, landing on the fluid bed gradually sinks into the sand. The material heats up and softens, its surface becoming covered with hot sand grains. Through the shearing forces of the fluid bed and “exchange” of sand grains takes place at the surface of the softened material; the abrasion of small particles and their decomposition begins. A methane and ethylene rich gas as well as a condensable liquid with a high percentage of aromatics are produced. The main part of the filler materials (carbon black and zinc oxide) is blown out of the fluid bed and can be separated in a cyclone. After 2 or 3 minutes the tire is completely pyrolyzed. What remains in the sand bed is a mass of twisted steel wires, which are removed by a tiltable grate extended into the fluid bed.

15.10.3 GASIFICATION (GASEOUS PRODUCT AND OXIDIZING ATMOSPHERE)

Gasification proceeds under higher temperatures (above 900°C) than pyrolysis and often under oxidizing conditions. It is essentially a two- or three-step incineration. An Italian pilot plant [42] has the following operating parameters:

Input per hour: 4200 kg of MSW, compacted and degassed

Output per kilogram charged:

660 kg of syngas

220 kg of slag

23 kg of metals

18 kg of salts

The compacted waste is pyrolyzed at 600°C and then fed to a gasifier at 2000°C and pressures of 20–65 bar. The **syngas** after cleaning is used to drive a gas turbine producing 300 kW of electricity.

15.11 INCINERATION WITH ENERGY RECOVERY

A one-step **incineration** with energy recovery is possible under a variety of circumstances. Among the many possibilities, three specific kinds of facilities can be differentiated: power plants, incinerators, and cement kilns. In a power plant, dry polymer waste is an additive to a standard fuel (coal, oil, or gas). In an incinerator, the usual feed is a mixture of polymers, paper, and other components of the MSW stream. Because paper and other cellulosic materials have a lower energy value and because water is evaporated, the total energy recovery is lower than from plastics or tire-burning power plants. In both power plants and incinerators, energy is recovered in the form of steam, which in turn is used to generate electricity. Also, in both, the disposition of gases and solid residues must be dealt with. However, burning waste in a cement kiln makes use of the energy to produce the cement, and the solid residues may be incorporated in the product.

15.11.1 POWER PLANTS

Most power plants have automatic feed mechanisms that will not accommodate odd shapes of solid feed. A mixture of chipped or powdered waste with coal or oil is preferred. For example, tires are combined with bituminous coal at the Jennison generating station near Bainbridge, New York [71]. The two generating units were built in 1945 and 1950 with a total capacity of 73 MW. Scrap tires are delivered to the power plant, where a chipper reduces them into 5 × 5 cm chips. The tires are delivered from various sources such as businesses, service groups, and municipalities that pay a fee to get rid of the waste. Before the unit could operate, state and local regulations presented hurdles to be overcome. The stoker boilers are fed by traveling chain grates, which have proved to be quite adaptable for conveying the mixture of chipped rubber and coal in a 1:4 ratio. With a boiler flame temperature of 1650°C, no problems have been reported with soot or odors. As in any power plant, fly ash is collected and sold to a cement manufacturer as a raw material. The metal from the tire chips melts into small clumps in the bottom ash and is removed by magnetic separation before storage. The bottom ash accumulates and is eventually used by local municipalities as a road traction agent, a necessity amidst the ice and snow of upstate New York winters. The average heat value of a 20-lb passenger car tire (13,000 Btu/lb) is equivalent to 30 lb of coal. Although the tires contain sulfur, the overall composition is favorable for clean combustion. When mixed plastics are used, a question often arises about HCl generation from PVC, with a consequent corrosion problem in older power plants. New plants can be designed with proper controls to minimize corrosion problems.

A California plant was built in 1987 to generate 15 MW using only tires as fuel [72]. The grate in this plant feeds whole tires into the boiler. The emission controls system is a vital part of the operation including removal of fly ash and bottom ash as well as flue gas desulfurization and thermal treatment of NO_x. The selling price of

power in 1989 was 8.3 cents per kilowatt-hour, giving total sales of about \$10 million from about 4.9 million tires. The wild fluctuations in the price of energy that have been seen over the years make the economics of any such plant problematical.

15.11.2 INCINERATION

Although **incinerators** have been in use for many years, the modern incinerator is a waste-to-energy facility with many features that older models do not possess [73]. In a typical plant (Figure 15.8), trucks deliver waste to a storage pit, from which it is loaded into a hopper above the charging chute. Hydraulic rams located at the bottom of the chute are used to push the fuel onto moving grates. On the grates, three successive stages are drying, combustion of volatiles, and a completion of the burning of solids. Steam is generated in the tubes lining the boiler. The three main streams leaving the incinerator are the ash from the bottom of the grate, the fly ash collected by precipitation or filtration, and the gases discharged after being scrubbed. Since the average heating value of MSW is less than half that of coal, an incinerator is not nearly as efficient a generator of power as a dedicated power plant. Arguments still rage over the desirability of building large, centrally located plants for the **mass burn** of MSW.

A rather negative view of MSW incineration has been detailed by the Environmental Defense Fund [74]. The arguments cited include the following:

1. *Expense.* To benefit from the economy of scale, most proposed incinerators are designed to handle refuse from a wide area. Construction costs typically are in the hundreds of millions of dollars. Local governments may have to participate in bond issues, special taxes, and tipping fees in order to build and maintain the operation.
2. *Solid residue (ash) disposal.* If the plant handles unsorted MSW, as much as 20%–30% by weight of the charge is noncombustible material. The resulting residue must be disposed of by land filling. There are concerns about leaching of heavy metals from the landfill into potable water sources.
3. *Air emissions.* Aside from CO₂, about which there is concern over the *greenhouse* effect, there are fears that other objectionable gases may be discharged.
4. *Effect on conservation.* A major objection by environmentalists is that mass-burn incineration removes any incentive by consumers and governments to get on with recycling, which is regarded as the most environment-friendly alternative.

15.11.3 CEMENT KILNS

Burning tires in a cement kiln is attractive, since the tires replace more expensive fuels. Usually the tires have to be reduced to pieces that are 5–15 cm long, in which form they are referred to in the trade as **tire-derived fuel**. A cement plant in California derives about 25% of its energy needs from shredded tires, the balance being coal [75]. The temperatures in cement kilns (1450°C), long residence times, and an excess of oxygen assure complete combustion. Moreover, even the steel from the tire beads can become part of the cement product and does not have to be removed as a separate stream.

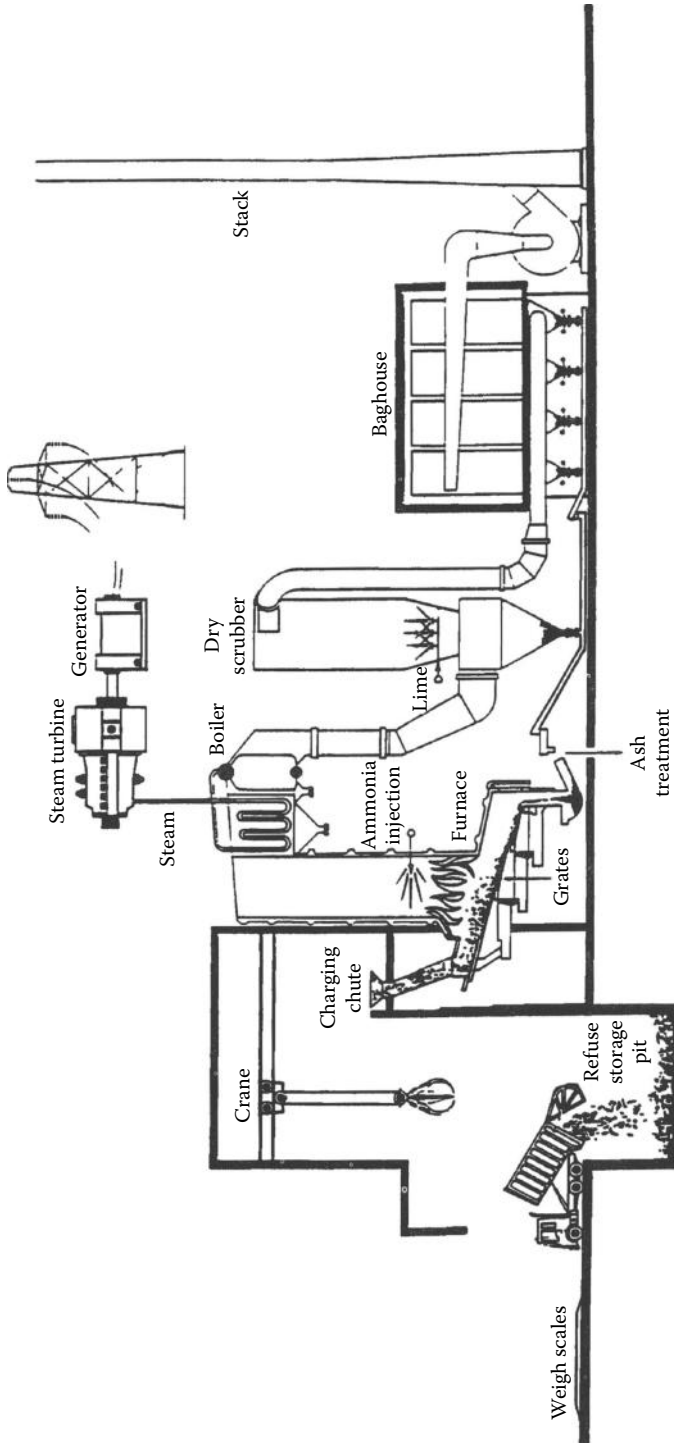


FIGURE 15.8 Refuse-to-energy incinerator at Commerce, California. (Data from Wheless, E., and S. Thalenberg, *The Design and Operation of an Ash Treatment System at the Commerce Refuse to Energy Facility*, in *Proceedings of the 1992 National Waste Processing Conference*, 1992, p. 165. Copyright The American Society of Mechanical Engineers. Used with permission.)

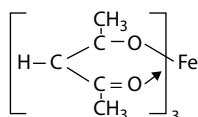
15.12 DEGRADABLE POLYMERS

Many people, including producers, consumers, and municipal waste collectors, would be very happy if postconsumer polymers would simply disappear without any particular effort on anyone's part. This is the attraction of the **degradable polymer**. Unfortunately, the reality is that even paper and food products do not *disappear*, as has become abundantly clear to those who have excavated landfills and found readable newspapers that are decades old [38]. There certainly are polymers that are truly degradable and there certainly are applications besides environmental concerns for which degradability is a valuable property. Despite the progress reported above and the push for developing polymers from renewable resources, many of which are biodegradable, there seems very little likelihood that the commodity resins used today are going to be entirely replaced by degradable materials soon.

There are many ways in which polymers may degrade (see Chapter 12). However, in developing *disposable* polymers, three main pathways can be distinguished: photooxidation, hydrolysis, and biodegradation.

15.12.1 PHOTOOXIDATION

A combination of sunlight and oxygen is capable of changing the structure of most hydrocarbons [76]. Although polyethylene is relatively stable under such circumstances, the incorporation of carbonyl groups in the main chain can increase the absorption of photonic energy in the ultraviolet range and also can provide a site at which chain scission will be favored. Additives have been used which will promote photooxidation even when they are not part of the polymer. One such additive is Fe(III)-acetylacetonate:



The additive may actually delay the apparent effects of oxidation, while hydroperoxide groups are formed. However, eventually the chain-scissioning process predominates and molecular weight decreases. The decrease in molecular weight leads to an increased vulnerability to biological attack. Thus, one often encounters photodegradation being recommended as an adjunct to biodegradation. **Photodegradable plastics** at one time seemed to be the answer to the problem of litter or, at least, to the problem of certain classes of litter. Some products that have been marketed include beverage rings, agricultural mulch, and hot drink lids.

15.12.2 HYDROLYSIS

Most polyesters, polyamides, and polyurethanes are susceptible to hydrolysis with a consequent decrease in molecular weight. Aliphatic polymers often hydrolyze more rapidly than aromatic polymers. Once again, the lower molecular-weight materials are subject to biological attack. The hydrolysis itself may be part of enzymatic attack on the main chains. Some polyurethanes based on polyester polyols are easily

hydrolyzed, especially if they are in the form of a foamed structure with a very large surface-to-volume ratio. However, most of the condensation polymers used in films, fibers, and castings do not hydrolyze on casual contact with water. Elevated temperatures and catalysts will accelerate the process.

15.12.3 MICROBIAL DEGRADATION (BIODEGRADATION)

The term **microbial degradation**, as used to describe the fate of plastics in the environment, embraces any change in physical properties brought about by burial in microbially active soil. Soil burial suffers as a laboratory technique for judging degradability because large samples are required and the conditions of exposure are not always reproducible. The **clear zone technique** [77] can be applied to water-immiscible polymers and gives relatively rapid (days rather than months) indications of change. The polymer is suspended in a nutrient agar medium poured into Petri dishes. The dilute suspension is hazy. As a colony of cells grows on the surface of the gel, a clear zone may occur in the medium surrounding the colony. From this, one can infer that the polymer has been metabolized. Usually this would occur by the excretion of an **extracellular enzyme** (or more than one) by the organisms. In the case of a polyester, the steps of metabolism might be hydrolysis followed by digestion with growth of cells or oxidation to carbon dioxide and water.

Another, more quantitative technique can be used to measure actual digestion rates. A thin layer of polymer is deposited on the bottom of a Petri dish (Figure 15.9) [77]. The dry film is weighed and then a layer of nutrient agar medium is poured over the polymer. The plate is then inoculated with a suspension of microorganism and incubated. The polymer is recovered after the incubation period and the loss in weight is measured. Sterile plates also are prepared for comparison. These distinguish nonmicrobial degradation such as hydrolysis from the truly microbe-mediated effects. In one test [78], several polyesters were compared after being exposed to the organism *Pullularia pullulans* for 21 days at 30°C (Figure 15.10). The polymers were similar in structure, but the rate of erosion differed significantly. At intrinsic viscosities above about 0.4 dl/g, the weight loss was hardly measurable.

15.12.4 COMMERCIAL AND NEAR-COMMERCIAL DEGRADABLE POLYMERS

A variety of products have been made from mixtures of photodegradable polyethylene and starch. A **pro-oxidant** based on transition metals and lipids might be added. It would appear that the starch part of the composite does degrade, but the polyethylene portion survives much longer, albeit in a weak and flimsy condition. A review

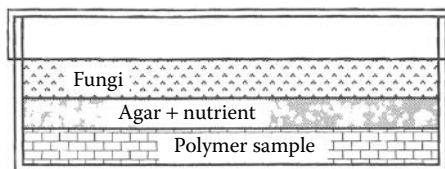


FIGURE 15.9 Quantitative measurement of polyester degradation. (Data from Fields, R. et al., *J. Appl. Polym. Sci.*, 18, 3571, 1974.)

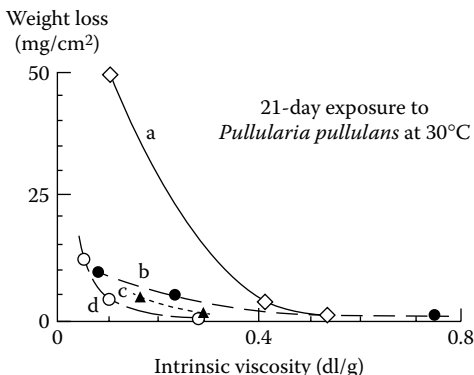


FIGURE 15.10 Degradation of polyesters: (a) copolymer of tetramethylene adipate and sebacate, 1:1 mole ratio; (b) homopolymer of adipate; (c) homopolymer of sebacate; (d) polycaprolactone. (Data from Fields, R. D., and F. Rodriguez, in J. M. Sharpley and A. M. Kaplan, eds., *Proceedings of the 3rd International Biodegradation Symposium*, p. 775, Applied Science, London, 1976.)

article [79] cited the following kinds of products as being marketed with claims to biodegradability (see also Table 15.7):

- Entirely starch-based polymers
- PLA and copolymers containing LA
- Polycaprolactone
- Water-soluble polymers; poly(vinyl alcohol) is said to biodegrade after dissolving unmodified, naturally occurring polymers

In the last category, PHB, a polyester produced by fermentation, has received a great deal of attention (see Section 15.5.1).

Cellulose (cotton) and natural rubber are biodegradable polymers that have had many uses over the years, almost none of them benefiting from biodegradability. In fact, the treatment of cotton to combat mildew and the addition of biocides to latex compounds is much more in the tradition of commercial uses than working in the opposite direction.

TABLE 15.7
Some Biodegradable Polymers

Monomer Name	Polymer Repeat Unit
Glycolic acid	—CH ₂ —CO—O—
Lactic acid	—CH(CH ₃)—CO—O—
Caprolactone	—CH ₂ —CH ₂ —CH ₂ —CH ₂ —CH ₂ —CO—O—
β-Hydroxybutyrolactone	—CH(CH ₃)—CH ₂ —CO—O—
β-Hydroxyvalerolactone	—CH(CH ₂ —CH ₃)—CH ₂ —CO—O—
Vinyl alcohol	—CH ₂ —CH(OH)—

15.12.5 APPLICATIONS

Almost all producers of degradable polymers aim for large-scale commodity markets such as packaging. Trash bags, grocery bags, and nonfood containers have been explored with marginal results. Certain niche applications, however, are much more successful. In the medical area, degradable sutures have been sold for many years. **Absorbable sutures** have been made from collagen (extracted from calf skins) and from synthetic polymers, notably the copolymer of GA and LA (see Table 15.7).

A polymer that erodes can be used as the host for a drug delivery system. As the polymer is removed from the surface, usually by biodegradation, the drug dispersed in the polymer becomes available in the body (see Section 13.7). An agricultural application with the same idea uses the slowly degrading polymer as a host to deliver pesticides, herbicides, or fertilizers, especially when combined in a tree planting container [80]. The construction of a facility for making a degradable polymer, PLA, from corn on a large scale is aimed at the packaging and fiber markets (see Section 17.2).

15.13 PROSPECTS

Certain aspects of conservation present paradoxical alternatives. The effort to reduce the amount of material in packaging, for example, often requires the use of a material that is more difficult to recycle. The use of an easily recyclable polymer may require the use of expensive raw materials or less efficient processing. A case in point is the modern automobile tire, which makes use of steel, inorganic or organic fibers, several different rubbery polymers, and a variety of compounding additives (see Section 11.2). A passenger car tire composed of one polymer without reinforcement or compounding ingredients has not yet been designed for highway use.

Energy recovery is attractive since it does not usually involve separation of components. In the case of some consumer items, the curb-side separation of polymers may be extended to all six currently identified plastics. This could make recycling processes for LDPE, PVC, PP, and PS as attractive as current programs for HDPE and PET.

There is a hierarchy of aims that consumer groups, polymer producers, and politicians might agree on with regard to polymer waste disposal:

- Reduce usage of polymers at the source by more efficient design.
- Reuse items.
- Recycle without separation (by melt processes).
- Recycle after separation (and design for ease of separation).
- Depolymerize.
- Convert to liquid fuels.
- Incinerate to recover energy.

When the entire **life cycle** of polymers is considered, it becomes obvious that no matter what steps are taken to reuse or recycle materials, the end products of the hydrocarbons (and other materials that are used to make polymers useful) are CO₂, water, energy, and some solid residues (Figure 15.11). Moreover, Figure 15.11 describes only some of the options that apply to polymers, primarily plastics, rubber, and fibers. Not

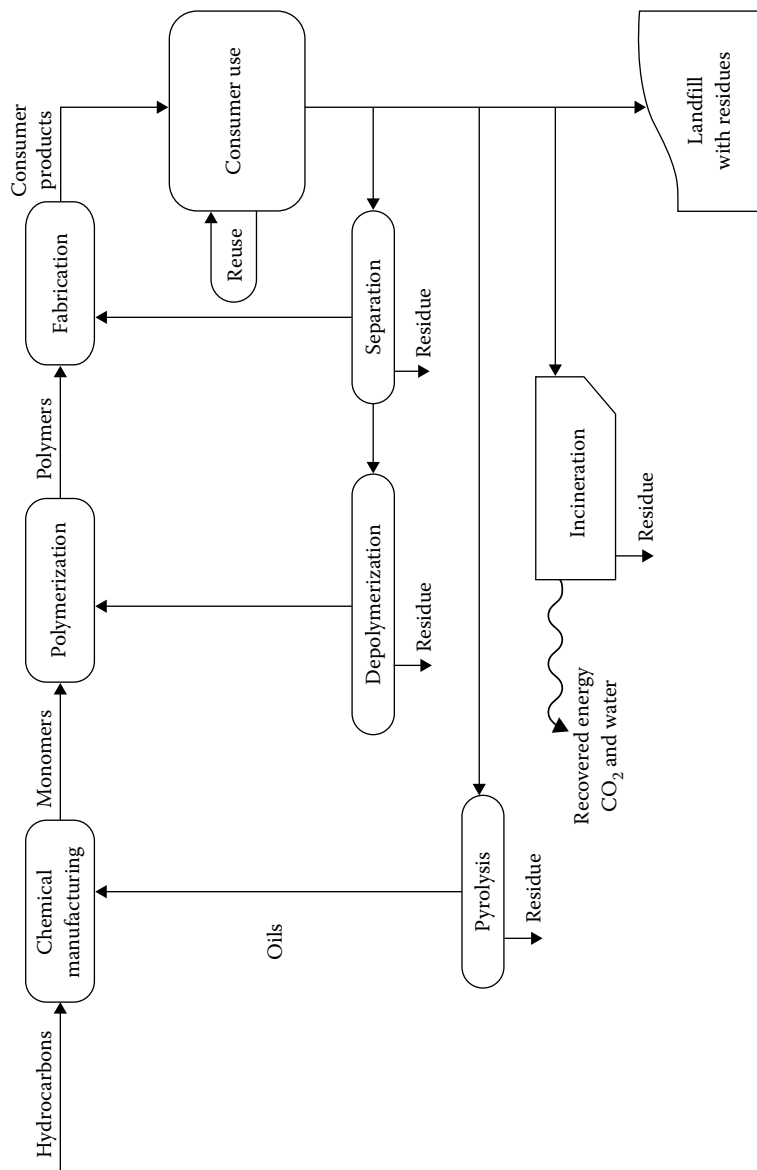


FIGURE 15.11 Polymer life cycle.

included are many other contributors to the waste stream, such as metal, glass, paper, yard wastes, manufacturing wastes, and sewage.

Every step in the process has inefficiencies that can be diminished but not eliminated. Also, every option has associated social and economic costs. Probably the one factor that overwhelms all other considerations is population growth. While some will think of this only in terms of their own country or community, the worldwide exponential growth of population together with the improvement in the standard of living should put the possible control of disposal by technical advances in perspective.

KEYWORDS

Cellulose
Pectin
Carrageenan
Chitin
Baratte
Xanthate
Cellophane
Cellulose nitrate
Cellulose diacetate
Ethyl cellulose
Hydroxyethyl cellulose
Silk
Fibrous proteins
Keratin
Fibroin
Collagen
Globular protein
Albumin
Casein
Zein
Ribonuclease A
Nucleic acid
Genomics
Nucleotide
DNA (deoxyribonucleic acid)
Polynucleotide
Chromosome
Genome
Poly(lactic acid) (PLA)
Poly(glycolic acid) (PGA)
Poly(hydroxyalkanoate) (PHA)
Poly(hydroxybutyrolactone) (PHB)

Suberin
Polyols
Triglycerides
Poly(propylene) carbonate (PPC)
Poly(acrylic acid)
Municipal solid waste (MSW)
Sanitary landfill
Postconsumer waste
Postconsumer recycle
Postindustrial waste
Downsizing
Rubberized asphalt
SPI container code
Flotation
Froth flotation
Fluidized bed
Cyclone
Electrostatic separation
Selective dissolution and precipitation
RPI process
Down-cycling
Plastic lumber
Repolymerization
Glycolysis
Devulcanization
Chemical recycling
Plastics-to-chemicals
Hydrogenation
Syncrude
Pyrolysis
Gasification
Syngas
Incineration
Mass-burn
Tire-derived fuel
Degradable polymer
Biodegradable polymer
Photodegradability
Microbial degradation
Clear-zone technique
Extracellular enzyme
Pro-oxidant
Absorbable suture
Life cycle

PROBLEMS

- 15.1** Suppose that a mausoleum were constructed in which the departed would be entombed in caskets made from compacted postconsumer polymer wastes with a density of 1000 kg/m^3 . Each casket would have a length of 3 m and an internal volume of 1 m^3 . The other two dimensions would be identical. If each of the 250 million people in the United States accumulates half of the total per capita output of polymers from 2000 (Table 1.1) for 80 years, what would be the necessary dimensions of the casket?
- 15.2** A small automobile averages about 30 mi/gal (12.75 km/l) of fuel. Assuming that the density of polyethylene is about 1.2 times that of gasoline and has a similar fuel value, the equivalent of how many shopping bags (6.0 g each) are required to move the automobile 1 mi (and also 1 km)? How many 1.75-g PS cups would be needed, assuming that the density of PS is 1.3 times that of gasoline, and the fuel value is slightly higher (say 1.2 times more than gasoline)?
- 15.3** A mixture of wet postconsumer plastic chips is received after removal of paper and metal. All of the six categories in Table 15.6 are included. Draw a flow sheet showing how the chips could be separated into four streams using three liquids. Include mixers, separators (filters or centrifuges), and dryers. Indicate any recycle streams. Liquids: water (1.00 g/cm^3), 20% NaCl in water (1.15 g/cm^3), and tetrahydrofuran (THF) (0.89 g/cm^3). THF is a solvent for PS and PVC at room temperature, but not for PET or polyolefins. Output streams: mixed polyolefin chips, PS chips, PET chips, and PVC as a solution in THF.
- 15.4** For the 15-MW California power plant mentioned in Section 15.11, what is the effectiveness of the plant expressed as power produced divided by the heat value of the fuel (tires)? The 4.9 million tires/year can be modeled as each weighing 20 lb with a heat value of 13,000 Btu/lb (1 Btu = 1055 J).
- 15.5** A plant is to be designed to produce styrene monomer from PS scrap. Current prices of PS and styrene monomer can be found in the *Chemical Marketing Reporter*. Suppose a plant to produce 10 million kg/year can be built for \$20 million and that plant cost scales with production to the power of 0.6. What is the minimum capacity plant (at the break-even point) that can produce monomer economically?
- Assumptions:
- Cost of clean PS scrap is one-third that of crystal molding PS.
 - Monomer recovery is 70% of scrap input.
 - Energy and disposal of residues costs \$0.08/kg scrap input.
 - Capital depreciation is 10% of the plant cost per year (10-year, straight-line depreciation). If no current prices are available, use the April 1995 prices of \$0.53/lb and \$0.47/lb for polymer and monomer, respectively.
- 15.6** If a product were made from the low-molecular-weight copolyester (Figure 15.10) with an intrinsic viscosity of 0.2 dl/g, how long would it take for article that is 1 mm thick to be completely digested? Remember that it would be attacked from both surfaces. Assume a polymer density of 1.1 g/cm^3 .

REFERENCES

1. Whistler, R. L., and J. N. BeMiller (eds.): *Industrial Gums*, Academic Press, New York, 1959.
2. Fieser, L. F., and M. Fieser: *Organic Chemistry*, 3rd edn., Heath, Boston, MA, 1963.
3. Warner, S. B.: *Fiber Science*, Prentice Hall, Englewood Cliffs, NJ, 1995, p. 105.
4. Brydson, J. A.: *Plastics Materials*, Van Nostrand, Princeton, NJ, 1966, p. 366.
5. Mitchell, P. H.: *A Textbook of Biochemistry*, 2nd edn., McGraw-Hill, New York, 1950, pp. 97, 98, 106.
6. Zhang, L., and M. Zeng: chap. 23 in M. N. Belgacem and A. Gandini (eds.), *Monomers, Polymers and Composites from Renewable Resources*, Elsevier, Amsterdam, The Netherlands, 2008.
7. Gutte, B., and R. B. Merrifield: *J. Am. Chem. Soc.*, 91:501 (1969); W. Sullivan: *New York Times*, January 17, 1969, p. 1; *Chem. Eng. News*, p. 15 (January 20, 1969).
8. Sryer, L.: *Biochemistry*, chap. 4, 4th edn., Freeman, New York, 1995; see also, special issue of *Nature* 421:396 (2003).
9. Averous, L.: chap. 21 in M. N. Belgacem and A. Gandini (eds.), *Monomers, Polymers and Composites from Renewable Resources*, Elsevier, Amsterdam, The Netherlands, 2008, p. 435.
10. Gupta, A. P., and V. Kumar: *Eur. Polym. J.*, 43:4053 (2001).
11. Zhang, R., and P. X. Ma: *Macromol. Biosci.*, 4:100 (2004).
12. Danhier, F., E. Ansorena, J. M. Silva, R. Coco, A. LeBreton, and V. Preat: *J. Control. Release.*, 161:505 (2012).
13. Ju, H. W., F. A. Sheikh, B. M. Moon et al.: *J. Biomed. Mater. Res. A*, 102(8):2713 (2014).
14. Holmes, P. A.: *Phys. Tech.*, 16:32 (1985).
15. Zhang, J.: *J. Appl. Polym. Sci.*, 91:1657 (2004).
16. *Chem. Eng. News*, January 23, 2012, p. 19.
17. Dawes, E. A. (ed.): *Novel Biodegradable Microbial Polymers*, Kluwer Academic Publishers, New York, 1990.
18. Holmes, P. A., L. F. Wright, and S. H. Collins: Beta-hydroxybutyrate polymers, European Patent Appl. No. EP 52 459 A1, May 26, 1982.
19. Sivestre, A. J., C. P. Neto, and A. Gandini: chap. 15 in M. N. Belgacem and A. Gandini (eds.), *Monomers, Polymers and Composites from Renewable Resources*, Elsevier, Amsterdam, The Netherlands, 2008.
20. Gandini, A., *Macromolecules*, 41:9491 (2008).
21. Cargill BiOH[®], <http://www.cargill.com/products/industrial/foam/>.
22. Tamano, K., K. S. Bruno, S. A. Karagiosis, D. E. Culley, S. Deng, J. R. Collett, M. Umemura, H. Koike, S. E. Baker, and M. Machida: *Appl. Microbiol. Biotechnol.*, 97:269 (2013).
23. Petrovic, Z. S.: *Polym. Rev.*, 48:109 (2008).
24. Luinstra, G. A.: *Polym. Rev.*, 48:192 (2008).
25. <http://empowermaterials.com/>.
26. Coates, G. W., and D. R. Moore: *Angew. Chem. Int. Ed.*, 43:6618 (2004); Cohen, C. T., and G. W. Coates: *J. Polym. Sci. A: Polym. Chem.*, 44:5182 (2006).
27. <http://www.novomer.com>.
28. US Patent 6,133,402.
29. www.pmahome.org/files/1713/6613/8001/Novomer_Paper_for_PMA_2013_vF.pdf.
30. Stephanopoulos, G.: *Science*, 315:801 (2007).
31. Singh, K. S., S. U. Ahmed, and A. Pandey: *Process Biochem.*, 15:991 (2006).
32. <http://www.novozymes.com/en/news/news-archive/Pages/BASF,-Cargill-and-Novozymes-achieve-milestone.aspx>.

33. Matos, C. T., L. Gouveia, A. R. C. Morais, A. Reis, and R. Bogel-Lukasik: *Green Chem.*, 15:2854 (2013).
34. <http://biosciences.dupont.com/industries/biomaterials/>.
35. <http://www.icis.com/Articles/2011/11/18/9509800/amyris+moves+toward+bio-isoprene+commercialization.html>from.
36. Characterization of Municipal Solid Waste in the United States: 2011 Facts and Figures Fact Sheet, U.S. Environmental Protection Agency, <http://www.epa.gov/osw/nonhaz/municipal/msw99.htm>.
37. Statistical Abstract of the United States, Tables 377 and 378, U.S. Census Bureau, Washington, DC, 2012.
38. Rathje, W., and C. Murphy: *Rubbish! The Archaeology of Garbage*, HarperCollins, New York, 1992, p. 4.
39. Hocking, M. B.: *Science*, 504:251 (1991).
40. Allen, D. T., and N. Bakshani: *Chem. Eng. Educ.*, 26:82 (1992), reprinted in *Chem. Tech.*, 22 (November 1993) and 53 (December 1993).
41. Fouhy, K.: *Chem. Eng.*, 100:30 (December 1993).
42. Culp, E.: *Mod. Plast.*, 69:10 (1992).
43. Rubber Manufacturers Association (www.rma.org).
44. Cain, M. E.: *Rubber Developments*, 45:66 (1992).
45. Leaversuch, R.: *Mod. Plast.*, 65:65 (June 1988).
46. Rathje, W., and C. Murphy: *Rubbish! The Archaeology of Garbage*, HarperCollins, New York, 1992, p. 102.
47. Plastic Container Code System, The Plastic Bottle Information Bureau, Washington, DC.
48. *Mod. Plast.*, 70:73 (1994).
49. *Recycling Today*, 32(8):38 (1994).
50. *Plast. Eng.*, 46(11):15 (1990).
51. Alter, H.: Recycling (plastics) in M. Grayson and D. Eckroth (eds.), *Kirk-Othmer Encyclopedia of Chemical Technology*, vol. 19, 3rd edn., Wiley, New York, 1982, p. 993.
52. *Chem. Eng. News*, 63:26 (October 21, 1985).
53. Smoluk, G. R.: *Mod. Plast.*, 65:87 (February 1988).
54. Environmental impact of Nitrile barrier containers, LOPAC: A case study, p. 24, Monsanto Co., St. Louis, MO, 1973.
55. *Chem. Eng.*, 91:22 (June 25, 1984).
56. *Mod. Plast.*, 57:82 (April 1980).
57. Perry, R. H., and D. W. Green: *Perry's Chemical Engineers Handbook*, 6th edn., McGraw-Hill, New York, 1986, pp. 21-42–21-44.
58. Rodriguez, F., L. M. Vane, J. J. Schlueter, and P. Clark: chap. 9 "Separation Steps in Polymer Recycling Processes," in G. F. Vandegrift, D. T. Reed, and I. R. Tasker (eds.), *Environmental Remediation*, ACS Symposium Series 509, ACS, Washington, DC, 1992.
59. Vane, L. M., and F. Rodriguez: chap. 11 "Selected Aspects of Poly(Ethylene Terephthalate) Solution Behavior," in G. D. Andrews and P. M. Subramanian (eds.), *Emerging Technologies in Plastics Recycling*, ACS Symposium Series 513, ACS, Washington, DC, 1992.
60. Sperber, R. J., and S. L. Rosen, *Polym. Eng. Sci.*, 16:246 (1976).
61. Sperber, R. J., and S. L. Rosen, *SPE ANTEC Tech. Papers*, 21:521 (1975).
62. Lynch, J. C., and E. B. Nauman: Presented at *SPE RETEC: New Developments in Plastics Recycling*, October 30–31, 1989; also U.S. Patent 5,278,282 (January 11, 1994).
63. *Mod. Plast.*, 70(10):79 (1993).
64. Leaversuch, R. D.: *Mod. Plast.*, 70(1):20 (1993).
65. Scheirs, J.: *Polymer Recycling*, Wiley, New York, 1998, p. 538.
66. Thayer, A. M.: *Chem. Eng. News*, 67(5):7 (1989).
67. Herbold, K.: *Kunststoffe: German Plastics*, 1989.

68. Milgrom, J.: chap. 3 in R. J. Ehrig (ed.), *Plastics Recycling*, Hanser Publishers, New York, 1992.
69. Farrissey, W. J.: chap. 10 in R. J. Ehrig (ed.), *Plastics Recycling*, Hanser Publishers, New York, 1992.
70. Kaminsky, W., and H. Sinn: *Hydrocarbon Proc.*, 59(11):187 (1980).
71. Tesla, M. R.: *Power Eng.*, 98(5):43 (1994).
72. Clark, C., K. Meardon, and D. Russell: *Scrap Tire Technology and Markets*, Noyes Data, Park Ridge, NJ, 1993.
73. Wheless, E., and S. Thalenberg: The Design and Operation of an Ash Treatment System at the Commerce Refuse to Energy Facility, *Proceedings of the 1992 National Waste Processing Conference*, American Society of Mechanical Engineering, New York, 1992.
74. Denison, R. A., and J. Ruston (eds.): *Recycling and Incineration*, Island Press, Washington, DC, 1990.
75. Clark, C., K. Meardon, and D. Russell: *Scrap Tire Technology and Markets*, Noyes Data, Park Ridge, NJ, 1993, p. 59.
76. Schnabel, W: *Polymer Degradation*, Hanser Publishers, New York, 1981, p. 124.
77. Fields, R. D., F. Rodriguez, and R. K. Finn: *J. Appl. Polym. Sci.*, 18:3571 (1974).
78. Fields, R. D., and F. Rodriguez: "Microbial Degradation of Polyesters," in J. M. Sharpley and A. M. Kaplan (eds.), *Proceedings of the 3rd International Biodegradation Symposium*, Applied Science, London, 1976, p. 775.
79. Nir, M. M., J. Miltz, and A. Ram: *Plast. Eng.*, 49(3):75 (1993).
80. Lindsay, K. F.: *Mod. Plast.*, 69(2):62 (1992).

GENERAL REFERENCES

- Albertsson, A.-C., and S. J. Huang (eds.): *Degradable Polymers, Recycling, and Plastics Waste Management*, Dekker, New York, 1995.
- Andrews, G. D., and P. M. Subramanian (eds.): *Emerging Technologies in Plastics Recycling*, ACS, Washington, DC, 1992.
- Bisio, A. L., and M. Xanthos (eds.): *How to Manage Plastics Waste*, Hanser-Gardner, Cincinnati, OH, 1995.
- Doi, Y., and K. Fukada (eds.): *Biodegradable Plastics and Polymers*, Elsevier, Amsterdam, The Netherlands, 1994.
- Ehrig, R. J. (ed.): *Plastics Recycling: Products and Processes*, Hanser-Gardner, Cincinnati, OH, 1992.
- French, A. D., and J. W. Brady (eds.): *Computer Modeling of Carbohydrate Molecules*, ACS, Washington, DC, 1990.
- Glass, J. E., and G. Swift (eds.): *Agricultural and Synthetic Polymers: Biodegradability and Utilization*, ACS, Washington, DC, 1990.
- Griffin, G.: *Chemistry and Technology of Biodegradable Polymers*, Chapman & Hall, New York, 1993.
- Hegberg, B. A., G. R. Brenniman, and W. H. Hallenbeck: *Mixed Plastics Recycling Technology*, Noyes Data, Park Ridge, NJ, 1992.
- Inagaki, H., and G. O. Phillips (eds.): *Cellulosics Utilization*, Elsevier, New York, 1989.
- Jellinek, H. H. G., and H. Kaachi (eds.): *Degradation and Stabilization of Polymers: A Series of Comprehensive Reviews*, vol. 2, Elsevier, New York, 1989.
- Kaplan, D. L., E. L. Thomas, and C. Ching (eds.): *Biodegradable Polymers and Packaging*, Technomic, Lancaster, PA, 1993.
- La Mantia, F. P. (ed.): *Recycling of Plastic Materials*, Chemtec, Toronto, Canada, 1993.
- La Mantia, F. P. (ed.): *Recycling of PVC and Mixed Plastics Waste*, ChemTec, Toronto, Canada, 1996.

- Milgrom, J., R. Stephenson, G. Mavel, and G. Vanhaeren: *Recycling Polyethylene, PET, and PVC*, Technomic, Lancaster, PA, 1992.
- Mobley, D. P. (ed.): *Plastics from Microbes*, Hanser-Gardner, Cincinnati, OH, 1994.
- Mustafa, N. (ed.): *Plastics Waste Management: Disposal, Recycling, and Reuse*, Dekker, New York, 1993.
- Rader, C. P., S. D. Baldwin, D. D. Cornell, G. D. Sadler, and R. F. Stockel (eds.): *Plastics, Rubber, and Paper Recycling: A Pragmatic Approach*, ACS, Washington, DC, 1995.
- Shalaby, S. W. (ed.): *BioPolymers: Designed-to-Degrade-Systems*, Hanser-Gardner, Cincinnati, OH, 1994.
- Swartzbaugh, J. T., D. S. Duvall, L. F. Diaz, and G. M. Savage: *Recycling Equipment and Technology for Municipal Solid Waste*, Noyes Data, Park Ridge, NJ, 1993.
- Tötsch, W., and H. Gaensslen: *Polyvinylchloride: Environmental Aspects of a Common Plastic*, Elsevier, New York, 1992.
- Vandegrift, G. F., D. T. Reed, and I. R. Tasker (eds.): *Environmental Remediation*, ACS, Washington, DC, 1992.

16 Carbon Chain Polymers

16.1 INTRODUCTION

Commercially significant polymers may be conveniently grouped in two broad classes: those with backbones containing only aliphatic carbon and those with backbones containing ring structures or additional atoms such as oxygen, nitrogen, sulfur, or silicon. Polymers in the first class usually are made by addition reactions at the double bond (or 1,4-polymerization at a conjugated double bond system). Polymers in the second class can be made by a variety of reactions, including condensation and ring scission.

Although the plastics industry uses both classes of polymers, most thermoset plastics are based on heterochain polymers such as the urethane, epoxy, and aldehyde condensation resins. Thermoplastics, however, are mainly based on carbon chain polymers (with the notable exceptions of polyesters, nylons, and a few others).

Two other polymer-based industries are found to depend more on one class than the other. The rubber industry uses both carbon chain and heterochain polymers. A generic classification of **elastomers** suggested by the American Society for Testing and Materials (ASTM) indicates no bias toward carbon chain polymers [1]. However, the seven heterochain rubbers listed in Appendix 16.A probably constituted less than 5% of the total rubber produced in 2000. The reasons for this situation appear to be economic and historical rather than fundamentally physical or chemical. Heterochain polymers of excellent strength, resilience, and durability have been designed, but never at a price that attracted widespread use.

The fiber industry historically has favored heterochain polymers [2]. Once again, a listing of the generic names of the **man-made fibers** includes both classes (Appendix 16.B). However, except for the **polyolefins** (mainly polypropylene), two heterochain polymers, nylon and polyester, dominate the fiber market. The naturally occurring fibers, cotton, wool, and silk, also are heterochain polymers. The reason for the dominance by heterochain polymers does have a physical and chemical basis. The *sine qua non* of fibers is a high T_m , together with a reasonable degree of crystallinity on stretching (drawing). The heterochain structure is higher in polarity than the carbon chain structure, and it can often be tailored to a suitable chain stiffness. The high polarity of the nitrile group in acrylics and the remarkable regularity of isotactic polypropylene and linear polyethylene permit these carbon chain polymers to compete successfully.

Within each of the two major classes, the polymers have been arranged in families. Carbon chain polymers are summarized in this chapter and heterochain polymers in Chapter 17. Although some properties and uses are mentioned, more details on individual polymers are in Appendices C and D.

16.2 THE POLYOLEFINS

Ethylene and propylene from petroleum-refining operations or natural gas are the cheapest raw materials for polymer production. Aside from being the starting materials for a variety of other monomers, they are combined in an impressive array of products (Appendix 16.C). Branched polyethylene, its chlorosulfonated, rubbery derivative, and butyl rubber date back to the 1930s and 1940s. The 1950s saw the introduction of linear polyethylene and isotactic polypropylene. Copolymers of ethylene with propylene and polar monomers came along in the 1960s, as did the isotactic polymer of 4-methylpentene-1. Further innovations in the 1990s stemmed from the introduction of metallocene and related catalysts that made new structures possible. Gas-phase and slurry polymerization processes have been used since the late 1960s [3,4].

16.2.1 SOME INDIVIDUAL POLYMERS

The range of properties that can be achieved within the olefin family goes from highly crystalline, linear polymers of high T_m to completely amorphous, rubbery materials that are branched or that can be cross-linked. Even among the homopolymers of ethylene a wide range of mechanical and processing behavior is available depending on molecular weight, molecular weight distribution, and branching. Linear polyethylene with a molecular weight above 10,000 or so is dense, reflecting its high crystallinity. Branching decreases crystallinity, as does copolymerization. The naturally occurring waxes recovered from petroleum include polyethylenes with molecular weights of a few hundred to 5000. Ethylene and many of its copolymers can be polymerized by free-radical initiation and also by various insertion schemes. The high-pressure, free-radical polymerization of ethylene and some copolymers was described in Section 5.3 as a form of solution polymerization since over half of the monomer acts as a solvent, remaining unreacted when polymer is recovered. The conditions are conducive to chain transfer from growing radicals to *dead* polymer resulting in extensive branching with consequent low crystallinity (Section 4.4). Thus, the polymer falls in the industrial category of low-density polyethylene (**LDPE**).

The same process can be used to make copolymers of ethylene with polar monomers such as vinyl acetate, ethyl acrylate, and maleic anhydride with decreased crystallinity and increased room-temperature flexibility. Some items in which this controlled degree of flexibility is useful are tubing, protective coatings (waxes and polishes), adhesives, and shoe soles. Copolymerization with acid-functional monomers followed by neutralization with a base (usually NaOH) gives the class of **ionomers**. Although still crystalline, the spherulite size is decreased, making films of ionomers much more transparent than those of polyethylene. As might be expected, the ionic groups facilitate adhesion and printing. The ionic groups act as somewhat labile cross-links in the melt, so that ionomer sheets are rubbery and can be vacuum-formed more easily than polyethylene.

Ziegler–Natta catalysts, metallocenes, and supported metal oxides (Phillips process) all are capable of producing high-density (or linear) polyethylene (**HDPE**) (see Section 4.7). These catalyst systems are sensitive to water and polar compounds, operate at moderate pressures, and usually are somewhat slower than most ionic systems. The single-site metallocene catalysts resemble the conventional Ziegler–Natta catalysts in that they can be used in many of the same polymerization processes that have been described. However, the metallocene catalysts have allowed a control over processing properties not previously attained. Very narrow molecular weight distributions coupled with long-chain branching make a polyethylene that is more shear thinning than older materials (see Section 4.7). Copolymerization with other α -olefins also can be coupled with control of molecular weight distribution so that materials ranging from highly crystalline to highly elastic have been brought to market.

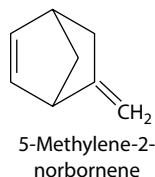
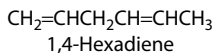
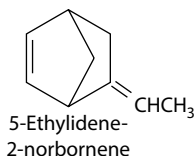
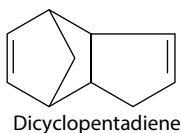
Gas-phase polymerization for ethylene was commercialized in 1968. Elimination of solvent recovery and catalyst removal as process steps gave significant economics. The process was described in Section 5.3 as an example of *solution* polymerization with insoluble initiator and polymer. It is used to produce HDPE, linear polymers with short branches by the copolymerization of ethylene with other branches of α -olefins (linear LDPE [**LLDPE**]), and polypropylene.

Ziegler–Natta type systems and metallocenes are used to produce a number of stereoregular polymers. Two of these, **isotactic polypropylene** and, in much smaller volume, **poly(4-methylpentene-1)**, are available commercially. Production parallels the schemes of Figures 5.7 and 5.8. Advances in catalyst preparation increased the purity of the isotactic portion in most processes so that removal of the atactic fraction is no longer needed. Also, productivity (kilogram of polymer gram of catalyst metal) usually is high enough so that removal of catalyst residues is seldom necessary.

The metallocene *single-site* catalysts (see Section 4.7) have been used in gas-phase and slurry reactors of various descriptions. The fact that metallocenes have been adapted to existing production lines has sped the introduction of the new polyethylenes into commercial markets. Other monomers that can be polymerized with metallocene catalysts include propylene, other α -olefins, and styrene.

Polyallomers are **block copolymers** of propylene with small amounts of ethylene. The lifetime of a single growing chain apparently is long enough that blocks can be achieved by a rhythmic alternation of ethylene and propylene in the monomer feed. The materials still are highly crystalline. However, when a **random copolymer** is made with almost equal amounts of ethylene and propylene, the product is amorphous and rubbery (ethylene-propylene-monomer [**EPM**] **rubber**). Peroxides can be used to cross-link either polyethylene or EPM by hydrogen atom abstraction followed by radical combination. The mechanism was outlined in Section 12.3. The cross-linking is done in a separate operation after the polymer has been made. The rubber is compounded and molded or extruded into its final shape before being cured. By incorporating a third monomer, which contributes a favored cross-linking site, a wider variety of cross-linking agents can be used. Some nonconjugated dienes are especially useful, since only one double bond polymerizes, leaving a pendant unsaturation that is reactive with the sulfur and sulfur-bearing vulcanizing systems

long used in the rubber industry. Some dienes used to the extent of about 3% in ethylene–propylene–diene monomer (**EPDM**) rubber are as follows:



Another rubbery material, **chlorinated polyethylene**, can be made directly from branched polyethylene by postchlorination. A major use of this material is as a polymeric plasticizer for poly(vinyl chloride) (PVC).

The production of polymers and copolymers of isobutylene was described in Section 5.3 as an example of solution polymerization with insoluble polymer. The lower molecular weight homopolymers are used in adhesives and the copolymer with isoprene is a commercial rubber.

16.2.2 SELECTED USES

Blow-molded containers made from polyethylene (squeeze bottles of LDPE and milk bottles of HDPE) and shrink-packaging film of polypropylene are everyday examples of large-volume uses. Gasoline tanks for many automobiles are blow-molded or rotation-molded from HDPE (see Section 14.8). Except for butyl rubber and chlorosulfonated polyethylene, the polyolefins are not easily dissolved at room temperature, so they have not been widely used in solvent coatings or adhesives. Melt coating or laminating of polyethylene on paper or cardboard is important for making containers for milk and other liquids. Ultra-high-molecular-weight, linear polyethylene (**UHMWPE**) cannot be fabricated by any of the usual molding techniques. Instead, powders are sintered together in a manner like powdered metals. One significant application of UHMWPE is as the socket material in hip replacement surgery. The gel spinning of UHMWPE to give highly oriented fibers was mentioned in Section 14.3. Butyl rubber had a large market in inner tubes before the advent of the tubeless tire. Most tubeless tires today have inner liners of chlorobutyl or bromobutyl rubber to enhance air pressure retention.

16.3 THE ACRYLONITRILE–BUTADIENE–STYRENE GROUP

Homopolymers and interpolymers from acrylonitrile, butadiene, and styrene offer a wide range of properties (Figure 16.1). The variety of processes used is outlined in Appendix 16.D. It has been pointed out (Section 1.3) that the synthetic rubber program during World War II established almost overnight a tremendous capacity

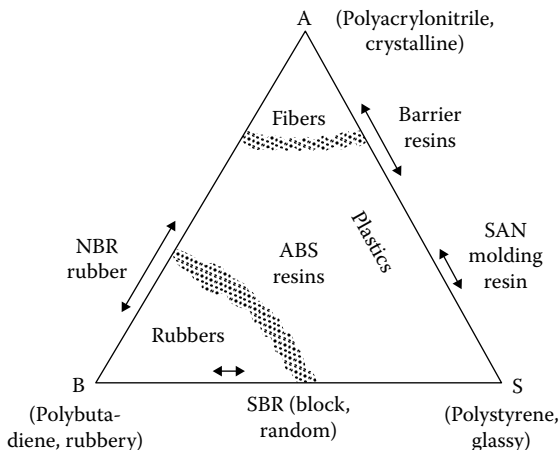


FIGURE 16.1 ABS compositions. Besides the homopolymers, interpolymers of the three building blocks give rise to numerous modifications. Locations indicated are only approximate.

for styrene and butadiene. Butadiene is made by the dehydrogenation of butane or butene from petroleum. Because benzene can be made from petroleum by catalytic reforming, much styrene owes its origin to petroleum too. Benzene is alkylated with ethylene (AlCl_3 , catalyst) and dehydrogenated to make styrene. The third member of the A–B–S triumvirate, acrylonitrile, can be made by several routes. A single-stage catalyzed reaction of propylene with ammonia and oxygen is popular.

16.3.1 SOME INDIVIDUAL POLYMERS

A discussion of the stereoregular homopolymers of butadiene is delayed until Section 16.4. The continuous process for making **styrene–butadiene rubber (SBR)** by emulsion polymerization has not changed in essential features over the past 30 years (Figure 16.2) [5,6]. It involves a series of 12 7000-gal reactors, each 20 ft tall and 90 in (inside) in diameter. Each reactor is compartmented and stirred, so that the emulsion passes from one end of the train to the other in a kind of plug flow. Residence time in each reactor is 1.0–1.25 h, and the heat removed in each may be as high as 132,000 Btu/h. Some *hot* rubber is made with a peroxide initiator at 50°C , but most SBR is *cold* rubber initiated by a redox couple at 5°C . A chain transfer agent, dodecyl mercaptan, is added to regulate the molecular weight. After reaching a conversion of about 75%, the reaction is short-stopped by the addition of hydroquinone, and unreacted monomers are removed without coagulation in vacuum flash tanks and falling-film strippers. The relative reactivities are such that butadiene is consumed more rapidly than styrene ($r_1 = 1.4$, $r_2 = 0.8$). Consequently, a feed concentration of about 30% styrene is used to achieve a 25% styrene polymer. About 70% of the SBR goes to make tires in which carbon black will be used as a reinforcement and oil as an extender plasticizer. Most producers sell SBR as master batches that have been compounded before coagulation. Common loadings are 37.5 or 50 parts (by weight) of oil per 100 of rubber and 40–75 parts of carbon black per 100 of rubber.

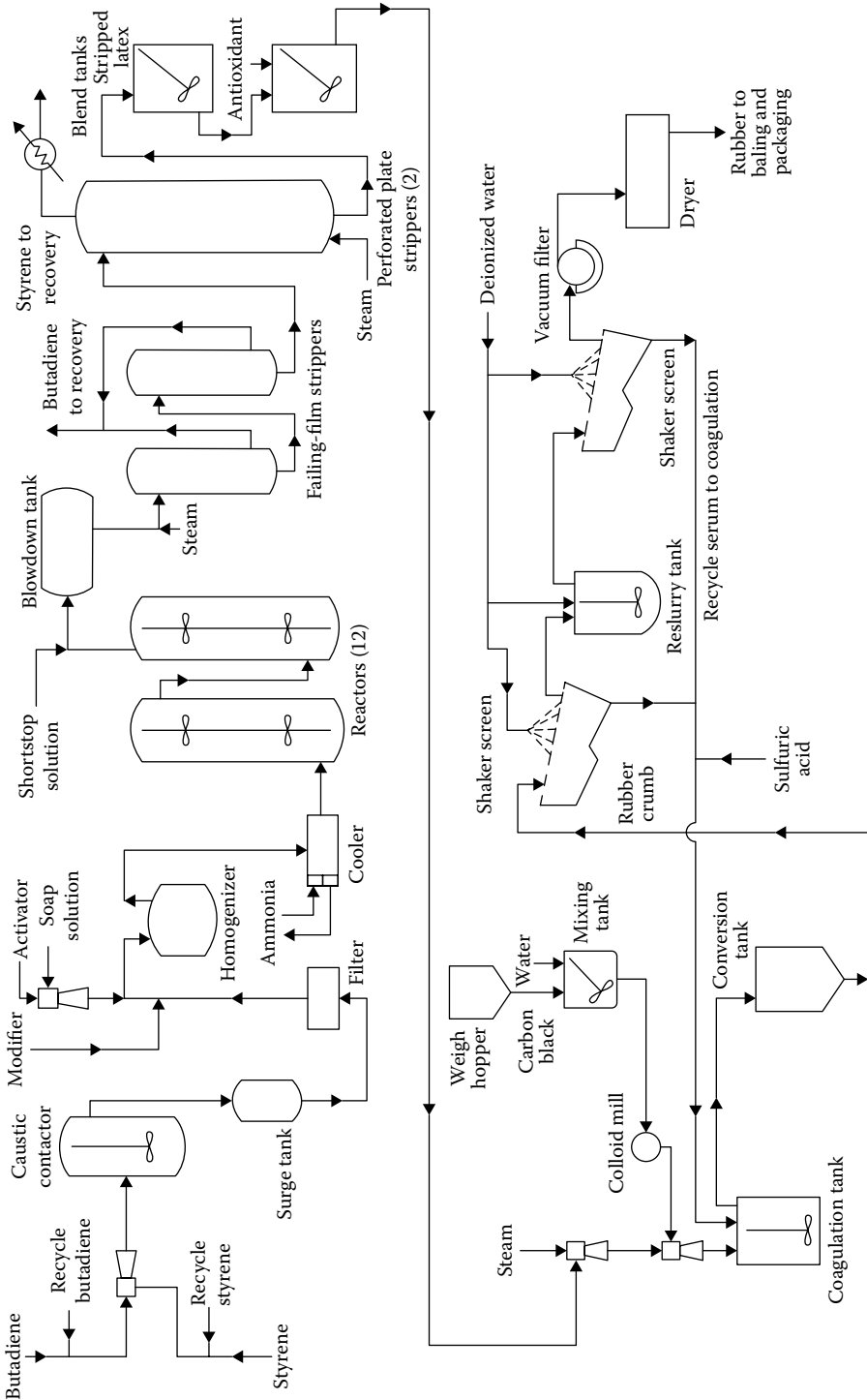


FIGURE 16.2 Continuous production of SBR. (Data from Winding, C. C., and G. D. Hiatt, *Polymeric Materials*, McGraw-Hill, New York, 383–387, 1961.)

SBR latexes have been used as paints and adhesives. Most are produced in batch operations. Higher styrene contents give somewhat better abrasion resistance (from a higher T_g), and conversions may be run almost to completion (with high molecular weights and branching), since film formation does not involve much polymer flow. Some latexes are intentionally cross-linked by copolymerizing a tetrafunctional monomer, divinyl benzene. These gelled latex particles act like organic fillers and are used to smooth out extrusion of linear rubber.

The production and properties resulting from the anionic terpolymerization in solution incorporating styrene, butadiene, and isoprene have been reviewed by Halasa [7]. The product, **SIBR**, can be tailored by monomer composition to give polymers with single or multiple glass transition temperatures. As noted earlier, block copolymers produced by rhythmic alternation of styrene and butadiene in the feed of anionic polymerization are quite different in mechanical behavior from conventional SBR (see Section 4.5).

Copolymerization of acrylonitrile with butadiene is usually carried out in free-radical emulsion polymerization with high conversion. Production is most often batchwise rather than continuous because so many modifications are marketed and the total volume is smaller than that of SBR. The outstanding property of **nitrile rubber (NBR)**, as it is called, is resistance to swelling in nonpolar solvents. With increasing acrylonitrile content, the cohesive energy density increases, so swelling in nonpolar, low-cohesive-energy-density solvents decrease (Section 2.5). The term *solvent-resistant rubber* is used, but it should be regarded cautiously because a polar rubber actually swells more than a nonpolar one in a polar solvent.

Most atactic **polystyrene** is produced by free-radical propagation in so-called bulk polymerization (in fact, a solution polymerization) described in Section 5.2.2.

For applications that require the crystal clarity of polystyrene, but where the chemical resistance and tensile strength are marginal, a copolymer of styrene with 20%–40% acrylonitrile is available (**SAN**). Some grades will bear more than twice the stress that conventional polystyrene does before crazing or cracking. Also, the T_g can be substantially higher, making kitchen articles that are *dishwasher safe*. Where clarity is not needed, polystyrene can be toughened by mechanically blending it with a rubbery polymer. Blends can be made by milling polystyrene with SBR on a hot mill or by coagulating latexes of the two ingredients together. However, it is more common to dissolve SBR or polybutadiene rubber in styrene monomer and then to polymerize in bulk. This results in some grafting along with homopolymerization. In these rubber-modified resins, maximum toughness is achieved by selecting the two components so that they are compatible enough to wet each other well but incompatible to the extent that the rubber will be present as discrete droplets about 50 μm in diameter within a continuous polystyrene matrix. The impact strength can be raised to over 1 ft-lb/in (53 J/m) of notch from the unmodified value of 0.3 by a rubber content of 10%.

The combination of all three monomers is different enough to result in a separate class of materials, the acrylonitrile–butadiene–styrene (**ABS**) resins. Simultaneous terpolymerization does not give the desired heterogeneity that goes along with high impact strength and general toughness. The two processes favored are a blending of latexes of styrene–acrylonitrile and acrylonitrile–butadiene copolymers or a grafting of styrene and acrylonitrile on a polybutadiene backbone in latex form. In the blending process, the butadiene–acrylonitrile copolymerization usually is short-stopped at about 75%

conversion and residual monomer is stripped before blending. The styrene–acrylonitrile copolymerization can be carried substantially to completion, as can the grafting of the two monomers on a polybutadiene latex. Typical recipes include, in each case, surfactants, a water-soluble peroxide, and a chain transfer agent (mercaptan). The three monomers representing glassiness (styrene), rubberiness (butadiene), and polarity (acrylonitrile) can be placed at the corners of a triangular composition diagram (Figure 16.1). Even the triangular diagram is not enough to catalog all the significant variations that are possible. Neither steric variations (tacticity and *cis–trans* isomerism) nor cross-linking is shown. As indicated earlier, both random and block copolymers of styrene and butadiene have the same ratio of monomers, but they differ in properties. On the diagram the *barrier* resins, which appear at high acrylonitrile content, are so called because of their low permeability to oxygen and carbon dioxide. Functional groups affect permeability strongly (Table 16.1). This is reflected in the series of styrene–acrylonitrile copolymers (Table 16.2). Such polymers are used as margarine tubs and vegetable oil bottles.

Even more complex are compositions that are physical mixtures of polymers. One important outlet for ABS resins is in blends (**alloys**) with other polymers such as nylons or polycarbonates. Polystyrene itself is blended with poly(propylene oxide). In each case, the blend can be tougher than constituent resins. Often these blends offer advantages of lower cost and easier fabrication.

Syndiotactic polystyrene is produced using metallocene catalysis and, unlike the atactic polymer, is highly crystalline with a T_m of 270°C. Most grades offered are glass-reinforced [8]. Alloying with nylon or other polymers improves processing. The heat deflection temperature under load is 256°C for an alloy with nylon that is reinforced with 30 wt% glass fiber. Some applications for the homopolymer and its alloys include heat-, steam-, and oil-resistant food containers; molded circuit boards; and radiator tanks for automobiles. Another development is the production of ethylene/styrene interpolymers [9]. A *constrained geometry* metallocene catalyst is used which makes *pseudo-random* copolymers, so called because a growing chain ending with styrene

TABLE 16.1
Effect of Functional Groups on Permeability

R Group in (–CH ₂ CHR–)	Permeability to Oxygen
–OH (dry)	0.002
–CN	0.035
–Cl	8.02
–F	15.0
–CH ₃	150
–C ₆ H ₅	416
–H	501

Source: *Environmental Impact of Nitrile Barrier Materials*, Monsanto Company, St. Louis, MO, July 19, 1973, pp. 24–25.

Note: Permeability is in units of cm³/day for an area of 100 in² and a driving force of 1 atm over a thickness of 0.001 in.

TABLE 16.2
Gas Permeability of Acrylonitrile–Styrene Copolymers

Weight % Acrylonitrile in Copolymer	Permeability to Oxygen	Permeability to Carbon Dioxide
0	416	1250
25	66.8	217
60	4.5	7.5
67	2.3	5.3
82	0.25	0.83
100	0.035	0.15

Source: *Environmental Impact of Nitrile Barrier Materials*, Monsanto Company, St. Louis, MO, July 19, 1973, pp. 24–25.

Note: See Table 16.1 for permeability of functional groups.

does not add another styrene, whereas a chain ending in ethylene can add styrene or ethylene [10]. As with most copolymers, a variety of products have been marketed.

Fibers bearing the generic name **acrylic fiber** contain at least 85% acrylonitrile. **Modacrylics** contain 35%–85% acrylonitrile. Most are familiar to the consumer by trademarked names such as Orlon, Acrilan, Creslan, and Dynel. These fibers appear in rugs, upholstery, and apparel. Acrylonitrile may be solution-polymerized in water from which the polymer precipitates or in a polar solvent such as acetonitrile. Varying amounts of comonomers are used to modify mechanical properties or to facilitate the dyeing of products. In spinning fibers from solution, a wet technique may be used with a water-miscible solvent spun into a water bath. Dry spinning with evaporation of solvent is another possibility (see Section 14.3).

16.3.2 SELECTED USES

About 75% of all polystyrene and 85% of ABS go into molded or extruded products. About 15% of the polystyrene appears as the familiar form of *expanded* (or foamed) packaging material. Not all of the A–B–S family are thermoplastics. Divinylbenzene–styrene copolymer, which is the basis for ion-exchange resins, is cross-linked and glassy. The cast polyesters, in which styrene monomer is polymerized in the presence of an unsaturated polymer, are discussed in Section 17.2. Styrene also finds use in the coatings industry as a modifier for other resins. Styrenated alkyds and oils are used, which undoubtedly make use of grafting to some extent. High-styrene SBR latexes find use as adhesives for carpeting. The interior water-based paints introduced right after World War II were made from SBR latexes. However, the vinyl and acrylic latexes now dominate the paint market.

16.4 THE DIENE POLYMERS

Although conjugated diene monomers are capable of exhibiting a functionality of four in polymerization reactions, the important examples are linear or branched polymers with residual unsaturation (Appendix 16.E). Natural rubber (*cis*-1,4-polyisoprene)

(NR) was harvested and used in the Western Hemisphere for centuries before it was introduced to Europe over 200 years ago. Because of the remoteness of the tropical climates where rubber could be grown, Germany in World War I and Germany, Russia, and the United States in World War II intensified research on duplicating the natural products on which so much of their transportation depended. Substitutes such as SBR were found, but synthesis of the stereoregular polymer was not accomplished until the 1950s and 1960s. There was no rush to put synthetic *natural* rubber into production, however, because by this time the *substitutes* had come to be appreciated for their own properties.

16.4.1 SOME INDIVIDUAL POLYMERS

NR is recovered as a latex by tapping trees. Although the process resembles maple sugar tapping, the latex is carried in a separate layer from the sap of the rubber tree. The latex contains about 35% rubber and another 5% of solids comprising proteins, sugars, resins, and salts. Most tree latex is coagulated and formed into sheets 3 or 4 mm thick. Major producers include Malaysia, Indonesia, Thailand, and Sri Lanka. Almost half of the world's supply today is sold in the form of technically specified rubber (TSR), which establishes standards for preparation, properties, and packaging. According to the Rubber Manufacturers Association, approximately 70% of all rubber used today is synthetic. Over the years, attempts to recover *cis*-polyisoprene from guayule have continued to receive the support of the US and Mexican governments [11]. **Guayule** is a shrub native to the southwestern United States and northern Mexico. Two major incentives for development of guayule are the goal of independence from an overseas source of raw materials as far as the Americas are concerned, and the productive use of arid and semiarid lands in the United States and Mexico.

The naturally occurring *trans*-1,4-polyisoprene is recovered as a latex from trees also. **Gutta-percha** and **balata** are obtained from trees in southeast Asia and South America, respectively. The unvulcanized material crystallizes enough to be quite dimensionally stable at room temperature. It may have been the first thermoplastic resin, since it was used as an electrical insulation for submarine cable in England and Germany [12] as long ago as 1848. A former application for the vulcanized gutta-percha, golf ball covers, indicates the typical properties of the polymer. A novel application is as a splint in orthopedics. The synthetic *trans*-1,4-polyisoprene made with Ziegler–Natta catalysts is preferred. Direct molding is used to customize the splint. When heated to 70°C or 80°C, the polymer becomes amorphous and a sheet can be handled and shaped quite easily. It can be held against the skin where it becomes dimensionally stable after a few minutes due to crystallization. It can replace plaster of Paris, which is the older material used for this purpose. The polymer has the advantages of being light, durable, attractive, and unaffected by water.

The remarkable degree of control over structure in diene polymers is illustrated in Table 16.3. These values are only a few selected from among hundreds found in the older literature. A commercially successful catalyst system may use similar systems, but economic considerations will modify the requirements. Predominantly *cis* polymers have the largest market, although *trans* polymers are available. The major

TABLE 16.3
Structure of Polymers from Conjugated Dienes

Monomer	Initiator	Polymer Structure (%)			
		<i>cis</i> -1,4	<i>trans</i> -1,4	1,2	3,4
Butadiene	Free radical: 50°C	19	60	21	
	Butyl lithium–hexane: 20°C	33	55	12	
	Cobalt chelate-AlEt ₂ Cl:				
	Al:Co = 5:20	99	1		
Isoprene	TiCl ₄ -AlR ₃ : Al/Ti < 1	6	91	3	
	Free radical: 50°C	15	75	5	5
	Butyl lithium–pentane	93	–	–	7
	TiCl ₄ -AlEt ₃ : Al/Ti > 1	96	–	–	4
	TiCl ₄ -AlEt ₃ : Al/Ti < 1	–	95	–	5

Source: Cooper, W., and O. Vaughan; in A. D. Jenkins (ed.): *Progress in Polymer Science*, vol. 1, Pergamon Press, New York, 1967, pp. 100, 107, 109, 128, 130.

differences between isoprene or butadiene polymerization by the Ziegler process and the process described for ethylene and propylene (Section 16.2) are that the reaction may be short-stopped at 80%–90% conversion, that monomers are less volatile and somewhat more difficult to recover, and that the polymer remains soluble in the medium and must be precipitated by adding a diluent. An efficient solvent recovery system is essential for economic operation.

The emulsion polymerization to make **polychloroprene rubber (CR)** by free-radical initiation dates back to the early 1930s. While the *trans*-1,4 structure predominates, it is not all head-to-tail and there is some branching. Most chloroprene is made by chlorination of butadiene followed by isomerization to give 3,4-dichlorobutene-1. Then hydrogen chloride is removed by aqueous sodium hydroxide. Continuous emulsion polymerization [13,14] uses a series of stirred reactors similar to SBR production, although only one is shown in Figure 16.3. A typical residence time is 2 h for 70% conversion at 40°C. Some grades are produced in batch reactors, and conversions can range up to 90%. Sulfur or sulfur compounds are included, possibly as antioxidants or as chain transfer agents. Several of the commercial rubbers probably have small amounts of comonomer such as styrene, acrylonitrile, or 2,3-dichloro-1,3-butadiene. Some latex is used directly for dipped goods and paints, but most of it is coagulated. Coagulation differs from the method used for SBR in that after neutralizing the emulsifier with acetic acid, the unstable latex is coagulated on the surface of a chilled, rotating drum. The strong film of polymer that forms rapidly can be pulled off the drum continuously, and washed and dried in film form before being gathered into a rope that is chopped into short pieces for packaging. The unvulcanized rubber crystallizes sufficiently to appear hard and horny, with little tendency to flow. Cross-linking can be carried out by heating with 5 parts ZnO and 4 parts MgO per 100 parts of rubber. As with any rubber, many other cross-linking combinations are used.

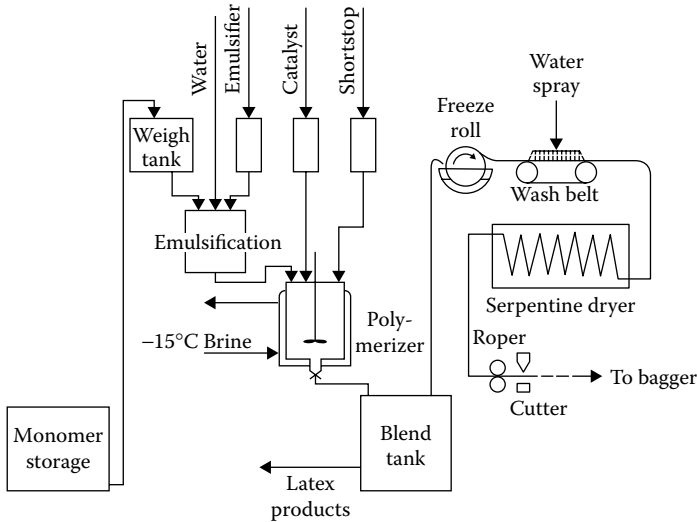
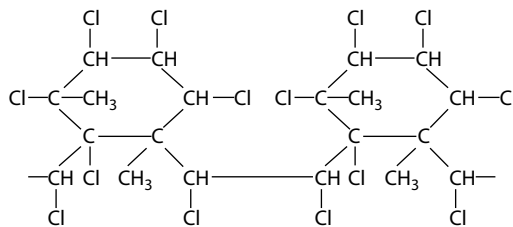


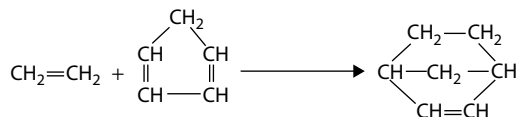
FIGURE 16.3 Schematic flow sheet for the polymerization and isolation of polychloroprene. (Data from Stewart, C. A., Jr. et al., *Chloroprene Polymers*, in H. F. Mark, ed., *Encyclopedia of Polymer Science and Engineering*, vol. 3, 2nd edn., 441, 1985; Johnson, P. R., *Rubber Chem. Technol.*, 49, 650, 1976.)

Two derivatives of NR that have been produced for many years are **cyclized rubber** and **chlorinated rubber**. The first of these may be produced in solution by heating with a strong acid such as H_2SnCl_6 . The structure that results resembles a ladder to some extent (Section 12.3). It is still quite soluble and finds use in adhesives and coatings. Chlorinated rubber (structure shown below) also is ladderlike. The product with about 65% chlorine has been used as a coating for many years.

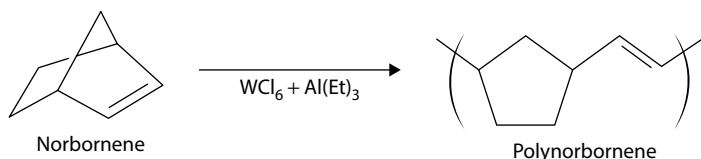


Two other derivatives that have received attention are thermoplastic NR (**TPNR**) blends and epoxidized NR (**ENR**). TPNRs often are blends of NR with polypropylene [15]. Applications include automotive components and floor tiles. ENR-50, with 50 mol% epoxidized double bonds, can be used where oil resistance or air impermeability is needed together with high strength [16]. Some applications include hoses and seals. The grafting of methyl methacrylate on NR has been carried out on a commercial scale by polymerizing the monomer in a rubber latex. The primary use of the grafted material is as an additive to improve flow of unmodified rubber.

Ring-scission polymerization of norbornene (1,3-cyclopentylenevinylene) produces a rubber, **polynorbornene**, that was introduced in 1976 in France and has since been offered in other countries. The monomer norbornene is made by the Diels–Alder condensation of ethylene with cyclopentadiene:

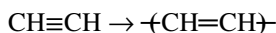


The ring-opening polymerization can be carried out by a variety of catalysts, for example, WCl_6 with aluminum triethyl [17].



There can be a considerable amount of *cis* configuration as well as the *trans* shown here. The commercial product is a high-molecular-weight (2×10^6) plastic with a T_g of 35°C . To be used as a rubber, plasticizing oils must be added to lower T_g . A fascinating feature of the material is its ability to absorb large amounts of oil and still remain a useful rubber. One mixing technique that can be used is dry blending of polymer and plasticizer, a method widely used with PVC. If the oil is added while the powdered polymer is tumbled, the final mixture remains a free-flowing powder that can be fed directly to an extruder. In a typical recipe (Table 16.4), the polymer is less than 20% of the final weight of the product. Some applications have been engine mounts, roll coverings, sealing materials, and taillight gaskets for automobiles [18].

Polyacetylene is another polymer with residual chain unsaturation:



Catalytic polymerization of acetylene gas on a glass surface gives a lustrous, silvery film with a fair amount of mechanical strength [19,20]. The polycrystalline films (mainly *trans* isomer) can be *doped* with small amounts of AsF_5 to give conductivities of over $100 \text{ (ohm-cm)}^{-1}$. For their work with doped **polyacetylene**, A. J. Heeger, A. G. MacDiarmid, and H. Shirakawa received the Nobel Prize in Chemistry in 2000.

Solid-state polymerization of some **diacetylenes** proceeds via a biradical to give a backbone in which a triple and a double bond remain for each four-carbon repeat unit in the chain [21,22].

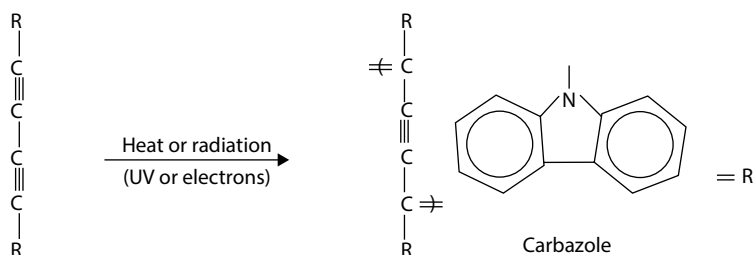


TABLE 16.4
Compound Based on Polynorbornene

Recipe	Parts by Weight
Polynorbornene (Norsorex: American Cyanamid Company)	100
Zinc oxide	5
Stearic acid	1
Carbon black	200
Aromatic oil	180
Paraffinic oil	20
Accelerator (<i>N</i> -cyclohexylbenzothiazole-2-sulfenamide)	5
Sulfur	1
Properties after molding 30 min at 150°C	
Tensile strength	20 MPa (2900 psi)
Elongation at break	320%
Hardness (Shore A)	55
Brittle temperature	-40°C

Source: Walker, D.: *Rubber Plast. News*, October 3, 1977, p. 1.

When R is the carbazole unit, large crystals of the monomer can be polymerized in the solid state to give macroscopic single crystals of the polymer with dimensions up to several centimeters. Often the colors that result in the highly conjugated unsaturated polymers are very striking. The heat of polymerization is high, about 37 kcal/mol. Some proposed uses for various diacetylenes are as time-temperature indicators, radiation indicators, nonlinear optical components, and holographic imaging media.

16.4.2 SELECTED USES

The dienes often compete with NR in many applications. Choices often are affected by relatively small changes in price. Tires consume about 70% of the polymers based on isoprene (synthetic and natural) and butadiene. Polychloroprene, while not suited for tires because of heat buildup, is the most widely used oil-resistant rubber. It is much more resistant to oxidation at high temperatures than the hydrocarbon dienes or SBR. More than any other polymer, it fits in the paradoxical category of being a general-purpose specialty rubber.

16.5 THE VINYL

The group designated as vinyl polymers usually excludes vinyl benzene (styrene), vinyl cyanide (acrylonitrile), and vinyl fluoride (Appendix 16.F). The observation recorded by Regnault in 1838, that vinylidene chloride is converted by exposure to sunlight in a sealed glass tube to an insoluble polymer, often is cited as the beginning

of polymer science. However, 100 years passed before commercial use began. In the 1930s, copolymers of vinyl acetate with vinyl chloride were introduced. They are more soluble than the homopolymers of vinyl chloride and are used in lacquers. The unique affinity of vinyl polymers for plasticizers was discovered at about the same time. No other thermoplastic matches the ability of **PVC** and its copolymers to form stable, dry, flexible solutions in nonvolatile liquids. Although triaryl phosphates and dialkyl phthalates dominate the plasticizer market today, hundreds of liquids are marketed as plasticizers. In Germany and the United States in the 1930s and 1940s, homopolymers were developed using suspension and emulsion techniques that yield useful plasticized (and unplasticized) items. Regardless of plasticization, virtually all PVC is compounded with additives to stabilize the polymer against dehydrohalogenation (see Section 12.3). Widely used heat stabilizers include metal soaps (Ba, Ca, Cd, Zn, and Sn) as well as organophosphites and epoxy compounds. Lead compounds also are effective stabilizers but they are less attractive from an ecological standpoint.

16.5.1 SOME INDIVIDUAL POLYMERS

Most **vinyl chloride** is polymerized by a batchwise suspension process. Jacketed, stirred reactors like the one in Figure 5.13 vary in size from 2,000 to 10,000 gal (8–40 m³).

Reactors are stainless steel or glass-lined and must handle a pressure of about 1.5 MPa (220 psi). An initiator soluble in the monomer, such as lauroyl peroxide, is added to monomer, which is dispersed in about twice its weight of water containing 0.01%–1% of a stabilizer such as poly(vinyl alcohol). Over a period of 8–15 h at 50°C–80°C, conversion may reach 80%–90%. Polymer precipitates within the monomer droplets to form a reticulated structure. If the unreacted monomer is blown off at the end of the period by reducing the pressure, porous particles are obtained that can adsorb large volumes of plasticizer. Dry-blend resins are those that can adsorb 20–40 parts of plasticizer per 100 parts of polymer and still remain as free-flowing powders. Mixing and handling such systems is easier than operating with sticky, semifluid mixtures. The suspension polymer can be dried in rotary dryers, in spray dryers, or in combination grinding mill-classifier dryers. Individual reactors with volumes of 200 m³ have been made with bottom-entering agitators [23]. The charge to one of these *supersized* reactors includes 100×10^3 kg of monomer. Much **PVC** goes into construction applications such as siding for houses and pipes. These require very little plasticization. Special suspension recipes are used with high conversion to give solid, nonporous resins. These are harder to dissolve in plasticizers. However, they are useful as additives in **plastisols**, since they do not increase the viscosity very much.

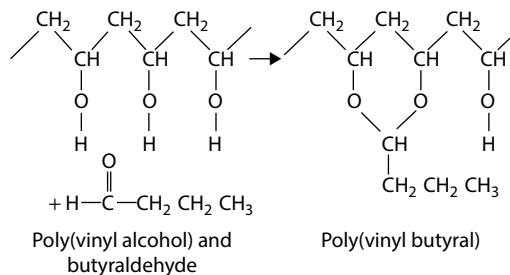
Dispersion (also called **plastisol** or **stir-in**) resins are made by emulsion polymerization in vessels similar to those used for suspension polymerization. The ease with which these polymers can be suspended in the plasticizer to give a free-flowing liquid is a result of the small particle size of the emulsion and the residual emulsifier. When the latex is spray-dried, most of the emulsifier remains on the surface of the particles (actually aggregates of latex particles) and helps the plasticizer to wet them. Plastisol molding was described in Section 14.8, and some effects of plasticization were described in Section 3.3. Emulsion polymerization of vinylidene chloride was mentioned in Chapter 5 as a case where stirring rate affects the kinetics.

Copolymerization of vinyl chloride with vinyl acetate or vinylidene chloride gives polymers of lower T_g and better solubility. The main advantage of propylene copolymers is said to be stability and clarity in unplasticized, blow-molded bottles. **Postchlorination** of PVC yields a material of higher T_g that has been recommended for pipes that can carry hot water without deforming.

The latexes that result from vinyl acetate polymerization have been used for exterior and interior water-based paints. Emulsion polymerization can be carried to high conversion fairly rapidly [24]. The rate is controlled by continuous addition of monomer. Rate of addition is limited primarily by rate of heat removal. A final heating to 90°C may be used to react the last bit of monomer. When the latex is to be used as an adhesive, a plasticizer may be added. The popular white glues for paper and wood often are partly hydrolyzed poly(vinyl acetate) suspensions plasticized with liquids such as castor oil.

Until the introduction of exterior latex paints, most **poly(vinyl acetate)** was hydrolyzed to alcohol and reacted to form the butyral adhesive layer for laminating safety glass. **Poly(vinyl alcohol)** is water soluble and has been mentioned frequently as the stabilizing agent in many suspension polymerizations. All the other customary uses (thickening agent, gelling agent, cosmetic ingredient) of water-soluble polymers are conceivable for poly(vinyl alcohol). Fibers are produced in Japan by extruding a concentrated aqueous solution of poly(vinyl alcohol) into a sodium sulfate solution containing sulfuric acid and formaldehyde, which acts as a cross-linking agent.

A continuous process for solution polymerization of vinyl acetate has been described [25]. The resulting polymer solution is rapidly converted by methanolysis in a subsequent continuous process to the corresponding **poly(vinyl alcohol)** when a strong base such as NaOH or sodium methoxide is added together with an excess of methanol. Various degrees of hydrolysis can be produced. The gelatinous poly(vinyl alcohol) precipitates as a slurry in the methanol. When butyraldehyde is reacted with poly(vinyl alcohol) suspended in ethanol with sulfuric acid as a catalyst (5–6 h, 80°C), an intramolecular condensation is favored. After rearrangements the **poly(vinyl butyral)** may contain fewer than 10% unreacted OH groups.



Poly(vinyl formal) can be made by direct reaction of formaldehyde with poly(vinyl acetate) in aqueous sulfuric acid. The cyclic intramolecular structure is formed again. Wire enamels have been a major use.

In order to make an ester of poly(vinyl alcohol) with pendant unsaturation, an indirect route once again is needed. One such commercial polymer is produced by the reaction of **cinnamoyl chloride** with poly(vinyl alcohol) dispersed in pyridine [26].

A dry film of the product can be deposited from a solution and easily redissolved. However, when it is exposed to light, extensive cross-linking insolubilizes the film. Lithographic plates are made by this photosensitive insolubilization. Poly(vinyl alcohol) itself also can be photoinsolubilized in the presence of chromate ions and by exposure to much higher intensities of ultraviolet light than the cinnamate [26]. Photoresists are also discussed in Section 13.5.

16.5.2 SELECTED USES

Some familiar items made from plasticized PVC include garden hoses, laboratory tubing, and numerous film products such as shower curtains, diaper covers, and rain-coats. Blow-molded bottles (for lubricating oil, shampoo, and other cleaning solutions) and sheet-formed packaging are made from unplasticized (*rigid*) vinyls. The construction industry makes use of large quantities of rigid PVC for pipe, plastic siding, and glazing. Although far outweighed by the chloride and acetate, several other vinyl monomers are homopolymerized industrially. **Poly(vinyl ethyl ether)** finds use in pressure-sensitive adhesives. **Poly(vinyl pyrrolidone) (PVP)** probably has its major market as a home-permanent wave-setting resin. It has unique complexing properties that make it valuable in some pharmaceutical and physiological applications. The iodine complex of PVP is an effective antiseptic that is much lower in toxicity than iodine itself. Also, about 7% PVP added to whole blood allows it to be frozen, stored at liquid nitrogen temperatures for years, and thawed out without destroying blood cells. **Poly(vinylidene chloride)** is molded into pipes and fittings for corrosion-resistant applications. However, it is probably most familiar in the form of a household plastic film, Saran Wrap (Dow Chemical Company, Midland, MI), which may be plasticized by acetyl tributyl citrate. Because it is a safe and stable barrier material with low-energy absorption, it is widely used as a cover for foods that are heated in microwave ovens.

16.6 THE ACRYLICS

Acrylic and methacrylic acid and their esters are included in the acrylic group (Appendix 16.G). Otto Röhm published his doctoral thesis dealing with acrylic compounds in 1901 in Germany. First in Germany (1927) and then in the United States (1931), he was associated with the commercialization of acrylic polymers as coating resins. Later in the 1930s, **poly(methyl methacrylate)** sheets and molding compounds became available. Latex paints based on ethyl acrylate for exterior application achieved importance in the 1950s and 1960s. Acrylonitrile has been mentioned previously in Section 16.3 as a fiber former and as a comonomer in oil-resistant rubber.

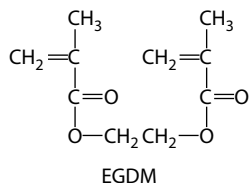
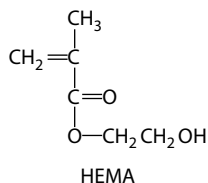
16.6.1 SOME INDIVIDUAL POLYMERS

Acrylates can be made by a single-step process from acetylene or a two-step process from ethylene oxide. Methacrylates can be made by selective oxidation of isobutylene followed by esterification or a two-step process starting with acetone.

The continuous bulk polymerization of methyl methacrylate was used as an example in Section 5.2. A stirred bulk polymerization like that used for styrene (Section 5.4) could be adapted for methyl methacrylate. A suspension process for poly(methyl methacrylate) was described in Section 5.4. The polymerization of **ethyl acrylate** most often is carried out in emulsion. A process such as that used for vinyl acetate is suitable (Section 16.4). Like vinyl acetate, the monomer is slightly water soluble, so *true* emulsion polymerization kinetics are not followed. That is, there is initiation of monomer dissolved in water in addition to that dissolved in growing polymer particles. Ethyl acrylate is distinguished by its rapid rate of propagation. Initiation of a 20% monomer emulsion at room temperature by the redox couple persulfate–metabisulfite can result in over 95% conversion in less than a minute. As with vinyl acetate polymerization, a continuous addition of monomer at a rate commensurate with the heat transfer capacity of the reactor is necessary in order to control the temperature.

A copolymer of ethyl acrylate with 5% chloroethyl vinyl ether has been marketed as an oil-resistant, high-temperature-stable, specialty elastomer. The pendant chlorine group gives a preferred cross-linking site with polyfunctional amines. The relatively high T_g of the rubber (about 28°C) can be lowered by plasticization, but this can be temporary if oils or solvents are in contact with the product and leach out the plasticizer. Interpolymers of ethyl acrylate with methyl methacrylate and with higher acrylates and methacrylates are widely used as latex paints and as additives for paper and textiles. The T_g of an interpolymers can be *tailored* for a particular application by varying the ratio of acrylate to methacrylate monomers.

Methacrylates are used in contact lenses. The hard lenses generally are made from poly(methyl methacrylate). Soft lenses were introduced in the 1970s and are made from cross-linked poly(2-hydroxyethyl methacrylate), also called **poly(HEMA)**. HEMA is copolymerized with hydrophilic monomers (primarily vinyl pyrrolidone) to increase water content and improve oxygen transfer. As it is used, poly(HEMA) is slightly cross-linked with ethylene glycol dimethacrylate (**EGDM**). It is a swollen hydrogel in contact with tears, but does not dissolve. In the late 1990s, silicone hydrogels that are biphasic soft lenses made of poly(dimethyl siloxane) (PDMS) and poly(HEMA) were developed. The silicone hydrogels provide increased tear resistance over the original poly(HEMA) hydrogels.



While the soft lenses require more care and may be of somewhat lower optical quality, they are usually more comfortable and easier to get accustomed to. Over 75% of contact wearers prefer them.

Hard contact lenses are machined to prescribed dimensions with a lathe from blanks sliced from prefabricated poly(methyl methacrylate) rods. Stresses must be

relieved to prevent deformation. Hydration of the lenses occurs after machining and finishing. The polymerization and fabrication processes for soft lenses are carried out by a casting operation. A spinning mold is used so that the outside diameter of the lens is determined by the mold surface and the inside diameter depends on the rotational speed of spinning that alters the free surface. Free-radical polymerization of the monomers–water mixture takes place in the mold. While poly(HEMA)-based hydrogels dominate the soft contact lens market, many other hydrogels have been tested and used in bioengineering and biomedical applications such as bioseparations, tissue engineering (such as soft tissue replacements in the human body), and drug delivery [27–29].

16.6.2 SELECTED USES

To the layman, the term acrylic plastic has become synonymous with poly(methyl methacrylate), although the trade names such as Plexiglas, Lucite, Perspex, and Acrylite might be even better known. The high light transmittance of poly(methyl methacrylate) has led to its use in a variety of decorative forms. Industrially, one single large market for molded, dyed polymers has been automotive exterior signal lenses. The toughness and stability of the polymer are important. In the automobile interior and in appliance panels, *internally lighted* numerals and letters can be molded in, since the transparent plastic transmits light so well that it is scattered only at interruptions such as raised or roughened surfaces. Aircraft glazing was formed from stretched sheets for many years, but polycarbonates are used more often now. Acrylics can be toughened by rubber addition in the manner of polystyrene, but with a sacrifice in light transmission.

Some other uses of acrylate and methacrylate interpolymers are as viscosity index improvers in lubricating oil, ion-exchange resins, textile additives, paper coating, thermosetting (baking) coatings, and polymeric plasticizers in PVC. (Cyanoacrylate adhesives were described in Section 13.4.)

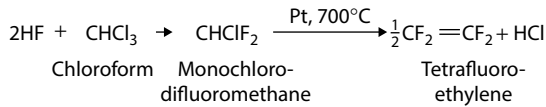
The water-soluble polymers of acrylamide, acrylic acid, and methacrylic acid probably are produced mainly by solution polymerization. Interpolymers of these monomers are used in sewage coagulation, drag reduction, adhesives, coatings, and textile and paper sizes. One major application has grown over the years: The ubiquitous disposable diaper often is based on *superabsorbent* salts of poly(acrylic acid).

16.7 THE FLUOROCARBON POLYMERS

Although many fluorocarbon polymers are commercially available (Appendix 16.H), poly(tetrafluoroethylene) (**PTFE**) is estimated to command about 90% of the market. This polymer, under DuPont's trade name, Teflon, has been made since the early 1940s. Both PTFE and poly(chlorotrifluoroethylene) were developed to meet wartime demands, especially for the corrosive processes involving separation of radioactive isotopes. Many other fluorinated polymers have been commercialized over the years.

16.7.1 SOME INDIVIDUAL POLYMERS

The combination of high-temperature stability, chemical resistance, and surface lubricity has made PTFE useful in many industrial applications and in coated kitchenware such as frying pans, cookie sheets, pots, and pans. In order to make the monomer, chloroform is treated with hydrofluoric acid to give an intermediate that is subjected to pyrolysis.



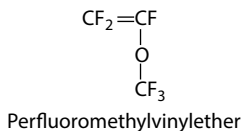
Emulsion polymerization of the monomer gives a latex that is used directly in some applications, notably in thin coatings. Suspension polymerization can be carried out to produce a granular product in the form of irregular particles [30]. Special techniques have been developed to process the polymer into useful items. The polymer is dense (2.2 g/cm^3), insoluble at temperatures below its T_m (327°C), and highly crystalline (see Figure 9.17 for thermal transitions). The favored method for forming resembles techniques developed for powdered metals. Particles are brought into intimate contact by high-pressure preforming or by suspension in an oil that is removed before fusing. The particles are sintered together by heating to 37°C followed by cooling. Thin coatings adhere well to metals, but the polymer is very hard to print on or to fasten to another surface by ordinary adhesives. Good adhesion usually requires a chemical alteration of the surface. A dispersion of sodium metal in kerosene will attack PTFE sufficiently to allow adhesion to metals and plastics. It is one of the few reagents that have any effect on this polymer. Semifinished forms that are available include tape, film, tubing, and fibers. The tape may be skived, that is, shaved from a molded cylinder. Extruded tape, made by sintering an extruded paste of powder in oil, is much smoother but somewhat more expensive. Spun fibers of PTFE also are quite expensive. However, a less costly process has been developed which produces fibrous porous shapes by a replicating technique.

Poly(chlorotrifluoroethylene) and the copolymer of fluorinated ethylene and propylene represent polymers that can be molded by conventional techniques while preserving a large measure of the chemical resistance and high-temperature stability of PTFE. There is a sacrifice in these properties, however. Films based on vinyl fluoride and vinylidene fluoride are much more stable than the corresponding chloride products. Their use has been recommended in outdoor applications where weather resistance and moisture containment are important as in moisture barriers in home building. While the fluorine-carbon bond is very strong in these polymers, the carbon-hydrogen bond is susceptible to oxidation, making them less chemically resistant than a fully fluorinated material. However, they are much more dimensionally stable, not having the multiple transitions near room temperature that are associated with PTFE's tendency to cold flow.

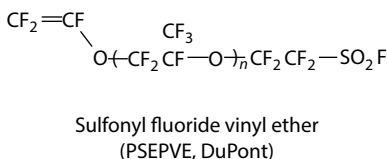
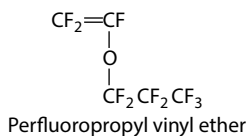
Rubbers based on fluoro- or chlorofluoropolymers make use of carbon-hydrogen bonds in a comonomer to provide cross-linking sites. Peroxides can be used to

abstract hydrogen atoms, leaving chain radicals to join in carbon–carbon links. However, amines such as hexamethylenediamine are used more often. One widely used fluorocarbon rubber (FPM) rubber can be cross-linked by heating with an alicyclic amine salt and magnesium oxide at 150°C for 30 min followed by a *post-cure* of 24 h at 200°C. The vulcanizate can be used for continuous service as high as 200°C and yet can be useful down to its brittle temperature of –40°C. Solvent and chemical resistance are excellent except for amines, ketones, and a few other polar chemicals.

In 1970, DuPont introduced a perfluoroelastomer under the trade name of Kalrez that is based on tetrafluoroethylene and perfluoromethylvinylether [31].



A third perfluorinated monomer (perhaps 1-hydropentafluoropropylene) provides a cross-linking site. The random copolymer has a molar ratio of 3:2 for the two major monomers, C_2F_4 and $\text{C}_3\text{F}_6\text{O}$, respectively, and a T_g of –12°C. The rubbery material and its cross-linked derivative are quite stable for months at 288°C. Two other monomers that have been used with C_2F_4 are a vinyl propyl ether and an ionic ether:



The first monomer has been used to modify PTFE to make it thermoplastic but with somewhat better stability than FEP based on perfluoropropylene (Appendix 16.H). The second monomer makes copolymers that are ionomers swelling in water. Films of copolymers (Nafion, DuPont) have been used as membranes in electrolytic cells and ion recovery units [32].

16.7.2 SELECTED USES

The workhorse of the fluorocarbon family, PTFE, is molded and extruded only by the special techniques mentioned previously. A familiar form of film is the tape used as a pipe thread *dope*. The cold flow of the polymer to seal the threaded pipe joint is a real advantage here. Fibers have been made from the polymer and woven into textile for special applications such as filter fabrics, protective clothing, surgical thread, and even dental floss. The rubbery copolymers are most often seen as O-rings and gaskets, but tubing and sheets are also available.

APPENDIX 16.A GENERIC CLASSIFICATION OF SOME COMMERCIAL ELASTOMERS

ASTM Designation	Common or Trade Name	Chemical Designation
IR	Synthetic NR	Synthetic polyisoprene
IIR	Butyl, Chlorobutyl	Isobutylene–isoprene
ACM	Acrylic	Polyacrylate
AU ^a	Urethane (IJR)	Polyurethane (polyester)
EU ^a	Urethane (UR)	Polyurethane (polyether)
BR	CBR, PBd	Polybutadiene
CO ^a	Hydrin (CO, ECO)	Polyepichlorohydrin
CR	Neoprene	Chloroprene
CSM	Hypalon (HYP)	Chlorosulfonyl polyethylene
FPM	EP elastomer	Ethylene propylene copolymer
EPDM	EP elastomer	Ethylene propylene terpolymer
ET	Thiokol A	Ethylene polysulfide
EOT ^a	Thiokol B	Ethylene ether polysulfide
FKM	Viton, Fluorel, Kel-F	Fluorinated hydrocarbon
NBR	Buna N, Nitrile	Butadiene–acrylonitrile
SBR	GR-S, Buna S	Styrene–butadiene
VMQ ^a	Silicone	Poly(dimethylsiloxane) with vinyl groups
PVMQ ^a	Silicone	Silicone rubber having methyl, phenyl, and vinyl groups
FVMQ ^a	Silastic LS	Silicone rubber having methyl, vinyl, and fluorine groups
CM	Plaskon CPE	Chlorinated polyethylene
NR	NR	Natural polyisoprene
YSBR	Kraton, Solprene	Block copolymers of styrene and butadiene

Source: ASTM Standard D-1418-99.

^a Heterochain polymers.

APPENDIX 16.B CLASSIFICATION AND PROPERTIES OF PRINCIPAL MAN-MADE FIBERS

Fibers	Characteristic Properties
Cellulosic fibers	
Rayon—composed of regenerated cellulose from wood and cotton fiber ^a	Easy to dye and finish, offers high moisture absorption, flexibility, soft hand, good drape, minimum tendency to develop static charges
Acetate and triacetate—composed of regenerated cellulose from wood and cotton fiber that has been treated with acetic acid ^a	Easy to dye, supple, fast drying, good drape, wrinkle resistant; heat-set triacetate has high resistance to shrinking, stretching, and wrinkling
Synthetic polymer fibers (noncellulosic)	
Acrylic—at least 85% by weight acrylonitrile-based polymer	Warmth without weight, durable, soft hand, shape retention, resistant to sunlight, weather, oil and chemicals
Modacrylic—at least 35% but not more than 85% acrylonitrile-based polymer	Resembles acrylic fibers; self-extinguishes when exposed to flame
Anidex—a manufactured fiber in which the fiber-forming substance is any long-chain synthetic polymer composed of at least 50% by weight of one or more esters of a monohydric alcohol and acrylic acid	Imparts permanent stretch and recovery properties of fabrics
Aramid—a manufactured fiber in which the fiber-forming substance is a long-chain synthetic polyamide in which at least 85% of the amide linkages are attached directly to two aromatic rings ^a	High strength, high-temperature stability
Novoloid—a manufactured fiber containing at least 85% by weight of a cross-linked novolac	Converts to carbon fiber at high temperatures, used in flame-protective garments
Nylon—a manufactured fiber in which the fiber-forming substance is a long-chain synthetic polyamide in which less than 85% of the amide linkages are attached directly to two aromatic rings ^a	Great strength, chemical resistance, high elasticity, durability, range of dyeability
Nytril—a manufactured fiber containing at least 85% of a long-chain polymer of vinylidene dinitrile where the vinylidene dinitrile content is no less than every other unit in the polymer chain	Soft and resilient, used in sweaters
Olefin—at least 85% by weight ethylene, propylene, or other olefin-based polymers; polypropylene most common	Lightest man-made fiber, low moisture absorption, high strength, chemical and soil resistance
Polyester—at least 85% by weight of an ester based on dihydric alcohol and terephthalic acid ^a	High strength, resistance to stretching and shrinking; dyes well; resists chemicals, crisp and resilient both wet and dry; fabric can be heat-set

(Continued)

Fibers

Saran—at least 80% by weight vinylidene chloride-based polymer

Spandex—at least 85% by weight of polyurethane^a

Vinal—a manufactured fiber in which the fiber-forming substance is any long-chain synthetic polymer composed of at least 50% by weight of vinyl alcohol units and in which the total of the vinyl alcohol units and any one or more of the various acetal units is at least 85% by weight of the fiber^a

Vinyon—at least 85% by weight vinyl chloride-based polymer

Characteristic Properties

Resistance to chemicals, sunlight, outdoor exposure, nonflammable

Easily dyed, strength and durability, high elastic recovery, resistance to chemicals

High resistance to chemicals

Resistance to chemicals; softens at low temperatures

Fibers from nonfibrous natural substances

Glass—composed of silicon dioxide and other components drawn from molten state

Great strength and resistance to heat, flame, and most chemicals; will not shrink, stretch, or absorb water

Metal—various metals and alloys drawn to fine-diameter fiber

Properties similar to metals from which they are drawn

Rubbet—natural or synthetic rubber drawn into fiber form

Elastic often is a core around which other fibers are wrapped

Azlon—manufactured from naturally occurring proteins in corn, peanuts, and milk^a

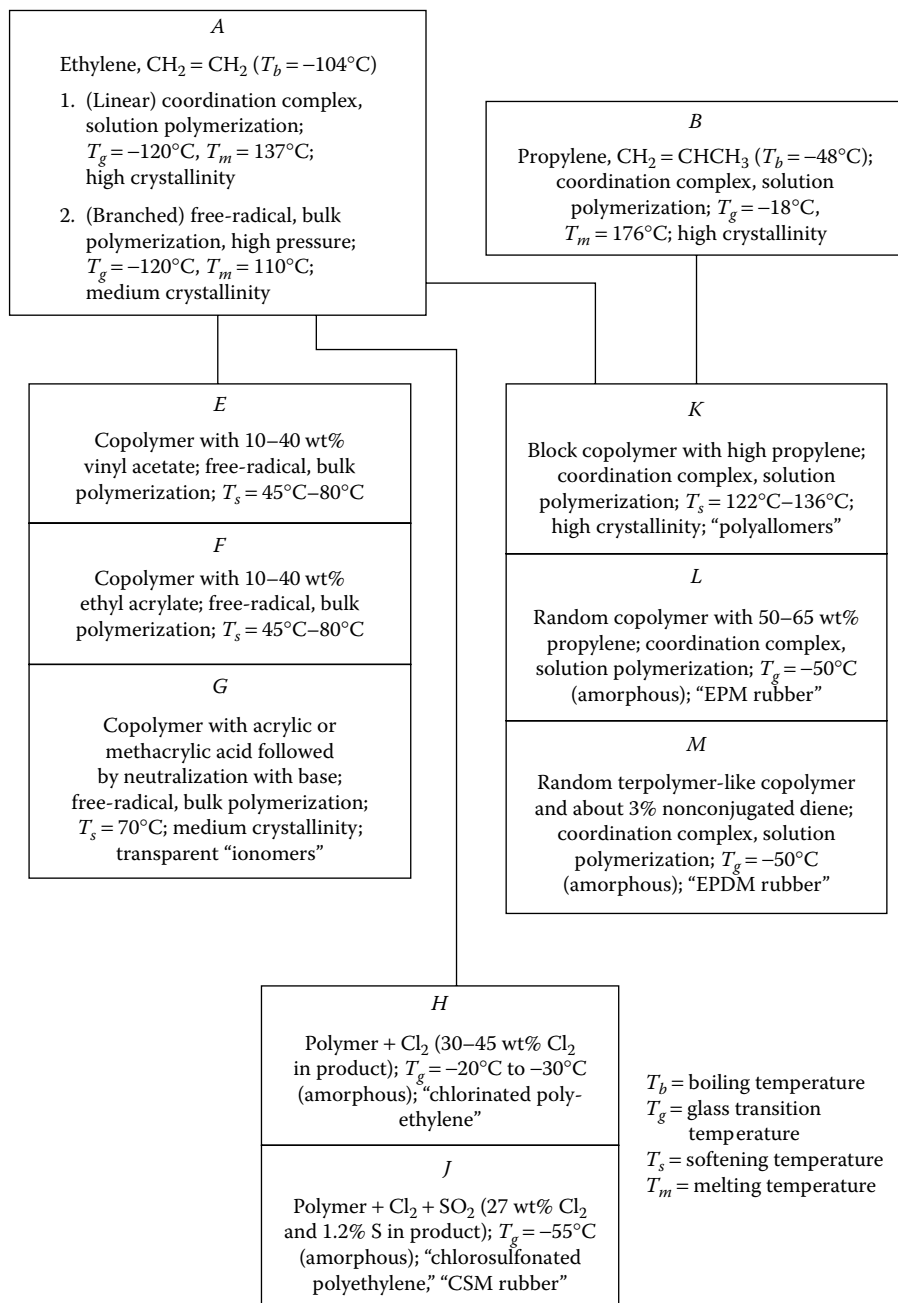
Soft feel, blends with other fibers, used like wool

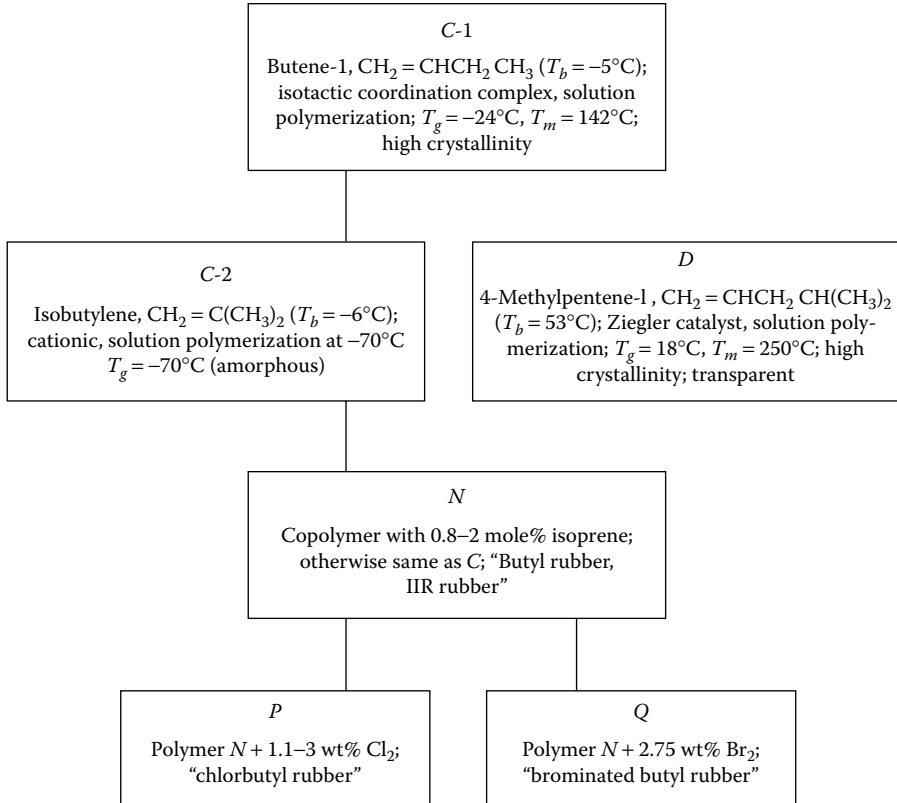
Source: Man-Made Fiber Producers Association, *Guide to Man-Made Fibers*, Washington, DC, 1977 (and subsequent editions).

Note: This fabrication is based on the Federal Trade Commission's Textile Fiber Products Identification Act, which assigns generic names to the various types of man-made fibers.

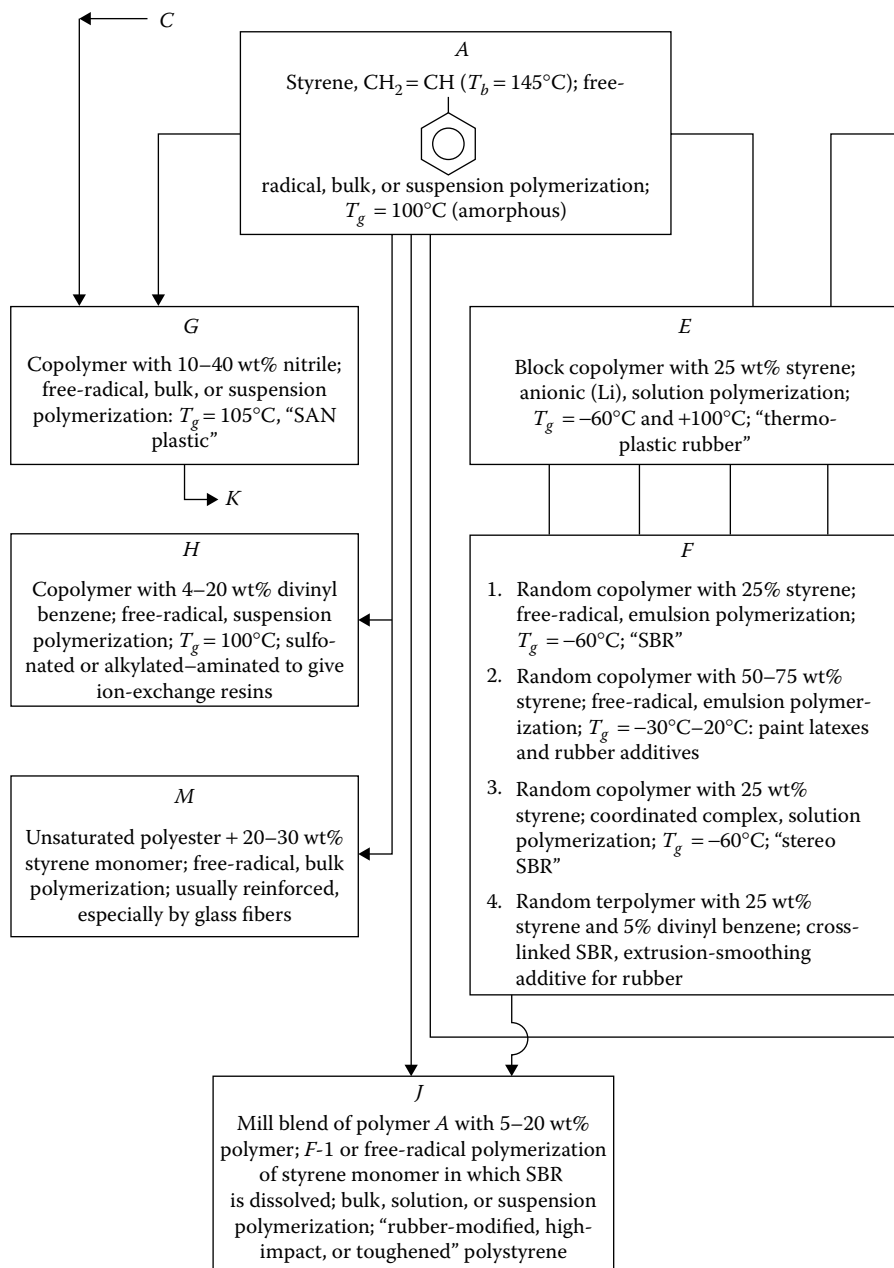
^a Heterochain polymers.

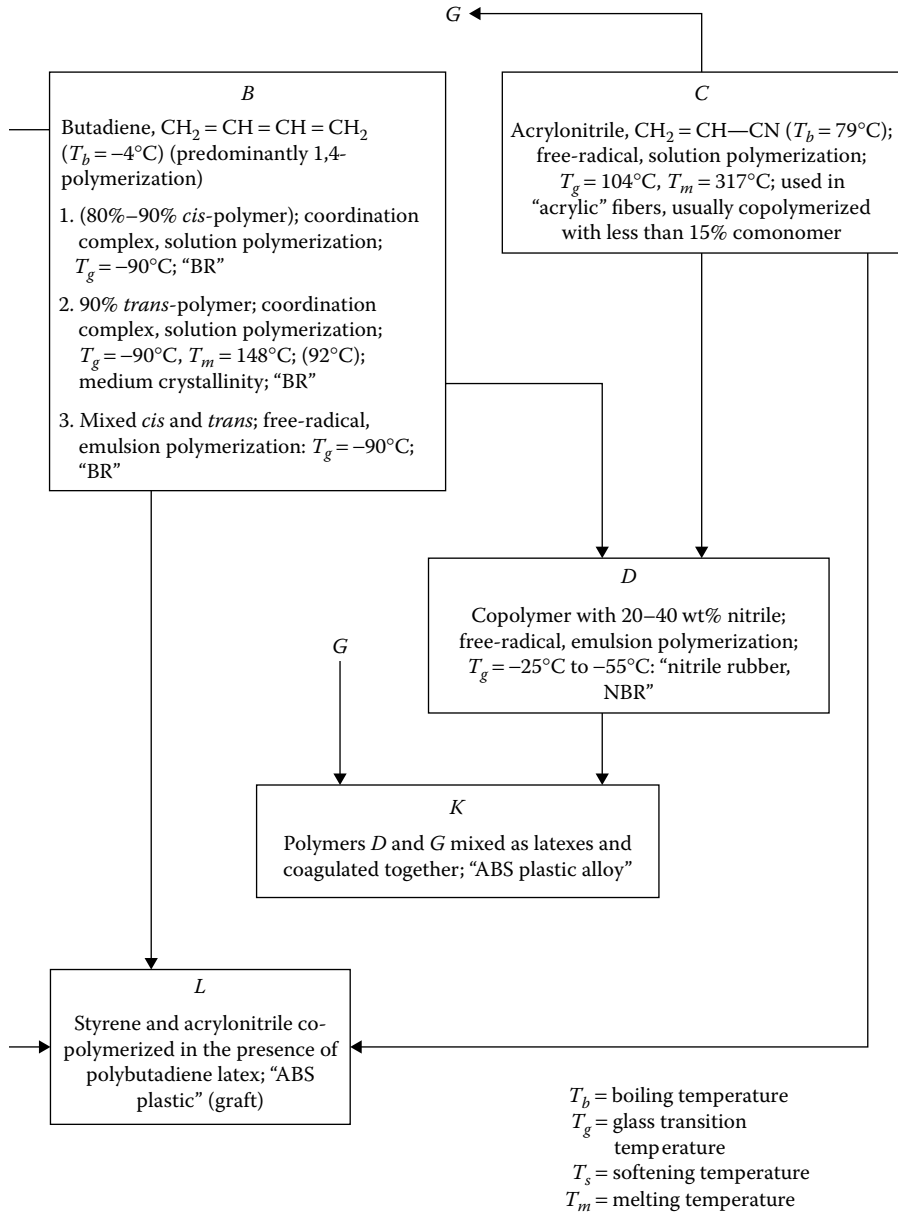
APPENDIX 16.C THE POLYOLEFINS



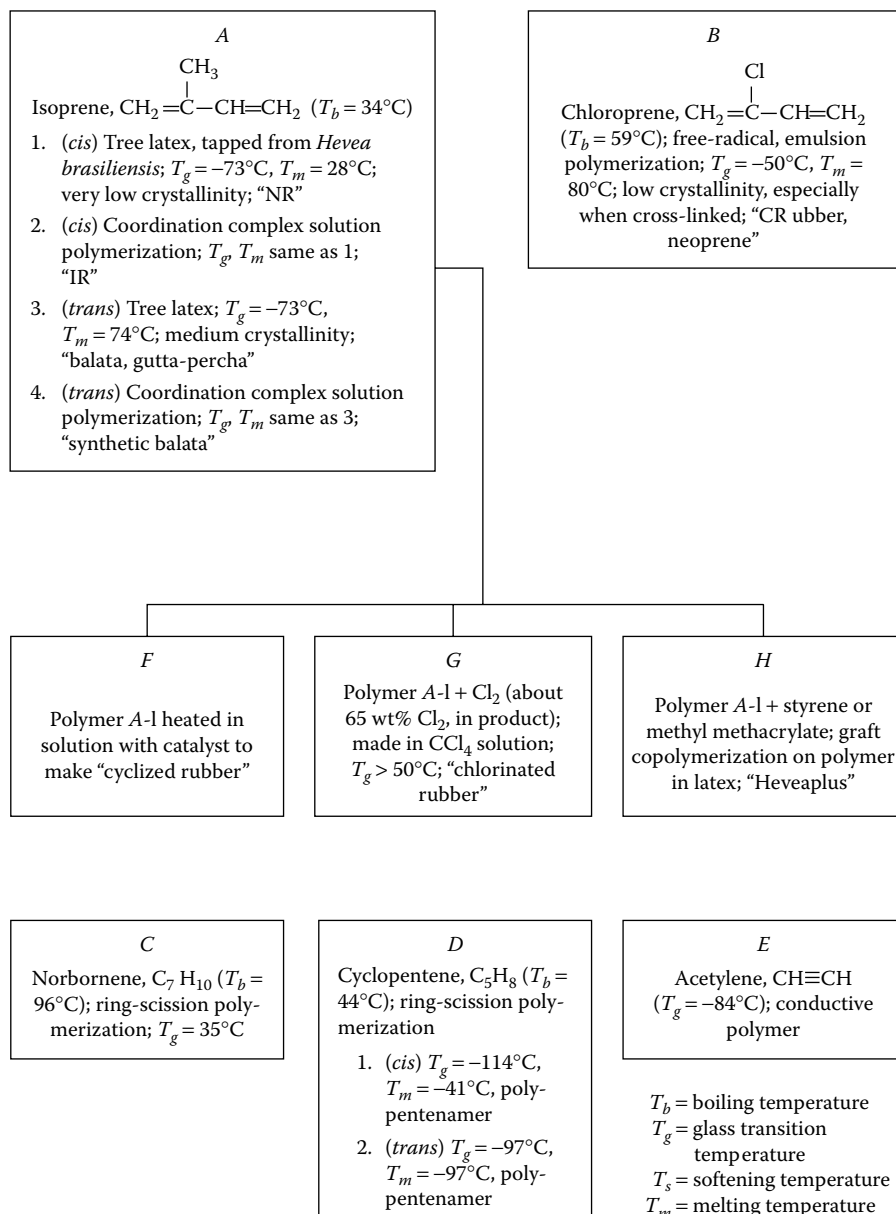


APPENDIX 16.D THE ACRYLONITRILE–BUTADIENE–STYRENE GROUP

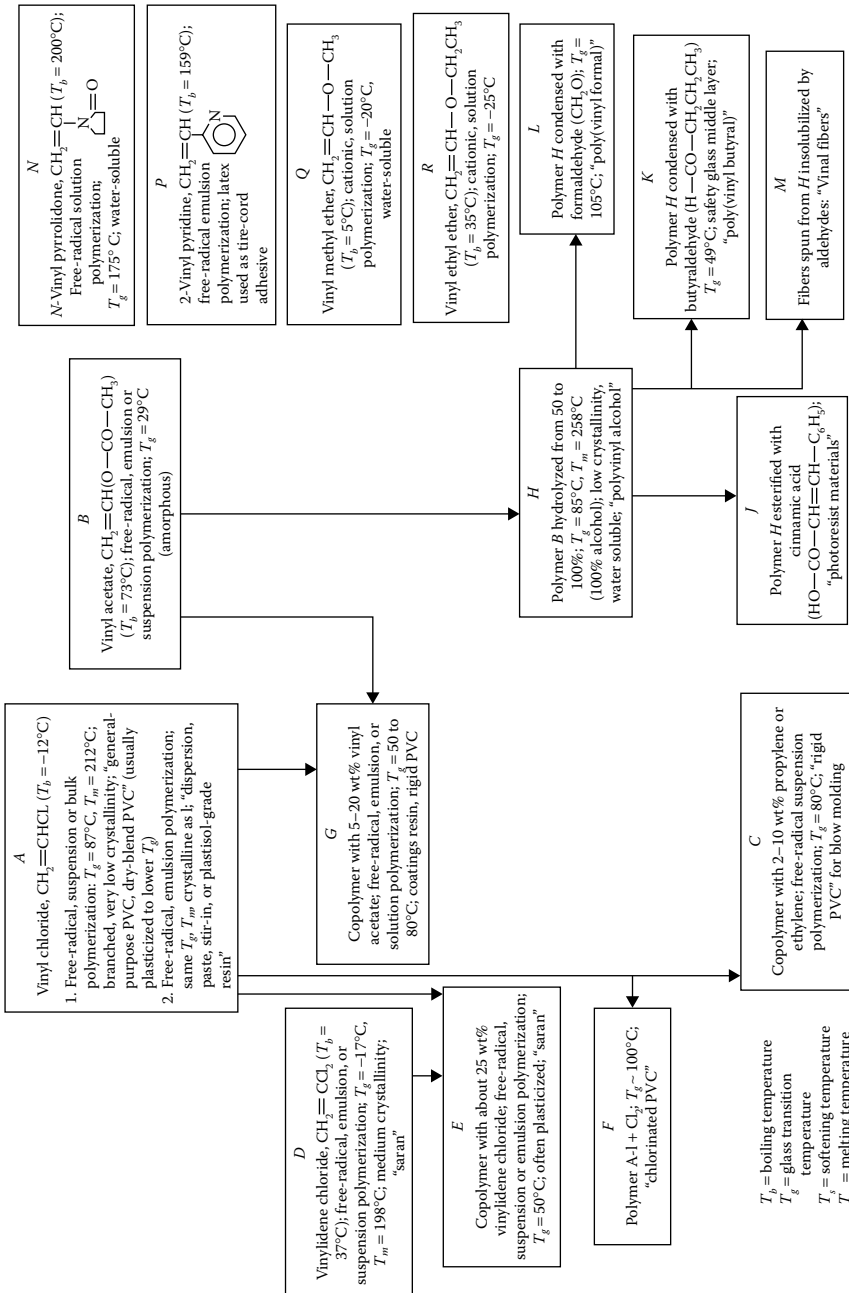




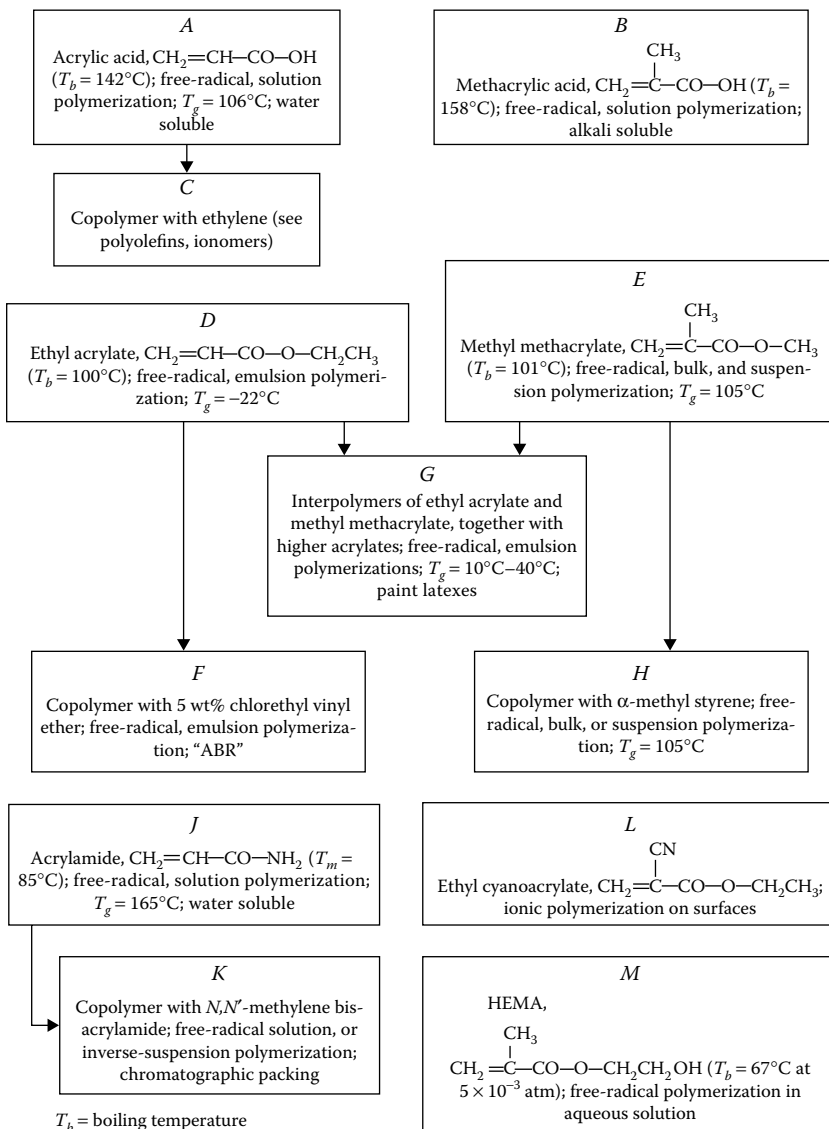
APPENDIX 16.E THE DIENES (BUTADIENE INCLUDED IN APPENDIX 16.D)



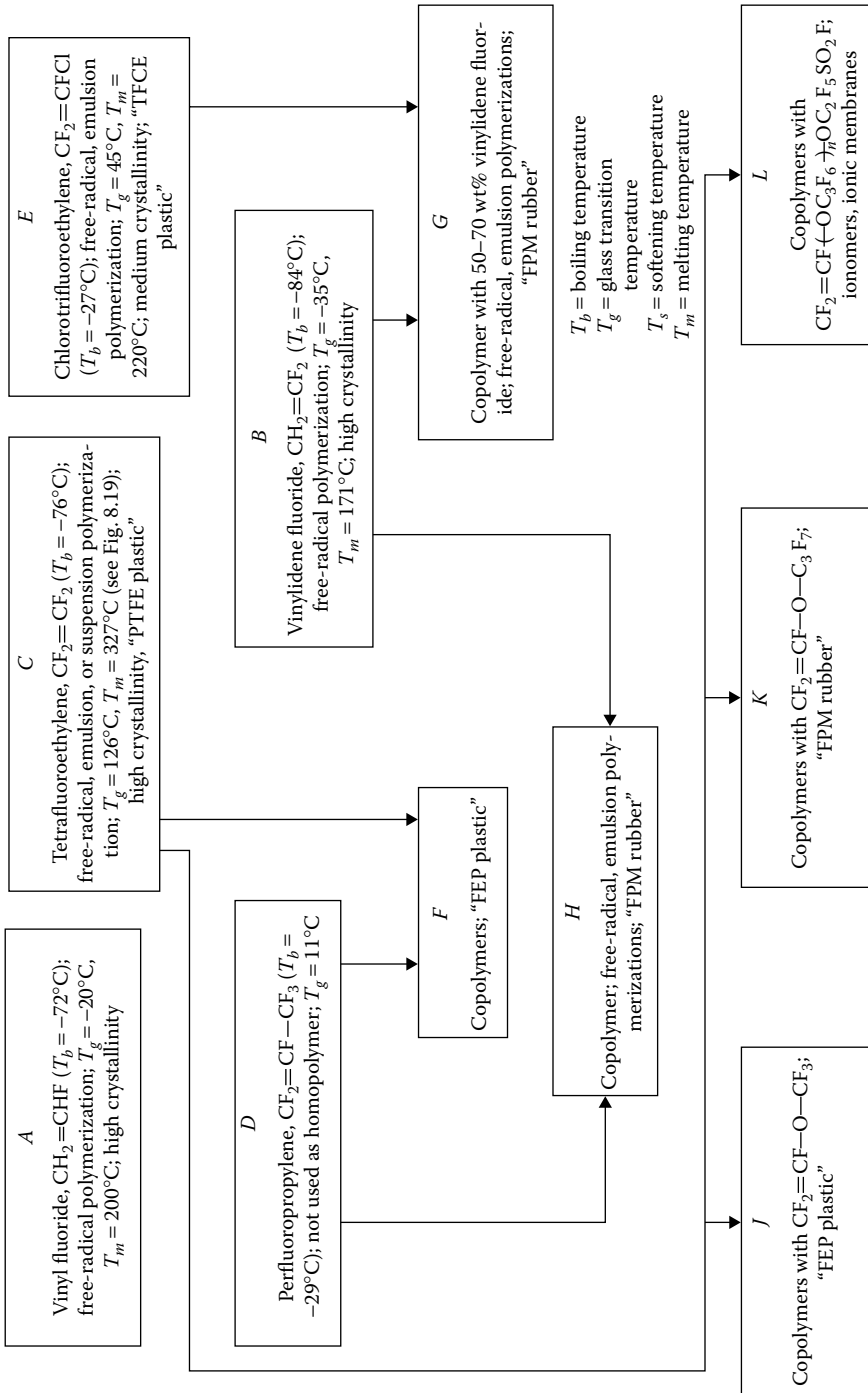
APPENDIX 16.F THE VINYLs



APPENDIX 16.G THE ACRYLICS

 T_b = boiling temperature T_g = glass transition
temperature T_s = softening temperature T_m = melting temperature

APPENDIX 16.H THE FLUOROCARBON POLYMERS



KEYWORDS

Polyolefins
Ionomer
LDPE
LLDPE
HDPE
UHMWPE
Isotactic polypropylene
Polyallomer
Chlorinated polyethylene
Chlorosulfonated polyethylene
ABS
SBR
SIBR
NBR
SAN
Nitrile rubber
Barrier resin
Cast polyester
Ion-exchange resin
NR
Guayule
Gutta-percha
Balata
Polychloroprene (CR)
Polynorbornene
Cyclized rubber
Polyacetylene
Diacytlyene
Dry-blend resin
Dispersion (plastisol) resin
Poly(vinyl butyral)
Granulation polymerization
HEMA
Poly(tetrafluoroethylene)

PROBLEMS

- 16.1 Describe two methods for coagulating a latex (note SBR and CR production).
- 16.2 Assuming 15% conversion per pass, calculate the energy needed to compress ethylene to 2000 atm and 100°C for the production of 1 lb of polymer. At \$0.03/kWh, is this a significant production cost?
- 16.3 Explain the origin of short- and long-chain branches in polyethylene produced at high pressures.
- 16.4 Why are so many synthetic rubbers copolymers?

- 16.5** What difference in structure might be expected between cold- (5°C) and hot-process (50°C) SBR?
- 16.6** Why are some ethylene–propylene copolymers stiff and crystalline (at room temperature), while others are soft and amorphous?
- 16.7** Vinyl acetate is polymerized, hydrolyzed, and reacted with butyraldehyde to give a soluble product.
- (a) Why is it not hydrolyzed first, then polymerized?
- (b) What is a major use of the product from each of the three steps?
- 16.8** A monodisperse triblock polymer has end blocks of styrene and a central block of butadiene (mixed *cis* and *trans*). If the density is 0.985 g/cm³ (25°C) and the molecular weight measured by osmometry is 100,000, what is the molecular weight and the degree of polymerization of each styrene end block? Assume additivity of volumes.
- Densities (g/cm³) at 25°C:
Polystyrene, 1.054; polybutadiene (mixture of *cis* and *trans*), 0.896.
- 16.9** In a test for carbon dioxide permeability, dishes containing pellets of NaOH are covered by films of acrylonitrile–styrene copolymers. The dish covers are 10.0 cm in diameter and the films are 50.0 μm thick. The samples are placed in a chamber with carbon dioxide at one atmosphere and 27°C. What is the expected weight gain in 7 days if the film is 67% acrylonitrile? See Table 16.2.
- 16.10** Under the conditions of Problem 16.9, how long would it take (in hours) for the dish to gain 0.100 g if the film were polystyrene?

REFERENCES

1. ASTM Standard D-1418-10a - Standard Practice for Rubber and Rubber Lattices. Nomenclature.
2. Man-Made Fiber Producers Association: *Guide to Man-Made Fibers*, Washington, DC, 1977 (and subsequent editions).
3. Vassily, C. (ed): *Handbook of Polyolefins*, 2nd edn., Dekker, New York, 2000.
4. Kaminsky, W.: chap. 1 in H. R. Kricheldorf (ed.), *Handbook of Polymer Synthesis*, Part A, Dekker, New York, 1992.
5. Winding, C. C., and G. D. Hiatt: *Polymeric Materials*, McGraw-Hill, New York, 1961, pp. 383–387.
6. Latimme, R. R.: Styrene-Butadiene Rubber, in R. E. Kirk, and D. F. Othmer (eds.), *Kirk-Othmer Encyclopedia of Chemical Technology*, vol. 22, 4th edn., 1997, p. 994.
7. Halasa, A. F.: *Rubber Chem. Technol.*, 70:295 (1997).
8. Qestra Crystalline Polymers—Data Sheets, Dow Chemical Co., Midland, MI, 2002.
9. Karjala, T. P., Y. W. Cheung, and M. J. Guest: *SPE ANTEC Proc.*, 2127 (1999).
10. Timmers, F. J.: (Dow Chemical Company), U.S. Patent 5,703,187 (1997).
11. McIntyre, D., H. L. Stephens, and A. K. Bhowmick: Guayule Rubber, in A. K. Bhowmick and H. L. Stephens (eds.), *Handbook of Elastomers*, Dekker, New York, 1988.
12. Stern, H. J.: *Rubber: Natural and Synthetic*, 2nd edn., Palmerton, New York, 1967, p. 12.
13. Stewart, C. A., Jr., T. Takeshita, and M. L. Coleman: Chloroprene Polymers, in H. F. Mark (ed.), *Encyclopedia of Polymer Science and Engineering*, vol. 3, 2nd edn., 1985, p. 441.
14. Johnson, P. R.: *Rubber Chem. Technol.*, 49:650 (1976).

15. Tinker, A. J.: *NR Technol.*, 18:30 (1987).
16. Gelling, I. R.: *NR Technol.*, 18:21 (1987).
17. Matsumoto, S., K. Komatsu, and K. Igarashi: chap. 21 in I. Saegusa and E. Goethals (eds.), *Ring-Opening Polymerizations*, ACS, Washington, DC, 1977, pp. 303–317.
18. Walker, D.: *Rubber Plast. News*, October 3, 1977, p. 1.
19. Shirakawa, H., and S. Ikeda: *Polym. J.*, 2:231 (1971).
20. Naarmann, H., and P. Strohrriegel: chap. 21 in H. R. Kricheldorf (ed.), *Handbook of Polymer Synthesis*, Part B, Dekker, New York 1992.
21. Chance, R. R.: Diacetylene Polymers, in J. I. Kroschwitz (ed.), *Encyclopedia of Polymer Science and Engineering*, vol. 4, 2nd edn., 1987, p. 767.
22. Bloor, D., and R. R. Chance (eds.): *Polydiacetylenes: Synthesis, Structure, and Electronic Properties*, Martinus Nijhoff, Leiden, The Netherlands, 1985.
23. Terwiesch, B.: *Hydrocarbon Processing*, 55:117 (November 1976).
24. Daniels, W.: Vinyl Ester Polymers, in H. F. Mark (ed.), *Encyclopedia of Polymer Science and Engineering*, vol. 17, 2nd edn., 1989, p. 393.
25. Marten, F. L.: Vinyl Alcohol Polymers, in H. F. Mark (ed.), *Encyclopedia of Polymer Science and Engineering*, vol. 17, 2nd edn., 1989, p. 181.
26. Kosar, J.: *Light Sensitive Systems*, Wiley, New York, 1965, pp. 66, 141–142.
27. Andrade, J. D. (ed.): *Hydrogels for Medical and Related Applications*, ACS, Washington, DC, 1976.
28. Peppas, N. A., Y. Huang, M. Torres-Lugo, J. H. Ward, and J. Zhang: *Ann. Rev. Biomed. Eng.*, 2:9 (2000).
29. Saltzman, M. W.: *Drug Delivery: Engineering Principles for Drug Therapy*, Oxford University Press, Oxford, 2001.
30. Gangal, S. V.: Tetrafluoroethylene Polymers, in H. F. Mark and J. I. Kroschwitz (ed.), *Encyclopedia of Polymer Science and Engineering*, vol. 16, 2nd edn., 1989, p. 577.
31. Arnold, R. G., A. L. Barney, and D. C. Thompson: *Rubber Chem. Technol.*, 46:619 (1973).
32. Savu, P. M.: Perfluoroalkanesulfonic Acids, in R. E. Kirk, and D. F. Othmer (eds.), *Kirk-Othmer Encyclopedia of Chemical Technology*, vol. 11, 4th edn., 1994, p. 558.

GENERAL REFERENCES

- Albright, L. E.: *Processes for Major Addition-Type Plastics and Their Monomers*, McGraw-Hill, New York, 1974.
- Arthur, J. C., Jr. (ed.): *Polymers for Fibers and Elastomers*, ACS, Washington, DC, 1984.
- Bhowmick, A. K., and H. L. Stephens (eds.): *Handbook of Elastomers*, Dekker, New York, 1988.
- Blackley, D. C.: *Synthetic Rubbers*, Elsevier Applied Science, New York, 1983.
- Bloor, D., and R. R. Chance (eds.): *Polydiacetylenes: Synthesis, Structure, and Electronic Properties*, Martinus Nijhoff, Leiden, The Netherlands, 1985.
- Brydson, J. A.: *Plastics Materials*, 4th edn., Butterworth, Woburn, MA, 1982.
- Buchholz, F., and A. Graham: *Modern Superabsorbent Polymer Technology*, Wiley, New York, 1997.
- Burgess, R. H. (ed): *Manufacturing and Processing of PVC*, Elsevier Applied Science, New York, 1981.
- Butters, G. (ed): *Particulate Nature of PVC*, Elsevier Applied Science, New York, 1982.
- Chien, J. C. W.: *Polyacetylene*, Academic Press, New York, 1984.
- Chung, T. C. (ed): *New Advances in Polyolefins*, Plenum Press, New York, 1993.
- Cowie, J. M. G. (ed.): *Alternating Copolymers*, Plenum Press, New York, 1985.

- Culbertson, B. M., and J. E. McGrath (eds.): *Advances in Polymer Synthesis*, Plenum Press, New York, 1985.
- Davidson, R. L. (ed): *Handbook of Water-Soluble Gums*, McGraw-Hill, New York, 1980.
- De, S. K., and A. K. Bhowmick (eds.): *Thermoplastic Elastomers from Rubber-Plastic Blends*, Prentice Hall, Englewood Cliffs, NJ, 1991.
- Dragutan, V., A. T. Balaban, and M. Dimonie: *Olefin Metathesis and Ring-Opening Polymerization of Cyclo-Olefins*, Wiley, New York, 1986.
- Dyson, R. W. (ed.): *Specialty Polymers*, Chapman & Hall (Methuen), New York, 1987.
- El-Aasser, M. S., and J. W. Vanderhoff (eds.): *Emulsion Polymerisation of Vinyl Acetate*, Elsevier Applied Science, New York, 1981.
- Elias, H.-G.: *Macromolecules, Synthesis, Materials, and Technology*, 2nd edn., Plenum Press, New York, 1984.
- Elias, H.-G., and F. Vohwinkel: *New Commercial Polymers: 2*, Gordon & Breach, New York, 1986.
- Erusalimskii, B. L.: *Mechanisms of Ionic Polymerization*, Plenum Press, New York, 1986.
- Finch, C. A. (ed): *Chemistry and Technology of Water-Soluble Polymers*, Plenum Press, New York, 1983.
- Flick, E. W. (eds.): *Industrial Synthetic Resins Handbook*, 2nd edn., Noyes, Park Ridge, NJ, 1991.
- Flick, E. W.: *Water-Soluble Resins: An Industrial Guide*, 2nd edn., Noyes, Park Ridge, NJ, 1991.
- Fontanille, M., and A. Guyot (eds.): *Recent Advances in Mechanistic and Synthetic Aspects of Polymerization*, Kluwer Academic Publishers, Norwell, MA, 1987.
- Glass, J. E. (ed.): *Water-Soluble Polymers*, ACS, Washington, DC, 1986.
- Glass, J. E. (ed): *Polymers in Aqueous Media*, ACS, Washington, DC, 1989.
- Harper, C. A. (ed): *Handbook of Plastics, Elastomers, and Composites*, 2nd edn., McGraw-Hill, New York, 1992.
- Hergenrother, P. M.: *High Performance Polymers*, Springer-Verlag, Berlin, Germany, 1994.
- Holden, G., N. R. Legge, R. P. Quirk, and H. E. Schroeder: *Thermoplastic Elastomers*, Hanser Publishers, Munich, Germany, 1996.
- Kaminsky, W., and H. Sinn (eds.): *Transition Metals and Organometallics as Catalysts for Olefin Polymerization*, Springer, New York, 1988.
- Karger-Kocsis, J. (ed.): *Polypropylene: Structure, Blends, and Composites*, Chapman & Hall, New York, 1994.
- Karian, H. G. (ed.): *Handbook of Polypropylene and Polypropylene Composites*, Dekker, New York, 1999.
- Kniel, L., O. Winter, and K. Stork: *Ethylene: Keystone to the Petrochemical Industry*, Dekker, New York, 1980.
- Koleske, J. V., and L. H. Wartman: *Poly(Vinyl Chloride)*, Gordon & Breach, New York, 1969.
- Krivoshai, I. V., and V. M. Skorobogatov: *Polyacetylene and Polyarylenes: Synthesis and Conductive Properties*, Gordon & Breach, New York, 1991.
- Legge, N. R., G. Holden, and H. E. Schroeder (eds.): *Thermoplastic Elastomers*, Macmillan, New York, 1987.
- Margolis, J. M. (ed): *Engineering Thermoplastics*, Dekker, New York, 1985.
- Martuscelli, E., and C. Marchetta (eds.): *New Polymeric Materials: Reactive Processes and Physical Properties*, VNU Science, Utrecht, The Netherlands, 1987.
- Meier, D. J. (ed): *Block Copolymers*, Gordon & Breach, New York, 1983.
- Miles, D. C., and J. H. Briston: *Polymer Technology*, Chemical Publishing, New York, 1979.
- Molyneux, P.: *Water Soluble Synthetic Polymers: Properties and Behavior*, 2 vols., CRC Press, Boca Raton, FL, 1984.
- Moore, E. P., Jr.: *Polypropylene Handbook*, Hanser Publishers, Munich, Germany, 1996.
- Morton, M. (ed.): *Rubber Technology*, 3rd edn., Van Nostrand Reinhold, New York, 1987.

- Nass, L. I. (ed.): *Encyclopedia of PVC*, vol. 3, 2nd edn., Dekker, New York, 1992.
- Nass, L. I., and R. F. Grossman: *Encyclopedia of PVC: Conversion and Fabrication Processes*, vol. 4, 2nd edn., Dekker, New York, 1997.
- Nass, L. I., and C. A. Heiberger (eds.): *Encyclopedia of PVC: Resin Manufacture and Properties*, vol. 1, 2nd edn., Dekker, New York, 1986.
- Nass, L. I., and C. A. Heiberger (eds.): *Encyclopedia of PVC: Compound Design and Additives*, vol. 2, 2nd edn., Dekker, New York, 1987.
- Peacock, A. J.: *Handbook of Polyethylene—Structures, Properties, and Applications*, Dekker, New York, 2000.
- Roberts, A. D. (ed.): *Natural Rubber Science and Technology*, Oxford University Press, New York, 1988.
- Roesky, H. W. (ed.): *Rings, Clusters, and Polymers of Main Group and Transition Elements*, Elsevier, Amsterdam, The Netherlands, 1989.
- Rubin, I. D.: *Poly-1-butene*, Gordon & Breach, New York, 1986.
- Sakurada, I.: *Polyvinyl Alcohol Fibers*, Dekker, New York, 1985.
- Scheirs, J. (ed.): *Modern Fluoropolymers—High Performance Polymers for Diverse Applications*, Wiley, New York, 1997.
- Schildknecht, C. E.: *Polymer Processes*, Wiley, New York, 1956.
- Schildknecht, C. E., and I. Skeist (eds.): *Polymerization Processes*, Wiley, New York, 1977.
- Seymour, R. B., and T. Cheng (eds.): *Advances in Polyolefins*, Plenum Press, New York, 1988.
- Seymour, R. B., and G. S. Kirshenbaum (eds.): *High-Performance Polymers: Their Origin and Development*, Elsevier, New York, 1986.
- Seymour, R. B., and H. F. Mark (eds.): *Applications of Polymers*, Plenum Press, New York, 1988.
- Svec, P., L. Rosik, Z. Horak, and F. Vecerka: *Styrene-Based Plastics and Their Modification*, Prentice Hall, Englewood Cliffs, NJ, 1989.
- Tess, R. W., and G. W. Poehlein (eds.): *Applied Polymer Science*, 2nd edn., ACS, Washington, DC, 1985.
- Titow, W. V.: *PVC Plastics: Properties, Processing, and Applications*, Elsevier, New York, 1990.
- Tötsch, W., and H. Gaensslen: *Polyvinylchloride: Environmental Aspects of a Common Plastic*, Elsevier, New York, 1992.
- Van der Ven, S.: *Polypropylene and Other Polyolefins: Polymerization and Characterization*, Elsevier, New York, 1990.
- Vasile, C. (ed.): *Handbook of Polyolefins*, 2nd edn., Dekker, New York, 2000.
- Walker, B. M., and C. P. Rader (eds.): *Handbook of Thermoplastic Elastomers*, 2nd edn., Van Nostrand Reinhold, New York, 1988.
- Wickson, E. J. (ed.): *Handbook of PVC Formulating*, Wiley, New York, 1993.
- Wilson, A. D., and H. J. Prosser (eds.): *Developments in Ionic Polymers—1*, Elsevier Applied Science, New York, 1982.
- Wilson, A. D., and H. J. Prosser (eds.): *Developments in Ionic Polymers—2*, Elsevier Applied Science, New York, 1986.

17 Heterochain Polymers

17.1 INTRODUCTION

The classification of polymers with backbones containing atoms other than aliphatic carbon calls for some arbitrary decisions. Ester, ether, and amide groups in the main chain distinguish some classes. However, polymers based on isocyanate or aldehyde reactions may contain a variety of groups, especially when network structures are produced. The silicones and phosphazenes form distinct families, at least in their commercial applications. Finally, this chapter concludes with brief summaries of two industrial categories based on physical properties rather than chemical composition. As the name implies, high-performance polymers (including both thermoplastic and thermoset materials) are usable at elevated temperatures. The other category is that of thermoplastic elastomers, which have rubbery properties at room temperature. Natural heterochain polymers such as cellulose-based polysaccharides, plant and animal polyesters, and proteins (polyamides) are discussed in Chapter 15.

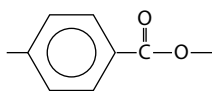
17.2 POLYESTERS

The **alkyd resins** (described in Section 13.4) were developed in the 1920s and 1930s as an outgrowth of the earlier cooked varnishes, which combined unsaturated oils with natural resins. Similar unsaturated polyesters were dissolved in styrene monomer to make casting and laminating resins in the 1940s. Films and fibers based on poly(ethylene terephthalate) (PET) were developed in England in the 1940s. During the 1950s, polycarbonates of bisphenol A were offered in Germany and the United States.

17.2.1 SOME INDIVIDUAL POLYMERS

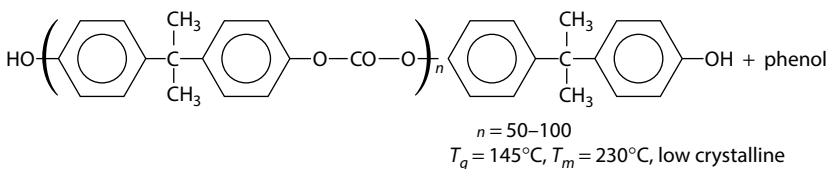
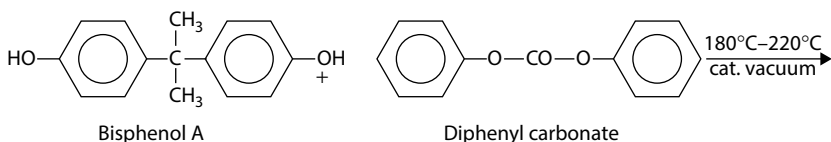
The condensation of an alcohol with an acid to give an ester with water as a by-product is a classical way to make polymers (Table 17.1, I). In alkyd resin cooking (Section 13.4), it was mentioned that additional reactions are those between anhydride and alcohol or epoxide and between free acid and alcohol and esters (transesterification). The simple polyester with its repeating dyadic structure can be dissolved in styrene (about 70 parts polyester to 30 parts styrene) and polymerized at room temperature by a free-radical route using a redox couple. (Methyl ethyl ketone peroxide plus cobalt naphthenate would be typical.) Glass-reinforced boat hulls and automobile bodies are made from such systems. In some cases, monomers more expensive than styrene can be justified. Methyl methacrylate, triallyl cyanurate, and diallyl phthalate have been suggested by various sources. Flammability

TABLE 17.1
(Continued) Polyesters

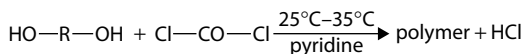


p-Oxybenzoyl polyester

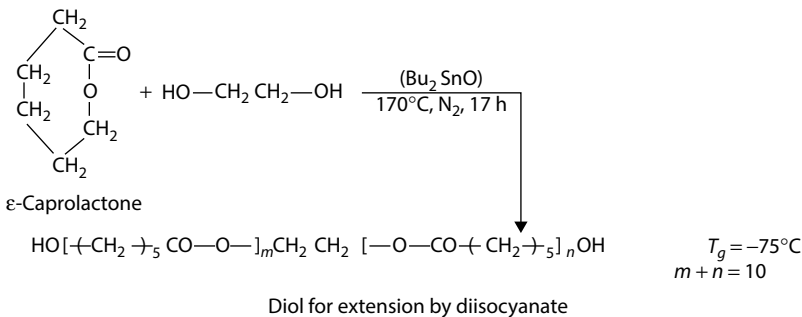
B. Polycarbonates



Also

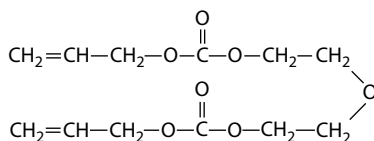


C. Polylactone



is a parameter that is important for all materials. Polyesters for casting resins can be modified by copolymerization with a chlorine-rich diacid to decrease flammability.

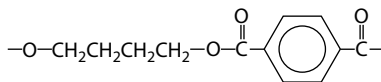
A combination of carbon chain and ester bonds results from the free-radical polymerization of diallyl diglycol carbonate ester. Polymerization proceeds more slowly than with corresponding divinyl monomers.



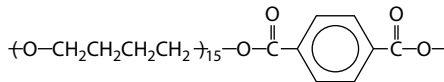
The network polymer obtained on complete conversion contains ester, ether, and carbon-chain linkages. The bulk polymerization proceeds in two steps, so that the actual casting of the final product starts with a prepolymerized syrup much as in the methyl methacrylate sheet process (see Section 5.2). The hard, abrasion-resistant, transparent character of the polymer, most popularly known as CR-39 (PPG Industries, Pittsburgh, PA), makes it suitable for optical applications such as cast lenses for eyeglasses [1].

Ester interchange is favored for terephthalates because the free acid is very insoluble and difficult to incorporate into a reaction system. Two stages are used: In the first, methanol is displaced from the terephthalic acid ester by the diol, and in the second, the excess diol is driven off at high temperatures and low pressures. A continuous process (Figure 17.1) starts with a molar ratio of dimethyl terephthalate to glycol of 1:1.7. Methanol is removed from the horizontally sectioned vessel over a period of 4 h with a rise in temperature to 245°C at a pressure of 1 atm. In two polycondensation reactors, the pressures are about 0.020 and 0.001 atm, and the exit temperatures are 270°C and 280°C, respectively. The resultant polymer melt is low enough in viscosity that pumps can be used to extrude fibers directly or to make chips as an intermediate form for storage.

Beverage bottles made of **PET** were made possible by the invention of stretch blow molding (see Section 14.8.3). The biaxial structure yields strong bottles of high clarity and strength. The most popular sizes are 2 l and 32 oz. Also in the 1970s, poly(butylene terephthalate) (**PBT**) became available. Although the T_g is 228°C compared to 265°C for PET, PBT is much easier to work with. Reinforced with glass fibers, both polymers compete with nylon and metal for such applications as gears, machine parts, small pump housings, and insulators. When the terephthalic acid is replaced by 2,6-naphthalene dicarboxylic acid, the T_g is raised by as much as 50°C. Oxygen permeability and ultraviolet (UV) resistance are also improved. However, the polymer, abbreviated as **PEN** for polyethylene naphthalate, crystallizes more slowly than PET that results in dimensional changes and warping of thick sections of molded parts. The polymer is more expensive than PET or PBT. Another related material is a **thermoplastic elastomer** made by using two diols differing in molecular flexibility:



Repeat unit in hard segment



Soft segment

The final polyester [3] with a molecular weight of about 30,000 is made up of soft, flexible segments (M_n about 1500) and an equal number of hard segments (M_n about 700). At a molding temperature above 200°C, the materials are thermoplastic. Below 150°C the *hard segments* crystallize to form massive cross-links similar to the glassy

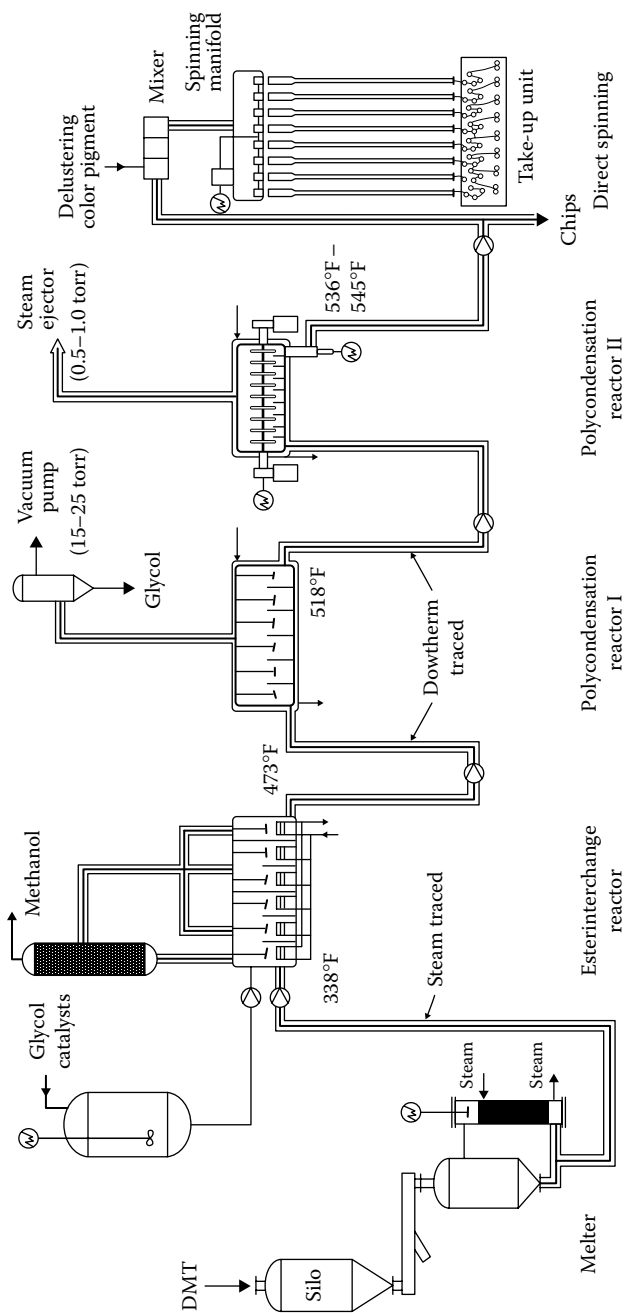


FIGURE 17.1 Continuous preparation of PET from dimethyl terephthalate (DMT). (Data from Ellwood, P., *Chem. Eng.*, 74, 98, 1967.)

domains in the styrene–butadiene or styrene–isoprene block copolymers (see Section 4.5). Between -50°C and 150°C , the materials are rubbery and can be used for molded tires, snowmobile tracks, wire and cable insulation, gaskets, seals, and other mechanical goods (see also Section 17.10).

Several aromatic polyesters (**polyarylates**) are made which have high T_g 's because of the stiff backbones containing many aromatic rings. They are part of a class of polymers termed **liquid crystal polymers** (see Section 3.13) because they can remain ordered in both the liquid and solid states. The nematic structure is typical, especially when the polymers are molded or extruded. Other commercial examples of liquid crystal polymers are the copolymers of *p*-hydroxybenzoic acid with 6,2-hydroxynaphthoic acid. **Poly(*p*-oxybenzoyl ester)** is a compact, linear, crystalline polymer that does not melt below its decomposition temperature of 550°C . Like poly(tetrafluoroethylene) (PTFE), the ester can be fabricated by compression sintering at temperatures above a crystal transition (330°C – 360°C). The polymer can be combined with PTFE (see Section 16.7) in a plasma-spray coating. Typically, a 1:3 ratio of polyester to PTFE is applied using an argon–hydrogen plasma. When powdered plastics are deposited and sintered on a metal surface, wear-resistant coatings with low coefficients of friction are produced.

Polycarbonate results when **bisphenol A** is combined directly with phosgene (Cl—CO—Cl) in the presence of a HCl acceptor such as pyridine. **Bisphenol A** is produced by the condensation of acetone with phenol (Table 17.1, IIB). Polycarbonate has been the favored material for compact discs (CDs). In thin sheets the plastic has extremely high impact strength. Both in the form of sheets and as molded lamp housings, it has been a favored material for high-resistant, rugged applications such as safety goggles and sports equipment. A silicone treatment for polycarbonate surfaces is claimed to make the abrasion resistance of the polymer approach that of ordinary inorganic window glass. Polyesters have also been produced by combining bisphenol A with isophthalic acid, *p*-hydroxybenzoic acid, or terephthalic acid.

A variety of aliphatic polyesters of molecular weight near 1000 are made with terminal hydroxyl groups to form the basis for urethane polymers. A ring-scission polymerization has been used for one such material (Table 17.1). A product that is less likely to crystallize on aging can be made if a copolymer of α -methyl caprolactone and caprolactone is made. Some commercially important polyesters produced by plants and animals are discussed in Chapter 15.

17.2.2 SELECTED USES

PET in fibers and bottles and polycarbonates in compact discs represent large-volume markets. As with most polymer families, there is a wide diversity of applications, many of which involve combinations with other materials. Aliphatic polyesters have been used as lubricants and vinyl plasticizers. Hydrolytic stability is a factor to be considered in many applications. As a rule, aryl acids and branched-chain diols resist hydrolysis. Fibers and films of terephthalic acid esters and polycarbonates are not particularly sensitive to moisture. Alkyd resins are so highly cross-linked in the final coating that water is not a major problem, although alkaline solutions of soaps and detergents can cause film failure. It is in the urethane foams that hydrolytic stability

has been a significant factor. Foams based on polyesters generally are more sensitive to alkaline conditions than are those based on polyethers.

17.3 POLYETHERS

Polymers of formaldehyde form spontaneously in aqueous solutions of the monomer, but a useful molding material was not marketed until the late 1950s. The three-membered ring of ethylene and propylene oxide opens readily and was used for low-molecular-weight surfactants in the 1940s. Urethane prepolymers became important in the 1950s; high-molecular-weight poly(ethylene oxide) became available in 1958; and rubbers based on epichlorohydrin came on the market in 1966. The epoxy resins from bisphenol A and epichlorohydrin were produced in the 1940s, and the high-molecular-weight phenoxy resins appeared in the 1960s. Polysulfide rubber was the first successful synthetic rubber in the United States back in the 1920s. The aromatic polyethers poly(phenylene oxide) and polysulfone appeared in the 1960s. Although polysaccharides and silicones could be regarded as polyethers, they will be treated separately.

17.3.1 SOME INDIVIDUAL POLYMERS

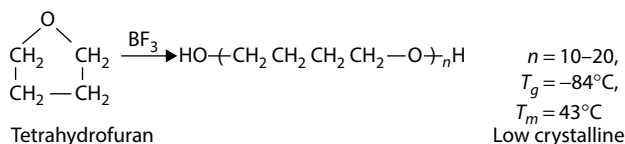
Monomers of formaldehyde vapor that can be dissolved in an inert hydrocarbon such as heptane along with an initiator. Initiators include Lewis acids such as BF_3 (Table 17.2, I.A) as well as amines, phosphines, arsines, stibenes, organometallic compounds, and transition metal carbonyls. The polymer is often referred to as acetal homopolymer, **polyacetal**, or poly(oxymethylene). All of these terms distinguish the useful, stable polymer from polyformaldehyde, the thermally unstable, waxy material that forms easily from the pure monomer. Because of the instability of the chain structure and its tendency to *unzip*, esterification of the end-group hydroxyls or end blocking with acetic acid is one answer (Table 17.2, I.A). Another is the copolymerization of formaldehyde with monomers that will interrupt the chain sequence. Ethylene oxide is one such monomer.

Polymers containing ethylene oxide have one prominent property, an affinity for water. Homopolymers, even with molecular weights in excess of a million, are soluble in water. Segmented, block copolymers with propylene oxide provide a wide range of materials with variable **hydrophilic–lipophilic balance** because the propylene oxide polymers are not water soluble above a molecular weight of about 500. Random copolymers of ethylene oxide and propylene oxide, homopolymers of propylene oxide, and homopolymers of tetrahydrofuran in the molecular weight range of 1000–3000 are often extended by reaction with diisocyanates in making foams, rubbers, and spandex-type fibers (Table 17.2).

Epoxy resins make use of several different reactions. To make the simplest member of the series, 2 mol of epichlorohydrin is reacted with 1 mol of bisphenol A at 60°C with flake NaOH added to neutralize the HCl that is formed. Actually, more than 2 mol of epichlorohydrin is charged, and the excess is removed after the reaction. Higher molecular-weight resins call for sturdy equipment to agitate the molten polymer. In the *taffy* process (Figure 17.2), epichlorohydrin and bisphenol A are

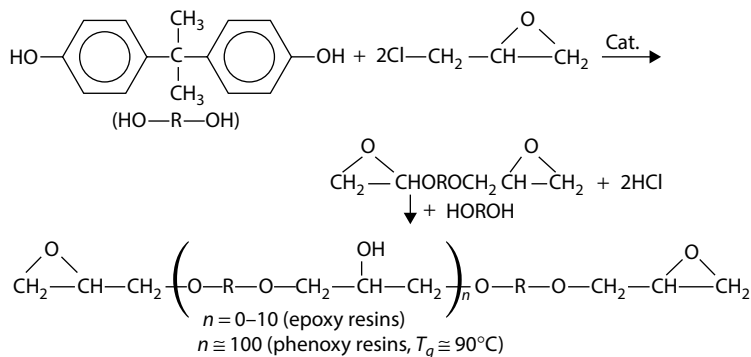
TABLE 17.2
(Continued) Polyethers

H.



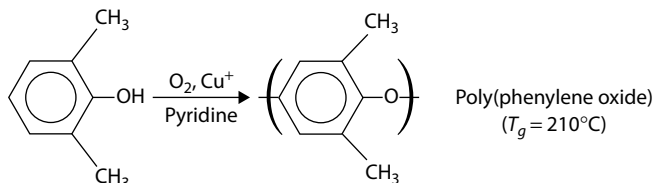
Tetrahydrofuran

I.



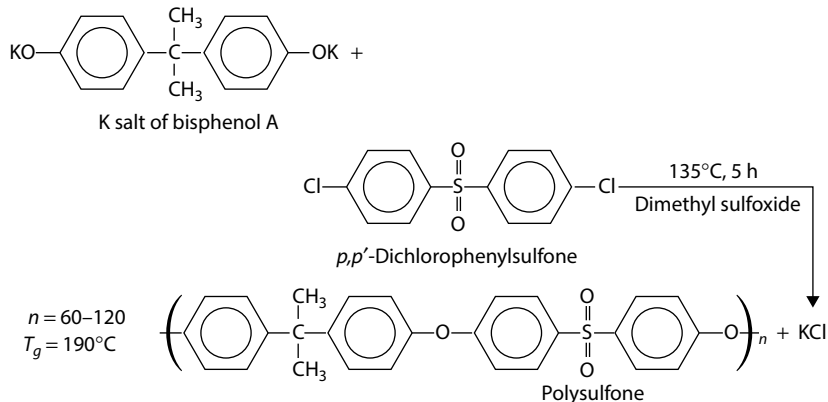
II. Condensation Polymerization

A.



2,6-Dimethylphenol

B.



(Continued)

TABLE 17.2
(Continued) Polyethers

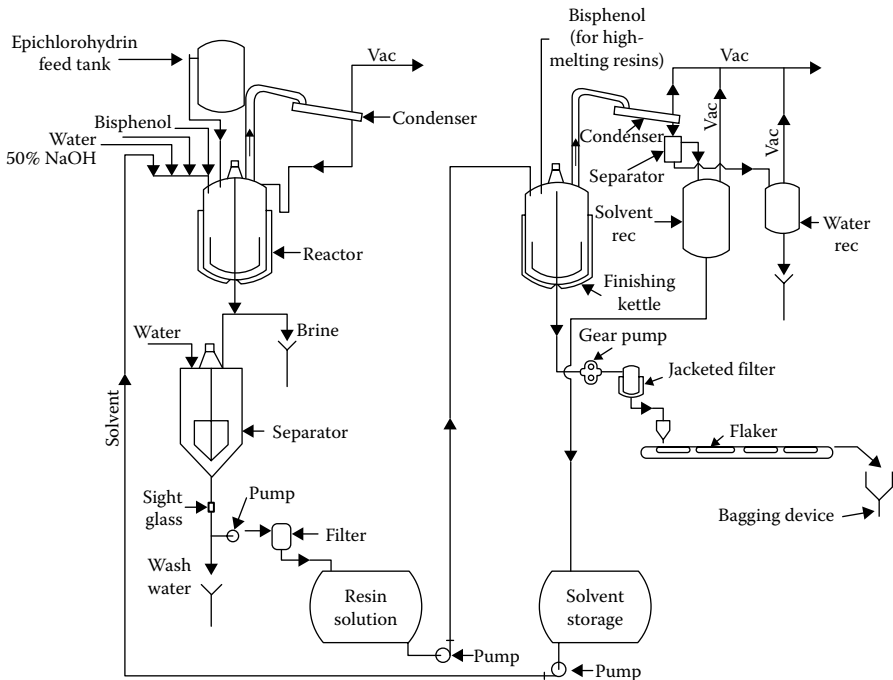
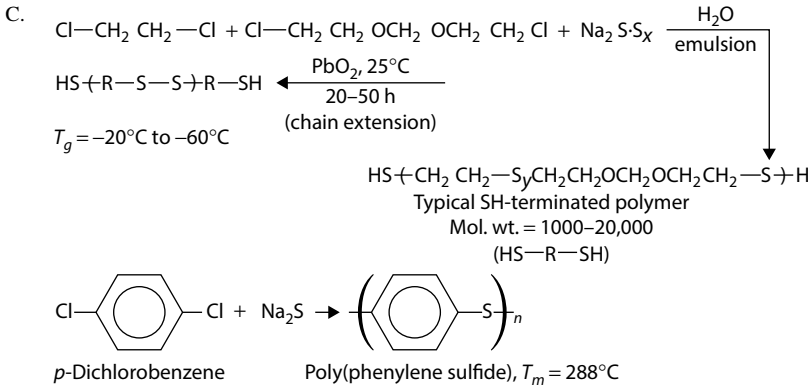


FIGURE 17.2 Equipment and process for solid epoxy resin. (Data from Hutz, C. E.: in W. M. Smith (ed.), *Manufacture of Plastics*, Reinhold, New York, 507, 1964.)

charged to the reactor with flake NaOH and a small amount of inert solvent. The temperature is allowed to rise to 90°C or 95°C . The taffy, which forms rapidly, is an emulsion of about 30% concentrated brine in molten polymer (perhaps containing some solvent). Several cycles of washing with water are followed by stripping of solvent and water under a vacuum at 150°C . Very high molecular weights can

be made by reacting low-molecular-weight polymers with additional bisphenol A with the aid of a catalyst. It can be seen that both condensation and ring scission are used for these materials. The largest use of epoxy resins (adhesives, coatings, laminates) calls for a *curing* through the oxirane rings. Popular *curing agents* include acid anhydrides and polyamines, which form ester and imine bonds, respectively. Polyfunctionality leads to network structures of high thermal stability. A number of other epoxy compounds have been made by treating an unsaturated structure with peracetic acid. Some are complex, such as epoxidized soybean oil, which is widely used as a plasticizer–stabilizer for poly(vinyl chloride). Specialty rubbers have been made from epichlorohydrin (Table 17.2, I.D).

To be useful at elevated temperatures, thermoplastic polymers must combine chain stiffness (for a high T_g) with thermal stability in order to carry out molding at temperatures higher than the projected use temperature. Phenylene groups in the polymer backbone contribute both of these properties. In **poly(phenylene oxide)**, a novel oxidative coupling technique is applicable which gives a chemically stable thermoplastic resin (Table 17.2, II.A). The polymer is difficult to process. A number of alloys (polymer blends) with polystyrene are marketed (**Noryl**, GE Plastics, Pittsfield, MA), which combine dimensional stability and processability. The **poly-sulfones** also combine phenylene groups in a backbone to yield a thermoplastic molding material useful up to temperatures of 140°C–170°C (Table 17.2, II.B). Alloys of polysulfones with **acrylonitrile–butadiene–styrene** (ABS) resin form a separate family of materials.

The aliphatic thioethers (**polysulfides**) are unique among condensation polymers in being produced in an emulsion polymerization. The rank x (Table 17.2, II.C) has an influence on the number of sulfur atoms in each polymer linkage. The tacky or liquid polymers are cast or applied as pastes in the case of sealants. The sulfur analog of poly(phenylene oxide) is **poly(phenylene sulfide)** (Table 17.2, II.C), which can be made by a condensation reaction between *p*-dichlorobenzene and sodium sulfide. The highly crystalline polymer is solvent resistant and has a low coefficient of friction. It can be injection molded at about 300°C and can also be used as a powder spray coating.

17.3.2 SELECTED USES

The importance of regularity, polarity, and chain stiffness becomes apparent in the uses of polyethers. Of the common polyethers, only polyformaldehyde, poly(ethylene oxide), and the polymer based on 2,2-dichloromethylpropylene-1,3-oxide are crystalline. Since poly(ethylene oxide) is water soluble, only the remaining two polyethers are useful structural materials. Phenoxy, phenylene oxide, and sulfone polymers are useful thermoplastics because the chain stiffness contributed by aromatic rings in the backbone raises T_g well above room temperature. Polysulfones are used in the manufacture of membranes for gas separations (Section 13.6). The aliphatic ether backbone is more conducive to low T_g 's that are suitable for rubbery applications. Fully cured epoxy resins are dimensionally stable network polymers. Low-molecular-weight polymers of ethylene oxide [often abbreviated as **PEG** for **poly(ethylene glycol)**] are often listed as ingredients of

shampoos, lotions, and medications along with PEG esters. Epoxy adhesives were described in Section 13.4.

17.4 POLYAMIDES AND RELATED POLYMERS

The use of silk, a protein fiber recovered from the cocoons of the silkworm, goes back to antiquity. Many attempts have been made to produce a synthetic material with similar characteristics. Rayon, a regenerated cellulose fiber (Section 15.2), was made in the 1890s. However, in the 1930s a team of chemists at DuPont led by W. H. Carothers investigated the properties of aliphatic polyesters at some length before discovering that an aliphatic polyamide of the same molecular weight as the polyester would have a much higher T_m and could be spun into a useful apparel fiber suitable for many of the same applications as natural silk. Nylon 6,6, made from a dyad of a diamine and a diacid each with six carbons, was commercialized before 1940 and continues to grow in importance today. Nylon 6, based on the ring-scission polymerization of ϵ -caprolactam, was produced in Europe before it was introduced to the United States in the 1950s. The 1960s brought the aromatic nylons and polyimides. The dragline silk of certain spiders combines high strength with great toughness. Production of the same material in transgenic plants and animals made possible by gene-splicing techniques is an active field of research with some products such as sutures already being marketed (Section 15.5.1).

17.4.1 SOME INDIVIDUAL POLYMERS

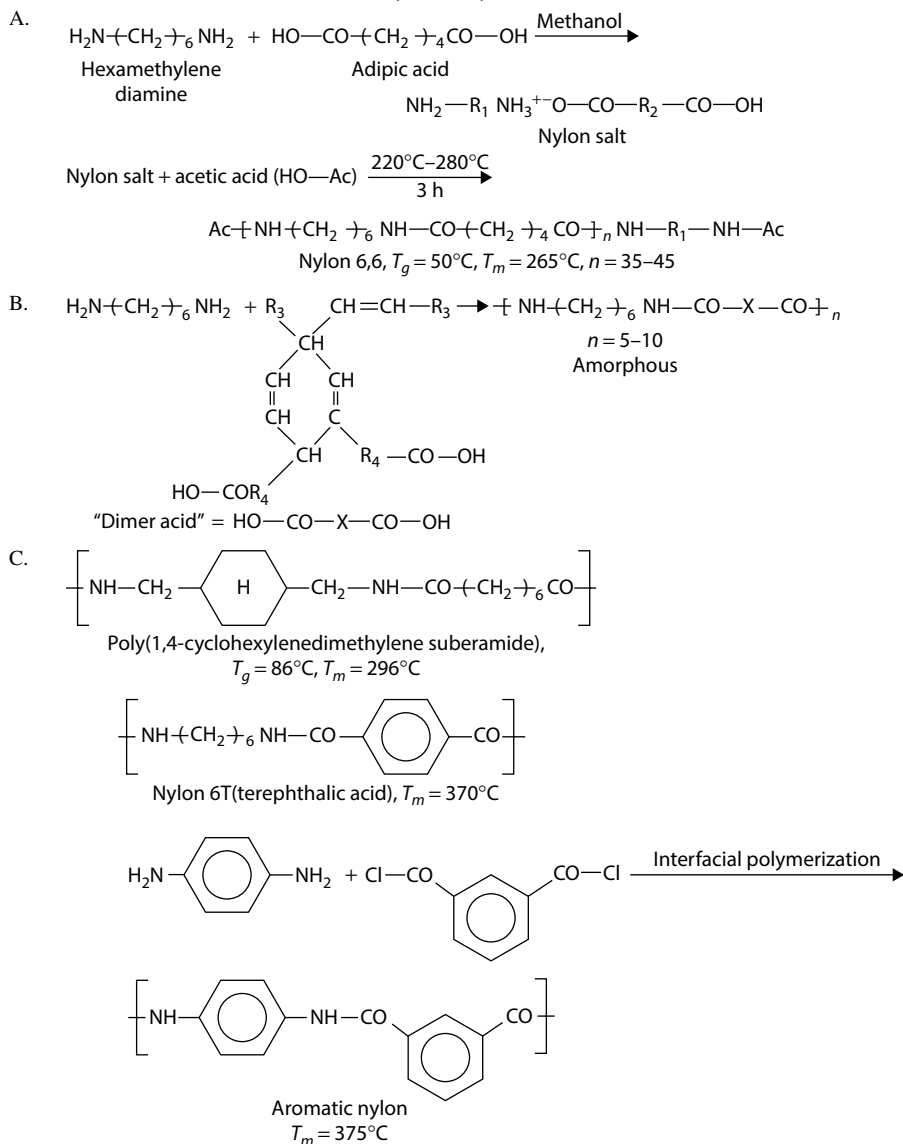
The best known synthetic polyamides are the **nylons**. The term **nylon** originally was a trademark for the polyamide based on hexamethylene diamine and adipic acid (Table 17.3). Later on it became a generic term. The numerals following the name designate the number of carbon atoms in the chain between successive amide groups. The dyadic nylons have two numbers: the first for the diamine and the second for the diacid. Monadic nylons such as polycaprolactam require only one number. Although they have been studied as protein models, the synthetic nylon 2 polymers have not been commercialized as fibers or plastics. While some new polymers have been introduced over the years (nylon 4, nylon 1,1, nylon 1,2), nylon 6,6 and nylon 6 have been produced for a longer time and dominate the markets for synthetic polyamides, especially as fibers.

The first step in making dyadic nylons is the formation of a salt of amine and acid (without condensation). The second step involves actual polycondensation [5]. In a batch process, salt solution is concentrated to about 75% solids before being charged along with a chain terminator such as acetic acid into an autoclave, whereas residence time of several hours and a temperature of up to 280°C yield a polymer with a molecular weight of 12×10^3 – 15×10^3 . A continuous process for nylon 6,6 was described in Section 5.2.

Not all nylons are highly crystalline. The polyamide based on dimerized fatty acids (Table 17.3, I.B) is soluble in common solvents and contains residual unsaturation. It is used as a coating material and a reactive curing agent for epoxy resins in coatings and adhesives. Ordinary nylon 6,6 is soluble only in highly polar

TABLE 17.3
Polyamides and Polyimides

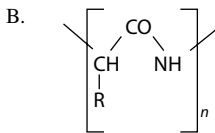
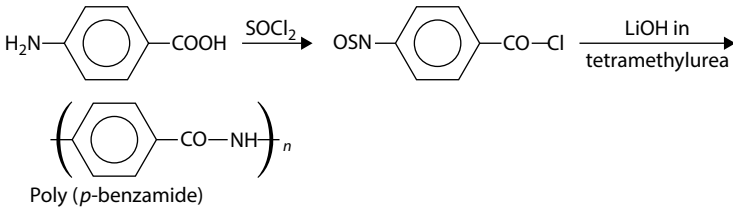
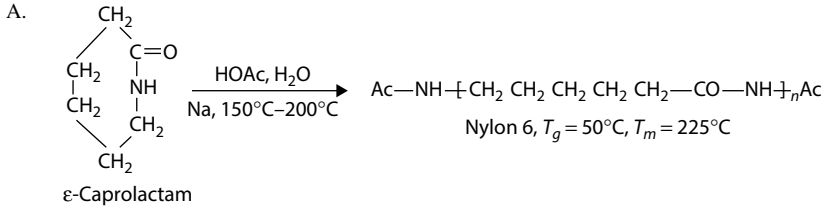
I. Dyadic Polyamides



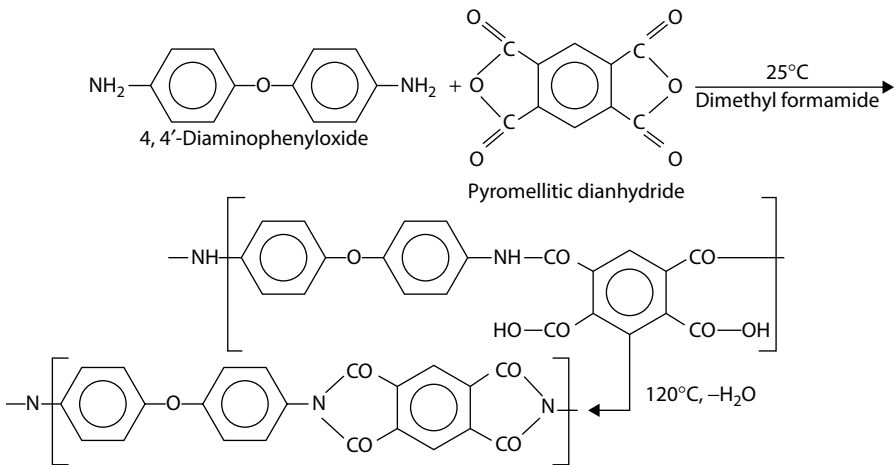
(Continued)

TABLE 17.3
(Continued) Polyamides and Polyimides

II. Monadic Polyamides



III. Polyimides

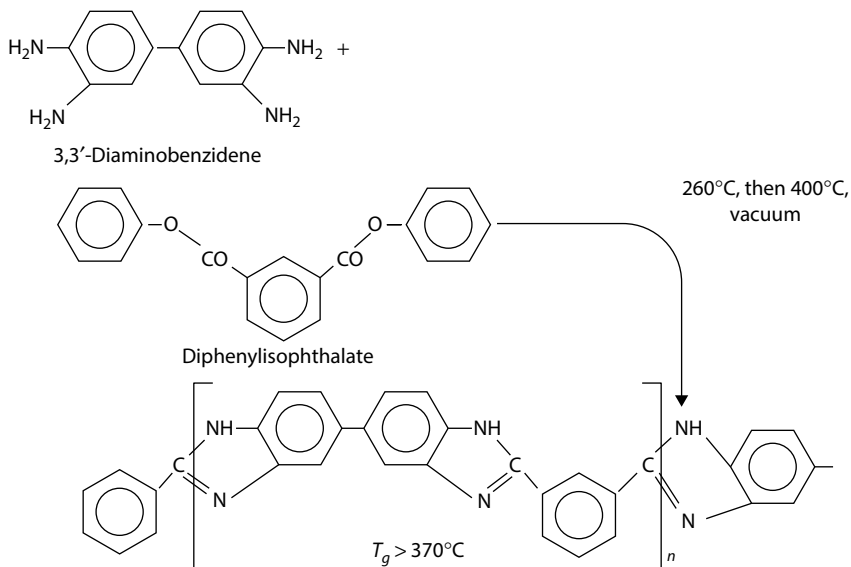


Stable at 420°C (air), 500°C (vacuum).
 Tensile strength at 260°C is two-thirds that at 25°C.

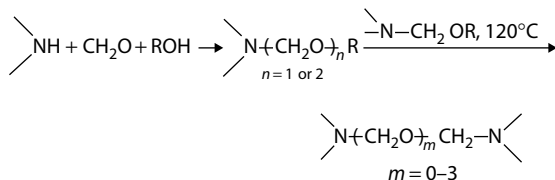
(Continued)

TABLE 17.3
(Continued) Polyamides and Polyimides

IV. Polybenzimidazoles

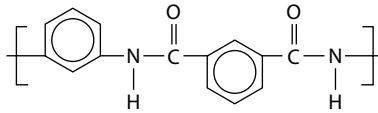


solvents such as 90% formic acid or metacresol. Treatment of nylon with formaldehyde and an alcohol while the polymer is dissolved in 90% formic acid (phosphoric acid is added as a catalyst) results in the N-alkylated derivative, which is soluble in methanol and ethanol and can be used in coatings [6]. The coatings can be cross-linked by baking in the presence of an acid (20 min at 120°C with 2% citric acid is typical).

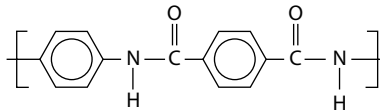


Other commercially available nylons such as nylon 610 (using sebacic acid, HO—CO—(CH₂)₈CO—OH) are based on aliphatic dyads. The T_g and T_m can be increased by incorporating cyclic or aromatic structures into the backbone. The nylons in Table 17.3, I.C, can be made by interfacial polymerization (see Section 5.3), since the amide formation is rapid between aroyl chlorides and aromatic amines. Two aromatic nylons (**aramids**), poly(*p*-phenylene terephthalamide) and poly(*m*-phenylene

isophthalamide), with a very rigid backbone have become familiar by the trade names **Kevlar** and **Nomex** (DuPont), respectively. Both have found use as high-strength, high-temperature-resistant fibers.



poly(*m*-phenylene isophthalamide), Nomex (DuPont)



poly(*p*-phenylene terephthalamide), Kevlar (DuPont)

Kevlar is a liquid crystal polymer that can be wet-spun from concentrated sulfuric acid into dilute acid. The rigid molecules undergo a great deal of flow orientation during spinning. High-temperature stability and high strength have led to a variety of applications for the fibers including body armor, belt material in radial tires, and reinforcement for high-tech composites.

Nylon 6 is made by a ring-scission polymerization that results in an equilibrium mixture of high-molecular-weight, linear polymer and cyclic monomer. High-strength fibers require removal of the unreacted monomer. This can be done in a continuous process (Figure 17.3) that starts with molten caprolactam. Titanium dioxide can be added at the very start, since it is inert during the reaction and serves as a delusterant in the final fiber. After a residence time in the reactor of about 18 h at 260°C, the melt viscosity reaches about 100 Pa·s. The unreacted monomer (about 10% of the batch) is removed and recovered in a falling-film evaporator at 260°C–280°C at an absolute pressure of about 0.001 atm. Large cast pieces of nylon 6 can be produced directly from monomer by using a catalyst such as sodium metal or a Grignard reagent [8].

The **polyimides** and **polybenzimidazoles** (Table 17.3, II and IV) combine chain stiffness with thermal stability. A two-step synthesis is usually required. In the first step a linear, soluble, and fusible polymer is made by forming amide links. At this stage the polymer can be cooled and stored, and then later heated and fabricated into a final shape such as a film, a fiber, or a molded object. In the second step, at a higher temperature than that used in the first step, heterocyclic ring structures are made by intramolecular condensation. While the structures shown in Table 17.3 predominate, some intermolecular cross-linking occurs and the materials are nominally thermosetting. They have the disadvantage of not being easily formed compared to the aromatic polyamides. However, in general, they preserve their strength and flexibility to higher temperatures than that can be attained by the true thermoplastics. The reaction of an aromatic diamine with maleic anhydride results in a **bismaleimide** that combines the reactivity of the double bonds with the chemical stability of the aromatic imide structure.

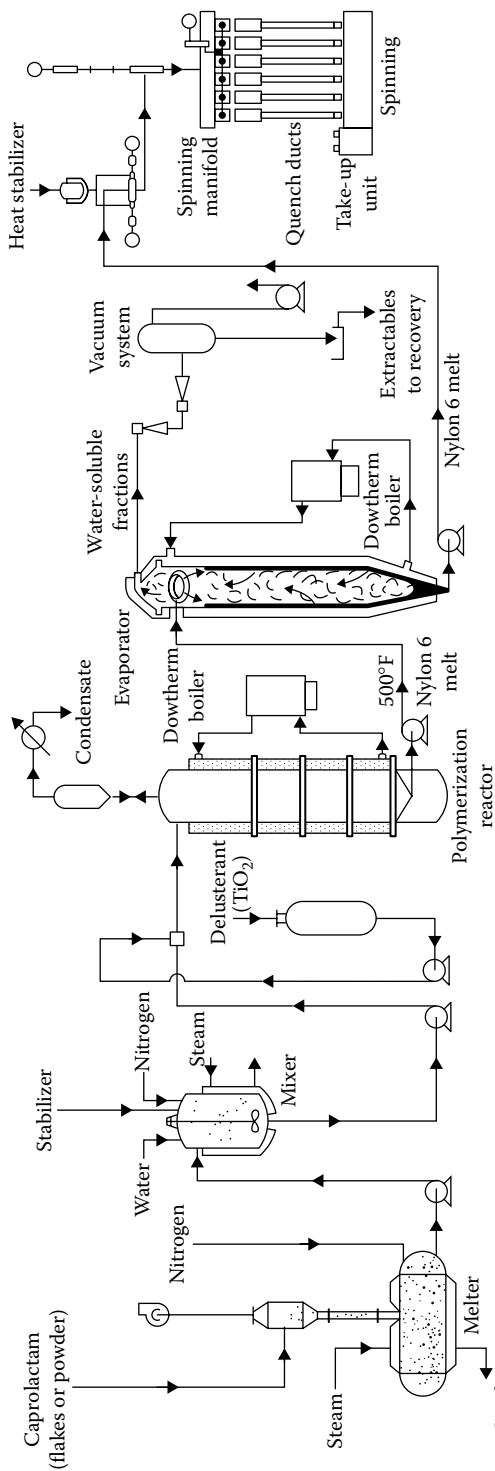
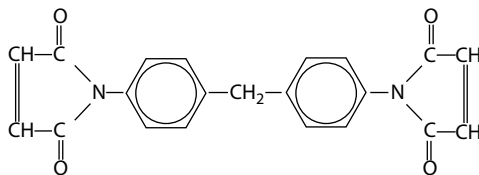


FIGURE 17.3 Nylon 6 production. (Data from *Chem. Eng.*, 73, 178, 1966.)



Bismaleimide based on methylene dianiline

Since the homopolymers tend to be brittle, coreactants are used with the bismaleimides to improve strength and toughness. Also, coreactants such as amines or allyl phenols make the starting material more processable by lowering the melting point of the mixture. A major use of bismaleimides has been in printed-circuit boards. With glass fiber reinforcement, the compression molding of the board typically proceeds in two stages: an initial stage of 175°C–230°C for 1–4 h followed by a postcure at 230°C for another 4 h. The high-temperature properties of such composites generally are superior to those of most epoxy-based composites. Aircraft structural components have also been made especially with lightweight reinforcements such as aromatic polyamides or carbon fibers.

17.4.2 SELECTED USES

Aromatic polyamides have been used for flame-resistant garments for firefighters and astronauts and as lightweight body armor for military and law enforcement agents. In some tests, seven layers of fabric made from an aromatic polyamide were sufficient to protect against the effect of most common handguns. Such a *bulletproof vest* weighs less than 2 kg. Fiber type, fabric weave, and garment design are all factors in making such a product.

Nylon 6,6 and nylon 6 accounted for most of the 4 million ton nylon fibers as well as the 2.7 million ton nylon plastics used in 2011. Some of the large-volume fiber products include carpets, apparel, and tire cord. Smaller markets include strings for guitars, tennis racquets, and fishing lines. Molded and extruded nylons are used in automotive, electronics, and electrical parts. Other applications of amorphous nylons include coatings and adhesives.

17.5 ALDEHYDE CONDENSATION POLYMERS

Historians disagree about the birthday of plastics. Some contend that cellulose nitrate in the 1860s started it all, but purists hold out for 1907, when Dr. Leo H. Baekeland patented the resins based on phenol and formaldehyde, an entirely synthetic polymer composition. In this book, we have included cellulose-based polymers as produced from natural resources (Section 15.2). The synthetic urea–formaldehyde resins were introduced in the 1930s, opening up the possibility of light colors that were impractical in phenolics. Sterilizable, rugged plastic dinnerware based on melamine resins made a great impact on the market after World War II. The exciting growth of thermoplastics in the 1950s tended to overshadow the thermosets. But in the 1960s it was found that urea and melamine resins could be used to impart permanent press to

cottons and other fabrics. The phenolic resins were found to perform well as abrasive materials in reentering space vehicles. Over the intervening years so many markets became important for the aldehyde condensation polymers that no single use can be said to dominate the market for any one polymer. Coatings and adhesives, laminating adhesives for plywood, bonding agents for grinding wheels and fiberglass filters, and paper-treating agents all claim significant portions of the production of aldehyde condensation polymers.

17.5.1 SOME INDIVIDUAL POLYMERS

A typical **one-stage phenolic resin** might be made in a vessel of the type shown in Figure 5.13. An excess of formaldehyde (as a 40% solution in water) with the phenol and an alkaline catalyst (NH_3 or Na_2CO_3) is refluxed for an hour or so (Table 17.4). A charge of 1.5 mol aldehyde per mole of phenol is typical. A branched, water-soluble, hydroxyl-bearing polymer of low molecular weight called a **resole** is formed. Dehydration by heating under a vacuum may take 3 or 4 h. The polymer is removed and cooled. Casting resins, bonding resins, and resins for laminating paper and wood are made this way. The product, when heated with further dehydration, will cross-link completely to give a hard, infusible network.

A two-stage resin is also used to obtain fusible **novolak** resin. The molten, low-molecular-weight dried polymer is cooled, and the glassy product is crushed, blended with a lubricant and an *activator* and filler, and then rapidly mixed on differential rolls. The resultant blend is quickly cooled and made into a molding powder by cutting and blending. The activator is usually hexamethylenetetramine (structure in Table 17.4, III). Compression molding yields a hard, dense, thermoset network. Wood flour (ground wood) is a popular filler, but numerous other fillers, including cellulose fibers and glass fibers, are used. Brake linings for automobiles are one important use for the fiber-reinforced material.

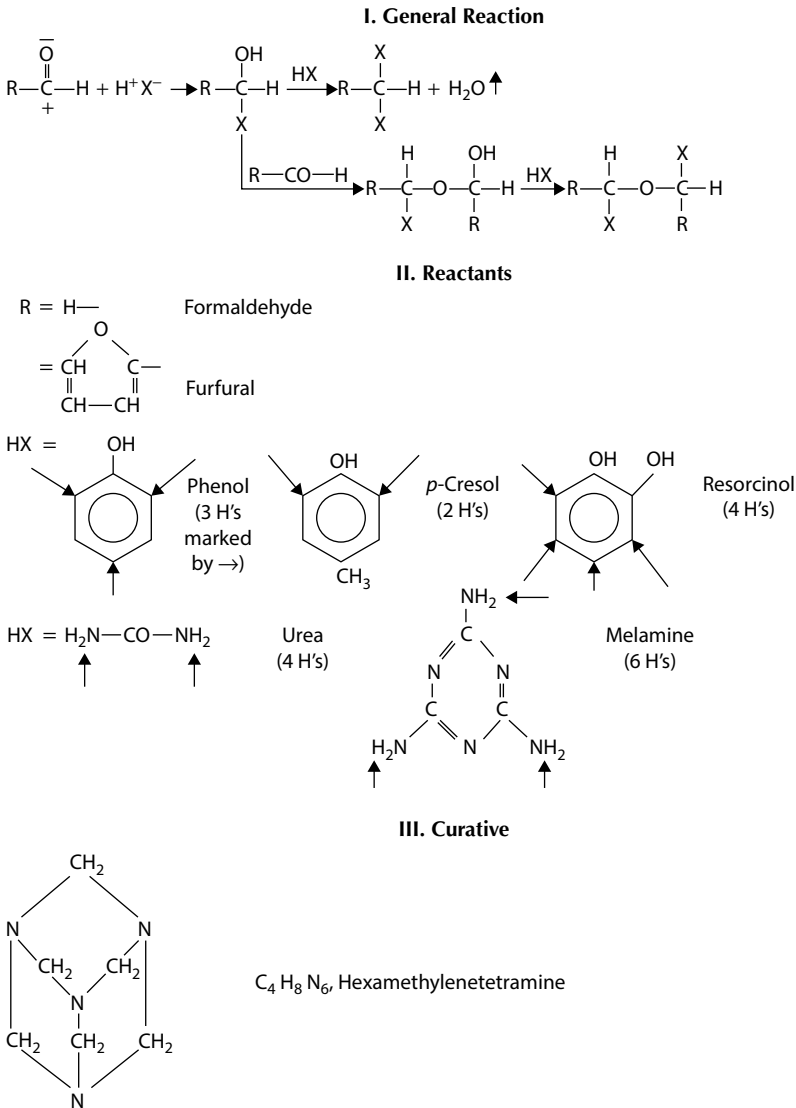
In **melamine** molding resin production, the filler may be added to the wet syrup from the reaction kettle without removing water, rather than being mixed with dry resin as in the case of the phenolic resin. The mixture is then dehydrated, ground, mixed, and finally converted into a molding powder. A molar ratio of 2:1 (formaldehyde to melamine) and a pH of 8.6 are maintained until condensation has proceeded to the desired point as evidenced by insolubility of a sample in cold water. To make an unfilled resin for laminating paper, the syrup is spray-dried after reaching the required viscosity. The dried powder is redissolved by the consumer in order to impregnate layers of paper.

Like the polyamides, the melamine or urea condensation products can be N-alkylated with formaldehyde and an alcohol such as methanol or butanol. The resulting compositions have good solubility in common solvents and are used in textile treatment and protective coatings.

17.5.2 SELECTED USES

As mentioned above, no single use dominates the aldehyde resin market. Over a period of many years, dozens of minor variations in the resins have been produced. Substitution

TABLE 17.4
Aldehyde Condensation Products



of furfural for formaldehyde adds ethenic functionality. In many applications, the resins act as binders or adhesives for plywood or other wood products. Phenolic resins have been used to coat fibrous glass insulation (giving it its characteristic pink color). Ion-exchange resins have been made from phenolic resins by sulfonation and the other reactions that are used with polystyrene resins (see Section 16.3).

17.6 POLYMERS BASED ON ISOCYANATE REACTIONS

During World War II, products in all the major categories of Table 17.5 were investigated in Germany. It was not until the 1950s that **urethane foam** was produced in the United States on a large scale. Flexible foam continues to be an important product, even though many other items are made on a commercial scale. Foams were discussed in Section 14.9. The diols and polyols used usually are polyethers, although polyesters are preferred for some applications such as textile backings because they adhere more readily to the substrates. Similar reagents are used in reaction injection molding (Section 14.8).

17.6.1 SOME INDIVIDUAL POLYMERS

Cast urethane elastomers can be made by a variety of routes similar to those used for foams (Table 17.5). A popular scheme with polyester diols is to make a prepolymer with excess diisocyanate and then to chain-extend or cross-link the prepolymer with a small molecule such as a diamine or a polyol. Two such reactants are shown in Table 17.5, IV. **Thermoplastic urethane elastomers** have been called **virtually cross-linked** polymers because they appear at room temperature to be cross-linked and thus resist creep and have rather low hysteresis. However, the cross-links are microphase-separated domains of the urethane polar segments of the **poly(urethane)** and disappear as the temperature is raised, so that the polymer can be molded or extruded like an ordinary thermoplastic resin (see Section 17.10). The cross-links may be hydrogen bonds between urethane groups as well as allophanate bonds. They re-form on cooling. A typical elastomer is made by combining a polyester diol (adipic acid with 1,4-butanediol) with methylene-bis-diisocyanate (**MDI**). The segmented nature of the polymer, with polyester sections separating

TABLE 17.5
Isocyanate Reaction Polymers

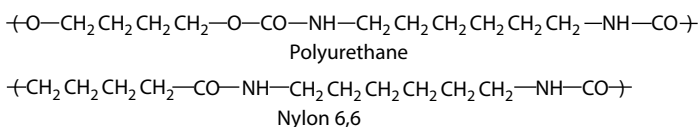
I. Products

- A. Foams
 - Flexible or rigid depending mainly on branched structure of diol
 - “Prepolymer” or “one-shot”
 - Polyester or polyether diol
 - B. Elastomers
 - Cast
 - Thermoplastic
 - Millable, vulcanizable
 - C. Fibers
 - Nylon-like
 - Spandex, elastic
 - D. Adhesives and coatings
-

(Continued)

the urethane links, allows the cross-links to form at isolated points with flexible chains leading from one cross-link to the next. Covalent cross-links can be introduced into such an elastomer by heating the elastomer with a peroxide. Several *millable, vulcanizable* gums are marketed that incorporate some unsaturation in the diol (polyester or polyether) allowing conventional sulfur-type curing as is used in vulcanizing natural rubber.

One nylon like fiber has been produced in Germany for some time based on 1,4-butanediol and hexamethylene diisocyanate. The structure resembles nylon 6,6 except for two additional oxygens per repeating dyad. Their properties are similar except that the urethane has lower water adsorption and somewhat better electrical and mechanical stability on aging.



Elastic fibers that are at least 85% by weight of polyurethanes have the generic name **spandex**. The fibers may be produced by wet-spinning (see Section 14.3). One commercial fiber appears to be a prepolymer based on MDI and poly(tetrahydrofuran) that has been chain-extended with a diamine. The fibers find use in foundation garments, surgical hose, and swimsuits. In these applications, they appear to have displaced natural rubber thread that was made by slitting extruded, vulcanized rubber sheets.

In coatings and adhesives, isocyanates may be used as reactive species at room temperature, or by modification, at high temperatures. Most *urethane* varnishes, however, are probably solutions of alkyd resins modified by reaction of free hydroxyl groups with diisocyanates.

17.6.2 SELECTED USES

Except for the nylon-like urethane fiber, most isocyanate polymers are characterized by a segmented structure in which the rather polar urethane groups act as cross-links and the connecting chains are varied in stiffness and polarity depending on the application. In the elastomeric and coatings applications, the one property most often cited as being superior for polyurethanes over other materials is abrasion resistance. Pneumatic tires said to outlast conventional rubber tires have been constructed from unfilled cast elastomers. Other properties such as traction and cost presumably have kept them from becoming commercially available. Solid tires for forklift trucks and the ubiquitous in-line skates and skateboards often are made from cast polyurethanes. A major product group for the isocyanate-based polymers has been flexible foams for bedding, furniture, and rug underlays. Reaction injection molding (Section 14.8), which produces parts with densities about 80%–90% of the corresponding solid materials, is widely used for automobile parts such as bumpers and grills.

17.7 SILICONES

The need during World War II for a heat-resistant, flexible electrical insulating material accelerated development of the silicones on the basis of research previously done by Kipping (England) and Hyde (the United States). The Dow Corning Corporation (1943) and General Electric Company (1946) were the first producers of fluids and rubber based on silicones.

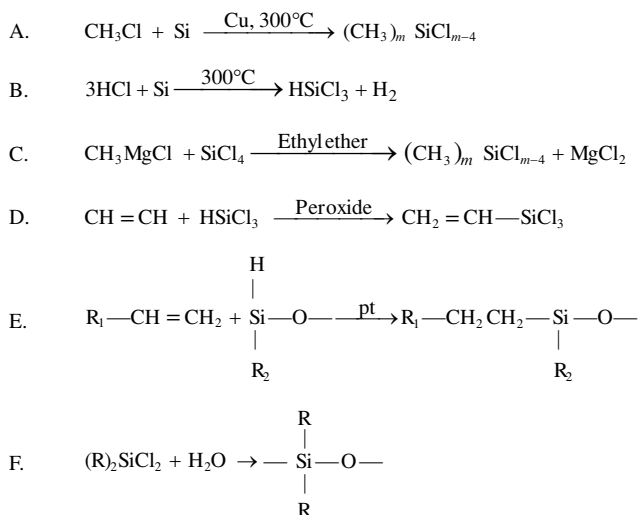
17.7.1 SOME INDIVIDUAL POLYMERS

In addition to the heat resistance commonly associated with silicones, the low-temperature flexibility inherent in the Si—O bond (Section 2.2) and the low surface tension of silicones suit them for many applications despite their relatively high cost (Table 17.6). Most silicone monomers start with reactions of silicon metal

TABLE 17.6

Silicones

I. Monomer Production



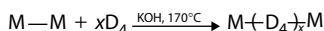
II. Product Classes

- A. Fluids
- B. Rubber
 - Dimethyl siloxane
 - Methyl-phenyl copolymer
 - Fluoramethyl siloxane
- C. Resins
- D. Surfactants
- E. Coupling agents

or SiCl_4 derived from $\text{Cl}_2 + \text{SiC}$. Originally, the Grignard synthesis was widely used commercially (Table 17.6, I.C). The *direct* reaction of alkyl and aryl chlorides with silicon metal is favored today (Table 17.6, I.A and I.B). In either case, monomers of variable functionality are formed and are often separated prior to hydrolysis (Table 17.6, I.F). Since a monochlorotrialkyl silane, ClSiR_3 , has only one hydrolyzable group, we can abbreviate it in the hydrolyzed form as M-. Because the free hydroxyls are not very stable, the major product of hydrolysis is $\text{R}_3\text{Si-O-SiR}_3$, abbreviated M-M. The difunctional group, R_2SiO , is abbreviated by D, $\text{RSiO}_{1.5}$ by I, and SiO_2 by Q.

An interesting feature of the hydrolysis of dichlorosilanes is the formation of many stable ring structures. In addition to the cyclic tetramer, D_4 , simple mixing of $(\text{CH}_3)_2\text{SiCl}_2$ with alkaline water leads to appreciable quantities of D_3 , D_5 , D_6 , and so on. Vapor-liquid chromatography is able to confirm the presence in hydrolyzate of rings up to D_{40} . Production of many silicone compounds starts with redistilled hydrolyzate, which is predominantly D_4 .

By heating D_4 together with the appropriate amount of M-M in the presence of a strong base (KOH) or acid (H_2SO_4), an equilibrium composition may be reached in which the molecular weight of the linear portion is regulated by the amount of end groups (M) added.



Neutralization of catalyst followed by vacuum distillation can give a linear fluid with most of the cyclic species removed. The relationship between melt viscosity and molecular size is shown in Figure 7.17. Poly(dimethyl siloxane)s, **PDMS**, with viscosity at room temperature of up to 100,000 centistoke are used as lubricants, antifoaming agents, and additives for cosmetics, pharmaceutical preparations, and hundreds of other consumer products. A distinguishing property of PDMS is a low viscosity temperature coefficient (**VTC**) compared with that of hydrocarbon lubricants.

$$\text{VTC} = 1 - \left(\frac{\text{viscosity at } 210^\circ\text{F}}{\text{viscosity at } 100^\circ\text{F}} \right) \quad (17.1)$$

The effect is lost, however, when phenyl, ethyl, or other groups are substituted for methyl (Table 17.7).

When D_4 is heated to 170°C with a small amount of KOH and no added end blocker, high-molecular-weight gums are produced. The molecular weight distribution corresponds roughly to the *most probable* distribution (Section 6.2) for the linear portion. The cyclic species form a separate distribution. Gel permeation chromatography (Section 6.4) shows the initial distribution and the distribution after neutralization of catalyst and vacuum stripping (Figure 17.4). No redistribution seems to occur in the linear portion, and most of the cyclic species are removed. Most commercial gums are copolymers with 0.2%–0.6% vinylmethylsiloxane. The vinyl group provides a preferential cross-linking site with peroxides. The tensile strength of unfilled, cross-linked silicone rubber is only a few hundred pounds per square inch at best. Fillers, especially finely divided silica, raise this into the range of 1,200–2,000 psi

TABLE 17.7
Temperature Dependence of Viscosity for Polysiloxanes

Substituents	Viscosity at 25°C (cs) ^a	VTC (Equation 17.1)
Dimethyl (M–M)	0.65	0.31
Dimethyl (MD, M)	2.0	0.48
Dimethyl	10	0.57
Dimethyl	10 ²	0.60
Dimethyl	10 ³	0.62
Dimethyl	10 ⁴	0.61
Dimethyl	10 ⁵	0.61
Methylphenyl	482	0.38
Methylethyl	1300	0.71
Diethyl	800	0.90
Methylhydrogen	25	0.50

Source: Barry, A. J., and H. N. Beck, in F. G. A. Stone and W. A. G. Graham (eds.), *Inorganic Polymers*, Academic Press, New York, 1962.

Note: For comparison, a typical mineral oil would have a viscosity of 110 cs and a VTC of 0.9.

^a 1 cs = 1 mPa·s divided by density (g/cm³).

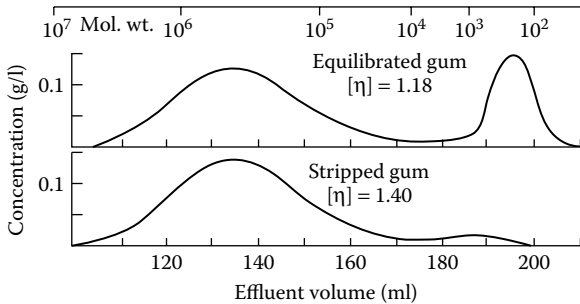
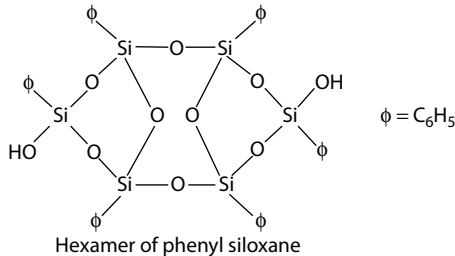


FIGURE 17.4 Gel permeation chromatographs of equilibrated and vacuum-stripped dimethyl siloxane gums. (Data from Rodriguez, F., R. A. Kulakowski, and O. K. Clark, *Ind. Eng. Chem. Prod. Res. Dev.*, 5, 121, 1966.)

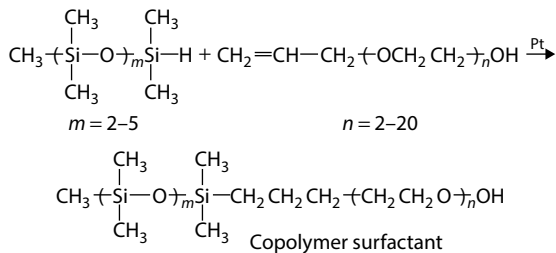
(8–14 MPa). Even with the vinyl comonomer and cross-linking, dimethyl siloxanes become stiff at -54°C because of crystallization. The stiffening temperature is brought close to the glass transition temperature (-110°C) by copolymerization with phenylmethyl siloxane or diphenyl siloxane (see Section 3.5). Some silicone fluids with hydrolyzable or reactive end groups have been compounded with fillers and catalysts to make room-temperature vulcanizing (RTV) rubber. An example of a one-package system that converts to a rubber on exposure to moist air was given in Section 13.4.

Silicone resins for coatings resemble some phenol–formaldehyde polymers in that polymerization takes place in two stages. A trifunctional monomer such as phenyltrichlorosilane may be hydrolyzed to the relatively stable hexamer (and related structures modified by comonomers for better solubility).



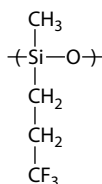
This compound when heated alone or with carboxylic acids and esters will undergo further condensation and rearrangement to give heat-stable, network polymers.

Surfactants based on block copolymers of dimethylsiloxane with poly(ethylene oxide) are unique in regulating the cell size in polyurethane foams. One route to such polymers uses reaction I.E in Table 17.6 between a polysiloxane and an allyl ether of polyethylene oxide [11]. Increasing the silicone content makes the surfactant more **lipophilic** (oil-loving), whereas increasing the poly(ethylene oxide) content makes it more **hydrophilic** (water-loving).



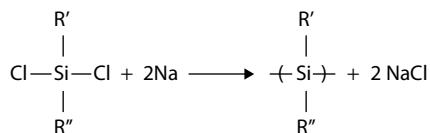
Coupling agents used to change the surfaces of silica and glass fillers (see Section 10.9) are substituted alkoxy silanes in monomeric form. They may polymerize on the surface of the filler, or they can be copolymerized with other organic monomers.

The incorporation of bulky groups into the silicone chain would be expected to raise T_m and T_g . Attempts have been made to do this without sacrificing the high-temperature stability of the silicones. One such material is *p*-bis(dimethylhydroxysilyl) benzene, made from *p*-dibromobenzene and $(\text{CH}_3)_2 \text{SiCl}_2$ by the Grignard reaction [12]. Copolymers with dimethylsiloxane are also possible. Fluorosilicone elastomers are based on trifluoropropylmethyl siloxane:

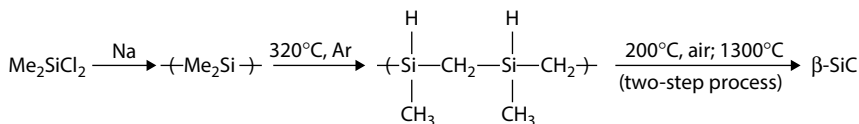


Such elastomers have some of the solvent resistance associated with fluorocarbon polymers. It would seem that a more highly fluorinated monomer would be better. Unfortunately, fluorines on carbons next to or one carbon away from silicon generally lead to thermal or hydrolytic instability [13].

Chains of silicon atoms (**polysilanes**) differ in many properties from those with alternating silicon and oxygen (polysiloxanes). On exposure to UV or ionizing radiation, for example, most polysiloxanes undergo cross-linking, whereas the polysilanes usually undergo chain scission. Stable organopolysilanes can be prepared by the reaction of a silyl dihalide with sodium [14,15]:



where R' and R'' can be various alkyl or aryl groups. In one example, when R' is *p*-*tert*-butylphenyl and R'' is methyl of high molecular weight, a soluble polymer can be produced. This polymer has some interesting properties for potential applications as a photoresist because it undergoes extensive random chain scission under UV light [15]. Some other uses proposed for polysilanes include electrically conducting materials (when doped with arsenic pentafluoride) and impregnating agents for ceramic materials. It has also been shown that poly(dimethylsilane) can be converted to poly(carbosilane) and eventually to β -silicon carbide:



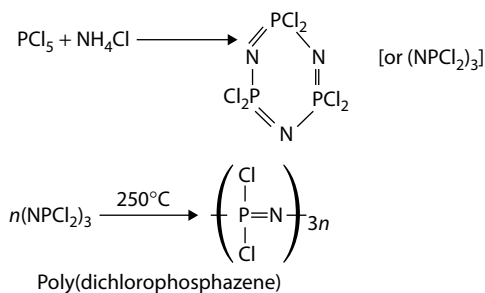
A number of companies that include Dow Corning, Gelest, and Wacker Chemie specialize in the production of a large variety of silicone and silane products for commercial and research usage.

17.7.2 SELECTED USES

It was pointed out above that silicone fluids are used as additives in many products. Their use alone is limited; high-temperature laboratory baths and special lubricants are examples. Silicone sealants, adhesives, molded rubber products, specialty coatings, and surfactants also find large markets.

17.8 POLYPHOSHAZENES

Although polymers with the —P=N— backbone were produced as long ago as the 1890s by ring-scission polymerization of $(\text{NPCl}_2)_3$, moisture hydrolyzes the polymer to a brittle material.



In the 1960s and 1970s, H. R. Allcock used the dichloro-polymer as a precursor for various derivatives and there are now hundreds of stable polyphosphazenes known [16,17].

17.8.1 SOME INDIVIDUAL POLYMERS

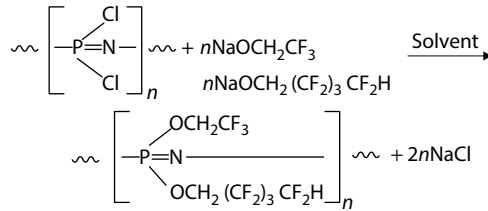
The polymerization of the cyclic trimer proceeds at about 250°C–270°C in a vacuum over a period of 20–40 h with reflux (Table 17.8). Precipitation of the polymer in hexane or pentane leaves unreacted trimer and some other low-molecular-weight species in solution. Yields may range from 15% to 75%.

The chlorine atoms on the backbone of the polymer may be replaced by organic groups such as alkoxy, aryloxy, or amino groups. Most of these derivative polymers do not exhibit the hydrolytic instability of the parent polymer. In order to carry out the substitution, the chlorine-bearing polymer is added dropwise to a solution containing sodium alkoxide or aryloxy in a solvent such as tetrahydrofuran or benzene. A commercial rubber (**PNF**, Firestone Tire and Rubber Company) is based on alkoxides of trifluoroethyl alcohol or heptafluoroisobutyl alcohol [18].

TABLE 17.8
Some Polyorganophosphazenes

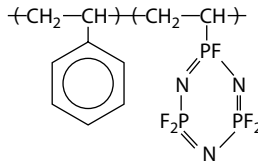
Repeat Group in Compound	T_g (°C)	Solvent
—N=PCl ₂ —	–63	Benzene
—N=P(OCH ₃) ₂ —	–76	Methanol
—N=P(OCH ₂ CH ₃) ₂ —	–84	Alcohols
—N=P(OCH ₂ CF ₃) ₂ —	–66	Ketones
—N=P(OC ₆ H ₅) ₂ —	–8	Benzene
—N=P(NH—C ₆ H ₅) ₂ —	91	Benzene
—N=P(N(CH ₃) ₂) ₂ —	–4	Aqueous acid
—N=P(NC ₅ H ₁₀) ₂ —	19	Benzene

Source: Allcock, H. R., *Angew. Chem. Int. Ed. (English)*, 16, 147, 1977.



The product is referred to as a **phosphonitrilicfluoroelastomer**, a *semiorganic* rubber. The useful range is from the T_g of -68°C up to about 175°C . PNF can be cross-linked by peroxides, sulfur, or high-energy electrons. The outstanding properties of the rubber are excellent oil and fuel resistance, good dynamic properties, and good abrasion resistance making it suitable for the manufacture of O-rings and seals. Disadvantages are water resistance that is only fairly good and price higher than that of fluorosilicones.

Numerous other derivatives have been reported in the literature. A few examples are tabulated (Table 17.8). In addition to those with phosphazene in the backbone, some contain —P=N— in side groups. The reaction of styrene with a vinyl-substituted trimer gives a copolymer that is flame retardant in a standard test and that can be used as foam for fire-resistant insulation [19].



17.8.2 SELECTED USES

Aside from the commercial fluoroelastomer mentioned above, many applications for polyphosphazenes have been proposed. In particular, recent studies have looked at modified polyphosphazenes as potential biomedical materials [20,21]. Phosphazenes with hydrophilic side chains in water exhibit a lower critical solution temperature (LCST) (Section 3.3) and their hydrogels have been considered for controlled drug release and other biomedical applications [22–24]. However, no large-scale use has yet emerged.

17.9 ENGINEERING RESINS AND HIGH-PERFORMANCE POLYMERS

In industrial practice, polymer categories may be based on a variety of considerations. Producers of polymers may well use a compositional basis like the one used in the various sections here and in Chapter 16. Raw materials and techniques for many products may be common to one such group. However, users of polymers often create categories by performance properties such as those summarized in Section 11.1. Within a major industry, polymers compete on a price and performance basis. As an example, in the

rubber industry one can differentiate among general-purpose rubbers (for tires, wire, and cable insulation), specialty rubbers (oil resistant, ozone resistant, heat resistant), and thermoplastic elastomers (which need no covalent cross-linking step).

The term **engineering resin** has been used to designate a group of mainly heterochain thermoplastics that compete with some die-cast metals such as zinc, aluminum, and magnesium in plumbing parts, hardware, and automotive parts [25]. Generally speaking, the engineering resins command a higher price than the *commodity plastics*. Most people would agree on the selection shown in Table 17.9 and Figure 17.5. The polyimide is included by some even though it is not melt processible. All of the polymers included here can be used without reinforcement, but glass fibers, aramid fibers, or mineral reinforcement generally improves dimensional stability at elevated temperatures (see Table 10.2). The flexural modulus and tensile strength as a function of temperature are included for some of these materials in Figures 17.6 and 17.7.

TABLE 17.9
Selected Engineering Thermoplastics

Formula Index (Figure 17.5)	Polymer (Abbreviation)	Trade Name(s)	Distortion Temperature under Load, Neat (Reinforced) (°C)
1	Polyetheretherketone (PEEK)	Victrex	165 (282)
2	Polyamideimide (PAI)	Torlon	274 (278)
3	Polyarylsulfone	Udel	174
4	Polyarylsulfone	Victrex	203
5	Polyarylsulfone	Astrel	274
6	Polyimide (not melt processible)	Kapton	245 + (350)
7	Polyetherimide (PEI)	Ultem	200 (223)
8	Polyphenylenesulfide (PPS)	Ryton	111 (241)
9	PET	Valox, Rynile	150 (224)
10	PBT	Valox	130 (160)
11	Polyarylate, aromatic polyester	Ardel, Durel	170
12	Polycarbonate (PC)	Lexan, Merlon	130 (142)
13	Polyacetal	Delrin	136 (155)
14	Polyacetal	Celcon	110 (165)
15	Nylon 6,6	Zytel	100 (250)
16	Nylon 6	Zytel	80 (205)
17	Modified poly(phenyleneoxide) (PPO)	Noryl	90 (160)

Source: Clagett, D. C.: Engineering Plastics, in H. F. Mark, and J. I. Kroschwitz, *Encyclopedia of Polymer Science and Engineering*, vol. 6, Wiley, New York, 94, 1986. Copyright Wiley-VCH Verlag GmbH & Co. KGaA. Reproduced with permission.

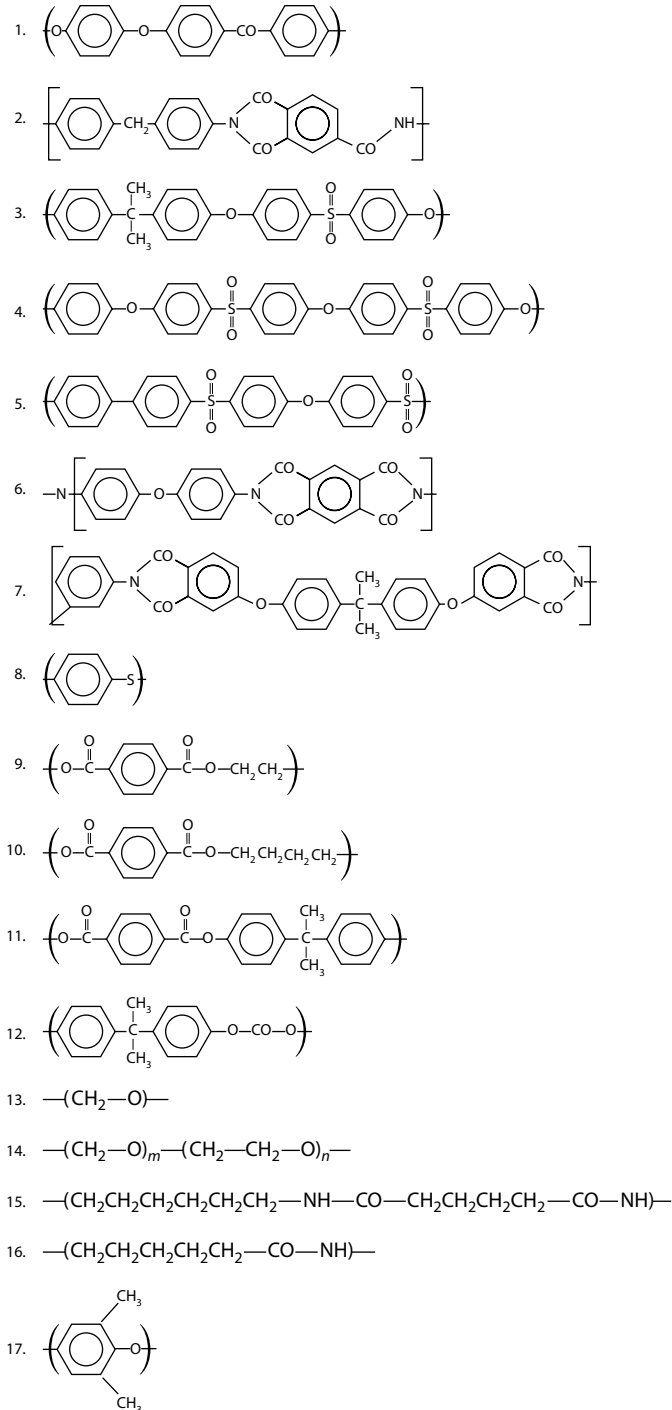


FIGURE 17.5 Chemical formulas for engineering thermoplastics (see Table 17.9).

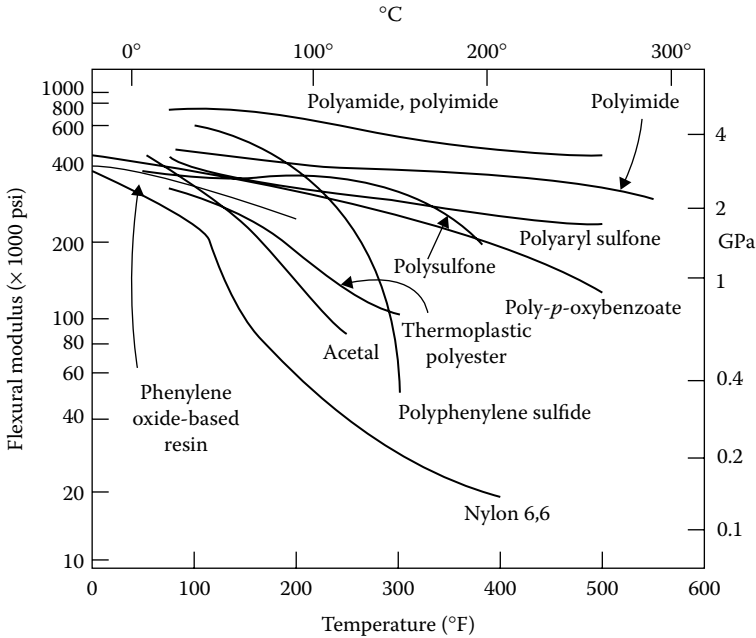


FIGURE 17.6 Flexural modulus of selected molding resins (unreinforced). (Data from Raia, D. D., *Plast. World*, 31, 75, September 17, 1973.)

Because of the high temperatures needed to process many of these resins, the screws and barrels of extruders, and injection-molding machines have to be coated with wear-resistant liners.

A list of materials regarded as **high-performance polymers** (Table 17.10) overlaps the list of Table 17.9 to some extent, but also includes thermosets such as epoxy, phenolic, and silicone molding resins. As with most molded plastics, high-temperature performance is enhanced by reinforcement with glass, boron, or carbon or aramid fibers. The thermosets are seldom used without reinforcement. Several are included in Figures 17.6 and 17.7.

17.10 THERMOPLASTIC ELASTOMERS

It has been noted in several places (Sections 4.6, 17.1, and 17.5) that certain thermoplastic polymers can be quite elastic (rubbery) at room temperature. They form a distinct class of materials, the **thermoplastic elastomers (TPEs)**, which have been defined (ASTM D1566) as “a family of rubber-like materials that, unlike conventional vulcanized rubber, can be processed and recycled like thermoplastic materials.” The typical structure of these materials is the coexistence of *soft* domains that give rubbery behavior with *hard* domains that act as heat-labile cross-links. Although the thermoplastic elastomers compete in many of the applications traditionally assigned to conventional rubbers, the sensitivity of the cross-links to heat makes them unsuitable for an application such as automobile tires, where the

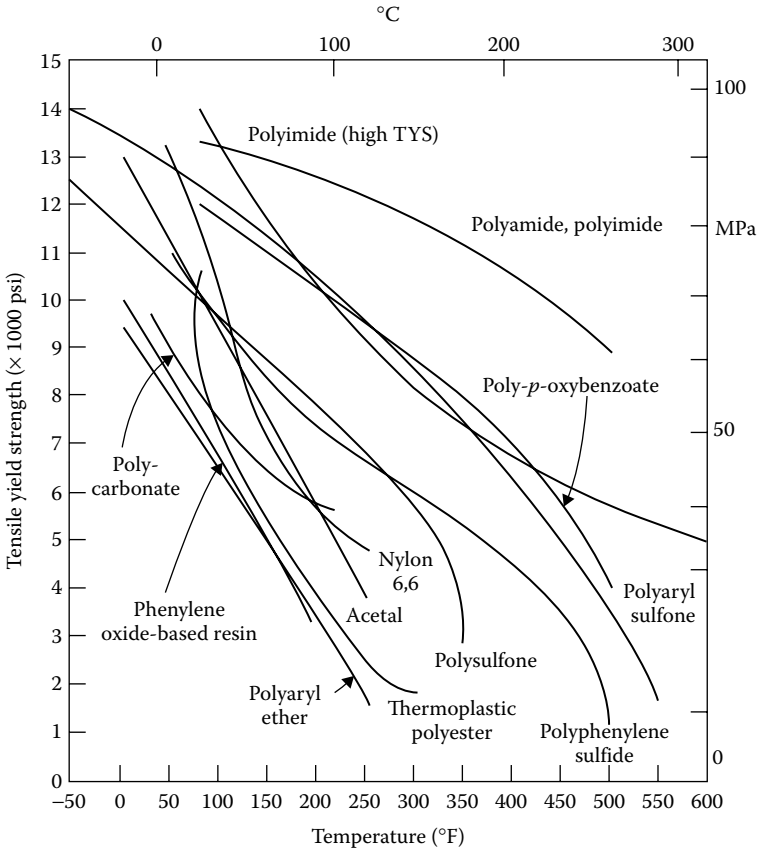


FIGURE 17.7 Tensile yield strength (TYS) of selected molding resins (unreinforced). (Data from Raia, D. D., *Plast. World*, 31, 75, September 17, 1973.)

repeated flexing invariably leads to high temperatures. However, the ease of processing and the possibility of recycling material both make TPE very attractive from an economic standpoint.

Payne and Rader [28] cite three generic classes of TPEs. In the first class they put the **block copolymers**. These include the styrene–butadiene–styrene triblocks, copolyesters, polyurethanes, and polyamides. The latter result when aromatic diamines are used in the hard segments and aliphatic diamines are used in the soft segments, both in combination with aliphatic dicarboxylic acids. The mechanical properties, processing conditions, and solvent resistance differ for the various copolymers. Within each type, a spectrum of hardness values is obtainable by variation of the size and chemical composition of the segments.

The second class is made up of **elastomer/thermoplastic** blends, abbreviated **TEO**. Typical of this class is a dispersion of 20–30 parts of rubber based on ethylene–propylene–diene monomer (EPDM) in a continuous phase of 70–80 parts of a plastic such as isotactic polypropylene. Partial covalent cross-linking of the

TABLE 17.10
Properties of Some High-Performance Plastics

	Tensile Strength (MPa)	Flexural Modulus (GPa)	Heat Deflection Temperature (°C at 1.8 MPa)	Continuous Use Temperature (°C)
Polyimide				
Thermoplastic	118	3.3	132–138	290
Thermoset	62–90	–	>245	–
Thermoset, filled	19–39	22	290–350	260
Poly(amide–imide)				
Unfilled	92	5	280	290
Filled	78–90	5–8	285–295	290
Polyarylsulfone	90	2.7	–	260
Aromatic polyester	17	7.1	–	–
Aromatic copolyester	70	3.1	>315	300
Aromatic polyamide	115	4.4	–	–
Polyphenylene sulfide				
Unfilled	70	4.1	137	205–260
Filled	145	15	>215	205–260
Silicone resin, filled	25–45	7–17	>480	>315
Poly(tetrafluoroethylene)	15–35	–	–	260
Epoxy (mineral-filled)	70–140	17–30	120–260	–
Phenolic (glass fiber filled)	35–125	14–23	150–315	–

Source: Markle, R. A., chap. 39 in J. K. Craver, and R. W. Tess (eds.), *Applied Polymer Science*, American Chemical Society, Washington, DC, 1975.

Unfilled unless designated otherwise.

EPDM particles, which may be less than 10 μm in diameter, results in improved elastic recovery and solvent resistance. Another example of the second class is a dispersion of particles of nitrile rubber in a continuous phase of a poly(vinyl chloride) (PVC) compound.

The third class consists of **elastomeric alloys (EAs)**, which are defined as [28] “highly vulcanized rubber systems with the vulcanization having been done dynamically in the melted plastic phase.” The difference between the highly cross-linked EA and the uncross-linked or loosely cross-linked TEO can appear as a fivefold improvement in ultimate tensile strength and much improved elastic recovery. Evidence has been presented to show that bonding occurs between the phases when the cross-linking is done in the melted plastic [29]. Some other EAs are made with isotactic polypropylene as the continuous phase by dispersing and dynamically cross-linking nitrile rubber, natural rubber, or butyl rubber.

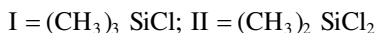
KEYWORDS

Alkyd resin
Ester interchange
PET
PBT
PEN
Thermoplastic elastomer
Polyarylate
Liquid crystal polymers
Poly(*p*-oxybenzoyl ester)
Bisphenol A
Polycarbonate
PHB
Polyacetal
Hydrophilic–lipophilic balance
Epoxy resin
Poly(phenylene oxide)
Polysulfone
Polysulfide
Poly(phenylene sulfide)
PEG
Nylon
Polyamide
Polybenzimidazoles
Bismaleimide
One-stage resin
Resole
Two-stage resin
Novolak
Melamine
Urethane foam
Reaction injection molding
Thermoplastic urethane elastomer
Spandex
PDMS
VTC
RTV
Lipophilic
Hydrophilic
Coupling agents
Polysilanes
Polyphosphazenes
Phosphonitrilic fluoroelastomer
Engineering resin
High-performance plastics

Thermoplastic elastomer, TPE
 Elastomer/thermoplastic blend, TEO
 Elastomeric alloy, EA
 TEO
 EA

PROBLEMS

17.1 How many grams of I and II are needed to make 100 g of a PDMS oil with $M_n = 10,000$?



17.2 Explain why 2,5-dimethyl phenol gives a high-molecular-weight polymer when oxidized but only a low-molecular-weight material with formaldehyde.

17.3 In the *equilibrium* polymerization of tetrahydrofuran, how can residual monomer be removed without depolymerizing the linear polyether?

17.4 What polymers make use of bisphenol A? What properties does it contribute to the polymers?

17.5 A fabricated sample of *cast unsaturated polyester* has the following properties:

(a) It becomes somewhat less stiff at 100°C.

(b) It does not flow, even at 300°C.

(c) It becomes somewhat weaker on soaking in hot, dilute sodium hydroxide. Explain how each of these properties is related to the chemical structure of the sample.

17.6 Both propylene oxide and styrene oxide can be polymerized to give isotactic polymers that can crystallize.

(a) Write formulas for the two polymers.

(b) Identify the asymmetric carbons.

(c) Which of the two polymers would you expect to have the highest T_g ? Why?

17.7 Why are most of the new thermoplastics with high heat distortion temperatures heterochain polymers rather than carbon chain polymers? Why is not ring-scission polymerization used more often for them?

17.8 In a certain country with an *emerging* economy, a governmental decision has been made to establish a polymer industry based on native resources. No oil refineries or coal tar operations exist. Cotton (pure cellulose) and sugar are the major raw materials. In addition, electrolytic processes can be used, since hydroelectric power abounds. Your first step is to set up plants to produce from sugar, sequentially: ethyl alcohol, acetic acid, and butadiene. From electrolysis you now have NaOH, Cl_2 , HCN, and HCl. Sulfuric and nitric acids are also produced locally.

Outline the steps necessary to establish consumer product plants for the following (including reactions where possible):

Cellulose acetate film

cis-Polybutadiene rubber (to be used in tires)

Nylon 6,6 (fibers and molding compound)

(Where you have to import materials, say so.) Outline briefly the feasibility of producing at least two other polymers and give some idea of where they might be useful. Remember that an intermediate in butadiene production can be 1,3-butanediol. Ethyl chloride is also possible.

17.9 A synthetic copolymer of glycine and valine is found to contain 0.210% nitrogen (by weight). What is the ratio of monomers (by weight) in the copolymer?

17.10 A cloth specimen is found by qualitative examination with a microscope to be a mixture of silk, wool, and cotton. Explain how an elemental analysis for nitrogen and sulfur could give the actual proportions of the three fibers by weight. What would be the percent nitrogen and percent sulfur (by weight) if the three fibers were present in equal weights?

REFERENCES

1. Schildknecht, C. E.: Diallyl and Related Polymers, in H. F. Mark, and J. I. Kroschwitz, *Encyclopedia of Polymer Science and Engineering*, vol. 4, Wiley, New York, 1986, p. 779.
2. Ellwood, P.: *Chem. Eng.*, 74:98 (1967).
3. Witsiepe, W. K.: *Polym. Preprints*, 13:588 (April 1972).
4. Hutz, C. E.: in W. M. Smith (ed.), *Manufacture of Plastics*, Reinhold, New York, 1964, p. 507.
5. Winding, C. C., and G. D. Hiatt: *Polymeric Materials*, McGraw-Hill, New York, 1961, p. 228.
6. Brydson, J. A.: *Plastics Materials*, Van Nostrand, Princeton, NJ, 1966, p. 311.
7. *Chem. Eng.*, 73:178 (1966).
8. Butler, J. M., R. M. Hedrick, and E. H. Moftus: (Monsanto) U.S. Patent 3,018,273 (1962).
9. Barry, A. J., and H. N. Beck: chap. 3 in F. G. A. Stone, and W. A. G. Graham (eds.), *Inorganic Polymers*, Academic Press, New York, 1962.
10. Rodriguez, F., R. A. Kulakowski, and O. K. Clark: *Ind. Eng. Chem. Prod. Res. Dev.*, 5:121 (1966).
11. Kanner, B., W. G. Reid, and I. H. Petersen: *Ind. Eng. Chem. Prod. Res. Dev.*, 6:88 (1967).
12. Merker, R. L., and M. J. Scott: *J. Polym. Sci.*, A2:15 (1964).
13. Warrick, E. L., O. R. Pierce, K. E. Polmanteer, and J. C. Saam: *Rubber Chem. Technol.*, 52:437 (1979).
14. Miller, R. D., D. Hofer, D. R. McKean, C. G. Willson, R. West, and P. T. Trefonas, III: Soluble Polysilane Derivatives, in L. F. Thompson, C. G. Wilson, and J. M. J. Frechet (eds.), *Materials for Microlithography*, American Chemical Society, Washington, DC, 1984, p. 292.
15. Miller, R. D., D. Hofer, J. Rabolt, R. Sooriyakumaran, C. G. Wilson, G. N. Fickes, J. E. Guillet, and J. Moore: Soluble Polysilanes in Photolithography, in M. J. Bowden and S. R. Turner (eds.), *Polymers for High Technology*, American Chemical Society, Washington, DC, 1987, p. 170.
16. Allcock, H. R.: *Phosphorus-Nitrogen Compounds*, Academic Press, New York, 1972.
17. Allcock, H. R.: *Angew. Chem. Int. Ed. (English)*, 16:147 (1977).
18. Kyker, G. S., and T. A. Antkowiak: *Rubber Chem. Technol.*, 47:32 (1974).
19. DuPont, J. G., and C. W. Allen: *Macromolecules*, 12:169 (1979).
20. Deng, M., S. G. Kumbar, Y. Wan, U. S. Toti, H. R. Allcock, and C. T. Laurencin: *Soft Matter*, 6:3119 (2010).

21. Allcock, H. R., and N. Morozowich: *Polym. Chem.*, 3:578 (2012).
22. Allcock, H. R., S. R. Pucher, M. L. Turner, and R. J. Fitzpatrick: *Macromolecules*, 25:5573 (1992).
23. Allcock, H. R., S. R. Pucher, and A. G. Scopelianos: *Macromolecules*, 27:1 (1994).
24. Kim, J., C. Chun, B. Kim, J. M. Hong, J.-K. Cho, S. H. Lee, and S.-C. Song: *Biomaterials*, 33:218 (2012).
25. Claggett, D. C.: Engineering Plastics, in H. F. Mark, and J. I. Kroschwitz, *Encyclopedia of Polymer Science and Engineering*, vol. 6, Wiley, New York, 1986, p. 94.
26. Raia, D. D.: *Plast. World*, 31:75 (September 17, 1973).
27. Markle, R. A.: chap. 39 in J. K. Craver, and R. W. Tess (eds.), *Applied Polymer Science*, ACS, Washington, DC, 1975.
28. Payne, M. T., and C. P. Rader: *Elastomer Technology Handbook*, CRC Press, Boca Raton, FL, 1993.
29. Coran, A. Y, R. P. Patel, and D. Williams: *Rubber Chem. Technol.*, 55:116 (1982).

GENERAL REFERENCES

- Aharoni, S.: *N-Nylons: Their Synthesis, Structure and Properties*, Wiley, New York, 1997.
- Allcock, H. R.: *Chemistry and Applications of Polyphosphazenes*, Wiley, New York, 2003.
- Andrianov, A. K. (ed.): *Polyphosphazenes for Biomedical Applications*, Wiley, New York, 2009.
- Arthur, J. C., Jr. (ed.): *Polymers for Fibers and Elastomers*, ACS, Washington, DC, 1984.
- Ashida, K., and K. C. Frisch (eds.): *International Progress in Urethanes*, vol. 6, Technomic, Lancaster, PA, 1993.
- Baer, E., and A. Moet (eds.): *High Performance Polymers*, Hanser-Gardner, Cincinnati, OH, 1991.
- Bailey, F. E., Jr., and J. V. Koleske (eds.): *Alkylene Oxides and Their Polymers*, Dekker, New York, 1991.
- Bauer, R. S. (ed): *Epoxy Resin Chemistry II*, ACS, Washington, DC, 1983.
- Bessonov, M. I., M. M. Koton, V. V. Kudryavtsev, and L. A. Laius: *Polyimides*, Plenum Press, New York, 1987.
- Bessonov, M. I., and V. A. Zubkov (eds.): *Polyamic Acids and Polyimides: Synthesis, Transformations, and Structure*, CRC Press, Boca Raton, FL, 1993.
- Bhowmick, A. K., and H. L. Stephens (eds.): *Handbook of Elastomers*, Dekker, New York, 1988.
- Bhowmick, A. K., and H. L. Stephens (eds.): *Handbook of Elastomers*, 2nd edn., Dekker, New York, 2000.
- Blackley, D. C.: *Synthetic Rubbers*, Elsevier Applied Science, New York, 1983.
- Brydson, J. A.: *Plastics Materials*, 4th edn., Butterworth, Woburn, MA, 1982.
- Buist, J. M. (ed.): *Developments in Polyurethanes—I*, Elsevier Applied Science, New York, 1978.
- Carfagna, C. (ed.): *Liquid Crystalline Polymers*, Pergamon Press, New York, 1994.
- Carraher, C. E., Jr., and L. H. Sperling (eds.): *Renewable-Resource Materials*, Plenum Press, New York, 1986.
- Cassidy, P. E.: *Thermally Stable Polymers: Syntheses and Properties*, Dekker, New York, 1980.
- Cheremisinoff, N. P. (ed.): *Handbook of Engineering Polymeric Materials*, Dekker, New York, 1997.
- Clarson, S. J., and J. A. Semlyen (eds.) *Siloxane Polymers*, Prentice Hall, Englewood Cliffs, NJ, 1993.
- Culbertson, B. M., and J. E. McGrath (eds.): *Advances in Polymer Synthesis*, Plenum Press, New York, 1985.

- De, S. K., and A. K. Bhowmick (eds.): *Thermoplastic Elastomers from Rubber-Plastic Blends*, Prentice Hall, Englewood Cliffs, NJ, 1991.
- DiStasio, J. I. (ed.): *Epoxy Resin Technology (Developments since 1979)*, Noyes, Park Ridge, NJ, 1982.
- Dusek, K. (ed.): *Epoxy Resins and Composites, 1–4*, Springer-Verlag, New York, 1985–1986.
- Dusek, K. et al. (eds.): *Key Polymers*, Springer-Verlag, New York, 1985.
- Dyson, R. W. (ed.): *Specialty Polymers*, Chapman & Hall (Methuen), New York, 1987.
- Dyson, R. W. (ed.): *Engineering Polymers*, Chapman & Hall, New York, 1990.
- Elias, H.-G.: *Macromolecules: Synthesis, Materials, and Technology*, 2nd edn., Plenum Press, New York, 1984.
- Elias, H.-G., and F. Vohwinkel: *New Commercial Polymers—2*, Gordon & Breach, New York, 1986.
- Ellis, B. (ed.): *Chemistry and Technology of Epoxy Resins*, Chapman & Hall, New York, 1993.
- Feger, C., M. M. Khojasteh, and M. S. Htoo (eds.): *Advances in Polyimide Science and Technology*, Technomic, Lancaster, PA, 1993.
- Feger, C., M. M. Khojasteh, and J. E. McGrath (eds.): *Polyimides: Materials, Chemistry and Characterization*, Elsevier, Amsterdam, The Netherlands, 1989.
- Finch, C. A. (ed.): *Chemistry and Technology of Water-Soluble Polymers*, Plenum Press, New York, 1983.
- Flick, E. W.: *Epoxy Resins Curing Agents, Compounds, and Modifiers: An Industrial Guide*, Noyes, Park Ridge, NJ, 1987.
- Flick, E. W.: *Water-Soluble Resins: An Industrial Guide*, 2nd edn., Noyes, Park Ridge, NJ, 1991.
- Flick, E. W. (ed.): *Industrial Synthetic Resins Handbook*, 2nd edn., Noyes, Park Ridge, NJ, 1991.
- Fontanille, M., and A. Guyot (eds.): *Recent Advances in Mechanistic and Synthetic Aspects of Polymerization*, Kluwer Academic Publishers, Norwell, MA, 1987.
- Frisch, K. C., and D. Klemptner (eds.): *Advances in Urethane Science and Technology*, 12 vols., Technomic, Lancaster, PA, 1971–1992.
- Ghosh, M. K., and K. L. Mittal: *Polyimides—Fundamentals and Applications*, Dekker, New York, 1996.
- Glass, J. E. (ed.): *Water-Soluble Polymers*, ACS, Washington, DC, 1986.
- Glass, J. E. (ed.): *Polymers in Aqueous Media*, ACS, Washington, DC, 1989.
- Gum, W. F., Jr., W. Reise, and H. Ulrich (eds.): *Reaction Polymers*, Hanser-Gardner, Cincinnati, OH, 1992.
- Gupta, S. K., and A. Kumar: *Reaction Engineering of Step Growth Polymerization*, Plenum Press, New York, 1987.
- Hamerton, I. (ed.): *Chemistry and Technology of Cyanate Ester Resins*, Chapman & Hall, New York, 1994.
- Harper, C. A. (ed.): *Handbook of Plastics, Elastomers, and Composites*, 2nd edn., McGraw-Hill, New York, 1992.
- Hepburn, C.: *Polyurethane Elastomers*, Elsevier, New York, 1992.
- Hergenrother, P. M.: *High Performance Polymers*, Springer-Verlag, Berlin, Germany, 1994.
- Knop, A., and L. A. Pilato: *Phenolic Resins*, Springer-Verlag, New York, 1985.
- Koerner, G., M. Schulze, and J. Weis: *Silicones: Chemistry and Technology*, CRC Press, Boca Raton, FL, 1992.
- Kohan, M. I. (ed.): *Nylon Plastics Handbook*, Hanser, Munich, Germany, 1995.
- Krol, P.: *Linear Polyurethanes: Synthesis Methods, Chemical Structures, Properties and Applications*, VSP, Boston, MA, 2008.
- Kumar, A., and R. K. Gupta: *Fundamentals of Polymer Engineering*, 2nd edn., Dekker, New York, 2003.

- Lee, J. A., and D. L. Mykkanen: *Metal and Polymer Matrix Composites*, Noyes, Park Ridge, NJ, 1987.
- Legge, N. R., G. Holden, and H. E. Schroeder (eds.): *Thermoplastic Elastomers*, Macmillan, New York, 1987.
- LeGrand, D. G., and J. T. Bendler (eds.): *Handbook of Polycarbonate Science and Technology*, Dekker, New York, 1999.
- Lin, S.-C.: *High-Performance Thermosets*, Hanser-Gardner, Cincinnati, OH, 1993.
- Lucke, H.: *Aliphatische Polysulfide*, Huthig & Wepf, Basel, Switzerland, 1992.
- Margolis, J. M. (ed.): *Engineering Thermoplastics*, Dekker, New York, 1985.
- Margolis, J. M. (ed.): *Advanced Thermoset Composites*, Van Nostrand Reinhold, New York, 1986.
- Mark, J. E., H. R. Allcock, and R. C. West: *Inorganic Polymers: An Introduction*, Prentice Hall, Englewood Cliffs, NJ, 1992.
- Martuscelli, E., and C. Marchetta (eds.): *New Polymeric Materials: Reactive Processes and Physical Properties*, VNU Science, Utrecht, The Netherlands, 1987.
- May, C. A. (ed.): *Epoxy Resins*, 2nd edn., Dekker, New York, 1988.
- Meier, D. J. (ed.): *Block Copolymers*, Gordon & Breach, New York, 1983.
- Meltzer, Y. L.: *Water-Soluble Polymers (Developments since 1978)*, Noyes, Park Ridge, NJ, 1981.
- Meyer, B.: *Urea-Formaldehyde Resins*, Addison-Wesley, Reading, MA, 1979.
- Miles, D. C., and J. H. Briston: *Polymer Technology*, Chemical Publishing, New York, 1979.
- Mittal, K. L. (ed.): *Polyimides and Other High Temperature Polymers: Synthesis, Characterization, and Applications*, vol. 4, VSP, Boston, MA, 2007.
- Mittal, K. L. (ed.): *Polyimides and Other High Temperature Polymers: Synthesis, Characterization, and Applications*, vol. 5, VSP, Boston, MA, 2009.
- Mittal, V.: *High Performance Polymers and Engineering Plastics*, Wiley, Hoboken, NJ, 2011.
- Molyneux, P.: *Water Soluble Synthetic Polymers: Properties and Behavior*, 2 vols., CRC Press, Boca Raton, FL, 1984.
- Oertel, G. (ed.): *Polyurethane Handbook*, 2nd edn., Hanser-Gardner, Cincinnati, OH, 1993.
- Ray, N. H.: *Inorganic Polymers*, Academic Press, New York, 1978.
- Riew, C. K., and J. K. Gillham (eds.): *Rubber-Modified Thermoset Resins*, ACS, Washington, DC, 1984.
- Robinson, J. S. (ed.): *Fiber-Forming Polymers*, Noyes, Park Ridge, NJ, 1980.
- Rochow, E. G.: *Silicon and Silicones*, Springer-Verlag, New York, 1987.
- Roesky, H. W. (ed.): *Rings, Clusters, and Polymers of Main Group and Transition Elements*, Elsevier, Amsterdam, The Netherlands, 1989.
- Ropp, R. C.: *Inorganic Polymeric Glasses*, Elsevier, Amsterdam, The Netherlands, 1992.
- Schildknecht, C. E., and I. Skeist (eds.): *Polymerization Processes*, Wiley, New York, 1977.
- Schultz, J., and S. Fakirov: *Solid State Behavior of Linear Polyesters and Polyamides*, Prentice Hall, Englewood Cliffs, NJ, 1990.
- Serafini, T. T. (ed.): *High Temperature Polymer Matrix Composites*, Noyes, Park Ridge, NJ, 1987.
- Seymour, R. B., and G. S. Kirshenbaum (eds.): *High-Performance Polymers: Their Origin and Development*, Elsevier, New York, 1986.
- Seymour, R. B., and H. F. Mark (eds.): *Applications of Polymers*, Plenum Press, New York, 1988.
- Sheats, J. F., C. E. Carraher, Jr., and C. U. Pittman, Jr. (eds.): *Metal-Containing Polymeric Systems*, Plenum Press, New York, 1985.
- Tess, R. W., and G. W. Poehlein (eds.): *Applied Polymer Science*, 2nd edn., ACS, Washington, DC, 1985.
- Tomanek, A.: *Silicones & Industry*, Hanser-Gardner, Cincinnati, OH, 1992.

- Walker, B. M., and C. P. Rader (eds.): *Handbook of Thermoplastic Elastomers*, 2nd edn., Van Nostrand Reinhold, New York, 1988.
- Wilson, D., H. D. Stenzenberger, and P. M. Hergenrother (eds.): *Polyimides*, Chapman & Hall, New York, 1990.
- Wisian-Neilson, P., H. R. Allcock, and K. J. Wynne (eds.): *Inorganic and Organometallic Polymers II: Advanced Materials and Intermediates*, ACS, Washington, DC, 1995.
- Woods, G.: *The ICI Polyurethanes Handbook*, Wiley, New York, 1990.
- Zeldin, M., K. J. Wynne, and H. R. Allcock (eds.): *Inorganic and Organometallic Polymers*, ACS, Washington, DC, 1988.
- Ziegler, J. M., and F. W. G. Fearon: *Silicon-Based Polymer Science*, ACS, Washington, DC, 1990.

18 Analysis and Identification of Polymers

18.1 PURPOSE OF POLYMER ANALYSIS

A variety of situations call for the identification of polymers. A customer wishes to paint or glue an item or to use an object in a novel environment. It may be awkward or impossible to obtain the composition from the supplier. In another common case, it may simply be detective work to find a chemical reason why a competitor's product behaves differently from your own. Contaminants in fabrication plants can be very hard to trace. For example, a small amount of a highly unsaturated polymer, such as natural rubber, can prevent the proper cross-linking of a large amount of a more saturated material, such as butyl or ethylene propylene diene monomer (EPDM) rubber.

Many of the tests described as useful in identification are also run routinely as quality controls on known polymers. Although **infrared (IR) spectroscopy** is extremely helpful as an identification tool, it is also applied to the measurement of crystallinity and branching in some polymers (notably polyethylene). Physical testing, molecular weight determination, and electrical testing have been discussed previously. The larger polymer producers perform almost all of these tests routinely. The smaller, more specialized laboratories of many fabricators and consumers may not possess all of the instruments needed for these tests. Independent laboratories will perform them on a consulting basis. Where the instruments are expensive or the test method is quite involved, recourse to independent laboratories may be wise.

18.2 IR AND ULTRAVIOLET SPECTROSCOPY

The atoms constituting a molecule are in constant vibration. When the number of atoms in a molecule exceeds 10 or so, the number of possible modes of vibration becomes very large. Fortunately, many frequencies are characteristic of localized bonds. Thus, the absorption of light by the stretching of the C–H bond almost always occurs at frequencies between 2880 and 2900 cm^{-1} . Most IR spectrophotometers use a glowing light source to provide light with wavelengths from 2.5 to about 15 μm . An alternative system of nomenclature that is popular refers to the reciprocal of wavelength as **wave number** or frequency. A wavelength of 2.5 μm corresponds to a wave number or frequency of 4000 cm^{-1} , 10 μm is equivalent to 1000 cm^{-1} , and so on. In a classical machine, a rotating prism or diffraction grating breaks up the light from the source into a spectrum from which various wavelengths are progressively isolated with the aid of filters. A programmed slit compensates for the varying intensity of the source at different wavelengths.

In more recent IR spectrometers, the Fourier transform (FT) method is used. An interferogram is recorded that makes use of a Michelson interferometer. Information is collected in the time domain and converted by the computer to a frequency domain spectrum by means of an FT. From this interferogram and the known wavelengths of the exposing IR radiation (typically over the range of $4000\text{--}400\text{ cm}^{-1}$), the software will fit the interferogram to a series of spectral absorbances. The advantage of this method is the speed with which information can be collected, making **FTIR** ideal for kinetics studies. It is also possible to carry out signal averaging, thereby improving signal to noise in samples consisting of small quantities of material.

The sample may be a thin unsupported film (usually about 2 mm thick); a film evaporated on a nonabsorbing substrate such as NaCl; a solution held in a nonabsorbing cell (often made of NaCl); a pressed, clear wafer of the material to be analyzed mixed with KBr powder; or a mull of the material with a heavy paraffin oil held between NaCl flats. Other alkali and alkaline earth halides are used as substrates. Water and alcohols are not used as solvents generally, because they absorb strongly in the IR region and may corrode the substrates.

In a double-beam instrument, the absorption by H_2O and CO_2 vapors is canceled out. By using matched cells in such a machine, one can also compensate for the solvent. It must be remembered that even with compensation, high absorption by the solvent in both cells still reduces the sensitivity of the method at that particular frequency. By contrast, FTIR machines record a blank spectrum and subtract background during the computational portion of spectral analysis. Taking advantage of modern information handling, most FTIR spectrometers also hold sample spectra of a wide variety of organic materials and polymers. Thus, it is relatively simple to use IR spectroscopy to identify unknown polymers by spectral matching.

The positions of some characteristic absorption bands are summarized in Table 18.1. Although these are valuable in analyzing spectra, we can often learn much by regarding the entire spectrum as a kind of fingerprint. In this way, we can identify the common homopolymers rapidly by simple comparison with standard spectra. Copolymers, terpolymers, and mixtures introduce complications, although the spectra may be simply additive. Some bands are shifted by changes in environment. The OH and NH bands are moved by hydrogen bonding. In fact, the shift of the deuterated hydroxyl group (OD) band in deuterated methanol when it is mixed with another liquid is used as a measure of hydrogen bonding in classifying solubility and swelling data (Section 2.5).

In Figures 18.1 through 18.3, spectra for some common polymers are reproduced. Since these are transmission spectra, absorption bands appear as valleys. The characteristic band frequencies of Table 18.1 can be compared with specific polymers. The OH band appears in poly(vinyl alcohol) and not in polyethylene, for example. Spectra for the same polymer may appear differently depending on several factors. The thickness or concentration will affect the absolute value of absorption. Since the hydroxyl group in the poly(ethylene oxide) shown in Figure 18.3 occurs as an end group, the molecular weight will affect the intensity of that band relative to the bands for the ether and hydrocarbon bonds. In poly(vinyl alcohol) (Figure 18.2), an incompletely hydrolyzed sample will show vestiges of the acetate group remaining.

TABLE 18.1
Positions of Characteristic IR Bands

Group	Frequency Range (cm ⁻¹)
OH stretching vibrations	
Free OH	3510–3645 (sharp)
Intramolecular hydrogen bonds	3450–3600 (sharp)
Intermolecular hydrogen bonds	3200–3550 (broad)
Chelate compounds	2500–3200 (very broad)
NH stretching vibrations	
Free NH	3300–3500
Hydrogen-bonded NH	3070–3350
CH stretching vibrations	
≡C–H	3280–3340
=C–H	3000–3100
C–CH ₃	2872 ± 10.2962 ± 10
O–CH ₃	2815–2832
N–CH ₃ (aromatic)	2810–2820
N–CH ₃ (aliphatic)	2780–2805
CH ₂	2853 ± 10.2926 ± 10
CH	2880–2900
SH stretching vibrations	
Free SH	2550–2600
C≡N stretching vibrations	
Nonconjugated	2240–2260
Conjugated	2215–2240
C≡C stretching vibrations	
C≡CU (terminal)	2100–2140
C–C–C–C	2190–2260
C–C≡C–C≡CH	2040–2200
C=O stretching vibrations	
Nonconjugated	1700–1900
Conjugated	1590–1750
Amides	~1650
C=C stretching vibrations	
Nonconjugated	1620–1680
Conjugated	1585–1625
CH bending vibrations	
CH ₂	1405–1465
CH ₃	1355–1395, 1430–1470
C–O–C vibrations in esters	
Formates	~1175
Acetates	~1240, 1010–1040
Benzoates	~1275

(Continued)

TABLE 18.1
(Continued) Positions of Characteristic IR Bands

Group	Frequency Range (cm ⁻¹)
C—OH stretching vibrations	
Secondary cyclic alcohols	990–1060
CH out-of-plane bending vibrations in substituted ethylenic systems	
—CH=CH ₂	905–915, 985–995
—CH=CH—(<i>cis</i>)	650–750
—CH=CH—(<i>trans</i>)	960–970
C=CH ₂	885–895
	790–840

Source: Cole, A. R. H., in K. W. Bentley (ed.): *Elucidation of Structures by Physical and Chemical Methods, Part 1, Technique of Organic Chemistry*. 1963. vol. XI, Wiley, New York, 33ff. Copyright Wiley-VCH Verlag GmbH & Co. KGaA.

IR analysis can be applied to surfaces [3] and pyrolyzed fragments of polymeric materials [4] for purposes of identification. In particular, FTIR microscopes are useful for evaluating micron-sized regions of fiber, film, and coating samples. The FTIR microscope can be used as a conventional optical microscope, but, in addition, an IR spectrometer is attached to the microscope. It is possible to direct the image beam through the spectrometer and collect sample spectra. Of particular use is the fact that silicon wafers, the substrates used to build most microelectronics, are transparent in the IR. Thus, this substrate is ideal for use in thin film analysis.

In addition to the obvious use in identifying unknown polymers and the estimation of amounts of comonomers, impurities, or end groups in polymers, IR analysis, with some modification, has been used for measuring crystallinity and orientation of specific groups in crystalline polymers. Chemical reactions of polymers can be followed by the appearance or disappearance of functional groups such as oxygen groups in oxidation or free hydroxyl groups from hydrolysis.

The absorption of light in the near ultraviolet (wavelengths of 0.2–0.4 μm, 200–400 nm) arises from electronic excitation of the molecules. Two important features are that the ultraviolet absorption is generally indicative of multiple unsaturation and the absorption bands are often rather broad. One does not usually obtain a *fingerprint* with many individual bands as in the IR region. However, absorption in the ultraviolet region can be quite strong and can be carried out in aqueous solutions. The column effluent from chromatographic separations of some water-soluble polymers can be monitored by measuring the absorption at a single wavelength.

18.3 DIFFERENTIAL THERMAL METHODS

Very often the limiting parameter for the useful application of a polymer is dimensional or chemical stability. The temperatures at which physical transitions occur are important to the first criterion, and the temperature of the onset of chemical

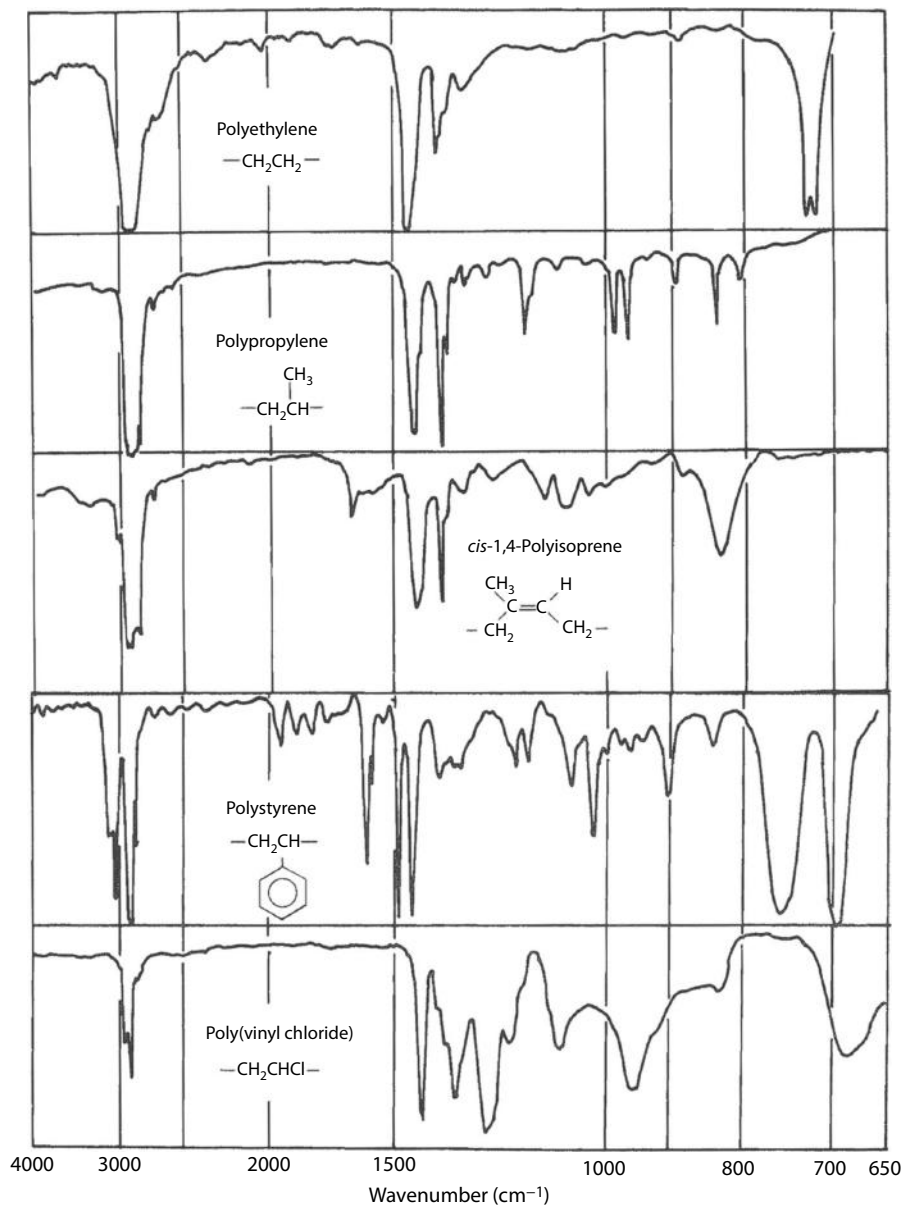


FIGURE 18.1 Typical transmission spectra in the IR region. The ordinate in each diagram is 0%–100% transmission. (Data from Nyquist, R. A., *Infrared Spectra of Plastics and Resins*, 2nd edn., Dow Chemical Co., Midland, TX, 1961.)

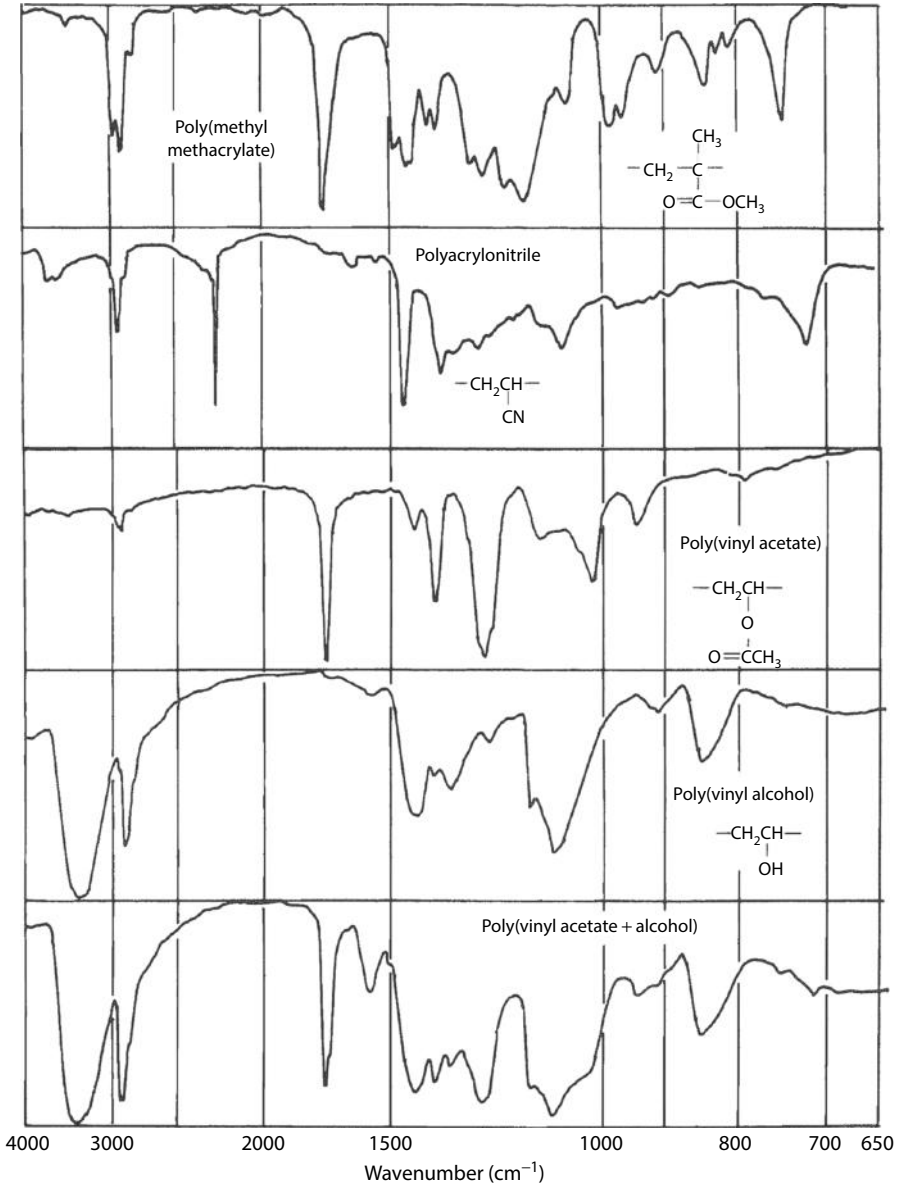


FIGURE 18.2 Typical transmission spectra in the IR region. The ordinate in each diagram is 0%–100% transmission. The incompletely hydrolyzed sample of poly(vinyl acetate) illustrates the additivity of spectra. (Data from Nyquist, R. A., *Infrared Spectra of Plastics and Resins*, 2nd edn., Dow Chemical Co., Midland, TX, 1961.)

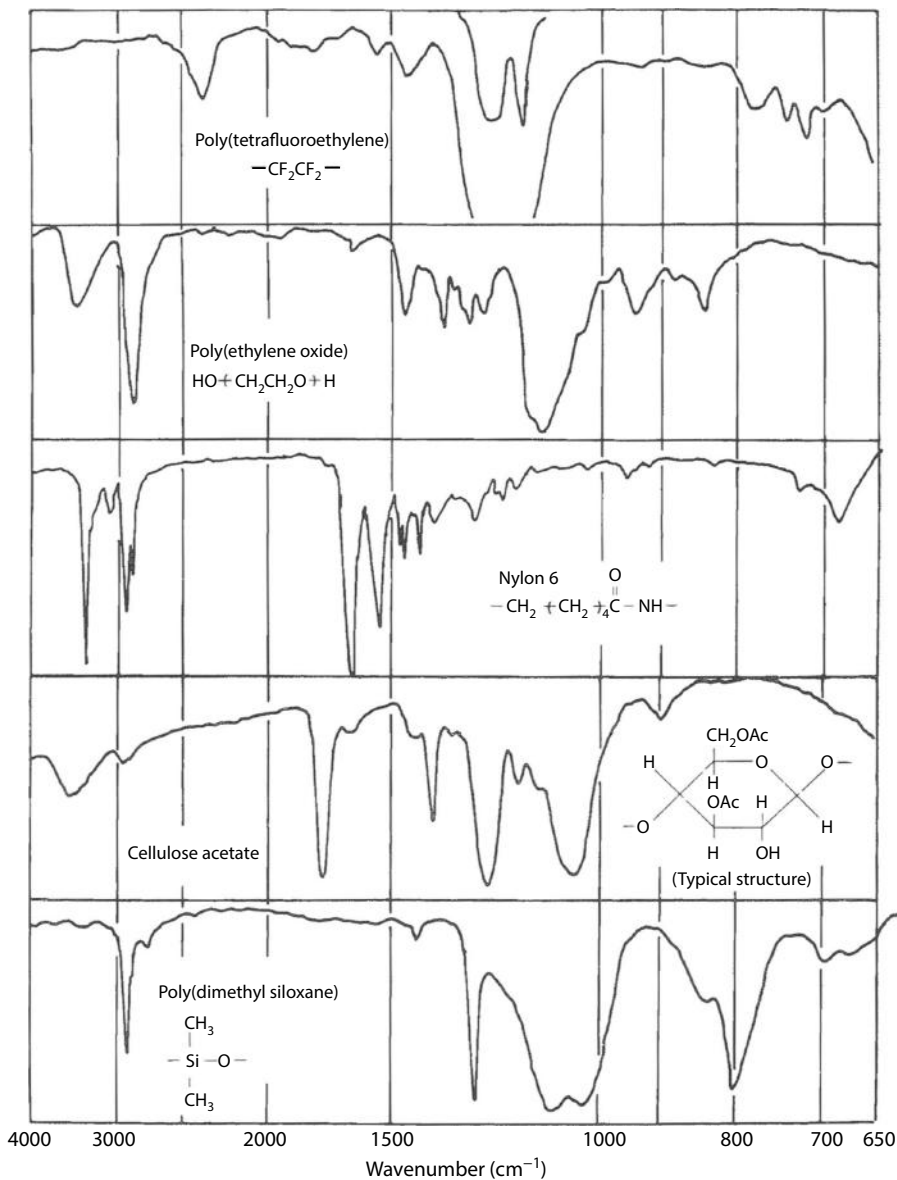


FIGURE 18.3 Typical transmission spectra in the IR region. The ordinate in each diagram is 0%–100% transmission. Since the cellulose acetate is made by hydrolysis of the triacetate, the structure shown is only one of many that may exist in the polymer. The average composition does correspond to the diacetate. (Data from Nyquist, R. A., *Infrared Spectra of Plastics and Resins*, 2nd edn., Dow Chemical Co., Midland, TX, 1961.)

reaction is important to the second criterion. Some subtle changes in structure can be observed when the polymer sample is compared to another material undergoing a similar heating process but not undergoing any transitions or reactions.

Differential scanning calorimetry (DSC) uses a servo system to supply energy to a sample and a reference material in such a way that both undergo a linearly rising temperature. The difference in energy supplied between the sample and the reference is a measure of various thermal events, the most common of which are glass transition, crystallization, and melting. Other processes can take place such as evaporation and chemical reactions. Although the most common test uses an increasing temperature, some processes such as crystallization and chemical reactions can be characterized by the energy supplied under isothermal conditions.

In one commercial instrument, the polymer sample is held in an aluminum pan with a crimped-on lid (Figure 18.4). The reference most often is simply an empty pan. Both the sample and the reference are heated to give a constant rate of temperature change by separate platinum resistance heaters, which are controlled by the signals from platinum resistance thermometers. The difference in power needed to keep both at the same temperature is amplified and provides the information on thermal events. For a properly calibrated DSC, the level of the power flux is a direct measure of the specific heat of the sample. Since the specific heat of a polymer melt is greater than that of the corresponding glass, a discontinuity is expected at T_g . When crystallization or melting occurs, the area under a peak represents the enthalpy change.

A sample mass of 5–15 mg and a heating rate of 10°C–40°C/min are typical conditions. As indicated in Section 3.8, DSC has become accepted as a standard measure of T_g (ASTM D3418). In an illustrative example (Figure 18.5), mixtures of poly(vinyl chloride) (PVC) with a plasticizer, di-2-ethylhexylphthalate, are sealed in aluminum pans. At the rapid rate of temperature increase used, each test requires only 5 or 10 min.

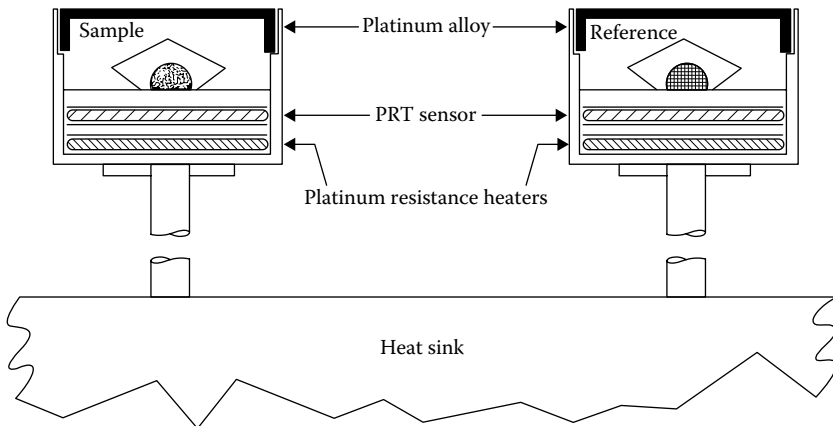


FIGURE 18.4 Differential scanning calorimeter (power compensation type). The platinum resistance thermometer (PRT) sensor detects a small error signal between the programmed temperature and the sample temperature and calls for more or less power to each heater to keep both holders on program. The difference in power required between the sample and the reference is amplified and recorded. (Courtesy of PerkinElmer Corporation, Norwalk, CT.)

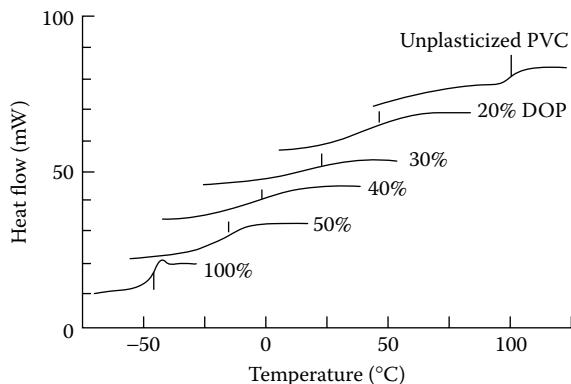


FIGURE 18.5 The glass transition for plasticized PVC as determined by DSC. The heating rate was 40°C/min. (Reprinted from Brennan, W. P. et al., *Amer. Lab.*, 20, 36, 1988; copyright by International Scientific Communications, Inc.)

The transitions seen for mixtures like these are not as clear-cut as those for the pure components. As indicated in Section 3.6, it is not unusual for the transition zone for mixtures to be broader than it is for individual components. The T_g measured by DSC at a fast heating rate (Figure 18.5) is substantially higher than the flex temperature of Figure 3.10, which corresponds to a much longer timescale of testing. Some other typical effects can be seen when a partly crystalline polymer is examined (Figure 18.6). A *thermoplastic polyester* exhibits a melting transition at about 250°C. The sample cooled at 20°C/min shows very little change at the expected glass transition point (77°C). The sample quenched from the melt, having a greater amorphous fraction, shows a substantial shift in heat flow at 77°C and crystallization at 135°C followed by melting at 250°C (refer also to Figures 3.23 and 3.24).

Some workers have superimposed a sinusoidal pattern on the heating rate in order to derive a more detailed information from the heat flow pattern [7]. Many other applications have been found for DSC, including the study of kinetics of polymerization or cross-linking, absorption, adsorption and desorption, and almost every other possible thermal event.

In conventional **differential thermal analysis (DTA)**, the temperature at the center of the sample is compared with a reference material (often powdered alumina) as both are heated at a uniform rate. Any change in the sample's specific heat as at T_g , any structural change that is endothermic or exothermic as at T_m , or chemical reactions will show as changes in the temperature difference between sample T_s and reference T_r . A primitive instrument consists of thermocouples inserted in the sample and the reference. The sample and the reference material are held in a heated metal block at a controlled temperature T_0 . As T_0 is raised (a rate of 10°C/min is common), T_s and T_r follow perhaps by as little as 0.1°C. If an endothermic reaction takes place, T_s will lag behind T_r temporarily. If an exothermic reaction takes place, T_s will exceed T_r temporarily. Superficially, DTA resembles DSC in that temperatures of a sample and a reference material are increased at almost the same rate. However, in DTA the difference in temperature, ΔT , is the measured quantity rather than the difference in

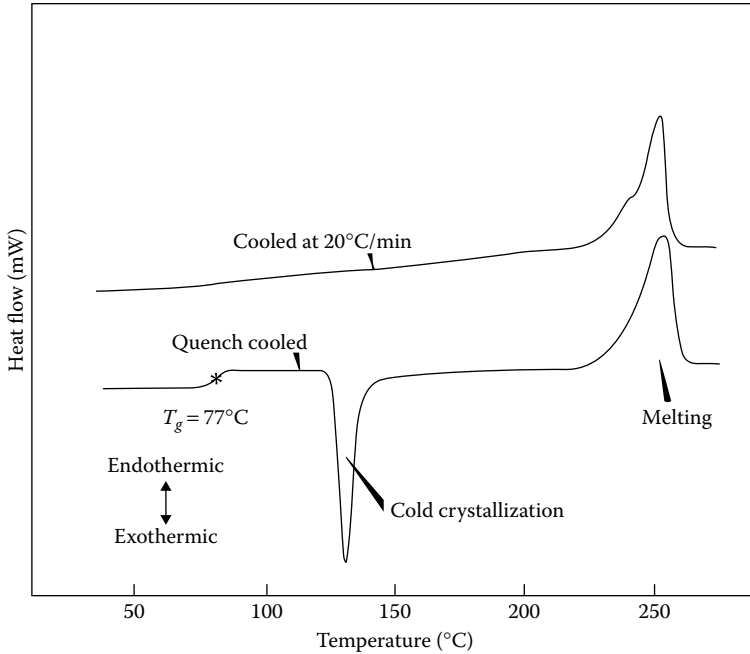


FIGURE 18.6 Samples of a thermoplastic polyester show different DSC traces depending on preparation kinetics. (Data from Brennan, W. P., *Characterization and Quality Control of Engineering Thermoplastics by Thermal Analysis*, Instrument Division, PerkinElmer Corporation, Norwalk, CT, 1977.) Rapid quenching yields a sample that, on heating, shows a distinct glass transition as well as crystallization and melting. The heating rate was 20°C/min. (Courtesy of PerkinElmer Corporation, Norwalk, CT.)

energy being supplied. If an endothermic event such as crystallization takes place, the sample temperature will lag slightly behind the reference temperature, giving a peak in the ΔT versus T (average) plot similar in appearance to that in Figure 18.6. The method is a sensitive one for detecting T_m , but the area under the peak is not easily related quantitatively to the enthalpy change.

18.4 OTHER METHODS OF THERMAL ANALYSIS

In **thermogravimetric analysis (TGA)**, a sample is weighed continuously as the temperature is raised. Volatilization, chemical reaction, and dehydration are some of the processes that affect the sample weight. When many compounds have to be screened for their applicability in a high-temperature environment, TGA may be the only test needed. For example, if a rubbery gasket material is needed for short-term service at 300°C, the limitation on most materials will not involve T_g or T_m . Moreover, the chemical stability may be affected by fillers, cross-linking agents, antioxidants, plasticizers, and lubricants. Whether the test is run in a vacuum or an atmosphere of air or oxygen will be important. When TGA is combined with DTA

or when the gases evolved are examined by gas chromatography, IR spectroscopy, or mass spectroscopy, an even more complete picture of the mechanism of reaction can be put together.

Somewhat related is **torsional braid analysis** [8]. In this method a glass braid is impregnated with the polymer or polymer precursors. The treated braid is made to be the restoring element in a torsion pendulum. A programmed temperature rise is imposed and the dynamic mechanical properties of the system are followed. Both changes in rigidity and damping can be correlated with physical and chemical changes in the polymer structure.

Commercial equipment is available for monitoring other properties as a function of temperature. In **dynamic mechanical analysis (DMA)**, tensile or shear modulus and loss are measured. In **dielectric analysis**, dielectric constant and loss tangent are followed. Both provide information about the time response of polymers by applying an oscillating field at a predetermined frequency. At each temperature, the mechanical or electric field test is run at a number of frequencies covering two or more decades. Mechanical frequencies up to 200 Hz are common. Electrical tests can cover greater ranges, say 10–10,000 Hz.

In both types of measurements, time–temperature superposition allows a further generalization of the results obtained over a wide frequency range. The loss modulus or loss tangent measured by either technique provides information about transition processes going on in a polymer film. Although some machines use a continuous temperature scan, others raise the temperature in steps of 5°C or so, allowing the samples, which are often larger than those used for DSC, to come to a more uniform temperature. The continuous scan will usually reflect a rate-dependent behavior so that the loss peaks will occur at higher temperatures at higher rates. Frequency multiplexing increases the amount of information from a single scan. A more detailed explanation of dynamic mechanical measurements is given in Section 9.3.

Dielectric spectroscopy measures the dielectric properties of a medium placed in an electric field as a function of frequency. Practically in an experiment, a polymer film of known thickness is placed between two metal electrodes and then an AC electric field is applied across the polymer film at a known frequency. The measured response is related to the interaction of the external electric field with an electric dipole present in a sample, expressed in terms of its permittivity. This measurement can be used to describe a number of important characteristics of polymers.

Polymers are used as insulators and low dielectric materials in electronic applications, and understanding the dielectric properties of polymers can be important. In a modern microelectronic device, the circuits may operate at very high frequencies and in so doing apply rapidly oscillating electric fields to a dielectric medium surrounding a device. In the case of polymers used as the dielectric medium, for example, as an insulator, chemical functions with notable dipoles present in a polymer may respond to this electric field and adversely affect the dielectric properties of the polymer. At lower frequencies, this is not especially significant, but at very high frequencies such as those used by today's microelectronics, properties can change. For example, polymer insulators used in the gigahertz regime must be especially stable, and often only fluorinated polymers have sufficiently low dielectric response to be used.

In addition to determining technologically useful characteristics of polymers, dielectric spectroscopy can provide information on the nature of a polymer and the relaxation processes present in a polymer material. This response involves the actual movement of dipoles in response to the alternating electric field and is related to the motion of segments involved in the relaxation behavior of polymers. Just as with DMA there is an *in-phase* response and an *out-of-phase* response, and the mathematics describing the dielectric response is similar to the mechanical response described in Section 9.2.4. When the out-of-phase component is high, there is energy loss and this is associated with a transition. Such motional response is related to the movement of monomeric units, side groups on the polymers, or short segments of the polymer chain. These movements are related to the glass transition of polymers. The loss response associated with the glass transition is known as the α -transition, whereas others at lower temperatures are known as the β -, γ -, and δ -transitions. These additional transitions are due to localized motion of the dipole vector. In particular, dielectric spectroscopy has been very useful for identifying sub- T_g transitions that play a role in long-time relaxation and aging processes in polymers.

Thermally stimulated current (TSC) has been used to characterize various thermal processes [9]. In this method, a sample is subjected to a high voltage that orients dipoles in the material. The temperature is lowered with the voltage applied, trapping the polarized dipoles. When the sample is reheated, small currents are detected as the material relaxes. TSC can be operated in such a way as to obtain a complete map of relaxation times versus temperature. Even thin films of coatings and adhesives are conveniently studied by this method.

18.5 NUCLEAR MAGNETIC RESONANCE SPECTROSCOPY

When a compound containing hydrogen is placed in a strong magnetic field and irradiated with a radio-frequency signal, it is found that energy absorption occurs at discrete frequencies. Transitions between different nuclear spin orientation levels are taking place in the hydrogen atom. Fortunately, few of the other nuclei found in organic compounds have a net magnetic moment and spin, so that except for fluorine, chlorine, and certain isotopes of carbon, nitrogen, and oxygen, the only effects seen are those of the protons. It is fortunate, also, that the exact frequency at which energy is absorbed is very sensitive to the atomic environment of the proton. Thus, a scan of absorption versus frequency for a molecule such as ethanol, for example, gives three widely separated peaks with areas in the ratio of 1:2:3. Tetramethylsilane, in which all the protons are equivalent, is often used as an internal standard and assigned a frequency value δ of 0. Most other protons have values of δ between 0 and 10, revealing various degrees of **chemical shift** of the fundamental frequency by the environment.

In practice, about 0.5 ml of polymer solution (say 10% in an aprotic solvent such as deuterium-labeled chloroform) is placed in a thin glass tube between the poles of a strong magnet having field strengths of up to several teslas. A radio-frequency field is imposed on the sample at right angles to the magnetic field. Various devices are used to detect the absorption of energy at resonance as the protons undergo changes in spin orientation level.

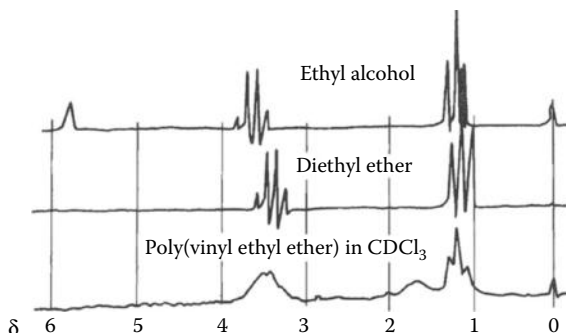


FIGURE 18.7 Comparison of the proton magnetic resonance spectra of ethanol, diethyl ether, and poly(vinyl ethyl ether). (Data from Slichter, W. P., *J. Chem. Educ.*, 45, 10 1968.)

Some typical **nuclear magnetic resonance (NMR)** spectra (Figure 18.7) show the broadening of the peaks in the polymer compared with small molecules because of the lower mobility in the polymer. Of course, the hydroxyl peak at $\delta = 5.8$ appears only in the alcohol in this series. The chain CH peak in the polymer underlies the CH_2 multiplet at $\delta = 3.4\text{--}3.7$ and is not seen separately.

Current NMR machines are based on FT methods. In these newer machines, a sample is placed in a strong magnetic field and a radio-frequency pulse is directed to the sample. The sample becomes excited, and depending on the local magnetic environment in the sample, the various nuclei relax at different rates. The spin relaxation is monitored by the spectrometer and the free induction decay (FID) signal is recorded. This time-domain information is converted to a frequency domain signal by an FT. The advantage of this method is that a variety of pulse sequences can be applied that enhance the detection of specific nuclei. It is also possible to use signal averaging to improve the signal-to-noise ratio of data so that low-abundance isotopes such as ^{13}C can be more easily detected. Examples of ^1H and ^{13}C NMR spectra of polystyrene are shown in Figures 18.8 and 18.9. While the ^1H spectra show rather broad lines, the ^{13}C NMR spectrum is a series of narrow lines. Note that the chemical shift range is greater in the ^{13}C NMR spectrum. Typically, ^{13}C spectra are not integrated because the relative area of each peak is highly variable and depends on such factors as the nuclear Overhauser effect (NOE) for enhancement of weak signals [11].

One of the principal applications of NMR spectroscopy is compositional analysis. The chemical shift reveals the nature of the nucleus, while integration of the area of each peak provides quantitative information about the relative content of each nucleus. Furthermore, it is possible to gain information about the local molecular environment because the magnetic fields of the neighboring nuclei will induce small changes in the chemical shift that can be detected by the NMR.

While the information about chemical coupling is often used to provide information about neighboring chemical groups, with strong enough magnetic fields it is possible to detect isotactic/atactic ratios, monomer sequence distributions in copolymers, and other configurational variations in polymers. Each of these features becomes easier to detect with a stronger magnetic field. The latest NMR spectrometers have magnetic fields as high as 20 T. Using such machines, it is relatively easy

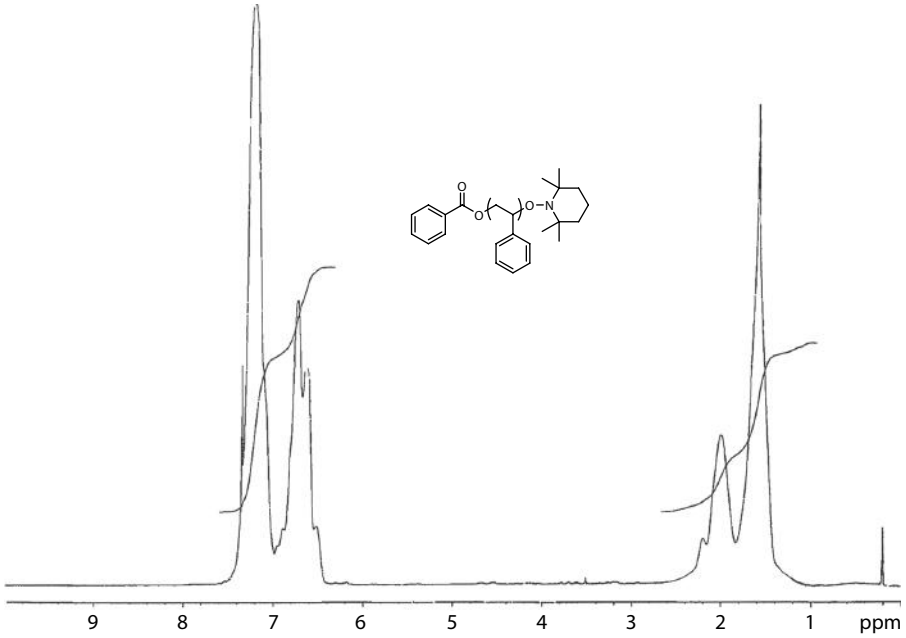


FIGURE 18.8 ^1H NMR spectrum of polystyrene prepared via living radical polymerization. (Courtesy of Dr. Luisa Andruzzi, Cornell University, Ithaca, New York.)

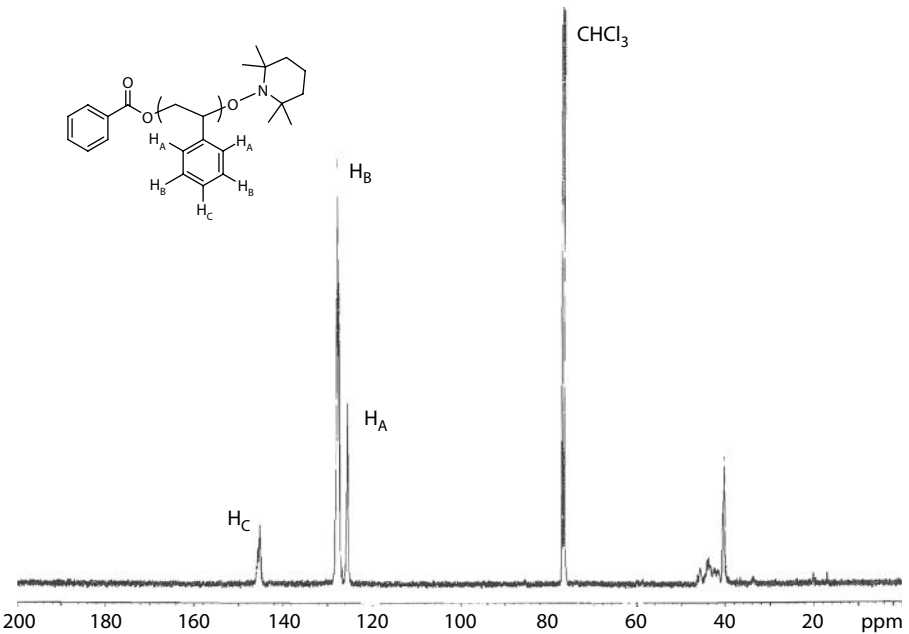


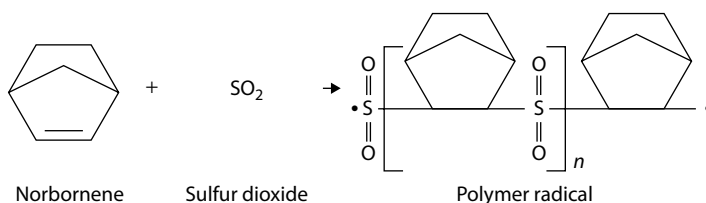
FIGURE 18.9 ^{13}C NMR spectrum of polystyrene prepared via living radical polymerization. (Courtesy of Dr. Luisa Andruzzi, Cornell University, Ithaca, New York.)

to characterize the relative abundance of sequences of as many as seven monomer units (heptads). NMR is also very sensitive to changes in molecular mobility and can be used to monitor diffusion in polymers.

While the measurements of polymers described above were carried out in solution, it is often desirable to carry out studies on polymers in the solid state. The relatively new method of solid-state NMR spectroscopy uses very high sample rotational velocities spinning at a *magic angle* and cross-polarization to make it possible to resolve specific features in the spectra. These features in the technique compensate for the different relaxation times in the solid state. The magic-angle spinning eliminates the effect of anisotropic orientation in the sample. **Solid-state NMR** has been used to establish the detailed solid structure of syndiotactic polypropylene in combination is **X-ray diffraction (XRD)** sometimes called wide angle X-ray diffraction [WAXD]). A narrowing of the resonance peak is typical at phase transitions, making it possible to use NMR to measure T_g and T_m when solid polymers are heated.

A related technique using microwave frequencies is capable of detecting the changes in energy levels due to the magnetic moment of electrons. Such **electron paramagnetic resonance (EPR)**, also called **electron spin resonance (ESR)**, can be studied when there is a net unpaired electronic magnetic moment in the molecule being investigated. Several molecules exist that possess stable radicals, but probably the most common representatives are the nitroxides. These molecules are used as the capping agent in living radical polymerization. They are also used as radical labels in ESR measurements of mobility and orientation in polymers. Free radicals from polymerization or oxidation, especially long-lived ones trapped in the glassy solid state, can also be measured. In most free-radical polymerizations, the radical concentration is down around 10^{-8} mol/l and is difficult to detect by EPR. The bulk copolymerization of norbornene and sulfur dioxide, however, appears to proceed with radical concentrations of around 10^{-5} mol/l, so that detection of radicals at room temperature over a period of hours and weeks is feasible [12].

The structure of these *living* polymers is postulated as



18.6 X-RAY METHODS

There are a number of useful characterization methods that make use of XRD and scattering techniques [13]. The typical wavelength used for X-ray studies is ~ 0.15 nm, a wavelength about the dimension of the carbon–carbon bond. Based on the diffraction theory, the X-ray methods can probe the presence of structures as small as this bond distance, making X-ray methods ideal for studying organization of polymers. This section briefly describes these techniques and provides a description of the information that can be provided by using these methods. They include **XRD** (powder and

fiber methods), **small-angle X-ray scattering (SAXS)**, and grazing-incidence (GI) SAXS. The small-angle methods are well suited for investigating the larger structures found in block copolymers, whereas XRD is appropriate for the smaller structures found in crystalline materials.

XRD makes use of the ability of crystalline materials to diffract X-rays. By measuring specific angles and intensities, it is possible to build a three-dimensional representation of electron density within the crystal. From electron density, the location of atoms and chemical bonding in a crystalline material can be surmised. X-rays can be considered as waves of electromagnetic radiation and interact with the regular arrays of atoms found in crystals. Each electron in the crystal acts as a scatterer and a regular array of scatterers will produce waves of scattered X-rays that interact through destructive and constructive interference. It is the constructive interference that is important in XRD since the scattered waves add in a few specific directions in a manner described by Bragg's law (see Figure 18.10):

$$2d \sin\theta = n\lambda$$

where:

d is the spacing between diffracting planes of atoms

θ is the incident angle made by the atomic layers and the X-ray beam

n is any integer

λ is the wavelength of the beam

Normally, the diffracted intensities are recorded on a flat film or detector a fixed distance from the sample. The two-dimensional images provide information about atomic spacing and, if a single crystal, the orientation of the atoms in the sample. When a single crystal is not available, then a sample consisting of randomly oriented small crystals is used and the resulting image is known as a powder diffraction pattern. This pattern consists of rings whose diameter depends on the spacing of the atomic planes.

Polymers are typically not in the form of single crystals, but are a combination of amorphous and crystalline materials (Section 3.10). Thus, the two-dimensional XRD

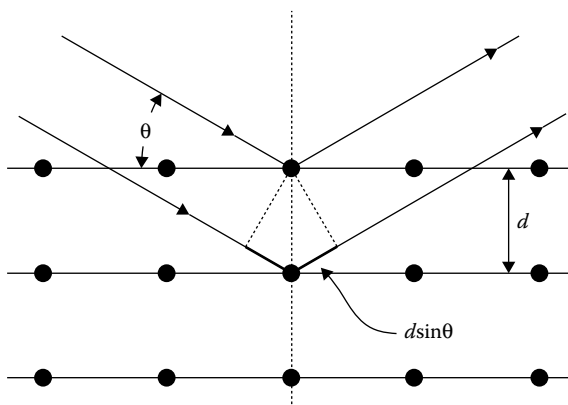


FIGURE 18.10 Layers of atoms create planes from which XRD takes place. The angle θ and the distance between layers (d) are the key variables in Bragg's law.

pattern from a synthetic polymer resembles that of a **powder diffraction** pattern with the rings present providing information about the internal spacing of the polymer crystals. If a polymer is drawn into a fiber, there is a high probability that the crystals in the polymer will become partially oriented. In that case, the **fiber diffraction** pattern is in the form of arcs rather than rings. This fiber pattern has uniaxial symmetry, that is, the fiber can be rotated along the fiber axis and the pattern will remain the same. The perfection of orientation can be characterized by the **Herman's orientation function** which is given by

$$f = \frac{\overline{3(\cos^2\theta)} - 1}{2}$$

where:

f is the orientation parameter

θ is a value related to the angle the diffracted arc makes (and not the θ used above)

The smaller the arc, the higher the orientation. If f is 1, then the fiber is completely oriented; if f is 0, then it is randomly oriented; and if f is -0.5 , then orientation is perpendicular to the fiber direction. Orientation may also be present because a polymer has liquid crystalline properties and an orientation parameter may be similarly calculated. A combination of FTIR and XRD has been recently used in the analysis of the complex morphology of biaxially oriented syndiotactic polystyrene films [14].

Larger structures may be present than those related to crystal spacing dimensions and may sometimes be detectable using **SAXS**. In block copolymers, it is possible to form uniformly sized periodic structures due to the phase separation of different blocks that are on the order of 5–245 nm. These phases lead to electron density differences that can be detected by X-ray scattering, but given the dimensions of the phases, they will cause scattering that can only be detected at very small angles, typically 0.1° – 10° . These structures do not have the physical perfection of crystals, so the resulting spatial averaging leads to a loss of information in SAXS compared to crystal diffraction. As a result of the very small angles, the sample-to-detector distance is quite large and the resulting signal is weak unless a strong source is used or very long data acquisition times are involved. Often a synchrotron X-ray source with its very high intensity is a convenient means for SAXS measurements [15].

Figure 18.11 shows XRD/X-ray scattering at wide and small angles of a block copolymer with a liquid crystalline block. This sample is a lamellar block copolymer in which a liquid crystalline (LC) block organizes its smectic phase perpendicular to the lamellar layers. The outer arcs are due to the smaller liquid crystalline layers and the inner arcs are for the lamellar spacings. From this figure, it is possible to get information about layer thickness and the orientation parameter of both the liquid crystalline groups and the lamellae.

A complementary X-ray technique suited for probing the structure of thin films makes use of grazing-incidence geometry in the technique known as GISAXS. Using a synchrotron X-ray source due to the need for an intense beam, this method has become of increasing use to probe block copolymers in thin films. The high intensity enables near-real-time diffraction studies and has been used to study the ability to enhance structural order in block copolymers during annealing processes.

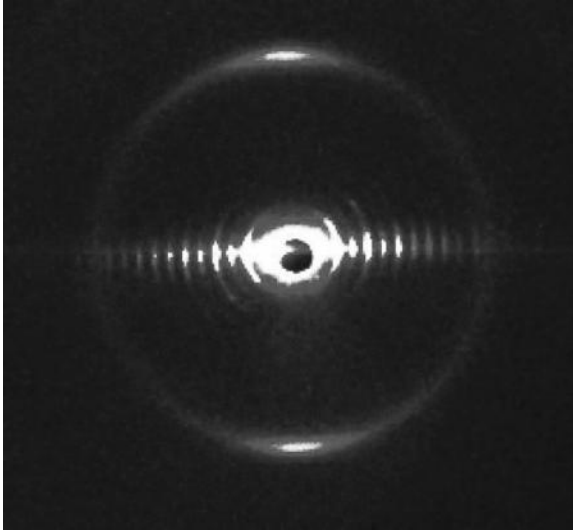


FIGURE 18.11 Combined SAXS and WAXD X-ray pattern of a bulk sample of a liquid crystalline block copolymer.

18.7 MISCELLANEOUS SPECTROSCOPIC METHODS

Many methods of analysis have been extended to polymer systems. Some techniques include the following:

1. **Raman spectroscopy** for analyses of polymer morphology in crystalline structures and of chain-stretching motions in lamellar regions [16]. This technique is based on **inelastic scattering of photons** as opposed to the elastic Rayleigh light scattering (Section 6.7) where the scattered light has the same frequency as the incident light. In Raman scattering, the frequency of scattered light is lower (Stokes band, stronger) or higher (anti-Stokes band, weaker) due to the interaction of light with the polarization of the molecules.
2. **Neutron scattering** that extends static light-scattering techniques to the measurements of radius of gyration in melts and interaction parameter in blends. The technique is based on the difference of scattering efficiencies between hydrogen atoms and deuterium atoms. For melts, some of the molecules need therefore to be deuterated, and for mixtures, one of the species must be partially deuterated [17]. Dynamic neutron scattering allows for the analysis of movements of small chain segments [18].
3. Various methods of analyzing surfaces for chemical composition and physical texture. **Electron spectroscopy for chemical analysis** and **Auger analysis** [19] are techniques that have been used to identify chemical species in thin films. In **Rutherford backscattering** spectrometry incident He^+ ions are scattered elastically by nuclei. The energy spectrum thus obtained can

provide a quantitative measure of various elements as a function of depth. **Atomic force microscopy** can reveal the contours of a surface on an atom-by-atom basis [20].

18.8 CHEMICAL TESTS AND IDENTIFICATION SCHEMES

There are many ways by which polymers may be identified. In textile fibers, microscopic examination of the cross section and texture may be sufficient for the more complex, naturally occurring polymers. Solubility and staining tests can also be used [21]. Unpigmented polymer films can often be characterized by simple tests. Polyethylene and polypropylene are lighter than water, whereas PVC, polystyrene, and polyester are heavier. PVC does not support a flame, whereas the others do. A scheme that uses density, burning, and a few other simple tests has been used to distinguish among a variety of plastics [22]. A more complete picture demands other tools [23]. When a polymer or compound ingredient can be extracted and made into a film or pressed wafer, the IR spectrum may be the most direct and most powerful tool available. As a general rule, it is best to try to separate a sample suspected of being a mixture by extraction before attempting to carry out chemical tests. Plasticizers, antioxidants, surfactants, and other small molecules are usually not bound chemically to the polymer and should be removed by preliminary treatment. The detailed unraveling of the composition of a plasticized, stabilized, and pigmented polymeric article like the typical PVC garden hose is not an undertaking for the impatient or unsophisticated investigator.

KEYWORDS

Infrared spectra (IR)
Wave number
Fourier transform infrared (FTIR)
Differential scanning calorimetry (DSC)
Differential thermal analysis (DTA)
Thermogravimetric analysis (TGA)
Torsional braid analysis
Dynamic mechanical analysis (DMA)
Dielectric analysis
Thermally stimulated current (TSC)
Chemical shift
Nuclear magnetic resonance (NMR)
Electron paramagnetic resonance (EPR)
Electron spin resonance (ESR)
X-ray diffraction (XRD)
Small-angle X-ray scattering (SAXS)
Powder diffraction
Fiber diffraction
Hermann's orientation function
Raman spectroscopy

Inelastic scattering of photons
Neutron scattering
Electron spectroscopy for chemical analysis
Auger analysis
Rutherford backscattering
Atomic force microscopy

PROBLEMS

- 18.1** Three samples of flexible tubing are subjected to the following tests:
- Held in burner flame. Tubes A and C burn.
 - Soaked overnight in chloroform. Tube A swells, B becomes very stiff and somewhat smaller on drying out, and C is unaffected.
 - Immersed in a lead nitrate solution, A turns black; B and C are unaffected.
- Which of the three is vulcanized rubber, polyethylene, or plasticized PVC?
- 18.2** Try to identify the group associated with the four most prominent absorption bands in poly(vinyl acetate). Use Table 18.1 as a guide.
- 18.3** One characteristic property by which unmodified polystyrene can often be identified is the clattering sound made by dropping a molded piece on a hard surface. An inexpensive protractor or comb tossed on a table top can be identified this way. What factors might be involved in causing this property?
- 18.4** How would microscopic observation of the cross section of a fiber sample differentiate between nylon 6 and rayon?
- 18.5** A sample of rubber shows no flow in a creep experiment, indicating that it is cross-linked. It contains no fillers. What additional simple tests might be run to decide whether the material is natural rubber, styrene-butadiene rubber, or acrylonitrile-butadiene rubber?
- 18.6** You are given a material to identify. It is in the form of a stiff, transparent sheet about 0.01 in thick. It burns slowly with a smell of vinegar. It dissolves completely in acetone. Is it polyethylene, polypropylene, PVC, poly(vinyl acetate), nylon 6, or cellulose diacetate?

REFERENCES

- Cole, A. R. H.: in K. W. Bentley (ed.), *Elucidation of Structures by Physical and Chemical Methods, Part 1, Technique of Organic Chemistry*, vol. XI, Wiley, New York, 1963, pp. 33ff.
- Nyquist, R. A.: *Infrared Spectra of Plastics and Resins*, 2nd edn., Dow Chemical Co., Midland, TX, 1961.
- Willis, H. A., and V. J. I. Zichy: in D. I. Clark and W. J. Feast (eds.): *Polymer Surfaces*, Wiley, New York, 1978.
- Gross, D.: *Rubber Chem. Technol.*, 48:289 (1975).
- Brennan, W. P., R. B. Cassel, and M. P. DiVito: *Amer. Lab.*, 20(1):32 (1988).
- Brennan, W. P.: *Characterization and Quality Control of Engineering Thermoplastics by Thermal Analysis*, Instrument Division, PerkinElmer Corporation, Norwalk, CT, 1977.

7. Reading, M.: *Trends Polym. Sci.*, 1:248 (1993).
8. Gilham, J. K.: *Polym. Eng. Sci.*, 19:749 (1979).
9. Matthiesen, A., F. McIntyre, J. P. Ibar, and J. Saffell: *Amer. Lab.*, 23(1):44 (1991).
10. Slichter, W. P.: *J. Chem. Educ.*, 45:10 (1968).
11. Neuhaus, D., and M. P. Williamson: *The Nuclear Overhauser Effect in Structural and Conformational Analysis*, 2nd edn., Wiley, New York, 2000.
12. Zutty, N. L., and C. W. Wilson, III: *Tetrahedron Lett.*, 1963(30):2181 (1963).
13. Roe, R.-J.: *Methods of X-Ray and Neutron Scattering in Polymer Science*, Oxford University Press, New York, 2000.
14. Rizzo, P., and A. R. Alburnia: *Macromol. Chem. and Phys.*, 212:1419 (2011).
15. Chu, B., and B. S. Hsiao: *Chem. Rev.*, 101:1727 (2001).
16. Koenig, J. L.: *Spectroscopy of Polymers*, Elsevier, Amsterdam, The Netherlands, 1999.
17. Higgins, J. S., and H. C. Benoît: *Polymers and Neutron Scattering*, Clarendon Press, Oxford, 1994.
18. Doster, W., S. Cusack, and W. Petry: *Phys. Rev. Lett.*, 65:1080 (1990).
19. Ferguson, I. F.: *Auger Microprobe Analysis*, Institute of Physics, Bristol, 1989.
20. Atomic Force Microscopy, TM Microscopes, Sunnyvale, CA.
21. Mlynar, M.: Qualitative evaluation of nonwoven samples using DuPont fiber identification stain no. 4 and Microscopy, *Int. Nonwovens J.*, 9:2 (2000); see also ASTM D276.
22. TexLoc, Ltd., Fort Worth, TX. http://www.tensiontech.com/papers/fiber_id/.
23. Braun, D.: *Simple Methods for Identification of Plastics*, 4th edn., Hanser-Gardner, Cincinnati, OH, 1999.

GENERAL REFERENCES

- Brandolini, A. J., and D. D. Hills: *NMR Spectra of Polymers and Polymer Additives*, Dekker, New York, 2000.
- Braun, D.: *Simple Methods for Identification of Plastics*, 4th edn., Hanser-Gardner, Cincinnati, OH, 1999.
- Campbell, D., R. A. Pethrick, and J. R. White: *Polymer Characterization: Physical Techniques*, 2nd edn., CRC Press, Boca Raton, FL, 2000.
- Cheremisinoff, N. P., and P. N. Cheremisinoff (eds.): *Handbook of Advanced Materials Testing*, Dekker, New York, 1995.
- Craver, C. D., and T. Provder (eds.): *Polymer Characterization: Physical Property, Spectroscopic, and Chromatographic Methods*, ACS, Washington, DC, 1990.
- Crompton, T. R.: *Introduction to Polymer Analysis*, Smithers Rapra Technology, Akron, OH, 2009.
- De Rosa, C., and F. Auriemma: *Crystals and Crystallinity in Polymers*, Wiley, Hoboken, NJ, 2014.
- Fawcett, A. H. (ed.): *Polymer Spectroscopy*, Wiley, New York, 1996.
- Garton, A.: *Infrared Spectroscopy of Polymer Blends*, Hanser-Gardner, Cincinnati, OH, 1992.
- Hunt, B. J., and M. I. James (eds.): *Polymer Characterization*, Chapman & Hall, New York, 1993.
- Ishida, H. (ed.): *Fourier Transform Infrared Characterization of Polymers*, Plenum Press, New York, 1987.
- Koenig, J. L.: *Spectroscopy of Polymers*, Elsevier, Amsterdam, The Netherlands, 1999.
- Kuptsov, A. H., and G. N. Zhizhin: *Handbook of Fourier Transform Raman and Infrared Spectra of Polymers*, Elsevier, Amsterdam, The Netherlands, 1998.
- Mark, J. E., K. Ngai, W. W. Graessley, L. Mandelkern, E. Samulski, J. L. Koenig, and G. Wignall: *Physical Properties of Polymers*, 3rd edn., Cambridge University Press, Cambridge, 2004.
- Mathot, V. B. F. (ed.): *Calorimetry and Thermal Analysis of Polymers*, Hanser-Gardner, Cincinnati, OH, 1994.

- Mitchell, J., Jr. (ed.): *Applied Polymer Analysis and Characterization*, Hanser-Gardner, Cincinnati, OH, 1992.
- Murthy, N. S.: in F. H. Chung, and D. K. Smith (eds.): *Advances in Industrial Applications of X-Ray Diffraction*, Dekker, New York, 2000.
- Pham, Q. T., R. Pétiaud, H. Waton, and M.-F. Llauro-Darricades: *Proton and Carbon NMR Spectra of Polymers*, Wiley, Hoboken, NJ, 2004.
- Provdor, T., M. W. Urban, and H. G. Barth (eds.): *Hyphenated Techniques in Polymer Characterization: Thermal-Spectroscopic and Other Methods*, ACS, Washington, DC, 1995.
- Runt, J. P., and J. J. Fitzgerald (eds.): *Dielectric Spectroscopy of Polymeric Materials—Fundamentals and Applications*, ACS, Washington, DC, 1997.
- Sawyer, L., and D. T. Grubb: *Polymer Microscopy*, Chapman & Hall (Methuen), New York, 1987.
- Schmidt-Rohr, K., and H. W. Spiess: *Multidimensional Solid-State NMR and Polymers*, Academic Press, New York, 1994.
- Schröder, E., G. Müller, and K.-F. Arndt: *Polymer Characterization*, Hanser-Gardner, Cincinnati, OH, 1989.
- Spells, S. J. (ed.): *Characterization of Solid Polymers: New Techniques and Developments*, Chapman & Hall, New York, 1994.
- Turi, E. A. (ed.): *Thermal Characterization of Polymeric Materials*, 2nd edn., 2 vols., Academic Press, New York, 1997.
- Urban, M. W. (ed.): *Attenuated Total Reflectance Spectroscopy of Polymers—Theory and Practice*, ACS, Washington, DC, 1996.

Appendix A

LIST OF SYMBOLS

Symbol	Common Unit	Definition or Label	Sections Where First Used
A	cm ² , in ²	Area	7.2
A_t	m ²	Total surface area of particles	5.5
A'	–	Constant	7.2
A_u	cm ²	Area, original unstretched	9.8
A, A_p, A_i, A_t	s ⁻¹	Collision frequency factors	4.4
A_2	dl·mol/g ²	Second virial coefficient	6.6
A_3	dl ² ·mol/g ³	Third virial coefficient	6.6
Å	–	Angstrom unit (10 ⁻¹⁰ m)	–
B, B'	Variable	Used as an arbitrary constant	–
B	–	Factor in modulus equation (Equation 9.52)	9.6
B	m	Specimen thickness	10.3
C_1, C_2	Pa	Constants in Equation 8.44	9.8
C_∞	–	Chain stiffness	7.4
C_f	farad	Capacitance	11.6
C_i, C_s	–	Chain transfer constant	4.4
C_{ij}	–	Expansion coefficient of the strain energy function	9.8
C_t	–	Couette contribution to Bagley correction	8.3
CED	cal/cm ³	Cohesive energy density	2.6
D	m	Specimen depth	10.3
D	–	Abbreviation for bifunctional unit	17.7
D, D_L, D_A, D_v	mm, cm, in	Diameter or average diameter	6.1
D_c	mm	Capillary diameter	8.3
D_s	–	Optical dispersion	11.7
D_b	cm	Barrel diameter inside extruder	14.1
De	–	Deborah number	7.2
D_3, D_4, \dots	–	Representation of cyclic trimer, tetramer, etc. of dimethyl siloxane	17.7
D_{12}	cm ² /s	Binary diffusion coefficient	11.8
ΔE_v	cal	Internal energy of vaporization	2.5
E	Pa	Young's modulus	9.1
E_a, E_i, E_p, E_t	kcal/mol	Activation energies	4.4
$E(\theta)$	Pa	Distribution of relaxation times	9.5
$E(t)$	Pa	Time-dependent modulus	9.2

(Continued)

Symbol	Common Unit	Definition or Label	Sections Where First Used
E_i	Pa	Modulus of individual element	9.5
E_r	Pa	Modulus measured in stress relaxation mode	12.3
E_t	Pa	Modulus measured intermittently	12.3
E_T	Pa	Modulus of an array of elements	9.5
E^*	Pa	Complex modulus	9.2
E'	Pa	Real part of complex modulus	9.2
E''	Pa	Imaginary part of complex modulus	9.2
F	N	Normal force, thrust force	8.5, 8.6
F_1, F_2	–	Mole fractions of monomers 1 and 2	4.10
F_i	cal-cm ³	Molar attraction constant of group i	2.6
ΔG_{el}	J	Elastic contribution to the free energy of mixing	2.5
ΔG_{gel}	J	Free energy of swelling of a network	2.5
ΔG_m	J	Free energy of mixing	2.5
G	Pa	Shear modulus	9.1
G_c	Pa	Cross-link contribution to the modulus	9.8
G_c	J/m ²	Fracture work (energy) per unit area	10.3
G_e	Pa	Entanglement contribution to the modulus	9.8
G_e	Pa	Equilibrium shear modulus in Equation 9.99	9.8
G_{ph}	Pa	Shear modulus of the phantom network	9.8
G_N^0	Pa	Rubbery plateau shear modulus	7.5, 9.6
ΔH_f	J/mol	Enthalpy of fusion per mole, pure solvent	6.6
ΔH_m	J	Enthalpy of mixing	2.5
H_p	hp	Horsepower	14.1
ΔH_p	J/mol	Enthalpy of polymerization per mole	5.1
ΔH_u	J/mol	Enthalpy of fusion per mole for polymer repeat unit	3.11
ΔH_v	J/mol	Enthalpy of vaporization per mole	2.6
$\bar{H}(\log \theta)$	Pa-s	Distribution of relaxation times	9.5
$[I]$	mol/l	Initiator concentration	4.4
I_i	–	Strain invariant variables	9.8
I_s	lumen	Scattered light intensity	6.7
I_0	lumen	Incident light intensity	6.7
I_m, I_v	g-cm ²	Moment of inertia	9.2
J	Pa ⁻¹	Compliance	9.1
J', J''	Pa ⁻¹	Storage and loss compliance	9.8
J_i	mol/cm ² -s	Molar flux of species i	11.8
K	s ^{-1/n}	Constant in Avrami's Equation 3.29	3.10
K	–	Light-scattering intensity lumped constant	6.7
K	Pa-s ⁿ	Power-law fluid consistency	7.2

(Continued)

Symbol	Common Unit	Definition or Label	Sections Where First Used
K	$(\text{J/m}^2)\cdot(\text{g/mol})^{-1/2}$	Prefactor in the Lake–Thomas theory	10.8
K	–	Extruder geometric factor	14.1
K'	$(\text{cm}^3/\text{g})\cdot(\text{mol/g})^3$	Mark–Houwink–Sakurada coefficient	7.4
K''	cm^3	Geometric factor in Equation 9.33	9.3
K_{Ic}	$\text{MPa}\cdot\text{m}^{1/2}$	Critical stress intensity factor or fracture toughness	10.7
K_0	s^{-1}	Constant rate of strain	9.2
K_c	–	Dielectric constant	11.6
L	cm	Length	7.7, 9.1
L_T	μm	Total length of fully stretched out polymer chain	7.4
L_c	nm	Contour length of an entangled chain	7.5
L_u	cm	Unstressed length	9.1
\mathcal{L}	–	Langevin function	9.8
M	–	Used as an abbreviation for a monofunctional unit	17.7
M	g/mol	Molecular weight	6.1
$[\text{M}]$	mol/l	Monomer concentration	4.4
$[\text{M}\cdot]$	mol/l	Concentration of radical chains	4.4
M_c	g/mol	Critical molecular weight at cross-over to entangled polymer behavior	7.5
M_e	g/mol	Molecular weight of polymer chain segments between entanglement points	7.5
M_i	g/mol	Molecular weight of species i in a polydisperse polymer	6.7, 7.4
M_n	g/mol	Number-average molecular weight	4.3, 6.1
M_v	g/mol	Viscosity-average molecular weight	7.4
M_w	g/mol	Weight-average molecular weight	6.1
M_0	g/mol	Molecular weight of repeat unit	6.2
M_i, M_1, M_2, \dots	g/mol	Molecular weight of specific components	6.1, 6.6
N	–	Number of moles of lattice sites	Appendix 2.A
N	cm^{-3}	Seed concentration	3.10
N	–	Number of beads in bead-spring model	9.6
N	–	Number of samples	10.1
N	mol/cm^3	Moles of elastic polymer chains per unit volume	2.5, 9.8
N	mol/cm^3	Concentration of monomer units per unit volume	12.3
N	RPM	Screw rotation rate	14.1
N_{AV}	mol^{-1}	Avogadro's number	6.6
N_e	mol/cm^3	Density of trapped entanglements	9.8
N_i	–	Mole fraction of i	2.5

(Continued)

Symbol	Common Unit	Definition or Label	Sections Where First Used
N_p	mol/l	Concentration of particles per unit volume	5.5
$N, N_i, N_1, N_2,$ $N_E, N_A, N_D, N_0,$ N_c, N_s	mol	Number of moles of specific components	4.7, 4.10, 6.3, 12.3
N_1, N_2, N_3	Pa	First, second, and third normal stress difference	8.2
N_{Re} or Re	–	Reynolds number	7.8
$(N_{Re})_{crit}$	–	Critical Reynolds number	8.4
P	Pa	Pressure, injection pressure	7.3, 14.6
$P(\theta)$	–	Scattering intramolecular interference function	6.7
PDI	–	Polydispersity index	6.1
(P_x)	–	Probability of mole fraction of x -mer	6.2
P_{12}	cm ³ (STP)/cm·s·atm	Gas permeability coefficient in a polymer	11.8
Q	–	Constant in Price–Alfrey scheme	4.10
Q	cm ³ /s	Volumetric flow rate, melt flow rate	7.3, 14.6
\bar{Q}	cm ³ /s	Average volumetric flow rate	7.3
Q, Q_c	kg/h	Extruder capacity	14.1
$Q(\theta)$	–	Scattering intermolecular interference function	6.7
R	cal/mol·deg	Gas constant	2.5
R	mm	Capillary radius	8.3
R	cm	Distance from sample to detector	6.7
\bar{R}	nm	Polymer end-to-end vector	7.4
$\langle \bar{R} \rangle$	nm	Ensemble averaged end-to-end vector	7.4
R_g	nm	Radius of gyration	6.7
R_G	nm	Center-of-mass position vector	7.4
R_h	nm	Hydrodynamic radius	7.2
R_p	mol/l·s	Rate of polymerization	4.4
R_1, R_2	cm	Radii of inner and outer cylinders in Couette flow device	8.4
R_3, R_4	ohm	Electrical resistance	11.6
$[R\cdot]$	mol/l	Concentration of initiator radicals	4.4
$[R_s]$	mol/l	Concentration of initiator seeds	4.5
R_0	–	Light scattering Rayleigh ratio	6.7
S	J/K	Entropy	9.8
S	cm ³ (STP)/cm ³ ·atm	Equilibrium gas solubility parameter in a polymer	11.8
ΔS_m	J/K	Entropy of mixing	2.5
$[S]$	mol/l	Surfactant concentration	5.5
T	K, R	Absolute temperature	–
T	N·m	Torque exerted by deformed fluid	8.4

(Continued)

Symbol	Common Unit	Definition or Label	Sections Where First Used
T_f	K	Freezing temperature of pure solvent	6.6
T_g	K	Glass transition temperature	3.5, 7.6
T_m	K	Melting temperature	3.4
T_m^0	K	Melting temperature, pure polymer	3.11
T_R	K	Reference temperature	7.6
U, V	cm/s	Speed of moving plane in planar Couette flow apparatus	7.2
U_p	W	Power used in dielectric heating	11.6
V	mm ³ , cm ³	Scattering volume	6.7
V	cm ³	Volume	2.5, 9.1
V	cm ³ /g	Specific volume	7.5
V	L	Volume of fluid in viscometer	7.3
V_f	cm ³ /g	Free volume	7.6
V_g	cm ³ /mol	Molar volume of solvent as vapor	2.6
V_0	cm ³ /g	Specific volume extrapolated to 0 K	7.6
V_p	nm ³	Volume occupied by a single polymer molecule	7.5
V_r	cm ³	Effluent volume	6.4
$V_r(M)$	cm ³	Effluent volume for molecular weight M	6.4
V_u	cm ³ /mol	Molar volume of the polymer repeat unit in the liquid state	3.11
V_u	cm ³	Original dry volume	9.8
V_0	cm ³ /mol	Molar volume of lattice sites	3.3
V_1, V_2	cm ³ /mol	Molar volume of solvent, molar volume of polymer	2.5
W	J	Stored energy, fracture work	9.8, 10.3
W_i	g	Weight of component i	6.1
W_x	g	Weight of x -mer	6.2
Wi	–	Weissenberg number	7.2
X	–	Ratio of f_1/f_2	4.10
Y	–	Ratio of F_1/F_2	4.10
Z_c	–	Degree of polymerization at cross-over to entangled polymer behavior in melts	7.5
\bar{Z}_w	–	Weight-average degree of polymerization	7.5
a	–	Mark–Houwink–Sakurada exponent	7.4
a	nm	Statistical segment length	7.2
a	–	$x_n/(x_w - x_n)$	6.3
a	cm	Thickness	9.1
a	m ²	Surface area of a particle	5.5
a	nm	Equilibrium spring length in bead-spring model	9.6
\bar{a}	nm	Average statistical segment length	7.4
a_s	m ²	Area occupied by a mole of surfactant	5.5

(Continued)

Symbol	Common Unit	Definition or Label	Sections Where First Used
a_T	nm	Diameter of reptation tube	7.5
a_T	—	Shift factor (Equation 9.40)	9.4
b	—	$\langle \cos \phi \rangle$	7.4
b	cm	Width	9.1
c	gm/dl, g/cm ³	Concentration	6.6
c	g/cm ³	Polymer concentration in solution	7.4
c	cm/s	Velocity of light in vacuum (3.00×10^8 cm/s)	12.1
c_p	cal/g·°C	Specific heat	12.5
c	cm	Crack length	10.7
c^*	g/cm ³	Overlap concentration for polymer chains in solution	7.5
d	mm	Gap	7.2
d	mm	Capillary diameter	7.3
d	cm	Plate spacing, sample thickness, distance between atomic planes	8.5, 11.6, 18.6
e	—	Polarity parameter in Price–Alfrey scheme	4.10
e	—	Bagley's end correction	8.3
f	—	Fraction of reactive initiators	4.4
f	—	Functionality of monomer	4.2, 4.8
f	N	Force	7.2
f	—	Number of arms per branch point	7.4
f	—	Herman's orientation function	18.6
f_1, f_2	—	Mole fraction in monomer feed	4.10
f', f'_g	—	Fractional free volume at temperature T or T_g	7.6
f_i	—	Friction factor	7.8
f^*	—	Functionality of cross-links	8.2
g	m/s ²	Gravitational acceleration	7.2, Appendix 8.A
g	—	Size contraction factor for branched polymer molecules	7.4
\hat{g}	—	Ratio of intrinsic viscosity of branched and linear polymer molecules with the same total molecular weight	7.4
\hat{g}_{ic}	J/s	Strain energy release rate	10.7
g_{star}	—	Size contraction factor for starlike polymer molecules	7.4
h	cm	Height	6.6, 10.3
\bar{h}	cm	Average head driving flow in viscometer	7.3
i	—	Subscript referring to component i	2.6.3
i	—	Denoting imaginary part of a complex variable, square root of -1	9A.2

(Continued)

Symbol	Common Unit	Definition or Label	Sections Where First Used
k	(N·m)/K	Boltzmann's constant	7.5
k_c	cal/cm·s·°C	Thermal conductivity	11.5
k_e	J	Kinetic energy correction	10.3
$k, k_1, k_t, k_p, k_2, k_3, k_4, k_{11}, k_{12}, k_{22}, k_{21}$	Variable	Rate constants	4.4, 4.10
k'	–	Constant in the Huggins equation	7.4
k''	–	Constant in Kraemer equation	7.4
k'_L	–	Parameter in Lyons–Tobolsky formula	7.5
l	cm	Capillary length	7.3
m_c/m_0	–	Mass fraction of crystallizable polymer	3.10
m	kg	Mass	7.2
m	g	Masses used in torsional pendulum	9.3
m	mol/l	Concentration of polymer molecules	12.3
n	–	Total number of lattice sites	Appendix 2.A
n	–	Exponent of time in Avrami's equation (Equation 3.29)	3.10
n	–	Shear thinning exponent or power-law index	7.2
n	–	Unit normal vector	7.6
n	–	Sample index number	10.1
n, n_C, n_D, n_F	–	Refractive index	6.7, 11.7
n_1, n_2	–	Number of solvent molecules, number of polymer molecules	Appendix 2.A
\dot{n}	s ⁻¹	Rate of nuclei generation	3.10
p	–	Number of segments per polymer molecule in a blend	3.3
p	–	Fraction of monomer converted to polymer, extent of reaction	4.8, 6.2
p	Pa	Pressure	7.3
p_F	–	Fraction of monomer converted to polymer at gelling point for bifunctional monomer B and polyfunctional monomer F	4.8
p_{atm}	Pa	Atmospheric pressure	8.3
p_c	nm	Packing length	9.6
P_1, P_0	Pa	Pressure at inlet and outlet of capillary tube	8.3
q	cm ⁻¹	Scattering wavevector of light	6.7
q	–	Number of entangled chain segments required to produce cross-over to entangled polymer flow behavior	7.5

(Continued)

Symbol	Common Unit	Definition or Label	Sections Where First Used
q	–	Equals to $1/n$, where n is the power-law index	8.4
\dot{q}_T	Kg/(m·s ³)	Energy dissipation rate per unit volume	7.2
r_1, r_2	–	Relative reactivity ratios	4.10
r	cm	Radial coordinate	8.3
L_i	nm	Segment end-to-end vector	7.4
r_{gm}	cm	Geometric mean radius	8.4
$\left(\overline{r^2}\right)^{1/2}$	nm	Root-mean-squared end-to-end distance	7.4
$\left(\overline{r_0^2}\right)^{1/2}$	nm	Root-mean-squared end-to-end distance in a theta solvent	7.4
s	–	Shear-thinning exponent in Ellis model	7.2
s	–	Slippage parameter for coupled drag model of entangled polymers	7.5
s	–	Standard deviation	10.1
$\langle s^2 \rangle$	nm ²	Mean-squared radius of gyration	7.4
$\langle s^2 \rangle_{br}$	nm ²	Mean-squared radius of gyration for a branched polymer	7.4
t	s	Time	4.4
t_f	s	Characteristic flow time	7.2
t_{fill}	s	Mold-filling time	14.7
u	cm/s	Velocity	7.2
\bar{u}, \bar{v}	cm/s	Average velocity	7.8
u_e	J	Energy loss per cycle	9.2
v	m ³	Particle volume	5.5
v	nm ³	Excluded volume	7.4
v^0	nm ³	Excluded volume parameter	7.4
v_c	μm/s	Polymer center-of-mass velocity	7.2
v_s	μm/s	Slip velocity	8.3
v_1, v_2	–	Volume fractions of components 1 and 2	2.5, 3.4
$v_{1,c}, v_{2,c}$	–	Critical volume fractions of components 1 and 2	3.4
v_2^*	–	Overlap polymer volume fraction in solution at cross-over to entangled solution properties	7.5
w	N or lb _f	Weight	10.3
w_i	–	Weight fraction of species i in a polymer blend	3.5
w_i, w_x	–	Weight fraction of species i or x -mer in a polydisperse polymer	6.2, 7.4
x	–	Degree of polymerization of polymer chain (also x_w, x_n , etc.); also ratio of polymer size to solvent size	4.4, 6.2, 7.2, Appendix 2.A

(Continued)

Symbol	Common Unit	Definition or Label	Sections Where First Used
x_c	–	Degree of polymerization of polymer chain segments between entanglements	7.5
x_1, x_2, \dots	–	Mole fraction of component 1, 2, ...	2.5
x, y, z	cm	Position vector components	7.2
y	cm	Distance	7.2
$z(t)$	cm	Melt front position	14.6
Γ	$(\mu\text{m})^{-3}$	Number of polymer molecules per unit volume	7.5
$\Gamma(a + 1)$	–	Gamma function of $a + 1$	6.3
Δ	–	Signifies difference	2.4
Δ	–	Logarithmic decrement	9.3
Λ	–	Factor in Equation 9.93	9.8
Π	–	Product sign	Appendix 2.A
Σ	–	Summation sign	2.6.3
Y	–	Coupling–disproportionation factor	4.4
Φ_v	$\text{dl/mol}\cdot\text{cm}^3$	Flory–Fox parameter = $2.1 \pm 0.2 \times 10^{21} \text{ dl/mol}\cdot\text{cm}^3$	7.4
Ψ_1, Ψ_2, Ψ_3	$\text{Pa}\cdot\text{s}^2$	First, second, and third normal stress coefficients	8.2
Ω	rad/s	Angular velocity at radial location R	8.4
Ω_M	–	Number of possible configurations on a lattice	Appendix 2.A
Ω_1, Ω_2	–	Probabilities of states 1 and 2	9.8
α	–	In Equation 4.45, $\alpha = r_2/(1 - r_2)$	4.10
α	–	Expansion coefficient for polymers in solution	7.4
α	K^{-1}	Difference in volumetric coefficient of thermal expansion for polymer melt and polymer in the glassy state	7.6
α	rad, degrees	Cone angle	8.6
$\alpha, \alpha_1, \alpha_2, \alpha_3$	–	Extension ratio, also in x -, y -, and z -directions	9.1, 9.8
α_r	–	Relative volatility in Equation 4.40	4.10
β	–	Enthalpic contribution to Flory's interaction parameter or lattice parameter	2.5
β	–	A constant, function of r_1 and r_2 in Equation 4.45	4.10
β	–	Ratio of linear connector molecular weight to total molecular weight of a multiarm, long-chain branched polymer	7.4
β	mol/g	Fitted viscosity constant in Equation 7.65	7.6
β	–	Normalization factor	9.8

(Continued)

Symbol	Common Unit	Definition or Label	Sections Where First Used
γ	—	A constant, function of r_1 and r_2 in Equation 4.45	4.10
γ	—	Hydrogen-bonding index	2.6
γ	—	Shear strain	7.2
γ_c	dynes/cm	Critical surface tension	12.4
γ_{Rc}	—	Contribution of fluid elasticity to Bagley correction	8.3
$\dot{\gamma}$	s^{-1}	Shear rate	7.2
$\dot{\gamma}^*$	s^{-1}	Critical shear rate for onset of non-Newtonian flow behavior	7.2
$\dot{\gamma}^{**}$	s^{-1}	Critical shear rate for transition to <i>upper Newtonian</i> viscosity plateau	7.2
$\dot{\gamma}_{gm}$	s^{-1}	Shear rate at geometric mean radius	8.4
$\dot{\gamma}_a$	s^{-1}	Apparent shear rate	8.3
$\dot{\gamma}_R$	s^{-1}	Wall shear rate	8.3
δ	—	A constant, function of r_1 and r_2 in Equation 4.45	4.10
δ	—	Loss angle	9.2
$\delta, \delta_1, \delta_2$	$(\text{cal}/\text{cm}^3)^{1/2}$ (Hildebrand)	Solubility parameters, also referred to solvent and polymer, respectively	2.5
$\delta_T, \delta_d, \delta_p, \delta_h$	$(\text{cal}/\text{cm}^3)^{1/2}$	Total, nonpolar, polar, and hydrogen-bonding solubility, respectively	2.5
$\sin \delta$	—	Power factor	11.6
$\tan \delta$	—	Dissipation factor	9.2, 11.6
ϵ	—	Elongation ($\epsilon = \gamma - 1$)	9.1
ϵ_1, ϵ_2	—	Elongation of components 1 and 2 in Maxwell model	9.2
$\dot{\epsilon}$	s^{-1}	Characteristic deformation rate or rate of elongation	7.7
ζ	—	Number of moles of elastic polymer strands	2.5
ζ_m	(N·s)/m	Monomeric friction coefficient	7.2
ζ_p	(N·s)/m	Polymer friction coefficient	7.2
ζ_{PT}	(N·s)/m	Friction coefficient for curvilinear motion of polymer in a tube	7.5
η	Pa·s, poise	Apparent shear viscosity	7.2
η_0	Pa·s, poise	Zero-shear viscosity	7.2
η_e	—	Entanglement slip coefficient	9.8
η_s	Pa·s, poise	Solvent viscosity	7.2
η_∞	Pa·s, poise	Shear viscosity in the upper Newtonian flow regime	7.2

(Continued)

Symbol	Common Unit	Definition or Label	Sections Where First Used
η^p	Pa-s, poise	Polymer contribution to the viscosity of a polymer solution	7.2
$[\eta]$	cm ³ /g	Intrinsic viscosity	7.4
$[\eta]_i$	cm ³ /g	Intrinsic viscosity of component i in a multicomponent mixture	7.4
$\overline{[\eta]}$	cm ³ /g	Average intrinsic viscosity of a multicomponent mixture	7.4
η_r	–	Reduced viscosity	7.4
η_r	–	Relative viscosity	7.8
η_{sp}	–	Specific viscosity	7.4
η_E	Pa-s, poise	Elongational viscosity	7.7
η_R, η_g	Pa-s, poise	Viscosity at T_R and T_g	7.6
η'	Pa-s, poise	Dynamic viscosity	9.2
θ, θ_f	K	Theta temperature or Flory temperature	7.4
θ	Degrees, rad	Supplement of bond angle	7.4
θ	s	Relaxation time	9.2
θ	Degrees	Light-scattering angle, incident X-ray beam angle	6.7, 18.6
θ_c	Degrees	Contact angle	13.4
θ_i	s	Rouse relaxation time	9.6
θ'	Degrees, rad	Bond angle	7.4
ι	–	Exponent relating \hat{g} and g	7.4
κ	–	Ratio of outer and inner cylinder radii	8.4
λ	Variable	Wavelength of light or other electromagnetic waves	6.7, 12.1
λ	s	Fluid relaxation time	7.2
λ	–	Coefficient in Equation 9.93	9.8
λ_{CR}	s	Constraint-release relaxation time	7.5
λ_{rep}	s	Reptation relaxation time	7.5
λ_1	s	Longest polymer relaxation time	7.2
μ, μ_1, μ_2	J	Chemical potential, also referred to solvent and polymer, respectively	3.3
μ	m ³ /s	Particle growth rate	5.5
μ	Pa-s, poise	Shear viscosity	7.2
μ	–	Geometric factor in Equation 9.4	9.1
ν	m ² /s	Kinematic viscosity	7.3
ν	–	Poisson's ratio	9.1
ν_n	Variable	Kinetic chain length	4.4
π	Pa	Osmotic pressure	6.6
ρ	g/cm ³	Density	3.10, 6.6, 7.2

(Continued)

Symbol	Common Unit	Definition or Label	Sections Where First Used
ρ_i	–	Ratio of reactive groups on reactant i to all groups that react the same way in the system	4.8
ρ_r	ohm-cm	Volume resistivity	11.6
ρ_r	Radicals/s	Rate of radical generation	5.5
σ	–	Steric factor	7.4
σ	Pa	Tensile stress	9.1
σ_b	Pa	Stress at break	10.1
σ_f	Pa	Stress at fracture	10.7
$\sigma_n(n)$	Pa	Stress at break for n th sample	10.1
$\bar{\sigma}_b$	Pa	Modal strength for sample population	10.1
σ_i	Pa	Stress in element i	9.5
σ_0	Pa	Fixed stress	9.2
σ_T	Pa	Total stress of an array of elements	9.5
τ	s	Time of particle formation	5.5
τ, τ_s	Pa	Stress, shear stress	7.2
τ_e	s ⁻¹	Characteristic time of stress relaxation in Equation 9.99	9.8
τ_{gm}	Pa	Shear stress at geometric mean radius	8.4
τ_{ij}	Pa	Component of the stress tensor	8.2, Appendix 8.A
τ_r, τ_w	Pa	Shear stress at radial location r or capillary wall ($r = R$)	8.3
$\tau_{R,t}, (\tau_w)_t$	Pa	True wall shear stress	8.3
τ_0	Pa	Yield stress	7.2
φ	Degrees	Conformation bond angle	7.4
φ	–	Volume fraction of polymer in solution (Figure 6.5)	6.4
$[\varphi]$	mol/l	Concentration of ester bonds	12.3
χ	–	Polymer–solvent interaction parameter	2.5
χ_c	–	Critical value of the interaction parameter	3.3
χ_H	–	Enthalpic contribution of the interaction parameter	2.5
ψ'	Degrees	Angle of twist	9.1
ω	rad/s	Frequency	9.2
ω_c	Hz (cycles/s)	Frequency	11.6

Appendix B

**TYPICAL PROPERTIES OF POLYMERS USED
FOR MOLDING AND EXTRUSION**

	ASTM Test Method	ABS Medium Impact	Acetal	Cellulose Acetate	Poly (Tetrafluoroethylene)	Poly(Vinyl Fluoride) (Film)	Poly(Vinylidene Fluoride)	Ionomers	Nylon 6,6 (Moisture-Conditioned)
Specific gravity	D792	1.03–1.06	1.42	1.22–1.34	2.14–2.20	1.38–1.40	1.77–1.78	0.93–0.96	1.13–1.15
Refractive index	D542		1.48	1.46–1.50	1.35			1.51	1.53
Tension strength (GPa)	D638, 651	40–50	65–80	13–60	15–35	41–110	25–50	25–35	75
Elongation (%)	D638	5–25	9.5–12	1.9–9.0	2–5	100–250	12–600	350–450	300
Tension modulus (GPa)	D638	2–3	3.6	0.45–2.80	0.40	2.1–2.6	1.0–5.5	0.14–0.40	
Compressive strength (MPa)	D695	70–85	125	20–55	12		55–110		
Flexural strength (MPa)	D790	75–90	95	15–110	12–65		65–95		40
Impact strength, notched Izod (J/m)	D256	160–320	70–120	50–420	160		135–4300	320–800	110
Hardness, Rockwell	D785	R107–115	M94–R120	R34–125			R79–85		R120
Hardness, Shore								D50–65	
Flexural modulus (GPa)	D790	2.5–2.8	2.6–3.0	–	D50–55		1–8		1.2–2.8
Compressive modulus (GPa)	D695	1.4–3.1	4.6						
Thermal conductivity ((cal/s·cm·K) × 10 ⁴)	C177	4.5–8.0	5.5	4–8	6.0		2.4–3.1	5.8	5.8
Specific heat (cal/g·K)	–	0.3–0.4	0.35	0.3–0.4	0.25			0.55	0.4

Linear thermal expansion coefficient ($K^{-1} \times 10^6$)	D696	8-10	10	8-18	10	12	8.0
Continuous use temperature ($^{\circ}C$)	-	71-93	90	60-105	290	70-95	80-150
Deflection temperature ($^{\circ}C$) (at 0.45 MPa)	D648	102-107	124	50-100	121	38	180-240
Volume resistivity (ohm-cm)	D257	$2.7 \times E 16$	$1 \times E 15$	$1 \times E 10-14$	Greater than E 18	$2 \times E 14$	E 14-E 15
Dielectric strength (V/mm)	D149	15-20	20	10-20	20	35-45	15-18
Dielectric constant (1 kHz)	D150	2.4-4.5	3.7	3.4-7.0	Less than 2.1	2.4	3.9-4.5
Dissipation factor (1 kHz)	D150	0.004-0.007	0.004	0.01-0.07	Less than 0.0002	0.0015	0.02-0.04
Deleterious media	D543	Concentrated oxidizing acids, OS	SA, SB	SA, SB	None	SA	SA
Solvents ($25^{\circ}C$)	-	Ketones, esters, CH	None	Ketones, esters, CH	None	None	Phenol, formic acid

(Continued)

ASTM Test Method	Nylon 6		Polycarbonate		High-Density Polyethylene		Low-Density Polyethylene		Linear Low-Density Polyethylene		Ultra-High-Molecular-Weight Polyethylene		Polypropylene		Poly(Methyl Methacrylate)	
Specific gravity	D792	1.12–1.14	1.2	0.940–0.965	0.910–0.925	0.918–0.94	0.94	0.90–0.91	1.17–1.20							
Refractive index	D542		1.586	1.54	1.51			1.49								
Tension strength (GPa)	D638, 651	70	65	20–40	4–16	15–38	40–50	30–40	50–75							
Elongation (%)	D638	300	110	20–130	90–800	100–965	350–525	100–600	2–10							
Tension modulus (GPa)	D638	0.7	2.4	0.4–1.2	0.10–0.25			1.1–1.6	2–6							
Compressive strength (MPa)	D695		85	20–35				35–55	80–125							
Flexural strength (MPa)	D790	35	95	7				40–55	90–130							
Impact strength, notched Izod (J/m)	D256	150	850	25–1000	No break	No break	No break	20–50	15–25							
Hardness, Rockwell	D785	R119	M70	D60–70	D40–51	D55–56	R50	R80–102	M85–105							
Hardness, Shore				0.7–1.8	0.06–0.4	0.3–0.7	D61–63	1.2–1.7	2.9–3.2							
Flexural modulus (GPa)	D790	1.0	2.3	0.7–1.8	0.06–0.4		0.9–1.0	1.0–2.1	2.6–3.2							
Compressive modulus (GPa)	D695	1.7	2.4													
Thermal conductivity ((cal/s-cm-K) × 10 ⁴)	C177	5.8	4.7	11–12	8.0			2.8	4–6							

Specific heat (cal/g·K)	–	0.38	0.3	0.55	0.55	0.46	0.35
Linear thermal expansion coefficient ($K^{-1} \times 10^6$)	D696	8.0–8.3	6.8	11–13	10–22	13–20	5–9
Continuous use temperature ($^{\circ}C$)	–	80–120	121	120	80–100	70–82	60–88
Deflection temperature ($^{\circ}C$) (at 0.45 MPa)	D648	150–185	138	60–88	38–49	225–250	80–107
Volume resistivity (ohm-cm)	D257	E 12–E 15	$2.1 \times E 16$	Greater than E 16	Greater than E 16	Greater than E 16	Greater than E 14
Dielectric strength (V/mm)	D149	17–20	15	18–20	18–40	28	15
Dielectric constant (1 kHz)	D150	4.0–4.9	3.02	2.30–2.35	2.25–2.35	2.2–2.6	3.0–3.6
Dissipation factor (1 kHz)	D150	0.011–0.06	0.0021	Less than 0.0005	Less than 0.0005	Less than 0.0018	0.03–0.05
Deleterious media Solvents (25 $^{\circ}C$)	D543	SA Phenol, formic acid	Bases, SA Aromatic, CH	SOA None	SOA None	SOA None	SB, SOA Ketones, esters, CH, aromatic

(Continued)

Linear thermal expansion coefficient (K ⁻¹ × 10 ⁶)	D696	5.2-5.6	6-8	3.4-21	5-10	7-25	65
Continuous use temperature (°C)	-	150-175	66-77	60-79	65-80	65-80	
Deflection temperature (°C) (at 0.45 MPa)	D648	180	75-100	75-95	57-82		75
Volume resistivity (ohm-cm)	D257	5 × E 16	Greater than E 16	Greater than E 16	Greater than E 16	E 11-E.15	Greater than E 16 E 10-E 14
Dielectric strength (V/mm)	D149	17	20-28	12-24	17-50	12-40	17-22
Dielectric constant (1 kHz)	D150	3.13	2.4-2.65	2.4-4.5	3.0-3.3	4-8	3.45-3.5 5.7-7.3
Dissipation factor (1 kHz)	D150	0.001	0.0001-0.0003	0.0004-0.002	0.009-0.017	0.07-0.16	0.005-0.007 0.02-0.05
Deleterious media Solvents (25°C)	D543	None Aromatic	SOA Aromatic, CH	SOA Aromatic, CH	None Ketones, esters, aromatic, CH	None Same as rigid	

(Continued)

	ASTM Test Method	Epoxy (Bisphenol) (w/Glass Fiber)	Melamine-Formaldehyde (w/Glass Fiber)	Phenol-Formaldehyde (w/Glass Fiber)
Specific gravity	D792	1.5–2.0	1.5–2.0	1.7–2.0
Refractive index	D542			
Tension strength (GPa)	D638, 651	35–135	35–70	50–120
Elongation (%)	D638	4	0.6	0.2
Tension modulus (GPa)	D638	20	11–17	13–23
Compressive strength (MPa)	D695	125–275	135–240	110–480
Flexural strength (MPa)	D790	40–200	100–160	80–400
Impact strength, notched Izod (J/m)	D256			
Hardness, Rockwell	D785	M100–112	M115	E54–101
Hardness, Shore				
Flexural modulus (GPa)	D790	15–30		8–25
Compressive modulus (GPa)	D695			20–25
Thermal conductivity ((cal/s·cm·K) × 10 ⁴)	C177	4–10	10–11.5	8–14
Specific heat (cal/g·K)	–			

Linear thermal expansion coefficient ($K^{-1} \times 10^6$)	D696	11–50	15–28	8–34
Continuous use temperature ($^{\circ}C$)	–			
Deflection temperature ($^{\circ}C$) (at 0.45 MPa)	D648	Greater than 225	Greater than 375	Greater than 350
Volume resistivity (ohm-cm)	D257	E 15–E 16	E 11	$3 \times E 10$
Dielectric strength (V/mm)	D149	10–20	5–15	6–16
Dielectric constant (1 kHz)	D150	3.0	7.0	4.5
Dissipation factor (1 kHz)	D150	0.004	0.015	0.019
Deleterious media Solvents ($25^{\circ}C$)	D543	–		

Source: Based on manufacturers' data as reported in *Modern Plastics Encyclopedia* and other sources.

ABS, acrylonitrile-butadiene-styrene; ASTM, American Society for Testing and Materials; CH, chlorinated hydrocarbon; OS, organic solvent; SA, strong acid; SB, strong base; SOA, strong oxidizing acid.

Appendix C

TYPICAL PROPERTIES REPORTED FOR SOME COMMERCIAL TEXTILE FIBERS

Fiber Identification		Breaking Tenacity (g/denier)		Elongation at Break(%)		Density (g/cm ³)	Water Absorbed ^a (%)	Thermal Stability
		Standard	Wet	Standard	Wet			
Generic Name	Description							
Rayon (regular viscose)	Regenerated cellulose	1.9–2.3	1.0–1.4	20–25	24–29	1.48–1.54	11–13	Loses strength at 150°C, decomposes at 175°C–240°C
Rayon (high-tenacity viscose)	Regenerated cellulose	4.9–5.3	2.8–3.2	11–14	13–16	1.48–1.54	11–13	Similar to regular viscose
Acetate	Cellulose diacetate	1.2–1.4	0.8–1.0	25–45	35–50	1.32	6.3–6.5	Sticks at 175°C–205°C, softens at 205°C–230°C, melts at 260°C
Acetate	Cellulose triacetate	1.1–1.3	0.8–1.0	26–40	30–40	1.3	3.2	Melts at 300°C
Spandex	Segmented polyurethane	0.8–1.0	–	400–800	–	1.2	1.3	Sticks at 215°C
Fluorocarbon	Poly(tetrafluoroethylene)	0.9–2.1	0.9–2.1	19–140	19–140	2.1	Nil	Melts at about 288°C
Polyester	Poly(ethylene terephthalate)	2.0–9.5	2.0–9.5	12–55	12–55	1.38–1.39	0.4	Sticks at 230°C, melts at 250°C
Acrylic	Polyacrylonitrile	2.0–3.0	1.6–2.7	30–45	30–50	1.17	1.5	Shrinks 5% at 253°C
Nylon	Nylon 6	2.0–9.0	1.7–8.2	16–50	19–60	1.14	2.8–5.0	Melts at 216°C, decomposes at 315°C
Nylon	Nylon 66	2.3–9.8	2.0–8.0	15–65	18–70	1.13–1.14	4.0–4.5	Sticks at 230°C, melts at 250°C–260°C
Aramid	<i>Kevlar</i> (duPont)	18–30	22	1.5–4.2	2.5–4	1.44–1.47	1.2–4.3	Decomposes at 500°C
Aramid	<i>Nomex</i> (duPont)	2.3–5.1	–	25–32	20–30	1.38	4.5	Decomposes at 370°C
Olefin	LDPE	1.0–3.0	1.0–3.0	20–80	20–80	0.92	Nil	Softens at 105°C–115°C, melts at 110°C–120°C

(Continued)

Fiber Identification		Breaking Tenacity (g/denier)		Elongation at Break(%)		Density (g/cm ³)	Water Absorbed ^a (%)	Thermal Stability
Generic Name	Description	Standard	Wet	Standard	Wet			
Olefin	HDPE	3.5–7.0	3.5–7.0	10–45	10–45	0.95	Nil	Softens at 115°C–15°C, melts at 125°C–138°C
Olefin	<i>Spectra</i> (Honeywell), gel-spun polyethylene	30–35	30–35	2.7–3.6	2.7–3.6	0.97	Nil	Melts at around 145°C
Olefin	Polypropylene	2.5–5.5	2.5–5.5	14–150	14–150	0.91	0.01	Softens at 140°C–175°C, melts at 160°C–177°C
Cotton	Cellulose	3.0–4.9	3.0–5.4	3–10	–	1.54	7–8.5	Decomposes at 150°C
Wool	Protein	1.0–2.0	0.8–1.8	20–40	–	1.32	11–17	Decomposes at 130°C
Silk	Protein	3.5	2.8	20	–	1.34	10	<i>Safe iron limit</i> , 145°C

Source: Based on information from manufacturers reported in *Textile World* and other sources. Tensile strength (MPa) = tenacity (g/d) × density × 88.3.

^a at 21°C, 65% relative humidity.

HDPE, high-density polyethylene; LDPE, low-density polyethylene.

Appendix D

MAJOR MARKETS FOR SELECTED PLASTICS AND RUBBER

Polymer	Total Use ^a (millions of kg)	Major Markets
Carbon-Chain Polymers		
LDPE	3506	27% packaging film, 25% bags and other extruded products and coatings, 6% molding
LLDPE	4478	26% packaging film, 22% bags and other extruded products and coatings, 10% molding
HDPE	7092	2% packaging film, 29% bags and other extruded products, 44% molding
Polypropylene	6051	28% other extruded products, 35% injection molded
PVC	6632	11% calendering and coating, 81% extruded products (pipe, siding, wire, etc.), 4% molding
Polystyrene	3009	32% molding, 43% extrusion, 14% expanded (foams)
ABS and other styrenics	805	50% molding, 35% extrusion
Poly(methyl methacrylate)	682	32% cast and extruded sheet, 15% molding, 24% coatings
EPDM and EPR	346	44% transportation, 18% roofing, 18% oil additives, 10% wire
SBR ^b	874	77% tires, 5% other transportation, 15% mechanical goods
NBR	89	48% mechanical goods, 15% molded products, 15% latex products (gloves, etc.), 15% adhesives
CR	64	25% transportation, 30% mechanical goods, 25% adhesives
Heterochain Polymers		
PET (non-fibers)	2323	60% molded bottles, 6% film and sheet
PBT	71	50% transportation
Urethane	2809	26% construction, 28% transportation, 14% furniture, 9% carpeting
Polycarbonate	232	20% blends with ABS, 25% transportation, 27% optics and glazing
Nylon (non-fibers)	271	39% transportation, 12% films
Acetals	65	29% transportation, 26% consumer products, 7% hardware

(Continued)

Polymer	Total Use^a (millions of kg)	Major Markets
Phenol-formaldehyde	1455	49% plywood, 19% other bonding, 13% glass insulation coating
Melamine-formaldehyde	145	37% coatings, 32% laminates
Urea-formaldehyde	273	88% wood adhesives
Epoxy	300	40% coatings, 5% adhesives, 20% molding (composites)

Source: Estimates based on *Modern Plastics, Chemical Marketing Reporter, SRI Reports*.

^a 77% emulsion polymer, 23% solution polymer.

^b North America in 2000.

ABS, acrylonitrile–butadiene–styrene; CR, chloroprene rubber; EPDM, ethylene propylene diene monomer; EPR, ethylene propylene; HDPE, high-density polyethylene; LDPE, low-density polyethylene; LLDPE, linear low-density polyethylene; NBR, nitrile-butadiene rubber; PET, poly(ethylene terephthalate); PBT, poly(butylene terephthalate); PVC, poly(vinyl chloride); SBR, styrene butadiene rubber.

Appendix E

EQUIVALENTS FOR SELECTED SI QUANTITIES

Quantity	SI Unit	Value in cgs Units	Value in British Units
Mass	kg	1.000×10^3 g	2.200 lb _m
Length	m	1.000×10^2 cm	3.281 ft
Area	m ²	1.000×10^4 cm ²	10.76 ft ²
Volume	m ³	1.000×10^6 cm ³ , or 1.000×10^3 liter	35.31 ft ³ or 264.2 gal (US)
Force	N (newton)	1.000×10^5 dyn	0.2248 lb _f
Energy	J (joule), N·m	1.000×10^7 erg or 0.2389 cal	0.7376 ft·lb _f or 0.9481×10^{-3} Btu
Pressure, stress	Pa (pascal), N·m ⁻²	10.00 dyn	1.450×10^{-4} lb _f /in ² , psi
Viscosity	Pa·s	10.00 P (poise)	6.72 lb _m /ft·s
Power	W (watt), J/s	1.000×10^7 erg/s or 14.34 cal/min	1.341×10^{-3} hp or 3.413 Btu/h
Specific heat	J/kg·K	2.389×10^2 cal/g·°C	2.389×10^2 Btu/lbm·°F
Heat transfer coefficient	W/m ² ·K	0.2389 cal/m ² ·s·°C	0.1761 Btu/ft ² ·h·°F
Impact strength	J/m		1.873×10^{-2} ft·lb _f /in
Gas constant	8.314 J/K·mol	0.08206 liter·atm/K·mol	

Maintaining a balance between depth and breadth, the *Sixth Edition of Principles of Polymer Systems* continues to present an integrated approach to polymer science and engineering. A classic text in the field, the new edition offers a comprehensive exploration of polymers at a level geared toward upper-level undergraduates and beginning graduate students.

Revisions to the sixth edition include:

- A more detailed discussion of crystallization kinetics, strain-induced crystallization, block copolymers, liquid crystal polymers, and gels
- New, powerful radical polymerization methods
- Additional polymerization process flow sheets and discussion of the polymerization of polystyrene and poly(vinyl chloride)
- New discussions on the elongational viscosity of polymers and coarse-grained bead-spring molecular and tube models
- Updated information on models and experimental results of rubber elasticity
- Expanded sections on fracture of glassy and semicrystalline polymers
- New sections on fracture of elastomers, diffusion in polymers, and membrane formation
- New coverage of polymers from renewable resources
- New section on X-ray methods and dielectric relaxation

All chapters have been updated and out-of-date material removed. The text contains more theoretical background for some of the fundamental concepts pertaining to polymer structure and behavior, while also providing an up-to-date discussion of the latest developments in polymerization systems. Example problems in the text help students through step-by-step solutions and nearly 300 end-of-chapter problems, many new to this edition, reinforce the concepts presented.

K22345